BC

Province of British Columbia
Ministry of Energy, Mines
and Petroleum Resources

MINERAL RESOURCES DIVISION
Geological Survey Branch

GEOLOGICAL FIELDWORK 1991

A Summary of Field Activities and Current Research

Editors: B. Grant and J.M. Newell

PAPER 1992-1

MINERAL RESOURCES DIVISION
Geological Survey Branch

British Columbia Cataloguing in Publication Data

Main entry under title:
Geological fieldwork. — 1974–

(Paper. ISSN 0226-9430)
Annual.
Issuing body varies: 1974–1980, Geological Division; 1981–1985, Geological Branch; 1986– . Geological Survey Branch.
Subseries, 1979– , of: Paper (British Columbia. Ministry of Energy, Mines and Petroleum Resources)
"A summary of field activities of the Geological Division, Mineral Resources Branch."
ISBN 0381-243X=Geological fieldwork

1. Geology — British Columbia — Periodicals. 2. Geology, Economic — British Columbia — Periodicals. 3. Mines and mineral resources — British Columbia — Periodicals. I. British Columbia. Geological Division. II. British Columbia. Geological Branch. III. British Columbia. Geological Survey Branch. IV. British Columbia. Ministry of Energy, Mines and Petroleum Resources. V. Series: Paper (British Columbia. Ministry of Energy, Mines and Petroleum Resources)

QE187.G46 557.11'05
Rev. Dec. 1987

VICTORIA
BRITISH COLUMBIA
CANADA

January 1992

PREFACE

The 1991 edition of *Geological Fieldwork: A Summary of Field Activities and Current Research* is the seventeenth in this annual publication series. It contains reports on activities and project results in a year in which the Geological Survey Branch underwent a substantial reorganization in order to better serve the needs of an increasingly broad-based client group. The base budget of the Branch for the 1991/92 fiscal year was $7.45 million, a modest increase over the previous year. An additional $505 000 was allocated for economic development projects as B.C.'s share of an anticipated renewed Canada-British Columbia Partnership Agreement on Mineral Development (MDA-2).

The diversity of the Branch's current programs is reflected in the highlights of this year's volume which include:

- Reports on four 1:50 000-scale geological mapping programs, two in the Stikine district of northwestern British Columbia and two in the northern Quesnel trough, both areas of strong exploration activity for alkalic porphyry copper-gold deposits.
- Reports on mineral potential studies of candidate parks in the Babine Mountains, Cascade and Kakwa recreation areas carried out at the request of the Ministry of Environment, Lands and Parks, in accordance with the requirements of Section 19 of the *Mineral Tenure Act.*
- Reports covering work in the wind-up year of studies of the metallogenesis of the Rossland mining camp and of skarn deposits throughout the province, and the initiation of a new project to study deposits transitional between the porphyry and epithermal environments.
- The expanding role of the Branch's Environmental Geology Section is reflected in papers covering such diverse topics as: the on-going Regional Geochemical Survey program; geological hazards in the Peace River district; the study of neotectonics on Vancouver Island, with particular reference to the evaluation of potential seismic risks; geochemical prospecting techniques applicable to areas thickly mantled by Quaternary deposits with complex stratigraphy; the Quaternary geology of gold placers in the Atlin district; and construction aggregate resources in the Sooke area of southern Vancouver Island.
- Progress reports ongoing studies of the quality of British Columbia coals and potential coalbed-methane resources.
- A report on the magnesite resources of southeastern British Columbia.
- A progress report on the application of digital geographical information systems (GIS) to assessment of mineral resource potential and land-use planning.
- A new section that includes nine papers reporting on the results of research by the Mineral Deposit Research Unit (MDRU) at The University of British Columbia on the metallogenesis of the Iskut River area and related topics.

The continued success of the British Columbia Geoscience Research Grant Program and cooperative projects with the Geological Survey of Canada is evidenced by the inclusion of sixteen papers by external authors, in addition to the nine papers submitted by the MDRU. Topics covered include: the results of on-going research on the metallogenesis of the Silver Queen vein deposits at Owen Lake; paleomagnetism and its implications in unravelling the tectonic history of the Cordillera; the mineralogy of the footwall alteration zone beneath the Sullivan orebody: and other petrographic, mineralogical geochemical and structural geology studies at a number of locations throughout the province.

This volume of *Fieldwork* contains 58 papers, an increase of more than 27 per cent over last year but fifteen short of the record established by the 1989 edition. As always, meeting the January publication deadline demands a concerted and unstinting effort from our editorial and publications staff. We acknowledge the efforts of Doreen Fehr, Janet Holland and Shannon Ferguson for formatting and page layout, John Newell for timely editing, and Brian Grant for managing the entire process and plugging any holes that appeared. This is the tenth edition that Doreen Fehr has worked on and she has carried a particularly heavy load this year as her colleague, Janet Holland, was hospitalized quite early in the process. We also thank the staff of the Queen's Printer for their cheerful cooperation and enthusiasm, without which everyone else's efforts would be largely in vain.

W.R. Smyth
Chief Geologist
Geological Survey Branch
Mineral Resources Division

TABLE OF CONTENTS

TABLE OF CONTENTS *(Continued)*

PETROLOGY OF PRE TO SYNTECTONIC EARLY AND MIDDLE JURASSIC INTRUSIONS IN THE ROSSLAND GROUP, SOUTHEASTERN BRITISH COLUMBIA (82F/SW)

By Kathryn P.E. Dunne (née Andrew) and Trygve Höy

KEYWORDS: Regional geology, Rossland Group, Jurassic plutons, Eagle Creek Plutonic Complex, Rossland monzonite, Rossland sill, monzogabbro, Silver King intrusions.

INTRODUCTION

Early and Middle Jurassic plutons are recognized throughout the Rossland Group in southeastern British Columbia. They are important in understanding the tectonics and metallogeny of the group. They host a variety of mineral deposits, including the mesothermal veins of the Rossland gold-copper camp and vein and alkali porphyry deposits south and west of Nelson.

The purpose of this paper is to present data on four main intrusive suites in the Trail map area and to relate these suites to the Rossland Group or to the early deformational history of the area. The paper reviews field data, presents new petrographic and geochronological data, and discusses mineralizing events.

REGIONAL SETTING

The Rossland Group is exposed in a broad arcuate belt in the Trail map area, bounded to the east, north and west by granitic rocks of the Late Jurassic Nelson batholith and in fault contact with lower Paleozoic rocks of the Kootenay Arc on the south (Figure 1-1-1). The group forms the eastern boundary of Quesnellia and is similar in composition to rocks of the Nicola and Takla groups.

The Rossland Group is Early Jurassic in age (Frebold and Little, 1962; Frebold and Tipper, 1970; Tipper, 1984). It comprises a basal succession of dominantly fine-grained clastic rocks of the Archibald Formation, volcanic rocks of the Elise Formation and overlying clastic rocks of the Hall Formation. The Ymir Group underlies the Elise Formation in the Nelson area; its upper part is correlative with the Archibald Formation.

The Rossland and Ymir groups are intruded by a number of different plutons including a suite of synvolcanic intrusions, syncollisional early-Middle Jurassic plutons, the Middle to Late Jurassic Nelson intrusions, the Middle Eocene Coryell intrusions and numerous felsic and mafic Tertiary dikes.

EAGLE CREEK PLUTONIC COMPLEX

The Eagle Creek Plutonic Complex, referred to as 'pseudodiorite' (Mulligan, 1952), straddles the Kootenay River 3 kilometres west of Nelson. It is generally a medium to coarse-grained mafic intrusion, in part gneissic; however, it grades into leucocratic hornblende syenite (Mulligan, 1951) and locally incorporates coarse ultramafic phases (Mulligan, 1951, 1952; Little, 1982a, b; Lindsay, 1991). It is described as metadiorite by Lindsay on the basis of extensive petrography and rock geochemistry at the Moochie occurrence. It is suggested that the term Eagle Creek, originally proposed by Mulligan (1951), be retained.

Contacts of the Eagle Creek Plutonic Complex with the Rossland Group rocks are generally sharp, locally marked by coarse-grained clinopyroxenites. The southwest part of the complex is cut by the Mount Verde fault, a steep, westerly-dipping, listric normal fault that records a period of extension just prior to intrusion of the Nelson batholith (Figure 1-1-1; Höy and Andrew, 1989a, b).

The age of the Eagle Creek Plutonic Complex is not known. It is cut by the Nelson granodiorite (*ca.* 165 Ma) and by the Silver King shear zone, a wide zone of shearing along the margins and extending into the core of the Hall Creek syncline. This shearing and deformation is dated at about 180 Ma, the age of syntectonic intrusion (*see* section on Silver King intrusions). Its relationship to the surrounding Rossland Group rocks (*ca.* 190–200 Ma) is less clear. However, based on similarity with the Rossland monzonite and its pretectonic age, it is possible that the complex may be cogenetic with Rossland Group volcanism

PETROGRAPHY

The Eagle Creek Plutonic Complex is a composite intrusion with phases varying from equigranular to porphyritic and mafic to ultramafic. The mafic phases contain 10 to 30 per cent plagioclase (An_{5-84}) and minor (1 to 15%) microcline (Plate 1-1-1, Table 1-1-1). Primary quartz ranges up to 5 per cent. Most mafic minerals are variably altered to chlorite and carbonate; unaltered mafic minerals are rare and include euhedral augite (5–15%), hornblende (3%) and green biotite (10–30%). Apatite occurs frequently as an accessory mineral in the mafic phases. The ultramafite contains at least 25 per cent augite, 10 per cent amphibole and abundant alteration of remaining mafic minerals to chlorite.

The complex is variably altered and sheared close to the Silver King shear zone (Figure 1-1-1). Plagioclase is commonly saussuritized, sericitized and/or replaced in part by chlorite. Muscovite, chlorite and calcite overprint and surround plagioclase and microcline (Lindsay, 1991) and segregated albite and epidote show fine-grained cataclastic textures.

On Streckeisen's (1973) quartz-alkali feldspar-plagioclase diagram (Figure 1-1-2) phases of the Eagle Creek Plutonic Complex fall within the monzonite, quartz monzonite, quartz monzodiorite, quartz gabbro and diorite/gabbro fields. Diorite or gabbro are the most common phases in the field and because of regional metamorphism, may be referred to as metadiorite/gabbro.

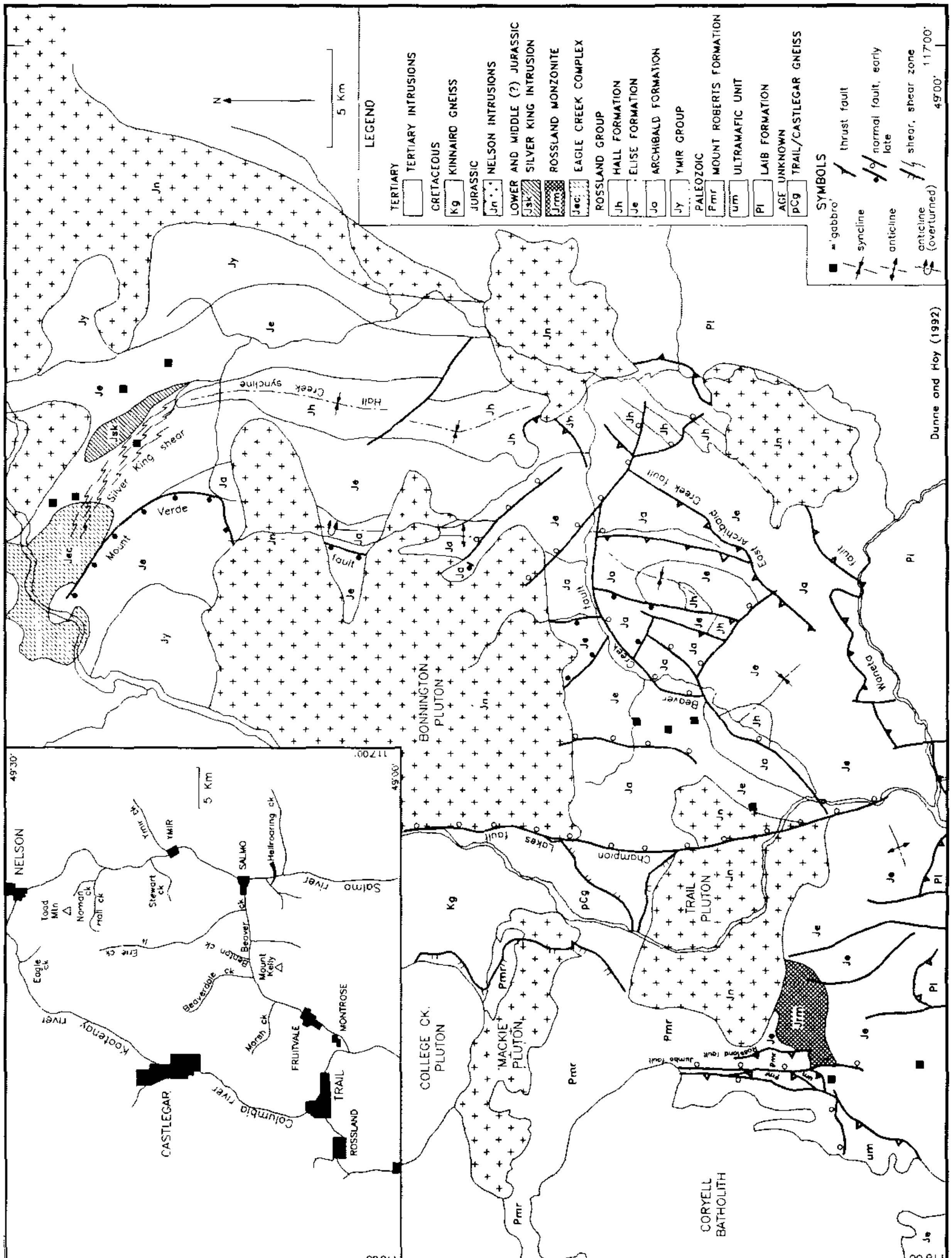

Figure 1-1-1. Distribution of Early and Middle Jurassic intrusions and main geologic and physiographic features of the Trail map area (082F/SW). 'Gabbro' intrusions are located by small squares.

Plate 1-1-1. Microcline crystal, 635 microns, in gabbro phase of the pseudodiorite (field of view = 1.48 mm).

Ultramafic phases along the margins of the complex are coarse-grained clinopyroxenite. They have similar mineral assemblages to the metadiorite/gabbro (Mulligan, 1951), comprising dominantly augite with lesser green amphibole rimming and replacing the augite, and secondary chlorite (Plate 1-1-2). Symplectite texture, comprising iron ore, probably ilmenite, intimately intergrown with clinopyroxene in a vermicular fashion, is seen in the ultramafic phases (Plate 1-1-3). Minor saussuritized plagioclase is noted in some localities (Mulligan, 1951).

Certain phases of the Eagle Creek Plutonic Complex, such as the monzonitic to syenitic rocks and clinopyroxenites, suggest affinities to Alaskan-type mafic-ultramafic complexes (Nixon, 1990). However, silica-oversaturated rocks such as the quartz monzonites, diorites and gabbros are more akin to calcalkaline plutonic suites.

Mineral Prospects

Several mineral deposits and showings occur within or adjacent to the Eagle Creek Plutonic Complex. These include porphyry copper-gold showings such as the Toughnut and Moochie occurrences and copper-gold-lead veins. Mineralization at the Toughnut zone adjacent to the complex includes disseminated chalcopyrite, tetrahedrite and pyrite in potassic-altered, carbonate and sericite-rich lower Elise Formation volcanic rocks .

The Moochie occurrence, within the complex, is characterized by disseminated chalcopyrite, magnetite and pyrite within locally potassic-altered metadiorite. Magnetite commonly encloses irregular lenses of ilmenite and cataclastic aggregates of chalcopyrite and magnetite are also noted (Lindsay, 1991). The occurrence is locally overprinted by the Silver King shear zone.

The Star and Granite Poorman occurrences are vein deposits within the complex. Quartz veins at the Star deposit carry patches of chalcopyrite, pyrite, malachite and

TABLE 1-1-1
PETROGRAPHIC COMPARISON OF TYPICAL LOWER TO MIDDLE JURASSIC INTRUSIONS IN THE ROSSLAND GROUP, TRAIL MAP AREA, SOUTHEASTERN BRITISH COLUMBIA

	Pseudodiorite (metadiorite/ gabbro)	Silver King Intrusions	Rossland Monzonite	Rossland Sill	'Gabbro' Nelson Area	'Gabbro' Fruitvale Area	'Gabbro' Rossland Area
Plagioclase	10–30	30–60	40–60	30–40	15–45	30–45	20–55
(An content)	5–84	28–60	38–48	48–54	50–67	54–69	55
Orthoclase	0	0	20–25	25	5–25	0–25	0
Microcline	1–15	0	0	0	0	0	0
Quartz	1–5	1–2	1–2	0	2–5	0	0
Augite	5–15	0	3–15	10	0	10–20	7–25
Hornblende	3	0–3	0–30	10	0–7	0–5	0
Biotite	10–30	0	5–15	10	1–25	0	0–1
Chlorite	2–35	10–15	5–25	1	5–20	0–20	10–40
Epidote	2–20	1–5	0	0	0–15	0–15	0–10
Sericite	10–20	5–60	0	0	0–35	0–35	0
Carbonate	7–25	5–30	0	0	0–10	0	0
Apatite	0–1	0–1	1	1	0–1	0–1	0–1
Sphene	0	0	0–1	0	0	0	0
Opaques	0–10	0–3	1–5	1	0–3	0–5	0–7
Matrix	0	0–60	0	0	0–25	0–35	0

Analyses incorporate, in part, work by Beddoe-Stephens and Lambert (1981), Fyles (1984), Lindsay (1991) and Mulligan (1951).

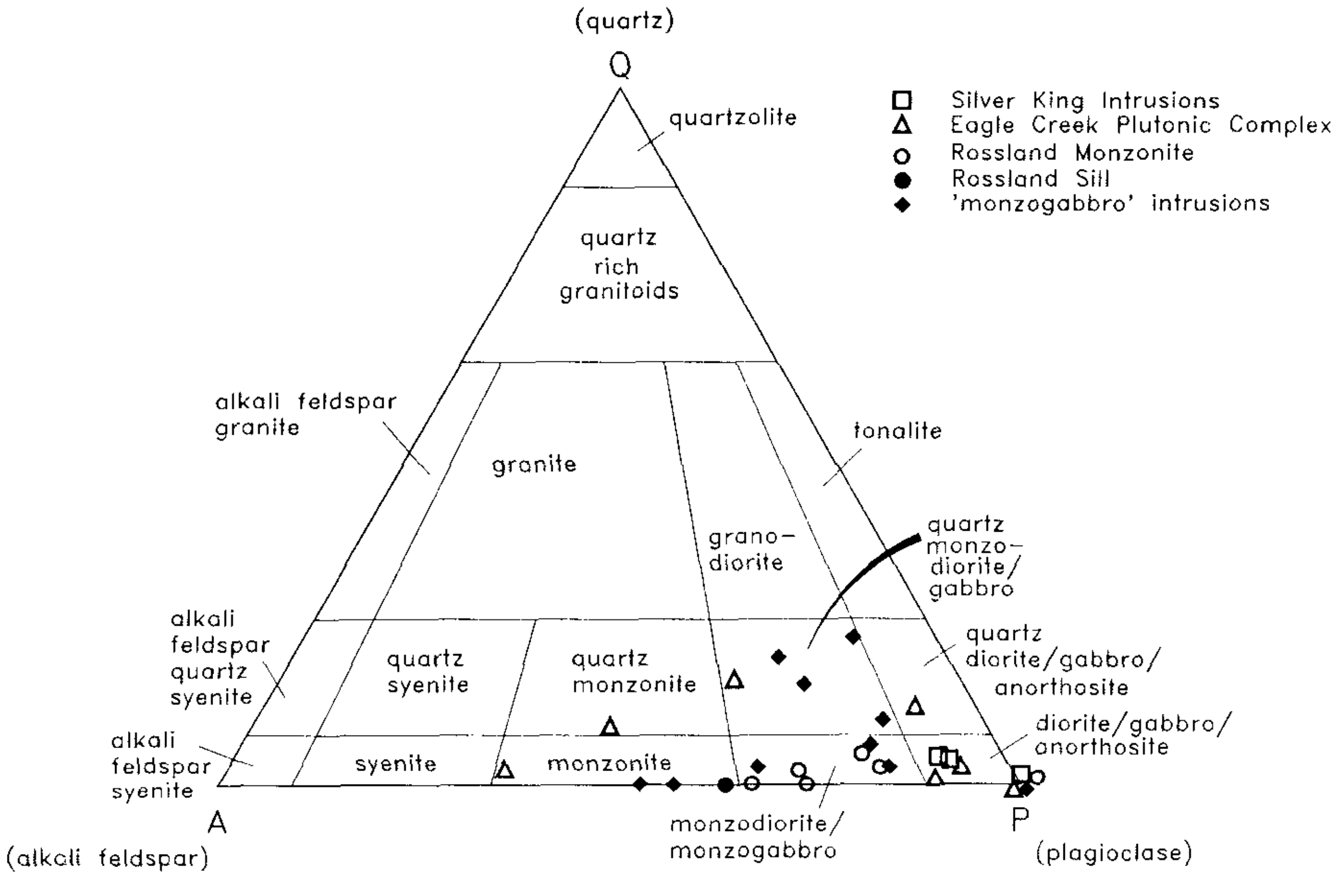

Figure 1-1-2. Quartz-alkali feldspar-plagioclase diagram of Early and Middle Jurassic intrusions in the Trail map area.

galena. The Granite Poorman mine (Dawson, 1889) is characterized by veins of quartz carrying pyrite, galena, chalcopyrite, sphalerite, minor scheelite and free gold.

ROSSLAND MONZONITE

The Rossland monzonite is centred on the town of Rossland and extends north to Monte Cristo and Columbia-Kootenay mountains and east to the vicinity of Lookout Mountain. A small fault slice of Rossland monzonite is exposed on the northwest slopes of Red Mountain. Contact relationships with the Rossland Group vary from sharp to locally gradational over several hundreds of metres, obscured by a wide thermal aureole (Fyles, 1984). The Rossland monzonite and Rossland mining camp have been studied by many previous workers including Drysdale (1915), Bruce (1917), Gilbert (1948), Little (1960, 1963, 1982b), Fyles (1984) and Höy and Andrew (1991a,b). Veins in the gold camp and their relationship to the monzonite and structures are discussed by Höy *et al.* (1992, this volume), molybdenum-skarn deposits on Red Mountain are reviewed by Webster *et al.* (1992, this volume) and studies of ultramafic bodies in fault slices just west of Rossland are outlined by Ash and MacDonald (1992, this volume).

The age of the Rossland monzonite is interpreted as Early Jurassic (*ca.* 190 Ma; J. Gabites, personal communication, 1991) suggesting that it is cogenetic with the Rossland Group (Höy *et al.*, 1992). It is cut on its west side by the Rossland fault, an east-directed thrust, and by the steeply dipping, north-trending Jumbo fault (Fyles, 1984; Höy and Andrew, 1991a,b). The Trail pluton, part of the Late Jurassic plutonic suite, obscures the Rossland monzonite contact to the north (Figure 1-1-1).

The Rossland monzonite hosts a number of different vein deposits, including the famous Le Roi, Centre Star and Evening Star mines. Gold-copper-lead-zinc veins hosted by the Elise Formation such as the Bluebird and Mayflower deposits occur mainly south of Rossland. Bonanza gold veins, including the Midnight deposit, occur adjacent to ultramafic bodies southwest of Rossland. Gold-copper skarn mineralization occurs within the Rossland monzonite adjacent to some of the main and north belt veins (Höy *et al.*, 1992).

PETROGRAPHY

The Rossland monzonite is an inequigranular intrusion. It comprises 40 to 60 per cent euhedral to subhedral andesine (An_{38-48}), with rare labradorite (An_{62-68}) in the Crown Point area, and 10 to 25 per cent orthoclase. Primary mafic minerals are only partially preserved, typically as ragged grains. Augite is replaced by hornblende in some areas but, more commonly, biotite replaces both hornblende and augite. Remnant augite comprises 3 to 15 per cent anhedral, often

Plate 1-1-2. Symplectite texture: ilmanite or magnetite and clinopyroxene intimately intergrown in a vermicular fashion in a coarse-grained clinopyroxenite phase of the pseudodiorite (field of view = 1.48 mm).

Plate 1-1-3. Coarse-grained augite crystals are pervasively rimmed and replaced by chlorite in coarse-grained clinopyroxenite phase of the pseudodiorite (field of view = 1.48 mm).

poikilitic crystals mantled by biotite and chlorite. Magnetite and apatite are ubiquitous accessory minerals; sphene is rare. Quartz, if present, ranges from 1 to 2 per cent as late, resorbed crystals which may indicate a subvolcanic origin for the intrusion (Table 1-1-1). This mineralogy indicates that the Rossland monzonite is dominantly a monzodiorite (Figure 1-1-2). Other phases include monzonite, and a large biotite clinopyroxenite xenolith is exposed at the Centre Star deposit.

Studies of metamorphism by Fyles (1984) define a wide thermal aureole around the intrusion. The northern margin, near Columbia-Kootenay Mountain, and the southern margin, south of Rossland, have a zone of well-indurated biotite hornfels, 300 to 500 metres wide, that is locally bleached, silicified and contains pyroxene and garnet (Fyles, 1984). Alteration of mafic minerals in the monzonite to ragged hornblende, biotite and chlorite may be due to superimposed regional metamorphism.

ROSSLAND SILL

The Rossland sill is exposed on the eastern slope of Red Mountain near Rossland. It has a similar mineral assemblage to the Rossland monzonite. The sill is fragmental in part, with blocks up to a metre wide with the same composition as the matrix (Fyles, 1984). Texturally, it is inequigranular to porphyritic with 30 to 40 per cent euhedral, sausseritized, oscillatory zoned calcic andesine to sodic labradorite (An_{48-54}) and 25 per cent orthoclase. Mafic minerals (30%) comprise nearly equal proportions of augite, a blue-green amphibole and biotite. The blue-green amphibole is probably secondary hornblende and may be described as uralite. The augite is oscillatory zoned and is often rimmed with hornblende (Plate 1-1-4). Accessory apatite in the sill has distinct mineral cores (Plate 1-1-5).

Symplectite textures of magnetite or ilmenite and clinopyroxene are common in the Rossland sill (Plate 1-1-6). On Monte Cristo Mountain, opaque oxide has symplectite textures and is mantled by biotite.

EARLY JURASSIC MONZOGABBRO UNIT

A number of monzogabbro/gabbro sills or small stocks occur throughout the exposures of the Elise Formation and are interpreted to be high-level syn-Rossland Group intru-

Plate 1-1-4. Augite rimmed by hornblende in the Rossland sill (field of view = 1.48 mm).

Plate 1-1-5. Accessory apatite crystal, 30 microns, with distinct mineral core in biotite from the Rossland sill (field of view = 185 microns).

sions. Previously referred to as 'diorite (Jdi)' (Andrew *et al.*, 1991), the sills are renamed on the basis of detailed petrography. They are typically tabular, lensoid or sill-like, several tens of metres thick and can often be traced for several kilometres. Others are subrounded, discordant plutons. They are fine to medium grained and often porphyritic with 30 to 40 per cent plagioclase phenocrysts in a dark green-grey matrix. They are petrographically distinct from the Eagle Creek Plutonic Complex, Rossland monzonite and Silver King intrusions. Monzogabbro stocks can occur anywhere within the Elise Formation but tend to be mainly in the upper part. Locations of monzogabbros studied in this report are plotted on Figure 1-1-1.

The best-documented example of an Early Jurassic monzogabbro is the Shaft intrusion, a tabular, locally brecciated complex up to 50 metres in width and 5 kilometres in strike length. It has pervasive propylitic alteration that hosts disseminated chalcopyrite, pyrite and magnetite (Andrew and Höy, 1989).

Petrography

Monzogabbros in the Nelson area have the widest diversity of mineral assemblages. Most are found intruding both upper and lower Elise Formation rocks up to 5 kilometres south and west of Nelson, in the plateau areas east of Toad Mountain and in the vicinity of Morning Mountain. They are characterized by 15 to 45 per cent labradorite (An_{50-67}), rarely saussuritized, a significant orthoclase component (5 to 25%), and minor quartz (2 to 10%). Primary mafic minerals are rarely seen (Plate 1-1-7), as they are commonly altered to hornblende, biotite, chlorite and epidote. Often, the unit has a fine-grained matrix of feldspar and chlorite with up to 1 per cent apatite and 1 per cent magnetite and pyrite. The Nelson area intrusions fall within the monzonite, (quartz) monzogabbro and quartz gabbro fields on Streckeisen's (1973) quartz-alkali feldspar-plagioclase diagram (Figure 1-1-2).

The Shaft intrusion exposed 3 kilometres south of Nelson is a fine to medium-grained, locally porphyritic monzogabbro. It is brecciated and locally sheared. It contains 30 to 45 per cent labradorite (An_{50-64}), 5 to 10 per cent orthoclase and 2 to 3 per cent quartz. It ranges in composition from quartz gabbro to quartz monzogabbro and monzogabbro. The feldspars are variably saussuritized and sericitized (10 to 25%). Biotite, chlorite and epidote have totally replaced any augite or hornblende phenocrysts. Apatite and

Plate 1-1-6. Symplectite texture of magnetite (?) – clinopyroxene mantled by biotite in the Rossland sill (field of view = 370 microns).

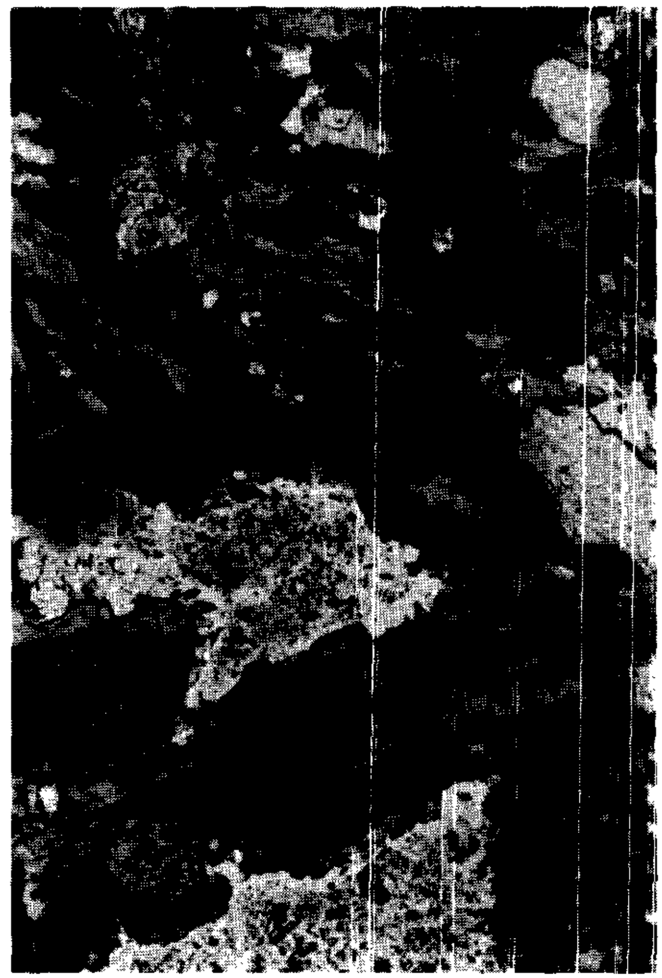

Plate 1-1-7. Hornblende, chlorite and epidote in 'gabbro from the Nelson area (field of view = 1.4 mm).

sphene are present as accessory minerals. Opaques include chalcopyrite, pyrite and magnetite. Hematite and malachite are common oxide minerals.

A number of monzogabbros in the Elise Formation north and east of Fruitvale are quartz-poor but have diverse feldspar compositions. They are characterized by 30 to 45 per cent labradorite (An_{48-72}), rarely concentrically zoned or saussuritized, and varying orthoclase content (0 to 35%); quartz is generally absent. Augite is usually preserved but variably altered to hornblende and chlorite. These monzogabbros may have a fine-grained matrix of feldspar, biotite and chlorite. Accessory apatite is rarely seen and 2 to 5 per cent opaque minerals, mainly pyrite, are present. The Fruitvale area monzogabbros plot within the monzonite, monzogabbro and gabbro fields (Streckeisen, 1973; Figure 1-1-2).

Monzogabbros in the Rossland area are quartz-poor and alkali-feldspar poor. Most are found in the Elise Formation south of Rossland on Tamarac Mountain or Deer Park Hill. They are characterized by 50 to 55 per cent euhedral labradorite and bytownite (An_{58-88}), typically saussuritized, minor orthoclase and no quartz. Augite is still preserved but variably altered to biotite and chlorite. Apatite is rare and up to 7 per cent opaque minerals, mainly pyrite occur in the matrix. These monzogabbros are mainly within the gabbro field on Figure 1-1-2.

SILVER KING INTRUSIONS

The Silver King intrusions are a suite of dominantly feldspar porphyries in the Nelson area. The main body is traced southeast from Giveout Creek, 1 to 5 kilometres south of Nelson (Figure 1-1-1). Several lenses of the Silver King porphyry outcrop on the west slopes of Mount Elise and border the main Silver King intrusion.

Outcrops of the Silver King intrusion are typically cream coloured and form resistant ridges. Contacts with Rossland Group rocks are either sharp and discordant or intensely sheared.

The Silver King intrusion is sheared along its margins. Commonly, smaller lenses are strongly foliated or sheared sericite phyllites that superficially resemble foliated felsic volcanic rocks. These contact relationships and the foliated to massive nature suggest that the Silver King intrusions are a pre to syntectonic suite.

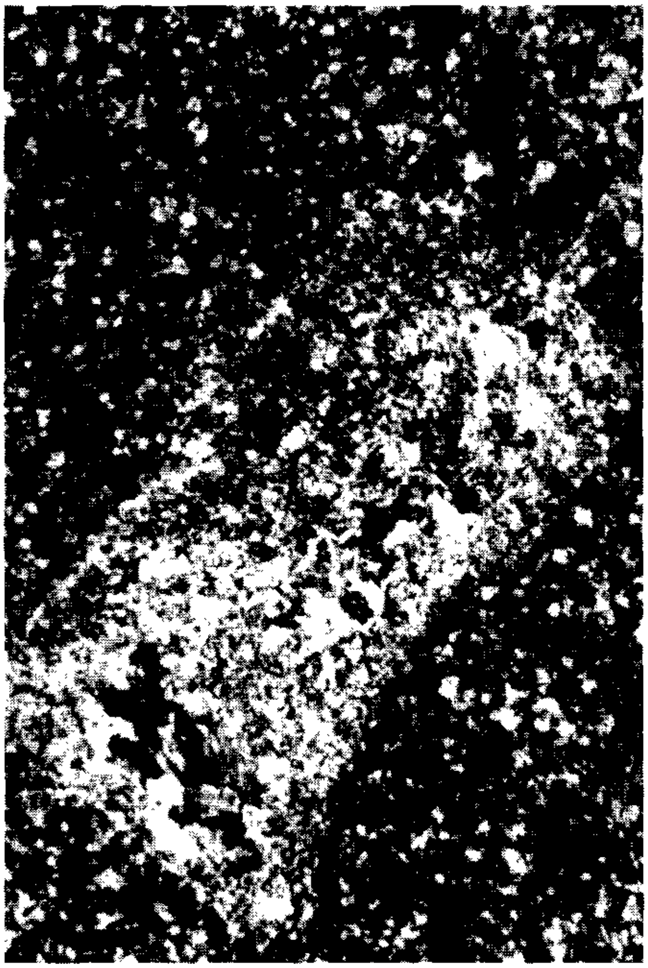

Plate 1-1-8. Intensely saussuritized plagioclase phenocrysts with inner zones replaced by clusters of sericite needles in a fine-grained matrix of feldspar and secondary quartz, Silver King intrusion (field of view = 1.48 mm).

Plate 1-1-9. Cataclastic fabric in the Silver King intrusion; platey minerals rotated into parallelism and rounded feldspar boudins in a protomylonite (field of view = 1.48 mm).

A stratabound conglomerate-breccia unit, the Silver King breccia (Mulligan, 1951, page 117), characterized by clasts of feldspar porphyry, outcrops in Gold Creek and the drainage basin south of Cottonwood Lake. It is described as an epiclastic unit of the Elise Formation by Höy and Andrew (1988), and is characterized by abundant to ubiquitous 10 to 15-centimetre clasts of plagioclase porphyry. These porphyry clasts were weathered from a high-level subvolcanic intrusion within the Elise Formation. Farther south, only the distal portions of the apron is exposed. The clasts are not, as previously described (Höy and Andrew, 1988), derived from weathering of Silver King intrusions; the intrusions are now known to be much younger than the Elise Formation.

Petrography

Silver King rocks are porphyritic, characterized by 10 to 30 per cent euhedral to subhedral plagioclase (An_{28-60}) phenocrysts, 5 to 10 millimetres in size (Table 1-1-1) in a fine-grained greenish grey groundmass. Quartz content ranges from 1 to 2 per cent; grains are commonly resorbed which may indicate a high-level of intrusion. Generally, primary mafic minerals are not preserved although acicular secondary hornblende needles are locally observed. Accessory sphene and ilmenite are common (Mulligan, 1951); apatite is rare.

The Silver King intrusion has been strongly altered and sheared. Plagioclase twinning is commonly obscured by intense saussuritization and the inner zones of the phenocrysts are replaced by clusters of sericite needles (Plate 1-1-8). Mafic minerals are almost totally replaced by chlorite and calcite. The groundmass comprises abundant secondary albite (?), epidote, carbonate and often 10 to 50 per cent interlocking aggregates of quartz grains and sericite 'mats'. A cataclastic fabric is typically seen in thin section. This varies from shearing and parallelism of platy minerals to rotation of feldspar boudins in a protomylonite (Plate 1-1-9).

A quartz-sericite-carbonate schist on the Great Western property, initially assumed to be part of the Elise Formation (Höy and Andrew, 1989c), is interpreted to be a small, strongly sheared Silver King intrusion. This occurrence is unusual as it contains 2 to 3 per cent scattered tourmaline crystals. The interpretation that this lens is part of the Silver King plutonic suite has important implications because it means that the Elise Formation is strictly intermediate to mafic in composition with no recognized felsic members.

The Silver King intrusions fall within the diorite/gabbro field on Streckeisen's (1973) quartz-alkali feldspar-plagioclase diagram (Figure 1-1-2). As the porphyry has virtually no mafic minerals and plagioclase is generally $An_{<50}$, it is classified as a leucodiorite porphyry.

GEOCHRONOLOGY

Preliminary U-Pb analyses of zircons from Silver King intrusions give dates that range between 178 to 182 Ma (J. Gabites, personal communication, 1991). The intrusions are interpreted to have been emplaced contemporanous with the early phase of deformation in Rossland Group rocks (Höy *et al.*, 1992). Other synorogenic intrusions in the Kootenay Arc of southern British Columbia include the Cooper Creek stock (*ca.* 180 Ma; Klepacki, 1985), a small discordant pluton northwest of Kaslo, and the Aylwin Creek stock south of Silverton. The Aylwin Creek stock, in Rossland Group volcanic rocks in a roof pendant of the Nelson batholith, hosts copper-gold-silver mineralization on the Willa property. Preliminary U-Pb data indicate an intrusive age of approximately 184 Ma (W.J. McMillan, personal communication, 1991).

MINERALIZATION

A genetic connection between some of the satellite phases of the Silver King intrusions and certain ore deposits has been suggested by Drysdale (1915, page 32). Deposit types associated with the Silver King intrusions include shear-related copper-gold and copper-zinc-silver, and vein lead-zinc-silver-gold.

The California prospect is a vein deposit in the Silver King intrusion near its northern contact with the Elise Formation and Nelson batholith. Quartz veins contain pyrite, galena, sphalerite and free gold. The Great Western occurrence (Höy and Andrew, 1989c), Kena occurrence and Silver King mine are examples of shear-related deposits.

The largest producer hosted by Silver King intrusions is the Silver King mine, after which the intrusions were named. It began production in 1896 and attracted wide attention to the Nelson area. The Silver King orebody is believed to have been a shear-related silver-lead-zinc-gold deposit although its origins are still debated more than 100 years after its discovery. Mineralization, within three main shear-controlled veins, is characterized by galena, chalcopyrite, pyrite and tetrahedrite with minor sphalerite, bornite and stromayerite (a gold-copper sulphide) near the east contact of the Silver King intrusions with highly sheared Elise Formation mafic volcanic flows. The gangue is quartz, carbonate and siderite in sericite schist, a strongly sericitized and sheared Silver King intrusion. Shearing is right lateral as indicated by C-S fabric kinematic indicators.

SUMMARY AND DISCUSSION

This paper presents preliminary data, based largely on field relations, descriptive petrology and preliminary U-Pb dating, on Early and Middle Jurassic plutons in the Rossland Group. More definitive statements, particularly regarding the relationship of magmatism to tectonism, must await analysis of chemical data and additional U-Pb dating.

At least four suites of Early to Middle Jurassic intrusions, associated with or within the Rossland Group, are exposed in the Trail map area. The Early Jurassic Eagle Creek Plutonic Complex west of Nelson, the Rossland monzonite and small monzogabbros throughout the Elise Formation are interpreted to be coeval with the Rossland Group, whereas the early Middle Jurassic Silver King intrusions are interpreted to be synorogenic, related to collision of the eastern margin of Quesnellia with North America (*see* Höy *et al.*, 1992).

The Rossland monzonite is dominantly a monzodiorite with at least one large xenolith of biotite clinopyroxenite. Preliminary U-Pb analysis of zircons suggests a date of approximately 190 Ma (Höy *et al.*, 1992). It is pretectonic, overprinted by regional metamorphic alteration assemblages and skarn alteration associated with Middle Jurassic plutons.

The Eagle Creek Plutonic Complex may be similar to the Rossland monzodiorite. It is associated with clinopyroxenite phases as well as hornblende syenite, monzonite and gabbro. It is pretectonic, with local development of a penetrative fabric due to shearing in the Silver King shear zone.

It is suggested that these intrusions are comagmatic with arc volcanics of the Rossland Group. They were both emplaced along major structures, and are both associated with mineralization – gold-copper veins in the Rossland area and dominantly alkali porphyry gold-copper prospects in the Eagle Creek Plutonic Complex. The ubiquitous presence of both apatite and magnetite in these intrusions is common in Upper Triassic – Early Jurassic arc complexes elsewhere in Quesnellia and Stikinia. These intrusive complexes have phases that are typically calcalkaline as well as phases that resemble feldspar-bearing rocks found associated with Alaskan-type complexes in the Cordillera (Nixon *et al.*, 1989; Nixon, 1990).

Small widely scattered monzogabbros are inferred to be high-level synvolcanic intrusions. They are restricted to the Elise Formation, have diffuse, commonly brecciated margins, and may be associated with minor copper-gold-magnetite mineralization.

The Silver King intrusions occur south of Nelson in strongly deformed eastern exposures of the Rossland Group. They are interpreted to be synorogenic, related to convergence of Quesnellia with North America. Small intrusions and margins of large intrusions are penetratively foliated or intensely sheared. Other intrusions, petrologically similar to the Silver King intrusions and assumed to be comagmatic, are discordant, massive or only locally foliated. The preliminary age of these intrusions – *ca.* 178–182 Ma – coupled with a 180 Ma date on a post-tectonic intrusion, the Cooper Creek stock farther north in the Kootenay Arc (Klepacki, 1985), dates this early collisional event.

ACKNOWLEDGMENTS

We would like to thank our field assistants (1987–1990) for their cheerful and able help: H. Blyth, J. Drobe,

M. Fournier, M. Holmes, E. Höy, H. Karam, D. Lindsay and C. Lund. Discussions with C. Ash, J. Fyles, D. Lefebure, G. Nixon and P. Simony were valuable in our synthesis of ideas regarding these pre to syntectonic intrusive rocks in the Rossland Group.

The paper was reviewed by J.M. Newell, G.T. Nixon and B. Grant.

REFERENCES

Andrew, K.P.E. and Höy, T. (1989): The Shaft Showing, Elise Formation, Rossland Group; *in* Exploration in British Columbia 1988, *B.C. Ministry of Energy, Mines and Petroleum Resources*, pages B21-28.

Andrew, K.P.E., Höy, T. and Simony, P. (1991): Geology of the Trail Map Area, Southeastern British Columbia; *B.C. Ministry of Energy, Mines and Petroleum Resources*, Open File 1991-16.

Ash, C. H. and Macdonald, R.W.J. (1992): Listwanite Project – Update; *in* Geological Fieldwork 1991, Grant, B. and Newell, J.M., Editors, *B.C. Ministry of Energy, Mines and Petroleum Resources*, Paper 1992-1, this volume.

Beddoe-Stephens, B. and Lambert, R. St. J. (1981): Geochemical, Mineralogical and Isotopic Data Relating to the Origin and Tectonic Setting of the Rossland Volcanic Rocks, Southeastern British Columbia; *Canadian Journal of Earth Sciences*, Volume 18, pages 858-868.

Bruce, E.L. (1917): Geology and Ore Deposits of Rossland, British Columbia; *B.C. Ministry of Energy, Mines and Petroleum Resources*, Bulletin 4.

Dawson, G.M (1889): Report on a Portion of the West Kootenai District, British Columbia; *Geological Survey of Canada*, Annual Reports 1888-1889.

Drysdale, C.W. (1915): Geology and Ore Deposits of Rossland, British Columbia; *Geological Survey of Canada*, Memoir 77, pages.

Frebold, H. and Little, H.W. (1962): Paleontology, Stratigraphy, and Structure of the Jurassic Rocks in Salmo Map-area, British Columbia; *Geological Survey of Canada*, Bulletin 81.

Frebold, H. and Tipper, H.W. (1970): Status of the Jurassic in Canadian Cordillera of British Columbia, Alberta and Southern Yukon; *Canadian Journal of Earth Sciences*, Volume 7, pages 1-21.

Fyles, J.T. (1984): Geological Setting of the Rossland Mining Camp; *B.C. Ministry of Energy, Mines and Petroleum Resources*, Bulletin 74, 61 pages.

Gilbert, (1948): Rossland Camp; *in* Structural Geology of Canadian Ore Deposits, *Canadian Institute of Mining and Metallurgy*, Jubilee Volume, pages 189-196.

Höy, T. and Andrew, K.P.E. (1988): Preliminary Geology and Geochemistry of the Elise Formation, Rossland Group, between Nelson and Ymir, Southeastern British Columbia; *in* Geological Fieldwork 1987, *B.C. Ministry of Energy, Mines and Petroluem Resources*, Paper 1988-1, pages 19-30.

Höy, T. and Andrew, K.P.E. (1989a): The Rossland Group, Nelson Map Area, Southeastern British Columbia; *in* Geological Fieldwork 1988, *B.C. Ministry of Energy, Mines and Petroluem Resources*, Paper 1989-1, pages 33-43.

Höy, T. and Andrew, K.P.E. (1989b): Geology of the Rossland Group, Nelson Map-area, Southeastern British Columbia; *B.C. Ministry of Energy, Mines and Petroleum Resources*, Open File 1989-1.

Höy, T. and Andrew, K.P.E. (1989c): The Great Western Group, Elise Formation, Rossland Group; *in* Exploration in British Columbia 1988, *B.C. Ministry of Energy, Mines and Petroleum Resources*, pages B15-19.

Höy, T. and Andrew, K.P.E. (1991a): Geology of the Rossland Area, Southeastern British Columbia; *in* Geological Fieldwork 1990, *B.C. Ministry of Energy, Mines and Petroleum Resources*, Paper 1991-1, pages 21-31.

Höy, T. and Andrew, K.P.E. (1991b): Geology of the Rossland-Trail Map Area, Southeastern British Columbia; *B.C. Ministry of Energy, Mines and Petroleum Resources*, Open File Map 1991-2.

Höy, T., Dunne, K.P.E. and Wehrle, D. (1992): Tectonic and Stratigraphic Controls of Gold-Copper Mineralization in the Rossland Camp, Southeastern British Columbia; *in* Geological Fieldwork 1991, Grant, B. and Newell, J.M., Editors, *B.C. Ministry of Energy, Mines and Petroleum Resources*, Paper 1992-1, this volume.

Klepacki, D.W. (1985): Stratigraphy and Structural Geology of the Goat Range Area, Southeastern British Columbia; unpublished Ph.D. thesis, *Massachusetts Institute of Technology*, 268 pages.

Lindsay, D.D. (1991): Geology, Geochemistry and Petrography of the Moochie Cu-Au Occurrence, Nelson, British Columbia; unpublished B.Sc. thesis, *Carleton University*, 51 pages.

Little, H.W. (1960): Nelson Map Area, West-half, British Columbia; *Geological Survey of Canada*, Memoir 308, 205 pages.

Little, H.W. (1963): Rossland Map-area, British Columbia; *Geological Survey of Canada*, Paper 63-13.

Little, H.W. (1982a): Geology, Bonnington Map-area, British Columbia; *Geological Survey of Canada*, Map 1571A.

Little, H.W. (1982b): Geology, Rossland-Trail Map Area, British Columbia; *Geological Survey of Canada*, Paper 79-26, 38 pages.

Mulligan, R. (1951): The Geology of the Nelson (Bonnington) and adjoining part of Salmo Map Areas, British Columbia; unpublished Ph.D. thesis, *McGill University*, 202 pages.

Mulligan, R. (1952): Bonnington Map Area, British Columbia; *Geological Survey of Canada*, Paper 52-13, 37 pages.

Nixon, G.T. (1990): Geology and Precious Metal Potential of Mafic-Ultramafic Rocks in British Columbia: Current Progress; *in* Geological Fieldwork 1989, *B.C. Ministry of Energy, Mines and Petroleum Resources*, Paper 1990-1, pages 353-358.

Nixon, G.T., Ash, C., Connelly, J.N. and Case, G. (1989): Alaskan-type Mafic-Ultramafic Rocks in British

Columbia: The Gnat Lakes, Hickman and Menard Creek Complexes; *in* Geological Fieldwork 1988, *B.C. Ministry of Energy, Mines and Petroleum Resources*, Paper 1989-1, pages 429-442.

Streckeisen, A.L. (1973): Plutonic Rocks: Classification and Nomenclature Recommended by the IUGS Subcommission on the Systematics of Igneous Rocks; *Geotimes*, Volume 18, 26 pages.

Tipper, (1984): The Age of the Jurassic Rossland Group of Southeastern British Columbia; *in* Current Research, Part A, *Geological Survey of Canada*, Paper 84-1A, pages 631-632.

Webster, I.C.L., Ray, G.E. and Pettipas, A.R. (1992): Investigations of Selected Mineralized Skarns in British Columbia; *in* Geological Fieldwork 1991, Grant, B. and Newell, J.M., Editors, *B.C. Ministry of Energy, Mines and Petroleum Resources*, Paper 1992-1, this volume.

NOTES

STRATIGRAPHIC DATING OF FAULT SYSTEMS OF THE CENTRAL HUGHES RANGE, SOUTHEAST BRITISH COLUMBIA (82G/12)

By Alastair I. Welbon and Raymond A. Price
Queen's University

(Contribution No. 5, Sullivan-Aldridge project)

KEYWORDS: Regional geology, stratigraphic variation, structural control, Purcell Supergroup, Lower Paleozoic, reactivation.

INTRODUCTION

In southeastern British Columbia the northward-plunging Purcell anticlinorium is segmented by several major northeast-trending transverse faults (Rice, 1937; Leech, 1962; Höy, 1982). These faults have various senses of offset and show evidence of reactivation. They have been active at various times including the Middle Proterozoic (Höy, 1982; McMechan and Price, 1982), Late Proterozoic (Lis and Price, 1976), Early Paleozoic and Early Cretaceous (Leech, 1958, 1962; Benvenuto and Price, 1979). Within the Purcell anticlinorium there are several significant mineral deposits, some of which are cut by these transverse structures. The largest of these, the Sullivan lead-zinc "sedex" deposit, is cut by an extensional structure, the Kimberley fault, which has been linked to the Lewis Creek fault across the Rocky Mountain Trench and into the Hughes Range.

The Hughes Range between Skookumchuck (49°55′) and Bull River (49°30′) (Figures 1-2-1 and 2) forms the east wall of the Rocky Mountain Trench. It is the uplifted footwall block of the Rocky Mountain Trench normal fault, and is the offset counterpart of the east flank of the Purcell anticlinorium, the main part of which lies west of the trench in the hangingwall of the normal fault. In the Hughes Range, the Middle Proterozoic Purcell Supergroup rocks, which host the Sullivan deposit on the west side of the trench, are overlain unconformably by a Lower Paleozoic carbonate platform succession. The stratigraphic sequence comprising the Hughes Range has been overthrust, along the Lussier Creek fault, onto the thick Lower Paleozoic shale-carbonate facies that is characteristic of the western Main Ranges and Western Ranges of the southern Canadian Rockies (Leech, 1958).

Several northeast-trending transverse faults cut the Purcell succession and parts of the Lower Paleozoic succession in the Hughes Range. Relationships along unconformities within and at the base of the Lower Paleozoic strata provide evidence of the nature and timing of displacement on these faults. Field mapping of the faults and unconformities bounding three Lower Paleozoic formations have been the main focus of this study.

The Lussier Creek fault trends north for most of its length, but at the south end of the Hughes Range swings northeast, parallel to the transverse faults in the Purcell anticlinorium. Towards the Rocky Mountain Trench, the fault merges with an old transverse fault, the Boulder Creek fault (Figure 1-2-1).

The preliminary results presented here are the product of fieldwork on this project which was carried out in June, July and August, 1991. In addition to field mapping and data collection, samples have been collected for geochronologic (K-Ar) studies to constrain ages of volcanic sequences and postorogenic granites. A new facility at Queen's University is being used to produce computer-generated geological maps of the area. Geographic information systems (GIS) technology is being used to store multiple data sets and analyse fault configurations and paleogeography in the region.

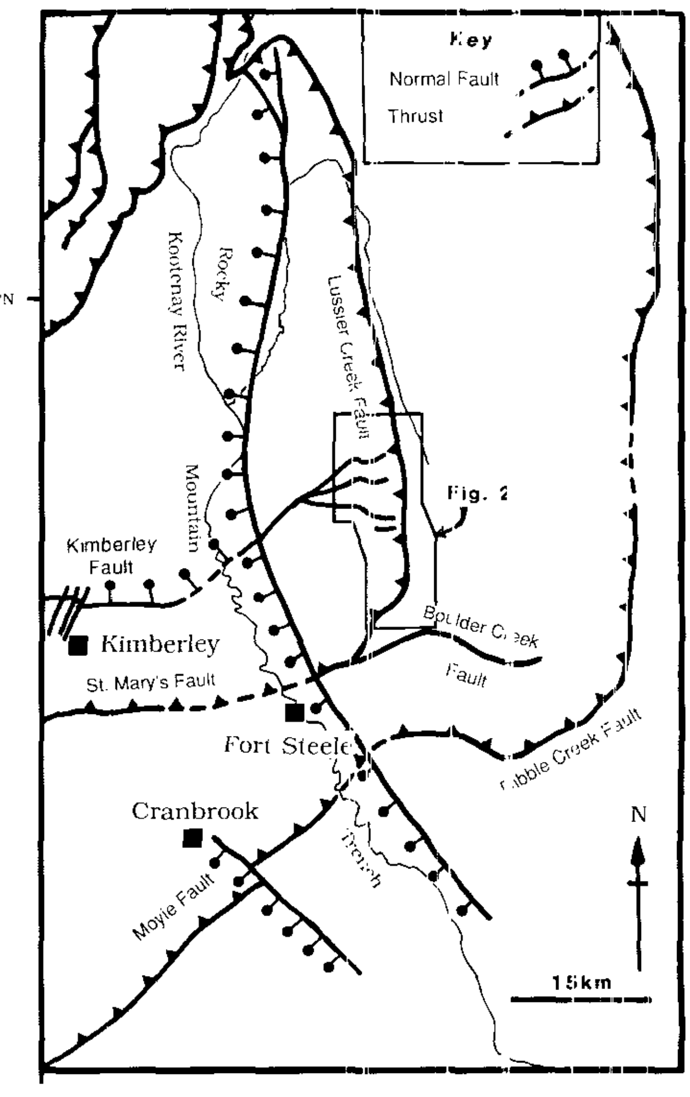

Figure 1-2-1. Location map of the study area. The figure also shows major faults in the region.

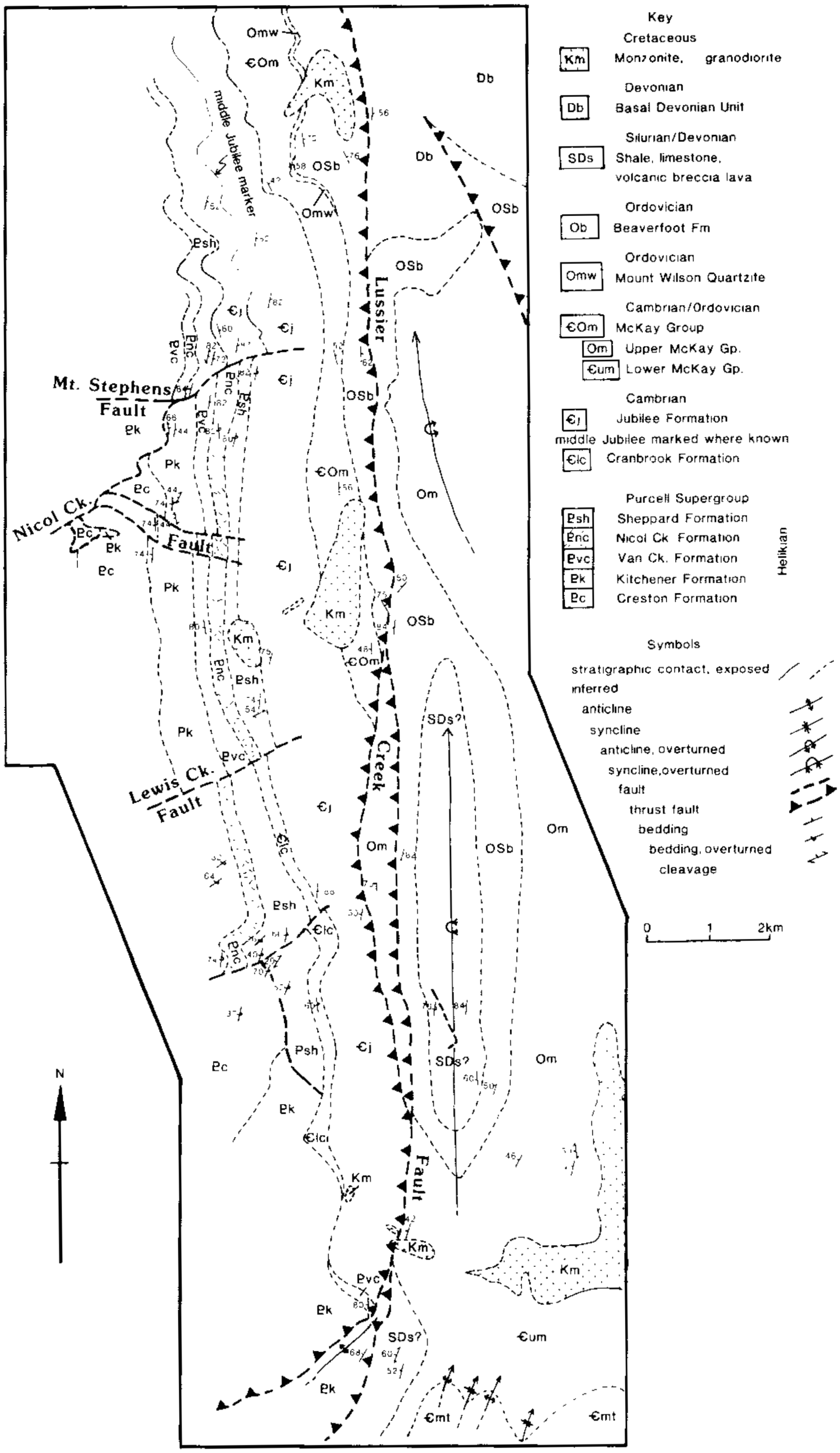

Figure 1-2-2. Geological map of the study area. The data are from 1991 field work, plus Höy (1979, 1988, and personal communication) and Leech (1958, 1960).

REGIONAL GEOLOGY

The Hughes Range lies in the western part of the Cordilleran fold and thrust belt (Figure 1-2-1). It is underlain by the Lussier Creek fault, a major eastward-verging thrust. The fault is part of the regional thrust-fault system that separates east-verging structures of the Purcell anticlinorium to the west, from the west-verging structures of the Porcupine Creek fan structure to the east (Price, 1981, 1986).

Transverse, northeast-trending fault structures are characteristic of this part of the Cordillera (Höy, 1982). They segment the Purcell anticlinorium and extend across the Rocky Mountain Trench into the western Rockies. The two main transverse structures, the St. Mary - Boulder Creek fault to the north, and the Moyie - Dibble Creek fault to the south, are both northwest-dipping, right-hand reverse faults. Profound variations in stratigraphic relationships beneath the sub-Cambrian unconformity indicate that the St. Mary fault follows the locus of a Late Proterozoic structure along which the northwest side was downdropped (Lis and Price, 1976). Similar variations in stratigraphic relationships beneath the Upper Devonian Fairholme Group indicate that the Moyie and Dibble Creek faults follow the locus of an Early Paleozoic structure that was downdropped to the northwest (Leech, 1958; Benvenuto and Price, 1979; McMechan and Price, 1982).

PREVIOUS WORK

Interest in the geology of the Hughes Range (Figures 1-2-1 and 2) and the surrounding areas was initially driven by the discovery of placer gold deposits of the Wild Horse Creek during the 1800s. Exploration interest has continued ever since.

The first detailed work in the range was in the Wild Horse River region (Rice, 1937). The whole of the Hughes Range was mapped at a scale of 1 inch to 2 miles and was published by the Geological Survey of Canada in 1958 (Leech, 1958). The first detailed mapping was by Höy, who demonstrated the influence of faulting on the deposition of the Purcell Supergroup (Höy, 1982, 1985; Carter and Höy, 1987).

STRATIGRAPHY OF THE HUGHES RANGE

The Purcell Supergroup

The Purcell sequence in the Hughes Range, where complete, consists of ten formations and reaches a thickness of approximately 7 kilometres (Höy, 1985, in preparation). The lowermost seven formations are exposed in the central Hughes Range, northeast of Fort Steele. Only the upper part of this succession was studied during this project.

The lowest part of the succession comprises the Fort Steele Formation, a sequence of quartzites, argillites and conglomerates which are only found east of the Rocky Mountain Trench. It is overlain by the Aldridge Formation which is a thick (up to 6 km) sequence of fine-grained turbidites that consist of quartzite, quartz wacke and argillite.

The Creston Formation, which overlies the Aldridge Formation, is the stratigraphically lowest formation exposed in the study area. It consists of green, thickly bedded quartzites and argillites and is approximately 2 kilometres thick. A thick carbonate sequence, the mainly buff-weathering, thickly bedded Kitchener Formation, overlies the Creston Formation and is a distinctive marker unit.

The upper part of the Purcell Supergroup consists of dominantly shallow-water argillaceous clastic and carbonate rocks, with a distinctive volcanic sequence in the middle. The Van Creek Formation (McMechan *et al.*, 1980) which is up to 850 metres thick, consists of green and purple siltites and argillites which become tuffaceous at the top. It is overlain by the Nicol Creek Formation (McMechan *et al.*, 1980) which contains dark green, basaltic and andesitic lavas and tuffs, commonly in association with argillites, siltites and sandstones. The lavas are generally amygdaloidal, which helps to distinguish them from thick sills that cut the Creston and Kitchener formations.

The Sheppard Formation lies with sharp contact on the Nicol Creek Formation, and is the uppermost part of the Purcell Supergroup exposed in the study area (Figure 1-2-2). It is a series of red and green dolomitic siltstones and dolomitic sandstones, with a distinctive stromatolitic dolomite near the top. Clast-supported breccias occur within the formation near faults, and may indicate Sheppard-age syntectonic sedimentation.

At the northern end of the Hughes Range, north of the study area, younger parts of the Purcell Supergroup (Gateway, Phillips and Roosville formations) and part of the Windermere Supergroup are preserved under the sub-Cambrian unconformity.

Lower Paleozoic Rocks

Contrasting Lower Paleozoic sequences occur in the hangingwall and footwall of the Lussier Creek fault. The hangingwall sequence is a relatively thin (*ca.* 2.5 km) carbonate platform sequence; whereas the footwall sequence is a thick (*ca.* 6 km) shale-carbonate sequence. Both the hangingwall and footwall successions begin with Lower Cambrian siliciclastic formations, but these are laterally variable.

Four unconformity-bounded formations are found in the hangingwall of the Lussier Creek fault. They range in age from Cambrian to Ordovician and they vary in thickness along strike. The two oldest, the Cranbrook and Jubilee formations, are offset by transverse northeast striking synsedimentary faults, which do not offset the younger formations. The distribution of the Cranbrook Formation is controlled by the sense of displacement on these faults, and by erosion prior to deposition of the Jubilee Formation.

The Lower Cambrian Cranbrook Formation which forms the base of the Lower Paleozoic sequence, is dominated by white quartzite and includes major components of quartz wacke and conglomeratic sandstone (as much as 60% locally). The Cranbrook Formation, although widespread elsewhere north of the Moyie - Dibble Creek fault, is absent beneath the Jubilee Formation throughout most of the map area. It is preserved locally beneath the sub-Jubilee unconformity adjacent to the transverse faults in the central Hughes Range. The shale-dominated Eager Formation, which is also widespread regionally in the hangingwall of the Moyie - Dibble Creek Fault, is absent from the study area.

The base of the carbonate sequence is marked by the Middle to Upper Cambrian Jubilee Formation (Leech, 1958), which is characteristically a well-bedded limestone/ dolomite in its lower part, but more massive in its upper part. In the northern part of the study area, there is a rusty weathering dolomitic unit in the middle part of the Jubilee Formation that is a good marker horizon. Evidence of synsedimentary tectonism was found towards the base of the formation in the form of extensional structures within layers of sediment, and sediment dikes along fault traces.

The McKay Group (Leech, 1958) is a shaley limestone at its base, but becomes progressively more characteristic of carbonate platform facies toward the top, with intraformational conglomerates, peloidal wackestones, nodular limestones and bioclastic grainstones. To the north of the field area, the Middle Ordovician Mount Wilson quartzite unconformably overlies the McKay Group (Leech, 1954; Norford, 1969). Elsewhere this quartzite is absent and carbonates make up the top of the group.

The Beaverfoot Formation, an Upper Ordovician and Lower Silurian carbonate platform deposit (Norford, 1969), rests unconformably on the McKay Group except where the Mount Wilson quartzite is present. It consists of thick-bedded dolomitic limestones and dolomite and is characterized by chert nodules and a mottled texture. The top of the formation is truncated by the Lussier Creek fault; but north of the study area it is overlain by Middle Devonian gypsum, shale and carbonate rocks (Leech, 1958).

The Paleozoic rocks in the footwall to the Lussier Creek fault differ significantly from those in the hangingwall. The Purcell sequence is overlain by the quartzites of the Cranbrook Formation which grade upwards into the shale of the Eager Formation (Leech, 1958). The overlying succession comprises the shales of the Tanglefoot unit (Thompson, 1962), the McKay Group, Beaverfoot Formation and a "Silurian-Devonian unit" (Leech, 1960).

The Tanglefoot unit has a thick, laminated, basinal carbonate-rich shale at its base and consists of sandstones and possible storm-influenced limestones at the top. It appears to be a deep-water equivalent of the Jubilee limestones and dolomites. The top of the McKay Group is similar to that in the hangingwall of the Lussier Creek fault and contains nodular limestones. The lower part is a shaley limestone and is very thick (greater than 1 km). The Beaverfoot Formation is of similar thickness and appearance to the hangingwall Beaverfoot.

The Silurian-Devonian unit has been described in detail by Leech, (1958). Examination in the field shows it to be series of shaley limestones overlain by laterally discontinuous volcaniclastic rocks, basaltic lavas and tuffs, above which are more shaley limestones and to the south, bioclastic limestones. The sedimentary sequence is characterized by slump structures (up to 1 m), breccias containing many dolomitic and volcanic clasts and small-scale synsedimentary faults. In addition to a major north-trending syncline containing this unit (Leech, 1958), this unit has been found in the immediate footwall of the Lussier Creek fault in the extreme south of the map area. In the north of the study area it overlies the Beaverfoot Formation, while in the south it overlies the McKay Group.

STRUCTURE

Three main sets of faults occur in the study area; older northeast-trending transverse faults which generally only cut the Purcell and lower part of the Lower Paleozoic sequences; north-trending thrust faults; and north-trending normal faults that are associated with the Rocky Mountain Trench normal fault.

TRANSVERSE STRUCTURES

Five transverse faults cross the central Hughes Range. These are from north to south; the Mount Stephens, Nicol Creek, Lewis Creek, and two unnamed faults. The three named faults merge southwestward towards the Rocky Mountain Trench, and can be correlated across the trench with the Kimberley fault, which cuts the Sullivan ore deposit. Stratigraphic relationships at the sub-Jubilee unconformity show that these faults were active prior to deposition of the Jubilee Formation. They were tilted or overturned during the development of the Purcell anticlinorium, the east flank of which is the hangingwall of the Lussier Creek fault. They cut bedding at high angles, and therefore must have been steeply dipping when they formed.

The sense of stratigraphic separation changes from one fault to another and in the case of some faults, along their length. The Mount Stephens and Nicol Creek faults have reverse separations; separation on the Lewis Creek fault is normal. The two unnamed faults have complex relationships. The northernmost has a reverse-sense offset at its tip, but has a normal offset farther down its length. The other abuts the first and appears to be overlapped by the sub-Cambrian unconformity. The sense of displacement is uncertain.

A late, low-angle, west-side-down normal fault connects the Nicol Creek and Mount Stephens faults (Höy, 1979). As these faults are lateral structures bounding the hangingwall block to this normal fault, they must incorporate a component of offset related to displacement on the normal fault. Thus some of the apparent offsets observed along faults are the result of only partial reactivation of old faults by new structures.

AGE OF FAULTING

By comparing fault offsets of bedding above and below various regional unconformities, the relative timing of some of the offset history can be established. At the east end of the Mount Stephens fault, near where it dies out in the Jubilee Formation, both upper Purcell rocks and the Jubilee Formation show a reverse sense of offset relative to the horizontal datum provided by the bedding. The fault does not offset the upper part of the Jubilee Formation, but local thinning of the overlying McKay Formation above the fault

(Figure 1-2-2) may be either a compaction effect, or the result of continued displacement. This constrains the last age of offset on this fault to the Cambrian. A greater offset at the level of the Purcell Supergroup compared to the offset of the Jubilee Formation indicates that there was additional reverse offset prior to deposition of the Jubilee. This may be related to tectonic activity during deposition of the Sheppard Formation, as evidenced by changes of thickness and facies (*see* Stratigraphy section).

The Nicol Creek fault also has a reverse offset, and relative to the horizontal datum provided by the bedding, it appears to die out upward into the Jubilee Formation. The Lewis Creek fault is marked by normal offset of the upper part of the Purcell Supergroup and the base of the Jubilee Formation, and also dies out within the Jubilee Formation. Cranbrook strata are preserved beneath the Jubilee Formation in the hangingwall; but the Jubilee Formation is unconformable on the Sheppard in the footwall (Figure 1-2-2). This shows that the fault was active during the interval between the deposition of the Cranbrook and Jubilee Formations.

The northern unnamed transverse fault has a thick Cranbrook succession in the hangingwall, including a facies containing a conglomeratic wacke, suggesting Early Cambrian extension. The southern fault is truncated by the sub-Cambrian unconformity and overlain by the Cranbrook Formation, indicating faulting took place prior to Cambrian sedimentation.

Synsedimentary faulting is recorded at several stratigraphic levels in the Hughes Range. Höy (1982, in preparation) reported block faulting during deposition of the Aldridge Formation. Thickness and facies-change patterns are indicative of faulting during deposition of the Sheppard Formation. Both reverse and normal offset occurred during the Cambrian. In the footwall of the Lussier Creek fault, there is evidence of extensional faulting during the deposition of the Silurian-Devonian unit. Regionally, the overlap at the base of the Upper Devonian Group onto different stratigraphic sequences indicates significant Middle to Late Devonian tectonic activity (Benvenuto and Price, 1979).

North-Striking Major Thrusts

The second important set of faults in the region are north-trending thrusts in both the hangingwall and footwall of the Lussier Creek fault. Those in the hangingwall are east verging, but those in the footwall are part of the west flank of the structural fan of the Porcupine Creek anticlinorium and verge to the west (Price, 1986). The Lussier Creek fault itself has a northerly trend along most of its length, but swings into a northeast orientation at the south of the map area where it converges with the Boulder Creek fault (Leech, 1958), a reactivated older transverse structure.

The timing of displacement of the north-trending faults is constrained by the fact that they cut rocks as young as Devonian (Leech, 1958), but are pinned by monzonitic to granodioritic intrusions of mid-Cretaceous age (Höy and van der Hayden, 1988). A few additional small intrusive bodies were discovered in the study area during 1991 (Figure 1-2-2).

CONCLUSIONS

Northeast-trending transverse structures in the hangingwall of the Lussier Creek fault were active during Aldridge time and subsequently during deposition of the Nicol Creek (Höy, 1982) and Sheppard formations. Reactivation of these structures took place during the Cambrian, prior to deposition of the Jubilee Formation and, at least locally, during deposition of the lower part of the Jubilee Formation. The tectonic setting during late Purcell and Cambrian time is not clear. Both reverse and normal offsets along steep faults during the Cambrian point to strike-slip motion, with localized transpression and transtension. A similar tectonic regime may have operated during late Purcell time, but because of the large time interval between the Middle Proterozoic and the Cambrian it must have been a separate tectonic event.

Similar pre-Devonian structures with a northeast orientation, which occur in the Bull River area, define a step on the northwest flank of "Montania", which was a continental platform during Early Paleozoic time (Benvenuto and Price, 1979). The Moyie - Dibble Creek fault system followed this older structure. The positioning of the Lussier Creek fault and its deflection to a northeast trend may be indicative of a similar structural inheritance.

ACKNOWLEDGMENTS

The senior author acknowledges a William E. White Postdoctoral Fellowship and also financial support from a Queen's University Advisory Research Council Grant, and a Natural Sciences and Engineering Research Council Operating Grant #0092417 to R.A. Price. A visit by D.A. Archibald to the field area and his discussions are appreciated. Lorrence Toffolo and Wild Horse River Outfitters are thanked for logistical help. S. Castonguay provided assistance in the field.

REFERENCES

Benvenuto, G.L. and Price, R.A. (1979). Structural Evolution of the Hosmer Thrust Sheet, Southeastern British Columbia; *Bulletin of Canadian Petroleum Geology*, Volume 27, pages 360-394.

Carter, G. and Höy, T. (1987): Geology of the Skookumchuck Map Area, Southeastern British Columbia; *in* Geological Field Work 1986, *B.C. Ministry of Energy, Mines and Petroleum Resources*, Paper 1987-1, pages 143-156.

Höy, T. (1979): Geology of the Estella - Kootenay King Area, Hughes Range, Southeastern British Columbia; *B.C. Ministry of Energy, Mines Petroleum Resources*, Preliminary Map 36.

Höy, T. (1982): The Purcell Supergroup in Southeastern British Columbia; Sedimentation, Tectonics and Stratiform Lead-Zinc Deposits; *in* Precambrian Sulphide Deposits, *Geological Association of Canada*, Special Paper 25, pages 127-147.

Höy, T. (1985): The Purcell Supergroup, Fernie West-half, Southeastern British Columbia, Part A, Stratigraphy - Measured Sections; *B.C. Ministry of Energy, Mines and Petroleum Resources*, Bulletin 76, 79 pages.

Höy, T. (in preparation): The Middle Proterozoic Purcell Supergroup in the Fernie West-half Map Area, Southeastern British Columbia; *B.C. Ministry of Energy, Mines and Petroleum Resources*, Bulletin.

Höy, T. and van der Hayden, P. (1988): Geochemistry, Geochronology, and Tectonic Implications of Two Quartz Monzonite Intrusions, Purcell Mountains, Southeastern British Columbia; *Canadian Journal of Earth Sciences*, Volume 25, pages 106-115.

Leech, G.B. (1954): Canal Flats, British Columbia; *Geological Survey of Canada*, Paper 54-7.

Leech, G.B. (1958): Fernie Map-area, West Half, British Columbia; *Geological Survey of Canada*, Paper 58-10.

Leech, G.B. (1960): Fernie, (West Half), Kootenay District, British Columbia; *Geological Survey of Canada*, Map 11-1960.

Leech, G.B. (1962): Structure of the Bull River Valley near Latitude 49°35'; *Journal of the Alberta Society of Petroleum Geologists*, Volume 10, pages 396-407.

Lis, M.G. and Price, R.A. (1976): Large Scale Block Faulting During Deposition of the Windermere Supergroup (Haydrynian) in Southeastern British Columbia; *Geological Survey of Canada*, Paper 76-1A, pages 135-136.

McMechan M.E. and Price, R.A. (1982): Transverse Folding and Superposed Deformation, Mount Fisher Area, Southern Canadian Rocky Mountain Thrust and Fold Belt; *Canadian Journal of Earth Sciences*, Volume 19, pages 1011-1024.

McMechan, M.E., Höy, T. and Price, R.A. (1980): Van Creek and Nicol Creek Formations (New): A Revision of the Stratigraphic Nomenclature of the Middle Proterozoic Purcell Supergroup, S.E. British Columbia; *Bulletin of Canadian Petroleum Geology*, Volume 28, pages 542-558.

Norford, B.S. (1969): Ordovician and Silurian Stratigraphy of the Southern Rocky Mountains; *Geological Survey of Canada*, Bulletin 176, 87 pages.

Price, R.A. (1981): The Cordilleran Foreland Thrust and Fold Belt in the Southern Canadian Rocky Mountains; *in* Thrust and Nappe Tectonics, McClay, K.R. and Price, N.J., Editors, *The Geological Society of London*, Special Publication No. 9, pages 427-448.

Price, R.A. (1986): The Southeastern Canadian Cordillera: Thrust Faulting, Tectonic Wedging, and Delamination of the Lithosphere; *Journal of Structural Geology*, Volume 8, pages 239-254.

Rice, H.M.A. (1937): Cranbrook Map Area, British Columbia; *Geological Survey of Canada*, Memoir 207.

Thompson, T.L. (1962): Stratigraphy, Tectonics, Structure and Gravity in the Rocky Mountain Trench Area, Southeastern B.C.; unpublished Ph.D. thesis, *Stanford University*.

TECTONIC SIGNIFICANCE OF STRATIGRAPHIC AND STRUCTURAL CONTRASTS BETWEEN THE PURCELL ANTICLINORIUM AND THE KOOTENAY ARC, EAST OF DUNCAN LAKE (82K): PRELIMINARY RESULTS

By Marian J. Warren and Raymond A. Price
Queen's University

KEYWORDS: Regional geology, Purcell anticlinorium, Kootenay Arc, stratigraphy, deformation, Horsethief Creek Group, Hamill Goup, Mohican Formation, Badshot Formation, intrusions.

INTRODUCTION

The main goal of this study is to elucidate the nature and tectonic significance of the profound stratigraphic and structural changes that occur between the crest of the Purcell anticlinorium and the Kootenay Arc.

Reconnaissance (1:250 000) mapping by Reesor (1973) outlined conspicuous contrasts between the thick basal Paleozoic (Hamill-Badshot) succession that overlies the Windermere Supergroup in this area and the thin, condensed early Paleozoic succession with overlapping Upper Devonian strata that occurs immediately to the east in the Purcell Mountains. Reesor also described the abrupt contrast between the tight upright fold structures in this area and the refolded, west-verging, recumbent isoclinal folds that occur immediately to the west in the Kootenay Arc. He also showed that several small granitic plutons in the area were probably emplaced while folding was still underway.

The rocks exposed in this area (Figure 1-3-1) record both the Late Proterozoic to early Paleozoic birth and development of the Cordilleran miogeoclinal passive margin of North America (Bond and Kominz, 1984; Bond *et al.*, 1985), and the Late Mesozoic to Early Cenozoic deformation, regional metamorphism and granitic plutonism resulting from collisions between North America and a series of allochthonous terranes that have been accreted to it (Monger *et al.*, 1982).

Systematic detailed geological mapping (1:50 000 and greater) was begun during July and August of 1991 within an area of about 900 square kilometres in the western Purcell Mountains, between Duncan Lake and the headwaters of Toby and Jumbo creeks (Figure 1-3-2). This will link the detailed mapping along the Kootenay Arc by Fyles (1964) to the detailed mapping by Root (1987) and Pope (1990) in the central and eastern Purcell Mountains.

The main objectives of this study are:

- To establish the nature and tectonic significance of the stratigraphic relationships between the thick sequence of Windermere. Hamill and Badshot strata in the study area and the condensed onlapping early Paleozoic succession that occurs on "the Windermere high" in the adjacent area, below the Mount Forster thrust fault, in the central and eastern Purcell Mountains (Root, 1985);
- To establish the nature, evolution and regional tectonic significance of the change in structural style between the study area and the adjacent areas in the Kootenay Arc and the central Purcell Mountains;
- To establish the relative time relationship between the intrusion of granitic plutons and the deformation and metamorphism;
- To determine the pressure and temperature conditions under which the plutons were emplaced and the surrounding rocks were deformed;
- To date the plutons, the metamorphism and the deformation.

STRATIGRAPHY

HORSETHIEF CREEK GROUP

Mapping during the 1991 field season was concentrated primarily in the upper part of the Horsethief Creek Group; mapping will be extended east of the Purcell divide in 1992 to include the base of the Horsethief Creek Group and the Toby Formation, which unconformably overlies the Purcell Supergroup. Five mappable units were identified within the middle to upper part of the Horsethief Creek Group (Figure 1-3-3). In ascending order, these units are: (Ht1) a dark limestone and calcareous argillite; (Ht2) a light green-grey argillite and muscovite-quartz schist: (Ht3) a coarser grained, dark grey-green, micaceous quartzite and quartzose schist, capped by (Ht4) a sequence of interbedded light grey or white grits, quartzites and thin carbonates to the east, and by (Ht5) interbedded grits and dolostone-clast conglomerate to the west. The lower units are laterally continuous, but the upper units are not. The total thickness of these units is estimated at 2.0 to 2.5 kilometres.

Ht1: DARK LIMESTONE AND ARGILLITE

This unit is well exposed in the western part of Howser Creek and in Tea Creek. It consists of dark grey, thinly to thickly bedded limestone or marble, locally argillaceous, and commonly pyritiferous. The carbonate is interbedded with dark argillite. The base of the unit was not observed. The upper contact with overlying argillite was not directly observed, but appears to be abrupt. Minimum thickness of this unit is estimated at 200 to 300 metres.

Ht2: LIGHT GREY-GREEN ARGILLITE

This unit is a largely homogeneous sequence of light grey or grey-green argillite. It lies stratigraphically above the dark limestone and marble (Ht1). Where not too severely deformed, bedding is visible as subtle lighter and darker

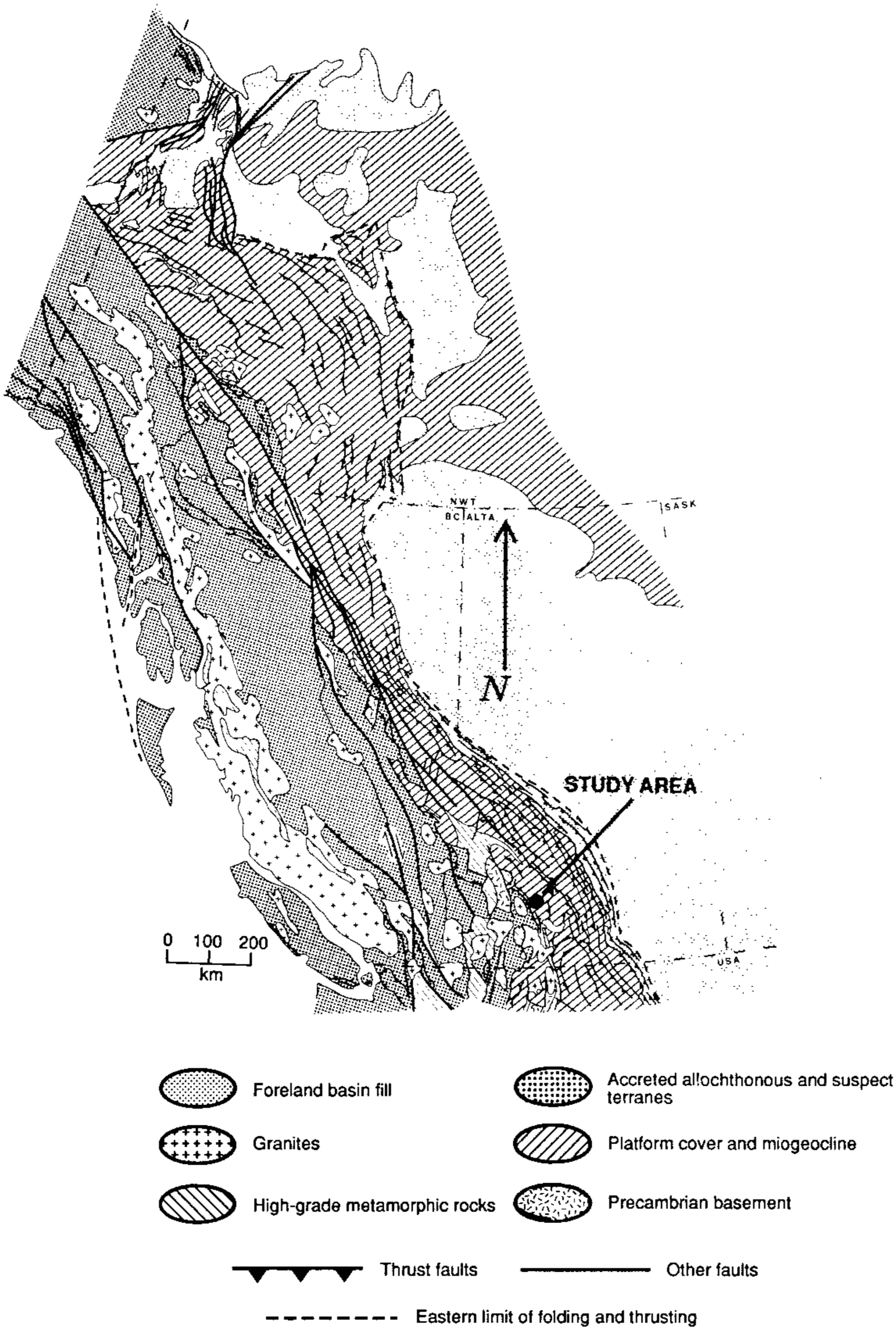

Figure 1-3-1. Tectonic map of the Canadian Cordillera showing location of the study area. Modified after Douglas (1968) and Price (1986).

grey bands, 1 to 10 centimetres thick. No changes in grain size or composition between beds are discernible in hand specimens. Pyrite is abundant and rusty orange weathering is characteristic. Toward the west, or locally within high-strain zones, this unit is a silvery quartz-muscovite schist, locally containing biotite porphyroblasts. The argillite is recessive and forms valleys, such as those cut by the north and south forks of Glacier Creek. This unit is generally poorly exposed. It is more strongly deformed than the overlying grits and quartzites, and an estimated thickness of about 1000 metres may be in error due to significant tectonic thickening or thinning, as strain is concentrated in the less competent argillites relative to the grits and overlying quartzites.

Ht3: DARK GREEN-GREY QUARTZITE AND QUARTZOSE SCHIST

The grey-green argillite grades upward into a coarser grained dark schist or quartzite. Colour and texture are variable from a grey, competent muscovite-rich quartzite, to a dark green, quartz-muscovite-(chlorite) schist or quartzite in which tectonic fabrics are well expressed. Laterally discontinuous grit horizons, several centimetres to several metres thick, contain white and blue quartz pebbles up to 4 millimetres in diameter. Feldspar clasts are very rarely observed with the naked eye. Other primary sedimentary structures were not observed. This unit is absent north of Jumbo Pass, on the east side of the Purcell divide. Estimated thickness ranges from 0 to 500 metres.

Ht4: INTERBEDDED WHITE GRITS AND QUARTZITES

Toward the top of Unit Ht3, dark quartzites are interbedded with increasingly abundant light-coloured quartzose grits. The transition to a sequence dominated by interbedded grits and quartzites occurs over an interval as thick as 100 metres. Contacts between light and dark horizons are sharp. Where Unit Ht3 is absent, the contact between the grits and the underlying Ht2 argillite is extremely sharp. The grits are composed dominantly of pebbles of white quartz, with less abundant pebbles of blue, grey, and rare, distinctive red quartz. Feldspar is rare, but locally comprises 2 to 3 per cent of the clasts. Toward the contact with the overlying Hamill Group, beds of coarse-grained white quartzite are increasingly abundant. In general, this sequence becomes finer grained and more mature upward. Sedimentary structures are more common toward the top, and include abundant trough crossbeds, planar-tabular crossbeds, pebbly channels up to 1 metre across, pebbly graded beds, and possible hummocky cross-stratification. A distinguishing feature of this sequence is the occurrence of two to three, metre-thick, tan and orange dolostone beds, about 100 metres below the base of the Hamill Group. Individual beds are laterally continuous over at least a few hundred metres.

Ht5: INTERBEDDED DOLOSTONE-CLAST CONGLOMERATE, ARGILLITE AND GRIT

This unit is well exposed west of Macbeth Icefield, where it overlies Unit Ht3, and underlies the Hamill Group. Structureless beds, up to 10 metres thick and laterally continuous only over tens of metres, contain abundant orange-tan-weathering dolostone cobbles and boulders, in a "matrix" of white, blue and grey quartz pebbles, rarer feldspar pebbles, muscovite and carbonate. Locally, thin conglomerate beds are rich in pelitic clasts. Within individual beds, clasts are poorly sorted. The conglomerates are interbedded with quartzose grits and minor grey argillites. Graded beds, 10 centimetres to 1 metre thick, are common in the grits. Trough crossbeds are observed more rarely. West of Macbeth Icefield, Unit Ht5 is approximately 200 metres thick, but the true thickness is difficult to estimate due to the effects of tight folds. Elsewhere, the unit is less than 50 metres thick, although it has not been traced along strike to the north of the icefield. Unit Ht5 may be a lateral equivalent of Unit Ht4.

CONTACT BETWEEN HORSETHIEF CREEK AND HAMILL GROUPS

The contact between the Horsethief Creek and Hamill groups varies significantly in the study area. It was studied at several localities, primarily within the Glacier Creek drainage. The Hamill Group quartzite was observed in contact with three Horsethief Creek Group map units, Ht5, Ht4 and Ht3. In all of these localities the contact is interpreted as sedimentary, but it may be tectonic in the lower part of Howser Creek, where it is not well exposed, and also west of Macbeth Icefield, where there is shearing parallel to the contact.

Where the Hamill Group overlies the white grits and quartzites of Unit Ht4, the contact is gradational and commonly difficult to map. The transition between the grit and massive orthoquartzite typically occurs over several tens of metres, and quartzose grit or quartz-cobble beds occur within the lower several tens of metres of the base of the Hamill Group.

Where the Hamill Group overlies Unit Ht3, the dark quartzite and schist, the contact is more abrupt, marked by a 1 to 10-metre transition to a light grey orthoquartzite. Crossbeds and grit horizons appear to be less common in the quartzite than when it overlies Horsethief Creek grits.

The contact is most abrupt above the dolostone-clast conglomerate and grit of Unit Ht5 west of Macbeth Icefield, where beds at the base of the Hamill Group appear to truncate bedding in the conglomerate at a low angle. The overlying Hamill contains grit units, as well as laterally continuous dark grey vitreous quartzites, several metres thick.

HAMILL GROUP

Stratigraphic subdivision of the Hamill Group is made difficult by lateral variations, faulting and lack of complete traversable sections in very rugged topography. Several distinct map units are recognized within the group, but correlation of units between different areas is tenuous (Figure 1-3-3). The sequence described in this study area, however, bears some marked similarities, as well as several differences, to those described by Höy (1974) to the south, in the Kootenay Arc, and by Devlin (1989) to the north, in the Dogtooth Range.

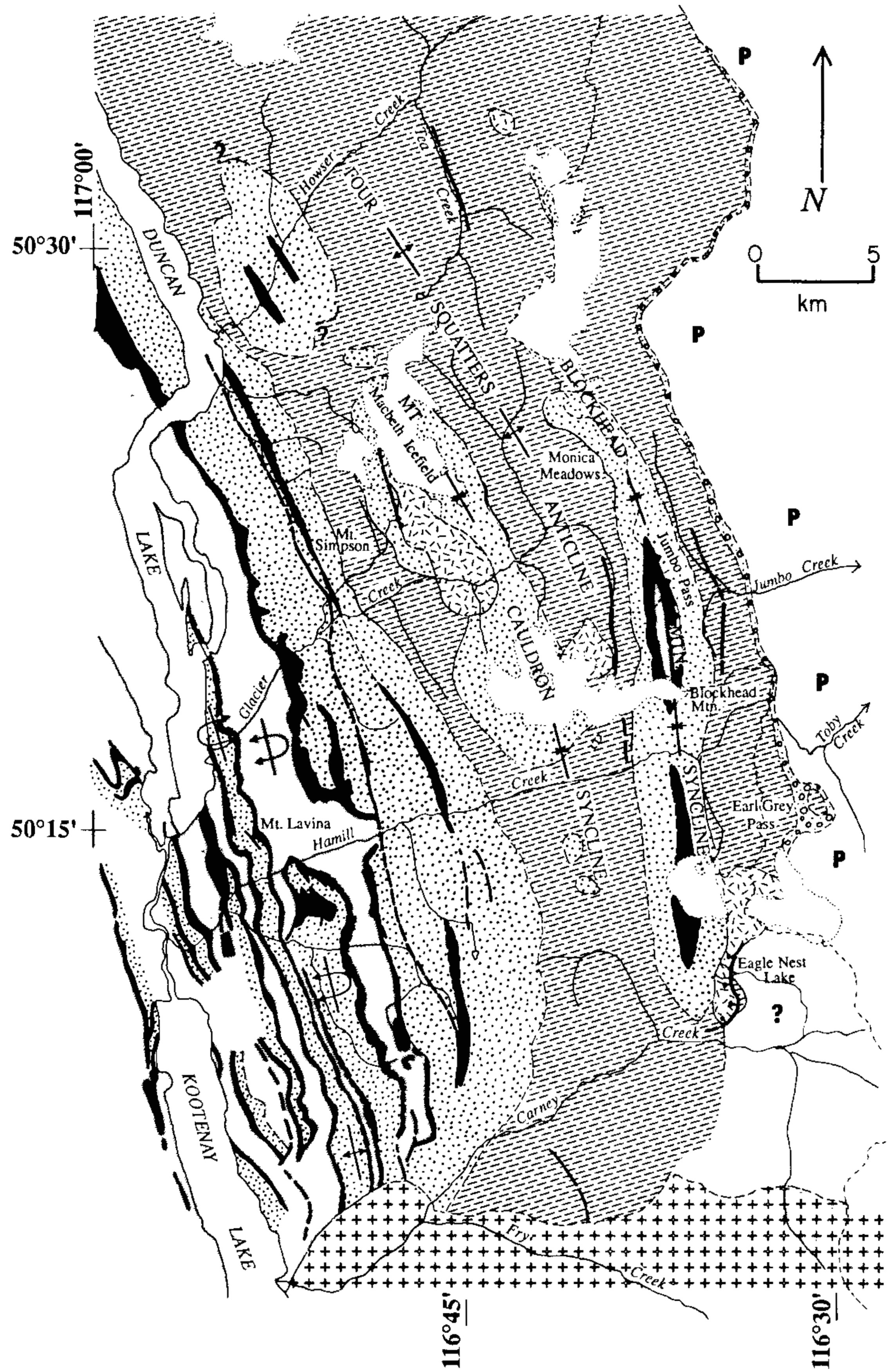

Figure 1-3-2. Geological map of the study area and adjacent segment of the Kootenay Arc. Modified after Reesor (1973). See facing page for legend.

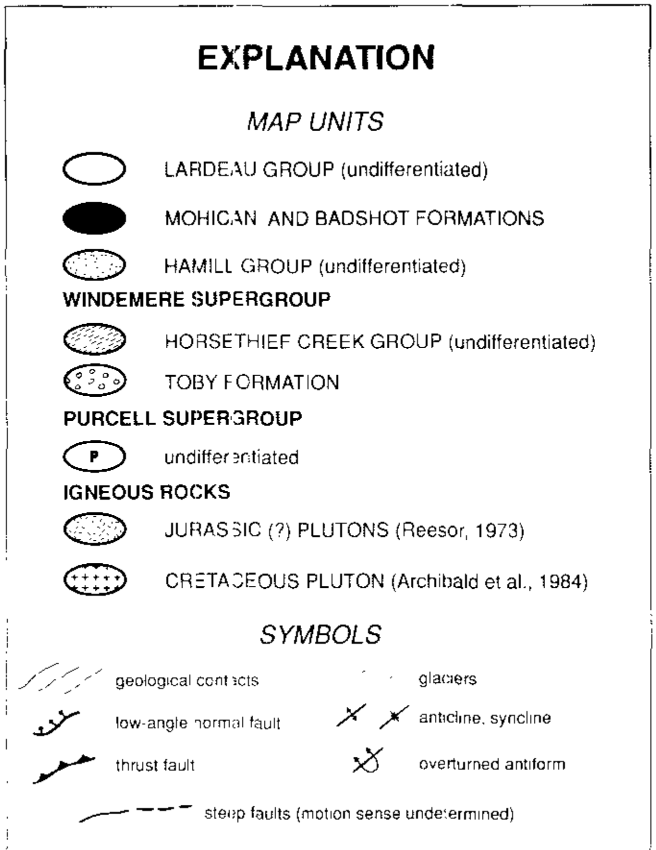

The Hamill Group (Walker and Bancroft, 1929) lies stratigraphically above the Horsethief Creek Group, and below the Badshot Formation. It is characterized by thick, mature quartzites in the Glacier Creek drainage, but a section to the north and west near Howser Creek contains more variable and generally less mature rock types, and locally abundant mafic metavolcanic rocks. Reconnaissance suggests that there may be a similar, although less marked, change to the south into Hamill Creek. These variations may reflect abrupt changes across faults, rather than lateral gradations.

In the upper part of Glacier Creek, the total thickness of the Hamill Group is estimated to be from 900 to 1500 metres, including the Mohican Formation. The estimated thickness of 1500 metres may be due to stratigraphic repetition by thrust faults.

Hm1: LIGHT GREY CROSSBEDDED ORTHOQUARTZITE

The base of the Hamill Group is characterized by a thick sequence of light grey, clean quartzite, characterized by large trough crossbeds. Truncation surfaces are 5 to 50 centimetres apart, and planar. Flow directions are difficult or impossible to measure because three-dimensional exposures are rare, but crossbeds indicate a variety of flow directions. Estimated thickness of this unit is 300 to 500 metres.

Hm2: PELITIC SCHIST, SEMIPELITE AND METAVOLCANICS

A less mature sequence, Unit Hm2, overlies the crossbedded quartzite of Unit Hm1. It consists of interbedded quartz-muscovite-biotite-(chlorite)-(garnet) schist, local biotite-chlorite-(plagioclase)-(hornblende)-(garnet)-(calcite) mafic schist in layers 1 to 10 metres thick, some impure quartzite and carbonate, and minor pebble or cobble conglomerate. Contact relationships suggest that the mafic rocks were emplaced as both dikes and flows. Thin horizons of quartz-muscovite-hornblende-garnet schist may reflect a volcanic source, and rare mafic clasts are found in conglomerate lenses associated with the mafic schists. Quartzite and pelite are interbedded on a scale of 5 centimetres to 5 metres. Total thickness is very loosely estimated at 0 to 250 metres. The lower contact appears to be abrupt; the upper contact is gradational.

Hm3: MASSIVE WHITE ORTHOQUARTZITE

A distinctive, brilliant white, structureless, fine to medium-grained orthoquartzite occurs in a few localities in sharp contact above the amphibolite or biotite schist of Hm2. Parting surfaces thinly coated with fine-grained muscovite are 10 centimetres to 1 metre apart. East of Mount Lavina, on the ridge between the Glacier and Hamill creek drainages, this unit overlies Unit Hm2. In other localities, its stratigraphic position is not yet clear. Its maximum thickness is approximately 200 metres.

Hm4: INTERBEDDED DARK AND LIGHT QUARTZITE AND SEMIPELITE

Unit Hm4 consists of a heterogeneous sequence of dark grey quartzite, black quartzose muscovite-(biotite) schist, and less common white quartzite beds. Bed thicknesses range from a few centimetres to ten metres. Sedimentary structures are rare, but subtle graded bedding occurs in the quartzose schist, and crossbeds in the light quartzite. Both upper and lower contacts are gradational, although the lower contact with Unit Hm3 is more abrupt. Estimated maximum thickness is 1000 metres near Blockhead Mountain. A minimum thickness of about 100 metres, south of Mount Simpson, reflects significant tectonic attenuation, probably along an isoclinal fold limb.

MOHICAN FORMATION

The Mohican Formation (Fyles and Eastwood, 1962) represents a transition between quartz-rich sediments of the Hamill Group and carbonate-rich rocks of the Badshot Formation. Much of the Mohican Formation is characterized by light to medium grey, brown-weathering quartz-muscovite schist and interbedded thin tan metasiltstones. The base contains quartzite beds which decrease in abundance and thickness upwards. Metre-thick dolostone beds become more abundant toward the top and the schist becomes more calcareous upwards.

The most striking feature of the Mohican Formation is the occurrence of three closely spaced orthoquartzite beds about 50 to 100 metres below the Badshot Formation, in the core of the Blockhead Mountain syncline. Each of the beds is

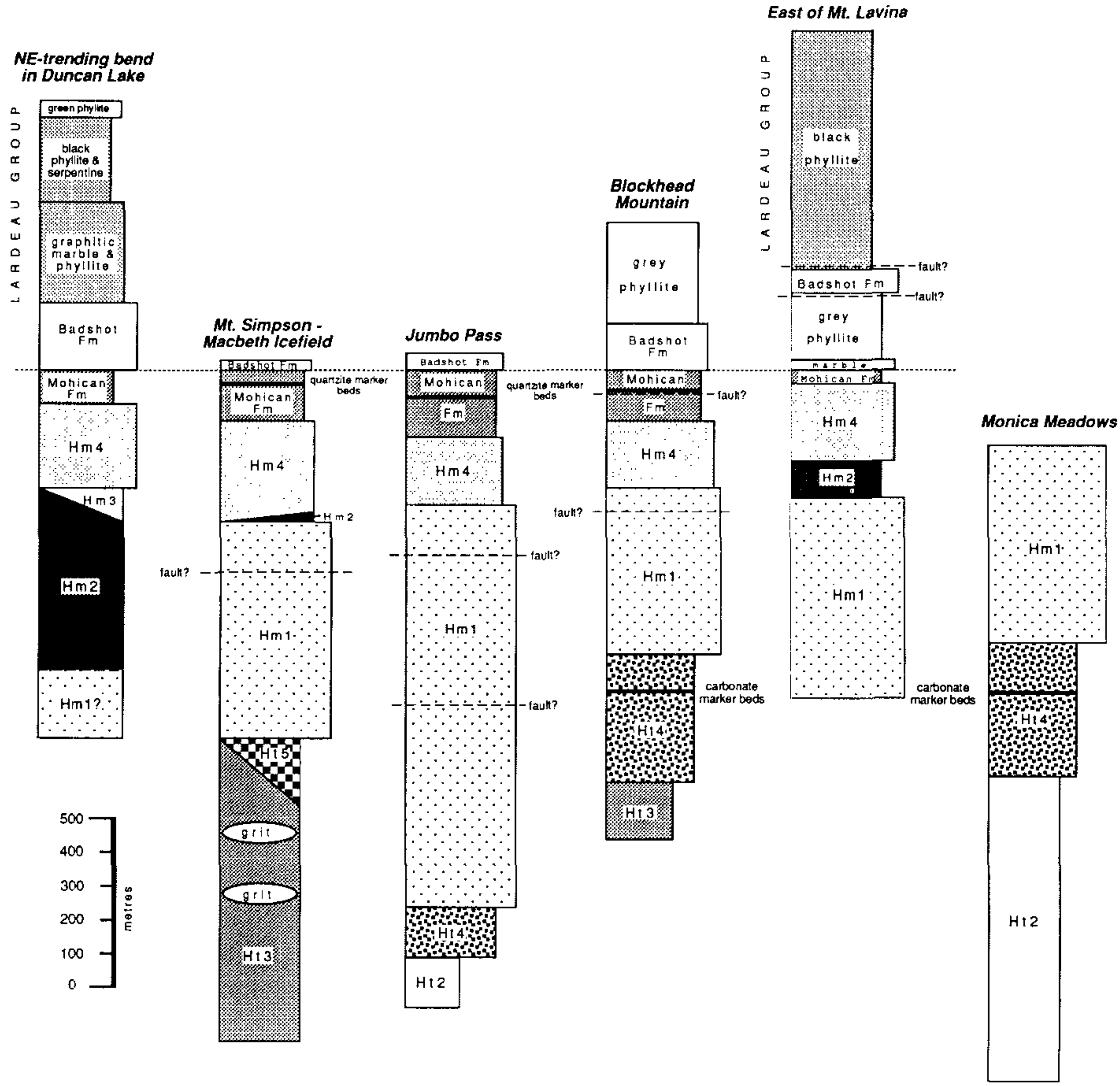

Figure 1-3-3. Stratigraphic columns from the study area showing approximate thicknesses of map units. Upper and lower limits of columns represent limit of exposure or truncation along a fault. Column locations are identified in Figure 1-3-2.

about 5 metres thick, and contains abundant trough crossbeds, very similar to those observed at the base of the Hamill Group. The three beds are a very prominent marker horizon in cliff faces, and can be traced along the entire exposure of Mohican Formation in the Blockhead Mountain syncline, a distance of 20 kilometres. A white quartzite, 5 metres thick, was also mapped in Mohican schist beneath the Badshot Formation near Mount Simpson, and may represent a tectonically thinned equivalent to the west.

The thickness of the Mohican Formation is difficult to estimate because of tectonic thickening and thinning. Within the highly strained rocks of the Kootenay Arc, Unit Hm4 and the Mohican Formation are commonly indistinguishable.

Badshot Formation

The Badshot Formation (Walker and Bancroft, 1929) stratigraphically overlies the Mohican Formation of the Hamill Group. It is characterized by two rock types in the study area, which are not separated into mappable units. Most abundant, and most characteristic, is a cliff-forming, white to medium grey, commonly laminated marble or dolomitic marble. At the eastern edge of the area mapped by Fyles (1964), marble horizons tens of metres thick may be separated by grey, locally calcareous schist. The schist varies in thickness from several metres to 100 metres. It is possible, however, that a single carbonate horizon has been duplicated by faulting or folding, and the schist belongs to either the underlying Mohican Formation or overlying Index Formation.

Phyllite in the Core of the Blockhead Mountain Syncline

A homogeneous, silvery grey phyllite overlies the dolomitic marble of the Badshot Formation in the core of the Blockhead Mountain syncline. Root (1987) tentatively mapped this unit as the lower Index Formation of the Lardeau Group. The grey phyllite, however, differs in appearance from the lower Index Formation exposed to the west along Duncan Lake. The lower Index phyllite or schist is characteristically black, commonly graphitic, and contains abundant black or graphitic marbles above the contact with the Badshot Formation.

Lardeau Group

The Index Formation of the Lardeau Group is well exposed in tight map-scale folds within the Kootenay Arc on the east side of Duncan and Kootenay lakes (Fyles, 1964). The formation as mapped by Fyles includes: black, commonly graphitic, phyllite or schist of the lower Index Formation, with interbedded black marble at the base; and green phyllite or quartz-muscovite-chlorite schist, with quartzose laminations, of the upper Index Formation. It is not a goal of this study to remap the Lardeau Group in this area, but two observations which differ from those of Fyles are worth noting.

Southeast of Mount Lavina, plagioclase-actinolite or hornblende-biotite-chlorite-(epidote) greenstone, 20 to 30 metres thick, is intercalated with green and beige, laminated muscovite-chlorite-quartz schist. This sequence is exposed in the core of a syncline and appears to stratigraphically overlie the upper Index Formation.

The lower Index Formation, between the mouths of Glacier and Howser creeks, contains at least one thin ultramafic to mafic unit, which varies in composition and texture from a green talc-chlorite-(antigorite)-(magnesite)-(calcite) schist to an equigranular to well-foliated plagioclase-hornblende-biotite-(chlorite) gneiss or schist with strongly sheared chloritic schistose margins. The unit is up to 30 metres thick, and has been traced south for approximately 3 kilometres from the bend in Duncan Lake (E. Lawrence, personal communication), parallel to the dominant schistosity. Repetitions of this unit may be the result of isoclinal folding which also deforms the dominant schistosity.

STRUCTURE

The overall map pattern outlined by Fyles (1964) and Reesor (1973) has not been changed significantly as a result of this study. However, several important new observations contribute to the understanding of the kinematics of deformation in this part of the Kootenay Arc and adjacent Purcell anticlinorium.

Sequence of Deformation

Three main phases of deformation are recognized in the study area: (1) early large-scale west-verging recumbent folds (Fyles, 1964); (2) a dominant phase of upright or east-verging folds, associated with steep ductile shear zones and a pervasive subhorizontal north-south stretching lineation; and (3) a late crenulation or spaced cleavage which is probably not correlative across the entire area

Prograde metamorphism up to garnet grade accompanied Phase I or the early part of Phase II deformation. Retrograded garnet porphyroblasts show that the garnet isograd is considerably farther east than shown by Reesor (1973). Widespread retrograde metamorphism probably occurred late in Phase II deformation.

Minor folds related to Phase I, previously thought to be confined to the Kootenay Arc (Reesor, 1973), are preserved in competent rocks as far east as Jumbo Pass These folds form Type 3 interference patterns with younger, upright Phase II folds, but do not affect the map pattern as they do in the Duncan Lake region.

Phase II fold axes are parallel to a distinctive subhorizontal lineation. It is expressed in quartzose rocks as mullions or quartz rods at a wide range of scales, as an intersection lineation or mica and quartz mineral lineation in schistose rocks, as boudinage in rocks of variable rheology, and as strongly stretched clasts in grits and conglomerates. Aspect ratios of stretched clasts are as high as 50:1. The plunge is most commonly shallow to 330° to 340°, although domains of southeasterly plunge are not uncommon. The lineation is pervasive within the strongly deformed, overturned sequence of Hamill Group, Badshot Formation and Lardeau Group to the west, but is very well developed in high-strain zones as far east as the Purcell divide.

The Phase II schistosity or cleavage also decreases in intensity from west to east, but is locally stronger in ductile shear zones, parallel to the axial surfaces of map-scale structures. A variety of complex folds and faults are clearly outlined in the Blockhead Mountain syncline by the three marker beds within the Mohican Formation, and indicate that the syncline is internally complex. These structures include megascopic boudinage, duplexes and large-amplitude, repeated isoclinal folds. The Phase II fabric varies in orientation from east-dipping to west-dipping. A pattern to variations in orientation of Phase II structures has not been recognized yet. The variation may be due to fanning of Phase II structures, changes in orientation with structural level, or disturbance by Phase III structures.

The Phase III deformation is coaxial with Phase II in the western part of the area (Fyles, 1964), but cuts obliquely across earlier structures in the eastern part of the area.

Transition From Purcell Anticlinorium to Kootenay Arc

Fyles' (1964) mapping provided thorough documentation of the complex fold style in the vicinity of Duncan and northern Kootenay lakes. A largely inverted sequence represents the lower, overturned limb of a large southwest-verging recumbent fold, which closes west of Duncan Lake. This structure is isoclinally refolded by younger, tight, upright folds (Fyles, 1964). Reesor (1973) reported a "sudden change of folding intensity" several kilometres east of Duncan Lake, within the westernmost exposed Horsethief Creek Group. This change separates rocks of the western Purcell anticlinorium from the more complexly deformed rocks of the Kootenay Arc to the west. To the east, Reesor (1973) documented an upright stratigraphic succession, deformed only by less tight, upright or steeply east-verging folds. It is important to note that the geometric relationships shown on Reesor's (1973) compilation map allow no place for the upright limb of the west-verging recumbent structure mapped by Fyles to "root" to the east.

A well-developed ribbon mylonite zone has been traced from the west flank of Mount Simpson, north of Glacier Creek, to south of Hamill Creek. To the north, the stratigraphy is disrupted at the edge of Duncan Lake, suggesting that the fault continues. The fault lies primarily within the Hamill stratigraphy, but juxtaposes different parts of the Hamill Group. The regional subhorizontal lineation, including stretched pebbles, is particularly well developed in this zone. Shear-sense indicators observed in outcrops within the fault zone include C-S fabrics and strongly asymmetric minor folds. The dominant shear sense is dextral, although in many places indicators are ambiguous or lacking. The amount of fault displacement cannot be estimated.

Along strike to the south, a similar change in fold style is also marked by a fault zone, the West Bernard fault of Höy (1977) or the Seeman Creek fault of Leclair (1988). East-verging reverse motion was inferred in the Riondel area, but conclusive evidence was lacking (Höy, 1974).

Relationships Between Intrusive Rocks and Deformation

Three types of intrusive rocks are found in the study area: small, elongate and locally deformed hornblende biotite granodiorite plutons (Jurassic?; Reesor, 1973), foliated felsite dikes which are common in the western part of the study area, and larger two-mica quartz monzonite plutons (Cretaceous Fry Creek batholith; Reesor, 1973; Archibald *et al.*, 1984). Field relationships indicate that the elongate plutons and the felsite dikes were intruded during the latter part of Phase II deformation. The dike margins, foliation and elongate xenoliths are parallel to the Phase II schistosity and axial surfaces. The dikes, however, are not themselves folded, and the dike foliation is not as strong as that within competent country rocks. The dikes are commonly boudinaged, with stretching subparallel to the regional subhorizontal lineation. Veins associated with the elongate plutons are folded by the Phase II deformation, but not nearly as tightly as are the host sediments. Some veins completely cut the Phase II fabric at low angles. The western margin of the Glacier Creek stock is very weakly foliated compared to the country rock, although the adjacent Hamill quartzite shows evidence of intense ductile deformation during Phase II deformation.

Minor folds in the country rock are parallel to the contact with the Fry Creek batholith within 0.5 metre of the contact, but the batholith completely crosscuts the map-scale structures. The north-south subhorizontal mineral lineation is evident in the country rock, but nowhere in the pluton. The western part of the pluton, however, near the mouth of Fry Creek canyon, displays a moderately southeast-dipping quartz-muscovite schistosity, and a west-dipping quartz lineation. Eocene Ar-Ar dates from the western part of the pluton suggest that it has been affected by Eocene extension (Archibald *et al.*, 1984).

A spectacular ductile fault zone separates the southern tail of the Toby stock from the upper part of the Horsethief Creek Group to the east of the stock. A strong west-plunging mineral lineation, including hornblende, is developed on a west-dipping mylonitic fabric and shear-sense indicators imply west-side down. Boudinage is dramatic on a variety of scales. This fault is also suspected to be Eocene, and it is hoped that Ar-Ar dating of oriented hornblendes will help to constrain the age of deformation.

SUMMARY AND PRELIMINARY CONCLUSIONS

- The middle to upper part of the Horsethief Creek Group is characterized by a sequence of five mappable units, which may represent a transition from deep to shallow water. The base of the Hamill Group appears to be gradational at some localities, but not at others; and to overlap the top three units of the Horsethief Creek Group.
- The internal stratigraphy of the Hamill Group can be correlated quite closely with that described by Höy (1974) in the Riondel area to the south, and less closely with that described by Devlin (1989) in the Dogtooth Range to the north; however, in the Glacier Creek area, immature clastic sediments and volcanic rocks are much less significant in the middle of the Hamill Group than in the regions to the north and south.
- A prominent subhorizontal stretching lineation associated with the development of Phase 2 structures is pervasive within the Kootenay Arc, and widespread at least as far east as the Purcell divide.
- A well-developed, steep ductile mylonite zone separates rocks of the Kootenay Arc from upright rocks of the Purcell anticlinorium. Evidence suggests that motion was dominantly strike-slip, although an earlier history may be masked.
- Low-angle ductile normal faulting has affected the southeastern part of the area and may be associated with regional Eocene extension.

ACKNOWLEDGMENTS

Funding for this project is provided by British Columbia Geoscience Research Grant RG91-05, Natural Sciences and Engineering Research Council Research Operating Grant OGP0092417 awarded to R. A. Price, and a Queen's University School of Graduate Studies research travel grant awarded to M. Warren. Natalie Sweet provided cheerful assistance in the field. The British Columbia Ministry of Forests, in Nelson and Kaslo, is thanked for providing up-to-date copies of maps. We are grateful for the services of Pemberton Helicopter Services, Ltd. in Meadow Creek, and Canadian Helicopters, Ltd. in Nelson. Thanks to Dugald Carmichael of Queen's University for comments in the field, and for introducing M.W. to the thrill of helicopters. M.W. is grateful to many residents of the West Kootenays, particularly John Carter, for useful information and warm hospitality.

REFERENCES

Archibald, D. A., Krogh, T. E., Armstrong, R. L. and Farrar, E. (1984): Geochronology and Tectonic Implications of Magmatism and Metamorphism, Southern Kootenay Arc and Neighbouring Regions, Southeastern British Columbia. Part II: Mid-Cretaceous to Eocene; *Canadian Journal of Earth Sciences*, Volume 21, pages 567-583.

Bond, G. and Kominz, M. A. (1984): Construction of Tectonic Subsidence Curves for the Early Paleozoic Miogeocline, Southern Canadian Rocky Mountains: Implications for Subsidence Mechanisms, Age of Breakup and Crustal Thinning; *Geological Society of America*, Bulletin, Volume 95, pages 155-173.

Bond, G.C., Christie-Blick, N., Kominz, M.A. and Devlin, W.J. (1985): An Early Cambrian Rift to Drift Transition in the Cordilleran of Western North America; *Nature*, Volume 315, pages 742-746.

Devlin, W.J. (1989): Stratigraphy and Sedimentology of the Hamill Group in the Northern Selkirk Mountains, British Columbia: Evidence for Latest Proterozoic - Early Cambrian Extensional Tectonism; *Canadian Journal of Earth Sciences*, Volume 26, No. 3, pages 515-533.

Douglas, R.J.W. (Compiler) (1968): Geological Map of Canada; *Geological Survey of Canada*, Map 1374A.

Fyles, J.T. (1964): Geology of the Duncan Lake Area, Lardeau District, British Columbia; *B.C. Ministry of Energy, Mines and Petroleum Resources*, Bulletin 49, 87 pages.

Fyles, J.T. and Eastwood, G.E.P. (1962): Geology of the Ferguson Area, Lardeau District, British Columbia; *B.C. Ministry of Energy, Mines and Petroleum Resources*, Bulletin 45, 92 pages.

Höy, T. (1974): Structure and Metamorphism of Kootenay Arc Rocks Around Riondel, British Columbia; unpublished Ph.D. thesis, *Queen's University*.

Höy, T. (1977): Stratigraphy and Structure of the Kootenay Arc in the Riondel Area, Southeastern British Columbia; *Canadian Journal of Earth Sciences*, Volume 14, pages 2301-2315.

Leclair, A.D. (1988): Polyphase Structural and Metamorphic Histories of the Midge Creek Area, Southeast British Columbia: Implications for Tectonic Processes in the Central Kootenay Arc; unpublished Ph.D. thesis, *Queen's University*, 264 pages.

Monger, J.W.H., Price, R.A. and Templeman-Kluit, D.J. (1982): Tectonic Accretion and the Origin of Two Metamorphic and Plutonic Welts in the Canadian Cordillera; *Geology*, Volume 10, pages 70-75

Pope, A. (1990): The Geology and Mineral Deposits of the Toby - Horsethief Creek Map Area, Northern Purcell Mountains, Southeast British Columbia (82K); *B.C. Ministry of Energy, Mines, and Petroleum Resources*, Open File 1990-26.

Price, R.A. (1986): The Southeastern Canadian Cordillera: Thrust Faulting, Tectonic Wedging, and Delamination of the Lithosphere; *Journal of Structural Geology*, Volume 8, pages 239-254.

Reesor, J.E. (1973): Geology of the Lardeau Map-area, East-half, British Columbia; *Geological Survey of Canada*, Memoir 369, 129 pages.

Root, K.G. (1985): Reinterpretation of the Age of a Succession of Paleozoic Strata, Delphine Creek, Southeastern British Columbia; *in* Current Research, Part A, *Geological Survey of Canada*, Paper 85-1A, pages 727-730.

Root, K.G. (1987): Geology of the Delphine Creek Area, Southeastern British Columbia: Implications for the Proterozoic and Paleozoic Development of the Cordilleran Divergent Margin; unpublished Ph.D. thesis, *University of Calgary*, 446 pages.

Walker, J.F. and Bancroft, M.F. (1929): Lardeau Map-area, British Columbia, General Geology; *in Geological Survey of Canada*, Memoir 161, pages. 1-16.

NOTES

PETROLOGY OF THE GOLDEN CLUSTER LAMPROPHYRES IN SOUTHEASTERN BRITISH COLUMBIA (82N)

By O.J. Ijewliw
Queen's University

KEYWORDS: Petrology, lamprophyre, diatreme, dike, pipe, Golden, kimberlite.

INTRODUCTION

Lamprophyre diatremes and dikes of probable Paleozoic age occur in three areas of eastern British Columbia. These are: the Ospika River diatreme in the north (Pell, 1986, 1987a, b), a cluster of diatremes and dikes near Golden (Ijewliw, 1986, 1987; Pell, 1986, 1987a, b; Ijewliw and Schulze, 1988) and another cluster in the Cranbrook - Bull River area in the south (Leech, 1958, 1964, 1965, 1979; Grieve, 1981, 1982; Ijewliw, 1986, 1987; Pell, 1986, 1987a, b; Hall *et al.*, 1989; Hall 1991; Helmstaedt *et al.*, 1988). These three groups of diatremes are aligned in a north-northwest belt northeast of the Rocky Mountain Trench within the Western and Main ranges of the Rocky Mountain fold and thrust belt They vary, however, with respect to their rock types, stratigraphic position, time of emplacement and structural setting.

The nothern Ospika pipe and the central Golden cluster are lamprophyres of the ultramafic, calcalkaline or alkaline branches, whereas the diatremes of the southern Cranbrook - Bull River cluster, with the exception of the Cross kimberlite, are more difficult to classify due to severe alteration. Some of them resemble limburgites or olivine melilitites (Grieve, 1981; Ijewliw, 1986, 1987; Pell, 1986, 1987b; Hall, 1990).

Since the 1970s, diatreme facies rocks in eastern British Columbia have generated some exploration interest due to their presumed similarity to kimberlites, possible carriers of diamonds (Pell, 1986). In this note the chemical composition of clinopyroxenes and spinels in two of the Golden cluster lamprophyres, HP and Mons Creek pipes are examined in order to better understand the igneous processes.

GEOLOGICAL SETTING

The Golden cluster lamprophyres extend over a curvilinear distance of about 55 kilometres along a southeasterly trend. They occur at distances ranging from 40 to 90 kilometres north of the town of Golden, British Columbia (Table 1-4-1) and are located on NTS map 82N. The lamprophyres lie within a single structural unit in Cambro-Ordovician carbonate strata, west of the west-dipping Mons Creek fault. Its continuity is unbroken by any major faults. Each location comprises a diatreme or breccia phase(s) with associated or crosscutting dikes. The degree of preservation varies from the relatively well preserved HP pipe and the relatively fresh Mons Creek float samples; to the moderately preserved Bush River site, which retains both primary minerals and clearly discernible pseudomorphs of altered minerals; to the severely altered rocks at Valenciennes River and the tuffisitic rocks on Lens Mountain in which primary textures and mineralogy are no longer discernible.

Classification of the Golden cluster diatremes (Table 1-4-2) is based primarily on the extensive work of Rock (1977, 1984, 1986, 1987, 1989) and the IUGS recommendations (Streckeisen, 1979) regarding lamprophyre nomenclature. Based on a survey of the lamprophyre literature, Rock (1987) prepared a scheme for lamprophyre definition, distinction and nomenclature. The definition stated that essential mineral phases should include amphiboles, biotites, phlogopites and other volatile-rich minerals such as halides, carbonates, sulphates and zeolites, in addition to feldspars and quartz with coexisting magnesium-rich mafic minerals, olivine and clinopyroxene. Neither feldspars nor quartz occur as phenocrysts and olivine does not occur in the groundmass (Rock, 1977, 1984, 1987).

MINERAL CHEMISTRY

The chemical composition of fresh, cognate minerals occurring in the Golden cluster lamprophyres was determined in order to assist in lamprophyre classification as, to a limited extent, a given rock type contains minerals within a limited compositional range. Additionally, mineral compositions may elucidate the igneous processes occurring during the evolution of a given rock. Mineral chemical data from the HP and Mons Creek pipe clinopyroxenes and spinels are characteristic for each pipe.

Mineral chemical compositions were determined using an ARL SEMQ microprobe at Queen's University. Structural formulae for clinopyroxenes were calculated based on six

TABLE 1-4-1
LOCATIONS OF THE GOLDEN CLUSTER LAMPROPHYRES

Pipe	Latitude and Longitude	Elevation
Bush River	52°05'00"N & 117°23'00"W	2195 m (7200 ft)
Lens Mountain	51°54'15"N & 117°07'30"W	2794 m (9200 ft)
Mons Creek	51°49'30"N & 117°00'30"W	2225 m (7300 ft)
Valenciennes River	51°47'00"N & 116°58'30"W	2591 m (8500 ft)
HP Pipe	51°41'30"N & 116°57'15"W	2195 m (7200 ft)

TABLE 1-4-2
GOLDEN CLUSTER LAMPROPHYRE CLASSIFICATION

Location	Name	Branch
Bush River	olivine kersantite	Calcalkaline
Mons Creek	biotite camptonite	Alkaline
Valenciennes River	camptonite	Alkaline
HP Pipe	aillikite	Ultramafic

oxygens, assuming a $(W)_{1-p}(X,Y)_1+_pZ_2O_6$ stoichiometry, where: W = Ca,Na,K; X = Mg,Fe^{2+},Mn; Y = Fe^{3+}, Al-VI, Ti, Cr; Z = Si, Al-IV (Deer *et al.*, 1978). Using the methods of Deer *et al.* (1966), cations were normalized to four and, using either oxygen deficiency or charge balance considerations, the Fe^{3+} cation component was calculated. Structural formulae for spinels were calculated based on four oxygens, assuming an XY_2O_4 stoichiometry, where: X=Mg,Fe^{2+},Mn; Y=Cr,Al,Fe^{3+},Ti (Deer *et al.*, 1962). Cations were normalized to three and the Fe^{3+} cation component was calculated as for the clinopyroxenes.

HP Pipe Homogeneous Clinopyroxenes

Contrary to expectations, the HP pipe clinopyroxene chemical compositions are independent of whether they are from the breccia or dike phases and are also independent of size, that is, megacryst, macrocryst or phenocryst sizes. Consequently, all of the chemical data are grouped together. Seventy-five clinopyroxene grains were analysed. A majority, 87 per cent (65 out of 75 grains) of the HP pipe clinopyroxes are not zoned. Microprobe testing confirmed that the grains are homogeneous where optical zoning is not seen.

In hand sample, the HP pipe clinopyroxenes can be easily divided, on the basis of colour, into the bright green diopsides and the black diopsides and salites. This distinction is reflected in the chemical analyses; the green clinopyroxenes are chrome diopsides with an average of 1.0 weight per cent Cr_2O_3 and the black diopsides and salites are virtually devoid of chromium.

Thin-section colour is also correlated with chemical composition. Pyroxenes with green pleochroism have the highest amounts of FeO (11.3–15.7 wt.%), those with pink pleochroism have the highest TiO_2 contents (1.9–2.8 wt.%) and those with pink and green pleochroism are high in both iron and titanium. Nonpleochroic, clear or white grains are highest in MgO (12.3 -17.0 wt.%). The highest aluminum values are in the 13.11 to 14.52 weight per cent Al_2O_3 range and the highest sodium values range from 2.02 to 2.33 weight per cent Na_2O.

The HP pipe has three groups of clinopyroxenes. They are distinct with respect to Mg, Fe, Mg# [Mg# = Mg/(Mg+Fe(total)+Mn)] and chrome contents, but there is overlap in the other major elements. The high-Mg# diopside group [Mg# > 0.90] is chrome rich, green in hand sample and white in thin section. The intermediate-Mg# diopside group, [Mg# = 0.78 – 0.88] is chrome poor, black-brown in hand sample and pale tan or green pleochroic in thin-section. Both the high and intermediate-Mg# clinopyroxene groups have a negative correlation between Mg# and Ti cations (Figure 1-4-1). The low-Mg# salite group, [Mg# = 0.45–0.68] is also chrome poor, black-brown in hand sample and green in thin-section. This group's values have too much scatter to unequivocally establish a trend (Figure 1-4-1).

Lamprophyre clinopyroxenes (excluding those of kimberlites) tend to be in the diopside, salite or augite fields (Rock, 1987). Comparing the HP pipe clinopyroxene compositions with those of different lamprophyre branches as well as anhydrous, ultramafic rocks given by Rock (1987) and Bergman (1987) reveals that the chrome diopsides of the high-Mg# group correspond closely to those from alpine-type peridotites and are intermediate in composition between lamproite and kimberlite clinopyroxenes (Bergman, 1987; Rock, 1987). They also correspond to the ultramafic lamprophyre clinopyroxenes of Rock (1987) within one or sometimes two standard deviations. The intermediate-Mg# group, the chrome-poor diopsides, corresponds to the ultramafic lamprophyre clinopyroxenes of Rock (1987). The low-Mg# group, the salites, corresponds to the alkaline and the ultramafic lamprophyre clinopyroxenes within one or two standard deviations (Rock, 1987), as well as to clinopyroxenes from alkaline olivine basalts and alkaline intrusives (Bergman, 1987).

Thus, it appears that at least the intermediate-Mg# clinopyroxenes of the HP pipe support the designation of this rock within the ultramafic lamprophyre branch and that the other clinopyroxene groups have elemental values in common with other undersaturated alkaline rocks and lamprophyre branches. The chemical discontinuities and distinct trends make it unlikely that the three clinopyroxene groups are part of one system. The origins of the three groups and their relationship to each other are discussed in the following section.

Chrome diopsides are commonly considered to have originated from disaggregated peridotites (Brooks and Printzlau, 1978; Wass, 1979). However, the HP pipe high-Mg# chrome diopsides are chemically distinct from clinopyroxene xenoliths and xenocrysts occurring in lamproites, kimberlites, alkali olivine basalts and lamprophyres in the amounts of silica, aluminum, iron and calcium (Bergman, 1987). The HP high-Mg# chrome diopsides range in size up to 2 to 3 centimetres in diameter and are significantly larger than average lherzolite clinopyroxenes which are less than 30 millimetres in diameter (Eggler *et al.*, 1979). The HP pipe chrome diopsides are unlikely to have derived from disaggregated peridotites as they differ in chemical composition and are much coarser grained. They are also thought to be cognate to the HP pipe system(s) because the rims of the zoned grains are of a similar composition. The small variations in Mg# and the other major

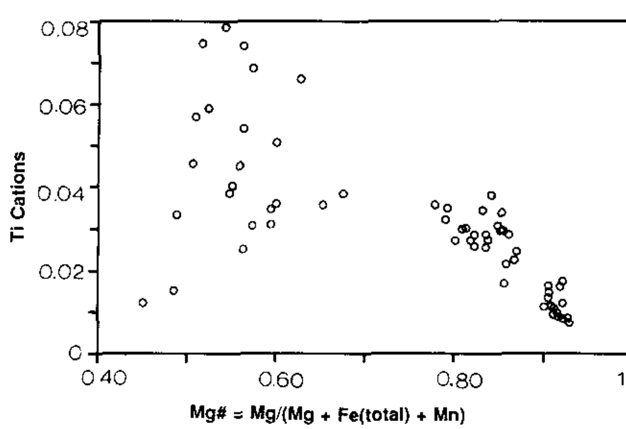

Figure 1-4-1. HP pipe homogeneous clinopyroxenes. Mg# versus Ti cations. The high and intermediate Mg# groups have negative correlations with titanium contents.

elements measured, and the clear correlations, suggest that a small degree of fractionation occurred in this group.

The intermediate-Mg# chrome-free diopside group corresponds in composition to those from ultramafic lamprophyres (Rock, 1987) and is considered to be cognate to the HP pipe system. The wide variation and distinct negative correlations between Mg# and Ti cations (Figure 1-4-1) indicate that this clinopyroxene group may have crystallized in a fractionating liquid which was becoming progressively enriched in iron, aluminum and titanium. A similar pattern exists among chrome-poor megacrysts in the Colorado-Wyoming kimberlites and was also attributed to fractionation (Eggler *et al.*, 1979). Gurney *et al.* (1979) similarly noted a linear trend of increasing TiO_2 with increasing FeO from the Monastery kimberlite pipe in South Africa. Malaita alnoite (ultramafic lamprophyre) contains subcalcic diopsides and augites with fractionation trends similar to this intermediate-Mg# HP group and these cognate clinopyroxenes are chemically distinct from xenolithic lherzolite clinopyroxenes found in the same pipe (Nixon and Boyd, 1979). Therefore, it is suggested that fractional crystallization is the dominant process controlling the trends in the intermediate-Mg# clinopyroxene group.

The low-Mg# salite group has the most variability in both Mg# and component elements and no clear negative correlation with Ti cations (Figure 1-4-1). Salites or green clinopyroxenes of slightly varying chemical compositions are found in a variety of alkaline hydrous and nonhydrous rocks. Explanations for their occurrence include that they may be xenocrysts from other magma systems (Pe-Piper, 1984; O'Brien *et al.*, 1988; Pe-Piper and Jansa, 1988), or xenocrysts from disaggregated xenoliths (Barton and van Bergen, 1981).

When zoned, the HP salites have irregular, rounded and lobate green cores with narrow, subhedral, white overgrowths and correspondingly sharp compositional changes from a high-iron core to a low-iron rim. There is a distinct gap in the iron and magnesium contents between the intermediate and low-Mg# (gap is Mg# 0.68–0.78) clinopyroxene groups. Average weight per cents of the other major elements are distinct beyond one standard deviation. Reverse zoning and compositional gaps suggest that the green salites are most likely accidental inclusions from another system encountered en route by the HP intrusion.

In summary, the three distinct clinopyroxene populations in the HP pipe comprise: the high-Mg#, cognate chrome diopsides fractionating from a new primitive melt; intermediate-Mg#, chrome-free diopsides in a fractionating system; and, low-Mg#, xenocrystic salites.

HP Pipe Zoned Clinopyroxenes

The cores of the zoned grains correspond in composition to the low and intermediate-Mg# unzoned clinopyroxenes, whereas the rims correspond to the intermediate and high-Mg# unzoned grains (compare Figure 1-4-2 to Figure 1-4-1). The gap in Mg# between the low and intermediate-Mg# zoned cores is similar to the gap in the unzoned grains. The gap between the high and intermediate-Mg# groups is not as evident in the rims. The zoned clinopyroxenes are thus a particular subset of the three groups of homogeneous clinopyroxenes and can be ascribed to the same lamprophyre branches as the corresponding Mg# indicates. There is a preponderance of clinopyroxene zones within the intermediate-Mg# group which also supports the designation of the HP pipe within the ultramafic lamprophyre branch.

The zoned grains do not differ texturally from the homogeneous clinopyroxenes. They vary in size and occur both in the breccia and dike phases but are slightly more prevalent in the dikes. Only 13 per cent (10 out of the 75) of the HP pipe clinopyroxenes examined show optical and chemical zoning. These grains have green or pink cores and white rims. Only two zones, core and rim, are apparent except for a single grain where four zones are noted.

The zoned clinopyroxenes are characterized by iron-rich cores and very narrow magnesium-rich rims. Figure 1-4-2 shows that the cores which are particularly rich in titanium also have rims which are relatively enriched in these elements. Similarly, the cores which are relatively poor in magnesium also have relatively magnesium-poor rims. The most magnesium-rich and titanium-poor rims are similar to the high-Mg# chrome diopside group (Figure 1-4-2). Therefore, it is postulated that a new magma batch, in equilibrium with the high-Mg# clinopyroxene group, entered the system, reacted with the previously formed diopsides and xenocrystic salites and formed rims of intermediate composition. It is suggested that the new magma pulse may have triggered the eruption of the HP system.

Only the high-Mg#, homogeneous clinopyroxene group has appreciable chrome. The cores of the zoned grains are all chrome free, whereas some of the rims are enriched in chrome. This corroborates the idea of an influx of primitive magma because chrome cannot remain residual in a system during fractional crystallization.

Mons Creek Clinopyroxenes

Thirteen clinopyroxenes were analysed on the microprobe: nine complexly zoned phenocrysts and simply zoned groundmass grains and four homogeneous groundmass

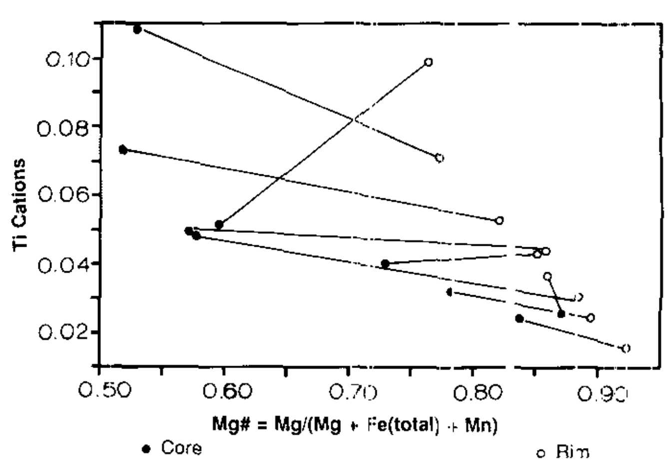

Figure 1-4-2. HP pipe zoned clinopyroxenes, Mg# versus Ti cations. The rims are magnesium and titanium enriched.

grains. Zoning traverses were made at 30 to 100-micron intervals and resulted in 2 to 22 spots being analysed per grain, depending on the complexity of the optical zoning. Despite such detailed examination, chemical distinctions are only noted on the scale of core, mantle and rim variations. The composition of the groundmass grains spans the range of compositions of the individual zones of the zoned clinopyroxenes.

Whereas the Mons Creek clinopyroxenes are more complexly zoned than those from the HP pipe, there are some similarities. If chrome is present in the Mons Creek clinopyroxenes, it commonly occurs in the rims or mantles (0.83–1.20 wt.% Cr_2O_3). This is similar to the HP pipe chrome diopsides. The cores of the larger zoned grains and the unzoned groundmass grains are relatively chrome poor (<0.40 wt.% Cr_2O_3) and some grains are entirely chrome free. Colour in thin section is related to chemical composition in that the green portions are particularly iron rich (8.23–12.19 wt.% FeO) but less so than the iron-rich grains from the HP pipe. The brown portions are particularly titanium rich (1.93–2.77 wt.% TiO_2), similar to HP pipe values, and the highest values occur in the mantles and rims. The highest magnesium values are in the 15.13 to 16.58 weight per cent MgO range, similar to HP pipe values, and occur in the grain mantles and cores. The highest aluminum values range from 9.30 to 10.43 weight per cent Al_2O_3 which is lower than in the HP pipe, and the highest sodium contents are 0.91 to 1.10 weight per cent Na_2O which is also lower than for the HP pipe. There are oscillations in all elements.

The Mons Creek clinopyroxenes have a complexity of zoning variations. At least six patterns can be discerned and two of these, Patterns 3 and 5 will be examined in this paper. Pattern 3 is a combination of simple reverse zoning, that is, increasing magnesium and chrome from core to mantle, followed by simple normal zoning, increasing iron, aluminum and titanium from mantle to rim (Figure 1-4-3). Simple reverse zoning is attributed to the entrainment of xenocrysts or previously crystallized grains in a more primitive melt, whereas, simple normal zoning is considered to be the result of fractionation. This pattern of zoning directions could occur in a grain entrained in a more primitive melt with subsequent overgrowths of more fractionated material. Pattern 5 is a combination of simple normal zoning, from core to mantle, followed by anomalous normal zoning, increasing iron but decreasing aluminum and titanium from mantle to rim (Figure 1-4-4). Anomalous normal zoning occurs as the last stages in grains exhibiting complex zoning patterns. The source of this outer material may be the melting of iron-rich, titanium, aluminum-poor xenocrysts or their entraining material possibly as a result of a cognate grain with fractionated overgrowths coming into contact with a xenocrystic melt.

In summary, these variations in the zoning directions and patterns indicate a relatively prolonged period of crystal interaction with fractionated, primitive and xenocrystic melts. It is postulated that there were at least two pulses of melting. Following the first melting episode, crystallization of clinopyroxenes occurred with later overgrowths of fractionated material (normal zoning). A second melting episode is inferred from the primitive overgrowths on previously crystallized grains (reverse zoning). Fractionation of the second melt also occurred as evidenced by the normally zoned groundmass grains. Both melts produced clinopyroxenes of similar composition and similar fractionation patterns. Xenocrysts, distinct in chemical composition (Fe-rich, Al and Ti-poor) from the cognate grains, were entrained and subsequently rimmed with fractionated or primitive melt. The xenocrysts or their enclosing melt also interacted with the cognate grains, rimming them in turn (anomalous zoning). Such complex interactions among melt episodes and xenocrystic material suggest a prolonged time period for all the events to have transpired and sufficient turbulence or convection to have allowed the mixing.

The compositions of the Mons Creek clinopyroxenes range from the HP intermediate-Mg# group to midway towards the low-Mg# group. The outstanding difference

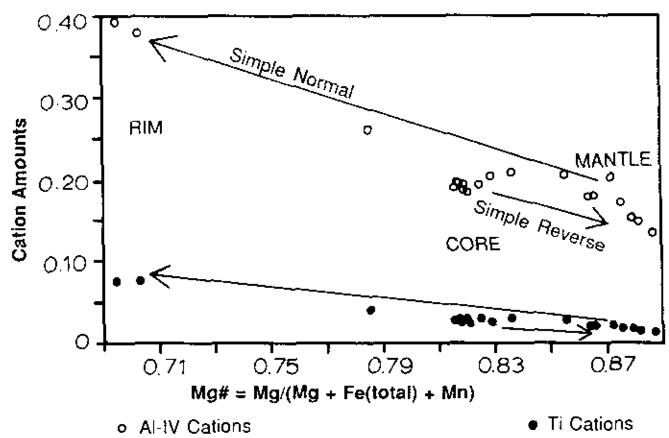

Figure 1-4-3. Mons Creek complexly zoned clinopyroxenes. Pattern 3, simple reverse zoning (with Mg# up, Al-IV, Ti down) followed by simple normal zoning (with Mg# down, Al-IV, Ti up) from core through mantle to rim.

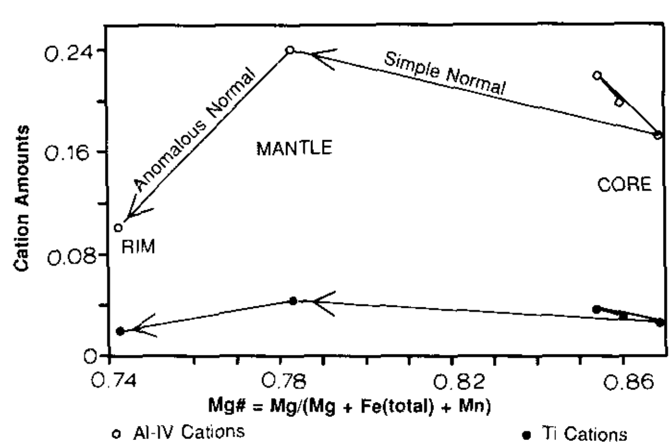

Figure 1-4-4. Mons Creek complexly zoned clinopyroxenes, Pattern 5, simple normal zoning (with Mg# down, Al-IV, Ti up) followed by anomalous normal zoning (with Mg# down, Al-IV, Ti down) from core through mantle to rim.

between the HP and Mons Creek pipes is the degree of zoning. At the HP pipe, the zoning is simple with very narrow rims upon rounded and resorbed cores. These rims are the reaction product of the xenocrystic or fractionated cores and primitive rimming material. At Mons Creek, on the other hand, the zoning is multiple, and sometimes oscillatory. It is the product of repetitive interaction among xenocrystic, fractionated and primitive melts. This suggests that the HP pipe was emplaced very shortly after the primitive magma pulse, whereas the Mons Creek diatreme had a comparatively much longer residence time prior to ascent to the surface.

In both the Mons Creek and the HP pipes, the lowest Mg# green clinopyroxene groups are considered to be xenocrysts. They have been rimmed by the cognate melt, but only at Mons Creek has a melt similar in composition to the xenocrysts also rimmed the cognate grains.

Golden Cluster Spinels

Twenty-seven grains, nine phenocrysts and eighteen groundmass spinels from the HP pipe were analysed. Eight phenocryst spinels were checked for zoning and found to be homogeneous except for one grain with a magnesium-rich core and iron-rich rim. Breccia and dike-phase spinels are neither optically nor chemically distinct from each other.

The HP spinels plot within the magnesiochromite quarter at the base of the spinel prism. They show some variation in chrome and aluminum and very little variation in iron and magnesium (Figure 1-4-5). Chrome contents range from 44.20 to 50.60 weight per cent Cr_2O_3 and titanium ranges from 0.57 to 1.18 weight per cent TiO_2.

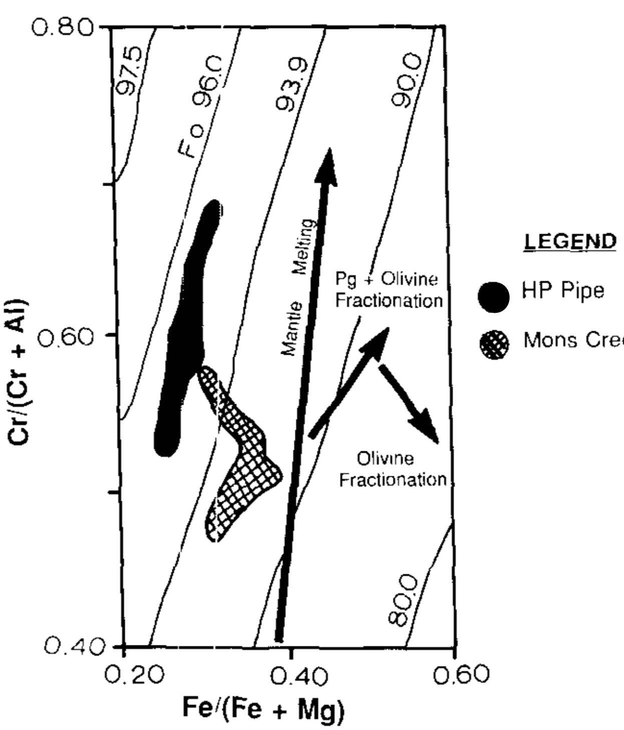

Figure 1-4-5. Comparison of HP and Mons Creek spinel compositional trends to the interpretations of Dick and Bullen (1984) for anhydrous mafic rocks.

Ten spinels, six phenocryst and four groundmass grains from Mons Creek were analysed and examined for zoning from core to rim. There are no consistent zoning patterns, although one grain has a high-chrome, low-aluminum core and another has a high-magnesium, low-iron core.

Mons Creek spinels fall predominantly within the magnesiochromite quarter at the base of the spinel prism, are homogeneous, except for two values, and show a modest variation in chrome and aluminum and in the iron/magnesium component (Figure 1-4-5). A bimodal distribution of Cr# is seen: a high-Cr# group (>0.54) has a negative correlation with Fe^{2+}#, and a low-Cr# group (<0.52) has a positive correlation with Fe^{2+}#. Chrome ranges from 36.52 to 45.12 weight per cent Cr_2O_3 with one sample measuring at 53.24 weight per cent Cr_2O_3. Titanium does not exceed 0.91 weight per cent TiO_2.

In the HP and Mons Creek pipes, the spinels are optically similar but have distinct chemical trends characteristic of each pipe. They are disseminated throughout the groundmass and are not intergrown with, or included within, other minerals.

The Golden cluster magnesiochromites differ from typical, ultramafic lamprophyre titanomagnetites (Rock, 1986; Bergman, 1987). However, they are closer in composition to the subset of ceylonites, chromites or magnesiochromites from specific, ultramafic lamprophyres, especially aillikites (Mitchell, 1983; Rock, 1986). The magnesiochromite spinels from lamprophyres of extreme composition, kimberlites and lamproites, also have some similarities to the Golden cluster magnesiochromites (Mitchell, 1985). Additionally, the Golden magnesiochromite values and trends resemble those from the nonhydrous, ultramafic, alpine-type peridotites (Irvine, 1967; Bergman, 1987). Either they crystallized from a hydrated, peridotitic mantle melt or are merely xenocryts from disaggregated peridotites.

For most spinels, there is a small increase in Fe^{2+}# accompanied by a larger increase in Cr#. A combination of Irvine's (1965) thermodynamic treatment and data from Jackson (1969), using the base of the spinel prism, shows some possible interpretations of these trends (Figure 1-4-5). Spinel chemical compositions in equilibrium with olivine forsterite content isopleths are shown. Proposed mechanisms are partial mantle melting characterized by a significant variation in Cr# and very little variation in Fe^{2+}#, (very steep slope), plagioclase plus olivine and fractionation (shallower slope), or olivine fractionation alone (shallow slope and an inverse relationship between Cr# and Fe^{2+}#).

High-chromium spinels are not usually found with high-iron, high-aluminum silicates but rather with high-magnesium silicates such as olivine (Dick and Bullen, 1984). When olivine and spinel fractionate, there is a decrease of magnesium and chrome in the melt and liquidus phases, resulting in a decrease in Mg# (increase in Fe^{2+}) and Cr# of the spinels. When plagioclase also fractionates, aluminum decreases in the melt and Cr# of the spinels goes up (Dick and Bullen, 1984). Allan *et al.* (1988) also concluded that coprecipitation of olivine and plagioclase causes the magma to increase in Fe^{2+} and decrease in aluminum in mid-ocean ridge basalts of the Lamont seamount chain, and thus the coprecipitating spinels will tend towards higher Cr#

and Fe^{2+}#. Haggerty (1979), on the other hand, concluded that higher pressure spinels in spinel lherzolites are more aluminous because chrome is preferentially incorporated into clinopyroxene and at lower pressure the spinels are more chromiferous because aluminum is incorporated into plagioclase. This implies some coprecipitation of spinels and clinopyroxenes.

If hydrous rocks, such as lamprophyres, allowed the coprecipitation of spinels and clinopyroxenes, the iron enrichment and chrome depletion would be similar to the olivine fractionation pattern as the magnesium-iron partitioning is similar in both olivines and clinopyroxenes. Chrome in the melt would also be sharply depleted by being incorporated into both the clinopyroxenes and spinels. Therefore an olivine-plus-spinel fractionating pattern might be indistinguishable from a clinopyroxene-plus-spinel fractionating pattern in a hydrous melt.

The compositional ranges of the Golden magnesiochromites are not extensive. Nevertheless, the chemical trends exhibited by each pipe are characteristic and indicative of various igneous processes. The slopes and directions of Cr# versus Fe^{2+}# plots among the magnesiochromites imply a number of different processes. The HP magnesiochromite trend is ambiguous. The steep slope, moderate variation in Cr# and increasing forsterite content of equilibrium olivines lies between the slope indicating increased partial melting of the mantle and the slope indicating fractionation (Figure 1-4-5). The variation in HP clinopyroxene chemistry suggests that a differentiating magma was incorporated into a more primitive batch, perhaps generated by an increase in mantle partial melting, just prior to ascent. Thus, the increase in the Cr# of the HP magnesiochromites might simply reflect an increase in partial melting of the mantle.

The HP clinopyroxene trends also suggest fractionation, but this is not clearly evident for the spinel trend, as shown in Figure 1-4-5. To test for evidence of fractionation among the HP spinels, it is necessary to look at other chemical parameters. If increasing Cr# is due to increased partial melting, then there should be no correlation with Ti# [(Ti/Ti+Cr+Al)] or Fe^{3+}# [$Fe^{3+}/(Fe^{3+}+Cr+Al)$]. Titanium contents might even be expected to decrease with increased mantle partial melting. Additionally, as increasing Fe^{3+}# implies increased oxygen fugacity and/or lower confining pressures, increased partial melting should yield uniform Fe3+#. But, Figures 1-4-6 and 1-4-7 and Table 1-4-3 show a clear positive correlation between Cr# and Ti# and a modest positive correlation between Cr# and Fe^{3+}#. Increasing both Ti# and Fe^{3+}# is consistent with fractionation. Titanium is an incompatible element and is incorporated into minerals during the latter stages of crystallization. The amount of Fe^{3+} also increases as crystallization proceeds. Therefore, the increases in Ti# and Fe^{3+} support the fractionation hypothesis among the HP magnesiochromites.

The Mons Creek magnesiochromite trend is bimodal (Figure 1-4-5). The lower Cr# lobe has both increasing Fe^{2+}# and Cr# which is consistent with an interpretation of an olivine-plus-plagioclase fractionation. The higher Cr# lobe shows decreasing Cr# with increasing Fe^{2+}# consistent with olivine fractionation. Plagioclase is found in the groundmass, and only rarely are olivines or olivine pseudomorphs found among the phenocryst phases at Mons Creek. The clinopyroxenes also show a bimodal chemical pattern, with either increasing or decreasing aluminum and titanium relative to Mg#, and zoning is either "normal" or "reverse". Thus both the magnesiochromites and clinopyroxenes suggest either two different processes or they are the result of two provenances with mixing of two initially separate magmas.

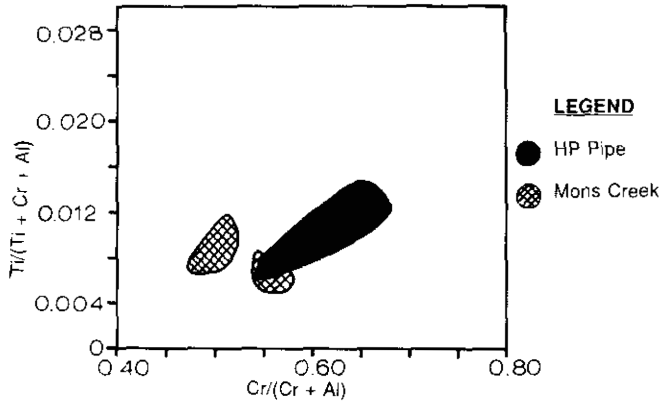

Figure 1-4-6. Plot of Cr# verus Ti# indicating a positive correlation for HP spinels and a negative correlation for Mons Creek high-Cr# spinels.

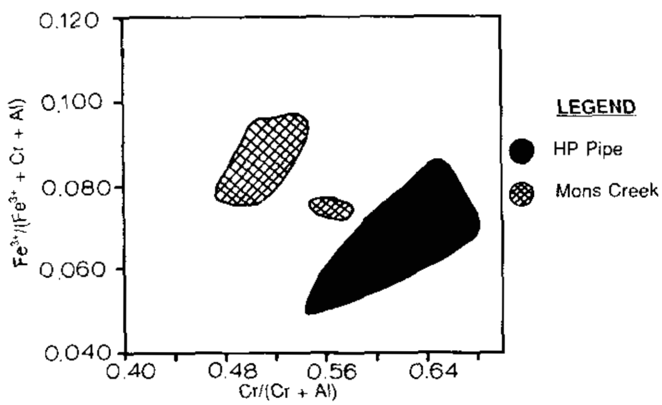

Figure 1-4-7. Plot of Cr# versus Fe^{3+}# indicating a positive correlation for the HP and Mons Creek low-Cr# spinels and a negative correlation for the high-Cr# spinels.

Other bimodal patterns exist among the Mons Creek magnesiochromites. In the Cr# versus Fe^{3+}# graph, a positive correlation is found at lower Cr# values and a negative correlation at higher Cr# values (Figure 1-4-7; Table 1-4-3). The positive correlation segments at lower Cr# suggest plagioclase-plus-olivine fractionation similar to the interpretation in Figure 1-4-5. The negative correlation segments at higher Cr# may reflect the olivine fractionation process similar to the interpretation in Figure 1-4-5. The higher Cr# magnesiochromites are in equilibrium with olivine of higher forsterite content. Possibly this group of magnesiochromites is the result of increased mantle melting followed by olivine fractionation. This lends support to the hypothesis of increased partial melting with increasing Cr#. Mixing of

TABLE 1-4-3
SPINEL CORRELATIONS

	Fe^{2+}# vs Cr#	Cr# vs Ti#	Cr# vs Fe^{3+}#	Fe^{2+}# vs Ti#
HP Pipe	0.68	0.69	0.42	0.24
Mons Creek high Cr	-0.91	-0.56	-0.53	0.47
low Cr	*0.59*	*0.21*	*0.37*	*0.39*

fractionated material with more primitive chrome and magnesium-rich material is consistent with the clinopyroxene trend for the Mons Creek pipe.

The Mons Creek high-Cr# spinels exhibit a negative correlation between Cr# and Ti#, also consistent with an increased mantle melting interpretation, while the low-Cr# lobe has a very low correlation with Ti#. Taking both lobes together indicates an overall negative correlation between Cr# and both Ti# and Fe^{3+}#. These trends are consistent with an increased mantle melting interpretation.

In summary, the chemical trends of the Mons Creek magnesiochromites exhibit both fractionation and increased mantle melting processes similar to the conclusions reached from the clinopyroxene chemical trends.

The chemical composition and trends of the Golden lamprophyre magnesiochromites are similar to those in ultramafic lamprophyres, lamproites and peridotites. Spinel compositions and trends do not unequivocally indicate their origins, as there is much variation within each rock type. The magnesiochromites may be merely disaggregations from a solid peridotitic rock or they may be crystallization products from a hydrated (metasomatized) peridotitic melt which formed the lamprophyre. In either case their chemical composition would be similar. Clear evidence of entrained xenoliths was not seen in thin section. The grains occur singly or rarely as inclusions in olivine pseudomorphs, are subhedral to rounded, and range from phenocryst to microphenocryst in size, all of which may be evidence of crystallization from a melt. Although compatible with a xenocrystic interpretation, the inferences drawn from spinel chemical trends are consistent with inferences drawn from cognate clinopyroxene trends: fractionation and increased mantle partial melting at the HP and Mons Creek pipes.

SUMMARY OF IGNEOUS PROCESSES

In the HP pipe, the combined chemical trends of the pyroxenes and spinels corroborate the idea that two processes are involved Fractionation is clearly indicated by the inverse relationship of Mg# versus Ti cations in high and intermediate-Mg# clinopyroxene trends and is supported by the spinel chemical trends of increasing Ti# and Fe^{3+}#. The subsequent influx of primitive magma, as a result of increased partial mantle melting prior to emplacement, is indicated by the reversely zoned clinopyroxenes and by the increased chrome contents of the spinels.

Mineral chemical data from the Mons Creek pipe are somewhat more complex. The Mons Creek clinopyroxenes have oscillatory zoning indicative of at least two magma pulses, fractionation and mixing involving both cognate and xenocrystic material. The spinel data also indicate a bimodal origin and two distinct fractionation patterns. Both the HP and the Mons Creek pipes incorporate high-iron clinopyroxene xenocrysts.

ACKNOWLEDGMENTS

The author wishes to thank Dan Hora and Jennifer Pell of *the British Columbia Geological Survey Branch for their* generous support over the years in terms of research funding, field guidance and consultation. Herb Helmstaedt of Queen's University has patiently supervised the wrapping up of the M.Sc. thesis from which this article is drawn. This project was partly funded by the 1985–1990 Canada/B.C. Mineral Development Agreement through a research grant to Queen's University. Queen's Graduate Fellowships are also gratefully acknowledged.

REFERENCES

Allan, J.F., Sack, R.O. and Batiza, R. (1988): Cr-rich Spinels as Petrogenetic Indicators: MORB-type Lavas from the Lamont Seamount Chain, Eastern Pacific; *American Mineralogist*, Volume 73, pages 741-753.

Barton, M. and Van Bergen, M.J. (1981): Green Clinopyroxenes and Associated Phases in a Potassium-rich Lava from the Leucite Hills, Wyoming; *Contributions to Mineralogy and Petrology*, Volume 77, pages 101-114.

Bergman, S.C. (1987): Lamproites and Other Potassium-rich Igneous Rocks: A Review of Their Occurrence, Mineralogy and Geochemistry; *in* Alkaline Igneous Rocks, Fitton, J.G. and Upton, B.C.J., Editors, *Geological Society*, Special Publication No. 30, pages 103-190.

Brooks, C. K. and Printzlau, I. (1978): Magma Mixing in Mafic Alkaline Volcanic Rocks: The Evidence from Relict Phenocryst Phases and Other Inclusions; *Journal of Volcanology and Geothermal Research*, Volume 4, pages 315-331.

Deer, W.A., Howie, R.A. and Zussman, J. (1962): Rock-forming Minerals, Volume 5, Nonsilicates; *Longmans Press*, London, 371 pages

Deer, W.A., Howie, R.A. and Zussman, J. (1966): An Introduction to the Rock Forming Minerals; *Longmans Press*, London, 528 pages.

Deer, W.A., Howie, R.A. and Zussman, J. (1978): Rock-forming Minerals: Volume 2A, Second Edition, Single-chain Silicates; *Longmans Press*, London, 668 pages.

Dick, H.J.B. and Bullen, T. (1984): Chromian Spinel as a Petrogenetic Indicator in Abyssal and Alpine-type Peridotites and Spatially Associated Lavas; *Contributions to Mineralogy and Petrology*, Volume 86 pages 54-76.

Eggler, D.H., McCallum, M.E. and Smith, C.B. (1979): Megacryst Assemblages in Kimberlite from Northern Colorado and Southern Wyoming: Petrology, Geothermometry-Barometry, and Areal Distribution; *in* The Mantle Sample: Inclusions in Kimberlites and Other Volcanics, Boyd, F.R. and Meyer H.O.A., Editors, Proceedings of the Second International Kimberlite Conference; *American Geophysical Union*, Washington, Volume 2, pages 213-226.

Grieve, D.A. (1981): Diatreme Breccias in the Southern Rocky Mountains; *in* Geological Fieldwork 1980, *B.C. Ministry of Energy, Mines and Petroleum Resources*, Paper 1981-1, pages 96-103.

Grieve, D.A. (1982): 1980 – Petrology and Chemistry of the Cross Kimberlite (82J/2); *in* Geology in British Columbia, 1977-1981, *B.C. Ministry of Energy, Mines and Petroleum Resources*, pages 34-41.

Gurney, J.J., Jakob, W.R.O. and Dawson, J.B. (1979): Megacrysts from the Monastery Kimberlite Pipe, South Africa; *in* The Mantle Sample: Inclusions in Kimberlites and Other Volcanics, Boyd, F.R. and Meyer, H.O.A., Editors, Proceedings of the Second International Kimberlite Conference; *American Geophysical Union*, Washington, Volume 2, pages 227-243.

Haggerty, S.E. (1979): Spinels in High Pressure Regimes; *in* The Mantle Sample: Inclusions in Kimberlites and Other Volcanics, Boyd, F.R. and Meyer, H.O.A., Editors, Proceedings of the Second International Kimberlite Conference; *American Geophysical Union*, Washington, Volume 2, pages 183-196.

Hall, D.C. (1991): A Petrological Investigation of the Cross Kimberlite Occurrence, Southeastern British Columbia, Canada; unpublished Ph.D. thesis, *Queen's University*, 536 pages.

Hall, D.C., Helmstaedt, H.H. and Schulze, D.J. (1989): The Cross Diatreme, British Columbia, Canada: A Kimberlite in a Young Orogenic Belt; *in* Kimberlites and Related Rocks, Volume 1, Their Composition, Occurrence, Origin and Emplacement, Ross, J., Editor, *Geological Society of Australia*, Special Publication 14, pages 97-108.

Helmstaedt, H.H., Mott, J.A., Hall, D.C., Schulze, D.J. and Dixon, J.M. (1988): Stratigraphic and Structural Setting of Intrusive Breccia Diatremes in the White River – Bull River Area, Southeastern British Columbia; *in* Geological Fieldwork 1987, *B.C. Ministry of Energy, Mines and Petroleum Resources*, Paper 1988-1, pages 363-368.

Ijewliw, O.J. (1986): Comparative Mineralogy of Three Ultramafic Diatremes in Southeastern British Columbia – Cross, Blackfoot and HP; unpublished B.Sc. thesis, *The University of British Columbia*, 61 pages.

Ijewliw, O.J. (1987): Comparative Mineralogy of Three Ultramafic Breccia Diatremes in Southeastern British Columbia, Cross, Blackfoot and HP; *in* Geological Fieldwork 1986, *B.C. Ministry of Energy, Mines and Petroleum Resources*, Paper 1987-1, pages 273-282.

Ijewliw, O.J. and Schulze, D.J. (1988): The HP Pipe, a Preliminary Report (82N/10); *in* Geological Fieldwork 1987, *B.C. Ministry of Energy, Mines and Petroleum Resources*, Paper 1988-1, pages 369-374.

Irvine, T.N. (1965): Chromian Spinel as a Petrogenetic Indicator, Part 1, Theory; *Canadian Journal of Earth Sciences*, Volume 2, pages 648-672.

Irvine, T.N. (1967): Chromian Spinel as a Petrogenetic Indicator, Part 2, Petrologic Applications; *Canadian Journal of Earth Sciences*, Volume 4, pages 71-103.

Jackson, E.D. (1969): Chemical Variation in Coexisting Chromite and Olivine in Chromitite Zones of the Stillwater Complex; *in* Magmatic Ore Deposits, Wilson, H.D.B., Editor, *Economic Geology*, Monograph 4, pages 41-47.

Leech, G.B. (1958): Fernie Map-area, West-half, British Columbia; *Geological Survey of Canada*, Paper 58-10, 40 pages.

Leech, G.B. (1964): Kananaskis Lakes (West-half) (82J W 1/2) Map Area; *Geological Survey of Canada*, Paper 64-1, 30 pages.

Leech, G.B. (1965): Kananaskis Lakes (West-half) (82J W 1/2) Map Area; *Geological Survey of Canada*, Paper 65-1, 77 pages.

Leech, G.B. (1979): Kananaskis Lakes Map-area; *Geological Survey of Canada*, Open File 634.

Mitchell, R.H. (1983): The Ile Bizard Intrusion, Montreal, Quebec – Kimberlite or Lamprophyre?: Discussion; *Canadian Journal of Earth Sciences*, Volume 20, pages 1493-1496.

Mitchell, R.H. (1985): A Review of the Mineralogy of Lamproites; *Geological Society of South Africa*, Transactions, Volume 88, pages 411-437.

Nixon, P.H. and Boyd, F.R. (1979): Garnet Bearing Lherzolites and Discrete Nodule Suites from the Malaita Alnoite, Solomon Islands, S.W. Pacific, and their Bearing on Oceanic Mantle Composition and Geotherm; *in* The Mantle Sample: Inclusions in Kimberlites and Other Volcanics, Boyd, F.R. and Meyer, H.O.A., Editors, Proceeedings of the Second International Kimberlite Conference, *American Geophysical Union*, Washington, Volume 2, pages 400-423.

O'Brien, H.E., Irving, A.J. and McCallum, I.S. (1988): Complex Zoning and Resorption of Phenocrysts in Mixed Potassic Mafic Magmas of the Highwood Mountains, Montana; *American Mineralogist*, Volume 73, pages 1007-1024.

Pell, J. (1986): Diatreme Breccias in British Columbia; *in* Geological Fieldwork 1985, *B.C. Ministry of Energy, Mines and Petroleum Resources*, Paper 1986-1, pages 243-253.

Pell, J. (1987a): Alkalic Ultrabasic Diatremes in British Columbia: Petrology, Geochronology and Tectonic Significance; *in* Geological Fieldwork 1986, *B.C. Ministry of Energy, Mines and Petroleum Resources*, Paper 1987-1, pages 259-272.

Pell, J. (1987b): Alkaline Ultrabasic Rocks in British Columbia: Carbonatites, Nepheline Syenites, Kimberlites, Ultramafic Lamprophyres and Related Rocks; *B.C. Ministry of Energy, Mines and Petroleum Resources*, Open File 1987-17, 109 pages.

Pe-Piper, G. (1984): Zoned Pyroxenes from Shoshonite Lavas of Lesbos, Greece: Inferences Concerning Shoshonite Petrogensis; *Journal of Petrology*, Volume 25, pages 453-472.

Pe-Piper, G. and Jansa, L.F. (1988): The Origin of Complex Mantling Relationships in Clinopyroxene from the New England Seamounts; *Canadian Mineralogist*, Volume 26, pages 109-116.

Rock, N.M.S. (1977): The Nature and Origin of Lamprophyres: Some Definitions, Distinctions and Derivations; *Earth Science Reviews*, Volume 13, pages 123-169.

Rock, N.M.S. (1984): Nature and Origin of Calcalkaline Lamprophyres: Minettes, Vogesites, Kersantites and Spessartites; *Royal Society of Edinburgh*, Transactions, Earth Sciences, Volume 74, pages 193-227.

Rock, N.M.S. (1986): The Nature and Origin of Ultramafic Lamprophyres: Alnoites and Allied Rocks; *Journal of Petrology*, Volume 27, pages 155-196.

Rock, N.M.S. (1987): The Nature and Origin of Lamprophyres: An Overview; *in* Alkaline Igneous Rocks, Fitton, J.G. and Upton, B.G.J., Editors, *Geological Society*, Special Publication No. 30, pages 191-226.

Rock, N.M.S. (1989): Kimberlites as Varieties of Lamprophyres: Implications for Geological Mapping, Petrological Research and Mineral Exploration; *in* Kimberlites and Related Rocks, Volume 1, Their Composition, Occurrence, Origin and Emplacement, Ross, J., Editor, *Geological Society of Australia*, Special Publication 14, pages 46-59.

Streckeisen, A. (1979): Classification and Nomenclature of Volcanic Rocks, Lamprophyres, Carbonatites, and Melilitic Rocks: Recommendations and Suggestions of the IUGS Subcommission on the Systematics of Igneous Rocks; *Geology*, Volume 7, pages 331-335.

Wass, S.Y. (1979): Multiple Origins of Clinopyroxenes in Alkali Basaltic Rocks; *Lithos*, Volume 12, pages 115-132.

NOTES

CASCADE RECREATION AREA, PRELIMINARY GEOLOGY AND MINERAL POTENTIAL (92H/2, 3, 6, 7)

By H.R. Schmitt and V.M. Koyanagi

KEYWORDS: Regional geology, Cascade Recreation Area, mineral potential, Methow basin, stratigraphy, intrusions, economic geology, Punchbowl Lake, Granite-Scheelite.

INTRODUCTION

Location And Access

The Cascade Recreation Area is located 30 kilometres southeast of Hope, in the Hozameen Ranges of the northern Cascade Mountains. The 167 square kilometre recreation area encompasses the headwaters of the Tulameen and Skaist rivers, and Snass Creek adjacent to the northwest boundary of E.C. Manning Provincial Park and the Skagit Valley Recreation Area (Figure 1-5-1).

Vehicle access to the southwest boundary is possible along Highway 3, to the north boundary via the Podunk Creek logging road into Whitecloud Creek and the upper Tulameen River, and along the east boundary via Whipsaw Creek and a seasonal four-wheel-drive road to Granite Mountain. In the recreation area a network of rehabilitated historic trails (Whatcom, Dewdney, Hope Pass) and former grazing trails provide excellent foot or horseback access along major valley bottoms. Valley Helicopters Ltd. in Hope provide the closest helicopter charter service.

Project Terms Of Reference

The field component of a two-year mineral potential study of the Cascade Recreation Area was completed in 1991. The study is required under Section 19 of the *Mineral Tenure Act* to provide government and industry with detailed mineral potential information, and to initiate the time-limited exploration period prior to Cabinet decision on proceeding to park status.

The objectives of fieldwork in 1991 were:

- To complete geological mapping of the entire recreation area at a scale of 1:20 000.
- To examine, map and sample all known mineral occurrences, and prospect for new occurrences.
- To augment the 1990 stream-sediment survey with additional samples from unsampled drainages.
- To establish lithologic, stratigraphic and structural controls on mineralization.

This initial report on 1991 fieldwork includes a preliminary geological map, generalized rock descriptions and initial lithogeochemical analyses. Results of 1990 fieldwork were reported by Schmitt and Stewart (1990). Full descriptions of mineral occurrences and interpretation of stream-sediment geochemistry will be presented in the final report which is scheduled for publication in spring, 1992.

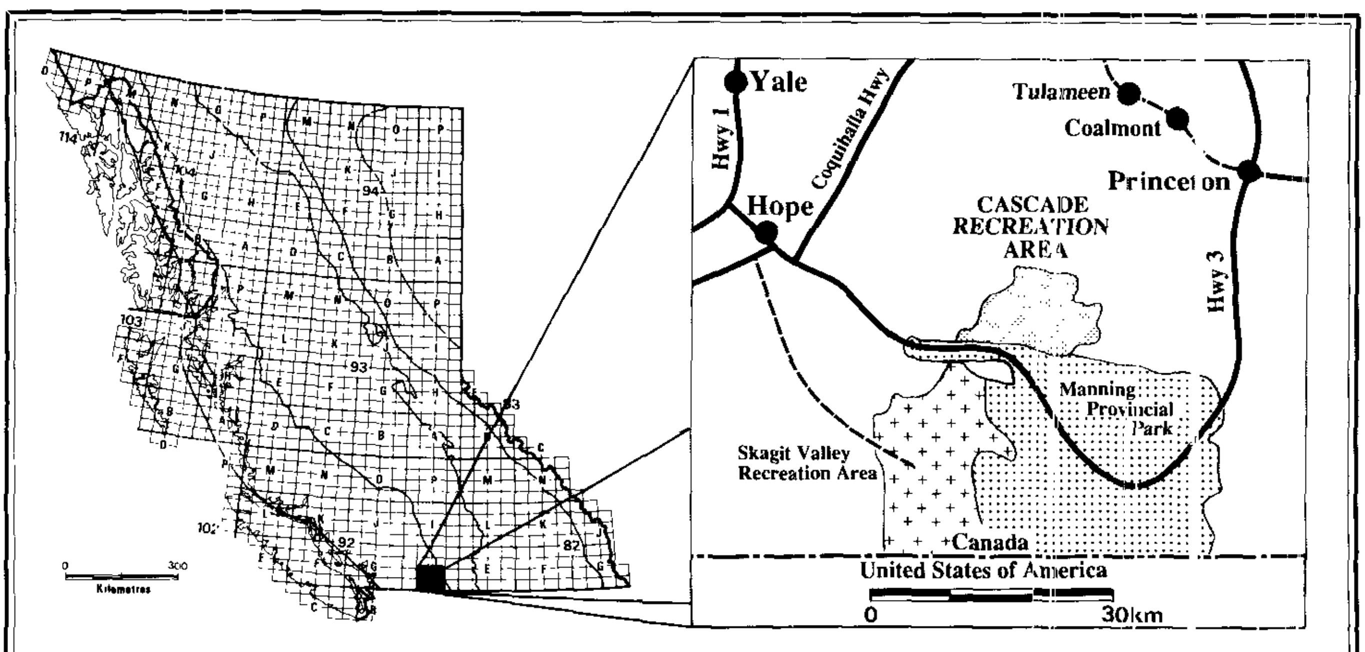

Figure 1-5-1. Location of Cascade Recreation Area, NTS 92H/2, 3, 6, and 7, in relation to Hope, Princeton, Manning Provincial Park and major transportation corridors.

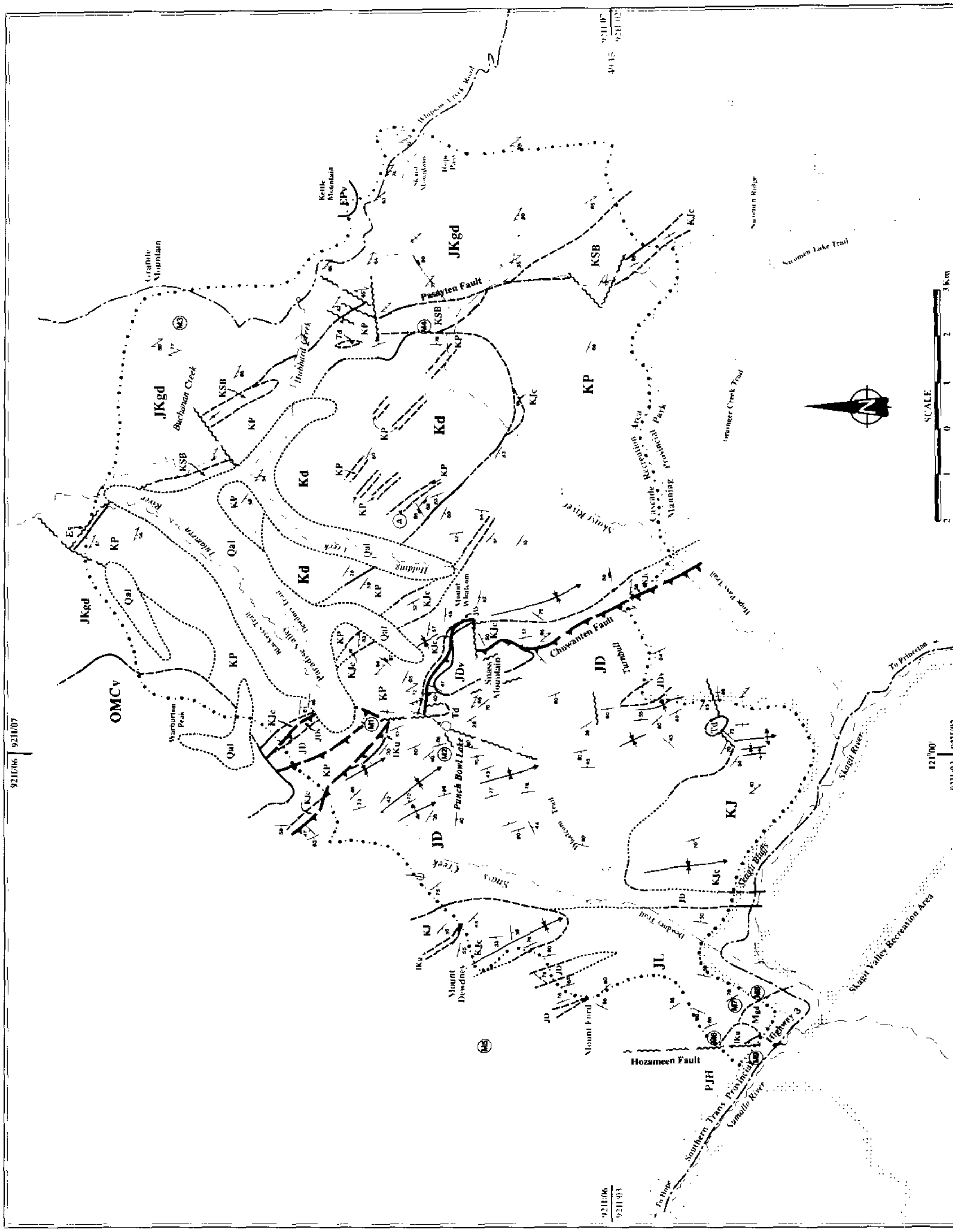

Figure 1-5-2. Geology and location of mineral occurrences in the Cascade Recreation Area, NTS 92H/2,3, 6, and 7.

LEGEND

LAYERED ROCKS

QUATERNARY

Qal	*UNCONSOLIDATED GLACIAL TILL AND POORLY SORTED ALLUVIUM*

LATE OLIGOCENE TO EARLY MIOCENE

COQUIHALLA VOLCANICS

OMCv	*HORNBLENDE ANDESITE, TRACHYTE, DACITE, BRECCIA, ASH FLOW TUFF*

EOCENE

PRINCETON GROUP

EPv	*MAFIC TO INTERMEDIATE DIKES AND FLOWS, CHARACTERISTICALLY COARSE HORNBLENDE PHYRIC*
Es	*PURPLE TO MAROON, QUARTZ-EYE LITHIC SANDSTONE*

LATE EARLY, EARLY LATE CRETACEOUS

PASAYTEN GROUP

KP	*QUARTZ MUSCOVITE ARKOSE, MINOR SILTSTONE AND CHERT PEBBLE CONGLOMERATE, NONMARINE FACIES EQUIVALENT TO THE UPPER PART OF THE JACKASS MOUNTAIN GROUP*

LATE EARLY CRETACEOUS

SPENCES BRIDGE GROUP

KSB	*INTERMEDIATE TO MAFIC, MAROON, PURPLE AND GREEN CRYSTAL-LAPILLI TUFFS AND FLOWS, VOLCANIC CONGLOMERATE, MINOR WACKE, SILTSTONE, SANDSTONE*

JACKASS MOUNTAIN GROUP

KJ	*UNDIFFERENTIATED SANDSTONE, ARGILLITE, CONGLOMERATE, (KJc) GRANITIC-COBBLE CONGLOMERATE*

EARLY AND MIDDLE JURASSIC

LADNER GROUP

JL	*ARGILLITE, SLATE, SILTSTONE, TYPICALLY RUSTY*

DEWDNEY CREEK FORMATION

JD	*LAPILLI CRYSTAL TUFF, MINOR FOSSIL BEARING TUFFACEOUS ARGILLITE, SILTSTONE, SANDSTONE, CONGLOMERATE, RARE LIMESTONE, (JDv) HYDROCLASTIC BRECCIA, VOLCANICLASTICS, FLOWS, AGGLOMERATES, (JDs) FOSSIL BEARING TUFFACEOUS ARGILLITE, WACKE, (JDt) CRYSTAL, LITHIC AND LAPILLI TUFF*

PERMIAN TO JURASSIC

HOZAMEEN GROUP

PJH	*UNDIFFERENTIATED CHERT, GREENSTONE, LIMESTONE*

INTRUSIVE ROCKS

TERTIARY

Td	*PLAGIOCLASE-HORNBLENDE-BIOTITE DIORITE, GRANODIORITE, APLITE*

MIOCENE

Mgd	*BIOTITE-HORNBLENDE GRANODIORITE (SUMALLO STOCK)*

LATE CRETACEOUS OR YOUNGER

lKu	*ULTRAMAFIC ROCK, GABBRO*

LATE CRETACEOUS

Kd	*PLAGIOCLASE-HORNBLENDE-BIOTITE PORPHYRITIC DIORITE (SKAIST RIVER STOCK)*

LATE JURASSIC AND EARLY CRETACEOUS

EAGLE PLUTONIC COMPLEX

JKgd	*FOLIATED GRANITE, GRANODIORITE, QUARTZ-BIOTITE GNEISS, PEGMATITE, AMPHIBOLITE*

SYMBOLS

Potassium-argon isotopic age locality	A
Mineral Showing or Prospect	M1
Cascade Recreation Area Boundary	
Manning Provincial Park Boundary - Skagit Valley Recreation Area Boundary	
Trail	
Road	

The Cascade Recreation Area was designated in 1987 to protect and manage heritage, wildlife and recreation values. A no-staking mineral reserve was placed over the area in 1987 as an interim measure until Cabinet provided further direction on mineral potential assessment and park designation. On September 3, 1991 the no-staking mineral reserve was removed, and the area became open to 1-post claim staking by application. Specific no-staking mineral reserves remain over parts of the Dewdney and Whatcom heritage trails and Punchbowl Lake basin

REGIONAL GEOLOGIC SETTING

The project area is located in the northern Cascade belt between the Coast Plutonic Complex to the west and the Intermontane Belt to the east. It is underlain mostly by the Methow basin containing Jurassic to Late Cretaceous sedimentary and volcanic rocks of the Ladner, Jackass and Pasayten groups deposited in a back-arc to nonmarine setting (Davis *et al.*, 1978; Anderson, 1976; Ray, 1990). The internal structure of the basin is dominated by northeast-directed thrusting of the Ladner Group onto younger rocks along the Chuwanten fault. The Methow basin is bounded on the west by the Hozameen fault which separates the basin from the Permian to Jurassic Hozameen Complex of the Bridge River Terrane, and on the east by the Pasayten fault which separates the basin from the Cretaceous Eagle Plutonic Complex of Quesnellia (Monger *et al.*, 1982; Monger, 1989; Greig, 1988; McGroder and Miller 1989; Whitney and McGroder, 1989). Eocene clastic rocks (Greig, 1988) and Oligocene to Miocene Coquihalla volcanic rocks (Berman and Armstrong, 1980) unconformably overlie the Methow basin, but are minor components of the project area.

Three periods of regional plutonism are tentatively recognized in the Cascade Recreation Area: Late Jurassic to late Early Cretaceous formation of the Eagle Plutonic Complex (Greig, 1988); Late Jurassic(?) to Early Tertiary emplacement of numerous mafic to felsic dikes, sills and stocks during crustal shortening, uplift, thrust faulting and folding; and Early Miocene intrusion of the dioritic Sumallo stock into the Hozameen fault (Armstrong *et al.*, 1987). Many of the dikes, sills and minor intrusions in the Ladner Group are of uncertain age, but probably post-Toarcian.

GEOLOGY OF THE RECREATION AREA

A preliminary geological map of the recreation area is shown in Figure 1-5-2. Seven lithostratigraphic units are recognized, including two previously unrecognized; a sandstone of presumed Eocene age (Greig, 1988; Monger, 1989), and a volcanic-epiclastic sequence tentatively assigned to the Cretaceous Spences Bridge Group. These two sequences occur along the west margin of the Eagle Plutonic Complex. In addition, a 20 square kilometre intrusion, named the Skaist River stock, was delineated in the east-central part of the recreation area. Isotopic dating of a hornblende separate is presently in progress. Detailed mapping has determined that both the Chuwanten and Pasayten faults are structurally complex with important implications for localizing intrusive activity and mineral potential. The following descriptions will be augmented by chemical. petrographic and paleontological analysis for the final mineral potential report.

Stratified Rocks

Stratified rocks range in age from Permian to Miocene. They generally strike northwest with moderate to steep southwest dips and, east of the Hozameen fault, record progressive infill and subsequent deformation of the Methow trough.

HOZAMEEN COMPLEX – UNIT PJH

The Permian to Jurassic Hozameen Complex is a deformed oceanic assemblage, which together with its northern faulted extension, the Bridge River Complex, comprise the Bridge River Terrane (Monger, 1970; Haugerud, 1985; Potter, 1986; Schiarizza *et al.*, 1989).

The Hozameen Complex underlies less than 100 hectares of the southwest corner of the recreation area, north of Highway 3. It consists of interlayered, massive light grey-buff to pinkish, black-streaked recrystallized chert, massive dark green hornblende-phyric greenstone and minor metasediments. Adjacent to the Hozameen fault these rocks are strongly deformed, commonly brecciated and have a prominent planar fabric oriented 160/75° west which parallels the strike of the fault. Pyrite is ubiquitous as narrow discontinuous stringers and disseminations in abundant fractures and small felsic segregations or dikes along the fault trace. Hozameen Complex rocks and the fault were intruded by the Early Miocene Sumallo stock but no obvious thermal overprinting is evident.

LADNER GROUP – UNITS JL, JD

Jurassic Ladner Group strata underlie most of the Snass Creek basin between the Hozameen and Chuwanten faults. They are the oldest sediments in the Methow basin (Ray, 1990) and are divisible in the recreation area into an Early Jurassic (Pliensbachian and Toarcian), marine clastic sequence (Unit JL), and an overlying Middle to Late Jurassic volcanic-rich sequence of the Dewdney Creek Formation (Unit JD). The contact between the two sequences is best exposed north of Mount Ford where it is represented by a gradual facies change from predominantly fine-grained turbiditic siltstones to tuffaceous sandstones and lapilli tuff interbedded with siltstones. This facies change marks the onset of Dewdney Creek Formation volcanic activity.

The Ladner Group distribution is currently shown on regional maps as two parallel, northwest-striking belts separated by a belt of Jackass Mountain Group sediments (Monger, 1989). New mapping information shows an uninterrupted stratigraphic interval of Ladner Group rocks, with the Jackass Mountain sediments in the northwest extension of the south-plunging Gibson Pass syncline. The syncline is completely eroded in its central part by Snass Creek, exposing the underlying Ladner Group. Further revisions to the distribution of Ladner Group rocks, and definitive recognition of the late Oxfordian to late Tithonian Thunder Lake sequence (Coates, 1974; O'Brien, 1986) may be possible with final age determinations of macrofossils collected from various localities. Ladner Group strata are thrust northeast onto both Jackass and Pasayten Group coarse to fine clastics along the Chuwanten fault.

Unit JL: Early Jurassic Ladner Group sediments crop out south of Mount Dewdney and west of Snass Creek where they comprise a section possibly 1500 metres thick that strikes north-northwest and dips 40° to 80° northeast. The easterly derived marine sediments were deposited as a west-facing prism of turbidites, submarine fan and related channel deposits (Ray, 1990). They consist of thinly laminated to medium-bedded, siliceous siltstones, slates, silty argillites, wackes and minor sandstones and chert-bearing grit to pebble conglomerates. Siliciclastic rocks fracture conchoidally and display slaty, bedding-parallel cleavage, or less commonly, well-developed pencil cleavage. The sediments range in colour from pale cream-buff to dark grey-brown with characteristic pale brown to gossanous weathering derived from ubiquitous oxidized, finely disseminated pyrite. Greenish and green-brown units with cherty and plagioclase-hornblende-phyric clasts predominate near the top of the sequence, marking progressive influx of Dewdney Creek Formation tuffaceous material.

Sedimentary structures include soft-sediment slumping, ripple marks, small-scale crossbedding and ball, pillow and flame features in thinly laminated silty units.

Regional deformation is manifest as well-developed foliation subparallel to bedding planes, and the presence of upright, tight to isoclinal folds, and local east-verging kink folds. Ladner sediments adjacent to the Hozameen fault and Sumallo stock exhibit intense small-scale folding and thermal metamorphism to quartz-biotite hornfels interbedded with a saccharoidal (re-crystallized?) cherty siltstone.

The presumed thickness of the Early Jurassic sequence is uncertain owing to few distinct marker units and the possibility of fold repetition. In the Coquihalla region Ray (1990) estimated the thickness of the Ladner Group to be 2000 metres, which is consistent with our observations in the recreation area.

A sequence of fine-grained clastic rocks with many lithological similarities to the Ladner Group Unit JL is exposed in a narrow belt in the hangingwall of the Chuwanten fault but is tentatively assigned to the Dewdney Creek Formation (Unit JDs below).

Dewdney Creek Formation – Units JD, JDs, JDt, JDv

The upper part of the Ladner Group is represented by the Toarcian to Bajocian Dewdney Creek Formation (O'Brien, 1986; Coates, 1974; Cairnes, 1924). The formation is characterized by epiclastic volcanic and volcanic-derived marine sediments, tuffs and breccia developed during tectonic uplift of the immature Methow basin (O'Brien, 1986).

Dewdney strata underlie the central Snass Creek and east Snass Creek basins, southwest of the Chuwanten fault, and have a possible accumulated thickness of over 2000 metres, even accounting for fold repetition. A small duplex thrust slice of Dewdney rocks also underlies an area northwest of lower Punchbowl Creek.

In the recreation area, the Dewdney Creek Formation is divisible into at least four members: a lower fossiliferous, locally pyritic clastic sequence (Unit JDs); a distinctive volcanic-rich unit (Unit JDv); a massive crystal, lithic and lapilli tuff (Unit JDt); and an upper sequence of turbiditic and tuffaceous clastics, tuffs, and rare carbonate (Unit JD). The division between Units JDt and JD is poorly defined and is distinguished largely by the relative frequency of certain lithologic units. Units JDt and JD are intruded by basic to felsic sills and dikes. Cairnes (1924) originally recognized three distinct crystal-lithic tuff divisions in the Dewdney Creek type section in Dewdney Creek, which was revised by O'Brien (1986) to include tuffaceous strata in the Manning Park area. The Cascade Recreation Area may contain the most complete section of Dewdney Creek Formation yet recognized, with extensive representatives of both sections described earlier by Cairnes and O'Brien. On Figure 1-5-2 contacts between Units JD, JDs and JDt are omitted for clarity.

Unit JDs: An intensely folded sequence of fossiliferous argillites, tuffaceous siltstones and wackes is exposed in a north-tapering belt immediately above the Chuwanten fault from Punchbowl basin southeast. These rocks are locally pyritic, pale brown-buff to dark grey argillites. The unit has many lithological and structural similarities with the Ladner Group Unit JL but its stratigraphic position is uncertain pending further dating of the ammonite and bivalve fauna. Its stratigraphic contact with the overlying Unit JDv is mostly conformable but locally is unconformable, or faulted (Plate 1-5-1).

Unit JDv: Unit JDv crops out immediately north, east and southeast of Snass Mountain, and as minor belts north of Punchbowl Creek and west of Turnbull Lake. The unit is characterized by massive-weathering, medium to coarse-textured andesitic hydroclastic breccia, epiclastic flows, agglomerate, plagioclase-hornblende-phyric flows and subvolcanic intrusions(?), crystal-lithic tuff, minor tuffaceous wacke and rare limestone. Plate 1-5-2 shows an example of an andesitic hydroclastic breccia unit from Mount Whatcom. These rocks show *in situ* fragmentation textures considered to be diagnostic of non-explosive injection into wet sediments (Hanson, 1991). The textural and contact relationships of the various lithologies indicate a complex marine depositional environment close to one or more volcanic vents. The contact relationship with underlying strata is variable and is locally an unconformity, a fault or a possible disconformity. It is apparent that Unit JDv behaved in a structurally competent manner during thrusting along the Chuwanten fault, relative to underlying fine-grained sediments of Unit JDs. The deformation contrast between these two units may have been instrumental in the location and propagation of the Chuwanten fault in Ladner stratigraphy. Similar lithologic and field relationships exist for the volcanic breccia unit described on Blackwall Peak in Manning Park (Coates, 1974; O'Brien, 1986).

Unit JDt: Medium to thick-bedded crystal-lithic lapilli and crystal tuff, minor volcanic-pebble conglomerate and tuffaceous wacke crop out as prominent cliffs in a belt extending 5 kilometres from the headwaters of Snass Creek to the ridges west and south of Turnbull Lake. The rocks are predominantly medium green and light grey-green with subordinate brown colours, and are characterized by small (mm to 1 cm) ovoid to subangular cherty and feldspar-porphyritic lapilli and fine-grained lithic clasts of volcanic and argillaceous material set in a cherty tuffaceous matrix of quartz, feldspar and chlorite. Conglomerate and gritty tuffaceous wacke interbeds may represent periods of relative volcanic quiescence when reworking of lapilli-bearing units occurred.

The member is similar to the lower and intermediate Dewdney Creek series of Cairnes (1924), and the Dewdney Creek Formation rocks described by Ray (1990) in the central Sowaqua Creek drainage. If these units are correlative, then collectively they would indicate widespread volcanic activity in the Middle to Late Jurassic Methow basin.

Unit JD: Undivided Dewdney Creek Formation, Unit JD, contains a diverse assemblage of sparsely fossiliferous, turbiditic, thinly laminated to medium-bedded tuffaceous siltstone, argillite and wacke interbedded with coarser lapilli and lithic tuffaceous sediments, and most of the units described in Unit JDt. Most rocks exhibit bedding-parallel cleavage and a penetrative foliation striking 160°. A range of colours are present, from light green-grey to buff, brown and black. The beds exhibit a wide array of sedimentary structures, mostly indicating stratigraphic tops are up. Deformation is manifest as gentle warping and broad, upright open folds, to tight isoclinal and disrupted chevron folds, local shearing and block faulting. Fold axes typically plunge southeast and are generally difficult to trace for more than 2 kilometres along strike. The unit is intruded by a variety of aplite, diorite and gabbro dikes and sills, typically less than 5 metres thick and rarely exposed for more than 20 metres along strike.

JACKASS MOUNTAIN GROUP – UNIT KJ

Early Cretaceous Jackass Mountain Group marine sediments were mapped in three belts: from Mount Dewdney, southeast to Skagit Bluffs along Highway 3; and as the southwest and northeast limbs of a southeast-plunging syncline (proposed name – Turnbull Creek syncline) including a belt 50 to 500 metres wide with a strike length of 7 kilometres in the footwall of the Chuwanten fault, and a belt 100 to 500 metres wide extending over 8 kilometres from Paradise Meadows to upper Skaist River (Figure 1-5-2). In the recreation area the group is divisible into two members: a sequence of thin to medium-bedded fine to medium-grained wackes, sandstone, arkose and argillaceous clastics, with minor conglomerate (Unit 8 of Coates, 1974), and a massive polymictic cobble conglomerate with minor intercalated sandstone and siltstone beds (Unit 9 of Coates, 1974).

The western exposures of Jackass Mountain Group comprise a southeast-plunging syncline (possible northwest extension of Gibson Pass syncline of Coates 1974) which has been completely eroded in its central part by the deep valley of Snass Creek. The sequence includes wacke, arkose, siltstone, argillite and massive, fine to coarse-grained conglomerate containing subrounded to well-rounded granitic, gneissic, volcanic, chert and argillaceous clasts. The stratigraphically lowest part of this sequence, exposed on the north slopes of Mount Dewdney and north of Skagit Bluffs, contains fossiliferous arkose, siltstone,

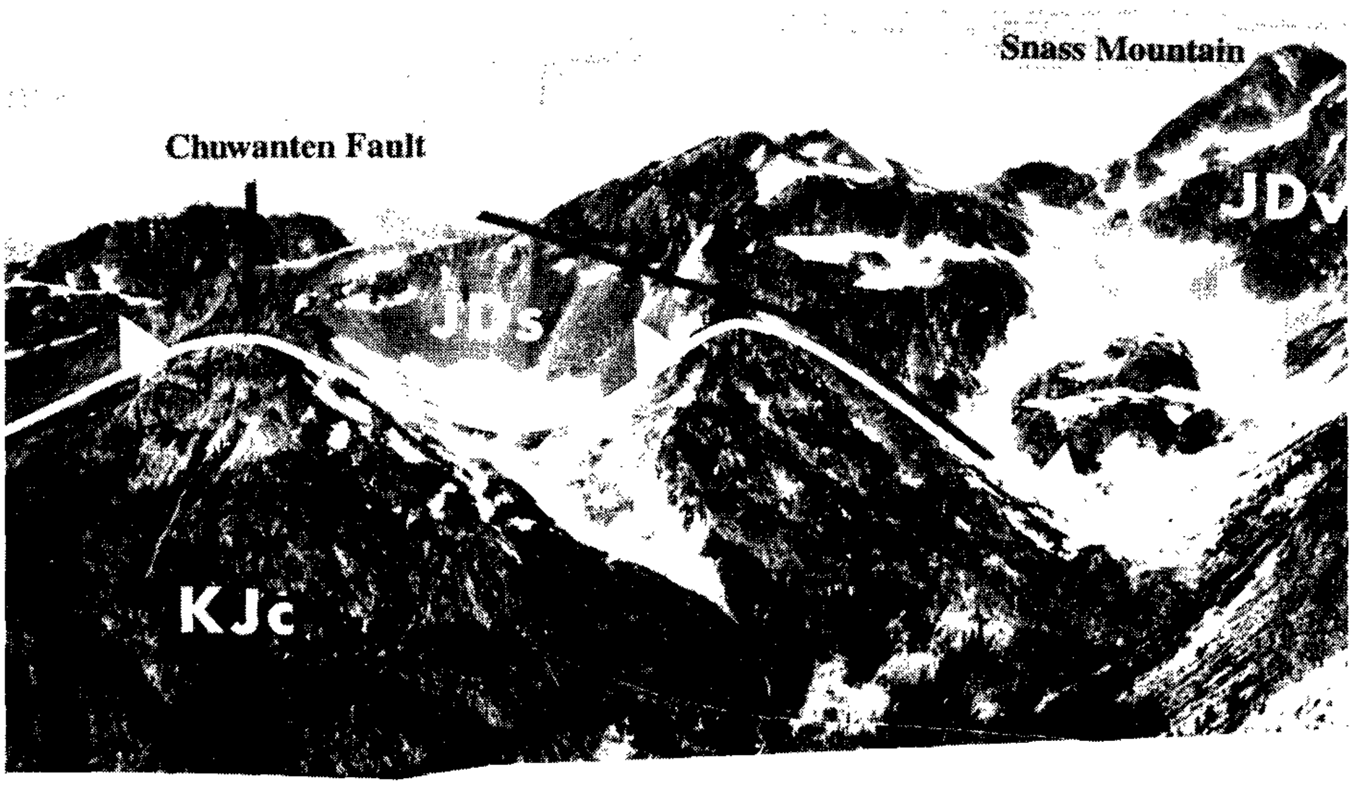

Plate 1-5-1. Photomosaic looking southwest at the Chuwanten fault; lower Dewdney Creek Formation Unit JDs and

argillite and rare limestone pods, and may be equivalent to the Dewdney Creek Formation of Coates (1974, Unit 3) and Thunder Lake sequence of O'Brien (1986) and Monger (1989). Age determinations of a sparse faunal collection from these rocks will hopefully help in stratigraphic interpretation.

Massive, granite-cobble conglomerate beds up to 100 metres thick are interbedded with minor sandstone, arkose and siltstone in the footwall of the Chuwanten fault. Plate 1-5-3 is an example of imbricate polymictic conglomerate from north of Snass Mountain. Similar conglomerates 1.7 kilometres to the southeast, contain locally abundant limestone clasts up to 30 centimetres across. A strongly sheared carbonate bed, 2 metres thick, is exposed in sheared polymictic conglomerate at possibly the same stratigraphic level, 1.5 kilometres northeast of Snass Mountain.

Jackass Mountain Group strata in the northeast limb of the Turnbull Creek syncline consist of polymictic conglomerate as above, but with volumetrically greater proportions of interbedded light green-brown sandstone, arkose and siltstone. The coarser strata exhibit abrupt facies changes indicative of channelized deposits. The beds are exposed intermittently for over 8 kilometres from Paradise Meadows to Skaist River. Their textural and lithological similarity, and stratigraphic position, may indicate time-stratigraphic equivalence with the adjacent nonmarine Pasayten Group sandstone and arkose (Coates, 1974). Unfortunately, most of the Jackass and Pasayten strata are characteristically unfossiliferous.

PASAYTEN GROUP - UNIT KP

The term Pasayten Group (Rice, 1947; Coates, 1974) has been used to describe predominantly nonmarine sandstones and siltstones of Albian age which overlie, and are partly time-stratigraphic equivalents of the upper Jackass Mountain Group. We recognize Pasayten Group rocks as a broad belt striking northwest and generally dipping moderately southwest, underlying the central and east-central parts of the recreation area.

Two broad divisions of the Pasayten Group are distinguishable. The lower sequence consists of predominantly thin to thick-bedded quartz-muscovite-biotite sandstone, arkose, siltstone and argillite, with minor wacke and tuffaceous beds. The upper sequence consists almost entirely of massive, light grey-buff, well-indurated quartz-muscovite-biotite sandstone with minor arkose, siltstone, and minor argillite and polymictic conglomerate. The lowermost, predominantly eastern member is equivalent to Coates' uppermost Jackass Mountain Group, Unit 10, whereas our uppermost member is correlative with Coates' entire Pasayten Group. Our definition parallels more recent usage (Monger, 1989) which restricts the Pasayten Group to areas east of the Chuwanten fault, and the Jackass Mountain Group to areas west of the fault.

SPENCES BRIDGE GROUP - UNIT KSB

A northwest-trending belt of previously unmapped volcanic and related epiclastic and sedimentary rocks, up to 1 kilometre wide, is exposed almost continuously over a

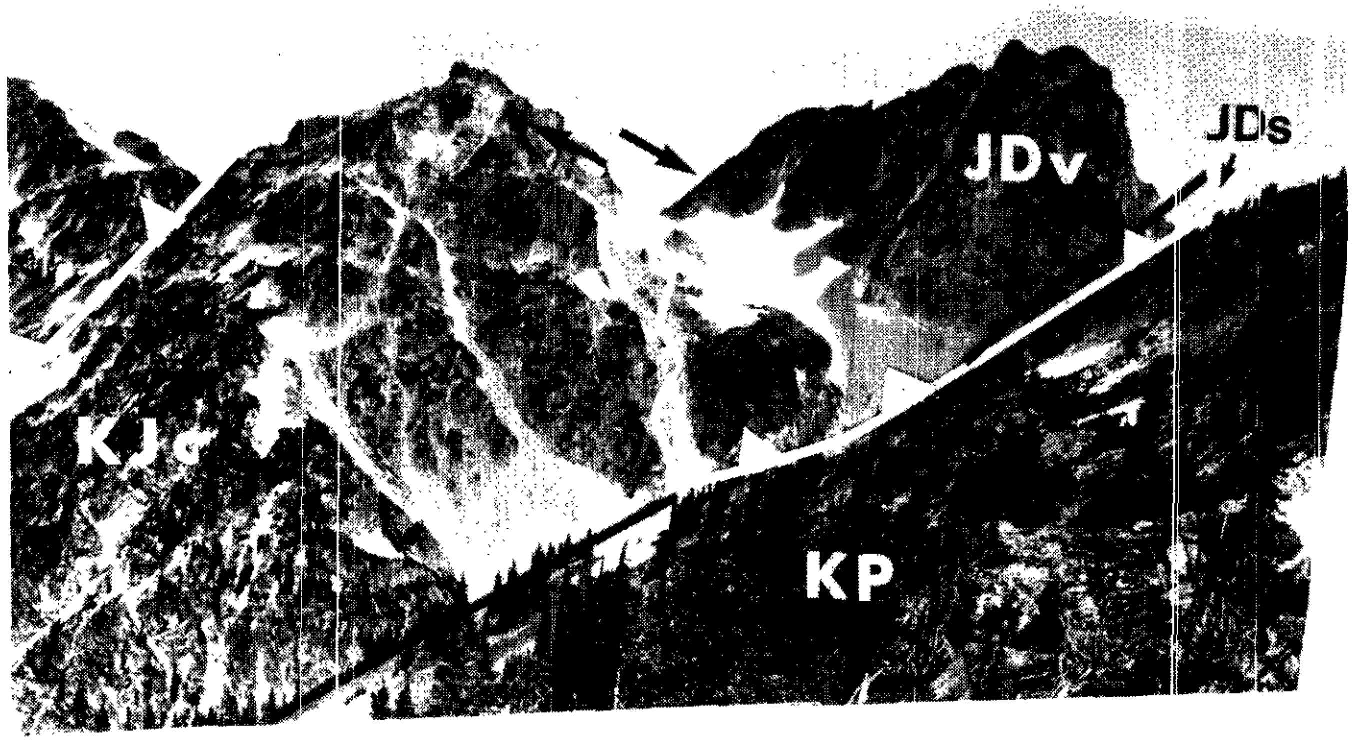

volcanic Unit JDv are thrust towards the viewer over Jackass Mountain Group massive cobble conglomerate, Unit KJc.

strike length of 11 kilometres along the west margin of the Eagle Plutonic Complex. The belt consists of green-brown and purple amygdaloidal basaltic(?) and dark green, crowded plagioclase-phyric flows, varicoloured green and maroon epiclastic units with angular to subrounded clasts up to 30 centimetres across, tuffaceous wacke, cherty tuff, argillite and minor basic intrusions. The volcanic flows exposed at the Manning Park boundary are weakly magnetic and contain numerous microfractures and shears with propylitic, quartz-chlorite-epidote alteration and minor veinlets. These rocks strike mostly northwest and have steep southwest dips, whereas north of the Skaist River north-south oriented beds dip steeply east, and north of Hubbard Creek, northwest-striking beds are near vertical. Beds may be locally overturned as evidence for stratigraphic tops is not equivocal.

The Pasayten fault marks the belt's eastern contact against the Eagle Plutonic Complex; evidence of intense shearing and quartz-sericite alteration along this contact is exposed 1.5 kilometres north of the Skaist River. The belt is apparently terminated by a northeast-trending Tertiary(?) fault south of Buchanan Creek. The contact between this unit and the Albian(?) sediments to the west is partly faulted in the south, but appears to be unconformable elsewhere. Exposures of wacke and volcanic sandstone along the west margin in the southern segment of the belt locally contain muscovite and biotite, whereas adjacent Albian(?) arkosic strata locally contain rare purple lithic fragments. The lithologic evidence implies at least some synchronous deposition of the two units.

The foregoing contact relationships and regional comparisons suggest a pre-Santoniar, post-Jurassic age. Immediately north of the Skaist River the volcanic unit is intruded by the early Late Cretaceous (Santonian?) Skaist River stock (Unit Kd, described below). By comparison with recent studies of Thorkelson and Rouse (1989), and McGroder (1989), we conclude that the unit most closely resembles the Pimainus Formation of the Albian Spences Bridge Group.

In the Cascade Recreation Area, Spences Bridge Group rocks were apparently deposited in a narrow, north-tapering structural depression marginal to the Eagle Plutonic Complex, possibly extending discontinuously southeast into Washington State (Monger, 1989; McGroder, 1989). These rocks provide intriguing new evidence for mid-Cretaceous volcanic activity west of the Mount Lytton – Eagle Plutonic Complex, possibly related to down-dropping along the Pasayten fault (Monger, 1989, marginal notes).

PRINCETON GROUP – UNITS Es; EPv

Limited exposures of Eocene Princeton Group occur immediately west of the Tulameen River, and on the peak of Kettle Mountain.

The northern exposure (Unit Es) consists of reddish to maroon, quartzose lithic sandstone about 100 metres thick, in fault contact with the Eagle Plutonic Complex. Similar rocks have been described and palynologically dated as Eocene at Vuich Creek, 15 kilometres to the northwest (Greig, 1988) and 60 kilometres to the north in the Pig Lake

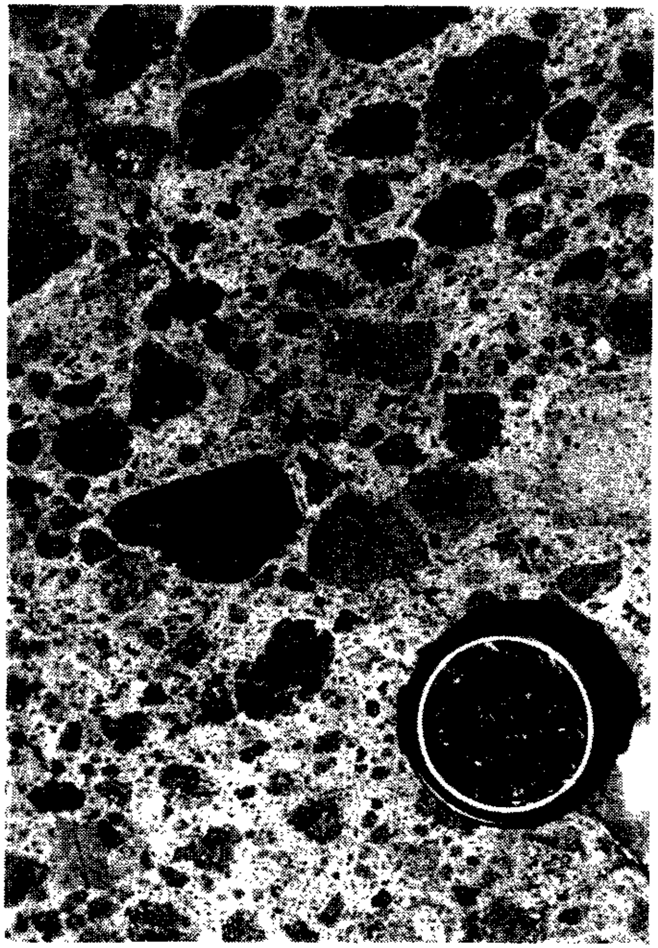

Plate 1-5-2. Dewdney Creek Formation andesitic hydroclastic breccia (Unit JDv) located above the Chuwanten fault 1.5 kilometres northeast of Snass Mountain. Fragmentation and resorption textures developed during non-explosive intrusion into marine sediments.

Plate 1-5-3. Jackass Mountain Group polymictic cobble conglomerate (Unit KJc) from 1 kilometre north of Snass Mountain, adjacent to dextral fault offsetting Chuwanten thrust fault (*see* Figure 1-5-2).

graben along the Coldwater fault system (Thorkelson, 1988).

Kettle Mountain is underlain by a prominent subcircular body of dark greenish black hornblende augite(?) basalt porphyry (Unit EPv). Columnar fracture patterns suggest that the rock was intruded into the surrounding Eagle plutonic rocks although a talus apron conceals the contact area. Intrusives of similar age were mapped by Preto (1972) in the Copper Mountain area, and small dikes of similar appearance occur in the headwaters of Buchanan Creek. The intrusive is an interesting physiographic feature, comprising a roche moutonnée covered by scattered glacial erratics of the Eagle Plutonic Complex.

COQUIHALLA VOLCANICS - UNIT OMCv

The north-central boundary of the recreation area, in the vicinity of Mount Warburton, is underlain by Oligocene to Miocene volcanics of the Coquihalla Volcanic Complex. The dominant rock type is a fresh, pale green-grey trachytic hornblende andesite that forms prominent, unstable cliffs and a large talus apron. The Coquihalla volcanics were investigated in detail by Berman and Armstrong (1980) who concluded that they are part of the Pemberton volcanic belt formed in response to subduction of the Juan de Fuca plate.

QUATERNARY DEPOSITS - UNIT QAL

Paradise Valley and the lower reaches of Holding and Hubbard creeks are infilled with unconsolidated glacial deposits of clay to cobble-sized material, and mantled by organic deposits. Partly stratified drumlinoid ice-contact deposits are found along the margins of these areas. Although not indicated on the geology map, the bottoms of other narrow valleys, such as the Skaist River and Snass Creek, are also filled with discontinuous deposits of similar material, locally mantled by distal parts of postglacial colluvium and talus aprons.

A thin veneer of locally derived glacial till, colluvium and immature soils covers most slopes and rounded ridge crests. Glacial erratics are widely deposited on all exposed ridges. The source of ultramafic erratics near Snass Mountain is thought to be the Tulameen Ultramafic Complex, indicating that a minimum 22 kilometres of southwest-directed ice transport has occurred.

Intrusive Rocks

Prior to this mapping project only two intrusive bodies and several dikes of uncertain age were indicated on published regional maps of the recreation area: the Miocene Sumallo stock, the Cretaceous Eagle Plutonic Complex, and the Lightning Creek intrusions (Cairnes, 1920, 1944; Rice, 1947; Monger, 1989). Exploration work in the Punchbowl Lake area had delineated small diorite bodies, and Monger (*1989; personal communication, 1990*) reported diorite dikes northeast of Snass Mountain for which he had determined an early Late Cretaceous date. This project has delineated: a large (20 square kilometres) diorite stock that intrudes the Pasayten Group sediments and is referred to as the Skaist River stock; several 50 to 100-hectare diorite plugs, and numerous gabbro, diorite and minor ultramafic and felsic dikes and sills.

EAGLE PLUTONIC COMPLEX – UNIT JKgd

The late Jurassic(?) to Cretaceous Eagle Plutonic Complex underlies the eastern part of the recreation area in a belt ranging from 1 to 3 kilometres wide, and forms the core of the Skaist, Kettle and Granite Mountain uplands. Its western boundary is in fault contact with Pasayten, Spences Bridge and Princeton groups along the Pasayten fault and later Tertiary faults.

Greig (1988) recognized three major units in the complex; muscovite granite, gneissic granodiorite and heterogeneous gneiss. In the recreation area, foliated hornblende biotite granodiorite and heterogeneous amphibolitic to granitic gneiss are the dominant units, however, in the Granite Mountain area, the proportions of pegmatite and muscovite granite increase. Foliations and planar fabrics strike mostly northwest with steep to moderate southwest dips, although in some sections dip reversals are numerous. Deformation is manifest as tight isoclinal and ptygmatic folding, boudinaging of quartz veins and pegmatites, and possibly mylonitization. In the Pasayten fault and related cross-faults, the plutonic rocks are present as well-developed quartz sericite schists. *North of the recreation area and immediately south* of Cunningham Creek, alongside the Podunk Creek road, Eagle plutonic rocks were forcefully intruded by the Coquihalla Volcanic Complex to form a breccia zone 500 metres wide. Angular fragments of Eagle complex up to 0.5 metre across, and smaller fragments of Cretaceous sediments, are preserved in a pinkish brown vitrophyric ash-rich *matrix displaying fiammé textures.*

SKAIST RIVER STOCK – UNIT Kd

A plagioclase-hornblende-biotite-porphyritic diorite stock (Plate 1-5-4) has been delineated between the northern bend of the Skaist River and the ridge east of Paradise Valley (Figure 1-5-2). The body is elliptical in outline, with a northwest elongation, and has a maximum width of 3.8 kilometres and maximum exposed length of 7 kilometres. Where the contact with enveloping sediments *is observed it is generally sharp and steeply dipping with* only minor hornfelsing or shearing apparent. Thin to medium-bedded Cretaceous sediments, up to 200 metres thick and traceable along strike for up to 2 kilometres, are preserved at high elevations in the central parts of the stock, and less commonly in the low-elevation exposures west of the Skaist River.

The stock exhibits considerable uniformity in internal structure, texture and composition. It is generally light grey-buff to light green-buff and contains equant to stubby lath-*shaped plagioclase and fresh to weakly chloritized* hornblende phenocrysts averaging 3 to 5 millimetres in length, and subhedral to euhedral 1 to 4-millimetre biotite in a fine-grained light olive-buff groundmass. The most common texture is a weakly trachytic crowded porphyry, with local gradations to less crowded and less trachytic varieties. Along its eastern margins, a possible weak zonation is discernible, with biotite phenocrysts increasing at the expense of hornblende.

The stock was sampled for isotopic dating of hornblende *and a separate has been prepared and submitted to* The University of British Columbia. Monger (1989) reported a Santonian age (85.7 Ma; K-Ar) for hornblende from a diorite "dike" which appears to have been collected along the south-central margin of the stock, close to where we collected our sample. Thus, intrusion may have occurred shortly after final deposition of the Albian Pasayten Group sediments during a period of crustal thickening resulting from northeast-directed thrusting (McGroder, 1989; Haugerud *et al.*, 1991). It is interesting to note that a lithologically similar dike dated at 84.8 Ma (Monger, 1989) is exposed in a roadcut 16 kilometres to the northwest, near Vuich Creek, suggesting that early Late Cretaceous magmatism in the northern Methow basin may be more widespread than previously recognized. Petrological and chemical analyses are in progress on these rocks.

Unit lKu: Diorite, gabbro and ultramafic dikes and sills intrude Jurassic and Early Cretaceous strata primarily in the western half of the study area. These are generally less than 5 metres wide but may extend for many tens of metres. Four *notable exceptions are described.*

Adjacent to the Hozameen fault a locally serpentinized, medium to coarse pyroxenitic gabbro with dimensions of 300 by 500 metres, is exposed as a fault-bounded(?) sliver which was tectonically emplaced, or intruded into the Ladner Group sediments. The rock is dark green-brown and contains clusters of radiating clinopyroxene and sporadic concentrations of pyrite and pyrrhotite. Its margins are variably sheared, serpentinized and silicified, however the actual contact with the Ladner Group was not observed.

Northwest of Punchbowl Creek a medium-grained hornblende gabbro sill, up to 20 metres thick and over 1 kilometre in length, intrudes Dewdney Creek Formation tuffaceous sediments in the hangingwall of the Chuwanten fault. The eastern end of the sill strikes into the Punchbowl Creek fault zone, whereas the northwest end crosses upper Snass Creek and may be related to a similar body which crops out 500 metres northwest of the recreation area boundary. Intrusion of the sill was accompanied by shearing, silicification and pyritization of surrounding sediments; traces of chalcopyrite were noted.

A hornblende gabbro dike 5 metres wide by over 50 metres long intrudes Jackass Mountain siltstone, argillite and sandstone 3 kilometres east of Skagit Bluffs. The western contact of the dike is weakly serpentinized adjacent to a

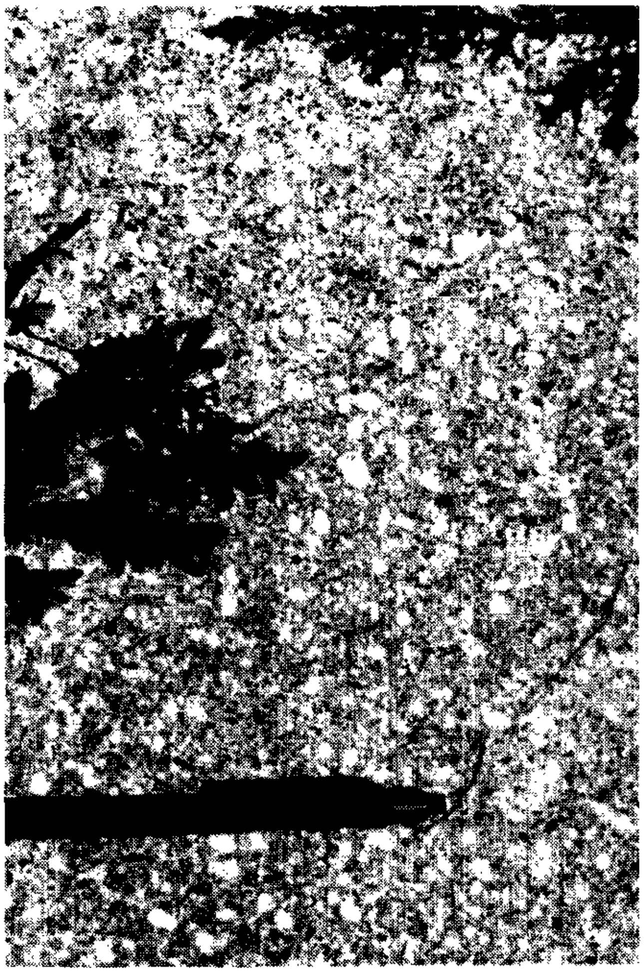

Plate 1-5-4. Skaist River stock plagioclase-hornblende-biotite diorite illustrating typical crowded porphyritic texture.

listwanitic zone of quartz-carbonate veining and brecciation 0.2 to 0.5 metre wide. Adjacent sediments are pyritic. The dike apparently intruded a minor fault zone which was active subsequent to intrusion and veining.

On the northeast slopes of Mount Dewdney several gabbroic to ultramafic sills have intruded Jackass Mountain Group sediments, causing sporadic pyritization. The largest sill is up to 50 metres thick and appears to extend for over 1 kilometre along strike, into the upper Sowaqua Creek drainage. It is dark greenish black and varies from fine to coarse grained, suggesting cumulate textures.

SUMALLO STOCK – UNIT Mgd

A massive hornblende biotite granodiorite stock, exposed over an area of 100 hectares, intrudes the Hozameen fault, Hozameen complex, Ladner Group and the ultramafic unit 1 kilometre north of the confluence of the Sumallo and Skagit rivers. The contact of the stock with most of these rocks is concealed although there is some evidence for sharp and irregular contacts with some diking and quartz veining. The stock was first dated by Coates (in Wanless *et al.*, 1967) who determined a 84 Ma age, but was recently redetermined by Armstrong *et al.* (1987) to be 19.9 to 22 Ma (Early Miocene). Several mineral occurrences are associated with the Sumallo stock.

OTHER INTERMEDIATE TO FELSIC INTRUSIONS – UNIT Td

Several small intrusive bodies of dioritic to granitic composition were mapped in the recreation area. These include: two hornblende diorite bodies adjacent to Punchbowl Lake; an equigranular hornblende granodiorite of unknown dimensions (possibly several hundred metres across) underlying the headwaters of east Snass Creek, and a smaller, but similar body on the ridge between lower Whatcom and Dewdney trails; and several prominent granodiorite to aplite dikes west of Snass Mountain and east of Mount Dewdney.

STRUCTURE

The dominant structural fabrics and elements of the recreation area trend northwest and reflect late Mesozoic, northeast tectonic convergence and crustal shortening. All stratified rocks, except for Unit OMCv, and most intrusive rocks, have northwest-trending planar foliations and lineations.

Folding is best developed in rocks west of the Chuwanten fault and typically occurs as northeast-verging upright to inclined isoclinal and chevron folds. Folding intensity increases adjacent to the fault. Two broad, shallow southeast-plunging synforms are developed in Cretaceous strata: the northwest extension of the Gibson Pass syncline (Coates, 1974) which underlies Mount Dewdney and the slopes northeast of Skagit Bluffs; and a similar feature, referred to as the Turnbull Creek syncline, that occurs northeast and parallel to the Chuwanten fault. Strongly deformed, gently south-dipping strata, including thin, boudined limestone beds in the nose of this syncline, were mapped 1.75 kilometres northeast of Snass Mountain.

The principal faults in the Cascade Recreation Area are the northwest-trending Hozameen, Chuwanten and Pasayten faults. East to northeast-striking Tertiary normal faults are found in many areas and may control the physiographic depressions drained by the Skaist and upper Tulameen rivers, and Snass Creek.

The Hozameen fault trends across the southwest corner of the recreation area where it separates Hozameen complex from Ladner Group sediments and is intruded by the Miocene Sumallo stock. The steep west-dipping fault is characterized by a zone of high strain and brecciation, and its development may have been accompanied by tectonic emplacement of the adjacent ultramafic body, analogous to the Coquihalla River area (Ray, 1990). Precise timing of the fault movement is uncertain, however, Ray concluded that its regional importance as a gold exploration target is related to a long period of recurrent movement, mainly during the Cretaceous.

The Chuwanten thrust fault strikes northwest through the central part of the recreation area. Along its length the Ladner Group is thrust northeast over Early Cretaceous Jackass Mountain and Pasayten Group sediments. Field evidence suggests that the fault propagated along a detachment zone defined by the brittle-ductile contrasts between thin-bedded argillaceous and massive volcanic units in the Ladner Group.

The thrust zone is complex as shown on Figure 1-5-2. It changes from a simple, steep southwest-dipping planar geometry in the southeast, to a segment of steep and north-east dips east of Snass Mountain, complicated by dextral shear along east-trending wrench faults. It eventually splays into a system of imbricate thrust sheets northwest of Paradise Valley. Deformation in the lower hangingwall of the thrust is manifest as tight east-verging to upright and partly overturned isoclinal drag folds, shearing, locally intense stretching and pencil lineations, and development of coplanar quartz and carbonate veins. The thrust has localized a number of intrusions including gabbro to diorite dikes and sills and the Punchbowl Lake area diorite. Pronounced quartz-pyrite alteration is present in sediments and intrusions adjacent to the thrust in the Punchbowl Creek area.

The fault is traceable for more than 80 kilometres south-east into Washington State where it becomes the Canyon Creek thrust fault and terminates in the Canyon Creek tear fault (McGroder, 1989). It is also traceable for over 75 kilometres northwest to Boston Bar, where it terminates in the Fraser fault system. The regionally significant Treasure Mountain lead-silver-zinc-copper-gold deposit occurs in a splay of the fault (Meyers and Hubner, 1989).

The third major fault in the recreation area is the Pasayten fault which places the Cretaceous Eagle Plutonic Complex against the Methow basin stratigraphy. The fault trace lies up to 1.5 kilometres northeast of its previously indicated position on regional maps (Monger, 1989). It is best exposed southeast of Hubbard Creek where pale buff to grey-green quartz sericite schists and stongly fractured, quartz-sericite-pyrite-carbonate-altered sediments characterize the fault zone. The Pasayten fault has been disrupted by east to northeast-trending Tertiary(?) faults.

GEOCHEMISTRY

Information on the distribution of trace elements in bed-rock and surficial materials is an integral component in determining prospective metallogenic environments. The geochemical sampling component of this mineral potential study included the following:

- Detailed drainage-sediment (moss mat and silt) and water geochemistry, with an average density of one sample per 1.5 square kilometres.
- Lithogeochemical sampling of known and newly located mineral occurrences, alteration and shear zones.
- Collection of representative rock types for major and trace element determinations.

The initial drainage-sediment sampling conducted under contract in 1990 resulted in collection of samples from 74 sites. Chemical analyses for the standard Regional Geochemical Survey (RGS) suite of trace elements were visually interpreted and assisted in guiding mapping and prospecting in 1991. In-fill sampling during mapping resulted in the collection of an additional 72 samples. Representative samples of mineralized and altered zones, and common lithologies, were collected during mapping, for chemical analysis and to assist with interpretation of the silt and moss-mat geochemical data. The final project report will include sample location maps, multi-element plots highlighting anomalous drainages and data interpretation

ECONOMIC GEOLOGY

The tectonostratigraphic setting of the Cascade Recreation Area contains metallogenic environments typical of deformed, convergent terrane margins. Mineral deposit types recognized include:

- Base and precious metal veins associated with regional and local faults.
- Gold-bearing base metal veins, disseminations and listwanite(?) associated with ultramafic and gabbro intrusions.
- Precious and/or base metal veins, disseminations and skarns associated with mafic to felsic intrusions.
- Polymetallic quartz veins in metamorphosed granitoids and supracrustals.
- Base metal sulphides in pyritic sediments.

Table 1-5-1 summarizes the mineral occurrences in the recreation area, and is based on field examination and literature review. A number of minor occurrences and zones of quartz-carbonate alteration, shearing and pyritization which are not documented in the table will be described in the final report. Three key areas of mineralization are described below.

PUNCHBOWL LAKE AREA (MINFILE 92HSW151, AND UNDOCUMENTED)

Mineralization in the Punchbowl Lake area was discovered by R. Rabbitt in 1984 and preliminary exploration was carried out until 1987 when the recreation area was designated and no further exploration permitted. Two areas of mineralization reported by Cardinal (1986a, b) and Kallock (1987) were geologically mapped and resampled (Figure 1-5-3). To date neither of these prospects has been geophysically surveyed or drilled.

The Punchbowl Creek occurrence (M1 – Figure 1-5-2) is located approximately 1 kilometre north of Punchbowl Lake and 500 metres south of Paradise Meadows where the creek has deeply incised the lower valley. The area is underlain by thin to medium-bedded Pasayten Group siltstones, argillite and arkose intruded by altered hornblende diorite dikes or plugs. There are few exposures of the intrusive(s) away from the creek so dimensions are uncertain. Structures are dominated by a zone of high strain parallel to the creek. It appears to have caused dextral offset of the main Chuwanten fault trace, and may be the terminus for a zone of imbricate thrust faulting to the northwest (see Figure 1-5-2). Sediments along the creek strike north with steep to vertical dips, compared to northwest strikes and moderate southwest dips away from the creek. Sediments are sheared, intensely fractured and pervasively silicified and pyritized for over 200 metres along the creek. Adjacent to the main intrusive body, bedding-parallel and crosscutting shears contain narrow, discontinuous quartz veins with variable amounts of pyrite and arsenopyrite, and trace amounts of chalcopyrite, sphalerite and galena. Trace element analyses of the samples plotted in Figure 1-5-3 indicate anomalous concentrations of gold, zinc, lead, copper, arsenic and tungsten (Table 1-5-2). Pyrite veinlets in silicified Unit KP contain up to 267 ppb gold, 0.1 per cent zinc, and 5200 ppm lead.

The Punchbowl Fault occurrence (M2 – Figure 1-5-2) is located 500 metres west of Punchbowl Lake on the ridge crest at the head of a prominent gully. The gully follows an east-trending fault which splays into several minor faults on the ridge, where it is intruded by two small, irregular shaped hornblende diorite plugs. The hostrocks are thin-bedded Dewdney Creek tuffaceous argillite, sandstone and lapilli tuff, which have been moderately hornfelsed and weakly pyritized up to several metres away from the diorite contact. A prominent northwest fault splay has localized a quartz-ankerite vein 30 centimetres wide which can be traced for 200 metres along strike. Trenching on the vein has exposed irregular blebs, streaks and disseminations of pyrite, chalcopyrite, galena, sphalerite and arsenopyrite. Samples plot-

TABLE 1-5-1
SUMMARY OF MINERAL OCCURRENCES IN THE CASCADE RECREATION AREA

MAP NO.	MINFILE NAME	COMMODITIES	REFERENCE	UTM Zn 10 EAST	UTM Zn 10 NORTH	DESCRIPTION
M1	Punch Bowl	Zn,Ag,Au,Pb,Cu	Schmitt and Stewart, 1991	646432	5461859	hornblende diorite intrudes Pasayten Group sediments; py, cpy, gn and sp occur as blebs and disseminations in qtz veins, shears and fractures.
M2	Punch Bowl Fault K.C.M.	Au,Ag,Cu,Pb,Zn	Schmitt and Stewart, 1991; Cardinal, 1985	645550	5460500	qtz veins are developed along the faulted contact between several diorite dikes and Dewdney Creek Formation fine-grained volcaniclastics; py, gn, cpy and sp occur in qtz veins and hornfelsed Dewdney Creek rocks.
M3	Granite Scheelite	Au,Ag,Cu,Zn,Pb	this report, Brown, 1980	654966	5467408	mineralized qtz occurs along the contact of qtz-albite-muscovite pegmatite and hornblende-biotite amphibolite in the Eagle Plutonic Complex; mineralization consists of disseminated py, gn, sp and cpy; assays returned elevated Au, Ag, Cu, Pb and Zn values.
M4	Skaist River	Cu	this report	654469	5461147	semimassive and disseminated py and cpy occur in sheared and altered Spences Bridge Group volcaniclastics near the contact with the Skaist River diorite stock.
M5	Ford	Au,Ag	Barde, 1984	639295	5459572	qtz veins up to 15 cm in width cut Hozameen Group sediments and return trace Ag, Au, Cu, Pb and Zn values.
M6	Forks	Ni	M.M. ANN RPT 1938	639585	5454512	a serpentinized ultramafic body intrudes Hozameen Group rocks east of the Hozameen fault; po is disseminated throughout; significant Ni values are reported.
M7	Dingo	Ag,Cu,Au,Mo	M.M. ANN RPT 1927	640446	5454101	a Miocene granodiorite stock intrudes Ladner Group sediments east of the Hozameen fault; small sheared zones within the intrusion contain mo and cpy mineralization; assays returned significant Ag and Cu values and trace Au.
M8	Silver Queen	Ag,Pb,Zn,Au,Cu	M.M. ANN RPT 1915	640559	5453641	Ladner sediments east of the Hozameen fault are intruded by a Miocene granodiorite stock; nodules and narrow stringers of gn, cpy, py and po in qtz are hosted by the intrusive; assays returned Au, Ag, Cu, Pb and Zn values.
M9	Mammoth	Ni,Ag,Au,Cu,W,Mo	EMPR Property Files	639266	5453546	a 15-metre-wide zone of altered limestone of the Hozameen Group near the Hozameen fault hosts disseminated po, py, aspy and cpy mineralization; a 0.9-metre calcsilicate vein hosts scheelite and po mineralization with minor amounts of sp, pyr and mo.

Abbreviations:

Ag - silver, ANN RPT - annual report, As - arsenic, aspy - arsenopyrite, A.R. - assessment report, Au - gold, cpy - chalcopyrite, Cu - copper, EMPR - Energy, Mines and Petroleum Resources, gn - galena, M.M. - Minister of Mines, mo - molybdenite, Mo - molybdenum, Ni - nickel, Pb - lead, po - pyrrhotite, py - pyrite, pyr - pyrolusite, qtz - quartz, sp - sphalerite, W - tungsten, Zn - zinc ted on Figure 1-5-3 are anomalous in base and precious metals (Table 1-5-2). The highest concentrations of metals occur in quartz veins in the fault splay. Hornfelsed sediments contain anomalous tungsten and slight enrichments in zinc. A recent assessment report documents a broad zone of anomalous zinc and arsenic in soils, suggesting the possible presence of additional mineralized structures (Kallock, 1987).

GRANITE SCHEELITE (MINFILE 92HSE101 – M3 FIGURE 1-5-2)

Gold-silver mineralization has been explored and evaluated at the Granite-Scheelite prospect intermittently since about 1942 (Stevenson, 1942; Brown, 1980). The mineralized vein system is well exposed for 175 metres along strike, in a series of trenches and an adit on upper Buchanan Creek. In 1969 Silver Tip Explorations Ltd. advanced an adit 50 metres along the vein system and conducted a milling test of 132 tonnes of ore, the results of which are unknown (*Geology, Exploration and Mining in British Columbia 1969*, p. 282). Detailed surface sampling of trenches and a five-hole drilling program were carried out by Long Lac Mineral Exploration Ltd. in 1980 to test the gold and silver potential of the vein system under option from Northern Lights Resources Ltd. (Brown, 1980). Long Lac relinquished the option after concluding that there was limited economic potential. Apart from limited interest in tungsten during the war years there is no record of base metal geochemical analyses from this property despite recognition of chalcopyrite, galena and sphalerite mineralization.

The prospect is underlain by chloritized hornblende, biotite and garnet-bearing amphibolites of the Eagle Plutonic Complex which have been intruded by one or more quartz-albite-muscovite pegmatite dikes, and later diabase dikes of possible Princeton Group affinity (Figure 1-5-4). A series of parallel and bifurcating mineralized quartz veins up to 1 metre wide are parallel to the contact zone of the pegmatite and amphibolite and locally offset by minor faults. The main vein system strikes 150° and dips steeply northeast. All rocks have undergone high strain, with development of schistose and fine-grained recrystallized equivalents.

Mineralization occurs as blebs, small lenses and disseminations of pyrite, galena, sphalerite and chalcopyrite, principally in the quartz veins but also disseminated in adjacent amphibolites and quartz-sericite schists. Sulphide concentrations are erratic along the strike length of the main vein system. Table 1-5-3 lists our preliminary analyses of selected vein samples. High gold values of 60 grams per tonne and silver values of nearly 2000 grams per tonne occur in narrow quartz veins carrying chalcopyrite, sphalerite and galena. Mineralization has an interesting polymetallic signature, including anomalous antimony, cadmium and bismuth, which may reflect a volcanic origin of the amphibolitic unit (Nelson *in* Brown, 1980) and offer new possibilities for regional exploration in similar amphibolitic units in the Eagle Plutonic Complex.

SKAIST RIVER

A previously undocumented mineral occurrence was found during mapping in 1991 along the southeast contact of the Skaist River stock, 500 metres north of the Skaist River (Figure 1-5-2, M4). The main stock and satellite dikes of hornblende biotite diorite intrude thin to medium-bedded tuffs and tuffaceous siltstone, wacke and argillite of the Cretaceous Spences Bridge Group. Mineralization consists of a sheared quartz vein 15 to 30 centimetres wide by 1.5 metres long with massive to banded pyrite and trace chalcopyrite. The exposure is on a steep, outcrop and talus-covered slope. Down slope, along strike, the volcaniclastics are pervasively hornfelsed and pyritized. From the air a weakly gossanous zone can be seen to extend to the east and up slope, suggesting potential for additional alteration and mineralization. Chemical analyses of mineralization are in progress.

SUMMARY

A two-year mineral-potential field study of the Cascade Recreation Area was completed in 1991. The 16 780 hectare recreation area was mapped at a scale of 1:20 000, prospected and geochemically sampled in order to provide a comprehensive mineral potential database for private industry and government decision makers. Publication of the final report and interpretation of this study, scheduled for early 1992, will initiate a further minimum 10 year exploration period in the recreation area. Exploration during this period will be jointly administered by the Ministries of Energy, Mines and Petroleum Resources and of Environment, Lands and Parks.

The Cascade Recreation Area is underlain by a thick succession of Mesozoic marine and nonmarine sedimentary and volcaniclastic rocks of the Methow basin between the Hozameen Complex (Bridge River Terrane) to the west and Eagle Plutonic Complex to the east. Accretionary tectonics and associated plutonism during the Late Jurassic and throughout the Cretaceous resulted in the development of a number of intrusion and structure-associated metallogenic environments. The area's mineral potential has been substantially upgraded through: delineation of the Skaist River stock; recognition of a belt of previously unmapped Spences Bridge Group volcanics and derived clastics; definition of the structural complexity and intrusive activity along the Chuwanten fault, mapping of mafic and ultramafic bodies along the Hozameen and Chuwanten faults and within Ladner Group sediments; and an improved geochemical database.

Potential for the following mineral deposit types is recognized: quartz-carbonate veins containing gold, silver, copper, lead and zinc, associated with regional (Hozameen, Chuwanten, Pasayten) and related minor faults, with mineralization hosted by various rock types; quartz veins, disseminations, and skarns containing a variety of base and precious metals associated with intrusive rocks ranging from diorite to pegmatite; and veins and disseminations of nickel and gold-bearing sulphides associated with gabbro and ultramafic rocks.

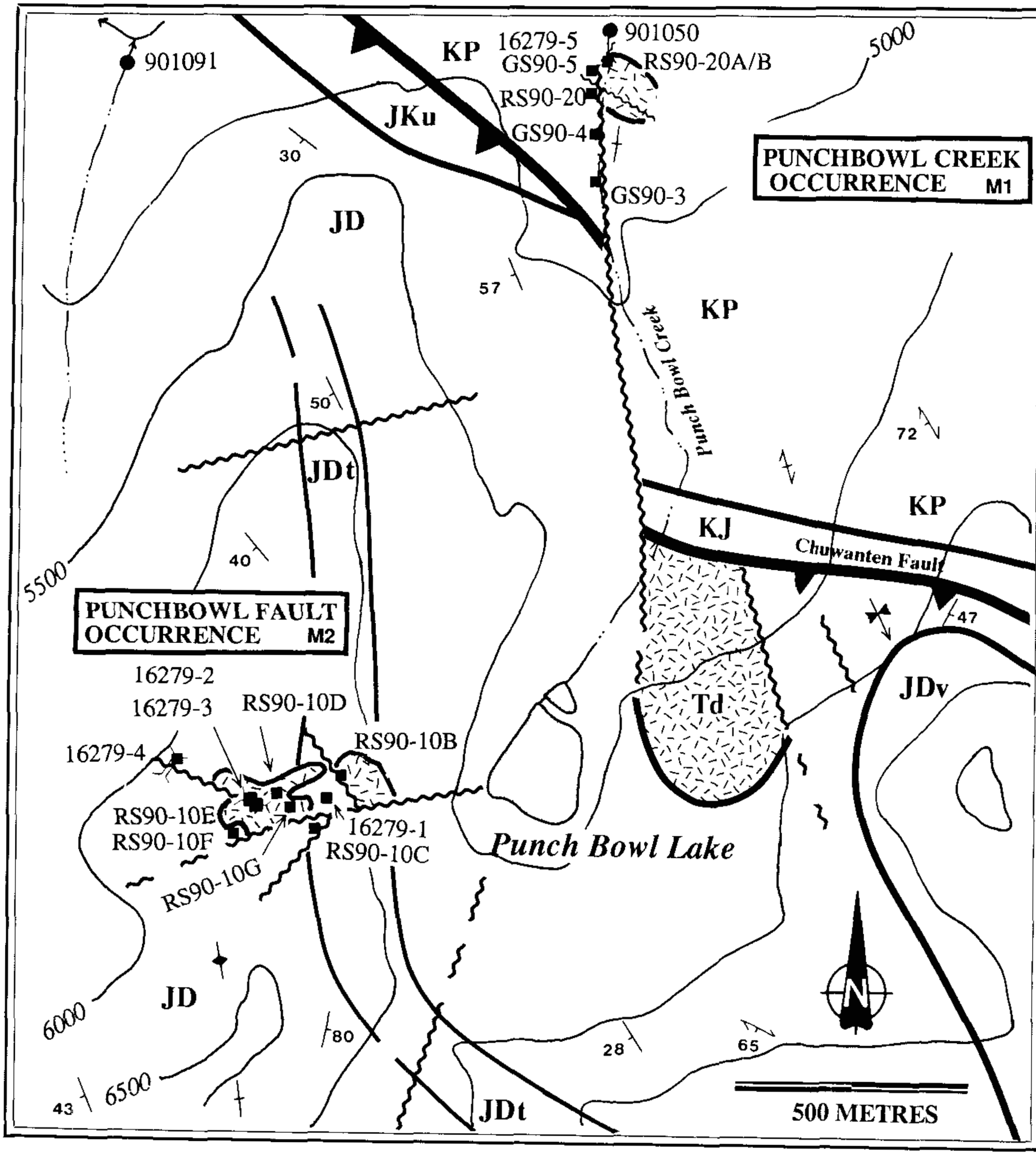

Figure 1-5-3. Geology, location and lithogeochemical sample sites at Punchbowl Creek and Punchbowl Fault occurrences (M1 and M2, Figure 1-5-2). Sample analyses and descriptions in Table 1-5-2.

ACKNOWLEDGMENTS

The writers gratefully acknowledge the contributions of the following individuals to this project: Paul Wilton and Rick Meyers for discussions on regional geology; the late Dr. Armstrong for drawing to our attention new isotopic ages for the Sumallo stock; Dr. Ray Lett for expediting chemical analyses; Dr. Howard Tipper for fossil age determinations; Fred, Carol, Pat and Ron of Valley Helicopters for exemplary service; Magnus Bratlein of Huldra Silver Inc. for permission to visit and sample Treasure Mountain; George Ralph and Manning Park staff of the Ministry of Environment, Lands and Parks for their support and cooperation during fieldwork; and Graeme McLaren and John Newell for timely manuscript reviews.

REFERENCES

Anderson, P. (1976): Oceanic Crust and Arc-trench Gap Tectonics in Southwestern British Columbia; *Geology*, Volume 4, pages 443-446.

Armstrong, R.L.A., Greig, C.J., Harakal, J. and Runkle, D. (1987): Isotopic Age Date for Sumallo Stock; Geochronology Files, *The University of British Columbia.*

Berman, R.G. and Armstrong, R.L.A. (1980): Geology of the Coquihalla Volcanic Complex, Southwestern British Columbia; *Canadian Journal of Earth Sciences*, Volume 17, pages 985-995.

Barde, B. (1984): Geological and Geochemical Report, Ford 1, 2, 3, 4, 5, and 6 Mineral Claims New Westminster Mining Division, NTS 92H/3W; *B.C. Ministry of Energy, Mines and Petroleum Resources*, Assessment Report 13270, 13 pages.

Brown, R.F. (1980): Long Lac Mineral Exploration Diamond Drilling Report, Gransil Claims I and II, Granite-Scheelite 1, Granite Mtn. Area, Similkameen Mining District, NTS 92H/7W; *B.C. Ministry of Energy, Mines and Petroleum Resources*, Assessment Report 8503, 25 pages.

TABLE 1-5-2
SELECTED TRACE ELEMENT ANALYSES OF PUNCHBOWL FAULT AND PUNCHBOWL CREEK MINERALIZATION

Sample Number	Au (ppb)	Ag	Cu	Pb	Zn	As	Sb	W	Ni
PUNCHBOWL FAULT OCCURRENCE:									
RS90C-10B	<5	<0.6	44	<3	51	65	1.0	2[illegible]0	140
RS90C-10C	<5	<0.6	59	3	122	8	2.2	[illegible]8	120
RS90C-10D	<5	<0.6	31	6	116	54	2.0	1[illegible]0	<50
RS90C-10E	624	406	440	970	0.36%	130	100	1[illegible]0	<50
RS90C-10F	<5	<0.6	34	<3	207	71	2.1	[illegible]6	<50
RS90C-10G	5	<0.6	76	6	88	14	0.6	[illegible]8	280
16279-1	5	1.2	54	73	165	53			
16279-2	215	>100	310	7200	770	1100			
16279-3	190	>100	118	1700	600	5700			
16279-4	10	0.2	35	9	206	73			
PUNCHBOWL CREEK OCCURRENCE:									
GS90-3	<5	<0.6	31	5	58	9	0.6	[illegible]2	<50
GS90-4	<5	<0.6	99	<3	58	4	0.4	[illegible]4	<50
GS90-5	267	4	60	43	420	1600	0.9	[illegible]0	<50
RS90C-20	19	2	94	35	136	14	1.3	110	<50
RS90C-50N	13	1	59	11	130	42	0.8	1[illegible]0	<50
RS90C-50NA	126	8	36	12	0.10%	310	4.5	[illegible]9	110
RS90C-50NB	14	2	28	11	169	45	1.4	[illegible]6	<50
RS90C-60N	5	0.6	2	<3	290	14	0.7	[illegible]0	63
16279-5	85	13	253	5200	>10,000	160			

All values in ppm unless otherwise indicated
Au, As, Ni, Sb and W determined by instrumental neutron activation analyses (INAA)
Ag, Cu, Pb and Zn determined by atomic absorption spectrometry (AAS)

Sample descriptions:

RS90C-10B; sheared Unit JDt at diorite contact
RS90C-10C; sheared Unit JDt with disseminated pyrite
RS90C-10D; hornfelsed tuffaceous siltstone Unit JD
RS90C-10E; sulphide-bearing quartz vein in fault zone
RS90C-10F; 10-metre chip sample pyritic hornfelsed Unit JDt
RS90C-10G; pyritic hornblende diorite Unit Td
GS90-3; pyritic silicified siltstones Unit KP
GS90-4; pyritic silicified siltstones Unit KP
GS90-5; pyrite veinlets in silicified siltstones Unit KP
RS90C-20; pyritic, propylitic altered diorite Unit Td
RS90C-50N; pyritic siltstones Unit KP
RS90C-50NA; pyrite vein in silicified siltstone Unit KP
RS90C-50NB; pyrite veins in silicified Unit KP
RS90C-60N; pyrite veins in silicified Unit KP

Samples reported in Kallock (1987):

16279-1; lapilli tuff Unit JDt
16279-2; quartz-galena float near fault
16279-3; mineralized quartz vein in fault zone
16279-4; quartz-limonite veinlets in Unit JDt, average of 4 samples across 10 metres
16279-5; pyrite veinlets in silicified Unit KP sediments

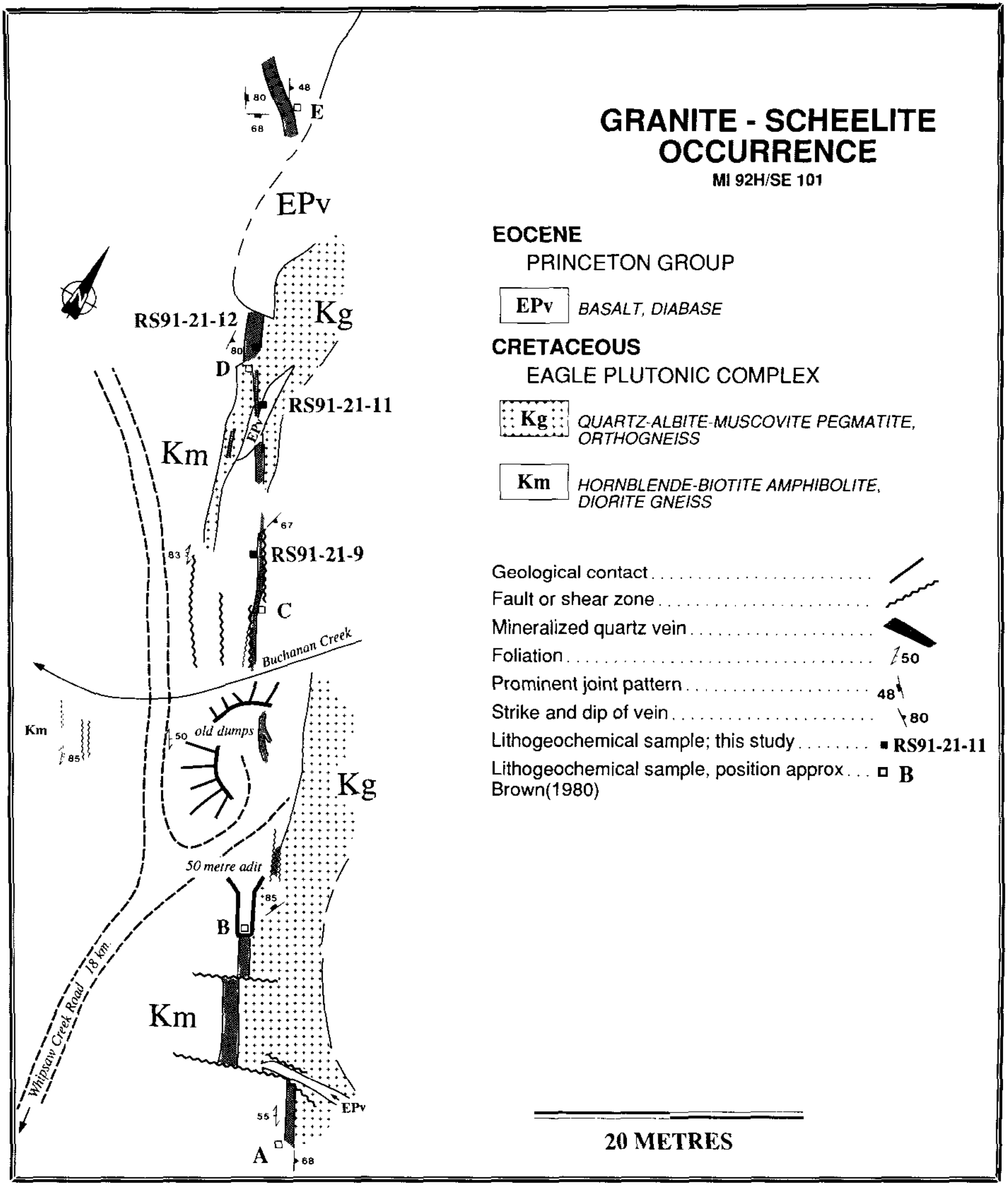

Figure 1-5-4. Geology and lithogeochemical sample sites at the Granite-Scheelite occurrence (MINFILE 92HSE101 and M3, Figure 1-5-2). Sample analyses and descriptions in Table 1-5-3.

Cairnes, C.E. (1920): Dewdney Trail between Beaver Lake and Nine-mile Creek; *Geological Survey of Canada*, Summary Report, Part A, pages 108A-123A.

Cairnes, C.E. (1924) Coquihalla Area, British Columbia; *Geological Survey of Canada*, Memoir 139, 187 pages.

Cairnes, C.E. (1944): Hope; *Geological Survey of Canada*, Map 737A, 1:253 440.

Cardinal, D.G. (1985): A Preliminary Geological Report on the K.C.M. Claim Group, Similkameen and New Westminster Mining Divisions, NTS 92H/6E, 7W; *B.C. Ministry of Energy, Mines and Petroleum Resources*, Assessment Report 14693, 14 pages.

Cardinal, D.G. (1986a): Reconnaissance Geochemical and Geological Assessment Report on the Punch Bowl Claim Group, Similkameen and New Westminster Mining Divisions, NTS 92H/6E, 7/W; *B.C. Ministry of Energy, Mines and Petroleum Resources*, Assessment Report 15146, 13 pages.

Cardinal, D.G. (1986b): Reconnaissance Geochemical and Geological Assessment Report on the K.C.M. Claim Group, Similkameen and New Westminster Mining Divisions, NTS 92H/6E, 7/W; *B.C. Ministry of Energy, Mines and Petroleum Resources*, Assessment Report 15212, 14 pages with maps.

Coates, J.A. (1974): Geology of the Manning Park Area, British Columbia; *Geological Survey of Canada*, Bulletin 238, 177 pages.

Davis, G.A., Monger, J.W.H. and Burchfield, B.C. (1978): Mesozoic Construction of the Cordilleran "Collage", Central British Columbia to Central California; *in* Mesozoic Paleogeography of the Western United States, Howell, D.G. and McDougall, K.A., Editors, *Society of Economic Paleontologists and Mineralogists, Pacific Section*, Pacific Coast Paleogeography Symposium 2, pages 1-32.

Greig, C.J. (1988): Geology and Geochronometry of the Eagle Plutonic Complex, Hope Map-area, Southwestern British Columbia; *in* Current Research, Part E, *Geological Survey of Canada*, Paper 88-1E, pages 177-183.

Hanson, R.E. (1991): Quenching and Hydroclastic Disruption of Andesitic to Rhyolitic Intrusions in a Submarine Island-arc Sequence, Northern Sierra Nevada, California; *Geological Society of America Bulletin*, Volume 103, pages 804-816.

Haugerud, R.A. (1985): Geology of the Hozameen Group and the Ross Lake Shear Zone, Maselpanik Area, North Cascades, Southwest British Columbia; *University of Washington*, unpublished Ph.D. thesis, 263 pages.

Haugerud, R.A., Van der Heyden, R., Tabor, R.W., Stacey, J.S. and Zartman, R.E. (1991): Late Cretaceous and Early Tertiary Plutonism and Deformation in the Skagit Gneiss Complex, North Cascade Region Washington and British Columbia; *Geological Society of America Bulletin*, Volume 103, pages 1297-1307.

TABLE 1-5-3
SELECTED TRACE ELEMENT ANALYSES OF GRANITE-SCHEELITE OCCURRENCE

Sample Number	Au (ppb)	Ag	Cu	Pb	Zn	As	Sb	W	Cd	Mo	Bi
RS91-21-9[a]	56 900	2000			7450	8	78	<4		<5	
RS91-21-9[b]		>100	5870	>10 000	6710			120	104	12	144
RS91-21-11[a]	112	10			463	29	2	9		130	
RS91-21-11[b]		6.2	833	50	382			10	1	155	2
RS91-21-12[a]	7850	56			19 600	6	3.8	<4		<5	
RS91-21-12[b]		60	3840	390	>10 000			30	246	3	50
A-A (0.46m)	16 930	464									
A-B (0.3m)	1440	9.9									
B-A (0.94m)	7130	146									
B-B (1.5m)	3290	37									
C-A (0.46m)	63 350	123									
C-B (1.22m)	5420	22.5									
D-A (0.76m)	19 680	107									
D-B (1.07m)	2060	45									
E-A (0.76m)	25 780	111									
E-B (0.9m)	3570	42.5									

All values in ppm unless otherwise indicated

[a] analyses by instrumental neutron activation (INAA)

[b] analyses by inductively coupled plasma emission spectroscopy (ICP) following total digestion

Sample descriptions:

RS91-21-9; 15 cm quartz vein with galena, chalcopyrite and pyrite

RS91-21-11; sheared pyritic amphibolite adjacent to quartz vein

RS91-21-12; 0.6 m wide quartz vein with sphalerite, pyrite, chalcopyrite and minor galena

Samples collected by Phendler, 1979 (A series) and Hogan, 1980 (B series) as reported in Brown (1980, Assessment Report 8503)
Sample locations approximately the same, analytical method not reported.

A; mineralized quartz in shear zone
B; mineralized quartz vein in adit face
C; mineralized quartz veins in trenches
D; quartz veins in trench
E; quartz vein in exposed face, north end of vein

Kallock, P. (1987): Geological and Geochemical Investigations, Punch West, Puch East, K.C.M. West and K.C.M. East Mineral Claims, Snass Creek – Tulameen River Area, Hope, B.C., Similkameen and New Westminster Mining Divisions, NTS 92H/6E 7W; *B.C. Ministry of Energy, Mines and Petroleum Resources,* Assessment Report 16279, 14 pages.

McGroder, M.F. (1989): Structural Geometry and Kinematic Evolution of the Eastern Cascades Fold-belt, Washington and British Columbia; *Canadian Journal of Earth Sciences,* Volume 26, pages 1586-1602.

McGroder, M.F. and Miller, R.B. (1989): Geology of the Eastern North Cascades; *in* Geologic Guidebook for Washington and Adjacent Areas, N.L. Joseph *et al.*, Editors, *Washington Division of Geology and Earth Resources,* Information Circular 86, pages 97-118.

Meyers, R.E. and Hubner, T.B. (1990): Preliminary Geology of the Treasure Mountain Silver-Lead-Zinc Vein Deposit; *in* Exploration in British Columbia 1989, *B.C. Ministry of Energy, Mines and Petroleum Resources,* pages 95-103.

Monger, J.W.H. (1970): Hope Map-area, West-half, British Columbia; *Geological Survey of Canada,* Paper 69-47, 75 pages.

Monger, J.W.H. (1989): Geology, Hope, British Columbia; *Geological Survey of Canada,* Map 41-1989, 1:250 000, Sheet 1 to 4 and accompanying notes.

Monger, J.W.H., Price, R.A. and Templeman-Kluit, D.J. (1982): Tectonic Accretion and the Origin of the Two Major Metamorphic and Plutonic Welts in the Canadian Cordillera; *Geology,* Volume 10, pages 70-75.

O'Brien, J. (1986): Jurassic Stratigraphy of the Methow Trough, Southwestern British Columbia; *in* Current Research. Part B, *Geological Survey of Canada,* Paper 86-1B, pages 749-756.

Potter, C.J. (1986): Origin, Accretion, and Post-accretionary Evolution of the Bridge River Terrane, Southwestern British Columbia; *Tectonics,* Volume 5, pages 1027-1041.

Preto, V.A. (1972): Geology of Copper Mountain; *B.C. Ministry of Energy, Mines and Petroleum Resources,* Bulletin 59, 87 pages plus plates and maps.

Ray, G.E. (1990): The Geology and Mineralization of the Coquihalla Gold Belt and Hozameen Fault System, Southwestern British Columbia; *B.C. Ministry of Energy, Mines and Petroleum Resources,* Bulletin 79, 97 pages plus maps.

Rice, H.M.A. (1947): Geology and Mineral Deposits of the Princeton Map-area, British Columbia; *Geological Survey of Canada,* Memoir 243, 136 pages.

Schiarizza, P., Gaba, R.G., Glover, J.K. and Garver, J.I. (1989): Geology and Mineral Occurrences of the Tyaughton Creek Area (92O/2, 92J/15, 16); *in* Geological Fieldwork 1988, *B.C. Ministry of Energy, Mines and Petroleum Resources,* Paper 1989-1, pages 115-130.

Schmitt, H.R. and Stewart, G.G. (1990): Preliminary Geology and Mineral Potential of the Cascade Recreation Area, (92H/2, 3, 6, 7); *in* Geological Fieldwork 1990, *B.C. Ministry of Energy, Mines and Petroleum Resources,* Paper 1991-1, pages 47-55.

Stevenson, J.S. (1942): Tungsten Deposits of British Columbia; *B.C. Ministry of Energy, Mines and Petroleum Resources,* Bulletin 10, page 116.

Thorkelson, D.J. (1988): Eocene Sedimentation and Volcanism in the Fig Lake Graben, Southwestern British Columbia; *Canadian Journal of Earth Sciences,* Volume 26, pages 1368-1373.

Thorkelson, D.J. and Rouse, G.E. (1989): Revised Stratigraphic Nomenclature and Age Determinations for Mid-Cretaceous Volcanic Rocks in Southwestern British Columbia; *Canadian Journal of Earth Sciences,* Volume 26, pages 2016-2031.

Wanless, R.K., Stevens, R.D., Lachance, G.R. and Edmonds, C.M. (1967): Age Determinations and Geological Studies, K-Ar Isotopic Ages, Report 7; *Geological Survey of Canada,* Paper 66-17.

Whitney, D.L. and McGroder, M.F. (1989): Cretaceous Crustal Section through the Proposed Insular-Intermontane Suture, North Cascades, Washington; *Geology,* Volume 17, pages 555-558.

KAKWA RECREATION AREA: NORTHEASTERN BRITISH COLUMBIA GEOLOGY AND RESOURCE POTENTIAL (93H/15, 16, 93I/1, 2)

By J. Pell, J.L. Hammack, B. Fletcher and W.D. Harris
Geological Consultants

KEYWORDS: Regional geology, Kakwa Recreation Area, resource assessment, stratigraphy, coal, dimension stone, phosphate, lead-zinc, barite, mineral potential.

INTRODUCTION

The Kakwa Recreation Area encompasses approximately 128 000 hectares (1280 km^2) of wilderness land immediately west of the Alberta border and approximately 70 kilometres north of the town of McBride, British Columbia, at latitude 54°00′ north, longitude 120°20′ west (Figure 1-6-1). It is the northernmost part of a contiguous, northwest-trending belt of parks and wilderness areas that includes Yoho National Park and Mount Robson Provincial Park in British Columbia, and Banff and Jasper National Parks and Willmore Wilderness Area in Alberta. The area is quite remote and access is generally on horseback, on foot, or by helicopter or float plane. An old logging road, along the McGregor River valley, leads to the southern and western edge of the recreation area and an extension leads into the area; however, wash-outs along this road have made it impassable to vehicles. Trails suitable for dirt bikes and all-terrain vehicles lead into the northeastern part of the area from Sherman Meadows, in Alberta.

Relief in Kakwa is considerable, with elevations ranging from less than 915 metres (3000 feet) in the Jarvis Creek valley, along the western edge of the area, to over 3050 metres (10 000 feet) at Mount Ida (3190 m) and Mount Sir Alexander (3275 m). Much of the terrain is very steep and cliffs are common. There are large icefield near Mount

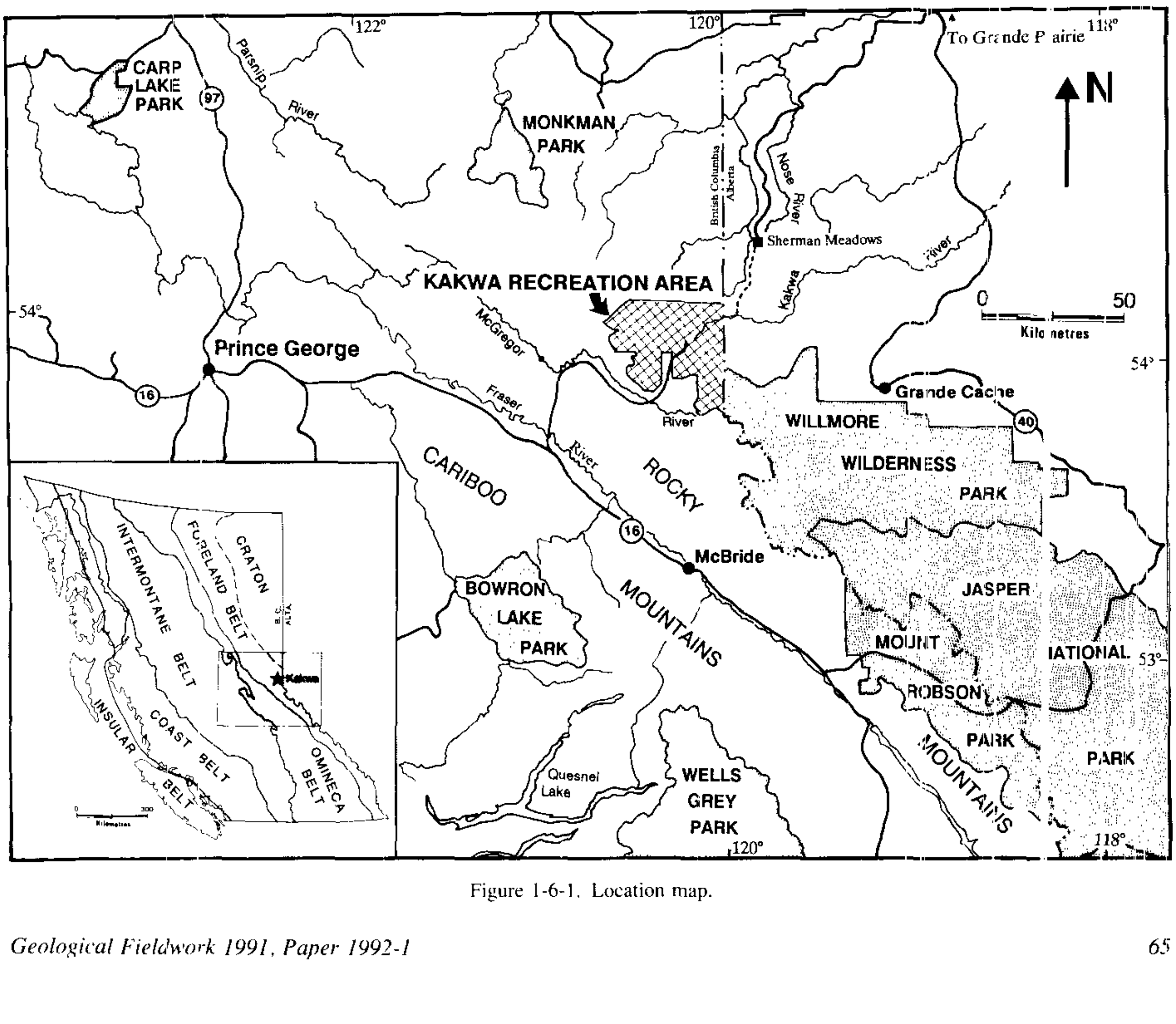

Figure 1-6-1. Location map.

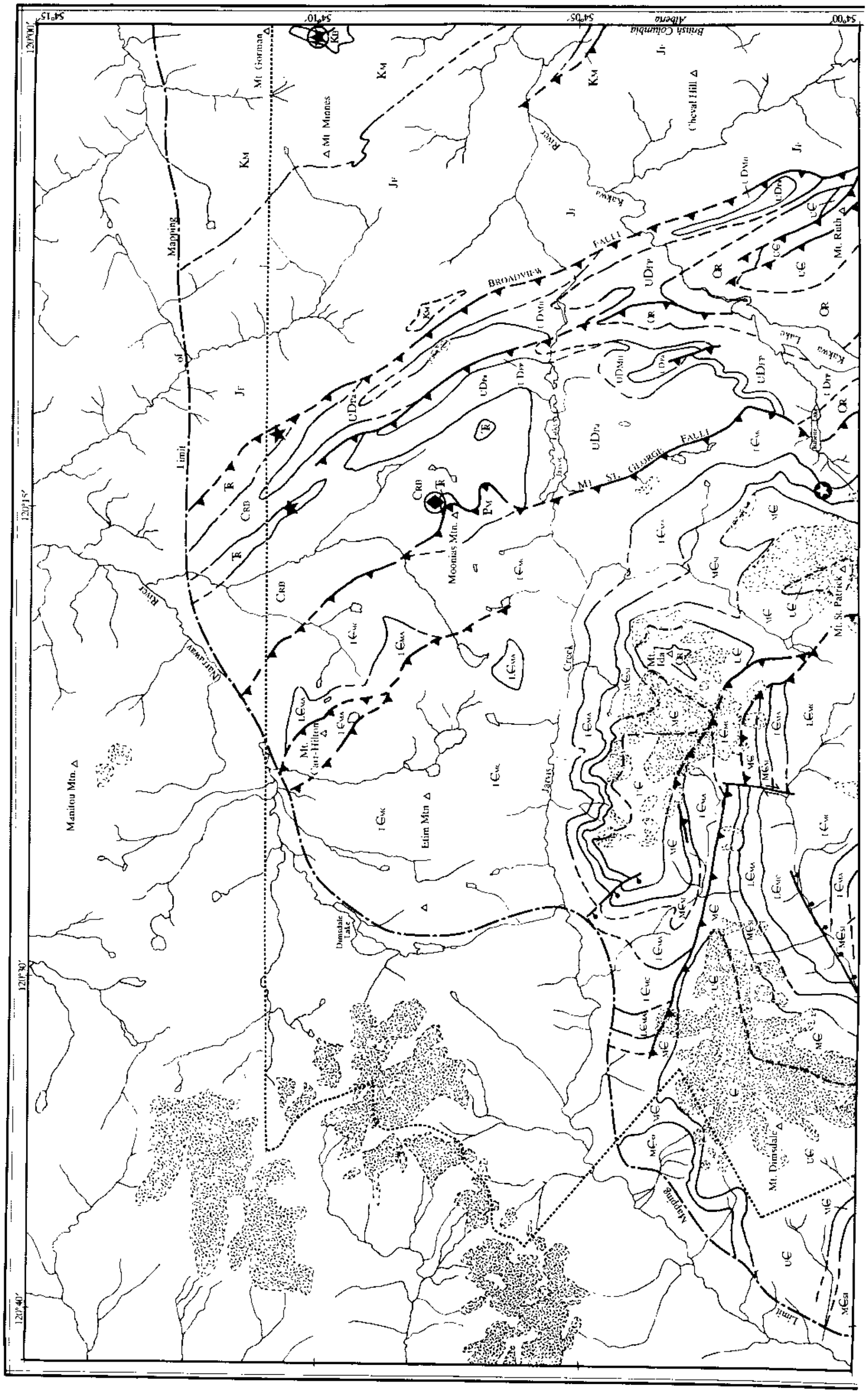

Limit of Mapping
Narraway River
Manitou Mtn.
Mt. Gorman
Mt. Minnes
Cheval Hill
British Columbia
Alberta
Kakwa River
BROADVIEW FAULT
MT. ST. GEORGE FAULT
Kakwa Lake
Mt. Ruth
Moonias Mtn.
Mt. St. Patrick
Jarvis Creek
Mt. Ida
Etlim Mtn
Dimsdale Lake
Mt. Dimsdale

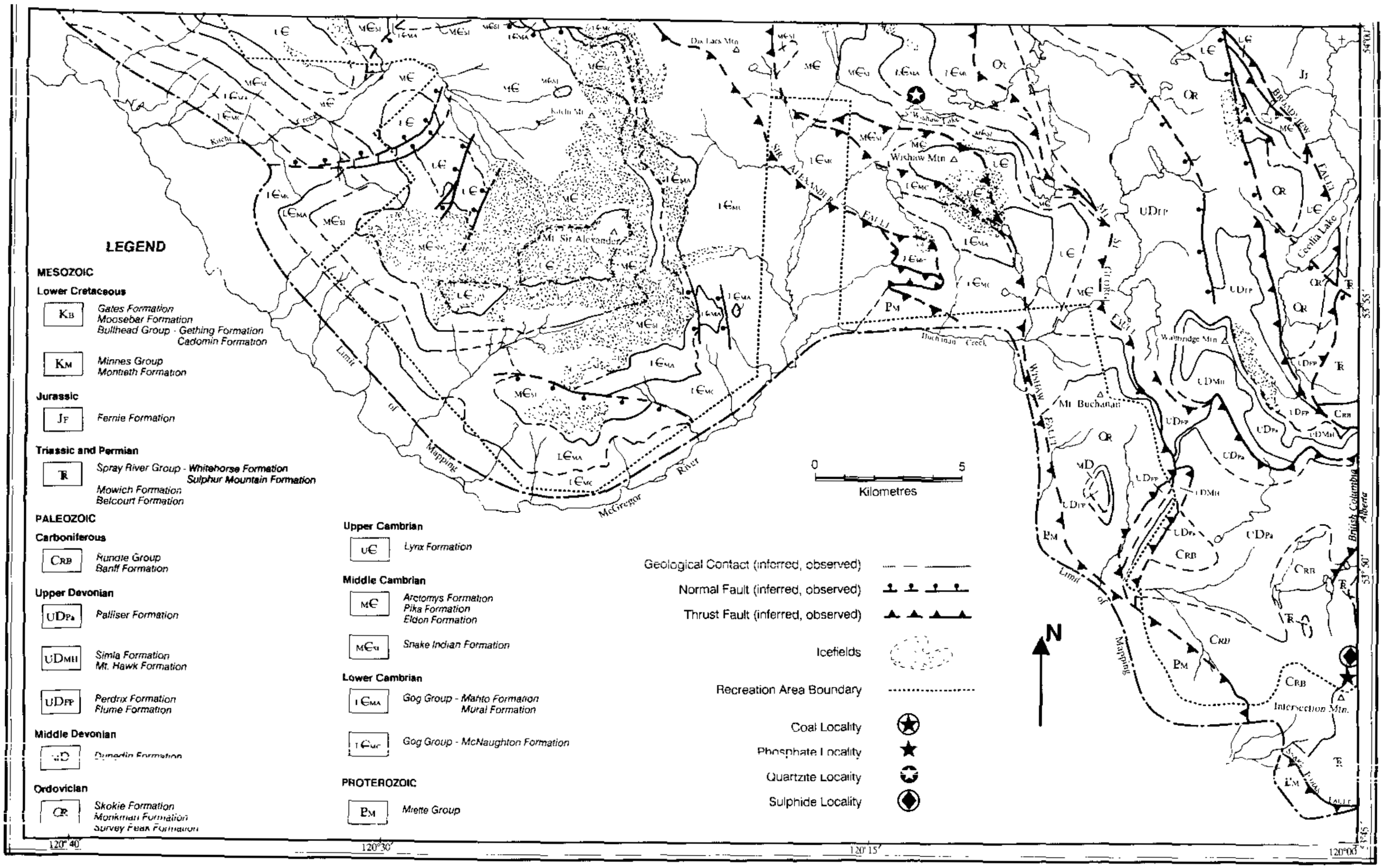

Figure 1-6-2. Generalized geology, Kakwa Recreation Area; compiled from mapping by J. Pell, J.L. Hammack, B. Fletcher and W.D. Harris, 1991 and from McMechan, 1986 and McMechan and Thompson, 1985.

Ida, Mount Sir Alexander and Mount Dimsdale and along the northwestern boundary of the recreation area.

There has been very little exploration work in Kakwa, in part due to its remoteness. There are coal leases in the northeastern part of the region and some oil and gas permits were also held there in the early 1980s. Quartzite, near the centre of the region, has been examined for its potential as a building stone. A lead-zinc-barite showing is located a few kilometres north of the recreation area and a gypsum prospect a short distance to the southeast. Although there has been limited activity, the geology indicates that a number of potentially economic commodities could exist within the boundaries of the recreation area, including coal, phosphate, gypsum, lead, zinc, barite and dimension stone. Kakwa Recreation Area is currently under consideration for upgrade to Class "A" park status and, prior to its reclassification, the mineral potential of the area must be evaluated, which is the focus of this project.

GEOLOGICAL SETTING

Kakwa lies within the Foreland tectonostratigraphic division of the Canadian Cordillera and is underlain by a sequence of carbonate and clastic sedimentary rocks ranging from Late Precambrian to Early Cretaceous in age. Folds and southwest-dipping, northeasterly directed thrust faults are the dominant structures in the region. Major thrust sheets contain strata which generally young to the northeast. Previous work in the area includes regional mapping by Campbell, Mountjoy and Young (1973), McMechan (1986), McMechan and Thompson (1985) and Taylor and Stott (1979).

STRATIGRAPHY

Upper Proterozoic (Hadrynian)

Rocks of the Hadrynian Miette Group are exposed in the hangingwall of the Mount St. George fault in the Moonias Mountain area; the Snake Indian and Wishaw faults near Intersection Mountain; and the Mount Sir Alexander and Wishaw faults south of Wishaw Mountain (Figure 1-6-2). Only the upper parts of this unit are exposed within the study area and detailed observations were possible only in the Moonias Mountain and Intersection Mountain areas.

At Moonias Mountain two lithologic units were observed. The lowest comprises a relatively resistant, thickly bedded, medium brown weathering quartzite-granule to pebble conglomerate, quartz wacke and medium grey quartz arenite, interbedded with brown and grey-weathering argillite and minor light grey quartz arenite. Minimum thickness for this unit is 300 metres. The conglomerate is composed of well-rounded quartzite pebbles supported by a matrix of medium-grained, poorly sorted quartz wacke. This lower unit is overlain by in excess of 200 metres of thinly bedded, dark brown-grey argillite with thin silty interbeds. Silty beds are locally crosslaminated and show graded bedding. One thick unit within the argillite has abundant tan-weathering dolostone breccia blocks of probable olistostromal origin. These blocks are up to 6 metres in diameter and stand out in relief against the more recessive argillite.

In the Intersection Mountain area, rocks of the Miette Group include a well-bedded, cliff-forming unit consisting of medium orange-brown-weathering, dark grey, calcareous quartzite-granule conglomerate and quartz wacke with interbedded medium to dark grey phyllite. This unit is underlain by a thick, poorly exposed, dark grey phyllite.

Lower Paleozoic

Lower Paleozoic strata underlie a significant proportion of Kakwa Recreation Area (Figure 1-6-2) and comprise a conformable sequence that disconformably overlies Proterozoic rocks. The Lower Cambrian Gog Group, which forms the base of this succession, consists of the McNaughton, Mural and Mahto formations (Table 1-6-1). The McNaughton Formation is a resistant, rusty to dark-weathering unit that forms a thick and fairly monotonous sequence dominated by medium to thick-bedded light grey quartzites. These quartzites are often laminated or crosslaminated; thin black shale layers and granule to pebble-conglomerate beds are present locally. In some areas crosslaminations are stained pinkish, giving the rock an attractive banded appearance. In the area south and west of Wishaw Mountain, black siltstones and argillites are interbedded with the quartzites and locally form units tens of metres thick that contain thin quartzite interbeds. The McNaughton Formation is largely devoid of fossils; however, trace fossils such as worm tubes *(Scolithus)* and meandering patterns on bedding planes, suggestive of worm trails, occur in the upper parts of the unit. In the Kakwa area, the McNaughton Formation is estimated to be approximately 1500 metres thick (McMechan, 1990; Slind and Perkins, 1966).

The Mural Formation is a reddish brown, recessive unit predominantly consisting of silty and sandy dolostones, dolomitic quartzites, shales and minor limestone. Its contact with the underlying McNaughton Formation is gradational and consists of a zone of interbedded light grey quartzites, dolomitic quartzites and dolostones. The Mural Formation begins where dolomitic rocks dominate over quartzites. Orange to tan dolostones, dolomitic quartzites and grey quartzites characterize the lower part of the formation, while grey and greenish grey shales, grey crystalline limestones, dolostones and lesser amounts of quartzite are more common in the upper part. Dolomitic quartzite beds often grade up-section into sandy dolostones. *Scolithus* worm tubes are common in the sandy layers (Plate 1-6-1). This formation is 225 to 300 metres thick in the Kakwa region.

The Mahto Formation is a grey to maroon, resistant unit, overlying the recessive Mural Formation. In the Kakwa area it is approximately 300 to 350 metres thick. It consists of light grey to creamy beige, pink and maroon, medium to thick-bedded quartzites with minor amounts of interbedded brown and dark grey sandy shales, dolomitic quartzites and siltstones. As with the other units of the Gog Group, fossils are restricted to *Scolithus* worm tubes. Quartzites are generally fine to coarse grained and, locally, granule-conglomerate layers are present. Colours of the quartzites vary from solid greys, pinks and maroons to very attractive, intricately swirled and banded patterns in shades of maroon, pink and creamy white (Plate 1-6-2).

TABLE 1-6-1
TABLE OF FORMATIONS

LOWER CRETACEOUS		
Gates Fm:	(>110 m)	sandstone, carbonaceous shale, coal
(Middle and Torrens River members, in descending order)		
Moosebar Fm:	(35-50 m)	shale, minor sandstone
BULLHEAD GROUP		
Gething Fm:	(25-80 m)	sandstone, siltstone, coal
Cadomin Fm:	(±25 m)	conglomerate
——— unconformity ———		
MINNES GROUP		
Gorman Creek Fm:	(650-1000 m)	sandstone, siltstone, minor coal
UPPER JURASSIC AND LOWER CRETACEOUS		
Monteith Fm:	(200-400 m)	sandstone, siltstone, shale
JURASSIC		
Fernie Fm:	(250-900 m)	shale, silty sandstone, siltstone
——— unconformity ———		
TRIASSIC		
SPRAY RIVER GROUP		
Whitehorse Fm:	(130-400 m)	dolostone, limestone, evaporites
(Winnifred, Brewster and Starlight evaporite members, in descending order)		
Sulphur Mountain Fm:	(405-475 m)	siltstone, silty limestone
(Llama, Whistler and Vega-Phroso members, in descending order)		
——— unconformity ———		
PERMIAN		
Mowich Fm:	(±10 m)	sandstone, conglomerate at base
Belcourt Fm:	(>10 m)	limestone, conglomerate at base
——— unconformity ———		
UPPER CARBONIFEROUS		
Hanington Fm:	(0-5 m)	limestone w/basal pebble conglomerate
——— unconformity ———		
LOWER CARBONIFEROUS		
RUNDLE GROUP:	(±400 m)	limestone, dolostone
(Mt. Head, Turner Valley, Shunda & Pekisko formations, in descending order)		
UPPER DEVONIAN AND LOWER CARBONIFEROUS		
Exshaw & Banff fms:	(180-260 m)	shale, minor limestone
——— unconformity ———		
UPPER DEVONIAN		
Palliser Fm:	(±530 m)	limestone (fossil-poor)
——— unconformity ———		
Simla Fm:	(60-70 m)	limestone, biostromal
Mount Hawk Fm:	(90-140 m)	limestone, fossiliferous
Perdrix Fm:	(85-470 m)	laminated shale
Flume Fm:	(75-145 m)	limestone, stromatoporoid biostrome
——— unconformity ———		
MIDDLE DEVONIAN		
Dunedin Fm*:	(±60 m)	limestone, siltstone, conglomerate
——— unconformity ———		
MIDDLE ORDOVICIAN		
Unnamed unit*:	(>75 m)	dolostone, quartzite and limestone
Skoki Fm:	(110-380 m)	dolostone, minor limestone
LOWER ORDOVICIAN		
Monkman quartzite:	(30-75 m)	quartzite, dolomitic quartzite
Survey Peak Fm:	(450-600 m)	silty dolostone, limestone, shale
UPPER CAMBRIAN		
Lynx Fm:	(600-800 m)	limestone, dolostone, calc-argillite
MIDDLE CAMBRIAN		
Arctomys Fm:	(50-100 m)	red shale, silty shale, dolostone
Pika Fm:	(80-100 m)	limestone, dolostone
Eldon Fm:	(350-375 m)	limestone, dolostone
Snake Indian Fm:	(±400 m)	limestone, red shale, siltstone
LOWER CAMBRIAN		
GOG GROUP		
Mahto Fm:	(300-350 m)	maroon, pink, grey quartzite, dolostone
Mural Fm:	(225-300 m)	dolostone, quartzite, limestone, shale
McNaughton Fm:	*(±1500 m)*	*quartzite, granule conglomerate*
——— unconformity ———		
UPPER PROTEROZOIC		
MIETTE GROUP		
Upper Miette:	(>300 m)	argillite, sandstone, conglomerate

* Mt. Buchanan area only

Plate 1-6-1. Subvertical *Scolithus* worm tubes in Lower Cambrian quartzites within the Mural Formation. Section viewed is perpendicular to bedding.

Plate 1-6-2. Intricately swirled colour-banding patterns in Lower Cambrian Mahto Formation quartzites. Banding parallels solution fronts. Symbol indicates bedding orientation.

The Middle Cambrian Snake Indian Formation is a recessive to ribbed-weathering unit with colourful banding in shades of tan, red, green and grey, and overlies the Mahto Formation quartzites (Plate 1-6-3). The lower part of the formation is more recessive and tan weathering; it consists of thin-bedded red, green and grey shales, with tan-coloured dolostone, silty limestone layers and minor sandstone interbeds. The upper part of the formation is ribbed weathering, with thick resistant grey limestone units separated by recessive bands of brightly coloured shales and thinly interbedded dolostones. The limestones are variably thin to thick bedded, wavy bedded to nodular and commonly show evidence of bioturbation, with dolomitized burrows. The top of the formation is marked by the last thick, recessive, brightly coloured shale and dolostone (Mountjoy and Aitken, 1978). In the Kakwa area, this formation is approximately 400 metres thick.

Massive, cliff-forming, dark grey limestones of the Eldon Formation overlie the Snake Indian shales and carbonates (Plate 1-6-3). These limestones vary from thin bedded and nodular to thick bedded and often are bioturbated, with dolomitized worm burrows and beds a common feature (Plate 1-6-4). The dominant lithology is lime mudstone, however, oolitic grainstones also occur locally. The Eldon Formation is approximately 350 to 375 metres thick in the Kakwa area and is overlain by approximately 80 to 100 metres of ribbed-weathering strata of the Pika Formation.

In much of the area, the base of the Pika Formation is placed at the base of a yellow-orange dolostone unit between the massive Eldon limestones and the overlying, wavy, thin to medium-bedded lime mudstones. These limestones are commonly bioturbated, locally contain dolomitized worm burrows and are sometimes interbedded with thin grey shales. In the Mount Sir Alexander area, the Pika Formation consists of two distinctive units. The lower unit comprises an orange to buff-weathering, recessive sequence of medium grey lime mudstone, that commonly contains dolomitized laminae and worm burrows. The top of the lower sequence is marked by approximately 5 metres of interbedded grey-brown to orange-brown argillite and grades into an upper, massive, more resistant unit comprising medium to light grey, laminated lime mudstones that are locally oolitic and display lode casts, graded beds and crosslaminations.

The top of the Middle Cambrian sequence is marked by the Arctomys Formation, a distinctive, red-weathering recessive unit, 50 to 100 metres thick. It comprises blood-red and minor amounts of dark green dolomitic shale and silty shale and thin bedded, tan-weathering dolostone. Mud cracks, salt crystal casts and ripple marks are common.

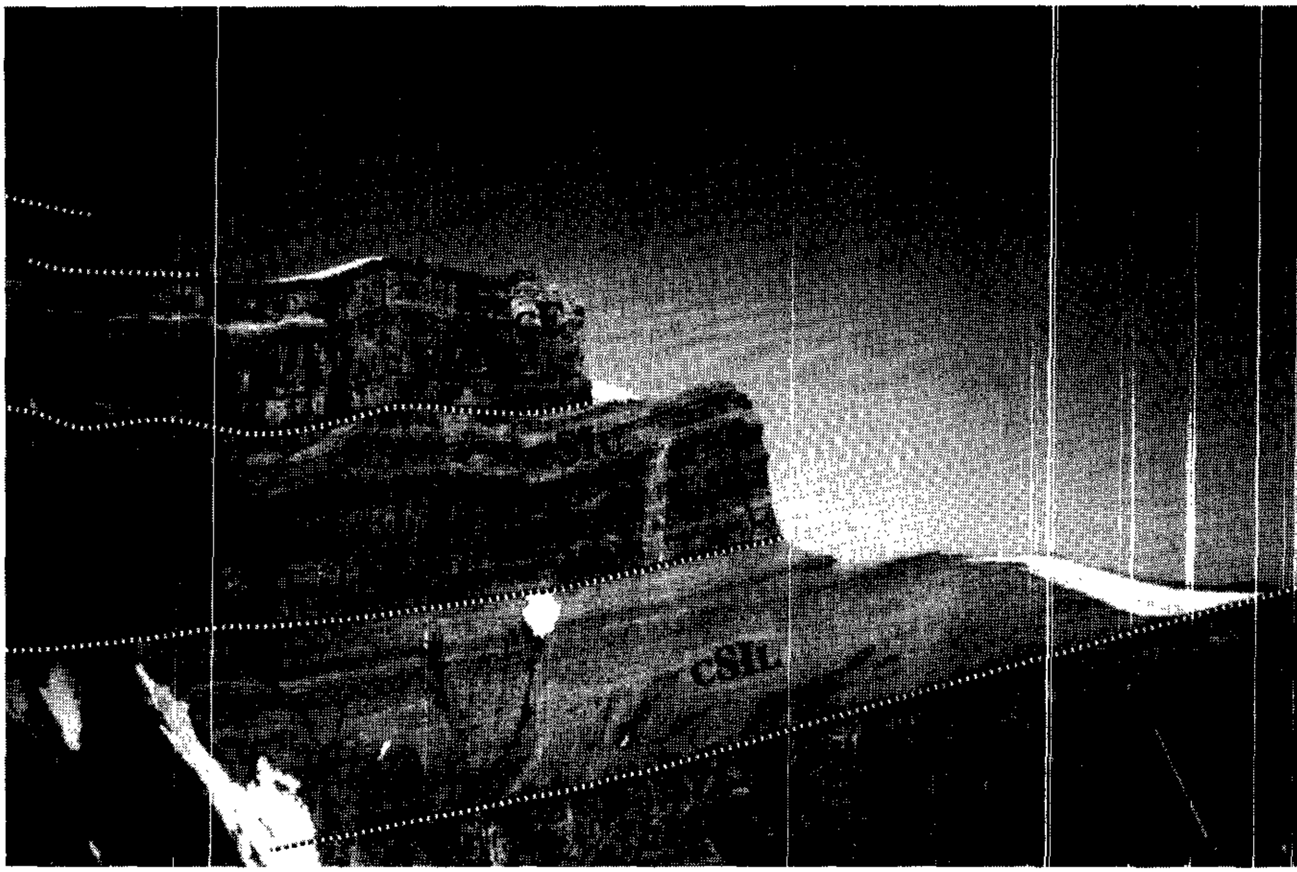

Plate 1-6-3. The exposed Cambrian section on the east flank of Mount St. Patrick, as viewed from the southeast. The lowest unit exposed is the massive, cliff-forming Lower Cambrian Mahto Formation (cMh) which is overlain by the recessive Middle Cambrian lower Snake Indian Formation (cSIl). The colour-banded and slightly ribbed-weathering upper Snake Indian formation (cSIu) forms the next cliff step and is overlain by a cliff-forming ledge of the Middle Cambrian Eldon Formation (cE). Recessive strata of the Middle Cambrian Pika and Arctomys formations (cPA) form the next step and the uppermost ledge, seen only in the far upper left corner of the photograph, is cliff-forming Upper Cambrian Lynx Formation (cLx).

The Upper Cambrian Lynx Formation is a resistant, cliff-forming unit that crops out at the peaks of most of the highest mountains in the area and is characterized by well-defined buff and grey colour-banding and bedding (Plate 1-6-5). It conformably overlies recessive shales of the Arctomys Formation and is estimated to be 600 to 800 metres thick (McMechan, 1986). The lower part of this formation consists of medium-bedded, buff, grey and locally orange-weathering, very fine grained dolostones with interbeds of fine to coarse-grained quartz arenites and sandy dolostones, light grey siltstones and minor, medium-bedded, grey limestones. The sandstones are often crossbedded and may contain dolostone chips (Plate 1-6-6). The dolostones are locally stromatolitic and characterized by sedimentary structures such as layers of flat-pebble conglomerate, burrows, lode casts, slump folds and disrupted bedding. Beds containing nodules of white chert are also present locally. The upper part of the Lynx Formation is dominated by limestone. Its base is marked by 50 to 100 metres of relatively recessive, greenish grey to grey-weathering calcareous argillite with limestone nodules. This is overlain by tan to grey-weathering, wavy bedded to nodular, argillaceous or silty limestones with thin to thick beds of more resistant grey limestone.

The Lower Ordovician Survey Peak Formation is a resistant unit that conformably overlies Upper Cambrian strata. It is 450 to 600 metres thick and has approximately 30 to 70 metres of recessive, light greenish grey to silvery weathering, strongly cleaved, calcareous shale and shaley limestone with interbeds of limey flat-pebble conglomerate at its base. Burrows and feeding traces on bedding planes are locally very common. The remainder of the unit comprises resistant, buff to orange-weathering, silty dolostones, dolomitic siltstones and blue-grey-weathering limestones. Grey argillite partings are common in this part of the sequence and flat-pebble conglomerates are present locally. The siltstones and dolostones are wavy bedded and have a very rough weathered surface, with more resistant, whispy laminae. They are interbedded with silty, thin-bedded to massive limestones that are generally nodular to wavy bedded and can be partially dolomitized. Both the dolostones and limestones locally show evidence of bioturbation, containing burrows and feeding trails that are sometimes silicified. Some layers are rich in fossil debris; brachiopod and trilobite fragments are common.

The Survey Peak Formation is overlain by the Lower Ordovician Monkman Quartzite Formation. The Monkman is a resistant, light grey weathering marker unit that aver-

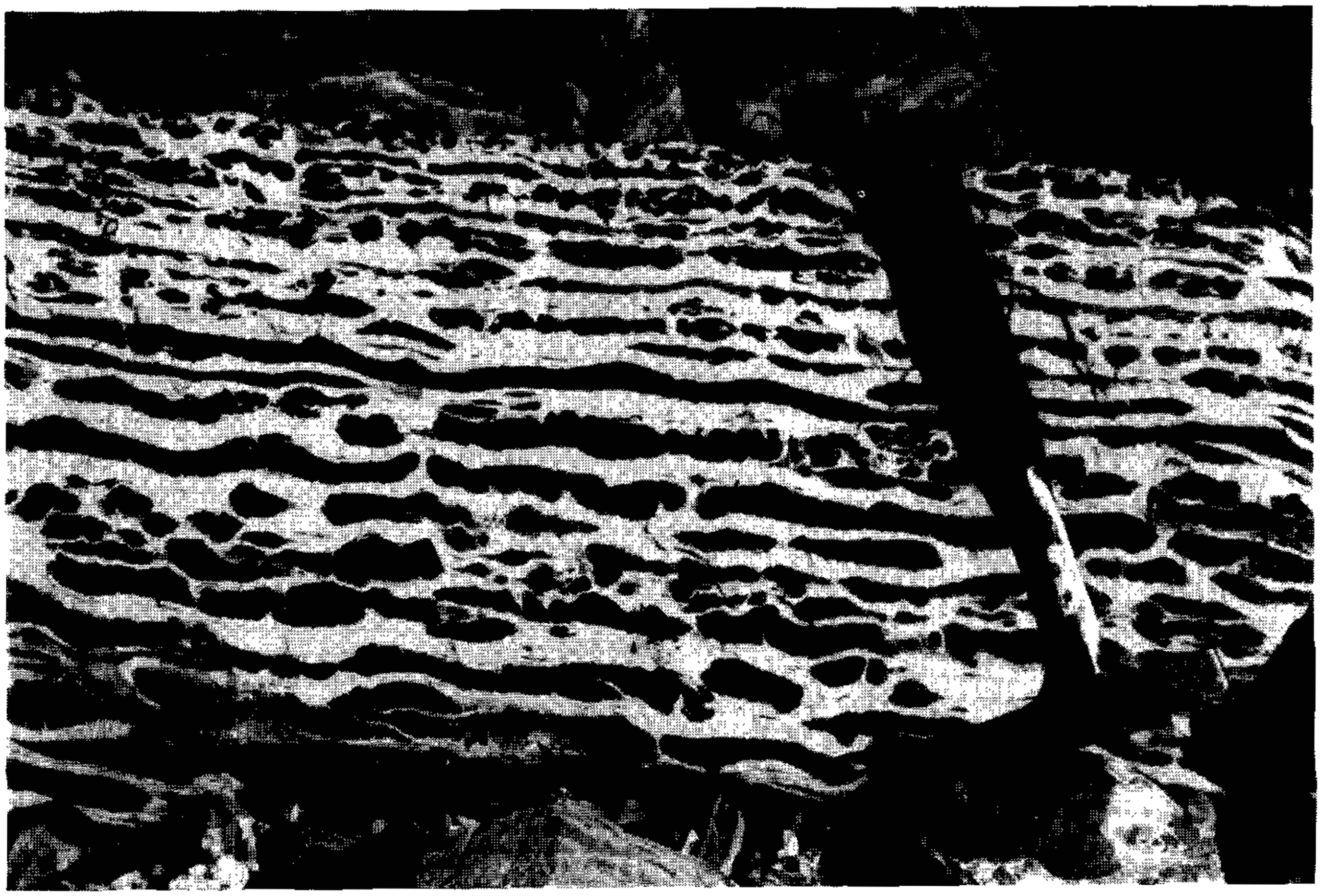

Plate 1-6-4. Dolomitized layers and worm burrows (light grey) are commonly found within thin-bedded Eldon Formation lime mudstone units (darker grey).

ages between 30 and 100 metres thick and comprises fine to medium-grained, thin-bedded to massive, light grey to buff-weathering quartzites and dolomitic quartzites. Crossbedding, ripple crosslaminations and burrows are common features.

Middle Ordovician strata, assigned to the Skoki Formation, overlie the Monkman quartzites. The Skoki is a resistant, tan-weathering formation characterized by monotonous, medium to thick-bedded, finely crystalline dolostones. For the most part, the dolostones are rather featureless, however, locally they can contain oncolites, stromatolites, intraclasts, mud cracks and rare chert nodules. Minor amounts of wavy bedded to nodular limestone are present in this formation and gastropods are found locally. Thick-bedded, crosslaminated, sandy dolomite horizons can also occur.

The youngest Lower Paleozoic rocks observed in the Kakwa area are an unnamed unit composed of medium-bedded to massive dolomitic quartz arenite and dolostone. This unit was mapped in the Mount Buchanan area where it conformably overlies the Skoki Formation (Figure 1-6-2). Medium-bedded to massive, medium to light grey, fine-grained dolomitic quartz arenite predominates and has a distinctive medium yellow-tan to buff-orange weathered surface. This sandstone is locally interbedded with medium-bedded, medium to light grey and orange-weathering, finely crystalline dolostone. True thickness could not be determined but is not less than 75 metres.

Middle Paleozoic

The middle Paleozoic sequence in the Kakwa area is dominated by carbonate rocks exposed in a thrust sheet which is bounded on the east by the Broadview fault and on the west by the Mount St. George and Wishaw faults (Figure 1-6-2).

The lowest unit in the middle Paleozoic package is the the Middle Devonian Dunedin Formation which disconformably overlies Ordovician strata. It is exposed at only one location within the study area, approximately 3 kilometres south of Mount Buchanan (Figure 1-6-2) where it is estimated to be approximately 60 metres thick (McMechan and Thompson, 1985). It is characterized by two distinct lithologies, an upper, resistant limestone-dominated package and a lower, less resistant sequence dominated by clastic rocks. The upper package consists of thick-bedded, medium grey and yellow-buff-weathering, medium grey lime mudstones and wackestones with minor interbeds of medium orange-brown weathering, light grey, fine-grained quartz arenite and siltstone. The lower clastic sequence

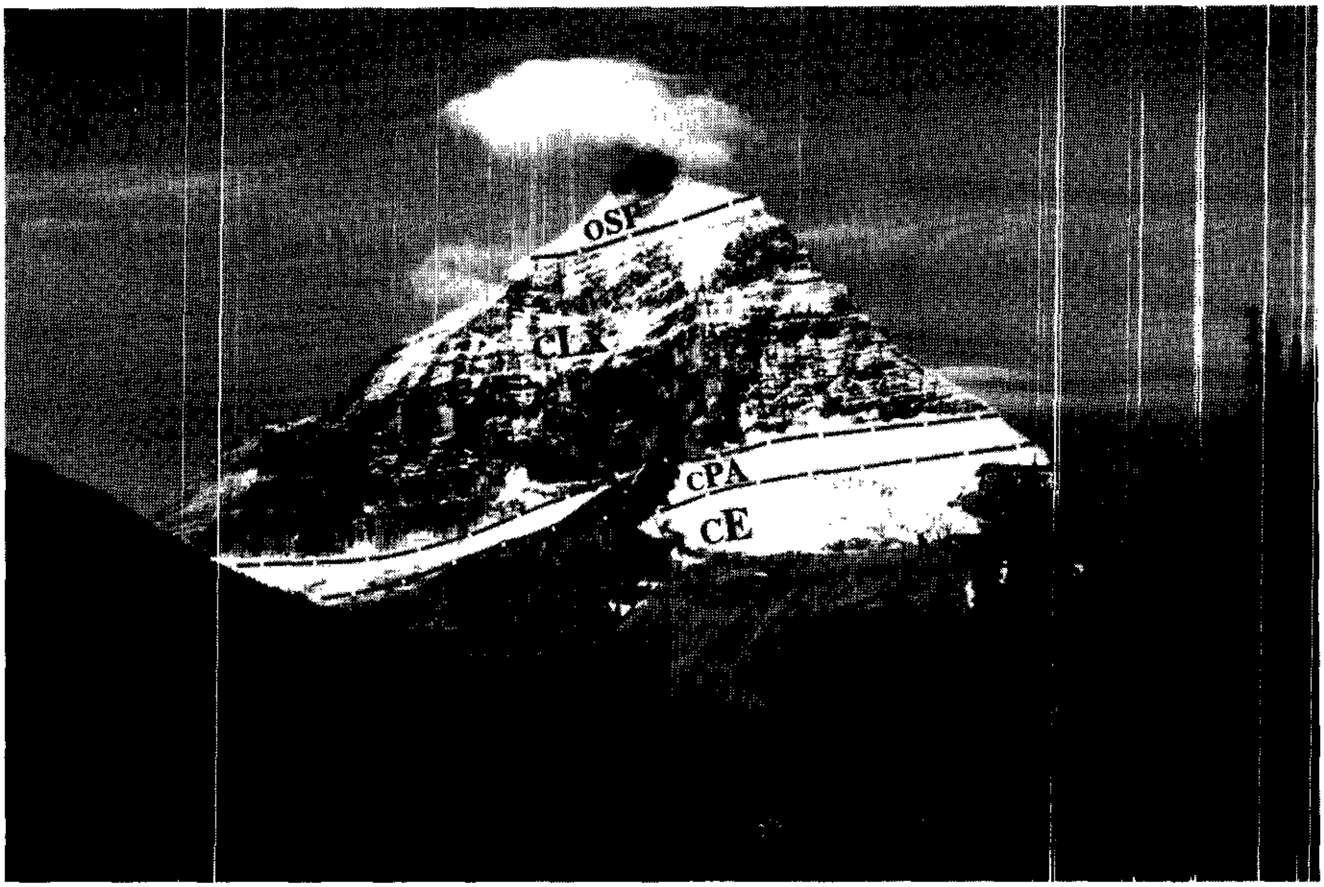

Plate 1-6-5. The Cambrian and Ordovician section exposed at Mount Ida, as viewed from Jarvis Lakes. The main cliff-forming unit, that comprises the bulk of the mountain, is the Upper Cambrian Lynx Formation (cLx); it is overlain by more recessive strata of the Ordovician Survey Peak Formation (oSP), which cap the mountain. Recessive strata of the Middle Cambrian Arctomys and Pika formations (cPA) that underlie Lynx strata, are poorly exposed, outcropping on the small spur between the two icefields. The Middle Cambrian Eldon Formation (cE) forms the lowest cliffs, immediately above the scree slope.

consists of medium orange-brown weathering, fine to coarse-grained, light grey quartz arenite and siltstone. Elsewhere, the Dunedin Formation includes a basal quartz-pebble conglomerate (McMechan and Thompson; 1985), however, this was not observed in the study area.

Upper Devonian Fairholme Group strata unconformably overlie the Dunedin Formation. The Fairholme Group comprises the Flume, Perdrix, Mount Hawk and Simla formations of Frasnian age (Table 1-6-1). The Flume Formation is generally 75 to 85 metres thick, however, in the Mount Buchanan area it is in excess of 145 metres (Geldsetzer, 1982). Where the whole sequence is exposed, as in the area east of Mount Buchanan, the Flume Formation consists of a thin quartzose sandstone unit overlain by a thin unit of red and green calcareous shales followed by a stromatoporoid biostrome which is sharply overlain by shaley limestones. The biostrome, which can be in excess of 100 metres thick, generally consists of medium to thick-bedded, grey to buff to chocolate-brown weathering limestones and patchily interspersed dolostones. Large, mound-shaped stromatoporoids in apparent life position; smaller, detached specimens; fenestral stromatoporoids and corals were all noted (Plate 1-6-7). Fossils are locally silicified. The overlying shaley limestones generally form a dark grey weathering, relatively recessive, thin-bedded to nodular unit that becomes increasingly shaley up-section. They commonly contain abundant corals and crinoids and extremely abundant brachiopods; locally, they weather to form brachiopod gravels.

The Perdrix Formation has a gradational contact with the underlying Flume Formation. It is characterized by greyish green to black shales with thin, calcareous interbeds that are recessive and generally very poorly exposed. Thickness of the Perdrix Formation is estimated at between 185 and 470 metres (Geldsetzer, 1982); lack of good exposure, and faulting, make true thickness estimations difficult.

The Mount Hawk Formation conformably overlies the Perdrix shales and consists of cliff-forming grey limestones, often with a ribbed weathering pattern. In the Kakwa area, it is characterized by thick ledges of massive limestone with intervening zones of thin-bedded to nodular limestone and shaley limestone. This formation is invariably very fossiliferous; however, weathered surfaces are locally coated with a crust of light grey lime, which obscures their fossiliferous nature. Gastropods, rugosan and colonial corals are the dominant macrofossils; brachiopods were also noted

Plate 1-6-6. Lime mudstone chips in a crossbedded dolomitic sandstone bed from the lower part of the Lynx Formation.

locally. The nodular limestone units predominantly consist of skeletal mudstones and wackestones; skeletal wackestones and grainstones comprise the more massive beds. In the Kakwa area, the Mount Hawk Formation is 90 to 140 metres thick (Geldsetzer, 1982).

The Simla Formation conformably overlies the Mount Hawk and averages 60 to 70 metres in thickness. It comprises a sequence of massive, thick-bedded, resistant, light grey limestones, interbedded with lesser, thin-bedded limestones. Grainstones are the dominant lithology (Geldsetzer, 1982). Like the Mount Hawk Formation, Simla limestones are very fossiliferous, with colonial corals, bryozoans and crinoids the dominant organisms. Brachiopods occur locally and gastropods were noted in a few places. In some locations, light grey, limy encrustations obscure the fossiliferous nature of these rocks; in other areas, silicification enhances the fossils. Thin bands and nodules of black chert occur in some sections. In the Kakwa area, lithological similarities between the Simla and Mount Hawk formations often make recognition of the contact difficult and it is often easier to distinguish the units from a distance due to the lighter weathering colour of the Simla limestones.

The Palliser Formation, of Famennian age, consists of a thick succession of monotonous limestones which disconformably overlie the Simla Formation. In the Kakwa area, this formation is approximately 530 metres thick. Its base is marked by a thin, brown-weathering fossil "hash" layer containing whole and fragmented gastropods, brachiopods and crinoids. The lower part of the formation consists of recessive to ribbed-weathering, thin, wavy bedded to nodular lime mudstones, with some medium-bedded limestone ledges which grade upwards from grainstones to mudstones (Geldsetzer, 1982). These strata are often mottled light grey, dark grey and buff weathering. Rare oolitic beds (oolitic shoals) containing lime-mud intraclasts are present locally. Fossils are uncommon, with only rare brachiopods and scleractinian corals being noted near the base of the formation. Locally, flat-pebble conglomerate beds, with a reddish, iron oxide coating, are also present.

The upper part of the Palliser Formation consists of more resistant, thin to medium-bedded, grey to grey-brown mottled limestones. Its base is defined by approximately 10 metres of black and grey, rhythmically laminated lime mudstones, which are in sharp contact with underlying lower Palliser lithologies. This marker unit is overlain by thin-bedded lime mudstones and shaley limestones that give way, up-section, to monotonous, medium-bedded lime mudstones and pelletal grainstones. Macrofossils are rare in this part of the section, with brachiopods and crinoid osciceles occasionally present; trace fossil markings are common

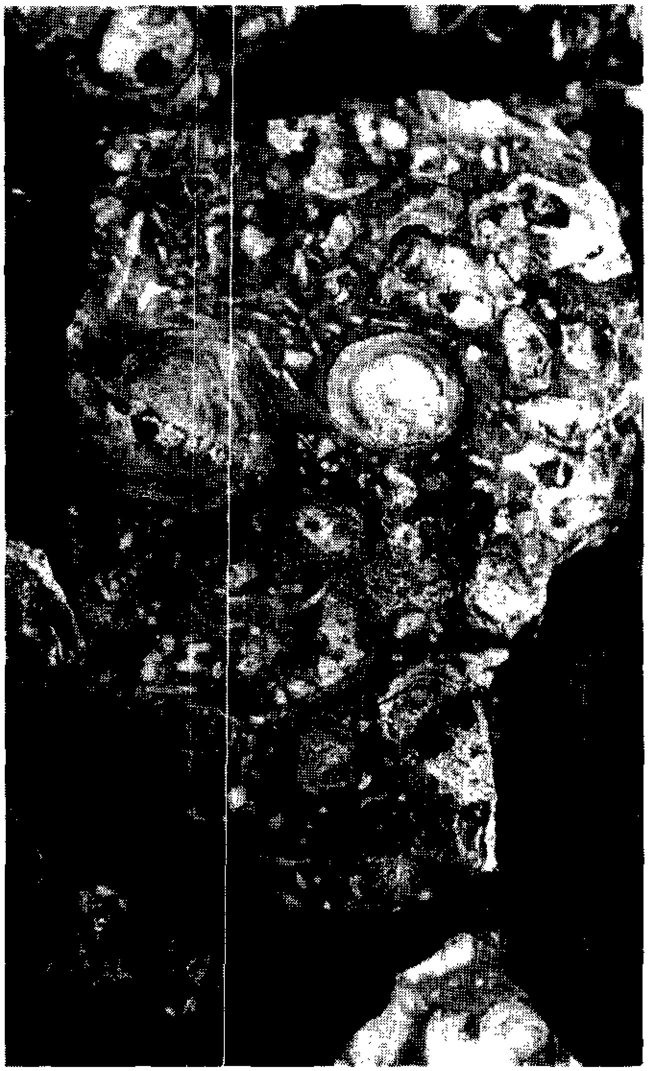

Plate 1-6-7. Detached and fragmented stromatoporoids in the Upper Devonian (Frasnian) Flume Formation.

on bedding planes in the lower part of this section. Nodules of black chert also occur locally.

Upper Paleozoic

The Upper Paleozoic sequence comprises a basal clastic, shale-dominated package, overlain by a thick sequence of carbonate rocks, capped by thin sandstones and chert-pebble conglomerates. Terrigenous clastic rocks of the Banff and Exshaw formations, which are predominantly Lower Carboniferous in age, form the base of this sequence and unconformably overlie the Palliser Formation. These units, which cannot be subdivided in the Kakwa area, are recessive and poorly exposed. They consist predominantly of black shales with thin interbeds of lime wackestone and grainstone and minor sandstone; carbonate content of this unit increases up-section until carbonate rocks dominate and the strata are assigned to the Rundle Group. A thickness of 180 to 260 metres has been estimated for the combined Banff and Exshaw formations (McMechan, 1986).

Two carbonate units of Carboniferous age are present within the study area; the widespread Lower Carboniferous Rundle Group, and the thin, discontinuous, Upper Carboniferous Hanington Formation. The latter is typically absent due either to nondeposition or erosion as part of a widespread sub-Permian disconformity. The only known occurrence of the Hanington Formation within the study area is at the type section, approximately 3 kilometres east of Moonias Mountain (Bamber and Macqueen, 1979; Figure 1-6-2). Rundle Group rocks crop out in the southeastern and north-central parts of the recreation area (the Intersection Mountain area and northeast of Moonias Mountain; Figure 1-6-2) and reach a thickness of approximately 400 metres.

The Rundle Group is subdivided into four formations in this area. From oldest to youngest, they are the Pekisko, Shunda, Turner Valley and Mount Head formations. The Pekisko, Shunda and Turner Valley formations are very similar in character. All are variably thin to thick bedded, light to medium grey weathering and consist of medium grey skeletal grainstones, wackestones and packstones with minor lime mudstone. Crinoidal debris is the most abundant skeletal constituent. Chert nodules are typically absent, however, they are locally abundant. The overlying Mount Head Formation is predominantly composed of light grey weathering, light to dark grey, fine-grained dolostone which is locally petroliferous. Chert nodules and chert beds are very common. Macrofossils are common in all of the formations of the Rundle Group. The most common types include rugosan, scleractinian and lithostrotion corals: brachiopods, gastropods and echinoderms are also present.

Rocks of the Hanington Formation disconformably overlie those of the Rundle Group. At the type section, this unit consists of medium to thick-bedded, partially dolomitized skeletal wackestone, packstone and lime mudstone. Chert nodules and layers are locally common and a thin bed of chert-granule to pebble conglomerate is found at its base. The unit is 5 metres thick, and is lithologically very similar to the overlying Belcourt Formation of Permian age. Division has been made primarily on the basis of microfossil interpretation which has established an Upper Carboniferous age for this formation (Bamber and Macqueen, 1979).

Permian strata disconformably overlie rocks of the Lower Carboniferous Rundle Group and the Upper Carboniferous Hanington Formation. Two lithologically unique units characterize the Permian of the area, the Upper Permian Mowich Formation sandstones and the Lower Permian Belcourt Formation gritty limestones and conglomerates. The Belcourt Formation appears to be absent over much of the study area, but where exposed it is separated from the overlying Mowich Formation by a mid-Permian disconformity (Bamber and Macqueen, 1979).

Belcourt Formation rocks were observed at one locality, approximately 3 kilometres east of Moonias Mountain (Figure 1-6-2). Here, thick-bedded medium grey weathering chert-pebble conglomerate with a carbonate matrix is interbedded with, and grades into, thick-bedded, medium grey weathering gritty lime mudstone, clean lime mudstone, skeletal packstone and wackestone. Finely crystalline dolostone predominates toward the top of the unit. Chert pebbles are dark to light grey in colour and are well rounded. Gastropods and brachiopods are locally abundant. The true thickness of this unit could not be established, but is not less than 10 metres.

The Mowich Formation is by far the more extensive of the two units within the study area. It is a light brown-buff weathering, light to medium grey, medium to fine-grained quartz arenite. Outcrops are commonly lichen covered, giving the rocks a dark grey to black appearance. The unit is typically less than 10 metres thick, and is most easily distinguished by its dark colour and its unmistakable stratigraphic position between the thick succession of massive grey carbonates of the Rundle Group and the thick orange to brown-weathering siltstone sequence of the Triassic Sulphur Mountain Formation.

Mesozoic

Triassic Spray River Group strata (Sulphur Mountain and Whitehorse formations), which crop out in the northern and eastern regions of Kakwa Recreation Area (Figure 1-6-2), unconformably overlie Permian rocks. The older Sulphur Mountain Formation is a moderately resistant unit that weathers a characteristic dark reddish brown to brownish orange colour. It has been subdivided into the Vega-Phroso, Whistler and Llama members, in ascending order. In the Kakwa area, the Vega-Phroso siltstone member is approximately 245 to 270 metres thick and comprises a shaley to flaggy weathering sequence of dolomitic and calcareous siltstone, fine-grained sandstone, silty limestone and shale (Gibson, 1975). It is quite platey near the base and becomes increasingly flaggy up-section. Ammonites are relatively common; pelecypods were also noted in some sections and, in one location, moderately well preserved fish fossils were found (Pell and Hammack, 1992, this volume). The Whistler Member, where present, is generally 10 to 20 metres thick and consists of dark grey to black-weathering siltstone, silty limestone, silty shale, dolostone, phosphorite and phosphatic pebble conglomerate (Gibson, 1975). Ammonites, pelecypods, and locally brachiopods, occur in this member and are commonly phosphatic. The Llama Member is characterized by relatively resistant, orange-brown-weathering, thin to thick-bedded dolomitic quartz siltstones, silty limestones and dolostones that contain pelecypods and rare ammonite fossils, and locally, reptile bones. Where it occurs, it is approximately 150 to 185 metres thick.

The Whitehorse Formation conformably overlies the Sulphur Mountain Formation and is a variable sequence of recessive to moderately resistant, buff to light grey to yellowish grey weathering dolostones, limestones and sandstones, with minor amounts of siltstone, intraformational conglomerate and evaporite. Regionally, it can be divided into the Starlight evaporite member, the Brewster limestone member and the Winnifred Member with cumulative thicknesses of between 130 and 400 metres (Gibson, 1972, 1975). Limited exposure in the Kakwa area makes subdivision of the Whitehorse Formation difficult. The most common lithologies encountered were very porous, sugary, buff

Plate 1-6-8. Disharmonic chevron folds in Lower Cretaceous Minnes Formation strata, north of Mount Minnes.

grainstones, buff and grey fossiliferous grainstones, massive, light grey weathering quartz wacke and medium-crystalline dolostones that often had a very strongly petroliferous odor when broken. Chert layers and lenses and intraformational breccia horizons were also observed.

The Jurassic Fernie Formation is a recessive, poorly exposed unit with an estimated thickness of 250 to 900 metres that, on a regional scale, unconformably overlies carbonate rocks of the Triassic Whitehorse Formation (McMechan, 1986). In the Kakwa area, it crops out east of the Broadview fault (Figure 1-6-2) and is always in fault contact with older strata. The lower part of the Fernie Formation consists of dark grey and black shale with minor sandstone; very thin to thin-bedded, greyish brown weathering siltstone, silty sandstone and shale with local, more resistant silty sandstone units in the upper part of the formation.

The Upper Jurassic to Lower Cretaceous Monteith Formation conformably overlies Fernie Formation strata. It is a resistant, light greyish brown to yellowish brown weathering marker unit, approximately 200 to 400 metres thick, that predominantly consists of very fine grained laminated sandstones. Wood fragments and crinoids with star-shaped stems *(Pentacrinites?)* are locally present in these sandstones.

The Gorman Creek Formation of the Lower Cretaceous Minnes Group (also referred to as the Nikanassin Formation) conformably overlies Monteith Formation sandstones in the northeastern part of the Kakwa area. It comprises a thick, orange-brown, ribbed-weathering succession of interlayered sandstone, siltstone, mudstone and carbonaceous shale. Thin coal beds, averaging 30 to 50 centimetres in thickness, are common in the upper part of this formation. Sandstones are generally buff weathering, fine to coarse grained, carbonaceous and often display ripple crosslaminations or crossbedding. Dark chert grains are common constituents of the sandstones. The thickness of this formation is estimated at 650 to 1000 metres (McMechan, 1986).

Conglomerates and sandstones of the Lower Cretaceous Bullhead Group (Cadomin and Gething formations) unconformably overlie Minnes Group strata east of Mount Minnes (Figure 1-6-1). The Cadomin Formation is a cliff-forming unit, approximately 25 metres thick, that comprises clast-supported, multilithic conglomerates with pebble to cobble-sized clasts in a sandy matrix. The Gething Formation conformably overlies the Cadomin conglomerates and consists of a ribbed-weathering sequence of orange-brown crosslaminated sandstones, carbonaceous siltstones and carbonaceous shales. In the Kakwa area it is 45 to 50 metres thick and its top is marked by a fairly thick (2.5 to 3 m) coal seam (Pribyl, 1979).

The Moosebar Formation conformably overlies Gething strata. It is a recessive unit, 35 to 55 metres thick, that is comprised of grey to tan-weathering shales with thin, rusty weathering siltstone interbeds. In the Kakwa area, it is conformably overlain by approximately 110 metres of Lower Cretaceous Gates Formation strata, which comprise the youngest sediments in the region. The Torrens River Member of the Gates Formation comprises approximately 12 metres of thin to thick-bedded, crosslaminated sandstones and is overlain by a ribbed-weathering succession of fine to coarse-grained carbonaceous sandstones, siltstones and shales assigned to the "Middle" Gates Member. Three moderately thick coal seams (ranging from 2 to 6 m) are present within this unit (Pribyl, 1979).

STRUCTURE

The Kakwa area can be broadly divided into three structural domains with differing structural styles. The eastern domain includes the area underlain by Jurassic and Cretaceous strata, east of the Broadview fault (Figure 1-6-2). The rocks in this region are relatively incompetent; shales and thin-bedded sandstones are the dominant lithologies. Folds are predominantly chevron style with short wavelengths, small amplitudes and highly variable axial planes (Plate 1-6-8). They tend to be disharmonic. Axial traces of the folds trend southeasterly and are subparallel to the bounding faults.

The central domain is bounded by the Broadview fault to the east and, to the west, by the Wishaw fault in the vicinity of, and south of Mount Buchanan and by the Mount St. George fault to the north of Mount Buchanan (Figure 1-6-2). Numerous minor thrusts occur within this major sheet; in most cases they are not more than 10 kilometres in strike length and are either splays off the major bounding faults or terminate along strike with displacement transferred into folds. In the southern part of the area, south of Wallbridge Mountain, northerly directed thrusts with east-west strikes cross the main structural grain. Two northwest-trending, west-side-down normal faults, with strike lengths in excess of 5 kilometres, are also present within the central domain. Normal faults post-date the thrusts and many of the thrusts are either offset or truncated by them.

The central block is predominantly underlain by Middle and Upper Paleozoic strata; some Ordovician rocks are present near the centre of the belt and Triassic units crop out in the north and south. The units carried within this thrust sheet are dominated by carbonates and most are fairly competent; however, intervening, thick incompetent (shaley) units also occur within the sequence. Map-scale folds, with northwest-trending axial traces are present within this domain and are fairly continuous along strike. They are generally quite tight and vary in orientation from upright to overturned, both along their axial trace and in cross-section (Plate 1-6-9). Some smaller scale folds are also present. They are not continuous along strike and are clearly conical in nature. With folds of all scales, disharmony occurs between competent and incompetent units.

The western domain lies west of Wishaw fault in the vicinity of, and south of Mount Buchanan and west of the Mount St. George fault, north of Mount Buchanan. A structurally complex zone of small thrust slivers and overturned folds occupies the region north of Mount Buchanan, between where the Mount St. George and Wishaw faults are clearly the eastern bounding structures of this package (Figure 1-6-2). The southern and western boundary of this domain is defined by the Snake Indian - Back Range fault system (McMechan, 1986), which lies outside the area mapped.

This domain is underlain by Cambrian quartzites and carbonate rocks that are predominantly medium to thick

Plate 1-6-9. Upright to overturned folds in Upper Devonian strata, northeast of Kakwa Lake. The recessive Perdrix Formation (dPx) is exposed at the base of the cliffs and is overlain by the cliff-forming Mount Hawk and Simla formations (dSMh) that cannot be easily differentiated in this section. The Palliser Formation (dP) is exposed at the top of the ridge; a slightly more recessive unit at the base of the Palliser forms a slight step above the Simla and Mount Hawk strata.

bedded and quite competent. Proterozoic Miette Group strata are exposed, in a number of locations, in the immediate hangingwall of the east-bounding faults. The dominant structures in this part of the area are open folds and broad warps with east or southeast-trending axial traces and northerly directed thrusts with east to east-southeast traces. Normal faults are also prominent within this block, particularly in the southwestern area, near Mount Sir Alexander. Most strike westerly and southwesterly. Small drag folds are often associated with the normal faults. The east-west structural trends within this domain are anomalous on a regional scale.

ECONOMIC GEOLOGY

Coal

Coal licenses are held in the northeastern corner of Kakwa Recreation Area, covering the ridge south of Mount Gorman. This area is underlain by a shallow, south-dipping sequence of Lower Cretaceous strata that contains four significant coal seams. The lowest seam is reportedly 2.4 to 3 metres thick and occurs at the top of the Gething Formation. The overlying Gates Formation, the top of which has been eroded, hosts three seams that were trenched in the late 1970s and are reported to be 1.8 to 2.7, 3.6 to 6, and 5.5 to 6 metres thick, respectively (Pribyl, 1979). The coal-bearing strata cap the ridge and the seams, which contain an estimated 4 to 4.5 million tonnes of coal, could be exploited at stripping ratios of between 1:1 and 15:1 (Pribyl, 1979).

Coal seams also occur within the Lower Cretaceous Minnes Formation in the Mount Minnes and Mount Gorman areas, in the northeastern part of the Kakwa area. Several seams are present, particularly in the upper part of this formation; however, they are generally less than 1 metre thick and not of serious economic interest under current conditions.

Dimension Stone

Quartzites of the Lower Cambrian Mahto Formation, that crop out in the centre of Kakwa Recreation Area near Babette and Wishaw lakes, were examined in the late 1970s and early 1980s for their potential use as dimension stone.

At that time, roads were extended to the prospects from existing logging roads in the McGregor River valley. At Babette Lake the strata were drilled, while at Wishaw Lake an attempt was made to quarry test blocks. The only mineral claims currently held within the recreation area cover these stone prospects.

The Mahto Formation, at the Babette Lake prospect, consists of fine to medium-grained, locally crossbedded quartzites that vary from creamy white to dark maroon in colour; some beds are uniform in colour, while others have quite attractive colour banding. Some of the colour banding is parallel to sedimentary laminations and crosslaminae and may reflect a depositional feature, however, much of the banding appears to be unrelated to original sedimentary features and forms intricately swirled patterns that may be related to solution fronts (Plate 1-6-2). Beds slightly more than a metre thick are common. Large blocks, in the 1 to 2 cubic metre size range, are found in talus beneath cliff outcrops. At Wishaw Lake, the Mahto quartzites are creamy white or beige to light pink in colour; most of the colour banding at this location is parallel to laminations and crosslaminations. Bedding thicknesses range from 50 centimetres to just over a metre; beds up to 2 metres thick are reported (Hora, 1984). Quarried blocks, 2 to 2.5 cubic metres in size, are present on site, however, there are no blocks in the size range preferred by industry (1.4x1.6x3 m) on site at this time.

When cut into slabs and polished, the quartzite from these prospects has a colour and textural qualities comparable to high-quality, commercially exploited marble and strength comparable to high-quality granite (Hora, 1984). Due to the extreme hardness of this material, however, it is more difficult and hence, more expensive to finish than either marble or granite. Also of concern, is the variable porosity of these quartzites. In some places, the rock is well cemented and has low porosity, while in others it is quite porous, stains easily and would not produce an acceptable product unless treated with some type of sealant coating to reduce staining. The distribution of porous, and therefore, less desirable material within these prospects has not been documented (Z.D. Hora, personal communication, 1991).

PHOSPHATE

Phosphorite beds are found within the Whistler Member of the Triassic Sulphur Mountain Formation at three locations around Kakwa. In the northern part of the area mapped, near the boundary of the recreation area, phosphatic rocks occur near the core of a syncline in the Sulphur Mountain Formation (Figure 1-6-2). At this location, the phosphatic horizon is 10 to 15 centimetres thick and is exposed in a rubbly outcrop associated with calcareous siltstones and silty limestones. The phosphorite is dark grey or bluish to white weathering, with a dark brown to black fresh surface. It has a gritty texture, a petroliferous odor and contains abundant ammonite and pelecypod fossils. Purple fluorite is present as veinlet infillings and fracture coatings. Grab samples of these phosphorites contained 21 to 23 per cent P_2O_5 (Samples 1097A and B, Table 1-6-2).

To the east of this occurrence, on the east limb of the adjacent anticline, phosphatic rocks again outcrop. At this locality, approximately 12 centimetres of phosphate rock overlies thin to medium-bedded, grey argillaceous limestone and calcareous siltstone. The phosphate horizon is black to dark brown in colour, has a nodular texture and contains abundant ammonite fossils. It is overlain by 90 centimetres of grey, silty limestone, which is, in turn, overlain by 18 centimetres of phosphatic shale and siltstone. Sixteen centimetres of very fissile black shales overlie the phosphatic shale and the sequence is capped by more grey limestones. The lower nodular and fossil-rich phosphate horizon is moderately high grade, containing approximately 22 per cent P_2O_5, while the upper horizon of phosphatic shales and siltstones contains between 8 and 11 per cent P_2O_5 (Samples 1091 and 1094, Table 1-6-2). The entire phosphatic interval is only 1.2 metres thick in this area and limestones comprise a greater proportion of it than do phosphorites and phosphatic shales.

A third phosphate occurrence was found in the southeastern corner of Kakwa Recreation Area, near Intersection Mountain. It outcrops on a cliff face and is estimated to be no more than a metre in thickness. Nodular and fossiliferous phosphorites with fluorite-coated fracture surfaces were found in talus beneath the outcrops. Grab samples from this area contain between 18 and 20 per cent P_2O_5 (Samples 1251A and B, Table 1-6-2).

TABLE 1-6-2
ANALYSES OF TRIASSIC PHOSPHORITES

Sample	Sample Type/ Thickness	P_2O_5 %	Lithology	Location
1079A	Grab/Bulk	23.12	Fossiliferous P_2O_5	North Ridge-West
1079B	Grab	21.77	P_2O_5 w/fossils & fluorite	North Ridge-West
1091A	Grab	10.97	Phosphatic shale	North Ridge-East
1091B	Grab	8.04	Impure P_2O_5, silty w/fossils	North Ridge-East
1094A	12 cm	22.58	Nodular P_2O_5 w/fossils	North Ridge-East
1094B	18 cm	9.40	Phosphatic shale	North Ridge-East
1251A	Grab	18.70	Nodular phosphate	Intersection Mt.
1251B	Grab	20.06	P_2O_5 w/fossils & fluorite	Intersection Mt.

P_2O_5 analyzed by gravimetric assay method

CARBONATE-HOSTED VEIN AND REPLACEMENT SHOWINGS

Vein and replacement showings in carbonate rocks, although not common in the Kakwa area, were discovered in six locations. Southeast of Mount Ida, an orange-weathering, irregular dolomitized zone is exposed in light grey limestones near the top of the Middle Cambrian Snake Indian Formation. Coarse-grained dolomite occurs in veins and solution-collapse breccia infillings within the dolomitized rocks. Small shear zones, dominantly consisting of fine-grained calcite, are also present in this area. To the west of Mount Ida, an irregular zone of altered and recrystallized dolomite, cut by coarse-grained dolomite veins, occurs within limestones of the Middle Cambrian Eldon Formation. No evidence of potentially economic commodities, such as lead, zinc or magnesite was found in either area (Table 1-6-3), although correlative strata in southeastern British Columbia are known to host economic deposits in similar environments (Grieve and Höy, 198 ; Simandl and Hancock, 1991).

In the southern part of the area, southeast of Mount Buchanan, coarse-grained dolomite occurs in veins and open-space fillings in a brecciated zone within Ordovician Skoki dolostones. East-northeast of Mount Buchanan coarse-grained calcite veins containing minor amounts of barite cut irregularly dolomitized zones in Upper Devonian Mount Hawk limestones. These veins are narrow and appear to be barren; they are not particularly widespread (Table 1-6-3).

Barite veins and replacement zones, over a metre wide, were found in Rundle Group carbonate rocks at two locations, near the upper part of the unit. One site is in the northernmost part of the area mapped, approximately 2 kilometres north of the recreation area boundary and the other is near Moonias Mountain, north of Jarvis Lakes. In both localities, the veins consist predominantly of coarse-grained white barite; at the northern location carbonate inclusions and rusty vugs are common within the vein. Samples collected from these veins did not contain appreciable amounts of base metals (Table 1-6-3); however, the rusty material from the northern locality could not be adequately sampled and in both cases the material analyzed was predominantly pure barite. The Belcourt zinc prospect, located approximately 6 kilometres north of the recreation area, occurs in the same stratigraphic position and also consists of barite veins with patchily distributed zinc mineralization. This showing is reported to contain up to 2 per cent zinc (Lenters, 1980); grab samples of gossanous material and altered dolomitic wallrock, collected during a brief visit to the showing, contain 0.35 and 0.65 per cent zinc, respectively, while baritic vein material does not contain appreciable zinc values (Table 1-6-3).

Quartzite-Hosted Vein Showings

Quartz veins containing pyrite or associated with pyritic alteration halos were found in Lower Cambrian quartzites at two locations. A few kilometres south of Mount Ida, pyritic quartz veins associated with rusty, pyritic alteration halos cut McNaughton Formation strata. North of Kitchi Mountain, irregular quartz-pyrite veins, with alteration halos that locally contain 50 to 70 per cent pyrite occur within the Mahto Formation. No gold or base metals were noted in the limited samples collected from these veins (Table 1-6-3) even though veins in similar rocks, south of Jasper, are known to carry gold (Shaw and Morton, 1990).

Stratiform Sulphides

Apparently stratiform massive sulphide mineralization was found in fine-grained sandstones of the Permian Mowich Formation at two locations. Near Moonias Mountain, approximately 3.5 kilometres north of Jarvis Lakes, beds of pyrite 1 to 3 centimetres thick were discovered. In the southern part of the area, near Intersection Mountain, a gossanous zone, approximately 6 metres thick and 20 metres in strike length, occurs in what should be Mowich strata. In the same area, pieces of dark, bituminous sandstone containing up to 40 per cent pyrite were found in float beneath Mowich outcrops. Samples of pyrite-rich sandstones contain anomalous concentrations of zinc, up to 0.7 per cent (Table 1-6-3). Zinc mineralization in Permian sandstones has also been reported from the Belcourt showing, a few kilometres north of Kakwa (Lenters, 1980).

TABLE 1-6-3
CHEMICAL ANALYSES OF VEIN, REPLACEMENT AND STRATIFORM OCCURRENCES

SAMPLE	Au ppb	Ag ppm	Cu ppm	Pb ppm	Zn ppm	Fe %	DOMINANT MINERALS	LOCATION
Carbonate-hosted vein-replacement showings in Rundle Group strata								
1071	na	<0.2	2	<2	13	0.04	barite	North Ridge
2028	na	<0.2	<1	<2	12	0.04	barite	2.5 k N of Jarvis Lakes
BEL1	na	4.2	30	40	6462	1.24	dolomite	6 k N of Kakwa Rec. Area
BEL2	na	<0.2	<1	33	3549	>10.00	goethite	6 k N of Kakwa Rec. Area
BEL3	na	0.2	2	<2	43	0.32	barite	6 k N of Kakwa Rec. Area
Carbonate-hosted vein-replacement showings in other units								
1124A	na	<0.2	2	<2	<1	0.70	dolomite	4 k SE of Mt. Ida
1124B	na	<0.2	3	4	<1	0.75	calcite	4 k SE of Mt. Ida
1160	na	<0.2	2	<2	<1	0.30	dolomite	6 k W of Mt. Ida
1186A	na	0.2	2	<2	<1	0.10	calcite	3 k ENE of Mt. Buchanan
1186B	na	<0.2	1	<2	<1	0.02	barite	3 k ENE of Mt. Buchanan
2124	na	<0.2	2	4	<1	0.94	dolomite	3 k SE of Mt. Buchanan
Quartzite-hosted vein-replacement showings								
1100	6	<0.2	4	7	21	3.71	qz/py	3 k S of Mt. Ida
2078	6	<0.2	5	12	5	>10.00	pyrite	2 k N of Kitchi Mt.
Stratiform mineralization								
1252	6	<0.2	25	15	7190	5.98	pyrite	3.5 k N of Jarvis Lakes
1253	<5	<0.2	8	8	717	6.90	pyrite	Intersection Mountain
2164	<5	<0.2	6	13	1890	>10.00	goethite	Intersection Mountain

na = not analyzed; Au analyzed by fire assay with atomic absorption finish; all other elements analyzed by inductively coupled plasma technique, using HNO_3-HCl hot extraction.

DISCUSSION AND CONCLUSIONS

The Kakwa Recreation Area is underlain by strata which range in age from Late Precambrian to Early Cretaceous. The area can be divided into three domains with distinct stratigraphy and structural styles, bounded by major thrust faults. The eastern domain is underlain by Mesozoic rocks, predominantly shales and thin-bedded sandstones, and characterized by small, disharmonic chevron folds. The central domain predominantly contains middle and upper Paleozoic carbonate rocks with thick intervening shale units. Map-scale folds, which are common in this domain, are generally tight, upright to overturned structures that display some degree of disharmony between carbonate and shale-dominated sequences. Minor thrusts and normal faults are also present in this domain. The western domain contains thick-bedded lower Paleozoic quartzites and carbonate rocks and is characterized by broad open folds, small thrusts and abundant normal faults. Easterly structural trends are common in this domain, whereas the other two domains are dominated by northwesterly trends, more typical of the regional structures. The difference in structural styles between the three domains is largely controlled by the differences in competency and competency contrasts of the rock units. The east-west structural trends in the western domain represent a regional anomaly that may, in part, be related to the original shape of the sedimentary basin, where an anomalously thick section of Cambrian rocks was deposited on the south flank of the Peace River arch (McMechan, 1990).

A number of commodities of potential economic interest occur within Kakwa Recreation Area, including coal, phosphate, dimension stone, barite and zinc. Four thick coal seams occur in an erosional remnant of Lower Cretaceous strata that caps a small ridge in the northeastern corner of the area. The seams are up to 6 metres thick; however, they are of limited extent and constitute a fairly small tonnage of recoverable reserves. The phosphorite occurrences that were found within the recreation area, although worthy of note, are far too thin to be of economic interest at the present time. Approximately 50 kilometres to the north, in the Wapiti Lake area, phosphatic strata in the Sulphur Mountain Formation are reportedly up to 3.2 metres thick (Butrenchuk, in preparation; Legun and Elkins, 1986), which suggests that this interval does have potential and should not be overlooked.

Quartzite strata near the centre of the recreation area have been examined for their potential use in the building stone industry. They are very attractive rocks with colourful maroon, pink and cream banding and laminations; when cut and polished they produce a product comparable in appearance to commercially exploited marbles and in strength, to good quality granite. There are a number of problems with this stone, in some areas the rock is very porous and easily takes a permanent stain. If the showings were to be quarried, the porosity distribution would have to be mapped out and only the well-cemented material used, or the porous material coated with a sealant to reduce potential staining problems, which would increase costs. It is also doubtful whether large blocks of the size preferred by industry can be produced from the prospective sites. In some cases, smaller blocks might be utilized but again, this would result in increased costs. Distance to existing fabricating plants is another concern: trucking costs from the Kakwa area would be extremely high and a significant amount of road improvement would be necessary prior to shipping any material.

Zinc and barite showings occur near the upper contact of the Carboniferous Rundle Group and in the overlying Permian Mowich Formation in a number of locations within and immediately north of Kakwa. The barite occurs in veins and replacement zones approximately 1 metre wide within Rundle Group carbonate rocks; it is coarse grained and white in colour. In some areas, particularly to the north of the area, the barite veins cut extremely altered hostrocks and contain rusty vugs or gossanous (sulphide-rich) inclusions with anomalous zinc contents. Apparently stratiform sulphide mineralization occurs locally in the Permian sandstones that overlie the Rundle Group. These stratiform sulphides carry some zinc and may be related to the same system that produced the barite veins. The rocks straddling the Carboniferous-Permian boundary have some potential and should be prospected in more detail.

ACKNOWLEDGMENTS

We would like to thank Rolf Schmidt, Mineral Policy Branch, for doing the preliminary organization and budget for this project and the Ministry of Environment, Lands and Parks for providing the funding. Victor Koyanagi kindly provided assistance at the end of the field season. This paper has benefited from critical review by Bill McMillan and John Newell. Special thanks go to Bob Batchelor, Northern Mountain Helicopters, for providing us with excellent logistical support, good company and generally helping out in ways beyond the normal call of duty!

REFERENCES

Bamber, E.W. and Macqueen, R.W. (1979): Upper Carboniferous and Permian Stratigraphy of the Monkman Pass and Southern Pine Pass Areas, Northeastern British Columbia; *Geological Survey of Canada*, Bulletin, 301, 27 pages.

Butrenchuk, S.B. (in preparation): Phosphates in British Columbia; *B.C. Ministry of Energy, Mines and Petroleum Resources*, Open File.

Campbell, R.B., Mountjoy, E.W. and Young, F.G. (1973): Geology of the McBride Map-area, British Columbia; *Geological Survey of Canada*, Paper 72-35, 104 pages.

Geldsetzer, H.H.J. (1982): Depositional History of the Devonian Succession in the Rocky Mountains, Southwest of the Peace River Arch; *in* Current Research, Part C, *Geological Survey of Canada*, Paper 82-1C, pages 55-64.

Gibson, D.W. (1972): Triassic Rocks of the Pine Pass - Smoky River Area, Rocky Mountain Foothills and Front Ranges of British Columbia and Alberta; *Geological Survey of Canada*, Paper 71-30, 108 pages.

Gibson, D.W. (1975): Triassic Rocks of the Rocky Mountain Foothills and Front Ranges of Northeastern British

Columbia and West-central Alberta; *Geological Survey of Canada*, Bulletin 247, 61 pages.

Grieve, D.A. and Höy, T. (1981): Lead-Zinc Showings in Carbonate Rocks, Southern Rocky Mountains; *in* Geological Fieldwork 1980, *B.C. Ministry of Energy, Mines and Petroleum Resources*, Paper 1981-1, pages 105-110.

Hora, Z.D. (1984): Industrial Minerals and Structural Materials; *in* Geological Fieldwork 1983, *B.C. Ministry of Energy, Mines and Petroleum Resources*, Paper 1984-1, pages 213-218.

Legun, A. and Elkins, P. (1986): Wapiti Syncline Phosphate Potential; *in* Geological Fieldwork 1985, *B.C. Ministry of Energy, Mines and Petroleum Resources*, Paper 1986-1, pages 151-153.

Lenters, M.H. (1980): Report on Geological Mapping, Prospecting, Trenching and Geochemical Sampling, Belcourt Claims, Liard Mining Division; *B.C. Ministry of Energy, Mines and Petroleum Resources*, Assessment Report 8404, 26 pages.

McMechan, M.E. (1986): Geology of the Northeast McBride Map-area (93H/15, 16), British Columbia; *Geological Survey of Canada*, Open File 1229.

McMechan, M.E. (1990): Upper Proterozoic to Middle Cambrian History of the Peace River Arch: Evidence from the Rocky Mountains; *Bulletin of Canadian Petroleum Geology*, Volume 38A, pages 36-44.

McMechan, M.E. and Thompson, R.I. (1985): Geology of Southeast Monkman Pass Area (93I/SE), British Columbia; *Geological Survey of Canada*, Open File 1150.

Mountjoy, E.W. and Aitken, J.D. (1978): Middle Cambrian Snake Indian Formation [New], Jasper Region, Alberta; *Bulletin of Canadian Petroleum Geology*, Volume 26, Number 3, pages 343-361.

Pell, J. and Hammack, J.L. (1992): A New Triassic Fossil Fish Locality, Kakwa Recreation Area, Northeastern British Columbia (93I/1); *in* Geological Fieldwork 1991, Grant, B. and Newell, J.M., Editors, *B.C. Ministry of Energy, Mines and Petroleum Resources*, Paper 1992-1, (this volume).

Pribyl, A. (1979): Preliminary Report on the Geology of the Mt. Gorman and Coal Ridge Area B.C. Coal Licenses; *B.C. Ministry of Energy, Mines and Petroleum Resources*, Open File Coalfile Report 00549, 17 pages.

Shaw, R.P. and Morton, R.D. (1990): Gold Mineralization in Lower Cambrian McNaughton Formation, Athabasca Pass, Canadian Rocky Mountains: Structural, Mineralogical and Temporal Relationships; *Canadian Journal of Earth Sciences*, Volume 27, pages 477-493.

Simandl, G.J. and Hancock, K.D. (1991): Geology of the Mount Brussilof Magnesite Deposit, Southeastern British Columbia; *in* Geological Fieldwork 1990, *B.C. Ministry of Energy, Mines and Petroleum Resources*, Paper 1991-1, pages 269-278.

Slind, O.L. and Perkins, G.D. (1966): Lower Paleozoic and Proterozoic Sediments of the Rocky Mountains between Jasper, Alberta and Pine River, British Columbia; *Bulletin of Canadian Petroleum Geology*, Volume 14, No. 4, pages 442-468.

Taylor, G.C. and Stott, D.F. (1979): Geology of Monkman Pass Map-area (93I), Northeastern British Columbia; *Geological Survey of Canada*, Open File 630.

TRIASSIC FOSSIL FISH FROM THE SULPHUR MOUNTAIN FORMATION, KAKWA RECREATION AREA, NORTHEASTERN BRITISH COLUMBIA (93I/1)

By J. Pell and J.L. Hammack
Geological Consultants

KEYWORDS: Vertebrate paleontology, Triassic fossil fish, Kakwa Recreation Area, Wapiti Lake, Osteichthyes, ganoid fish, holosteans, coelacanths.

INTRODUCTION

Fossil fish have been known from the Triassic Sulphur Mountain Formation in western Canada since the beginning of this century, with the first specimens found at a locality near Banff, Alberta (Lambe, 1914, 1916). In 1947, fish fossils were discovered near Wapiti Lake, in northeastern British Columbia (Figure 1-7-1), by a group of researchers from the University of Wisconsin (Laudon *et al.*, 1949). Since that time, a number of expeditions have visited the Wapiti Lake area, which has proved to be a prolific collecting locality. More than one thousand specimens, many of which are articulated, representing 16 genera have been recovered and three distinct faunas recognized. Commercial collecting occurred in the area in the past; however, it is now considered a Provincial Heritage Site and is protected. Six sites from which fossiliferous material was collected *in situ* have been identified within a belt 2.5 kilometres long, south of Wapiti Lake; however, a single site in this area has produced most of the specimens (Brinkman and Neuman, 1987; Neuman, in press; Schaeffer and Mangus, 1976). Ichthyosaur reptiles were also found at four of the six sites (Callaway and Brinkman, 1989).

A second Triassic fossil fish locality in British Columbia, located approximately 50 kilometres south-southeast of Wapiti Lake, was encountered in Kakwa Recreation Area during the course of a mineral potential study, conducted in the summer of 1991 (Pell *et al.*, 1992, this volume). It was originally found by Dr. Barry Richards of the Geological Survey of Canada in the early 1980s (A. Neuman and B. Richards, personal communication, 1991), but has not previously been reported on. The area is remote and access is most easily attained by helicopter. Because of its location within a Provincial Recreation Area, the site is protected and open only to scientific study by application to the British Columbia Ministry of Environment, Lands and Parks.

A number of articulated specimens and numerous fossil fragments were collected during brief visits to the site. All samples were found on a scree slope beneath outcrops of the Sulphur Mountain Formation or in loose blocks scattered amongst the outcrop. In this vicinity, the Sulphur Mountain Formation is exposed in steep to cliffy outcrops that are flaggy weathering and unstable. Little time was spent on the outcrops themselves, due to their hazardous nature and, as a result, no fossils were found *in situ*.

GEOLOGICAL SETTING

The Sulphur Mountain Formation is exposed in a northwest-trending belt (Figure 1-7-1) that extends from north of Wapiti Lake, through Kakwa Recreation Area into Alberta, to the southeast of Kakwa (McMechan, 1986; McMechan and Thompson, 1985; Taylor and Scott, 1979). It is a moderately resistant, characteristically dark reddish brown to brownish orange weathering unit that unconformably overlies black, lichen-covered sandstones of the Permian Mowich Formation and is conformably overlain by buff and grey carbonate rocks of the Late Triassic Whitehorse Formation. The Sulphur Mountain Formation has been subdivided into the Vega-Phroso, Whistler and Llama members, in ascending order (Table 1-7-1).

In the Kakwa area, the Vega-Phroso siltstone member is 245 to 270 metres thick and comprises a shaley to flaggy weathering sequence of dolomitic and calcareous siltstone, fine-grained sandstone, silty limestone and shale that ranges in age from Early Triassic Griesbachian to Spathian (Gibson, 1975). It is platey near the base and becomes increasingly flaggy up-section. Ammonites are locally common within this member. However, they are generally poorly preserved, occurring as faint imprints on bedding planes. Well-preserved ammonites were rare finds (Plate 1-7-1). Chondrichthyian spines (*cf. Listracanthus* sp.) are common in some strata (Plate 1-7-2) and are believed to represent some part of the skin of ancient sharks (A. Neu-

TABLE 1-7-1
PERMIAN AND TRIASSIC STRATIGRAPHY

	Formation	Member	Stage	Series
SPRAY RIVER GROUP	Whitehorse Formation	Starlight Evaporite	Carnian	Late Triassic
	Sulphur Mountain Formation	Llama	Ladinian	Middle Triassic
		Whistler	Anisian	
		Vega-Phroso Siltstone	Spathian	Early Triassic
			Smithian	
			*Din/Grsb	
		unconformity		
	Mowich			Permian

*DIN/Grsb = Dienerian & Griesbachian
Table modified from Gibson, 1975

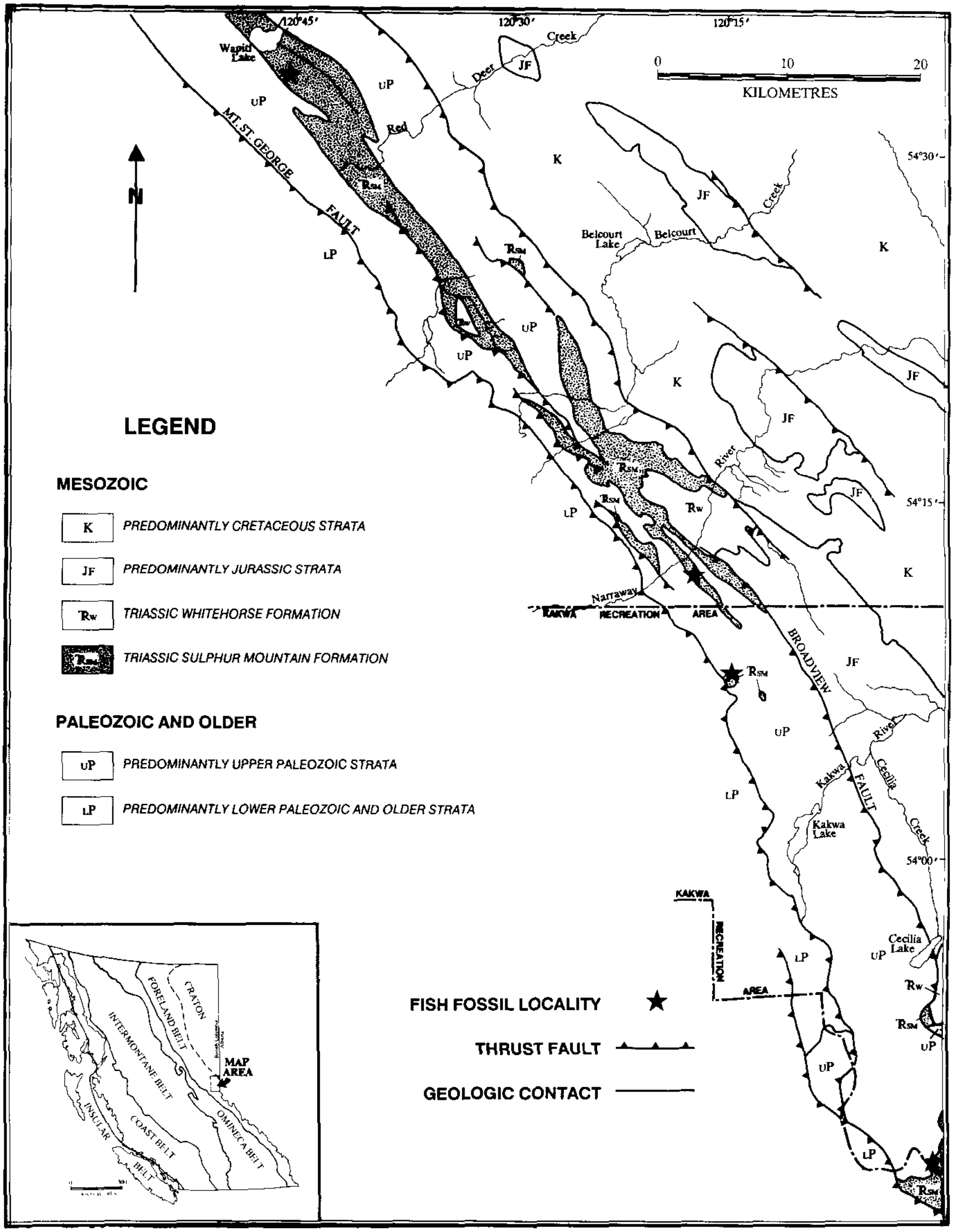

Figure 1-7-1. Distribution of Triassic Sulphur Mountain Formation strata in northeastern British Columbia.

Plate 1-7-1. Ammonite, from the Sulphur Mountain Formation in Kakwa. Such well-preserved specimens are a rarity in this area.

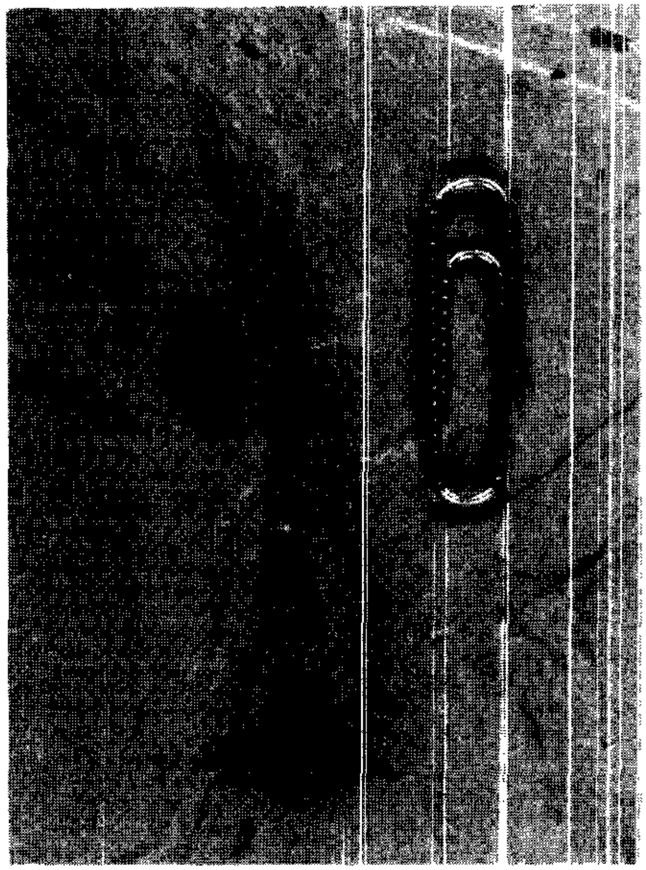

Plate 1-7-2. Chondrichthian spine (cf. *Listracanthus* sp.); such spines are believed to represent some part of the "skin" (shagreen is the correct term) of ancient sharks (paper clip scale is 3 centimetres).

man, personal communication, 1991). Pelecypods were also noted in some sections. Moderately well preserved fish fossils were found at one locality and fragmented fish were found in two other areas (Figure 1-7-1). Fish-bearing strata are estimated to be approximately 30 to 50 metres above the base of the section and probably correlate with similar strata in the Wapiti Lake area, which are Smithian in age (Schaeffer and Mangus, 1976; Tozer, 1967).

The Whistler Member, of Middle Triassic Anisian age, where present, is generally 10 to 20 metres thick and consists of dark grey to black-weathering siltstone, silty limestone, silty shale, dolostone, phosphorite and phosphatic pebble conglomerate (Gibson, 1975). Ammonites, pelecypods and, locally, brachiopods occur in this member and are commonly phosphatic. The Llama Member is characterized by relatively resistant, orange-brown-weathering, thin to thick-bedded dolomitic quartz siltstones, silty limestones and dolostones that contain pelecypods, rare ammonite fossils and, locally, reptile bones. It ranges from Middle Triassic late Anisian to late Ladinian in age. Where it occurs, it is approximately 150 to 185 metres thick.

At the best fossil fish site, only the Vega-Phroso siltstone member is exposed It overlies light grey quartz arenites of the Mowich Formation that locally form small cliffs at the base of the outcrop, above a talus slope. The upper members are eroded away or truncated by a northeasterly directed thrust fault that is located west of the main outcrop area (Pell *et al.*, 1992, this volume). The base of the exposed section is dark brown to grey-brown-weathering and very fissile to platey; flaggy, buff to orange-weathering calcareous siltstone layers crop out a few tens of metres above the base of the section. The ridge is steep and only the basal beds were examined closely.

Fish fossils were generally found on buff to orange-weathering slabs of calcareous siltstone that varied from 2 to 30 centimetres in thickness, scattered in the talus beneath the outcrop. Fossils were also found on relatively fresh, chocolate to dark grey-brown siltstone slabs. No fossil fish were observed in the basal, fissile shaley beds it is probable that they are derived from the thicker, flaggy weathering beds higher in the section.

THE FOSSIL FISH

Seven genera of fish, belonging to the Class Osteichthyes (bony fish) have been identified to date, from the Sulphur Mountain Formation in Kakwa Recreation Area (A. Neuman, personal communication, 1991). Since their first appearance in Early Devonian freshwater deposits, there have been two major groups of bony fish the subclass

Plate 1-7-3. *Bobasatrania canadensis;* complete specimen with distinct vertebral column. Specimen is 17 centimetres long (paper clip scale is 3 centimetres).

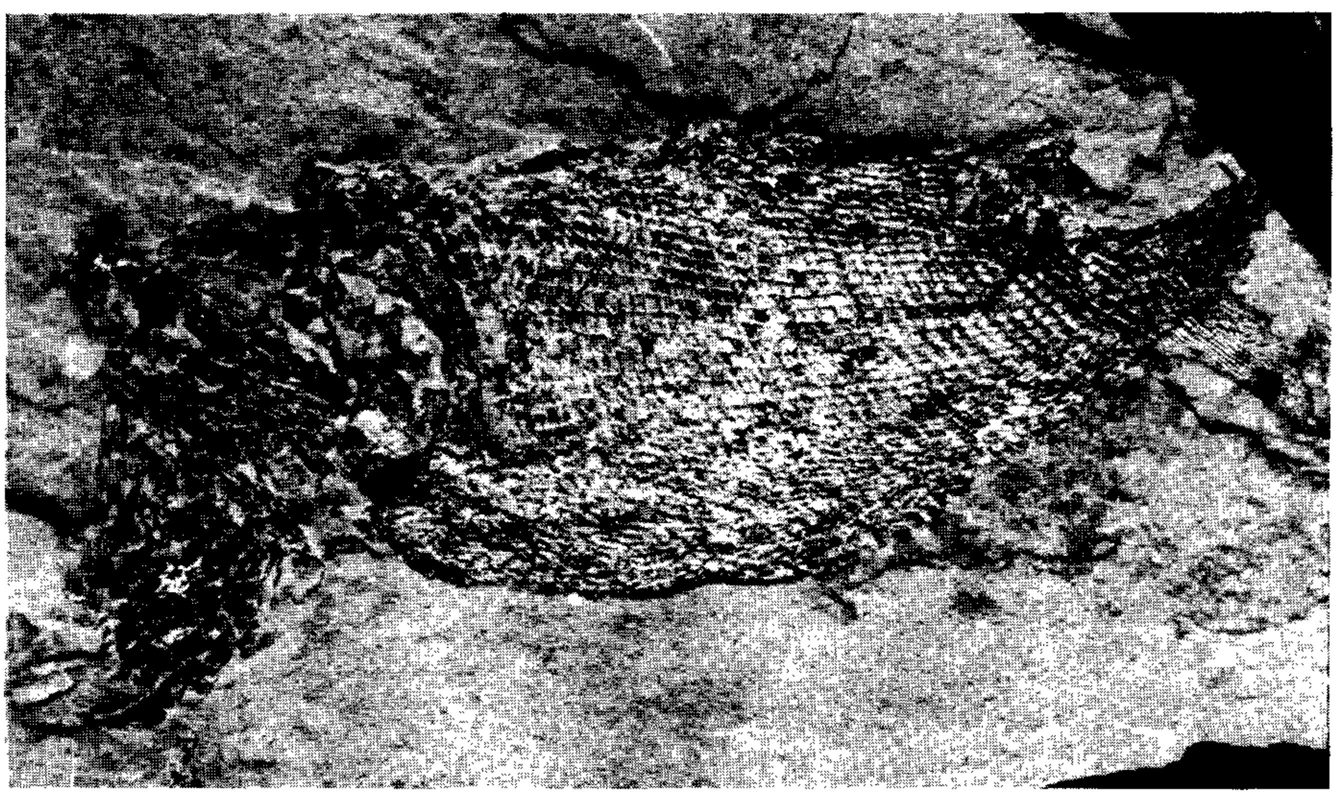

Plate 1-7-4. *Boreosomus* sp.; near-complete specimen; fins, other than caudal (tail) are missing. Specimen is approximately 25 centimetres long.

Actinopterygii, or ray-finned, and the subclass Sarcopterygii, or fleshy finned (Table 1-7-2). The fin structure is fundamentally different in these two subclasses, as implied by their names. Ray-finned fish have fan-like fins with thin, bony rods for support, like most of the modern fish with which we are familiar, while the fleshy or lobe-finned fishes have stout fins with a strong internal skeleton and muscles (Dodson and Dodson, 1976). Both subclasses are represented in the Triassic deposits from Kakwa.

Ray-finned fish can be further subdivided into infraclasses Chondrostei and Neopterygii (Table 1-7-2). Chondrosteans, or ganoid fish, generally have cartilaginous skeletons, a vertebral column that is upturned at the posterior end and a tail with a heterocercal structure (*i.e.* asymmetrical with a larger upper lobe). They are characterized by the possession of heavy, rhombic, enamel-coated ganoid scales that fit together edge to edge, with very little overlap, and form a heavy, stiff armour. Lungs were present to supplement the gills and jaw muscles were generally small and weak. Many of the more primitive members, such as the Palaeonisciformes, also had well-ossified (bony) skulls. Chondrosteans were common until the end of the Triassic; only a few specialized members of this group, such as the sturgeon (*Acipenser* and *Scaphirhynchus*) and spoonbills (*Polyodon*), have survived to the present (Dodson and Dodson, 1976).

Four genera of ganoid fish (Table 1-7-2) have been identified from the Kakwa area, *Bobasatrania*, *Boreosomus*, *Australosomus* and *Saurichthys*. The first two genera are typical or "primitive" chondrosteans, while the latter two are more advanced and sometimes referred to as "subholosteans" (A. Neuman, personal communications 1991). One of the more common genera found at Kakwa was *Bobasatrania;* some of the most distinctive and best-preserved specimens are examples of this genus. *Bobasatrania* has a distinctive "diamond" shape and exhibits many of the typical chondrostean features such as the curved vertebral column with an upturned end and the asymmetrical tail (Plate 1-7-3). Most good specimens are 15 to 20 centimetres in length; however, pieces of individuals that may belong to this genus, measuring up to a metre in size, were found. Members of the other genera were uncommon; only one specimen of *Boreosomus* (Plate 1-7-4) and rare examples of the other taxa were found.

Members of infraclass Neopterygii first appeared in the Permian. One line, the holosteans, became dominant in the Triassic, but by the Cretaceous, had passed their peak and were on the decline toward their present low numbers (there are only two surviving members of this group, *Amia*, the bowfin and *Lepisosteus*, the garpike). The holosteans had more efficient jaw leverage than chondrosteans and had swim-bladders rather than lungs. Their vertebral columns

TABLE 1-7-2
CLASSIFICATION OF FISHES, INCLUDING TAXA FOUND IN KAKWA RECREATION AREA

PHYLUM:				CHORDATA			
SUBPHYLUM:				VERTEBRATA			
Superclass:				PISCES			
Class:	Agntha (Ord. to Perm. & Present) Jawless fish (lampreys)	Placodermi (Devonian & Carboniferous) Jawed, armoured fish	Chondrichthyes (Devonian to Present) Sharks	Osteichthyes (Dev. to Present) Bony fish			
Subclass:				Actinopterygii Ray-finned fish		Sarcopterygii Fleshy/lobe-finned	
Infraclass:				Chondrostei (E. Devonian >>) Ganoid fish	Neopterygii (Permian >>) Holosteans & Teleosts (Modern fish)	Crossopterygii (E. Devonian >> Rhipidistans & Coelacanths	Dipnoi (E. Dev. >>) Lungfish
Order Family *Genus:*				Paleonisciformes Boreosomidae *Boreosomus* Bobasatraniidae *Bobasatrania*	Parasemionotiformes Parasemionotidae *Watsonulus* *Albertonia*	Coelacanthiformes Coelacanthidae *Whiteia*	
				Pholidopleuriformes Pholidopleuridae *Australosomus*			
				Saurichthyiformes Saurichthyidae *Saurichthys*			

Modified from Dodson and Dodson, 1976 and Andy Neuman, personal communication, 1991.

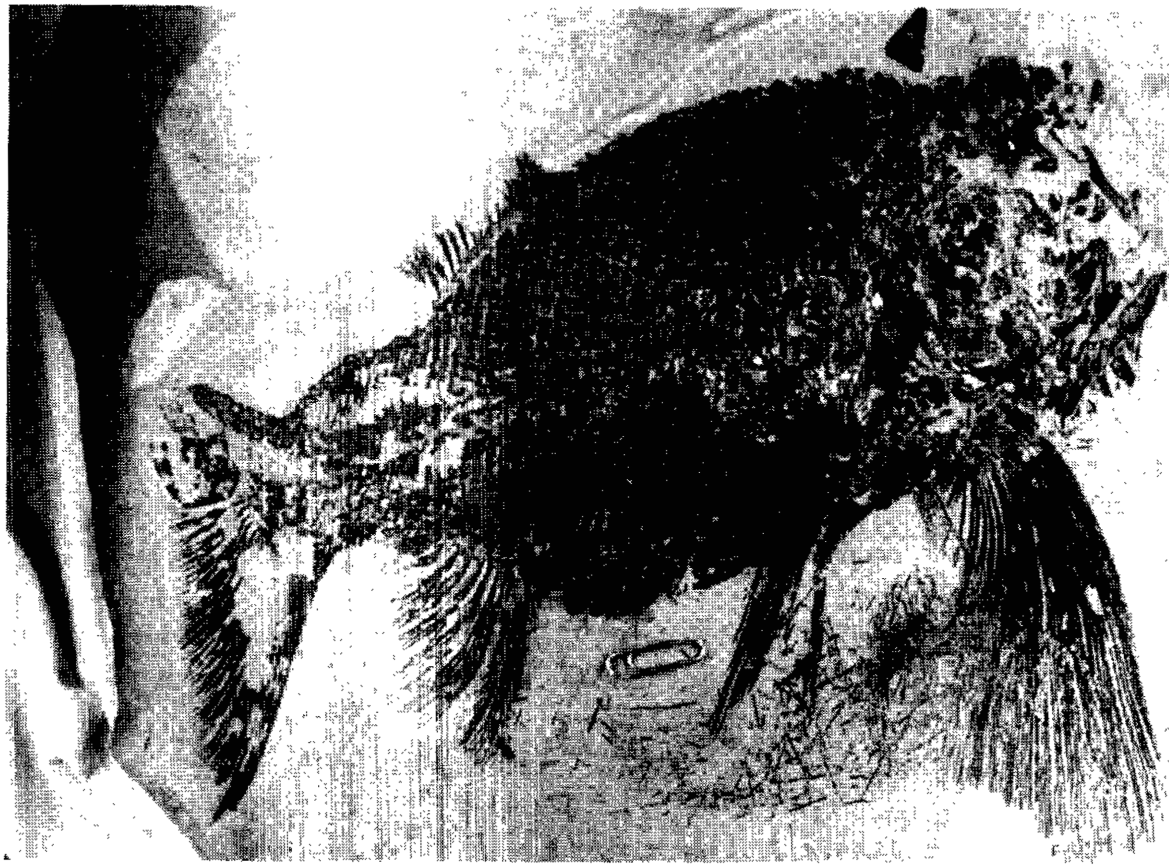

Plate 1-7-5. *Albertonia cupidinia;* near-complete fish with well-developed pectoral fin and poorly preserved skull. Note distinctive, well-preserved ganoid scales. Specimen is 33 centimetres long (paper clip scale is 3 centimetres).

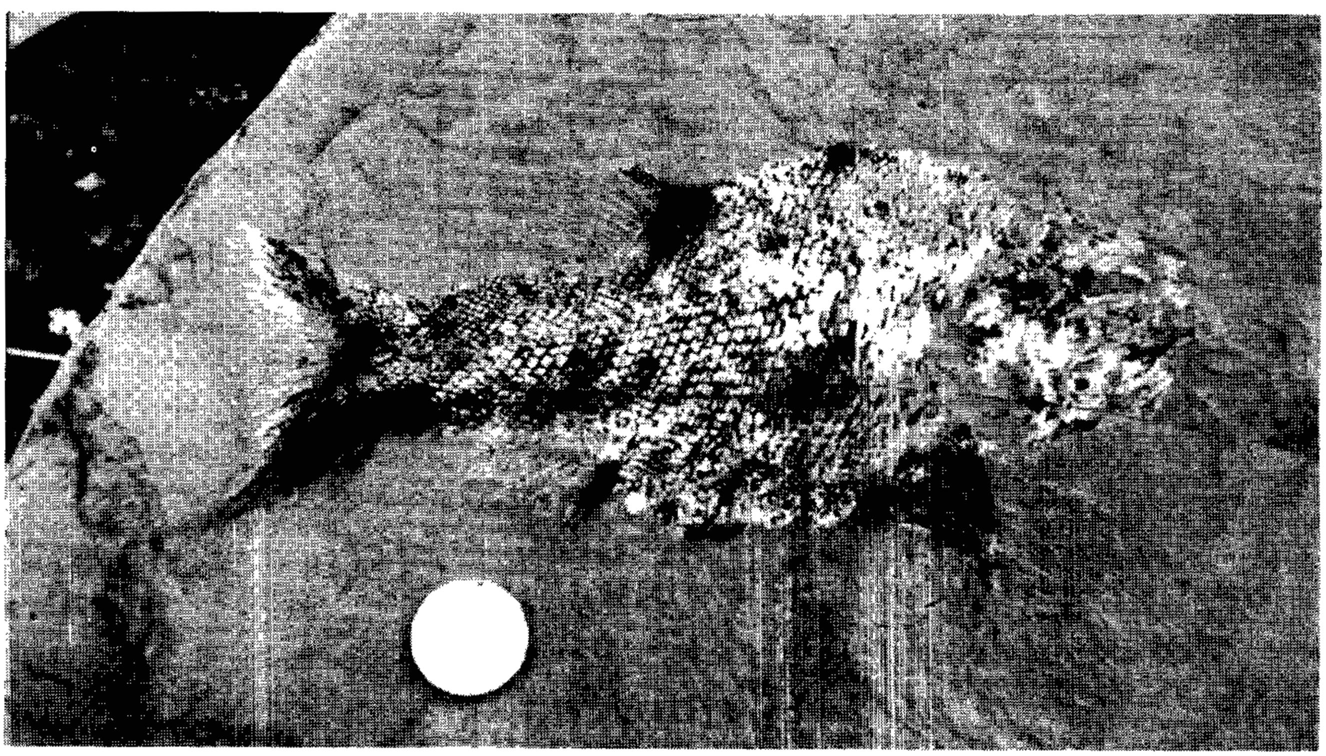

Plate 1-7-6. *Albertonia* sp.; complete fish. Pectoral fin is not as well preserved as in previous specimen. "Loony" for scale is 2.5 centimetres in diameter.

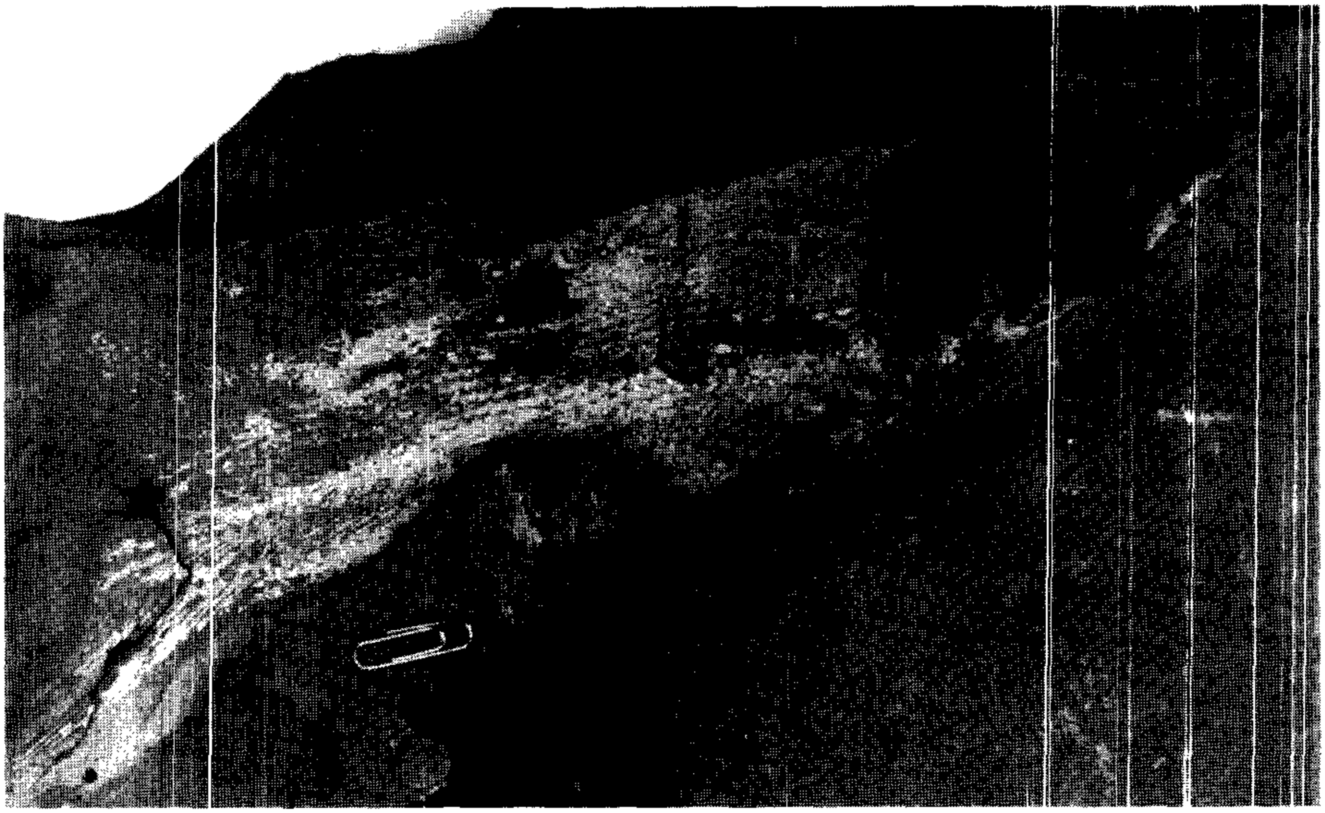

Plate 1-7-7. Coelacanthidae *Whiteia* sp.; near-complete fish, part of caudal (tail) fin missing. Note delicate scale p ttern and small, fleshy lobe at base of pelvic fin. Specimen is 35 centimetres long (paper clip scale is 3 centimetres .

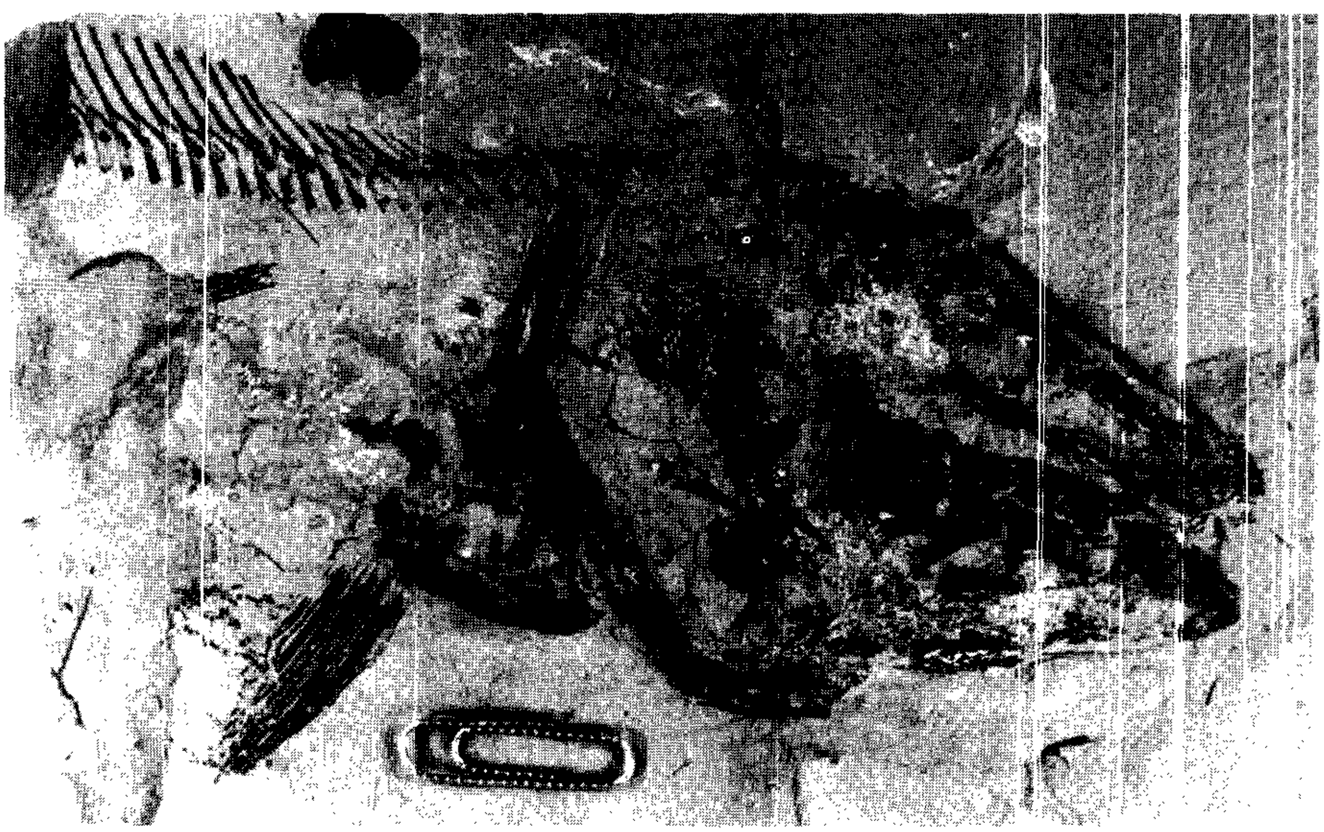

Plate 1-7-8. Coelacanthidae *Whiteia* sp.; skull (paper clip scale is 3 centimetres).

were ossified and, although still slightly upturned at the posterior end, terminated in a more symmetrical tail. Primitive holosteans still retained the ganoid scales, while the more advanced members lost their ganoine covering (Dodson and Dodson, 1976). The other main line, the teleosts, first appeared in the Jurassic, were dominant in the Cretaceous and today comprise more than 95 per cent of the fishes of the world. They are characterized by an entirely bony skeleton, thin, flexible scales that are chips of bone, a versatile jaw mechanism and a symmetrical tail that is conducive to fast swimming.

Two genera of holostean fish, *Albertonia* and *Watsonulus* have been identified from samples collected in the Kakwa area (A. Neuman, personal communication, 1991). Specimens of *Albertonia* are quite abundant; a number of well-preserved individuals were collected. Only one poorly preserved specimen of *Watsonulus* was found. *Albertonia* is one of the largest fish commonly found in the area, individuals measuring 30 to 35 centimetres in length are not uncommon. It has a distinctive form, with a deep body, well-developed ganoid scales, a slightly upturned vertebral column, a large tail and, commonly, elongated pectoral fins (Plates 1-7-5 and 6). It is a unique fish that is fairly easily recognized by the layperson, particularly when the pectoral fins are well preserved.

Lobe-finned fish of subclass Sarcopterygii originated in fresh water in Early Devonian times and from the very beginning comprised two groups, the Dipnoi, or lungfish and the Crossopterygii (Table 1-7-2). Two orders of Crossopterygii exist, the rhipidistians, from which amphibians are believed to have evolved and the coelacanths. From the Devonian to the Permian, coelacanths existed in fresh water; in the Triassic they spread into shallow seas where they persisted until the Cretaceous. They were believed to have been extinct for 75 million years until 1939, when a living coelacanth was caught by a fisherman off the coast of Madagascar. Coelacanths, like other sarcopterygeans, have skull patterns that are completely different from ray-finned fishes and have cosmoid scales, with a dentine-like inner layer rather than the superficial enamel layer present in ganoid scales. Coelacanths generally do not have ossified vertebrae (Dodson and Dodson, 1976).

One genus of coelacanth, *Whiteia*, has been identified from the Triassic deposits in the Kakwa area (A. Neuman, personal communication, 1991). Articulated specimens are between 35 and 75 centimetres long; numerous fragments of coelacanth fossils were also found. *Whiteia* is unique in that the scales, when preserved, are more delicate and less distinct, and tassel-like adornments are common around the tail. The skull structure is different from the actinopterygeans, with the eye socket set farther back. The fleshy nature of the fins can also be discerned in some specimens (Plates 1-7-7 and 8).

CONCLUSIONS

The discovery of well-preserved fish fossils within the Triassic deposits in Kakwa Recreation Area may be significant as there are fewer than 20 areas throughout the world in which similar fossils have been found and only six localities which have yielded more than five genera (Neuman, in press; Schaeffer and Mangus, 1976). Already seven genera from the Class Osteichthyes and one from Chondrichthyes have been identified from Kakwa; more specimens are currently being studied and it is possible that additional taxa will be recognized. It also must be reiterated that specimens were all obtained from a scree slope and that no extensive, systematic sampling effort has yet been made at this site. More work is needed at the Kakwa fossil locality, to accurately identify all taxa present and to locate the stratigraphic position of the fossiliferous horizons; a museum collecting expedition appears to be warranted.

ACKNOWLEDGMENTS

We would like to thank Andy Neuman of the Royal Tyrrell Museum of Paleontology in Drumheller for identifying specimens collected in Kakwa and his colleague Don Brinkman for supplying background reference material; both Andy and Don also provided helpful discussion as did Barry Richards of the Institute of Sedimentary and Petroleum Geology in Calgary. Betsy Fletcher and Wade Harris provided excellent assistance in the field and helped in the collection of specimens. A special thanks goes to Bob Batchelor and Northern Mountain Helicopters who provided us with excellent support; also Bob, thanks to his keen eyes, patience and interest, found quite a few of the specimens that are the basis of this collection.

REFERENCES

Brinkman, D.B. and Neuman, A.G. (1987): Lower Triassic Vertebrates from the Sulphur Mountain Formation, Wapiti Lake, British Columbia (abstract); *Geological Association of Canada/Mineralogical Association of Canada*, Joint Annual Meeting, Program with Abstracts, Volume 12, page 26.

Callaway, J.M. and Brinkman, D.B. (1989): Ichthyosaurs (Reptilia, Ichthyosauria) from the Lower and Middle Triassic Sulphur Mountain Formation, Wapiti Lake Area, British Columbia, Canada; *Canadian Journal of Earth Sciences*, Volume 26, pages 1491-1500.

Dodson, E.O. and Dodson, P. (1976): Evolution: Process and Product; *D. Van Nostrand Company*, New York, 440 pages.

Gibson, D.W. (1975): Triassic Rocks of the Rocky Mountain Foothills and Front Ranges of Northeastern British Columbia and West-central Alberta; *Geological Survey of Canada*, Bulletin 247, 61 pages.

Lambe, L.M. (1914): Description of a New Species of Platysomus from the Neighborhood of Banff, Alberta; *Transactions of the Royal Society of Canada*, Series 3, Section 4, Volume 8, pages 17-23.

Lambe, L.M. (1916): Ganoid Fish from near Banff, Alberta; *Transactions of the Royal Society of Canada*, Series 3, Section 4, Volume 10, pages 35-44.

Laudon, L.R., Deidrick, E., Grey, E., Hamilton, W.B., Lewis, P.J., McBee, W., Spreng, A.C. and Stoneburner, R. (1949): Devonian and Mississippian Stratigraphy, Wapiti Lake Area, British Columbia, Canada; *Bulletin of the American Association of Petroleum Geology*, Volume 33, pages 1502-1552.

McMechan, M.E. (1986): Geology of the Northeast McBride Map-area (93H/15, 16), British Columbia; *Geological Survey of Canada*, Open File 1229.

McMechan, M.E. and Thompson, R.I. (1985): Geology of Southeast Monkman Pass Area (93I/SE), British Columbia; *Geological Survey of Canada*, Open File 1150.

Neuman, A.G. (in press): Summary of Geology and Update of Faunal List with Emphasis on Fishes: Lower Triassic Sulphur Mountain Formation, Wapiti Lake Area, British Columbia; *Royal British Columbia Museum*, Contribution Series.

Pell, J., Hammack, J.L., Fletcher, B. and Harris, W.D. (1992): Kakwa Recreation Area, Northeastern British Columbia: Geology and Resource Potential (93H/15, 16, 93I/1, 2); *in* Geological Fieldwork 1991, Grant, B. and Newell, J.M., Editors. *B.C. Ministry of Energy, Mines and Petroleum Resources*, Paper 1992-1, this volume.

Schaeffer, B. and Mangus, M. (1976): An Early Triassic Fish Assemblage from British Columbia. *Bulletin of the American Museum of Natural History*, Volume 156, Article 5, pages 515-564.

Taylor, G.C. and Stott, D.F. (1979): Geology of Monkman Pass Map-area (93I), Northeastern British Columbia; *Geological Survey of Canada*, Open File 630.

Tozer, T.N. (1967) A Standard for Triassic Time; *Geological Survey of Canada*, Bulletin 156, 103 pages.

NOTES

MINERAL POTENTIAL INVESTIGATIONS IN THE BABINE MOUNTAINS RECREATION AREA (PARTS OF 93L/14E, 15W AND 93M/2W)

By R.G. Gaba, P.J. Desjardins and D.G. MacIntyre

KEYWORDS: Regional geology, mineral potential, Babine Mountains Recreation Area, porphyry, veins, silver, gold, copper, molybdenum.

INTRODUCTION

The Babine Mountains Recreation Area encompasses approximately 32 400 hectares of alpine and subalpine terrain within the central Babine Range east of Smithers, in west-central British Columbia. At the request of the Ministry of Environment, Lands and Parks, a mineral potential study of the region was conducted in accordance with Section 19 of the *Mineral Tenure Act* during late July and early August, 1991. The geoscience information collected will be used to guide government land-use decisions regarding conversion of the recreation area to Class "A" park status. The final results of the study will be released as a Ministry of Energy, Mines and Petroleum Resources, Geological Survey Branch report early in 1992.

The program was designed to augment geological mapping and metallogenic studies in the area, conducted by MacIntyre *et al.* (1987) and MacIntyre and Desjardins (1988a, b, unpublished data). Their database and geological map were the starting points for the project. Geological mapping of the northern part of the Babine Mountains Recreation Area, which was not included in the previous investigation, was also completed, including a small region northwest of Harold Price Creek. Regionally extensive belts of pyritic and limonite-stained altered rocks were examined and sampled. Rocks with anomalous precious metal concentrations, identified by previous studies (MacIntyre and Desjardins, 1988b), were re-examined and sampled. Field studies also included examination of selected metallic mineral prospects and deposits and general prospecting in areas of favourable geology. During the program three previously undocumented polymetallic vein occurrences were found: these are informally referred to as the "Silver King Lake", "Rhyolite" and "Little Joe Lake South" showings. These new showings were mapped in detail and sampled.

Consulting geochemist John Gravel collected stream-sediment and water samples from 39 sites to supplement the existing Regional Geochemical Survey (RGS) database for the area. The methods used to collect and analyze the samples were in accordance with standards set by the RGS program. The results of this survey will be included in the final report.

GEOLOGY OF THE BABINE MOUNTAINS RECREATION AREA

The Babine Mountains Recreation Area covers the central part of the Babine Range within the Skeena Mountains. This region is part of the Stikine Terrane; exposed lithologies include: subaerial to submarine calcalkaline volcanic, volcaniclastic and sedimentary rocks of the Lower to Middle Jurassic Hazelton Group; sedimentary rocks of the Middle to Upper Jurassic Bowser Lake Group and Lower Cretaceous Skeena Group; and calcalkaline continental volcanic-arc rocks of the Upper Cretaceous Kasalka Group. Upper Cretaceous to Lower Tertiary volcaniclastic rocks occur sporadically throughout the area. Intermediate to felsic dikes and stocks are Late Cretaceous to Early Tertiary in age (Figure 1-8-1). More detailed subdivisions and descriptions of rock units are outlined by MacIntyre and Desjardins (1988a).

The structural setting of the Babine Range is similar to that of the basin-and-range physiographic province of the southwest United States: the range is dominated by a series of northwest-trending tilted horsts and grabens. Skeena Group and Kasalka Group rocks are preserved in graben structures that are underlain by thick successions of Hazelton Group and Bowser Lake Group(?) strata. The rocks are generally folded: fold axes trend and plunge moderately to the southeast (MacIntyre *et al.*, 1987). Folds are less common in the northern part of the range where the structural style is dominated by southwest-dipping fault blocks.

Regional extension is thought to have developed during the Late Cretaceous, with associated extensive volcanism and stratovolcano development. Compression during Tertiary time caused reverse movement along older high-angle normal faults and resulted in upward thrusting and folding of subsided fault blocks. Major east to northeast-trending faults, also probably of Tertiary age, truncate and offset the dominant northwest-trending structural fabric of the range.

GEOLOGICAL MAPPING OF THE NORTHERN PART OF THE RECREATION AREA

Geological mapping of the northern part of the recreation area, (part of NTS 93M/2W) not previously mapped by the British Columbia Geological Survey Branch was completed (Figure 1-8-1). Rocks in this area are porphyritic andesite flows with interbedded epiclastic and tuffaceous sedimentary rocks of the Upper Cretaceous Kasalka Group. Minor pyritic and limonite-stained altered rocks contain small quartz-ankerite veins, but no other metallic minerals.

In addition, a small region northwest of Harold Price Creek (part of NTS 93M/3E) and outside the recreation area was examined and mapped. This area is underlain by massive augite-porphyritic basalt flows that are correlated with the Lower Cretaceous Rocky Ridge formation. The rocks show no indications of alteration and no quartz veins were seen; the region is therefore considered to be of low mineral-resource potential.

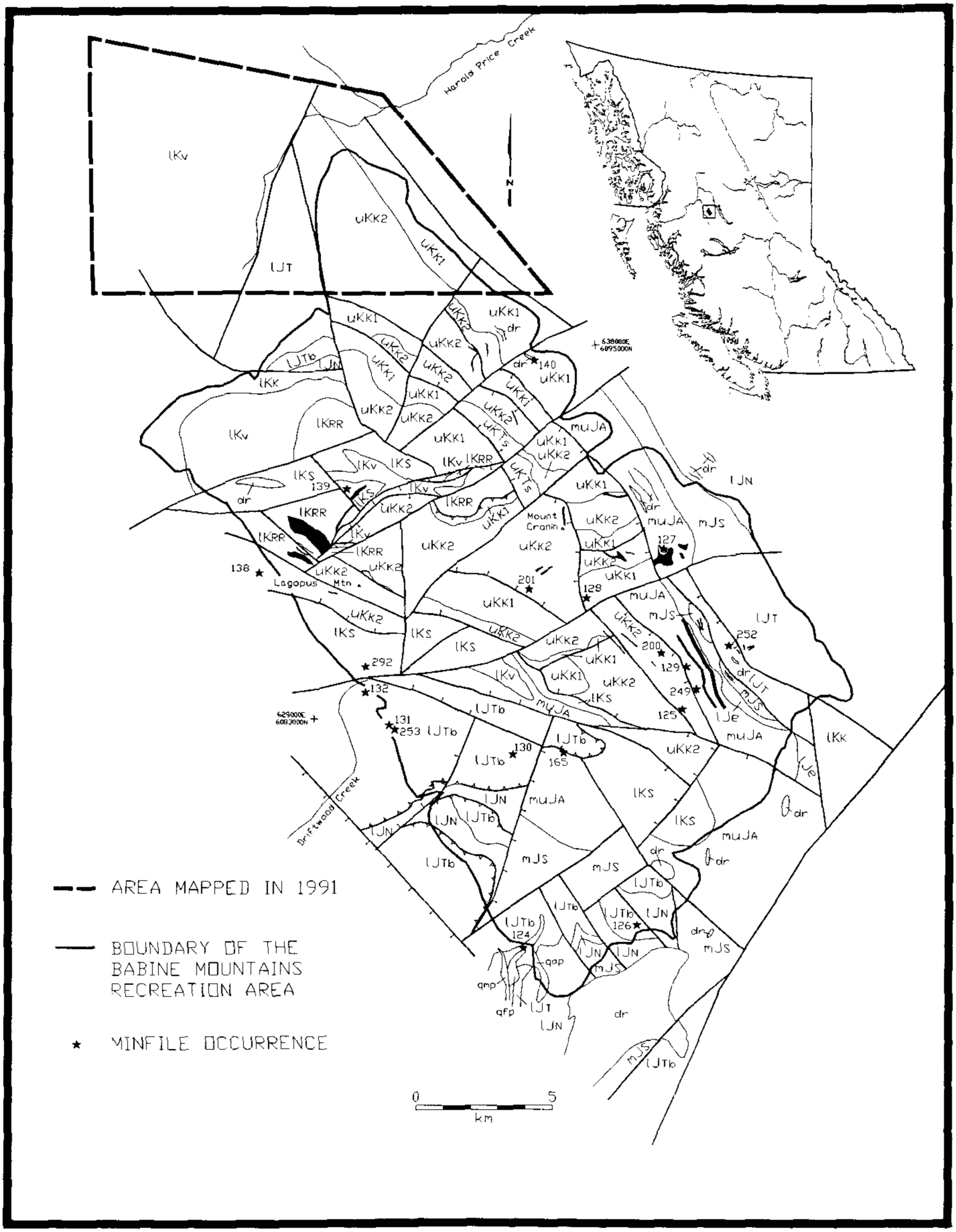

Figure 1-8-1. Simplified geology of the Babine Mountains Recreation Area (parts of 93L/14E,15W and 93M/2W) and the distribution of mineral occurrences (MINFILE numbers are preceeded by 093L-).

KNOWN MINERAL RESOURCES

MINERAL DEPOSIT TYPES

Mineral deposits and prospects within and adjacent to the Babine Mountains Recreation Area (Figures 1-8-1 and 2) are divided into three distinct groups (Table 1-8-1): silver-rich polymetallic veins, basalt-hosted copper-silver veins and porphyry copper-molybdenum (±gold) deposits associated with quartz diorite and quartz feldpsar porphyry intrusions.

Historically the area is known as a silver camp, with lesser lead, zinc and copper production; ancillary gold and cadmium were also recovered as byproducts (Table 1-8-2). Most of the metals have come from high-grade polymetallic veins at the Cronin mine, mainly during the period 1951 to 1974. Potentially economic ore reserves that remain at the Cronin mine were recently outlined by Southern Gold Resources Limited (Table 1-8-1; Quin, 198?). Less extensive polymetallic deposits and basalt-hosted copper-silver veins supported small-scale mining operations between 1917 and 1940; access trails to many of these prospects are now used as mountain bike and hiking trails.

THE BIG ONION PROSPECT

The Big Onion prospect, a low-grade large-tonnage calc-alkaline porphyry copper-molybdenum deposit on the south side of Astlais Mountain, is the most promising mineral property presently being explored within the bounds of the recreation area. The area was initially staked as the Cimbria group in 1918 and has subsequently received attention from many individuals and exploration groups. Efforts by Canadian Superior Exploration Limited during the middle 1970s,

TABLE 1-8-1
KNOWN METALLIC MINERAL OCCURRENCES WITHIN THE BABINE MOUNTAINS RECREATION AREA

MINFILE No. (093L)	Property Name	Deposit Type	Commodities	Property Status
124	Big Onion	porphyry Cu-Mo	Cu,Mo,[Au]	developed prospect[1]
125	Silver Pick	polymetallic vein	Ag,[Au],Cu,Zn;Pb	past producer
126	Mert	porphyry Cu-Mo	Cu,Mo,[Ag]	showing
127	Cronin	polymetallic vein	Ag,[Au],Pb,Zn;Cd,Cu	past producer[2]
128	Hyland Basin	polymetallic vein	Ag,[Au],Pb;ZN	past producer
129	Lorraine	polymetallic vein	Ag,Pb;Zn,Cu	past producer
130	Jud	basalt-hosted copper-silver vein	Cu,Ag	showing
131	Drift	basalt-hosted copper-silver vein	Cu,Ag;Pb	past producer
132	Driftwood	basalt-hosted copper-silver vein	Ag,[Au],Cu,Pb,Zn	past producer
138	AG	polymetallic vein	Ag,Pb;Zn	showing
139	Reiseter Creek	polymetallic vein	Cu,Pb;Zn	showing
140	Debenture	polymetallic vein	Ag,Pb,Zn	prospect
165	Shamrock	basalt-hosted copper-silver vein	Ag,Cu	showing
200	Silver Saddle	polymetallic vein	Ag,Au,Pb;Cu	showing
201	Silver King mine	polymetallic vein	Ag,[Au],Pb;Zn,Cu	past producer
249	Native	polymetallic vein	Ag,Pb,Zn	showing
252	Fisher	porphyry Cu	Cu	showing
253	Home	basalt-hosted copper-silver vein	Ag;Cu,Pb,Zn	showing
292	Viking	pyrite veinlets	[Ag,Au]	showing

[1] Reserves of 80 to 100 Mt with an approximate grade of 0.42% Cu, 0.02% MoS_2, plus minor Au.
[2] Reserves of 47 kt with an approximate grade of 428 g/t Ag, 1.7 g/t Au, 0.16% Cu, 8.0% Pb, 8.0% Zn.

TABLE 1-8-2
HISTORICAL METAL PRODUCTION WITHIN THE BABINE MOUNTAINS RECREATION AREA

MINFILE No. (093L)	Property Name	Gold (grams)	Silver (grams)	Copper (kg)	Lead (kg)	Zinc (kg)	Cadmium (kg)
125	Silver Pick	466	209 230	886	420	836	
127	Cronin	8 772	8 169 918	10 394	1 367 178	1 517 881	18 012
128	Hyland Basin	342	84 880		3 396	397	
129	Lorraine		19 448		3 175		
131	Drift		132 779	4 711			
132	Driftwood	93	21 928	109	327	245	
201	Silver King mine	62	41 865	107	3 490	348	
	Total	**9 735**	**8 680 048**	**16 207**	**1 377 986**	**1 519 707**	**18 012**

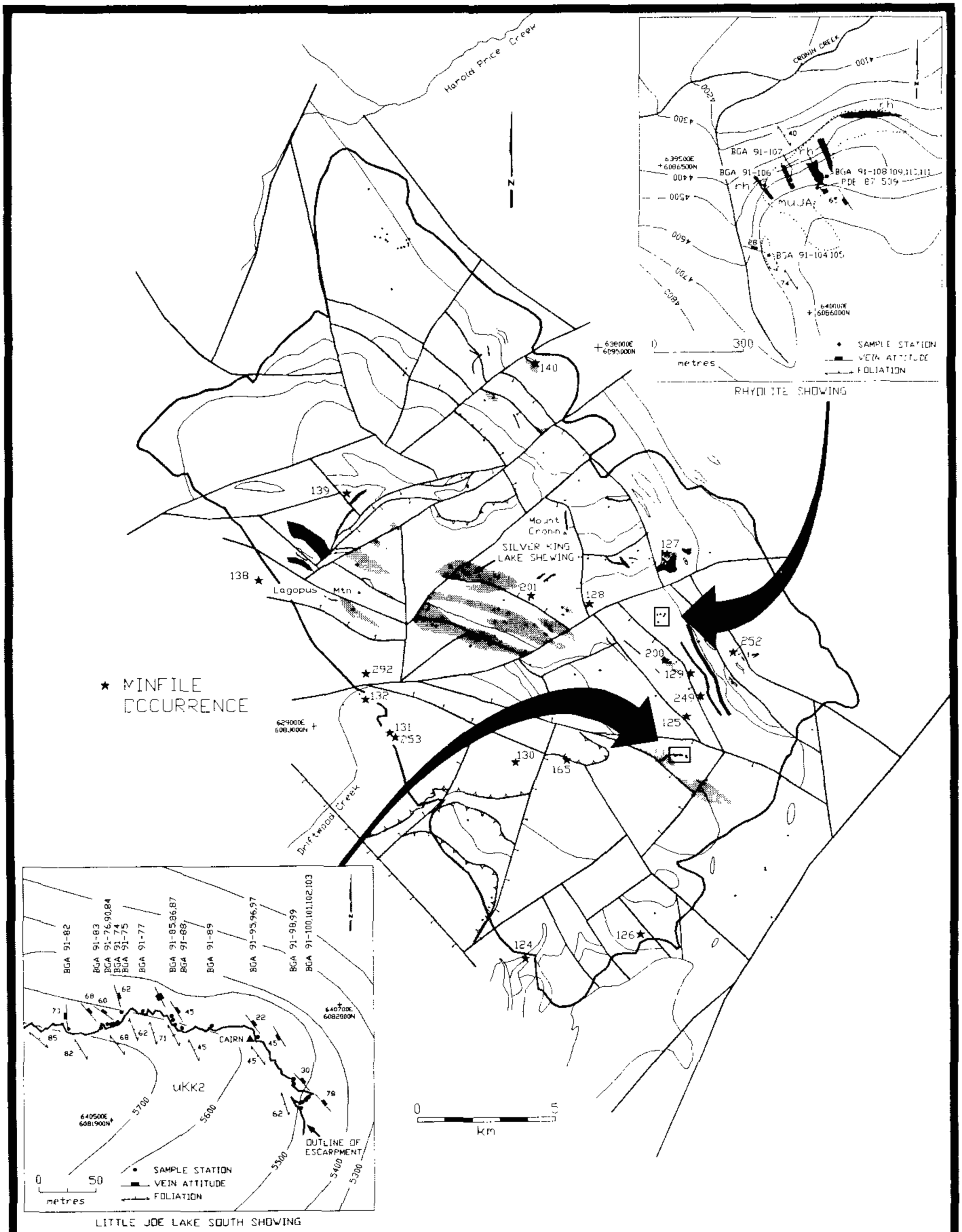

Figure 1-8-2. Distribution of lithogeochemical sample stations (represented by dots) and location of mineral occurrences; shaded areas represent pyritic and limonite-stained rocks. Insets are geological sketch maps of the "Rhyolite" and "Little Joe Lake South" showings with locations of sample stations; assays of samples collected at the showings are presented on Tables 1-8-3 and 4. The "Silver King Lake" showing is at the centre of the map area.

LEGEND

SEDIMENTARY AND VOLCANIC ROCKS

UPPER CRETACEOUS AND LOWER TERTIARY

uKTs — *tuffaceous sandstone*

UPPER CRETACEOUS

KASALKA GROUP

uKK2 — *hornblende-feldspar-phyric flows and breccias*

uKK1 — *lahars, lapilli tuffs and conglomerate; epiclastic rocks*

LOWER CRETACEOUS

SKEENA GROUP

lKS — *undifferentiated Skeena Group*

lKRR — *Red Rose formation: shale, orange-weathering siltstone well-bedded micaceous wacke and conglomerate*

lKv — *Rocky Ridge formation: green and maroon phyllitic tuff, minor augite-phyric basalt flows; phyllite*

lKK — *Kitsuns Creek formation: quartz-chert-pebble conglomerate, sandstone and shale*

MIDDLE TO UPPER JURASSIC

BOWSER LAKE GROUP

muJA — *Ashman Formation: argillite; sandstone and siltstone*

LOWER TO MIDDLE JURASSIC

HAZELTON GROUP

mJS — *Smithers Formation: fossiliferous feldspathic sandstone, greywacke and siltstone*

lJe — *Eagle Peak formation: red tuffs and basalt flows*

lJN — *Nilkitkwa Formation: conglomerate, siltstone and shale*

lJT — *Telkwa Formation: dacitic to basaltic flows and pyroclastic rocks*

lJTb — *amygdaloidal basalt flows*

INTRUSIVE ROCKS

LATE CRETACEOUS TO EARLY TERTIARY

rhyolite intrusions

qmp — *quartz monzonite porphyry*

dr — *diorite*

qfp — *quartz feldspar porphyry*

qdp — *quartz diorite porphyry*

and most recently by Varitech Resources Limited, have quantified reserves of copper and molybdenum (Table 1-8-1). Early in 1991 Varitech signed an option agreement whereby it can earn a 100 per cent interest in the property by spending $4 million on exploration over a 4-year period. Planned exploration during the first 2 years will include a diamond-drilling program designed to reconfirm grades previously outlined by the Canadian Superior percussion-drilling program, and expand reserves. Varitech plans to "twin" previous percussion-holes by drilling parallel diamond-drill holes with a larger diameter and to a greater depth than before. It has been suggested that the percussion-drilling program yielded lower-than-actual grades due to poor recovery from the fractured and altered hostrocks and an apparent concentration of metallic minerals, specifically bornite, at the bottom of the percussion-drill holes due to inadequate flushing after drilling each sample interval (J. Baker, personal communication, 1991).

POTENTIAL FOR UNDISCOVERED RESOURCES

The field-based component of this study gathered information to help assess the potential for undiscovered mineral resources within the recreation area. Although the region has been extensively prospected and explored during the past 90 years, there is still the possibility that some mineral wealth has gone undetected during that time. The goal here is to identify areas with significant mineral potential to ensure that the region is thoroughly tested before it is considered for reclassification as park land with no mineral exploration allowed.

The methods used to identify areas of interest included lithogeochemical sampling of alteration zones, and delineation and prospecting of regions deemed favourable for mineral deposits. Analysis of stream sediments is also a part of this evaluation, the results of which will form part of the final report.

A total of 244 rock samples was collected from the area during previous (MacIntyre and Desjardins 1988a,b) and present studies. Of these, 113 were taken from regionally extensive pyritic and limonite-stained altered rocks that form spectacular red-brown gossans across the central part of the area (Figure 1-8-2). These zones are essentially bleached sericitic schists and phyllites derived from volcanic and sedimentary rocks of the Upper Cretaceous Kasalka Group. The rocks contain abundant disseminated pyrite, some of which has altered to limonite. The rocks also exhibit breccia textures and are locally veined by quartz or quartz and epidote. The alteration zones, which are a few hundred metres wide, are semicontinuous for several kilometres along a west-northwest strike. They are coincident with shear zones of probable post-Late Cretaceous age that are truncated by northeast-trending Tertiary faults (Figure 1-8-2).

With few exceptions, samples taken from outcrop contain only background levels of precious and base metals; this is in agreement with the experience of local prospectors (Joe L'Orsa, personal communication, 1991). However, the altered rocks have not been tested at depth by diamond drilling and might contain metals beneath the leached rocks exposed at surface.

Previously Undocumented Mineral Occurrences

Three previously undocumented mineral occurrences were found during the course of prospecting and regional lithogeochemical sampling. All are within 1 or 2 kilometres of known prospects or mines and are on ground held in good standing by Vancouver-based companies. However, there are no indications of surface work at any of these showings and they may represent new occurrences with interesting exploration potential.

SILVER KING LAKE SHOWING

The "Silver King Lake" showing is at the head of Silver King Lake basin at an elevation of 1965 metres, approximately 2 kilometres northwest of the Silver King mine (MINFILE 093L 201; Figure 1-8-2). The showing consists of a quartz vein 3 centimetres wide, exposed for 2 metres along strike within feldspar-porphyritic andesite of the Upper Cretaceous Kasalka Group. Hostrocks are mylonitic to schistose and form lenticular zones within otherwise massive volcanic rocks. The foliated rocks have an easterly strike and a south dip, generally parallel to the regionally extensive pyritic and limonite-stained rocks.

The vein consists of vuggy, crystalline quartz and contains irregular blebs of galena, chalcopyrite and pyrite, 1 millimetre to several centimetres in size. A sample of the vein submitted for assay returned 11 ppb gold, 16 grams per tonne silver, 564 ppm copper, 1.59 per cent lead, 370 ppm zinc and 13 ppm cadmium. This vein is typical of the polymetallic veins of the region.

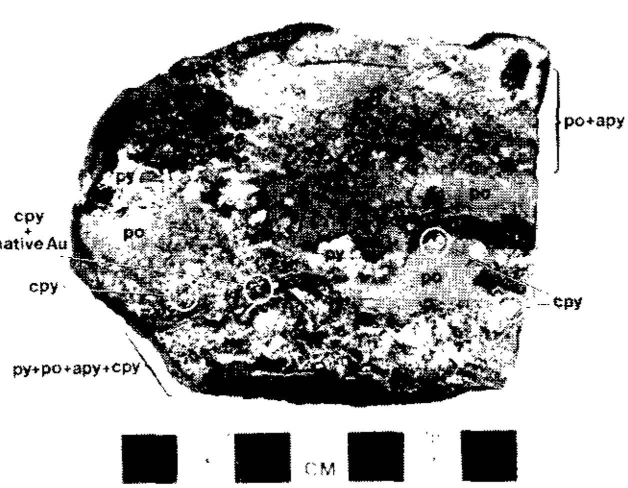

Plate 1-8-1. Polished slab of massive sulphide vein (sample BGA91-111) from the "Rhyolite" showing. Chalcopyrite, arsenopyrite and microscopic native gold are associated with quartz veinlets (dark grey) within massive to banded intergrowths of pyrrhotite, pyrite and arsenopyrite.

RHYOLITE SHOWING

The "Rhyolite" showing is near the headwaters of Cronin Creek, approximately 2 kilometres south of the Cronin mine (MINFILE 093L 127) and 1.5 kilometres northwest of the Lorraine prospect (MINFILE 093L 129; Figure 1-8-2). This site, initially sampled in 1987 in the course of regional geological mapping by MacIntyre and Desjardins (1988b), contains up to 4.32 grams per tonne gold in rhyolite veined by quartz, pyrite and arsenopyrite (sample PDE87-539 in Figure 1-8-2 inset and Table 1-8-3). The area was briefly re-examined during the present study to document the nature and distribution of the mineralization.

The showing consists of sulphide veins and stockworks within and adjacent to rhyolite dikes that cut black argillite of the Middle to Upper Jurassic Ashman Formation (Figure 1-8-2 inset). The sulphide concentrations are predominantly pyrrhotite and pyrite, with lesser arsenopyrite, chalcopyrite and specularite, minor sphalerite and microscopic native gold (Plate 1-8-1). The assemblage forms massive banded veins up to 15 centimetres wide that are spatially associated with rhyolite and disseminations and stockworks of sulphides within rhyolite. These are exposed over an area of approximately 25 square metres. Samples of sulphide veins and stockworks submitted for assay returned up to 13.2 grams per tonne gold and 86 grams per tonne silver, and appreciable copper and zinc concentrations (Table 1-8-3).

Argentiferous polymetallic mineralization (quartz veins with coarsely intergrown pyrite, sphalerite, galena, chalcopyrite, boulangerite and tetrahedrite) at both the Cronin mine and the Lorraine prospect (north and south of the Rhyolite showing) is closely associated with rhyolite intrusions. The area between these two past-producers is riddled with dikes and irregular bodies of rhyolite – an obvious place to expect similar mineralization. Veins at the "Rhyolite" showing also have a spatial association with rhyolite, but are mineralogically and texturally distinct from assemblages at the Cronin and Lorraine: "Rhyolite" veins contain abundant pyrrhotite and arsenopyrite with significant associated gold (a higher temperature assemblage), and occur as pod-like veins of almost massive sulphide, possibly manto-style veins?.

LITTLE JOE LAKE SOUTH SHOWING

The "Little Joe Lake South" showing is exposed in the prominent north-facing cliff of the ridge south of the easternmost lake at the headwaters of Little Joe Creek. This area is approximately 1.2 kilometres south of the Silver Pick prospect (MINFILE 093L 125; Figure 1-8-2). Sulphide-bearing quartz-ankerite veins are exposed along the ridge escarpment for more than 250 metres within massive to foliated porphyritic andesite and tuff of the Upper Cretaceous Kasalka Group. The foliated rocks strike northwest and dip steeply to moderately southwest or northeast. Within the area of extensive quartz veining, the hostrocks are schists and phyllites speckled with fine-grained ankerite (or limonite after ankerite). In contrast to similar vein deposits nearby, rhyolite and other intrusions are not in evidence.

TABLE 1-8-3
ASSAY RESULTS OF SAMPLES COLLECTED FROM THE "RHYOLITE" OCCURRENCE

Sample No.	Au	Ag	Cu	Pb	Zn	Cd	As	Sb
BGA91-104	4	<0.4	24	5	133	0.3	78	0.4
BGA91-105	23	<0.4	4	3	47	<0.3	310	<0.1
BGA91-106	<2	<0.4	5	6	53	<0.3	12	0.8
BGA91-107	<2	<0.4	15	9	134	0.6	22	1.3
BGA91-108	5370	12	213	54	68	0.3	62000	77
BGA91-108*	3950							
BGA91-109	11600	7	555	33	138	2.0	140000	250
BGA91-109*	9490							
BGA91-110	12800	38	273	138	28	<0.3	99000	99
BGA91-110*	13200							
BGA91-111	12300	86	1.09%	50	0.12%	24	31000	67
BGA91-111*	10500							
PDE87-539	4320	2	37	25	90			

Units and analytical methods:

Au in ppb; all other elements in ppm, except where noted in per cent (%).

Au, As and Sb by neutron activation (Actlabs, Ancaster, ON).

All other elements by atomic absorption spectrophotometry (MEMPR Analytical Sciences Laboratory, Victoria, B.C.).

* analysis by classic fire assay (Chemex Laboratories, Vancouver, B.C.).

Sample descriptions:

BGA91-104 quartz vein with py, lm (15 cm thick/exposed for 7 m), BGA91-105 quartz vein with py, ank (10 cm/2 m), BGA91-106 rhyolite with lm; BGA91-107 rhyolite with lm; BGA91-108 sulphide-quartz vein with py, apy, cpy (3 cm/2 m), BGA91-109 sulphide-quartz vein with py, apy, cpy, sp (1–3 cm/1 m); BGA91-110 sulphide-quartz stockwork with py, apy, cpy, gn (30 cm/2–3 m); BGA91-111 solid sulphide vein composed of po, py, apy, cpy, spec, sp, trace microscopic native Au (15 cm/unknown – sample not in-situ); PDE87-539 rhyolite with lm, py, apy. Abbreviations: ank=ankerite, apy=arsenopyrite, cpy=chalcopyrite, gn=galena, lm=limonite, po=pyrrhotite, py=pyrite, sp=sphalerite, spec=specularite.

The quartz veins are generally 2 to 10 centimetres wide and are exposed along strike for an average of 3 to 5 metres along the face of the escarpment. The thickest and most sulphide-rich vein is 25 centimetres wide and is exposed intermittently for 20 metres (stations BGA91-76, 90, 84 in Figure 1-8-2 inset). Vein quartz is massive and milky white to slightly banded or blotchy with respect to the distribution of sulphides and ankerite (or pockets of limonite after ankerite). Cockscomb quartz and vuggy textures are present but not common. Ankerite (and limonite) veinlets and slices of ankeritized wallrock subparallel to the vein walls give an impression of poorly developed ribbon texture.

Metallic minerals within the veins include: galena, sphalerite, tetrahedrite, boulangerite, chalcopyrite, specularite and pyrite, and occur as irregular concentrations several millimetres to 2 centimetres in size. The vein assemblages are similar to those at the Cronin mine, but the abundance of metallic minerals within the veins is much less than at Cronin.

Aside from a generally pervasive ankeritic component to the host phyllite, alteration adjacent to the veins is negligible; small amounts of chlorite (±sericite) are present along or close to the vein margins, but seem to be part of the vein rather than a product of wallrock alteration.

The quartz veins have variable morphology, and their relationships with the host phyllites indicate that there are several generations of veins, each related to intervals of progressive structural deformation. Veins that comprise the west part of the Little Joe Lake South showing are almost all concordant with host phyllite and are variably deformed. The thickest and most sulphide-rich vein is also approximately concordant within the phyllite, but is internally drag folded and probably thickened. Fold structures within the vein, defined by the alignment of acicular boulangerite, probably formed during shearing and dilation along foliation.

Other veins that closely follow the foliation of the hostrocks are planar to slightly warped. They contain irregular clots of sphalerite and galena, and have irregular margins, but are generally not internally deformed. These veins were probably emplaced during the latest stages of shearing and dilation along the foliation.

Veins that comprise the east part of the prospect are largely discordant to foliation. Many are flat to gently north-dipping and occur in regularly spaced vein sets within the phyllites. The veins, which are generally undeformed and have sharp contacts, occupy planar dilations perpendicular to the foliation of the hostrocks. Blebs of galena and sphalerite, 1 to 2 centimetres in diameter, are common within veins, many of which are less than 5 centimetres wide. Veins in similar structural settings are slightly warped or folded and the host phyllites deformed. Drag-folding in the phyllites suggests down-dip, or normal movement along fractures (now occupied by quartz veins); movement was probably synchronous with vein emplacement.

Quartz veins also occupy crescent-shaped fractures where slip along foliation has induced shear folding and accompanying dilation perpendicular to the foliation direction. Veins that occupy these dilatant zones are irregular in width and continuity, but are commonly widest in the fold crests. Quartz concentrations of this type, which reach widths of up to 50 centimetres, are riddled with irregular blebs and veinlets of sphalerite, galena and chalcopyrite.

Veins were sampled wherever it was safe to do so. The largest vein (stations BGA91-76, 90, 84 in Figure 1-8-2 inset) contains up to 104 grams per tonne silver and 8.25 per cent lead, whereas other veins contain up to 26 grams per tonne silver (Table 1-8-4).

CONCLUDING REMARKS

Preliminary results of this study are as follows:

- The northern part of the recreation area, including the region to the northwest of Harold Price Creek, is underlain by rocks that are not likely hosts of metallic mineral deposits. This is exemplified by the lack of alteration and lack of mineral showings in the area. This area is considered to have low mineral-resource potential.
- The central part of the recreation area contains most of the known mineral occurrences, some of which have yielded economically extractable quantities of metals. Most of the important past-producers and prospects are concentrated in the east-central region, roughly coincident with the distribution of rhyolite in the area. The detection of two previously undocumented mineral showings within the area during this study indicates that the region still has high mineral resource potential. The most important new occurrence is the Rhyolite showing because of its significant gold content.
- Surface samples collected from regionally extensive belts of pyritic and limonite-stained rocks that traverse the central part of the recreation area do not contain significant concentrations of economic metals, but have minor associated polymetallic mineralization (*e.g.*, the Silver King Lake showing). Proper evaluation without diamond drilling is difficult because of the immense size of the region occupied by the altered rocks. Undetected metal deposits may be present beneath the leached capping of iron-rich altered rocks. For this reason the area is considered to have an intermediate rank of resource potential.
- The southernmost part of the recreation area covers a known resource of copper with molybdenum and gold at the Big Onion deposit. This area has very high mineral resource potential.

ACKNOWLEDGMENTS

The authors would like to thank R. Lett and the Analytical Services section of the British Columbia Geological Survey Branch for accurate and prompt geochemical analyses. We also benefited from discussions and field trips with: G.P. McLaren, M.L. Malott, D.V. Lefebure and D.J. Alldrick of this Ministry; T.A. Richards, consultant; P. Peto of Varitech Resources, Ltd.; J.F. Baker of J.T. Thomas Diamond Drilling; C.J. Sampson, geological consultant; and J. L'Orsa, prospector. T. Brooks and L. Ledoux of Canadian Helicopters in Smithers provided safe and punctual helicopter service. The manuscript was improved by the editorial pens of W.J. McMillan and J.M. Newell.

TABLE 1-8-4
ASSAY RESULTS OF SAMPLES COLLECTED FROM THE "LITTLE JOE LAKE SOUTH" OCCURRENCE

Sample No.	Au	Ag	Cu	Pb	Zn	Cd	As	Sb
BGA91-74	<5	10	66	0.41%	0.38%	22	8	220
BGA91-75	<5	0.4	16	18	163	0.6	<2	20
BGA91-76	<12	32	163	2.53%	0.14%	10	<2	1400
BGA91-77	<5	0.6	4	16	39	<0.3	3	2.6
BGA91-82	<5	<0.4	11	19	71	<0.3	4	4.2
BGA91-83	<38	17	413	1.83%	1.07%	60	110	4100
BGA91-84	<36	28	73	1.80%	0.27%	22	<8	5600
BGA91-85	<5	<0.4	4	15	34	<0.3	4	2.1
BGA91-86	12	0.6	15	30	83	0.5	15	3.1
BGA91-87	<5	0.4	19	63	70	0.4	4	1.7
BGA91-88	<5	0.4	53	66	22	0.3	3	3.4
BGA91-89	<5	<0.4	3	66	57	0.3	<2	2.3
BGA91-90	<5	95	112	8.25%	0.14%	11	<2	500
BGA91-90DUP	7	104	115	8.25%	0.12%	10	14	510
BGA91-95	26	11	53	0.60%	0.36%	31	2.9	8.7
BGA91-96	15	6	110	0.18%	3.40%	300	2.0	6.7
BGA91-97	<2	0.4	9	228	98	1.5	2.1	2.7
BGA91-98	<2	2	10	687	470	3.0	1.9	5.8
BGA91-99	2	6	36	869	0.12%	11	3.7	18
BGA91-100	5	3.5	69	168	730	2.9	6.1	40
BGA91-101	<2	<0.4	3	20	135	1.0	5.1	0.8
BGA91-102	2	1.4	7	38	43	0.3	5.7	5.0
BGA91-103	52	26	337	0.25%	2.60%	140	77	110

Units and analytical methods:

Au in ppb; all other elements in ppm, except where noted in per cent (%).

Au, As and Sb by neutron activation (Actlabs, Ancaster, ON).

All other elements by atomic absorption spectrophotometry (MEMPR Analytical Sciences Laboratory, Victoria, B.C.).

Sample descriptions:

BGA91-74 quartz vein with gn, boul, sp, tet, mal, cpy (10–15 cm thick/exposed for 5 m); BGA91-75 quartz vein with lm, gn (40 cm/3 m); BGA91-76 quartz vein with lm, gn, boul, sp, tet, mal, cpy (3 veins 2–25 cm/20 m); BGA91-77 quartz vein with lm, py, sp (35 cm/3 m); BGA91-82 quartz vein with lm, py, gn (80–100 cm/12 m); BGA91-83 quartz vein with lm, tet, sp, gn, mal (10–25 cm/8 m); BGA91-84 quartz vein with lm, gn, boul, sp, tet, mal, cpy (3 veins 2–25 cm/20 m); BGA91-85 to 87 quartz vein with lm, py, sp, gn (15–20 cm/20 m); BGA91-88 quartz vein with lm, py sp (40–50 cm/3 m); BGA91-89 quartz vein with lm, py, tet, gn (10 cm/1 m); BGA91-90 quartz vein with lm, gn, boul, sp, tet, *mal, cpy (3 veins 2–25 cm/20 m); BGA91-95 quartz vein with lm, gn, sp, py (2–5 cm/1.5 m); BGA91-96 quartz vein with lm, sp, gn, py (2–6 cm/1.5 m); BGA91-97 quartz vein with* lm, gn (50 cm/5 m); quartz vein with lm, gn (100 cm/8 m); BGA91-99 quartz vein with lm, gn (1–40 cm/5 m); BGA91-100 quartz vein with lm, mal, gn, sp, cpy, py (5–20 cm/5 m); BGA91-101 quartz vein with lm, gn sp (1–50 cm/3 m); BGA91-102 quartz vein with lm, gn, sp (1–30 cm/5 m); BGA91-103 quartz vein with lm, mal, gn, cpy, py (3–10 cm/3 m). Abbreviations: boul=boulangerite, cpy=chalcopyrite, gn=galena, lm=limonite, mal=malachite, py=pyrite, sp=shalerite, tet=tetrahedrite.

REFERENCES

MacIntyre, D.G., Brown, D., Desjardins, P. and Mallett, P. (1987): Babine Project (93L/10,15); *in* Geological Fieldwork 1986, *B.C. Ministry of Energy, Mines and Petroleum Resources,* Paper 1987-1, pages 201-222.

MacIntyre, D.G. and Desjardins, P. (1988a): Babine Project; *in* Geological Fieldwork 1987, *B.C. Ministry of Energy, Mines and Petroleum Resources,* Paper 1988-1, pages 181-194.

MacIntyre, D.G. and Desjardins, P. (1988b): Geology of the Silver King – Mount Cronin Area; *B.C. Ministry of Energy, Mines and Petroleum Resources,* Open File 1988-20.

Quin, S.P. (1987): Cronin Mine Project: Summary Report for the 1987 Exploration Program for Southern Gold Resources; *B.C. Ministry of Energy, Mines and Petroleum Resources,* Assessment Report 16721, 36 pages.

NOTES

REGIONAL GEOLOGICAL MAPPING IN THE NATION LAKES AREA (93N/2E, 7E)

By JoAnne Nelson, Kim Bellefontaine, Chris Rees and Mary MacLean

KEYWORDS: Regional geology, porphyry Cu-Au, alkaline intrusions, Takla Group, Inzana Lake formation, Witch Lake formation, Chuchi Lake formation, Hogem intrusive complex, Takla intrusions, alteration halos.

INTRODUCTION

The Nation Lakes area of central British Columbia is located approximately 75 kilometres north of Fort St. James and is accessed by well-maintained logging roads from Fort

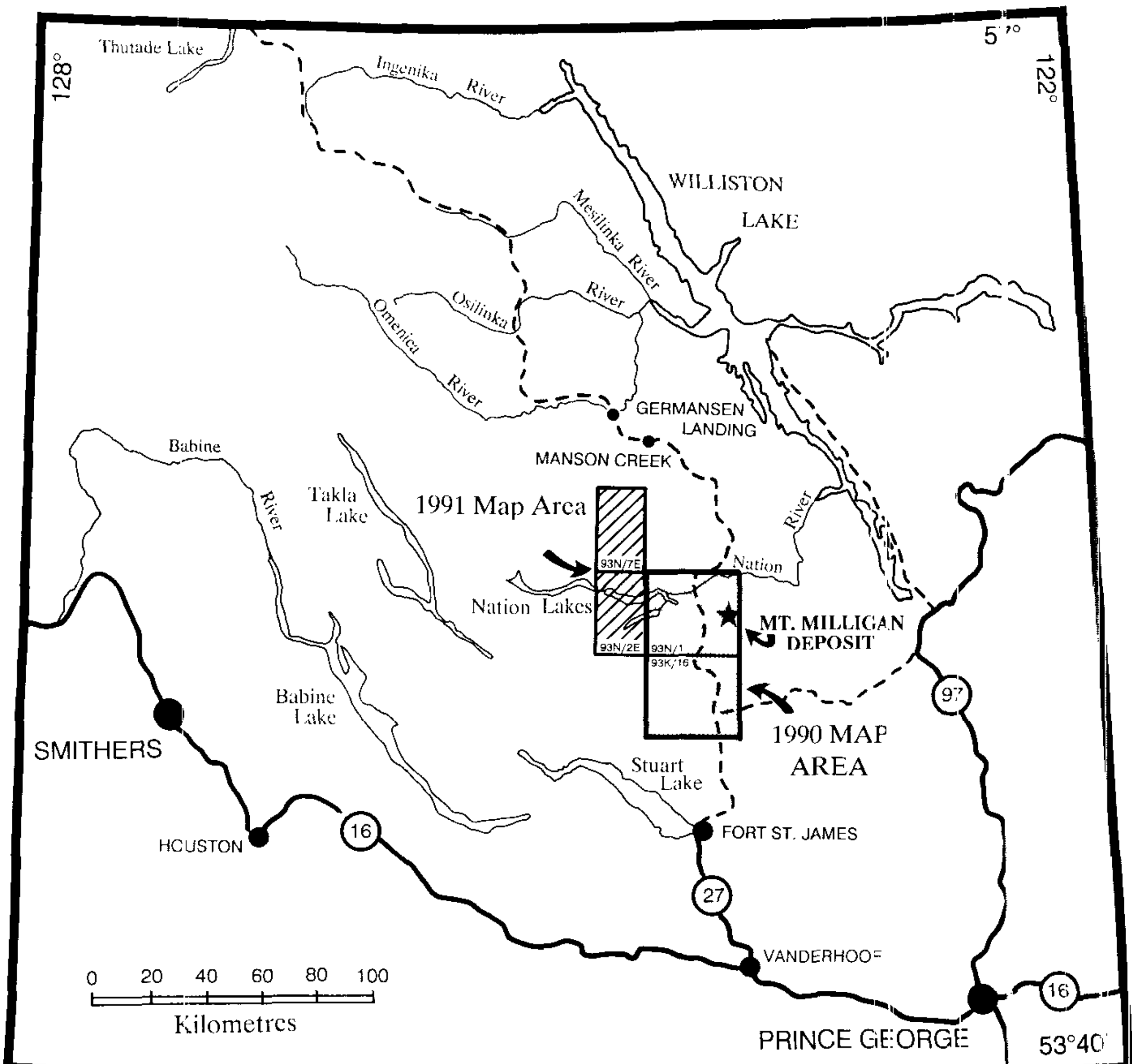

Figure 1-9-1. Location map, Nation Lakes project area.

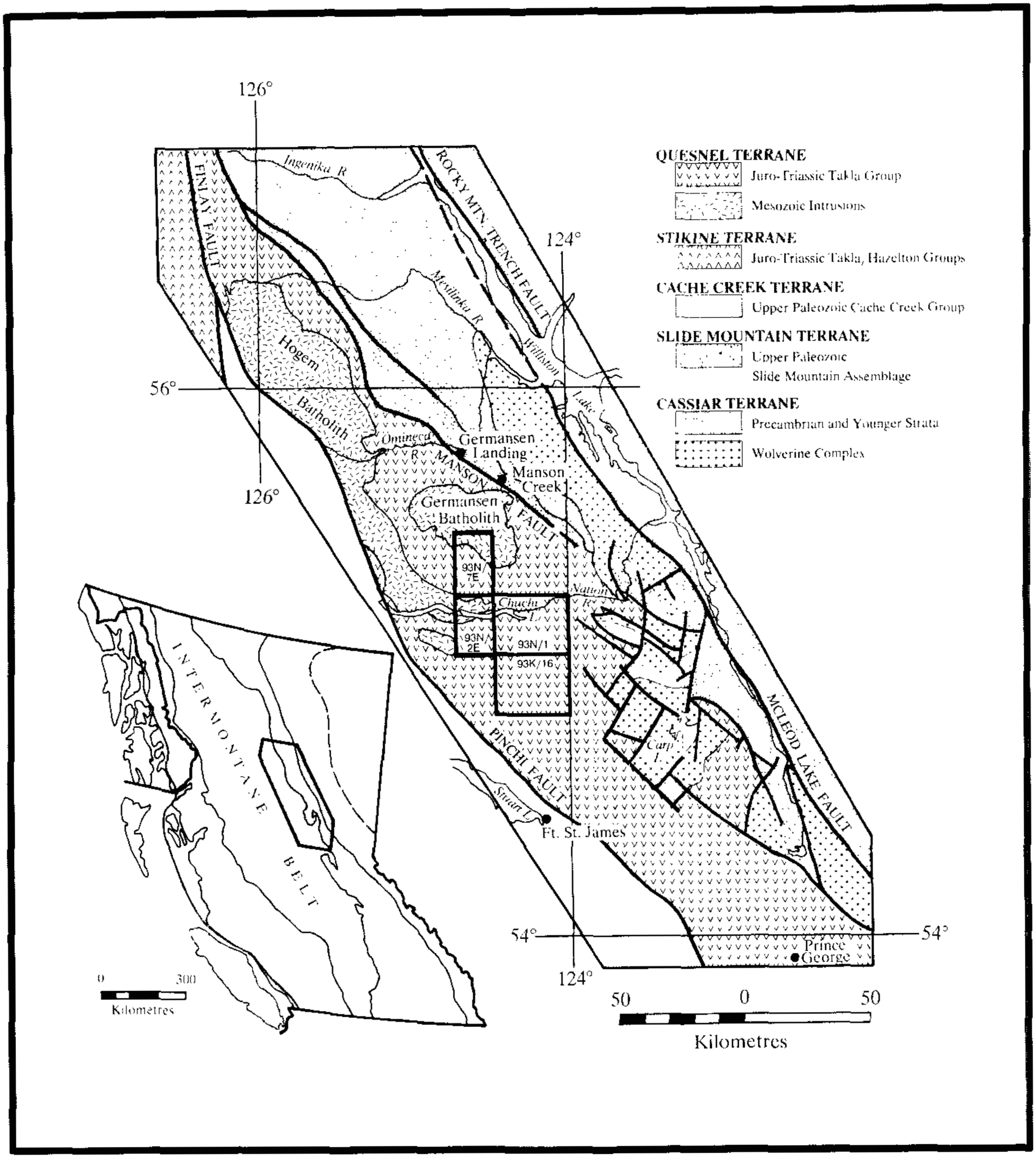

Figure 1-9-2. Tectonic setting of the Nation Lakes area.

St. James and Mackenzie (Figure 1-9-1). The Nation Lakes regional mapping project was started in 1990 to provide 1:50 000-scale geological maps to aid mineral exploration in the area, principally for alkaline porphyry copper-gold deposits similar to Mount Milligan. At time of writing (November, 1991) feasibility studies for Mount Milligan are still in progress, with results anticipated in early 1992.

Results of 1990 fieldwork on mapsheets 93N/1 and 93K/16 (Nelson *et al.*, 1991a, b) included:

- The establishment of a fourfold stratigraphic subdivision of the Takla Group.
- The identification of numerous Takla intrusions and associated alteration halos and mineralization.
- The delineation of a series of fault strands related to the Manson–MacLeod Lake transcurrent fault system, that divide the area near the Mount Milligan deposit into sets of horsts and grabens.

During 1991, this work was continued as mapping was extended to the west and north onto map sheets 93N/2E and 93N/7E (Figure 1-9-1). The resulting 1:50 000 maps are available as Open File 1992-4 (Nelson *et al.*, 1992).

REGIONAL SETTING

The Nation Lakes map area is part of the Quesnel Terrane and is underlain by Triassic-Jurassic island-arc rocks of the Takla Group (Monger *et al.*, 1990). The region is bordered by two major transform fault systems: the Manson–MacLeod Lake fault, which separates the Mesozoic volcanics from Paleozoic and younger strata to the east, and the Pinchi fault, which separates them from the oceanic Cache Creek Group to the west (Figure 1-9-2). Parts of two regional-scale batholiths are exposed in the map area. The southern end of the Early Jurassic and younger Hogem batholith intrudes the alkalic Takla volcanics on the shores of Chuchi Lake, and the southwestern margin of the Cretaceous Germansen batholith outcrops sparsely in the lowlands of the northeastern corner of 93N/7. The Takla Group volcanics are also intruded by roughly coeval, high-level, alkaline plutons which are responsible for the development of porphyry systems rich in copper and gold. For a more detailed discussion of the alkaline porphyry Cu-Au association and regional geological correlations refer to Nelson *et al.* (1991a).

GLACIAL GEOLOGY

The geomorphology of the Nation Lakes area bears a strong glacial imprint, particularly from the Fraser glaciation, the most recent ice advance. Glacial straie trend east to northeasterly, and large-scale glacial grooves are aligned at about 060°. Northeasterly regional ice-flow from the Coast Mountains was deflected by smaller ice masses originating in the Skeena Mountains to the north and the Cariboo Mountains to the south, resulting in flow directions that varied through time (Plouffe, 1991). Till and fluvioglacial deposits are thickest in the lowlands south and southwest of Witch Lake. Elsewhere, in most areas, scattered outcrops emerge from blanket to veneer till and outwash. Perched glacial channels occur on hillsides and are incised into the highest plateaus.

STRATIGRAPHY

TAKLA GROUP

Regional mapping of 93K/16 and 93N/1 during 1990 resulted in the subdivision of the Takla Group into four informal formations. From base to top these are the Rainbow Creek, Inzana Lake, Witch Lake and Chuchi Lake formations. The basal Rainbow Creek formation is comprised of dark grey and black basinal shales and siltstones correlative with the Triassic black phyllite unit near Quesnel. The Inzana Lake formation consists of interbedded distal and proximal pyroclastic volcanics and basinal sediments. It is overlain by, and interfingers with, the Witch Lake formation, which is dominated by augite-porphyritic volcanics and agglomerates. These rocks pass upward into plagioclase and augite-bearing fragmental rocks and flows of the Chuchi Lake formation.

Work done during the summer of 1991 shows an overall continuity of this stratigraphy with the addition of important facies transitions between and within the formations. In the eastern half of the Chuchi Lake map area (93N/2E), epiclastic sediments of the Inzana Lake formation interfinger eastwards with augite porphyry agglomerates of the Witch Lake formation from its base to near its assumed top. The Chuchi Lake formation has a much greater lithologic and petrologic diversity than previously thought, including augite and even olivine-phyric basalt flows and augite-plagioclase-phyric agglomerates as well as plagioclase and plagioclase-augite-phyric latites. Continuity within the Chuchi Lake formation is maintained by a sedimentary marker, erroneously denoted as Late Triassic in age [uTrCL(c); Nelson *et al.*, 1991a, b], which extends westward for 15 kilometres in 93N/7. Three Early Jurassic ammonite collections were made from this unit.

WITCH LAKE-INZANA LAKE RELATIONSHIPS

The Inzana Lake formation represents a submarine environment on the fringes of a dominantly augite-phyric. explosive basalt centre, such as is represented by the Witch Lake formation. Witch Lake agglomerates overlie Inzana Lake sediments in the nose of the regional anticline near Mudzenchoot Lake in 93N/1 (Nelson *et al.*, 1991a, b), and this contact extends westward into 93N/2 (Figure 1-9-3). However, south of Chuchi Lake in 93N/2, the monotonous Witch Lake augite porphyry agglomerates give way westward along strike to epiclastic sediments (dust tuffs, sandstones and siltstones) identical to the Inzana Lake formation (Figure 1-9-3). This contact is interpreted to be the western edge of a major basaltic edifice. The edifice extends eastwards to Mount Milligan, where it is truncated by the Cretaceous to Early Tertiary Great Eastern fault, and southwards to near Cripple Lake, where it may interfinger with Inzana Lake sediments under thick till (Nelson *et al.*, 1991a, b).

East of Klawli Lake (93N/7), Witch Lake lapilli tuffs and agglomerates interfinger with finer grained epiclastic sediments and appear below the south-dipping Chuchi Lake formation (Figure 1-9-4). Their inferred thickness is between 500 and 1300 metres, compared with more than

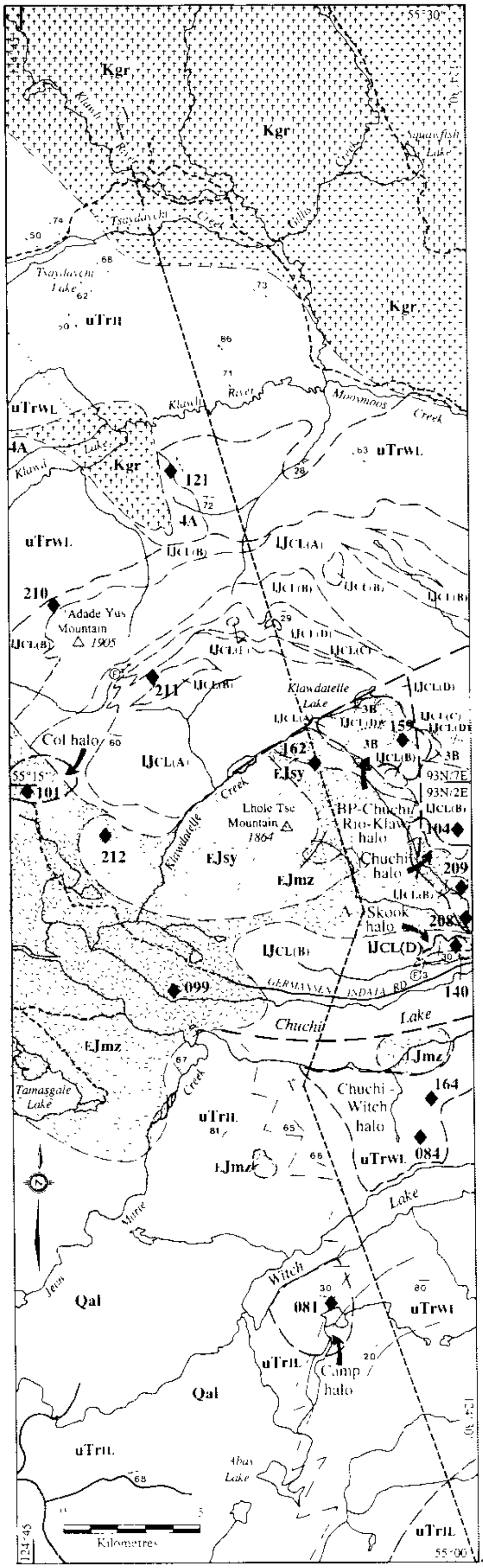

Figure 1-9-3. Generalized geology of 1992 project area, 93N/2 East Half and 93N/7 East Half.

LEGEND

LAYERED ROCKS

QUATERNARY

Qal — *UNCONSOLIDATED GLACIAL TILL AND ALLUVIUM*

UPPER TRIASSIC - JURASSIC

TAKLA GROUP

lJCL — **CHUCHI LAKE FORMATION: (A)** *HETEROLITHIC AGGLOMERATE;* **(B)** *PLAGIOCLASE ± AUGITE PORPHYRY ANDESITE, LATITE AND DACITE FLOWS;* **(C)** *AUGITE/HORNBLENDE + PLAGIOCLASE ± OLIVINE BASALT FLOWS;* **(D)** *INTERVOLCANIC SEDIMENTS. SANDSTONE, SILTSTONE, SHALE, CHERTY TUFF;* **(E)** *CONGLOMERATE*

uTrWL — **WITCH LAKE FORMATION:** *AUGITE (± PLAGIOCLASE ± HORNBLENDE) PORPHYRY AGGLOMERATE, LAPILLI TUFF AND EPICLASTIC SEDIMENTS*

uTrIL — **INZANA LAKE FORMATION:** *VOLCANIC SANDSTONE, SILTSTONE, CHERTY TUFF, MUDSTONE, ARGILLITE, LAPILLI TUFF AND AUGITE PORPHYRY AGGLOMERATE*

INTRUSIVE ROCKS

MIDDLE TO LATE CRETACEOUS

GERMANSEN BATHOLITH

Kgr — *COARSE-GRAINED GRANITE, EQUIGRANULAR TO ORTHOCLASE MEGACRYSTIC*

EARLY JURASSIC

HOGEM INTRUSIVE COMPLEX

EJsy — *MEDIUM-GRAINED SYENITE ± QUARTZ*

EJmz — *COARSE-GRAINED EQUIGRANULAR MONZONITE*

EARLY JURASSIC?

SYN-TAKLA INTRUSIONS*

1 — **GRANITE SUITE: (1A)** *COARSE TO MEDIUM-GRAINED, EQUIGRANULAR GRANITE;* **(1D)** *RHYODACITE/DACITE*

2 — **SYENITE SUITE: (2A)** *COARSE TO MEDIUM-GRAINED, EQUIGRANULAR SYENITE;* **(2B)** *CROWDED PLAGIOCLASE-PORPHYRITIC SYENITE;* **(2C)** *MEGACRYSTIC SYENITE*

3 — **MONZONITE SUITE: (3A)** *COARSE TO MEDIUM-GRAINED, EQUIGRANULAR MONZONITE;* **(3B)** *CROWDED PLAGIOCLASE-PORPHYRITIC MONZONITE;* **(3C)** *MEGACRYSTIC PLAGIOCLASE MONZONITE,* **(3D)** *SPARSELY PORPHYRITIC LATITE*

4 — **DIORITE/MONZODIORITE SUITE: (4A)** *COARSE TO MEDIUM-GRAINED, EQUIGRANULAR DIORITE/MONZODIORITE;* **(4B)** *CROWDED PLAGIOCLASE-PORPHYRITIC DIORITE;* **(4C)** *MEGACRYSTIC PLAGIOCLASE (± AUGITE)-PORPHYRITIC DIORITE;* **(4D)** *SPARSELY PORPHYRITIC ANDESITE*

5 — **GABBRO/MONZOGABBRO SUITE: (5A)** *COARSE TO MEDIUM-GRAINED, EQUIGRANULAR GABBRO/MONZOGABBRO*

6 — **ULTRAMAFIC SUITE: (6A)** *COARSE-GRAINED EQUIGRANULAR LAMPROPHYRE*

* Not all lithologic types are present in the map area; however the complete listing is retained for consistency with Nelson *et al.*, 1991a and 1991b.

SYMBOLS

geologic contact (approximate, inferred)

lithologic contact (approximate, inferred)

facies relationship (inferred)

fault (approximate)

bedding (tops known, tops unknown, overturned) — 50 50 50

foliation — 78

area of alteration

mineral occurrence and MINFILE number — 164

fossil locality — F3

elevation in metres — 1905

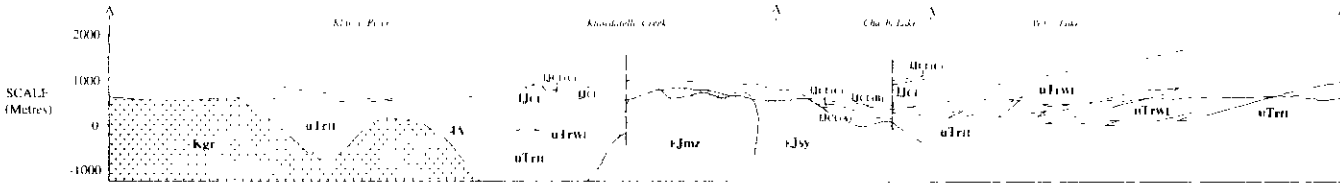

Figure 1-9-4. Geologic cross-section of 93N/2 East Half and 93N/7 East Half. The location of section A-A'-A''-A''' is on Figure 1-9-3.

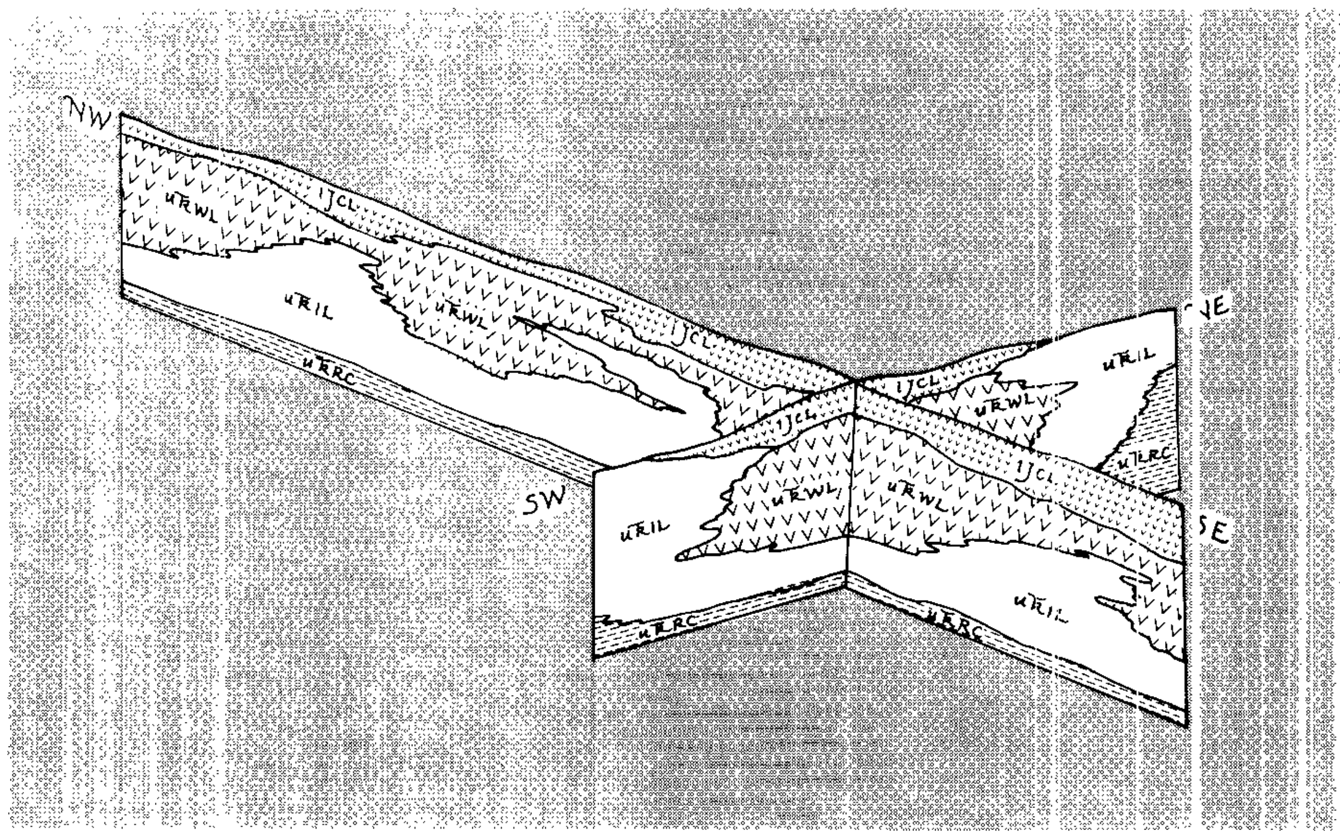

Figure 1-9-5. Sketch showing generalized Takla Group facies relationships along and across the arc axis. Augite-phyric basalts of the Witch Lake formation form coalescing piles along the arc axis. The dominantly epiclastic Inzana Lake formation underlies these piles, interfingers with them, and also dominates the fore arc and back arc. The basinal Rainbow Creek formation becomes more prominent further into the back-arc region.

5 kilometres of Witch Lake stratigraphy south of Chuchi Lake. This area may lie near the northern extent of the volcanic pile. Overall, the volcanic edifice extends over 1000 square kilometres in this region and probably formed by coalescing fissure eruptions.

These facies relationships demonstrate that the Witch Lake and Inzana Lake formations are lithostratigraphic rather than time-stratigraphic units. Simple stratigraphic columns generally depict the centres of basaltic edifices, such as the Mount Milligan area (Nelson *et al.*, 1991a) and near Quesnel (Bailey, 1989). Figure 1-9-5 provides a more general view of the early Takla arc, in which discrete basaltic centres are surrounded by blankets of epiclastic products in the fore-arc and back-arc areas as well as longitudinally between centres.

AGE OF THE INZANA AND RAINBOW CREEK FORMATIONS

Two preliminary conodont ages from the Tezzeron Creek map area (93K/16) help to constrain the onset of Takla volcanism. One, from the pre-volcanic Rainbow Creek formation near Dem Lake is late Carnian; the other, from the Inzana Lake formation, is Norian (M.J. Orchard, personal communication, 1991).

THE CHUCHI LAKE FORMATION

The Chuchi Lake formation north of Chuchi Lake (93N/1) consists of heterolithic plagioclase± augite-phyric lahars and lesser maroon plagioclase-phyric latite and trachyte flows, with a single west-northwesterly striking sandstone-siltstone unit near the northern border of the map area (Nelson *et al.*, 1991a, b). This marker horizon dips moderately south and extends northwestwards under cover towards the BP-Chuchi and Rio-Klaw properties, where sediments outcrop minimally but are intersected in many drill holes. North of Klawdetelle Creek, the sediment horizon is exposed in the cirques of 'Adade Yus Mountain (Figure 1-9-3), where it dips gently south and strikes nearly east-west, with an estimated thickness of 250 metres. It pinches out into volcanic flows toward the west. The sediments include brown-weathering sandstone, siltstone, dark grey shale and variable amounts of cherty, pale green dust-tuff.

The external relationships of the sedimentary marker illustrate the petrologic and lithologic variability of the Chuchi Lake formation (Figure 1-9-6). On 'Adade Yus Mountain (Figure 1-9-6A), a lower sedimentary interval 10 metres thick is interbedded with green and maroon amygdaloidal clinopyroxene±plagioclase-phyric and aphanitic basalt flows 150 metres below the main sedimentary unit. The major interval of sediments is overlain by heterolithic agglomerates with plagioclase±augite, augite±plagioclase, plagioclase±acicular hornblende porphyry clasts and locally altered and pyritized monzonite fragments. This unit is indistinguishable from the heterolithic agglomerate that lies below the sediments.

East of 'Adade Yus Mountain (Figure 1-9-6B), the sediments contain abundant fine-grained tuff and overlie a green porphyritic agglomeratic flow unit with plagioclase laths up to 1 centimetre in size and lesser augite. The sediments coarsen upwards into thick sandstone beds with abundant rip-up clasts of shale. These are overlain by pebbly grit and conglomerate with clasts of pink glassy flow-banded trachyte, welded trachytic tuff, quartz-jasper veins, subvolcanic intrusions and strongly epidotized volcanic rocks which represent both local and exotic source rocks. These conglomerates are overlain by heterolithic agglomerate.

In 93N/1 (Figure 1-9-6D), the sediments lie between identical heterolithic lahars. This package overlies an augite(-olivine)-phyric basalt flow (or flows?) that underlies much of the prominent ridge along the southern border of 93N/8. It may correlate with the flows below the sediments on 'Adade Yus Mountain. On the BP-Chuchi property (Figure 1-9-6C), the sediment package overlies and also interfingers with heterolithic agglomerates and lapilli tuffs that contain abundant crowded porphyry intrusive clasts. They are discussed further in the property description. The sediments are capped by a distinctive suite of plagioclase and augite-phyric intermediate flows with large phenocrysts. The flow unit continues south, interrupted by an apophysis of the Hogem batholith, to the Skook claims (Figure 1-9-6E). There volcanic flows overlie sandstones, siltstones

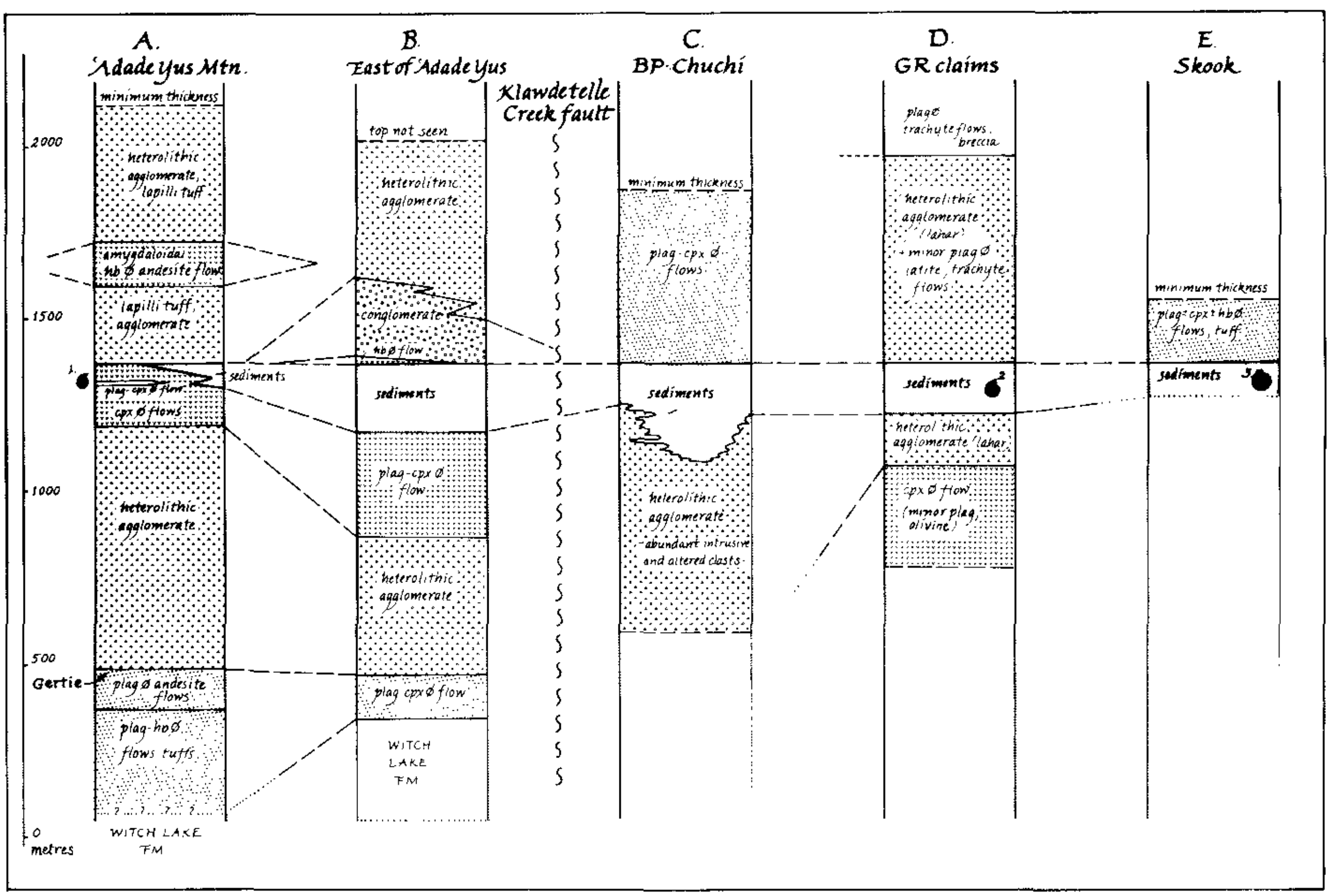

Figure 1-9-6. Selected stratigraphic columns through the Chuchi Lake formation.

and white-weathering cherty tuffs with limy nodules. In the cross-section (Figure 1-9-4) the Skook sediments are interpreted as an inlier of the main sedimentary marker.

In contrast to the underlying Witch Lake formation, the Chuchi Lake formation is characterized by extreme variability in rock composition and texture. The 1650 metres of Chuchi Lake stratigraphy are composed predominantly of heterolithic volcanic agglomerates, plagioclase and plagioclase $\pm$ augite-phyric latites and andesites, lesser augite (and even olivine)-phyric basalts and trachytes. Internal facies variations within the flows are also pronounced. Local flow packages show consistency in textures and even in the shapes of phenocrysts. They grade laterally into heterolithic agglomerates and lahars which represent much broader textural and compositional parentage. Flows are especially prominent from the north shore of Chuchi Lake to Klawdatelle Creek and northwestwards towards 'Adade Yus Mountain. A major volcanic centre may be masked by the intrusive rocks of the Hogem batholith.

The basal contact of the Chuchi Lake formation is exposed on one ridge in east-central 93N/7. Augite-porphyry lapilli tuffs pass transitionally upwards into slightly maroon, heterolithic plagioclase $\pm$ augite-phyric agglomerates. At this locality there is no suggestion of unconformable relationships between the two formations. However, at one locality between Chuchi and Witch lakes, a few outcrops of maroon plagioclase-porphyritic flows and fragmentals occur within an area otherwise underlain by dark green augite-porphyritic agglomerates and volcanic sediments of the Witch Lake formation. The maroon rocks are archetypical of the Chuchi Lake formation and may represent its base. If this interpretation is correct, then the base of the Chuchi Lake formation here is morphologically irregular and lithologically abrupt and thus may be a local unconformity. Alternatively, these rocks may represent part of a Witch Lake centre, deposited in conditions more typical of the Chuchi Lake formation (i.e., above wave base) or could belong to the Chuchi Lake formation proper and be a fault-bounded sliver, although there is no supporting evidence for the latter.

AGE OF THE CHUCHI LAKE FORMATION

Three collections of ammonites and two collections of brachiopods were made from the sedimentary marker in the Chuchi Lake formation. Collection 91-1 is from the 10-metre interval below the main marker on 'Adade Yus Mountain (Figures 1-9-3, 1-9-6A, Plate 1-9-1). Collection 91-2 is from map sheet 93N/8, 200 metres north of the western extent of the sedimentary unit as shown in Figure 1-10-4a of Nelson *et al.* (1991a). Collection 91-3 is from a stream gully 2 kilometres from the eastern border of 93N/2 and 500 metres north of the Germansen-Indata road (Figure 1-9-3). The ammonites were identified by Howard Tipper of the Geological Survey of Canada. Collections 91-1 and 91-2 are probably of early Pliensbachian age, and Collection 91-3 is of late Pliensbachian age (H.W. Tipper, personal communication, 1991; Table 1-9-1). These fossil collections demonstrate that Chuchi Lake formation volcanism continued at least as late as Pliensbachian time. This is the youngest documented age of volcanism in Quesnellia. The uppermost volcanic units near Quesnel, and the augite porphyries of the Elise Formation near Rossland, are overlain by sediments of Pliensbachian age (Bailey, 1989; Höy and Andrew, 1989; Tipper, 1984).

This Early Jurassic age for the Chuchi Lake formation indicates that the Takla Group in the Nation Lakes area spans the Triassic-Jurassic boundary. The Inzana Lake formation is, at least in part, of Norian age. The Slate Creek formation near Manson Creek (Ferri and Melville, in preparation) and the basal Takla sediments between the Pinchi fault and the Hogem batholith (Armstrong, 1949) are also Late Triassic. At this point, no regional unconformities that might correspond to the Triassic-Jurassic boundary have been recognized in the Takla Group in this area. The contact between the Inzana Lake and Witch Lake formations is transitional, as is the basal contact of the Chuchi Lake formation with the one exception noted above. The upper and lower contacts of the sedimentary marker unit show interbedding of sediments, flows and fragmental rocks. At the easternmost exposure of the sedimentary marker in 93N/1, 10 metres of brown sandstones and siltstones are interbedded with lahars. Wood fragments occur within both the sandstones and the lahars, and two brachiopods were discovered in the matrix of the underlying lahar. In summary, field evidence in the Nation Lakes area suggests a continuous Triassic-Jurassic volcanic sequence, with a volcanic lull during Pliensbachian time.

STRUCTURE

The structural fabric of the 1991 map area is simple, with few faults and only one regional fold. The lack of faults is in strong contrast to the Mount Milligan area, which is transected by strands of the Manson–MacLeod Lake fault system. The present map area, in central Quesnellia, is relatively unaffected by the Manson–MacLeod Lake or the Pinchi transcurrent faults.

A northwesterly trending regional anticline underlies the western part of 93K/16 and 93N/1 (Nelson *et al.*, 1991a, b). Its hinge zone and part of the western limb continues into 93N/2. Interfingering Witch Lake and Inzana Lake formations strike northeasterly and dip gently to moderately northwest (Figure 1-9-3). This regional-scale fold is not present north of Chuchi Lake; instead, an approximately homoclinal panel of Chuchi Lake formation dips gently to the south. A fault is therefore inferred under Chuchi Lake, based on these differences in stratigraphy and structural trends. The preferred interpretation for the disappearance of the anticline north of Chuchi Lake, is that the fault may have formed at a point of structural weakness along the plunge depression of the anticline. The open nature of the fold, and the gentle dips of bedding on both sides of Chuchi Lake, support the idea that the fold opens further to the north and loses its identity. Movement on the Chuchi Lake fault probably predated emplacement of the Hogem intrusive complex, since it does not offset the strong magnetic anomaly associated with the monzonite. Also, the fault may have acted as a guide for the satellite body of coarse-grained monzonite exposed on the south side of Chuchi Lake at the east end of the map area.

Other significant faults in the area include an east-northeasterly trending fault along Klawdetelle Creek and a northerly striking fault on the BP-Chuchi property that terminates against the Klawdetelle fault. Both of these structures offset the sedimentary marker unit in the Chuchi Lake formation. The Klawdetelle fault also seems to have exerted control over the northwestern margin of the Chuchi syenite, a late phase of the Hogem intrusive complex. Therefore this fault, like the Chuchi Lake fault, was probably active between Takla Group deposition and intrusion of the Hogem batholith.

The excellent exposures on, and east of, 'Adade Yus Mountain provide good control on the attitudes of regional bedding and the often strongly discordant orientations of individual beds within them. The Chuchi Lake formation as a whole is only gently warped in these exposures, in spite of the tight folds observed in thin-bedded sediments. In a more general sense, the complicated structural history unravelled from the Inzana Lake formation in 93K/16 (Nelson *et al.*, 1991a, b) is not shared by the Witch Lake and Chuchi Lake volcanic units: the Takla Group is disharmonically folded. Regional-scale structures are broad and open while incompetent layers such as the Inzana Lake formation are intensely deformed. Because of the conflicts between local and regional bedding attitudes, major contacts were used exclusively in construction of the cross-section of the project area (Figure 1-9-4).

Sporadic zones of strong northwesterly trending foliation, separated by areas with weaker fabrics, occur in the Inzana Lake formation around Tsaydaychi Lake and between the Klawli River and the Germansen batholith. In thin section, the foliation consists of strongly oriented actinolite needles and, less commonly, biotite trains that wrap around relict augite phenocrysts. Within a kilometre of the Germansen batholith, inside its thermal aureole, the foliation is overprinted by randomly oriented actinolite and biotite, and the matrix has a finely granular texture. The sporadic development of foliation resembles the structural style seen near fault strands in the Mount Milligan area (Nelson *et al.*, 1991a). Such a fault, perhaps part of the Manson Creek system, may have controlled the southwestern margin of the Germansen batholith. In addition, parts of the batholith margin, for example north of Moosmoos Creek, show post-solidus deformation and foliation. Microscopically the foliation is due to recrystallization of igneous biotite to finer grained trains, accompanied by subgrain formation in feldspars and neoblast recrystallization along grain boundaries. Thus, strain in this area both preceded and postdated intrusion of the Cretaceous Germansen batholith.

INTRUSIONS

TAKLA INTRUSIONS

Relatively fine-grained mafic to intermediate hypabyssal intrusions occur in several areas within the Takla Group.

Plate 1-9-1. Lower sedimentary bed on 'Adade Yus Mountain, at the early Pliensbachian ammonite locality.

Their textures and alkalic character link them to the Takla Group; moreover hypabyssal clasts of these intrusions are abundant in parts of the Chuchi Lake formation. The intrusions are classified using the scheme developed by Nelson *et al.* (1991a); that is on the basis of their textures and compositions. Some intrusions are described in more detail in connection with their associated alteration halos. The intrusions are grouped from north to south and include the following:

(1) The older phase of the intrusion around Klawli Lake. This syn-Takla hypabyssal complex is made up of a variety of textural and compositional variants including equigranular diorite with 0 to 5 per cent quartz (4A), a border phase of microdiorite which is sometimes interbanded on a centimetre scale with a more leucocratic igneous phase giving the rock a fallacious gneissic appearance (4A), and rare biotite lamprophyre (6A; new classification, coarse-grained, equigranular ultramafite) comprised entirely of altered mafic minerals. Fragments of the equigranular diorite occur in the surrounding volcanic agglomerates, indicating that intrusion was contemporaneous with volcanism. Contact metamorphism has converted pyroxenes to amphiboles and hornfelsed the volcanic country rocks. The later potassium feldspar megacrystic granite intrusive phase has generated a contact aureole both in the intrusion and in the volcanic rocks around it. This body is probably related to the Germansen batholith and is discussed below.

(2) A small, pink, crowded plagioclase±acicular hornblende monzonite porphyry (3B) that occurs in a glacial gully 4 kilometres north of Klawdetelle Lake. Its margins are composed of intrusive breccias with clasts of monzonite and volcanic lithologies (Plate 1-9-2).

TABLE 1-9-1
FOSSIL IDENTIFICATIONS

REPORT J7-1991-HWT

Report on three collections of Jurassic fossils, collected in 1991, from the Manson Creek map area (93N), British Columbia, submitted by Joanne Nelson, BCMEMPR.

Field No.:	91JN-19-4	GSC Loc. No: C-189721
Locality:	North of Chuchi Lake, Skook claims. In an east-west gully 0.5 km north of main logging road. UTM 403200E 611700N; 93N/2.	
Identifications:	*Leptaleoceras* aff. *accuratum* (Fucini) *Leptaleoceras* sp. *Fuciniceras?* sp. *Arieticeras* cf. *algovianum* (Oppel)	
Age and comments:	Late Pliensbachian. Lower part of the Kunae zone. This is a first occurrence of the late Pliensbachian in the Fort St. James area. Important new information for Quesnellia Terrane.	

Field No.:	91JN-93N8W	GSC Loc. No.: C-189719
Locality:	Clearcut north of Chuchi Lake, GR claim group. UTM 410550E 6123275N; 93N/8W.	
Identifications:	*Amaltheus* sp. *Fanninoceras?* sp. *Leptaleoceras* aff. *accuratum* (Fucini) *Arieticeras?* sp.	
Age and comments:	Late Pliensbachian. Lower part of the Kunae zone. Almost certainly equivalent to collection C- 89721	

Field No.:	91CRE-7-3	GSC Loc. No.: C-189720
Locality:	'Adade Yus Mountain north of Chuchi Lake. UTM 392875E, 6128050N; 93N/7E.	
Identifications:	*Tropidoceras* sp. *Acanthopleuroceras?* sp. *Metaderoceras evolutum* (Fucini) *Gemmellaroceras??* sp. *Phricodoceras???* sp. bivalves	
Age and comments:	Early Pliensbachian. Whiteavesi zone. Material is compressed but the assemblage is clearly early Pliensbachian in age and almost certainly Whiteavesi zone; i.e., mid-early Pleinsbachian.	

H.W. Tipper Research Scientist R.I. Thompson Subdivision Head 15 November 1991	Cordilleran Division Geological Survey of Canada 100 West Pender Street Vancouver, B.C. CANADA

(3) A very small plug or dike of equigranular, medium-grained, grey-green hornblende monzonite (3A) located 3.5 kilometres southeast of 'Adade Yus Mountain.
(4) The intrusive complex south of Klawdetelle Lake on the BP-Chuchi and Rio-Klaw properties (MINFILE 093N 159). Numerous small plutons and sills of crowded plagioclase-porphyritic monzonite (3B) and crowded plagioclase±acicular hornblende monzonite (3B) intrude the sedimentary unit in the Chuchi Lake formation. In terms of textures and compositions, these intrusions very closely match the suite at the Mount Milligan deposit. Fragmental rocks that contain abundant crowded-porphyry monzonite clasts, as well as altered clasts, are associated with these plutons.
(5) The crowded plagioclase-porphyritic monzonites (3B) on the Rio-Witch property (MINFILE 093N 164) between Chuchi and Witch Lakes. They are associated with finely milled intrusive breccias.
(6) A swarm of large hornblende-porphyritic dikes (4C) on the Camp property (MINFILE 093N 081) south of Witch Lake. The large blocky hornblende crystals in these dikes link them texturally with the dikes on the Tas property (MINFILE 093K 080; Nelson *et al.*, 1991a, b). Similar dikes, and also crowded plagioclase porphyries (3B) and one intrusive breccia occur as far as 5 kilometres southeast of the main Camp showing.

The Hogem Intrusive Complex

The southeastern end of the Hogem batholith outcrops on the north and south shores of Chuchi Lake. It comprises at least three main phases, each phase consisting of many textural and compositional variants. This intrinsic variability suggests that the Hogem batholith is better described as an intrusive complex. The earliest and most mafic phase forms a few outcrops at the northern margin of the complex 1.5 kilometres from the eastern border of 93N/2. It consists of layered gabbro and pyroxenite, cut by hornblende-plagioclase-epidote-magnetite pegmatite stringers and pods. Dikes of coarse pegmatitic monzonite and syenite establish this mafic marginal phase as older than the remainder of the complex.

Medium to coarse-grained equigranular monzonite dominates the second Hogem phase. It outcrops on the shores of Chuchi Lake and on the Col property (MINFILE 093N 101). In some areas the pluton appears uniform, but overall this phase is highly variable and includes textures ranging from fine grained to pegmatitic, equigranular to porphyritic and compositions spanning gabbro, monzogabbro, monzodiorite, diorite (±quartz) and syenite. These lithologies appear to grade into each other, although in some areas the more mafic lithologies are cut by felsic dikes. Porphyritic monzonite contains phenocrysts of plagioclase, hornblende and augite. Biotite can occur either as regular plates or as large oikocrysts and magnetite contents range up to 7 per cent.

The latest phase of the Hogem intrusive complex underlies Lhole Tse Mountain (also called Chuchi Mountain) and is referred to as the Chuchi syenite (Garnett, 1978). It includes syenite and quartz syenite, with quartz ranging up to 7 per cent. True granite is very rare. The predominant texture of the Chuchi syenite is medium grained, equigranular to aplitic, with hornblende and/or biotite ranging from 2 to 10 per cent. Medium to coarse-grained phases with megacrystic orthoclase are also present. They show that orthoclase was on the liquidus when the syenite was forming. This is in direct contrast to the less-evolved monzonite phase where potassium feldspar does not form phenocrystic phases. Dikes of syenite cut the coarse-grained monzonite on the flanks of Lhole Tse Mountain and on the Col property and xenoliths of monzonite occur in syenite; therefore the Chuchi syenite is the latest phase of the Hogem intrusive complex in the area.

Garnett (1978) reported K-Ar ages for the older parts of the Hogem intrusive complex ranging from 206 to 178 Ma (converted to new decay constants), corresponding to Sinemurian to Bajocian faunal zones. The older age is perhaps coeval with early Chuchi Lake volcanism, while the younger age postdates the collision of Quesnellia with the margin of ancestral North American.

Plate 1-9-2. Mixed monzonite-volcanic breccia along the steep margins of a small intrusion 4 km north of Klawdetelle Lake.

Germansen Batholith and Klawli Stock

The northeastern corner of 93N/7 is an area of very sparse outcrop underlain by Cretaceous granite of the Germansen batholith (106±4 Ma, K-Ar biotite; Ferri and Melville, in preparation). Unlike the Hogem intrusive complex, the Germansen batholith displays a monotonous uniformity of composition and texture. It is coarse grained, with 25 to 35 per cent plagioclase, 25 to 40 per cent orthoclase, 20 to 30 per cent quartz and 7 to 15 per cent biotite and hornblende. Orthoclase forms megacrysts in about half of the outcrops visited. Magmatic crystal-alignment fabrics are not present. In a few areas near its southern margin, a subsolidus foliation characterized by wispy quartz stringers is evident. Unlike the Hogem monzonite, the Germansen batholith is only weakly magnetic.

The Klawli stock is texturally and compositionally identical to the Germansen batholith. It intrudes the core of the early dioritic Takla intrusion near Klawli Lake and mimics its shape. The Klawli stock is composed of unvarying coarse-grained granite with 20 per cent pink orthoclase megacrysts 1.5 to 2 centimetres in length and 5 to 10 per cent mafics (hornblende±biotite). We concur with Armstrong (1949) that the Germansen batholith and the Klawli stock belong to the same intrusive suite and are probably both Cretaceous in age.

METAMORPHISM

Regional metamorphism in the area increases from prehnite-pumpellyite grade in the Chuchi Lake formation near Klawdetelle Creek to lower greenschist grade in the Inzana Lake formation north of the Klawli River. The transition may be partly a function of stratigraphic depth; also, metamorphic grade increases in a northeasterly direction towards the Manson–MacLeod Lake fault zone in the Mount Milligan area (Nelson *et al.*, 1991a) and may show a similar pattern here.

Contact metamorphic textures are of two types. Very fine grained, flinty hornfelses with lavender shades are due to submacroscopic biotite concentrations and occur in the aureoles of the syn-Takla intrusions. Near the Germansen batholith and Klawli intrusion, and in places near the Hogem intrusive complex, coarse-grained hornfelses are developed with macroscopic actinolite and biotite, and patches, segregations and vesicle fillings of epidote, in some areas with garnet. The garnet probably formed at the expense of epidote as a result of the reaction: epidote + quartz = grossular-andradite + anorthite + magnetite + water. Planar fabrics are associated with the thermal peak in the inner contact aureole of the Klawli intrusion. They result from crystallographic alignment of biotite; the overall texture is granoblastic. These fabrics contrast strongly with the pre-intrusive deformation noted north of the Klawli River. They are consistent with forceful emplacement of the Klawli intrusion.

ALTERATION AND MINERALIZATION

Four halos of pervasive alteration are associated with syn-Takla intrusions in the map area. They range from well-defined to somewhat speculative porphyry copper-gold systems. The most prominent is the BP-Chuchi/Rio-Klaw halo, with roughly 30 million tonnes of geological reserves. Second most important is the Witch halo, currently being explored by Rio Algom Exploration Inc. This large halo is partly on 93N/1 (Nelson *et al.*, 1991a, b) and partly on 93N/2, where the Moss showing is located. The Skook halo lies north of Chuchi Lake. In it, a zone of potassic alteration is associated with a swarm of crowded monzonite porphyry dikes. It was drilled by BP Resources Canada Ltd. in 1991. In the Camp halo south of Witch Lake, minor amounts of chalcopyrite and malachite occur in a hornfelsed zone.

Two alteration halos are developed within the Hogem batholith: the western half of the Chuchi halo north of Chuchi Lake, and the Col halo west of Chuchi Mountain. In these, coarse-grained, pink secondary potassium feldspar occur with magnetite and copper sulphides in veins and pegmatites along discrete fractures.

In addition to alteration halos, two new mineral showings are highlighted. The Gertie and Hannah showings are not associated with large alteration systems but are indicative of porphyry and perhaps porphyry-related mineralization.

BP-Chuchi/Rio-Klaw Halo (Minfile 093N 159, Chuchi Lake)

This extensive intrusive complex and alteration halo lies in the southeastern corner of 93N/7, south of Klawdetelle Creek. The centre of the system is on the Phil claims, where BP Resources Canada Ltd. has been drilling since 1989 (Wong, 1990). The northern extension on the Klaw claims was drilled by Rio Algom Exploration Inc. in 1990 and 1991 (Campbell, 1990a, 1991). The alteration system is bounded to the east by a north-trending fault, and to the north by the fault in Klawdetelle Creek. Within it, crowded plagioclase-porphyritic monzonite stocks intrude the sedimentary horizon in the Chuchi Lake formation [lJCL(?)] and blossom out into sill swarms (Wong *et al.*, 1991). In many instances in drill core, hornfelsed sedimentary rocks show soft-sediment deformation and are intimately intercalated with monzonite: this association is considered by some BP geologists to indicate intrusion of the monzonites while the sediments were still unlithified (Russ Wong, personal communication, 1990), although further study is necessary to document this. The fine-grained, well-bedded sandstones, siltstones and tuffs grade downwards into massive coarse lapilli tuffs and agglomerates. In many cases, intrusive clasts form a large percentage of the fragmental material. Crowded plagioclase porphyry clasts with small blocky plagioclase crystals less than 2 millimetres across are common, and identical to the later porphyries that intrude the sediments. Clasts with pink secondary potassium feldspar, magnetite and epidote are also present.

Abrupt changes occur in the relative percentage of sedimentary rocks and fragmental material between closely spaced drill holes (Bernie Augsten, personal communication, 1991). Possible interpretations of this include rapid facies changes or local faulting. In the valley of Klawdetelle Creek, drill intersections of monotonous black argillites contain virtually no coarse components (Campbell, 1991).

The strong difference between these sections and the fragmental-rich sedimentary sections farther south and west may constitute evidence for facies changes over less than 2 kilometres.

On the ridge 1 kilometre south of the main mineralized area, the sedimentary section is overlain by a suite of plagioclase-augite and augite-plagioclase-phyric flows and minor, thin crystal tuffs of identical composition. These flows contain plagioclase laths 0.6 to 1 centimetre long, commonly synneused to give a ragged appearance to their terminations; and blocky augite crystals up to 0.8 centimetre in diameter. A partly brecciated plagioclase-augite porphyry dike with this distinct appearance cuts the crowded-porphyry monzonite in BP diamond-drill hole 1991-53.

The geological relationships described here point to an intimate relationship between the hypabyssal intrusions and sedimentation (Figure 1-9-7). Some intrusions predate the sedimentary unit, as clasts of them occur in and are also interbedded with the underlying fragmental units. Other intrusions cut the sediments but not the overlying flows. A possible feeder dike to the flows cuts one of the monzonites. The predominance of sills over dikes suggests that they were intruded before lithification was complete, as is observed with synsedimentary igneous activity in, for instance, the Guaymas Basin. It is also possible, albeit not proven, that the sills plastically deformed the sediments around them. The abundance of intrusive material in the surface fragmentals probably resulted from surface venting of intrusive breccias into the sedimentary basin.

In light of the geological evidence that sedimentation, intrusion and porphyry-style copper-gold mineralization were roughly coeval, the Early Jurassic, Pliensbachian fossil ages of the sedimentary horizon would also date the BP-Chuchi porphyry system. As at Mount Milligan (Dale Sketchley, personal communication, 1991), the presence of sediments in this system may have helped to enhance the size and intensity of the altered area, by providing a permeable zone for lateral expansion of the intrusions and the hydrothermal cells. Bailey (1988) cites alteration of Pliensbachian sediments by the Bullion Pit stock near the Quesnel River, dated as 193 Ma by K-Ar on biotite. This porphyry system may have been approximately coeval with the BP-Chuchi system.

Both the monzonite and the sediments at BP-Chuchi are extensively altered. Secondary potassium feldspar occurs in pink veinlets in the monzonite with magnetite, pyrite and chalcopyrite. The sedimentary rocks show a strong biotite hornfels overprint, with subsequent mottling by potassic and propylitic alteration. Hairline veinlets with bleached selvages and magnetite veinlets and disseminations are also characteristic of alteration. Rough geological reserves for this system are about 50 million tonnes with grades between 0.21 and 0.40 per cent copper and 0.21 and 0.44 gram per tonne gold (Digger Resources Inc., news release, October 17, 1991).

CHUCHI-WITCH HALO (MINFILE 093N 084 MOSS; MINFILE 093 164, WITCH)

This broad alteration halo spans the border of 93N/2 and 93N/1 between Chuchi and Witch lakes and covers an area of 3 by 5 kilometres (Nelson *et al.*, 1991a, b). Most of it lies on the Chuchi claims of Rio Algom Exploration Inc. (Campbell, 1990b; Campbell and Donaldson, 1991). Vol-

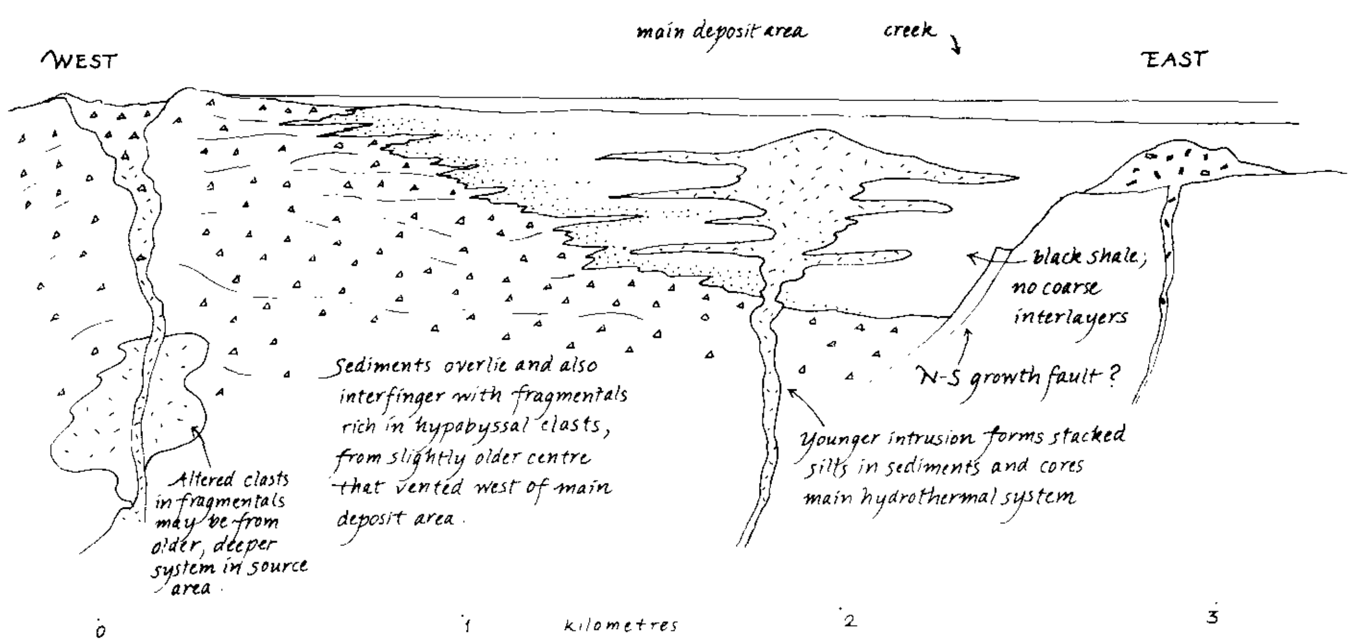

Figure 1-9-7. Cartoon of unit relationships around the BP-Chuchi deposit in Pliensbachian time. The anomalous thickness of sediments near the deposit is explained by half-graben development, with movement occurring on the north-trending fault located along the creek between the deposit and the "multi-element zone" to the east. To the west, the sediments pinch out against an edifice built of fragmental deposits, including intrusive debris, from a centre that predates the main intrusion.

canic rocks of the Witch Lake formation, including augite-porphyritic flows and fragmentals, aphanitic volcanics and minor tuffs, host the alteration system. In it, biotite hornfelsing is widespread. It is overprinted by patchy potassic and propylitic alteration. Pyrrhotite, pyrite and minor chalcopyrite occur throughout the halo. Secondary magnetite is locally abundant. Skarn occurs in several areas at the expense of limy tuffaceous sediments. Skarn minerals include epidote, garnet and diopside. In one thin section from 93N/1 diopside skarn is overprinted by secondary potassium feldspar.

In comparison to the BP-Chuchi/Rio-Klaw halo, the volume of exposed hypabyssal intrusive rock is very small. Crowded plagioclase-porphyritic monzonite forms tiny scattered stocks and dikes with associated intrusive breccias. The breccias are easily confused with surface fragmentals, except that they are more disorderly and the clasts are entirely intrusive. This region is also intruded by several phases of the Hogem intrusive complex including coarse-grained equigranular monzonite, sericite-bearing potassium feldspar pegmatite and coarse-grained syenite.

The best surface mineralization on the property is at the Moss showing. It consists of minor fracture coatings and blebs of chalcopyrite associated with abundant pyrite and pyrrhotite in a gossanous host (Campbell and Donaldson, 1991). Propylitic, potassic and carbonate alteration are so intense that original lithologies are not distinguishable.

Camp Halo (Minfile 093N 081, Camp)

The Camp halo is developed in fine-grained dust-tuffs and siltstones of the Inzana Lake formation where it interfingers with augite porphyry agglomerates of the Witch Lake formation. A swarm of coarse hornblende-phyric dikes cuts the sediments. Pyrrhotite and pyrite are abundant in altered biotite hornfels and minor chalcopyrite and malachite occur as disseminations and along fracture surfaces. The main altered outcrops that constitute the Camp showing were trenched and drilled in the winter of 1990-1991 by Noranda Exploration Company, Limited. The area south of them is covered by extensive Quaternary alluvium. An RGS stream-sediment sample from a glacial gully 2 kilometres south of the showing returned 309 ppm copper, 1100 ppb mercury and 1.5 ppm silver. The sample location is in an obscure drainage plugged by numerous beaver dams. The only surficial materials are organic muck and glaciofluvial gravels exposed in stream banks. Thus the significance of this sample is in doubt. Five kilometres farther southeast, large hornblende-phyric dikes identical to those at the showing are accompanied by crowded plagioclase-porphyritic monzonite stocks and one body of intrusive breccia. It is possible that the Camp showing is part of a much more extensive halo that lies under thick Quaternary cover.

Skook Halo (Minfile 093 140, Skook; Minfile 093N 208, Rig Breccia; Minfile 093N 209, GG)

The Skook alteration system contains several small showings and occurs primarily within the sedimentary unit of the Chuchi Lake formation near its contact with the Hogem intrusive complex. The CL11 zone is the area of most intense alteration and highest density of crowded monzonite porphyry intrusions. It is exposed in an east-trending gully in a logging cut. The sediments are bleached and hornfelsed; alteration minerals include potassium feldspar, chlorite, pyrite, sericite, epidote, biotite, calcite and minor tourmaline (Campbell, 1988). These rocks contain disseminated pyrite, pyrrhotite and minor chalcopyrite and bornite. White-weathering siliceous tuffs with limy nodules are baked and have developed weak skarn alteration minerals such as garnet and chlorite. A polymetallic quartz vein contains sphalerite, galena and chalcopyrite. The best assay results on grab samples from this locality are 13.4 ppm gold, 16.6 ppm silver and 2.3 per cent zinc (Campbell, 1988). The South zone lies 250 metres south of this vein and consists of a silicified zone in volcanics that contains quartz, calcite, pyrite and chalcopyrite. The GG polymetallic vein and the Rig Breccia zone are also hosted within the overlying flows and are probably part of an epithermal vein system near the Takla-Hogem contact.

Col Halo (Minfile 093N 101, Col)

The Col property (Col and Kael claims) of Kookaburra Gold Corporation is located 5 kilometres north of the west end of Chuchi Lake, straddling the boundary between map sheets 93N/2 and 93N/7. The main copper-gold showings are situated near the southern end of the Hogem intrusive complex. They are hosted by alkaline intrusive rocks near the contact with volcanic flows of the Chuchi Lake formation. Medium to coarse-grained hornblende monzonite, fine to medium-grained pink syenite, aplite and pegmatite are the main intrusive phases. Copper mineralization including chalcopyrite, bornite and malachite is concentrated along steep, 140°-trending parallel fractures, enveloped by salmon-pink potassium feldspar rich alteration 1 to 4 centimtres thick. These zones may also contain quartz, minor magnetite and hairline seams of tremolite/actinolite and chlorite. Some outcrops are so heavily striped with alteration that they take on a gneissic appearance. While some of the zones appear to be late magmatic syenitic dikes, most appear to be the result of metasomatic alteration of the monzonite. A later crosscutting set of steep fractures strikes 050°, but contains only minor mineralization. A trench on the Col showings averaged 2.2 ppm gold and 3.16 per cent copper over a 4-metre interval (Nebocat and Rotherham, 1988).

Chuchi Halo (Minfile 093N 104, SRM)

The eastern tail of the Hogem intrusive complex in 93N/2 contains sparse, fracture-controlled chalcopyrite with pink orthoclase, epidote and magnetite. Scattered blebs of chalcopyrite are also present in flows of the Chuchi Lake formation near the margin of the intrusive complex. Chalcedonic quartz breccia veins and small swarms of quartz veinlets contain minor pyrite. In 93N/1 barren orthoclase veins and areas of abundant pyrrhotite in salt-and-pepper monzodiorite characterize the eastern edge of the Chuchi halo (Nelson *et al.*, 1991a). This system resembles other disseminated and vein-hosted mineralization (such as the

Col and Skook halos) near the contact between the Hogem intrusive complex and the Takla Group volcanics.

THE GERTIE SHOWING (MINFILE 093N 210)

The Gertie copper showing was found on July 3, 1991, during this regional mapping program. It lies on the Jan 5 and 6 claims approximately 5 kilometres south of Klawli Lake and is hosted by volcanic flows of the Early Jurassic Chuchi Lake formation. The showing consists of two large outcrops spaced roughly 1 kilometre apart. The westernmost outcrop is exposed along a glacial gully. An amygdaloidal, maroon and grey, plagioclase-phyric flow hosts disseminated and fracture-controlled malachite and minor azurite. Pink calcite (rhodochrosite?) and jasperoid quartz occur as vesicle infillings. An assay on a single grab sample from this locality returned 0.2 per cent copper. A brecciated zone in a more greenish and aphanitic area of the outcrop contains minor chalcopyrite and has areas of bleaching and hairline fractures with chlorite envelopes. Multidirectional vuggy quartz veinlets are also present and some contain malachite. An altered and bleached intrusive body outcrops 150 metres south of the gully. It contains a crackle breccia that grades into a matrix-supported breccia with milled fragments of intrusive floating in a hematite-rich matrix; no sulphides were visible at this locality.

Native copper blebs 1 by 2 centimetres in size are associated with carbonate and jasper in open-space fillings and occur within a highly amygdaloidal part of the same flow package 75 metres north of the gully. Two, zones of strong propylitic alteration (epidote, chlorite), 1-metre wide, cut the outcrop and contain disseminated malachite.

The eastern outcrop is 1.2 kilometres northeast of the native copper showing. Brecciated green, grey and maroon crystal-lapilli tuff contains disseminated malachite, chalcocite and possibly tetrahedrite. A grab sample from this outcrop assayed 1.08 per cent copper and 17.5 grams per tonne silver.

Stratigraphically, the Gertie showing is located near the top of a maroon flow package that is overlain by massive and monotonous green-grey heterolithic agglomerates. The stratigraphy strikes 070° and dips gently to the south. The regional attitude of bedding suggests that the easternmost outcrop could be a strike extension of the main Gertie showing. The open-space nature of the mineralization points to a flow-top hosted copper occurrence. This showing resembles several other native copper occurrences in the Takla Group including some in the Hydraulic map area near Quesnel and the Sustut Copper deposit in north-central British Columbia. Native copper is hosted in Norian maroon augite-phyric alkali basalts west of Morehead Lake (Bailey, 1987). The Sustut Copper deposit is hosted by the Triassic Moosevale formation, the upper part of Takla Group. Disseminations and veinlets of chalcocite, bornite, chalcopyrite, pyrite and native copper occur in green and maroon volcaniclastics, volcanic breccia, and conglomerates at the transition between marine basaltic volcanism and non-marine intermediate volcanism (Church, 1975; Monger, 1977). Similar occurrences are also present in the Hazelton Group. Small discontinuous pods of high-grade copper and silver are hosted by amygdaloidal and brecciated flow tops of subaerial basalts in the Early Jurassic Telkwa Formation (MacIntyre and Desjardins, 1988; D. MacIntyre, personal communication, 1991). All of these occurrences are in subaerial volcanic flows. Their mineralogy and open-space character suggest that they are products of late-phase hydrothermal fluids related to volcanic activity (Church, 1974).

Although, in itself, the Gertie showing is not directly indicative of a porphyry system, this occurrence may attest to a favourable environment for mineral deposits. The overlying heterolithic agglomerate package hosts altered and mineralized porphyritic monzonite clasts (Hannah, MINFILE 093N 211) and cobbles of epithermal quartz. The volcanic flows that host the Gertie are also on strike with the Klawli showing (MINFILE 093N 032). Although this showing was not visited during the course of 1991 mapping, its potential significance warrants a short description. It is described as a system of mineralized calcite-quartz veins in a brecciated shear zone cutting altered porphyritic and amygdaloidal andesites (Shaede, 1987). Significant minerals include chalcopyrite, malachite, sphalerite, galena and pyrite. The best grab-sample assays reported include 6.7 per cent copper, 1200 grams per tonne silver and 14 grams per tonne gold (Shaede, 1987).

THE HANNAH SHOWING (MINFILE 093N 211)

The Hannah showing occurs approximately 3.25 kilometres southeast of 'Adade Yus Mountain. It is an area of abundant altered and mineralized monzonite fragments within green, heterolithic volcanic agglomerates of the Early Jurassic Chuchi Lake formation. Up to 2 per cent of the fragments are fine grained and rusty weathering and contain disseminated pyrite and pyrrhotite (Plate 1-9-3).

Plate 1-9-3. Rusty, pyritic monzonite fragment in heterolithic agglomerate, 2.5 km northwest of the Hannah showing. Fragment is 4 cm in diameter.

Many of the clasts, including some crowded monzonite porphyry, are bleached and potassically? altered. Assays on grab samples from an area rich in rusty fragments yielded results up to 840 ppb gold and 224 ppm copper (David Cook, personal communication, 1991). The heterolithic agglomerates associated with the Hannah showing appear to have tapped a mineralized porphyry system.

DISCUSSION AND CONCLUSIONS

The Pliensbachian fossil ages (Table 1-9-1) for the sedimentary unit in the Chuchi Lake formation roughly date the middle of the later, more evolved part of the Takla Group; they may also date the crowded monzonite porphyries that are key to the alkalic porphyry copper-gold deposits, although U-Pb zircon ages are needed to establish this.

The Takla Group between Fort St. James and Germansen Landing represents the most protracted volcanic interval so far documented in Quesnellia, from Carnian to late Pliensbachian. Mixed latite-basalt-trachyte volcanism of the Chuchi Lake formation postdates the Rossland volcanics and the youngest preserved volcanic unit near Quesnel. It is coeval with and even younger than some parts of the Hazelton Group. Thus volcanism was "alive and well" in Quesnellia during Hazelton time. The major difference between the Jurassic volcanic history of Quesnellia and Stikinia is less one of timing than of style: while the chemistry of the Hazelton Group is dominantly calcalkalic, the later part of the Takla Group is mildly alkalic, with strong evolutionary ties to the earlier augite porphyries.

ACKNOWLEDGMENTS

Our thanks and appreciation go to the fine BP team, Chris Bates, Russ Wong, Tucker Barrie, Russ Barnes and Bernie Augsten, for the quality of their insights and willingness to share them.We are also indebted to Bill McMillan and Bob Lane, who bashed bush and broke rocks with us. And thanks to pilot Kraig Hancocks, for being there and being safe.

REFERENCES

Armstrong, J.E. (1949): Fort St. James Map-area, Cassiar and Coast Districts, British Columbia; *Geological Survey of Canada*, Memoir 252.

Bailey, D.G. (1987): Geology of the Hydraulic Map Area NTS 93A/12; *B.C. Ministry of Energy, Mines and Petroleum Resources*, Preliminary Map No. 67.

Bailey, D.G. (1988): Geology of the Central Quesnel Belt, Hydraulic, South-central British Columbia; *in* Geological Fieldwork 1987, *B.C. Ministry of Energy, Mines and Petroleum Resources*, Paper 1988-1, pages 147-153.

Bailey, D.G. (1989): Geology of the Central Quesnel Belt, Swift River, South-central British Columbia (93B/16, 93A/12, 93G/1); *in* Geological Fieldwork 1988, *B.C. Ministry of Energy, Mines and Petroleum Resources*, Paper 1989-1, pages 167-172.

Campbell, C. (1988): Preliminary Geochemical and Geological Report on the Skook 3-6 Mineral Claims; *B.C. Ministry of Energy, Mines and Petroleum Resources*, Assessment Report 18073.

Campbell, E.A. (1990a): Klawli Option; Geology, Geophysics and Geochemistry; *B.C Ministry of Energy, Mines and Petroleum Resources*, Assessment Report 19719.

Campbell, E.A. (1990b): Witch Option; Geology, Geophysics and Geochemistry, 1989; *B C. Ministry of Energy, Mines and Petroleum Resources*, Assessment Report 19720.

Campbell, E.A. (1991): Klawli Option; Geology, Geophysics and Geochemistry; *B.C Ministry of Energy, Mines and Petroleum Resources*, Assessment Report 20612.

Campbell, E.A. and Donaldson, W.S. (1991): Witch Option; Geology, Geophysics and Geochemistry, 1990: *B.C. Ministry of Energy, Mines and Petroleum Resources*, Assessment Report 20899.

Church, B.N. (1974): Geology of the Sustut Area; *in* Geology, Exploration and Mining in British Columbia 1973, *B.C. Ministry of Energy, Mines and Petroleum Resources*, pages 411-455.

Church, B.N. (1975): Geology of the Sustut Area; *in* Geology, Exploration and Mining in British Columbia, 1974, *B.C. Ministry of Energy, Mines and Petroleum Resources*,, pages 305-310.

Ferri, F. and Melville, D. (in preparation): Geology of the Germansen Landing–Manson Creek Area; *B.C. Ministry of Energy, Mines and Petroleum Resources*, Bulletin.

Garnett, J.A. (1978): Geology and Mineral Occurrences of the Southern Hogem Batholith; *B.C. Ministry of Energy, Mines and Petroleum Resources*, Bulletin 70.

Höy, T. and Andrew, K. (1989): The Rossland Group, Nelson Map-area, Southeastern British Columbia; *in* Geological Fieldwork 1988, *B.C. Ministry of Energy, Mines and Petroleum Resources*, Paper 1989-1, pages 33-44.

MacIntyre, D.G. and Desjardins, P. (1988): Babine Project; *in* Geological Fieldwork 1987, *B.C. Ministry of Energy, Mines and Petroleum Resources*, Paper 1988-1, pages 181-193.

Monger, J.W.H. (1977): The Triassic Takla Group in McConnell Creek Map-area, North-central British Columbia; *Geological Survey of Canada*. Paper 76-29.

Monger, J.W.H., Wheeler, J.O., Tipper, H.W., Gabrielse, H., Harms, T., Struik, L.C., Campbell, R.B., Dodds, C.J., Gehrels, G.E. and O'Brien, J. (1990): Cordilleran Terranes; *in* The Cordilleran Orogen: Canada, Chapter 8, Upper Devonian to Middle Jurassic Assemblages, Gabrielse, H. and Yorath, C.J., Editors, *Geological Survey of Canada*, Geology of Canada, Number 4.

Nebocat, J. and Rotherham, D. (1988): Geochemical, Geological and Physical Work Report, Col Claim Group; *B.C. Ministry of Energy, Mines and Petroleum Resources*, Assessment Report 18123.

Nelson, J., Bellefontaine, K., Green, K. and MacLean, M. (1991a): Regional Geological Mapping Near the Mount Milligan Copper-Gold Deposit (93K/16, 93N/1); *in* Geological Fieldwork 1990, *B.C. Ministry of Energy, Mines and Petroleum Resources*, Paper 1991-1, pages 89-110.

Nelson, J., Bellefontaine, K., Green, K. and MacLean, M. (1991b): Geology and Mineral Potential of the Wittsichica Creek and Tezzeron Creek Map-areas (NTS 93N/1, 93K/16); *B.C. Ministry of Energy, Mines and Petroleum Resources*, Open File 1991-3.

Nelson, J., Bellefontaine, K., MacLean, M. and Rees, C.J. (1992): Geology and Mineral Potential of the Chuchi Lake East Half (93N/2) and Klawli Lake East Half (93N/7) Map-areas; *B.C. Ministry of Energy, Mines and Petroleum Resources*, Open File 1992-4.

Plouffe, A. (1991): Preliminary Study of the Quaternary Geology of the Northern Interior of British Columbia; *in* Current Research, *Geological Survey of Canada*, Paper 91-1A, pages 7-14.

Shaede, E. (1987): Geochemical and Petrographic Report on Gold Supplemental Claim Group; *B.C. Ministry of Energy, Mines and Petroleum Resources*, Assessment Report 16865.

Tipper, H.W. (1984): The Age of the Rossland Group of Southeastern British Columbia; *in* Current Research, Part A, *Geological Survey of Canada*, Paper 84-1A, pages 631-632.

Wong, R. (1990): Assessment Report on the 1989 Ground Geophysical and Diamond Drilling Program on the Phil 13 Claim Group; *B.C. Ministry of Energy, Mines and Petroleum Resources*, Assessment Report 20018.

Wong, R., Barrie, C.T., McClintock, J., Campbell, E.A. and Lane, R. (1991): Porphyry Copper-Gold Mineralization in the Chuchi Lake Area, Omineca Mining Division, North-central British Columbia; *Canadian Institute of Mining and Metallurgy*, Bulletin, Volume 84, Number 947, page 88; abstract of paper delivered at CIMM Annual General Meeting April 30, 1991.

PALEOMAGNETISM OF THE MIDDLE CRETACEOUS GERMANSEN BATHOLITH, BRITISH COLUMBIA (93N/9, 10)

By P.J. Wynne, E. Irving, Pacific Geoscience Centre, Geological Survey of Canada and F. Ferri, B.C. Geological Survey Branch

(GSC Contribution No. 37391)

KEYWORDS: Paleomagnetism, Germansen batholith, paleomagnetic aberrancy, tilt, translation.

INTRODUCTION

Paleomagnetic data from intrusive rocks of the Coast Belt are aberrant (Symons, 1977; Monger and Irving, 1980; Beck *et al.*, 1981a, b; Irving *et al.*, 1985). The aberrancies can be interpreted as tilting, 30° to the southwest (Symons, 1977; Beck and Noson, 1972; Irving *et al.*, 1985; Butler *et al.*, 1989); as northward displacement of about 2000 kilometres and clockwise rotation of 60° about a vertical axis (Beck and Noson, 1972; Irving, *et al.*, 1985; Umhoefer, 1987; Umhoefer *et al.*, 1989) or as a combination of these two processes (Irving and Wynne, 1990; Irving and Thorkelson, 1990; Umhoefer and Magloughlin, 1990). One result from the Axelgold intrusion (Monger and Irving, 1980; Armstrong *et al.*, 1985) also shows a similar aberrancy, indicating that this phenomenon extends eastward into the Intermontane Belt. The purpose of this paper is to describe results obtained from a study of the Germansen batholith (Figure 1-10-1), also in the Intermontane Belt, which was undertaken to further investigate this aberrancy.

The rocks of the Germansen batholith are generally, but not everywhere, too felsic to serve as good recorders of the paleofield. Also, as this work shows, many outcrops have been struck by lightning which has affected their magnetization. The results presented here, therefore, are not definitive, but provide information pertinent to the "tilt versus translation" debate regarding the origin of aberrant paleomagnetic results from mid-Cretaceous plutons in the Cordillera.

GEOLOGY AND SAMPLING

The Germansen batholith intrudes Upper Triassic to Lower Jurassic sedimentary and volcanic rocks of the Takla Group (Figure 1-10-2). It is a large body (600 km^2) composed mainly of foliated hornblende biotite granodiorite. It commonly contains large (3 cm) potassium feldspar phenocrysts aligned parallel to foliation. Ferri and Melville (1989) suggest that, because the foliation parallels the intrusive contact and is also associated with a steep mineral lineation, it may be related to the emplacement of the batholith. Hence the fabric is probably a "hot" phenomenon, predating the acquisition of magnetization.

Granodiorite near Mount Germansen (the locality here informally referred to as Radiometric Ridge) has been dated at 106±3 Ma and 86±3 Ma (K-Ar ages from hornblende and biotite respectively; Meade, 1975). The younger age may reflect partial resetting by Tertiary intrusions nearby. Biotite from a two-mica granite from near Mount Gillis yielded a K-Ar age of 107±4 Ma (Ferri and Melville, 1989). Hence the batholith is considered to be mid-Cretaceous in age.

We sampled the batholith in three localities, collecting 18 hand samples from the apophysis on the southeast margin, 23 drill cores on Radiometric Ridge, and 12 hand samples from an isolated knoll west of Mount Gillis (Figure 1-10-2). Samples from the apophysis are fine to medium grained, weakly foliated, equigranular hornblende biotite granodiorite. The foliated hornblende biotite granodiorite from Radiometric Ridge and the knoll west of Mount Gillis contains large potassium feldspar phenocrysts (2 by 5 cm) and is more leucocratic than the apophysis granodiorite.

METHOD

In the laboratory, up to three cores were taken from each hand sample and two specimens were cut from each core; about 100 cores or 180 specimens altogether. After the natural remanent magnetization (NRM) of the specimens was measured, a pair of specimens from one out of three hand samples was chosen for detailed stepwise demagnetization. One specimen was thermally demagnetized, the other was demagnetized using alternating fields. The response of these specimens to demagnetization was used to determine the treatment for the remainder; namely, three levels between 20 and 100 milliteslas. A line fitting program (LINEFIT) was used to calculate the direction of magnetization removed over the treatment steps.

PALEOMAGNETIC OBSERVATIONS

WELL-GROUPED MAGNETIZATION

Interpretable data were obtained from 55 per cent of the collection (100 specimens). The majority of these specimens are from the apophysis and all are normally magnetized. After the removal of a small, low coercivity component, the directions become well grouped, defining an end-point, and the magnetization decays along a straight line to the origin (Figure 1-10-3). The direction of the magnetization removed along the straight-line segment, from 10 to 100 milliteslas, is labelled RV in Figure 1-10-3 and was calculated using LINEFIT.

Low coercivity components are common in the collection and are interpreted to be the product of lightning. They are best removed using alternating field demagnetization. To illustrate this the demagnetization of two specimens from the same core is shown in Figures 1-10-4 and 1-10-5. During thermal demagnetization the direction of the B specimen starts to migrate towards the northeast quadrant but no end point is achieved (Figure 1-10-4). During AF demagne-

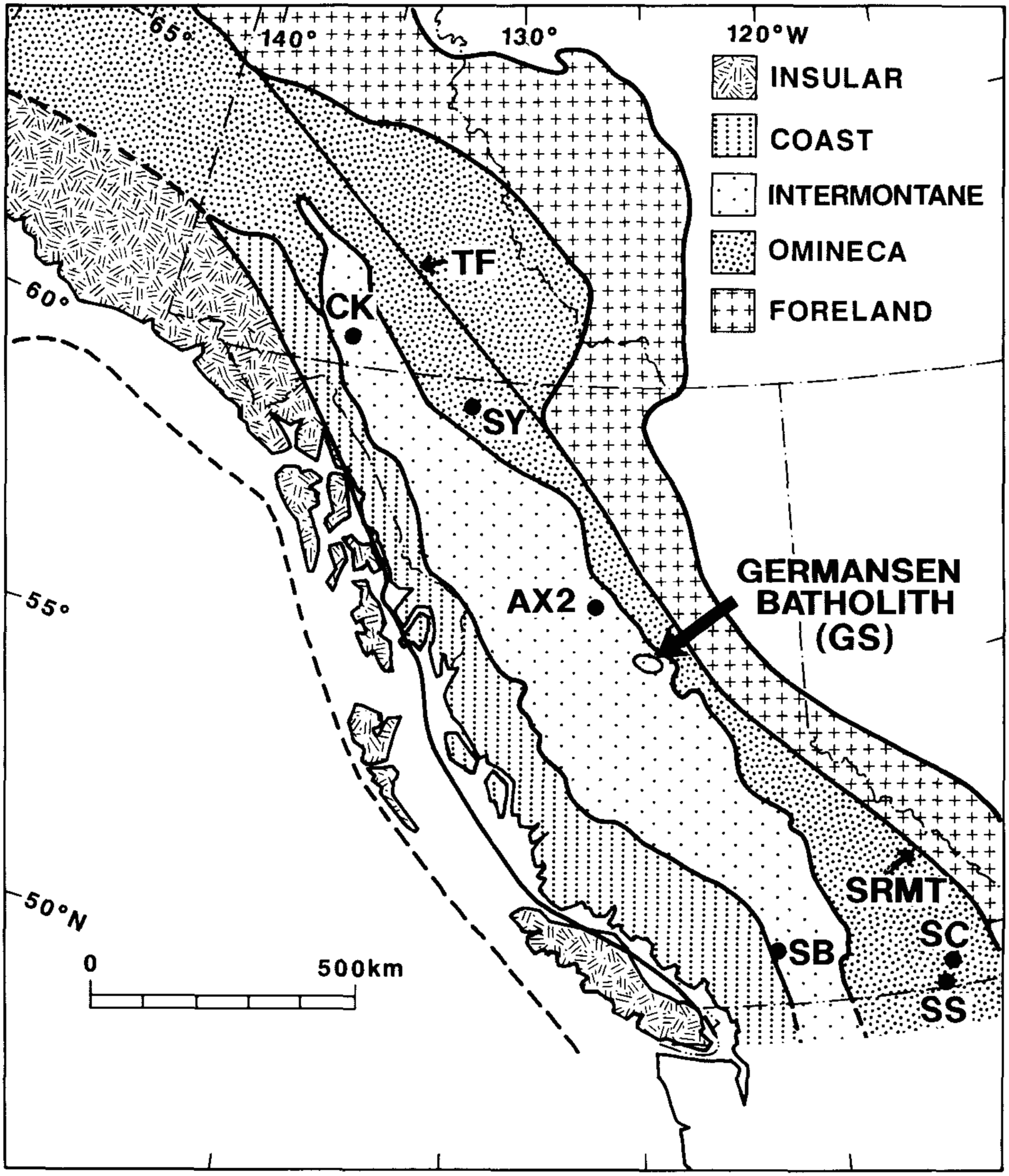

Figure 1-10-1. Location of the Germansen batholith, morphogeological belts and previous paleomagnetic studies in the Intermontane and Omenica belts.

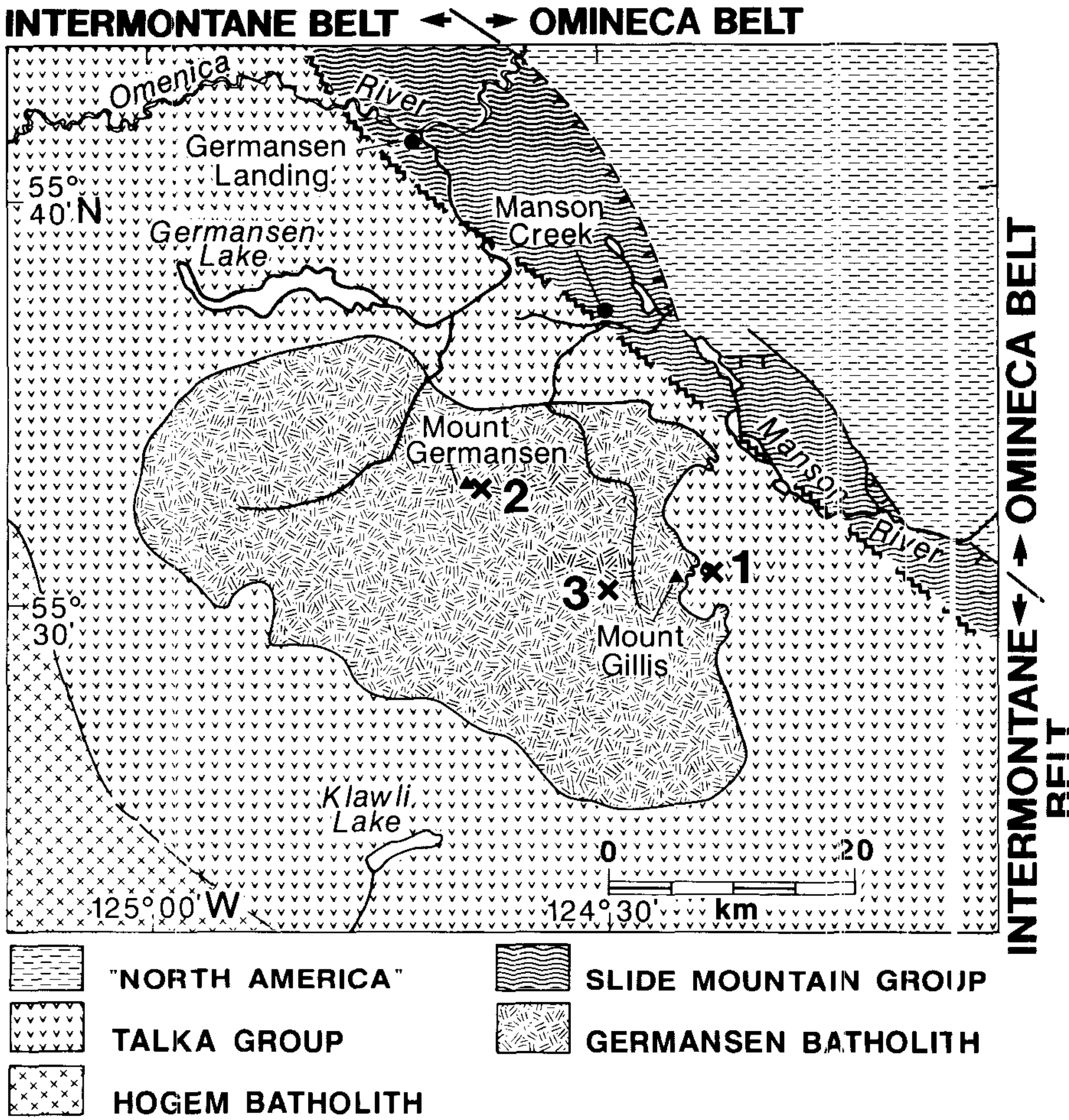

Figure 1-10-2. Local geology map and sampling localities as follows: (1) apophysis, (2) Radiometric Ridge, (3) knc l west of Mount Gillis. Geology modified from Armstrong, 1949; Ferri and Melville, 1988, 989.

tization, by 30 milliteslas, the intensity of the A specimen dropped to 10 per cent of the NRM intensity as the lightning-induced component was removed (Figure 1-10-5). The orthogonal plot shows a sharp change in direction between 10 and 20 milliteslas. Between 30 and 90 milliteslas a rough end-point is attained and a linear decay to the origin of the orthogonal plot is defined. Apparently, lightning has superposed a magnetization but has not destroyed the underlying stable magnetization.

Figure 1-10-6 illustrates more generally the effect of removing the lightning component. Disparate clusters of NRM directions, corresponding to specimens from three hand samples, are shown. These move into a well-defined group after alternating field demagnetization (Figure 1-10-6). Each point in the cluster of cleared directions represents the magnetization removed from a single specimen in the range 10 to 100 milliteslas, as calculated using LINEFIT.

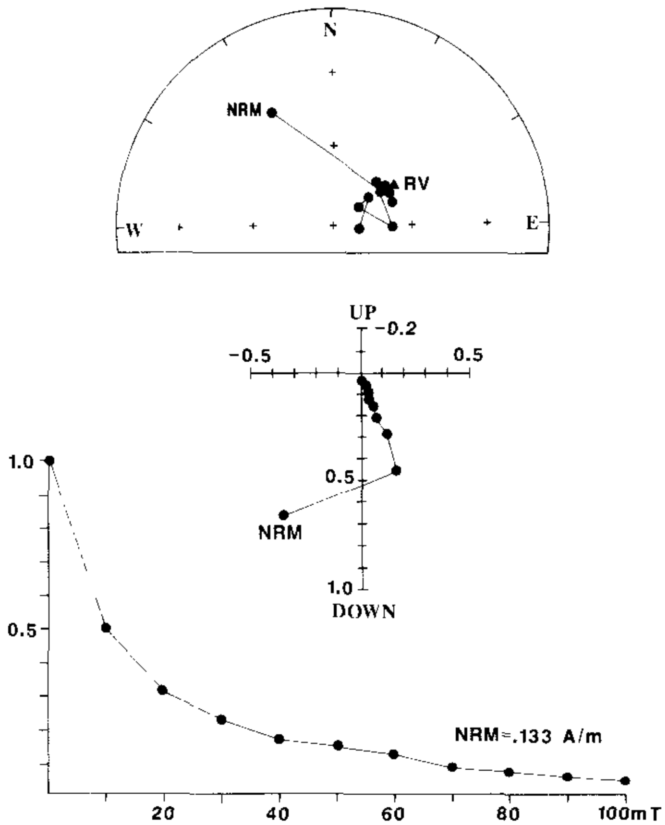

Figure 1-10-3. Alternating field demagnetization of a specimen from the apophysis. Changes in direction (top), orthogonal plot (centre), changes in intensity (bottom) are shown. **RV** is the magnetization removed along the straight-line segment going to the origin of the orthogonal plot.

The results for specimens with interpretable magnetization, organized by localities, are summarized in Table 1-10-1. Averages were calculated giving unit weight to the mean direction of specimen pairs from each core.

Random Magnetization

Twenty-four per cent of the collection (44 specimens) have very strong NRM intensities (3.39 A/m) that fall to a few per cent after demagnetization in alternating fields of 10 to 20 milliteslas. While some specimens show end-points, the directions are inconsistent within a single hand sample. For this reason they were not included in the analysis. Lightning has apparently completely overprinted the magnetization and no underlying stable magnetization could be retrieved.

Ill-defined Magnetization

The remainder of the specimens in the collection (22%, 38 specimens) have a non-linear decay. The strong NRM intensity (1.5×10^{-1} A/m) decreases sharply to 10 per cent at 10 milliteslas and remains little changed for the rest of the treatment interval. For a given specimen the directions at subsequent treatment steps remain in one quadrant, forming a loose cluster. The specimens appear to have a small stable magnetization, but it is not well defined and consequently they were not included in the analysis. The majority of these specimens are from the two more felsic localities, Radiometric Ridge and the knoll west of Mount Gillis.

TABLE 1-10-1
SUMMARY OF MEAN DIRECTIONS

Location	H(S)C	D°, I°	k	α_{95}	α_{63}
1. Apophysis	16(64)48	045,72	14	6	3
2. *Radiometric Ridge*	–(16)9	030,67	6	22	11
3. Knoll east of Mt. Gillis	10(20)17	060,74	6	16	8
Germansen Average					
4. Cores	–(100)74	045,72	10	6	3
5. Localities	–3	043,71	189	9	3
6. K *expected*	–	328,78	—	3	—

NOTES: H(S)C, number of hand samples (specimens) cores, unit weight given to cores. Cores were drilled at Radiometric Ridge. D°, I° are declination, inclination of the mean direction, k, precision parameter for directions; α_{95}, radius of the circle of confidence ($P = 0.05$); α_{63} is the standard error = $81\,(kN)^{-1/2}$, where N is the number of data used in the average (number of cores or localities in this table). K expected is the direction for the Germansen batholith predicted using the mid-Cretaceous cratonic reference paleopole of Globerman & Irving (1988).

RESULTS – TILT OR TRANSLATION?

The mean directions of the three localities have normal polarity. Their standard error circles overlap so the directions are not significantly different from one another (Figure 1-10-7) but are significantly different from the expected Cretaceous direction (Table 1-10-1). This difference can be accounted for either by post-emplacement tilt, by northward displacement and rotation about a vertical axis, or some combination of these two. No mapping has been done of bathozonal mineral assemblages in the contact aureole of the Germansen batholith so no estimate of paleohorizontal is available.

Table 1-10-2 summarizes, in terms of both apparent tilts and apparent displacements and/or rotations, the paleomagnetic results obtained from Cretaceous rocks in the Omineca and Intermontane belts. Ninety-five per cent errors are quoted. The two entries for the Axelgold intrusion have been calculated first with respect to present horizontal (AX1) and then (AX2) after correction for tilt using crystal layering as an estimate of paleohorizontal (Monger and Irving, 1980; Armstrong *et al.*, 1985). The latter yields the more modest aberrancy and is used in the following discussion.

Results from two studies in the Omineca Belt indicate that no tilting had occurred (SC, SY). The aberrancy in paleomagnetic directions of the Summit stock (SS) is that expected from the tilt of bathozones mapped in the metamorphic aureole around the batholith. The tilt has been considered to be a product of Eocene extension (Irving and Archibald, 1990). In the Intermontane Belt the dips of the two bedded sequences (CK, SB) are variable. When these are corrected to paleohorizontal, the paleomagnetic directions remain aberrant. The Axelgold (AX2) and Germansen (GS) aberrancies can be expressed as the product of 18 to 20° tilts down to the west-southwest. The apparent tilts are smaller but are in the same direction as those required to produce the observed magnetization directions in plutons of the Coast Plutonic Complex and the North Cascades Range (30° to the west-southwest) (Beck and Noson, 1972; Irving *et al.*, 1985; Butler *et al.*, 1989; Irving and Wynne, 1990).

If the results are cast as the product of rotation and displacement then in the southern Omineca Belt the Skelly Creek batholith suggests a clockwise rotation; Summit stock (after tilt correction indicated by bathozones) shows a small counter-clockwise rotation; neither show any significant displacement. In the north the Sylvester allocthon shows displacement but no significant rotation. Within errors, the SY result is consistent with an estimate of 900 kilometres dextral offset along the Tintina and Northern Rocky Mountain Trench fault which is situated just to the east of the Sylvestor allocthon (Figure 1-10-1).

In the Intermontane Belt results from the Late Cretaceous Carmacks Group show no rotations. The rotations observed in the mid-Cretaceous studies are remarkably similar; clockwise, between 58° and 75°, with the Germansen showing the greatest rotation. An apparent northward displacement of the Germansen batholith is indicated, but it is of borderline significance at $P = 0.05$. The rest (AX2, CK, SB) show northward displacements which are again very similar. Figure 1-10-8 shows the aberrances calculated as displacements. The error arrows of the figure give the probability distribution. The probability is highest at the mean (centre) and decreases away from it. It is interesting to note that if the compositional layering is a reasonable estimate of paleohorizontal, then the aberrancy of the Axelgold direction is the product of both tilt and northward translation with rotation. The directions obtained from bedded rocks SB and CK are best explained as the product of translation with and without rotation, respectively (Irving and Thorkelson, 1990; Marquis and Globerman, 1988).

These new data indicate that a second pluton in the Intermontane Belt is aberrant and confirms that paleomagnetic aberrancies are a feature of intrusions in both the Intermontane and the Coast belts. Although each result is

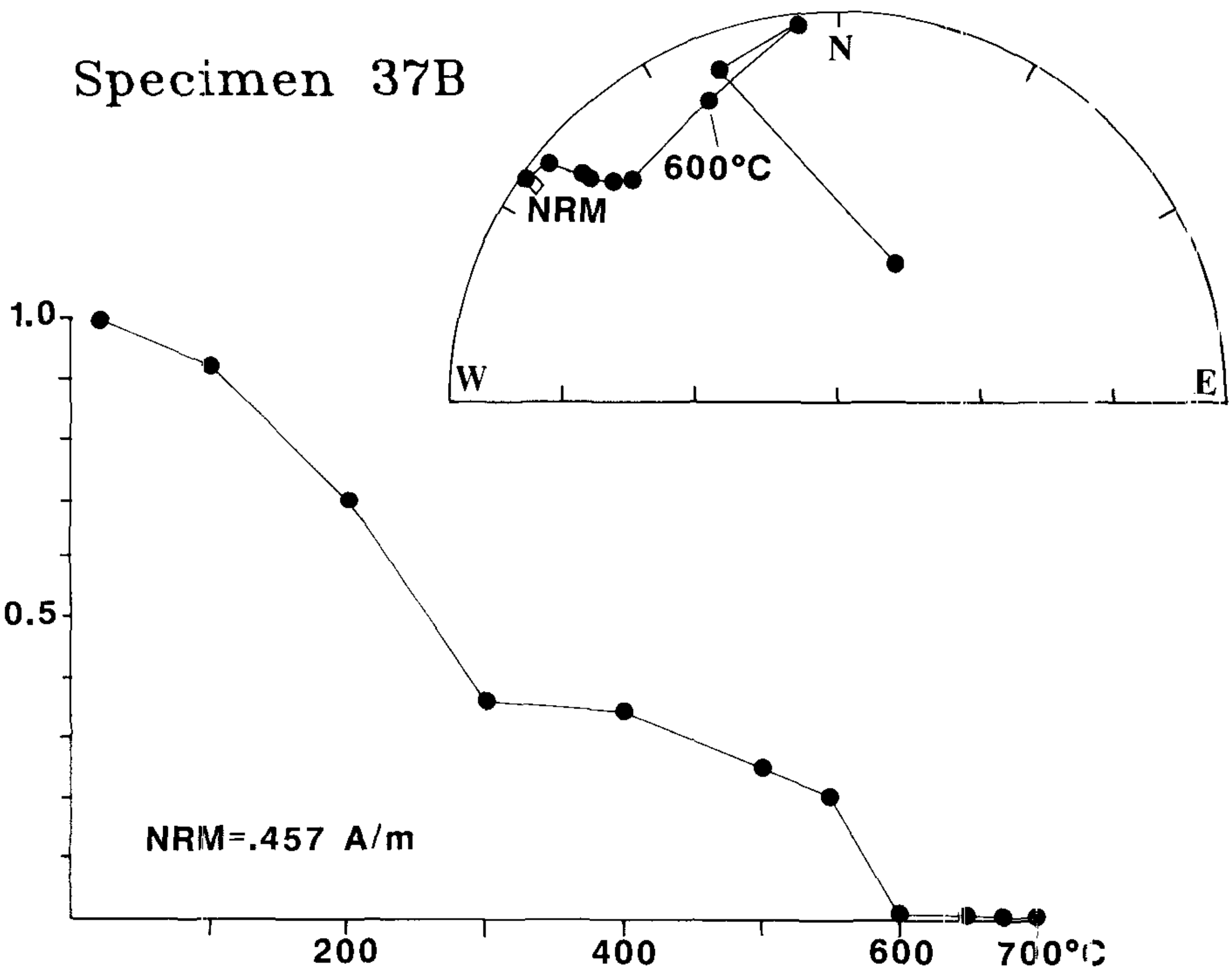

Figure 1-10-4. Specimen 37B, from the apophysis: thermal demagnetization with changes in direction above, changes in intensity below. An end-point is not achieved.

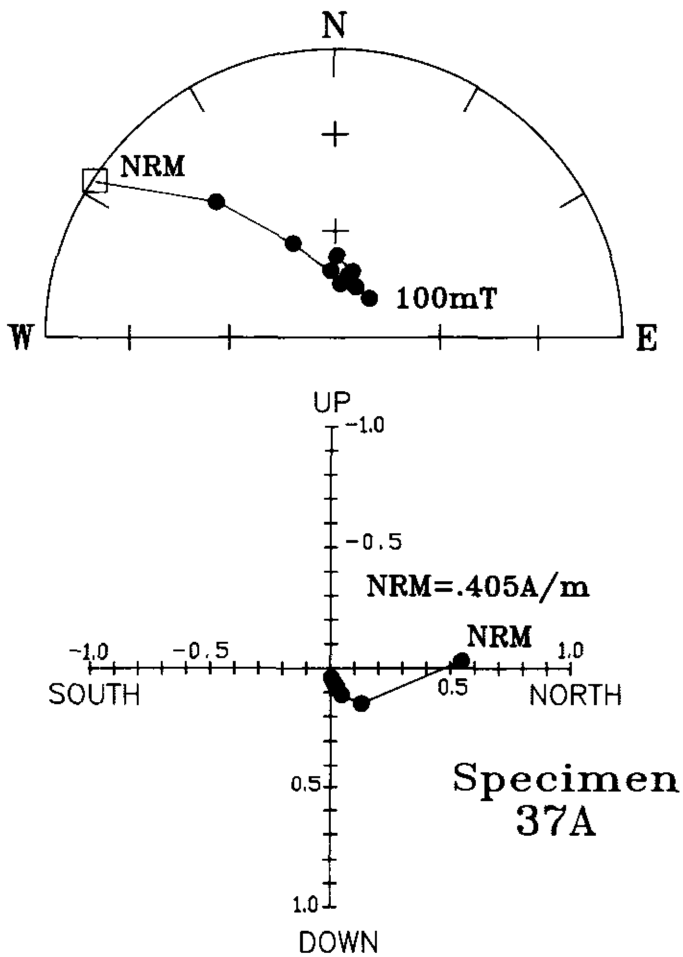

Figure 1-10-5. Specimen 37A, from the apophysis: alternating field demagnetization with changes in direction above, orthogonal plot below. An end-point is achieved.

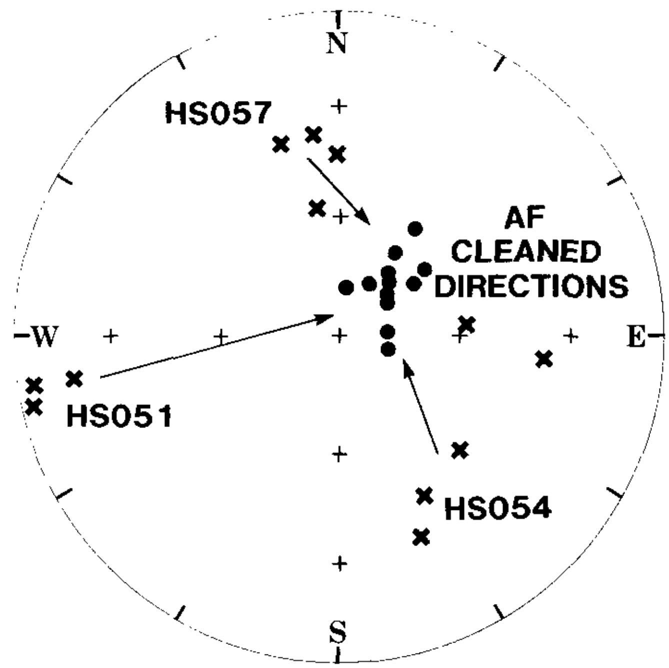

Figure 1-10-6. Directions of magnetization in specimens from three hand samples. NRM directions (crosses) are widely scattered, the "cleaned" directions (solid dots) are well grouped. All are down directions, plotted on the lower hemisphere.

TABLE 1-10-2
SUMMARY OF PALEOMAGNETIC WORK ON CRETACEOUS ROCKS DONE IN THE INTERMONTANE AND OMENICA BELTS

Rock Unit	Belt	Apparent tilt Dip°,DDA°	Apparent displacement RR°	RPD°
SC Skelly Creek	OM	<5,-	-17±17	-01±08
SS Summit Stock	OM	24,west	14±11	-01±06
SY Sylvester Allocthon	OM	flat lying	-05±20	08±07
AX1 Axelgold 1	IM	28,234	-65±14	27±06
AX2 Axelgold 2	IM	18,237	-58±12	16±07
CK Carmacks	IM	variable	-06±20	14+07
SB Spences Bridge	IM	variable	-66±12	16±07
GS Germansen	IM	20,256	-75±23	12±12

NOTES: OM, IM Omineca, Intermontane belts: Apparent tilt is given as the dip and down-dip azimuth (DDA) of the tilt required to produce the observed directions from that expected (down 28° at 234°); Apparent displacement is given as RR, relative rotation (clockwise rotation is negative) and RPD, relative paleolatitudinal (northward relative motion is positive). RR and RPD errors (P = 0.05) have been calculated using the method of Demarest (1983). Calculations for this table were made using the mid-Cretaceous cratonic reference paleopole of Globerman and Irving 1988 (71°N, 196°E, A_{95}=4.9) except for the Carmacks. For the Carmacks a late Cretaceous cratonic reference paleopole, 79°N, 190°E, N=5, K=326, A_{95}=4.2° (Wynne *et al.*, 1992) was used. To convert RPD from degrees to kilometres, multiply by 111.3. References: SC, SS Irving and Archibald, 1990; SY, Butler *et al.*, 1988; AX1, AX2 Monger and Irving, 1980, Armstrong *et al.*, 1985; CK, Marquis and Globerman, 1988; SB, Irving and Thorkelson, 1990. GS is calculated using localities unit weight, line 5, Table 1-10-1. The GS paleopole is 66°N, 054°W, A_{95} = 15°, K = 70.

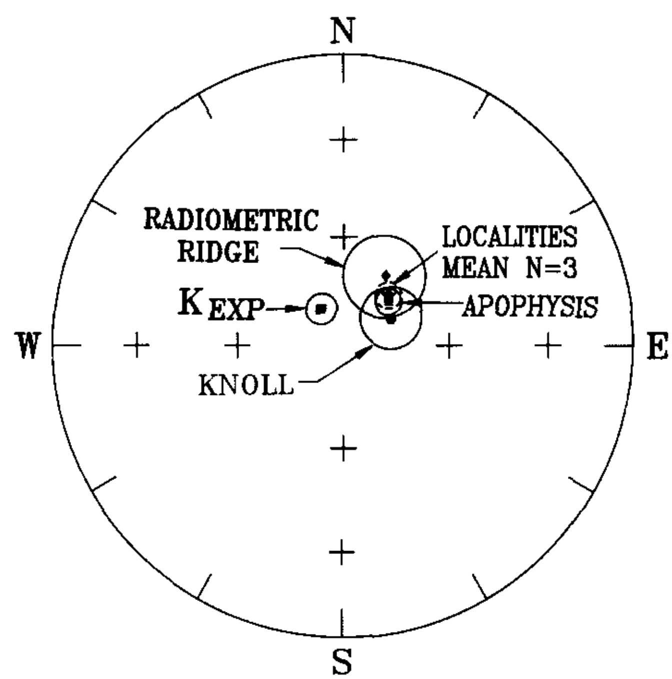

Figure 1-10-7. Locality mean directions. Specimen pair given unit weight. All three are significantly different (P=.05) from K_{exp}, the expected mid-Cretaceous direction (Globerman and Irving, 1988). Standard error (63) ellipses are shown.

subject to considerable error, the apparent displacements within the Intermontane Belt are all from the south and of similar magnitude (>1000 km). The apparent displacements are comparable to those observed in bedded Cretacous rocks. An alternative explanation (which does not agree with data from bedded rocks) is that tilts 20° to the west-southwest have taken place. This is about 10° less than the apparent tilts for Coast Belt plutons. Finally the Germansen data could be the product of both tilt and rotation/displacement like its neighbour (AX2), 100 kilometres to the northwest.

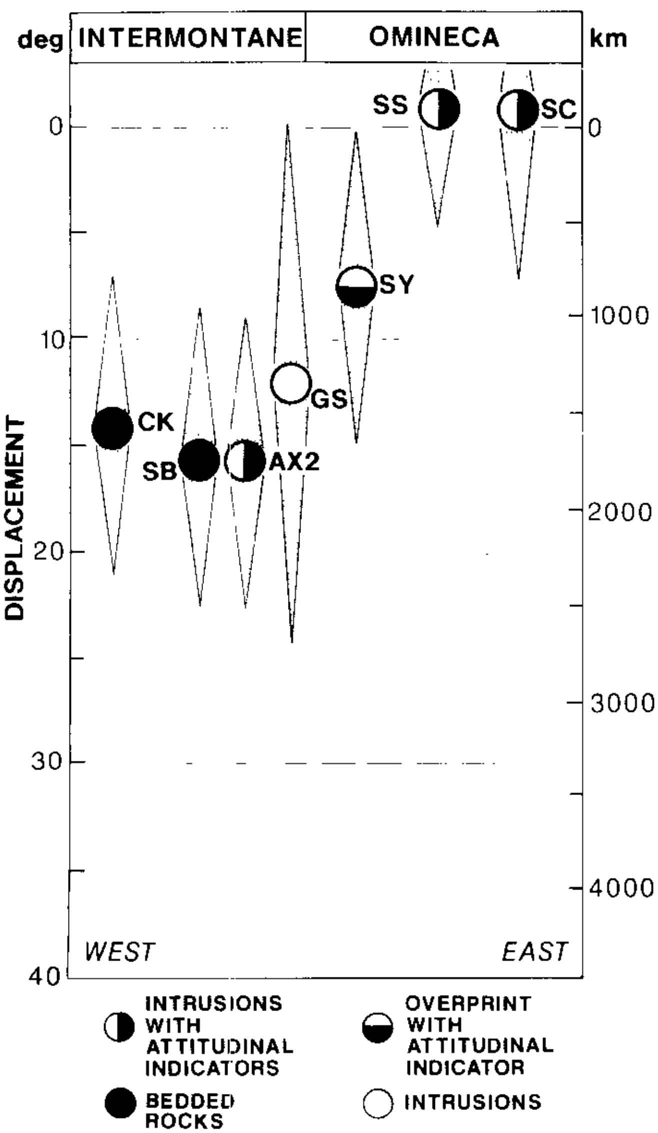

Figure 1-10-8. Displacement diagram showing paleomagnetic studies from the Intermontane and Omenica belts. Labelling is the same as in Figure 1-10-1. GS calculated using the combined localities average, line 5, Table 1-10-1. P=0.05 error arrows are shown as calculated using Demarest's (1983) method.

ACKNOWLEDGMENTS

Our thanks to Kirsten Nicolsen for her cheerful and able assistance in the field and to C.J. Yorath for his review of this paper.

REFERENCES

Armstrong, J.E. (1949): Fort St. James Map Area, Cassiar and Coast Districts, British Columbia; *Geological Survey of Canada*, Memoir 252. 210 pages.

Armstrong, R.L., Monger, J.W.H. and Irving, E. (1985): Age of Magnetization of the Axelgold Gabbro, North-central British Columbia; *Canadian Journal of Earth Sciences*, Volume 22, pages 1217-1222.

Beck, M.E., Jr., Burmester, R.F., Engebretson, D.C. and Schoonover, R. (1981a): Northward Translation of Mesozoic Batholiths of Western North America: Paleomagnetic Evidence and Tectonic Significance; *Geofisica International*, Volume 20, pages 144-162.

Beck, M.E., Burmester, R.F. and Schoonover, R. (1981b): Paleomagnetism and Tectonics of the Cretaceous Mt. Stuart Batholith of Washington: Translation or Tilt?; *Earth and Planetary Science Letters*, Volume 56, pages 336-342.

Beck, M.E. and Nosan, L. (1972): Anomalous Paleolatitudes in Cretaceous Granitic Rocks; *Nature*, Volume 235, pages 11-13.

Butler, R.F., Gehrels, G.E., McClelland, W.C., May, S.R. and Klepacki, D. (1989): Palaeomagnetic Poles from the Canadian Coast Plutonic Complex: Regional Tilt Rather than Large-scale Displacement?; *Geology*, Volume 17, pages 691-694.

Butler, R.F., Harms, T.A. and Gabrielse, H. (1988): Cretaceous Remagnetization in the Sylvester Allochthon: Limits to Post-105 Ma Northward Displacement of North-central British Columbia; *Canadian Journal of Earth Sciences*, Volume 25, pages 1316-1322.

Demerest, M.M. (1983): Error Analysis for the Determination of Tectonic Rotation from Paleomagnetic Data; *Journal of Geophysical Research*, Volume 88, pages 4321-4328.

Ferri, F. and Melville, D.M. (1988): Manson Creek Mapping Project (93N/09); *in* Geological Fieldwork 1987; *B.C. Ministry of Energy Mines and Petroleum Resources*, Paper 1988-1, pages 169-180

Ferri, F. and Melville, D.M. (1989): Geology of the Germansen Landing Area, British Columbia (93N/10, 15); *in* Geological Fieldwork 1988, *B.C. Ministry of Energy, Mines and Petroleum Resources*, Paper 1989-1, pages 209-220.

Globerman, B.R. and Irving, E. (1988): Mid-Cretaceous Paleomagnetic Reference Field for North America: Restudy of 100 Ma Intrusive Rocks from Arkansas; *Journal of Geophysical Research*, Volume 93, pages 11,721-11,733.

Irving, E. and Archibald, D.A. (1990): Bathozonal Tilt Corrections to Paleomagnetic Data from Mid-Cretaceous Plutonic Rocks: Examples from the Omenica Belt, British Columbia; *Journal of Geophysical Research*, Volume 95, pages 4579-4585.

Irving, E. and Thorkelson, D.J. (1990): On Determining Paleohorizontal and Latitudinal Shifts: Paleomagnetism of Spences Bridge Group, British Columbia; *Journal of Geophysical Research*, Volume 95, pages 19, 213-19, 234.

Irving, E., Woodsworth, G.J., Wynne, P.J. and Morrison, A. (1985): Paleomagnetic Evidence for Displacement from the South of the Coast Plutonic Complex, British Columbia; *Canadian Journal of Earth Sciences*, Volume 22, pages 584-598.

Irving, E. and Wynne, P.J. (1990): Paleomagnetic Evidence Bearing on the Evolution of the Canadian Cordillera; *Philosophical Transactions of the Royal Society of London*, Volume A 331, pages 487-509.

Marquis, G. and Globerman, B.R. (1988): Northward Motion of the Whitehorse Trough; Paleomagnetic Evidence from the Upper Cretaceous Carmacks Group; *Canadian Journal of Earth Sciences*, Volume 25, pages 2005-2016.

Meade, H.D. (1975): Geology of the Germansen Lake Area; *B.C. Ministry of Energy, Mines and Petroleum Resources*, Preliminary Map 19.

Monger, J.K.H. and Irving, E. (1980): Northward Displacement of North-central British Columbia; *Nature*, Volume 288, pages 289-294.

Symons, D.T.A. (1977): Paleomagnetism of Mesozoic Plutons in the Westernmost Coast Complex of British Columbia; *Canadian Journal of Earth Sciences*, Volume 14, pages 2127-2139.

Umhoefer, P.J. (1987): Northward Translation of "Baja British Columbia" Along the Western Margin of North America; *Tectonics*, Volume 6, pages 377-394.

Umhoefer, P.J., Dragovich, J., Cary, J. and Engebretson, D.C. (1989): Refinements of the "Baja British Columbia" Plate-tectonic Model for Northward Translation Along the Margin of Western North America; *in* Deep Structure and Past Kinematics of Accreted Terranes, Hillhouse, J.W., Editor, *Geophysical Monograph 50*, IUGG Volume 5, pages 101-111.

Umhoefer, P.J. and Magloughlin, J.F. (1990): Comment on "Discordant Paleomagnetic Poles from the Canadian Coast Plutonic Complex: Regional Tilt Rather than Large-scale Displacement?"; *Geology*, Volume 18, pages 800-801.

Wynne, P.J., Irving, E., Schulze, D.J., Hall, D.C. and Helmstaedt, H.H. (1992): Paleomagnetism and Age of Three Canadian Rocky Mountain Diatremes; *Canadian Journal of Earth Sciences*, in press.

GEOLOGY OF THE USLIKA LAKE AREA, NORTHERN QUESNEL TROUGH, B.C. (94C/3, 4, 6)*

By F. Ferri, S. Dudka and C. Rees

KEYWORDS: Regional geology, Quesnel trough, Cassiar Terrane, Harper Ranch Terrane, Slide Mountain Terrane, Quesnel Terrane, Hogem batholith, Uslika Formation, Sustut Group, strike-slip faults, metamorphic rocks, porphyry copper-gold, carbonate-hosted lead-zinc.

INTRODUCTION

The Aiken Lake project is a 1:50 000-scale mapping program under the Canada - British Columbia Partnership Agreement on Mineral Development (1991-1995) and is located in the northern Quesnel trough. It will consist of three years of field mapping, covering an area centred on Aiken Lake and extending southward to Uslika Lake and northward to Johanson Lake (Figure 1-11-1). The mapping will focus on the northernmost limit of Mesozoic volcanics within the Quesnel trough, Upper Paleozoic oceanic volcanics and sediments, and Lower Paleozoic carbonates. The area has known porphyry copper-gold occurrences, carbonate-hosted lead-zinc mineralization and the potential for economic mineral concentrations. The project will provide geological base maps that will detail the geology and facilitate the search for new mineral occurrences. Other goals are to update the mineral inventory data base and place known mineral occurrences within a geological framework. To assist in achieving these objectives, stream-sediment samples were collected from creeks in the map area and analysed according to Regional Geochemical Survey (RGS) procedures. Lithogeochemical samples of prospective lithologies were also collected.

During the 1991 field season, mapping was concentrated near Uslika Lake and included most of map sheet 94C/3 and parts of map sheets 94C/4 and 94C/6. The centre of the map area is located approximately 200 kilometres north of Fort St. James (Figure 1-11-1). Road access is by the gravel, all-season Omineca mining access road from Fort St. James, or a similar forestry access road which originates at the southern end of Williston Lake. These roads follow the Osilinka and Tenakihi drainages and connect to numerous secondary logging roads in the area. Approximately 50 per cent or more of the area will be accessible by logging roads by the end of 1991.

The map area is contiguous with that of the Manson Creek mapping project (Ferri and Melville 1988, 1989, 1990a and b, in preparation; Ferri *et al.*, 1988, 1989). This

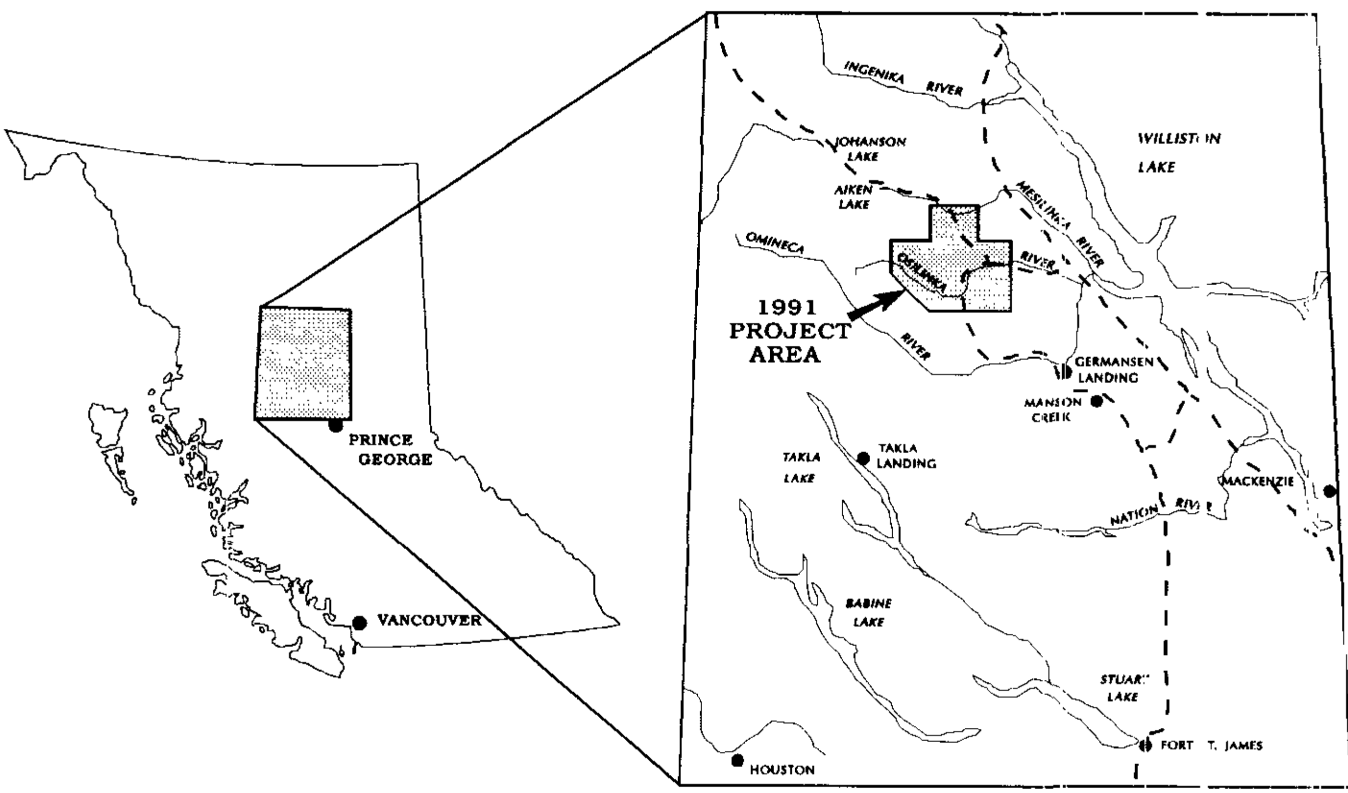

Figure 1-11-1. Location of the map area.

* Canada - British Columbia Partnership Agreement on Mineral Development.

work represents the most recent geological material published for the area. Initial mapping of the Aiken Lake region was carried out by Roots (1954) at 4-mile scale. The east half of the Mesilinka sheet was mapped by Gabrielse (1975) and mapping to the south was published at 6-mile scale by Armstrong (1949). Detailed geological studies of Paleozoic rocks within the map area were completed by Monger (1973) and Monger and Paterson (1974) and were summarized, in part, by Monger (1977). Garnett (1978) carried out an in-depth study of the southern Hogem intrusive complex and Meade (1975) mapped Takla Group rocks in the Germansen Lake area.

REGIONAL GEOLOGY

The project area straddles the boundary between the Intermontane and Omineca tectonostratigraphic belts of the Canadian Cordillera. It is underlain by accreted volcanic rocks of the Intermontane Superterrane and displaced rocks of North American affinity (Wheeler and McFeely, 1987, Figure 1-11-2).

Parts of at least four terranes are present in the map area. The easternmost are displaced continental rocks of the Cassiar Terrane. To the extreme west lies the Mesozoic island-arc terrane of Quesnellia. These are separated by two Upper Paleozoic terranes; the volcanic(arc?)-sedimentary Harper Ranch Terrane and the oceanic Slide Mountain Terrane.

Strata of the Cassiar Terrane include the Upper Proterozoic Ingenika Group through to the Devono-Mississippian Big Creek Group. The rocks are predominantly clastic with carbonates more abundant higher in the stratigraphy. The structurally and stratigraphically lower parts of this sequence are polydeformed and metamorphosed to sillimanite grade and outcrop as core complexes (Wolverine, Butler).

The Slide Mountain Terrane to the west lies structurally above the Cassiar Terrane. It is represented by the Pennsyl-

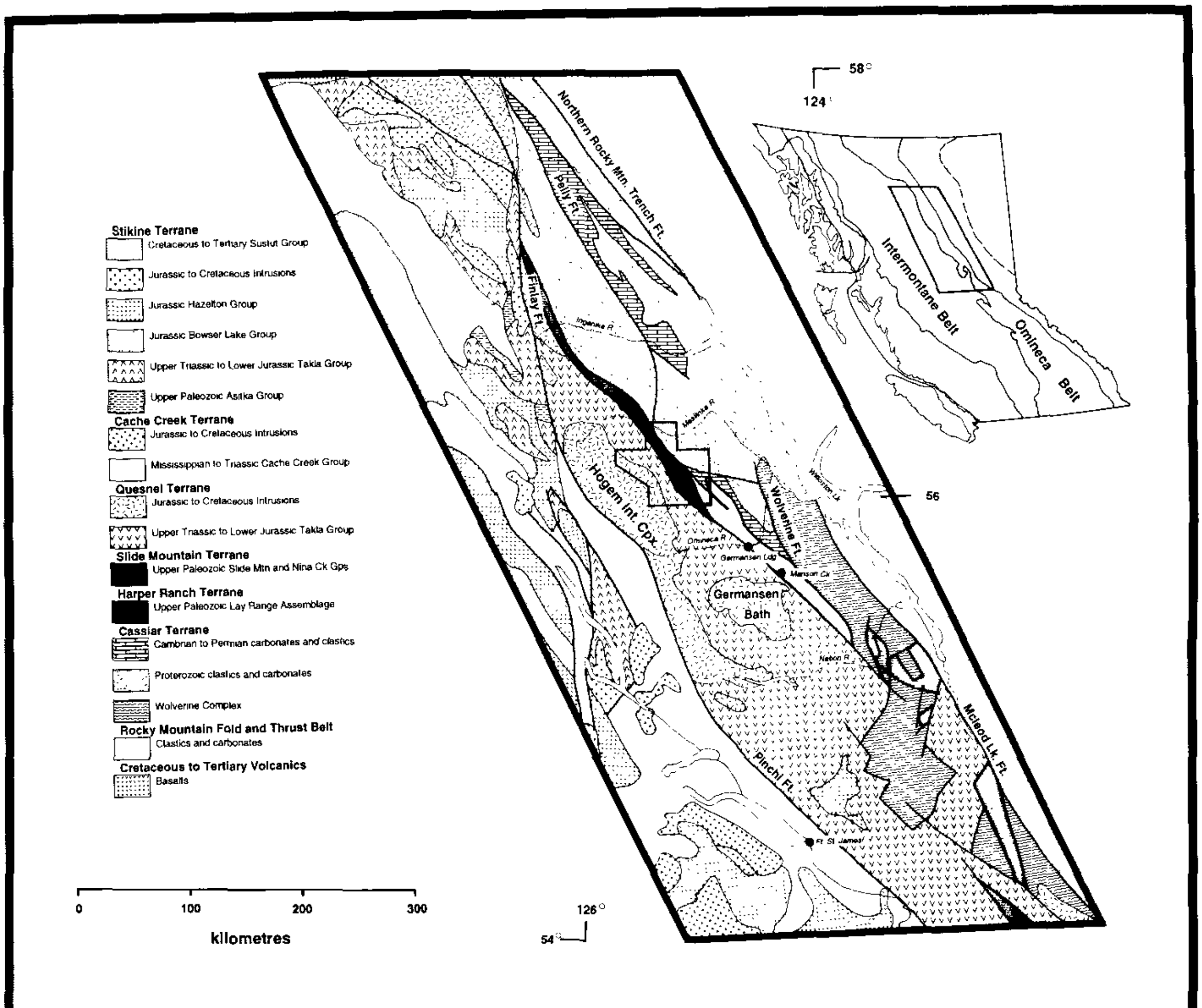

Figure 1-11-2. Regional geological setting of the Uslika Lake map area.

vanian to Permian Nina Creek Group (Ferri and Melville, in preparation). This package is composed of oceanic volcanic and sedimentary rocks (pillow basalts and cherty sediments) which have been thrust onto North American rocks.

The Quesnel Terrane is represented by the Upper Triassic to Lower Jurassic Takla Group (Roots, 1954). This is a volcanic and sedimentary arc sequence which is intruded along its western margin by the Triassic to Cretaceous Hogem intrusive complex (Garnett, 1978) and related intrusions. The eastern part of Quesnellia is further subdivided, in this area, into the Harper Ranch Terrane (Wheeler and McFeely, 1987). This terrane is represented by the enigmatic Upper Paleozoic Lay Range assemblage, a package of volcanic and sedimentary rocks with predominantly arc affinities. Traditionally it has been included with the Quesnel Terrane but in the study area it displays links with the Nina Creek Group and contains sedimentary rocks of continental origin.

STRATIGRAPHY

Descriptions of layered rocks are organized by terrane, beginning with rocks of North American affinity, and ending with the overlap assemblages that postdate accretion of the Intermontane Superterrane to the craton (Figure 1-11-3; Table 1-11-1).

NORTH AMERICAN CASSIAR TERRANE

INGENIKA GROUP (LATE PROTEROZOIC)

Proterozoic rocks in the map area were originally subdivided into two units by Roots (1954): the lower Tenakihi Group and the succeeding Ingenika Group. Subsequent workers in the area found the differences between the two units too ambiguous and proposed that use of the term Tenakihi Group be dropped and that all Proterozoic rocks in the area be included in the Ingenika Group (Mansy and Gabrielse, 1978). Furthermore, Mansy and Gabrielse proposed a four-fold subdivision for the Ingenika Group which is, in ascending order, the Swannell, Tsaydiz, Espee and Stelkuz formations. All four formations are recognized in the study area. Rocks originally termed the Tenakihi Group by Roots are equivalent to the upper part of the Swannell Formation whereas Roots' succeeding Ingenika Group equates to the Tsaydiz, Espee and Stelkuz formations.

The Ingenika Group is areally the dominant unit of the Cassiar Terrane exposed in the Uslika Lake area. It occupies the north and northeastern parts of the map. Its thickness is unknown, due to poor structural and stratigraphic control, but it is estimated to be at least several kilometres thick if the ridge on Beveley Mountain represents a continuous sequence of lower Swannell clastics. It is composed of quartz and feldspathic wackes, impure quartzite, sandstone, siltstone, slate, limestone and their metamorphosed equivalents. The Ingenika Group was examined in a cursory manner in the course of this study, and the following observations were made.

SWANNELL FORMATION

The Swannell Formation was examined along the ridges east and west of Beveley Mountain. These rocks form the southwest flank of a broad F_3 anticline. They appear to comprise an uninterrupted southwest-dipping panel with an estimated thickness of 1.5 kilometres or more. They are faulted against the upper part of the Ingenika Group to the southwest. The Swannell Formation in this area consists of grey to tan, thin to thickly bedded impure quartzite in sequences several metres thick, interlayered with lesser, thin to moderately bedded garnet-bearing biotite-muscovite-feldspar-quartz schists. The impure quartzite contains up to 20 per cent feldspar and mica. The schists are commonly chloritized and contain a weak to moderate crenulation.

This unit is very similar to the upper part of the Swannell Formation described farther south in the Nina Lake area (Ferri and Melville, 1990; in preparation). To the south the upper Swannell is estimated to be only 300 metres thick whereas it is some 1500 metres thick at Beveley Mountain. This suggests tectonic thickening (which is entirely possible considering the monotonous nature of the lithologies and the polyphase deformation which has affected these rocks) or stratigraphic thickening to the northwest.

TSAYDIZ FORMATION

The Tsaydiz Formation was observed in only a few localities; along the north side of the Osilinka River south of Beveley Mountain and northwest of Jim May Creek in a possible southwesterly overturned panel of rock.

It consists of greenish grey to dark grey slates and phyllites, interlayered with thinly bedded, buff to brown-weathering limestone to calcareous phyllite. Green-grey sandstones and siltstones, blue-quartz-bearing feldspathic wackes and buff-brown-weathering, blue-grey impure laminated limestone are of lesser importance.

The thickness of the unit is not known as it was mapped only in scattered outcrops below timberline and its basal contact is not observed. Structural sections in the Beveley Mountain area suggest a minimum thickness of 200 metres.

ESPEE FORMATION

The Espee Formation is well exposed in a northwest-plunging fold pair along a ridge immediately southwest of Beveley Mountain. A thick, northeast-dipping carbonate unit northwest of Jim May Creek has also been tentatively assigned to the Espee Formation. The formation is composed of thin to moderately bedded, tan to buff-weathering, dark grey to white or mottled limestone and dolomitic limestone which in some localities is coarsely recrystallized to a white marble. Very thin phyllite laminae (less than 2 mm) sometimes separate the limestone into layers. The Espee Formation is at least 400 metres thick in the Beveley Mountain area.

STELKUZ FORMATION

The Stelkuz Formation is poorly exposed on the southwest flank of Beveley Mountain, on the down-thrown side of the Camp fault. It is composed of green-grey, crenulated phyllite to quartzitic phyllite or schist, sometimes interlayered with impure quartzite beds up to 20 centimetres thick. White to bluish grey, clean limestone with micaceous partings is also found in this area and can be several metres

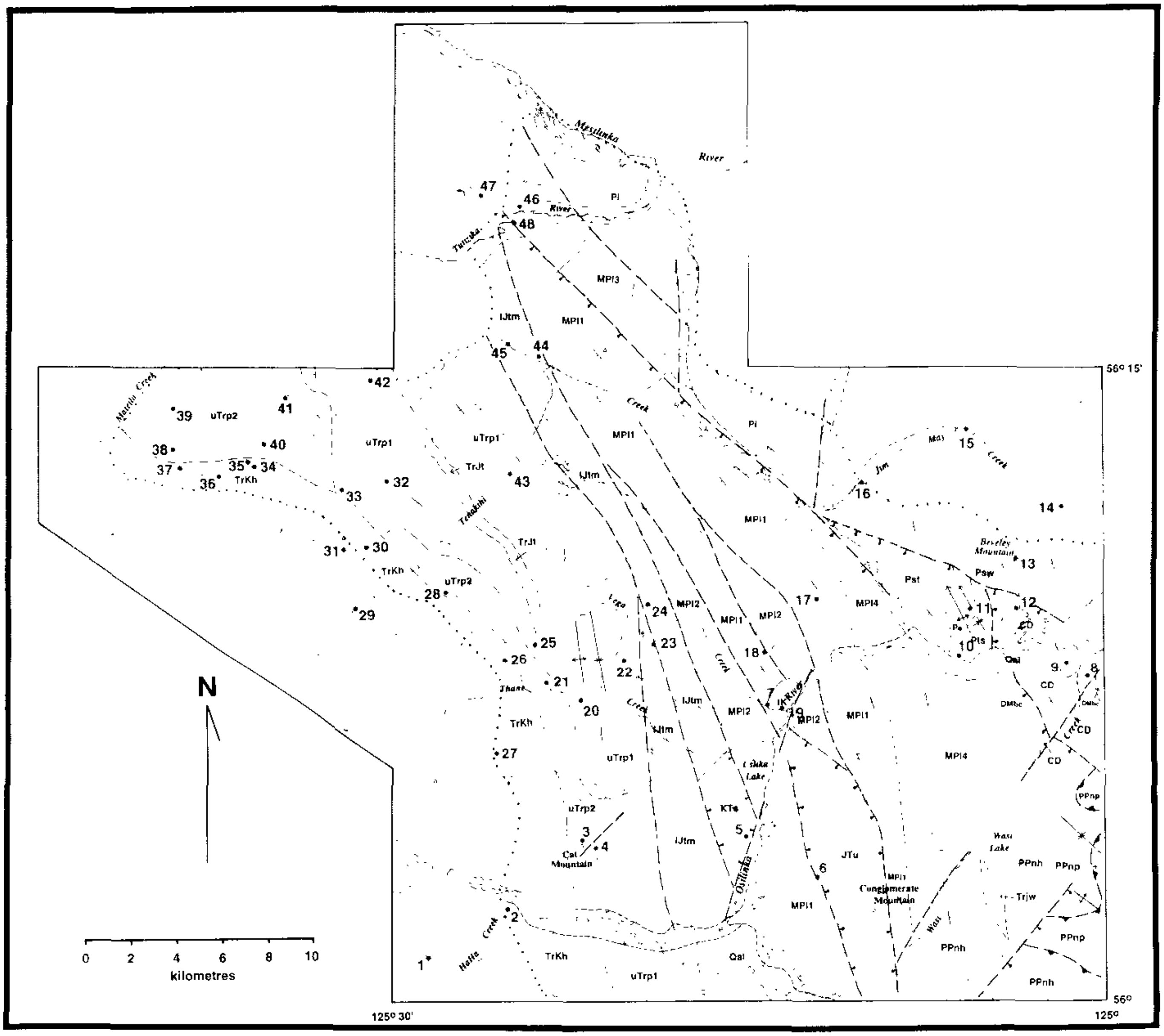

Figure 1-11-3. Geology of the map area including location of mineral occurrences.

thick. Dark blue-grey to black graphitic phyllite, slate and fine siltstone, approximately 100 metres thick, are exposed west of Beveley Mountain in the hangingwall of the Camp fault. This lithology is not typical of the Stelkuz Formation or other formations in the Ingenika Group but has been placed within the Stelkuz Formation due to its position on the northeast side of southwest-side-down normal fault along the lower parts of the Tenakihi Creek valley. This fault separates rocks of the Cassiar and Harper Ranch terranes.

PALEOZOIC SUCCESSION

A succession of Paleozoic carbonate and clastic rocks, upwards of 2 kilometres thick, is exposed in the northeastern part of the map area, and spans the Early Cambrian to Early Mississippian time periods. Areally these rocks are of minor importance in the map area, but locally and regionally, they contain significant lead-zinc-silver deposits within several of the carbonate horizons. Carbonate rocks of this succession were originally equated with the Cache Creek Group by Roots (1954) and Armstrong (1949). Monger (1973), Monger and Paterson (1974) and Gabrielse (1975) realized the distinct nature of these rocks and noted their similarities to units exposed in the Cassiar Mountains. Mapping by Ferri and Melville (1990) further corroborated this and led them to equate many of these units with similar lithologies in the Cassiar Mountains. It is now proposed that local names be applied to these units, due to their localized extent and differences with lithologies of similar age elsewhere in the Cassiar Terrane (Ferri and Melville, in preparation).

LAYERED ROCKS

Quaternary

Qal — *alluvium, sands, gravels*

Upper Cretaceous to Tertiary
Sustut Gp

KTs — *sandstone, conglomerate, siltstone, coal*

Lower Cretaceous

lK — *conglomerate, sandstone, siltstone, argillite, minor coal*

Lower Jurassic to Lower Tertiary

JTu — ***USLIKA FM:****heterolithic boulder conglomerate, lesser sandstone*

Lower Jurassic
Takla Gp

lJtm — *maroon to grey basalts, agglomerates, tuffs, plagio-lase and augite phyric*

Upper Triassic

uTrp2 — ***PLUGHAT MOUNTAIN FM:** augite phyric agglomerates, basalts, tuffs*

uTrp1 — ***PLUGHAT MOUNTAIN FM:** tuffs, tuffaceous, silt-stone, argillite, agglomerate minor limestone*

Pennsylvanian to Permian
Nina Creek Gp

PPnp — ***PILLOW RIDGE FM:** massive to pillowed basalt, lesser chert, argillite, gabbro*

PPnh — ***MOUNT HOWELL FM:** argillite, chert, gabbro, minor basalt, wacke, felsic tuff*

Mississippian to Permian
Lay Range Assemblage

MPl1 — *green, maroon tuffs to siltstones, agglomerate, basalt, argillite, gabbro, minor limestone*

MPl2 — *basalt, gabbro, serpentine, minor amphibolite, chert, chlorite, schist*

MPl3 — *black argillite, shale, phyllite, limestone, argillaceous limestone, sandstone, quartzite*

MPl4 — *grey, quartz-feldspar (dacite) tuff, minor argillite, sandstone*

Upper Devonian to Lower Mississippian
Big Creek Gp

DMbc — *dark grey to blue grey shales, argillites, minor siltstones, siltite*

Lower Cambrian to Middle Devonian
Atan Gp, Razorback Gp,
Echo Lake Gp, Otter Lakes Gp

CD — *limestone, dolomite, lesser shale, quartzite argillaceous limestone*

Upper Proterozoic
Ingenika Gp

Pi — ***Undivided:** impure quartzite, schist, phyllite, limestone,feldspathic wacke,arkosic sandstone*

Pst — ***STELKUZ FM:** phyllite, slate, sandstone, siltstone, graphitic slate*

Pe — ***ESPEE FM:** limestone, dolomite, dolomitic limestone, marble*

Pts — ***TSAYDIZ FM:** green-grey slates, phyllites, limestone, marble, argillaceous limestone*

Psw — ***SWANNELL FM:****impure quartzite, sandstone, schist, garnet-mica schist,*

INTRUSIVE ROCKS

Late Triassic to Cretaceous
Hogem Intrusive Complex

TrKh — *monzonite, quartz monzonite, syenite, quartz syenite*

Late Triassic to Early Jurassic
Tenakihi Intrusive Body

TrJt — *monzodiorite, diorite or gabbro*

Middle Triassic to Lower Jurassic (?)
Wasi Lake Ultramafic Body

TrJw — *serpentine, gabbro, minor listwanite, aplite*

Geologic Contact(defined, assumed)....................

Fault ....

Normal Fault(defined, assumed)..............................

Thrust Fault(defined, assumed)..............................

Strike and dip direction of bedding.........................

Strike and dip direction of bedding, overturned.....

Strike and dip of foliation..

Limit of quaternary cover..

Limit of mapping..

Mineral Occurrence.. 23

TABLE 1-11-1
MINERAL OCCURRENCES IN THE USLIKA MAP AREA

Map Number	Style of Mineralization	MINFILE Number	Occurrence Name	Commodities	Geological Description
1	Porphyry Cu	094C 097	REM	Cu, Pb, Ag	Sulphide mineralization includes disseminated chalcopyrite, pyrite, and rare bornite and galena hosted in the Duckling Creek syenite complex within the Late Jurassic to Early Cretaceous Hogem intrusive complex.
2	Vein and shear	094C 058	HaHa Creek,	Au, Cu	Small quartz veins in sheared quartz diorite carrying a small amount of free gold and chalcopyrite, malachite and pyrite are hosted in a vertical shear parallel to HaHa Creek within the Hogem intrusive complex.
3	Porphyry Cu-Au and vein	094C 069	CAT	Cu, Au, Fe, Ag	The original showings on the ridge top consist of magnetite and pyrite in boxwork quartz veins which are host to native copper, native gold, cuprite, chalcopyrite, tetrahedrite and bornite mineralization. Recent work has concentrated on the alkalic porphyry Cu-Au potential of propylitic and potassic-altered volcanics of the Takla Gp., located east of the original showings.
4	Porphyry Cu	094C 100	Kiwi	Cu	Malachite staining on fracture surfaces of fragmental augite-feldspar porphyry of the Takla Gp.
5	—	094C 061	Uslika coal	coal	Thin lenses (<1-15 cm) of impure silty/sandy lignite to sub-bituminous coal hosted in sandstones and conglomerates of the Sustut Gp.
6	—	094C 101	Energy	coal	Same as #5
7	—	094C 102	Fuel	coal	Same as #5
8	Stratabound carbonate-hosted base metals	094C 103	Critter	Zn, Ba?	Disseminated sphalerite with possible barite found in recrystallized and brecciated sections of light to dark grey dolomite of the Otter Lakes Fm.
9	Stratabound carbonate-hosted base and precious metals	094C 024	Carie/ PAR	Pb, Zn, Ag, Ba	Dolomitized carbonate breccia, possibly of the Espee Fm., hosts disseminated and massive galena, disseminated sphalerite, hydrozincite and smithsonite with pyrite and barite.
10	Fracture controlled veins	094C 104	Quarry	Pb, Zn, Cu, Au, Sb	Recrystallized and dolomitized limestones of the Espee Fm. host quartz vein mineralization. Minerals identified in hand samples include sphalerite, galena, cerussite, chalcopyrite, boulangerite, malachite, azurite and possibly stibnite. Fire assays on two grab samples from this location returned values of 890 ppb and 385 ppb Au.
11	Vein/ replacement?	094C 038	Regent	Pb, Ag	An irregular pod-shaped vein of massive crystalline galena is hosted in Espee Fm. dolomite and limestone (assay: 1575 g/t Ag, 83.53% Pb).
12	Carbonate-hosted base and precious metals and fracture controlled vein/ replacement	094C 023	Beveley	Pb, Zn, Ag, Ba	Disseminated to massive galena, sphalerite, barite and argentiferous galena occur in veins and veinlets in fractures and shears within the Mt. Kison Fm. of the Atan Gp., the Echo Lake Fm. and possibly the Otter Lakes Fm. in several zones on the Beveley prospect. Mineralization appears to be localized in minor folds, flexures and warps on larger scale folds.
13	Shear-controlled quartz vein	094C 105	Gael	Ag, Au, Cu	Disseminated fine-grained argentite and arsenopyrite are hosted by a shear-controlled quartz vein within the Swannell Fm. of the Inginika Gp.
14	Vein breccia	094C 057	Silver	Ag, Au, Pb, Zn	A quartz breccia vein within sheared quartzite, phyllite, argillite and siliceous sericite schist of the Inginika Gp. hosts disseminated argentiferous galena and pyrite with minor sphalerite and gold.
15	Shear-controlled vein breccia	094C 022	Ruby	Au, Ag, Pb, Zn, Mo	A stockwork of small quartz veins in a multiply brecciated shear cutting the Swannel Fm. hosts disseminated to massive pyrite, molybdenite, sphalerite, chalcopyrite, galena, tetrahedrite, arsenopyrite, pyrargyrite, polybasite, native silver and minor gold.
16	Placer	094C 026	Jim May Creek	Au	Placer gold occurs in reworked glacial deposits 1.5-3.65 m above bedrock and from a buried preglacial channel.
17	Shear-controlled vein	094C 106	Range	Au, Cu	Massive basalt of the Lay Range assemblage is sheared, locally altered to epidote and silicified. Malachite staining, about 1% pyrite and 1300 ppb Au are present.
18	Shear-vein	094C 107	Surprise	Cu	Volcanic sediments, sandstones, siltstones and cherty argillites of the Lay Range assemblage are strongly brecciated and cut by a quartz-ankerite vein 10-15 cm thick which is stained with malachite.
19	Placer	094C 028	Vega creek	Au	Small placer workings near the mouth of Vega creek.
20	Shear controlled	094C 044	Thane creek	Hg	Mafic volcanics of the Takla Gp. are cut by a carbonatized fault zone which contains minor cinnabar.
21	Shear-vein	094C 020	Thane	Cu, Fe, Au	Silicified fault, fracture and shear zones up to 1.2 m wide in the Takla Gp. near the contact with the Hogem intrusive complex are mineralized with disseminated and massive pods of chalcopyrite, pyrite, magnetite, specularite and a little gold.
22	Cu-Au vein	094C 076	Dave	Cu, Au	Propylitically altered andesitic flows of the Takla Gp. are cut by a silicified fracture zone 1 m wide carrying chalcopyrite, magnetite, specularite and minor gold.
23	Shear	094C 043	Beg	Hg, Cu	A strongly fractured, silicified and carbonatized shear zone carries cinnabar, pyrite and minor chalcopyrite as disseminations and fracture fillings. The hostrocks are flows, breccias and tuffs of the Takla Gp.

TABLE 1-11-1
MINERAL OCCURRENCES IN THE USLIKA MAP AREA — *Continued*

Map Number	Style of Mineralization	MINFILE Number	Occurrence Name	Commodities	Geological Description
24	Cu-Au porphyry/ shear/ vein	094C 021	Vega	Cu, Au, Hg	Disseminated chalcopyrite, bornite and pyrite occur in andesitic flow breccias of the Takla Gp. These volcanic rocks are propylitically and potassically altered. Calcareous and siliceous andesite breccia associated with a major northwest-trending shear zone contains minor disseminated cinnabar.
25	Vein/ shear	094C 019	Pluto	Cu, Au	Lenses of massive arsenopyrite, pyrite, magnetite and specularite, with minor chalcopyrite and gold, occur in quartz-carbonate-healed fracture zones (up to 1 m wide) within Takla rocks adjacent to the contact with the Hogem intrusive complex.
26	Porphyry Cu	094C 108	MJW	Cu	Malachite and azurite staining with specularite, pyrite and possible chalcopyrite in strongly fractured and locally silicified dark green chloritized and hornfelsed volcanics. The mineralized zone is up to 7 m across. This is possibly a xenolithic raft of the Takla Gp. within the monzonites of the Hogem intrusive complex.
27	Vein	094C 109	Claw	Cu	Malachite staining occurs with massive crystalline specularite and magnetite in a vein 15 cm wide found in rubble on a ridge top underlain by Hogem monzonite.
28	Porphyry Cu/vein	094C 110	Bottle	Cu	Multiple occurrences of chalcopyrite, chalcocite, malachite and azurite in brecciated quartz-chacedony veins in ankerite-veined and altered zones (up to 1 m wide) in Takla volcanics. Occurrences are very near the contact with the Hogem intrusive complex.
29	Vein/ disseminated	094C 072	Gail	Cu, Mo	Quartz vein with pyrite, chalcopyrite, molybdenite and bornite cuts biotite K-feldspar monzodiorite of the Hogem intrusive complex.
30	Vein/ porphyry	094C 049	Copper 5	Cu	Hogem monzonites host quartz veins with magnetite, chalcopyrite, malachite and azurite in altered and mineralized zones up to 1.5 m wide. One zone is exposed for 8 m along strike and is open down dip, but seems to pinch out up dip. Numerous occurrences were noted.
31	unknown	094C 048	Tenakihi Creek	Cu	The area is underlain by monzonites of the Hogem batholith.
32	Vein	094C 111	Snow	Cu	Fractured argillite and siltstone of the Takla Gp. host an epidote-calcite vein (up to 15 cm wide) with 1–3% disseminated chalcopyrite and malachite and azurite staining. The wallrock is also stained with malachite and azurite.
33	Vein	094C 112	DM	Cu	Fractured tuffs of the Takla Gp. are cut by epidote veining with malachite staining. Also malachite staining in the wall rocks.
34	Vein	094C 113	Yak	Cu	Fine and coarse-grained Hogem monzonite is cut by numerous small ankerite veins in a zone 5-6 m wide. Chalcopyrite, malachite and azurite are disseminated throughout and coat fracture surfaces. Local mafic segregations in the monzonite are more strongly mineralized than the felsic sections. The zone strikes approximately 130° and can be traced for 50–75 m to the east and apparently to the northwest across a small cirque into mineral showing #35.
35	Vein	094C 114	Koala	Cu	Same as #34 with 1-2% chalcopyrite and malachite.
36	Vein/ disseminated	094C 018	Matetlo	Cu, Au	A fracture zone 40 m wide hosts at least five quartz veins, each up to 25 cm wide, containing massive coarse-grained pyrite with chalcopyrite. Epidote, malachite, azurite and chrysocolla occur as vein selvages and are disseminated in fractures in Hogem granodiorite.
37	Vein/ disseminated	094C 115	Intrepid	Cu	Ankerite and quartz veins with chalcopyrite and malachite disseminated and as fracture filling found in several locations within the Hogem monzonite near the contact with Takla Gp. volcanics.
38	Vein	094C 116	Bill	Cu	Epidotized zone in fine-grained Hogem monzonite. Contains epidote veins with pyrite, malachite and azurite in two zones up to 10 m across.
39	Disseminated/ porphyry Cu	094C 117	Yeti	Cu	Malachite staining found on fracture surfaces with minor sulphides (pyrite±chalcopyrite) in an augite porphyry flow of the Takla Gp.
40	Disseminated/ porphyry Cu	094C 118	Dragon	Cu	Minor malachite staining on some fracture surfaces, minor amounts of epidote and up to 5% pyrite blebs in a dike of aplitic granite 2 m wide which cuts the Takla Gp. volcanics.
41	Vein/ disseminated	094C 099	Mat 1	Au, Cu	Pyrite, hematite, minor chalcopyrite and an unidentified silver mineral are hosted in a quartz-carbonate vein 1.1 m wide within a volcanic breccia of the Takla Gp. The vein is exposed over 100 m of strike length and a 34 cm chip sample across the vein returned 400 g/t Ag.
42	Disseminated	094C 119	Tough	Cu	Chalcopyrite in lithic crystal tuff of the Takla Gp.
43	Vein/ disseminated	094C 071	Oy	Cu	Takla volcanics contain chalcopyrite and minor specularite as fracture coatings, within quartz veins and as minor disseminations.
44	Disseminated	094C 120	CR	Cu	Epidote alteration and malachite staining are found in massive maroon amygduloidal basalt flows of the Takla Gp.

TABLE 1-11-1
MINERAL OCCURRENCES IN THE USLIKA MAP AREA — *Continued*

Map Number	Style of Mineralization	MINFILE Number	Occurrence Name	Commodities	Geological Description
45	Vein/Disseminated	094C 121	Nuthatch	Cu	Same as #44 except carbonate veining present and flows are locally sheared and fractured. Minor azurite present. Mineralized zone is at least 15 m across.
46	Vein?	094C 015	Stranger	Au	Pyrite occurs in quartz-calcite veins which cut Permian calcareous black slatey argillite.
47	unknown	094C 041	Mercury 1	Hg	Carbonatized fault zone contains a little cinnabar (in Lay Range volcanics?)
48	unknown	094 042	Mercury 2	Hg	Same as #47.

ATAN GROUP (EARLY CAMBRIAN)

Rocks of Early Cambrian age were originally placed within the Ingenika Group by Roots (1954). Gabrielse (1975), working in the east half of the Mesilinka map area, partially separated these rocks from the Proterozoic succession, based on their age and similarities to Early Cambrian rocks elsewhere in the Cordillera. More detailed mapping by Ferri and Melville (1990) distinguished the Lower Cambrian succession from the Proterozoic sequence. Similar rocks were mapped in the present study area.

The Atan Group is subdivided into two formations in the project area; the lower Mount Brown Formation and the upper Mount Kison Formation. No fossils were found by the authors but archaeocyathids of possible Early Cambrian age were collected south of Beveley Mountain by D. Craig (personal communication, 1991).

Mount Brown Formation is poorly exposed in the extreme eastern part of the map area, south of Beveley Mountain and north of the Osilinka River. The best exposures are along the main logging road and old access roads leading to the abandoned camp on the Beveley showings. The base of the unit is not seen within the map area and only the upper few hundred metres are exposed. The unit consists of moderately to thickly bedded, grey-brown and maroon impure quartzite and sandstone, interlayered with thin to thickly bedded dark grey to grey-green phyllite and siltstone. Limestone nodules up to 40 centimetres long were seen within the phyllite-siltstone sequences. Some of the thinner sandstone layers contain horizontal worm burrows.

Mount Kison Formation is poorly exposed in the map area. It crops out on the north side of the Osilinka River, just south of Beveley Mountain. Grey, recrystallized limestone east and west of the mouth of Wasi Creek may also belong to this unit. The formation consists of grey to white mottled limestone with thin, wavy to indistinct bedding. In some localities the unit consists of finely crystalline grey limestone layers, 3 to 5 centimetres thick, interlayered with coarser, darker grey, discontinuous limestone and slightly argillaceous limestone beds 0.5 to 2 centimetres thick. South of Beveley Mountain, this carbonate is commonly coarsely recrystallized and sometimes dolomitized.

RAZORBACK GROUP (CAMBRIAN TO ORDOVICIAN)

The Razorback Group is a name now applied to rocks previously called the Kechika and Road River groups in the Nina Creek area by Ferri and Melville (1990a, b). It is approximately 75 metres thick and comprises shale, argillaceous dolomite and dolomite. It is recessive and poorly exposed. Exposures were found only along road cuts or in trenches in the Beveley Mountain area and on the east side of Wasi Creek. The age of the unit is based on its position above Lower Cambrian carbonates of the Atan Group and below Lower Silurian carbonates and shales of the Echo Lake Group (Ferri and Melville, in preparation).

In the Beveley Mountain area, rocks assigned to the Razorback Group outcrop along the road leading to the mineral showings. They are dark grey and grey, thinly layered shales which grade upwards into thin and thickly bedded argillaceous limestone. Strongly brecciated and recrystallized dolomite and limestone can also be seen along the road.

On the east side of Wasi Creek, rocks tentatively assigned to the Razorback Group were exposed in trenches on the PAR mineral claims. The exposed sequence is upwards of 75 metres thick. Dark grey to silvery argillite and shale, with sections of white and greenish white sericitic phyllite and schist up to several metres thick, pass upward into dark grey, thinly bedded calcareous argillites which in turn grade upward into dark grey, thinly layered argillaceous to dolomitic limestone. This section is similar to sections of the Razorback Group seen in the Nina Creek area (Ferri and Melville, 1990), the only difference is the presence of sericitic phyllite in the Wasi Creek area.

ECHO LAKE GROUP (MIDDLE ORDOVICIAN TO EARLY DEVONIAN)

The Echo Lake Group crops out north and south of the Osilinka River in the eastern part of the map area. Near Wasi Creek it is continuous with Lower Silurian to Lower Devonian carbonates mapped by Ferri and Melville (1990, in preparation) and was originally equated with the Sandpile Group. Similar carbonates with corals of possible Siluro-Devonian age (Roots, 1954) are exposed immediately south of Beveley Mountain.

The Echo Lake Group is some 700 metres thick near Beveley Mountain and northwest of Wasi Creek, and upwards of 500 metres thick south of Wasi Creek. These estimates are based on structural cross-sections and may be affected by structural thickening. It consists of buff-weathering, pale grey to medium grey, thin to massively bedded, medium-grained sugary dolomite and limestone. There is sporadic quartz replacement of layers up to several centimetres thick. Bioclastic limestone, oolite and carbonate breccia horizons are also present within the sequence. West of Wasi Creek, the Echo Lake Group is characterized by discontinuous or thinly interlayered, light and dark grey mottled dolomite. Dark grey and grey graptolitic argillite up to 70 metres thick is exposed at the base of the sequence and is associated with planar-bedded limestone and argillaceous limestone.

This unit lacks the sandy dolomite and quartzite which characterize it in the Nina Lake and Trail Creek areas (Ferri and Melville, 1990; in preparation). This suggests a facies transition to the northwest, perhaps reflecting deposition in deeper water.

This unit was previously believed to range in age from Early Silurian to Early Devonian (Ferri and Melville, 1990a, b; in preparation), but Middle Ordovician graptolites were recovered from the basal argillites southeast of Wasi Creek (B.S. Norford, personal communication, 1991). This new age span for the Echo Lake Group is comparable to the lithologically similar Sandpile Group in the Cassiar Mountains (Gabrielse, 1963).

Otter Lakes Group (Middle Devonian)

The Otter Lakes Group was originally mapped as the McDame Group by Ferri and Melville (1990a, b). It is important locally as it carries significant amounts of disseminated galena and sphalerite. It has been recognized in the Wasi Creek area, where it is from 200 to 300 metres thick, and can be traced southeastward into the End Lake map area. The Otter Lakes Group also outcrops on the north side of Wasi Creek along the down-thrown side of a northwest-trending normal fault. The twin-holed columnal osicles within this unit make it no younger than Middle Devonian and conodont fossils collected in the End Lake map area restrict it to the Middle Devonian (Ferri and Melville, in preparation). It is characterized by thin to medium-bedded, grey to dark grey, fetid, fine to medium-grained crystalline dolomite and limestone with fossiliferous horizons. It is also typified by vugs filled with pyrobitumen, graphite or calcite. The unit is sometimes coarsely recrystallized and appears quite massive. Fossiliferous sections contain crinoid fragments, rugosan corals, bryozoa and amphipora.

Big Creek Group (Late Devonian to Early Mississippian)

Shales, argillites and minor siltstone in the Wasi Creek area are assigned to the Big Creek Group. These were originally included in the Cache Creek Group by Roots (1954). Similar rocks in the Nina Lake area were termed the Earn Group by Ferri and Melville (1990) due to their remarkable similarities with lithologies in the Cassiar Mountains. In the Nina Creek area, these rocks are bracketed as Upper Devonian to Lower Mississippian as they overlie the Middle Devonian Otter Lakes Group and contain Lower Mississippian conodonts in the upper parts of the section (Ferri and Melville, in preparation).

The Big Creek Group is upwards of 500 metres thick and is characterized by dark grey, blue-grey and black, thin to very thinly bedded, platy to wavy shales, argillites and siltstones. Slates and argillites predominate east of Wasi Creek whereas siltstones and siltites are more common to the west.

Slide Mountain Terrane

Nina Creek Group (Pennsylvanian to Permian)

Rocks of the Nina Creek Group in the map area were placed with the Cache Creek Group by Roots (1954) due to their similar age and lithologies. Monger (1973), Monger and Paterson (1974) and Gabrielse (1975) noted their distinctive characteristics and separated the various lithologies. Detailed mapping by Ferri and Melville (1988, 1989, 1990a) in the Manson Creek and Germansen Landing areas led them to assign these rocks to the Slide Mountain Group because of similarities to rocks of comparable age and lithology in southern British Columbia. It has now been suggested (Ferri and Melville, in preparation) that this assemblage be termed the Nina Creek Group due to its restricted extent and slight differences with other rocks of the Slide Mountain Terrane.

The Nina Creek Group outcrops in the mountainous area east of the Wasi Lake - Wasi Creek valley. It can be divided into two formations within the study area; the lower Mount Howell Formation and the succeeding Pillow Ridge Formation. The Mount Howell Formation is equivalent to the Middle Division (PPsmm) of the Slide Mountain Group as defined by Ferri and Melville (1990a, b) and the Pillow Peaks Formation equates with their Upper Division (PPsmu). Each of these formations spans the Pennsylvanian to Permian interval (Ferri and Melville, in preparation), indicating that they are in structural contact with each other. The combined thickness of the two units is difficult to determine due to faulting and folding, but a minimum of some 3 kilometres is estimated.

Pillow Ridge Formation (Pennsylvanian to Permian)

The Pillow Ridge Formation is exposed in thin fault slices within broad folds along the southeastern boundary of the map area. It is approximately 500 to 1000 metres thick and is characterized by grey-green and green massive and pillowed basalt. The basalt is microcrystalline and it commonly contains narrow veins of chlorite and epidote. Siliceous sediments, intruded by sill-like bodies of gabbro, are locally associated with these basalts. The sediments are dark grey to black, thin to moderately bedded, wavy banded argillite and siliceous argillite, interbedded with moderately to thickly bedded, varicoloured chert (green, grey, cream) and ribbon chert. Gabbro forms sill-like bodies up to several metres thick and contains equal amounts of fine to medium-grained plagioclase and pyroxene phenocrysts, the latter sometimes with glomeroporphyritic textures.

Mount Howell Formation

The Mount Howell Formation is at least 2 kilometres thick and is composed predominantly of sediments with lesser volcanic and igneous rocks. It crops out east of Wasi Lake and good exposures are seen in the creek valleys that drain into Wasi Lake and Wasi Creek and along the high ridges to the southeast.

The structurally lower part of the unit is typified by dark grey to black, thin to moderately bedded, wavy banded argillite with lesser cherty argillite, quartz wacke and quartz-(feldspar)-bearing tuff. The quartz wacke occurs as grey to grey-brown lenses and beds with up to 80 per cent fine to medium quartz grains in a silty to muddy matrix. The quartz-feldspar tuff crops out in several localities and may be several hundred metres thick. It is found as subcrop along the west-facing slopes south of Wasi Lake and in sections 10 metres thick along the canyon in the lower part of the creek that flows into the northeast side of Wasi Creek as it exits Wasi Lake. This tuff is light grey to grey, sericitic, and contains up to 80 per cent quartz and feldspar grains with lesser muscovite and argillite rip-up clasts. Quartz wackes and tuffaceous sequences make up less than 10 per cent of the unit. These rocks may have continental affinities.

The upper part of the Mount Howell Formation contains significantly more siliceous sediments which are interlayered with thin basaltic flows and intruded by gabbro. The sediments are grey to dark grey, thin to moderately bedded, wavy banded argillites and siliceous argillites which are interlayered with grey siltstones and grey to cream-coloured, thin to thickly bedded cherts and ribbon cherts. Fine to medium-grained gabbro sills, up to several hundred metres in thick, intrude the sediments. Basalts are massive to pillowed, green to grey-green, amygdaloidal (chlorite, quartz) and are possibly up to tens of metres thick. Sections of green mafic ash-tuff are associated with the basalts.

Harper Ranch Terrane (Lay Range Terrane?)

LAY RANGE ASSEMBLAGE

The Lay Range assemblage includes Upper Paleozoic tuffs, argillites, mafic to ultramafic igneous rocks, grits, limestone and chert (Roots, 1954). These rocks derive their name from their excellent exposure in the Lay Range (between Lay Creek and the Swannell River; Roots, 1954).

This is an enigmatic sequence within the map area. The tuffs and agglomerates are very similar to lithologies in the Plughat Formation of the Takla Group, yet an older age precludes any direct relationship. The Lay Range assemblage has some affinities with the time-equivalent Nina Creek Group. Massive to pillowed basalts and related cherty sediments are similar to lithologies in the Mount Howell Formation, but no interfingering of the two packages is seen, suggesting a fault contact between them.

The lower parts of the tuffaceous sequence contain quartz-rich detritus and its lower contact appears conformable with the upper part of a dacitic tuff unit, which may be part of the Cassiar stratigraphy. Furthermore, argillites, grits, quartzites and limestones in the structurally lower parts of the Lay Range assemblage have more similarities to North American rocks than with any other package within the map sheet.

No definitive fossils were found in the Lay Range assemblage during the 1991 field season. Bryozoa, brachiopod and crinoid ossicle fragments were recovered from tuffaceous beds. Roots (1954) describes fossils from this package which indicate a Mississippian to Permian age. Permian conodonts have been recovered from calcareous beds within the tuffs on the north side of Vega Creek (M.J. Orchard, personal communication, 1991). Ross and Monger (1978), working in the Lay Range, recovered middle Pennsylvanian fusulinids from limestones in the lower parts of the assemblage. The dacitic tuff unit bears a strong resemblance to lower Mississippian tuffs in the Germansen Landing area (Ferri and Melville, in preparation) suggesting a possible Mississippian lower age limit.

The Lay Range assemblage is subdivided into four lithologic divisions; the structurally lowest is the dacitic tuff unit followed by the argillite-grit-limestone unit which is succeeded by the mafic tuff unit which in its upper part contains a faulted sequence of basalts, gabbro and serpentinite which makes up the mafic-ultramafic subdivision.

Dacitic Tuff Unit

Grey to dark grey, massive quartzofeldspathic tuff outcrops over a large area west of the Wasi Creek - Wasi Lake valley. This unit commonly contains a weak to strong penetrative cleavage. Fine to coarse-grained quartz, feldspar and rare mica clasts constitute up to 30 per cent of the rock with quartz being dominant. Very minor occurrences of grey to dark grey phyllite are associated with the tuffs. Quartz feldspar wackes and arkosic sandstones occur along strike with the tuffs northwest of the mouth of Tenakihi Creek. These clastic rocks are also characterized by a strong penetrative fabric.

The dacitic tuff unit is very similar in appearance to a felsic tuff in the Germansen Landing area (Ferri and Melville, 1989; Ferri *et al*, 1989), now termed the Gilliland tuff and dated as Lower Mississippian (U-Pb; Ferri and Melville, in preparation). In the south these rocks have been grouped with argillites of the Mississippian to Permian Cooper Ridge Group, which is part of the Cassiar stratigraphy (Ferri and Melville, in preparation). In the present map area, the dacitic tuff unit appears to sit structurally above argillites assigned to the Big Creek Group. The argillites may be in part equivalent to the Cooper Ridge Group. Furthermore, arkosic sandstone beds within the dacitic tuff unit also suggest a North American affinity. If this is the case, tuffaceous argillites southeast of the Wasi Creek valley may also be part of the Cooper Ridge Group, suggesting that North American stratigraphy lies below the Nina Creek Group southeast of Wasi Lake.

South of the mouth of Tenakihi Creek the upper contact of this package appears to pass into lithologies of the mafic tuff unit which, together with the preceeding argument, suggests a link between North American stratigraphy and that of the Lay Range assemblage.

Argillite-grit-limestone Unit

Black argillite, shale, phyllite, dark grey to black limestone, quartzite and quartz feldspar wackes are exposed along the Tutizika River, and along road cuts to the north and south. These rocks are unlike any other lithologic package in the area. They have been grouped with the Lay Range assemblage due to their position structurally below the Lay Range tuffs and primarily on the basis of their resemblance to similar sequences described in the Lay Range (Roots, 1954). These rocks are in fault contact with the mafic tuff unit.

Strongly folded and faulted, thin to moderately bedded, dark grey to black graphitic argillite and siliceous argillite are interlayered with dark grey to black shale and phyllite in sequences up to 100 metres thick along the Tutizika River. These rocks are sometimes interlayered with brown-grey quartz feldspar wackes which contain pebbly sections carrying clasts of opalescent blue quartz.

Several sequences of massive, blue-grey pebbly quartzite up to 30 metres thick occur within these argillites. The quartzites are also distinguished by the presence of opalescent blue quartz grains which is a characteristic of North American clastic sequences. Observed contacts are conformable with the surrounding argillites.

Dark grey to black, finely crystalline and laminar limestone and argillaceous limestone up to 50 metres thick occurs within this argillite sequence. Laminar bedding is 0.1 to 3 centimetres thick and wraps around coarsely recrystallized zones up to 20 centimetres in diameter, suggesting that some of these limestone sequences have been tectonized. In one locality along the Tutizika River, large boudins or 'knockers' of limestone up to several metres thick and 5 metres long occur within the argillites.

Mafic Tuff Unit

Green to light green and maroon tuff, tuffaceous siltstone, lapilli tuff, agglomerate, basalt and lesser argillite, chert, gabbro and limestone form the most distinctive sequence within the Lay Range assemblage. These rocks appear very similar to the Plughat Mountain Formation of the Takla Group, but are commonly distinguished from Takla tuffs by their more intense greenish colour, the presence of quartz clasts and generally more penetrative deformation. It forms two linear belts of rocks some 1 to 5 kilometres wide on both sides of the Uslika Formation in the south and can be traced northwestward to the Tutizika River. Faulted equivalents of these rocks are exposed along the Vega Creek valley and are tectonically interleaved with younger clastic rocks.

Thick sequences of green, thin to thickly bedded, very fine tuffs and tuffaceous siltstones are the dominant lithologies within this unit. The beds commonly display sedimentary grading and load features. These units are interlayered with grey to dark grey argillaceous beds and rare grey to cream chert and limestone.

Tuffs are massive to thickly bedded, fine to coarse grained and are composed of lithic clasts (basalt), pyroxene and feldspar crystal fragments and fragments of chert, argillite and quartz. Some are reworked and better classified as volcanic sandstones or wackes. Rare conglomerate beds up to 1 metre thick, consisting of argillite, chert, quartz and volcanic(?) clasts, are also observed. Northeast of Vega Creek, maroon basaltic(?) clasts are abundant in the tuffs. Green, dark green and maroon basalt, amygdaloidal basalt, and pyroxene-feldspar-phyric basalt clasts predominate within lapilli tuffs and agglomerate. Graded, quartz-rich sands and wackes are a minor but conspicuous part of the tuff sequence. They are quite common northwest of the confluence of Tenakihi Creek and the Osilinka River. The coarser tuffs and lapilli tuffs sometimes contain fragments of bryozoa, crinoid ossicles and brachiopods.

Dark green, massive to amygdaloidal basalt flows from 1 to 10 metres thick, are occasionally found within these tuffs. They are well exposed along a road cut on the north side of the Osilinka River, 3 kilometres upstream from the confluence of Tenakihi Creek.

Dark green and green, fine to medium-grained gabbro sills were observed in several localities within the tuffs. They are up to 100 metres thick and traceable for several kilometres.

This unit is bounded by a strike-slip fault system on its southwest side. Its northeast margin is not well exposed but in one locality it appears that its lower parts become more argillaceous and pass into lithologies typical of the dacitic tuff unit. This transition occurs in an area with scattered outcrops and does not rule out the presence of a major fault separating the two units.

Mafic-ultramafic Unit

Basalt, gabbro and serpentinite are exposed along the high ridges northeast of Vega Creek and to the southeast across the Osilinka River valley where they are cut by a northwest-trending strike-slip fault north of Conglomerate Mountain. The unit pinches out to the northwest where it is last observed along the banks of a northeast-flowing creek, southwest of Tenakihi Creek. This package is a fault-bounded structural sequence in the middle of the mafic tuff unit.

Dark green, massive to pillowed, olivine(?)-bearing basalts form the structurally highest and lowest parts of this package northwest of the Osilinka River. They contain thin lenses of grey to cream chert, fine to medium-grained gabbro and serpentinite. Mafic tuffs are associated with basalt in the lowest fault slice.

Fine to very coarsely crystalline gabbro is associated with serpentinite northwest and southeast of the Osilinka River. It may be mylonitized and contain a strong fabric parallel to the unit boundaries. Amphibolite and foliated basalt are associated with gabbro and serpentinite southeast of the Osilinka River.

Quesnel Terrane

TAKLA GROUP (LATE TRIASSIC TO EARLY JURASSIC)

The Takla Group occupies the western half of the map area and is well exposed along the mountains extending from Cat Mountain to Matetlo Creek. It is bounded on the west by the Hogem intrusive complex and to the east by a series of northwest-trending strike-slip faults and related graben structures. The Takla exposure is relatively narrow in the southern part of the map area and then widens to the northwest as the Hogem intrusive contact swings to the west. Roots (1954) noted that the eastern base of the Takla Group is marked by a conglomerate unit 30 metres thick. It has been mapped in several localities and, from this and descriptions by Roots, it is probably a younger conglomerate sequence belonging to either the Uslika Formation or the Sustut Group and has been preserved in one of the many grabens in the area.

Two units are recognized within the Takla Group; augite-phyric volcanics and tuffaceous sediments of the Plughat Mountain Formation and maroon to green-grey basalts and related volcaniclastic rocks of an unnamed unit which may be equivalent to the Early Jurassic Chuchi Lake Formation of Nelson *et al.* (1992, this volume). The Plughat Mountain Formation (Ferri and Melville, in preparation) is the name applied to the thick pile of Takla Group basalts exposed below Plughat Mountain, east of Manson Creek. These rocks lie above Middle to Upper Triassic slates and argillites of the Slate Creek Formation (Ferri and Melville, *ibid.*). Units recognized within the Takla Group are very similar to those described by Nelson *et al.* (1991, 1992, this volume) who have carried out detailed mapping immediately to the south in the Chuchi Lake area.

Plughat Mountain Formation [Late Triassic, Norian(?)]

The Plughat Mountain Formation forms the western two-thirds of the Takla Group exposure. It occupies a south to southwest-dipping panel of rocks which is in fault contact with the Early Jurassic maroon volcanics to the east. Two subdivisions of the formation can be made; an easterly, and in part, lower sequence of predominantly tuffs, tuffaceous sediments with lesser agglomerate, argillite, siltstone and carbonate (Unit 1) and a western, and in part, upper sequence of augite and plagioclase-phyric massive to agglomeratic* basalts (Unit 2). Unit 1 is equivalent to Unit 2 of Ferri and Melville (1989) and the Inzana Lake Formation of Nelson *et al.* (1991, 1992, this volume). Unit 2 is equivalent to Units 3 and 4 of Ferri and Melville (1988) and the Witch Lake Formation of Nelson *et al.* (1991, 1992, this volume).

We believe that Units 1 and 2 of the Takla Group are time equivalent; Unit 1 represents a distal, volcaniclastic and epiclastic facies derived from a volcanic centre to the west which is represented by Unit 2. In such a setting, facies changes can be abrupt and, in some places, one facies may lie stratigraphically over the other. In the northwestern part of the map area, coarse volcaniclastic rocks of Unit 2 overlie tuffs of Unit 1, whereas in the south these two units interfinger in a manner similar to that seen in the Germansen Landing area by Ferri and Melville (1989). The epiclastic sequence of Unit 1 is locally interrupted by small intrusive bodies and related volcanics as seen south of Tenakihi Creek.

Diagnostic fossils have not been collected from the Plughat Mountain Formation in the map area. Rocks of similar lithology have been dated to the southwest and are Late Triassic (middle Norian; K. Bellefontaine, personal communication, 1991).

Unit 2 is characterized by grey to greenish grey augite and augite-plagioclase-phyric agglomerates and coarse lapilli tuffs with lesser massive flows, tuffs and tuffaceous sediments. It is well developed in the northern part of the map area whereas in the southeast only thin remnants of it are found near the contact of the Hogem intrusive complex. Agglomerates and flows are massive on outcrop scale and bedding or flow tops are seen only rarely. Clasts in the agglomerates are mostly porphyritic basalt with rare monzonite. Occasionally basalt clasts show a wide variation in the percentage and size of phenocrysts, indicating that numerous volcanic horizons were sampled prior to their deposition. Augite phenocrysts, up to 1 centimetre in diameter, constitute from 10 to 40 per cent of the rock. Plagioclase phenocrysts up to 0.5 centimetre in length are subordinate to augite and range from to 5 to 20 per cent. Both large clasts and flows may be amygdaloidal with infills of chlorite, calcite and prehnite(?). Grey-green, massive to poorly bedded crystal tuffs are subordinate to the agglomerates. Grey to greenish, moderately to thickly bedded tuffaceous siltstones and grey and dark grey argillites are a minor constituent of this facies.

Unit 1 consists of grey to greenish tuffs, tuffaceous siltstones and argillites, lesser lapilli tuffs and agglomerates, argillite and argillaceous limestone. The finer clastic units appear reworked. The tuffs are moderately to massively bedded, fine to coarse grained and composed of crystal (augite and plagioclase) and lithic fragments. They commonly contain lapilli fragments of predominantly augite-plagioclase-phyric basalts with lesser argillite, limestone and tuff. These tuffs are interlayered with grey to dark grey, thinly to thickly bedded tuffaceous siltstones which contain sections of dark grey argillite. Occasional beds of dark grey argillaceous limestone, 10 to 50 centimetres thick, occur

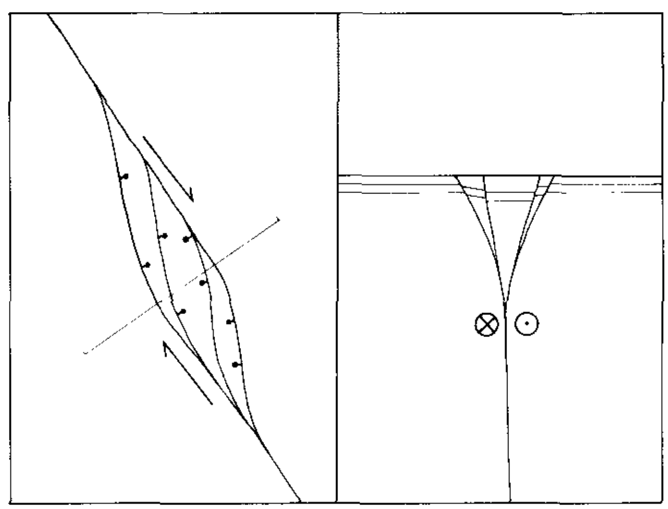

Figure 1-11-4. Diagramatic representation of strike-slip graben systems. (a) Plan view showing how motion is transferred between en echelon strike-slip faults along a graben system (negative flower structure). Movement on the bounding blocks of the main fault zone, in conjunction with the bend in the fault system, causes the blocks to drop within the transfer zone. Note that if motion were reversed on the faults, the grabens would be horsts (positive flower structure). (b) Cross-sectional view showing how the faults merge at depth.

* Agglomerate is used here solely as a descriptive term for primary volcaniclastic units with clasts greater than 64 mm and has no genetic implications.

within the more argillaceous sequences. Coarse lapilli tuffs and agglomerates of Unit 2, tens of metres thick, are interfingered with the finer grained clastics.

A small monzonite body and related subvolcanic rocks are found within this facies south of the big bend in Tenakihi Creek. An intrusive breccia is associated with this body and the coarse lapilli tuffs and agglomerates contain abundant intrusive clasts very similar in appearance to the intrusion. This monzonite may be related to a small volcanic centre within Unit 1.

MAROON VOLCANICS (LOWER JURASSIC)

A series of maroon to dark grey volcanics outcrops in the eastern part of the Takla Group and appears to lie stratigraphically below tuffs of the Plughat Mountain Formation. These are quite distinct from lithologies of the Plughat Mountain Formation and Roots (1954) recovered Early Jurassic ammonites, making them younger. This implies that these volcanics have been structurally emplaced. They are bounded on both sides, and are cut by, a series of steep, northwest-trending faults with possible strike-slip motion. These faults are associated with negative flower structures (or grabens, *see* Structure section, Figure 1-11-4; Woodcock and Fischer, 1986). It is believed that these younger volcanics have been preserved within one of these structures.

The age and composition of the volcanics is very similar to rocks of the Early Jurassic Chuchi Lake Formation which lies above rocks of the Witch Lake Formation in the Chuchi Lake area (Nelson *et al.*, 1992, this volume).

Grey-brown and maroon magnetic basalts outcrop along the Tutizika River and continue southwards to Tenakihi Creek and southeastwards to Thane Creek. These basalts are aphanitic or plagioclase and pyroxene phyric. They are commonly massive, amygdaloidal (with infills of calcite and chlorite) and may contain flow-top breccia. Typically plagioclase is the dominant phenocryst and constitutes up to 20 per cent of the rock.

The basalts are associated with dark grey to greenish polymictic agglomerates and tuffs which are exposed along a ridge south of the big bend in Vega Creek and continue south of Thane Creek. In the Vega Creek area the clasts are composed of augite-plagioclase-phyric, plagioclase-phyric and augite-phyric basalts, and syenite and monzonite which appear very similar to Hogem intrusive complex lithologies. The clasts are somewhat rounded and reworked. Roots (1954) described large feldspar porphyry clasts up to 60 centimetres in diameter in the vicinity of the Vega showing. Augite-plagioclase-olivine(?) and/or hornblende-phyric basalt flows and agglomerates are common south of Thane Creek.

YOUNGER ROCKS (OVERLAP ASSEMBLAGES?)

USLIKA FORMATION (EARLY JURASSIC? TO EARLY TERTIARY)

Massive to thickly bedded, well-indurated, coarse pebble to boulder conglomerate and minor sandstone crop out along the ridges of Conglomerate Mountain. It is green to grey-green with rounded to well-rounded clasts up to 40 centimetres in diameter. Clasts are composed of granitic material (primarily monzonite, syenite(?) and gabbro) with white to grey quartzite, grey to black chert, volcanic material (green, aphanitic basalt, augite-plagioclase porphyries and tuff) and lesser argillite and rare schistose rock. Massive sandstone layers range in thickness from 10 centimetres to over 2 metres. Rare cross-bedding indicates a northwesterly flow. The northern and southern margins of this unit are sheared, suggesting that it may be a fault sliver.

The age of the conglomerate is difficult to deduce as no macroscopic fossils have been found. Roots (1954) correlated chert-pebble conglomerate, sandstone, argillite and coal in the Vega Creek valley with the Uslika Formation. Fossils in the valley indicate an Early Cretaceous (Aptian) age (Roots, *ibid.*). Sediments on the northwest side of the Osilinka River do not resemble rocks of the Uslika Formation and may not be correlatable. Eisbacher (1974) correlated Late Cretaceous to Early Tertiary rocks of the Sustut Group within the map area (south of Thane Creek) with rocks of the Uslika Formation, but we see little resemblance and feel this correlation is invalid.

The age of the Uslika Formation can be inferred from a study of the clast composition. All clasts are locally derived, with quartzite from the Atan Group, chert from the Nina Creek Group, syenite and monzonite clasts from the Hogem intrusive complex and volcanic clasts from the Takla Group. The youngest rocks in this suite are the granitics from the Hogem intrusive complex and the Takla volcanics. Thus the conglomerate can be no older than Early Jurassic, based on the youngest ages of the Takla Group and K-Ar ages for monzonite and granodiorite reported by Garnett (1978). Younger granitic phases (Late Cretaceous) are not present. Uplift and erosion of the Atan quartzite to the west may have occurred as early as late Early Jurassic (Ferri and Melville, in preparation).

Roots (1954) describes minor occurrences of schistose and gneissic clasts. Locally, metamorphic cooling ages are as old as Middle Jurassic with a predominance of Late Cretaceous to Early Tertiary ages within the metamorphic complexes (Ferri and Melville, in preparation). All that can be confidently stated about the age of this unit is that it ranges from Early Jurassic to Early Tertiary.

SUSTUT GROUP (LATE CRETACEOUS TO EARLY TERTIARY)

Sandstone, conglomerate and siltstone assigned to the Sustut Group outcrop within fault-bounded areas on either side of the Osilinka River valley, west of Conglomerate Mountain. The finer grained rocks are grey-green to brown or red-brown, thin to thickly bedded and very friable. They commonly contain abundant coaly lenses and plant fossils dated as Late Cretaceous and Early Tertiary (Roots, 1954). Pebble conglomerate layers 1 to 2 metres thick and composed of chert, quartzite, grey and maroon argillite, grey-green basalt and tuff, vein quartz and schist clasts are associated with these lithologies.

The two bodies of Sustut Group rocks are bounded by northwest-trending strike-slip faults and it is suggested that these rocks are preserved within a negative flower structure (*see* Structure section). Sustut rocks west of the Osilinka River are strongly fractured at their contact with intensely fractured rocks of the Lay Range assemblage. They are also in contact with fractured rocks of the Uslika Formation south of Conglomerate Mountain. The northern contact of the body south of Thane Creek may rest unconformably on the Early Jurassic volcanics but such a contact was not observed.

CONGLOMERATE AND SANDSTONE ALONG VEGA CREEK (EARLY CRETACEOUS)

Grey-brown and maroon pebbly conglomerate, sandstone and argillite are exposed along Vega Creek and as a large body at its confluence with the Osilinka River. The conglomerate is composed of granite, basalt, tuff, quartzite, chert and argillite clasts. Fine to coarse-grained sandstone and siltstone layers up to 1 metre thick are found within the conglomerate and contain plant remains and very thin lenses of black coal.

Strongly sheared, black to dark grey argillite and siltstone outcrop at several localities along the lower reaches of Vega Creek. These argillites contain lenses of coal up to several centimetres thick and nodules of sandstone with abundant plant fossils. Roots (1954) collected Lower Cretaceous fossils from one such locality. Fossil collections made during this study are inconclusive and suggest an age from Late Jurassic to Late Cretaceous (E. McIver, personal communication, 1991).

These sediments do not resemble rocks of the Uslika Formation and though they look similar to those of the Sustut Group, their older age precludes this. Roots (1954) equates the conglomerate along Vega Creek with that of the Uslika Formation. If this correlation is correct these conglomerates and sandstones must represent a different facies of the Uslika Formation.

INTRUSIVE ROCKS

Intrusive rocks in the map area are subdivided into four groups: the Hogem intrusive complex; the Tenakihi body; monzonite to syenite porphyry stocks, dikes and sills within the Takla Group; and subvolcanic quartz and/or feldspar porphyry to felsite dikes and sills. All are part of the Omineca intrusive suite as defined by Roots (1954). Many of the intrusions mapped by Roots (*ibid.*) within the Lay Range assemblage are actually gabbroic bodies of probable upper mantle derivation (*i.e.* ophiolite).

HOGEM INTRUSIVE COMPLEX (LATE TRIASSIC TO CRETACEOUS)

The Hogem igneous suite consists of numerous intrusive bodies of distinct ages (Garnett, 1978). It has been suggested that the name Hogem batholith be replaced by the term Hogem intrusive complex (Nelson *et al.*, 1992, this volume). Several rock types outcrop at the edge of the complex. Field observations indicate a predominantly quartz-poor, alkali-rich suite. Rocks vary in composition between gabbro, diorite, monzonite, syenite and alkali-feldspar syenite. Gabbro and monzonite appear to be the oldest intrusive phases and are cut by stocks and dikes of syenite or alkali-feldspar syenite. Typically, an intrusive breccia is present at the contact with the Takla Group. Strong hornfelsing and granitization of the Takla Group extends several hundred metres to over a kilometre away from the contact with the intrusive rocks. The hornfelsing is accompanied by moderate to intense flattening or mylonitization of the Takla rocks indicating that ductile flow was occurring at the contact in response to emplacement of the batholith. The hornfelsing is also important economically in that it is almost always associated with copper-gold mineralization (see section on Mineralization). Both the monzonitic and syenitic phases of the Hogem intrusive complex carry copper mineralization, although it is more prevalent in the syenite end members.

The age of the Hogem rocks is not precisely known in the map area. It is post-Late Triassic based on its crosscutting relationships with the Takla Group. Potassium-argon dating by Garnett (1978) south of the Omineca River suggests an Early to Middle Jurassic age for the syenitic phases. Monzonite is related to early mafic phases of the complex and has been dated Late Triassic to Early Jurassic (Garnett, *ibid.*). Younger granitic phases are Early Cretaceous (Garnett, *ibid.*).

MONZONITE

Tan, brown and pinkish megacrystic monzodiorite, monzonite and quartz monzonite is the most abundant phase in the Hogem intrusive complex. Pinkish feldspar megacrysts up to 2 centimetres long constitute up to 30 per cent of the rock. Accessory minerals are hornblende, biotite and magnetite.

SYENITE

Pink to tan, very fine to coarse-grained syenite and quartz syenite form dikes and small stocks in the monzonite and the Takla volcanics. They are usually magnetic and contain hornblende as an accessory mineral. Syenite grades into the alkali-feldspar syenite described below. Pegmatitic phases of this lithology were observed at the contact with the Takla volcanics.

ALKALI-FELDSPAR SYENITE

Pink, fine to medium-grained alkali-feldspar syenite and alkali-feldspar quartz syenite also intrude the monzonite suite described above. These rocks contain magnetite and hornblende as accessory minerals.

MONZONITE AND SYENITE IN THE TAKLA GROUP (LATE TRIASSIC TO MIDDLE JURASSIC)

Small stocks and dikes of porphyritic monzodiorite, monzonite and syenite intrude the tuffs and agglomerates of the Takla Group close to the Hogem intrusive complex. These bodies are barely discernable at a scale of 1:50 000, but their association with copper-gold mineralization warrants their mention.

Porphyritic to crowded porphyritic syenite to monzonite outcrop at the top of Cat Mountain. These intrusions are tan to beige, with phenocrysts of plagioclase set in a very fine grained matrix of potassic feldspar and hornblende. The phenocrysts may constitute over 30 per cent of the rock. These bodies are sometimes strongly altered to chlorite, epidote and potassium feldspar in association with copper and gold mineralization. Another lenticular body of similar rocks (although lacking the alteration), up to 1 kilometre in length, was mapped southeast of Matetlo Creek. It has hornfelsed the Takla Group agglomerates around it.

Numerous dikes and small stocks of megacrystic monzonite or syenite intrude the Takla rocks throughout the area. They are grey to greenish in colour with 5 to 20 per cent plagioclase phenocrysts set in a finely crystalline groundmass of potassium(?) feldspar and hornblende. These bodies may also exhibit a crowded porphyry texture.

These rocks are assumed to be Late Triassic to Early Jurassic in age as they appear to be concentrated near the margin of the Hogem intrusive complex and are similar in composition to Hogem phases of this age.

TENAKIHI INTRUSIVE COMPLEX (LATE TRIASSIC TO EARLY JURASSIC)

A sill-like body up to 1 kilometre in thickness and traceable for over 10 kilometres is exposed at the headwaters of Tenakihi Creek. It may continue to the northwest beyond the present limit of mapping. It is composed of fine to coarse-grained diorite and monzodiorite, commonly with layered, cumulate textures. Layering is roughly parallel to bedding in the surrounding tuffs. The rocks are typically massive, and predominantly coarse grained with 30 to 70 per cent pyroxene and hornblende. Cumulate layers can be as thin as 10 centimetres or up to several metres thick. These cumulate textures were seen sporadically along the length of the body.

This body may be related to the Hogem intrusive complex and may be Early Jurassic in age. Another possibility is that the Tenakihi intrusive complex is related to the Alaskan-type ultramafic intrusions in the area, the most prominent of which is the Polaris Complex in the Lay Range. Recent geochronometry on these Alaskan-type intrusions has yielded Middle Triassic to Early Jurassic ages (G.T. Nixon, personal communication, 1991).

WASI ULTRAMAFIC COMPLEX (EARLY JURASSIC OR OLDER)

A lenticular ultramafic body some 4 kilometres long and 1 kilometre wide at its centre, is exposed within Nina Creek Group rocks along a ridge south of Wasi Lake. It is composed predominantly of dark green serpentinite and medium to coarse-grained gabbro. The serpentinite is commonly quite massive and may contain large crystals of pyroxene. The gabbro contains between 30 and 50 per cent green pyroxene. It is commonly massive and may exhibit a weak foliation and listwanite alteration. A small tan-coloured aplite dike cuts this body along the ridge crest.

Examination of the northeast contact of the ultramafite indicates that it is intrusive. Ultramafic and gabbroic bodies of Alaskan affinities intrude the time-equivalent Lay Range assemblage north of the map area and recent geochronometry suggests a Middle Triassic to Early Jurassic age (G.T. Nixon, personal communication, 1991).

TERTIARY(?) INTRUSIONS

Tan, beige, pink or white hypabyssal quartz feldspar porphyry (dacite) sills intrude schists of the Swannell Formation near Beveley Mountain and rarely rocks of the Takla Group. Numerous bodies in the Beveley Mountain area vary from a few centimetres to over 100 metres in thickness. Quartz and feldspar phenocrysts constitute up to 5 per cent of the rock. Biotite or hornblende are accessory minerals. A single occurrence of these felsites was seen within the Takla Group in the northwest corner of the map area. A small dacitic stock is described by Roots (1954) within Swannell schists southwest of Beveley Mountain.

These rocks appear quite fresh and are assumed to be younger than other lithologies in the area. They are very similar to hypabyssal intrusions described by Ferri and Melville (1988) in the Manson Creek area which have been dated as Early Tertiary (Ferri and Melville, in preparation).

STRUCTURE

The character of deformation within the map area is quite diverse and attests to the disparate tectonic histories of the different terranes. Deformation is strongest, and most complex, within the Cassiar Terrane and least developed in rocks of the Quesnel Terrane. Some elements of folding and faulting are common to more than one terrane and must reflect deformation during and after accretion

The most prominent structural features are northwest-trending faults. They are well developed in and around the Vega Creek valley and separate or cut rocks of the Takla Group and Lay Range assemblage. Large areas of brittly deformed and altered rock are also seen along Thane Creek and the gorge at the big bend in Tenakihi Creek. Evidence from several localities indicates strike-slip and dip-slip movement. Furthermore, rocks between the fault zones are younger than the surrounding rocks, suggesting preservation within graben-like structures. These faults are believed to be part of a negative flower structure and produced by the northward translation on the Manson fault zone (Woodcock and Fischer, 1986; Figure 1-11-4). This northward shift and concurrent splaying in the fault zone allows the blocks within the splayed zone to drop as the strata on either side of the main fault move past each other. This mechanism reconciles strike-slip and dip-slip motion within a single structural system. The southern extent of these faults coincides with the extrapolated northwestern extension of the Manson fault zone and related faults along the Discovery Creek valley. The number and spacing of the faults decreases to the northwest, reflecting their more northwestward trend and loss of the dip-slip component.

The Uslika Formation is bounded by two of these faults and the position of these younger rocks against older rocks of the Lay Range suggests dip-slip movement. They dip steeply towards each other and contain both brittle and ductile deformational features. The north bounding fault is well exposed and is expressed by a zone of deformed Uslika and Lay Range lithologies several metres thick. Slickensides on this fault zone show both subhorizontal and moderately south to southwest-plunging orientations which together indicate left-lateral motion for the strike-slip component. This is in complete discord with strike-slip motion on the Manson fault zone, and other major fault zones in the region, which is right-lateral (Ferri and Melville, in preparation; Gabrielse, 1985). Alternatively, if strike-slip motion is right-lateral along this fault zone, the southwest-plunging slickensides suggest up-dip movement. Most of the motion on the bounding faults of the Uslika Formation must be down-dip as they place younger against older rocks. Any up-dip motion may be quite late and minor in magnitude.

The age of these structures is difficult to deduce. Rocks of the Uslika Formation, Sustut Group and conglomerates along Vega Creek are found within some of the graben structures. There is no evidence for syntectonic deposition of any of these clastic sequences. If there was syntectonic deposition, then fault movement has occurred from Early Jurassic to Early Tertiary time. Alternatively, if the clastic sequences are only preserved within younger graben structures, then movement is only as old as the youngest clastic package, which in this case would be Early Tertiary (Sustut Group). Evidence elsewhere in the northern Canadian Cordillera suggests regional strike-slip motion in Cretaceous and Early Tertiary time (Gabrielse, 1985).

Several other prominent faults transect the map area. A major northwest-trending southwest-side-down normal fault (Camp fault) drops Early Paleozoic carbonate stratigraphy against higher grade metamorphic rocks of the Swannell Formation in the Beveley Mountain area. It may continue down the Tenakihi Creek valley, separating Lay Range from Swannell rocks. Several other parallel structures cut Nina Creek and Lower Paleozoic stratigraphy in the Wasi Creek area.

The Uslika Lake and Wasi Lake valleys form prominent lineaments and suggest the presence of northeast-trending normal(?) faults with only minor displacement. These faults die out away from the strike-slip fault structures, suggesting a genetic link.

Cryptic and visible thrust faults cut rocks of the Nina Creek Group. Northeast-verging thrust faults are seen southeast of Wasi Lake where sediments of the Mount Howell Formation are placed on top of volcanics of the Pillow Ridge Formation. The Nina Creek Group sits structurally above rocks of the Cassiar Terrane, carried on a cryptic, northeast-verging, layer-parallel thrust fault (Ferri and Melville, in preparation). This thrust separates rocks of the Slide Mountain Terrane from those of the Cassiar Terrane in the map area. A similar thrust separates the two formations of the Nina Creek Group (Ferri and Melville, *ibid.*).

The structurally and stratigraphically lower parts of the Cassiar Terrane are polydeformed and affected by a prograde metamorphic event which reaches upper greenschist grade in the map area. At least three phases of deformation affect the metamorphosed rocks. An early synmetamorphic folding event (D_1) produced isoclinal folds with bedding transposed parallel to foliation. A second period of folding (D_2) also produced isoclinal folds with crenulated S_1 schistosity in their hinges. This folding was rarely seen and may in fact be related to D_1 deformation and produced by local instabilities in the flow regime during D_1 deformation, leading to the refolding of S_1 schistosity. An upright series of open folds and associated short-wavelength crenulations is locally produced by the third phase of deformation (D_3). These may be related to the large northwest-trending antiform in the Swannell Formation north of Beveley Mountain. The vergence of these structures is not known. Bedding and S_1 schistosity are overturned to the southwest on the north side of the Tutizika River and north of Jim May Creek, suggesting southwest-verging D_1 or D_2 structures. This is only seen locally and typically structures verge to the northeast as seen in the Germansen Landing and Manson Creek areas (Ferri and Melville, 1988, 1989, 1990a). Southwesterly directed structures are consistent with similarly oriented structures mapped by Bellefontaine (1990) in the Ingenika Range north of the study area.

The relationship of these structures to higher structures within the Cassiar and other terranes is not known. Large-scale northeast-verging thrust faults in the Nina Creek Group and other packages may be related to D_1 and D_2 deformation as suggested by Ferri and Melville (in preparation).

The Slide Mountain Terrane is characterized by kilometre-scale open folds that affect the entire package. Macroscopic, open to tight chevron folds can be seen within the lower argillites of this package and are associated with an axial planar, penetrative cleavage.

Rocks of the Lay Range assemblage are steeply dipping and, based on top reversals, tightly folded and generally overturned to the southwest. The monotonous nature of this sequence does not allow the delineation of any large-scale structures and only rarely were outcrop-size folds observed. A penetrative cleavage is present in the more argillaceous members but only rarely developed in the tuffs. Commonly, large clasts within the tuffs are flattened parallel to the steeply dipping bedding, suggesting tight to isoclinal folding. Faults of unknown origin appear to separate the various main lithologies of the Lay Range. Those that separate the mafic and ultramafic rocks north of Vega Creek may be part of the strike-slip fault system, although this is not certain on the basis of currently available data.

Rocks of the Quesnel Terrane (Takla Group) west of the graben structure, form a moderately southwest-dipping homoclinal succession interrupted by local upright folds.

METAMORPHISM

Metamorphism is most intense in Cassiar rocks where garnet-grade assemblages are found within the Swannell Formation. The grade drops off to lower greenschist within younger stratigraphy where biotite and chlorite isograds can be discerned locally. Textural relationships between large porphyroblasts and the other fabric elements indicate that their formation coincided roughly with D_1 deformation. These relationships are similar to those described by Ferri and Melville (1990a) and by Parrish (1976) and Bellefontaine (1990) to the north. Garnets and biotite porphyroblasts are retrogressed to chlorite, muscovite and quartz in various localities, suggesting a late retrogression event of uneven distribution.

This prograde metamorphic event has been dated as Middle Jurassic by Ferri and Melville (in preparation) with the later retrogression possibly related to Tertiary uplift, as suggested by the prevalence of Early Tertiary ages in these rocks to the south (Gabrielse, 1975; Ferri and Melville, *ibid.*).

Metamorphic grade of rocks of the Slide Mountain and Lay Range terranes is lower to subgreenschist and the Takla Group has been metamorphosed to prehnite-pumpellyite grade.

ECONOMIC GEOLOGY

Mineral prospects are numerous and of various types within the map area, including porphyry copper-gold and carbonate-hosted lead-zinc showings, shear-controlled veining, placer deposits and minor coal occurrences. The following discussion describes the characteristics of each type of occurrence. For a brief description of individual prospects refer to Table 1-11-1; the locations of the showings are plotted on Figure 1-11-3.

The Takla Group hosts the majority of the known mineral occurrences; abundant small copper showings are found along the length of the Hogem-Takla contact. Mineralization in the Takla Group is related to syenite and monzonite intrusions, probably related to the Hogem intrusive complex, and shear zones, possibly related to the Manson fault zone mapped south of this area (Ferri and Melville, 1989).

The Upper Proterozoic and Lower to Middle Paleozoic carbonates in the northwest part of the map area also host numerous base and precious metal prospects.

Lay Range volcanics and sediments host two newly discovered shear-related copper-gold showings and maroon basalt flows of the Takla Group (Chuchi Lake Formation?) host copper mineralization in the northwest part of the map area.

Thin coal seams are present in the Upper Cretaceous Sustut Group. Placer gold is known on Jim May and Vega Creeks (Roots, 1954).

PORPHYRY COPPER-GOLD PROSPECTS

Porphyry copper-gold prospects are exemplified by the Cat Mountain and Vega showings. Disseminated and fracture-filling chalcopyrite with secondary malachite, azurite and chalcocite occur within the intrusive rocks and the coarse-fragmental basaltic augite porphyry flows, finer pyroclastics and volcanic sediments of the Takla Group. Propylitic and potassic alteration characterize mineralized zones.

Syenomonzonite porphyry and hornblende diorite bodies on the Cat property are believed to be satellites of the Hogem intrusive complex. The porphyries are cut by numerous faults. Some of these faults appear to postdate alteration and mineralization (Anomaly fault) while others are mineralized. This suggests a complex structural history which may involve reactivation of early, and possibly, synintrusive structures.

Massive, gossanous magnetite-quartz veins and boxwork host copper and coarse visible gold mineralization at the summit of Cat Mountain (BET claims). Magnetite-rich zones, like the MBX zone at Mount Milligan, often occur in alkaline porphyry systems. Similar magnetite-quartz veins were found in other locations close to the Takla-Hogem contact north of Cat Mountain.

MINERALIZATION RELATED TO THE HOGEM CONTACT

Copper mineralization (chalcopyrite, malachite, azurite, bornite, chalcocite) occurs along the Hogem-Takla contact. Copper is associated with ankerite veining, as disseminated blebs of chalcopyrite along fracture surfaces, disseminated throughout the host and in magnetite±specularite veins containing massive to disseminated chalcopyrite±bornite. Mineralization occurs in zones from a few centimetres to several metres wide cutting augite porphyry flows and tuffs, the Hogem monzonites and other peripheral phases of the intrusive complex. Prospects around the fringes of the Hogem intrusive complex are associated with swarms of syenitic dikes, potassium feldspar alteration and metasomatization of the Takla Group and the intrusive complex suggesting the roots of a porphyry system (Garnett, 1978).

CARBONATE-HOSTED MINERALIZATION

Two types of carbonate-hosted mineralization occur in the map area; disseminated and replacement lead-zinc mineralization of possible Mississippi Valley type and lead-zinc veins.

Mineralization in the Otter Lakes limestone occurs as replacement of dolomite or as open-space fillings. Mineralization appears stratabound and is found in pods or blebs. The mineralogy consists of fine-grained galena (which may be argentiferous), sphalerite (yellow-brown to red-brown) and pyrite. Similar mineralization is found along this horizon southeast of the map area (Ferri and Melville, 1990a).

The Beveley prospect, on the south slope of Beveley Mountain, is a series of occurrences of disseminated and massive galena, sphalerite, acanthite, tetrahedrite and barite which appear to have been emplaced in veins cutting the carbonates of the Middle Ordovician to Early Devonian Echo Lake Group. Mineral inventory calculations indicate approximately 100 000 tonnes grading 36.13 grams per tonne silver, 1.42 per cent lead and 2.24 per cent zinc (Coveney, 1981).

Southeast of the Beveley prospect, across the Osilinka River, lead-zinc-silver-barite veins carbonate rocks at the Carie showing. This occurrence was not visited, but it appears similar to the Beveley (Fahrni, 1979).

The Quarry showing (No.10), a new mineral prospect found in a limestone quarry at the base of Beveley Mountain, consists of several mineralized quartz veins cutting a dolomitized section of the Espee Formation. Quartz veins up to 20 centimetres wide appear to occur in a conjugate system with mineralization present throughout the veins but strongest at vein intersections. Coarsely crystalline minerals include galena, sphalerite, cerussite, chalcopyrite, boulangerite, stibnite and tetrahedrite. Two grab samples returned analyses of 890 ppb and 385 ppb gold.

SHEAR-CONTROLLED VEINING

Grits, impure quartzites and quartz-feldspar-garnet schists of the Ingenika Group at the top of Beveley Mountain host the Gael showing, a shear-controlled gold-silver-copper vein. The mineralized zone is clearly visible due to the yellow scorodite staining on the rocks. The hostrocks are strongly brecciated and silicified within the mineralized zone.

The Mississippian to Permian Lay Range assemblage is host to two copper-gold occurrences. Malachite staining on fracture surfaces was found in sheared, epidote-altered basalt flows on a ridge-top west of the mouth of Tenakihi Creek. A gold analysis of 1300 ppb was obtained from a grab sample. Fine-grained sediments northeast of Vega Creek are cut by quartz-ankerite veins carrying malachite.

Mercury mineralization (cinnabar) is reported at several locations within the Takla Group (Roots, 1954), always in sheared zones associated with ankerite veining and alteration. These strike-slip shear zones are most likely a northern extension of the Manson fault zone mapped to the southeast (Ferri and Melville, 1989).

The HaHa Creek showing consists of free gold in small quartz veins and copper mineralization in shears within the Hogem intrusives (Roots, 1954).

The Pluto showing consists of massive arsenopyrite and pyrite within strongly sheared Takla Group rocks along a tributary of Thane Creek. This occurrence has been known since the 1940s (Roots, 1954) and contains significant amounts of gold.

Minor Coal Occurrences

Late Cretaceous Sustut Group sandstones and conglomerates host discontinuous, low-grade coal seams up to 45 centimetres thick (Roots, 1954). Early Cretaceous sandstones, siltstones and argillites exposed along Vega Creek contain coaly lenses 5 to 10 centimetres thick.

CONCLUSIONS

- The map area covers parts of the Cassiar, Slide Mountain, Harper Ranch and Quesnel terranes.
- The Lay Range assemblage has characteristics which are consistent with an arc or back-arc setting and has similarities with the Nina Creek Group.
- The Takla Group comprises both Upper Triassic and Lower Jurassic units which are equivalent to recognized units farther south.
- The area is transected by a major northwest-trending system of strike-slip faults and associated graben structures.
- Mineral occurrences are diverse and abundant within the map area. Most are porphyry copper-gold prospects within the Takla Group and at the Hogem-Takla contact. Significant carbonate-hosted lead-zinc mineralization is found in Paleozoic rocks.

ACKNOWLEDGMENTS

The authors would like to thank Dan Meldrum and Marcus Willson for cheerful (and sometimes hilarious), enthusiastic and highly competent assistance in the field. Special thanks are given to Bud and Esther of the Uslika Road House for making our stay more hospitable. We also thank Northern Mountain Helicopters, particularly Keith Buchanan and Blair Savage, for excellent service. We would also like to acknowledge the input from Bert Struik, Jim Monger and Kim Bellefontaine for some of the ideas in this paper and acknowledge Kim for her much needed assistance during the final preparation of the manuscript. The manuscript also benefited from careful review by John Newell.

REFERENCES

Armstrong, J.E. (1949): Fort St. James Map Area, Cassiar and Coast Districts, British Columbia; *Geological Survey of Canada*, Memoir 252, 210 pages.

Bellefontaine, K. (1990): The Tectonic Evolution of the Ingenika Group and its Implications for the Boundary Between the Omineca and Intermontane Belts, North-central British Columbia; unpublished M.Sc. thesis, *McGill University*, 94 pages.

Coveney, C.J. (1981): Report on the Beveley Property; *B.C. Ministry of Energy, Mines and Petroleum Resources*, Assessment Report 8734.

Eisbacher, G.H. (1974): Sedimentary History and Tectonic Evolution of the Sustut and Sifton Basins, North-central British Columbia; *Geological Survey of Canada*, Paper 73-31, 57 pages.

Fahrni, K.C. (1979): Report on the Wasi Project; *B.C. Ministry of Energy, Mines and Petroleum Resources*, Assessment Report 7611.

Ferri, F. and Melville, D.M. (1988): Manson Creek Mapping Project (93N/9); *in* Geological Fieldwork 1987, *B.C. Ministry of Energy, Mines and Petroleum Resources*, Paper 1988-1, pages 169-180.

Ferri, F. and Melville, D.M. (1989): Geology of the Germansen Landing Area, British Columbia (93N/10, 15); *in* Geological Fieldwork 1988, *B.C. Ministry of Energy, Mines and Petroleum Resources*, Paper 1989-1, pages 209-220.

Ferri, F. and Melville, D.M. (1990a): Geology Between Nina Lake and Osilinka River, North-central British Columbia (93N/15, North Half and 94C/2, South Half); *in* Geological Fieldwork 1989, *B.C. Ministry of Energy, Mines and Petroleum Resources*, Paper 1990-1, pages 101-114.

Ferri, F. and Melville, D.M. (1990b): Geology Between Nina Lake and Osilinka River, British Columbia, 93N/15 (North Half) and 94C/2 (South Half); *B.C. Ministry of Energy, Mines and Petroleum Resources*, Open File 1990-17.

Ferri, F. and Melville, D.M. (in preparation): Geology of the Germansen Landing - Manson Creek Area; *B.C. Ministry of Energy, Mines and Petroleum Resources*, Bulletin.

Ferri, F., Melville, D.M., Malensek, G.A. and Swift, N.R. (1988): Geology of the Manson Lakes Map Sheet, 93N/9; *B.C. Ministry of Energy, Mines and Petroleum Resources*, Open File 1988-12.

Ferri, F., Melville, D.M. and Arksey, R.L. (1989): Geology of the Germansen Landing Area, 93N/10 and 93N/15; *B.C. Ministry of Energy, Mines and Petroleum Resources,* Open File 1989-12.

Garnett, J.A. (1978): Geology and Mineral Occurrences of the Southern Hogem Batholith; *B.C. Ministry of Mines and Petroleum Resources,* Bulletin 70, 75 pages.

Gabrielse, H. (1963): McDame Map-area, Cassiar District, British Columbia; *Geological Survey of Canada,* Memoir 319, 138 pages.

Gabrielse, H. (1975): Geology of Fort Grahame E1/2 Map-area, British Columbia; *Geological Survey of Canada,* Paper 75-33, 28 pages.

Gabrielse, H. (1985): Major Dextral Transcurrent Displacements along the Northern Rocky Mountain Trench and Related Lineaments in North-central British Columbia; *Geological Society of America,* Bulletin, Volume 96, pages 1-14.

Mansy, J.L. and Gabrielse, H. (1978): Stratigraphy, Terminology and Correlation of Upper Proterozoic Rocks in Omineca and Cassiar Mountains, North-central British Columbia; *Geological Survey of Canada,* Paper 77-19, 17 pages.

Meade, H.D. (1975): Geology of the Germansen Lake Area; *B.C. Ministry of Energy, Mines and Petroleum Resources,* Preliminary Map 19.

Monger, J.W.H. (1973): Upper Paleozoic Rocks of the Western Canadian Cordilleran; *Geological Survey of Canada,* Paper 73-1 Part A, pages 27-28.

Monger, J.W.H. (1977): Upper Paleozoic Rocks of the Western Canadian Cordillera and their Bearing on Cordilleran Evolution; *Canadian Journal of Earth Sciences,* Volume 14, pages 1832-1859.

Monger, J.W.H. and Paterson, I.A. (1974): Upper Paleozoic and Lower Mesozoic Rocks of the Omineca Mountains; *in* Report of Activities, *Geological Survey of Canada,* Paper 74-1, Part A, pages 19-20.

Nelson, J., Bellefontaine, K., Green, K. and MacLean, M. (1991): Regional Geological Mapping near the Mount Milligan Copper-Gold Deposit (93N/1 93K/16), *in* Geological Fieldwork 1990, *B.C. Ministry of Energy, Mines and Petroleum Resources,* Paper 1991-1, pages 89-110.

Nelson, J., Bellefontaine, K., Rees, C. and MacLean, M. (1992): Regional Geological Mapping in the Nation Lakes Area, 93N/2 East Half and 93N/7 East Half; *in* Geological Fieldwork 1991, Grant, B. and Newell, J.M., Editors, *Ministry of Energy, Mines and Petroleum Resources,* Paper 1992-1.

Parrish, R.R. (1976): Structure, Metamorphism and Geochronology of the Northern Wolverine Complex near Chase Mountain, Aiken Lake Map-area, British Columbia; unpublished M.Sc. thesis, *The University of British Columbia,* 89 pages.

Roots, E.F. (1954): Geology and Mineral Deposits of Aiken Lake Map-area, British Columbia; *Geological Survey of Canada,* Memoir 274, 246 pages.

Ross, C.A. and Monger, J.W.H. (1978): Carboniferous and Permian Fusulinaceans from the Omineca Mountains, British Columbia; *Geological Survey of Canada,* Bulletin 267, pages 43-64.

Wheeler, J.O. and McFeely, P. (1987): Tectonic Assemblage Map of the Canadian Cordillera; *Geological Survey of Canada,* Open File 1565.

Woodcock, N.H. and Fischer, M. (1986): Strike-slip Duplexes; *Journal of Structural Geology,* Volume 8, Number 7, pages 725-735.

NOTES

STRUCTURES ALONG FINLAY–INGENIKA FAULT, McCONNELL CREEK AREA, NORTH-CENTRAL BRITISH COLUMBIA (94C/5; 94D/8, 9)

By G. Zhang and A. Hynes
McGill University

KEYWORDS: Regional geology, Takla Group, Johanson Lake, stratigraphy, Goldway Peak, Osilinka Ranges, Kliyul Creek, Dortatelle Creek, Wrede Range, Aiken Lake, Sustut Lake, Hogem Ranges, transcurrent faulting, stretching lineation.

INTRODUCTION

The study area is located in the vicinity of Johanson Lake, some 350 kilometres north-northwest of Prince George, bounded to the northeast by the north-northwest-trending Lay fault and to the southwest by Willow Creek. The north-northwest-trending Finlay-Ingenika fault, one of the very prominent dextral strike-slip fault systems of north-central British Columbia (Gabrielse, 1985), passes through the western half of the study area.

The main aims of the project are to examine the structures on both sides of the Finlay-Ingenika fault, to provide geological evidence for the dextral transcurrent displacement and to study local deformation associated with it. Geological mapping in parts of map sheets 94C/5 and 94D/8, 9 at a scale of 1:5000, was conducted in 1990 and 1991. Preliminary results from the fieldwork of 1990 were reported last year (Zhang and Hynes, 1991). This report provides considerably more data on the nature of the deformation, and extends the mapped region southeast towards Aiken Lake and to the Hogem Ranges west of the Finlay-Ingenika fault.

Throughout the region, exposure on prominent ridges is excellent. Although primary access is possible via the gravel road from either Mackenzie or Fort St. James to Johanson Lake and the Cheni mine, the nature of the terrain necessitates use of a helicopter for camp moves.

REGIONAL GEOLOGY

The map area lies within the Intermontane Belt, one of the five morphogeological belts of the Canadian Cordillera (Wheeler and McFeely, 1987), and straddles the Quesnellia and Stikinia tectonostratigraphic terranes (Monger, 1984). North and south of the study area, Stikinia rocks are separated from those of Quesnellia to the east by the Cache Creek Terrane, a subduction-related assemblage, and bounded to the east by the Slide Mountain Terrane, a deep-water oceanic assemblage. These terranes were amalgamated by latest Triassic to earliest Jurassic time, forming a composite terrane, "Terrane I", which accreted to the ancient margin of North America in Jurassic time (Monger, 1984). Dextral strike-slip faulting took place extensively along the eastern margin of Terrane I, and possibly part of the Omineca metamorphic belt, during the late Cretaceous (Gabrielse, 1985). The Finlay-Ingenika fault, which lies between the Quesnellia and Stikinia terranes in the study area, is one of the dextral strike-slip faults on which the transcurrent motion occurred.

Quesnellia and Stikinia terranes in the study area are characterized by volcanic, volcaniclastic and sedimentary rocks of the Upper Triassic Takla Group. West of the Finlay-Ingenika fault the Takla Group was subdivided into three formations during 1:250 000 mapping of the McConnell Creek map area (Lord, 1948; Church, 1974, 1975; Richards, 1976a, b; Monger, 1977; Monger and Church, 1977). The lower Dewar Formation is dominated by volcanic sandstone, siltstone and argillite, and is overlain by a middle Savage Mountain Formation consisting of submarine, massive volcanic breccia and pillow lava with minor volcanic siltstone at the top. The upper Moose Valley Formation is predominantly reddish marine and nonmarine volcaniclastic rocks (Monger, 1977; Monger and Church, 1977). East of the Finlay-Ingenika fault the Takla Group remains undivided (Monger, 1977). It consists mainly of greenish grey, dark and pale grey volcanic, volcaniclastic and sedimentary rocks. No conclusive stratigraphic correlations have been made between the Takla Group rocks on either side of the fault (Minehan, 1989a, b). The Takla Group rocks east of the fault are extensively intruded by multiphase, early Jurassic to Cretaceous dioritic rocks (Woodsworth, 1976).

STRATIGRAPHY OF THE TAKLA GROUP EAST OF FINLAY–INGENIKA FAULT

Takla Group rocks east of the Finlay-Ingenika fault are predominantly volcaniclastic. They include some porphyritic rocks that are possibly volcanic flows and feeders, and minor sedimentary rocks. Stratigraphic successions and rock assemblages vary greatly from one locality to another. The stratigraphy and petrology have therefore been described separately for three different regions of the study area: the northwest (the Wrede Range), southwest (west of the Dortatelle fault) and southeast (between the Dortatelle fault and Kliyul Creek) (Zhang and Hynes, 1991, Figure 1-12-2).

In the southeastern region, a stratigraphic success on about 1500 metres thick along the east-trending ridges west of Aiken Lake (Figure 1-12-1) is lithologically very similar to that observed on the ridges between the Dortatelle fault (Monger, 1977) and Kliyul Creek (Zhang and Hynes, 1991; Figure 1-12-1). A lowest Unit 1 is dominated by grey volcanic sandstone. Most of this unit is covered by vegeta-

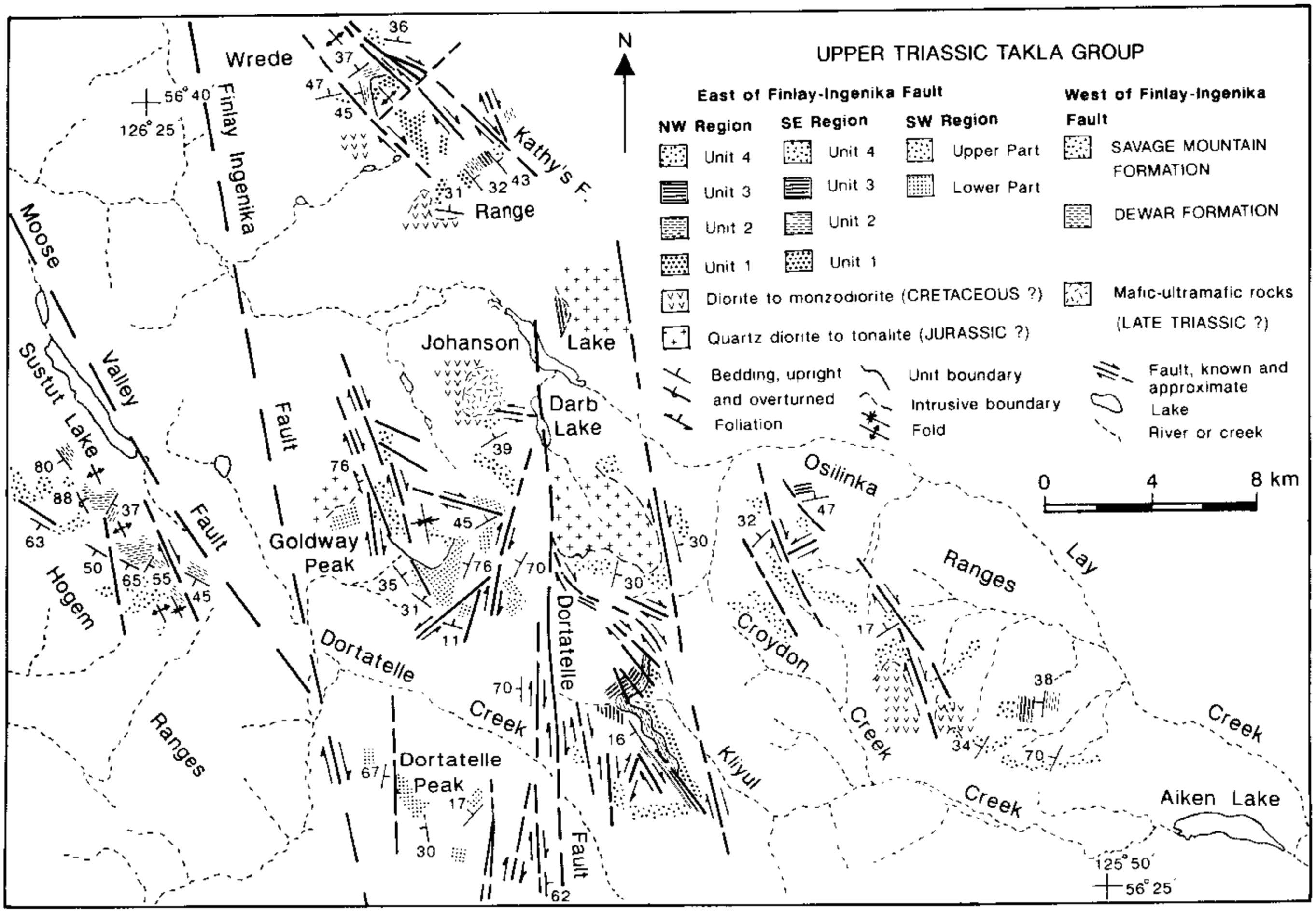

Figure 1-12-1. Generalized geology of the Johanson Lake area.

tion but a minimum thickness of 400 metres can be estimated west of Kliyul Creek. The top of this unit displays abundant recessive patches of carbonate. Unit 2 is up to 170 metres thick west of Kliyul Creek and attains a thickness of about 430 metres west of Aiken Lake. It consists of reddish weathering, black argillite with siltstone laminae and 2 to 10-centimetre layers or lenses of dark grey or black limestone. This unit also contains minor interbedded, grey volcanic sandstone and siltstone, ranging in thickness from 30 centimetres to several metres. Unit 3 is well exposed on the ridges west of both Kliyul Creek and Aiken Lake. The lower part is dominated by greenish grey volcanic siltstone which contains abundant fragments of dark grey or purplish, well-bedded limestone, ranging from several centimetres to several metres in diameter. Small-scale, slumping folds, generally several tens of centimetres in wavelength, are common in the fragments of the well-bedded limestone west of the Kliyul Creek, but not observed in those west of Aiken Lake. Fossils of brachiopods, bivalves and possibly some ammonites were found in the carbonate clasts west of Aiken Lake. The upper part is greenish grey or pale grey, medium-layered (10 to 20 cm) volcanic sandstone interbedded with dark grey or black, thin-layered limestone or black, dark grey to grey argillite (west of Aiken Lake). The thickness of this unit is up to 440 metres west of Kliyul Creek and 400 metres west of Aiken Lake. These limestone-rich beds are very widespread and useful marker horizons in the region. Unit 4 consists mainly of greenish grey, massive volcanic breccia and sandstone with minor clinopyroxene and clinopyroxene-plagioclase porphyries and is well exposed on the ridges east of the Dortatelle fault and northeast of Croydon Creek. The greenish grey breccias are compositionally heterogeneous and dominated by fragments of clinopyroxene and clinopyroxene-plagioclase porphyries. The fragments are angular to subrounded, commonly sitting in a porphyritic matrix with the same composition as the fragments, and average less than 20 centimetres in diameter. The breccias are usually poorly bedded and poorly sorted. The porphyritic rocks contain phenocrysts of either euhedral clinopyroxene or both euhedral clinopyroxene and anhedral plagioclase, commonly less than 5 millimetres in diameter but locally as much as 1 centimetre. The porphyritic rocks are generally several tens of centimetres to several metres thick and interbedded with the volcanic breccias, but sometimes occur as feeders where they cut the laminations of the volcaniclastic rocks, for example, on the ridges west of Aiken Lake. Rocks of this unit are very resistant and commonly cliff forming.

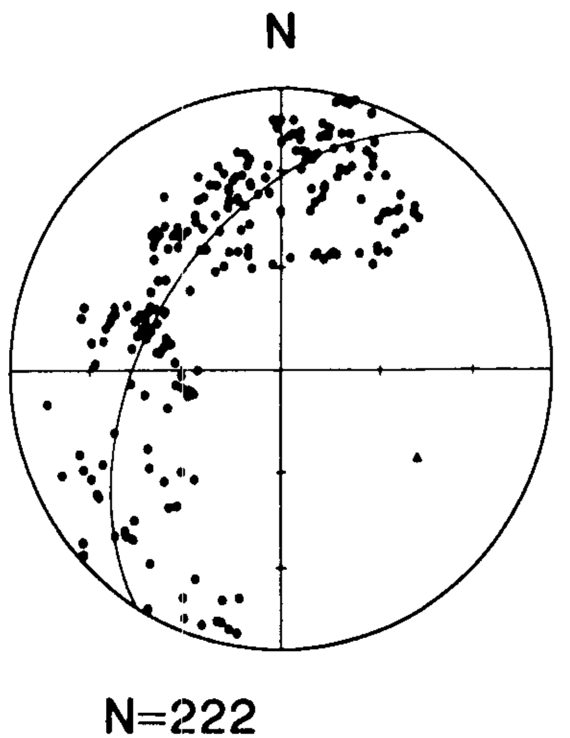

Figure 1-12-2. Stereonet plot of bedding planes from the Hogem Ranges. Solid circles: poles to bedding planes; open triangle: minimum eigenvector; great circle: plane normal to the eigenvector; N: number of measurements. Eigenvectors calculated using methods of Mardia (1972).

TAKLA GROUP WEST OF FINLAY-INGENIKA FAULT

Rocks of the Takla Group west of the Finlay-Ingenika fault are exposed in the Hogem Ranges (Figure 1-12-1) and are divided into two formations in the study area: Dewar and Savage Mountain (Richards, 1976a; Monger, 1977; Monger and Church, 1977).

The Dewar Formation is well exposed along the northern slopes of the Hogem Ranges. The lower part of the formation is dominated by reddish weathering, dark grey to black, locally graphitic and pyritic argillite with lenses of dark grey marly limestone. The upper part is mainly black argillite interbedded with pale grey volcanic sandstone and siltstone, with minor breccia containing fragments of argillite and volcanic sandstone. Beds ranging in thickness from laminae to 70 centimetres are common. The base of this formation is not exposed but a minimum thickness of 500 metres can be estimated.

The Savage Mountain Formation is characterized by massive, dark grey volcanic breccia with minor volcanic sandstone and siltstone. The fragments in the breccias are angular to subrounded and range in diameter from several centimetres to 40 centimetres. They consist of dark grey, reddish grey and dark purple clinopyroxene and clinopyroxene-plagioclase porphyries. The matrix of the breccias is predominantly clinopyroxene or clinopyroxene-plagioclase porphyritic. This unit contains locally conspicuous, coarse-grained, "bladed" feldspar porphyry. At the base of the formation one horizon contains clasts of purplish grey limestone and argillite with brachiopod and bivalve fossils. Rocks of this formation are very resistant and form high peaks in the area.

INTRUSIVE ROCKS

The Takla Group rocks east of the Finlay-Ingenika fault contain abundant intrusions associated with the Alaskan-type Johanson Lake mafic-ultramafic complex (Nixon and Hammack, 1990), and many dioritic to monzodioritic bodies occur north and south of Johanson Lake and north of Kliyul Creek. There are also many intermediate to felsic dikes and sills, typically less than 3 metres thick. These intermediate to felsic rocks are probably related to the Hogem batholith and early Jurassic to Cretaceous in age (Lord, 1948; Richards, 1976a; Woodsworth, 1976).

DEFORMATION

Rocks in the study area experienced deformation associated predominantly with dextral, transpressive displacement along the Finlay-Ingenika fault. Steeply dipping or vertical strike-slip faults (Figure 1-12-1) cut the rocks into a number of fault-bounded, weakly deformed blocks, in which cleavages and small-scale shear zones are the only visible structures. These characteristics are typical of continental crustal deformation associated with large-scale transcurrent faulting (*e.g.*, Nelson and Jones, 1986; Geissmar *et al.*, 1989; Ron *et al.*, 1986, 1990). In addition, there are some large-scale, open to medium folds with axes trending northwest to north-northwest (Figure 1-12-1).

FOLDS

Four large-scale folds have been recognized. The Wrede Range anticline and Goldway Peak syncline occur in the Wrede Range and Goldway Peak regions, respectively (Figure 1-12-1) and have been described previously (Zhang and Hynes, 1991). The Sustut Lake anticline and syncline are exposed in the Hogem Ranges area, immediately south of Sustut Lake (Figure 1-12-1).

The Sustut Lake syncline, which lies to the northeast of the anticline, involved only the black argillite and grey volcanic sandstone and siltstone of the Dewar Formation. Its northeastern limb is truncated by a north-northwest-trending, dextral strike-slip fault. The Sustut Lake anticline has the black argillite and grey volcanic sandstone and siltstone of the Dewar Formation in its core and dark grey volcanic breccia of the Savage Mountain Formation on both limbs. The southwestern limb dips steeply southwest and is locally vertical, or even overturned (Figure 1-12-1). Secondary, outcrop-scale folds are also developed. They are either symmetrical or asymmetrical in cross-section and very common in the well-bedded sedimentary rocks of the Dewar Formation (Plate 1-12-1d). Poles to bedding planes in the region fall on a great circle (Figure 1-12-2) and delineate a cylindrical fold axis trending at 122° with a plunge of 41°. The age of formation of the folds is unknown.

They were truncated by the faults and may therefore have developed during the early stages of the dextral transpression (*cf.* Wilcox *et al.*, 1973; Sylvester, 1988).

FAULTS

Subvertical or vertical strike-slip faults are the most widespread structural features in the study area. They are abundant along and near the Finlay-Ingenika fault, and become fewer and shorter away from it. On the ridges immediately west of Aiken Lake, for example (Figure 1-12-1), they are rarely seen. This spatial relationship of the strike-slip faults to the Finlay-Ingenika fault suggests that deformation in the study area was associated closely with the transcurrent motion on the Finlay-Ingenika fault and was largely restricted to a narrow belt, about 30 kilometres wide, adjacent to the major fault (Figure 1-12-1).

Based on the attitudes and slip senses, the faults were divided into four groups: dextral strike-slip faults trending northwest, north-northwest and north-northeast, and sinistral strike-slip faults trending east-northeast. All the faults can be readily interpreted as a resulting from dextral motion on the Finlay-Ingenika fault (Zhang and Hynes, 1991). The attitudes and slip senses of north-northeast and east-northeast-trending fault sets are consistent with their formation as Riedel (R) and conjugate Riedel (R′) shears, respectively, related to the main motion on the Finlay-Ingenika fault (*cf.* Tchalenko, 1970; Keller *et al.*, 1982; Sylvester, 1988). The northwest-trending faults generally display two stages of displacement. The earlier is dip-slip with a thrust sense, and the later is horizontal, dextral. The thrusts are thought to have developed in association with the initiation of dextral displacement on the Finlay-Ingenika fault (*cf.* Sylvester, 1988), with the dextral, strike-slip motion superimposed once the fault was fully established. Faults in the north-northwest-trending group are parallel to, and have the same slip senses as, the Finlay-Ingenika fault. They are inferred to have formed as secondary shears of the Finlay-Ingenika fault. At several localities, for example south of Darb Lake and north of Dortatelle Creek, dioritic dikes are incorporated in mylonitic zones associated with the faults, indicating that fault motions occurred after emplacement of the extensive dioritic plutons in the study area.

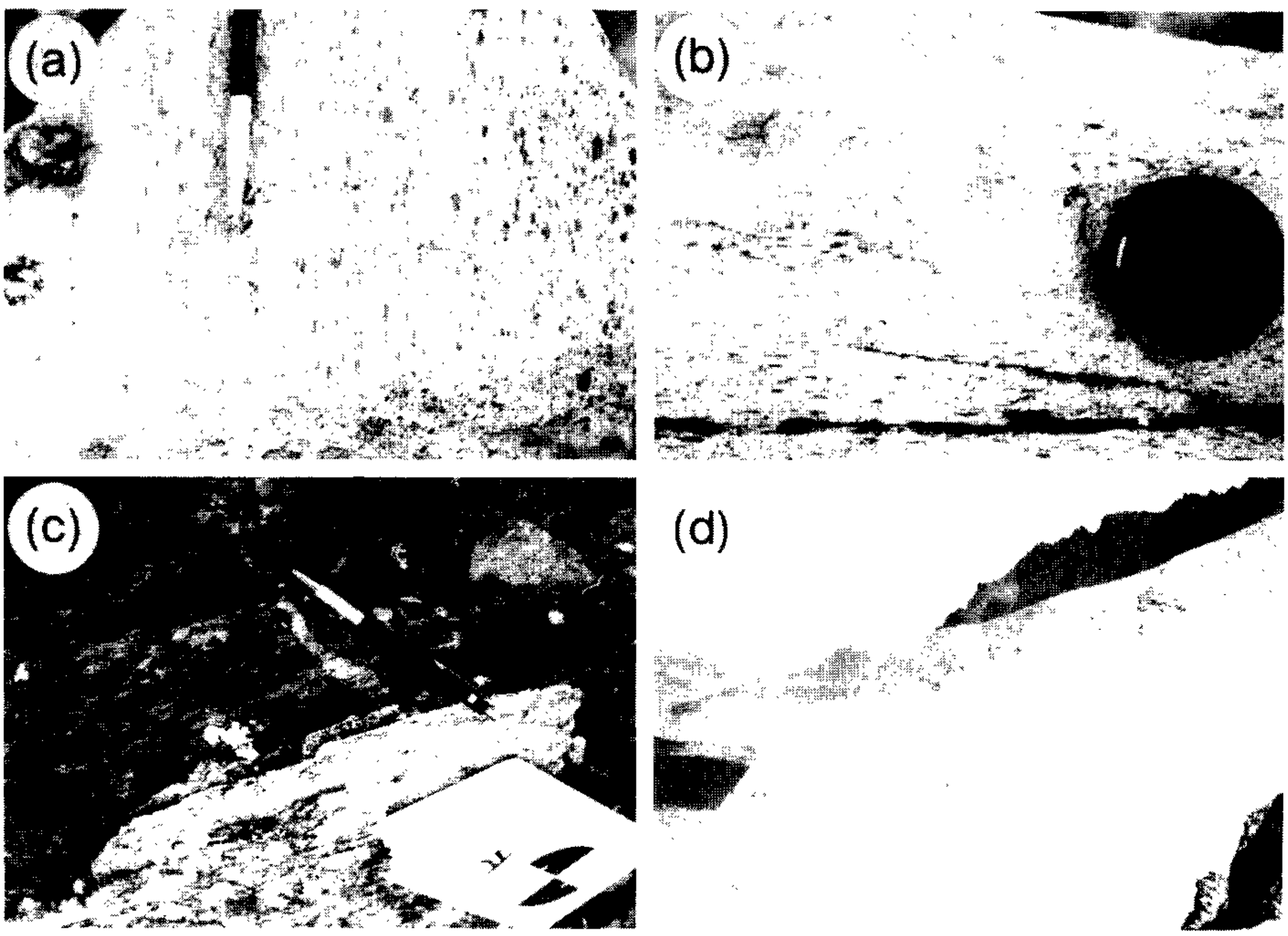

Plate 1-12-1(a). Primary mineral lineation in clinopyroxene porphyry; (b) Mineral stretching lineation in the north-northwest-trending faults east of Dortatelle Creek, looking northeast down. (c) North-northwest-trending fault west of Aiken Lake, pencil parallel to the extensional fissure filled with calcite fibres, book parallel to the fault plane, looking southwest down; (d) Outcrop-scale folds in well-bedded sedimentary rocks of the Dewar Formation in the Hogem Ranges, looking north.

The faults cut the Takla Group into fault-bounded, weakly deformed blocks, ranging in size from several square kilometres to tens of square kilometres (Figure 1-12-1). With progressive displacement on the Finlay-Ingenika fault, deformation was apparently concentrated in the previously formed fault zones, while the fault-bounded blocks remained only very weakly deformed. Cleavage is the only visible deformation outside the fault zones but within the fault zones rocks are strongly deformed and sheared into protomylonite to mylonite with a variety of kinematic indicators and fabrics, by which slip senses on the faults were determined.

Kinematic Indicators and Fabrics

S-C mylonites (Berthé *et al.*, 1979; Lister and Snoke, 1984; Shimamoto, 1989) are present in most of the faults, especially as they pass through the greenish grey clinopyroxene or clinopyroxene-plagioclase porphyries or volcanic breccias. They provide one of the most useful kinematic indicators in the study area. The C surfaces are predominantly closely spaced, displacement discontinuities or zones of relatively high shear strain, while the S surfaces are characterized by alignment of phyllosilicate minerals such as chlorite (Zhang and Hynes, 1991, Plate 1-12-1c). Angles between the C and S surfaces vary from 40°± (in slightly deformed domains) to 0°± (in strongly deformed domains). Hundreds of the C and S surfaces were measured along the Dortatelle fault and the fault east of Goldway Peak, and intersections of them are always subvertical or vertical, suggesting that horizontal displacement was predominant in the study area.

Drag folds, developed in mylonitic foliation, are common features in the strike-slip fault zones, and also provide kinematic indicators. Such folds in the Dortatelle fault zone, for example, are tight and asymmetrical, ranging in wavelength from less than 1 centimetre to several tens of centimetres. Axial planes of the folds are subvertical, striking northwest, with fold axes trending northwest and plunging 70° to 80°, and have an angle of 35°± to the fault plane. This geometry is consistent with that of the S-C fabrics and indicative of dextral strike-slip.

Extensional fissures (Ramsay and Huber, 1983) are common along the strike-slip faults and even between some cleavage planes. They are commonly filled with fibrous tremolite or calcite that grew either perpendicular or subperpendicular to the walls, especially where they cut volcanic breccias or porphyries. Typical relationships are exhibited in the north-northwest-trending fault on the ridge west of Aiken Lake (Plate 1-12-1c). Here, slickenlines marked by fibrous crystals of calcite on the fault plane display a dextral strike-slip sense, and six extensional fissures filled with calcite fibres were measured along the fault. Figure 1-12-3 plots the structural data and local, tectonic principal strains (e_1, e_2, and e_3) which were determined based on the assumption that the motion on the fault is simple shear. It is obvious from the plot that the principal strain e_2, which is determined by the intersection of the fault plane and mean extensional fissure plane (Fisher, 1953), is approximately perpendicular to the slickenline (the angle between them on the fault plane is 88°). The slickenlines and extensional fissures are therefore in excellent agreement with dextral strike-slip on the fault. Furthermore, the Fisher's mean (Fisher, 1953) of poles to the fissures moved away from the maximum principal strain e_1 (Figure 1-12-3), indicative of clockwise rotation of the fissures as a result of progressive incremental straining after their formation.

In addition to the above principal kinematic indicators, other fabrics such as stretching lineations and foliations are well developed in the fault zones. There are two types of mineral lineation in the study area: primary and secondary. The primary mineral lineations occur only in the clinopyroxene or clinopyroxene-plagioclase porphyries, and were observed at two localities on the ridge between Dortatelle and Kliyul creeks. They are due to the alignment of prismatic crystals of clinopyroxene and hornblende(?) (Plate 1-12-1a). No evidence of deformation has been found although some mineral grains are partially or entirely replaced by chlorite or epidote, which may have obscured such evidence. In its absence, these lineations are tentatively attributed to primary processes. The secondary lineations are characterized by stretched mineral grains, now predominantly chlorite (Plate 1-12-1b) and are confined to fault zones, especially in the north-northwest-trending faults on the ridge between the Dortatelle and Kliyul creeks (Figure 1-12-1). The minerals are commonly stretched subhorizontally into ribbons up to several centimetres long, while on the vertical section they have subrounded shapes. The stretching lineations (Plate 1-12-1b) cut the contacts

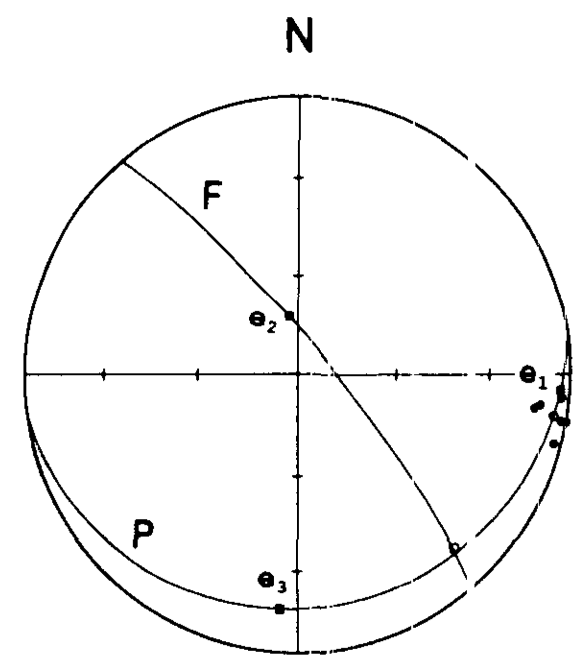

Figure 1-12-3. Stereonet plot of structural data from the north-northwest-trending fault on the ridge west of Aiken Lake. Solid circles: poles to the extensional fissure planes; solid square: principal strains (e_1, e_2 and e_3); open circle: Fisher's mean of poles to the extensional fissure planes; F: the fault plane; P: the principal plane normal to the intermediate principal strain (e_2).

between clinopyroxene-plagioclase porphyry and volcanic breccia, and minerals in different clasts of the breccia are aligned in the same direction, indicative of their deformational origin.

Foliations are the most common fabrics in or along the faults, and are characterized by parallel alignment of either phyllosilicate minerals or flattened fragments of volcanic breccia. Progressive development of cleavage due to flattening of volcanic breccia fragments is well developed in an area of about one square kilometre, bounded to the west by a north-northwest-trending, dextral strike-slip fault immediately north of the Goldway Peak. In the eastern part of this area fragments of clinopyroxene and clinopyroxene-plagioclase porphyries, in which phenocrysts of euhedral clinopyroxene and wispy plagioclase are relatively fresh, undeformed and randomly distributed, are only slightly flattened and may indeed have experienced deformation only during pyroclastic flow (Plate 1-12-2a). Passing westwards, a demonstrably tectonic flattening is superimposed, giving rise to a marked increase in the elongation ratio of fragments (Plate 1-12-2b), the local development of foliation, and deformation of a mafic dike (Plate 1-12-2d), which locally truncates the primary fabrics. In the western part of the area fragments are very strongly deformed, and foliations are extensive and penetrative in the breccia where the phenocrysts of euhedral clinopyroxene were no longer present (Plate 1-12-2c). The mean flattening plane strikes 335° and dips 73° northeast and makes an angle of 10° with the fault plane to the west, indicating that a clockwise rotation of 35° occurred, which is in good agreement with the estimate of rotation of cleavage (see below).

Outside the fault zones, rocks exhibit only a weakly developed spaced (typically at intervals of 2 to 10 cm) cleavage. The cleavage is steeply dipping and generally occurs in conjugate sets. It is interpreted to have formed at an early (pre-faulting) stage of the deformation, and its attitudes are used to constrain motions in the area since formation of the faults.

Statistics of Cleavage

Statistics of regionally distributed cleavage have been made at 24 sites within the fault-bounded blocks. Conjugate cleavages measured from the block northeast of Croydon Creek (Zhang and Hynes, 1991; Figure 1-12-3a in Zhang and Hynes, 1991) show orientations consistent with those to be expected in a stress field due to the initiation of dextral transcurrent motion on the Finlay-Ingenika fault (*cf.* Tchalenko, 1970; Keller *et al.*, 1982; Sylvester, 1988). If the regional cleavage was uniformly distributed before the

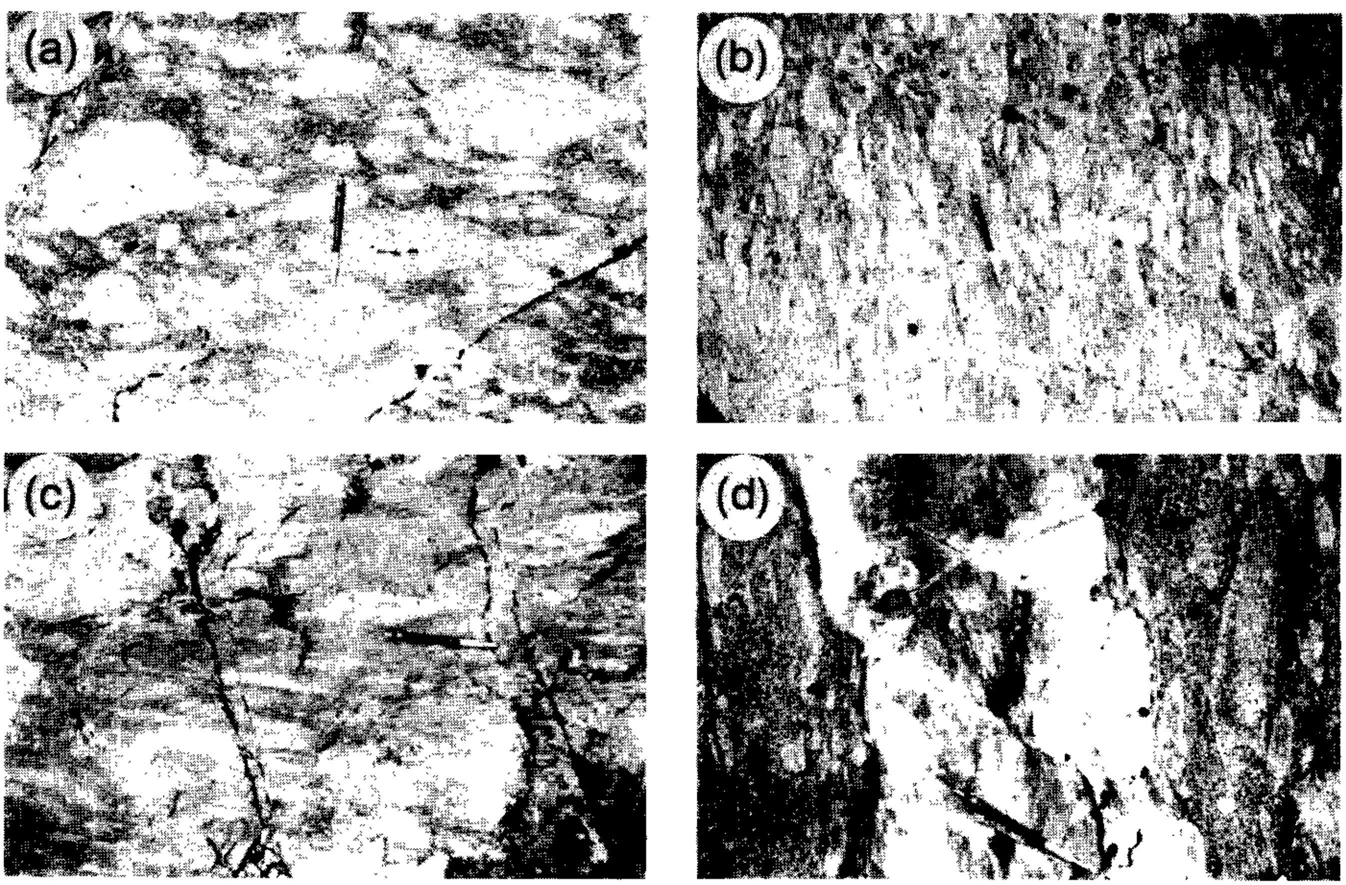

Plate 1-12-2 (a, b and c). Flattened fragments of volcanic breccia moving progressively westwards towards a dextral fault, looking northeast, north-northwest and northeast down, respectively; (d) Deformed mafic dike in the same region as (b), pencil parallel to the shear planes with thrust slip sense, looking north-northwest.

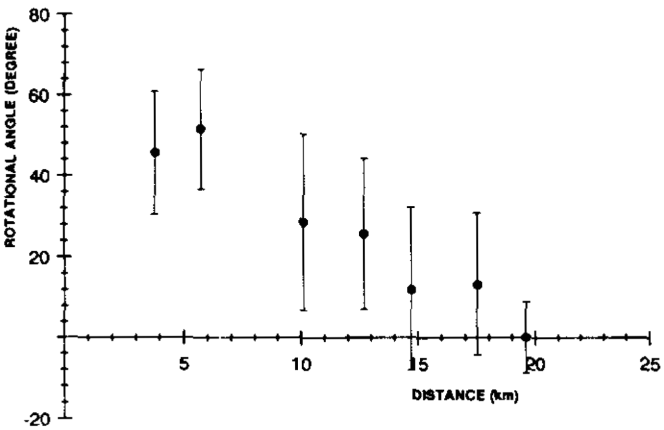

Figure 1-12-4. Variation of block rotational angle with distance away from the Finlay-Ingenika fault. The error bars represent the 95 per cent confidence circles for the rotational angles.

widespread strike-slip faulting in the study area, the variation of orientations of the cleavage can be used to indicate the block rotation. Based on this assumption, the rotational axes and angles for six sites were determined by comparing the mean attitudes for the regional cleavages with those from the block northeast of Croydon Creek. The mean rotational axis is subvertical, and the amount of block rotation varies over the study area, reaching its maximum (51.6±14.9°) close to the Finlay-Ingenika fault and minimum (0.0±9.0°) about 20 kilometres away from the fault (Figure 1-12-4).

CONCLUSIONS

The structures observed along the Finlay-Ingenika fault are dominated by subvertical to vertical, dextral strike-slip faults trending northwest, north-northwest and north-northeast, and sinistral strike-slip faults trending east-northeast. The faults are distributed in a narrow belt, about 30 kilometres wide, adjacent to the Finlay-Ingenika fault. This distribution, together with the attitudes and slip senses of the strike-slip faults, strongly suggests that the deformation developed in association with dextral, transcurrent motions on the Finlay-Ingenika fault. As displacement on the Finlay-Ingenika fault progressed, the deformation was apparently concentrated in the previously formed fault zones, while the fault-bounded, weakly deformed blocks were rotated clockwise about subvertical axes in response to the transcurrent motions. Statistics of regional cleavage indicate that the amount of block rotation varies over the study area, decreasing away from the major fault. This variable rotation of blocks is similar to that described by Nelson and Jones in the Las Vegas Range (1986) and in contrast to the uniform rotation described and modelled elsewhere (*e.g.*, Ron *et al.*, 1986; Hudson and Geissman, 1987; Geissman *et al.*, 1989; Ron *et al.*, 1990). Such rotations may characterize many parts of the Intermontane Belt and could in part explain the apparent disparities between the paleomagnetic declinations observed from the western allochthonous terranes and North America (Monger and Irving, 1980; Irving *et al.*, 1985; Rees *et al.* 1985; Irving and Wynne, 1990). We are currently conducting paleomagnetic studies to test this assertion.

ACKNOWLEDGMENTS

This research was made possible by grants from the British Columbia Ministry of Energy, Mines and Petroleum Resources and the Natural Sciences and Engineering Research Council. Their support is gratefully acknowledged.

REFERENCES

Berthé, D., Choukroune, P. and Jegouzo, P. (1979): Orthogneiss, Mylonite and Non-coaxial Deformation of Granites: The Example of the South American Shear Zone; *Journal of Structural Geology*, Volume 1, pages 31-42.

Church, B.N. (1974): Geology of the Sustut Area; *in* Geology, Exploration and Mining in British Columbia 1973, *B.C. Ministry of Energy, Mines and Petroleum Resources*, pages 411-455.

Church, B.N. (1975): Geology of the Sustut Area; *in* Geology, Exploration and Mining in British Columbia 1974, *B.C. Ministry of Energy, Mines and Petroleum Resources*, pages 305-309.

Fisher, R.A.S. (1953): Dispersion on a Sphere: *Royal Society of London*, Proceedings, Series A, 217, pages 295-305.

Gabrielse, H. (1985): Major Dextral Transcurrent Displacements Along the Northern Rocky Mountain Trench and Related Lineaments in North-central British Columbia; *Geological Society of America*, Bulletin, Volume 96, pages 1-14.

Geissman, J.W., Harlan, S.S. and Wawrzyniec, T.F. (1989): Strike-slip Faulting and Block Rotation in the Lake Mead Fault System; *Geology*, Volume 17, pages 1057-1058.

Hudson, M.R. and Geissman, J.W. (1987): Paleomagnetic and Structural Evidence for Middle Tertiary Counterclockwise Block Rotation in the Dixie Valley Region, West-central Nevada; *Geology* Volume 15, pages 638-642.

Irving, E. and Wynne, P.J. (1990): Paleomagnetic Evidence Bearing on the Evolution of the Canadian Cordillera; *Royal Society of London*, Philosophical Transactions, A 331, pages 487-509.

Irving, E., Woodsworth, G.J., Wynne, P.J. and Morrison, A. (1985): Paleomagnetic Evidence for Displacement from the South of the Coast Plutonic Complex, British Columbia; *Canadian Journal of Earth Sciences*, Volume 22, pages 584-598.

Keller, E.A., Bonkowski, M.S., Korsch, R.J. and Shlemon, R.J. (1982): Tectonic Geomorphology of the San Andreas Fault Zone in the Southern Indio Hills, Coachella Valley, California; *Geological Society of America*, Bulletin, Volume 93, pages 46-56.

Lister, G.S. and Snoke, A.W. (1984): S-C Mylonite; *Journal of Structural Geology*, Volume 6, pages 617-638.

Lord, C.S. (1948): McConnell Creek Map-area, Cassiar District, British Columbia; *Geological Survey of Canada*, Memoir 251, 72 pages.

Mardia, K.V. (1972): Statistics of Directional Data; *Academic Press*, London and New York, pages 212-339.

Minehan, K. (1989a): Takla Group Volcano-sedimentary Rocks, North-central British Columbia; *in* Geological Fieldwork 1988, *B.C. Ministry of Energy, Mines and Petroleum Resources*, Paper 1989-1, pages 227-232.

Minehan, K. (1989b): Paleotectonic Setting of Takla Group Volcano-sedimentary Rocks, Quesnellia, North-central British Columbia; unpublished M.Sc. thesis, *McGill University*, 102 pages.

Monger, J.W.H. (1977): The Triassic Takla Group in McConnell Creek Map-area, North-central British Columbia; *Geological Survey of Canada*, Paper 76-29, 45 pages.

Monger, J.W.H. (1984): Cordilleran Tectonics: A Canadian Perspective; *Bulletin Societé Géologique de France*, Volume 7, pages 255-278.

Monger, J.W.H. and Church, B.N. (1977): Revised Stratigraphy of the Takla Group, North-central British Columbia; *Canadian Journal of Earth Sciences*, Volume 14, pages 318-326.

Monger, J.W.H. and Irving, E. (1980): Northward Displacement of North-central British Columbia; *Nature*, Volume 285, pages 289-293.

Nelson, M.R. and Jones, C.H. (1986): Paleomagnetism and Crustal Rotations along a Shear Zone, Las Vegas Range, Southern Nevada; *Tectonics*, Volume 6, pages 13-33.

Nixon, G.T. and Hammack, J.L. (1990): Geology and Noble Metal Geochemistry of the Johanson Lake Mafic-Ultramafic Complex, North-central British Columbia; *in* Geological Fieldwork 1989, *B.C. Ministry of Energy, Mines and Petroleum Resources*, Paper 1990-1, pages 417-424.

Ramsay, J.G. and Huber, M.I. (1983): The Techniques of Modern Structural Geology; *Academic Press*, London and New York, Volume 1, 307 pages.

Rees, C.J., Irving, E. and Brown, R.L. (1985): Secondary Magnetization of Triassic-Jurassic Volcaniclastic Rocks of Quesnel Terrane, Quesnel Lake, B.C.; *Geophysical Research Letters*, Volume 12, pages 498-501.

Richards, T.A. (1976a): McConnell Creek Map Area (94D/E), Geology; *Geological Survey of Canada*, Open File 342.

Richards, T.A. (1976b): Takla Group (Reports 10-16): McConnell Creek Map Area (94D, East Half), British Columbia; *Geological Survey of Canada*, Paper 76-1a, pages 43-50.

Ron, H., Aydin, A. and Nur, A. (1986): Strike-slip Faulting and Block Rotation in the Lake Mead Fault System; *Geology*, Volume 14, pages 1020-1023.

Ron, H., Nur, A. and Eyal, Y. (1990): Multiple Strike-slip Fault Sets: A Case Study From the Dead Sea Transform; *Tectonics*, Volume 9, pages 1421-1431.

Shimamoto, T. (1989): The Origin of S-C Mylonites and a New Fault-zone Model; *Journal of Structural Geology*, Volume 11, pages 51-64.

Sylvester, A.G. (1988): Strike-slip Faults; *Geological Society of America*, Bulletin, Volume 100, pages 1666-1703.

Tchalenko, J.S. (1970): Similarities Between Shear Zones of Different Magnitudes; *Geological Society of America*, Bulletin, Volume 81, pages 1625-1640.

Wheeler, J.O. and McFeely, P. (1987): Tectonic Assemblage Map of the Canadian Cordillera; *Geological Survey of Canada*, Open File 1565.

Wilcox, R.E., Harding, T.P. and Seely, D.R. (1973): Basic Wrench Tectonics; *American Association of Petroleum Geologists*, Bulletin, Volume 57, pages 74-96.

Woodsworth, G.J. (1976): Plutonic Rocks of McConnell Creek (94 D West Half) and Aiken Lake (94 C East Half) Map-area, British Columbia; *Geological Survey of Canada*, Paper 76-1A, pages 26-30.

Zhang, G. and Hynes, A. (1991): Structure of the Takla Group East of the Finlay-Ingenika Fault, McConnell Creek Area, North-central B.C. (94D/8, 9); *in* Geological Fieldwork 1990, *B.C. Ministry of Energy, Mines and Petroleum Resources*, Paper 1991-1, pages 121-129.

PALEOMAGNETISM AND ANISOTROPY OF MAGNETIC SUSCEPTIBILITY OF THE TOODOGGONE FORMATION, BRITISH COLUMBIA (94E)

By H.C. Palmer
The University of Western Ontario
W.D. MacDonald
State University of New York

KEYWORDS: Paleomagnetism, magnetic susceptibility, Toodoggone Formation.

INTRODUCTION AND OBJECTIVES

The Toodoggone Formation is a succession of subaerially erupted ash flows, lava flows and associated pyroclastic rocks in north-central British Columbia that was constructed along the eastern margin of the Stikine Terrane in Early to Middle Jurassic time (Diakow, 1990; Diakow *et al.*, 1991). A field sampling program was conducted in late July and early August of 1991 with the objective of deciphering important geologic processes from the patterns of magnetic characteristics recorded in these strata (Figure 1-13-1). The specific magnetic characteristics are the natural remanent magnetization (NRM) and the anisotropy of magnetic susceptibility (AMS).

Paleomagnetic directions provide two pieces of regional tectonic information. Primary paleomagnetic inclinations, when compared to reference inclinations estimated from time-equivalent rocks of the North American craton, provide evidence for or against latitudinal displacement. Paleomagnetic results from Hazelton Group rocks exposed farther south in the Intermontane Belt suggest no detectable northward displacement (Irving and Wynne, 1990; Vandall and Palmer, 1990). Data from the Toodoggone Formation would serve to substantiate the results of previous workers and extend the conclusion to a larger part of the Stikine Terrane. Departures from the expected paleodeclination, also estimated from time-equivalent rocks of the craton, provide evidence for block rotation which may accompany fault displacement. Rotations about vertical axes, manifested by declination anomalies, appear to characterize Hazelton rocks at the latitude of 55°N near the eastern and western margins of the Stikine Terrane (Monger and Irving, 1980; Vandall and Palmer, 1990). Paleomagnetic results from the Toodoggone River area would test whether this mode of deformation also characterizes the Stikine Terrane at higher latitudes.

The paleomagnetic method depends on the remanent magnetic properties of rocks. A second magnetic property, magnetic susceptibility and its anisotropy, is proving useful in determining the fabric of rocks. With respect to ash-flow tuffs, the minimum susceptibility axis commonly coincides with the pole to foliation and the maximum susceptibility axis is aligned along the direction of flow (Ellwood, 1982; Knight *et al.*, 1986; MacDonald and Palmer, 1990; Palmer *et al.*, 1991; Hillhouse and Wells, 1991). The presumption is that nonspherical magnetite particles achieve a preferred dimensional alignment in the horizontal flow phase of ash-flow emplacement. This dimensional alignment is expressed by the anisotropy of magnetic susceptibilty and is measured in the same samples used for the paleomagnetic work. The AMS method offers the potential of inferring the locations of source vents of ash flows when allowance is made for possible rotations inferred from the paleomagnetic data.

FIELDWORK

Outcrops along and near the private road network maintained by Cheni Gold Mines Inc. and International Shasta Resources Inc. were examined with the object of: (1) examining stratigraphic variations in the magnetic parameters of the Toodoggone Formation, (2) selecting outcrops free of visible hydrothermal alteration, and (3) locating outcrops where flow-compaction foliations or flow contacts could be observed. The latter data are needed to provide a paleohorizontal reference for the axial and vector magnetic data. Criteria (2) and (3) were met at eight outcrops. At two outcrops in Metsantan lava flows attitudes could not be determined with certainty but samples were nevertheless collected for polarity information. At each of these ten outcrops, five to eight independently oriented core samples were obtained using sun and magnetic compasses and a clinometer. Four outcrops are of the Metsantan member, two of the Attycelley member and four of the Saunders member, the stratigraphically highest member of the Toodoggone Formation. Ash-flow tuffs from the lowest member of the formation were not examined because of inaccessibility.

LABORATORY METHODS

One or more standard paleomagnetic specimens were prepared from each of the 63 oriented cores. All cores were cut into specimens with height to diameter ratios of 0.85. Measured volumes and masses of all specimens were used to calculate dry-weight densities, the outcrop means of which are recorded in Table 1-13-1. Subsequent to measurement of initial natural remanent magnetization, but prior to demagnetization experiments, the anisotropy of magnetic susceptibility was measured in the specimens employing a Sapphire Instruments SI-2 low-field instrument. Four repeat measurements of each of six orientations was made. After the susceptibility measurements were completed, the specimens were stored inverted in the earth's field to provide a

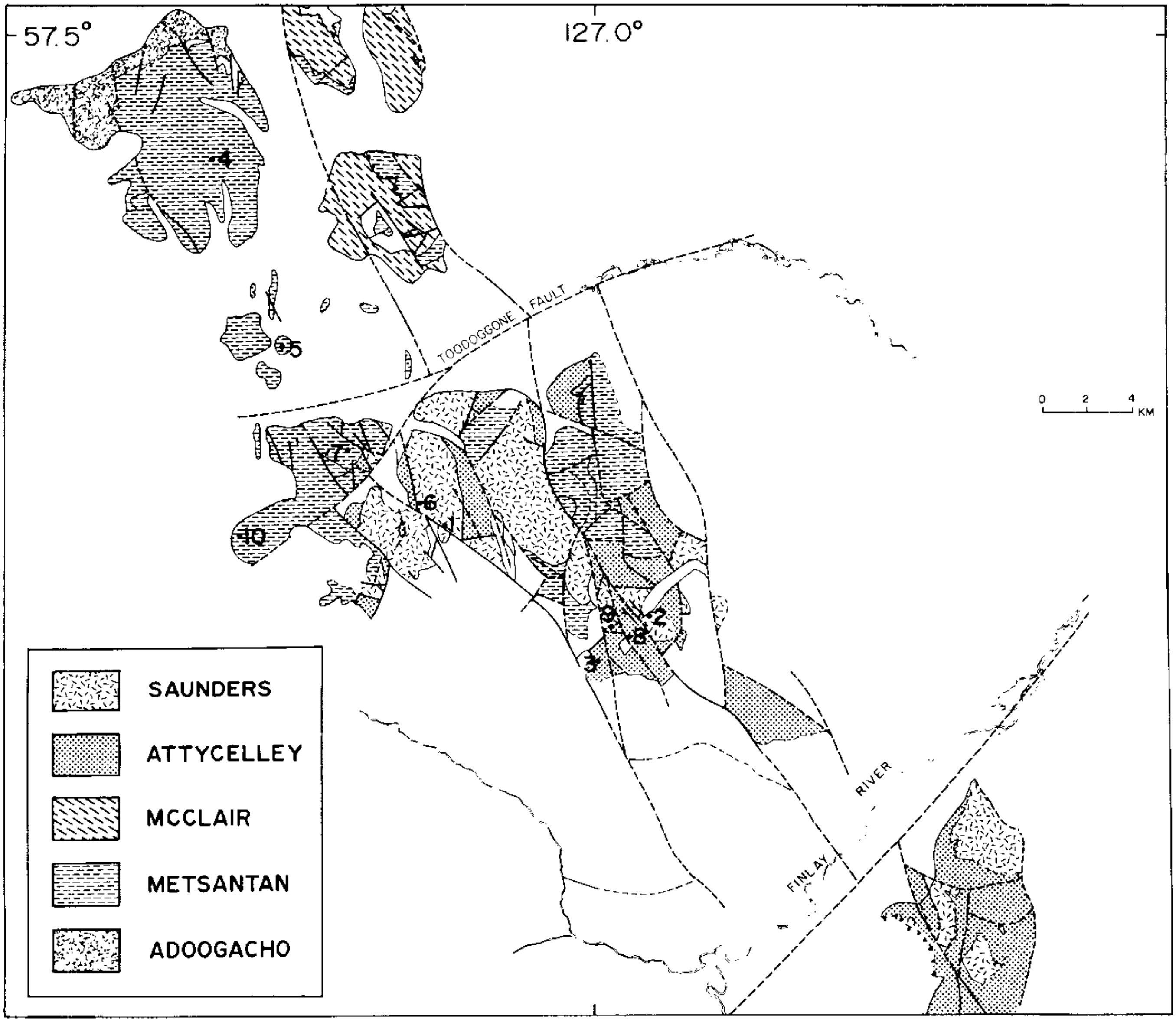

Figure 1-13-1. Geological map of the Toodoggone mining district simplified from Map 1 of Diakow (1990). Numbers identify the locations of sample sites.

storage test of remanence stability. Demagnetization experiments testing the stability of the natural remanent magnetism have yet to be carried out. The results that we present here are those of the AMS measurements and the field-measured structural elements.

RESULTS AND CONCLUSIONS

Foliation is very weakly developed in these rocks; at many localities none is visible in outcrop. In many ash-flow tuffs, collapsed pumice fragments form a eutaxitic structure and thus define a flow-compaction foliation. Although the Toodoggone tuffs are well compacted (*see* densities in Table 1-13-1), most are pumice-poor, crystal-rich tuffs.

The AMS axial ratios (Table 1-13-1) emphasize two points: the magnetic anisotropy is weak and the fabrics are oblate. These results are not unexpected given the weakly developed foliations noted above and the general absence of observed lineations in these rocks.

The bulk susceptibilities (Table 1-13-1) have a broad range of values. In magnetite-bearing rocks we find that the anisotropy of magnetic susceptibility cannot be measured with accuracy when the bulk susceptibility is less than 0.5×10^{-3} SI units. However the outcrops in the Toodoggone Formation with values of bulk susceptibility below this value have reddened feldspars or were characterized by a pink drilling return water, suggesting that hematite is the magnetic phase in these rocks of low susceptibility.

Additional experiments will be carried out to test whether the AMS patterns (Figure 1-13-2) are meaningful. Outcrops 5 and 10 are lava flows for which AMS axes are not likely to be well grouped; indeed they are not (Figure 1-13-2).

TABLE 1-13-1
ANISOTROPY OF MAGNETIC SUSCEPTIBILITY DATA, TOODOGGONE FORMATION

Unit	Site	ρ	K (10^{-3})	K_1/K_2	K_2/K_3	K_1 D°	K_1 I°	K_2 D°	K_2 I°	K_3 D°	K_3 I°
Saunders	1	2.63	43.4	1.014	1.044	281	07	190	03	091	84
Saunders	2	2.71	37.0	1.011	1.024	250	21	354	35	135	53
Attycelley	3	2.65	.366	1.016	1.015	346	24	069	12	148	48
Metsantan	4	2.50	.813	1.012	1.018	062	03	343	14	213	84
Metsantan	5	2.56	.288	1.013	1.021	357	00	084	21	250	68
Saunders	6	2.50	11.8	1.007	1.023	251	41	342	04	081	51
Metsantan	7	2.51	8.42	1.008	1.018	279	22	188	05	074	65
Attycelley	8	2.66	35.7	1.008	1.050	325	50	096	30	204	24
Saunders	9	2.70	7.09	1.009	1.013	056	24	320	13	204	70
Metsantan	10	2.55	.190	1.019	1.017	323	05	045	35	224	62

Notes:
ρ is the average density of the samples at the site in g/cm^3.
K is the site-mean volume susceptibility in SI units $\times 10^{-3}$; $k = (K_1+K_2+K_3)$
K_1, K_2, K_3 are axes of maximum, intermediate, minimum susceptibility, respectively.
D°, I° are declination and inclination in degrees, respectively, of the axial means which are computed by the method of Scheidegger (1965).
K_1/K_2 and K_2/K_3 are ratios of susceptibilities along the axes indicated.

Outcrop 3, which also has weak bulk susceptibility, has dispersed AMS axes (Figure 1-13-2) but the mean of the minimum axes (K_3, Table 1-13-1) agrees quite well with the pole to foliation at this site (Figure 1-13-2). This suggests that a signal is recovered although it may be contaminated by random noise.

Where the bulk susceptibilities are high, the AMS patterns are generally more coherent (Figure 1-13-2). At outcrops 1, 4 and 6 there is good agreement between K_3 axes and field-measured foliation F. Outcrops 2 and 7 show small angular offsets between K_3 axes and foliation (Figure 1-13-2); this may reflect a particle imbrication. Outcrops 8 and 9 have well-defined magnetic fabrics but the visible fabrics are complex. At outcrop 8, a secondary shear fabric may dominate the primary fabric; at outcrop 9, two foliations were measured, one of which penetrated volcanic clasts. Here there is no correspondence between field-measured fabric and the AMS axes (Figure 1-13-2).

The best groupings of the maximum susceptibility axes (K_1) are at outcrops 1, 2, 8 and 10. At outcrops 6, 7 and 9 the maximum and intermediate axes form girdle distributions. These latter patterns are common in rocks with small magnitude differences between K_1 and K_2 axes; that is oblate fabrics. Such data are best represented by tensor averaging methods (Ernst and Pearce, 1989); those results will be published at a future date. In a preliminary analysis we have taken the preliminary axial averages of K_1 axes (Table 1-13-1) and rotated these by the the value of dip about the line of strike of the field-measured foliations.

Assuming no initial dip is present, this procedure restores the K_1 axes to the paleohorizontal. The azimuths of the K_1 axes may then be used to infer paleoflow and the data presented in the form of a rose diagram (Figure 1-13-3). The dominant 'flow' modes have an east-west trend suggesting a north-south array of source vents. Diakow (1990, page 114) inferred that the Saunders member was erupted from a regional fracture system thought to coincide closely with the Saunders-Wrich fault which trends 330°. Thus our results are in general agreement with his inference.

Our future work will include measurements of the paleomagnetism to evaluate the possibility of regional and local rotations and latitudinal displacements. Work on the AMS and its significance to source areas and to structural movements will also be continued. These results will be compared with the paleomagnetic results for a better understanding of the volcanic and structural processes which have affected this region of the Stikine Terrane.

ACKNOWLEDGMENTS

We thank Cheni Gold Mines, Inc. for permission to use the road from Moosevale to the Lawyers minesite. We thank Northern Mountain Helicopters, Inc. for the use of their camp at Sturdee. The AMS measurements were ably performed by Dagmar Lacina at the University of Western Ontario.

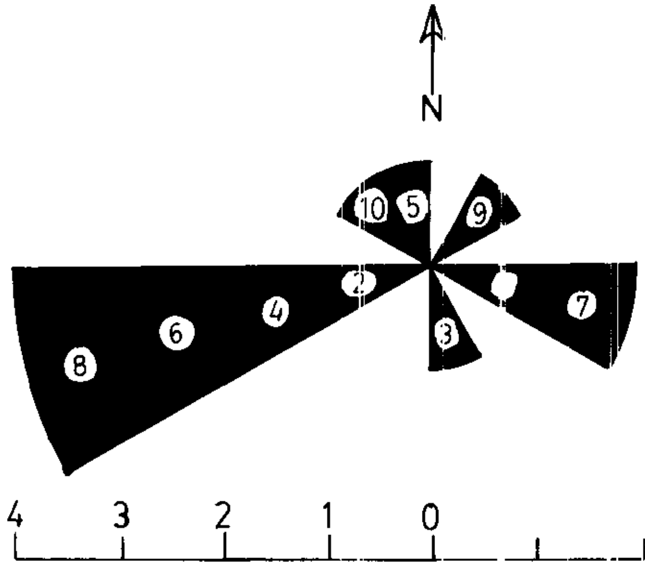

Figure 1-13-3. Rose diagram of downward directions of average K_1 axes corrected for tilt of foliation; numbers in sectors refer to outcrops. The radius of each sector is proportional to the number of observations. Six of the ten outcrops are consistent with east-west flow axes.

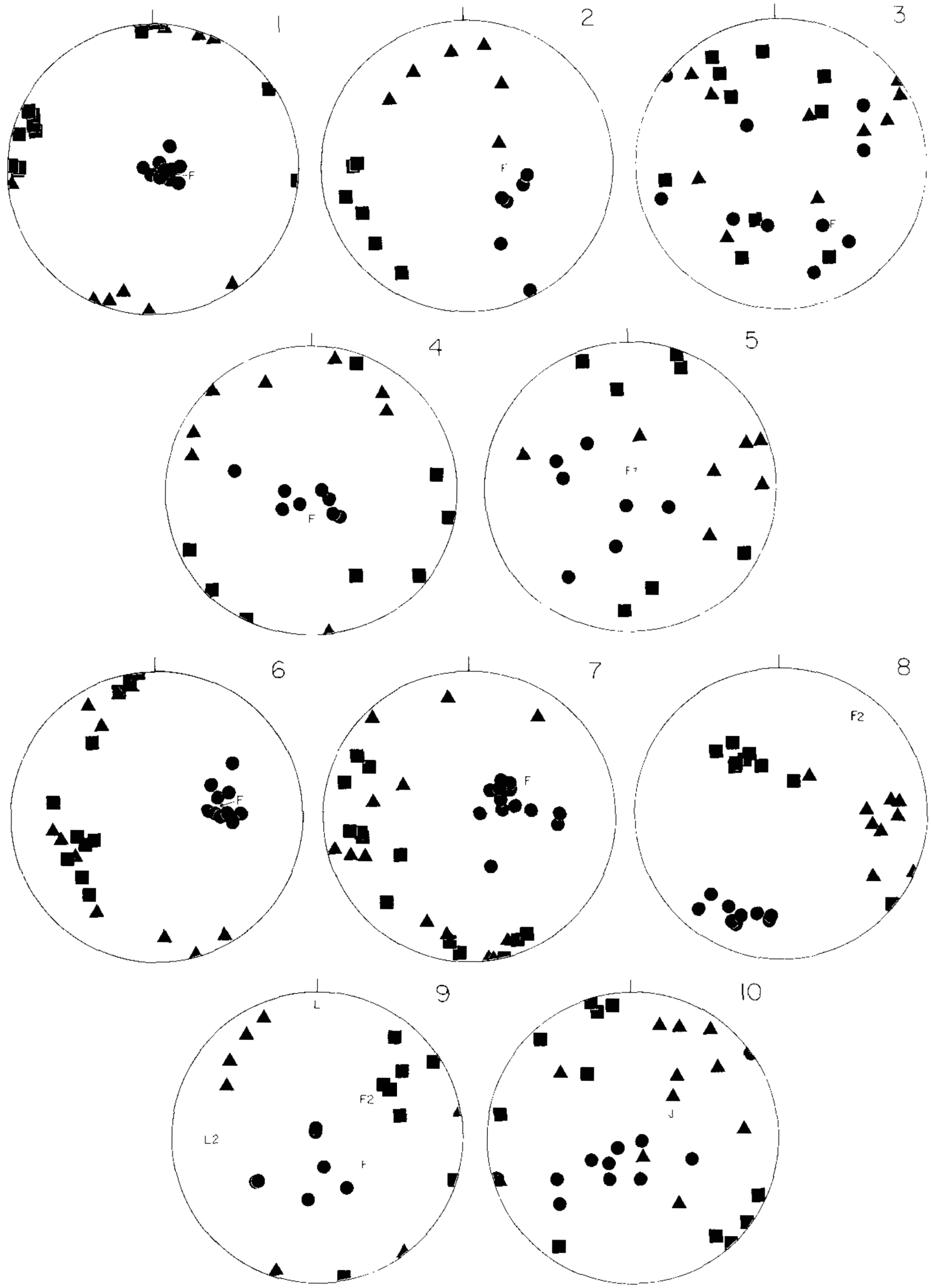

Figure 1-13-2. Equal-area stereograms showing K_1 axes (squares), K_2 axes (triangles) and K_3 axes (circles) at each of the ten sampled outcrops. F and L are field-measured foliation and lineation respectively. F_2 is foliation interpreted to be secondary. At outcrop 9, L_2 is the lineation defined by the intersection of F and F_2. At outcrop 10 only a slabby jointing is present and its pole is indicated by J.

REFERENCES

Diakow, L.J. (1990): Volcanism and Evolution of the Early and Middle Jurassic Toodoggone Formation, Toodoggone Mining District, British Columbia: unpublished Ph.D. thesis, *The University of Western Ontario*, 177 pages.

Diakow, L.J., Panteleyev, A. and Schroeter, T.G. (1991): Jurassic Epithermal Deposits in the Toodoggone River Area, Northern British Columbia: Examples of Well-preserved, Volcanic-hosted, Precious Metal Mineralization; *Economic Geology*, Volume 86, pages 529-554.

Ellwood, B.B. (1982): Estimates of Flow Directions for Calc-alkaline Welded Tuffs and Paleomagnetic Data Reliability from Anisotropy of Magnetic Susceptibility Measurements: Central San Juan Moutains, Southwest Colorado; *Earth and Planetary Science Letters*, Volume 59, pages 303-314.

Ernst, R.E. and Pearce, G.W. (1989): Averaging of Anisotropy of Magnetic Susceptibility Data; *in* Statistical Applications in the Earth Sciences, Agterberg, F.P. and Bonham-Carter, G.F., Editors, *Geological Survey of Canada*, Paper 89-9, pages 297-305.

Irving, E. and Wynne, P.J. (1990): Paleomagnetic Evidence Bearing on the Evolution of the Canadian Cordillera; *Philosophical Transactions of the Royal Society of London*, Volume A331, pages 487-509.

Knight, M.D., Walker, G.P.L., Ellwood, B.B. and Diehl, J.F. (1986): Stratigraphy, Paleomagnetism, and Magnetic Fabric of the Toba Tuffs: Constraints on the Sources and Eruptive Styles; *Journal of Geophysical Research*, Volume 91, pages 10355-10382.

Hillhouse, J.W. and Wells, R.E. (1991): Magnetic Fabric, Flow Directions, and Source of the Lower Miocene Peach Springs Tuff in Arizona, California, and Nevada; *Journal of Geophysical Research*, Volume 96, pages 12443-12460.

Monger, J.W.H. and Irving, E. (1980): Northward Displacement of North-central British Columbia *Nature*, Volume 285, pages 289-293.

MacDonald, W.D. and Palmer, H.C. (1990) Flow Directions in Ash-flow Tuffs: A Comparison of Geological and Magnetic Susceptibility Measurements, Tshirege Member (Upper Bandelier Tuff), Valles Caldera, New Mexico, U.S.A.; *Bulletin of Volcanology*, Volume 53, pages 45-59.

Palmer, H.C., MacDonald, W.D. and Hayatsu, A. (1991): Magnetic, Structural and Geochronologic Evidence Bearing on Volcanic Sources and Oligocene Deformation of Ash Flow Tuffs, Northeast Nevada; *Journal of Geophysical Research*, Volume 96, pages 2185-2202.

Scheidegger, A.E. (1965): On the Statistics of the Orientation of Bedding Planes, Grain Axes, and Similar Sedimentological Data; *United States Geological Survey*, Professional Paper 525-C, pages 164-167.

Vandall, T.A. and Palmer, H.C. (1990): Canadian Cordilleran Displacement: Paleomagnetic Results from the Early Jurassic Hazelton Group, Terrane 1, British Columbia; *Geophysical Journal International*, Volume 103, pages 609-619.

NOTES

GEOLOGY OF THE MORE CREEK AREA, NORTHWESTERN BRITISH COLUMBIA (104G/2)

By J.M. Logan, J.R. Drobe and D.C. Elsby

KEYWORDS: Regional geology, More Creek, Stikine assemblage, Stuhini Group, Mount Dilworth equivalent felsite, porphyry copper-gold, massive sulphides.

INTRODUCTION

This paper summarizes 1:50 000-scale mapping of the geology and mineral occurrences of the More Creek (NTS 104G/2) map sheet in northwest British Columbia (Figure 1-14-1). This work adjoins 1989 mapping of the Forrest Kerr (104B/15) map sheet (Logan *et al.*, 1990a, b), 1988 mapping of Sphaler Creek (104G/3) map sheet (Logan and Koyanagi, 1989; Logan *et al*, 1989), and mapping published by Souther (1972) and Brown and Gunning (1989a, b; Figure 1-14-1). The geology was mapped at a scale of 1:25 000, compiled at 1:50 000, and will be released as Open File 1992-5 (Logan *et al.*, 1992). Samples were collected for geochemical analysis (base and precious metals, major and trace elements), isotopic dating, macrofossil and conodont identification. Results will be released at a later date.

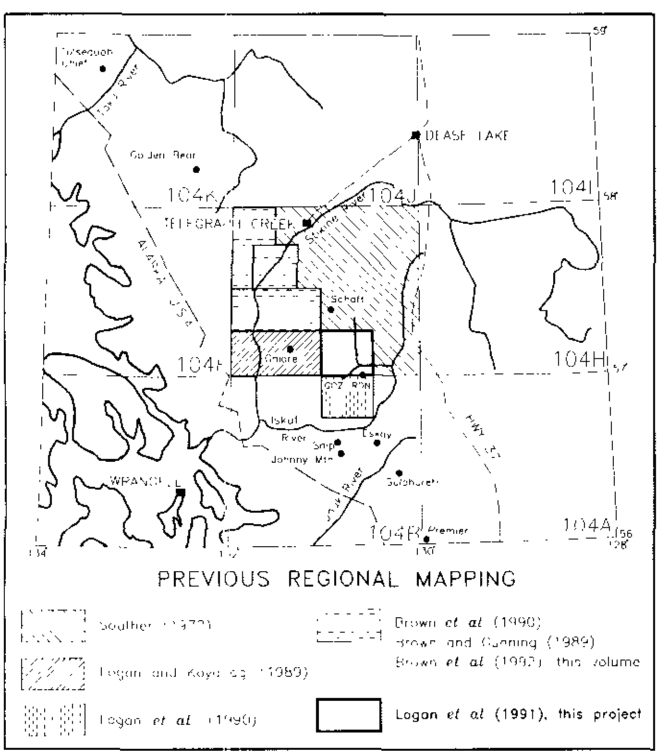

Figure 1-14-1. Location map showing previous and current field areas for Iskut North (Logan *et al.*) and Stikine (Brown *et al.*) projects.

The More Creek map area lies wholly within the Boundary Ranges of the Coast Mountains. The area is mountainous except for the high plateau around and to the south of Arctic Lake. West of Mess Creek, there is a significant increase in relief and the mountains are more rugged. The contrast in topography across Mess Creek decreases to the south and ends near its headwaters. More Creek is the main drainage in the area. It flows to the south along the Forrest Kerr fault linear, and then east after joining with a major northeast-flowing tributary, the south fork of More Creek. More Creek drains into the Iskut River off the eastern edge of the map area. Hankin Peak is the highest point in the area with an elevation of over 2560 metres.

Access to the area is by helicopter from Bob Quinn Lake airstrip, located 400 kilometres north of Smithers on Highway 37.

REGIONAL GEOLOGY AND PREVIOUS WORK

The study area lies along the margin of the Intermontane and Coast belts and is underlain by rocks of the Stikine Terrane. At this latitude, Stikinia is comprised of four unconformity-bounded, tectonostratigraphic packages (Anderson, 1989): Paleozoic volcanic and sedimentary rocks of the Stikine assemblage (Monger, 1970, 1977; Brown *et al.*,1991); Mesozoic volcanic-plutonic arc assemblages, represented in the Triassic by the Stuhini Group and in the Jurassic by the Hazelton Group (Alldrick and Britton, 1988; Anderson and Thorkelson 1990; Logan and Koyanagi, 1989b); a Middle and Upper Jurassic overlap assemblage, the Bowser Lake Group (Evenchick, 1991) and the Mesozoic to Cenozoic Coast Plutonic Complex (Woodsworth *et al.*, 1989; Anderson and Bevier, 1990). Upper Cretaceous to Tertiary transtensional continental-arc assemblages of the Sloko Group, and Neogene to Recent postorogenic bimodal plateau flows of the Edziza and Spectrum ranges (Souther, 1971; Souther and Symons, 1974) overlie these earlier island-arc assemblages.

The most economically important exploration targets are porphyry copper-gold deposits, peripheral mesothermal precious metal veins, and gold-enriched polymetallic massive sulphide deposits.

Earliest geological mapping in the area was carried out by F.A. Kerr along the Stikine and Iskut rivers (Kerr, 1948). Additional work by the Geological Survey of Canada includes: mapping on the Telegraph sheet as part of Project Stikine (1957), studies of the Tulsequah sheet (Souther, 1971), Telegraph sheet (Souther, 1972) and the Edziza volcanic complex (Souther, 1970, 1988; Souther and Symons, 1974). Read *et al.* (1989) conducted feasibility studies for B.C. Hydro and Power Authority between 1980 and 1983.

STRATIGRAPHY

STIKINE ASSEMBLAGE

The Stikine assemblage forms the basement to Stikinia and includes all Late Paleozoic rocks peripheral to the Bowser Basin (Monger, 1977). These rocks underlie the western third of the map area and range in age from pre-Early Devonian to Early Permian. In the More Creek area, the Stikine assemblage can be further divided into five main packages. From the oldest up, they are: an Early Devonian and older, penetratively deformed, intermediate to mafic metavolcanic tuff, recrystallized limestone, graphitic schist and quartz sericite schist package; a variably and overall lesser deformed Carboniferous and older mafic volcanic and carbonate package; latest Early Carboniferous to earliest Late Carboniferous crinoidal limestones, which overlie the volcanic flows and clastic rocks about 5 kilometres to the south, on the Forrest Kerr map sheet; pre-Early Permian, thick-bedded, granite-bearing volcanic conglomerate, grading into lapilli tuff near the upper contact; and Early Permian packstone.

DEVONIAN AND OLDER

West and south of the headwaters of Mess Creek is an arcuate belt of penetratively foliated, polydeformed metavolcanic and metasedimentary rocks 3 to 5 kilometres wide. These rocks comprise a structurally complex succession of schistose to foliated felsic and mafic volcaniclastics with interbedded sericite and chlorite schist, graphitic and siliceous phyllite and limestones (Holbek, 1988; Barnes, 1989; Logan and Koyanagi, 1989; Logan *et al.*, 1990a). Structurally, and presumably stratigraphically lowest, is a metasedimentary package of intermixed chloritic, graphitic and maroon phyllite with interbedded quartz sericite schist (**DSgs** and **DSqs**). Intermediate to mafic, purple and green tuffs and flows (**DSst**) overly the metasediments. Contacts are gradational. Massive to variably schistose sills of metadiorite and chlorite schist are intercalated with purple and green chloritic tuff and sericite schist.

A thick section of variably deformed intermediate volcanics and numerous limestone members of variable thickness (**DSfv** and **DSlm**) overlies the metasedimentary rocks in angular discordance (Barnes, 1990). Interbedded recrystallized limestones contain *Favosites* sp. at least as old as late Early Devonian (A. Pedder, personal communication, 1991). The volcanic rocks are predominantly green, plagioclase-phyric tuffs, amygdaloidal flows and volcaniclastic rocks, with subordinate purple and maroon tuff, black siltstone and felsic tuff. Relatively thin beds and lenses of carbonate are intercalated with the volcanics. The limestones are white to light grey, thinly foliated, locally variegated and recrystallized. Interbeds of black to dark grey micrite and green calcareous tuffaceous siltstone are common. Intraformational limestone conglomerates and breccias, buff and orange dolomite, and cherty siltstone horizons also occur. Thicker units of limestone which are, in part, structurally thickened, are medium bedded, light grey and recrystallized (**DSlm**). Thin interbedded siliceous layers weather positive and outline folds in otherwise massive, amorphous bone-white marble. Limestone units clearly display the polyphase nature of deformation affecting these rocks, particularly in Unit **DSfv,** where competency contrast between volcanic and carbonate rock is high.

CARBONIFEROUS OR OLDER

Above the Devonian and older unit is a more mafic sequence of variably foliated andesitic to basaltic volcanic rocks (**CSv**). These rocks occupy the higher peaks south and east of the headwaters of Mess Creek and are correlated with rocks which underly Mississippian limestone in the Forrest Kerr map area. The lower contact with Devonian and older volcanics (**DSfv**) was not defined. Carboniferous and older volcanic rocks are thought to be comprised of an upper basaltic pillow and breccia-flow unit, and a lower intermediate to felsic plagioclase-phyric succession of volcaniclastic rocks; the lower unit may in fact be the intermediate to felsic volcanics of the Devonian package (**DSfv**).

In the southwestern corner of the map area (Figure 1-14-2), a section of weakly to unfoliated, well-stratified and graded volcaniclastics more than 400 metres thick is exposed on the flank of a nunatak. The section includes maroon, hematitic and manganiferous lapilli and crystal tuffs, maroon pillow-basalt flows and breccias, and felsic dacitic to rhyolitic lapilli tuffs. Thin-bedded ash-tuff, tuffaceous sandstone and conglomerate are interspersed with the pillowed and breccia flows; sedimentary structures indicate tops are up. Mafic volcanics and patchy limestone lenses overlie these volcaniclastics.

The upper volcanic package is characteristically a dark green, massive pile of mafic pillowed flows, flow breccia and hyaloclastite. Flows are aphyric or weakly porphyritic and commonly amygdaloidal. Scoriaceous pillows and bombs(?) occur within thick interbedded finely vesicular basalt lapilli tuff and hyaloclastite debris flows. The latter are characterized by pale green angular to globular-shaped fragments with narrow quench-alteration rims in a limy, green-grey matrix.

UPPER CARBONIFEROUS

Early Upper Carboniferous (Bashkirian) reefal limestone conformably overlies hyaloclastite in the northwest corner of the Forrest Kerr map area (Logan *et al.* 1990b). At Round Lake, 8 kilometres west of Mess Creek, these same limestones are penetratively deformed and structurally thickened to more than 500 metres. Similar discontinuous limestone mounds (**CSlm**) are interbedded with hyaloclastites, epiclastics and flows on both sides of South More Creek. These are neither thin bedded nor as continuous as the Devonian limestones (**DSlm**). They have been sampled for conodonts and are tentatively included with the Upper Carboniferous package.

PERMIAN

West and south of Arctic Lake is a fault-complicated succession of sedimentary rocks greater than 400 metres thick. It comprises, from oldest to youngest, conglomerate, limestone, siltstone, sandstone and tuffaceous conglomerate (Plate 1-14-1). Preliminary macrofossil identifications from the limestone give Early Permian ages (E.W. Bamber, personal communication, 1991). Souther (1972) included the conglomerates from this area in his Unit 13, a Lower Jurassic succession of polymictic conglomerate, granite-boulder conglomerate and sandstone. Stratigraphic relationships indicate that these conglomerates are older than the limestone and may correlate with Upper Carboniferous to Lower Permian conglomerates (Logan and Koyanagi, 1989) recognized south of Round Lake and northwest of Newmont Lake (Logan *et al.*, 1990b).

The lowermost unit is a maroon and grey, polymictic boulder to cobble conglomerate which is conspicuous west of Arctic Lake. Volcanic clasts predominate but quartz grains and granitic clasts are diagnostic components. Rounded to subangular clasts include, in order of abundance; intermediate to mafic plagioclase-porphyritic and plagioclase-hornblende porphyritic-andesite, lapilli-crystal tuff, coarse-grained granite, quartz feldspar porphyry, diorite and minor basalt. The uppermost sections of this conglomerate are finer grained, maroon, quartz-rich tuff and tuffaceous siltstone. Well-bedded limestone overlies this unit; the contact is sedimentary and conformable. The limestone forms prominent limonite and hematite-stained bluffs, which trend north along the east side of Mess Creek. High-angle normal faults have offset and tilted the stratigraphy. Areas of significant alteration are coincident with fault structures and dikes. The limestone comprises less than 200 metres of massive and medium to thin bedded grey packstone and light brown dolomite. It lies in depositional contact with either maroon tuffs and sediments or quartz-rich Mississippian granite. It contains an abundant Early Permian fauna of rugose and tabulate corals, pelecypods, productoid and rhynchonellid brachiopods and fusulinacean foraminifers. In places corals are preserved in growth positions indicating a reefal (reef mound?) environment.

Middle Triassic

An unnamed package of Middle Triassic fine clastic rocks overlies the Paleozoic Stikine assemblage and separates it from the Upper Triassic Stuhini Group. A section of limy sediments 175 metres thick paraconformably overlies Lower Permian limestone west of Arctic Lake (Figure 1-14-2 and Plate 1-14-1). The lowermost 100 metres consists primarily of black, medium-bedded, planar-laminated, fetid, limy siltstone and fine sandstone. Elliptical concre-

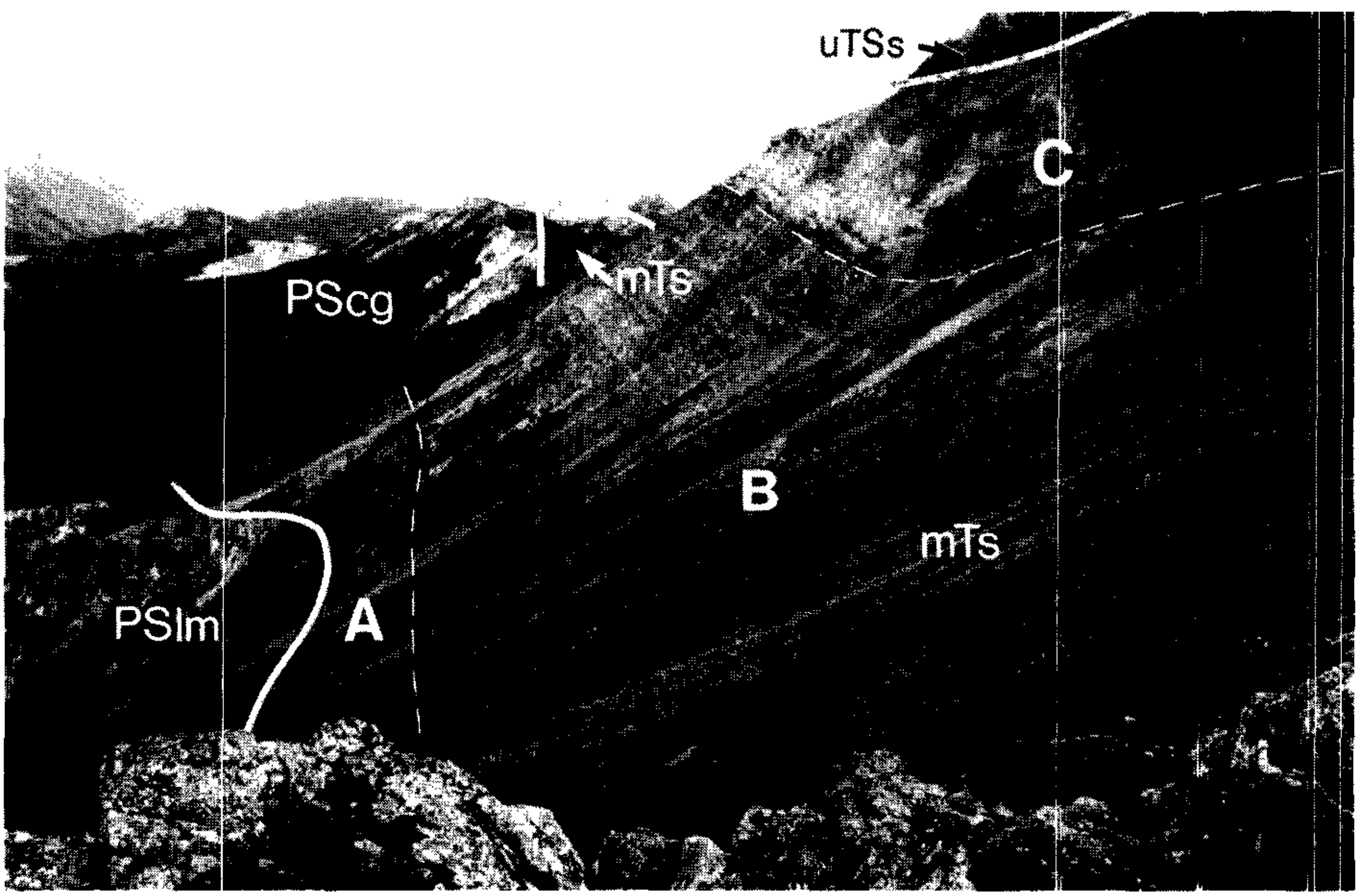

Plate 1-14-1. Well-bedded pre-Permian to Upper Triassic section exposed 4 kilometres southwest of Arctic Lake (viewed north down Mess Creek). Sediments are kinked and gently warped about a northeast-trending axis. Normal faulting has down dropped and preserved Middle Triassic sediments (mTs) in graben structures within Permian maroon quartz-rich granite conglomerate (PScg) to the north. PSlm=fossiliferous Permian limestone; mTs=Middle Triassic sediments, A=quartose sandstone, B=limy, fetid sandstone-siltstone, C=interbedded sandstone and siltstone; uTSs=Upper Triassic Stuhini Group conglomerate with potassium feldspar crystal-tuff horizons.

LEGEND

LAYERED ROCKS

QUATERNARY

Qal	*glacial till and alluvium*
Qob	*olivine basalt scoria, flow and flow breccia*

TERTIARY OR YOUNGER

Tb	*basalt flow, breccia and lapilli tuff*

LOWER AND MIDDLE JURASSIC

HAZELTON GROUP

mJHsl	*siltstone-sandstone, crystal-lapilli tuff and rhyolite-lapilli tuff, limy sandstone*
mJHb	*basalt flow, breccia and tuff, grey scoriaceous, aphyric to sparsely plagioclase-phyric, horizons of interbedded thin black shale and white tuff*
lJHv	*purple and green basaltic andesite lapilli tuff and flows, locally pillowed, plagioclase and augite-phyric flows*
lJHr	*rhyolite, ash-flow lapilli tuff and flow-layered lava, silicified conglomerate and tuff*
lJHsn	*tan-weathering sandstone, plagioclase crystal tuff, peperite flows, siltstone, carbonaceous plant fragments common*
lJHsl	*black graphitic siltstone, stratiform diagenetic pyrite to several per cent, thin interbeds of tan and grey sandstone*

UPPER TRIASSIC

STUHINI GROUP

uTSv	*medium to thin-bedded, pale green-grey tuffs, tuffaceous siltstone, orange-weathering* *augite-phyric and aphyric basalt flows, tuff and sills*
uTSs	*thick, poorly bedded green-grey tuffaceous, augite-bearing sandstone/siltstone, common granule and pebble conglomerate, thin-bedded black limestone*
uTSsn	*well-bedded feldspathic sandstone, greywacke and siltstone; limestone-bearing conglomerates and very thin-bedded siltstone*
uTSsl	*massive, black to grey-brown, calcareous siltstone, thin-bedded and laminated with fine-grained sandstone, typically undulose cross-stratified*

MIDDLE TRIASSIC ?

mTs	*limy, fetid sandstone, siltstone, concretionary sandstone and shale; thin bedded, carbonaceous and pyritic*

STIKINE ASSEMBLAGE

PERMIAN

PSlm	*bioclastic packstone, lesser buff silty dolomitic units; medium-bedded to massive, grey*
PScg	*cobble to boulder, maroon, grey and orange conglomerate and sandstone; clasts are granite, quartz-feldspar porphyry, plagioclase phyric andesite and lapilli-crystal tuff, minor diorite and basalt clasts, tuffaceous near upper contact with limestone*

CARBONIFEROUS OR OLDER

CSlm	*limestone, crinoidal limestone, massive to thickly bedded, medium grey*
CSv	*basalt and andesite pillowed flow and breccia, hyaloclastite, lapilli and ash tuff; massive to weakly foliated, dark green to grey*

DEVONIAN AND OLDER

DSfv	*intermediate to felsic plagioclase phyric tuffs, flow breccia, minor flows; light green to grey, minor limestone*
DSlm	*deformed coralline limestone; massive to thinly bedded, grey to buff*
DSst	*bright green chlorite and red-purple schistose tuff and minor flows, interbedded tuffaceous and siliceous dust-tuff and common thin-bedded recrystallized limestone*
DSqs	*quartz sericite schist; white to pale green-grey with crenulated foliation*
DSgs	*black graphitic schist*

INTRUSIVE ROCKS

EARLY JURASSIC AND YOUNGER

eJd	*medium-grained equigranular diorite and gabbro, plagioclase and pyroxene groundmass*
eJmz	*fine-grained and potassium feldspar porphyritic monzonite, granodiorite*

LATE TRIASSIC OR YOUNGER

lTum	*serpentinized peridotite*

PERMIAN OR YOUNGER

Pmz	*monzonite; dark grey-brown, pink weathering; plagioclase-hornblende porphyry*

MISSISSIPPIAN OR YOUNGER

Mg	*coarse to medium-grained, biotite and hornblende granodiorite, tonalite, and granite*
Md	*medium-grained hornblende diorite, quartz diorite; compositional layering (amphibolite-tonalite) common; locally foliated and gneissic, especially near margins*

DEVONIAN ?

lDd	*weakly foliated to schistose diorite; dark green and equigranular, grades into chlorite schist with crenulated foliation*

SYMBOLS

Geological contact (depositional, intrusive)............
Fault (normal, thrust)............
Limit of mapping............
Bedding............
Foliation (S_{1+2}, S_3)............
Dykes............
Fold axes............
Fossil locations............
Glaciers............

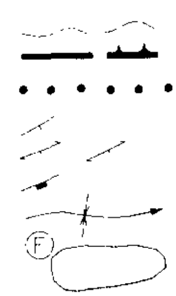

tions of coarsely crystalline siderite are common. Based on lithology, these sediments are correlated with Middle Triassic sediments exposed east of Galore Creek (Souther, 1972; Logan and Koyanagi, 1989). A discontinuous thin-bedded, quartz-bearing tuffaceous sandstone/greywacke occupies the base of the section. It overlies Lower Permian limestone and is interbedded with fetid black limestone at its upper contact. The clastic component increases in size and proportion up section; micrite and limy siltstone grade into thinly interbedded siltstone and sandstone. The sandstone package is 75 metres thick, and consists of medium-bedded buff to orange sandstone with thin interbeds of black and grey siltstone. The sandstone weathers concentrically and contains carbonized wood fragments. Rare bivalves from siltstones in this package have been submitted for identification.

Black, carbonaceous siltstone containing approximately 0.5 per cent finely disseminated pyrite, stockworks of white calcite veinlets, and numerous elliptical concretions, outcrops in the eastern edge of the map area in structurally low positions. The incompetent nature of these rocks accounts for their characteristically tight disharmonic parallel folding. On the basis of lithology, they are correlated with the calcareous siltstones west of Arctic Lake.

Upper Triassic Stuhini Group

Upper Triassic Stuhini Group rocks in the More Creek area comprise a thick package of predominantly volcanic arc derived sediments, limestones and intercalated intermediate to mafic volcanic rocks. These rocks correspond, in part, to the eastern facies of Anderson (1989). Rocks of the

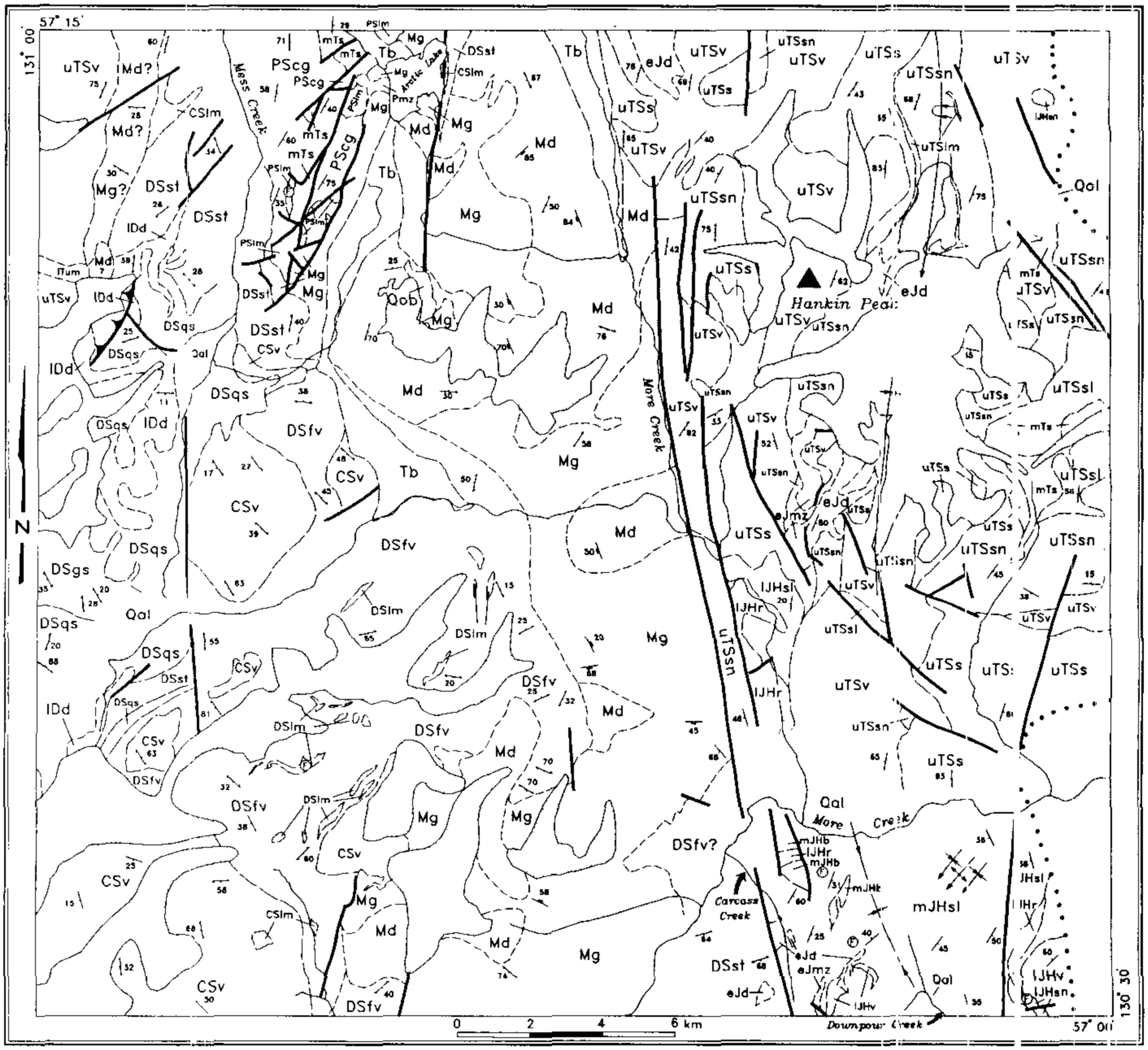

Figure 1-14-2. Simplified geology of the More Creek area (104G/2). *See* facing page for legend.

Stuhini Group crop out east of the Forrest Kerr fault north of More Creek and west of Mess Creek in the northwest corner of the map area (Figure 1-14-2). The best-exposed stratigraphic sections are on the northeast and southwest flanks of Hankin Peak, and approximately 10 kilometres south of Hankin Peak on the Lucifer claims. These rocks have been divided into five mappable units. From oldest to youngest, they are: massive, thin-laminated, black and brown siltstone (**uTSsl**); khaki feldspathic sandstone and greywacke (**uTSsn**); grey recrystallized limestone and cherty siltstone (**uTSlm**); thick-bedded augite-bearing greywacke and sharpstone conglomerate (**uTSs**); and augite-phyric and aphyric flows, related tuffs and epiclastics (**uTSv**).

West of Arctic Lake, in gradational contact with the Middle Triassic siltstone-sandstone package, is a discontinuous unit of finely laminated, pale green cherty siltstone 1 to 2 metres thick. Overlying the siltstone is a dark green polymictic pebble to cobble conglomerate (**uTSs**). The contact is sharp, parallels bedding and appears to be depositional. Clasts are well rounded to angular and include limestone, marble, augite and hornblende-phyric volcanics, basalts and chert. In contrast to the pre-Permian conglomerates that contain granite and free quartz, this conglomerate contains augite grains. Tuffaceous sections within the conglomerate contain coarse (0.5–2 cm) white and pink potassium feldspar laths, which comprise about 5 per cent of the rock. This tuffaceous conglomeratic unit crops out west and north of Arctic Lake, in an isolated occurrence 6 kilometres north of the confluence of More and South More creeks, on the west side of More Creek, and on the Lucifer property, north of More Creek.

East of Forrest Kerr fault, the lowermost unit (**uTSsl**) is a planar-laminated siltstone interbedded with undulose to wavy cross-stratified sandstone. The unit crops out as dark grey to black, massive or thickly bedded, calcareous siltstone with light brown, orange-weathering sandstone interbeds. Common sedimentary structures include load and flame structures, soft-sediment slumping and trough crossbeds; graded bedding is less common. This unit is overlain by a well-bedded sequence of khaki feldspathic sandstone, thin interbedded dark grey siltstone to fine sandstone, poorly sorted dark grey arkosic greywacke and limestone-bearing conglomerate (**uTSsn**). Sandstone commonly contains lithic clasts and laminated siltstone rip-up clasts. Interbedded with these rocks are planar-laminated, olive-grey, dark green and black, thin-bedded siliceous siltstones and fine sandstones. Limestone conglomerate and polymictic limestone-bearing conglomerate are distinctive green, yellow or maroon-weathering coarse clastic units. Angular to rounded light grey limestone clasts in a buff matrix of coarse, tuffaceous and limy sand comprise up to 85 per cent of some outcrops. Subordinate volcanic sandstone and siltstone make up the remainder. Polymictic conglomeratic layers of variable thickness contain mixed angular and rounded fragments up to 20 centimetres (average 5 cm) in diameter. Clasts include maroon and grey pyroxene and plagioclase-phyric andesite, black siltstone and limestone. Star-shaped (isocrinus?) crinoids, of Triassic or younger age, occur within limestone clasts. White-weathering, grey, recrystallized, massive to medium-bedded limestone (**uTSlm**) crops out as discontinuous units, less than 50 metres thick, throughout the stratigraphy. The limestone is bioclastic, containing sparse crinoids and various pelecypod and brachiopod fossil fragments. A package of siltstone and ribbon chert (to 50 m thick) overlies the limestone and in places is interbedded with it. The siltstone and chert are variegated; black, green, yellow and grey. Recessive dark grey and black silty limestone may represent basinward facies equivalents of the bioclastic limestone. Thick-bedded tuffaceous sandstones, sharpstone conglomerates and thin-bedded black limestones (**uTSs**) comprise a succession 300 metres thick east of Hankin Peak. The sandstones are light green, augite-bearing, medium-grained, well-sorted arkoses; in places, they texturally resemble pyroxene diorite intrusive bodies. These massive green tuffaceous sandstones are typically chaotic slump or debris-flow deposits of poorly sorted greywacke or sharpstone conglomerate. Thick and numerous sharpstone conglomerate horizons occur within this unit. The matrix of the sharpstone conglomerate is most commonly arkosic; clasts include laminated siltstone, bedded sandstone, chert, limestone and rare aphyric volcanics. The clasts are angular to subangular, average 2 centimetres, and are as large as 10 centimetres in diameter. Bivalves, possibly Late Triassic Monotis or Middle Triassic Daonella, are present in thin siltstones and in clasts from interbedded sharpstones north of the Lucifer claims. Sharpstone conglomerate with an argillaceous matrix is exposed east of Hankin Peak. Thin-bedded black to dark grey argillaceous limestone is interbedded with tuffaceous sandstones north of Twin glaciers. The limestone contains belemnites and ammonites; the siltstone and sandstone contain bivalves.

Upper Triassic volcanic rocks (**uTSv**) are volumetrically subordinate to the previously described sedimentary rocks. Intermediate volcaniclastics and epiclastics predominate, intermediate and mafic flows are subordinate. North of More Creek, maroon and dark green plagioclase-phyric lapilli tuff is interbedded with white to brown-weathering, medium-grained feldspathic volcanic sandstone. Subangular lapilli and reworked, well-rounded 1 to 2-centimetre fragments are plagioclase and hornblende phyric in a pyroxene crystal rich matrix. The tuffs and epiclastics are stratified but thick bedded, and generally difficult to distinguish from one another. Coarse polylithic block-tuffs containing plagioclase-phyric andesite, dacite and maroon hornblende plagioclase andesite are distinctive within the thick section of interbedded ash and lapilli tuff and reworked epiclastic rocks. Northwest and northeast of Hankin Peak, maroon augite-phyric and plagioclase-hornblende-phyric flows and flow breccias are interlayered with pyroxene-rich crystal and lapilli tuffs. The flows contain augite phenocrysts to 10 millimetres in size and stubby plagioclase phenocrysts to 3 millimetres in size in a purple and green mottled groundmass. West of Mess creek is a pile of maroon amygdaloidal plagioclase and pyroxene-phyric basalt flows, breccias and tuffs, and dun-weathering, olivine-rich basaltic tuffs 800 metres thick. These are intruded by trachytic sills of coarse-bladed plagioclase and pyroxene porphyries, probable feeders to overlying volcanics. East of Hankin Peak, interlayered maroon and green ash and lapilli tuff, massive plagioclase-phyric andesite, and scoriaceous flow breccias overlie thin bedded, pyritic siltstone and sandstone.

North of Hankin Peak, weak to variably foliated volcanic, tuffaceous and epiclastic rocks crop out in creek valleys. Lithologically this package is identical to rocks of the Upper Triassic Stuhini Group. Chlorite phyllites and schists are locally developed, and generally occur structurally below less-deformed pale green, fine-grained distal tuffs. This area may contain pre-Triassic rocks, but insufficient work has been completed to be certain.

Lower to Middle Jurassic

Lower and Middle Jurassic sedimentary and volcanic rocks (Souther, 1972; Read *et al.*, 1989) crop out mainly south of More Creek and east of Forrest Kerr fault (Figure 1-14-2). In general, the Lower to Middle Jurassic stratigraphy comprises a lower succession of dominantly siltstone and sandstone, a middle succession of massive rhyolitic and intermediate volcanic rocks and an upper sequence of siltstone, tuff and basalt breccias and flows. The area south of More Creek is bisected by a southerly flowing tributary of Downpour Creek. Read *et al.* (1989) report Early Jurassic (late Toarcian) fossils from the ridge west of this tributary. Fossils collected from the same general location (this study) have been interpreted as Middle Jurassic (Bathonian; Poulton, 1991). East of the tributary, Souther (1972) reports fossils with Middle Jurassic (middle Bajocian) ages from three localities along the lower slopes of the ridge. At the east end of the ridge a fault-bound package contains Early Jurassic (Sinemurian) fossils. Lithology and fossil distribution indicate a general synclinal form for the Jurassic strata south of More Creek.

The stratigraphically lowest, but structurally highest Lower Jurassic rocks occur northeast of Downpour creek. At this location at least 200 metres of massive and thin-bedded black siltstone and minor standstone (**lJHsl**) are conformably overlain by at least 50 metres of tan to rusty weathering sandstone and minor pebble conglomerate (**lJHsn**). These sediments are conformably overlain by a resistant volcanic succession of rhyolite (**lJHr**) and andesitic flows and tuffs (**lJHv;** Plate 1-14-2). The rhyolitic rocks are about 120 metres thick and consist of a basal welded ash-flow tuff and an upper flow-layered, aphyric, white and rusty weathering rhyolite flow. The ash-flow tuff contains pale green aphanitic and finely flow-layered lapilli, which average 3 to 6 millimetres in size, in a white to pale grey siliceous matrix. The exact relationship of the ash-flow tuff to the overlying flow-layered rhyolite is not known, but it appears to be conformable. Pebble conglomerate adjacent to

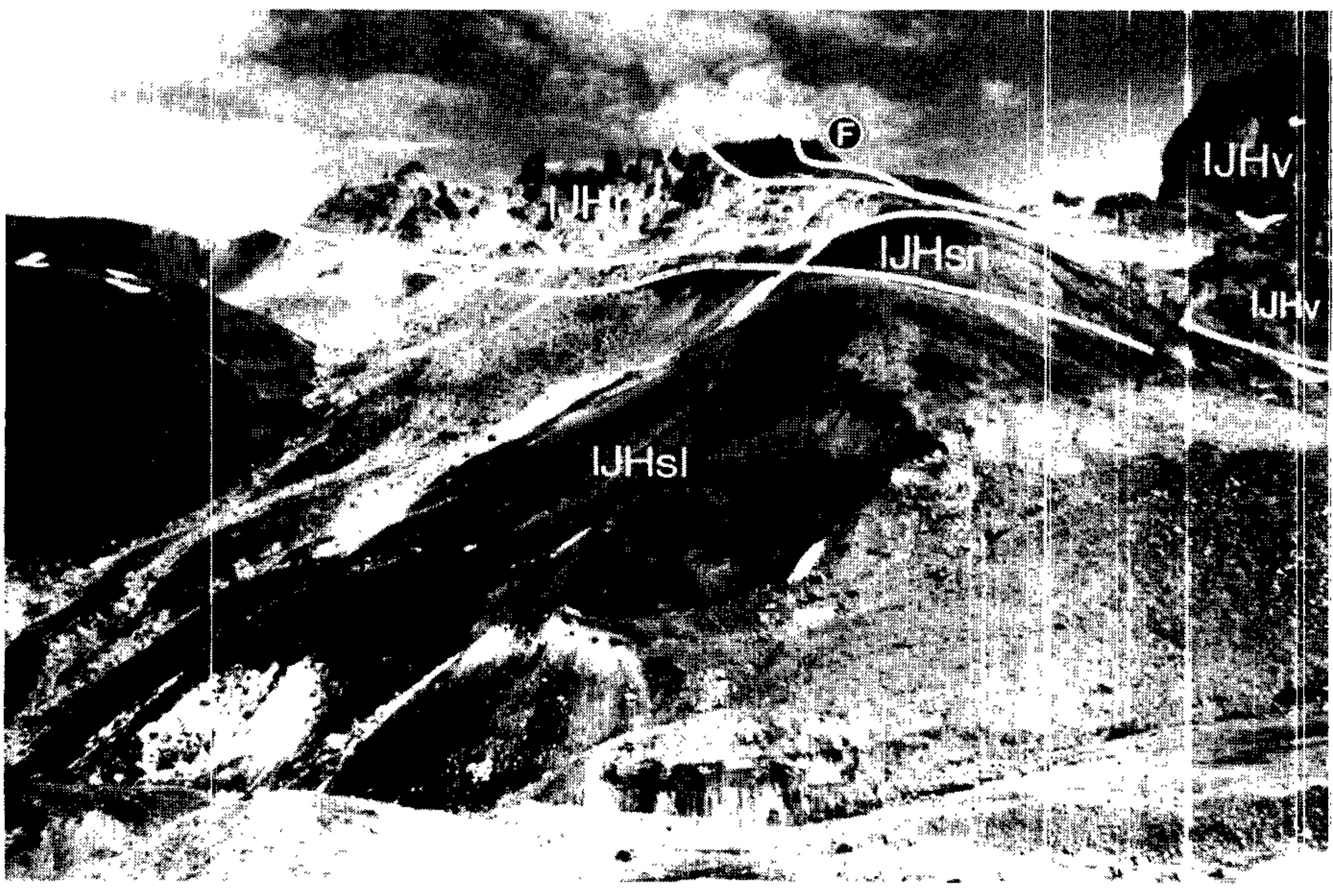

Plate 1-14-2. Lower Jurassic stratigraphic section 8 kilometres southeast of confluence of South More and More Creeks, viewed northeastward. Thin-bedded black siltstone and sandstone (lJHsl) are conformably overlain by tan sandstones and minor conglomerates (lJHsn). Conformably overlying these sediments is a white and rusty weathering, silicified rhyolite flow and tuff unit (lJHr). Maroon plagioclase-phyric andesite flow, breccia and tuff (lJHv) form the top of the section. Separating Unit lJHr from Unit lJHv is a sandstone and conglomerate unit, 10 to 20 metres thick which contains Sinemurian fossils.

the rhyolite and up to 5 metres above is intensely silicified and has a characteristic pale bluish green hue. The conglomerate is unaltered where it is in apparent fault-contact with the rhyolitic rocks. Souther (1972) mapped these rhyolitic rocks as Late Cretaceous to Tertiary dikes. However, because they are pyroclastic, at least in part, they are now interpreted as a Jurassic extrusive unit. Silicification of adjacent sedimentary rocks may be due either to primary synvolcanic or secondary hydrothermal fluid circulation, or both.

About 10 to 20 metres of fossiliferous sandstone, conglomerate, and a variety of green, thin-bedded tuffs and tuffaceous sediments (included with **lJHsn**) overlie the rhyolitic rocks. The sediments and tuffs have rapidly changing inclinations, apparently due to faulting and folding. A fossil from this horizon returned a mid-Early Jurassic (Sinemurian) age (Poulton, 1991).

The rhyolite unit and adjacent sediments are overlain by maroon plagioclase-phyric andesitic flows, breccias and tuffs (**lJHv**). These volcanic rocks were originally mapped by Souther (1972) as Triassic in age. However, their stratigraphic position indicates they are Early Jurassic, unless contact relationships with the underlying sediments are structural. Poorly formed pillows occur in the andesite. The rocks weather maroon-grey and contain about 30 per cent euhedral, felty plagioclase phenocrysts. Debris-flow deposits more than 30 metres thick and containing subrounded clasts of green-grey aphyric to plagioclase-phyric andesite in a maroon matrix overlie the pillowed and fragmental rocks. These grade upward into a thick sequence of massive to poorly bedded dark green-grey and reddish grey andesitic tuffs. Most fragments have narrow rims that weather a lighter shade of grey. The green-grey tuffs contain about 30 to 40 per cent euhedral, equant plagioclase crystals and lapilli-sized fragments containing chloritized augite phenocrysts. Similar tuffs and augite-phyric flows crop out on the ridge between Carcass and Downpour creeks, in the vicinity of the Early Jurassic fossil locality of Read *et al.* (1989).

Several isolated outcrops of thin-bedded siltstone and sandstone, conglomerate, felsic tuff, and flow-layered rhyolite occur on both the east and west sides of More Creek, a few kilometres north of the confluence with the south fork. Lithology suggests that these rocks correlate with Units **lJHsn** and **lJHr.** On the west side, moderately west-dipping, white-weathering, resistant rhyolite breccias and tuffs overlie thin-bedded deformed sediments. The felsic rocks are well stratified and graded; tuffs contain pink, flow-layered angular fragments of rhyolite and aphanitic grey, white and blue-green fragments. On the east side of More Creek, about 30 metres of felsic, orange-weathering lapillis crystal tuff crops out and appears to be, at least structurally, overlain by thinly interbedded carbonaceous siltstone and sandstone. The tuff contains about 1 per cent quartz grains and grey andesitic lapilli to 3 centimetres in size. Two aphyric, sparsely amygdaloidal rhyolite or dacite flows, 5 to 7 metres thick, occur within the tuffs. The carbonaceous black siltstone and tan, well-sorted, feldspathic sandstone which overlie the tuffs are poorly indurated and deeply weathered. Carbonaceous plant stems and leaves are ubiquitous.

Sedimentary rocks of possible Early Jurassic age also form isolated outliers within Triassic rocks on ridges a few kilometres southeast and northeast of Hankin Peak.

East of the Forrest Kerr fault, near Carcass Creek, is a thick succession of massive and thin-bedded siltstone (**mJHsl**). Numerous lenses of crystal tuff and lapilli tuff, from about 5 to 30 metres thick, are interbedded with these siltstones. The lapilli tuffs contain mainly pale grey rhyolitic fragments that average 1 centimetre in diameter. The crystal tuffs are typically maroon weathering and contain up to 30 per cent plagioclase crystal fragments averaging 2 to 4 millimetres in size; finely vesicular basaltic lapilli to 7 millimetres in size are common. These intermediate volcaniclastic rocks are similar to Unit **lJHv** and may represent the gradational change from a dominantly volcanic facies to a sedimentary one. Rare sandy limestones are interbedded with the tuff and siltstone. A fossil assemblage from one locality high on the ridge, returned a Middle Jurassic (probable Bathonian) age (Poulton, 1991). The volcanic component of these Bowser Lake Group age-equivalent rocks is problematic.

South of More Creek, about 200 metres of dark grey, fine-grained, aphyric basaltic rocks (**mJHb**) are interbedded with graphitic and pyritic siltstones. These basaltic volcanic rocks structurally underlie folded siltstone, but may overlie them stratigraphically. An ammonite was collected from interbedded tuffaceous sandstone near the top(?) of the volcanic sequence and yielded an early Middle Jurassic (Aalenian) age (Poulton, 1991). Flows are most abundant, but coarse fragmental rocks, similar to basaltic hyaloclastite in pillowed successions, also occur. Fragments are mainly scoriaceous lapilli and block-size clasts. The volcanic rocks are generally dark grey but are bleached light grey where pyritized. A sequence of thin, alternating black siltstone and white tuff, 10 metres thick, is interbedded with massive to thick-bedded basaltic fragmentals. These rocks resemble the 'pajama bed' rocks of the Troy Ridge facies of the Salmon River Formation (Anderson and Thorkelson, 1990).

Tertiary and Younger

Flat-lying, columnar-jointed basaltic flows (**Tb**) underlie the plateau north and south of Arctic Lake and at the north end of More Creek. The flows occupy north-trending valleys in the area extending for about 10 kilometres south of Arctic Lake. The distribution of the flows indicates that the paleosurface was similar to present topography. They unconformably overlie diorite of probable Mississippian age, Paleozoic schists and poorly consolidated sediments of unknown age. Souther (1972) assigned a Late Tertiary to Pleistocene age to these rocks based on correlations with similar rocks to the north, near Mount Edziza. A sample is currently being analyzed by the K-Ar isotopic dating method.

Dark grey basalt with a maximum of 2 to 3 per cent plagioclase, 1 per cent clinopyroxene, less than 1 per cent magnetite and rare olivine phenocrysts is the most common rock type. The mineralogy varies little in all the exposures examined. Phenocrysts are vitreous and unaltered. Fragmental aphyric rocks only occur in one outcrop at the south edge of Arctic Lake. Flows are vesicular near their tops and bases, and individual lava flows are identifiable where the flows are dissected by More Creek.

Quaternary

South of Arctic Lake, basaltic scoria, angular debris and lava flows (**Qob**) form a small knob built on Mississipian granitic rocks (Figure 1-14-2). The basalt contains an average of 5 per cent vitreous olivine and less than 1 per cent each of clinopyroxene and plagioclase; the phenocrysts range up to 5 millimetres in size. Several small dikes, all less than a metre wide, cut the scoria deposits. Along the flanks of the knob, the scoria are cemented, forming beds about 30 centimetres thick. The north side of the knob comprises mainly thin lava flows, underlain by weakly indurated, till-like sediments (diamictite) with rounded cobbles of granite and diorite to 10 centimetres in diameter. Minor stratified tuff is also present.

Souther (1972) correlated these olivine-bearing scoria and basalt flows with olivine basalt and related pyroclastic rocks of Pleistocene age (radio-carbon dated at 1340 years B.P.; Souther, 1970). They contain more olivine and fewer plagioclase phenocrysts than the Tertiary basalt flows around Arctic Lake and in More Creek.

INTRUSIVE ROCKS

Intrusive rocks have been subdivided into six age groups on the basis of intrusive relationships. The present designation favours a maximum age of intrusion. Thus, for example, the potassium feldspar megacrystic syenite intrusives that cut Late Triassic Stuhini Group rocks are assigned a Late Triassic and younger age. These ages will be refined with K-Ar, Ar-Ar step-wise heating, and U-Pb dating techniques now in progress.

Devonian (?)

Weakly foliated to schistose diorite sills and stocks (**lDd**) intrude Devonian schistose rocks west of and at the headwaters of Mess Creek (Figure 1-14-2). These are interpreted to be the oldest intrusions in the More Creek map area. Equigranular, medium-grained textures are preserved where the intrusions are not deformed. Undeformed chlorite metadiorite grades into strongly deformed chlorite schist in which intrusive textures have been destroyed. The massive, textureless nature of these schists helps distinguish them from similar chloritic, schistose mafic tuffs and flows, in which some primary textures are generally preserved.

Mississippian and Younger

An elongate, north-trending composite pluton of dioritic to granitic composition occupies the central third of the More Creek map area. It is bounded on the east by the Forrest Kerr fault zone, is overlain by Late Paleozoic rocks and intrudes mid-Paleozoic rocks to the west. It does not seem to crop out west of Mess Creek. The pluton extends 3 kilometres to the north of the map area where it is covered by Tertiary basalts, and to the south onto the Forrest Kerr map sheet (Figure 1-14-2). The Forrest Kerr pluton is mineralogically similar, consisting of a more mafic diorite phase at its northern end; it is also roughly the same size as the More Creek pluton. Biotite from a granitic phase in the Forrest Kerr map area gave a K-Ar isotopic age of 346±10 Ma. Step-heating $^{40}Ar/^{39}Ar$ analyses of hornblende separates from the mafic phase indicate excess argon and a minimum apparent cooling age of Early Permian. Nowhere in either map area was this intrusion seen to intrude rocks younger than Permian; southwest of Arctic Lake, Permian limestone and marble appear to unconformably overlie the pluton. The contact may also be structural in part. Weakly to moderately foliated outliers and possible dikes with mineralogy and textures similar to the main pluton (where it is undeformed) intrude deformed Mississippian or older rocks east of Mess Creek. The pluton has been sampled for U-Pb dating of zircons.

The earliest phase of the pluton is an equigranular medium-grained hornblende diorite (**Md**). Hornblende and plagioclase are the dominant constituents, though, in places, 1 to 2 per cent biotite coexists with the hornblende. In some outcrops, quartz is present to 5 per cent or less; it forms "eyes" averaging 4 millimetres in size, which often have a distinct blue colour. In other outcrops, hornblende forms pegmatitic clusters and rows of elongate crystals up to 20 centimetres long. Amphibolite forms irregular lenses and pods with diffuse margins which grade into more typical hornblende diorite. Parts of the intrusion are compositionally layered, with variations in hornblende to plagioclase ratios, phenocryst size, and alternating homogeneous diorite and intrusive breccia zones tens of metres thick. Deformed zones within the body are gneissic.

At one locality, massive coarse-grained hornblende gabbro grades into hornblendite with hornblende crystals aligned perpendicular to compositional layering, and equigranular clinopyroxene hornblendite, clinopyroxenite and biotite hornblendite. This pod of ultramafic rock (**Mum**) is about 200 metres square in area and is intruded by, and apparently suspended within, a later granitic phase. Layering within the hornblende gabbro is defined by zones slightly more rich in plagioclase, averaging 10 to 50 centimetres in width, and typically 3 to 5 metres in length. The boundaries are usually diffuse with hornblende crystals protruding into the plagioclase matrix from the enclosing hornblendite. Hornblende is mainly fresh and unaltered, but epidote veins are common and disseminated epidote occurs in places. Poikilitic hornblende encloses clinopyroxene in the clinopyroxene hornblendite and magnetite in the biotite hornblendite. Biotite books in the latter are up to 2 centimetres in size and green in colour, but are not chloritized. The textures and mineralogy are consistent with Alaskan-type ultramafic bodies (G.T. Nixon, personal communication, 1991).

Granodiorite, tonalite and granite (**Mg**) comprise the granitic phase of the pluton. Textures are usually medium to coarse grained and equigranular. Quartz is usually the coarsest mineral, and typically forms "eyes" making up between 10 and 30 per cent of the rock. Potassium feldspar occurs as anhedral, slightly finer grains between plagioclase crystals. Chloritized and rare pristine biotite is present from about 2 to 10 per cent; hornblende is uncommon. Contacts with the diorite are commonly irregular and curviplanar, with complex interfingering. Intrusive breccia textures of angular blocks of amphibolite suspended in diorite and diorite suspended in granite can be followed into areas where the granite clearly crosscuts the diorite. The contact between granitic rocks and diorite has been drawn as close to such a transition zone as possible. Where the diorite appears to be suspended as blocks within the granitic phase (*i.e.* an intrusive breccia), the outcrop was mapped as granite.

Near the south edge of the map area, a large complex of mainly plagioclase-phyric andesite dikes intrudes Mississippian volcanic rocks and Mississippian granite. Plagioclase occurs as phenocrysts from 2 to 5 millimetres in size. Some dikes have seriate and equigranular textures. Pyroxene is the only mafic phase and is usually interstitial to plagioclase or forms finer, less abundant phenocrysts; augite porphyry is uncommon. Most dikes are weakly propylitized.

Numerous fine-grained aphyric and aphanitic dikes and a variety of plagioclase porphyry diorite dikes cut the main Mississippian diorite-granite pluton. Most of them are less than 3 metres wide, but a few larger dikes are exposed above the south fork of More Creek and east of Arctic Lake.

Permian or Younger

A small porphyritic monzonite stock (**Pmz**) is exposed in several isolated outcrops northwest of Arctic Lake and in the lower reaches of a small creek draining west into Mess Creek. Sharp intrusive contacts with Permian limestone are exposed west of Arctic Lake. The stock appears to intrude granite of Mississippian age, but no clear contact was observed. The pluton is post-Permian, based on intrusive relationships, and correlated on its textural and compositional similarity with porphyritic monzonite near Newmont Lake in the Forrest Kerr map area. In outcrop, the monzonite weathers light pink and is brown or greenish purple on fresh surfaces. It is characterized by about 10 per cent plagioclase and 15 to 20 per cent oxidized hornblende phenocrysts in an aphanitic, hematized matrix.

Late Triassic and Younger

Stocks, sills and dikes of intermediate to felsic composition intrude Late Triassic rocks east of Forrest Kerr fault and Early Jurassic rocks south of More Creek.

Serpentinized peridotite plugs (**lTum**) and fault slices crop out southwest and west of Arctic Lake. The intrusions are medium grained, equigranular and olive-green on fresh surfaces. They weather dun to dark green and commonly have zones of pervasive, rusty weathering carbonate veins. Where exposed, contacts with adjacent Permian limestone and Triassic sedimentary rocks are faults.

Dikes of coarsely porphyritic syenite (**lTs**) are very common cutting Late Triassic rocks between Hankin Peak and More Creek. They range from a metre to over 20 metres in width. Tabular phenocrysts of potassium feldspar in the syenite range in size from 2 to over 30 millimetres and average 20 per cent of the rock. They are grey, pink or, where chloritized, green. The crystals often impart a trachytic texture to the rock. The groundmass of these dikes is either grey or pink, and equigranular or aphanitic. Sedimentary rocks are often hydrothermally altered adjacent to the syenites and copper mineralization commonly occurs within and adjacent to the dikes.

Early Jurassic and Younger

About 6 kilometres south of Hankin Peak, a series of diorite sills (**eJd**) up to 100 metres wide intrudes Late Triassic siltstones and sandstones. They are fine to medium grained and equigranular with subequal amounts of plagioclase and pyroxene. Contacts with the enclosing sedimentary rocks are often well exposed and knife sharp. The only contact effect is an increase in the induration of the sediments and minor addition of epidote and chlorite. Some of the sills have poorly developed columnar joints. A similar diorite sill intrudes both siltstone and green andesitic tuffs 2 kilometres east of Hankin Peak. It has a distinct felty texture imparted by 40 to 50 per cent plagioclase laths to 4 millimetres in length; equigranular textures are also common. North of Hankin Peak, propylitized, equigranular diorite appears to intrude Late Triassic volcanic rocks. Relationships with the volcanic rocks are confusing because intrusive textures repeatedly grade in and out of pyroclastic textures.

A stock of monzonite to syenite (**eJmz**) intrudes siltstones and volcanic rocks in the same area as the diorite sill swarm, 6 kilometres south of Hankin Peak. The intrusion is mainly light grey to pink-weathering, equigranular, medium-grained monzonite, but grades into medium-grey weathering, seriate-textured syenite near its base. Phenocrysts of potassium feldspar range up to 1 centimetre in size. Fine, chloritized biotite occurs to about 2 per cent. A similar stock intrudes Early Jurassic rocks south of More Creek on the GOZ/RDN property.

South of More Creek, numerous dikes and sills of dark green-grey, fine to coarse-grained gabbro (Read *et al.*, 1989) intrude Early and Middle Jurassic siltstone and sandstone. Textures vary with the size of the intrusions. Smaller dikes (less than about 2 metres in width) are fine grained and equigranular. Larger dikes and stocks, though mainly equigranular, are commonly felty textured with slender laths of plagioclase to 4 millimetres in length. Anhedral pyroxene is interstitial to the plagioclase laths. Some stocks are coarse grained and weather light grey with 10 to 20 per cent dark green chloritic clinopyroxene to 5 millimetres in size. These intrusions are thought to be feeders to the basaltic pillow lavas and flow breccias of Unit **mJHb.**

Lamprophyre dikes intrude Late Triassic rocks east of Forrest Kerr fault. A 2-metre dike also intrudes Late Triassic (?) rocks southwest of Arctic Lake, and another 1-metre dike intrudes an andesitic dike complex of probable Mississippian age or younger near the south edge of the map area. The dikes are up to 10 metres wide and have conspicuous biotite phenocrysts up to 2 centimetres in size. The matrix grain size averages 2 to 4 millimetres.

A basaltic dike 1.5 metres wide, with 2 to 5 per cent vitreous plagioclase and a pristine grey groundmass, intrudes schists along the east side of the headwaters of Mess Creek. This is the only dike noted which has a lithology identical to the Tertiary or younger basalt flows, and is probably a feeder to them.

STRUCTURE

The structural grain of the map area is controlled by north-trending faults. Polyphase deformation has affected all rocks; those west of the Forrest Kerr fault are affected by an earlier phase not present in younger rocks east of the fault. In general, Paleozoic rocks are penetratively deformed, metamorphosed and affected by four phases of folding. Early, low-angle ductile shearing in Paleozoic rocks has interleaved panels of largely undeformed rocks with more deformed rocks of similiar age. Movement along these shear zones is east-directed and associated with early isoclinal folding. The age and relationships of thrusting are unknown. The anisotropic deformation of Mesozoic rocks reflects the competency contrasts between volcanic and sedimentary units and Paleozoic metamorphic rocks. South of More Creek, rocks as young as Early and Middle Jurassic are affected by two macroscopic, nearly orthogonal fold events.

FOLDS

Read *et al.* (1989) describe three phases of folding in the Iskut River and More Creek areas: a post-Early Permian to pre-Middle Triassic phase (D_1), a post-Middle to Late Jurassic phase (D_2), and similarly aged phase (D_3), which is orthogonal to D_2. Holbek (1988) and Elsby (1992, this volume) recognized an additional phase of folding (D_4) within Paleozoic rocks west of Mess Creek and west of Forrest Kerr Creek, respectively.

The earliest deformation (D_1) is characterized by a prominent, northeast-striking, moderately northwest-dipping penetrative foliation. This foliation is axial planar to northwest-trending, mesoscopic, recumbent isoclinal folds, which have an overall east vergence. Development of axial planar foliation (S_1) is prominent in schists west of Mess Creek and coincided with lower greenschist grade metamorphism. Triassic and younger rocks lack these first-phase folds and foliations. Associated with D_1 are numerous discrete west-dipping layer-parallel ductile shear zones which separate packages of deformed and largely undeformed rocks. Shearing along these zones is east directed.

The second phase (D_2) deforms and transposes S_1 in Paleozoic rocks and (?) deforms bedding (S_0) in Mesozoic rocks. It is accompanied by lower greenschist grade metamorphism and characterized by northwest-trending recumbent to moderately upright, southeast-plunging isoclinal to open folds in Paleozoic rocks and upright northwest-trending open folds in Mesozoic rocks. Second phase cleavage (S_2) in Paleozoic rocks is a southwest-dipping, locally developed axial planar cleavage. In the Mesozoic rocks, S_2 is characterized by fracture and crenulation cleavage.

The third phase (D_3) is characterized by mesoscopic, disharmonic upright, open to tight crenulation folds and kink bands which deform all earlier structures. Fold axes plunge gently westward, axial planes dip steeply south. Third phase cleavage (S_3) is defined by a strong crenulation cleavage in Paleozoic rocks and a fracture cleavage in Mesozoic rocks. No significant fold development associated with (D_3) is recognized in the Paleozoic rocks. East of Forrest Kerr fault, D_3 is characterized by typically open, upright, east and northeast-trending folds. The third deformation accompanied north-south compression.

The fourth phase (D_4) folds are moderate to open north-trending upright mesoscopic to macroscopic structures with fold wavelengths up to several kilometres. Folds are mainly north or south plunging, chevron or open box-folds and minor kink bands. Folds are similar in Paleozoic and Mesozoic rocks. Folding close to the Forrest Kerr fault is tight, disharmonic and asymmetric and becomes progressively more open eastward, away from the fault. Everywhere S_4 is developed as spaced crenulation and fracture cleavage.

FAULTS

Regional-scale faults strike north (Souther, 1972) and control the distribution of tectonostratigraphic packages. Other fault trends are mainly northeasterly to northwesterly. East and northeasterly trending structures are important controls for Mesozoic mineralization. The Forrest Kerr fault trends northerly and separates Mesozoic volcanic and sedimentary rocks on the east from Paleozoic metavolcanic and metasedimentary rocks and coeval granitic plutons on the west (Figure 1-14-2). The fault is generally vertical to steeply east dipping. Slickensides measured on the fault plane plunge 24° at 181° and indicate a left-lateral strike-slip component of movement. Read *et al.* (1989) suggest a minimum of 2 kilometres of east-side-down and 2.5 kilometres of left-lateral oblique-slip motion on the fault north of the Iskut River. The deep-rooted nature of this north-trending structure is evidenced by the peralkaline character of the Mount Edziza volcanic complex (Souther and Symons, 1974), which is typical of melts produced by crustal rifting. Normal faulting has displaced flows as young as 20 000 years but movement occurred before 1340 years B.P. (Souther, 1970).

The abrupt topographic contrast across Mess Creek marks a north-trending fault zone which separates the rugged high peaks of Late Triassic volcanics on the west from Paleozoic rocks of the Arctic Lake plateau east of Mess Creek. North-northeast-trending splay faults and block faults are related to the regional trend. These faults have produced an abrupt escarpment on the east side of Mess Creek and control alteration and copper gold mineralization on the Bam 8 and Bam 10 claims. The Mess Creek fault was active from Early Jurassic to Recent time (Souther and Symons, 1974).

Northerly trending, gently-dipping ductile thrust faults are exposed west of Mess Creek (Holbek, 1988 and this study). These zones occur within sericite and chlorite-sericite schists and are related to east-directed ductile shearing active during D_1 deformation and probably continued into D_2. On the BJ property the competency contrast between quartz-sericite schist (DSqs) and metadiorite (JDd) has localized easterly directed thrusting along this contact.

EXPLORATION ACTIVITY

The major exploration activity in 1991 was focused west of the map area at the Galore Creek alkaline porphyry copper-gold deposit. Kennco Explorations (Canada) Limited began reassessing the geology and mineral potential of

TABLE 1-14-1
MINERAL OCCURRENCES IN THE MORE CREEK MAP AREA 104G/2

Type Prob. Age	MINFILE Name 104G	Host	Commodity	Description	Reference
STRATABOUND VEINS					
Early Jurassic	GOZ/RDN	lJHr, eJmz	Au, Ag, Zn, Cu, Pb	Gold-enriched chalcopyrite, sphalerite, galena, pyrite and arsenopyrite-bearing veins hosted in silicified and pyritized Mount Dilworth equivalent. Mineralization and alteration related to coeval subvolcanic feldspar porphyritic monzonite intrusives. WEDGE ZONE 11.6 g/t Au over 4.4 m SOUTH BOUNDARY ZONE 23.9 g/t Au over 11.6 m MAIN GOSSAN ZONE 18.6 g/t Au over 0.4 m	Savelle (1990)
STRATIFORM MASSIVE SULPHIDE					
Devonian-Mississippian	FOREMORE	DSst, DSfv DSlm	Zn, Pb, Cu, Ag	Laminated sphalerite and galena occurs in felsic volcanic horizons within foliated package of grphitic schists, argillites and intermediate to mafic volcanics of Devonian-Mississippian age. Mineralized boulders include pyrite, sphalerite and chalcopyrite-rich varieties. Cu% Pb% Zn% Ag g/t Au g/t Fe% chalcopyrite-rich (n=12) 2.3 0.5 6.2 186 1.5 16 sphalerite-rich (n=29) 0.22 3.5 10.2 96 1 16 pyrite-rich (n=112) trace 1 6.2 78 nil 23	Barnes (1989), Mawer (1988)
GOLD-COPPER PORPHYRY					
Late Triassic - Early Jurassic 79	LITTLE LES, TWO MORE	uTSs, lTs	Cu, Au, Ag	Disseminated and veinlet chalcopyrite mineralization in a propylitic-pyrite alteration zone associated with potassium feldspar porphyry syenite dikes grab sample, 5.9% Cu and 13.1 g/t Au.	Bobyn (1990), Folk (1981)
Late Triassic-Early Jurassic	LUCIFER	uTSv, lTs	Cu, Au	Structurally controlled propylitic alteration zone (1 x 2 km) coincident with potassium feldspar porphyry syenite dike swarm. Mineralization includes chalcopyrite, galena and gold in quartz-carbonate pyrite veins.	Baerg and Wong (1991)
Late Triassic-Early Jurassic	BIS BISKUT	uTSsn, lTs	Au, Au, Cu, Pb, Zn	Quart-sericite-pyrite-clay alteration zone (300 m x 50-100 m wide). All original textures obliterated by supergene leaching. Contains up to 5% pyrite, minor galena and arsenopyrite.	Brown (1990)
MESOTHERMAL GOLD-SILVER-QUARTZ VEINS					
Early Jurassic 27	BAM 8, ARCTIC	PScg, PSlm	Cu, Ag, Zn	Disseminated blebs and veinlets of tetrahedrite, minor chalcopyrite, pyrite, sphalerite and galena occupy fractures and breccia zones in limestone, sandstone and conglomerate. Mineralization and carbonate alteration follow northeasterly trending structures. INVENTORY Tonnes Cu% Ag g/t Southwest Zone 299 400 0.76 N.A. East Zone 4 540 2.45 17.83	Dearin (1983), Gillen *et al.* (1984), Rayner (1965), Souther (1972)
Early Jurassic 110	BAM 10	Mg, Md	Au, Ag, Bi, Sb	Gold and fine-grained pyrite occur in quartz and carbonate veinlets in fractured granite. Discontinuous mineralization occupies silicified and sericitized fault and shear zones in the granite. Gold values range from 8.57 g/t over 18.9 m in trench 86-1 to 1.72 g/t over 2.43 m in DDH 87-1, drilled to test the ground beneath Trench 86-1.	Diner (1987), Hewgill and Walton (1986), Walton (1986)
Early Jurassic 70	BJ	DSqs, lDd	Au, Cu, Pb, Zn, Ag	Mineralization includes mesothermal quartz veins and an iron carbonate breccia zone. Veins contain pyrite, tetrahedrite, chalcopyrite, sphalerite, trace arsenopyrite, galena, gold and prominent iron-carbonate alteration envelope. Northeast-trending quartz veins crosscut strata, iron carbonate breccia is strataform. Free gold occurs in creeks below the showing.	Folk (1986), Holbek (1982), Holbek (1988)
IRON-COPPER-GOLD SKARNS					
	DUNDEE, GLA	DSst, Mg, PP	Fe, Cu, Zn, Au	Iron-copper skarns develop where feldspar-porphyritic andesite dikes intrude granite and carbonate pendant rocks. Mineralization comprises magnetite and lesser pyrite, pyrrhotite, chalcopyrite, sphalerite and gold.	Webster *et al.* (1991)

the Central zone (125 million tonnes, 1.06% copper, 0.40 g/t gold and 7.7 g/t silver). Several properties in the More Creek map area were actively explored this year. Noranda Exploration Company Limited and joint venture partner High Frontier Resources Ltd. carried out mapping, prospecting, soil sampling, ground magnetic and electromagnetic surveys and drilled ten holes on the GOZ/RDN property. Drilling resumed in September with a total of 2000 metres projected for the entire 1991 program. Noranda also conducted mapping and sampling followed by magnetic and induced polarization surveys and two diamond-drill holes on the Lucifer property. Cominco Ltd. continued detailed lithostratigraphic and biostratigraphic mapping on the Foremore prospect, 15 kilometres up-ice from the 1990 drilling. Keewatin Engineering Ltd. carried out exploration on the Arctic claims which cover the Little Les mineral occurrence.

MINERAL PROSPECTS

Mineral showings and prospects are concentrated south of Hankin Peak, southwest of Arctic Lake, south of the headwaters of Mess Creek and adjacent to the Forrest Kerr fault. They can be grouped into the following categories: stratabound polymetallic massive sulphide; stratiform massive sulphide; porphyry copper-gold; gold-silver-quartz vein and replacement deposits; and iron-copper-gold skarn. Data on individual occurrences are summarized in Table 1-14-1; locations are shown on Figures 1-14-3 and 1-14-4.

At least two separate mineralizing events are postulated for deposits within the map area. Devonian limestone and volcanic rocks host conformable, massive polymetallic sulphide occurrences. Preliminary lead isotope data on boulders from the Foremore property define two clusters. On the Wrangellia growth curve these clusters correspond with a Devonian and possibly Mississippian model ages. These data points cluster with data from the Tulsequah Chief and Myra Falls deposits (M. Westcott, personal communication, 1991).

Alkalic porphyry copper-gold mineralization south of Hankin Peak is hosted by Late Triassic volcanics and subvolcanic intrusives. In the region this type of mineralization is generally latest Triassic to Early Jurassic in age. Lead isotope studies of galena samples from the GOZ/RDN property and a gold-bearing vein on the Foremore properties both plot in the Jurassic cluster (Godwin *et al.*, 1991). An Early Jurassic (194±6 Ma; Holbek, 1988) age for mineralization is inferred from K-Ar dating of chrome-bearing muscovite from a carbonate-sulphide vein on the BJ property.

Silver-rich base metal mineralization of Tertiary age is widespread to the east and elsewhere in northwestern British Columbia, but none has been recognized in the More Creek map area.

STRATABOUND-VEIN DEPOSITS

The GOZ/RDN property is located west of the Forrest Kerr fault, 5 kilometres south of the confluence of South More and More creeks, within an Early to Middle Jurassic package of volcanic and fine clastic rocks (Figure 1-14-3). In 1990, 1545.5 metres of diamond drilling was completed in 15 holes. The best results included 7.8 metres grading 7.88 grams per tonne gold and 4.4 metres of 11.65 grams per tonne gold.

The claims are underlain by maroon intermediate volcanic rocks comprising felsic tuffs and rhyolite flows which are overlain or interlayered with a sandstone-siltstone unit, basalt flows and tuffs. The hostrocks are age equivalents of the Mount Dilworth Formation and Eskay Creek facies of the Salmon River Formation. Mineralization consists of gold-enriched polymetallic quartz veins in silicified and pyritized rhyolite and felsic tuffs and subvolcanic porphyritic monzonite intrusions. The exploration target is a precious metal enriched polymetallic massive sulphide deposit similiar to Eskay Creek.

In 1991 exploration on the claims continued. Three areas of mineralization have received the most attention: the Wedge zone, the Main Gossan zone and the South Boundary zone. The most recent results released in the Northern Miner (September 16, 1991) report an 11.6-metre intersection in the South Boundary zone grading 2?.9 grams per tonne gold with minor base metals. This drill hole was collared in plagioclase-porphyritic andesitic rocks intruded by porphyritic-syenite dikes. The details of this mineralization are not known, however, the spatial and genetic association of gold and copper mineralization with porphyritic syenite dikes is a regional phenomena associated with Late Triassic to Early Jurassic porphyry deposits. The Main Gossan zone is a large, spectacular ferricrete gossan and argillic alteration zone associated with a subvolcanic monzonite intrusion. The gossan zone contains disseminated copper and gold. This style of mineralization may better fit a porphyry classification.

Stratabound mineralization consists of massive to brecciated quartz veins and stringer zones (Wedge Zone) hosted in silicified felsic volcanics of the Mount Dilworth Formation. The gold-enriched quartz veins strike north and generally dip easterly, parallel to the stratigraphy. The veins are narrow (about 1 metre) and contain from 5 to 10 per cent sulphides of copper, zinc, lead and arsenic in a quartz gangue. Drilling indicates the felsic succession is underlain by maroon, feldspar-porphyritic volcaniclastics, equivalent to the Betty Creek Formation, and black siltstones. Alteration and mineralization are related to coeval(?) subvolcanic porphyritic monzonite intrusions.

STRATIFORM MASSIVE SULPHIDE

Cominco's Foremore claims are located at the headwaters of the south tributary of More Creek, about 10 kilometres north of Forrest Kerr airstrip (Figure 1-14-3). The exploration target is the source of massive sphalerite and pyrite-bearing boulders. Electromagnetic conductors located below 120 metres of glacier ice were drill tested in 1990. Four holes were collared, three reached bedrock. Drilling intersected graphitic shear zones. The property is underlain by Stikine assemblage rocks: foliated basaltic flows, volcaniclastics, sediments and limestones as old as Early Devonian. Foremore float resembles Kuroko volcanogenic massive sulphide ore and similiar Devonian-Mississippian

Stikine assemblage rocks are potential exploration targets for deposits of the Kuroko type.

Several thousand mineralized boulders have been found on the Foremore claims in outwash plains at the eastern and northern lobes of the More Glacier. The distribution of polymetallic massive sulphide float suggests the source is beneath the main icesheet of the glacier. Boulders vary mineralogically, including pyrite-rich, zinc-rich, and copper-rich (Table 1-14-1) and texturally from massive to laminated. This mineral and textural variation suggests either a single zoned sulphide body or possibly several distinct bodies. Limestone boulders host massive sulphide replacements. One such boulder contains stromatoporoid *Favosites* sp. of Late Ordivician to Middle Devonian age (Logan *et al.*, 1990a).

In the North zone, felsic volcanic horizons host finely laminated and disseminated galena, sphalerite and pyrite mineralization. These felsic (quartz-eye) volcanics occur within a penetratively foliated sequence of graphitic schists, argillites and intermediate to mafic volcanics. Assay results from outcrop sampling average 87 ppb gold, 8 grams per tonne silver, 0.1 per cent copper, 0.3 per cent lead and 2.7 per cent zinc over an average sample width of 0.4 metre (Barnes, 1989)

Porphyry Copper-Gold Deposits

Porphyry deposits are regionally important exploration targets (*e.g.*, Galore Creek and Schaft Creek). Schaft Creek is a calcalkaline copper-molybdenum deposit of 1 billion

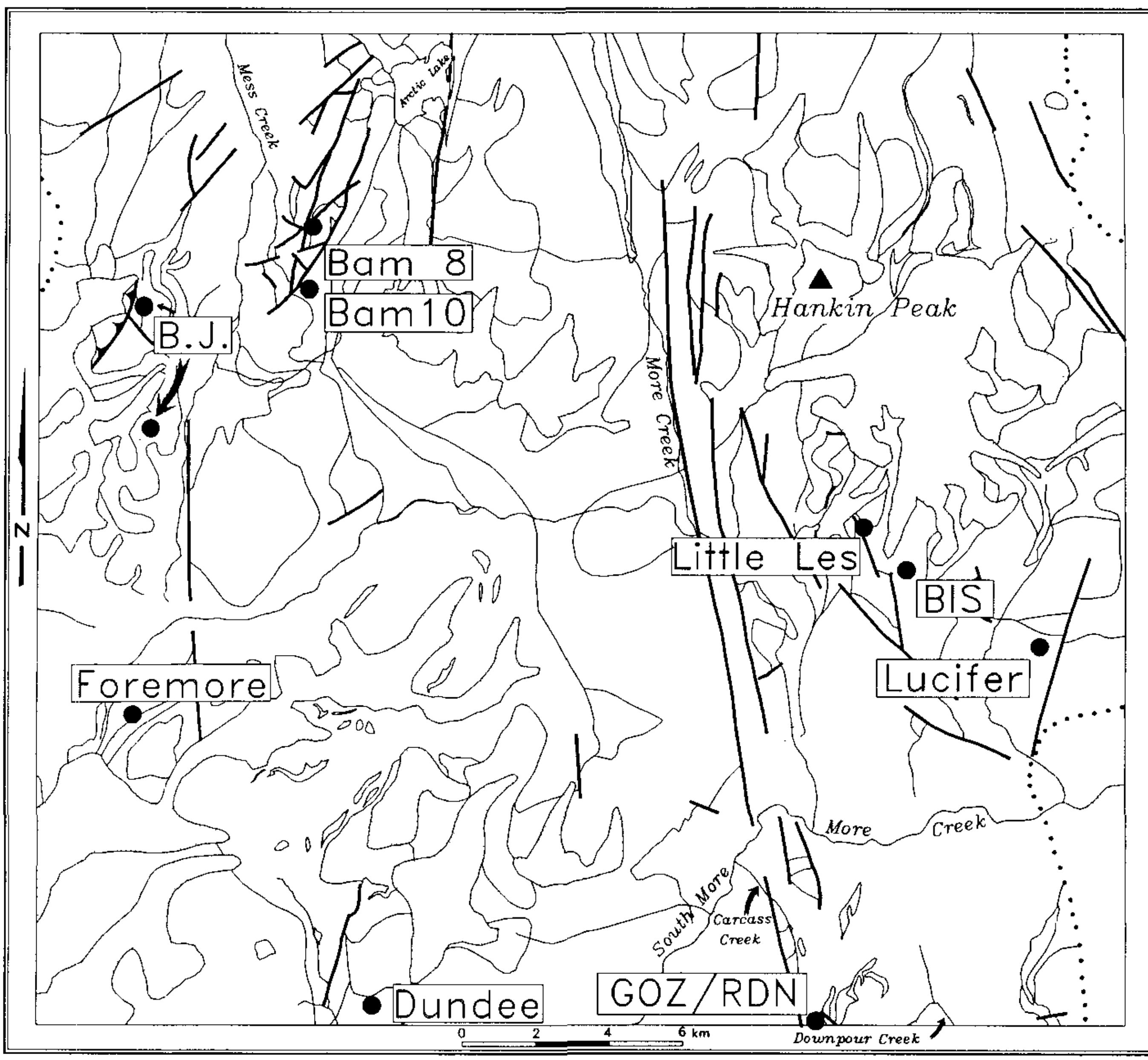

Figure 1-14-3. Mineral occurrence map showing locations of occurrences discussed in the text.

tonnes, which contains 0.12 gram per tonne gold. Galore Creek is an alkaline copper deposit of 125 million tonnes with a gold grade of 0.4 gram per tonne. The alkaline deposits are generally enriched in copper and gold and associated with high-level intrusions of potassium feldspar megacrystic syenite.

The Lucifer property is located 2 kilometres north of More Creek (Figure 1-14-3). Tuffaceous sediments, reworked tuffs and minor limestones of the Upper Triassic Stuhini Group underlie the claims. Maroon ash-tuffs and tuffaceous conglomerates containing coarse potassium feldspar crystals crop out high on the ridge west of the alteration zone. These lithologies are intruded by northerly trending megacrystic potassium feldspar porphyry dikes.

The area of interest occupies the headwall and steep upper reaches of a south-draining tributary of More Creek. It consists of a large (1 x 2 km) northerly trending limonite-carbonate-pyrite alteration zone. Weak silicification in the form of narrow stringer zones and veinlets crosscuts this chiefly propyllitic alteration zone. The alteration zone lies west of a northeast-trending fault and coincides with a northeast-striking swarm of megacrystic potassium feldspar porphyry dikes. Pyritic and propylitically altered and unaltered dikes crosscut the zone and indicate complex and episodic intrusive and mineralizing events. Mineralization consists of quartz-carbonate-pyrite veins containing chalcopyrite and galena. Results from the two 1991 diamond-drill holes do not explain the anomalous gold soil geochemistry of the alteration zone (R. Baerg, personal communication, 1991).

The Little Les (MINFILE 104G 079) limonitic gossan crops out 9 kilometres north of the confluence of More and South More creeks on the Arctic claims (Figure 1-14-3). It is derived from a pyrite-rich alteration envelope which flanks a 200 by 50 metre core zone of propylitically altered andesite flows and tuffs. Alteration and mineralization are related to intrusion by syenite porphyry dikes. Mineralization consists of 2 to 5 per cent disseminated and fracture-filling chalcopyrite and traces of galena and molybdenite.

Midway between the Lucifer and Little Les showings is the Bis occurrence (Figure 1-14-3), a substantial limonitic gossan easily visible from the air. This northeast-trending gossan, 300 metres long by 50 to 100 metres wide, is hosted in volcanics, tuffaceous sediments and limestone. The gossan consists predominantly of limonite, clay, sericite, pyrite and quartz. All original textures are obliterated. The gossan contains up to 5 per cent disseminated pyrite and traces of arsenopyrite and galena. A single grab sample from the gossan returned 16.1 grams per tonne gold (Bobyn, 1990). The gossan was mapped by Souther (1972) as a Late Cretaceous to Tertiary felsite dike. Bobyn (1990) interpreted the felsite as an Early Jurassic, Mount Dilworth equivalent (after Read *et al.*, 1989).

VEIN DEPOSITS

The Bam 8 prospect (MINFILE 104G 02?) is located 4 kilometres southwest of Arctic Lake on top of the eastern escarpment of Mess Creek valley (Figure 1-14-3). In 1967, diamond drilling defined the Southwest zone containing 299 400 tonnes grading 0.76 per cent copper and the East zone containing 4540 tonnes grading 2.45 per cent copper and 17.83 grams per tonne silver.

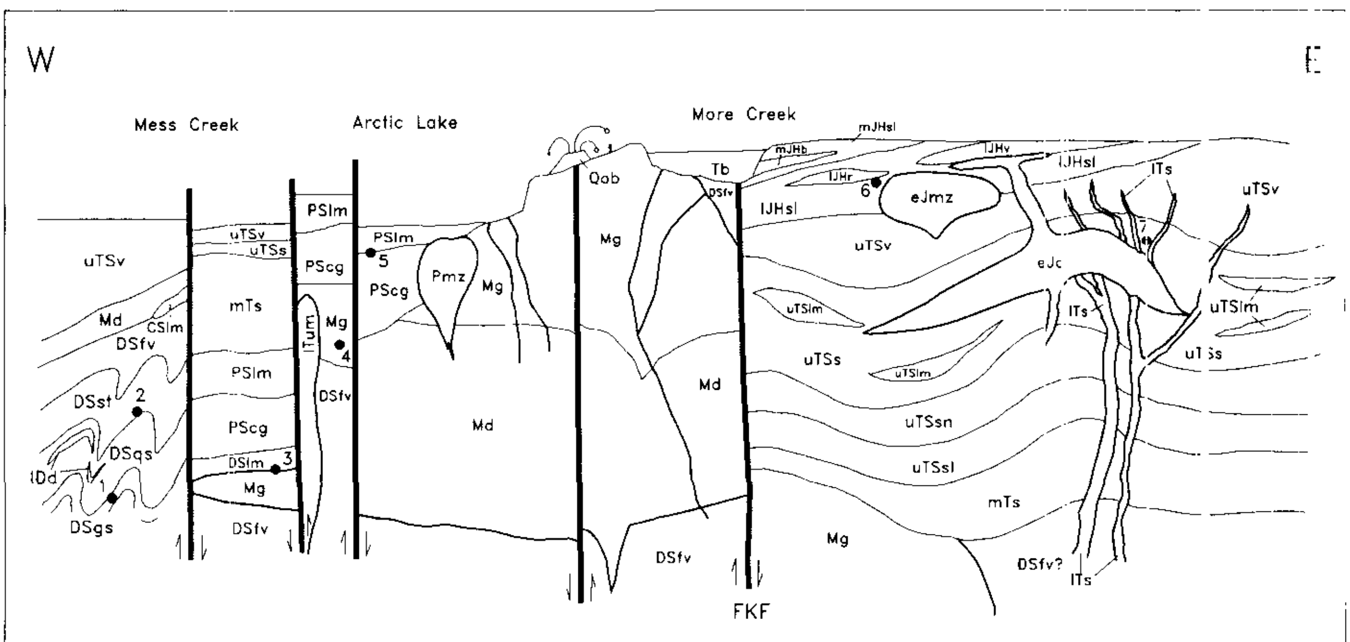

Figure 1-14-4. Schematic representation showing stratigraphic relationships of the various units across the northern part of the More Creek map area. Mineral occurrences are shown in their respective stratigraphic positions. See text and Figure 1-14-2 legend for description of units. Numbers correspond to mineral occurrences; 1=Foremore, 2=BJ, 3=Dundee, 4=Bam 10, 5=Bam 8, 6=GOZ/RDN, 7=Lucifer, Little Les and Bis. FKF=Forrest Kerr fault.

This property is underlain by green chlorite schists, purple schistose tuffs and flows and thin limestone (**DSst**) which are overlain by maroon polymictic granite-bearing cobble conglomerate (**PScg**). Thick-bedded Permian limestone (**PSlm**) and limonitic brecciated dolomitic limestone conformably overly the conglomerate and host most of the copper and silver mineralization. Overlying the carbonates are variably altered and mineralized, thin-bedded limy fetid sandstone and siltstone (**mTs**) and conglomerate (**uTSs**). Granite and diorite underlie much of the Arctic Lake plateau, east of the prospect. They do not intrude Permian or younger rocks and have been tentatively dated (K-Ar) as Early Mississippian. Fine-grained and porphyritic plagioclase hornblende monzonite dikes (**Pmz**) cut the granite and limestone. Serpentinized peridotite bodies are intruded along northeast-trending fault zones (**lTum**).

Mineralization consists of disseminations, stringers and east-northeast-trending veinlets of tetrahedrite, with minor chalcopyrite, pyrite, sphalerite and galena. Secondary minerals include azurite and malachite. Alteration includes dolomitization of limestone, carbonitization of volcanic rocks, dolomite, sandstone and conglomerate, and hydrothermal alteration and associated quartz veining in the granitic rocks (Gillan *et al.*, 1984). Alteration (limonitic orange cliffs) and mineralization are spatially related to north-trending regional faults and northeast-trending splays off them.

The Bam 10 showing (MINFILE 104G 110) is located 1 kilometre southwest of Bam 8 and is lower in the same stratigraphy. Strongly schistose flows, tuff and subordinate limestone (**DSst**) underlie the claims. Quartz-rich granite and diorite intrude these metavolcanics. The contact, which is in part structural, dips moderately westward. Diamond drilling in 1987 totalled 837 metres in nine holes. From drilling data, Diner (1987) recognized predictable and mappable alteration halos peripheral to mineralization, and that most mineralization occurs within 50 metres of the granite contact. Mineralized zones are poddy and associated with carbonate, chlorite and sericite alteration and silicification developed along north and northeast-trending faults in the granite. Mineralization consists of gold and fine-grained blebs of pyrite, chalcopyrite, galena and rare molybdenite in quartz and carbonate veinlets hosted within fractured, sericitized and silicifed granite.

The BJ showing (MINFILE 104G 070) is located west of Mess Creek (Figure 1-14-3). This occurrence is hosted by quartz-sericite schists (**DSqs**), part of a polydeformed and metamorphosed volcanic and sedimentary succession of Devonian to Mississippian age unconformably overlain by Upper Triassic volcanic and sedimentary rocks to the west.

Mineralization includes precious metal bearing mesothermal quartz veins and an iron-carbonate breccia zone. In addition, bull quartz veins parallel to foliation and related to greenschist metamorphism are common. These metamorphogenic veins contain minor pyrite but no precious metals. They are deformed, often recumbently folded and predate or are synchronous with early deformation. Younger, Early Jurassic (Holbek, 1988) quartz and carbonate veins trend east to northeast across an earlier foliation. Brown, limonitic-weathering carbonate alteration is commonly associated with faults, breccia zones and quartz veining. The veins contain pyrite, tetrahedrite, chalcopyrite, sphalerite and traces of arsenopyrite, galena, hematite and gold.

A zone of quartz veins is localized along the faulted contact between metadiorite (**lDd**) and chlorite-sericite schists (**DSqs**) on the Windy claim. Gold values average 0.34 gram per tonne with a single sample assaying 1.36 grams per tonne (Folk, 1986). An extensive iron carbonate breccia zone crops out on the Bee Jay claims, 5 kilometres to the south. Gold values range from 0.34 to 1.71 grams per tonne (Folk, 1986).

SKARN

The Dundee showing straddles the south fork of More Creek 13 kilometres southwest of its confluence with More Creek (Figure 1-14-3). The property is underlain by hornfelsed and silicified Paleozoic rocks intruded by a Mississippian or younger monzonite to biotite granite pluton. Mineralized skarns are developed where younger feldspar-porphyritic andesite dikes crosscut limestone bodies and the main intrusive body. There appear to be at least two stages of skarning; one is related to the main intrusion which surrounds the pendant rocks, the second to later dikes. Magnetite sulphide endoskarns occur in the pegmatitic diorite dikes. Coarse-grained diopside envelopes formed adjacent to the dikes. Pyrite and pyrrhotite mineralization is best developed in noncalcareous pendant rocks; garnet, diopside, epidote, magnetite and chalcopyrite skarns occur in limestone bodies. Webster and Ray (1991) provide a detailed description of the geology and skarn mineralization.

SUMMARY

The More Creek area is underlain by three fault-bounded stratigraphic packages which, from west to east, consist of the middle to late Paleozoic Stikine assemblage, an Early Carboniferous or younger granitic pluton and, separated by the Forrest Kerr fault zone, a Mesozoic volcanic-plutonic assemblage of Stuhini and Hazelton Group rocks (Figures 1-14-2 and 1-14-4). West of the Forrest Kerr fault the oldest rocks are a thick package of Early Devonian to Early Carboniferous metasedimentary and bimodal metavolcanic rocks intruded in part by early Mississippian (340±12 Ma, K/Ar) quartz monzonite to quartz diorite plutons (**Mg** and **Md**). A pre-Permian quartz-grain, granite-clast conglomerate (**PScg**) with tuff interlayers marks a profound post-Carboniferous unconformity. Clasts resemble the quartz-rich granite of the early Mississippian More Creek pluton. Early Permian limestones, the regional hallmark of the Stikine assemblage, are here no thicker than 200 metres. The limestone is overlain paraconformably by Middle Triassic sedimentary rocks. Rocks of the Late Triassic Stuhini Group conformably overly the Middle Triassic rocks.

East of the Forrest Kerr fault are Middle(?) Triassic rocks and possibly unrecognized Paleozoic rocks. North of More Creek, the Stuhini Group is a succession of chiefly volcanic arc derived sediments, reworked tuffs and subordinate flows more than 2000 metres thick. South of More Creek is an Early to Middle Jurassic succession of at least 1500 metres of thin-bedded sediments, tuffs, rhyolite and basalt.

The distribution of mineral occurrences, their stratigraphic positions and relationships to structure and intrusions are shown in Figure 1-14-4. Stratabound polymetallic sulphide mineralization is hosted by mid-Paleozoic rocks of the Stikine assemblage. Early Jurassic mineralization is manifest as: stratabound gold-enriched polymetallic massive sulphides in rocks correlated with the Eskay Creek facies of the Salmon River Formation; alkalic copper-gold porphyries in Upper Triassic Stuhini Group strata and feldspar porphyry dikes; mesothermal gold-quartz and silver-copper veins cutting Paleozoic metavolcanic and plutonic rocks. Pre-Mississippian(?) rocks host skarn mineralization, age constraints are not known.

ACKNOWLEDGMENTS

The authors would like to thank James Gough for his good natured and capable assistance in the field. Thanks also to Mike Savell and Rob Berg of Noranda Exploration Company Limited for sharing their alluvial fan, logistics and geological expertise, and Don Harrison for fossil submissions. Ron Batty and Darrell Adzich of Vancouver Island Helicopters provided safe, friendly and dependable flying. Wayne Bamber, Terry Poulton and Allan Pedder of the Institute of Sedimentary and Petroleum Geology in Calgary provided prompt and invaluable fossil identifications. This manuscript benefited from reviews by Bill McMillan, Brian Grant and John Newell.

REFERENCES

Alldrick, D.J. and Britton, J.M. (1988): Geology and Mineral Deposits of the Sulphurets Area (NTS 104A/15, 104A/12, 104B/8 and 104B/9); *B.C. Ministry of Energy, Mines and Petroleum Resources*, Open File 1988-4.

Anderson, R.G. (1989): A Stratigraphic, Plutonic, and Structural Framework for the Iskut River Map Area, Northwestern British Columbia; *in* Current Research, Part E, *Geological Survey of Canada*, Paper 89-1E, pages 145-154.

Anderson, R.G. and Bevier, M.L. (1990): A Note on Mesozoic and Tertiary K-Ar Geochronometry of Plutonic Suites, Iskut River Map Area, Northwestern British Columbia; *in* Current Research, Part E, *Geological Survey of Canada*, Paper 90-1E, pages 141-147.

Anderson, R.G. and Thorkelson, D.J. (1990): Mesozoic Stratigraphy and Setting for Some Mineral Deposits in the Iskut River Map Area, Northwestern British Columbia; *in* Current Research, Part E, *Geological Survey of Canada*, Paper 90-1E, pages 131-139.

Baerg, R. and Wong, T. (1991): Geological, Geochemical and Geophysical Report on the Lucifer Property; *B.C. Ministry of Energy, Mines and Petroleum Resources*, Assessment Report 21091.

Barnes, D.R. (1989): Geological-Geochemical Report, Foremore Group, Liard Mining Divison; *B.C. Ministry of Energy, Mines and Petroleum Resources*, Assessment Report 19379.

Bobyn, M.G. (1990): Geological Mapping, Prospecting and Geochemistry of the Arctic/Upper More Claim Group; *B.C. Ministry of Energy, Mines and Petroleum Resources*, Assessment Report 20667.

Brown, D.A. and Gunning M.H. (1989a): Geology of the Scud River Area, Northwestern British Columbia; *in* Geological Fieldwork 1988, *B.C. Ministry of Energy, Mines and Petroleum Resources*, Paper 1989-1, pages 251-267.

Brown, D.A. and Gunning M.H. (1989b): Geology, Geochemistry and Mineral Occurrences of the Scud River Area, Northwestern British Columbia (104G/5, 6); *B.C. Ministry of Energy, Mines and Petroleum Resources*, Open File 1989-7.

Brown, D.A., Greig, C.J. and Gunning M.H. (1990): Geology and Geochemistry of the Stikine River - Yehiniko Lake Area, Northwestern British Columbia (104G/11W, 12E); *B.C. Ministry of Energy, Mines and Petroleum Resources*, Open File 1990-1.

Brown, D.A., Harvey-Kelly, F.E.L., Neill, I. and Timmerman, J. (1992): Geology and Geochemistry of the Tahltan Lake and Parts of the Chutine River Map Areas, Northwestern British Columbia (104G/12W, 13); *B.C. Ministry of Energy, Mines and Petroleum Resources*, Open File 1992-2.

Brown, D.A., Logan, J.M., Gunning, M.H., Orchard, M.J. and Bamber, W.E. (1991): Stratigraphic Evolution of the Paleozoic Stikine Assemblage in the Stikine and Iskut Rivers Area, Northwestern British Columbia; *Canadian Journal of Earth Sciences*, Volume 28, pages 958-972.

Brown, R.F. (1990): Report on the Rock Geochemical Sampling in the Biskut Claim; *B.C. Ministry of Energy Mines and Petroleum Resources*, Assessment Report 19605.

Dearin, C. (1983): Evaluation of the Arctic Lake Property, Mess Creek Area; *B.C. Ministry of Energy, Mines and Petroleum Resources*, Assessment Report 11515.

Diner, Y. (1987): Geological, Geochemical and Geophysical Report on the Bam Claims; *B.C. Ministry of Energy, Mines and Petroleum Resources*, Assessment Report 17570.

Elsby, D.C. (1991): Structure, Ductile Thrusting and Mineralization within the Stikine Assemblage, South Forrest Kerr Area, Northwestern British Columbia (104B/10, 15); *in* Geological Fieldwork 1991, *B.C. Ministry of Energy, Mines and Petroleum Resources*, Grant, B. and Newell, J.M., Editors, Paper 1992-1, this volume.

Evanchick, C.A. (1991): Structural Relationships of the Skeena Fold Belt West of the Bowser Basin, Northwestern British Columbia; *Canadian Journal of Earth Sciences*, Volume 28, pages 973-983.

Folk, P. (1981): Geological and Geochemical Report on the More and Two More Claims; *B.C. Ministry of Energy, Mines and Petroleum Resources*, Assessment Report 9041.

Folk, P. (1986) Report on the Geology and Geochemistry of the Bee Jay Group of Claims; *B.C. Ministry of Energy, Mines and Petroleum Resources,* Assessment Report 14982.

Godwin, C.I., Pickering, A.D.R., Gabites, J.E. and Alldrick, D.J. (1991): Interpretation of Galena Lead Isotopes from the Stewart-Iskut Area (103O, P; 104A, B, G); *in* Geological Fieldwork 1990, *B.C. Ministry of Energy, Mines and Petroleum Resources,* Paper 1991-1, pages 235-243.

Gillan, J.F., Forster, D. and O'Donnell, M. (1984): Geological and Geochemical Evaluation of the Bam Claims; *B.C. Ministry of Energy, Mines and Petroleum Resources,* Assessment Report 12561.

Hewgill, W. and Walton, G. (1986): Geological, Geochemical, and Geophysical Report on the Bam Claims, *B.C. Ministry of Energy, Mines and Petroleum Resources,* Assessment Report 15827.

Holbek, P.M. (1982): Report on Geology and Soil Geochemistry of the BJ, Bee, Jay, Windy, Grey, Rainy, Day, Very, Fall, Valley Claims; *B.C. Ministry of Energy, Mines and Petroleum Resources,* Assessment Report 9692.

Holbek, P.M. (1988): Geology and Mineralization of the Stikine Assemblage, Mess Creek Area, Northwestern British Columbia; unpublished M.Sc. thesis, *The University of British Columbia,* 174 pages.

Kerr, F.A. (1948): Lower Stikine and Western Iskut River Areas, British Columbia; *Geological Survey of Canada,* Memoir 246, 94 pages.

Logan, J.M. and Koyanagi, V.M. (1989): Geology and Mineral Deposits of the Galore Creek Area, Northwestern B.C. (104G/3, 4); *in* Geological Fieldwork 1988, *B.C. Ministry of Energy, Mines and Petroleum Resources,* Paper 1989-1, pages 269-284.

Logan, J.M., Koyanagi, V.M. and Rhys, D. (1989): Geology and Mineral Occurrences of the Galore Creek Area, (104G/3, 4); *B.C. Ministry of Energy, Mines and Petroleum Resources,* Open File 1989-8

Logan. J.M., Koyanagi, V.M. and Drobe, J.R. (1990a): Geology of the Forrest Kerr Creek Area, Northwestern British Columbia (104B/15); *in* Geological Fieldwork 1989, *B.C. Ministry of Energy, Mines and Petroleum Resources,* Paper 1990-1, pages 127-140.

Logan, J.M., Koyanagi, V.M. and Drobe, J.R. (1990b): Geology, Geochemistry and Mineral Occurrences of the Forrest Kerr - Iskut River Area, Northwestern British Columbia (104B/10, 15); *B.C. Ministry of Energy, Mines and Petroleum Resources,* Open File 1990-2.

Mawer, A.B. (1988): Geological-Geochemical Report, Foremore Group; *B.C. Ministry of Energy, Mines and Petroleum Resources,* Assessment Report 18105.

Monger, J.W.H. (1970): Upper Paleozoic Rocks of the Stikine Arch, British Columbia; *in* Report of Activities, Part A, *Geological Survey of Canada,* Paper 70-1, pages 41-43.

Monger, J.W.H. (1977): Upper Paleozoic Rocks of Northwestern British Columbia; *in* Report of Activities, Part A, *Geological Survey of Canada,* Paper 77-1, Part A, pages 255-262.

Officiers of the Geological Survey of Canada (1957): Stikine River Area, Cassiar District, British Columbia; *Geological Survey of Canada,* Map 9-1957.

Poulton, T.P. (1991): Report on Seven Collections of Jurassic and Triassic(?) Fossils Collected by J. Logan and Colleagues in Telegraph Creek Map Area, B.C., in 1991 (NTS 104G/2); *Institute of Sedimentary and Petroleum Geology, Geological Survey of Canada,* Report No. J5-1991-TPP.

Rayner, G. (1965): Arctic Lake Examination, Bam Claim Group; *B.C. Ministry of Energy, Mines and Petroleum Resources,* Assessment Report 695.

Read, P.B., Brown, R.L., Psutka, J.F., Moore, J.M., Journeay, M., Lane, L.S. and Orchard, M.J. (1989): Geology of Parts of Snippaker Creek (104B/10), Forrest Kerr Creek (104B/15), Bob Quinn Lake (104B/16), Iskut River (104G/1), and More Creek (104G/2); *Geological Survey of Canada,* Open File 2094.

Savell, M. (1990): Geological, Geochemical, Geophysical and Diamond Drilling Report on the RDN and GOZ Mineral Claims; *B.C. Ministry of Energy, Mines and Petroleum Resources,* Assessment Report 20769.

Souther, J.G. (1970): Volcanism and its Relationship to Recent Crustal Movements in the Canadian Cordillera; *Canadian Journal of Earth Sciences,* Volume 7, pages 553-568.

Souther, J.G. (1971): Geology and Mineral Deposits of Tulsequah Map-area, British Columbia; *Geological Survey of Canada,* Memoir 362.

Souther, J.G. (1972): Telegraph Creek Map Area, British Columbia; *Geological Survey of Canada,* Paper 71-44, 38 pages.

Souther, J.G. (1988): Mount Edziza Volcanic Complex, British Columbia; *Geological Survey of Canada,* Map 1623A.

Souther, J.G. and Symons, D.T.A. (1974): Stratigraphy and Paleomagnetism of Mount Edziza Volcanic Complex, Northwestern British Columbia; *Geological Survey of Canada,* Paper 73-32, 48 pages.

Walton, G. (1986): Geochemical Survey, Bam Claims, *B.C. Ministry of Energy, Mines and Petroleum Resources,* Assessment Report 14859.

Webster, I.C.L. and Ray, G.E. (1991): Skarns in the Iskut River - Scud River Region, Northwest British Columbia; *in* Geological Fieldwork 1990, *B.C. Ministry of Energy, Mines and Petroleum Resources,* Paper 1991-1, pages 246-253.

Woodsworth, G.J., Anderson, R.G. and Armstrong, R.L. (1989): Plutonic Regimes in the Canadian Cordillera; *Geological Survey of Canada,* Open File 1983.

GEOLOGY OF THE CHUTINE RIVER – TAHLTAN LAKE AREA, NORTHWESTERN BRITISH COLUMBIA (104G/12W AND 13)

By D.A. Brown, F.E.L. Harvey-Kelly, I. Neill and J. Timmerman

KEYWORDS: Regional geology, Stikine River, Chutine River, Tahltan Lake, Stuhini Group, Stikine assemblage, Limpoke pluton, Rugged Mountain pluton.

INTRODUCTION

The third summer of 1:50 000-scale geological mapping was conducted in the Chutine River (104G/12W) and Tahltan Lake (104G/13) map areas. This work adjoins and locally updates mapping in the Yehiniko Lake and Scud River areas (Brown and Gunning, 1989a, b; Brown and Greig; 1990, Brown *et al.*, 1990). The project objectives are to provide new 1:50 000-scale geologic maps accompanied by up-to-date geochemical and mineral occurrence data, and an assessment of the mineral potential of the area. Geological highlights of the 1991 field season include the discovery of previously unrecognized phyllitic Stikine assemblage rocks north of the Barrington River; subdivision of the Stuhini Group; and identification of two small, previously unmapped Alaskan-type ultramafic bodies. Included here is a summary of preliminary observations and ideas, and a simplified version of the 1:50 000-scale geology map to be released as Open File 1992-2.

The study area was accessed by helicopter and float plane from Telegraph Creek, approximately 30 kilometres to the east (Figure 1-15-1). Previous geologic mapping was conducted by Kerr (1948) in the Stikine and Chutine river areas and by Souther (1959, 1972), who completed the entire Telegraph Creek (104G) 1:250 000-scale map area. Recent nearby mapping at 1:50 000-scale includes that by Logan and Koyanagi (1989a, b), Logan *et al.* (1990a, b; 1992a, b; Figure 1-15-1).

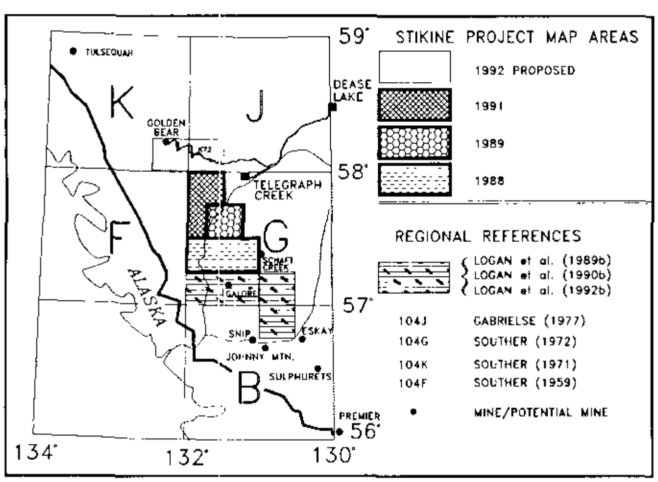

Figure 1-15-1. Location map for Stikine project with areas of previous work indicated.

The map area straddles the physiographic boundary between the dissected Tahltan Lake plateau on the east and the rugged, alpine-glaciated Coast Mountains on the west (Ryder, 1984). The plateau rolls gently between 1500 and 2000 metres elevation and is part of a large, late Tertiary erosional surface (Souther, 1971) covered by alpine vegetation and felsenmeer.

GENERAL GEOLOGIC SETTING

Strata of sedimentary and volcanic origin dominate the map area. They comprise the Paleozoic Stikine assemblage, eugeoclinal Late Triassic Stuhini Group and unnamed Miocene to Recent (?) rocks. In contrast, stratified rocks in the 1989 field area (Figure 1-15-1) to the southeast also include Early Jurassic Hazelton Group volcanic rocks, nonmarine clastic rocks of the Late Cretaceous to Tertiary (?) Sustut Group and continental volcanic rocks of the Eocene Sloko Group. Cutting these stratified rocks is a diverse suite of intrusive rocks ranging in age from Triassic to Eocene and in composition from granite to Alaskan-type ultramafite. For a more regional perspective of the geologic setting see Souther (1972) and Brown and Gunning (1989a).

STRATIGRAPHY

PALEOZOIC STIKINE ASSEMBLAGE (UNITS pPS, PS)

Four west-broadening structural culminations of Stikine assemblage rocks within the map area include those at Missusjay Creek, Chutine River, Barrington River and northwest of Little Tahltan Lake (Figure 1-15-2, 3). Two of those, Missusjay Creek and Chutine River are conspicuously outlined by thick, deformed Permian limestones. However, where these distinctive limestones are absent, correlation is less certain and based primarily on style and intensity of deformation which normally produces phyllitic fabrics and chevron folds in the sedimentary and volcanic rocks. Lithological and structural elements unique to each of these culminations are described below.

MISSUSJAY CULMINATION

The Missusjay culmination comprises a tight, southeast-verging syncline of Permian limestone underlain by phyllitic argillite, siltstone and siliceous siltstone (Unit pPSs; Brown *et al.*, 1990). The position of the contact and its relationship with Triassic rocks to the northwest remain uncertain.

CHUTINE ANTICLINE

The Chutine anticline was named by Kerr (1948) and is well exposed where dissected by the Chutine and Barring-

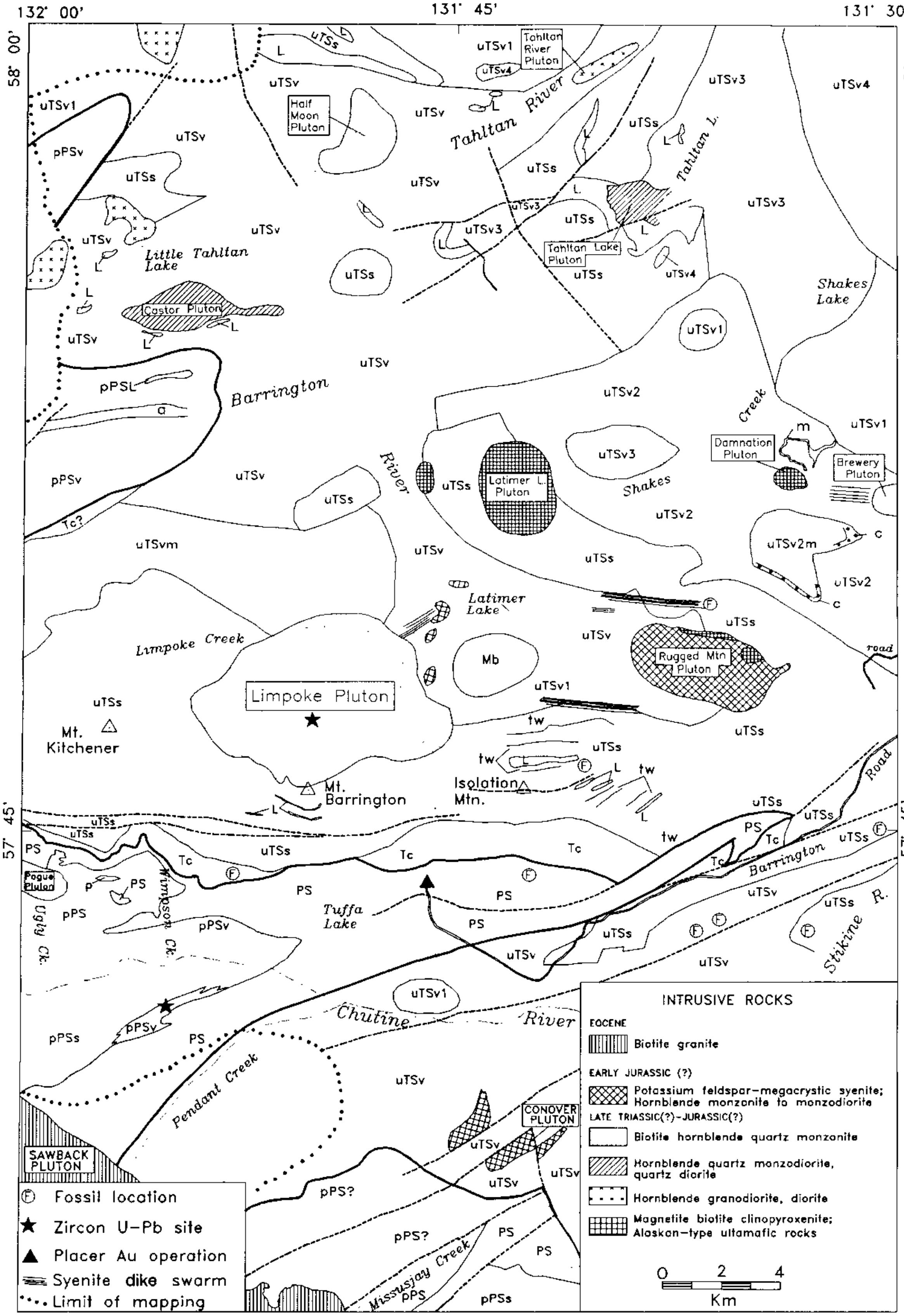

Figure 1-15-2. Simplified geology of the Chutine River – Tahltan Lake area (104G/12W and 13), for detailed map see Open File 1992-2. Geology shown beyond limits of mapping is from Souther (1972). Bolder contacts outline the Stikine assemblage.

STRATIFIED ROCKS

QUATERNARY

- Qal — Unconsolidated deposits

Miocene(?)–Recent(?)

- Mb — Basalt flows

UPPER TRIASSIC -- STUHINI GROUP

- uTSs — Undifferentiated sedimentary rocks; L=limestone; tw = tuffaceous wacke
- uTSv — Undifferentiated volcanic rocks; uTSvm = mafic volcanic and sedimentary rocks
  - 1 — Mafic volcanic rocks, augite phyric
  - 2 — Intermediate volcanic rocks; uTSv2m=maroon, c=conglomerate, m=marker unit
  - 3 — Tuffaceous wacke
  - 4 — Bladed plagioclase porphyry
- L — Discontinuous grey calcarenite

TRIASSIC

- Tc — Chert, siliceous siltstone, ash tuff

LOWER PERMIAN --STIKINE ASSEMBLAGE

- PS — Grey calcarenite, minor argillite, siltstone

PERMIAN OR OLDER

- pPS — Undifferentiated sedimentary and volcanic rocks
  Sedimentary facies (pPSs)
  Volcanic facies (pPSv); a=massive andesite, p=pillow basalt
  Recrystallized limestone (pPSL; age unknown)

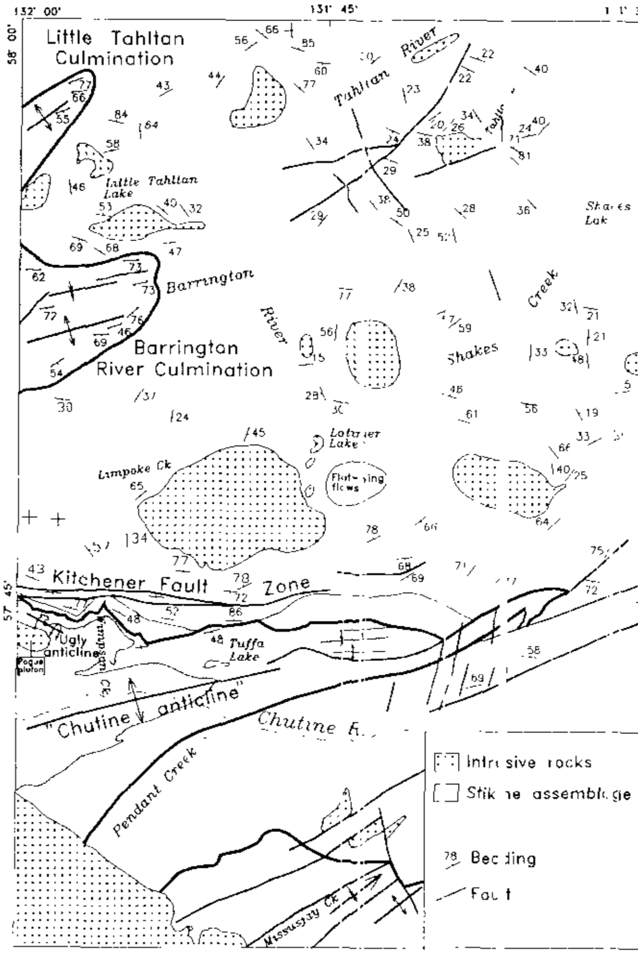

Figure 1-15-3. Structural elements of the Chutine River - Tahltan Lake area (104G/12W and 13), for detailed map see Open File 1992-2.

ton rivers. Chutine River exposures include northeast to east-trending Permian limestone structurally underlain by phyllitic volcanic and sedimentary rocks that form the core of the Chutine anticline. Complexly folded, well-bedded to massive, light and dark grey, recrystallized Permian limestone (Unit PS) forms conspicuous white cliffs north of the Chutine River. The simplified map pattern (Figures 1-15-2 and 3) resembles an east-striking anticline with an attenuated closure that extends east across the map area. In fact, lithologic units structurally above and below the limestone vary along strike, as does the thickness of the limestone itself, indicating structural and/or facies complications that are not addressed here. South of the Chutine River, green and maroon phyllitic plagioclase-rich andesitic lapilli tuff, a granitoid-bearing volcanic conglomerate (Unit pPSv), and argillite with siliceous siltstone layers (Unit pPSs) core the fold. Fabric intensity varies from schistose to unfoliated. The contact with Upper Triassic volcanic rocks along the southern limb is interpreted as a thrust fault (Brown *et al.*, 1990). The total structural thickness of Permian limestone, which is increased by folding and faulting, varies from less than 200 metres near Wimpson Creek to over 2800 metres east of Tuffa Lake. Locally the limestone contains rugose corals, brachiopods, bryozoans and crinoid stems. Conodonts, identified by M.J. Orchard (GSC, BCGS Report November, 1990), indicate an Early Permian (Artinskian - Sakmarian) age for the limestone.

A smaller structural culmination on the northwest limb of the Chutine anticline is here called the Ugly Creek anticline (Figure 1-15-3). It is outlined by Permian limestone which wraps around a core of rusty weathering, phyllitic siltstone, shale and minor, discontinuous, recrystallized limestone. It is an open fold, inclined to the north, with an amplitude of more than 150 metres (Plate 1-15-1).

One kilometre farther southeast, brown-weathering pillow basalt, less than 50 metres thick, is intercalated with phyllitic sedimentary rocks and tuff (p in Figure 1-15-2). Individual pillows are up to 2 metres long, with amygdaloidal cores, well-preserved chilled margins and intrapillow micrite. These subaqueous flows may correlate with a much thicker accumulation of pillow basalt exposed 15 kilometres to the southwest, between Triumph Creek and the Chutine River (104F/9; *cf.* Westcott, 1989a).

BARRINGTON RIVER AND NORTHWEST OF LITTLE TAHLTAN LAKE

Phyllitic tuff, siltstone, andesite and limestone exposed in the Barrington River valley and northwest of Little Tahltan Lake are correlated with the Stikine assemblage on the basis of their fabric and fold geometry (Unit pPS). Alternating centimetre to millimetre-scale layers of green, dark grey, white and maroon rocks grade from chlorite schist to unfoliated ash, lapilli tuff and siltstone and argillite. Concordant

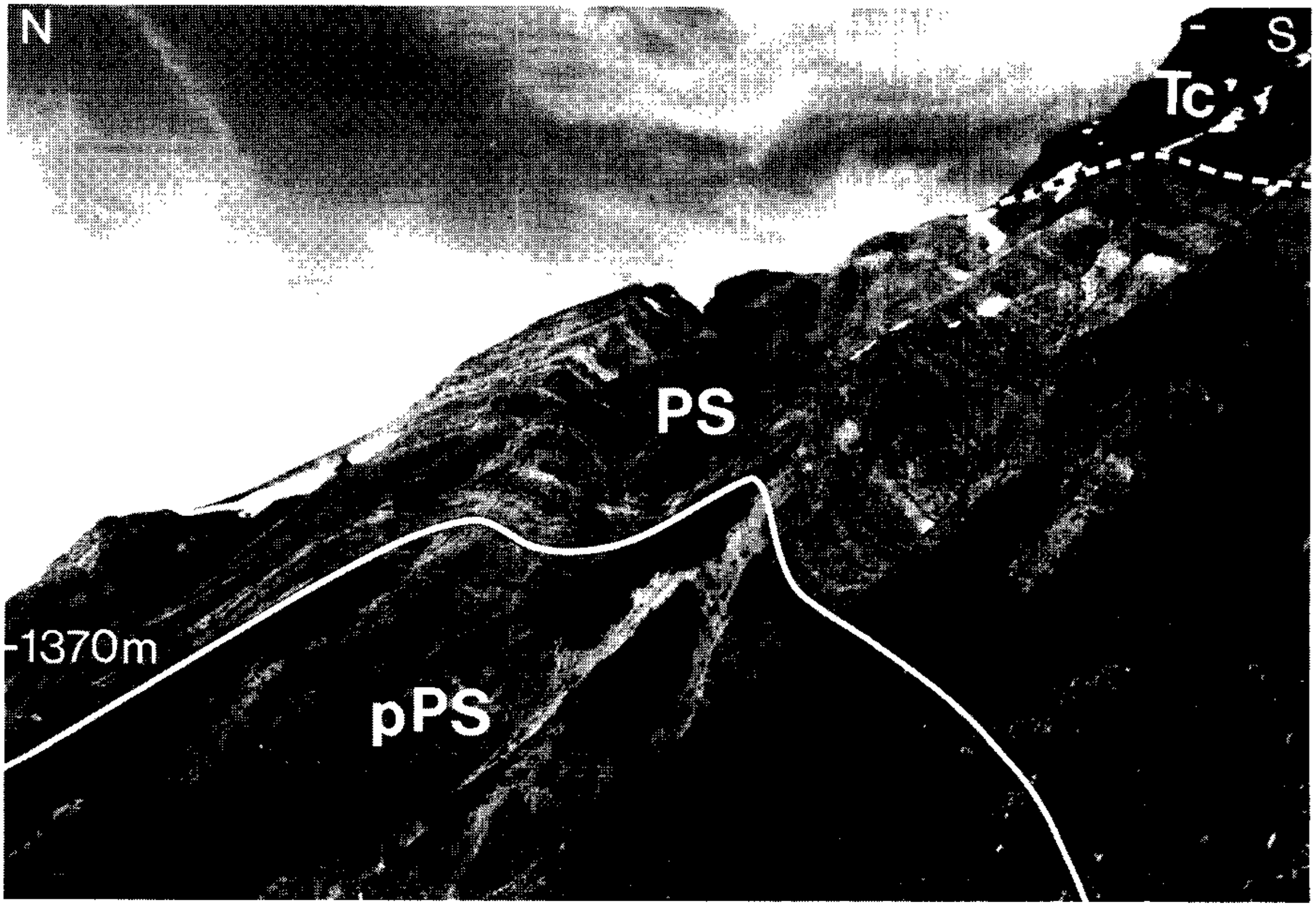

Plate 1-15-1. View to west of Ugly anticline. An open fold of well-bedded Permian limestone (**PS**) with a core of rusty weathering, phyllitic siltstone (**pPS**). Triassic chert (**Tc**) at the top right of the photograph, lies in steep fault contact to the north (dashed line).

and discordant, white quartz veins and sigmoidal quartz veins or pods are unique to these areas and are not present in other map units. They are presumably products of pre to syndeformational metamorphism. Locally, chlorite phyllite is intercalated and infolded with grey recrystallized limestone and limy tuff less than 75 metres thick. This pPS unit tends to form homogeneous, massive rounded outcrops, in contrast to the more irregular Stuhini Group exposures.

Although Barrington River and Little Tahltan Lake culminations have similar lithologies, their fold style and orientation differ significantly. Barrington River exposures display a uniform, south to southeast-dipping phyllitic fabric, fold closures are rare and cleavage commonly parallels bedding. Locally bedding-cleavage intersections suggest there is a major antiform somewhere along the valley, with secondary closures on the northern limb. In contrast, northwest of Little Tahltan Lake, phyllitic rocks are pervasively folded into moderately to steeply northwest-inclined folds with subhorizontal fold axes (Plate 1-15-2a, b). The centimetre to metre-scale, open to tight folds are north verging.

The eastern contact at the Little Tahltan culmination consists of a fault that places greenschist-grade, polydeformed phyllite against lower grade, steeply dipping Stuhini Group siltstone and volcanic rocks. Further investigation is required to determine whether the unmapped northern contact is an unconformity or a fault.

PERMO-TRIASSIC CONTACT RELATIONSHIPS

The Permo-Triassic contact is well exposed immediately north of the Ugly anticline, where it is sharp and believed to be a fault. At this location steeply north-dipping Permian limestone beds are overlain by concordant buff-weathering chert beds of Unit Tc (Plate 1-15-1). Farther east, near Tuffa Lake, the chert unit is absent and Stuhini Group tuffaceous wacke lies structurally on Stikine limestone. According to Kerr (1948) the limestone-chert contact may be unconformable where crossed by the Barrington River. However, at this locality, the competent chert is folded into chevrons, directly above the limestone.

TRIASSIC CHERT AND RELATED VOLCANO-SEDIMENTARY ROCKS (UNIT TC)

Unit Tc is dominated by buff, light to dark grey weathering chert but also includes siliceous siltstone and green and maroon ash tuff. These rocks crop out in four areas: near Wimpson Creek, east of Barrington River, along the Barrington road, and possibly on the southern limb of the

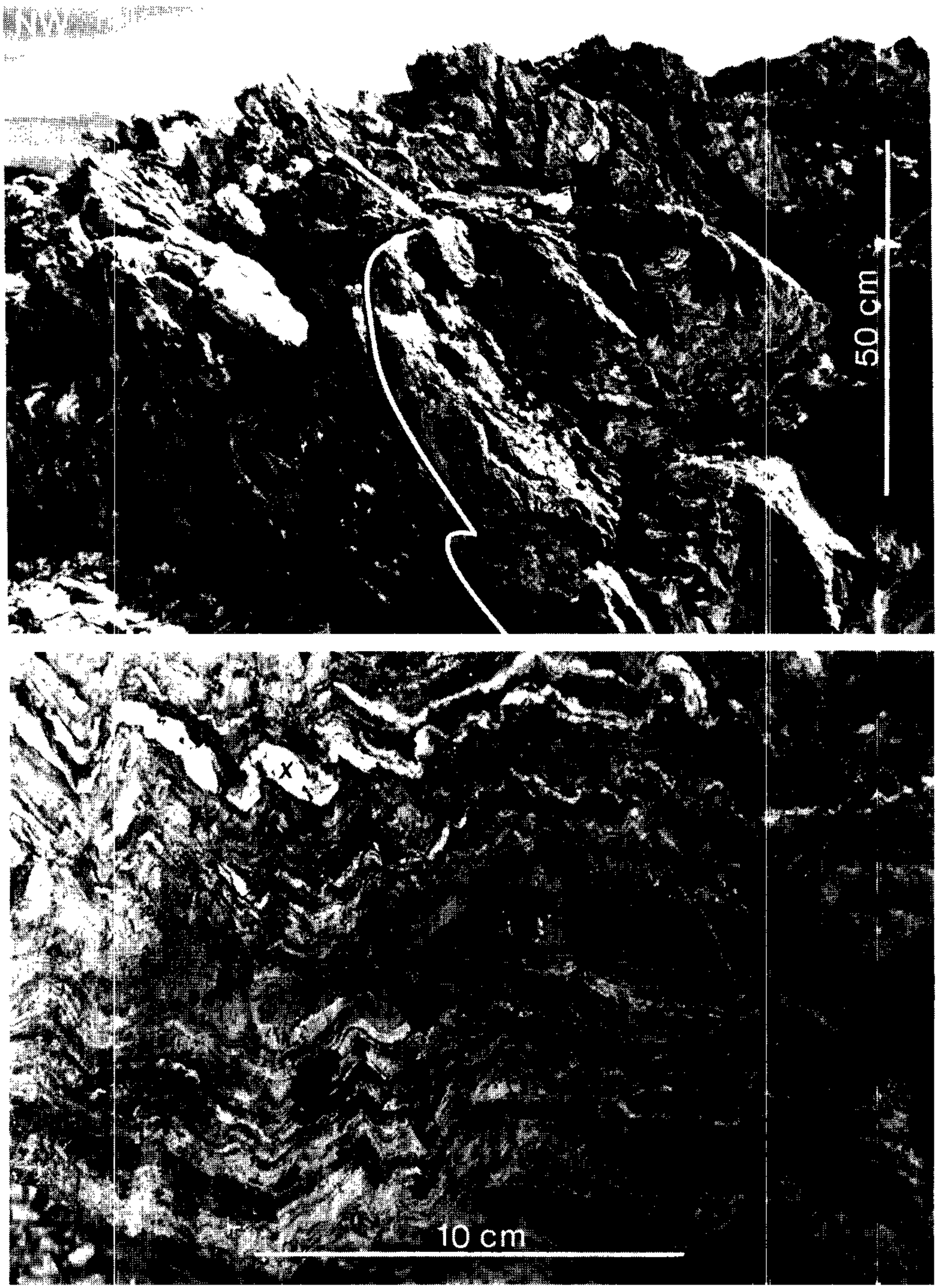

Plate 1-15-2. Characteristic deformation within Stikine assemblage phyllitic tuff in the Little Tahltan Lake structural culmination: (a) northwest-verging, tight, angular folds of green and grey phyllite, with axial planar cleavage and transposed bedding; (b) centimetre-scale, north-verging, rounded to chevron-style folds. The chlorite-sericite foliation (S_1) is coplanar to bedding (S_0) and both are folded, therefore, at least two phases of deformation are evident. Pre-deformation quartz vein that is parallel to bedding is shown in top left of the photograph (x).

Barrington River culmination. A maximum structural thickness of approximately 750 metres is exposed east of Wimpson Creek. Here the section is very well bedded, with parallel, centimetre-scale beds of chert separated by thin layers of chlorite and sericite phyllite. Barrington road exposures comprise bright green and red, laminated to bedded siliceous ash-tuff in thrust contact with overlying white Permian limestone. Prior to identification of Middle to Late Triassic radiolaria in the chert (early Ladinian-late Carnian; GSC Loc. No. C-167938; F. Cordey, personal communication, 1991), it was assumed to be Permian age because of the degree of deformation and the spatial association with Permian limestone.

Contacts with the Stuhini Group appear to be gradational. The chert unit becomes interbedded with progressively more tuffaceous wacke across the Kitchener fault zone (Figure 1-15-3). In the fault zone, the chert is characteristically deformed into chevron folds with up to 15-metre amplitudes. Where closures are not exposed, small bedding-cleavage intersection angles (<20°) also indicate tight folding. In contrast, folds are not evident in the monotonous tuffaceous wackes and they must have deformed by some other mechanism.

AGE OF DEFORMATION

Deformational events are currently being studied and interpreted. Preliminary observations suggest that although Stuhini strata dip more steeply than average near Stikine assemblage culminations, it is not certain that these structures are in fact post-Late Triassic. Chevron folded Unit Tc clearly indicates significant post-Ladinian-Carnian deformation. However, the difference in metamorphic grade, intensity of deformation and apparent truncation of phyllitic fabrics argues for a pre-Stuhini deformation. The minimum age of deformation is constrained by the Tertiary Sawback pluton that cuts all lithologies and structures (Figure 1-15-3), and possibly the unfoliated Pogue pluton, tentatively assigned a Late Triassic to Jurassic age, provides an older minimum age of deformation.

Upper Triassic Stuhini Group (Unit uTS)

Eighty per cent of the map area north of the Kitchener fault zone is underlain by the Stuhini Group, divided here into sedimentary and volcanic facies. The total thickness is at least 2500 metres. Sedimentary rocks include tuffaceous greywacke, siltstone, discontinuous limestone and minor shale. Volcanic-dominated facies are subdivided into mafic and intermediate flows and tuffs, tuffaceous wacke and bladed plagioclase porphyry. Contacts between units are gradational. Most, if not all, of the units are believed to be submarine, based on the presence of chert and limestone interbeds, and rare marine bivalves. No younger strata other than Miocene basalt flows (Unit Mb) overlie the Stuhini Group.

Fossil age control in the map area is meagre: Kerr (1948) collected Late Triassic bivalves, *Daonella* or *Halobia* (Figure 1-15-2) and 1989 collections from the immediate southeast, yielded late Carnian to early Norian and late Norian conodonts (M.J. Orchard, written communication, BCGS Report. November, 1990; *cf.* Brown *et al.*, 1990). However, 53 new samples were collected for microfossil extraction and six new macrofossil localities should constrain the age. Preliminary identification of a late Norian Monotis supports a Late Triassic age for this package (T. Poulton, personal communication, 1991).

SEDIMENTARY ROCKS (UNIT uTSs)

An east-trending belt of well-bedded sedimentary rocks, which has a maximum thickness of 1500 metres, extends from Mount Kitchener to Rugged Mountain. Other sediment-dominated areas shown in Figure 1-15-2 include Tahltan Lake, north of Little Tahltan Lake and north of Tahltan River. Sedimentary rocks are mainly brown weathering and are composed of thick to thin, parallel-bedded to laminated, tuffaceous siltstone, wacke and minor argillite and shale. Thinly interlayered tuffaceous wacke-siltstone and mudstone rhythmites, probably deposited as distal turbidites, are common. Trough crossbedding, normal grading and fining-upward volcaniclastic sequences occur throughout. Scour-and-fill structures, syndepositional growth faults, and angular argillite rip-up clasts point to an irregular paleodepositional surface. Several horizons of pale grey weathering, thick-bedded to massive, micritic limestone (up to 20 m thick) occur within the unit, between Mount Barrington and Isolation Mountain. Massive pyroxene crystal-lithic lapilli tuff, green ash-tuff and cherty tuff are subordinate to the sedimentary strata. Tuffaceous wacke and crystal-lithic lapilli tuff form massive, unbedded sections of the unit and increase in abundance to the east. Coarse, heterolithic pebble conglomerate contains siltstone, wacke, chert and limestone clasts. The limestone clasts are intraformational and not derived from the underlying Permian unit; successful extraction of conodonts from collected samples will help to verify this.

Stuhini Group rocks lack the penetrative fabrics that characterize the Paleozoic units. Structural deformation within Unit uTSs, in a gross sense, appears simple. For example, a monoclinal section is displayed between flat-lying strata at Mount Kitchener and vertical strata within the Kitchener fault zone. Locally, however, the unit is complexly deformed, such as south of the Damnation pluton where the strata are recumbently folded. Elsewhere bedding attitudes vary from gently to steeply dipping. Volcanic-dominated sections are generally massive and rarely foliated.

VOLCANIC ROCKS

Volcanic map units were differentiated on the basis of dominant lithology. Ubiquitous gradations between units require the subjective placement of many contacts. In general, Unit uTSs is overlain by intermediate volcanic rocks that grade upward and to the northeast into basaltic flows, breccia and tuff. Bladed plagioclase porphyry lies even farther to the north and northwest. All volcanic rocks are intermediate to mafic, no felsic units are apparent.

Mafic Volcanic Rocks (Unit uTSv1)

The most distinctive Stuhini Group lithology comprises mafic volcanic rocks, including clinopyroxene hornblende-phyric basaltic andesite flows and crystal-lithic lapilli tuff.

They are typically dark green, massive and contain distinctive, blocky clinopyroxene phenocrysts. Composition of the tuffs is similar to the flows. Lapilli to block size (2 to 75 cm) fragments are supported in a crystal-rich matrix. Monolithic amygdaloidal-basalt breccia, presumed to be autobrecciated flow, occurs locally. A pyroxenite clast in a lapilli tuff southwest of Shakes Lake suggests that the Latimer Lake ultramafic body, or a similar body, was unroofed and eroded during the deposition of this unit. Minor epidote-carbonate veinlets are common in the basalt.

Unlike typical orogenic andesites, basaltic flows and tuffs of Unit uTSv1 lack orthopyroxene, but they are clinopyroxene rich, which suggests a petrochemical tie to the Alaskan-type ultramafic bodies that are discussed later. Whole-rock major oxide data for rocks from the 1989 field area show that the clinopyroxenite-bearing flows are basalts with calcalkaline trends, that plot in the alkaline and subalkaline fields of Irvine and Baragar (1971).

Intermediate Volcanic Rocks (Unit uTSv2)

Massive, plagioclase-rich, andesitic block-tuff, tuff and flows dominate the section in the east-central part of the map area. Green and maroon, plagioclase-porphyritic andesite fragments are characteristic components. Andesitic compositions for the flows are inferred from the coexistence of plagioclase and hornblende. Crystal fragments of unstrained and embayed volcanic quartz found within an andesitic lapilli tuff are probably derived from dacitic rocks occurring somewhere in the sequence. This unit is similar to part of the Early Jurassic Unuk River Formation of the Hazelton Group, south of the Iskut River. However, diagnostic pyroxene-rich flows of the Stuhini Group overlie this unit, so it is thought to be Late Triassic in age.

Subunits include maroon volcanic rocks (uTSv2m) and a marker unit (m). Subunit uTSv2m has a lower division of brick-red, poorly sorted, heterolithic volcanic conglomerate (c) containing abundant limestone clasts and boulders, some measuring up to 10 metres in diameter (Plate 1-15-3). These are interpreted to be debris flows (lahars) that incorporated reefoidal limestone as it flowed down the flank of a Triassic stratovolcano.

A distinctive marker unit (m) comprises white to light grey, well-bedded, hornblende-rich epiclastic beds exposed on a ridge northwest of the Brewery pluton. Although the relatively flat-lying marker unit was not traced beyond this unnamed ridge, it provides distribution and attitude information about the otherwise massive strata in this area.

Tuffaceous Wacke (Unit uTSv3)

Olive-green medium-grained plagioclase-rich tuffaceous wacke forms massive outcrops from Shakes Lake to beyond the north edge of the map area. Like Unit uTSv2, it is massive and rarely bedded, but it lacks the lapilli and block size fragments. Contacts are gradational with intermediate volcanic rocks of Unit uTSv2.

Bladed Plagioclase Porphyry (Unit uTSv4)

Brown-weathering bladed plagioclase-phyric basalt or basaltic andesite flows dominate the northeast corner of the map area and form isolated exposures north of the Tahltan River. A bladed porphyry layer, interpreted to be a sill, is exposed on the cliff face 1 kilometre south of Tahltan Lake. A similar unit within the Takla Group of Quesnellia is discussed by Monger (1977).

Intercalated Mafic Volcanic and Sedimentary Rocks (Unit uTSvm)

This unit consists of interfingering sedimentary rocks (uTSs) and a mafic tuff (uTSv1), as exposed along the ridge north of Limpoke Creek. Here cliff faces are marked by prominent brown-weathering beds of sedimentary rocks which are intercalated with darker grey volcanic strata. This unit represents a south-to-north facies transition from a sediment to volcanic-dominated regime.

LIMESTONE HORIZONS (UNIT L)

Discontinuous fine-grained to aphanitic limestone units occur within both sedimentary and volcanic facies. They form prominent light grey outcrops in four areas: Mount Barrington - Isolation Mountain, west of Tahltan Lake, the Castor pluton area and north of the Tahltan River. Contacts are rarely exposed but they appear to be conformable. Unlike the Permian and older limestones, Late Triassic carbonate horizons are generally less than 30 metres thick and not recrystallized or foliated. West and south of Tahltan Lake the unit is uncharacteristically more than 100 metres thick, and here the limestone dips gently whereas in most other areas beds are steeply dipping. The limestone 25 metres thick that parallels the southern contact of the Castor pluton is well bedded and porcellaneous.

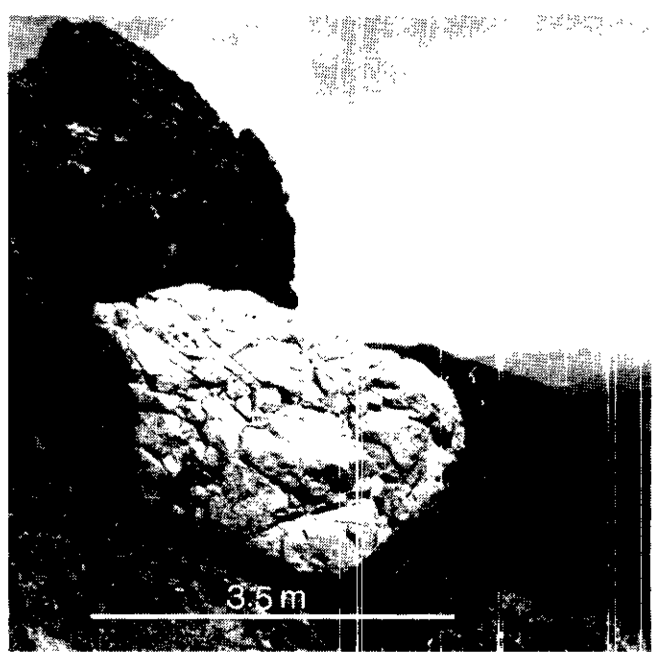

Plate 1-15-3. Huge angular limestone boulder, 3.5 metres in diameter, hosted in maroon volcanic conglomerate southwest of Brewery pluton. This boulder, too large to be transported by fluvial processes, must have been carried by a debris flow that incorporated reefoidal limestone. Such deposits indicate a high-energy, unstable and cannibalistic setting, possibly on the flank of a stratovolcano.

DEPOSITIONAL HISTORY OF UNIT Tc AND STUHINI GROUP

A preliminary synopsis of Stuhini Group evolution is presented below; however, it may change upon receipt of results from fossil and geochemical analyses. The first record of Triassic strata is the accumulation of chert (Unit Tc) deposited unconformably on Early Permian limestone and older strata (Figure 1-15-4). These siliceous oozes probably accumulated in a low-energy, pelagic environment, below the carbonate compensation depth. In modern oceans this is about 4 kilometres below sea level (Berger, 1974), however, other factors including high plankton productivity are know to produce shallower water chert accumulations (F. Cordey, personal communication, 1991). The gradational west-to-east change from chert to maroon ash-tuff may signify eastward shallowing of a Triassic sea. The chert sequence was gradually overwhelmed by an influx of fine tuffaceous material from a distal arc. Thick tuffaceous sediments continued to accumulate in the west, whereas in the east, interfingering basaltic and andesitic flows were an important component. Fringing carbonate reefs formed where volcanic edifices rose to within the photic zone, presumably during periods of volcanic quiescence. Limestone deposition as found north of the Tahltan River occurred at a transition from volcanic to sediment-dominated settings. Eventually the coarser, eastern proximal facies of flows, volcanic breccia and tuff prograded over the distal facies. The western migration of volcanism may have produced emergent volcanic islands.

MIOCENE (?) OR RECENT (?) FLOWS (UNIT Mb)

Previously unmapped, flat-lying columnar-jointed potassic andesite flows form isolated, cliff-face exposures (Plate 1-15-4) and benches in a densely forested area 1.6 kilometres south of Latimer Lake. The brown-weathering, amygdaloidal flows contain unaltered biotite and clinopyroxene phenocrysts set in a green-brown plagioclase microlite groundmass. Amphibole and clinopyroxene also occur as xenocrysts. Amygdules of intergrown quartz and calcite comprise 10 per cent of the rock. The series of flows, over 340 metres thick, is intermittently exposed from 670 to 1000 metres elevation. Individual flows are 4 to 6 metres thick. Local red-brown interflow conglomerate suggests fluvial reworking of some lava flows during lulls in volcanic activity.

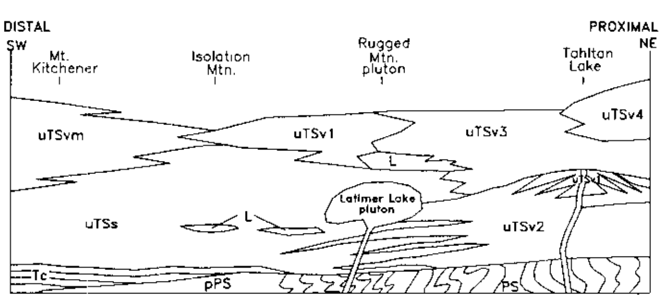

Figure 1-15-4. Schematic facies relationships of Stuhini Group strata in the map area. Map code descriptions are listed in the legend of Figure 1-15-2.

The closest correlative flows maybe the Recent Stikine River valley basalts (Souther, 1972), 20 kilometres to the east, or the Level Mountain flows (Gabrielse, 1977) 33 kilometres to the north-northwest. The source of the Latimer Lake flows is unknown.

QUATERNARY GEOLOGY

Cursory observations of glacial striations suggest at least three episodes of ice transport. A north-northwest or south-southeast ice movement above 1300 metres elevation contrasts with a north-northeast direction evident over the lower, rolling hills west of Shakes Lake. Large biotite granite erratics, probably derived from the Sawback pluton to the south, lie on a plateau at 1700 metres elevation and are probably the product of this northeasterly directed ice movement. Angular erratics of distinct tuff occur south of Tahltan Lake at 1000 metres elevation; they have been transported tens of metres from their source outcrop across a deep gully. This points to an additional period of southward-directed ice movement.

Broad, glaciated U-shaped valleys commonly display misfit drainages such as along the upper Tahltan River and demonstrate how Pleistocene glaciation has partially controlled the present drainage system. Clearly, more work is required to resolve the timing and limits of each ice advance and their Quaternary deposits. A study of the Quaternary geology is currently underway in the Telegraph Creek and Mount Edziza area by Ian Spooner, as part of a doctoral thesis at the University of Calgary.

INTRUSIVE ROCKS

Intrusive rocks underlie only 15 per cent of the project area. This is in marked contrast to the Scud River map area (104G/5, 6), where intrusions underlie about 75 per cent of the area. Furthermore, plutons in the Chutine River – Tahltan Lake area are quartz poor relative to those of Scud River. A maximum age limit for the plutonic rocks is provided by intrusive relationships with the Late Triassic Stuhini Group. It is difficult to determine minimum age constraints for the intrusions due to a lack of preserved younger strata. Uranium-lead and potassium-argon dating of the Limpoke pluton is in progress (Figure 1-15-2). Compositions of intrusive rocks were determined from cut, and potassium feldspar stained hand specimens and thin sections following the classification scheme of Streckeisen (1976). Plutons have been tentatively grouped into Late Triassic to Jurassic, Early Jurassic and Eocene episodes.

I-type plutonism (Pitcher, 1982) produced three Triassic to Jurassic calcalkaline plutonic suites and one Early Jurassic alkalic plutonic suite in the Chutine River – Tahltan Lake area (Figure 1-15-5). The two end-members probably represent separate, unrelated episodes, rather than a continuum or steadily evolving magma source. The calcalkaline plutons may be intrusive centres associated with island-arc volcanism. The more potassic, alkalic magma probably differentiated at relatively low crustal levels, and may be a

Plate 1-15-4. Flat-lying, columnar-jointed basalt flow, about 6 metres thick, 1.6 kilometres south of Latimer Lake. Tentatively correlated with the Level Mountain flood basalts.

product of crustal extension. In addition, in the central part of the map area, Alaskan-type ultramafic plutons are spatially associated with the alkaline suite.

Limpoke and Half Moon plutons (Suite A) are two-phase intrusions with biotite hornblende monzodiorite to biotite-hornblende quartz monzonite cores and hornblende-biotite quartz diorite to diorite border phases. The smaller, undifferentiated Pogue and Brewery plutons are included in this suite.

The Tahltan Lake and Castor plutons (Suite B) are also two-phase intrusions. They have a border phase of quartz diorite which grades into central cores of quartz monzonite (Tahltan Lake) to granodiorite-tonalite (Castor). They are quartz rich and potassic feldspar poor relative to Suite A. Hornblende is the only mafic mineral and is characteristically poikilitic. Skarns develop where these plutons intrude Stuhini limestone.

The Little Tahltan Lake and Tahltan River plutons (Suite C) have the broadest spectrum of compositions ranging from hornblende granodiorite to diorite. Biotite is locally present. Characteristically, carbonate and sericite replace feldspars and titanite (sphene) is abundant (1–2%). Small xenoliths of country rock are present.

Late Triassic (?) - Jurassic (?)

LIMPOKE PLUTON

The Limpoke pluton, an oblate body approximately 8 kilometres long, underlies 27 square kilometres immediately south of Limpoke Creek. Around the southern border, including the peak of Mount Barrington, a prominent, rusty weathering pyritic halo has attracted recent exploration interest. This two-phase, texturally heterogeneous pluton is dominated by a border phase of pale grey, medium to fine-grained, equigranular biotite-hornblende quartz monzonite. The centre of the intrusion is characterized by a coarse to medium-grained plagioclase-megacrystic, biotite hornblende monzodiorite with plagioclase phenocrysts, 1 to 2 centimetres in length, set in a fine-grained groundmass of potassic feldspar. The percentage of mafic minerals increases toward the outer margins of the pluton, with the colour index (M') ranging from about 18 to 40. Hornblende is the dominant mafic mineral, but dark brown biotite and dark green hornblende coexist at some localities. Clinopyroxene occurs with hornblende and biotite in one outcrop of monzodiorite. The intrusion contains up to 2 per cent magnetite as fine-grained opaque granules which are spatially associated with crystals of biotite

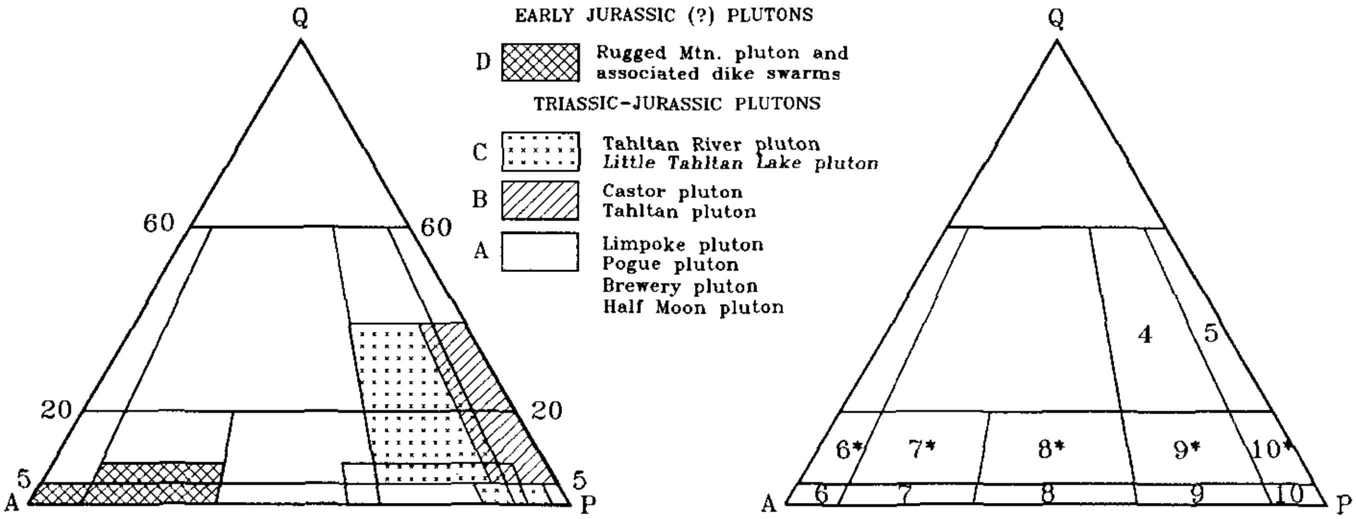

Figure 1-15-5. Comparison of compositions of plutons, plotted on Streckeisen (1976) diagram. Q=quartz, A=alkali-feldspar, P=plagioclase, 4=granodiorite, 5=tonalite, 6=alkali-feldspar syenite, 6*=quartz alkali-feldspar syenite, 7=syenite, 7*=quartz syenite, 8=monzonite, 8*=quartz monzonite, 9=monzodiorite, 9*=quartz monzodiorite, 10=diorite, 10*=quartz diorite.

and hornblende. Apatite is a common accessory mineral (up to 1%).

Dikes of varying composition cut the margins of the Limpoke pluton. Along the western contact, a set of aphanitic to coarse-grained pyroxene-biotite-hornblende granodiorite dikes have widths of up to 20 metres. The percentage of ferromagnesian minerals present increases with grain size; M′ is about 50 for the coarser grained dikes. Plagioclase is extensively altered to sericite and carbonate. These felsic dikes may represent a more hydrous phase of the Limpoke magma and they are probably similar in age to the pluton.

Leucocratic, potassium feldspar megacrystic syenite dikes intrude both the eastern and western borders of the Limpoke pluton and surrounding intercalated Late Triassic sedimentary and volcanic rocks. These dikes are analogous, both texturally and chemically, to syenite and alkali-feldspar syenite dikes that occur northwest of the Rugged Mountain syenite. The dikes are characterized by euhedral, tabular, potassium feldspar phenocrysts 1 to 2 centimetres long and smaller plagioclase laths, set in a groundmass of very fine grained interstitial potassium-feldspar. The phenocrysts are flow aligned, producing a subtrachytic texture. Hornblende and/or pyroxene (2 to 10%) occur as subhedral to euhedral prismatic grains.

HALF MOON PLUTON

The Half Moon pluton is a crescent-shaped body outcropping north of the Tahltan River. The centre of the pluton consists of equigranular medium to coarse-grained hornblende quartz monzodiorite. The quartz-poor and plagioclase-enriched border phase is composed of fine to medium-grained hornblende to hornblende-biotite quartz diorite. Mafic mineral contents range from 15 to 25 per cent. Plagioclase is saussuritized and chlorite alteration is pervasive though minor.

The waxy grey appearance of the plagioclase, the presence of biotite with hornblende, and the range in composition from quartz monzodiorite to quartz diorite are also characteristic features of the Limpoke pluton. These similarities suggest that the intrusions are related or share a common origin.

BREWERY PLUTON

The eastern edge of the map area is underlain by an isolated ridge of hornblende quartz monzodiorite which has been named the Brewery pluton. Further mapping is required to delineate its eastern boundary. The fresh surface has a colour index of 25 and an overall pinkish tone. Preliminary mapping suggests compositional affinities to the Limpoke pluton.

POGUE PLUTON

The Pogue pluton is a small, poorly exposed body southwest of the Limpoke pluton. It is composed of fine-grained, equigranular hornblende to biotite hornblende monzodiorite (M′=20). A subtrachytic texture defined by flow-aligned plagioclase is developed at the eastern contact. As with the Brewery pluton, compositional similarities suggest an affinity to the Limpoke pluton.

TAHLTAN LAKE PLUTON

The Tahltan Lake pluton underlies 3.5 square kilometres immediately west of Tahltan Lake. Hornblende quartz monzodiorite dominates the northern and western portions of the intrusion, while the eastern half is characterized by hornblende quartz diorite. Though compositionally varied, the fine to medium-grained, equigranular rocks are texturally homogenous.

Poikilitic hornblende is relatively unaltered and occurs as prismatic grains which enclose numerous, smaller equant plagioclase crystals. Colour index values range from 18 in the quartz monzodiorite to 30 in the quartz diorite. Oscillatory zoned plagioclase crystals are invariably saussuritized, giving a grey to greenish cast to the rocks. Accessory minerals include magnetite, apatite and zircon.

Hornblende granodiorite and diorite dikes cut sedimentary rocks adjacent to the southwestern edge of the coeval Tahltan Lake pluton. Distal dikes of crowded plagioclase-porphyritic *biotite-hornblende quartz monzonite* are exposed to the north and south of the pluton. White-rimmed, euhedral, equant and randomly oriented plagioclase crystals are set in an aphanitic groundmass. The textures are similar to those found in the Stuhini bladed plagioclase flows, possibly indicating that they are feeders to these flows. The third type of dikes adjacent to the pluton are composed of medium-grained, equigranular hornblende syenite. These outcrop to the south and southeast, and resemble those along the northern edges of the Castor and Rugged Mountain plutons.

CASTOR PLUTON

The Castor pluton is an eye-shaped, bimodal intrusion exposed north of the Barrington River and southeast of Little Tahltan Lake. It is dominated by a fine to medium-grained equigranular hornblende to biotite hornblende granodiorite. Along the eastern margin, the border phase is characterized by fine to medium-grained hornblende quartz diorite, to the west it is represented by fine-grained equigranular tonalite. The colour index ranges from 10 to 30 and plagioclase is weakly to moderately saussuritized. As in the Tahltan Lake pluton, hornblende poikilitically encloses smaller equant plagioclase crystals.

Several discrete, narrow mylonitic zones that consist of alternating foliated quartz diorite and chlorite schist occur along the southern margin of the Castor pluton. Adjacent Stuhini limestone and andesitic volcanics are also foliated. This local fabric may be a product of a larger east-trending fault system.

LITTLE TAHLTAN LAKE PLUTONS

The Little Tahltan Lake plutons are predominantly medium-grained, inequigranular hornblende granodiorite; most have medium to fine-grained quartz monzodiorite to hornblende diorite border phases. The colour index of the intrusive rocks directly northwest of Little Tahltan Lake ranges from 10 to 30. Hornblende is the dominant mafic mineral, accessory minerals include magnetite and titanite. Hornblende is altered to chlorite and epidote turbid, interlocking plagioclase laths and potassic feldspar crystals are completely replaced by carbonate and sericite. Overall, the intrusion is moderately to intensely altered. There is a faint foliation within the intrusion along its western margin; due west is a massive magnetite skarn which cuts adjacent Stuhini limestone and volcanic rocks.

TAHLTAN RIVER PLUTON

The Tahltan River pluton is an elliptical body that only outcrops along the banks of the Tahltan River, northwest of Tahltan Lake. It is a predominantly leucocratic, medium-grained equigranular hornblende to biotite-hornblende quartz monzodiorite (M′=10). Quartz and potassic feldspar are interstital. Alteration is moderate; hornblende is partially altered to chlorite, zeolites are present along joint surfaces and quartz-epidote veinlets crisscross parts of the outcrop.

The presence of small dioritic xenoliths, and accessory honey-coloured titanite and magnetite, in conjunction with the pluton's composition and degree of alteration, indicate affinities with the Little Tahltan Lake intrusions to the east.

ALASKAN-TYPE ULTRAMAFIC PLUTONS

Three small, Alaskan-type ultramafic plutons intrude Stuhini Group tuffaceous siltstone; two of these bodies had not been previously mapped. They form an east-trending group, 4 kilometres north and east of Latimer Lake, that parallels the Early Jurassic (?) Rugged Mountain pluton and related dike swarms. Their characteristics are well represented by the Latimer Lake pluton (Shakes iron deposit) which underlies a poorly exposed, forested area. Partially caved bulldozer trenches, from iron exploration in the 1960s (McIntyre, 1966), provide the only exposures of the pluton. The 1:50 000-scale aeromagnetic map of the area clearly outlines the pluton; it is the most anomalous feature in the map area (Map 9250G). The body consists of black, sugary textured, medium to fine-grained biotite magnetite clinopyroxenite. Cumulate clinopyroxenite and biotite are fresh and display faint millimetre-scale cumulate layering in thin section. Biotite also forms an intercumulate phase with magnetite. The clinopyroxenite is locally brecciated and infilled by potassium feldspar and coarse biotite. Part of the western flank of the Latimer Lake pluton includes intrusive breccia, consisting of pyroxenite fragments in hornblende diorite. Porphyritic syenite around the periphery of the body was noted by Souther (1972). A much smaller, unnamed satellitic ultramafic body, outcrops 2 kilometres farther west. The third body, the Damnation pluton is 10 kilometres to the east.

The intrusive relationships to the country rocks, absence of orthopyroxene and genetic association with syenite indicate that these bodies are Alaskan-type ultramafic plutons.

EARLY JURASSIC (?)

RUGGED MOUNTAIN PLUTON

The aptly named Rugged Mountain pluton, located immediately south of Rugged Mountain, covers about 14 square kilometres. It is a composite, pink to light grey, potassic body which intrudes Stuhini volcaniclastic rocks (Plate 1-15-5a). It is characterized by late phase, leucocratic, potassium feldspar megacrystic dike swarms (Plate 1-15-5b). Kerr (1948) referred to it as the "Shakes Creek mass" and described it in detail. Mapping and field observations during the 1991 field season will provide the basis for a B.Sc. thesis currently being undertaken by Ian Neill of The University of British Columbia.

The dominant phase consists of a biotite pyroxene alkali-feldspar syenite. Potassium feldspar phenocrysts range from

Plate 1-15-5. (a) View to northeast of Rugged Mountain syenite complex (z), dark mafic border phase (y) is partially preserved along the northern contact of the pluton, which intrudes Stuhini Group sedimentary rocks (x); (b) late-phase potassium feldspar megacrystic dike.

medium grained and equigranular to megacrystic. Mafic mineral contents range from 10 to 30 per cent in the central and eastern areas of the pluton, and increase from 50 to 80 per cent toward the border and western edge. Tabular and lath-shaped orthoclase phenocrysts range up to 7 centimetres in length. Ferromagnesian and accessory minerals, identified by Kerr, include biotite, aegirine-augite, bronzite, brown garnet and traces of magnetite, apatite and titanite. Pyroxenes are relatively fresh feldspars exhibit some sericite and chlorite alteration.

The Rugged Mountain alkali-feldspar syenite has a partially preserved biotite-clinopyroxenite border phase 10 to 15 metres wide, which outcrops along the northern edge of the intrusion. Similar material, with higher magnetite and biotite contents, occurs as a large, discrete body to the east (Plate 1-15-5a). Smaller pyroxenite bodies have also been mapped along the pluton's northeast and southeast borders. The contact between the pyroxenite and syenite is sharp and shows no evidence of faulting.

Forty kilometres to the northeast, the analogous Ten Mile Creek intrusion displays a better preserved clinopyroxenite border phase around a syenite core (Morgan, 1976). Pegmatitic syenite that cuts pyroxenite in this complex yields Early Jurassic K-Ar dates (Morgan, 1976), the Rugged Mountain pluton is thought to be coeval.

EOCENE

SAWBACK PLUTON

The Sawback pluton, exposed in the southwestern corner of the map area, is characterized by unaltered, medium to coarse-grained, massive biotite granite with well-developed joints. A Middle Eocene K-Ar date (48.0±1.7 Ma; biotite) was obtained for the pluton approximately 15 kilometres south of the present study area (Brown and Gunning, 1989b).

METAMORPHISM

Greenschist facies metamorphism has affected parts of the Stikine assemblage and, to a lesser extent, parts of the Stuhini Group. Most of the Stuhini Group rocks are zeolite facies or unmetamorphosed. Near the Damnation pluton, Stuhini basalts are metamorphosed to laumontite-prehnite grade; laumontite occurs in amygdules and in veinlets. Its stability limits the depth of burial for the Stuhini Group to less than 11 or 12 kilometres (Lion, 1971). The timing of metamorphism may be Middle to Late Jurassic, based on whole-rock K-Ar cooling ages.

STREAM-SEDIMENT GEOCHEMISTRY

Regional Geochemistry Survey (RGS) data were released for the Telegraph (104G) map sheet in July 1988 (RGS 104G) and include analyses of 141 silt and water samples collected from within the study area (Figure 1-15-6; Brown *et al.*, 1992). Numerous sample sites yielded anomalous geochemical results (i.e. exceeding the 95th percentile) that spurred a staking rush following the release. Subsequent follow-up exploration has located several and varied mineral occurrences, many peripheral to the Limpoke pluton.

MINERAL OCCURRENCES

There are eight mineral occurrences recorded in MINFILE for the Tahltan River map area (104G/13); they can be divided into six broad types: an actively mined placer gold deposit, porphyry copper showings, quartz-carbonate veins, gold-bearing massive sulphide zones, skarns and a cumulate magnetite deposit (Figure 1-15-6). Table 1-15-1 summarizes their geologic settings and lists key references. The occurrences that continue to be attractive exploration targets include; Barrington placer, Goat/Tuff, Poker and showings around the Limpoke pluton.

BARRINGTON RIVER PLACER OPERATION (MINFILE 104G 008)

Placer gold accumulations immediately south of the Barrington River canyon have been worked intermittently since the late 1920s. Reported gold recovery in 1933 was 3.1 kilograms and 6.8 kilograms in 1935 B.C. Annual Reports 1933, 1935). More recently, Barrington Gold Ltd. purchased the placer claims from Integrated Resources Ltd. and now operates the deposit on a seasonal basis. Test mining in 1990 produced 12.4 kilograms of gold from about 36 000 cubic metres of gravel (Integrated Resources Ltd., News Release, October 21, 1991) . The gold occurs as flakes less than 5 millimetres in diameter. Exploration for the lode source of the gold, thought to lie within the Barrington River or Limpoke Creek drainages and probably associated with marginal phases of the Limpoke pluton, is continuing.

GOAT/TUFF (MINFILE 104G 121)

The Goat claims (formerly Tuff property) are located due north of Tuffa Lake, near the headwaters of Cave Creek. In 1980, Du Pont of Canada Exploration Limited detected strongly anomalous gold in a heavy-mineral concentrate taken in the course of a regional stream-sediment sampling program in the region. A small massive sulphide pod (Little Cave Creek showing) was subsequently found and carried over 40 grams per tonne gold (Strain, 1981; Koreric, 1982a); numerous other pods have since been discovered. In 1986, Integrated Resources Ltd. restaked the area as the Goat claim group and has since conducted stream-sediment and soil sampling, geophysical surveys, prospecting, geologic mapping and some drilling (Van Angeren, 1991). Styles of mineralization include massive sulphide pods dominated by pyrrhotite with minor chalcopyrite; quartz-carbonate veins with pyrite and subordinate arsenopyrite and chalcopyrite; pluton-hosted massive magnetite with minor chalcopyrite veins (Lehtinen, 1989; Van Angeren, 1991).

POKER

A quartz-sulphide boulder train was traced from the Limpoke Creek valley to the southern edge of the Limpoke Glacier by Cominco Ltd. in 1988. Three types of mineralized boulders were identified – quartz-sulphide, massive pyrrhotite-pyrite-chalcopyrite-sphalerite-galena, and zinc-bearing quartz-carbonate (Westcott, 1989b). In 1990, Kee-

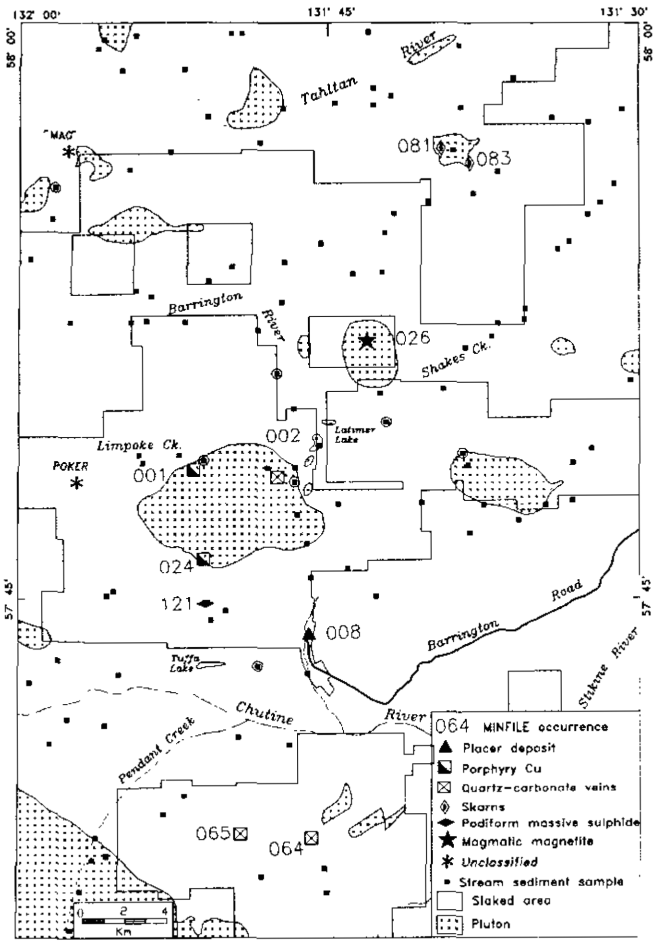

Figure 1-15-6. Mineral occurrence localities as recorded in the MINFILE database, approximate claim boundaries (October, 1991), RGS sample locations and British Columbia assessment report numbers in the Chutine River and Tahltan Lake map area. Solid squares denote RGS silt sample locations, encircled squares indicate gold anomaly sites (95th percentile). Mineral occurrences are grouped according to Table 1-15-1.

watin Engineering Inc. explored the south side of Limpoke Glacier and completed geochemical and geophysical surveys, geological mapping programs and four diamond-drill holes (Aspinall *et al.*, 1990).

Showings Peripheral to Limpoke Pluton

The Gordon showing (MINFILE 104G 002), located at the Limpoke Creek – Barrington River confluence, was examined by Kennco Explorations (Western) Ltd. (Hallof, 1966) and more recently (1990) by Homestake Mineral Development Company. Kennco conducted an induced polarization survey and prospected the area. The base metal mineralization is reported to consist of disseminated pyrite with minor chalcopyrite, bornite and malachite. Homestake's search for precious metal mineralization yielded geochemically low values (Marud, 1990c). The Poke showing was explored earlier by Kennco (Hallof, 1963).

Other Showings

The Tahltan Lake copper skarns (MINFILE 104G 081, 082) comprise a large alteration system 400 metres wide by 800 metres long (Marud, 1990a). Exoskarns and endoskarns consist of garnet, epidote, actinolite and diopside with smaller, rusty weathering patches of chalcopyrite, pyrite, magnetite and specular hematite. The northern portion of the skarn contains specular hematite while the southern part is principally magnetite with minor pyrite (Marud, personal communication, 1991). This gradation from reduced conditions close to the intrusive contact, to an oxidized regime distal to the intrusion is analogous to the Craigmont copper deposit (Rennie, 1962). At Craigmont some of the best copper grades occurred where both magnetite and hematite coexist in equal amounts (Rennie, *ibid*). Sulphide-bearing zones are 1 to 2 metres wide and up to 5 metres long (Marud, 1990a). The property was first staked and explored in 1973 by AMAX Exploration Inc. (Hodgson and LeBel, 1974) and is now owned by Homestake (Southam, 1991). A smaller skarn occurrence, VB 12 (MINFILE 104G 083), occurs near the lake shore.

Fifteen kilometres to the south, at Rugged Mountain, anomalous but relatively low copper and gold values are reported from the discontinuous clinopyroxenite border phase of the intrusion and isolated rusty weathering pyrite-malachite alteration zones (up to 2.32% Cu and 1.57 g/t Au; Marud, 1990b). Similarities to the setting of the Galore Creek alkaline porphyry copper-gold deposit prompted exploration of this body. However, the low geochemical values, combined with the lack of significant alteration zones at Rugged Mountain as compared to the Galore Creek deposit, suggest that the body has low mineral potential.

A new magnetite iron skarn ("MAG", Figure 1-15-6) was located in the northwest corner of the map area, where an altered granodiorite pluton intrudes Stuhini limestone and volcanic rocks. The massive magnetite pod is over 6 metres wide and 30 metres long.

MINERAL POTENTIAL AND EXPLORATION ACTIVITY

Mineral potential in the study area is varied and has been incompletely evaluated. Renewed interest in porphyry deposits and their peripheral vein systems has attracted mineral exploration companies to the region. Targets like the Galore Creek complex, the Wolverine showing on the edge of the Golden Bear road, and the Kaketsa Mountain porphyry system, suggest there is potential for copper-gold mineralization in the area. The contact zones around the Limpoke pluton remain prime exploration targets with silicified and pyritized float and placer gold reported in the area. Several RGS stream-sediment anomalies and small showings warrant further exploration.

Prominent iron-carbonate alteration zones between Tahltan and Shakes lakes appear attractive, however, sampling by industry has yielded poor results (Kasper, 1990). Similarly, a prominent rusty weathering syenite dike swarm on the northeast flank of Isolation Mountain has returned discouraging results (Dunn, 1990).

TABLE 1-15-1
GEOLOGY AND DESCRIPTIONS OF MINERAL OCCURRENCES

MINFILE No.	NAME	UTM Zone 9	MAP UNIT	DESCRIPTION	KEY REFERENCES
Placer gold occurrences:					
104G 008	Barrington River	335200E 6402600N	Qal	Placer gold deposits occur within unconsolidated gravel of the lower section of the Barrington River. Kerr (1948) suggested that the source of gold maybe related to the intrusive rocks which outcrop upstream along the Barrington River and Limpoke Creek.	EMPR AR 1925, '29, '31-3[illegible], '35; Kerr (1948)
Porphyry copper occurrences related to the marginal phase of the Limpoke pluton:					
104G 001	Poke	329920E 6410757N	uTSv	Disseminated chalcopyrite mineralization occurs along fracture zones within altered Stuhini Group volcanic rocks adjacent to the marginal phase of the Limpoke pluton.	EMPR AR 1963, '65; Halk (1963), Folk (1981) Kerr (1948), Souther (1972)
104G 002	Gordon	334119E 6410365N		Disseminated chalcopyrite mineralization is found throughout alkali feldspar syenite dike swarms which outcrop to the northeast of the Limpoke pluton.	EMPR AR 1930, '66; Halk (1966) Marud (1990c), Kerr (1948), Souther (1972)
104G 024	New Limpoke	330116E 6406383N		Disseminated chalcopyrite occurs predominantly within altered quartz monzonite to monzodiorite of the Limpoke pluton. Pyrite, pyrrhotite and molybdenite are also present in minor amounts.	EMPR AR 1965 Kerr (1948), Souther (1972)
Quartz - carbonate vein occurrences:					
104G 064	Conover Mt.	334512E 6392515N	uTSv	Slight evidence of mineralization, in the form of quartz, calcite and chalcopyrite veins has been observed at the contact between the Conover intrusions and surrounding volcanic rocks.	Kerr (1948), Davis (1988)
104G 065	Mist	331200E 6392700N	uTSv	Quartz veins associated with felsic and dioritic dikes intrude Stuhini Group mafic to intermediate volcanic rocks, cherts and siltstone,and contain minor pyrite, pyrrhotite and chalcopyrite. Gold is present in detectable but uneconomic quantities.	Eccles (1981), Korenic (1982b) Kerr (1948)
Skarn mineralization:					
104G 081, 082	VB 20, VB 5	342250E 6425670N	uTSs,L	Geologic setting and mineralization are similar for MINFILE 104G 081, 082, 083. Magnetite-pyrrhotite-chalcopyrite mineralized garnet, epidote, actinolite, and diopside-bearing skarns occur within Stuhini Group limestone and volcaniclastic rocks which have been intruded by a Triassic-Jurassic (?) hornblende diorite pluton. Pyrite and specular hematite mineralization is also present. A smaller skarn occurs near the lake (104G 083, VB 12)	EMPR GEM 1974; Hodgson et al. (1974) Marud (1990a), Southam (1991)
Podiform gold-bearing massive sulphide occurrences:					
104G 121	Tuff, Goat	331080E 6404200N	uTSs	Massive sulphide pods occur in Stuhini volcanics over an area of about 1200 x 1200 metres. These pods average less than 10 centimetres in width and are from 1 to 20 metres long. They are composed of pyrite with lesser arsenopyrite, chalcopyrite and pyrrhotite.	Strain (1981), Korenic (1982a) Lehtinen (1989), Van Angeren (1991) Kerr (1948)
Cumulate magnetite occurrences:					
104G 026	MH, Shakes Creek	338500E 6416500N	uTSv	Tuffaceous siltstone and andesite are intruded by magnetite-rich clinopyroxenite. Magnetite occurs interstitially throughout the rock as grains and blebs. The magnetite content varies but averages 15-19%. Two pyrite veins, 30 to 40 centimetres wide, cut the occurrence and carry minor chalcopyrite mineralization. Ultramafic intrusion is referred to as the Latimer Lake pluton.	EMPR AR 1965, '66; McIntyre (1966) Souther (1972) EMPR MP CORPFILE (Stikine Iron Mines Ltd., North Pacific Mines Ltd.)

Abbreviation: EMPR AR = Energy, Mines and Petroleum Resources Annual Report, GEM = Geology, Exploration and Mining.

ACKNOWLEDGMENTS

Fossil identifications by F. Cordey and T. Poulton provided key age constraints. Additional field observations by C. Aspinall, D. Marud, B. McClelland and W. McMillan greatly contributed to the final products and success of this project. Their data and comments were appreciated. Thanks are extended to W.J. McMillan, J.M. Newell, M.G. Mihalynuk and G.T. Nixon for improving the manuscript.

REFERENCES

Aspinall, N.C., Strain, D.M. and Blain, A. (1990): Assessment Report on Geological Mapping, Geochemical Sampling, Geophysical Surveying and Prospecting on the Poker Property; *B.C. Ministry of Energy, Mines and Petroleum Resources*, Assessment Report 20724.

Berger, W.H. (1974): Deep-sea Sedimentation; *in* The Geology of Continental Margins, Burke, C.A., Drake, C.L., Editors, *Springer*, New York, Heidelberg, Berlin, pages 213-241.

Brown, D.A. and Greig, C.J. (1990): Geology of the Stikine River – Yehiniko Lake Area, Northwestern British Columbia (104G/11W, 12E); *in* Geological Fieldwork 1989, *B.C. Ministry of Energy, Mines and Petroleum Resources*, Paper 1990-1, pages 141-151.

Brown, D.A., Greig, C.J. and Gunning, M.H. (1990): Geology and Geochemistry of the Stikine River – Yehiniko Lake Area, Northwestern British Columbia (104G/11W, 12E); *B.C. Ministry of Energy, Mines and Petroleum Resources*, Open File 1990-1.

Brown, D.A. and Gunning, M.H. (1989a): Geology of the Scud River Area, Northwestern British Columbia (104G/5, 6); *in* Geological Fieldwork 1988, *B.C. Ministry of Energy, Mines and Petroleum Resources*, Paper 1989-1, pages 251-267.

Brown, D.A. and Gunning, M.H. (1989b): Geology and Geochemistry of the Scud River Area, Northwestern British Columbia (104G/5, 6); *B.C. Ministry of Energy, Mines and Petroleum Resources*, Open File 1989-7.

Brown, D.A., Neill, I., Timmerman, J. and Harvey-Kelly, F. (1992): Geology and Geochemistry of the Chutine River and Tahltan Lake Areas, Northwestern B.C. (104G/12W, 13); *B.C. Ministry of Energy, Mines and Petroleum Resources*, Open File 1992-2.

Carmichael, R.G. and Holbek, P.M. (1989): 1989 Prospecting Report on the Rugged Mountain Property Canyon 25 Claim; *B.C. Ministry of Energy, Mines and Petroleum Resources*, Assessment Report 19072.

Davis, J.W. (1988): Geological and Geochemical Report on the MJ 1 to 16 Claims Stikine River Area; *B.C. Ministry of Energy, Mines and Petroleum Resources*, Assessment Report 18134.

Dunn, (1990): Latimer Lake Project, Report on Geological, Geochemical and Geophysical Programs on the Dole 1-4, Lake 1-4, Bake 1-4 and EN Claims; *B.C. Ministry of Energy, Mines and Petroleum Resources*, Assessment Report 20523.

Eccles, L. (1981): Geological and Geochemical Report on the Mist 1 and 2 Claims; *B.C. Ministry of Energy, Mines and Petroleum Resources*, Assessment Report 9218.

Folk, P. (1981): Geochemical Report on the Limp #2 Claim; *B.C. Ministry of Energy, Mines and Petroleum Resources*, Assessment Report 9092.

Gabrielse, H. (1977): Dease Lake Map Area; *Geological Survey of Canada*, Open File 707.

Hallof, P.G. (1963): Geophysical Survey of the Poke Claim Group; *B.C. Ministry of Energy, Mines and Petroleum Resources*, Assessment Report 535.

Hallof, P.G. (1966): Report on the Induced Polarization and Resistivity Survey on the Gordon Claim Group; *B.C. Ministry of Energy, Mines and Petroleum Resources*, Assessment Report 847.

Hodgson, C.J. and LeBel, J.L. (1974): South Tahltan Lake Property (#656 A) Magnetometer Survey; *B.C. Ministry of Energy, Mines and Petroleum Resources*, Assessment Report 5097.

Irvine, T.N. and Baragar, W.R.A. (1971): A Guide to the Chemical Classification of Common Volcanic Rocks; *Canadian Journal of Earth Sciences*, Volume 8, pages 523-548.

Kasper, B. (1990): Geological and Geochemical Report on the Rattle and Roll Claims; *B.C. Ministry of Energy, Mines and Petroleum Resources*, Assessment Report 19870.

Kerr, F.A. (1948): Lower Stikine and Iskut River Areas, British Columbia; *Geological Survey of Canada*, Memoir 246, 94 pages.

Korenic, J.A. (1982a): 1981 Assessment Report of Geological, Geochemical and Geophysical Work Performed on the Tuff 1 Claim; *B.C. Ministry of Energy, Mines and Petroleum Resources*, Assessment Report 10475.

Korenic, J.A. (1982b): 1981 Assessment Report of Geological, Geochemical and Geophysical Work Performed on the Mist 1 and 2 Claims; *B.C. Ministry of Energy, Mines and Petroleum Resources*, Assessment Report 10476.

Lehtinen, J. (1989): 1989 Geological and Geochemical Report of the Goat 1 to 11 Claims; *B.C. Ministry of Energy, Mines and Petroleum Resources*, Assessment Report 19439.

Lion, J.G. (1971): P-T Stabilities of Laumontite, Wairakite, Lawsonite, and Related Minerals in the System, $CaAl_2Si_3O_8$-SiO_2-H_2O; *Journal of Petrology*, Volume 12, pages 379-411.

Logan, J.M. and Koyanagi, V.M. (1989a): Geology and Mineral Deposits of the Galore Creek Area, Northwestern B.C. (104G/3, 4); *in* Geological Fieldwork 1988, *B.C. Ministry of Energy, Mines and Petroleum Resources*, Paper 1989-1, pages 269-284.

Logan, J.M. and Koyanagi, V.M. (1989b): Geology and Mineral Deposits of the Galore Creek Area (104G/3, 4); *B.C. Ministry of Energy, Mines and Petroleum Resources*, Open File 1989-8.

Logan, J.M., Koyanagi, V.M. and Drobe, J.R. (1990a): Geology of the Forrest Kerr Creek Area, Northwestern British Columbia (104B/15); *in* Geological Fieldwork 1989, *B.C. Ministry of Energy, Mines and Petroleum Resources*, Paper 1990-1, pages 127-139.

Logan, J.M., Koyanagi, V.M. and Drobe, J.R. (1990b): Geology of the Forrest Kerr Creek Area, Northwestern British Columbia (104B/15); *B.C. Ministry of Energy, Mines and Petroleum Resources*, Open File 1990-2.

Logan, J.M., Drobe, J.R. and Elsby, D. (1992a): Geology of the More Creek Area, Northwestern B.C. (104G/2); *in* Geological Fieldwork 1991, Grant, B. and Newell, J.M., Editors, *B.C. Ministry of Energy, Mines and Petroleum Resources*, Paper 1992-1, this volume.

Logan, J.M. and Drobe, J.R. (1992b): Geology, Mineralization and Geochemistry of the More Creek Area, Northwestern British Columbia (104G/2); *B.C. Ministry of Energy, Mines and Petroleum Resources*, Open File 1992-5.

Marud, D. (1990a): Report of Activities on the Tahltan Lake Property; *B.C. Ministry of Energy, Mines and Petroleum Resources*, Assessment Report 20149.

Marud, D. (1990b): Report of Activities on the Rugged Mountain Property; *B.C. Ministry of Energy, Mines and Petroleum Resources*, Assessment Report 20154.

Marud, D. (1990c): 1990 Assessment Report on the Gran 16 Claim; *B.C. Ministry of Energy, Mines and Petroleum Resources*, Assessment Report 20302.

McIntyre, J.F. (1966): Engineering, Geophysical and Geological Report, Shakes East and Shakes West Groups; *B.C. Ministry of Energy, Mines and Petroleum Resources*, Assessment Report 773.

Monger, J.W.H. (1977): The Triassic Takla Group in McConnell Creek Map Area, North-central British Columbia; *Geological Survey of Canada*, Paper 76-29, 45 pages.

Morgan, J.T. (1976): Geology of the Ten Mile Creek Syenite – Pyroxenite Pluton, Telegraph Creek, B.C.; unpublished B.Sc. thesis, *The University of British Columbia*, 42 pages.

Pitcher, W.S. (1982): Granite Type and Tectonic Environment; *in* Mountain Building Processes, Hsu, K.J., Editor, *Academic Press*, pages 19-40.

Rennie, C.C. (1962): Copper Deposits in the Nicola Rocks, Craigmont Mine, *Western Miner & Oil Review*, February, pages 50-52.

RGS 104G (1987): National Geochemical Reconnaissance 1:250 000 Map Series, Sumdum – Telegraph Creek, Northwestern British Columbia (NTS 104F-104G); *B.C. Ministry of Energy, Mines and Petroleum Resources*, RGS-19.

Ryder, J.M. (1984): Terrain Inventory for the Stikine – Iskut River Area (NTS 104F, 104G and parts of 104B and 104H); *B.C. Ministry of Environment, Land and Parks*, Technical Report 11, 85 pages.

Southam, P. (1991): 1990 Exploration Report on the Tahltan Lake Property (Canyon 1-20, TL-1, TL-2 and TL-3 Claims); *B.C. Ministry of Energy, Mines and Petroleum Resources*, Assessment Report 21320.

Souther, J.G. (1959): Chutine, British Columbia; *Geological Survey of Canada*, Map 7-1959.

Souther, J.G. (1971): Geology and Mineral Deposits of Tulsequah Map Area; *Geological Survey of Canada*, Memoir 362, 76 pages.

Souther, J.G. (1972): Telegraph Creek Map Area; British Columbia; *Geological Survey of Canada*, Paper 71-44, 38 pages.

Strain, D.M. (1981): Geological and Geochemical Report on the Tuff Claims; *B.C. Ministry of Energy, Mines and Petroleum Resources*, Assessment Report 9200.

Streckeisen, A. (1976): To Each Plutonic Rock Its Proper Name; *Earth Science Reviews*, Volume 12, pages 1-33.

Van Angeren, P. (1991): Assessment Report on the 1990 Exploration Results (Geology, Geochemistry and Drilling) of the Goat 4 to Goat 7 Claims; *B.C. Ministry of Energy, Mines and Petroleum Resources* Assessment Report 20988.

Westcott, M.G. (1989a): Geological and Geochemical Work on the TRI 5-7, 9 and RUSH 5-8, 17-20, 23-24 Claims; *B.C. Ministry of Energy, Mines and Petroleum Resources*, Assessment Report 19143.

Westcott, M.G. (1989b): Geological and Geochemical Work on the Poker 1-7 Claims; *B.C. Ministry of Energy, Mines and Petroleum Resources*, Assessment Report 19247.

NOTES

British Columbia Geological Survey
Geological Fieldwork 1991

STRUCTURE, DUCTILE THRUSTING AND MINERALIZATION WITHIN THE PALEOZOIC STIKINE ASSEMBLAGE, SOUTH FORREST KERR AREA, NORTHWESTERN BRITISH COLUMBIA (104B/10, 15)

By D.C. Elsby, Consulting Geologist

KEYWORDS: Structural geology, Stikine assemblage, West Lake thrust, deformation, brittle faults, ductile shear, veins

INTRODUCTION

This report summarizes results of detailed structural mapping completed during the 1991 field season in the north Iskut River region. The study area is located near the boundary between the Intermontane and Coast tectonic belts. Rocks of the Stikine Terrane underlie the area and comprise mid-Paleozoic island-arc successions which are overlain by sediments and volcanics of the Late Triassic Stuhini Group (Kerr, 1948; Souther, 1972; Read *et al.*, 1989; Logan and Koyanagi, 1989; Logan *et al.*, 1990, 1992). Unnamed Early to Middle Jurassic volcanics and sediments overlie Stuhini rocks. The island-arc successions are host to significant precious and base metal mineralization throughout the Iskut River region. These successions are overlain to the east by Middle to Late Jurassic sediments of the Bowser Basin (Wheeler *et al.*, 1988).

Exploration has outlined a number of mineral deposits of varying types which include: gold-bearing veins (Snip and Johnny Mountain), porphyry copper deposits (Schaft Creek and Galore Creek), volcanogenic massive sulphide (Eskay Creek) and skarn mineralization (McLymont).

This paper focuses on the nature and timing of superimposed ductile and brittle shearing within the Paleozoic Stikine assemblage and its relationships to the development of regional shear zones and mineralization in the area located on lower Forrest Kerr Creek straddling the boundary between map sheets 104B/10 and B/15 (Figure 1-16-1).

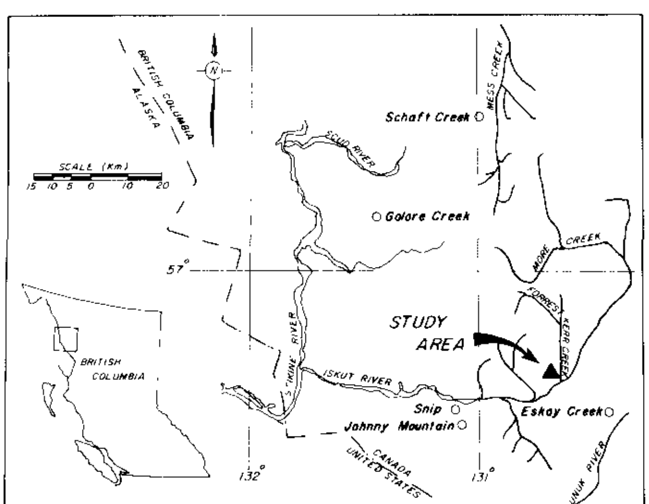

Figure 1-16-1. Location map of the north Iskut region showing position of study area.

REGIONAL GEOLOGY

Souther (1972), Read *et al.* (1989) and Logan *et al.* (1990) described rocks in the Forrest Kerr region as comprising three principal layered stratigraphic assemblages which are intruded by several generations of dioritic and granitoid igneous rock (Figure 1-16-1).

The oldest layered rocks within the study area are polydeformed and metamorphosed volcanics, volcaniclastics, and sediments of the Stikine assemblage. Microfossil data provide age limits which range from the Early Devonian to the Late Permian. Recent dating of extensive granitic and dioritic plutons within the Forrest Kerr area have returned radiometric dates as old as Mississippian (J.M. Logan, personal communication, 1991). These intrusions had previously been mapped as Jurassic in age (Souther, 1972; Logan *et al.*, 1990). Their exact age remains speculative.

Rocks of the Stikine assemblage are often unconformably overlain by deformed volcanics, volcaniclastics and sediments of the Upper Triassic Stuhini Group (Read *et al.*, 1989; Logan *et al.*, 1990, 1992). Where exposed, these rocks are variably deformed, complexly faulted and are nearly always in sharp faulted contact with underlying Paleozoic basement. Recent structural studies in the More Creek area (104G/2) to the north indicate that Stuhini rocks are generally unaffected by at least one early phase of folding only seen in Paleozoic strata (Holbek, 1988; Read *et al.*, 1989; Logan *et al.*, 1992). Most of the deformation recorded in Stuhini rocks is of a brittle nature with occasional scattered discrete high-strain zones of ductile-brittle shearing. Stuhini rocks are intruded by diorites, syenite porphyries and quartz monzonites of various ages. Quartz veins containing sulphides and associated precious metals occur adjacent to these intrusions in structurally favourable zones.

Unnamed Lower and Middle Jurassic and Middle to Upper Jurassic Bowser Lake Group rocks comprising sediments, volcanics and volcaniclastics unconformably overlie the Stuhini Group. These lithologies are brittly deformed and faulted and are intruded by minor dioritic sills and dikes with scattered syenite porphyry dikes injected along high-angle fault zones.

The above stratigraphy is cut by several generations of north-northeast-trending ductile and brittle fault zones. Four major fault or shear zones have been mapped in the Forrest Kerr area and have formed at different times in response to differing regional stress regimes. One of these, the West Lake thrust, an early ductile shear zone, trends through the study area and is the main focus of this report.

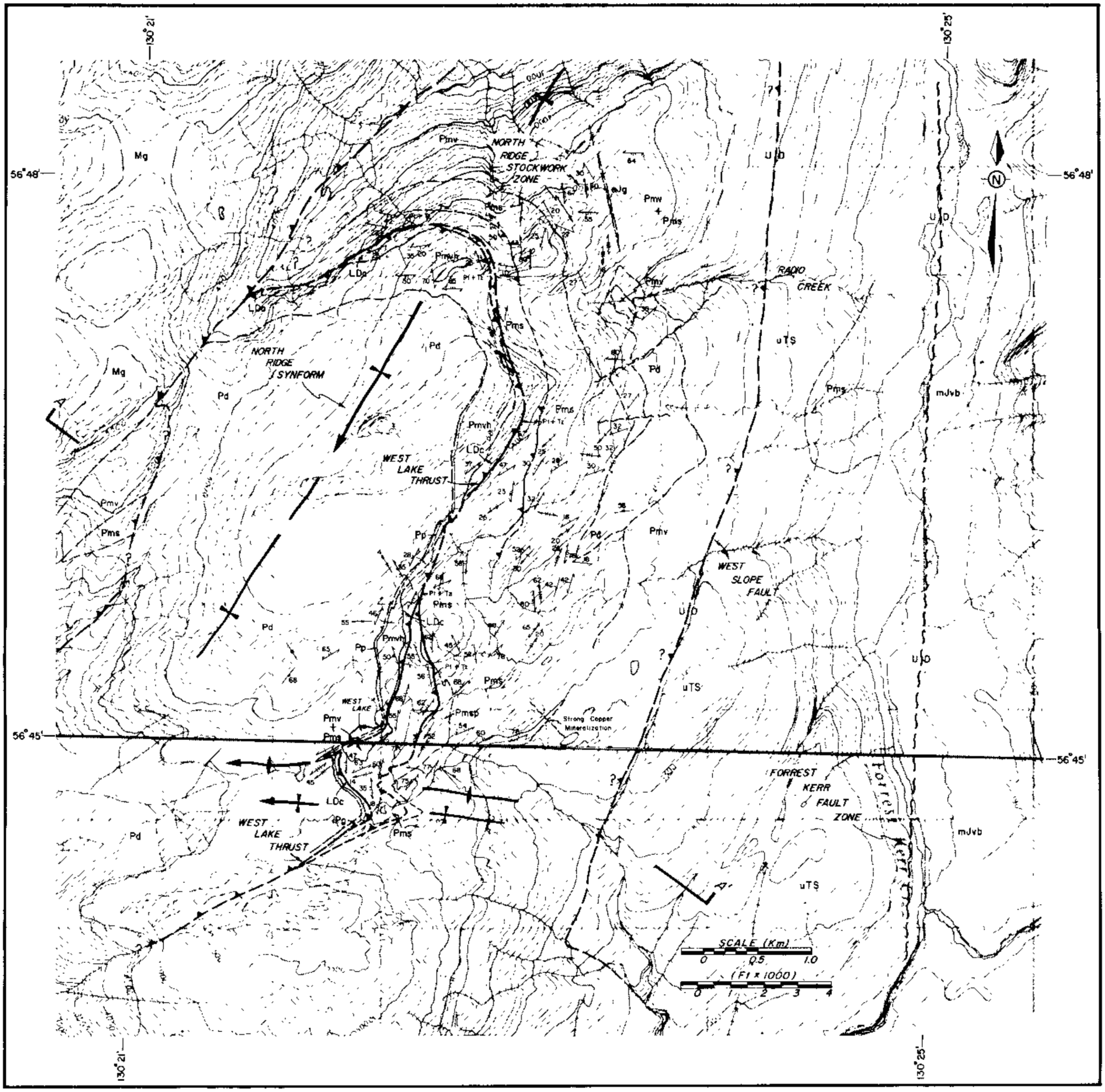

Figure 1-16-2. Geology map of the West Lake area. See facing page for legend.

LITHOLOGY

All layered rocks in the study area included in the Paleozoic Stikine assemblage are deformed by at least four phases of folding. Two principal lithologic packages have been defined within the area and are separated by the moderately to gently west-dipping West Lake thrust zone. Hangingwall rocks comprise a strongly deformed and metamorphosed Early Devonian and younger(?) package of volcanics, volcaniclastics and sediments containing distinctive carbonates. These deformed carbonates have been structurally emplaced over a footwall assemblage of Permian and older metavolcanics, metavolcaniclastics and metasediments. Both successions are intruded by quartz diorite of probable Paleozoic age (Read *et al.*, 1989; Logan *et al.*, 1990). In some areas, this intrusion is disturbed by the thrusting.

HANGINGWALL ASSEMBLAGE

LOWER DEVONIAN CARBONATES — LDc

Light grey to black, thin-bedded, strongly foliated marble, limestone and calcareous argillite and phyllite define

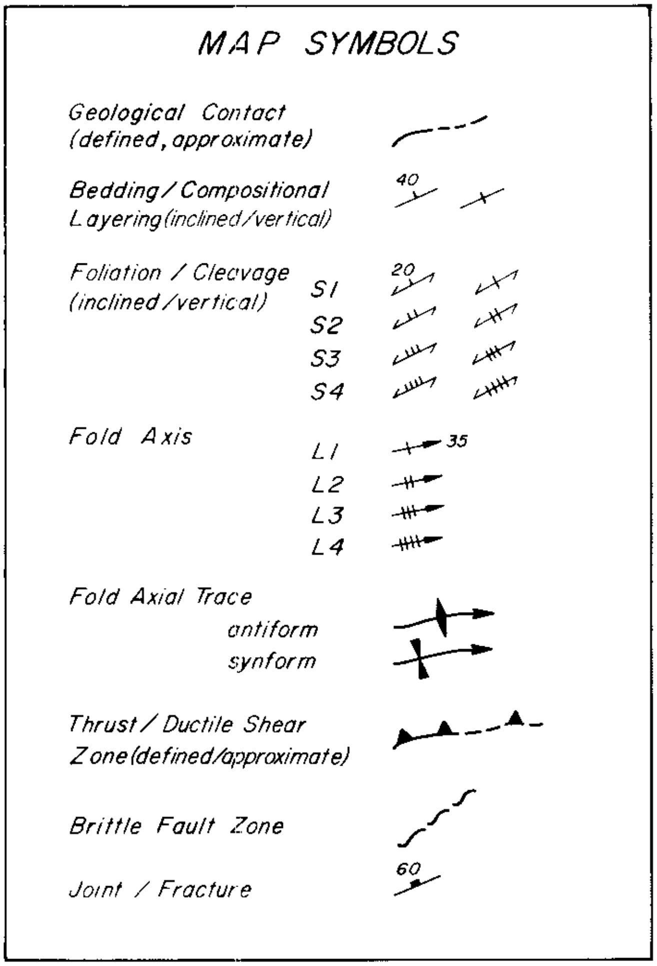

LEGEND

LAYERED ROCKS

MIDDLE TO UPPER JURASSIC

mJvb — PILLOW BASALT, FLOW BRECCIA, HYALOCLASTITE

UPPER TRIASSIC STUHINI GROUP

uTS — UNDIVIDED VOLCANICS AND SEDIMENTS

PALEOZOIC METAMORPHIC ROCKS (STIKINE ASSEMBLAGE)

LOWER DEVONIAN AND YOUNGER (?) HANGINGWALL ROCKS

Pp — FOLIATED GREY-GREEN PLAGIOCLASE PORPHYRY, MINOR BLACK PHYLLITIC SILTSTONE

Pmvh — FOLIATED VOLCANICS-VOLCANICLASTICS: LAPILLI, BLOCK, ASH TUFF SCHISTS AND PHYLLITES, ANDESITE FLOWS, SERICITE-QUARTZ SCHIST

LDc — THIN BEDDED FOLIATED GREY TO BLACK RECRYSTALLIZED LIMESTONE AND MARBLE, MINOR PHYLLITIC SILTSTONE

PERMIAN AND OLDER (?) FOOTWALL ROCKS

Tz — THRUST ZONE: BLACK SERICITE-QUARTZ SCHISTS AND MYLONITES

Pt — TAN BROWN TO GREY SERICITE-QUARTZ SCHISTS AND MYLONITES, BLACK CALCAREOUS-SERICITIC MYLONITES

Pms — GREY AND PURPLE SCHISTS, GREEN RIBBON CHERT, LAPILLI TUFF SCHIST, TAN THIN-BEDDED METASILTSTONE/SANDSTONE; GREY TO BLACK GRAPHITE-SERICITIC PHYLLITE (Pmsp)

Pmv — FOLIATED GREEN AND PURPLE PYROXENE-PHYRIC ANDESITE FLOWS, SCHISTOSE LAPILLI TUFF

INTRUSIVE ROCKS

EARLY JURASSIC

eJg — HORNBLENDE-BIOTITE K-FELDSPAR MEGACRYSTIC GRANITE, MINOR K-SPAR SYENITE PORPHYRY DIKES

PERMIAN AND OLDER (?)

Pd — FOLIATED HORNBLENDE-QUARTZ-DIORITE, GRANITE, FINE GRAINED BASALTIC DIKES

Mg — MISSISSIPPIAN (?) HORNBLENDE-BIOTITE GRANITE

the oldest and structurally lowest units within the study area (Figure 1-16-2). The carbonates range to in excess of 200 metres thick, are commonly fossiliferous and have been dated Early Devonian (Read *et al.*, 1989). This unit outcrops as a narrow, discontinuous north-trending, northwest-dipping band except in the north where large-scale synformal folding has changed this orientation to northeast (Figure 1-16-2). It structurally overlies and is separated from Permian and older metavolcanics and metasediments by narrow zones of ductile shearing and thrusting.

Thrust contacts dip moderately to gently west to northwest. Compositional layering within the carbonates is generally strongly folded and transposed parallel to early foliations related to thrusting. Intrafolial isoclinal folds are common and original stratigraphic directions are indeterminate due to the high degree of transposition and recrystallization. Minor quartz veining is prominent adjacent to the lower thrust contacts and represents at least two generations of hydraulic fracturing and fluid mobilization.

PALEOZOIC METAVOLCANICS (Pmvh)

Conformably overlying the Lower Devonian carbonates is a package of up to 500 metres of strongly flattened and sheared metavolcanics, metavolcaniclastics and metasediments of Early Permian to Early Devonian and older(?) age (Read *et al.*, 1989). The exact age and relationship of these strata to footwall Unit Pp of Read *et al.* (1989) and its equivalent, Unit Pmv of Logan *et al.* (1990) is uncertain. There is a possibility that Units Pmvh and Pmv are of different ages and they are therefore described separately. Strata generally dip to the southwest, vary from dark green to tan and grey-brown, and comprise phyllitic to schistose lapilli and block-tuffs, volcanic debris-flows phyllitic to schistose ash-tuff units, pyroxene-phyric andesitic flows, minor argillite and quartz-sericite schists. Layering within these units has been complexly folded and often transposed parallel to early foliations. These rocks are intruded and locally hornfelsed by a large body of Paleozoic(?) hornblende quartz diorite (Read *et al.*, 1989; Logan *et al.*, 1990). High-strain states during deformation and metamorphism have produced local mylonite zones related to thrusting in quartz-sericite schists.

FOLIATED FELDSPAR PORPHYRY — Pp

Foliated grey-green plagioclase porphyry containing minor black inclusions of phyllite occurs as a thin discontinuous unit separating Paleozoic metavolcanics from the large hornblende quartz diorite intrusion (Figure 1-16-2). This unit ranges to 20 metres in thickness and is typically strongly sheared and silicified along its trace. Both upper and lower contacts are often obscured by extensive iron carbonate alteration zones and are frequently interfoliated with Lower Devonian carbonates and Paleozoic metavolcaniclastics. The porphyry may represent a sheared, altered and recrystallized chilled margin of the diorite, though its genesis remains uncertain.

HORNBLENDE QUARTZ DIORITE — Qd

A large body of medium-grained equigranular hornblende quartz diorite intrudes all hangingwall units (Figure 1-16-2). Smaller quartz diorite bodies intrude footwall rocks and are classified as peripheral intrusions related to the main quartz diorite (Read *et al.*, 1989; Logan *et al.* 1990). In general, the quartz diorite comprises a heterogeneous mix of granitic and dioritic phases with quartz diorite as the dominant phase. Dark green diabase dikes of random orientation are scattered throughout the intrusion. Its eastern margin is in sharp contact with hangingwall units Pp, Pmvh and LDc. Here, the intrusion is cut by narrow discontinuous northeast-trending foliate zones related to ductile shearing. Locally, the intrusion is characterized by a braided, almost brecciated texture defined by angular amphibolite xenoliths within a sheared, more granitic matrix. The western margin of the quartz diorite is in thrust contact with an extensive granitic pluton of possible Mississippian age (Logan *et al.*, 1990; J.M. Logan, personal communication, 1991; Figures 1-16-2 and 3).

Paleozoic Footwall Assemblage

PERMIAN AND OLDER MAFIC METAVOLCANICS — Pmv

Mafic metavolcanics, primarily of pyroxene-phyric andesite flows and schistose lapilli tuffs ranging to in excess of 1500 metres thick, comprise the structurally lowest unit mapped within the study area. Andesitic flows are generally dark green to purple, moderately to weakly foliated and often massive. Lapilli tuffs are typically mottled green and purple and contain zones of high strain where lapilli are strongly attenuated within an early foliation plane (Logan *et al.*, 1990). Units within this package may be repeated by minor low-angle thrusting and include chlorite-sericite schists, grey phyllite, and minor recrystallized limestones.

PERMIAN AND OLDER METASEDIMENTS — Pms

Structurally and stratigraphically overlying the metavolcanics is a package of mixed metasedimentary and metavolcaniclastic rocks up to 700 metres thick. Strata within this unit are variable and discontinuous and comprise moderately west-dipping black graphitic and sericitic phyllites (Pmsp), green ribbon cherts, grey and purple phyllite and schists, grey to tan thin-bedded siltstone and sandstone, sericite-quartz phyllites and schists, siliceous ash-tuffs, purple schistose lapilli tuff and phyllitic to schistose volcanic breccia and debris flows. Original layering within most lithologies has been sheared and often transposed along early foliation planes, although bedding is preserved in scattered localities. Facing directions indicate these rocks are right way up.

SYENITE PORPHYRY DIKES — eJg (?)

Late-stage coarse felsic dikes containing porphyritic to megacrystic potassium feldspar outcrop randomly throughout the area. The age of these rocks is uncertain, but they may be related to Unit eJg of Logan *et al.* (1990), a potassium feldspar megacrystic granite which outcrops immediately south of the study area.

STRUCTURE

All layered rocks within the study area have been deformed and metamorphosed to lower to subgreenschist facies (Read *et al.*, 1989; Logan *et al.*, 1990). Four regionally significant phases of folding and shearing can be discerned locally. It is the superposition of these phases within areas of varied lithology which has produced the transposition of compositional layering and significant tectonic shortening observed throughout the area. Figures 1-16-2 and 3 illustrate map and cross-section geometry; Table 1-16-1 outlines the primary characteristics of each deformation event.

Folding

D_1 DEFORMATION

The geometry of the D_1 deformation is characterized by a northeast-trending penetrative transposed foliation, S_1,

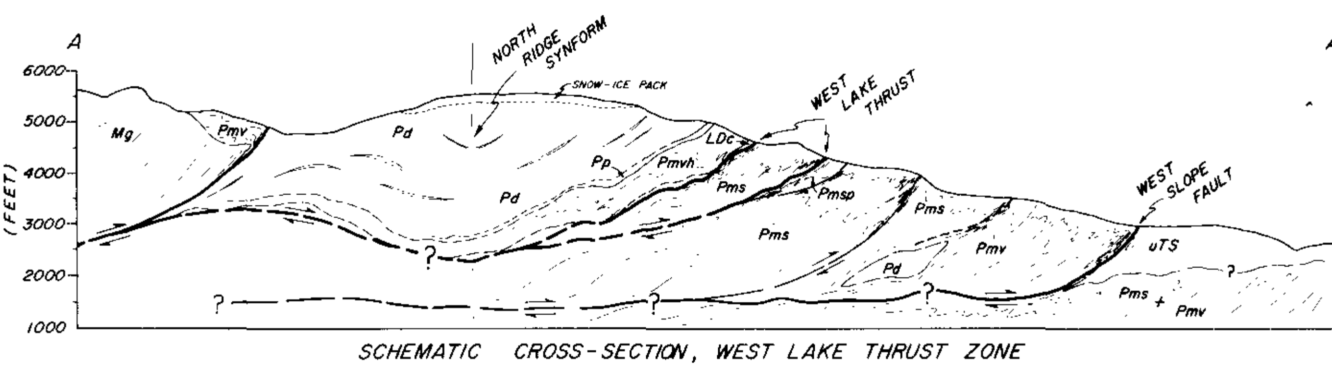

Figure 1-16-3. Cross-section, partly schematic, through the West Lake area.

which is axial planar to intrafolial isoclines and larger mesoscopic tight to isoclinal folds outlined by S_0 (Plate 1-16-1; Table 1-16-1). This early deformation is associated with regional metamorphism which has produced a recrystallized-mica fabric parallel to S_1. Axial planes generally dip moderately to gently northwest with shallow to moderately southwest-plunging fold axes. Phase-one minor folds are often asymmetrical from which a general southeast sense of vergence is deduced. Some minor folds display opposing senses of rotation which may indicate the presence of large-scale structures.

Approaching the West Lake thrust, F_1 folds and associated S_1 foliation are gradually rotated through nearly 30° into parallelism with the thrust zone, as a result of D_2 deformation (Figure 1-16-2).

D_2 DEFORMATION

The second phase of folding and its related foliation, S_2, are developed along a northeast trend and deform all earlier structures (Plate 1-16-2; Table 1-16-1). Axes of minor F_2 folds plunge gently to the southeast within moderately to gently northwest-dipping axial planes. Discrete zones of high ductile strain, in which F_1 and F_2 folds become progressively appressed, strongly attenuated and often transposed within S_2, are associated with the folding. Away from these zones, F_2 folds become more open and often display an asymmetry related to a southeast-directed sense of vergence.

Several major D_2 ductile strain zones define the northwest-dipping West Lake thrust (Figures 1-16-2 and 3). The thrust zone comprises discrete shear zones, 20 centimetres to 1 metre wide, in which both hangingwall and footwall units are completely transposed and have mylonite fabrics (Plate 1-16-3). The main zone and splays are flanked by subparallel bands of sericite-quartz schist, 3 to 10 metres thick, which contain isoclinal F_2 folds. East-vergent folding becomes progressively more open away from these bands. Other less sericitic shear zones occur throughout footwall rocks, but are not well developed in the hangingwall stratigraphy. Studies of deformed L_1 linear structures within F_2 folds indicate that the D_2 shear direction trends to the southeast at a high angle to F_2 hinge-lines. Based on these observations and previous work of Read *et al.* (1989) and Logan *et al.* (1990), the West Lake thrust is interpreted as having its latest movement directed to the southeast during late D_2 deformation.

D_3 DEFORMATION

Phase-three folding deforms the West Lake thrust with a trend almost orthogonal to F_1 and F_2 structures (Table 1-16-1). Phase-three folds and their related cleavage are developed along an east to southeast trend with steeply south-dipping axial planes and gently east- and west-plunging fold axes. A non-penetrative spaced cleavage typifies the S_3 fabric. Strong shearing along S_3 in the area

TABLE 1-16-1
DEFORMATION CHARACTERISTICS AND NOMENCLATURE FOR THE WEST LAKE AREA

Event	Characteristics	Nomenclature	Orientation (Original)
D_0	Compositional layering/bedding	S_0	variable, NE trending, generally NW dipping
D_1	Mesoscopic tight to isoclinal and intrafolial folds outlined by S_0, flattened, sheared, appressed; generally southeast verging	F_1	NE trending, NW dipping, variable
	Poorly developed mica-edge lineations, minor fold axes	L_1	SW plunging, 25/220
	Transposed regional axial-planar foliation associated with low-grade regional metamorphism	S_1	020-060/30 NW, variable
D_2	Mesoscopic, disharmonic shear folds outlined by S_0/S_1; generally planar limbs with thickened hinge regions; limbs are often sheared out along S_2 shear zones; generally southeast verging	F_2	NE trending, NW dipping
	Minor fold axes, mica-edge and mineral lineations	L_2	SW plunging 30/210, variable
	Well-developed penetrative axial-planar foliation and minor ductile shear zones	S_2	020-040/35 NW, variable
	— formation of low-angle thrust zones and associated mylonites, West Lake thrust		
	— associated with C and S-band microfabric development and peak metamorphism		
	— rotation of F_1 folds into parallelism with S_2 shear zones		
D_3	Mesoscopic to macroscopic upright, open to tight ductile-brittle folds, kink bands and crenulations	F_3	E to SE trending, variably N-S dipping, mod. to steep
	— macroscopic folding of the West Lake thrust		
	Minor fold axes, intersection lineations, S_1, S_2 with S_3	L_3	15/090, 270
	Nonpenetrative spaced cleavage, fracture cleavage	S_3	090-120/80 N-S
	— scattered vein mineralization along related fault and fracture zones		
D_4	Mesoscopic to macroscopic upright, open brittle buckle folds, and steep brittle faulting, minor chevron folds	F_4	NE to NW trending, variable steep E-W dip
	— synformal folding; warping of the West Lake thrust		
	Minor fold axes	L_4	20/360, 180
	Nonpenetrative fracture cleavages and brittle fault zones	S_4	160-200/80 E-W
	— scattered vein mineralization along related fault and fracture zones		

Plate 1-16-1. F_1 minor folds in sericite-graphite schist (footwall); looking northeast.

Plate 1-16-2. F_2 minor folds in thin-bedded metacherts and siltstones (footwall); view down-plunge, looking south.

surrounding West Lake has deformed the West Lake thrust and associated splays into upright, moderately open mesoscopic folds (Figure 1-16-2). In more competent lithologies, D_3 deformation is represented by kink banding and spaced fracture cleavages which provide structural control for localized iron carbonate alteration and vein mineralization. This deformation represents a ductile-brittle transitional phase associated with north-south compression.

D_4 DEFORMATION

Phase-four folds have an open, upright style and steeply dipping axial surfaces which trend almost orthogonal to F_3 structures (Figure 1-16-2; Table 1-16-1). All rock types and the West Lake thrust are involved in the northeast-trending, gently southwest-plunging North Ridge synform (Figure 1-16-3). Minor folds produce open buckling in more competent rocks and chevron folds in finer grained lithologies. S_4 is developed as a steep variably east to west-dipping fracture cleavage and as steep, minor brittle faults that locally provide structural control for polymetallic and precious metal bearing quartz veins and iron carbonate alteration.

FAULTING

With the exception of thrust faulting along the West Lake zone, little significant faulting was recognized within the map area. Several northwest-trending faults near Radio Creek have displaced quartz diorite contacts and are sites of scattered quartz and minor sulphide veining (Figure 1-16-2).

METAMORPHISM AND MICROFABRICS

All rock units within the area have undergone low-grade regional metamorphism to the lower greenschist facies. Muscovite and sericite laths are preferentially developed along S_1 and S_2 surfaces with only occasional weak alignment along S_3. Metamorphism initiated during D_1 deformation reached its peak late in the D_2 deformation. Fine-grained sericite schists contain the assemblage sericite-muscovite-chlorite-calcite-epidote. Early quartz veins are strongly deformed and recrystallized.

Microfabrics within thrust zones record a history of strong ductile shearing, mylonite development and dynamic recrystallization. Schists adjacent to the West Lake thrust contain prominent C fabrics defined by sericite and muscovite. Angular relationships between C and S_2 fabrics within these rocks vary between 5° and 10° with S_1 often completely transposed parallel to S_2. Polygonized and extremely attenuated quartz porphyroclasts outlined by sericite, define anastomosing elliptical shape-fabrics which define the S_2 foliation.

Deformed quartz occurs primarily within early hydraulic fractures and shows pronounced slip along incipient kink-band boundaries and the beginnings of ribbon-grain

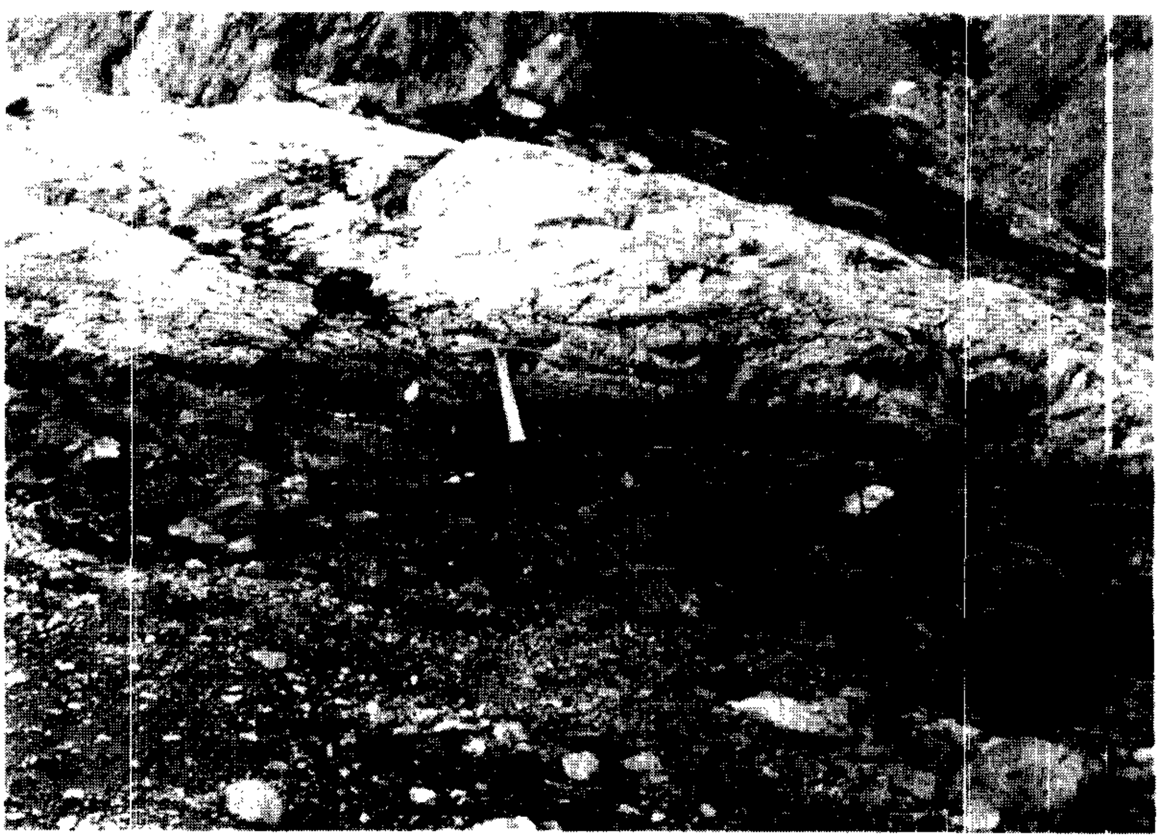

Plate 1-16-3. West Lake thrust zone; gently west-dipping hangingwall Lower Devonian carbonates structurally overlie footwall Permian and older sericite schists; looking west.

development. Strong recrystallization and recovery processes (diffusion-climb) have also polygonized quartz into subgrains outlined by sutured boundaries with individual subgrains having undulose extinction and mismatched birefringence.

Calcite within the main thrust zones and hangingwall carbonates is typically twinned and kinked with slip occurring along twin boundaries. The development of closely spaced twinning and incipient buckling of the twins is indicative of high stress. Minor zones of polygonization and subgrain development within larger calcite grains are also present.

ECONOMIC GEOLOGY

Mineral prospects and alteration zones are scattered throughout the study area, but are most concentrated in footwall metavolcanics. Quartz-vein stockworks and individual quartz veins with associated precious metal bearing sulphides occur in several localities and are the main exploration targets within the area (Figure 1-16-2). Iron carbonate alteration is widespread and occurs most prominently within D_3 and D_4 brittle fractures, along thrust-zone boundaries and in association with sulphide-bearing quartz vein systems. Numerous sigmoidal tension gashes filled with calcite and occasional quartz occur in all rock types and are indicative of progressive and complex deformation history.

VEINS

Strong fracturing and brittle shearing within metavolcanics provide structural control for iron carbonate alteration and quartz stockwork veining, the North Ridge stockwork zone, in the region north of Radio Creek (Figure 1-16-2). Many of the veins contain minor malachite, chalcopyrite, arsenopyrite, pyrite, azurite, galena, bornite, sphalerite and hematite.

Two generations of quartz veining are present: an early, deformed barren phase, and a later post-folding phase associated with iron carbonate alteration and sulphide precious metal mineralization. Early quartz vein systems, which are observed throughout the field area, crosscut bedding and are deformed by all four phases of folding. Microfabrics indicate significant pre to syn-F_1-F_2 hydraulic fracturing and incipient quartz veining. Quartz veins are strongly recrystallized and often transposed within S_1 and S_2 fabrics. Silica-rich fluid migration probably resulted from nearby Paleozoic intrusions and early dewatering and metamorphism of Paleozoic rocks.

Later quartz, sulphide and iron carbonate veining is controlled by orthogonal joints and brittle shears associated with F_3 and F_4 folding. S_4 fractures are pervasive in this area due to its position near the hinge zone of the North Ridge synform. Veins trend northeast, are typically undeformed and probably resulted from hydrothermal fluid convection from nearby intrusions. Similar quartz-sulphide veins and associated iron carbonate alteration occur in isolated late brittle joints and fault zones.

CONCLUSIONS

Paleozoic island-arc rocks in the south Forrest Kerr area are affected by an early phase of folding which is not seen in neighbouring Upper Triassic and Jurassic island-arc cover rocks. Phase-one folds are characterized by a transposed foliation and widespread east-vergent recumbent structures probably related to regional east-west compression during the Late Paleozoic to pre-Late Triassic. During this event metamorphism was initiated and as deformation progressed, was accompanied by the formation of low-angle ductile-brittle fault zones which accommodated localized strain in areas of varied lithology. This resulted in the formation of fault-bounded panels which remained relatively unstrained in comparison to more deformed rocks. This is a feature observed throughout the Forrest Kerr, More Creek and Mess Creek areas (Holbek, 1988; Read *et al.*, 1989; Logan *et al.*, 1990, 1992).

As deformation progressed into the Late Triassic and Jurassic, east-vergent F_2 folds were accompanied by increasing metamorphism and ductile shearing along established D_1, low-angle fault zones and F_2 axial plane surfaces. Shear directions during D_2 deformation trend southeast at a high angle to F_2 fold axes. Ductile fault zones such as the West Lake fault and numerous other thrusts developed subparallel to D_1 geometry and mylonite formed along their traces. The West Lake and West Slope faults place older Paleozoic stratigraphy over younger Paleozoic rocks, and Paleozoic rocks over Upper Triassic lithologies, respectively. Read *et al.* (1989) suggest an Early Cretaceous age for these faults. Estimates of movement along these structures remain ambiguous due to the lack of marker horizons.

Subsequent deformation records moderate to strong north-south compression that superimposed upright F_3 folding and fracturing on all rock types. This deformation represents a ductile-brittle transition during the last stages of waning metamorphism. Fourth-phase folding and faulting records a stress reorientation back to a dominantly east-west compression regime. This deformation produced widespread, inhomogeneous mesoscopic and macroscopic folds in cover rocks and more homogeneous folds in the Paleozoic stratigraphy. Deformation and recovery during this time may be associated in part with movement along large-scale regional faults such as the Forrest Kerr fault zone to the east of the study area.

Mineral prospects occur throughout the Iskut-Stikine region and in scattered locations within the field area. Quartz veins and stockworks derived from Jurassic and possibly older intrusives are controlled by F_3 and F_4-related joints and fractures. Sulphides and associated economic gold mineralization often accompany the quartz veining.

ACKNOWLEDGMENTS

The author gratefully acknowledges the British Columbia Geoscience Research Grant Program, Grant # RG91-26, for the financial support which made this fieldwork possible. I thank Doug Turnbull of Prime Resources Inc. and Mike Stammers of Pamicon Developments Limited, for the use of their geologic maps and camp facilities during the research.

I am grateful to Vancouver Island Helicopters for their prompt and safe flying and to James Gough for his assistance and enthusiasm. Finally, I wish to thank Jim Logan for his logistical support.

REFERENCES

Holbek, P.M. (1988): Geology and Mineralization of Stikine Assemblage, Mess Creek Area, Northwestern British Columbia; unpublished M.Sc. thesis, *The University of British Columbia*, 174 pages.

Kerr, F.A. (1948): Lower Stikine and Western Iskut River Areas, British Columbia; *Geological Survey of Canada*, Memoir 246, 94 pages.

Logan, J.M. and Koyanagi, V.M. (1989): Geology and Mineral Deposits of the Galore Creek Area, Northwestern B.C. (104G/3, 4); *in* Geological Fieldwork 1988, *B.C. Minstry of Energy, Mines and Petroleum Resources*, Paper 1989-1, pages 269-284.

Logan, J.M., Koyanagi, V.M., Drobe, J.R. (1990): Geology of the Forrest Kerr Creek Area, Northwestern British Columbia (104 B/15); *in* Geological Fieldwork 1989, *B.C. Ministry of Energy, Mines and Petroleum Resources*, Paper 1990-1, pages 127-139.

Logan, J.M., Drobe, J.R., Elsby, D.C. (1992) Geology of the More Creek Area, Northwestern British Columbia (104 G/2); *in* Geological Fieldwork 1990, Grant, B. and Newell, J.M., Editors, *B.C Ministry of Energy, Mines and Petroleum Resources*, Paper 1992-1, this volume.

Read, P.B., Brown, R.L., Psutka, J.F., Moore, J.M., Journeay, M., Lane, L.S. and Orchard, M.J. (1989): Geology of Parts of Snippaker Creek (104B/10), Forrest Kerr Creek (104B/15), Bob Quinn Lake (104B/10), Iskut River (104G/1), and More Creek (104G/2); *Geological Survey of Canada*, Open File 2094.

Souther, J.G. (1972): Telegraph Creek Map Area, British Columbia; *Geological Survey of Canada*, Paper 71-44, 38 pages.

Wheeler, J.O., Brookfield, A.J., Gabrielse, H., Monger, J.W.H., Tipper, H.W. and Woodsworth, G.J. (1988): Terrane Map of the Canadian Cordillera, *Geological Survey of Canada*, Open File 1894.

NOTES

PALEOZOIC STIKINE ASSEMBLAGE IN THE ISKUT RIVER AND CHUTINE RIVER REGIONS, NORTHWESTERN BRITISH COLUMBIA (104B/11, 12; 104F/9, 16)

By W.C. McClelland
University of California, Santa Barbara

KEYWORDS: Regional geology, Stikine assemblage, Yukon-Tanana Terrane, correlations.

INTRODUCTION

Paleozoic rocks included in the Stikine assemblage (Monger, 1977) are well exposed east of the Coast Belt between the Taku and Iskut rivers (Figure 1-17-1). Recent studies have provided insight into the age and stratigraphy of these Lower to Middle Devonian, Carboniferous and Permian strata in the Forrest Kerr – Newmont Lake and Scud River regions (*e.g.*, Anderson, 1989; Brown *et al.*, 1991). These studies provide a framework for interpretation and correlation of poorly known, Permian and older rocks described by Kerr (1948), Geological Survey of Canada (1957) and Souther (1959, 1972) in the Chutine River area and south of the Iskut River (Figure 1-17-1).

The nature of the contact between Paleozoic rocks of the Stikine assemblage and metamorphic rocks in the Coast Belt to the west is uncertain. Recent studies in southeastern Alaska suggest that metamorphic rocks west of and within the Coast Belt are correlative with the Yukon-Tanana and Nisling terranes (*e.g.*, Gehrels *et al.*, 1990, in press; Gareau, 1991; Rubin and Saleeby, 1991; Samson *et al.*, 1991; McClelland *et al.*, in press; Figure 1-17-1). Although the juvenile Sm-Nd isotopic signature of the Stikine Terrane is distinguished from the evolved signature characteristic of the Yukon-Tanana Terrane (Samson *et al.*, 1991), McClelland and Mattinson (1991) suggested that the Stikine assemblage may be partly correlative with mid-Paleozoic rocks in the Yukon-Tanana Terrane.

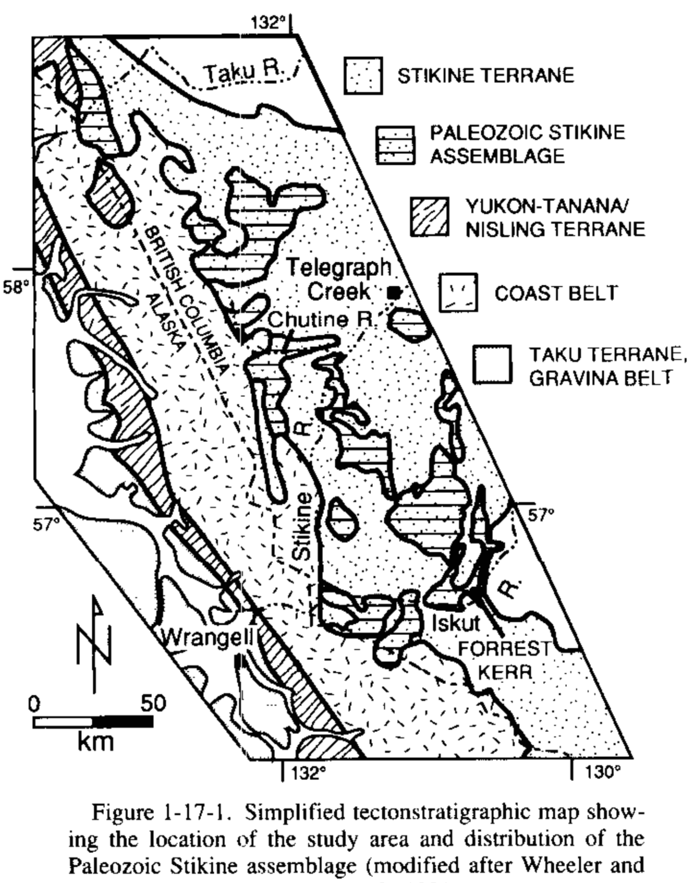

Figure 1-17-1. Simplified tectonstratigraphic map showing the location of the study area and distribution of the Paleozoic Stikine assemblage (modified after Wheeler and McFeely, 1987 and Brown *et al.*, 1991).

Fieldwork during 1991 focused on pre-Permian rocks of the Stikine Terrane to establish and compare the age, character and geologic relationships of the Stikinian basement with the Yukon-Tanana Terrane in southeastern Alaska. Permian and older rocks of the Stikine assemblage were examined in the Chutine River and Forrest Kerr regions and south of the Iskut River to provide a stratigraphic and structural framework for geochronologic and isotopic studies. The following article summarizes field observations from these areas. Results of conodont, macrofossil, geochronologic and isotopic studies in progress will be reported elsewhere. The preliminary descriptions following summarize the lithologic sections observed at these localities but will be revised as the results of structural analysis and fossil and geochronologic results demand.

ISKUT RIVER – CRAIG RIVER REGION (104B/11, 12)

Kerr (1948) and the Geological Survey of Canada (1957) outlined the regional distribution of metamorphic rocks that underlie limestone of known or suspected Permian age in the Stikine and Iskut region. Schistose to gneissic argillite, metavolcanic rocks, quartzite and limestone were reported and examined in this study south of the Iskut River at localities shown on Figure 1-17-2.

BRUNT CREEK

Brunt Mountain (Figure 1-17-2) is underlain by a massive section of clinopyroxene-porphyritic tuff, flows, volcaniclastic rocks and argillite of probable Late Triassic age (Kerr, 1948; Geological Survey of Canada, 1957). These volcanic rocks overlie a section of interlayered black argillite, siliceous tuff, fine-grained volcaniclastic rocks and discontinuous layers of light grey weathering, white marble. The marble layers may either be Permian in age, based on along-strike projection of limestone of probable Permian age exposed at the mouth of Brunt Creek and along the Craig River; or Triassic, based on comparison of this sequence with similar rocks in the Telegraph Creek area

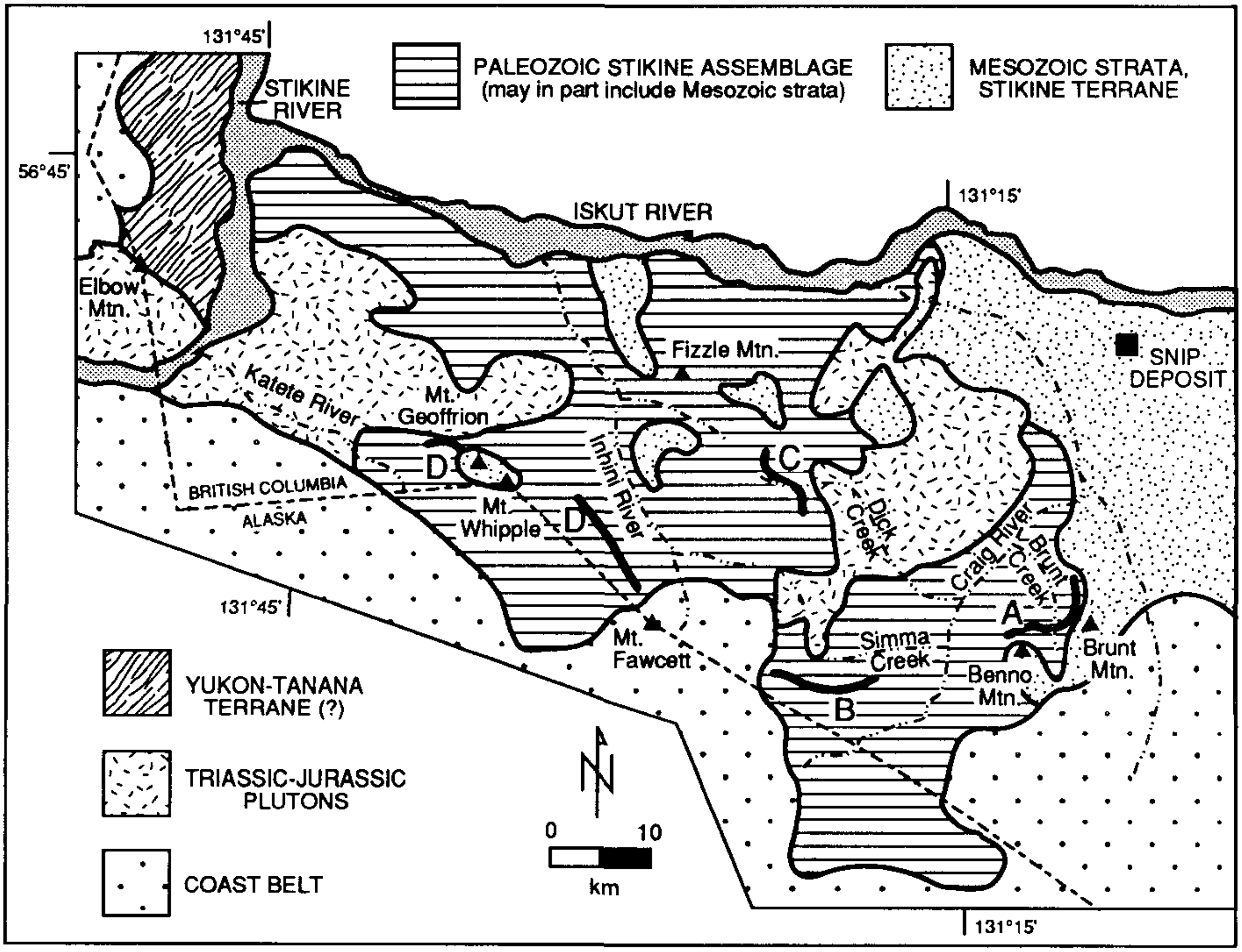

Figure 1-17-2. Location map of Iskut-Craig rivers study area showing the distribution of the Stikine assemblage (modified after Kerr, 1948 and Wheeler and McFeely, 1987) and general location of sections examined during this project.

(Souther, 1972; D.A. Brown, personal communication, 1991). In Brunt Creek, the marble-bearing section is underlain by phyllitic argillite and fine-grained volcaniclastic rocks with subordinate brown-weathering marble and mafic pillowed flows, fragmental rocks and tuff of uncertain but possible Carboniferous age. In Brunt Creek and north of Brunt Mountain, hornblende clinopyroxene gabbro and diorite that are inferred to be Late Triassic in age (Alldrick *et al.*, 1990) and appear compositionally similar to the uppermost volcanic sequence of probable Late Triassic age, intrude all of the above units.

Craig River – Simma Creek

The ridge between the Craig River and Simma Creek (Figure 1-17-2) is underlain by a thick sequence of garnet-biotite-white mica-feldspar-quartz schist derived from fine-grained quartzose, turbiditic strata and quartzite. Eastern exposures of the clastic sequence are intruded by foliated hornblende-biotite quartz diorite of unknown age. To the west, the quartzose turbidites grade upwards into a thick sequence of light green tuffaceous clastic rocks dominated by centimetre-scale beds of fine-grained sandstone, siltstone and mudstone. These rocks are in turn overlain by black argillite interlayered with dark brown marble and biotite-amphibole schist derived from mafic tuffs and flows. The argillite and volcanic section is capped by light grey weathering, white marble that is apparently laterally continuous with limestone of probable Permian age exposed along the Inhini River (Figure 1-17-2).

Quartz-rich clastic rocks at the base of this section are similar to continent-derived sediments of the Yukon-Tanana Terrane in southeastern Alaska (*e.g.*, Gehrels *et al.*, 1990). This correlation and the apparent depositional relationship between the quartzose clastic rocks and Permian rocks of the Stikine Terrane suggest that the Paleozoic Stikine assemblage either depositionally overlies or laterally grades into the Yukon-Tanana Terrane.

Dick Creek – Inhini River

East of the Inhini River, limestone of probable Permian age is faulted against a thick sequence of pyroxene crystal-lithic tuff and volcaniclastic rocks probably correlative with the Upper Triassic Stuhini Group (Figure 1-17-2). Nevertheless, the contact is probably a faulted depositional contact. Rocks conformably underlying the limestone in the unnamed creek south of Fizzle Mountain include tuffaceous siltstone and sandstone, siliceous siltstone, mafic tuff and minor brown-weathering limestone. North-dipping, massive Permian limestone along the north side of Dick Creek is underlain by probable Carboniferous interlayered green to brown tuffaceous siltstone, mafic flows, lapilli tuff and breccia. Thin limestone lenses within the volcanic section contain abundant crinoid fragments and rugose corals. Volcaniclastic rocks at the base of the unit grade downwards into light grey siliceous argillite. The upper part of the argillite contains a relatively thin (10 m) coarsely crystalline white marble. Exposures south of Dick Creek are dominated by a thick section of light green, tuffaceous to quartzose turbiditic rocks that are similar to the clastic rocks overlying the sequence of quartzose turbidites and quartzite south of Simma Creek. Centimetre-scale beds of fine-grained sandstone, siltstone and mudstone that make up the section may be Carboniferous or older as they appear to underlie the volcanic section exposed north of Dick Creek.

Mount Geoffrion – Mount Fawcett

Mount Geoffrion and Mount Whipple (Figure 1-17-2) are underlain by a thick sequence of probable Triassic mafic to intermediate, pyroxene, amphibole and plagioclase-bearing tuff, debris flows, volcaniclastic rocks and subordinate argillite that depositionally overlies massive light grey to white limestone of known Permian age (D.A. Brew, unpublished data). West of Mount Geoffrion, the limestone overlies centimetre-scale beds of fine-grained volcaniclastic rocks, tuff and argillite. The lower sequence contains at least two undated, massive limestone layers 5 to 20 metres thick. Probable Permian limestone along the ridge north of Mount Fawcett is underlain by mafic volcanic rocks, argillite and fine-grained tuffaceous clastic rocks. This section is similar to that below limestone of probable Permian age south of Simma Creek.

CHUTINE RIVER REGION (104F/9, 16)

Souther (1959) assigned rocks east of the Coast Belt in the Chutine River region to a metamorphic sequence that includes marble, quartzite and orthogneiss, a sequence of quartzose clastic rocks, mafic volcanic rocks and limestone. These rocks were examined at Chutine Lake and west of Triumph Creek, respectively (Figure 1-17-3). Penetratively deformed metamorphic rocks at Chutine Lake are derived from fine-grained turbiditic clastic strata and siliceous argillite intruded by granodioritic dikes. The ages of the metaclastic rocks and the granodiorite are unknown. These rocks are intruded by and locally faulted against plutonic rocks of probable Eocene age.

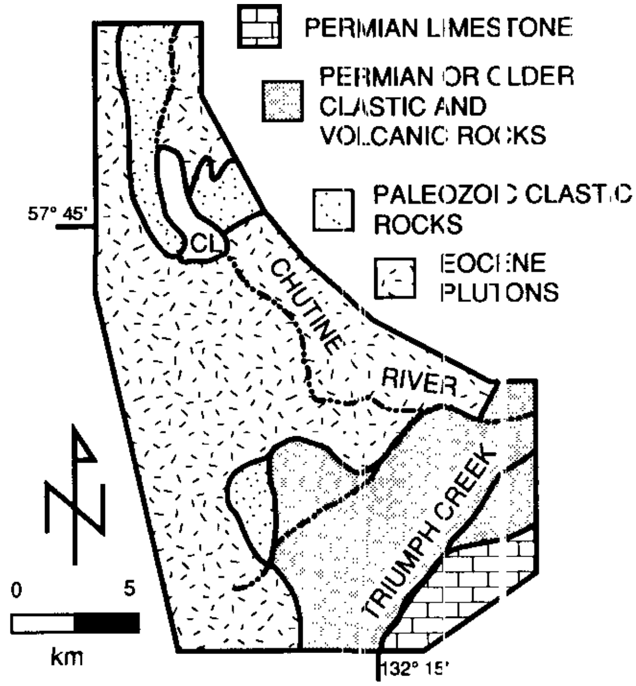

Figure 1-17-3. Generalized geologic map of the Chutine River area (modified from Souther, 1959) showing distribution of units discussed in text. CL-Chutine Lake Paleozoic Stikine assemblage (modified after Wheeler and McFeely, 1987 and Brown *et al.*, 1991).

West of Triumph Creek, the metaclastic section is overlain by a thick section of tuffaceous argillite, felsic tuff, limestone and mafic to intermediate flows, tuff and volcaniclastic rocks. Souther (1959) inferred a Triassic age for the volcanic portion of the section. A Permian or older age is more likely as these rocks are overlain by Permian limestone to the southeast (D.A. Brown, personal communication, 1991).

FORREST KERR REGION (104B/10, 15)

The Stikine assemblage exposed west of Forrest Kerr Creek (Figure 1-17-1) includes complexely deformed fine-grained clastic strata, siliceous argillite, limestone, mafic and felsic tuff, and mafic volcanic rocks (Anderson, 1989; Read *et al.*, 1989; Logan *et al.*, 1990a, b; Brown *et al.*, 1991). Massive limestone in the section has yielded Middle Devonian fossils (Anderson, 1989; Read *et al.*, 1989). It is interlayered with argillite, fine-grained tuffaceous clastic rocks, mafic volcanic rocks, intermediate fragmental rocks and intermediate to felsic tuff. This west-dipping section grades structurally down (to the east) into thinly bedded siliceous argillite and fine-grained clastic rocks, tuffaceous greywacke, maroon debris flows intermediate to felsic tuff and fine-grained tuffaceous clastic rocks. The age of this lower clastic sequence is uncertain, however, the section is similar to Permian or older clastic rocks that are depositionally overlain by Lower Permian limestone in the Scud River region (Brown and Gunning, 1989). Rocks of both sections are intruded by a dioritic to granitic complex that is interpreted as the marginal phase of large plutons to the west. These plutons may be Mississippian in age (J.M. Logan, personal communication, 1991) suggesting that the clastic section is Mississippian or older.

Read *et al.* (1989) and Logan *et al.* (1990b) suggested that the upper limestone-volcanic section structurally overlies the lower siliceous clastic section along a west-dipping thrust fault. Based on the apparent gradational contact between these two units, this fault probably does not have significant offset and the Forrest Kerr section may be alternatively interpreted as an overturned Middle Devonian to Permian sequence.

SUMMARY

The Paleozoic Stikine assemblage in the Iskut River - Craig River region of the Iskut River map area consists of (1) quartzose turbiditic strata, (2) fine-grained tuffaceous clastic rocks of uncertain age, (3) mafic volcanic rocks and argillite of probable Carboniferous age, and (4) Lower Permian limestone and mafic and subordinate felsic volcanic and volcaniclastic rocks. The structurally and inferred stratigraphically lowest unit of quartzose clastic rocks is similar and probably equivalent to continent-derived clastic strata of the Yukon-Tanana Terrane in southeastern Alaska, suggesting that parts of the Paleozoic Stikine assemblage may be correlative with Paleozoic rocks of this terrane. Clastic and volcanic rocks in the Chutine River are probably correlative with the Devonian to Permian rocks in the Forrest Kerr region and Units 2 and 3 listed above for the Iskut - Craig Rivers region.

ACKNOWLEDGMENTS

Fieldwork in the Iskut River map area was funded by the Geological Survey of Canada (Project 840046) through R.G. Anderson and by NSF grant EAR-8917316 (awarded to J.M. Mattinson). Fieldwork in the Chutine River region and sample collection in the Forrest Kerr region was supported by the British Columbia Ministry of Energy, Mines and Petroleum Resources through D.A. Brown and J.M. Logan, respectively. Additional funding for fieldwork and geochronologic studies was provided by the British Columbia Research Grant Program (RG91-19). Collaboration with R.G. Anderson, D.A. Brown and J.M. Logan was invaluable to the success of the project. The field observations outlined above are the result of coordinated mapping efforts of myself, M.H. Gunning and J. Rublee. Parts of this manuscript have greatly benefited from review by R.G. Anderson.

REFERENCES

Alldrick, D.J., Britton, J.M., MacLean, M.E., Hancock, K.D., Fletcher, B.A. and Hiebert, S.N. (1990): Geology and Mineral Deposits of the Snippaker Area; *B.C. Ministry of Energy, Mines and Petroleum Resources*, Open File 1990-16.

Anderson, R.G. (1989): A Stratigraphic, Plutonic, and Structural Framework for the Iskut River Map Area, Northwestern British Columbia; *in* Current Research, Part E, *Geological Survey of Canada*, Paper 89-1E, pages 145-154.

Brown, D.A. and Gunning, M.H. (1989): Geology and Geochemistry of the Scud River Area, Northwestern British Columbia (104G/5, 6); *B.C. Ministry of Energy, Mines and Petroleum Resources*, Open-File 1988-7.

Brown, D.A., Logan, J.M., Gunning, M.H., Orchard, M.J. and Bamber, W.E. (1991): Stratigraphic Evolution of the Paleozoic Stikine Aassemblage in the Stikine and Iskut Rivers Area, Northwestern British Columbia; *in* Contributions to the Geology and Geophysics of Northwestern British Columbia and Southeastern Alaska, Anderson, R.G., Editor, *Canadian Journal of Earth Sciences*, Volume 28, pages 958-972.

Gareau, S.A. (1991): The Scotia-Quaal Metamorphic Belt: A Distinct Assemblage with Pre-early Late Cretaceous Deformational and Metamorphic History, Coast Plutonic Complex, British Columbia; *in* Contributions to the Geology and Geophysics of Northwestern British Columbia and Southeastern Alaska; Anderson, R.G., Editor, *Canadian Journal of Earth Sciences*, Volume 28, pages 870-880.

Gehrels, G.E., McClelland, W.C., Samson, S.D. and Patchett, P.J. (in press): U-Pb Geochronology of Detrital zircons from the Yukon Crystalline Terrane in the Northern Coast Mountains Batholith, Southeastern Alaska; *Canadian Journal of Earth Sciences.*

Gehrels, G.E., McClelland, W.C., Samson, S.D., Patchett, P.J. and Jackson, J.L. (1990): Ancient Continental Margin Assemblage in the Northern Coast Mountains, Southeast Alaska and Northwest Canada; *Geology*, Volume 18, pages 208-211.

Geological Survey of Canada (1957): Stikine River Area, Cassiar District, British Columbia; *Geological Survey of Canada*, Map 9-1957.

Kerr, F.A. (1948): Lower Stikine and Western Iskut River Areas, British Columbia; *Geological Survey of Canada*, Memoir 246, 94 pages.

Logan, J.M., Koyanagi, V.M. and Drobe, J.R. (1990a): Geology of the Forrest Kerr Creek Area, Northwestern British Columbia; *in* Geological Fieldwork 1989, *B.C. Ministry of Energy, Mines and Petroleum Resources*, Paper 1990-1, pages 127-140.

Logan, J.M., Koyanagi, V.M. and Drobe, J.R. (1990b): Geology and Mineral Resources of the Forrest Kerr - Iskut River Area (104B/15); *B.C. Ministry of Energy, Mines and Petroleum Resources*, Open-File 1990-2.

McClelland, W.C. and Mattinson, J.M. (1991): U-Pb (Zircon) Constraints on the Age of the Yukon-Tanana Terrane in the Coast Mountains, Central Southeast Alaska and British Columbia (abstract); *Geological Society of America*, Abstracts with Programs, Volume 23, page A434.

McClelland, W.C., Gehrels, G.E., Samson, S.D. and Patchett, P.J. (in press): The Gravina Belt and Yukon-Tanana Terrane in Central Southeastern Alaska: Protolith Relations of Metamorphic Rocks along the Western Flank of the Coast Mountains Batholith; *Journal of Geology*.

Monger, J.W.H. (1977): Upper Paleozoic Rocks of the Western Canadian Cordillera and their Bearing on Cordilleran Evolution; *Canadian Journal of Earth Sciences*, Volume 14, pages 1832-1859.

Read, P.B., Brown, R.L., Psutka, J.F., Moore, J.F., Journeay, M., Lane, L.S. and Orchard, M.J. (1989): Geology of Parts of Snippaker Creek (104B/15), Forrest Kerr Creek (104B/15), Bob Quinn Lake (104B/16), Iskut River (104G/1), and More Creek (104G/2); *Geological Survey of Canada*, Open File 2094.

Rubin, C.M. and Saleeby, J.B. (1991): Tectonic Framework of the Upper Paleozoic and Lower Mesozoic Alava Sequence: A Revised View of the Polygenetic Taku Terrane in Southern Alaska; *in* Contributions to the Geology and Geophysics of Northwestern British Columbia and Southeastern Alaska, Anderson, R.G., Editor, *Canadian Journal of Earth Sciences*, Volume 28, pages 881-893.

Samson, S.D., Patchett, P.J., McClelland, W.C and Gehrels, G.E. (1991): Nd Isotopic Characterization of Metamorphic Rocks in the Coast Mountains, Alaskan and Canadian Cordillera: Ancient Crust Bounded by Juvenile Terranes; *Tectonics*, Volume 10, pages 770-780.

Souther, J.G. (1959): Chutine, Cassiar District, British Columbia; *Geological Survey of Canada*, Map 7-1959.

Souther, J.G. (1972): Telegraph Creek Map Area, British Columbia; *Geological Survey of Canada* Paper 71-44, 38 pages.

Wheeler, J.O. and McFeely, P. (1987): Tectonic Assemblage Map of the Canadian Cordillera; *Geological Survey of Canada*, Open File 1565.

NOTES

British Columbia Geological Survey
Geological Fieldwork 1991

PALEOMAGNETISM OF TOARCIAN HAZELTON GROUP VOLCANIC ROCKS IN THE YEHINIKO LAKE AREA (104G/11, 12): A PRELIMINARY REPORT

By T.A. Vandall, Pacific Geoscience Centre, G.S.C.,
D.A. Brown, B.C. Geological Survey Branch
and P.M. Wheadon, Consulting Geologist, Fulford Harbour, B.C.

(GSC Contribution No. 3191)

KEYWORDS: Paleomagnetism, block rotations, Hazelton Group, Toarcian volcanics, Yehiniko Lake, Chutine River.

INTRODUCTION

The first paleomagnetic study of Hazelton Group volcanic rocks included three localities in north-central British Columbia, near the eastern margin of the Intermontane Belt (Monger and Irving, 1980). A second, more recent study included two localities near the western margin of the Intermontane Belt and a third near the village of Telkwa (Vandall and Palmer, 1990; Figure 1-18-1). Both studies documented stable normal and reversed polarity magnetizations interpreted to be primary and Early Jurassic. The direction of magnetization at each of the six localities is different. However, within localities the data exhibit internally consistent directions of magnetization and, although declinations vary between each locality from 227° to 359°, inclinations are well grouped about an average of 53° (Vandall and Palmer, 1990). By comparing these results with the expected Early Jurassic direction for North America, inclinations were shown to be concordant. This indicates that rocks of the Early Jurassic Hazelton Group were at much the same latitude relative to the North American craton as they are now (Vandall and Palmer, 1990). In contrast, declinations for the Hazelton Group rocks are distinctly discordant, suggesting that large-scale block rotations about vertical axes have occurred between localities and relative to North America (Figure 1-18-1). One explanation for these block rotations is that they were generated by the process of accretionary tectonics which assembled former, discrete Jurassic island arcs along the ancient North American margin by at least Middle Jurassic time. The size and boundary relationships of these blocks is not yet known, and this information is critical to the assessment of possible rotation mechanisms.

The purpose of this investigation is to extend the geographic coverage of paleomagnetic data to assess the implications of these apparent large-scale block rotations and the apparent lack of latitudinal displacement relative to North America. Recent geochronometry and detailed mapping carried out around the Bowser Basin have advanced the concept that the Hazelton Group represents several volcanic episodes, perhaps related to discrete island arcs (*e.g.*, Anderson and Thorkelson, 1990; Brown and Greig, 1990; Diakow, 1990; MacIntyre *et al.*, 1989). As a consequence, paleomagnetism is ideally suited to provide a quantitative test of paleogeographic reconstructions and of tectonic settings of the Hazelton Group island arcs. In addition, Hazelton Group rocks studied to date exhibit periods of reversed polarity which may be chronologically and stratigraphically constrained in order to improve the current poor record of Early Jurassic magnetic polarity chrons. Establishing polarity zones would provide a powerful tool for stratigraphic correlation in the Hazelton Group.

In this report we outline the initial fieldwork, laboratory procedures in progress, preliminary results and proposed follow-up investigations for 1992.

GEOLOGY AND SAMPLING

The study area lies within northwestern Stikinia, approximately 20 kilometres east of the Coast Belt (Figure 1-18-1). Regionally, the stratigraphic succession includes Paleozoic limestones and island-arc volcanic rocks of the Stikine assemblage, Late Triassic and Early Jurassic island-arc volcanic and volcanogenic rocks of the Stuhini and Hazelton groups, and Late Cretaceous to Tertiary molasse sedimentary rocks of the Sustut Group. The Middle to Late Jurassic Bowser Lake Group is notably absent, due either to nondeposition or to erosion. Late Triassic, Early Jurassic, Middle Jurassic and Eocene plutons intrude all older units.

In the Iskut River area, 100 kilometres to the southeast, Anderson and Thorkelson (1990) divided the Hazelton Group into four formations. The lower three – the volcanogenic-dominated Unuk River, Betty Creek and Mount Dilworth formations – are overlain by the uppermost Salmon River Formation. In the Yehiniko Lake area, the well-exposed gently dipping Toarcian volcanic rocks of interest in this study are believed to be equivalent to the Salmon River Formation. Their late Early Jurassic age (Toarcian; Harland *et al.*, 1989) is well constrained by U-Pb and K-Ar geochronometry, and by macrofossils. A lower age constraint is provided by an andesite flow-breccia collected at locality IV shown in Figure 1-18-2, which yielded a zircon U-Pb age of 185±2 Ma (M.L. Bevier, written communication, 1991). An upper age constraint is provided by the "Saffron pluton" (formerly Yehiniko pluton) which intrudes the volcanic rocks and yields concordant hornblende and biotite K-Ar dates of 162±7 Ma (J. Harakal, written communication, 1990; Localities I and II, Figure 1-18-2). Further, intravolcanic sedimentary rocks contain Toarcian ammonite fragments, belemnites, brachiopods and scarce bivalves (Locality III, Figure 1-18-2; H.W. Tipper, Report J4-89-HWT, 1989).

In August, 1991, part of an exposure of gently northeast-dipping volcanic rocks, that form a section over 350 metres thick, was sampled in a prominent cirque at the headwaters of Kirk Creek (Figure 1-18-2). Access to the Kirk Creek area was by helicopter from Telegraph Creek, 40 kilometres to the north. Seven sites were sampled in the uppermost 80 metres of the section along the north face of the cirque (Plate 1-18-1; Table 1-18-1; Figure 1-18-3). Drilling was confined to the more massive flow units; site lithologies and stratigraphic positions are summarized in Figure 1-18-3 and Table 1-18-1.

The section comprises four divisions: (1) unstudied, lowermost flows and tuffs, (2) aphyric, amygdaloidal basalt flows overlain by mauve volcaniclastic beds, (3) rhyolite, and (4) porphyritic basaltic andesite flows. Division 2 comprises a northeastward-thickening wedge of basalt flows overlain by an equal thickness of epiclastic tuff beds. The flows, up to 5 metres thick, are dark brown to faintly maroon with characteristic abundant and large amygdules. Maroon flow-top breccia and chilled flow-contacts are common. The top half of this division is made up of thin to thick-bedded, poorly sorted and friable lithic-lapilli tuffs, that were not suitable for drilling. Lying on these epiclastic rocks is Division 3, consisting of conspicuous pink to buff-weathering, hematitic flow-banded and flow-folded aphanitic rhyolite (Figure 1-18-3; Plates 1-18-1 and 1-18-2). This

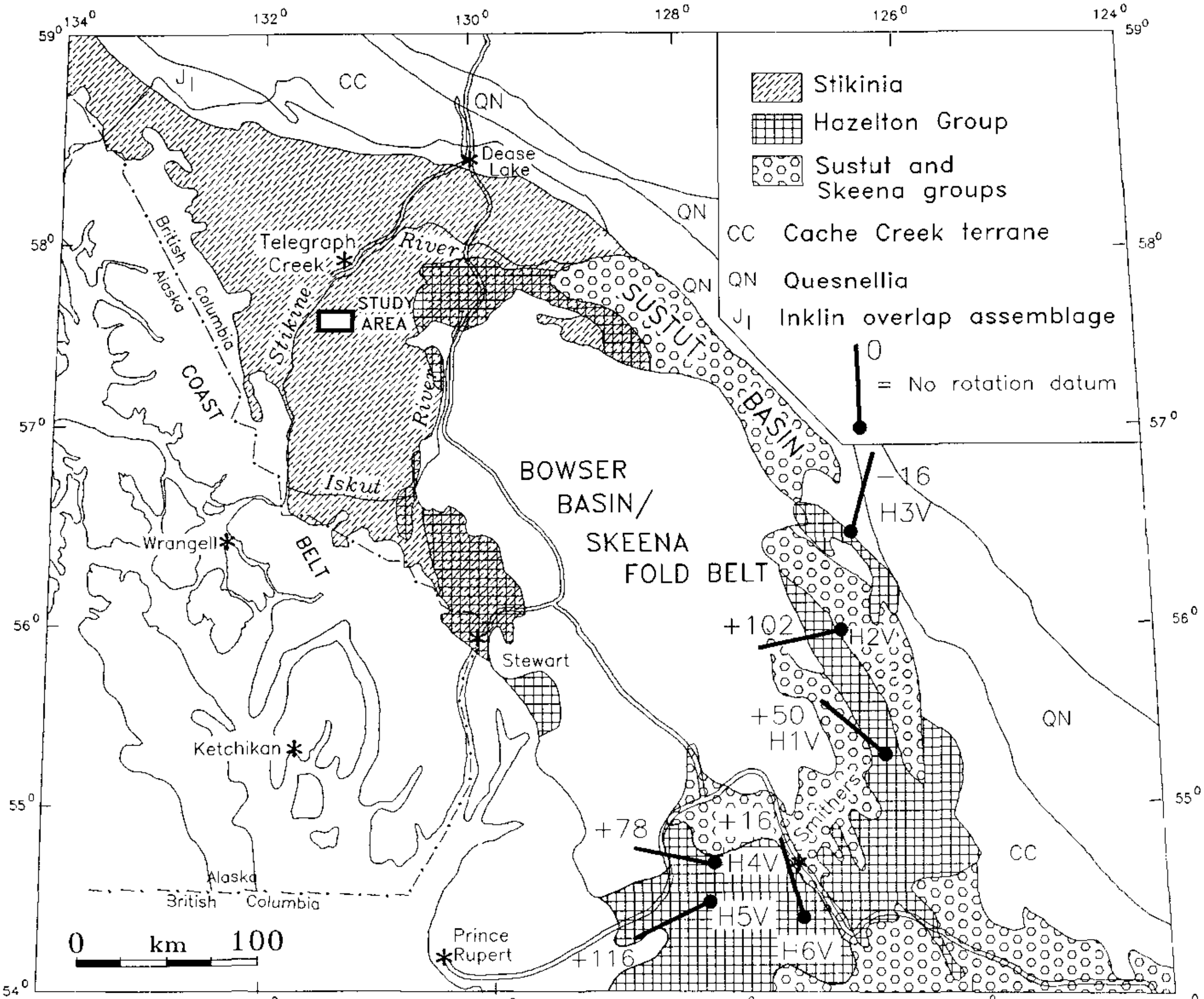

Figure 1-18-1. Regional distribution of Hazelton Group rocks within Stikinia with localities of previous paleomagnetic studies. Localities H1V, H2V, and H3V are from Monger and Irving (1980) and H4V, H5V, and H6V from Vandall and Palmer (1990). Bold lines and corresponding numbers outline the rotation relative to the craton, magnitude in degrees and sense of block rotation since original rock formation (0 or North is the concordant Early Jurassic datum of no relative rotation). Positive (negative) values are counterclockwise (clockwise). Rotation is assumed to be in the smallest angle sense. Block-rotation angles were determined from the observed locality declinations relative to the expected North American reference declination (Vandall, 1990). Geology simplified from Wheeler and McFeely (1987).

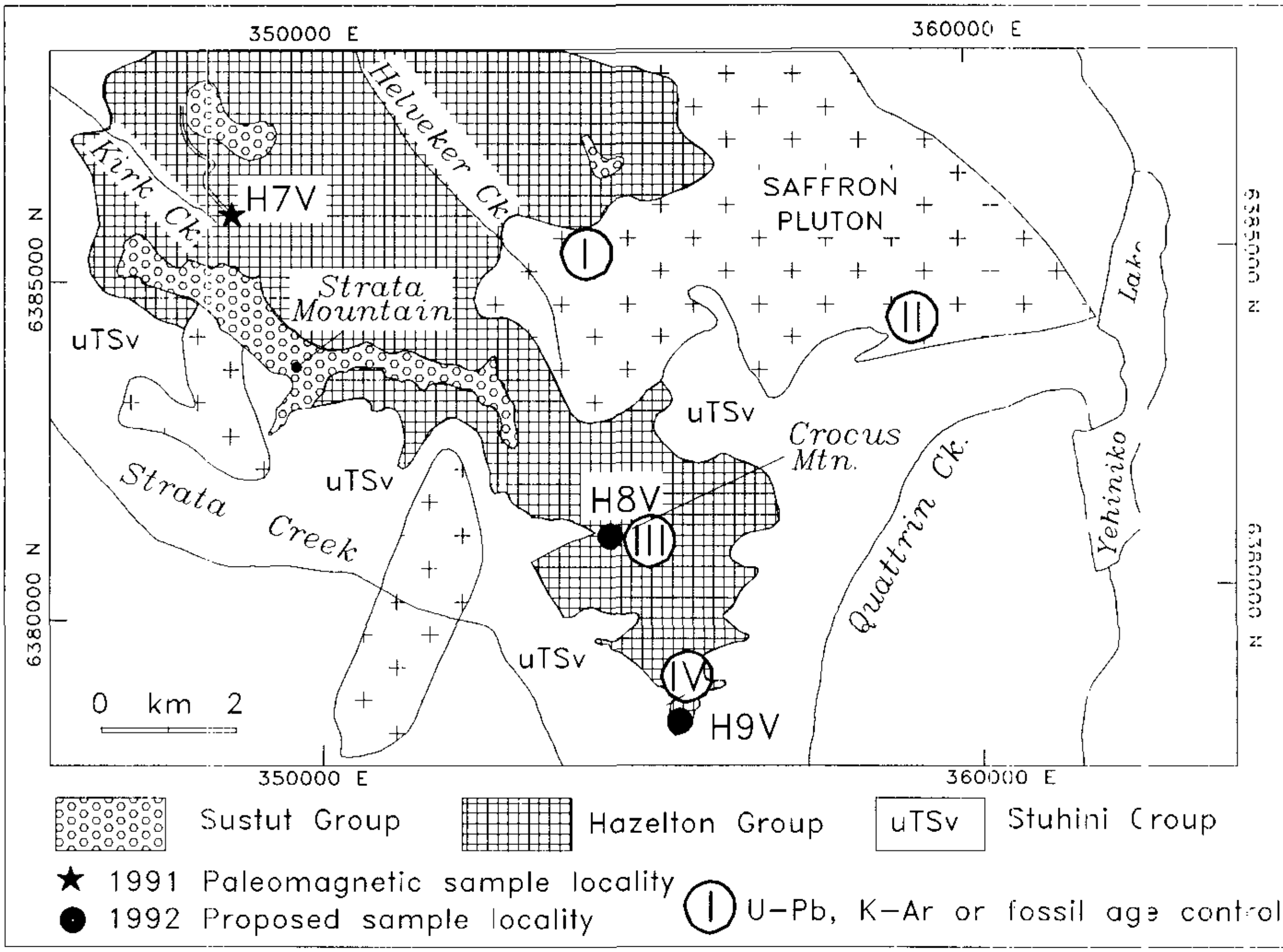

Figure 1-18-2. Simplified geologic setting of the study area with sample locality H7V from this study, and locations H8V and H9V which are targeted for sampling in the 1992 field season. See text for discussion of age control for sites. Geology modified from Brown *et al.* (1990).

TABLE 1-18-1
LOCATION AND LITHOLOGIC DATA FROM THE SEVEN SAMPLING SITES

Site**	Easting	Northing	Elevation	Flow Type
3	348923	6386299	1810 m	Plag.-px. por. andesite
2	348918	6386278	1795 m	Plag.-px. por. andesite
1	348871	6386202	1735 m	Basaltic andesite
5	348631	6386356	1685 m	Amygdaloidal basalt
4	348644	6386319	1670 m	Amygdaloidal basalt
6	348639	6386307	1664 m	Amygdaloidal basalt
7	348657	6386261	1658 m	Amygdaloidal basalt

UTM Zone 09, NAD83.

** Sites are listed in stratigraphic sequence from top to bottom.
Abbreviations: Plag. = plagioclase; por. = prophyritic; px. = pyroxene.

unit can be traced for over 2 kilometres along strike and is an important local marker; samples from the flow are currently being processed for zircon U-Pb dating. Division 4, dark grey plagioclase and coarse pyroxene-porphyritic flows with fractures subparallel to bedding, form the resistant ridge at the top of the section (Plate 1-18-3).

Metamorphic grade in the Kirk Creek area is low. Petrographic and x-ray diffraction data suggest that the volcanic rocks have undergone only zeolite facies metamorphism (Brown and Greig, 1990). In addition, the sample area is distant from the thermal contact aureoles of younger intrusive bodies which could potentially reset the primary magnetization.

Given their well-constrained age, low metamorphic grade and relatively undeformed character, these Toarcian volcanic rocks are ideal targets for paleomagnetic investigation.

METHODS

At each of the seven sites, seven to ten cores were drilled to a depth of about 10 centimetres, of these, only five to six

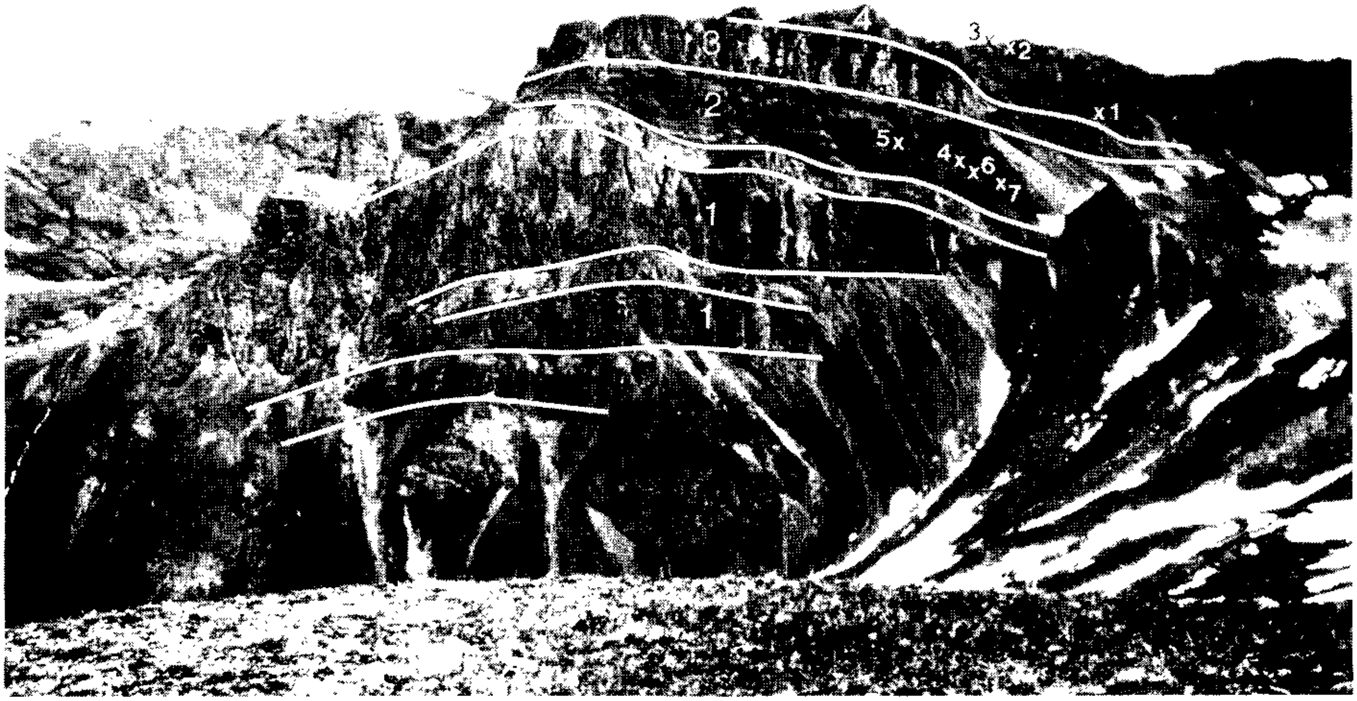

Plate 1-18-1. View to northeast of the Kirk Creek area where the paleomagnetic sites were sampled. The gently northeast-dipping Toarcian flows sampled are the uppermost 80 metres of the section.

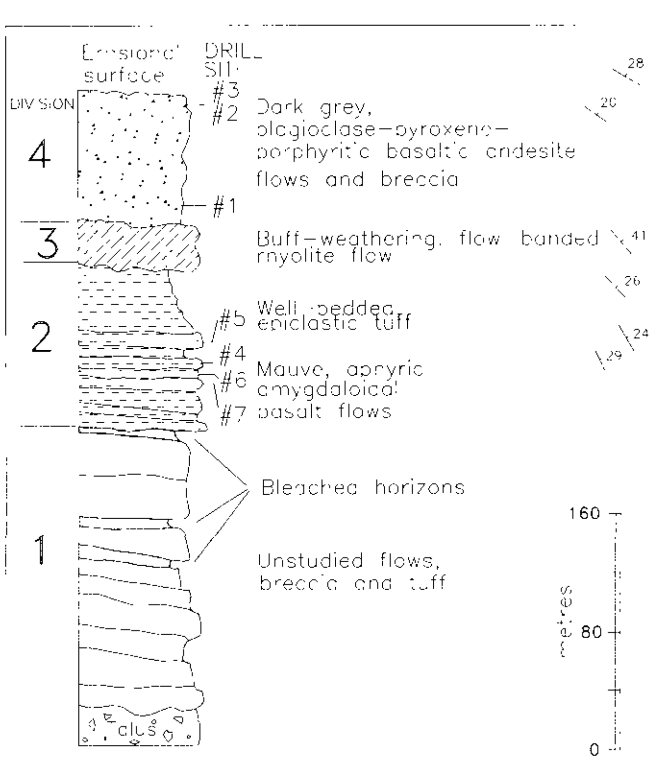

Figure 1-18-3. Schematic stratigraphic column for the Toarcian volcanic rocks in the Kirk Creek cirque, illustrating sample sites.

were recoverable due to the fractured and sometimes friable outcrop. Recoverable cores were oriented *in situ* using both sun and magnetic compasses in order to detect any possible local magnetic distortions; declinations agreed within a few degrees. Basal flow-contact and bedding attitudes were measured at each site. These measurements varied somewhat due to the irregular nature of the flow bottoms, however, the sequence as a whole strikes 300° and dips 20° northeast (Plates 1-18-2 and 1-18-3).

In the laboratory most cores were sliced into two specimens, however, a few provided only a single specimen due to rock fractures. Each specimen's remanent magnetization was analyzed using automated Schonstedt SSM spinner magnetometers, a TSD-1 thermal demagnetizer and an SI-4 static alternating field demagnetizer. In addition, each specimen's anisotropy of magnetic susceptibility (AMS) was measured using an SI-2 magnetic susceptibility instrument. These measurements permit the study of possible flow-induced anisotropies of the magnetic fabric, which may then be related to the measured *in situ* flow attitudes. After initial measurement of the natural remanent magnetization and AMS, each specimen was subjected to alternating field and/or thermal step demagnetization techniques. Specimens were demagnetized at progressively higher discrete alternating magnetic fields and/or temperatures between which their remanent magnetization was remeasured. These experiments isolate discrete components of the natural remanent magnetization in order to permit identification of characteristic stable remanence directions of geologic significance.

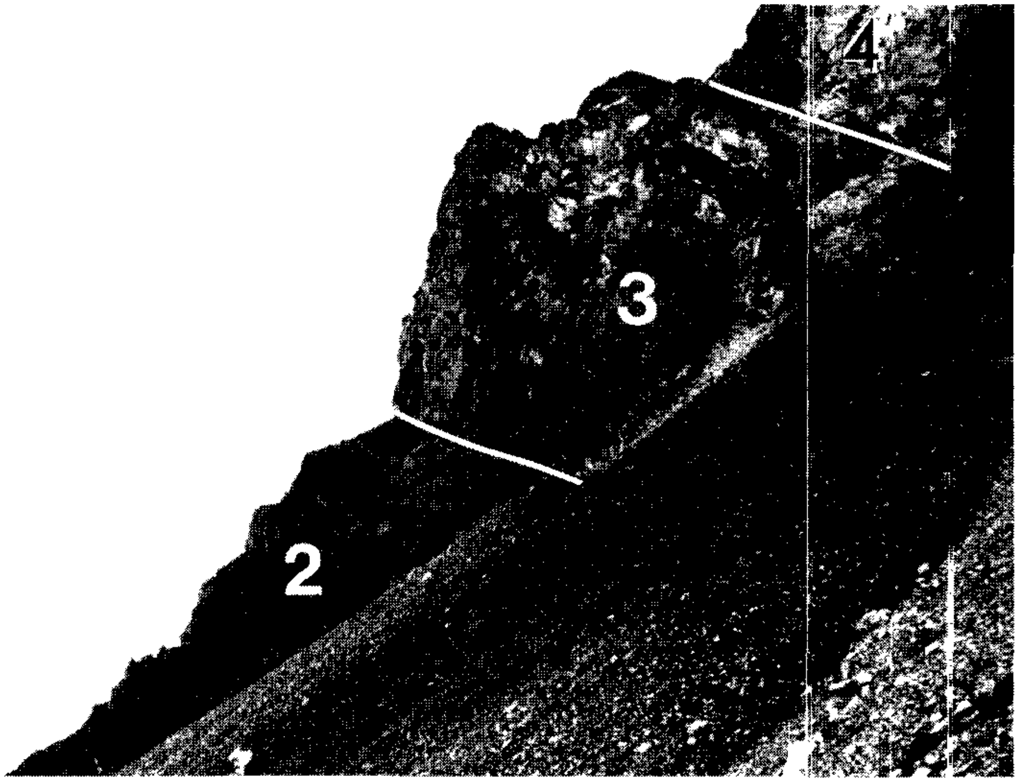

Plate 1-18-2. View to northwest of the gently northeast-dipping epiclastic beds of Division 2, that are directly overlain by the massive-weathering rhyolite flow (Division 3) that was sampled here for U-Pb dating.

Plate 1-18-3. View to southeast of the top of the section (drill site 3), basalt flows are 3 to 5 metres thick with faint and irregular columnar jointing. Erosional surface represents the dip slope.

DISCUSSION

Magnetic susceptibility data indicate that these rocks exhibit a small magnetic anisotropy averaging about 1.3 per cent. The dominant anistropy of magnetic susceptibility ellipsoid is prolate shaped with the axis of maximum magnetic susceptibility oriented near vertical. It is unlikely that this is a flow-induced orientation. More likely it is related to vertical columnar joint like patterns which reflect a history of contraction cooling and a stress regime that could have imparted the weak vertical lineation. Overall, anisotropy is weak and magnetic susceptibilities are large, averaging 17×10^{-3} SI, indicating the suitability of these rocks for paleomagnetic study.

The following discussion is based on step demagnetization analysis on 67 per cent of the collection. Analysis of all specimens subjected to demagnetization techniques indicates that samples from these Toarcian volcanic rocks are stable recorders of the earth's magnetic field. Both normal and reverse polarity magnetizations are present; reverse predominates. During progressive step demagnetization many specimens have a normal magnetic component removed to reveal a higher coercivity and unblocking temperature reversed direction (Figure 1-18-4). In paleomagnetic studies: coercivity is a measure of how strongly held a magnetization is within a rock at the magnetic domain level; (un)blocking temperatures are a measure of the ambient temperature at which a magnetization in a rock is acquired (removed). In all specimens with mixed-polarity magnetizations, the normal component exhibits lower coercivities and unblocking temperatures, and is removed during step demagnetization, yielding a reversed end-point direction. Reversed specimens subjected to thermal step demagnetizations are very stable, exhibiting high, discrete unblocking temperatures in the 550° to 650°C range, indicative of a probable primary magnetization which was acquired during cooling of the lava flows (Figure 1-18-5). In contrast, normal and mixed-polarity specimens subjected to thermal step demagnetization exhibit distributed unblocking temperatures over the entire 200° to 600°C range (Figure 1-18-6). Commonly, the normal component is substantially removed, to yield a hybrid, shallow-dipping, reversed direction (*e.g.*, Figure 1-18-6; demagnetization steps 500° to 550°C). However, in some specimens the normal component is completely removed, isolating the moderately dipping reversed direction (Figure 1-18-4; demagnetization steps 10 to 30 mT). This demonstrates the lower stability magnetic character of the normal polarity magnetization and suggests it is a secondary magnetic overprint. As the natural remanent direction of the normal component in many speci-

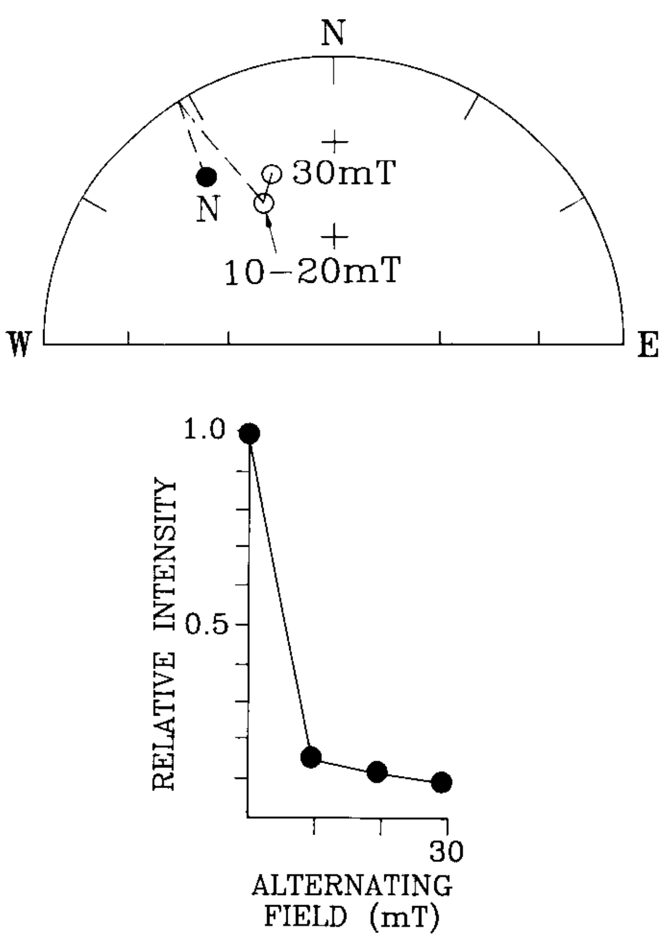

Figure 1-18-4. Example of alternating field demagnetization of a mixed-polarity specimen (Site #2) exhibiting the complete removal of a lower coercivity normal magnetization revealing a stable reversed direction. Direction changes above, intensity changes below. Closed (open) circles represent directions plotted in the lower (upper) hemishere of the equal-area stereonet. N represents the natural remanent magnetization direction (see text). (mT = milliteslas)

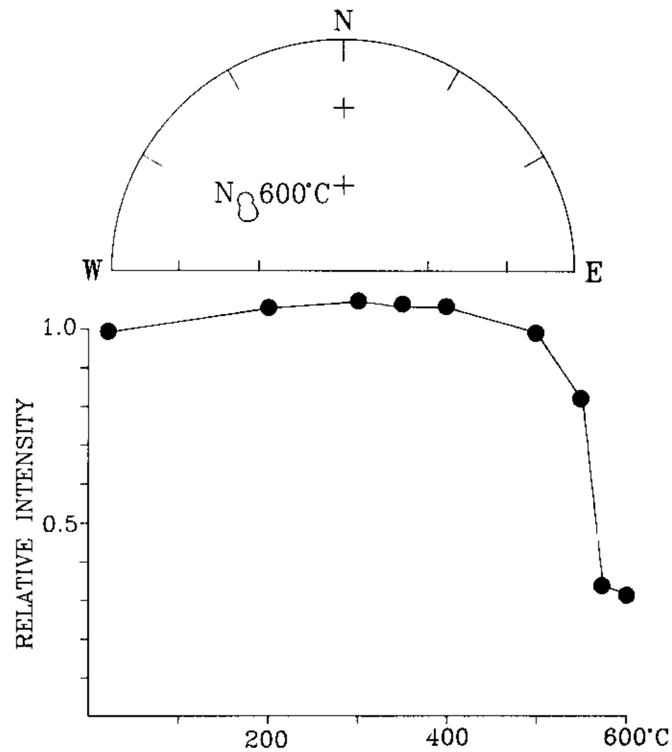

Figure 1-18-5. Example of thermal demagnetization of a high unblocking temperature reverse-polarity specimen (Site #5). Plotting conventions as in Figure 1-18-4.

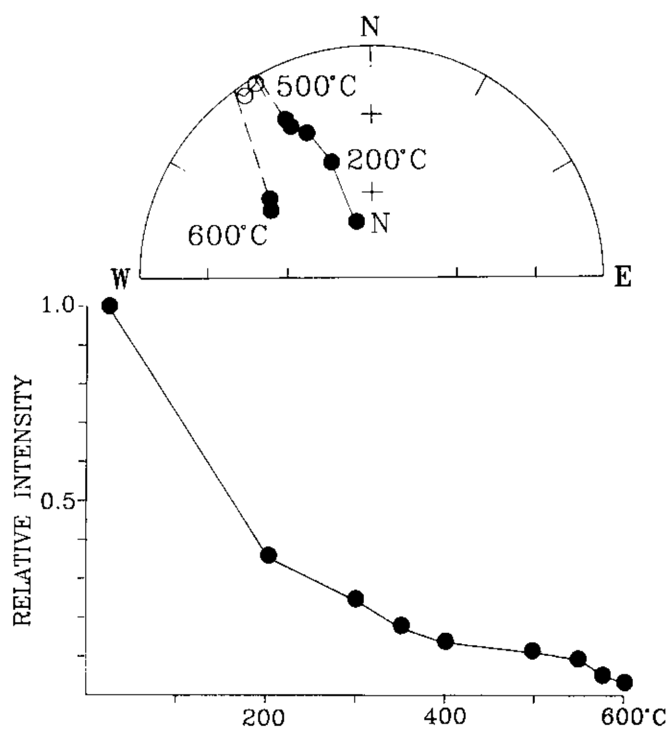

Figure 1-18-6. Example of thermal demagnetization of a mixed-polarity specimen (Site #3) exhibiting distributed unblocking temperatures. Directional changes reflect the removal of the normal magnetization. Natural remanent magnetization direction removed is close to the present earth's magnetic field direction. Plotting conventions as in Figure 1-18-4.

mens is quite steep, close to the present earth's magnetic field direction at this locality, it is probable that the normal component is a recent Brunhes overprint. This interpretation will be tested by future experiments. The uniquely different magnetic characters of the normal and reverse magnetizations are equally well defined by alternating field step demagnetization. Reverse-polarity specimens are very stable, with characteristically high coercivities in excess of 100 milliteslas (Figure 1-18-7). In contrast, normal or mixed-polarity specimens characteristically exhibit large directional changes and lower distributed coercivities (Figure 1-18-8).

Relative to present horizontal, the characteristic reversed magnetization is well grouped and directed north-northwest with an intermediate inclination. Tilt correction for the northeast-dipping attitude of the lava flows moves the north-northwest direction slightly steeper, and to the northwest. By rotating the reversed direction into its antipodal normal polarity position, a direct comparison can be made with the expected Early Jurassic direction [declination 341°, inclination 53° downwards (Figure 1-18-7) calculated using the cratonic reference pole of Vandall and Palmer (1990)]. The inference is that these rocks have undergone a very large rotation, possibly approaching 180° in post-Early Jurassic time. This observation is consistent with the large block rotations previously recognized by Monger and Irving (1980) and Vandall and Palmer (1990). However, these rocks appear to have undergone the largest documented Hazelton Group block rotation.

As the laboratory experiments and final analyses are not yet complete, a more detailed discussion and documentation of the results, and their implications, will be published at a later date.

As it has been demonstrated that these Toarcian volcanic rocks are very good magnetic recorders, additional sampling should be most fruitful. Plans for the 1992 field season include additional sampling in the lower part of the volcanic section in the Kirk Creek area, Crocus Mountain (H8V) and Strata Creek ridge (H9V; Figure 1-18-2). Suitable data from each of these sections would provide important field tests required to assess several outstanding questions. Is the reversed direction pre or post-tilting? Is this reversed polarity chron recognized in each section and can it be accurately dated? What is the consistency of these observations within the Yehiniko Lake area? Can constraints be placed on the size of individually rotated blocks? Can boundaries between rotated blocks be recognized paleomagnetically and geologically? The answers to these questions are critical to our understanding of the accretionary history of the Hazelton Group island arcs and the Intermontane Belt overall.

ACKNOWLEDGMENTS

Funding for this project was provided jointly by the Geological Survey Branch of British Columbia and the Geological Survey of Canada including B.C. Geoscience Research Grant RG91-29 to T. A. Vandall. The authors wish to extend their thanks to: Mary Lou Bevier (Geological Survey of Canada, Ottawa) who provided unpublished U-Pb

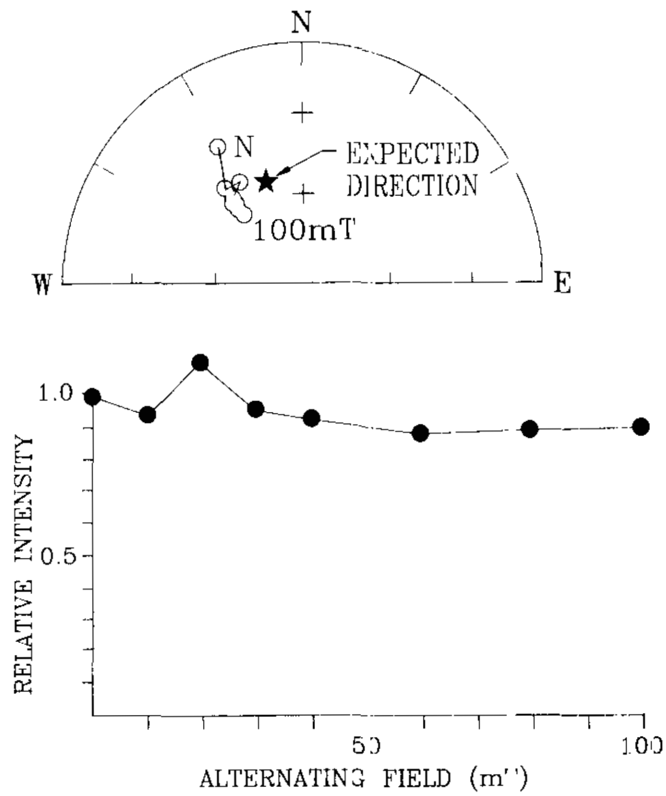

Figure 1-18-7. Example of alternating field (mT = milliteslas) demagnetization of a high-coercivity reverse-polarity specimen (Site #4). Plotting conventions as in Figure 1-18-4.

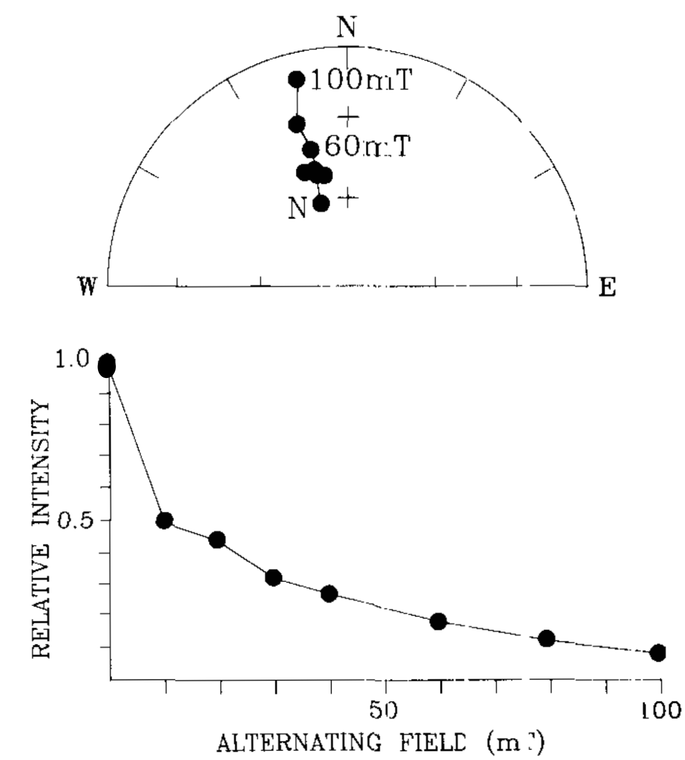

Figure 1-18-8. Example of alternating field demagnetization of a distributed low-coercivity normal-polarity specimen (Site #3). Plotting conventions as in Figure 1-18-4

age data for the area, Brian Sawyer and Linda Bedard (Geological Survey of Canada, Sidney) who provided magnetization diagrams, and Will Tompson (Trans North Helicopters) for his skill and perseverance which was greatly appreciated one windy August evening. Reviews by E. Irving, W.J. McMillan and J.M. Newell significantly improved this manuscript.

REFERENCES

Anderson, R.G. and Thorkelson, D.J. (1990): Mesozoic Stratigraphy and Setting for Some Mineral Deposits in Iskut River Map Area, Northwest British Columbia; *in* Current Research, Part E, *Geological Survey of Canada,* Paper 90-1F, pages 131-139.

Brown, D.A. and Greig, C.J. (1990): Geology of the Yehiniko Lake Area, Northwestern British Columbia (104G/11W and 12E); *in* Geological Fieldwork 1989, *B.C. Ministry of Energy, Mines and Petroleum Resources,* Paper 1990-1, pages 141-151.

Brown, D.A., Greig, C.J. and Gunning, M.G. (1990): Geology and Geochemistry of the Stikine River – Yehiniko Lake Area, Northwestern British Columbia (104G/11W, 12E); *B.C. Ministry of Energy, Mines and Petroleum Resources,* Open File 1990-1.

Diakow, L.J. (1990): Volcanism and Evolution of the Early and Middle Jurassic Toodoggone Formation, Toodoggone Mining District, British Columbia; unpublished Ph.D. thesis, *University of Western Ontario,* 178 pages.

Harland, W.B., Armstrong, R.L., Cox, A.V., Craig, L.E., Smith, A.G. and Smith, D.G. (1989): A Geologic Time Scale – 1989; *Cambridge University Press.*

MacIntyre, D.G., Desjardins, P. and Tercier, P. (1989): Jurassic Stratigraphic Relationships in the Babine and Telkwa Ranges (93L/10, 11, 14, 15); *in* Geological Fieldwork 1988, *B.C. Ministry of Energy, Mines and Petroleum Resources,* Paper 1989-1, pages 195-208.

Monger, J.W. and Irving, E. (1980): Northward Displacement of North-central British Columbia; *Nature,* Volume 285, pages 289-293.

Vandall, T.A. (1990): Paleomagnetic Constraints on Allochthonous Canadian Cordilleran Displacement: Results from Stikinia, British Columbia; unpublished Ph.D. thesis, *University of Western Ontario,* 156 pages.

Vandall, T.A. and Palmer, H.C. (1990): Canadian Cordilleran Displacement: Palaeomagnetic Results from the Early Jurassic Hazelton Group, Terrane I, British Columbia, Canada; *Geophysical Journal International,* Volume 103, pages 609-619.

Wheeler, J.O. and McFeely, P. (1987): Tectonic Assemblage Map of the Canadian Cordillera and the Adjacent Parts of the United States of America; *Geological Survey of Canada,* Open File 1565.

HIGHLIGHTS OF 1991 MAPPING IN THE ATLIN-WEST MAP AREA (104N/12)

By M.G. Mihalynuk and M.T. Smith

KEYWORDS: Regional geology, Peninsula Mountain suite, Table Mountain complex, Fourth of July batholith, Atlin Mountain pluton, Atlin Mountain fault, Cache Creek Complex, Laberge Group, Sloko Group, Late Cretaceous, Carmacks Group, Nahlin fault.

INTRODUCTION

A geological mapping and economic-oriented sampling program in the Atlin area (104N/12W) was conducted over a 2.5-week period in 1991 to compliment a program of similar duration in 1990 (Figure 1-19-1; Mihalynuk *et al.*, 1991). Primary objectives were: to address problems with interpretation of 1990 field observations that became apparent during follow-up laboratory analyses; to complete map coverage at 1:50 000 scale of map sheet 104N/12W; and to investigate critical contact relationships that bear on the tectometallogenic history of the area.

Inconsistencies between new isotopic data (Mihalynuk *et al.*, in preparation) and earlier field observations are addressed here. Newly defined lithologic and structural elements are described and structures related to the emplacement of the Cache Creek Complex, and high-angle brittle faults affecting younger rocks, are placed within a regional tectonic framework. Base and precious metal analyses were incomplete as of this writing but are touched on briefly.

PREVIOUS WORK

Previous geological mapping in the area dates back to Cairnes (1913), with the first systematic coverage by Aitken (1959) at 1:250 000 scale. Bultman (1979) mapped significant parts of the southern and western areas. Recently, mapping to the immediate east and west has been conducted at 1:50 000 scale (Bloodgood *et al.*, 1989; Mihalynuk *et al.*, 1990). The focus of this report is on new data from the 1991 field season; for more complete descriptions of geologic units in the Atlin area the reader is referred to the above mentioned reports.

GENERAL GEOLOGY

Rocks within NTS map area 104N/12W are divisible into eastern and western structural domains which are juxtaposed along the north-trending, high-angle Nahlin fault; all three tectonic elements are intruded by the Late Cretaceous Atlin Mountain pluton (Figure 1-19-2).

The oldest rocks in the eastern domain are Mississippian to Triassic oceanic crustal and sedimentary rocks of the Cache Creek Complex. These include ultramafite, basalt, limestone, chert, argillite and wacke, and probably a mixed ultramafic, gabbro and pillow basalt unit designated the Graham Creek igneous suite (Mihalynuk and Mountjoy, 1990). They are intruded by $171^{+1}/_{-5}$ Ma Mihalynuk *et al.*, 1991) synkinematic to postkinematic, polyphase, primarily granitic rocks of the Fourth of July batholith and related dike swarms. Unconformably overlying both are basal conglomerates of the Cretaceous Table Mountain volcanic complex, formerly included with the older Peninsula Mountain volcanic suite of possible Middle to Late Triassic age. In some localities the Table Mountain complex is underlain by Peninsula Mountain volcanic rocks, which are now thought to have a much more restricted distribution than indicated by Mihalynuk *et al.*, (1991).

Basinal wacke and shale of the Lower Jurassic Laberge Group dominate the western structural domain. Paleocene felsic to intermediate volcanic and epiclastic rocks of the Sloko Group sit with angular unconformity on the Laberge. Regionally, these rocks form an overlap sequence on the Cache Creek and Stikine terranes (Wheeler *et al.*, 1988).

NEW STRUCTURAL AND STRATIGRAPHIC DATA FROM THE EASTERN STRUCTURAL DOMAIN

CACHE CREEK COMPLEX

The Cache Creek Complex was mapped in greater detail in 1991, resulting in the assignment of two additional units and greater confusion regarding the structural style and distribution of lithotypes.

A newly defined unit, mapped along the western shore and inland of Torres Channel (Figure 1-19-3), is characterized largely by its chaotic internal fabric and is here referred to as the Nahlin structural unit. It consists primarily of strongly sheared, fine to medium-grained volcanic wacke and mudstone with an undetermined amount of sheared basalt, localized zones of black cataclastic rock and lenses of dioritic to ultramafic rock. The unit probably first underwent soft-sediment deformation, producing small, rootless folds and dismembered compositional layers on a millimetre to centimetre scale. An outcrop to regional-scale penetrative shear fabric was then superimposed. Anastomosing shears isolate angular to ellipsoidal domains generally less than 2 centimetres long. Shear surfaces are chloritized or calcified and contain randomly oriented slickensides. Shears are randomly oriented, although on an outcrop and larger scale a vague, high-angle, northwest-striking trend is evident. This unit may reflect the presence of a shear zone that crosses Torres Channel. A strand of the Nahlin fault is projected by Mihalynuk *et al.* 1991) through this same locality.

Another important component of the Cache Creek Complex is wacke with conglomerate lenses which contain chert, quartz, limestone, granitoid and rare serpentinite

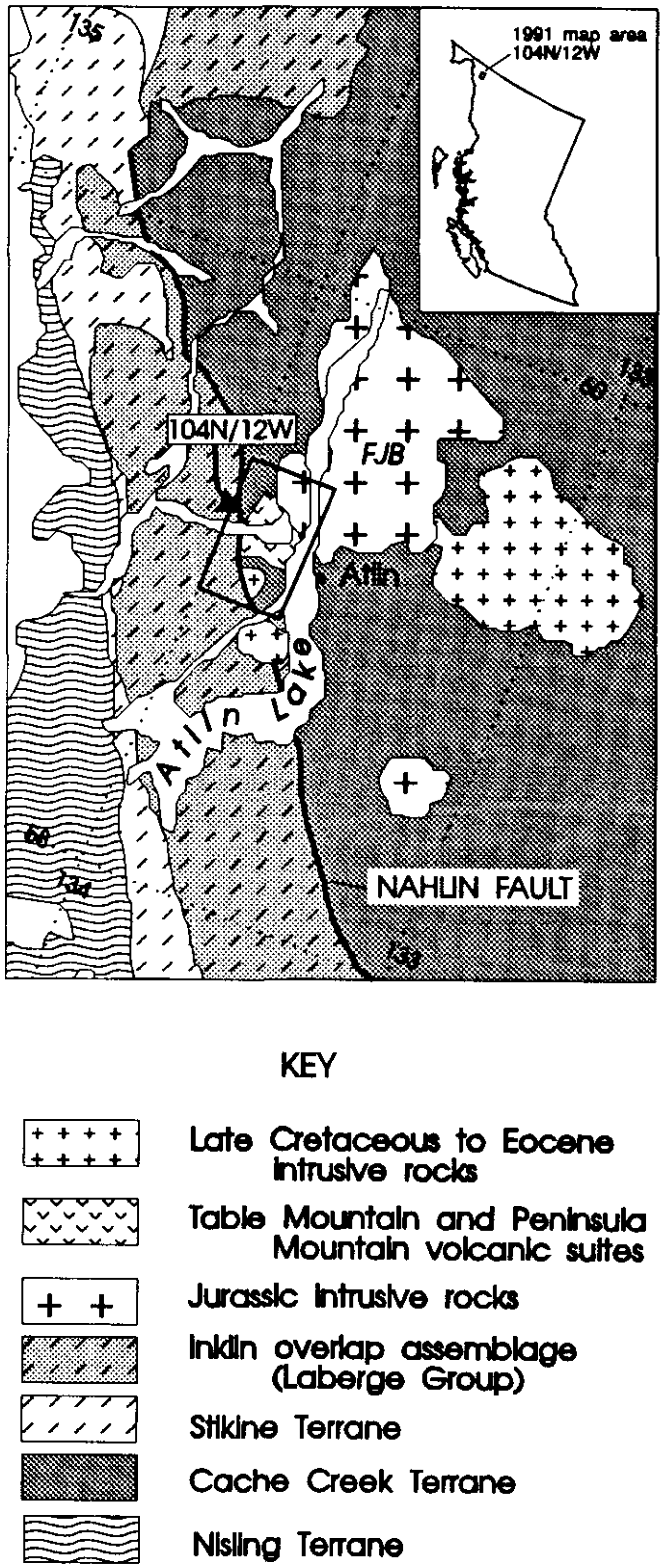

Figure 1-19-1. Location of the Atlin 104N/12W map sheet shown in relation to major tectonic features in northwestern British Columbia. Adapted from Wheeler *et al.*, 1988.

clasts. This unit is exposed at two localities south of Atlin River on the west shore of Atlin Lake (Figure 1-19-3), where it is intercalated with chert and argillite. A similar unit crops out along the northern shore of Graham Inlet (extreme western part of the map area) in association with pillow basalt. This unit in part reflects a continental sediment source and probably records interaction between the Cache Creek Terrane and ancestral North America.

Carbonate units provide one of the few markers that outline structures in the Cache Creek Complex. Carbonate bodies commonly form pods and lenses elongate in a north-northwest trend. On the northeast side of Teresa Island and nearby small islands (Figure 1-19-3), carbonate forms nearly flat-lying, massive sheets, folded about northwest-trending axes and cut by numerous moderate to high-angle faults. A different structural style characterizes the south side of the Atlin Mountain massif, where a kilometre-long, subhorizontal, east-trending, apparently cylindrical lens crops out in a cliff face.

The distribution of ultramafic rocks was mapped in greater detail as they are an important host to lode gold showings in the Atlin area. Those which do not appear on any previously published geological maps include a north-trending zone of listwanitized ultramafite at the north end of Torres Channel and a belt of tectonized harzburgite and serpentinite on the east flank of Atlin Mountain. Surface workings in the creek valley north of Torres Channel apparently followed a north-trending, opaline and coarsely crystalline quartz vein network in which individual veins are less than 10 centimetres thick. Ultramafite along the east flank of Atlin Mountain shows no sign of previous workings.

Fourth of July Batholith

The Fourth of July batholith is described fully by Aitken (1959) and features particular to the Atlin map area (104N/12W) are discussed by Mihalynuk *et al.* (1991). Mapping along its western margin in 1991 defined a north-northwest-trending, kilometre-wide belt of potassium feldspar megacrystic granite that extends from the north side of Deep Bay to the east side of Atlin Lake opposite Eight Mile Bay, and perhaps as far south as Como Lake in 104N/12E. It is bounded to the east by equigranular biotite hornblende granite and to the west by a mafic border phase. A later, alkali feldspar granite to alaskite "cupola" intrudes the border phase south of Deep Bay, and dikes of the same composition intrude the potassium feldspar megacrystic granite, the dioritic border phase and lamprophyre dikes.

Peninsula Mountain Volcanic Suite and Table Mountain Volcanic Complex

New isotopic and field data point to a much more restricted distribution of the Middle to Late Triassic(?) Peninsula Mountain volcanic suite than indicated by the preliminary mapping of Mihalynuk *et al.* (1991). We now assign a Late Cretaceous (~74 Ma) age to much of the section, based on new field data and Rb-Sr and U-Pb dates (Mihalynuk *et al.*, in preparation). Late Cretaceous volcanic rocks are present in the Whitehorse area to the north (vari-

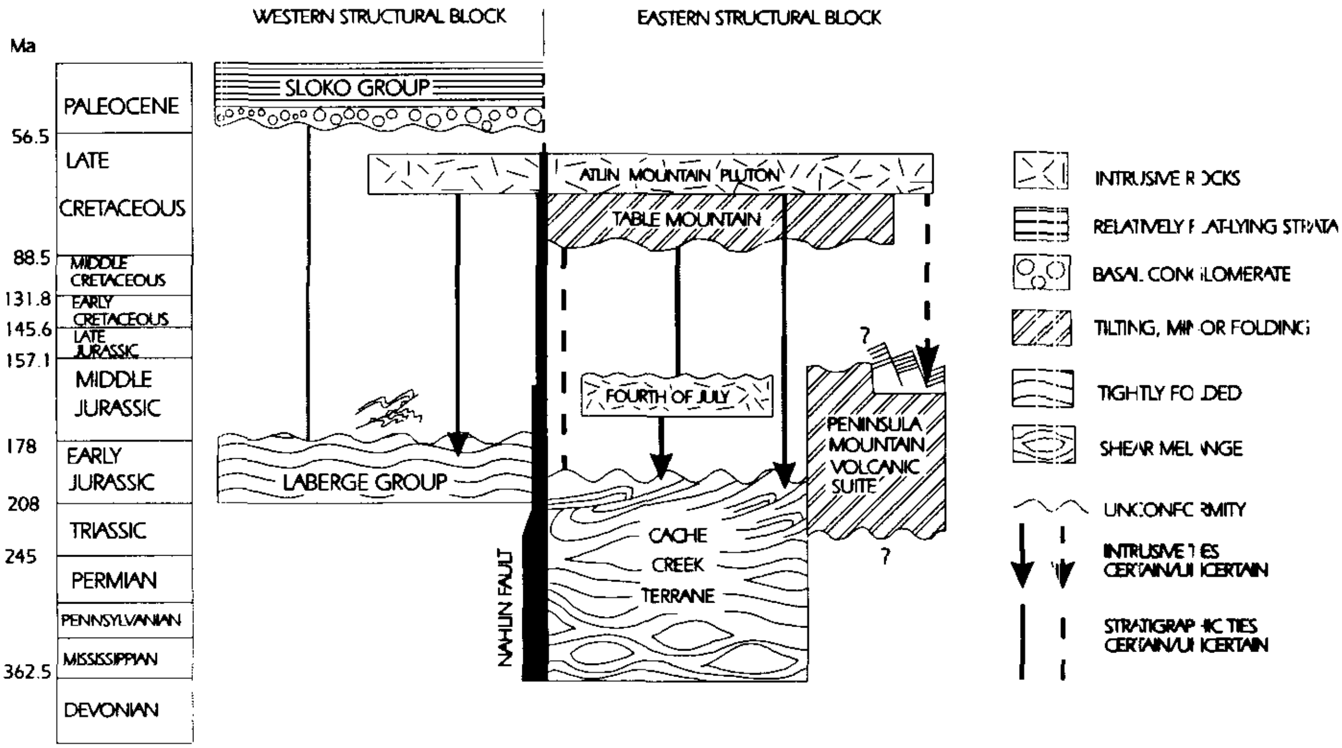

Figure 1-19-2. Box diagram illustrating age and geologic relationships in the map area. Age constraints are from Bultman (1979), Monger (1975), Mihalynuk *et al.* (1991; in press) and Cordey *et al.* (1991). Time scale is that of Harland *et al.* 1990). The width of the line representing the Nahlin fault is roughly proportional to the cumulative amount of offset experienced by adjacent units.

ously referred to as the Carmacks Group, Hutshi, and Mount Nansen volcanics; *e.g.*, Bultman, 1979; Wheeler and McFeely, 1987; Hart and Radloff, 1990), and the volcanic rocks on Table Mountain have been previously correlated with them (*e.g.*, Grond *et al.*, 1984; Bultman, 1979); this interpretation thus appears to be correct for at least part of the section. The name "Table Mountain volcanic complex" reflects the distribution of these Late Cretaceous volcanic rocks and coeval intrusions in the Atlin map area.

Peninsula Mountain Volcanic Suite

The older Peninsula Mountain suite is distinguished from the Table Mountain volcanic complex in the field by: a high degree of induration; the generally green colour of rocks; and epidote-chlorite-silica alteration. Distribution of the revised Peninsula Mountain volcanic suite corresponds mainly to the lowest unit and overlying indurated sediments of the suite as originally mapped by Mihalynuk *et al.* (1991). It includes: massive to sparsely pyroxene-phyric, dark green flow(?) rocks, some with altered, partially digested, cobble-sized clasts; strongly pyritic rhyolite flows and domes(?); and an epiclastic unit not described by Mihalynuk *et al.* (1991).

Rocks of the Peninsula Mountain epiclastic unit are strongly indurated, light weathering, chlorite-epidote-silica altered, and locally contain up to 1 per cent pyrite as irregular blebs. In places they are probably tuffites, with coarse ash layers and blocks of acicular hornblende plagioclase porphyry and rarely clasts of pyroxene porphyry and flow-banded rhyolite. Elsewhere the unit displays graded bedding in silt to gravel derived from feldspathic volcanic porphyry. Most clasts are subangular to subrounded. The unit is also characterized by the presence of interbedded, pyroxene-phyric amygdaloidal basalt flows.

Table Mountain Volcanic Complex

Rocks of the Table Mountain volcanic complex comprise the upper rhyolite, intermediate lapilli tuff and quartz-phyric ash-flow units of the former Peninsula Mountain volcanic suite of Mihalynuk *et al.* (1991), and a suite of felsic to intermediate intrusive rocks, previously unmapped or assigned to the Fourth of July intrusive suite.

As contrasted with the Peninsula Mountain suite, volcanic rocks of the Table Mountain Complex are typically less well indurated, orange, maroon or grey weathering, and have not undergone extensive chlorite-epidote alteration. Coarse, plagioclase-phyric volcaniclastic rocks (tuff, agglomerate and breccia) are volumetrically the most significant rock type.

The intrusive suite includes a small stock of orange to buff-weathering, feldspar-rich porphyry, exposed along approximately 2 kilometres of shoreline on the west side of Graham Inlet (Figure 1-19-3) and adjacent islands. Rocks similar in appearance crop out on the east side of Graham inlet and may be part of the same stock. Phenocrysts consist

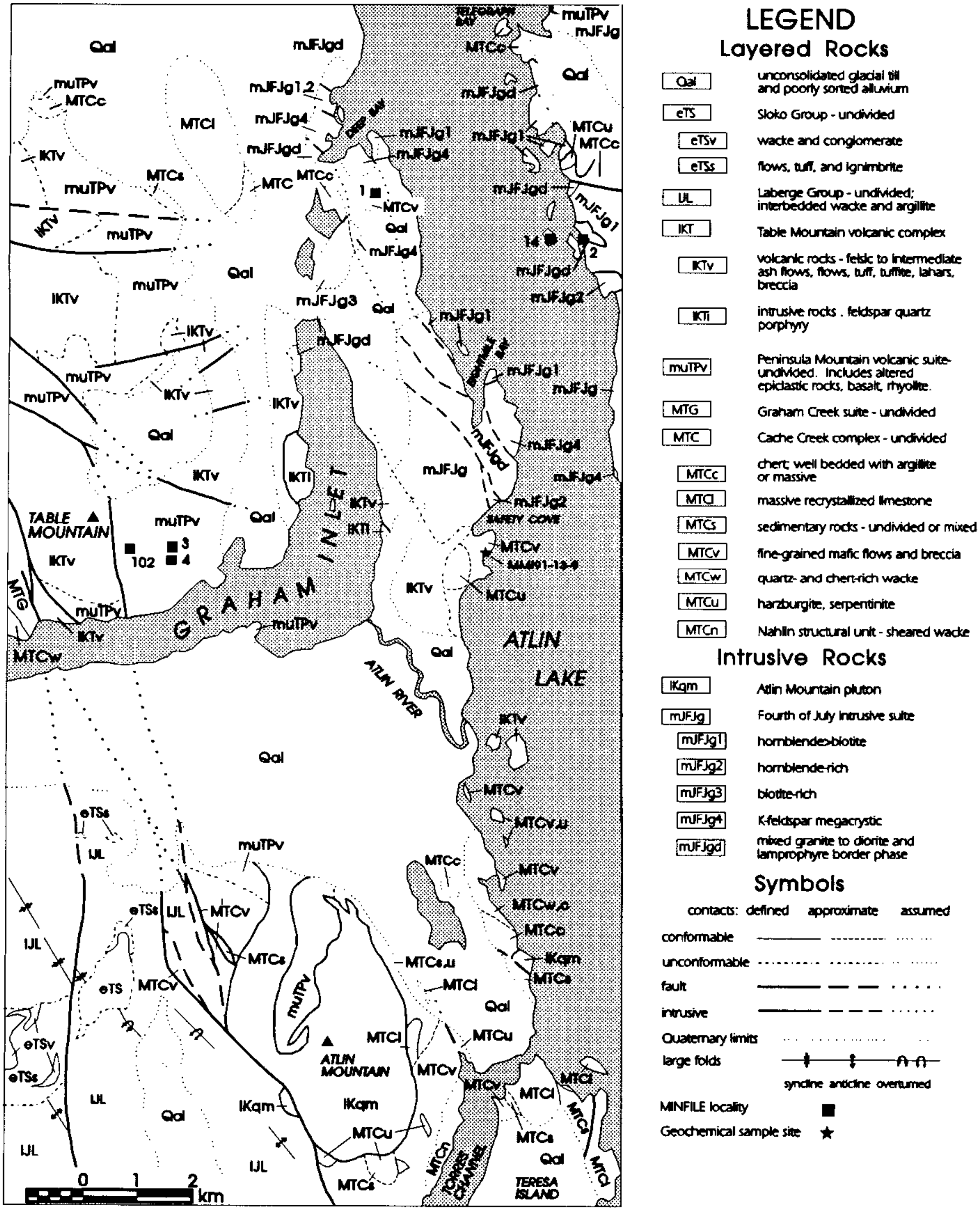

Figure 1-19-3. Generalized geologic map of the Atlin west map area, after Mihalynuk *et al.* (1991; 1992).

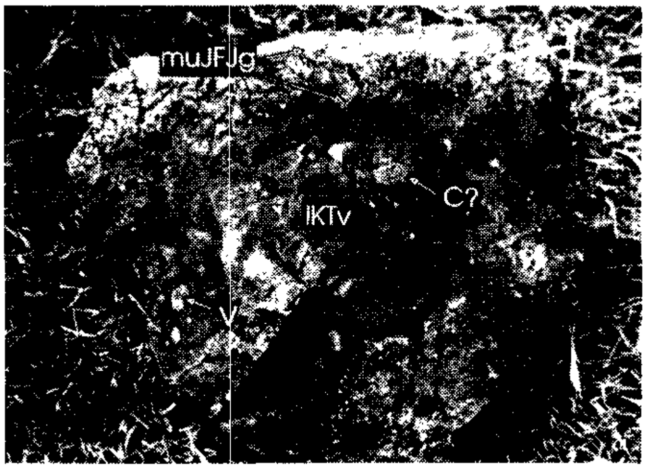

Plate 1-19-1. A sample of the contact between oxidized diorite of the Fourth of July batholith border phase (white, muJFJg) and basal volcaniclastic strata of the Table Mountain volcanic complex (lKTv). Clasts within the basal unit include chert (C?) of the Cache Creek Complex, porphyritic volcanic fragments probably derived from the Peninsula Mountain suite (V) and diorite derived from muJFJg. Elsewhere the unit also includes clasts of serpentinite and carbonate from the Cache Creek Complex.

of potassium feldspar (25–50%), plagioclase (50–60%, albite to oligoclase: glomeroporphyritic with potassium feldspar) and quartz (5–25%). Accessory minerals include biotite in altered booklets, hornblende, apatite and zircon. Quartz is clear and embayed, while all other components are partly altered to fine-grained chlorite, clay, opaque minerals and calcite. The fine-grained groundmass is holocrystalline and consists of potassium feldspar, oligoclase and quartz. Textural characteristics indicate that this stock is a relatively high-level intrusion. Exposures on islands and the adjacent shoreline are coarse, equigranular, and appear to represent more interior regions of the stock.

Dikes of the intrusive suite are typically orange or greenish weathering with medium to coarse, zoned (white, grey and pink) glomeroporphyritic feldspar comprising about 25% of the rock. Biotite booklets (5%) are medium grained, xenomorphic to idiomorphic and may be chloritized. Medium-grained quartz eyes comprise 2 to 5 per cent of the rock. Dikes have irregular margins and variable trends with east-west and northwest orientations most prominent. One dike, 9 to 25 metres thick, appears to have a northwest strike length of over 5 kilometres. Similar dikes cut the Cache Creek Complex on both the west and east sides of Atlin Lake.

The intrusive suite is coeval with the upper quartz-biotite-feldspar-phyric ash flows in the upper Table Mountain extrusive volcanic section. A hypabyssal to extrusive transition is well displayed about 3.5 kilometres north-northwest of Table Mountain.

Contact Relationships

Excellent unconformable relationships are observed between the basal Table Mountain units and the Fourth of July batholith. Altered pebbles of granodiorite mixed with porphyritic volcanic clasts overlie a red, oxidized paleoregolith (Plate 1-19-1) on the west side of Graham Inlet. West of Safety Cove, rhyolitic tuffs and flows overlie the Fourth of July batholith, with a basal granule conglomerate noted in several locations. These relationships support the post-Middle Jurassic (Late Cretaceous, Grond *et al.*, 1984; Mihalynuk *et al.*, in preparation) age for the Table Mountain volcanic complex. They also confirm the presence of two volcanic packages: the Table Mountain package and the older Peninsula Mountain suite which is intruded and thermally metamorphosed by the Fourth of July batholith at Telegraph Bay (Mihalynuk *et al.*, 1991) and perhaps at Safety Cove.

Contact relationships between the Peninsula Mountain suite and the Cache Creek Complex remain obscure (as discussed by Mihalynuk *et al.*, 1991), as all contacts observed to date are covered or have been disrupted by later faulting.

NEW STRATIGRAPHIC AND STRUCTURAL DATA FROM THE WESTERN DOMAIN

Structures in the Laberge Group

Laberge Group rocks underlie much of the southwestern part of the map area. Southeast of the map area the Laberge Group is upright and gently to moderately dipping about relatively open folds. In contrast, rocks in the map area often assume a steep, northwest-striking, upright to overturned orientation. Folds are tight to isoclinal and have steep to vertical axial planes. Fold axes trend southeast with a low to moderate plunge. Numerous joint sets and bedding-parallel shears further deform the Laberge rocks.

A north-trending fault mapped by Mihalynuk *et al.* (1991) south of Graham inlet, along the western margin of the map area, can be extended south to the southern edge of the map area. Slickenside striae on anastomosing shears in this fault zone indicate that latest movement was dominantly dextral strike-slip. Northwest-striking bedding planes within the fault zone contain moderately east-plunging slickenside striae with sinestral shear sense, consistent with overall dextral movement on this fault zone.

Sloko Group

The Sloko Group consists primarily of rhyolitic to andesitic flows, breccia, tuff and ignimbrite, and epiclastic rocks. It is essentially flat lying, and rests on a deeply incised paleosurface over deformed Laberge Group strata. A unit interpreted as a basal conglomerate unconformably overlies and is in part tectonically interleaved with the Laberge Group on the summit of a knob 3 kilometres south of Graham Inlet (2 kilometres east of the map border). It consists of very well rounded pebbles, cobbles and boulders of wacke, chert, argillite, greenstone, felsic plutonic rocks and feldspar-quartz-phyric volcanic rocks in a medium to coarse sand matrix. The range of lithologic types suggests derivation from the Laberge, Table Mountain and Cache

Creek units, as well as some of the units that intrude them. The conglomerate grades up-section into angular pebble conglomerate and breccia derived from felsic to intermediate volcanic rocks which are more typical of the Sloko Group.

RELATIONSHIPS BETWEEN STRUCTURAL DOMAINS

ATLIN MOUNTAIN PLUTON

The Atlin Mountain pluton intrudes the contact between the two structural domains. It is composed of homogeneous medium-crystalline, locally potassium feldspar porphyritic quartz monzonite, consisting of 10 to 25 per cent hornblende, biotite and magnetite, 10 to 15 per cent quartz, and 60 to 70 per cent feldspar. A finely crystalline phase is exposed along the eastern margin of the pluton and as dikes and sills adjacent to it. Intrusive relationships with the Cache Creek Complex and Peninsula Mountain suite are well documented; an intrusive relationship with the Laberge Group is also mapped west of the Atlin Mountain fault. The Atlin Mountain intrusion was assigned an early Tertiary age by previous workers (*e.g.*, Aitken, 1959; Bultman, 1979), but a preliminary two-point Rb-Sr isochron suggests a Late Cretaceous age (Mihalynuk *et al.*, in press).

ATLIN MOUNTAIN FAULT

The high-angle, east-dipping Atlin Mountain fault approximately follows the western margin of the Atlin Mountain pluton (Bloodgood and Bellefontaine, 1990). Regional relationships indicate that it is a strand of the Nahlin fault, a deep-seated, terrane-bounding structure thought to separate the Cache Creek from the Stikine Terrane.

North and south of the Atlin Mountain pluton, the fault juxtaposes the Laberge Group and Cache Creek Complex. South of the pluton, this fault is marked by a zone of mylonitized harzburgite with a shear fabric suggestive of dextral motion. There is extensive brecciation of the Laberge Group and a dense pattern of anastomozing shears in the Cache Creek Complex within 20 to 30 metres of the fault. The fault follows the contact between the Laberge Group and Atlin Mountain pluton northward, then cuts the Atlin Mountain pluton for approximately 1 kilometre, where it is a narrow, altered breccia zone generally only a few metres wide. Continuing northward, the fault once again follows the margin of the pluton. North of the pluton, it is manifest as an impressive zone of brittle and ductile deformation, locally over 100 metres wide, with limited evidence for dextral offset.

Latest movement, as evidenced by structures where the fault cuts the pluton, is brittle, and is restricted to less than a few kilometres laterally and vertically, as the pluton on either side of the fault is apparently not offset greatly. The present distribution of the Atlin Mountain pluton suggests that latest movement was east side down. Structures to the north and south suggest substantially more offset and mainly ductile deformation. The simplest explanation for the observed features is that most movement on the fault zone predated the Atlin Mountain pluton and that latest movement post-dated it. Rhyolite dikes, believed to be feeders to overlying Sloko Group volcanic rocks, cut the fault and thus limit the youngest motion along the strand to pre-56 Ma.

ECONOMIC GEOLOGY

Analyses of rock samples collected during 1991 are at this time incomplete, but one assay result is notably anomalous in gold (250 ppb Au). The sample was collected from a quartz vein, 10 centimetres wide, associated with a set of altered, northeast-striking, quartz feldspar porphyry dikes that intrude the Cache Creek Complex south of Safety Cove (Figure 1-19-3). A suite of samples collected to assess the paleoplacer potential of the basal Table Mountain conglomerate yielded no anomalous results. Complete analytical results are included in Mihalynuk *et al.* (1992).

CONCLUSIONS

Mapping in 1991, in conjunction with better age constraints (Mihalynuk *et al.*, in preparation) supports several important revisions and interpretations in the Atlin map area, including:

- The Peninsula Mountain volcanic suite of Mihalynuk *et al.* (1991) can be divided into two distinct suites: a lower, epidote-chlorite-altered suite, which predates the Fourth of July batholith and retains the name Peninsula Mountain suite; and an upper unit, the Table Mountain volcanic complex, which unconformably overlies the Fourth of July batholith and is dated as Late Cretaceous by U-Pb and Rb-Sr techniques.
- The Atlin Mountain pluton, which is apparently Late Cretaceous in age, intrudes the Cache Creek Complex, Peninsula Mountain suite and Laberge Group. It both cuts and is cut by the Atlin Mountain fault, a strand of the terrane-bounding Nahlin fault. This evidence suggests a long history of movement along the Nahlin fault, which was active from prior to Early Jurassic (Laberge overlap) to post-Cretaceous time.
- The Cache Creek Complex contains: a structural unit with steep shear fabrics that may be related to the Nahlin fault; sandstone and conglomerate derived in part from a granitic and/or continental terrain; and extensive units that are, on the whole, relatively flat-lying, as evidenced by the distribution of limestone bodies.

ACKNOWLEDGMENTS

Norm Graham of Discovery Helicopters Ltd. once again provided excellent logistical support. Jeff Nazarchuk and Rob Dutchak assisted in the field. Several of the interpretations in this report are supported by geochronological data supplied under contract by Janet Gabites at The University of British Columbia geochronology laboratory.

REFERENCES

Aitken, J.D. (1959): Atlin Map-area, British Columbia; *Geological Survey of Canada*, Memoir 307.

Bultman, T.R. (1979): Geology and Tectonic History of the Whitehorse Trough West of Atlin, British Columbia; unpublished Ph.D. thesis, *Yale University*.

Bloodgood, M.A., Rees, C.J. and Lefebure, D.V. (1989): Geology and Mineralization of the Atlin Area, Northwestern British Columbia (104N/11W and 12E); *in* Geological Fieldwork 1988, *B.C. Ministry of Energy, Mines and Petroleum Resources*, Paper 1989-1, pages 311-322.

Bloodgood, M.A. and Bellefontaine, K.A. (1990): The Geology of the Atlin Area (Dixie Lake and Teresa Island 104N/6 and Parts of 104N/5 and 12); *in* Geological Fieldwork 1989, *B.C. Ministry of Energy, Mines and Petroleum Resources*, Paper 1990-1, pages 205-215.

Cairnes, D.D. (1913): Portions of the Atlin District British Columbia: with Special Reference to Lode Mining; *Geological Survey of Canada*, Memoir 37, 129 pages.

Cordey, F., Gordey, S.P. and Orchard, M.J. (1991): New Biostratigraphic Data for the Northern Cache Creek Terrane, Teslin Map Area, Southern Yukon; *in* Current Research, Part E, *Geological Survey of Canada*, Paper 91-1E, pages 67-76.

Grond, H.C., Churchill, S.J., Armstrong, R.L., Harakal, J.E. and Nixon, G.T. (1984): Late Cretaceous Age of the Hutshi, Mount Nansen, and Carmacks Groups, Southwestern Yukon Territory and Northwestern British Columbia; *Canadian Journal of Earth Sciences*, Volume 21, pages 554-558.

Harland, W.B., Armstrong, R.L., Cox, A.V., Craig, L.E. and Smith, A.G. (1990): A Geologic Timescale 1989; *Cambridge University Press*, New York, 280 pages.

Hart, C.J.R. and Radloff, J.K. (1990): Geology of the Whitehorse, Alligator Lake, Fenwick Creek, Carcross, and Part of Robinson Lake Map Areas (105 D/11, 6, 3, 2 & 7); *Indian and Northern Affairs Canada*, Open File 1990-4, 113 pages.

Mihalynuk, M.G. and Mountjoy K.J. (1990) Geology of the Tagish Lake Area (104M/8, 9E); *in* Geological Fieldwork 1989, *B.C. Ministry of Energy, Mines and Petroleum Resources*, Paper 1990-1, pages 181-196.

Mihalynuk, M.G., Mountjoy, K.J., Currie, L.D., Lofthouse, D.L. and Winder, N. (1990): Geology and Geochemistry of the Edgar Lake and Fantail Lake Map Area, (104M/8, 9E); *B.C. Ministry of Energy, Mines and Petroleum Resources*, Open File 1990-4.

Mihalynuk, M.G., Mountjoy, K.J., McMillan, W.J., Ash, C.H. and Hammack, J.L. (1991): Highlights of 1990 Fieldwork in the Atlin Area, *in* Geological Fieldwork 1990, *B.C. Ministry of Energy, Mines and Petroleum Resources*, Paper 1991-1, pages 145-152.

Mihalynuk, M.G., Smith, M.T., Lefebure, D. and Gabites, J. (in press). Age of Emplacement and Basement Character of the Cache Creek Terrane as Constrained by New Isotopic Data; *Canadian Journal of Earth Sciences*.

Mihalynuk, M.G., Smith, M.T., Mountjoy, K.J., Nazarchuk, J.H., McMillan, W.J., Ash, C.H., Hammack, J.L. and Dutchak, R. (1992): Geology and Geochemistry of the Atlin (West) Map Area (104N/12W); *B.C. Ministry of Energy, Mines and Petroleum Resources*, Open File 1992-1.

Monger, J.W.H. (1975): Upper Paleozoic Rocks of the Atlin Terrane; *Geological Survey of Canada*, Paper 74-47, 63 pages.

Wheeler, J.O. and McFeely, P. (1987): Tectonic Assemblage Map of the Canadian Cordillera and Adjacent Parts of the United States of America; *Geological Survey of Canada*, Open File 1565.

Wheeler, J.O., Brookfield, A.J., Gabrielse, H., Monger, J.W.H., Tipper, H.W. and Wordsworth, G.J. (1988): Terrane Map of the Canadian Cordillera; *Geological Survey of Canada*, Open File 1894.

NOTES

COPPER-GOLD-SILVER DEPOSITS TRANSITIONAL BETWEEN SUBVOLCANIC PORPHYRY AND EPITHERMAL ENVIRONMENTS

By Andre Panteleyev

KEYWORDS: Economic geology, porphyry copper, epithermal, copper, gold, silver, magmatic, hydrothermal, acid-sulphate, high sulphidation, advanced argillic, steam heated, alunite, kaolinite, pyrophyllite, enargite.

INTRODUCTION

The many and varied types of intrusion-related mineral deposits in circum-Pacific volcanic arcs, including gold-rich porphyry and related epithermal types, have been discussed by Berger and Henley (1989), Sillitoe (1989, 1990, 1991a, b and in press), Hedenquist *et al.* (1990) and Sillitoe and Camus (1991). The similarity in geological environments of the many described porphyry copper, copper-gold, copper-molybdenum and epithermal precious metal deposits with those in the Canadian Cordillera is evident, but the scarcity of documented acid-sulphate high-sulphidation, advanced argillic-type epithermal deposits and mineralization in British Columbia is surprising. This lack of deposits is probably only apparent and not a geologic reality. It appears to be largely due to a lack of recognition and study of acid-sulphate-type deposits and their environments except for rare cases, for example, Clapp (1915), Bradford (1985) and Diakow *et al.* (1991).

A new project has been initiated to study the interrelationships of subvolcanic porphyry copper deposits and genetically related epithermal mineralization in British Columbia. Of particular interest are deposits with hydrothermal alteration of the kaolinite-alunite-quartz-pyrite-bearing **acid-sulphate** type (Hayba *et al.* 1985, Heald *et al.* 1987), also known as **high sulphidation** (Hedenquist, 1987) or a special case of **advanced argillic** (Meyer and Hemley, 1967). Similar mineralization and alteration suites have been described as: alunite-kaolinite (pyrophyllite), enargite-gold, enargite massive sulphide, high sulphur, Nansatu-type, epithermal quartz-alunite, alunitic quartzite (Russian terminology), volcanic-hosted copper-arsenic-antimony, Roseki clay or acidic zone (Japanese terminology) and hotspring gold-silver.

BACKGROUND

The spatial proximity of magmatic hydrothermal and some epithermal mineralization has been postulated in a number of geologic models (Sillitoe, 1983, 1988, 1989, 1991a; Mutschler *et al.*, 1985; Bonham, 1986, 1988; Panteleyev, 1986). This re-emphasizes Lindgren's concepts of a continuum in ore-forming hydrothermal environments in volcanic settings, from hydrothermal systems dominated by magmatic fluids at depth, to largely geothermal meteoric-groundwater systems near the surface. As stated by Henley (1991):

- "magmatic vapour from crystallizing plutons is critical to [mineralization in] the epithermal environment much as described for porphyry copper-molybdenum deposits."
- "in volcanic terranes the distinction of epithermal from porphyry-type environments of mineralization becomes largely one of convenience for exploration than one of reality." and ". . . a practical understanding of the relationship between magmatism and structural evolution is critical to the future of [epithermal] exploration . . .".

Some epithermal deposits are positioned above or marginal to subvolcanic intrusion-related porphyry-type mineralization. Although the relationship between porphyry copper deposits and adularia-sericite-type epithermal deposits is considered by some to be speculative, the genetic connection with acid-sulphate-type deposits is well established (Henley and Ellis, 1983; Henley, 1991; Sillitoe, 1991a, b). According to Sillitoe (1989, 1991a), the latter typically occur above porphyry copper mineralization, albeit they are laterally offset in some districts by structural channeling.

Acid-sulphate alteration with associated copper-gold-silver mineralization is characterized by zoned hydrothermal mineral assemblages containing abundant silica as quartz, chalcedony and opaline silica (cristobalite), kaolin (including kaolinite, dickite and halloysite) pyrophyllite, and alunite/natroalunite. Locally, white mica (sericite/illite), mixed-layer clays, andalusite, and rarely diaspore, corundum and dumortierite are present, commonly in zonal arrangement. In some deposits late-stage barite, gypsum, anhydrite, jarosite and native sulphur are common as well as minor boehmite, phillipsite, tourmaline and accessory topaz, rutile and zunyite. The principal ore minerals, in addition to abundant pyrite and/or hematite, are gold, electrum, chalcopyrite, copper sulphosalts (enargite – famatinite/luzonite), tetrahedrite/tennantite, bornite, chalcocite and covellite. Elevated values of gold, silver, arsenic and antimony are common in copper ores.

The advanced argillic alteration with its siliceous and aluminous mineral assemblages, commonly with the sulphate minerals alunite, gypsum and jarosite and rarely native sulphur, is a product of strongly oxidized, sulphur-rich, acidic hydrothermal fluids. It generally occurs at late stages of mineralization during declining hydrothermal activity. The acid-sulphate, advanced argillic alteration originates in three ways (Hayba *et al.*, 1985; Rye *et al.* 1989, Sillitoe, in press): from magmatic-hydrothermal fluids in which magmatic volatiles are evolved at depth from crystallizing magma and interact with surrounding groundwater as described by Henley and McNabb (1978) - the porphyry environment; near surface where steam-heated fluids occur above the water table due to vapour separation (boiling) caused by depressurization of ascending hydrothermal fluids – the epithermal environment; and by oxidation of sulphides in the supergene environment.

INTRUSION-RELATED EPITHERMAL PRECIOUS METAL DEPOSITS IN BRITISH COLUMBIA

This new project proposes to examine, describe and study prospective environments for these deposits in British Columbia. MINFILE has five listings for enargite-bearing deposits; three of these in the Taku-Sutlahine River area are related zones within a large hydrothermal alteration system at the Thorn and adjoining properties. Pyrophyllite has been documented at four locations (MacLean, 1988). These and other deposits mentioned in various reports, mainly company reports, are listed in Table 2-1-1.

During the summer of 1991, the Thorn property and a number of northern Vancouver Island occurrences considered to be the highest priorities were briefly examined. The presence of widespread enargite in quartz veins is confirmed at the Thorn property within a large area of pyritic, intensely leached, limonitic (jarositic), sericite alteration. On northern Vancouver Island silica-clay 'caps' and pyrophyllite-bearing breccias form extensive alteration zones in Bonanza Group volcanic rocks. More detailed work in these and other areas is planned for 1992.

TABLE 2-1-1
BRITISH COLUMBIA DEPOSITS WITH ACID-SULPHATE, ADVANCED ARGILLIC ALTERATION CONTAINING KAOLINITE±PYROPHYLLITE±ALUNITE AND/OR ENARGITE*

Location/Property Name	MINFILE	Published References
Sutlahine River area		
1. *THORN, DAISY, INK, Camp Creek	104K 031, 116	
2. *KAY, LIN, LIN 1-8	104K 030	
Iskut River Area		
3. *Johnny Mountain/ REG	104B 107	
4. Treaty Glacier	104B 078	Alldrick and Britton, 1991; J.F.H. Thompson, personal communication, 1991
Toodoggone River area		Diakow *et al.*, 1991
5. AL, Alberts Hump, Bonanza	94E 078, 79, 85, 91, 99	
6. Brenda (Jan alunite)	94E 107	
7. SHAS (Shasta)	94E 050	
8. Silver Pond	94E 069	
Central B.C.		
9. Equity Silver mine	93L 001	Cyr *et al.*, 1984; Wojdak and Sinclair, 1984; 'deep acid-sulphate' – Sillitoe, 1991a
Taseko River/Mt. McClure area		Bradford, 1985
10. Empress	92O 033	Company reports, Westpine Metals Ltd.
11. *Taylor-Windfall	92O 028	
Vancouver Island		
12. Expo (Hushamu, Mt. MacIntosh, HEP, Pemberton Hills)	92L 185, 240, 78, 308	Company reports, Moraga Resources Ltd., BHP-Utah Mines Ltd.; P.G. Dasler, personal communication, 1991
13. Red Dog	92L 200	Company reports, Moraga Resources Ltd., Crew Natural Resources Ltd.
14. Wanokana	92L 272	Company reports, Acheron Resources Ltd., P.G. Dasler, personal communication, 1991
15. Island Copper mine	92L 138, 158, 273	Cargill *et al.*, 1976; Perello, 1987; Company reports
16. Kyuquot Sound (Easy Inlet)	92L 072, 117	Clapp, 1915; MacLean, 1988
Southern B.C.		
17. Riverside	92INW087	MacLean, 1988
18. Pyro	92HSE131	MacLean, 1988

Note: * denotes occurrences containing enargite. Deposits with MINFILE numbers are summarized in MINFILE from various published and unpublished sources — mainly company reports and assessment reports filed with the Ministry.

SUMMARY

Zones of acid-sulphate high-sulphidation, advanced argillic alteration can host or overlie major precious metal and copper deposits. The discovery of even one major deposit in this environment can be a major economic bonanza. For example, at El Indio, Chile in 1975, the recognized economic potential of veins and breccias led to the discovery of ore reserves containing 140 tonnes of gold, 771 tonnes of silver and 0.4 million tonnes of copper in a 150 by 500-metre area (Jannas *et al.*, 1990). In addition, acid-sulphate advanced argillic alteration zones are near-surface features that can mark buried bulk-mineable porphyry copper-gold deposits such as the Island Copper orebody (Cargill *et al.*, 1976; Perello, 1987) or enargite-type copper-gold-silver deposits such as the Lepanto deposit in the Philippines and the related, newly discovered, Lepanto Far Southeast deposit with combined metal content of 526 tonnes gold and 3.45 million tonnes copper (Sillitoe, 1991a).

The target areas for this study are both areas of past exploration or newly discovered areas of interest in which hydrothermal clay-silica zones of acid-sulphate advanced argillic alteration have not been recognized or evaluated. The relationships of intrusive rocks, hydrothermally altered zones, structural controls for ore and mineralization might best be studied at a regional or district scale. As stated by Sillitoe 1991, page 202, in a summary of intrusion-related gold deposits: "An appreciation of the variety of gold deposit types in intrusion-centered systems, the geological parameters that controlled them, their mutual interrelationships and the resultant metal zoning patterns provide a cogent framework for gold exploration in volcano-plutonic arcs." With regard to recent discoveries in long-active mining districts, he further states: " No less than 25 of the 33 newly discovered [post-1979] deposits . . . are located in old mining districts. Furthermore, given that districts possess radii as great as 8 km, individual exploration targets can be large."

An invitation is extended to readers with personal knowledge of acid-sulphate, high-sulphidation, advanced argillic deposits in British Columbia to share information with the writer in order to inventory the deposits and identify the favourable geological environments.

ACKNOWLEDGMENTS

Keith Mounjoy provided affable, competent assistance in organizing this project and during the course of fieldwork. Gerald Carlson and J.R. Woodcock, consulting geologists, Vancouver, provided the writer with numerous reports and shared personal observations about the Thorn property. Information about various northern Vancouver Island properties and advice about site visits were offered by Peter G. Dasler and David Pawliuk of Daiwan Engineering Limited on behalf of Moraga Resources Limited and Arne O. Birkeland on behalf of Keewatin Engineering Incorporated. Access to EXPO property diamond-drill core and generous discussions at the mine-site were offered by John Fleming, Island Copper mine. Constructive comments about the content and style of this report were received from Dave Lefebure and John Newell.

SELECTED BIBLIOGRAPHY

Alldrick, D.J. and Britton, J.M. (1991): Sulphurets Area Geology (Parts of 104A/5W, 12W; 104B/8E, 9E); *B.C. Ministry of Energy, Mines and Petroleum Resources*, Open File 1991-21.

Berger, B.R. and Henley, R.W. (1989): Advances in the Understanding of Epithermal Gold-Silver Deposits, with Special Reference to the Western United States; *in* The Geology of Gold Deposits, the Perspective in 1988, *Economic Geology*, Monograph 6, pages 405-423.

Bonham, H.F., Jr. (1986): Models for Volcanic-hosted Epithermal Precious Metal Deposits; A Review; *in* Proceedings Symposium 5: Volcanism, Hydrothermal Systems and Related Mineralization, *International Volcanological Congress*, Auckland, pages 13-17.

Bonham, H.F., Jr. (1988): Models for Volcanic-hosted Precious Metal Deposits: A Review; *in* Bulk Mineable Precious Metal Deposits of the Western United States, Schafer, R.W., Cooper, J.J. and Vikre P.G., Editors, *Geological Society of Nevada*, Reno, pages 259-271.

Bradford, J.A. (1985): Geology and Alteration in the Taseko River Area, Southwestern British Columbia; unpublished B.Sc. thesis, *The University of British Columbia*, 122 pages.

Cargill, D.G., Lamb, J., Young, M.J. and Rugg, E.S. (1976): Island Copper; *in* Porphyry Deposits of the Canadian Cordillera, Sutherland Brown, A., Editor, *Canadian Institute of Mining and Metallurgy*, Special Volume 15, pages 206-218.

Clapp, C.H. (1915): Alunite and Pyrophyllite in Triassic and Jurassic Volcanics at Kyuquot Sound, British Columbia; *Economic Geology*, Volume 10, Number 1, pages 70-88.

Cyr, J.B., Pease, R.B. and Schroeter, T.G. (1984): Geology and Mineralization at Equity Silver Mine; *Economic Geology*, Volume 79, pages 947-968.

Diakow, L.J., Panteleyev, A. and Schroeter, T.G. (1991): Jurassic Epithermal Deposits in the Toodoggone River Area, Northern British Columbia – Examples of Well-preserved Volcanic-hosted, Precious Metal Mineralization; *Economic Geology*, Volume 86, pages 529-554.

Hayba, D.O., Bethke, P.M., Heald, P. and Foley, N.K. (1985): Geologic, Mineralogic, and Geochemical Characteristics of Volcanic-hosted Epithermal Precious-metal Deposits; *in* Geology and Geochemistry of Epithermal Systems, Berger, B.R. and Bethke, P.M., Editors, *Reviews in Economic Geology*, Volume 2, pages 129-167.

Heald, P., Foley, N.K. and Hayba, D.O. (198?): Comparative Anatomy of Volcanic-hosted Epithermal Deposits: Acid Sulfate and Adularia-Sericite Types; *Economic Geology*, Volume 82, pages 1-26.

Hedenquist, J. W. (1987): Mineralization Associated With Volcanic-related Hydrothermal Systems in the Circum-Pacific Basin; *in* Transactions of the Fourth Circum-Pacific Energy and Mineral Resources Conference, Singapore, Horn, M.K., Editor, *American Association Petroleum Geologists*, pages 513-524.

Hedenquist, J.W., White, N.C. and Siddeley, G., Editors (1990): Epithermal Gold Mineralization of the Circum-Pacific; Geology, Geochemistry, Origin and Exploration, Volumes I and II; *Journal of Geochemical Exploration*, Volume 35, 446 pages and Volume 36, 474 pages.

Henley, R.W. (1991): Epithermal Gold Deposits in Volcanic Terranes; *in* Gold Metallogeny and Exploration, Foster, R.P., Editor, *Blackie and Sons*, pages 13?-164.

Henley, R.W. and Ellis, A.J. (1983): Geothermal Systems Ancient and Modern: A Geochemical Review; *Earth Science Reviews*, Volume 19, pages 1-50.

Henley, R.W. and McNabb, A (1978): Magmatic Vapor Plumes and Ground Water Interaction in Porphyry Copper Emplacement; *Economic Geology* Volume 73, pages 1-20.

Jannas, R.R., Beane, R.E., Ahler, B.A. and Brosnahan, D.R. (1990): Gold and Copper Mineralization at the El Indio Deposit, Chile; *in* Epithermal Gold Mineralization of the Circum-Pacific: Geology, Geochemistry, Origin and Exploration, II, Hedenquist, J.W., White, N.C. and Siddeley, G., Editors, *Journal of Geochemical Exploration*, Volume 36, pages 233-267.

Meyer, C. and Hemley, J.J. (1967): Wall Rock Alteration; *in* Geochemistry of Hydrothermal Ore Deposits, Barnes, H.L., Editor, *Holt, Rinehart and Winston, Inc.*, pages 166-235.

MacLean, M. (1988): Talc and Pyrophyllite in British Columbia; *B.C. Ministry of Energy Mines and Petroleum Resources*, Open File 1988-19, 108 pages.

Mutschler, F.E., Griffen, M.E., Scott Stevens D. and Shannon, S.S. Jr. (1985): Precious Metal Deposits Related to Alkaline Rocks in the North American Cordillera – An Interpretive Review; *Geological Society South Africa*, Transactions, Volume 88, pages 366-37?.

Panteleyev, A. (1986): A Canadian Cordilleran Model for Epithermal Gold-Silver Deposits, *Geoscience Canada*, Volume 13, pages 101-11?; and *in* Ore Deposit Models, Roberts, R.G. and Sheahan, P.A., Editors, *Geoscience Canada*, Reprint Series 3, pages 31-44.

Perello, J.A. (1987): The Occurrence of Gold at Island Copper Mine, Vancouver Island, British Columbia; unpublished M.Sc. thesis, *Queen's University*, Kingston, 85 pages.

Rye, R.O., Bethke. P.M. and Wasserman, M.D. (1989): Diverse Origins of Alunite and Acid-Sulfate Alteration: Stable Isotope Systematics; *United States Geological Survey*, Open-File Report 89-5, 33 pages.

Sillitoe, R.H. (1983): Enargite-bearing Massive Sulfide Deposits High in Porphyry Copper Systems; *Economic Geology*, Volume 78, pages 348-352.

Sillitoe, R.H. (1988): Gold and Silver Deposits in Porphyry Systems; *in* Bulk Mineable Precious Metal Deposits of the Western United States, Schafer, R.W., Cooper, J.J. and Vikre, P. G., Editors, *Geological Society of Nevada*, Reno, pages 233-257.

Sillitoe, R.H. (1989): Gold Deposits in Western Pacific Island Arcs: The Magmatic Connection; *in* The Geology of Gold Deposits: The Perspective in 1988, Keays, R.R., Ramsay, W.R.H. and Groves, D.I., Editors, *Economic Geology*, Monograph 6, pages 274-291.

Sillitoe, R.H. (1990): Gold-rich Porphyry Copper Deposits of the Circum-Pacific Region – An Updated Overview; *in* Pacific Rim Congress 90, Gold Coast, Queensland, 1990, Proceedings, Volume 2, *Australian Institute of Mining and Metallurgy*, pages 119-126.

Sillitoe, R.H. (1991a): Intrusion-related Gold Deposits; *in* Gold Metallogeny and Exploration, Foster, R.P, Editor, *Blackie and Sons*, pages 165-209.

Sillitoe, R.H. (1991b): Gold Metallogeny in Chile; *Economic Geology*, Volume 86, pages 1187-1205.

Sillitoe, R.H. (in press): Gold-rich Porphyry Copper Deposits: Occurrence Model and Exploration Implications; *in* Proceedings 8th IAGOD Symposium, *IUGS/IAGOD Deposit Modeling Program Conference*, Ottawa, 1990.

Sillitoe, R.H. (in press): Epithermal Models, Geometric Controls and Shallow Features; *in* Proceedings 8th IAGOD Symposium, *IUGS/UAGOD Deposit Modeling Program Conference*, Ottawa, 1990.

Sillitoe, R.H. and Camus, F., Editors (1991): Gold Deposits of the Chilean Andes; *Economic Geology*, Volume 86, pages 1153-1345.

Wojdak, P.J. and Sinclair, A.J. (1984): Equity Silver-Copper-Gold Deposit: Alteration and Fluid Inclusion Studies; *Economic Geology*, Volume 79, pages 969-990.

AN INVESTIGATION OF SELECTED MINERALIZED SKARNS IN BRITISH COLUMBIA

By I.C.L. Webster, G.E. Ray and A.R. Pettipas

KEYWORDS: Economic geology, skarn, metallogeny, geochemistry, mineralogy, wrigglite.

INTRODUCTION

A number of skarn deposits and occurrences throughout the province were examined and sampled during the 1991 field season (Figure 2-2-1). The season represented the final part of a 4-year field program to map, study and compile data on some of the 700 or more mineralized skarns recorded in MINFILE. It is hoped to determine relationships between these skarns and their metal content, geochemistry, mineralogy, age, associated intrusions and lithostructural setting. Preliminary geochemical results and descriptions of the mineralized skarn samples collected this season are presented in Tables 2-2-1a and b. Whole-rock and additional trace element analytical results, together with data on microprobe analyses, will be published at a later date.

Earlier work in this program focused on the province's gold and iron skarns, such as those in the Hedley, Texada Island and Merry Widow camps, and in the Iskut River area; publications include those by Ray *et al.* (1988, 1991), Ettlinger and Ray (1989), Ray and Webster (1991), Webster and Ray (1991), and Ray and Dawson (in preparation). The 1991 research concentrated on some of British Columbia's copper, zinc-lead, tungsten, molybdenum and tin skarns (Figure 2-2-1). The final results of the study will eventually be published in bulletin form (Ray and Webster, in preparation).

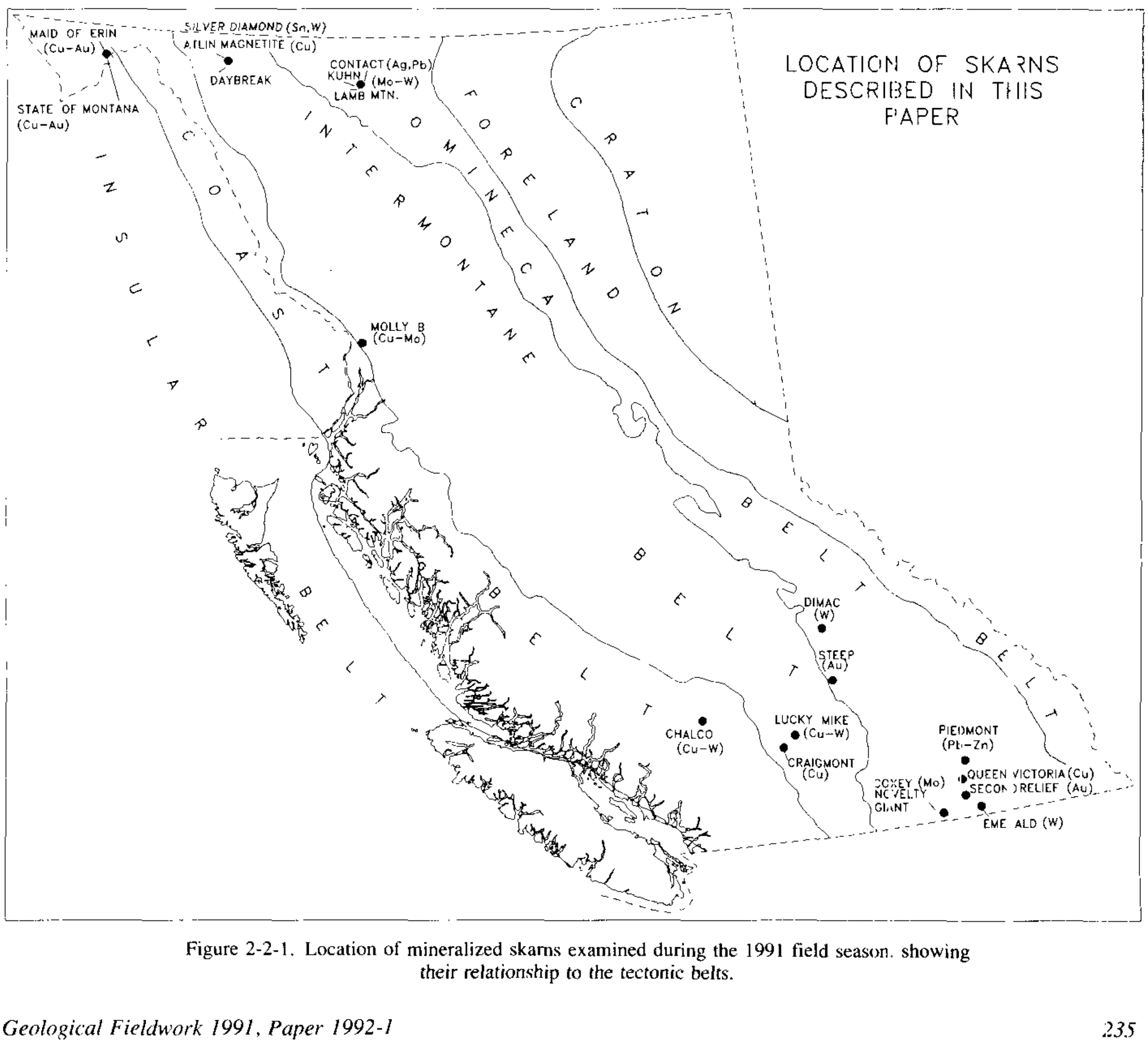

Figure 2-2-1. Location of mineralized skarns examined during the 1991 field season, showing *their relationship to the tectonic belts.*

TABLE 2-2-1a

PRELIMINARY GEOCHEMICAL RESULTS OF MINERALIZED SKARN GRAB SAMPLES. ALL UNITS ARE IN PPM EXCEPT WHERE STATED AS PPB OR PER CENT. VALUES PENDING FOR BLANK SPACES

LABNO	LOCATION	Ag	As	Au ppb	Ba	Bi	Cd	Ce	Co	Cr	Cu	Mn	Mo	Ni	Pb	Rb	Sb	Se	Th	W	Zn
043058	Maid of Erin			177	<100	1300		6	18	62						<30		48	0.5	19	
043059	Maid of Erin			89	<100			6	56	71						<30		48	0.5	4	
043060	Maid of Erin	0.8		<5	850	<5		100	13	70						68		<5	12.0	8	
043062	Maid of Erin	18		13	<100	22		18	42	44						<30		<5	0.6	33	
043063	Adams	2.2		41	200	53		12	14	36						<30		<5	2.3	8	
043064	Majestic	5		40	<100	101		5	210	46						<30		27	0.5	42	
043065	State of Montana			141	<100			11	16	69						<30		160	2.5	4	
043066	State of Montana			45	<100			6	46	62						<30		210	1.1	4	
043067	State of Montana	2		6	1500	<5		84	29	50						<30		<5	9.6	4	
043068	Lawrence	15		<5	<100	27		<3		29						<30		17	0.5	4	
043069	Rainy Hollow	<0.4		<5	280	<5		23	25	59						<30		<5	3.0	4	
043070	Rainy Hollow	<0.4		<5	320	<5		23		96						46		<5	3.6	4	
043072	Rainy Hollow	<0.4		<5	2800	<5		38	7	190						33		<5	5.2	4	
043073	Rainy Hollow	<0.4		<5	400	<5		40	19	98						34		<5	5.6	4	
043077	Chalco	2.2		27	<100	14		4	62	120						<30		<5	0.5	2600	
043078	Chalco	4		273	<100	77		<3	20	99						<30		<5	0.5	920	
043079	Chalco	3.2		287	<100	112		16	46	150						<30		<5	1.9	1200	
042818	Craigmont			19	<100			37		19						47		<5	0.5	86	
042548	Eric	<0.5	7	<2	<50	<5	<0.3	<3	23	70	0.10%	325	5	17	3	<5	2	<5	0.2	1	26
042544	Lucky Mike	22	13	61	110	<5	10	<3	75	160	1.13%	0.56%	29	7	3	<5	1	<5	1.0	450	540
042823	Molly B	1.6		39	1900	<5		14	36	100						55		<5	1.5	38	
042824	Molly B	10		55	<100	<5		8	620	58						<30		35	1.3	5800	
042825	Molly B	6		57	3000	<5		8	105	38						46		27	0.5	240	
042826	Oral M			4170	1600	<5		9	19	150						32		<5	1.3	11	
042827	Oral M			7910	3800	<5		7	7	110						100		<5	2.0	8	
043048	Atlin Magnetite	65		305	<100	68		<3	56	140						35		<5	<0.5	9	
043049	Atlin Magnetite	36		646	<100	210		<3	81	70						<30		<5	<0.5	39	
043050	Silver Diamond	185		25	110	396		<3	6	25						<30		9	<0.5	4	
043052	Silver Diamond	98		97	<100	2300		<3	58	82						150		<5	<0.5	3000	
043053	Silver Diamond	13		<5	330	37		<3	5	32						350		<5	<0.5	4600	
043054	Silver Diamond	31		55	<100	900		6	24	150						54		13	1.0	5500	
043055	Daybreak	23		42	<100	137		7	7	47						<30		<5	3.3	870	
043056	Daybreak	1		19	<100	70		14	8	44						<30		<5	3.1	550	
043057	Daybreak	0.4		49	<100	140		5	6	33						<30		<5	3.5	900	
042573	Coxey	1.5	36	35	2300	<5	<0.3	78	10	120	820	960	3.18%	56	38	170	1	<5	4.1	1900	62
042557	Coxey	4	13	110	1500	42	1	190	93	120	0.16%	0.114%	722	61	57	170	2	<5	11.0	160	131
042559	Coxey A pit	1.25	22	67	2600	<5	<0.3	51	92	87	0.135%	447	585	68	18	210	1	10	3.3	160	46
042560	Coxey E pit	8	30	220	1100	67	0.5	80	137	77	0.30%	891	0.46%	207	13	110	2	10	7.8	23000	74
042561	Coxey F pit	10	17	141	450	84	0.7	54	92	74	0.35%	0.18%	93	98	7	24	2	<5	2.1	4300	172
042563	Novelty	3	13.8%	47200	860	3500	<0.3	120	4.84%	100	11	82	1.40%	1.27%	23	150	103	35	3.9	30	6
042564	Novelty	1.5	4.11%	9070	550	1850	<0.3	26	0.11%	41	21	512	445	0.60%	20	41	15	9	3.1	65	43
042565	Novelty	0.75	4.48%	13000	2100	440	<0.3	32	0.48%	100	29	572	0.53%	186	31	240	47	28	1.6	39	27
042572	Novelty	3	12.6%	22900	1200	3800	<0.3	29	0.26%	73	9	295	0.17%	59	11	240	25	34	8.4	10	22
042568	Giant	2	30.5%	7530	1000	1400	0.8	27	1.26%	100	0.21%	73	1.06%	0.11%	16	75	59	100	3.6	17	40
042566	Vein - Coxey	143	136	16100	<50	80	775	<3	42	220	0.21%	647	7	8	3.71%	<5	54	<5	0.2	8	1.63%
042584	2nd Relief	2	17	356	110	<5	0.5	4	24	250	0.25%	175	7	16	13	8	0.6	<5	0.3	1	53
042585	2nd Relief	0.5	74	72	1000	<5	25	24	6	88	318	0.286%	5	7	20	84	2	<5	3.2	1	0.12%
042586	2nd Relief	2	259	119	77	<5	0.7	8	4	240	0.14%	488	23	10	13	14	2	<5	0.6	2	55
042588	2nd Relief	3	5.00%	10200	440	<5	510	17	9	100	0.107%	483	5	6	70	50	25	<5	2.5	4	1.78%
042556	Emerald W	<0.5	4	<5	93	8	1	55	10	110	32	2.40%	475	19	441	<5	1	<5	6.7	7900	470
042553	Dodger	19	1.78%	1380	160	<5	<0.3	6	140	90	720	0.19%	10	27	51	48	185	11	1.3	820	45
042554	Dodger	1	6	21	420	<5	<0.3	220	101	40	740	724	80	23	11	170	1	<5	19.0	14	65
042578	Queen Vic	76	5	602	<50	<5	15	<3	68	64	9.40%	0.45%	5	46	4	<5	<0.5	16	0.3	1	560
042579	Queen Vic	19	3	75	<50	<5	11	<3	40	37	2.07%	0.60%	5	55	5	<5	<0.5	<5	0.3	2	360
042580	Queen Vic	14	5	147	84	<5	3	<3	30	290	1.37%	595	5	41	17	12	<0.5	<5	0.2	3	120
042581	Piedmont	110	64	4	1100	<5	0.22%	10	12	97	770	0.98%	35	212	4.69%	100	135	7	2.0	2	12.4%
042582	Piedmont	124	2	3	61	350	0.24%	<3	43	17	950	741	5	610	4.18%	8	4	28	0.2	2	13.0%
042583	Piedmont	80	240	12	1500	<5	0.16%	9	12	80	480	0.99%	72	184	2.59%	81	111	12	0.9	7	9.20
042828	Steep	<0.4		23	<100	<5		44	147	79						<30		<5	10.0	19	
042829	Steep	1.4		23	<100	<5		180	45	96						<30		<5	18.0	12	
042819	Dimac			7	<100			52		43						71		<5	6.8	68000	
042820	Dimac			7	<100			18		130						<30		<5	2.9	23000	
042822	Dimac	<0.4		<5	<100	<5		23	18	57						<30		<5	6.4	70000	
043080	Contact	110		<5	<100	<5		<3	3	49						36		<5	0.5	15	
043082	Contact	162		6	420	<5		24	6	69						54		<5	5.2	24	
043083	Kuhn	1.4		<5	<100	10		420	14	390						380		<5	45.0	480	
043084	Kuhn	0.6		<5	260	<5		57	77	59						35		<5	6.7	35	
043085	Dead Goat	1		<5	250	<5		4	192	53						<30		<5	0.5	1800	
043086	Dead Goat	1.6		<5	340	35		<3	170	59						<30		<5	1.1	440	
043087	Lamb Mountain	1.2		<5	<100	<5		9	24	56						<30		<5	0.7	430	
043088	Lamb Mountain	<0.5		<5	260	17		33	14	46						530		<5	150.0	320	
043089	Lamb Mountain	<0.5		<5	250	<5		42	10	76						210		<5	34.0	1100	
043074	Unnamed	1.4		<5	<100	6		4	10	66						<30		<5	0.5	10	
043075	Unnamed	0.8		<5	<100	<5		13	15	120						34		<5	0.5	7	
043076	Unnamed	<0.4		<5	<100	<5		18	11	120						<30		<5	0.5	14	

TABLE 2-2-1b
DESCRIPTIONS OF SAMPLES LISTED IN TABLE 2-2-1a

LABNO	DEPOSIT	SAMPLE DESCRIPTION
043058	Maid of Erin	Bornite ore with yellowish green garnet.
043059	Maid of Erin	Massive bornite ore.
043060	Maid of Erin	Below deposit; rusty silicified float with disseminated po.
043062	Maid of Erin	Mineralization on road east of deposit.
043065	State of Montana	Massive bornite and garnet ore.
043066	State of Montana	Massive bornite and garnet ore.
043067	State of Montana	Disseminated po in banded garnet skarn.
043063	Adams	Minor py, po and aphl in siltstone and phyllite
043068	Lawrence	Sphl with minor cpy and gal with green garnet in marble.
043064	Majestic	Massive po vein with minor cpy and quartz veinlets.
043069	Rainy Hollow	Disseminated po in rusty siliceous siltstone on road into deposit
043070	Rainy Hollow	Disseminated po in rusty siliceous siltstone on road into deposit.
043072	Rainy Hollow	Disseminated po in schist; east side of Mineral Mountain.
043073	Rainy Hollow	Disseminated po in hornfelsed schist; Inspector Creek float.
043077	Chalco	Po, cpy and mgt in garnet pyroxene skarn.
043078	Chalco	Po, cpy and mgt in garnet pyroxene skarn.
043079	Chalco	Po and mo in skarn altered schist.
042818	Craigmont	Mgt, hem and cpy in epidote-chlorite skarn
042548	Eric	Mgt, hem, malachite and potassium feldspar in garnet skarn.
042544	Lucky Mike	Cpy, scht and calcite in brown garnetite.
042823	Molly B	Po in garnet-pyroxene skarn
042824	Molly B	Po, cpy and py in garnet-pyroxene skarn, mine dump
042825	Molly B	Sphl, po and cpy in pyroxene-garnet skarn; upper cut
042826	Oral M	Py and cpy in quartz vein.
042827	Oral M	Py and cpy in quartz vein.
043048	Atlin Magnetite	Mgt, cpy and po in garnet skarn
043049	*Atlin Magnetite*	*Mgt, cpy and azurite in garnet skarn*
043050	Silver Diamond	Coarse sphl,po and cpy mineralization
043052	Silver Diamond	Po, cpy and fluorite with sericite
043053	Silver Diamond	Black manganese in granular crystalline fluorite
043054	Silver Diamond	Sphl and gal veinlets with minor coarse py in quartz vein
043055	Daybreak	Wrigglite skarn
043056	Daybreak	Wrigglite skarn.
043057	Daybreak	Wrigglite skarn.
042557	Coxey	D pit; Po veinlets in pyroxene-amphibole skarn
042573	Coxey	Mo in pyroxene hornfels; uA pit
042559	Coxey	Mo and po matrix in diorite breccia; A pit
042560	Coxey	Mo and py veins in skarn, E pit.
042561	Coxey	Mo and py veins in skarn-altered siltstones, F pit.
042563	Novelty	Asp, mo, py ore with cobalt bloom
042564	Novelty	Asp and mo in silicified sedimentary breccia
042565	Novelty	Asp, cpy and cob ore
042572	Novelty	Asp in siliceous sediment.
042568	Giant	Asp, mo with minor po, py and garnet ore, upper adit dump
042566	Vein north of Coxey	Gal and py in thin, subhorizontal quartz vein.
042584	2nd Relief	Py, po, and cpy in quartz vein
042585	2nd Relief	Sulphide-rich pyroxene hornfels with minor garnet in wallrock.
042586	2nd Relief	Sulphide-rich quartz vein with dark green mineral.
042588	2nd Relief	Sphl and asp-rich quartz vein.
042556	Emerald W	Scht, and mo in garnet skarn inside portal
042553	Dodger	Po, py and asp at limestone-granite contact in portal
042554	Dodger	Po and py and equigranular quartz in granite at portal.
042578	Queen Victoria	Cpy and py in garnetite.
042579	Queen Victoria	Cpy and py in garnetite
042580	Queen Victoria	Sulphide-rich quartz vein
042581	Piedmont	Massive gal, sphl and po ore
042582	Piedmont	Massive po and sphl from inside adit.
042583	Piedmont	Gal sphl and po ore
042828	Steep	Po in garnet skarn
042829	Steep	Po and cpy in skarn
042819	Dimac	Po and scht in quartz-garnet skarn.
042820	Dimac	Coarse scht with po in garnet-pyroxene-quartz skarn
042822	Dimac	Scht and po in garnet-pyroxene-quartz skarn
043080	Contact	Mgt, po and sphl ore
043082	Contact	Mgt, po sphl ore.
043083	Kuhn	Mo and minor po in actinolite, garnet quartz skarn
043084	Kuhn	Po and cpy in float.
043085	*Dead Goat*	*Coarse po and py with minor sphl and mgt in coarse garnet skarn.*
043086	Dead Goat	Sphl and po in pyroxene skarn.
043087	Lamb Mountain	Minor po and cpy in actinolite skarn
043088	Lamb Mountain	Disseminated po in rusty, siliceous quartz monzonite
043089	Lamb Mountain	Disseminated po in rusty, siliceous quartz monzonite
043074	Unnamed	Garnet-pyroxene skarn with py and po (#6 in Figure 6).
043075	Unnamed	Garnet-pyroxene skarn with py and po (#6 in Figure 6).
043076	Unnamed	Endo skarn with py, po and mo (#5 in Figure 6).

Abbreviations; mo = molybdenite, py = pyrite, cpy = chalcopyrite, po = pyrrhotite, asp = arsenopyrite, hem = hematite, scht = scheelite, cob = cobaltite, gal = galena, sphl = sphalerite

Analytical methods:

Au,Ba,Ce,Cr,Rb,Se,Sn,Th,W; neutron activation, Activation Laboratories Ltd Ancaster, Ont

Ag,Bi,Cd,Co,Cu,Mn,Mo,Ni,Pb,Zn; atomic absorption spectroscopy. Anaytical Sciences Laboratory, B C Geological Survey Branch, M E M P R

As,Sb; atomic absorption-hydride generation, Anaytical Sciences Laboratory, B C Geological Survey Branch, M.E.M.P.R.

INSULAR BELT

A number of skarns, including the Maid of Erin and State of Montana deposits, are located in the Rainy Hollow area in the northwest corner of the province (Figure 2-2-1) approximately 70 kilometres northwest of Haines, Alaska. They occur within the Alexander Terrane and are hosted by Upper Paleozoic sediments that are intruded on the west and east by Oligocene rocks of the Tkope River intrusions (Campbell, 1983). A suite of Squaw-Datlaska gabbroic sills and dikes also occurs in the area (Figure 2-2-2). Skarn alteration and silicification, with zones of massive and disseminated sulphides, are exposed over a wide area. Intermittent underground mining took place, mostly at the Maid of Erin between 1907 and 1956; approximately 244 tonnes of copper, 1.5 tonnes of silver and minor gold were produced (Table 2-2-2). Minor production is also reported from the State of Montana claim. In addition to these two producers, several small skarn occurrences are exposed in old pits and exploratory adits in the area; they include the Lawrence, Adams, Victoria, Hibernia, Wonderful and Majestic skarns (McConnell, 1913; Hudson, 1927; Watson, 1948).

MAID OF ERIN (MINFILE 114P 007)

The Maid of Erin skarn lies less than 200 metres from the northeast margin of a hornblende-biotite quartz diorite body belonging to the Tkope River intrusions. This large massive stock, which underlies the skarn, is cut by numerous narrow, white quartz veins. The skarn is hosted by an altered and silicified package of tuff, argillite and marble that dips moderately northeastwards; these rocks are locally cut by narrow, endoskarn-altered sills and dikes that are believed to originate from the nearby diorite.

The endoskarn intrusions and exoskarn lenses largely comprise banded, massive and crystalline garnet with lesser pyroxene; banding in the exoskarn probably represents remnant bedding. The garnet includes pale brown, red, lime-green and yellow varieties, some of which are optically zoned. Several phases are recognized in the marble an early, brown garnet is overgrown, in turn, by dark green and yellow crystals. Also present are coarse, radiating crystals of vesuvianite and wollastonite as well as lesser epidote, sericite and biotite. The fine-grained biotite mainly occurs in remnant patches of dark, siliceous, hornfels-like rock that is cut by veinlets of pyroxene and later garnet. Watson (1948) reports the presence of zoisite, clinozoisite, monticellite, anorthite and blue gahnite spinel in the skarn.

Mineralization is found both in the exoskarn and endoskarn. It consists of veins and blebs of mainly bornite, chalcocite and lesser chalcopyrite with sporadic and minor azurite, black sphalerite, molybdenite and magnetite. Wittichenite (Cu_3BiS_3) has also been identified in some ore as well as trace covellite and native silver (Watson, 1948). Mineralized samples of sulphide-rich skarn contain high values of copper, silver and bismuth with some gold (Ettlinger and Ray, 1989; Table 2-2-1a). Extensive silicified and albitized zones containing disseminated pyrrhotite occur adjacent to the Maid of Erin skarn and on Mineral Mountain (Figure 2-2-2), however, samples of this material contained no gold (Table 2-2-1a).

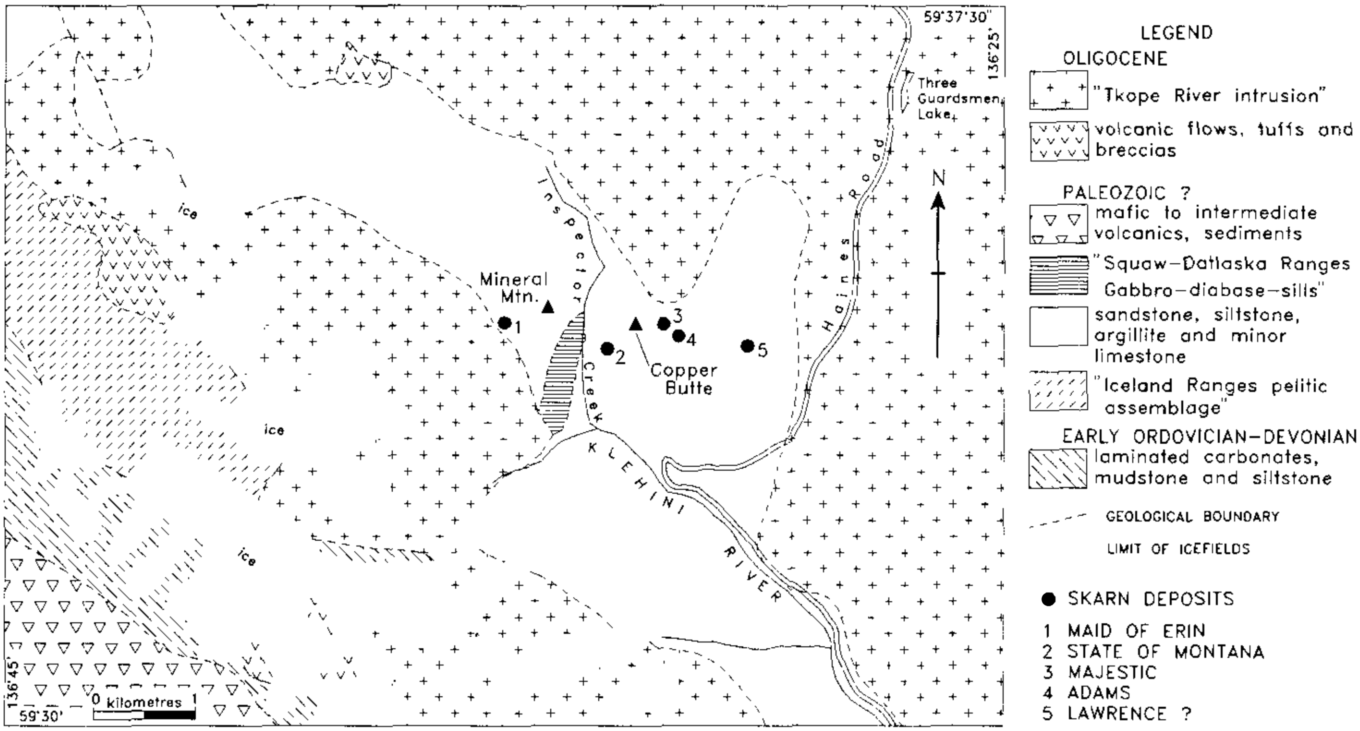

Figure 2-2-2. Geology and location of skarns in the Rainy Hollow area, northwest B.C. (geology after Campbell,1983).

TABLE 2-2-2
SKARNS VISITED DURING THE 1991 FIELD SEASON GIVING TECTONIC BELT, LITHOTECTONIC TERRANE AND PRODUCTION

Skarn name	Belt	Terrane	Ore (t)	Au (kg)	Ag (kg)	Cu (t)	Pb (t)	Zn (t)	Mo (t)	Fe (t)	W(t)
Maid of Erin	Ins	Alex	3 285	0.3	1 487	244	-	-	-	-	-
State of Montana	Ins	Alex	9	-	14	2	-	-	-	-	-
Victoria	Ins	Alex	none	-	-	-	-	-	-	-	-
Adams	Ins	Alex	none	-	-	-	-	-	-	-	-
Lawrence	Ins	Alex	none	-	-	-	-	-	-	-	-
Chalco	Cst	BrdgR	none	-	-	-	-	-	-	-	-
Craigmont	Int	Ques	29 325 342	78	242	402 704	-	-	-	141 634	-
Lucky Mike	Int	Ques	5	0.6	4.3	0.9	0.8	-	-	-	-
Molly B	Int	Stik	290	0.7	3.5	2	-	-	-	-	-
Oral M	Int	Stik	12	0.3	1.5	1	-	-	-	-	-
Silver Diamond	Int	Cache	none	-	-	-	-	-	-	-	-
Atlin Magnetite	Int	Cache	none	-	-	-	-	-	-	-	-
Day Break	Int	Cache	none	-	-	-	-	-	-	-	-
Coxey	Omn	SldMtn	1 035 509	-	-	-	-	-	1 749	-	-
Novelty	Omn	SldMtn	unknown production		-		-	-	-	-	-
Giant	Omn	SldMtn	*4 131	113	23	1.3	-	-	-	-	-
Second Relief	Omn	Ques	207 023	3 118	866	20	1	0.1	-	-	-
Emerald camp**	Omn	ANA	7 683 190	-	-	-	-	-	-	-	7 416
Queen Victoria	Omn	Ques	45 352	8	950	673	-	-	-	-	-
Piedmont	Omn	Ques	479	-	71	-	24	71	-	-	-
Steep	Omn	Koot	none	-	-	-	-	-	-	-	-
Dimac	Omn	Bark	105	-	-	-	-	-	-	-	105
Contact	Omn	Cass	25		10	0.02	2	-	-	-	-
Kuhn	Omn	Cass	none	-	-	-	-	-	-	-	-
Dead Goat	Omn	Cass	none	-	-	-	-	-	-	-	-
Lamb Mtn.	Omn	Cass	none	-	-	-	-	-	-	-	-

Abbreviations: Belts: Ins=Insular, Cst=Coast, Int=Intermontane, Omn=Omineca.
Terranes: Ques=Quesnellia, Stik=Stikinia, Cass=Cassiar, Bark=Barkerville, Alex=Alexander, Koot=Kootenay, SldMtn=Slide Montain, Cache=Cache Creek, ANA=Ancestral North America, BrdgR=Bridge River
* = Giant and California claims production.
** = Emerald Tungsten, Dodger, Feeney, Invincible: tungsten production figure from Jersey Mine records.

State of Montana (Minfile 114P 008)

The alteration and mineralization at this property are similar to that at the Maid of Erin skarn, approximately 1 kilometre to the east (Figure 2-2-2). The skarn consists mainly of green and brown garnet with minor amounts of coarse, radiating actinolite crystals. It is hosted by layered, steeply dipping marbles and siliceous and albitized metasediments close to small bodies of mafic diorite.

Mineralization appears to be confined to the green garnet skarn. It consists of veins and layers of massive bornite and chalcocite up to 10 centimetres thick; Watson (1948) notes that wittichenite occurs in bornite as microscopic grains. Like the Maid of Erin skarn, some of the silicified and albitized metasediments contain fine disseminated pyrrhotite.

Other Skarn Occurrences in the Rainy Hollow Area

The **Victoria, Adams and Lawrence** (MINFILE 114P 009, 010 and 011) occurrences are characterized by variable amounts of brown and green garnet with some minor wollastonite. Mineralization is dominated by black sphalerite with lesser galena (Hudson, 1927; Watson, 1948); some pods of massive pyrrhotite were also documented at the Adams where the skarn follows a marble-argillite contact, close to thin diorite sills. The Victoria skarn was not visited during this season because its location is uncertain.

The **Majestic** lies on the east side of Copper Butte (Figure 2-2-2) where it is hosted by grey marbles. At least two adits were driven on an east-trending zone of massive pyrrhotite. A narrow lens of crystalline brown and green garnet skarn is developed on the north side of the zone, between it and the marble.

The pyrrhotite zone contains garnet as well as rare veinlets of quartz and chalcopyrite. A pyrrhotite-rich sample from the Majestic is weakly anomalous in bismuth and cobalt but contains no gold (Table 2-2-1a).

To summarize, our examination of the Rainy Hollow area suggests that the numerous mineralized skarn deposits and occurrences are part of a major skarn system. This system, which probably resulted in a discontinuous but extensive alteration envelope that exceeds 1 square kilometre in outcrop area, covers parts of the Mineral Mountain and Copper Butte areas. It is uncertain whether it is related to the large Oligocene Tkope River intrusions or to a gabbroic sill suite forming part of the Squaw - Datlaska Ranges complex (Figure 2-2-2). The envelope contains copper and silver-rich skarn close to the Tkope River intrusion at the Maid of Erin deposit. Farther from the intrusion it contains some zinc-lead skarns as well as extensive alteration zones that are silicified and albitized with massive and disseminated pyrrhotite.

Past mining and exploration drilling at Rainy Hollow were concentrated on the proximal copper-rich skarn, while the possible existence of distal gold-rich and copper-poor skarn mineralization, similar to that at the Fortitude deposit in Nevada (Wotruba *et al.*, 1988; Myers, 1990), has largely been ignored. Although our samples of this pyrrhotite alteration were barren of gold (Table 2-2-1a), other features suggest that gold skarn mineralization could exist at Rainy Hollow. These features include the localized enrichment of gold, cobalt and bismuth in the hydrothermal system as well as the low Cu/Ag ratio (250) of the Maid of Erin ore; such a low ratio is atypical of most copper and iron skarns but is a characteristic of many gold-skarn systems (Ettlinger and Ray, 1989).

COAST BELT

Chalco (Minfile 92JNE043)

The Chalco 5 skarn is located 11 kilometres southeast of Bralorne in the Bridge River Terrane of southwestern B.C. (Figure 2-2-1). The area is underlain by biotite schist, banded amphibolite and marble of the Bridge River Group and the skarn is hosted by a northwest-trending pod of coarsely crystalline marble and schist 200 metres in length. An adit and open cut expose a section of marble containing a skarn zone up to 3 metres wide. The hornblende diorite Bendor batholith outcrops 100 metres to the north and is probably responsible for the skarn; it has yielded a Tertiary age of 64 Ma (Church and Pettipas, 1989). Small dikes of altered hornblende diorite crosscut the schist adjacent to the skarn.

Skarn minerals include coarse brownish red to black garnet with lesser pyroxene, actinolite and epidote. Garnet generally forms an interlocking mass of subhedral crystals up to 3 centimetres in diameter and often shows noticeable growth zoning; minor sericite is interstitial to the garnet. Locally the garnet skarn is banded with, or contains clots of, pyroxene and actinolite. Some crosscutting veins of quartz and carbonate contain euhedral crystals of garnet and pyroxene.

The disseminated metallic mineralization is sparse; it includes pyrrhotite, chalcopyrite and some magnetite with rare molybdenite. Geochemical analyses indicate sporadic minor enrichment in gold, bismuth and tungsten (Table 2-2-1a).

INTERMONTANE BELT

Craigmont Mine (Minfile 92ISE035)

The Craigmont copper skarn is situated in the Quesnel Terrane of southern British Columbia (Figure 2-2-1), approximately 13 kilometres northwest of Merritt. It is the largest copper skarn deposit in the province having produced over 400 000 tonnes of copper and 140 000 tonnes of magnetite iron ore (Table 2-2-2) from open-pit and underground workings. Mining took place between 1961 and 1982; since 1983 magnetite has been recovered from the tailings for use by the coal industry.

The Craigmont orebody was located on a major fault and was hosted mainly by volcanics, bedded tuffs and limestones of the Late Triassic Nicola Group adjacent to the southern margin of the Guichon Creek batholith. This batholith, which represents a high-level intrusion, was coeval with the Nicola Group volcanism and is associated with porphyry copper mineralization in the Highland Valley (McMillan, 1976, 1978). Quartz dioritic rocks of the batholith are exposed on the north wall of the open pit. They comprise dark, coarse-grained, epidote-altered rocks that contain up to 20 per cent hornblende.

The skarn silicate assemblage includes abundant chlorite, actinolite, epidote, calcite and quartz with minor red garnet and pink orthoclase. Sulphides occur mostly in the chlorite-actinolite exoskarn and the ore zones were generally concordant with the batholith margin and bedding in the Nicola Group. Exoskarn mineralization comprises masses and irregular veins of chalcopyrite up to 3 centimetres wide, together with magnetite and coarse specular hematite; pyrite is rare. Rennie (1962) notes that mineralization in the deposit was dominated by magnetite at its eastern end and by hematite farther west. The best copper grades occurred where there were equal amounts of magnetite and hematite. The mineral assemblages indicate that overall, the deposit formed in oxidized conditions although the magnetite to hematite zoning suggests that conditions towards the eastern end of the deposit were more reduced. Production data (Table 2-2-2) and geochemical analyses (Table 2-2-1a) indicate that this copper skarn has a very low gold content.

Minor amounts of endoskarn mineralization are observed; the altered diorite contains subcircular masses of chalcopyrite, up to 30 centimetres across, with patches of coarse, pink calcite and orthoclase, small euhedral quartz crystals and green epidote. This endoskarn includes thin magnetite layers that trend subparallel to the margins of the diorite, as well as rare, irregular veinlets of dark red garnet.

Two periods of mineralization are recognized (Johnson, 1973); an early magnetite-chalcopyrite assemblage, related to the main skarn-forming event, and later hematite-chalcopyrite mineralization that occurs mostly in chloritic shears. Some of the chalcopyrite veins are intergrown with pink orthoclase.

Morrison (1980) concluded that the metals were derived from the Nicola Group and not from the Guichon Creek batholith. However, the genetic relationship between the batholith and porphyry copper mineralization, and the spatial association of the skarn with the batholith margin suggests that the Craigmont deposit and the batholith are related. Moreover, approximately 2.5 kilometres east of the deposit, at the **Eric** occurrence (MINFILE 92ISE036), minor copper-magnetite mineralization is also developed along the batholith margin. This mineralization is associated with abundant orthoclase and lesser clinopyroxene, epidote, sphene and honey-coloured, optically isotropic garnet.

Lucky Mike Deposit (Minfile 92ISE027)

The Lucky Mike skarn is located approximately 20 kilometres north of Merritt within the Quesnel Terrane of southern British Columbia (Figure 2-2-1). Between 1917 and 1924 it produced minor amounts of silver, copper, lead and gold (Table 2-2-2). The area is underlain by Late Triassic Nicola Group volcanics, tuff and minor limestone (Moore and Pettipas, 1990). These contain a concordant, northerly striking zone of mineralized garnetite skarn that probably replaced a lens of clastic limestone. Both the footwall and hangingwall rocks comprise relatively fresh, massive andesitic crystal and lapilli tuffs with some agglomeratic layers. Locally, the hangingwall is occupied by a small body of hornblende-porphyritic mafic diorite; this intrusion is probably related to the skarn mineralization.

The garnetite zone is up to 3 metres wide and 30 metres long. It consists largely of medium-grained crystals of brownish red garnet. Irregular blebs of chalcopyrite, 2 to 3 centimetres long, are present in the garnetite; they are associated with patches of coarse calcite and quartz. Crystals of scheelite up to 0.5 centimetre across, as well as pyrite, pyrrhotite, sphalerite and magnetite are also present. Trace geochemical analyses of a mineralized grab sample are presented in Table 2-2-1a.

Molly B and Oral M (Minfile 103P 085)

The Molly B and Oral M deposits lie within the Stikine Terrane of northwestern British Columbia, close to the eastern margin of the Intermontane Belt (Figure 2-2-1). They are situated on the east side of the Bear River, opposite the town of Stewart. The Molly B adit was driven immediately above the river bank and the Oral M adit lies approximately 200 metres farther upslope. The geology and mineralization of the area are described by Grove (1971, 1986) and Alldrick (in preparation).

The Molly B deposit is a copper skarn whereas the Oral M is an auriferous, sulphide-rich quartz vein that cuts barren skarn and hornfels; both have had minor production of copper, gold and silver (Table 2-2-2). They are hosted by Early Jurassic Hazelton Group tuffs, argillites and minor limestones close to the intrusive contact of the Eocene granodioritic Hyder batholith. Extensive and irregular zones of biotite hornfels containing minor disseminated pyrrhotite occur in the vicinity of the two prospects. Hornfelsed tuffs are cut by veins of quartz and epidote, the cores of which locally contain pale brown garnet.

The Oral M prospect is a shear-hosted quartz vein that carries disseminated chalcopyrite, pyrite and gold; geochemical analyses on two vein samples are presented in Table 2-2-1a. The wallrock includes both hornfels and a garnet-dominant skarn with lesser pyroxene, actinolite and biotite. It is uncertain whether the mineralized quartz vein was genetically related to the formation of the wallrock skarn.

Close to the Molly B adit, massive to layered garnet-dominant skarn is associated with remnant, purplish coloured biotite hornfels that is cut by thin irregular pyroxene veinlets. An intense tectonic cleavage is developed locally; this is generally orientated subparallel to layering in the skarn which is believed to represent remnant bedding. Garnet forms veins, layers and pods up to 10 centimetres across. It occurs as euhedral light red, dark brown, amber and black crystals up to 1 centimetre in size. Pyroxene, epidote, actinolite, quartz and coarse carbonate are also present.

The skarn contains disseminations and irregular veins of pyrrhotite with lesser chalcopyrite, pyrite and molybdenite. Garnets in the sulphide-rich skarn are darker than those in the unmineralized skarn. Geochemical analyses of mineralized samples from the adit dump are anomalous in tungsten but, unlike the Oral M, they contain no gold (Table 2-2-1a).

Two dikes of unaltered leucocratic biotite granodiorite, up to 2 metres thick, are exposed in the Molly B adit. They are enveloped by banded garnet-pyroxene skarn, but it is uncertain whether the dikes are related to the skarn. However, float of endoskarn-altered intrusive was seen around the adit entrance. It consists of a coarse leucogranodiorite containing clots of red garnet and green epidote. Approximately 15 metres above the adit, several overgrown pits expose coarse garnet-pyroxene skarn with pyrrhotite, chalcopyrite and black sphalerite.

To summarize, the Oral M and Molly B deposits are distinct from one another in their morphology, mineralization and metal content. It is not known if they were coeval and related to the nearby Eocene Hyder pluton or whether they represent older Jurassic deposits as discussed by Alldrick (*in preparation*). The Oral M is a gold-bearing quartz vein, but it is uncertain whether it and the barren skarn-altered wallrock were formed during the same event. The Molly B, by contrast, is a gold-poor copper skarn that carries some local zinc, molybdenum and tungsten enrichment.

ATLIN CAMP

The **Silver Diamond, Atlin Magnetite** (MINFILE 104N 069 and 126) and the newly discovered **Daybreak** skarn occurrences are hosted by rocks of the Cache Creek Terrane, approximately 20 kilometres east-northeast of Atlin in northern British Columbia (Figure 2-2-1). They are spatially associated with the western margin of the Late Cretaceous Surprise Lake batholith where it intrudes calcareous rocks of the Cache Creek Group (Figure 2-2-3). The batholith consists largely of a leucocratic quartz monzonite.

The Silver Diamond skarn lies close to the southwest margin of a satellite stock of the Surprise Lake batholith (Figure 2-2-3) about 4.5 kilometres southwest of Ruby Mountain and west of Boulder Creek. It occurs mainly along the contact between a white, crystalline marble and altered greenstone and ultramafic rocks. Garnet is relatively uncommon and forms thin layers and veinlets of red and brown crystals. Variable amounts of pyroxene, fluorite, amphibole, biotite and sericite are also present. The greenstones adjacent to the skarn are bleached and silicified, whereas those adjacent to marble locally contain remnant patches of a dark biotite hornfels. Transition from marble to hornfels is often marked by the following mineral zoning: marble, garnet skarn, pyroxene skarn and hornfels.

The occurrence is characterized by pods, veins and irregular lenses of massive to disseminated sulphide, up to 1 metre wide, that are generally concordant with the marble contact. Locally, the greenstones are brecciated and cut by sulphide veinlets. Mineralization consists largely of pyrrhotite and sphalerite with minor chalcopyrite, pyrite and scheelite; some quartz-vein float with sphalerite and galena was noted at the occurrence. Locally, the colourless and purple fluorite is abundant. It occurs either as large crystalline masses that are stained with black manganese oxides and intergrown with sericite, or as isolated crystals growing within the massive sulphides. Analyses of mineralized samples (Table 2-2-1a) indicate that the Silver Diamond skarn is geochemically anomalous in silver, bismuth and tungsten.

There are reports in MINFILE of sporadic scheelite, cassiterite, molybdenite and tetrahedrite mineralization a short distance northeast of the occurrence.

The **Atlin Magnetite** skarn is situated approximately 8 kilometres northeast of the Silver Diamond prospect (Figure 2-2-3) between Ruby and Cracker creeks at about 1800 metres elevation. It is hosted by a deformed package of marble, sheared greenstone and talcose ultramafic rocks, approximately 200 metres south of their contact with the Surprise Lake batholith. In this area, the marginal phase of the batholith is a rusty-weathering quartz porphyry that hosts the Purple Rose uranium occurrence (MINFILE 104N 005); it lies approximately 250 metres north-northeast of the Atlin Magnetite skarn.

Skarn alteration and mineralization at the Atlin Magnetite occurrence are concentrated in marble layers close to their contact with sheared ultramafic rocks. Layers, masses and veins of garnet are present with lesser amounts of pyroxene, actinolite and coarse green epidote; minor late veins of rhodonite, and float containing coarse white wollastonite crystals, up to 2.5 centimetres long, were also seen. Garnets vary in colour from red, orange and yellow-green to dark green, brown, amber and black. Some of the sugary textured marbles contain euhedral crystals of black garnet up to 1 centimetre across.

Mineralization is dominated by layers and masses of magnetite, up to 0.5 metre thick, that are generally concordant with the foliated marbles. Magnetite is often intergrown with garnet although locally it is cut by garnet veins. Lesser amounts of chalcopyrite, pyrrhotite and sporadic pyrite occur with some azurite and abundant malachite staining. Geochemical analyses of mineralized samples indicate the skarn is weakly anomalous in silver and gold (Table 2-2-1a).

The **Daybreak** occurrence was recently discovered by an Atlin prospector, Mr. W. Wallis, and is of interest because it includes some ribbon-banded wrigglite skarn. It is situated at an elevation of 1550 to 1600 metres, east of Ruby Creek and 1 kilometre south of the Atlin Magnetite skarn (Figure 2-2-3) at UTM 595000E; 6620250N. The area is underlain by altered greenstone, schistose hornfelsic metasediment and minor mafic tuff and marble. These are intruded by several large, irregular sills and dikes of leucocratic quartz monzonite that are cut by narrow quartz veins, some of which carry minor fluorite. The sills and dikes are probably related to the nearby Surprise Lake batholith.

West and southwest of the occurrence there is a large area of garnet-pyroxene-biotite exoskarn, with lesser amounts of unaltered intrusive. This skarn contains layers and irregular veins of orange-red garnet and green pyroxene, up to 0.3 metre thick, that cut a schistose biotite hornfels. The eastern end of the skarn is covered by a scree that contains numerous large boulders of layered wrigglite skarn (Plate 2-2-1). Wrigglite was not seen in outcrop but some of the float represents frost-heaved boulders, suggesting that it subcrops in the immediate vicinity.

The wrigglite skarn is characterized by thin, rhythmic mineral layering; each layer is either green, brown or black depending upon the quantity of fluorite, vesuvianite, garnet or magnetite present. The layers, which are between

0.5 millimetre and 10 centimetres thick, are locally folded and sheared (Plate 2-2-1), and some are crosscut by veins of garnet. Rare vuggy cavities up to 10 centimetres in diameter are present; these are lined with elongate crystals of green clinozoisite. Microprobe and x-ray diffraction studies by the Geological Survey of Canada (S.B. Ballantyne, personal communication, 1991) indicate the wrigglite contains gahnite and trace cassiterite, and is enriched in beryllium. No beryl has yet been identified, and it is likely that much of the beryllium is contained as a non-essentail element within the vesuvianite and garnet.

The term "wrigglite" to describe rhythmically layered skarn was first used by Askins (1976) and later by Kwak and Askins (1981) although the texture has been recognized since the early part of this century. Kwak (1987) discusses the origin of wrigglite texture and notes it is a characteristic of iron and fluorine-rich tin skarns, most of which contain fluorine in excess of 9 per cent by volume. Wrigglite skarns are commonly associated with fault structures; unlike most tin skarns which generally form at deep levels, they are believed to develop under relatively near-surface conditions such as above the cupolas of high-level granites. Thus, its presence in the Daybeak skarn suggests the Surprise Lake batholith is a relatively high-level and structurally controlled intrusion. Moreover, the presence of the fluorine-beryllium-tin skarn assemblages at both the Daybreak and Silver Diamond occurrences are characteristic of highly evolved granitic melts derived from continental crust. This indicates the oceanic Cache Creek Terrane may be underlain by continental basement in the Atlin area.

OMINECA BELT

The **Coxey, Novelty** and **Giant** skarns are hosted by rocks of the Slide Mountain Terrane, and lie within the Rossland mining camp in southeastern British Columbia (Figure 2-2-1). The camp has a long mining history and many of its important deposits are on Red Mountain, west of Rossland township (Figure 2-2-4). Immediately east of Red Mountain, the geology is characterized by Early Jurassic Rossland Group supracrustal rocks and several suites of Jurassic intrusions. On Red Mountain, these rocks are structurally overlain by a thrust sheet comprising Pennsylvanian to Permian metasediments of the Mount Roberts Formation (Höy and Andrew, 1991a and b).

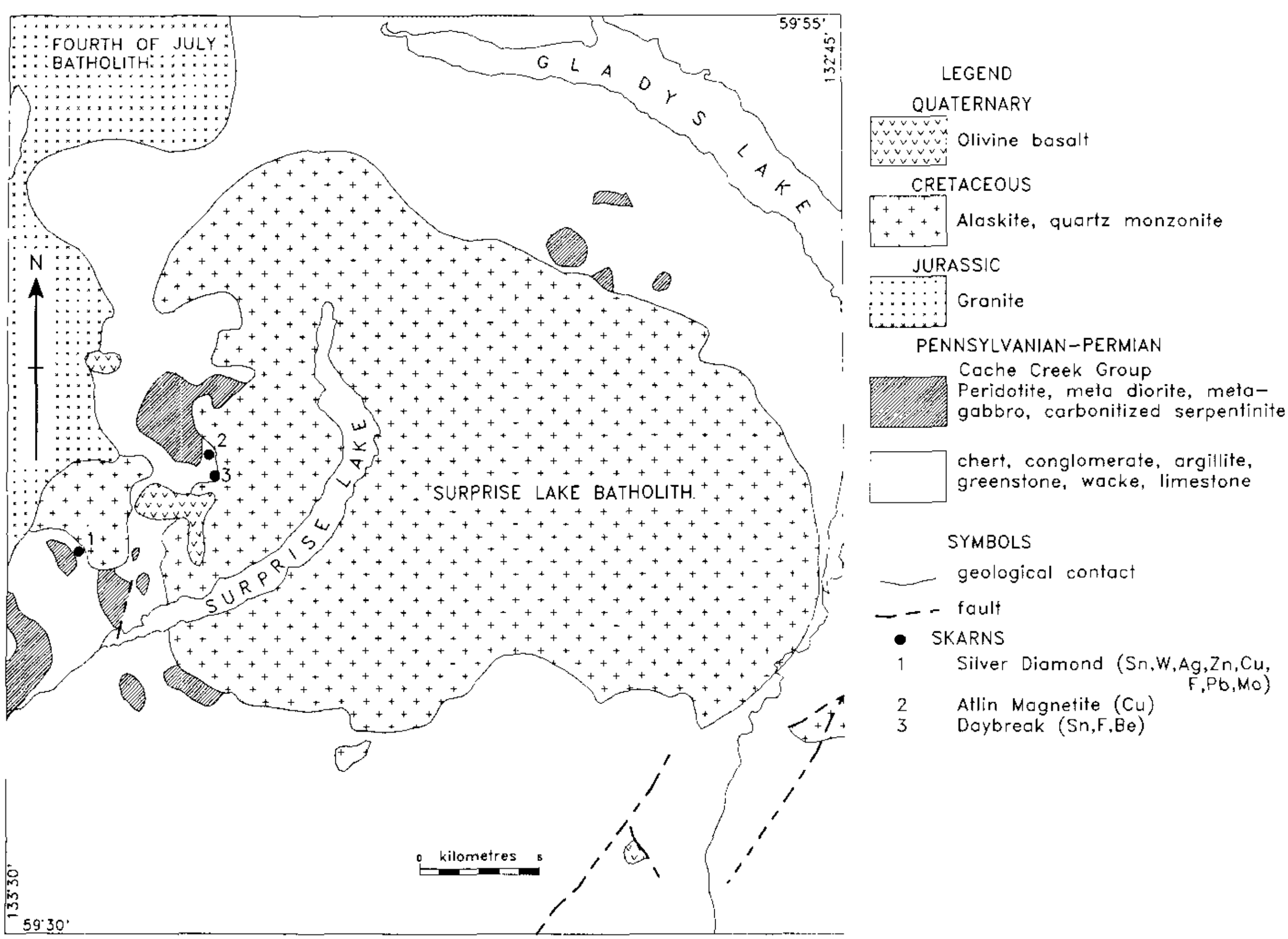

Figure 2-2-3. Geology and location of skarn occurrences associated with the Surprise Lake batholith, Atlin camp (geology after Aitken, 1960).

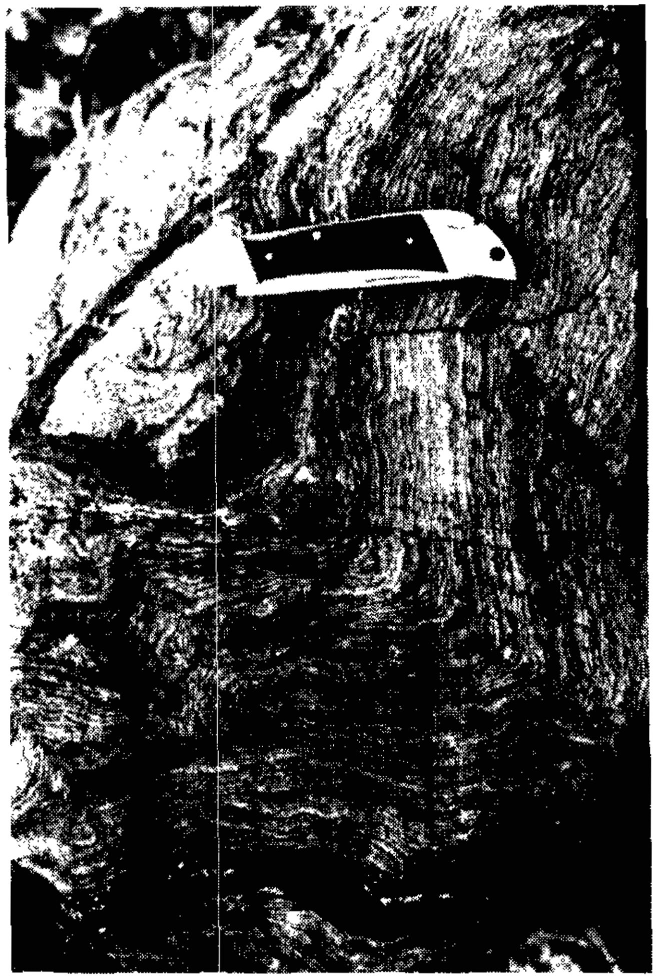

Plate 2-2-1. "Wrigglite" skarn with alternating layers rich in fluorite, magnetite, vesuvianite and grossular garnet. This skarn contains minor cassiterite and gahnite and is geochemically anomalous in beryllium (S.B. Ballantyne, personal communication, 1991). Daybreak tin skarn occurrence, Atlin camp, B.C.

Two types of mineralization are recognized in the camp; each in different hostrock packages, with contrasting mineralogies, and are believed to be of different ages (Dunne and Höy, 1992, this volume; Höy *et al.*, 1992, this volume). The oldest and most economically important deposits are in extensive, steeply dipping pyrrhotite-rich veins that contain gold, silver, arsenic and copper. The veins cut the Rossland Group sediments, volcanics and coeval plutonic rocks that underlie the lower eastern slope of Red Mountain. They were worked in numerous underground mines, mainly between 1890 and 1930, and include the Le Roi, I.X.L., Evening Star and Gertrude veins (Figure 2-2-4). Some of these vein deposits are associated with weak skarn alteration (Wilson *et al.*; 1990, Höy *et al.*, 1992, this volume).

The other major deposit type is younger than the veins and is represented by molybdenum skarns that were mined by open pit, mainly between 1966 and 1972; they include the Coxey, Novelty and the Giant orebodies. These are hosted by the thrust package of siltstones and tuffs belonging to the Mount Roberts Formation and in younger dioritic intrusions (Höy and Andrew, 1991a and b). There are, however, important geochemical differences between these molybdenum skarns; The Coxey orebodies are barren of gold while the Novelty and Giant deposits contain elevated values of gold, cobalt, bismuth, arsenic and nickel (Table 2-2-1a). It is not known if this variation represents a geochemical zoning in the molybdenum skarns, or whether the fluids responsible for the Novelty and Giant mineralization scavenged gold, arsenic and cobalt from the older vein mineralization in the underlying thrust plate.

The Mount Roberts Formation in the Rossland area also contains rare galena-sphalerite veins of unknown age. One narrow quartz vein with pyrite, galena and sphalerite outcropping north of Coxey (Figure 2-2-4) assayed 16 grams per tonne gold (Table 2-2-1a).

Geology of the Red Mountain Area

Early geological work in the Rossland area includes that by Drysdale (1915), Stevenson (1935), White (1949) and Little (1963). More recent publications include those by Little (1982), Fyles (1984), Höy and Andrew (1991a and b) and Höy *et al.*, (1992, this volume).

Two structural packages, separated by the easterly directed Rossland thrust fault (Figure 2-2-4), are recognized on the mountain (Höy and Andrew, 1991a and b). The oldest of these is the Permo-Carboniferous Mount Roberts Formation that comprises thin-bedded siltstones, bedded tuffs, minor volcanics and very rare, thin carbonate units. They form a subhorizontal to gently dipping sequence exposed on the upper part of Red Mountain. Structurally underlying these rocks are alkalic tuffs, volcanics and subvolcanic intrusions of the Early Jurassic Rossland Group.

A variety of intrusive rocks are recognized in the Red Mountain area. The oldest is the Rossland monzonite, an Early Jurassic pluton that is intrusive into and cogenetic with the Rossland Group (Dunne and Höy, 1992, this volume). It is probably genetically related to the gold-bearing sulphide veins and associated gold-skarn envelopes on the mountain, but it has not been mapped in the overlying Mount Roberts Formation. This and an inferred thrust contact between Mount Roberts Formation and Rossland monzonite south of Rossland, suggest a pre-faulting age for the Rossland monzonite.

A subsequent major plutonic event (*ca.* 165 Ma) resulted in the emplacement of the dioritic to monzonitic Rainy Day and Trail plutons. This event resulted in the extensive silicification, skarning and development of hornfels in the Mount Roberts Formation on Red Mountain (Fyles, 1984). A variety of equigranular to porphyritic quartz diorite sills and dikes, that cut both the Mount Roberts and underlying Rossland rocks, are believed to be related to this plutonism. They produced only localized barren garnet-pyroxene-epidote skarn in the lower structural package but resulted in the development of the molybdenum skarn orebodies in the Mount Roberts Formation.

Coxey Mine (Minfile 82FSW110)

The Coxey mine was worked from six open pits that extend from the lower western slopes almost to the summit of Red Mountain (Figure 2-2-4). Skarn alteration of the

Mount Roberts Formation increases towards the upper pits (E and F pits) as does the amount of sulphide mineralization. Here the skarn assemblage comprises veinlets of reddish brown garnet and green pyroxene. At a lower elevation, in pits D and B, garnet is rare but pyroxene and lesser biotite hornfels are abundant. Radiating crystals of actinolite are also locally present.

Mineralization consists primarily of molybdenite with minor scheelite; pyrite, pyrrhotite and chalcopyrite are generally uncommon. Analyses of five mineralized samples indicate enrichment in molybdenum, tungsten and copper, but no anomalous gold (Table 2-2-1a). Molybdenite generally occurs as thin smears, irregular patches and veinlets. In pits A and E, molybdenite is widely distributed in the exoskarn but at a slightly lower elevation, in pits A and uA, some mineralized endoskarn is seen. Molybdenite with pyrrhotite occurs along the margins of, and within, a brecciated dioritic body, particularly in the breccia matrix. The breccia mostly contains rounded to angular clasts of diorite up to 0.5 metre in diameter, many of which have bleached reaction rims. Adjacent to the country rocks however, it contains angular fragments of hornfelsed Mount Roberts Formation. Molybdenite is more abundant in the sedimentary breccia while pyrrhotite dominates in the dioritic breccia.

Molybdenite-rich mineralization is not always associated with pyrrhotite and pyrite, and the genetic relationship between the molybenite and the other sulphides is uncertain. Some pyrrhotite and pyrite are relatively early as they are cut and overgrown by veins of molybdenite. However, a later generation of coarse pyrite veining along late faults postdates the molybdenite.

Novelty (Minfile 82FSW107)

The Novelty open pit is at an elevation of 1370 metres on the south side of Red Mountain and south of the Coxey orebodies (Figure 2-2-4). Mineralization is hosted by thin-bedded and east-dipping metasediments of the Mount Roberts Formation. These are extensively silicified and hornfelsed with lesser amounts of epidote-pyroxene alteration and rare masses of brown, crystalline garnet. A small body of bleached, endoskarn-altered diorite cuts and brecciates the hornfelsed metasediments and the clasts of country rock have marked reaction rims.

Mineralization comprises irregular masses of anhedral arsenopyrite intergrown with minor pyrrhotite, molybdenite, cobaltite and pyrite. Some mineralized boulders are marked by minor chalcopyrite and erythrite staining; Fyles (1984) reports the presence of bismuthinite and uraninite. As well as gold, arsenic, cobalt, molybdenum and bismuth enrichment in the mineralization, geochemical analyses

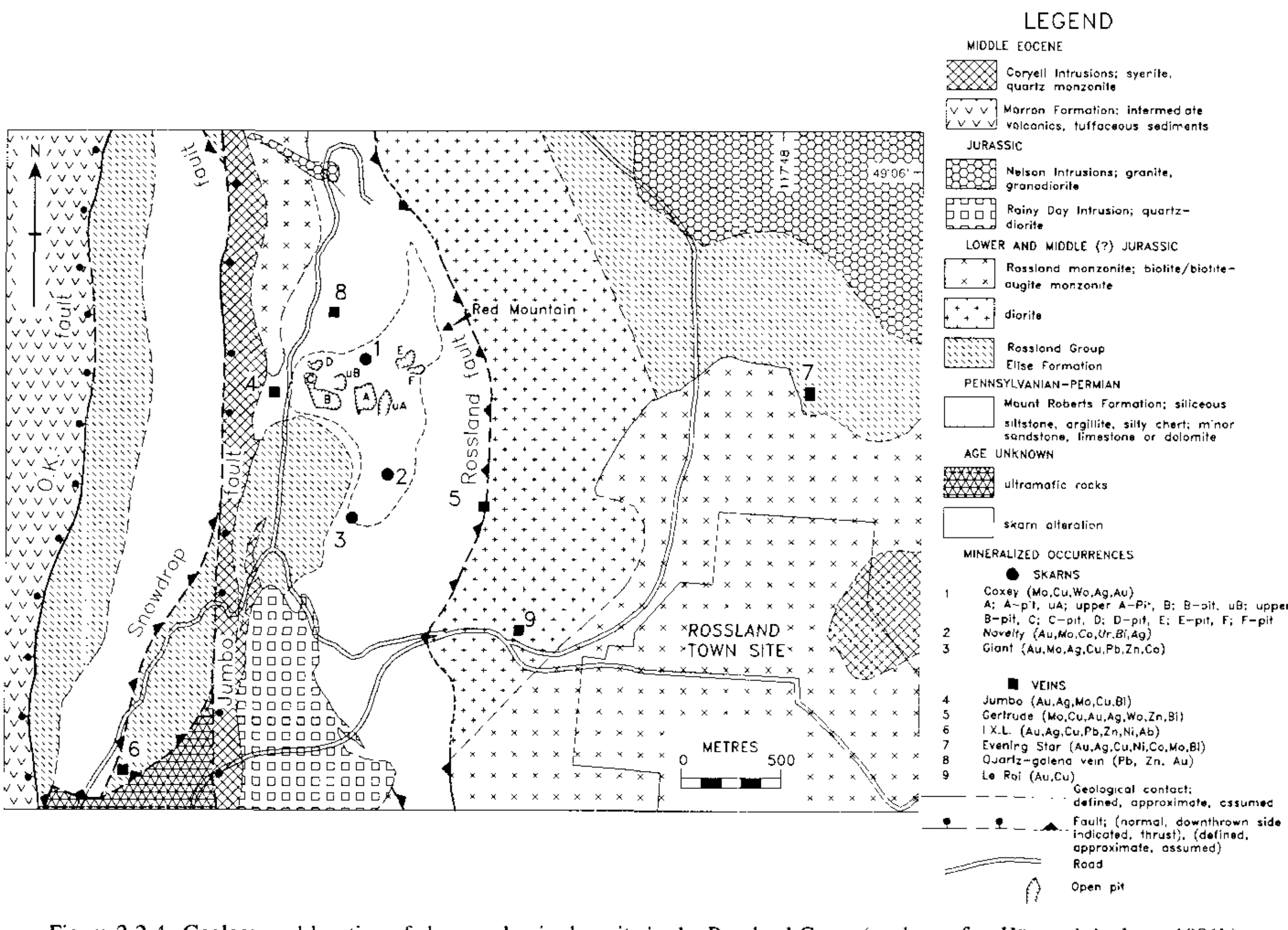

Figure 2-2-4. Geology and location of skarn and vein deposits in the Rossland Camp (geology after Höy and Andrew, 1991b).

indicate anomalous nickel (Table 2-2-1a), suggesting the presence of nickel arsenide minerals.

Giant Mine (Minfile 82FSW109)

The Giant mine, situated southwest of the Novelty deposit, produced copper, silver and gold (Table 2-2-2) from two adits between the years 1898 and 1903. The area is underlain by subhorizontal, thinly bedded, hornfelsed siltstone of the Mount Roberts Formation. No mineralization was seen in outcrop but rocks on the dump at the blocked entrance to the upper adit contain massive arsenopyrite intergrown with coarse molybdenite flakes, minor pyrrhotite and chalcopyrite. Minor garnet and some calcite veining occurs with the sulphides. Pyrrhotite-bearing rocks in the waste dump outside the lower adit contain epidote, lesser pyroxene, rare layers of brown garnet and narrow veins of quartz.

The geochemistry of an arsenopyrite-rich sample from outside the upper adit is similar to that of the Novelty mineralization; it contains anomalous gold, bismuth, cobalt and nickel (Table 2-2-1a).

Second Relief Mine (Minfile 82FSW187)

The Second Relief mine is located 42 kilometres south of Nelson in southeastern British Columbia (Figure 2-2-1). Hostrocks are Early Jurassic Rossland Group rocks close to their contact with Jurassic Nelson granodiorite (Höy and Andrew, 1989). Between 1900 and 1959 the mine produced gold and copper with minor lead, zinc and silver (Table 2-2-2). Mineralization is contained within several parallel northeast-striking, steeply dipping quartz veins that reach up to 4 metres in width. The veins also contain arsenopyrite, pyrite, pyrrhotite, chalcopyrite and magnetite with trace, sphalerite, molybdenum and native gold; minor garnet and epidote is also present.

The veins are surrounded by an extensive envelope of pervasive and siliceous garnet-pyroxene skarn alteration that overprints both the Rossland Group and the porphyritic diorite. The exoskarn also contains pyrrhotite, epidote, amphibole, clinopyroxene, carbonate, biotite and trace tourmaline; microprobe analyses indicate the garnets are iron rich and low in manganese (Ettlinger and Ray, 1989).

It is uncertain whether formation of the mineralized veins at the Second Relief mine was coeval and related to the skarn-altered wallrock. Some samples of sulphide-rich quartz vein contains anomalous gold, arsenic, copper and zinc, but the skarn-altered wallrock has no gold enrichment (Table 2-2-1a).

Emerald Tungsten Camp

The Emerald Tungsten camp, located 22 kilometres south of Salmo in southeastern British Columbia (Figure 2-2-1) is hosted by rocks of ancestral North America. It includes two Paleozoic, stratabound lead-zinc deposits worked at the **Jersey** and **Emerald Lead-Zinc** mines, as well as several Cretaceous tungsten skarn deposits that were worked from the **Emerald Tungsten** (MINFILE 82FSW010), **Feeney** (MINFILE 82FSW247), **Invincible** (MINFILE 82FSW218) and **Dodger** (MINFILE 82FSW011) mines (Figure 2-2-5). Between 1906 and 1972, 7.6 million tonnes of ore were mined from this camp (Table 2-2-2). Production records for the entire camp were grouped and reported as coming from the stratabound Jersey deposit; thus the comparative amount of metals obtained from the younger skarns and older stratabound deposits is uncertain. However, it is a reasonable assumption that no tungsten was derived from the Jersey or Emerald Lead-Zinc mines and none of the tungsten skarns produced any lead, zinc, silver or cadmium.

The geology of the camp is shown in Figure 2-2-5 and has been described by Hedley (1943), Ball *et al.* (1953), Rennie and Smith (1957) and Fyles and Hewlett (1959). Skarn is developed along the margins of the Cretaceous Emerald and Dodger stocks where they intrude the Early Cambrian Laib Formation, particularly along the contact of the Reeves limestone and the Emerald argillite. The stocks comprise a leucocratic, quartz-rich granite containing biotite and lesser muscovite. Close to the skarns they are cut by parallel sets of milky quartz veins up to 8 centimetres wide, as well as by veins of coarse pyrite and extensive patches of quartz-muscovite greisen.

Most of the skarn, which is dominated by garnet, is developed in the sedimentary rocks. The skarn includes both massive and banded varieties; the latter represents remnant bedding consisting of alternating layers rich in red and brown garnet, green pyroxene, quartz and carbonate. Locally, it contains layers of coarse wollastonite. The exoskarn is commonly cut by veinlets of amphibole, and includes minor amounts of epidote, orthoclase, sericite and biotite. Some remnant areas of dark, biotite-rich hornfels-like alteration are cut by pyroxene veinlets.

Three styles of mineralization related to the granitic stocks are identified: quartz veins, sulphide-rich pods and skarns. Some quartz veins cutting the stock are locally enveloped by thin, dark halos of altered feldspar and thicker patches of muscovite-rich greisen. Both the veins and the wallrock alteration contain coarse molybdenite and pyrite. Some quartz veins also contain elongate, dark tourmaline crystals.

Pods, lenses and irregular veins of massive to disseminated sulphide are locally developed within the granite close to its contact with either marble or exoskarn. One pyrrhotite-rich grab sample from a massive pod at the Dodger mine portal assayed anomalous gold, arsenic and tungsten (Table 2-2-1a).

Economic skarn mineralization is dominated by disseminated to irregular masses of scheelite that occur either with disseminated pyrrhotite or in sulphide-lean garnet skarn. Minor amounts of molybdenite were noted as well as rarer wolframite and powellite. Locally, the mineralized skarn is cut by late veinlets of pyrite. Geochemical analyses of a scheelite-bearing skarn sample from Emerald Tungsten adit are presented in Table 2-2-1a.

Queen Victoria Mine (Minfile 82FSW082)

The Queen Victoria copper skarn deposit is located approximately 12 kilometres west of Nelson within rocks of the Quesnel Terrane, (Figure 2-2-1). Intermittent open-pit

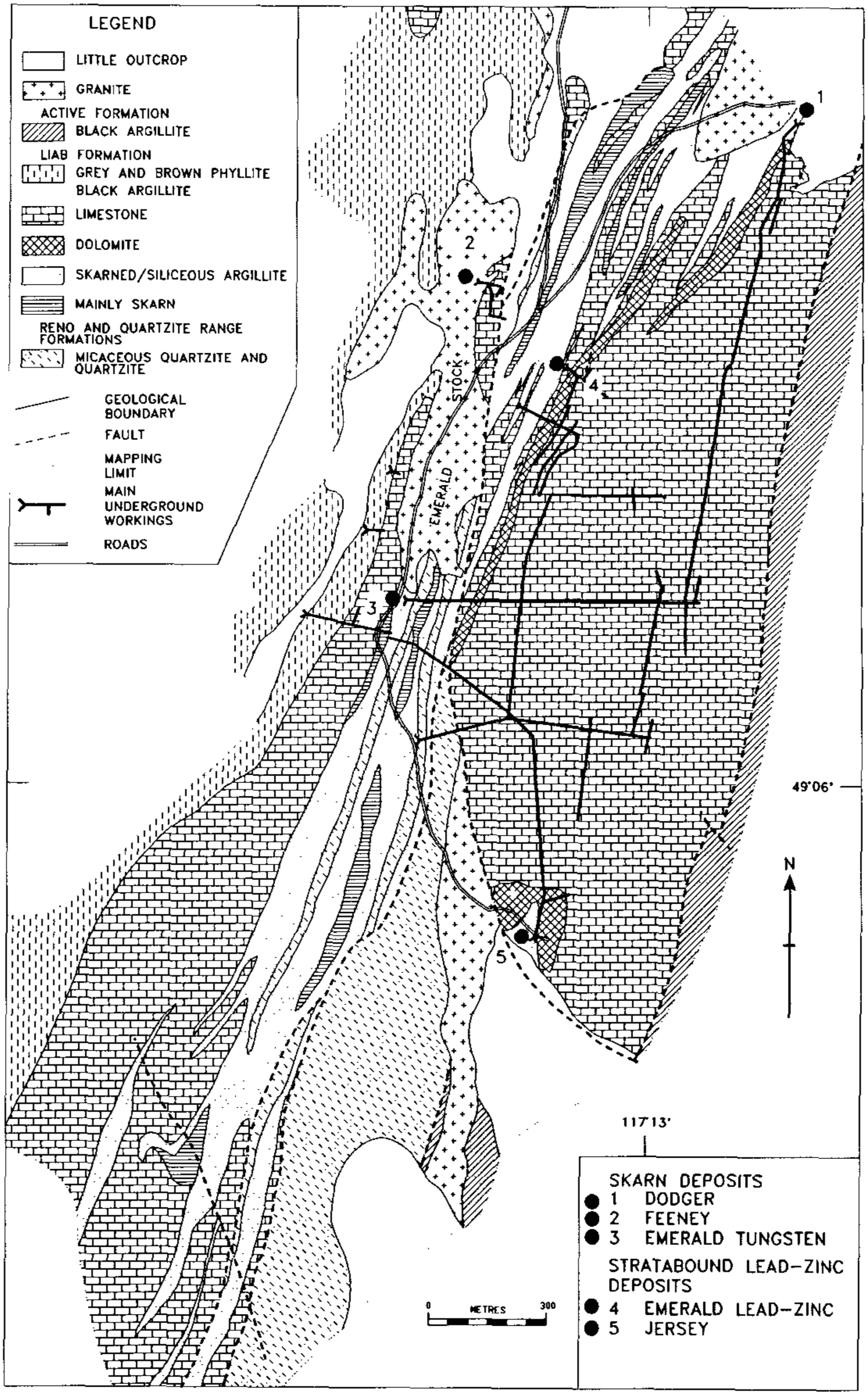

Figure 2-2-5. Geology of the Emerald Tungsten camp showing locations of the skarn deposits (geology after Fyles and Hewlett, 1959).

mining between 1907 and 1956 resulted in the production of copper with minor amounts of silver and gold (Table 2-2-2). The skarn is hosted by Early Jurassic sedimentary rocks of the Ymir Group close to its contact with a quartz diorite to granodiorite intrusion that is probably part of the Jurassic Nelson plutonic suite. Near the mine, this intrusion comprises a hornblende (25-35%) quartz diorite that is moderately bleached and veined with epidote; this body is cut by narrow, altered diorite dikes.

The deposit is hosted by limestone and impure calcareous sedimentary rocks that are interlayered with schistose quartzite and argillite. Most of the alteration appears to represent exoskarn although minor remnants of strongly altered porphyritic endoskarn are present.

The garnet-dominant exoskarn reaches 150 metres in length and 30 metres in width. It consists mainly of massive brown and red garnetite although towards the footwall, there is some subhorizontally layered, siliceous exoskarn, with remnant bedding. The garnetite is cut by several generations of veining. These include early bands and veins of green pyroxene and amphibole up to 10 centimetres wide. Some of these have dark centres containing pyroxene and amphibole and outer, light green margins that x-ray diffraction indicates contain actinolite, albite and microcline (M.Chowdry, personal communication, 1991). The garnetite is also cut by younger veins rich in either yellow-green, crystalline epidote or white quartz. The quartz veins, which reach 10 centimetres in thickness, contain lesser carbonate, crystalline epidote, black amphibole, pyrite and minor chalcopyrite. Locally they are enveloped by magnetite-rich zones that separate the vein from the garnetite host.

Mineralization consists of disseminations, masses and veins of chalcopyrite and pyrite, up to 40 centimetres thick, with minor bornite, magnetite and rare pyrrhotite. The high pyrite:pyrrhotite ratio of the ore suggests the Queen Victoria copper skarn formed in a relatively oxidized environment. Geochemical analyses of mineralized grab samples (Table 2-2-1a) indicate high copper values with a moderate silver but low gold content.

Piedmont Mine (Minfile 82FNW129)

The Piedmont lead-zinc skarn deposit is located 6 kilometres southeast of Slocan in rocks of the Quesnel Terrane, (Figure 2-2-1). Intermittent operations between 1928 and 1959 resulted in the production of minor zinc, lead and silver (Table 2-2-2). The Piedmont was the province's largest zinc-lead skarn producer and production was from underground and open-pit operations.

The mine area is largely underlain by an intrusive body of the Middle to Late Jurassic Nelson plutonic suite. It comprises multiple phases that include older mafic diorites intruded by both equigranular and potassium feldspar megacrystic, biotite hornblende granodiorite and quartz diorite; these form larger bodies as well as sills and dikes that vary from massive to weakly gneissic. Layers, disseminations and lenticular masses of mineralized exoskarn occur close to the contact between the batholith and several pendants of Late Triassic Slocan Group rocks; the latter comprise schistose quartzite, meta-argillite and minor brown marble. The largest mineralized pod, close to the old glory hole, is approximately 20 metres long and up to 3 metres thick (Allen, 1984). It lies adjacent to altered granodiorite dikes that are probably related to the nearby batholith.

The exoskarn is dominated by fine to coarse-grained black sphalerite and lesser galena in a matrix of red, yellow and green garnet, with quartz and patches of coarse calcite. Pyrrhotite generally forms crosscutting veinlets, however, in one adit it occurs intergrown with minor sphalerite in a narrow, massive sulphide zone. Most of the pyrrhotite postdates the sphalerite and galena although one post-pyrrhotite veinlet of coarse sphalerite was observed. Some coarse, euhedral crystals of sphalerite and galena form inclusions in the large calcite blebs. However, locally, the calcite is rimmed and separated from adjacent pyrrhotite by a narrow layer of sphalerite. Geochemical analyses of sulphide-rich grab samples (Table 2-2-1a) indicate high values of zinc, lead, cadmium and silver. The minor enrichment in antimony and copper suggests tetrahedrite may be present in the ore.

Steep Occurrence

The Steep skarn occurrence is located in southeastern British Columbia (Figure 2-2-1) on the west side of Adams Lake approximately 55 kilometres northeast of Kamloops. It is hosted by Paleozoic Sicamous Formation argillaceous limestones and black calcareous phyllites of the Kootenay Terrane (Schiarizza and Preto, 1984, 1987). A concordant zone of skarn alteration, that reaches several hundred metres in width, is traceable for at least 10 kilometres along strike (Ettlinger and Ray, 1989). It is structurally underlain by a strongly foliated unit that contains quartz phenocrysts, fine muscovite and quartz veinlets This unit is at least 500 metres thick and may represent a Devonian orthogneiss that generated the skarn. The orthogneiss contains lenses of less deformed granite.

The skarn assemblage includes garnet, clinopyroxene, epidote and amphibole with lesser biotite, sphene, chlorite, and apatite. Mineralization tends to be close to the outer margins of the skarn zone. It includes pyrrhotite and lesser chalcopyrite with magnetite, sphalerite, galena and trace gold (Miller *et al.*, 1988). The fine gold is associated with minute grains of native bismuth and bismuth tellurides.

Dimac (Silence Lake Mine; Minfile 82M 123)

The Dimac tungsten skarn is located (Figure 2-2-1), 37 kilometres northeast of Clearwater in rocks of the Barkerville Terrane. Minor tungsten production was recorded in 1982 (Table 2-2-2) from a small open-pit mine.

The area is underlain by east-northeast-striking, steeply dipping metasedimentary gneisses and schists of the Shuswap Metamorphic Complex. These amphibolite-facies rocks, which are strongly deformed and isoclinally folded, include some calcsilicate gneisses and thin marbles. The metasediments are cut by a postmetamorphic, Paleocene stock and some sills that vary in composition from granite to quartz monzonite to alaskite. The intrusions comprise a coarse to medium-grained, leucocratic two-mica granite that are generally massive although some sills are weakly foliated. The alaskitic rocks contain irregular segregations of coarse quartz, plagioclase, muscovite and rare biotite, the latter up to 1.5 centimetres in diameter, as well as small patches of greisen. This alteration is associated with quartz-sericite veins, up to 2 centimetres wide, that are bordered by narrow bleached halos.

Texturally, the exoskarn varies from massive to layered, the latter representing the replacement of remnant gneissic layering. At least three types of skarn are developed in calcsilicates adjacent to the intrusions: wollastonite-garnet-carbonate skarn, pyroxene-carbonate-quartz skarn and garnet-idocrase-quartz skarn. Scheelite is generally absent in the wollastonite skarn (White, 1989). Some of the garnet-idocrase skarn is extremely coarse grained and pegmatitic. It is dominated by large euhedral crystals of garnet, up to 7 centimetres across, and brownish green to amber vesuvianite that reaches 15 centimetres in length; these are often set in a matrix of white quartz (Plate 2-2-2). This skarn contains anhedral to subhedral scheelite, up to 1.5 centimetres across, that occurs either as clusters or scattered individual white crystals. Scheelite is also seen as small inclusions in both garnet and vesuvianite.

In outcrop, some of the large garnets are zoned from brown cores, containing small inclusions of quartz, scheelite and rare pyrrhotite, out to red rims that are inclusion free. Garnets are mostly red and brown but some dark brownish green to amber varieties were observed. They seldom form veins but mostly occur as isolated crystals, masses or layers, parallel to the remnant gneissic foliation. Vesuvianite forms massive bands and pods up to 5 centimetres thick, as well as isolated crystals.

The pyroxene-rich skarn varies from banded to massive; it contains small, euhedral hedenbergite crystals, generally in a carbonate matrix, together with variable amounts of scheelite, but garnet and wollastonite are uncommon. The wollastonite-rich skarn is commonly banded, consisting of alternating layers rich in garnet, pyroxene, amphibole and wollastonite. Coarse wollastonite, up to 5 centimetres long, commonly surrounds crystals of pink to red garnet, separating the garnet from carbonate.

Crystal relationships suggest that garnet formed early, followed by vesuvianite and wollastonite. However, some scheelite either predates, or was coeval with garnet as it occurs as inclusions in these crystals. Virtually no suphides were seen in the Dimac deposit apart from pyrrhotite that occurs either as minute, rare inclusions in garnet or as disseminations and veinlets in the quartz-garnet-vesuvianite skarn. A small coating of erythrite was noted on one outcrop and locally the skarn is cut by late veins of quartz and gypsum.

Geochemical analytical results on samples of scheelite-bearing skarn are presented in Table 2-2-1a. In addition, very large garnet and vesuvianite crystals were hand picked from the skarn for trace element analyses. X-ray diffraction analysis (with a detection limit of 15 ppm Sn) indicates that the vesuvianite and garnet contain up to 2106 and 317 ppm tin respectively. However, no anomalous tin values are recorded in the samples of scheelite-bearing skarn.

To summarize, the Dimac tungsten skarn is associated with a two-mica granite, is characterized by scheelite but carries virtually no sulphides except rare pyrrhotite. This suggests it developed in a reduced, low-sulphur system. The extremely coarse grained garnet, vesuvianite and scheelite crystals indicate that the skarn formed at a deep level and crystallized over a considerable length of time.

Cassiar Camp

Several skarns occur in the Cassiar area, north of Cassiar township in northern British Columbia (Figure 2-2-1) where they are hosted by rocks of the Cassiar Terrane; the geology of the area has been described by Panteleyev (1979, 1980) and Nelson and Bradford (1989). They include the **Contact, Dead Goat, Lamb Mountain** and **Kuhn** skarns as well as several unnamed mineralized skarn occurrences (Figure 2-2-6). The Contact and Dead Goat skarns are hosted by the Hadrynian Stelkuz Formation, comprising phyllites, quartzites and limestones, close to its contact with the eastern margin of the Late Cretaceous Cassiar stock. The stock is a coarse-grained, biotite-hornblende granite and quartz monzonite that contains potassium feldspar megacrysts. The

Plate 2-2-2. Coarse, euhedral garnet crystals in a quartz matrix, Dimac (Silence Lake) tungsten mine, Clearwater district, B.C.

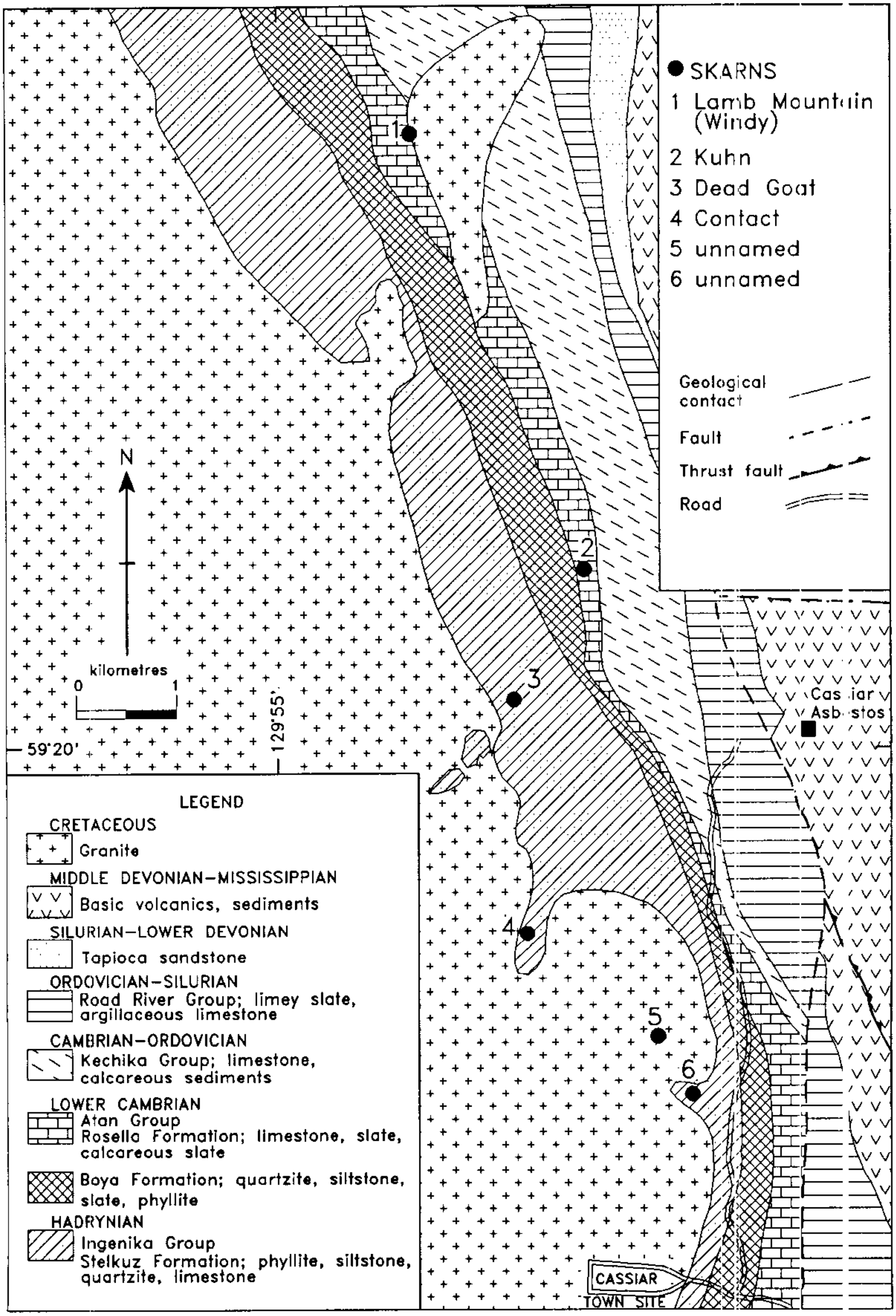

Figure 2-2-6. Geology and location of skarn occurrences in the Cassiar camp (geology after Nelson and Bradford, 1989).

Lamb Mountain and Kuhn skarns also lie close to the Cassiar stock and are hosted by limestone, dolostone and calcareous shale of the Lower Cambrian Rosella Formation (Nelson and Bradford, 1989).

Contact Mine (Telemark; MINFILE 104P 004)

The Contact skarn deposit is located 2 kilometres east of Cassiar asbestos mine (Figure 2-2-6). In 1956 it produced minor amounts of silver, lead and copper (Table 2-2-2). The main ore zone is a steeply dipping massive magnetite body that reaches 2 metres in thickness. This horizon, which is hosted by and concordant to layered marbles, lies approximately 200 metres east-southeast of the contact with the feldspar megacrystic Cassiar stock. Between the stock and the magnetite layer is a zone of layered garnet-pyroxene-biotite exoskarn 150 to 200 metres wide that represents altered, thinly bedded siltstones. This banded skarn contains remnant patches of biotite hornfels cut by veinlets of garnet and pyroxene; it is generally unmineralized except for minor disseminated pyrrhotite and late veins of pyrite.

The magnetite zone apparently formed at the outer margins of the skarn, probably along the contact between the skarn-altered siltstone unit and a limestone. It includes some patches of biotite hornfels and rare, coarse euhedral crystals of dark brown to black garnet. The western, footwall contact is concordant to the banded skarn, but its eastern hanging-wall contact is irregular and locally crosscutting; veinlets of magnetite have been injected into the adjacent marble. The massive magnetite is cut by blebs and veinlets of pyrrhotite, sphalerite, chalcopyrite and galena; galena tends to separate sphalerite from pyrrhotite. There are reports in MINFILE of trace molybdenite, arsenopyrite, tetrahedrite and bismuthinite (McDougall, 1954). Some of the marbles close to the skarn contain veins of rhodonite.

Kuhn (MINFILE 104P 071)

The geology and mineral assemblages of the Kuhn skarn has been described by Cooke and Godwin (1984). The skarn is hosted by a package of hornfelsed and silicified siltstones and argillites with minor coarse white marble; the biotite hornfels is cut by veinlets of pyroxene. The exoskarn assemblage comprises coarse actinolite, garnet and clinopyroxene. The garnets, which include pale or reddish brown, amber and black varieties, are commonly intergrown with actinolite and coarse, euhedral crystals of quartz. No endoskarn was identified.

The actinolite-rich skarn contains abundant disseminated pyrrhotite with minor pyrite, chalcopyrite and veins of coarse molybdenite. Cooke and Godwin (1984) report the presence of scheelite, powellite and fluorite.

Dead Goat (MINFILE 104P 079)

The area is underlain by hornfelsed argillite and some units of grey to white marble. The latter vary from massive and granular to layered and strongly deformed. The marble is associated with large masses of banded garnet-epidote-actinolite-pyroxene skarn up to 1 metre in thickness, that contain small, remnant patches of biotite hornfels. Some garnet crystals are coarse and euhedral and reach 1 centimetre in diameter; they vary in colour from pale brown to amber.

Mineralization includes patches of massive pyrrhotite cut by veins of pyrite. Also present are masses of black sphalerite with minor disseminated scheelite and magnetite. Marble adjacent to the skarn is cut by veinlets of rhodonite.

Lamb Mountain (Windy; MINFILE 104P 003)

This skarn is hosted by marbles and hornfelsed argillites close to the western margin of a small body of feldspar megacrystic quartz monzonite that represents a satellite intrusion of the Cassiar stock (Figure 2-2-6). Adjacent to the intrusion, the hornfels contains cordierite and is cut by irregular veinlets of pyroxene.

Two types of exoskarn are seen. One is dominated by very coarse actinolite that forms crystals up to 3 centimetres long. This actinolite skarn, which is developed immediately adjacent to the intrusion, contains minor epidote and clots of coarse calcite. The other type is a generally thin-banded garnet-pyroxene-epidote-quartz skarn, although some of the massive garnet bands exceed 1 metre in thickness. Garnet forms euhedral pale red, dark brown and amber-coloured crystals up to 1 centimetre in diameter. This skarn also contains some white elongate crystals, up to 2.5 centimetres, that x-ray studies indicate to be the scapolite mineral meionite (M. Chowdry, personal communication, 1992).

Mineralization in the exoskarn includes disseminated pyrrhotite, molybdenite, scheelite and rare chalcopyrite. The quartz monzonite immediately adjacent to the skarn is silicified and contain minor amounts of disseminated pyrrhotite.

Unnamed Skarns (Nos. 5 and 6, Figure 2-2-6)

Two unnamed skarns, marked by rusty weathering outcrops, are exposed north of Cassiar township (Figure 2-2-6) at elevations of 1740 and 1430 metres. It is uncertain whether the most northerly of the two skarns is hosted by the Cassiar stock or an altered metasedimentary screen within the intrusion. It contains actinolite and clinopyroxene with pyrrhotite and traces of fine molybdenite.

The other skarn farther south is hosted in calcareous metasediments close to the stock. It contains coarse subhedral reddish brown garnet, pyroxene, quartz and carbonate, with minor disseminated pyrrhotite. Geochemical analyses of samples from these two skarn show no evidence of gold, copper or tungsten mineralization (Table 2-2-1a).

ACKNOWLEDGMENTS

This project has benefited from stimulating discussions with Dan Wehrle, Vangold Resources Inc.; Ken Daughtry, Discovery Consultants; Jaroslav Jakubec, Cassiar Mining Corporation; William Wallace, prospector, Atlin; Bruce

Ballantyne, Geological Survey of Canada; Trygve Höy, Neil Church, Rick Meyers, Andre Panteleyev and Dani Alldrick, British Columbia Geological Survey Branch. The manuscript has benefitted from the editorial comments of John Newell. Thanks are expressed to Ray Lett and the staff of the Ministry Analytical Sciences Laboratory for timely results.

REFERENCES

Aitken, J.D. (1960): Atlin; *Geological Survey of Canada*, Map 1082A to accompany Memoir 307.

Alldrick, D.J. (in preparation): Geology and Metallogeny of the Stewart Mining Camp; *B.C. Ministry of Energy, Mines and Petroleum Resources*, Bulletin.

Allen, D.G. (1984): Geological Report on the Hope Prospect; for Chapleau Resources Ltd., *B.C. Ministry of Energy, Mines and Petroleum Resources*, Assesment Report 12980.

Askins, P.W. (1976): "Wrigglite" – An Unusual Fluorite-bearing Skarn, Mt. Garnet Region, North Queensland, Australia; unpublished M.Sc. thesis, *James Cook University*, 185 pages.

Ball, C.W., Wishaw, Q.C. and Mylrea, F.H. (1953): The Lead-Zinc and Tungsten Properties of Canadian Exploration Limited, Salmo, B.C.; *Canadian Institute of Mining and Metallurgy*, Transactions, Volume LVI, pages 241-242.

Campbell, R.B. (1983): Geology of the Tatshenshini River Map Area (114P); *Geological Survey of Canada*, Open File 926.

Church, B.N. and Pettipas, A.R. (1989): Research and Exploration in the Bridge River Mining Camp; *in* Geological Fieldwork 1988, *B.C. Ministry of Energy, Mines and Petroleum Resources*, Paper 1989-1, pages 105-114.

Cooke, B.J. and Godwin, C.I. (1984): Geology, Mineral Equlibria, and Isotopic Studies of the McDame Tungsten Skarn Prospect, North-central British Columbia; *Economic Geology*, Volume 79, Number 5, pages 826-847.

Drysdale, C.W. (1915): Geology and Ore Deposits of Rossland, British Columbia; *Geological Survey of Canada*, Memoir 77.

Dunne, K.P.E. and Höy, T. (1992): Petrology of Pre to Syntectonic Lower and Middle Jurassic Intrusions in the Rossland Group, Southeastern British Columbia (82F/SW); *in* Geological Fieldwork 1991, Grant, B. and Newell, J.M., Editors, *B.C. Ministry of Energy, Mines and Petroleum Resources*, Paper 1992-1, this volume.

Ettlinger, A.D. and Ray, G.E. (1989): Precious Metal Enriched Skarns in British Columbia: An Overview and Geological Study; *B.C. Ministry of Energy, Mines and Petroleum Resources*, Paper 1989-3.

Fyles, J.T. and Hewlett, C.G. (1959): Stratigraphy and Structure of Salmo Lead-Zinc Area; *B.C. Ministry of Energy, Mines and Petroleum Resources*, Bulletin 41.

Fyles, J.T. (1984): Geological Setting of the Rossland Mining Camp; *B.C. Ministry of Energy, Mines and Petroleum Resources*, Bulletin 74.

Grove, E.W. (1971): Geology and Mineral Deposits of the Stewart Area, British Columbia; *B.C. Ministry of Energy, Mines and Petroleum Resources* Bulletin 58, 219 pages.

Grove, E.W. (1986): Geology and Mineral Deposits of the Unuk River - Salmon River - Anyox Area; *B.C. Ministry of of Energy, Mines and Petroleum Resources*, Bulletin 63.

Hedley, M.S. (1943): Tungsten Deposits of British Columbia; *B.C. Ministry of Energy, Mines and Petroleum Resources*, Bulletin 10 (Revised), pages 35-148.

Höy, T. and Andrew, K.P.E. (1989): The Rossland Group, Nelson Map Area, Southeastern British Columbia (82F/6); *in* Geological Fieldwork 1988, *B.C. Ministry of Energy, Mines and Petroleum Resources*, Paper 1989-1, pages 33-43.

Höy, T. and Andrew, K.P.E. (1991a): Geology of the Rossland Area, Southeastern British Columbia, 82F/4E; *in* Geological Fieldwork 1990, *B.C. Ministry of Energy, Mines and Petroleum Resources*, Paper 1991-1, pages 21-31.

Höy, T. and Andrew, K.P.E. (1991b): Geology of the Rossland - Trail Area, Southeastern British Columbia; *B.C. Ministry of Energy, Mines and Petroleum Resources*, Open File 1991-2.

Höy, T., Dunne, K.P.E. and Wehrle, D. (1992) Tectonic and Stratigraphic Controls of the Gold-Copper Mineralization in the Rossland Camp, Southern British Columbia; *in* Geological Fieldwork 1991, Grant, B and Newell, J.M., Editors, *B.C. Ministry of Energy, Mines and Petroleum Resources*, Paper 1992-1, this volume.

Hudson, W.W. (1927): Report on the Maid of Erin, Elise, Victoria, War Eagle and Windsor Claims in the Rainy Hollow Area; *B.C. Ministry of Energy, Mines and Petroleum Resources*, Property File, 11 pages.

Johnson, A.E. (1973): Mineralogical and Textural Study of the Copper-Iron Deposits of the Craigmont Mines Ltd., South-central British Columbia; *B.C Ministry of Energy, Mines and Petroleum Resources*, Information Circular IC 303.

Kwak, T.A.P. (1987): W-Sn Skarn Deposit and Related Metamorphic Skarns and Granitoids; *in* Developments in Economic Geology, Volume 24; *Elsevier Publishing*, 450 pages.

Kwak, T.A.P. and Askins, P.W. (1981): The Nomenclature of Carbonate Replacement Deposits, with Emphasis on Sn-F (Be-Zn) "Wrigglite" Skarns; *Geological Society of Australia*, Volume 28, pages 123-136

Little, H.W. (1963): Rossland Map-area, British Columbia; *Geological Survey of Canada*, Paper 63-13 (Map 23-1963).

Little H.W. (1982): Geology of the Rossland-Trail Map-area, British Columbia; *Geological Survey of Canada*, Paper 79-26.

McConnell, R.G. (1913): Rainy Hollow Mineral Area, B.C.; *Geological Survey of Canada*, Summary Report, Sessional Paper No. 26, pages 29-33.

McDougall, J.J. (1954): The Telescoped Silver-Lead-Zinc Deposits of the Contact Group Mineral Claims, McDame Map Area, British Columbia; unpublished M.Sc. thesis, *The University of British Columbia*.

McMillan, W.J. (1976): Geology and Genesis of the Highland Valley Ore Deposits and the Guichon Creek Batholith; *in* Porphyry Deposits of the Canadian Cordillera, Sutherland-Brown, A., Editor, *Canadian Institute of Mining and Metallurgy*, Special Volume 15, pages 85-104.

McMillan, W.J. (1978): Geology of the Guichon Creek Batholith; *B.C. Ministry of Energy, Mines and Petroleum Resources*, Preliminary Map 30.

Miller, D.C., Wynne, F.L. and Daughtry, K.L. (1988): Report on the Geology and Mineralogy of the Steep Gold-skarn Property; *National Resources Exploration Ltd.*, unpublished report.

Moore, J.M. and Pettipas, A.R. (1990): Geology of the Swakum Mountain Area, Southern Intermontane Belt; *in* Geological Fieldwork 1989, *B.C. Ministry of Energy, Mines and Petroleum Resources*, Paper 1990-1, pages 73-82.

Morrison, G.W. (1980): Stratigraphic Control of Cu-Fe Skarn Ore Distribution and Genesis at Craigmont, British Columbia; *Canadian Mining and Metallurgical Bulletin*, August 1980.

Myers, G.L. (1990): Alteration Zonation of the Fortitude Gold Skarn Deposit, Lander County, NV; *Mining Engineering*, April 1990, pages 360-368.

Nelson, J.L. and Bradford, J.A. (1989): Geology and Mineral Deposits of the Cassiar and McDame Map Areas, British Columbia (104P/3, 5); *B.C. Ministry of Energy, Mines and Petroleum Resources*, Geological Fieldwork 1988; Paper 1989-1, pages 323-338.

Panteleyev, A. (1979): Cassiar Map-area (104/P); *in* Geological Fieldwork 1978, *B.C. Ministry of Energy, Mines and Petroleum Resources*, Paper 1979-1, pages 51-60.

Panteleyev, A. (1980): Cassiar Map-area; *in* Geological Fieldwork 1979, *B.C. Ministry of Energy, Mines and Petroleum Resources*, Paper 1980-1, pages 80-81.

Ray, G.E. and Dawson G.L. (in preparation): Geology of the Nickel Plate–Hedley Area; *B.C. Ministry of Energy, Mines and Petroleum Resources*, Bulletin.

Ray G.E. and Webster I.C.L. (1991): Geology and Mineral Occurrences of the Merry Widow Skarn Camp; *B.C. Ministry of Energy, Mines and Petroleum Resources*, Open File 1991-8.

Ray, G.E. and Webster, I.C.L. (in preparation): Mineralized Skarns in British Columbia; *B.C. Ministry of Energy, Mines and Petroleum Resources*, Bulletin.

Ray, G.E., Dawson, G.L. and Simpson, R. (1988): Geology, Geochemistry and Metallogenic Zoning in the Hedley Gold-skarn Camp; *in* Geological Fieldwork 1987, *B.C. Ministry of Energy, Mines and Petroleum Resources*, Paper 1988-1, pages 59-80.

Ray, G.E., Jaramillo, V.A. and Ettlinger, A.D. (1991): The McLymont Northwest Zone, Northwest British Columbia: A Gold-rich Retrograde Skarn? (104B); *in* Geological Fieldwork 1990, *B.C. Ministry of Energy, Mines and Petroleum Resources*, Paper 1991-1, pages 255-262.

Rennie, C.C. (1962): Copper Deposits in the Nicola Rocks, Craigmont Mine; *Western Miner and Oil Review*, February, 1962, pages 50-52.

Rennie, C.C. and Smith, T.S. (1957): Lead-Zinc and Tungsten Orebodies of Canadian Exploration Limited, Salmo B.C.; *Canadian Institute of Mining and Metallurgy*, Structural Geology of Canadian Ore Deposits, Volume II, pages 116-124.

Schiarizza, P. and Preto, V.A. (1984): Geology of the Adams Plateau–Clearwater Area; *B.C. Ministry of Energy, Mines and Petroleum Resources*, Preliminary Map 56.

Schiarizza, P. and Preto, V.A. (1987): Geology of the Adams Plateau–Clearwater–Vavenby Area; *B.C. Ministry of Energy, Mines and Petroleum Resources*, Paper 1987-2.

Stevenson, J.S. (1935): Rossland Camp; *B.C. Ministry of Energy, Mines and Petroleum Resources*, Annual Report 1935, pages E4-E11.

Watson, K.DeP. (1948): The Squaw Creek–Rainy Hollow Area, Northern British Columbia; *B.C. Ministry of Energy, Mines and Petroleum Resources*, Bulletin 25.

Webster, I.C.L. and Ray, G.E. (1991): Skarns in the Iskut River–Scud River Region, Northwest British Columbia; *in* Geological Fieldwork 1990, *B.C. Ministry of Energy, Mines and Petroleum Resources*, Paper 1991-1, pages 245-253.

White, W.H. (1949): Rossland South Belt; *B.C. Ministry of Energy, Mines and Petroleum Resources*, Annual Report 1949, pages 150-163.

White, G. (1989): Wollastonite Occurrences in British Columbia; *in* Geological Fieldwork 1988, *B.C. Ministry of Energy, Mines and Petroleum Resources*, Paper 1989-1, pages 483-496.

Wilson, G.C., Rucklidge, J.C. and Kilius, L.R. (1990): Sulfide Gold Content of Skarn Mineralization at Rossland, British Columbia; *Economic Geology*, Volume 85, pages 1252-1239.

Wotruba, P.R., Benson, R.G. and Schmidt, K.W. (1988): Geology of the Fortitude Gold-Silver Skarn Deposit, Copper Canyon, Lander County, Nevada; *in* Bulk Mineable Precious Metal Deposits of the Western United States; Schafer R.W., Cooper J.J. and Vikre P.G., Editors, Symposium Proceedings, *Geological Society of Nevada*, pages 159-171.

British Columbia Geological Survey
Geological Fieldwork 1991

TOWARDS A DEPOSIT MODEL FOR OPHIOLITE RELATED MESOTHERMAL GOLD IN BRITISH COLUMBIA

By C.H. Ash, R.W.J. Macdonald and R.L. Arksey

KEYWORDS: Economic geology, lode gold, listwanite, mesothermal veins, ophiolite, obduction, felsic magmatism.

INTRODUCTION

The Listwanite Project was initiated in 1989 to develop a regional metallogenic deposit model for mesothermal gold veins associated with ophiolitic ultramafic rocks in oceanic terranes throughout British Columbia. To date, investigations have been conducted in six lode-gold or related placer camps throughout the province. These include the: Atlin, Stuart–Pinchi Lakes, Bralorne, Cassiar (Erickson), Rossland and Greenwood areas (Figure 2-3-1). Most of the fieldwork has focused on the geology and potential source of gold placers in the Atlin camp (Ash and Arksey, 1990a, c). Results of this work, describing the origin and tectonic setting of the ophiolitic rocks and related gold mineralization will appear separately (Ash, in preparation).

This report summarizes the present understanding of the ophiolite–lode-gold association in British Columbia. It reviews the resource potential of this deposit type, the scientific approach taken and the current stage of development of the evolving deposit model. Detailed results will appear in an upcoming publication (Ash *et al.*, in preparation). An introduction to the listwanite–lode-gold association and a description of the deposit type have been given previously (Ash and Arksey, 1990b).

LISTWANITE – LODE GOLD RELATED DEPOSITS

Listwanite is a term applied to an alteration assemblage generated by carbon dioxide metasomatism of serpentinized ultramafic rocks. This alteration type is not only associated with most of the major mesothermal vein deposits in British Columbia (Figures 2-3-2 and 3), but also with many major mesothermal vein deposits in Phanerozoic and Archean gold camps worldwide. This relationship appears to be due primarily to similarities in tectonic history and involves using ultramafic and related plutonic rocks to delineate major structural breaks which act as a "first order control" for the development of mesothermal gold deposits (Groves, 1990).

The term listwanite has not been formally defined. It is loosely characterized as "a carbonatized ultramafic rock" (Buisson and Leblanc, 1986). The process of listwanitization produces a varying sequence of alteration products caused by differences in the intensity of alteration. A listwanite, therefore, consists of an alteration suite with the individual units of the suite best described in terms of their mineralogy. This suite commonly includes, in order of increasing intensity of alteration: talc-altered serpentinite; talc-carbonate; quartz-talc-carbonate; quartz-carbonate-mariposite and quartz-carbonate-mariposite-sulphides ± gold.

ECONOMIC SIGNIFICANCE

The economic significance of this deposit type in British Columbia is demonstrated by historic gold production (Schroeter *et al.*, 1989). Of the six gold camps producing more than 1 million ounces of gold (Figure 2-3-2), which together account for approximately 80 per cent of the gold produced in the province, three are mesothermal vein camps with a clear ophiolitic association. Five of the ten largest mesothermal vein deposits (Figure 2-3-3) have a currently defined ophiolitic association. Added economic significance for this deposit type lies in the fact that the majority of placer gold camps in British Columbia are closely associated with accreted oceanic terranes (Hodgson *et al.*, 1982).

APPROACH

Development of a deposit model has followed two main avenues of investigation:

(1) The lithotectonic setting of lode-gold deposits and associated ophiolitic rocks; and,

(2) The timing of lode-gold deposition relative to the tectonic and plutonic history of the host terrane.

These topics are addressed by combining regional reconnaissance and detailed geological mapping and, at specific properties, core logging and trench mapping was used to compliment surface data.

The existing geochronological database in areas of interest is being supplemented by additional radiometric dating in order to define the timing of plutonism and mineralization. Combined K-Ar and U-Pb isotopic dating techniques are being used to constrain the age of plutonic episodes thought to be associated with listwanitic alteration and gold mineralization. Where available, mariposite (fuchsite), a green chrome-bearing muscovite (phengite) commonly associated with carbonatized ultramafic rock, is being dated by Ar-Ar or K-Ar methods to obtain apparent mineralization ages.

In listwanites, the existence of a variety of green minerals other than, or in addition to mariposite, necessitates detailed mineralogical studies. Hand-picked concentrates are being studied optically and analyzed by x-ray diffraction for mineral identification and by inductively coupled plasma techniques for major and minor element content.

The potential for platinum group element (PGE) mineralization within this style of deposit is also being crudely assessed. A number of sulphide-rich samples from the various camps studied have, or are being analyzed to test for anomalous PGE concentrations.

REGIONAL GEOLOGICAL SETTING

All six areas investigated (Figure 2-3-1.) are either within accreted oceanic terranes or, as in the case of Rossland,

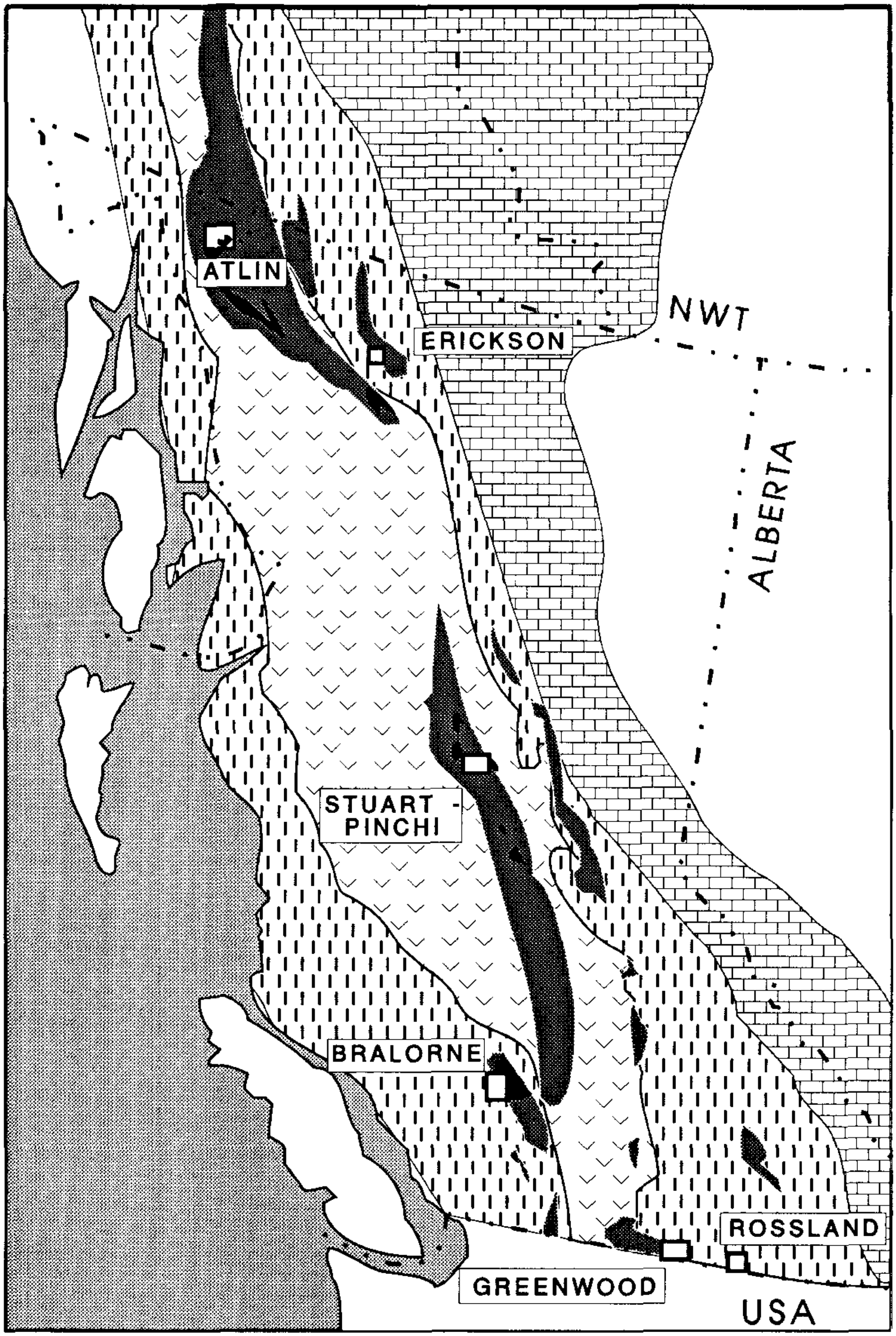

Figure 2-3-1. Study areas of the Listwanite Project in British Columbia.

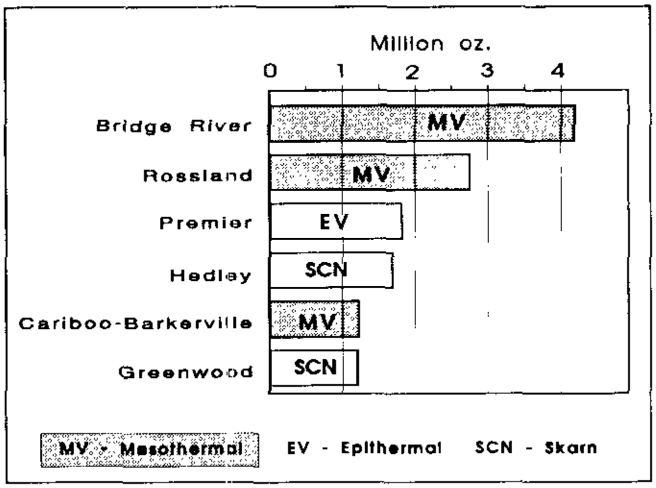

Figure 2-3-2. Top six gold-producing mines in British Columbia (data from Schroeter *et al.*, 1989).

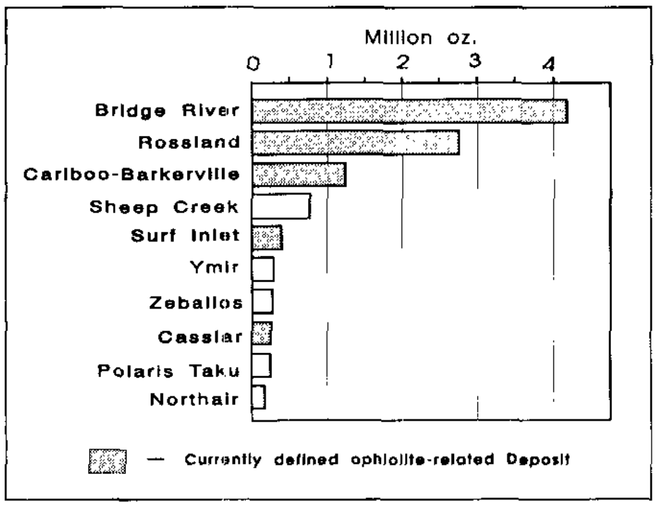

Figure 2-3-3. Top ten past-producing mesothermal gold vein deposits in British Columbia (data from Schroeter *et al.*, 1989).

overlie ophiolitic tectonic slivers along an accretionary structure (Rossland break; Fyles, 1984). Three of the camps are underlain by the Cache Creek Terrane and three by the Slide Mountain Terrane. The Cache Creek Terrane is a composite oceanic terrane which includes two distinctive elements; subduction-related accretionary complexes developed during the destruction of late Paleozoic to early Mesozoic oceanic crust (Monger *et al.*, 1982; Monger, 1984; Coney, 1989: Gabrielse and Yorath, 1989), and dismembered ophiolitic complexes emplaced by obduction of oceanic crust and upper mantle during final closure of the oceanic basin during collision.

Lithologically chaotic and tectonically mixed mélanges (Raymond, 1984) are a third important element of the Cache Creek Terrane and are imbricated with elements of both the accretionary and ophiolitic complexes. Mélanges are mappable on outcrop to regional scales throughout the terrane, and are interpreted as lithotectonic units intrinsic to both subduction and accretionary processes. In this regard, references to the Cache Creek as "a Tethyan-bearing mélange-like terrane" (Coney, 1989), or an "ophiolitic mélange" (Oldow *et al.*, 1989) truly reflect the large and small-scale lithological and structural complexities of the terrane as a whole.

The Slide Mountain Terrane is made up of allochthonous, dismembered, commonly imbricated, Devonian to Permian ophiolitic slices transported across a former continental margin during early Mesozoic time. Lithotectonic relationships common throughout the terrane (Nelson and Bradford, 1989; Klepacki and Wheeler, 1985) indicate classic inverted ophiolite stratigraphies (Gealey, 1980) resulting from the structural stacking of fault-bounded sections of dismembered oceanic crust and upper mantle during obduction. In comparison to the Cache Creek Terrane, the Slide Mountain Terrane has a conspicuous lack of subduction-related accretionary complexes.

DEPOSIT SETTING

Gold deposits investigated in each area are hosted by structures within or marginal to ophiolitic crustal and/or mantle lithologies. Having formed at oceanic crustal depths of 6 to 12 kilometres, the present tectonic setting of these lithologies suggests the presence of deep, through-going crustal structures along which reverse movement must have occurred. These structures, most likely active during collision and ophiolite obduction, are necessary to account for such significant vertical displacements.

All listwanite protoliths investigated are ophiolitic, upper mantle metamorphic harzburgite or crustal plutonic dunitic to wehrlitic ultramafic cumulates. These ultramafic rocks are commonly found in fault contact with mafic plutonic and volcanic members of a classic, dismembered ophiolitic suite (Anonymous, 1972; Coleman, 1977). These crustal rocks appear to be significant, as they provide competent lithologies suitable for the development of dilational fractures during the ore deposition process.

In most of the camps studied there is a spatial and apparent temporal association between mineralization and syn- to primarily post-accretionary felsic magmatism. The Erickson camp near Cassiar may be an exception, although a thermal metamorphic halo of appropriate age suggests that such an intrusion may be present at depth (Nelson, 1990). Felsic intrusive rocks are predominantly granodiorite; however, some compositional variability is evident as diorite and monzodiorite are also identified. Intrusions and magma injection are structurally controlled, a feature which is, in general, most evident at the deposit scale. Most appear to immediately postdate the main phase of accretionary deformation and intrude all oceanic lithologies. However, in the Rossland area the intrusion associated with mineralization, the Rossland monzonite, may predate collisional tectonism (Höy *et al.*, 1992, this volume).

In terms of tectonic setting and history, the most comprehensive picture to date has been developed for the Atlin area (Figure 2-3-4). Lode-gold mineralization throughout the camp is hosted by structures either within or marginal to a relatively flat-lying, dismembered and imbricated ophiolite complex. This complex overlies with marked

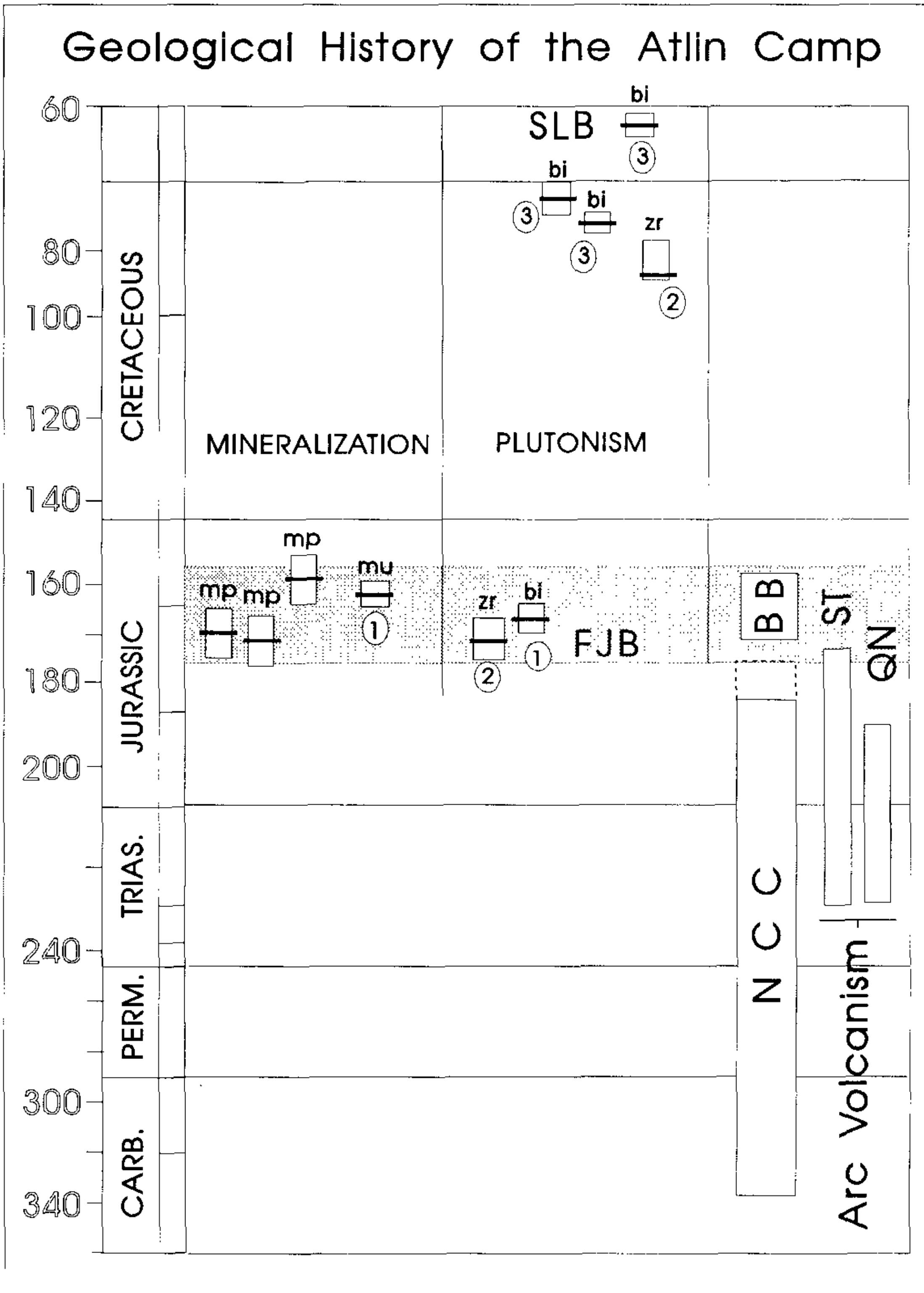

Figure 2-3-4. Geological history of the Atlin area.

FJB – Fourth of July batholith	BB – Bowser Basin	mp – mariposite/fuchsite	mu – muscovite
NCC – Northern Cache Creek	ST – Stikinia	zr – zircon	bi – biotite
SLB – Surprise Lake batholith	QN – Quesnellia		

References: 1 – Dawson (1988)
2 – Mihalynuk *et al.* (in preparation)
3 – Christopher and Pinsent (1979)

structural discordance, a lithologically variable, imbricated package of oceanic metasedimentary and metavolcanic rocks, interpreted to represent a remnant subduction accretionary complex (Ash, in preparation).

In Atlin, the timing of lode-gold mineralization, as inferred from mariposite radiometric ages (Figure 2-3-4), clearly reflects both the timing of oceanic closure and ophiolitic obduction as evidenced by: the ending of both oceanic crustal formation (Monger, 1984; Cordey, 1990) and arc volcanism (Tipper, 1984); and the shedding of oceanic material into the Bowser Basin (Monger, 1984). Felsic magmatism is spatially and temporally related to mineralization and tectonism. Throughout the camp most areas of listwanitic alteration with anomalous gold values are in close proximity or immediately adjacent to a felsic dike or stock.

Limited trace and rare-earth element chemistry from the Fourth of July batholith is consistent with intrusions found in a syn-collisional tectonic environment. Rubidium-strontium isotopic data for this suspected syn-collisional pluton (Mihalynuk *et al.*, in preparation.) indicates a primitive origin and supports partial melting of a stacked and hydrated oceanic crustal package as a possible source.

In both the Bralorne (Leitch, 1990) and Rossland camps (Höy *et al.*, 1992, this volume) gold deposits are spatially related to structurally controlled felsic intrusions which are contemporaneous with mineralization.

PRELIMINARY DEPOSIT MODEL

Lode-gold deposits within or marginal to ophiolitic terranes in British Columbia appear to be generated during and immediately following the period of oceanic accretion. They are hosted by accretionary structures and are spatially associated with both oceanic crust and mantle lithologies. Hostrocks are cut by syn-collisional felsic intrusions generated during the accretionary episodes. This model invokes leaching of gold from a tectonically thickened package of oceanic crustal rocks which is undergoing partial melting at deeper levels, producing the contemporaneous intrusion (Figure 2-3-5).

The structural configuration of the accreted package controls the geometry of the felsic intrusive rocks. Fluids are thermally driven by the heat of intrusion and are possibly supplemented by volatiles released from the intrusions. These fluids leach metals from the thickened oceanic package. Metals are then precipitated as the fluids move away from the magmatic heat source along pre-existing structures bounding and within the accreted ophiolite package.

EXPLORATION GUIDELINES

Systematic surface mapping that focuses on both the tectonic setting and the spatial distribution of the listwanitic alteration suite is extremely useful. The distinctive listwanite alteration assemblage occurs in linear arrays reflecting the structural control on the mineralizing system. Both alteration mineralogy and intensity vary systematically away from the controlling structure. The locus of significant mineralization is typically associated with silicified zones (veins or stockworks) at the core of the structural zone or in its related splays.

When evaluating the tectonic setting of the deposit type, it is critical to distinguish pre-accretionary, allochthonous, ophiolitic mantle and metamorphic or crustal plutonic rocks from those plutonic rocks which are syn to post-collisional and intrude the accreted oceanic package. Many reports and maps continue to interpret ophiolitic plutonic and metamorphic rocks throughout British Columbia as intrusions rather than fault-bounded tectonic slivers of oceanic crust and mantle. The most significant temporal relationship between the ophiolitic rocks and mineralization is that the tectonic emplacement of ophiolites by obduction generally occurs just prior to the mineralizing event. A classic example is the "Bralorne diorite" or "Bralorne intrusion" which hosted the largest lode-gold deposit in the Canadian Cordillera. This unit is the mafic plutonic portion of an obducted, dismembered ophiolitic assemblage, formed as part of the ocean crust and subsequently tectonically transported to its present position. It was not intruded into its present position as its name implies.

DISCUSSION

These preliminary results are consistent with current models for the development of mesothermal vein deposits in Archean greenstone belts (Barley *et al.*, 1989; Kerrich, 1989; Kerrich and Wyman, 1990) which promote vein development in association with periods of deformation, metamorphism and plutonism during terrane collision.

Current interpretations for the origin of greenstone belts invoke a prograde arc-trench model (Hoffman, 1990) in which:

"greenstone belts are viewed as remnants of fore-arc accretionary complexes, the volcanic/subvolcanic rocks being allochthonous island arcs, seamounts microcontinents, *etc.*, and the overlying sediments being indigenous trench turbidites and allochthonous pelagic and deep sea fan deposits."

The Paleozoic Cordilleran model presented here may be viewed as a well-defined Archean analogue in terms of tectonic history and mesothermal vein development.

CONCLUSION

Mesothermal vein deposits within and adjacent to accreted oceanic terranes are:

- Typically hosted within accretionary or related structures that are consistently defined by allochthonous ophiolitic plutonic or metamorphic lithologies which commonly host or are immediately associated with the vein system.
- Spatially and temporally associated with structurally controlled felsic intrusive rocks which are probably generated by crustal melting during an accretionary or collisional episode.

Accreted ophiolitic crustal or upper mantle lithologies, where intruded by structurally controlled syn-collisional felsic magmas, offer regional-scale targets for mesothermal lode-gold exploration.

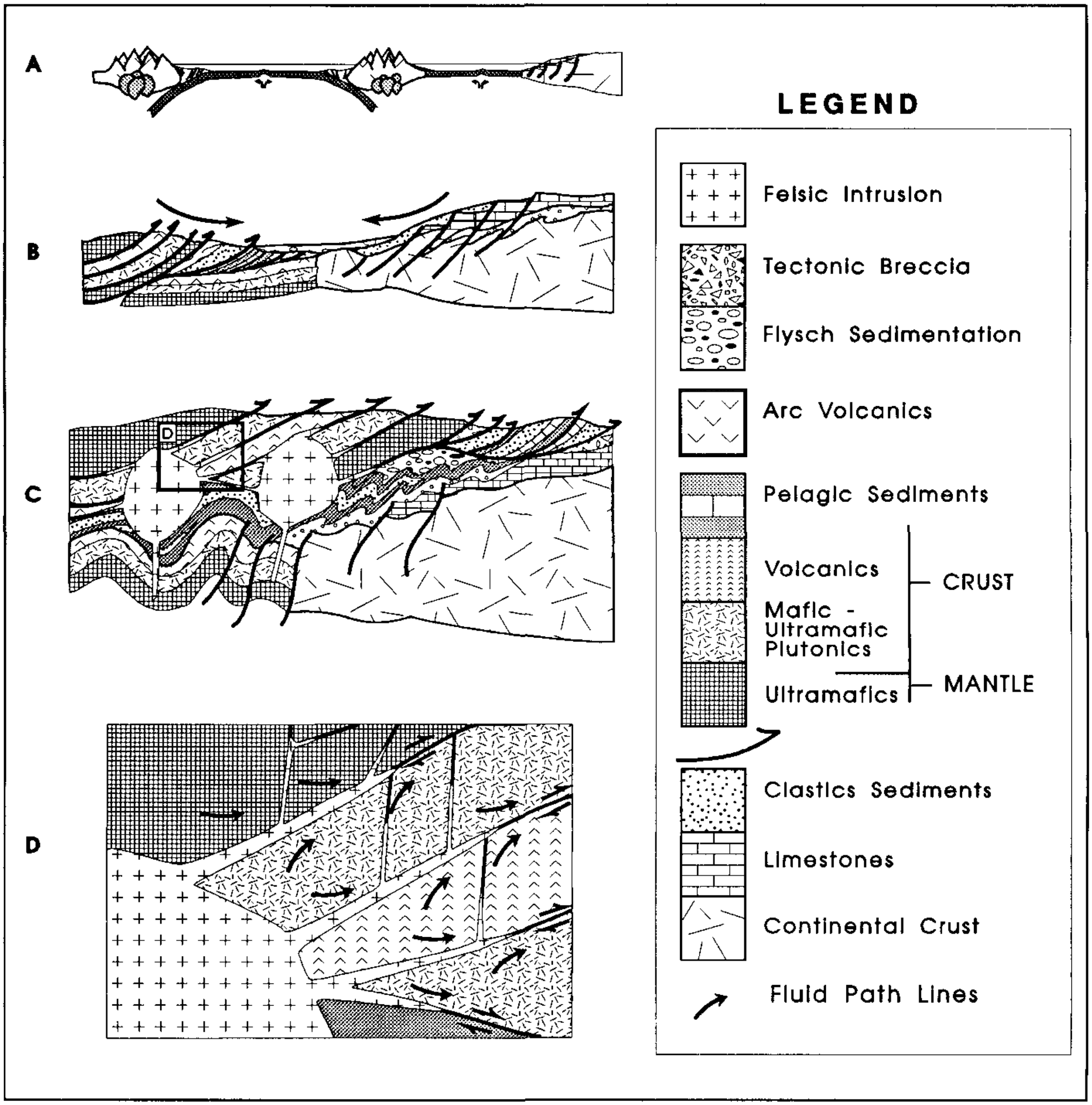

Figure 2-3-5. Schematic model for the development of ophiolite-related mesothermal vein deposits.
A. Development of oceanic crust and depleted mantle (Alpine-type ultramafics).
B. Decoupling of oceanic lithosphere and initiation of obduction with development of flysch sediments.
C. Crustal thickening causes partial melting and metamorphic dehydration of oceanic lithosphere to produce mineralizing fluids.
D. Fluids are thermally driven along pre-existing structures and deposit metals.

ACKNOWLEDGMENTS

The development of this model has involved the gracious contribution of many people. For eagerly providing information and ideas, field visits and the giving of their time and hospitality we are grateful. They include: Darcy Marud and Joanne Bozek (Homestake), Linda Dandy, John Harvey and Brad White in the Atlin area; Ursula Mowatt, Nick Callan, Ian Patterson and Chris Sampson in the Stuart Lake – Fort St. James area: Jim Fyles, Linda Lee and Vic Preto in Greenwood; Dan Wehrle and Trygve Höy in the Rossland camp; Jim Miller-Tait, Neil Church and Paul Schiarizza in the Bralorne area; Matt Ball and JoAnne Nelson in the Cassiar camp. This report has been improved by scientific reviews by Andre Panteleyev, Dave Lefebure, Trygve Höy, Dani Alldrick, JoAnne Nelson, Graham Nixon and Mitch Mihalynuk and editorial review by John Newell and Brian Grant.

REFERENCES

Anonymous (1972): Penrose Field Conference on Ophiolites, *Geotimes;* Volume 17, pages 24-25.

Ash C.H. (in preparation): Origin and Tectonic Setting of Ophiolitic Ultramafic rocks in the Atlin Area, Northwest British Columbia; *B.C. Ministry of Energy, Mines and Petroleum Resources,* Paper.

Ash, C.H. and Arksey R.L. (1990a): The Atlin Ultramafic Allochthon: Ophiolitic Basement within the Cache Creek Terrane; Tectonic and Metallogenic Significance; *in* Geological Fieldwork 1989, *B.C. Ministry of Energy, Mines and Petroleum Resources,* Paper 1990-1, pages 365-374.

Ash, C.H. and Arksey R.L. (1990b): The Listwanite – Lode Gold Association in British Columbia; *in* Geological Fieldwork 1989, *B.C. Ministry of Energy, Mines and Petroleum Resources,* Paper 1990-1, pages 359-364.

Ash, C.H. and Arksey R.L. (1990c): Geology and Tectonic Setting of the Atlin Ultramafic Allochthon; *B.C. Ministry of Energy, Mines and Petroleum Resources,* Open File 1990-22.

Ash, C.H., Macdonald R., Arksey, R., Renyolds, P. and Chaudhry, M. (in preparation.): Ophiolite-related Lode-gold Deposits in British Columbia; *B.C. Ministry of Energy, Mines and Petroleum Resources,* Bulletin.

Barley, M.E., Eisenlohr, B.N., Groves, D.I., Perring, C.S. and Vearncombe, J.R. (1989): Late Archean Convergent Margin Tectonics and Gold Mineralization: A New Look at the Norseman-Wiluna Belt, Western Australia; *Geology,* Volume 17, pages 826-829.

Buisson, G. and Leblanc, M. (1986): Gold-bearing Listwanites (Carbonatized Ultramafic Rocks) from Ophiolite Complexes; *in* Metallogeny of Basic and Ultrabasic Rocks, Gallagher, M.J., Ixer, R.A., Neary, C.R. and Prichard, H.M., Editors, *The Institution of Mining and Metallurgy,* pages 121-131.

Christopher, P.A. and Pinsent, R.H. (1979): Geology of the Ruby Creek and Boulder Creek Area Near Atlin (104/11W); *B.C. Ministry of Energy, Mines and Petroleum Resources,* Preliminary Map 2 with accompanying notes.

Coleman, R.G. (1977): Ophiolites, Ancient Oceanic Lithosphere?; *Springer-Verlag,* 229 pages

Coney, J.P. (1989): Structural Aspects of Suspect Terranes and Accretionary Tectonics in Western North America; *Journal of Structural Geology,* Volume 11, No. 1/2, pages 107-125.

Cordey, F. (1990): Radiolarian Age Determinations from the Canadian Cordillera; *in* Current Research, Part E, *Geological Survey of Canada,* Paper 90-1E, pages 121-126.

Dawson, K.M. (1988): Radiogenic Age and Isotopic Studies: Report 2; *Geological Survey of Canada,* Paper 88-2.

Fyles, J.T. (1984): Geological Setting of the Rossland Mining Camp; *B.C. Ministry of Energy, Mines and Petroleum Resources,* Bulletin 74, 61 pages.

Gabrielse, H. and Yorath, C.J. (1989): DNAG #4. The Cordilleran Orogen in Canada; *Geoscience Canada,* Volume 16, Number 2, pages 67-83.

Gealey, W.K. (1980): Ophiolite Obduction Mechanism; *in* Ophiolites, Proceedings International Ophiolite Symposium, Cyprus, 1979, Panayiotou, A., Editor, *Ministry of Agriculture and Natural Resources,* Geological Survey Department, Cyprus, pages 228-243.

Groves, D.I. (1990): Structural Setting and Control of Gold Deposits; *in* Greenstone Gold and Crustal Evolution, Roberts, F., Sheahan, P.A. and Green, S.B., Editors. *The NUNA Conference Volume,* pages 79-85.

Hodgson, C.J., Chapman, R.S.G. and MacGeehan, P.J. (1982): Application of Exploration Criteria for Gold Deposits in the Superior Province of the Canadian Cordillera; *in* Precious Metals in the Northern Cordillera, Levinson, A.A., Editor, *Association of Exploration Geochemists,* pages 174-206.

Hoffman, P.F. (1990): On Accretion of Granite-Greenstone Terranes; *in* Greenstone Gold and Crustal Evolution, Roberts, F., Sheaham, P.A. and Green, S.B., Editors, *The NUNA Conference Volume,* pages 32-45.

Höy, T., Dunne, K.P.E. and Wehrle, D. (1992): Tectonic and Stratigraphic Controls of Gold-Copper Mineralization in the Rossland Camp, Southeastern British Columbia; *in* Geological Fieldwork 1991, Grant, B. and Newell, J.M., Editors, *B.C. Ministry of Energy, Mines and Petroleum Resources,* Paper 1992-1, this volume.

Kerrich, R. (1989): Geochemical Evidence on the Source of Fluids and Solutes for Shear Zone Hosted Mesothermal Au Deposits; *in* Mineralization in Shear Zones, Bursnal, J.T., Editor, *Geological Association of Canada,* Short Course Notes, Volume 6, pages 129-197.

Kerrich, R. and Wyman, D. (1990): Geodynamic Setting of Mesothermal Gold Deposits: An Association with Accretionary Tectonic Regimes; *Geology,* Volume 18, pages 882-885.

Klepacki, D.W. and Wheeler, J.O. (1985): Stratigraphic and Structural Relations of the Milford, Kaslo and Slocan Groups, Goat Range, Lardeau and Nelson Map Areas, British Columbia; *in* Current Research, Part A, *Geological Survey of Canada,* Paper 85-1A, pages 277-286.

Leitch, C.H.B. (1990): Bralorne: A Mesothermal, Shield-type Vein Gold Deposit of Cretaceous Age in Southwestern British Columbia; *Canadian Institute of Mining and Metallurgy*, Bulletin, Volume 83, No. 941, pages 53-80.

Mihalynuk, M.G., Smith, M., Lefebure, D.V., and Gabites, J.E. (in preparation): Age of Emplacement and Basement Character of the Cache Creek Terrane as Constrained by New Isotopic Data; *Canadian Journal of Earth Sciences.*

Monger, J.W.H. (1984): Cordilleran Tectonics: A Canadian Perspective; *Bulletin de la Societe Geologique de France,* Volume 7.A XXVI, No.2, pages 255-278.

Monger, J.W.H., Price, R.A. and Tempelman-Kluit, D.J. (1982): Tectonic Accretion and the Origin of the Two Major Plutonic Welts in the Canadian Cordillera; *Geology,* Volume 10, pages 70-75.

Nelson, J.L. (1990): Evidence for a Cryptic Intrusion Beneath the Erickson-Taurus Gold-Quartz Vein System, Near Cassiar, B.C. (104P/4, 5); *in* Geological Fieldwork 1989, *B.C. Ministry of Energy, Mines and Petroleum Resources,* Paper 1990-1, pages 229-233.

Nelson, J.L. and Bradford, J.A. (1989): Geology and Mineral Deposits of the Cassiar and McDame Map Areas, British Columbia (104P/3, 5); *in* Geological Fieldwork 1988, *B.C. Ministry of Energy, Mines and Petroleum Resources,* Paper 1989-1, pages 323-338.

Oldow, J.S., Bally, A.W., Ave Lallemant, H.G. and Leeman, W.P. (1989): Phanerozoic Evolution of the North American Cordillera; United States and Canada; *in* The Geology of North America – An Overview, Bally, A.W. and Palmer, A.R., Editors, *Geological Society of America,* pages 139-232.

Raymond, L.A. (1984): Classification of Mélanges; in Mélanges: Their Nature, Origin and Significance, Raymond, L.A., Editor, *Geological Society of America,* Special Paper 198, pages 7-20.

Schroeter, T.G., Lund, C. and Carter, G. (1989): Gold Production and Reserves in British Columbia; *B.C. Ministry of Energy, Mines and Petroleum Resources,* Open File 1989-22, 86 pages.

Tipper, H.W. (1984): The Allochthonous Jurassic – Lower Cretaceous Terranes of the Canadian Cordillera and their Relation to Correlative Strata of the North American Craton; *in* Jurassic-Cretaceous Biochronology and Paleogeography of North America, *Geological Association of Canada,* Special Paper 27, pages 113-120.

TECTONIC AND STRATIGRAPHIC CONTROLS OF GOLD-COPPER MINERALIZATION IN THE ROSSLAND CAMP, SOUTHEASTERN BRITISH COLUMBIA (82F/4)

By T. Höy, B.C. Geological Survey Branch
K.P.E. Dunne (neé Andrew), Mineral Deposit Research Unit, U.B.C.
and D. Wehrle, Vangold Resources, Inc.

KEYWORDS: Economic geology, Rossland, gold-copper, mesothermal veins, Elise Formation, Rossland monzonite, growth faults, tectonics, Evening Star, Gertrude, Iron Colt, fluid inclusions.

INTRODUCTION

Historically, the Rossland camp (Figure 2-4-1) is the second largest lode gold producing district in British Columbia, with recovery of more than 84 000 kilograms of gold, 107 000 kilograms of silver and 54 295 tonnes of copper between 1894 and 1957. Molybdenum deposits on the western and southern slopes of Red Mountain, also regarded as being within the Rossland camp, produced 1.75 tonnes of molybdenum between 1966 and 1972.

The geology of the Rossland camp (Figure 2-4-2) has been the focus of a number of studies. Drysdale (1915) presented the first comprehensive description of many of the mines; Thorpe (1967), in an unpublished Ph.D. thesis, described vein and skarn mineralogy in detail and proposed a camp zonation. The regional geology of the Rossland-Trail area has been described by Little (1982) and Höy and Andrew (1991a), and in the vicinity of the camp itself, by Fyles (1984). Recent work by staff of the Geological Survey Branch has focused on Early and Middle Jurassic plutons (Dunne and Höy, 1992, this volume), ultramafic rocks south and west of Rossland (Ash and MacDonald, 1992, this volume), and molybdenum deposits on Red Mountain (Webster *et al.*, 1992, this volume).

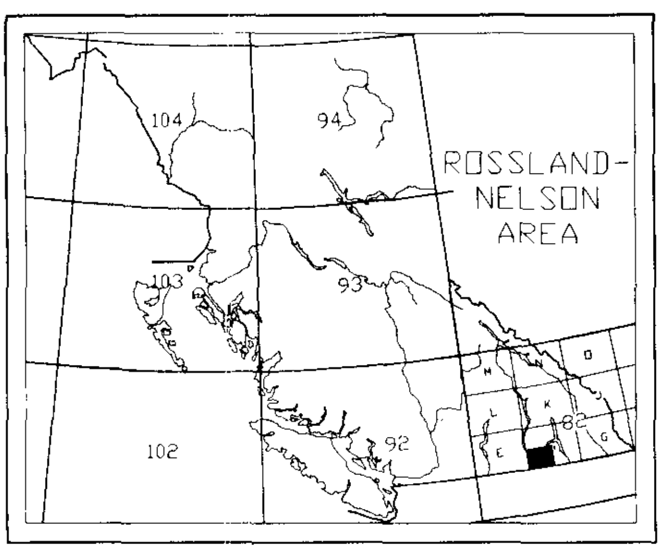

Figure 2-4-1. Location of the Rossland gold camp in southeastern British Columbia.

The field component of the Rossland project, from 1987 to 1990, concentrated on regional mapping of the Rossland Group from Nelson south to Salmo, and west to the town of Rossland. This mapping, with additions from P. Simony and J. Einersen (personal communication, 1990) has been incorporated into a 1:100 000 compilation map (Andrew *et al.*, 1991). The main purpose of the project is to better understand the regional controls and timing of the variety of mineral deposits that occur in the Rossland Group, including shear-related gold deposits southwest of Nelson, alkali porphyry copper-gold deposits such as the Katie, Moochie and Shaft, the numerous lead-silver-zinc and gold-copper veins, both copper and gold skarn deposits, and the vein system of the Rossland camp itself. Continuing work includes some detailed deposit descriptions, fluid inclusion studies, geochemical analyses and stable isotope work.

This paper is intended to serve as an overview of the geology of the Rossland camp, expanding on the preliminary report released in Fieldwork 1990 (Höy and Andrew, 1991a), to attempt to place constraints on the controls and timing of the deposit types that occur in the camp, and to present data on veins that are now being actively explored -- the Evening Star, Iron Colt and Gertrude.

REGIONAL GEOLOGY

The stratigraphic succession in the Rossland area is illustrated in Figure 2-4-3. The Mount Roberts Formation comprises a succession of dominantly fine-grained siliceous rocks, argillite, carbonate and minor greenstone of Pennsylvanian and possibly Permian age (Little, 1982). Although the Mount Roberts Formation has been assigned to the Harper Ranch Subterrane of the Quesnel Terrane (Monger and Berg, 1984), it may correlate with the westernmost assemblages of the Milford Group, which are assigned to the lower part of the Slide Mountain Terrane (Klepachi, 1985). The Mount Roberts Formation is exposed at Patterson near the United States border and in two thrust sheets just west of the Rossland gold-copper camp (Höy and Andrew, 1991a). It hosts the molybdenum skarn-breccia deposits on the western and southern slopes of Red Mountain.

The Rossland Group unconformably overlies the Mount Roberts Formation. It comprises coarse to fine clastic rocks of the Archibald Formation, volcanic rocks of the Elise Formation and generally fine clastic rocks of the overlying Hall Formation (Figure 2-4-3). The Rossland Group is Early Jurassic in age, bracketed by Sinemurian fossils in the

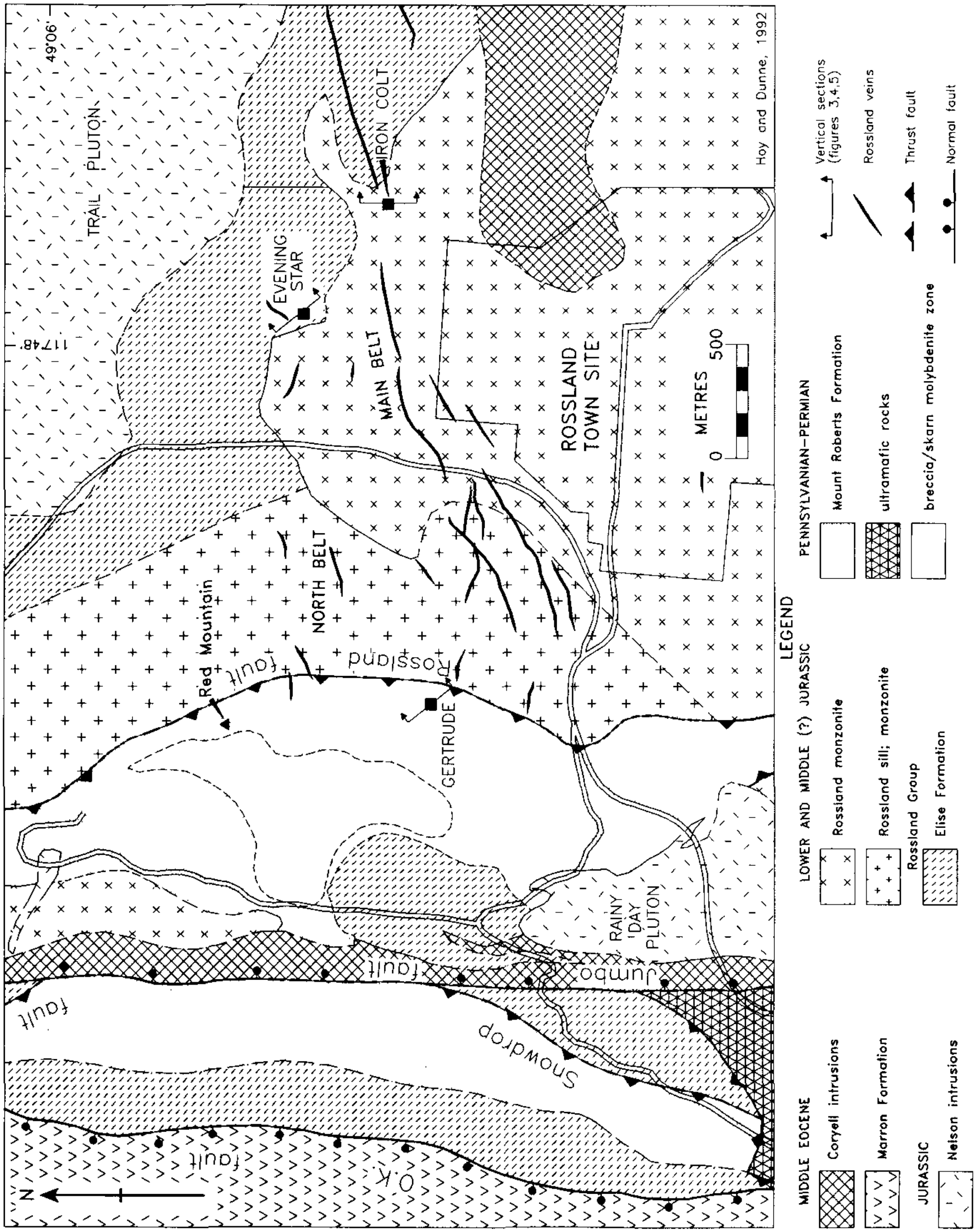

Figure 2-4-2. Geology of the Rossland area, showing distribution and orientation of the main and north copper-gold veins; geology after Höy and Andrew (1991b), Fyles (1984) and Drysdale (1915).

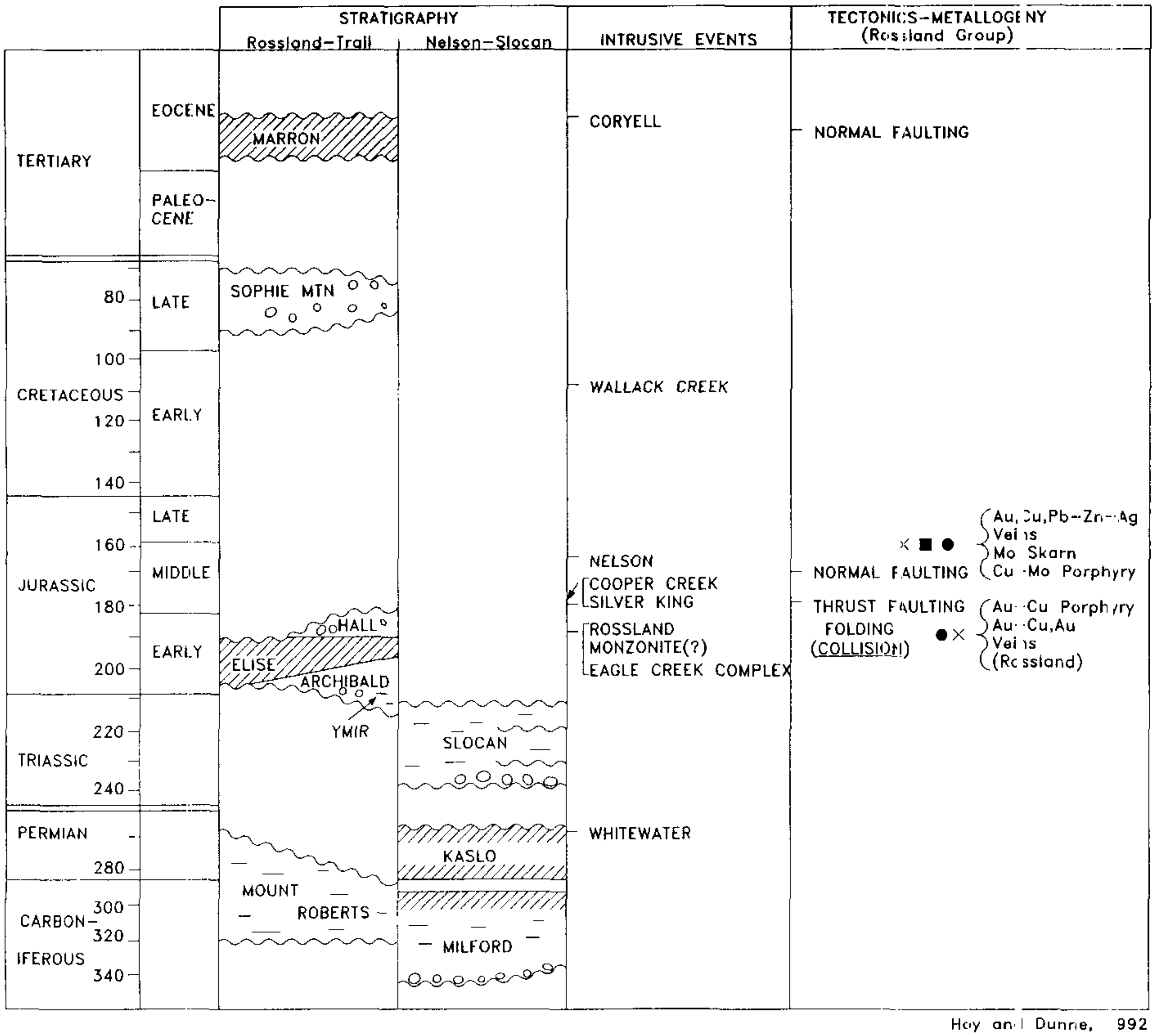

Figure 2-4-3. Summary diagram showing stratigraphy, intrusive events, tectonics and metallogeny of the Rossland Group.

Archibald (Frebold and Tipper, 1970; Tipper, 1984) and Pliensbachian and Toarcian macrofossils in the Hall (Frebold and Little, 1962).

The Archibald Formation is characterized by pronounced facies and thickness changes (Andrew *et al.*, 1990). It comprises coarse alluvial fan conglomerates near Fruitvale, proximal turbidites farther east in Archibald Creek and more distal turbidites and argillites farther north. In the Rossland area, the Archibald Formation is either missing or comprises a thin veneer of coarse conglomerates (Höy and Andrew, 1991a). These facies changes indicate that the Archibald Formation records deposition on a tectonic high in the Rossland-Trail area and in a fault-bounded structural basin located to the east. The faulted eastern boundary of the tectonic high has been the locus of later movements and intrusive activity, including Eocene normal faulting along the Champion Lake fault and a swarm of Eocene dikes that trend north from Waneta near the western banks of the Columbia River.

The Elise Formation is dominantly a volcanic succession. In the Nelson area, it is divisible into a lower unit of mafic augite-phyric flows overlain by an upper unit of pyroclastic rocks (Höy and Andrew, 1989). Elsewhere, mafic flows and tuffs occur throughout the succession. In the Rossland area, it comprises dominantly tuffaceous conglomerates, waterlain crystal and lapilli tuffs, and some interlayered argillite and siltstone. Basal Elise rocks, exposed just west of Waneta, thin and pinch out to the west along the eastern margin of the Rossland paleohigh.

The Hall Formation, the youngest formation in the Rossland Group, is exposed in the Nelson-Salmo area. Facies changes indicate that it was deposited in a shallow-marine, fault-bounded basin at the end of the explosive Elise volcanism (Andrew and Höy, 1991). It is absent in the Rossland area where Elise rocks are unconformably overlain by late Cretaceous conglomerates of the Sophie Mountain Formation or Eocene volcanic rocks of the Marron Formation, suggesting renewed up-lift of the paleohigh in late or post-Rossland time.

Intrusive rocks in the Rossland area include the Rossland monzonite, Rossland sill and a number of small gabbro stocks and sills that are compositionally similar to Elise volcanic rocks and are assumed to be synvolcanic (Dunne and Höy, 1992, this volume). The Rossland sill (Fyles, 1984), an intrusive diorite that underlies the eastern slopes of Red Mountain, has similar mineralogy to the Rossland monzonite and hosts a number of the Rossland veins. The Rossland monzonite intrudes the Rossland sill, but is cut by the Late Jurassic Trail pluton.

Preliminary U-Pb data on the Rossland monzonite (J. Gabites, personal communication, 1991) suggest a 190 Ma age, indicating it may be comagmatic with the Rossland Group. A small ultramafic body within the Rossland monzonite, a coarse-grained biotite clinopyroxenite at the Centre Star vein, suggests that the Rossland monzonite may be a more evolved phase of an Alaskan-type mafic-ultramafic complex. These complexes are typically coeval and cogenetic with their hostrocks (Nixon, 1990). The Eagle Creek Plutonic Complex west of Nelson, an early, pre-tectonic intrusion that may be coeval with the Rossland monzonite, also contains phases that resemble rocks associated with Alaskan-type complexes (Dunne and Höy, 1992).

ROSSLAND CAMP STRUCTURE AND TECTONICS

The structure of the Rossland area has been described by Fyles (1984), Little (1982) and Höy and Andrew (1991a). Three phases of deformation are recognized. Extensional tectonics in the Early Jurassic produced a block-faulted terrain, with a tectonic high in the Rossland area and a structural basin to the east. The western and northern margins of the tectonic high probably controlled the location and orientation of later thrusts and normal faults, as well as the northeast-trending Rossland break, a zone of structural weakness that is aligned with ultramafic bodies, the Rossland monzonite, the Rossland gold-copper veins and the southwestern extension of the thrust faults.

Compressional tectonics produced east-directed thrusts that carried Mount Roberts Formation, unconformably overlying Rossland Group and ultramafic bodies, over Rossland Group rocks that were deposited on the Rossland paleohigh. This phase of deformation probably correlates with the early compressive deformation recognized in more eastern exposures of the Rossland Group (Höy and Andrew, 1990) and records collision of the eastern edge of Quesnellia with cratonic North America. The age of this compressive deformation is early Middle Jurassic, defined by the syntectonic Silver King intrusive suite (*ca* 182-178 Ma; Dunne and Höy, 1992, this volume) and a post-tectonic intrusion (*ca* 180 Ma) in the Goat River area northwest of Kootenay Lake, called the Cooper Creek stock (Klepacki, 1985).

North-trending normal faults are related to a regional extensional event in southern British Columbia in the Eocene (Parrish *et al.*, 1988; Corbett and Simony, 1984).

ROSSLAND CAMP

The Rossland mining camp includes two separate and distinct deposit types: molybdenite deposits occur in brecciated and skarned Mount Roberts Formation sedimentary rocks on Red Mountain and gold-copper veins in structurally underlying Rossland Group rocks and the Rossland monzonite.

Considerable controversy exists regarding the timing and origin of Rossland gold-copper veins and their relationship with the molybdenite skarn deposits. Early workers (Drysdale, 1915; Gilbert, 1948) contended that sulphide mineralization postdated lamprophyre dikes, hence implying a Tertiary age. Little (1963) generally concurred with that conclusion, citing evidence of sulphide stringers cutting lamprophyre dikes.

Thorpe (1967) noted a camp zonation, with a central copper-gold zone that was centred on the main producing mines, an intermediate zone that contains deposits with a variety of sulphide mineralogies, including molybdenite, cobaltite and bismuthinite, and an outer zone defined by the presence of galena and tetrahedrite. Implicit in Thorpe's model is a genetic link between molybdenite deposits, gold-copper veins and the Rossland monzonite. Thorpe (*op cit.*) attributes heating and fluid generation to the underlying Trail pluton as well as the Rossland monzonite; however, preliminary U-Pb dating of the monzonite indicates a 190 Ma age, an intrusive event 25 million years earlier than the age of the Trail pluton.

Fyles (1984) first established that the Rossland monzonite is older than the Trail and Rainy Day plutons. He concluded that the molybdenum mineralization is associated with these younger plutons, but that the gold-copper veins have a more complex history, with mobilization and redeposition of Early Jurassic mineralization in the Middle Jurassic and Tertiary.

We propose a model that differentiates between early gold-copper vein mineralization and later molybdenum skarn mineralization. We concur with the conclusion that molybdenite deposits are spatially and genetically associated with the late Middle Jurassic Rainy Day and Trail plutons but believe that the copper-gold veins are related to the Early Jurassic Rossland monzonite. We argue that a compressional tectonic event separates these two mineralizing events; gold-copper veins formed prior to the thrust faulting, whereas molybdenite mineralization formed primarily in an upper thrust plate, after its emplacement on the Rossland sill, Rossland monzonite and Elise volcanic rocks.

GOLD-COPPER VEINS

The Rossland veins are dominantly pyrrhotite with chalcopyrite in a gangue of altered rock with minor lenses of quartz and calcite. Pyrite and arsenopyrite are common accessory sulphides. The veins are in three main groups referred to as the north belt, the main veins and the south belt. The north belt and main veins are shown on Figure 2-4-2; the south belt veins are within the Rossland Group several hundred metres to a kilometre south of the Rossland monzonite.

In the north belt, a zone of discontinuous veins extends eastward from the northern ridge of Red Mountain to Monte Cristo Mountain. The veins trend east and dip north at 60° to 70°. The largest, on the Cliff and Consolidated St. Elmo claims, is hosted by the Rossland sill. The Evening Star vein (Figure 2-4-2) is within Elise volcanic rocks near the eastern limit of the north belt.

The main veins form a continuous well-defined, steeply dipping fracture system that trends 070° from the southern slopes of Red Mountain northeastward to the eastern slopes of Columbia-Kootenay Mountain. More than 98 per cent of the ore shipped from the Rossland camp was produced from deposits in a central core zone between the large north-trending Josie and Centre Star dikes. These deposits included the Le Roi, Centre Star, Nickel Plate, Josie and War Eagle orebodies. The Gertrude is on a north-northwest-trending segment of the main vein system, straddling the Rossland thrust fault. The Iron Colt is within Rossland monzonite on an eastern extension of the main vein system.

The principal veins in the south belt, including the Bluebird and Mayflower, trend 110° and dip steeply north or south (Fyles, 1984).

EVENING STAR (82FSW102)

The Evening Star produced 56.7 kilograms of gold, 21.5 kilograms of silver and 1276 kilograms of copper from 2859 tonnes of ore during the periods from 1896-1908 and 1932-1939 (Fyles, 1984). This production was mainly from a wide and irregular northeast-trending vein of arsenopyrite, pyrrhotite, pyrite and chalcopyrite (Drysdale, 1915). The veins have a high cobalt content with danaite, a cobaltiferous arsenopyrite, identified and samples of the pyrrhotite containing 1.58 per cent cobalt and 0.67 per cent nickel oxide (Drysdale, *op cit.*). Sulphides are also disseminated in silicified, skarned country rock – siltstone and augite porphyry of the Elise Formation.

Recent drilling beneath the mined veins has intersected both thin, irregular veins and zones of mineralized and altered country rocks (Figure 2-4-4). These zones are at the immediate contact with the Rossland monzonite or in thin selvages between tongues of monzonite. The best intersection, in diamond-drill hole 88-37, (not shown on the plane of the section in Figure 2-4-4) contained 35.7 grams per tonne gold over 4.4 metres.

The zone intersected in drill hole 89-92 comprised dominantly diopside skarn with variable amounts of garnet and hornblende or actinolite. Petrographic analyses of three samples indicate that diopside is commonly partially replaced by epidote or actinolite; hornblende commonly has minor chlorite-epidote alteration. Calcite is interstitial and thin quartz-calcite veins with sulphides cut the skarn. Pyrrhotite is the dominant sulphide, occurring in massive, irregular veins, thin discontinuous veinlets and as disseminated grains in skarn. Chalcopyrite is intimately intergrown with pyrrhotite or occurs as finely dispersed grains. Only minor sphalerite was recognized, enclosed within pyrrhotite. Sample 92-392 contained isolated grains of arsenopyrite, also enclosed in pyrrhotite.

Chemical analyses of three skarn samples are given in Table 2-4-1. Gold content in Sample 92-385 is 1.9 ppm; high cobalt and arsenic values in this sample probably reflect the presence of cobalt-rich arsenopyrite. Lead and zinc values are low in all three samples.

FLUID INCLUSIONS

Fluid inclusions in quartz from the Evening Star vein were studied to better define the environment of deposition for this deposit as well as others in the Rossland Group (in progress). Quartz is an ideal mineral for study of fluid inclusions because it has high tensile strength and is stable under most metamorphic conditions in the crust. It is also readily mobilized by fluids and reprecipitated in veins and pods.

Samples from the Evening Star vein show 'wispy' textures (millions of healed microfractures) characteristic of veins generated at depths of greater than 4 kilometres (J. Reynolds, personal communication, 1991). Although most fluid inclusions are less than 1 micron some range from 6 to 12 microns in maximum dimension. They occur along healed fracture planes or as irregular, three-dimensional clusters and are secondary in origin. Secondary inclusions, formed by sealing and healing of fluid-filled fractures in minerals (Shelton and Orville, 1980; Smith and Evans, 1984), are common in rocks with low porosity or in environments in which grains are subject to tectonic or thermal stresses during or after growth (Crawford and Hollister, 1986).

Measurements were made on microfractures defined by secondary inclusions with uniform liquid to vapour ratios. These occur near or within quartz embayments in sulphide grains (Plate 2-4-1), or on similar microfractures with sulphides occuring along the plane of the fracture. Because the fluid inclusions in the ore minerals cannot be studied, one cannot state with confidence that the inclusions in the quartz embayments contain samples of the ore-forming fluid. However, the proximity of these inclusions to sulphide grains suggests at least a close temporal relationship to the ore fluid.

Three compositional types of fluid inclusions have been identified in quartz through observation of phases present at room temperature (21°C) and freezing (to −130°C) and heating (to 30°C) experiments.These are: an aqueous fluid of low salinity; a fluid of low salinity containing varying proportions of water and carbon dioxide; and a non-saline carbon dioxide rich fluid containing varying amounts of methane and nitrogen (Table 2-4-2).The compositions of fluid inclusions in Rossland Group veins (H_2O, CO_2 and $CH_4 + N_2$, in that order of abundance) are similar to those found in deep environments typical of mesothermal veins.

The wispy textures in quartz veins at the Evening Star deposit and abundant carbon dioxide and methane phases in fluid inclusions are typical of veins generated at depths of greater than 4 kilometres. Homogenization temperatures for

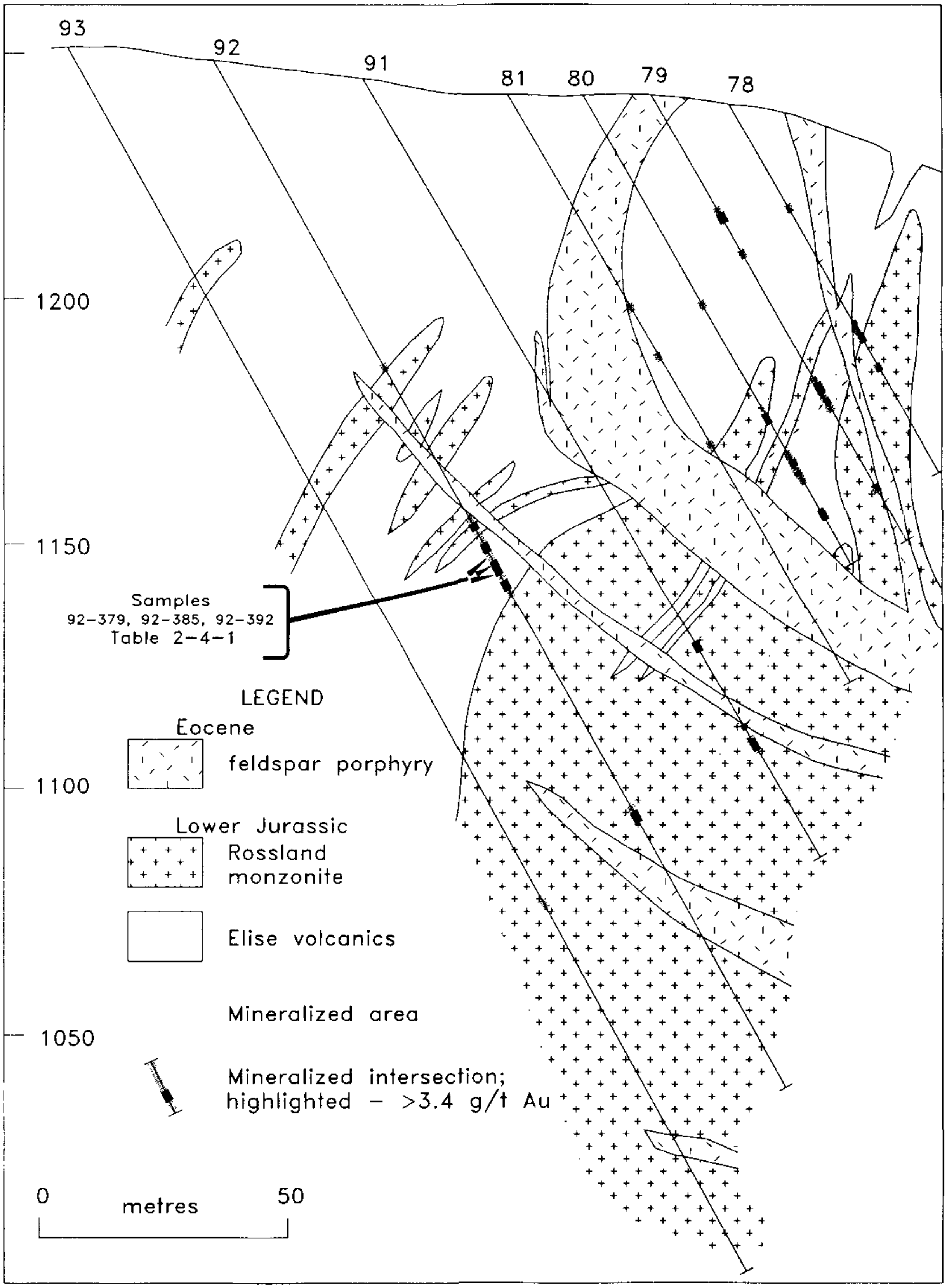

Figure 2-4-4. Vertical section through the Evening Star deposit, viewed to the northeast (*see* Figure 2-4-2 for location); section and data from D. Wehrle, Vangold Resources, Inc.

TABLE 2-4-1
ANALYSES OF SELECTED SAMPLES OF DRILL CORE FROM THE EVENING STAR AND GERTRUDE DEPOSITS

Sample No.	Au (ppb)	Ag (ppm)	Cu (ppm)	Pb (ppm)	Zn (ppm)	As (ppm)	Ba (ppm)	Co (ppm)	Cr (ppm)	Mo (ppm)	Ni (ppm)	Bi (ppm)	Fe (%)	Mn (ppm)	Cd (ppm)	Li (ppm)
92-379	313	0.75	0.20%	5	114	9	—	87	13	<5	8	8	26.4	0.40%	0.3	16
92-385	1920	<0.5	19	11	62	14	—	25	—	<5	2	24	10.5	0.44%	0.4	10
92-392	1210	2.5	0.19%	50	80	4500	220	438	62	<5	74	40	14	957	0.4	29
91-16-531	474	0.5	231	23	45	16	3300	45	120	<5	109	5	6.06	705	<0.3	20
91-16-546	26100	3.0	0.12%	12	108	32	350	53	130	25	122	104	10.1	996	1	26

Samples 92-379, 385, 392 from Evening Star; samples 91-16-546, 531 from Gertrude. Sample locations are shown on Figures 2-4-4 and 2-4-5.

Plate 2-4-1a. Microfractures in quartz (white) defined by secondary fluid inclusions, Evening Star vein (field of view = 93 microns).

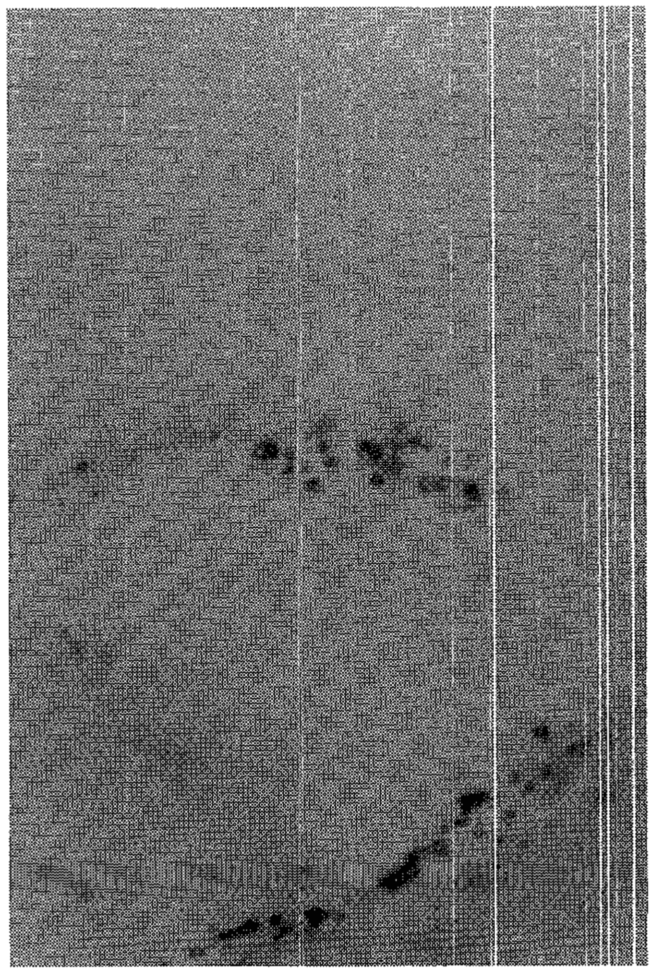

Plate 2-4-1b. Detail of microfractures, note uniform liquid to vapour ratios (field of view = 93 microns).

aqueous fluid inclusions range from 307 to 313°C; three-phase carbon dioxide and water inclusions homogenize at 350°C. These high temperatures are reasonable for mesothermal veins generated by either regional greenschist metamorphism or possibly contact metamorphism.

GERTRUDE (82FSW108)

Development of the Gertrude claim near the turn of the century consisted of a tunnel and prospect shaft (Drysdale, 1915). At that time, material on the dumps comprised pyrrhotite, chalcopyrite, pyrite, arsenopyrite and minor molybdenite. Recent drilling by Vangold Resources, Inc. has intersected a number of mineralized intervals, dominantly in augite monzonite of the Rossland sill at the contact of, or structurally beneath the overlying Mount Roberts Formation (Figure 2-4-5). The best intersection was 4.5 metres containing 14 grams per tonne gold.

The section through the Gertrude vein system in Figure 2-4-5 shows that the contact of the Mount Roberts Formation and Rossland sill is cut by lamprophyre and feldspar porphyry dikes of probable Tertiary age.

TABLE 2-4-2
TEMPERATURE (°C) AND COMPOSITION DATA FOR FLUID INCLUSIONS AT THE EVENING STAR PROPERTY, ROSSLAND AREA

Sample Number	CO_2 Melting	H_2O Initial Melting	H_2O Final Melting	Clathrate Melting	CO_2 Homogenization	H_2O Homogenization	Decrepitation	Salinity NaCl eq.wt. %
Type I: low-salinity aqueous inclusions								
1	—	–24.3	–3.0	—	—	313.1	—	4.9
2	—	–25	–3.4	—	—	307.8	—	5.5
3	—	—	—	—	—	312.8	—	—
Type II: CO_2-H_2O inclusions								
4	–57.4	—	–1.1	—	21.9	—	—	—
5	—	–26	–2.4	7	25.4	—	—	—
6	–57.4	—	–0.9	—	21.6	—	346	—
7	–58.5	—	–2.8	—	24.2	351.5	—	—
8	–57.3	—	—	—	10.8	—	—	—
9	–58.5	—	—	10.2	23.9	—	—	—
Type III: CO_2-CH_4 inclusions								
10	–58.7	—	—	—	13	—	—	—
11	–59.2	—	—	—	8.5	—	—	—
12	–57.1	—	—	—	7.1	—	—	—

Thermometric data was obtained using a Fluid-Inc. adapted U.S.G.S. gas-flow heating-freezing system.
Measurements of phase transitions in any inclusion between –65°C and +30°C were reproducible to ±0.2°C.
At >30°C, results are reproducible to ±1.0°C.

Mineralization is in steep north-dipping veins and veinlets that carry pyrrhotite and minor chalcopyrite. Skarn alteration up to several metres thick is associated with the veins. The skarn comprises mainly diopside with minor garnet, epidote, amphibole (hornblende), chlorite and garnet. Petrographic examination indicates that the diopside is early, commonly replaced by epidote and amphibole, and calcite is interstitial. The dominant sulphide is pyrrhotite, occurring in large irregular grains, disseminated, or in feathery veinlets. Chalcopyrite is intergrown with pyrrhotite but also occurs as small isolated grains in silicates.

Chemical analyses of two skarn samples from diamond-drill hole 91-16 are given in Table 2-4-1. Gold content in Sample 91-16-546 is 26 ppm and copper, 0.12 per cent.

IRON COLT (82FSW100)

The Iron Colt (Figure 2-4-2) is part of the eastern extension of the main vein system. This system continues eastward to the Columbia-Kootenay vein. Although the Iron Colt has had considerable underground development, it has had minimal production, with 186 grams of gold and 466 grams of silver recovered from 20 tonnes of ore (Fyles, 1984). The vein strikes north-northeast and dips steeply north (Drysdale, 1915). It comprises massive pyrrhotite with some chalcopyrite in altered Rossland monzonite.

Recent work on the Iron Colt includes diamond drilling in a joint venture by Antelope Resources, Ltd and Bryndon Ventures, Inc. Current work by Vangold Resources, Inc. includes continued drilling and rehabilitation of old underground workings.

A vertical section through the Iron Colt is illustrated in Figure 2-4-6. Steep north-dipping veins and associated alteration occur at the contacts of phases of the Rossland monzonite or in thin selvages of the Elise Formation within the monzonite. Mineralization is cut by Tertiary lamprophyre and feldspar porphyry dikes. The best assay, in diamond-drill hole 89-87, returned 243 grams per tonne gold over a 2.5 metre interval. Up-dip, in drill hole 90-1, a 1.8-metre interval assayed 8.2 grams per tonne gold. A second vein, approximately 20 metres to the south, assayed 3.77 grams per tonne gold in a 1.3 metre interval and 0.48 grams per tonne over 6.7 metres in drill holes 89-87 and 90-1, respectively (Figure 2-4-6). Other mineralized intersections included 14 grams per tonne gold over 4.6 metres in hole 91-16. These veins are surrounded by alteration zones a few metres wide that contain only minor disseminated sulphides.

SUMMARY AND DISCUSSION

The Rossland camp has many similarities with Archean mesothermal gold deposits or "greenstone gold deposits" (Hodgson *et al.*, 1982). It occurs in a dominantly mafic volcanic pile spatially associated with an oceanic assemblage (Mt. Roberts Formation), is associated with felsic intrusive rocks and ultramafic bodies, and occurs along a major structural break.

The origin of these mesothermal gold deposits is debatable (Kerrich, 1991; Pantaleyev, 1992), with most models relating mineralization to spatially associated intrusions (*see*, for example, Burrows *et al.*, 1986), discharge of metamorphic fluids (Kerrich, 1989), or possibly deep circulation of meteoric water (Nesbitt and Muehlenbachs, 1989). Most commonly, gold mineralization is interpreted to have formed in an accretionary tectonic setting, considerably later than the host volcanic rocks, with fluid flow focused by crustal faults (Kerrich and Wyman, 1990). Despite the apparent similar tectonic setting for Rossland Group rocks, on the eastern margin of an accreting plate, additional geochronological and isotopic data are necessary to conclude that Rossland mineralization is related to this accretionary process.

The Rossland gold-copper camp is within and along the margins of the Rossland monzonite. This has led recent

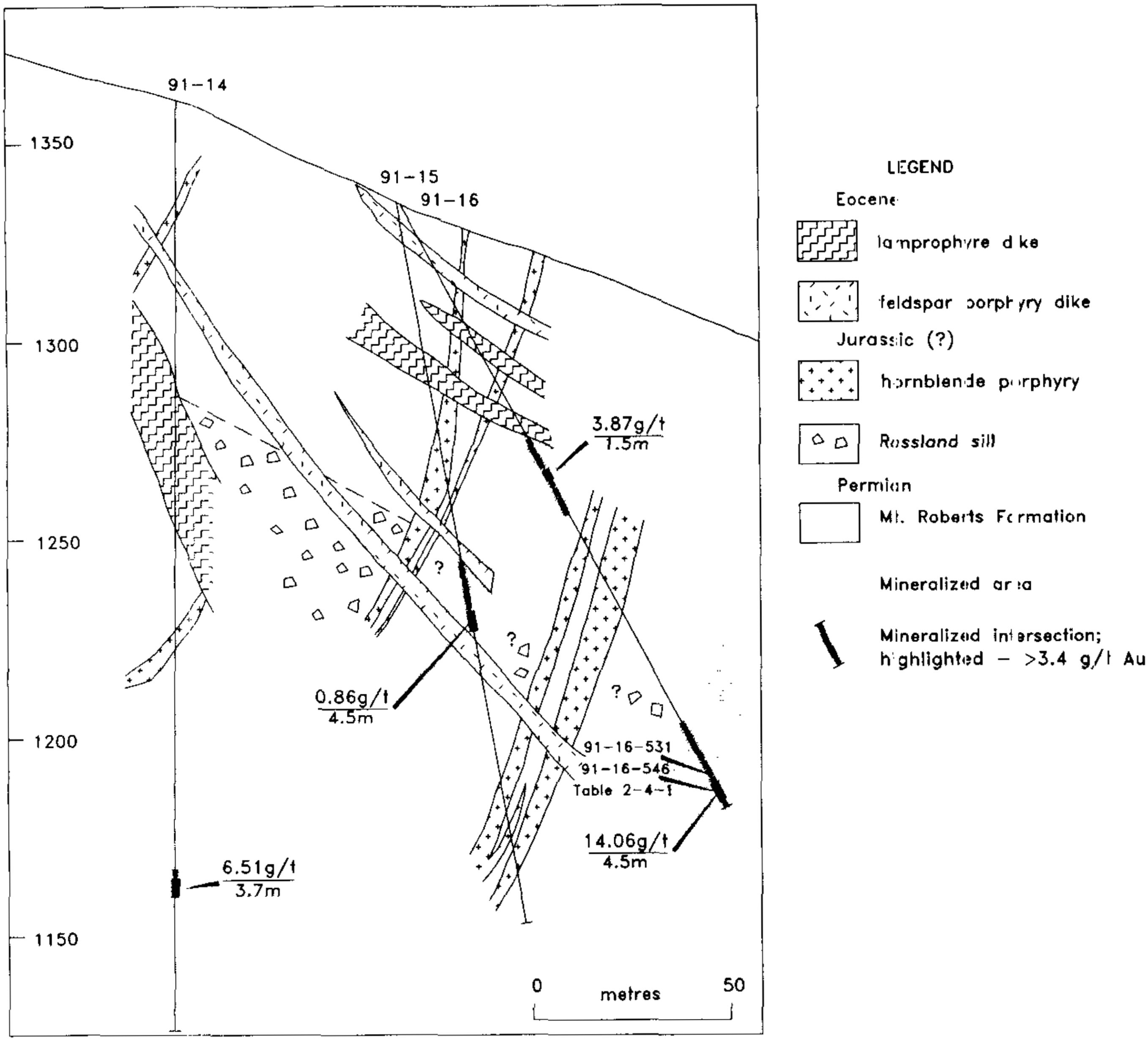

Figure 2-4-5. Vertical section through the Gertrude deposit, viewed to the northeast (*see* Figure 2-4-2 for location); section and data from D. Wehrle, Vangold Resources, Inc.

workers (Fyles, 1984; Thorpe, 1967) to relate the vein system to the intrusion. As well, the close spatial association of mineralization with thin selvages of Elise volcanic rocks in the Rossland monzonite (*see* Figures 2-4-4 and 6) and the association of veins with gold-copper skarn mineralization suggests a relationship with the intrusion. These features, as well as the massive, high sulphide content of the ore and relatively minor carbonate-quartz gangue contrast with more "typical" greenstone gold deposits.

Rare gold-copper veins that crosscut Tertiary dikes have been used as evidence for a Tertiary age of mineralization; however, these can be explained by remobilization and redeposition of sulphides during a widespread Tertiary thermal and tectonic event.

The tectonic history of the Rossland area includes Early Jurassic extensional tectonism that produced a fault-bounded tectonic high in the Rossland area. This paleohigh modified and locally controlled the distribution, thickness and facies of Rossland Group rocks. Furthermore, the early growth faults may have controlled the distribution of early comagmatic plutons, including the Rossland monzonite (*ca* 190 Ma), and the distribution of the Rossland vein system.

After intrusion of the Rossland monzonite (*see* Figure 2-4-3), thrust faults carried Mount Roberts Formation rocks eastward over Rossland Group rocks that were deposited on the Rossland paleohigh. As well, dunitic to wehrlitic ultramafic cumulates of probable oceanic affinity, perhaps part

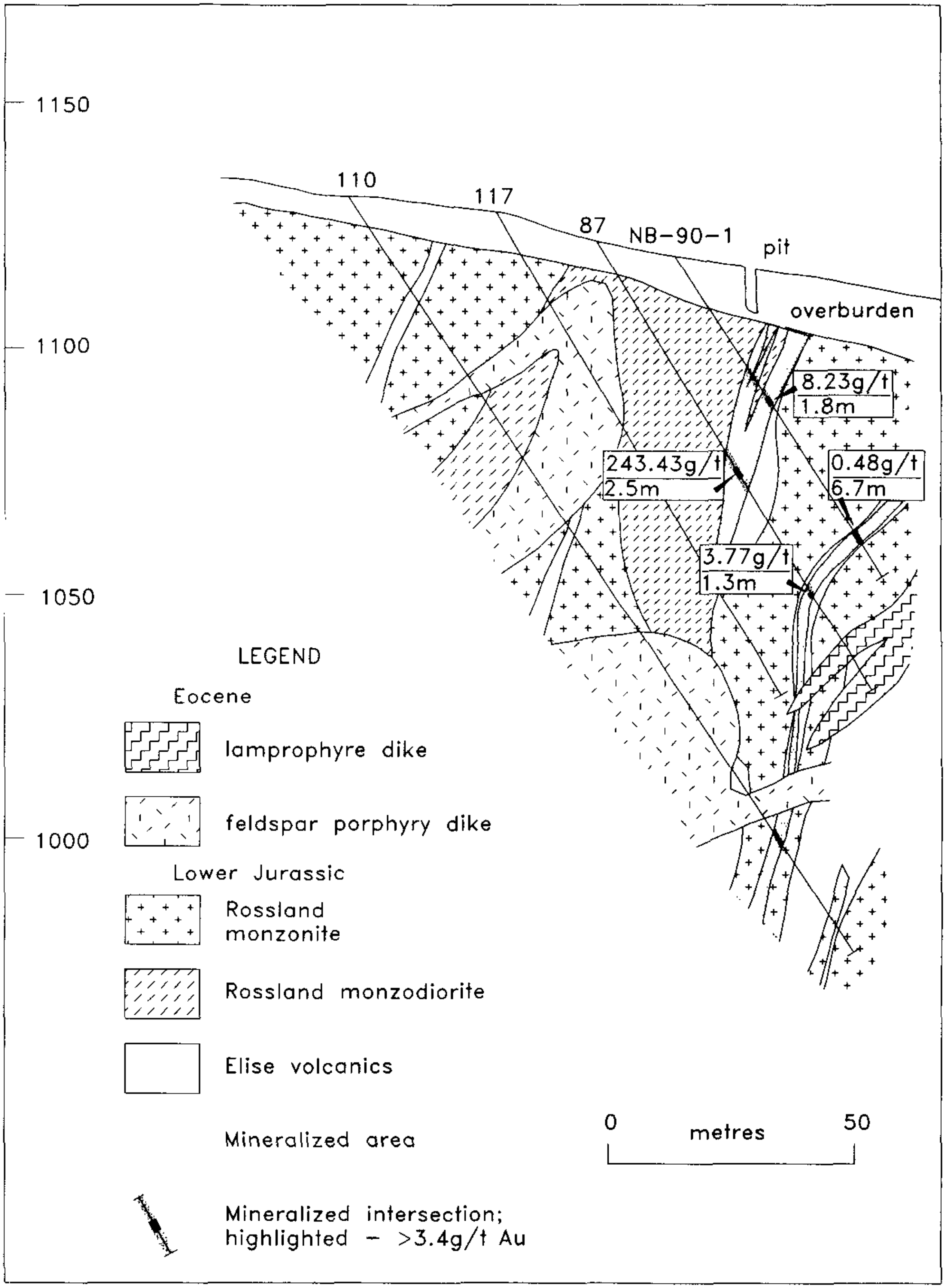

Figure 2-4-6. Vertical section through the Iron Colt deposit, viewed to the east (*see* Figure 2-4-2 for location); section and data from D. Wehrle, Vangold Resources, Inc.

of the Slide Mountain Terrane (C. Ash, personal communication, 1991; Ash and Macdonald, 1992), were thrust onto the high. These faults are probably related to widespread compressional tectonics as the eastern edge of Quesnellia impinged on cratonic North America (*ca* 182-178 Ma). They are parallel to and aligned with the northeast trend of the Rossland break, the Rossland monzonite and the Rossland veins, indicating the continued influence of deep crustal structures on tectonism and mineralization.

Early to Middle Jurassic post-tectonic intrusions (*ca* 165 Ma), including the Trail and Rainy Day plutons, cut the thrust faults. Molybdenite skarn and breccia mineralization is associated with these intrusions on the western and southern slopes of Red Mountain (Fyles, 1984; Webster *et al.*, 1992, this volume). To the east, thermal metamorphism, skarn alteration and molybdenite mineralization have locally overprinted Rossland gold-copper mineralization; elsewhere, gold and copper have been remobilized and deposited in rare, thin, late veins that cut the Mount Roberts Formation and molybdenite mineralization.

Extensional tectonics during the Eocene produced north-trending normal faults and a swarm of north-trending dikes. The dike swarm west of Waneta closely follows the inferred eastern faulted margin of the Rossland paleohigh; in the Rossland area, Tertiary faults follow the loci of earlier thrust faults and may be associated with extrusion of Marron Formation volcanic rocks (Figure 2-4-3).

In summary, Rossland gold-copper mineralization has a complex history. However, the fundamental control on mineralization appears to be deep crustal structures that were reactivated through time, controlling the distribution of Early Jurassic Rossland Group rocks, comagmatic (?) intrusions, gold-copper mineralization, Early to Middle Jurassic thrust faults, Middle Jurassic molybdenite mineralization, and Tertiary structures and associated igneous activity.

ACKNOWLEDGMENTS

We wish to acknowledge discussions with a number of geologists, including C.H. Ash, J.T. Fyles, D.V. Lefebure, R. Macdonald, G.T. Nixon, G.E. Ray, P. Simony and I.C.L. Webster. The editorial comments of B. Grant, J.M. Newell and D.V. Lefebure are appreciated. A. Pettipas and V. Koyanagi prepared the diagrams and tables. We would also like to thank J. Gabites for her preliminary U-Pb analysis of the Rossland monzonite, and Vangold Resources, Inc. for allowing us to publish some of its data.

REFERENCES

Andrew, K.P.E. and Höy, T. (1991): Geology of the Erie Lake Area with Emphasis on Stratigraphy and Structure of the Hall Formation, Southeastern British Columbia; *in* Geological Fieldwork 1990, *B.C. Ministry of Energy, Mines and Petroleum Resources,* Paper 1991-1, pages 9-20.

Andrew, K.P.E., Höy, T. and Drobe, J. (1990): Stratigraphy and Tectonic Setting of the Archibald and Elise Formations, Rossland Group, Beaver Creek Area, Southeastern British Columbia; *in* Geological Fieldwork 1989, *B.C. Ministry of Energy, Mines and Petroleum Resources,* Paper 1990-1, Pages 19-27.

Andrew, K.P.E., Höy, T. and Simony, P. (1991): Geology of the Trail Map-area, Southeastern British Columbia; *B.C. Ministry of Energy, Mines and Petroleum Resources,* Open File 1991-16.

Ash, C.H. and Macdonald, R.W.J. (1992): Listwanite Project – Update; *in* Geological Fieldwork 1991, Grant, B. and Newell, J.M. Editors, *B.C. Ministry of Energy, Mines and Petroleum Resources,* Paper 1992-1, this volume.

Burrows, D.R., Wood, P.C. and Spooner, E.T.C. (1986): Carbon Isotope Evidence for a Magmatic Origin for Archean Gold-Quartz Vein Ore Deposits; *Nature,* Volume 321, pages 851-854.

Corbett, C.R. and Simony, P.S. (1984): The Champion Lake Fault in the Trail-Castlegar Area of Southeastern British Columbia, *in* Current Research, Part A, *Geological Survey of Canada,* Paper 84-1A, pages 103-104.

Crawford, M.L. and Hollister, L.S. (1986): Metamorphic Fluids: The Evidence from Fluid Inclusions; *in* Fluid-Rock Interactions during Metamorphism, Advances in Physical Geochemistry 5, Walther, J.V. and Wood, B.J., Editors, *Springer Verlag,* pages 1-35.

Drysdale, C.W. (1915): Geology and Ore Deposits of Rossland, British Columbia; *Geological Survey of Canada,* Memoir 77.

Dunne, K.P.E and Höy, T. (1992): Petrology of Lower and Middle Jurassic Intrusions in the Rossland Group, Southeastern British Columbia; *in* Geological Fieldwork 1991, Grant, B. and Newell, J.M., Editors, *B.C. Ministry of Energy, Mines and Petroleum Resources,* Paper 1992-1, this volume.

Frebold, H. and Little, H.W. (1962): Paleontology, Stratigraphy, and Structure of the Jurassic Rocks in Salmo Map-area, British Columbia; *Geological Survey of Canada,* Bulletin 81.

Frebold, H. and Tipper, H.W. (1970): Status of the Jurassic in the Canadian Cordillera of British Columbia, Alberta, and Southern Yukon; *Canadian Journal of Earth Sciences,* Volume 7, Number 1, pages 1-20.

Fyles, J.T. (1984): Geological Setting of the Rossland Mining Camp; *B.C. Ministry of Energy, Mines, and Petroleum Resources,* Bulletin 74, 61 pages.

Gilbert, G. (1948): Rossland Camp; *in* Structural Geology of Canadian Ore Deposits, *Canadian Institute of Mining and Metallurgy,* Jubilee Volume, pages 189-186.

Hodgson, C.J., Chapman, R.S.G. and MacGeehan, P.J. (1982): Application of Exploration Criteria for Gold Deposits in the Superior Province of the Canadian Shield to Gold Exploration in the Cordillera; *in* Precious Metals of the Northern Cordillera, Levinson, A.A., Editor, *Association of Exploration Geochemists,* pages 173-206.

Höy, T. and Andrew, K. (1989): The Rossland Group, Nelson Map Area, Southeastern British Columbia; *in* Geological Fieldwork 1988, *B.C. Ministry of Energy, Mines and Petroleum Resources,* Paper 1989-1, pages 33-43.

Höy, T. and Andrew, K.P.E. (1990): Structure and Tectonics of the Rossland Group, Mount Kelly–Hellroaring Creek Area, Southeastern British Columbia; *in* Geological Fieldwork 1989, *B.C. Ministry of Energy, Mines and Petroleum Resources,* Paper 1991-1, pages 11-17.

Höy, T. and Andrew, K.P.E. (1991a): Geology of the Rossland Area, Southeastern British Columbia (82F/4E); *in* Geological Fieldwork 1990, *B.C. Ministry of Energy, Mines and Petroleum Resources,* Paper 1991-1, pages 21-31.

Höy, T. and Andrew. K.P.E., (1991b): Geology of the Rossland-Trail Area, Southeastern British Columbia (82F/4); *B.C. Ministry of Energy, Mines and Petroleum Resources,* Open File 1991-2.

Kerrich, R. (1989): Geodynamic Setting and Hydraulic Regimes: Shear Zone Hosted Mesothermal Gold Deposits; *in* Mineralization and Shear Zones, Bursnall, J.T., Editor, *Geological Association of Canada,* Short Course Notes, Volume 6, pages 89-128.

Kerrich, R. (1991): Mesothermal Gold Deposits: A Critique of Genetic Hypotheses; *in* Greenstone Gold and Crustal Evolution, Robert, F., Sheahan, P.A. and Green, S.B., Editors, Mineral Deposit Division, *Geological Association of Canada,* Nuna Conference Volume, pages 13-31.

Klepachi, D.W. (1985): Stratigraphy and Structural Geology of the Goat Range Area, Southeastern British Columbia; unpublished Ph.D. thesis, *Massachusetts Institute of Technology,* 268 pages.

Little, H.W. (1963): Rossland Map-area, British Columbia; *Geological Survey of Canada;* Paper 63-13.

Little, H.W. (1982): Geology, Rossland-Trail Map-area, British Columbia; *Geological Survey of Canada,* Paper 79-26, 38 pages.

Monger, J.W.H. and Berg, H.C. (1984): Lithotectonic Terrane Map of Western Canada and Southeastern Alaska; *in* Lithotectonic Terrane Maps of the North American Cordillera, Silberling, N.J. and Jones, D.L., Editors, *United States Geological Survey,* Open File Report 84-523.

Nesbitt, B.E. and Muehlenbachs, K. (1989): Geology, Geochemistry, and Genesis of Mesothermal Lode Gold Deposits of the Canadian Cordillera: Evidence for Ore Formation from Evolved Meteoric Water; *Economic Geology,* Monograph 6, pages 535-563.

Nixon, G.T. (1990): Geology and Precious Metal Potential of Mafic-Ultramafic Rocks in British Columbia: Current Progress; *in* Geological Fieldwork 1989, *B.C. Ministry of Energy, Mines and Petroleum Resources,* Paper 1990-1, pages 353-358.

Panteleyev, A. (1992): Gold in the Canadian Cordillera – A Focus on Epithermal and Deeper Environments; *in* Ore Deposits, Tectonics and Metallogeny in the Canadian Cordillera, *B.C. Ministry of Energy, Mines and Petroleum Resources,* Paper 1991-4 (in press).

Parrish, R.R., Carr, S.D. and Parkinson, D.L. (1988): Eocene Extensional Tectonics and Geochronology of the Southern Omineca Belt, British Columbia and Washington; *Tectonics,* Volume 7, pages 181-212.

Shelton, K.L. and Orville, P.M. (1980): Formation of Synthetic Fluid Inclusions in Natural Quartz; *American Mineralogist,* Volume 65, pages 1233-1236.

Smith, D.L. and Evans, B. (1984): Diffusional Crack Healing in Quartz; *Journal of Geophysical Research,* Volume 89, pages 4125-4135.

Thorpe, R.I. (1967): Mineralogy and Zoning of the Rossland Area; unpublished Ph.D. thesis, *University of Wisconsin.*

Tipper, H.W. (1984): The Age of the Jurassic Rossland Group of Southeastern British Columbia; *in* Current Research, Part A, *Geological Survey of Canada,* Paper 84-1A, pages 631-632.

Webster, I.C.L., Ray, G.E. and Pettipas, A.R. (1992): Selected Mineralized Skarns in British Columbia; *in* Geological Fieldwork 1991, Grant, B. and Newell, J.M., Editors, *B.C. Ministry of Energy, Mines and Petroleum Resources,* Paper 1992-1, this volume.

British Columbia Geological Survey
Geological Fieldwork 1991

RARE-EARTH ELEMENT GEOCHEMISTRY OF SELECTED SAMPLES FROM THE SULLIVAN Pb-Zn SEDEX DEPOSIT: THE ROLE OF ALLANITE IN MOBILIZING RARE-EARTH ELEMENTS IN THE CHLORITE-RICH FOOTWALL (82G/12)

By Eva S. Schandl, University of Toronto
and Michael, P. Gorton, Royal Ontario Museum

(Contribution No. 4, Sullivan-Aldridge project)

KEYWORDS: Economic geology, Sullivan mine, lithogeochemistry, rare-earth elements.

INTRODUCTION

This is a preliminary reconnaissance survey of rare-earth element (REE) geochemistry (supported by major and trace element geochemistry) of selected rock samples representing various alteration types at the sediment-hosted Sullivan lead-zinc sedex deposit, British Columbia.

We report the occurrence of very fine grained (<30µm) allanite (REE-rich epidote group mineral) in the chlorite-altered mineralized footwall, and in the albite-chlorite alteration zone at the Sullivan mine. The presence of allanite (Plate 2-5-1) identified in the mineralized, chlorite-altered footwall and the albite-chlorite altered hangingwall of the deposit is accompanied by an apparent increase in rare-earth element concentration in the footwall. The close textural relationship between chlorite, allanite, titanite, pyrrhotite, sphalerite and galena suggests that the crystallization of this assemblage was more or less contemporaneous. Thus, allanite formation was either contemporaneous with mineralization, or with post-ore alteration that was associated with some remobilization of the ore. The selective crystallization of the REE-rich epidote in the mineralized chlorite (±biotite) alteration zones implies one of two things: a rare-earth element gradient was superimposed on the rocks during alteration and mineralization, or less likely, the present rare-earth element concentration predated mineralization, and allanite may have formed after the light REE-rich phosphate, "metamorphic monazite", that reportedly occurs in the carbonaceous sediments of the Lower Aldridge Formation. In either case, as the abundance of allanite is accompanied by elevated rare-earth element values or significant rare-earth element fluctuation, combining detailed petrography with rare-earth element geochemistry could serve as a potential tool for identifying target areas that host mineralization. Allanite has been previously identified in the tourmalinitized footwall of the western part of the Sullivan ore zone by Campbell and Ethier (1984), in a biotite and garnet alteration zone within quartzite at North Star Hill by Delaney (1975), and in the granophyric part of the Purcell (Moyie) sills by Bishop (1974). Allanite grains in this study can be identified by their wide pleochroic halo which is the result of radiation damage to the host mineral by the decay of uranium (Plate 2-5-1). Because of the pleochroic halo around the grains, they may be mistaken for zircon.

Metamorphic monazite has been reported in the dark grey carbonaceous bands of siltite in the Aldridge Formation by Huebschman (1973). Fine-grained monazite was described as aggregates within the bands. The mode of occurrence of allanite in the chloritized and mineralized footwall in this study is significantly different. In the chloritized footwall, allanite overgrows or is intimately intergrown with pyrrhotite and galena, and the wide pleochroic halo around the grains suggests a high uranium content in the mineral (Plate 2-5-1).

ANALYTICAL TECHNIQUES

Rare-earth element geochemistry of selected rocks was determined by instrumental neutron activation analysis at the SLOWPOKE reactor at the University of Toronto. Sample preparation and analytical procedures followed the guidelines set out by Barnes and Gorton (1984). Major

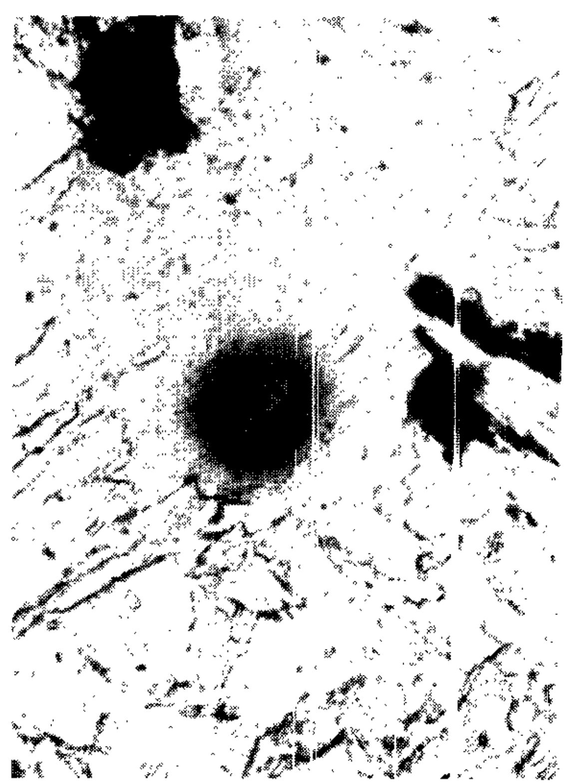

Plate 2-5-1. Allanite with pleochroic halo, in chlorite. Field: 2.3 mm. Plane polarized light.

TABLE 2-5-1
PETROGRAPHIC SUMMARY OF ANALYSED SAMPLES FROM AND AROUND THE SULLIVAN DEPOSIT

# and Loc.	Rock Type	Mineral Assemblage	Description
S-1 G-13-30	Pebble congl. (argillite)	qtz-carb-bio-ep-musc- gnt-po-sph-cp	Garnetized, fine-gr. siltstone
S-2 G-13-30	Moyie sill gabbro	amph-plag-ru-mag-ilm- ep-qtz-carb-po-cp	Epidote-amph. altered, coarse gr. gabbro
S-3 G-13-30	tourm. breccia	qtz-tourm-musc-bio-ru- mag-po	Fine-gr. siltstone repl. by tourmaline
S-4 P-10-4	chlorite rock crosscuts ore	chl-carb-gnt-po-mag-titan- all-zr	Chloritized, carbonatized siltstone
S-5 R-10-30	chlorite rock- footwall	chl-carb-po-gal-titan-all-ru sph-cp-boulangerite-zr	Med.-gr. chloritized, foliated titanite-rich siltstone/wacke
S-6 R-10-30	chlorite rock- footwall	chl-carb-titan-all-ru-bio- zr-qtz-apatite, scheelite	Med.-gr., foliated chloritized titanite-rich siltstone/wacke
S-8 N-10	'albitite'	ab-qtz-chl-py-mag-all-ru-zr	Med.-gr. albitized and chloritized siltstone/wacke
S-10 Moyie R.	Middle Aldridge Marker horizon	qtz-musc-carb-bio-mag-tourm	Very fine-gr. carbonaceous argillaceous siltstone
S-11 North Star Hill	Lower Aldridge siltstone	qtz-bio-chl-sphal-goeth-mag- gnt-all-zr	Very fine-gr. laminated argillaceous siltstone
S-14g Lumberton sill	Moyie sill gabbro	amph-plag-qtz-ep-mag- ilm.-ru-carb-bio-po-cp	Epidotized,amphibolitized coarse gr. gabbro
S-14p	'granophyre'	qtz-musc-ab-ep-chl-ru-mag-amph	sediment inclusion in gabbro

Underlining denotes dateable minerals. Abbreviations: ab:albite, all:allanite, amph:amphibole, bio: biotite, carb: carbonate, chl:chlorite, cp:chalcopyrite, ep:epidote, gal:galena, gnt:garnet, ilm:ilmenite, mag:magnetite, musc:muscovite, goeth=goethite, plag:plagioclase, po:pyrrhotite, py:pyrite, qtz:quartz, ru:rutile, sph:sphalerite, titan:titanite, tourm:tourmaline, zr:zircon.

TABLE 2-5-2
MAJOR, TRACE AND REE GEOCHEMISTRY OF SELECTED ROCKS FROM THE SULLIVAN MINE AND ITS AREA

#	S1	S2	S3	S4	S6	S8	S10	S11	S14g	S14p
SiO_2	61.7	51.4	66.1	30.5	26.2	59.8	68.1	65.9	50.5	62.0
TiO_2	0.20	1.15	0.55	0.63	0.80	0.72	0.65	0.58	0.72	0.44
Al_2O_3	5.22	13.0	11.3	15.0	17.8	17.8	16.5	13.0	14.6	13.8
Fe_2O_3*	3.68	13.4	12.7	20.4	20.2	4.67	3.25	7.30	10.3	5.75
MnO	1.00	0.32	0.02	1.08	0.72	0.07	0.04	0.16	0.15	0.09
MgO	1.63	6.01	1.76	17.4	18.4	2.68	1.20	1.34	8.36	3.99
CaO	13.4	8.52	0.21	2.45	0.60	0.68	0.19	0.06	10.0	7.88
Na_2O	0.06	1.34	0.72	0.02	0.03	9.24	1.01	0.07	1.59	3.09
K_2O	1.39	0.49	0.08	1.49	0.02	0.10	4.88	4.51	0.45	0.52
P_2O_5	0.09	0.11	0.11	0.11	0.08	0.09	0.13	0.08	0.07	0.06
LOI	9.54	2.31	2.93	8.23	10.05	2.70	2.62	6.23	2.70	1.77
TOTAL	98.0	98.1	96.6	97.4	95.4	98.7	98.8	99.4	99.5	99.5
(ppm)										
Cr	19	106	41	50	78	62	47	42	276	72
Co	6	37	21	2	0	3	7	13	37	22
Sc	3	44	8	10	16	16	13	10	38	20
Zr	174	91	328	343	362	338	266	350	50	243
Mo	0.50	0	1.40	1.10	1.40	1.50	0.30	1.80	0.20	0.20
Au	1.8	0.8	2.2	1.1	1.7	1.5	1.7	2.7	1.3	2.7
Rb	72	14	1	90	3	7	170	155	18	12
Ba	100	44	10	60	0	35	820	600	100	115
Th	4.40	1.90	10.90	11.40	17.70	15.40	13.00	11.00	1.50	7.30
U	1.10	0.33	2.90	3.20	4.50	4.10	3.60	3.00	0.10	1.30
La	23.00	8.10	22.40	10.20	67.70	17.90	36.20	62.40	5.60	19.70
Ce	51.80	20.60	50.40	21.90	147.10	45.30	76.40	143.60	11.00	46.10
Nd	20.90	9.40	20.80	10.00	57.70	24.10	27.00	53.00	5.40	19.70
Sm	5.15	3.22	5.00	2.80	12.80	9.00	6.30	11.90	1.84	5.47
Eu	0.82	1.08	1.12	0.99	3.85	1.30	0.84	2.48	0.55	0.99
Tb	0.94	0.83	0.83	0.48	1.68	1.30	0.87	1.10	0.36	1.00
Yb	3.00	2.30	3.50	2.50	6.86	4.65	3.94	4.10	1.55	3.45
Lu	0.44	0.39	0.54	0.44	1.00	0.74	0.60	0.62	0.24	0.58

* Total Fe expressed as Fe_2O_3, g=gabbro, p=sediment clot in gabbro.

element analysis was obtained on fused disks by x-ray fluorescence (X-Ray Assay Laboratory, Toronto). The rocks analyzed were collected during a visit to the mine in the fall of 1990. Samples were selected from alteration types that would most likely contain dateable hydrothermal accessory minerals such as rutile and titanite (Hamilton *et al.*, 1982; Leitch, 1991). Detailed petrographic study preceded analysis in order to determine the mineralogy and the textural relationships between alteration assemblages. Allanite was identified by electron microprobe. A summary of mineralogy, texture and the sample locations is given in Table 2-5-1, whole-rock geochemistry in Table 2-5-2 and microprobe analysis of selected allanite grains in Table 2-5-3.

REE GEOCHEMISTRY OF ALTERED ROCKS

Various rock types were selected for analysis in order to identify alteration type(s) associated with REE mobility and subsequently with the abundance of allanite. The samples included gabbro from the Moyie sills in the mine, pebble conglomerate in the footwall of the laminated ore, tourmalinized breccia, albitized sediment and chloritized sediment from the footwall. In addition, gabbro with a 'granophyric' inclusion was collected from the Lumberton sill at Moyie Lake, south of Cranbrook as well as Lower Aldridge siltstone from North Star Hill immediately south of the deposit, and siltstone from the lower Middle Aldridge marker unit (Hiawatha marker). The rare-earth element composition of the analyzed rocks is discussed below.

The two samples of Moyie sill gabbro have a flat rare-earth element pattern typical of rocks of tholeiitic basalt composition and it is in agreement with the tholeiitic basalt composition determined by trace and major element chemistry for most Moyie sills in southern British Columbia (Höy, 1989; Figure 2-5-1). However, there is a distinct chemical difference between the gabbro from the mine (S-2) and the gabbro from the Moyie Lake area (S-14g, Table 2-5-2); the former has higher rare-earth element concentration, it is higher in scandium and lower in chromium, rubidium and barium, which indicates that it is either a more fractionated equivalent of the gabbro from Moyie Lake, or that the two are unrelated. The comparable lanthanum:ytter-

TABLE 2-5-3
MICROPROBE ANALYSES* OF MINERALS FROM THE SULLIVAN MINE†

	ALLANITE		APATITE
SiO_2	32.16	31.19	0.0
Al_2O_3	17.53	17.92	0.0
CaO	10.80	9.61	54.61
FeO	13.94	14.72	0.46
P_2O_5	0.0	0.0	42.47
La_2O_3	5.09	4.58	0.0
Ce_2O_3	12.35	11.36	0.0
Nd_2O_3	3.54	4.32	0.0
SO_3	0.56	0.0	0.0
TOTAL	95.97	94.72	97.55

* Semiquantitative analyses due to the overlap of some REE peaks
† Analyses are from S-6 (chlorite footwall)

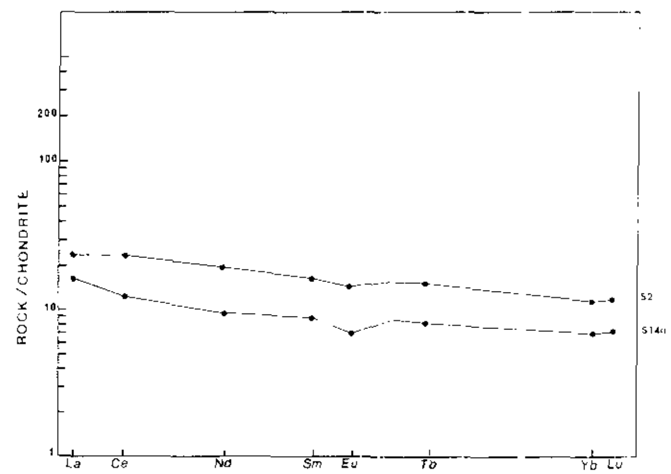

Figure 2-5-1. Rare-earth element pattern of gabbros from the Moyie sills.

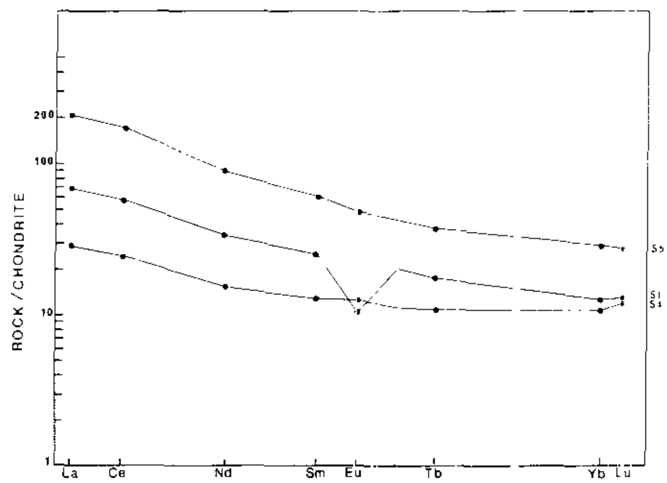

Figure 2-5-2. Rare-earth element pattern of pebble conglomerate (S1), chloritized footwall (S6) and chloritized rock in a fault (S4).

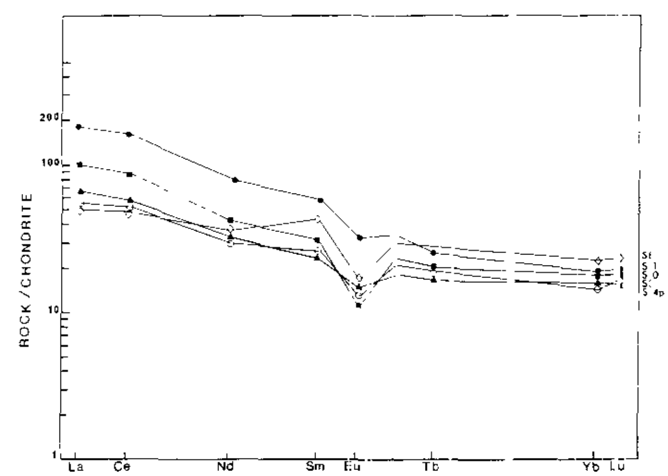

Figure 2-5-3. Rare-earth element pattern of altered sediments.

Plate 2-5-2a. Sediment inclusion ('granophyre') in the Lumberton sill gabbro. Both fields 5.8 mm. Crossed polars.

Plate 2-5-3. Allanite grains in chlorite-rich albitite. Field: 0.8 mm. Plane polarized light.

Plate 2-5-2b. Gabbro from the Lumberton sill.

Plate 2-5-4. Allanite and pyrrhotite in chlorite. Field: 0.8 mm. Plane polarized light.

bium ratios suggest that the rare-earth element abundances have not been disturbed in these rocks during extensive epidotization, and that the difference in their concentration is a primary feature. The 'granophyre' pod or inclusion (S-14p), 0.5 by 0.5 metre in size, in the Lumberton sill represents a fragment of fine-grained sediment (Plate 2-5-2a). Textural evidence and rare-earth element concentrations (Table 2-5-2) suggest a sedimentary precursor to this inclusion in the gabbro (Plate 2-5-2b). The low REE concentration in the gabbros, coupled with the absence of allanite, suggest that rare-earth mobility was insignificant within the gabbros during their emplacement and during subsequent hydrothermal alteration.

The sediments in the mine have been overprinted by various types of alteration, including tourmaline, chlorite, albite, garnet and pyrite (Hamilton *et al.*, 1982; Leitch and Turner, 1991; Leitch *et al.*, 1991). Although the mineralogy of some sediments may be distinctly different, the similarity in REE concentrations implies that the REE were 'fixed' in the rocks prior to alteration and were not disturbed subsequently. For example, S-1 (pebble conglomerate), S-3 (tourmalinized breccia), S-8 (albitized sediment with only minor chlorite) and S-14p (sediment fragment in gabbro) all display comparable rare-earth element trends (negative europium anomaly) and concentrations (Figures 2-5-2 and 3), but their mineralogy is significantly different (Table 2-5-1). This suggests that tourmalinitization, albitization, garnetization and epidotization of the rocks were not accompanied by significant mobilization of rare earths. It should be noted here that in the albitized sample, S-8, REE concentrations are not particularly high, and allanite grains are sparse, whereas in samples in which albite is accompanied by extensive chlorite alteration, the number of allanite grains increases five to tenfold (Plate 2-5-3).

The major element concentration in S4 and S6 basically reflects the extensive chlorite alteration observed in the rocks, thus the original nature of the rock is difficult to infer (Table 2-5-1). Looking at the elements least likely to have been disturbed by chloritization (Zr, Th), S4 and S6 are distinct in having unusually high zirconium and thorium concentrations. Furthermore, the zirconium and thorium concentrations in these samples cover the range of similarly high concentrations in the Aldridge sediments (Table 2-5-1). Thus we infer that S4 and S6 are chloritized sediments. S4 and S6 have significantly different rare-earth concentrations. However, as there is evidence for significant rare-earth mobility in the chlorite alteration zones, localized concentration and depletion associated with the chlorite alteration is expected.

The chlorite-rich sample (S-6) which was collected from the mineralized footwall of the orebody is distinguished by its elevated rare-earth concentration (Figure 2-5-2) and its lack of a negative europium anomaly. The high REE values are accompanied by the presence of allanite in the chlorite (Plates 2-5-4 and 5). The close textural association of chlorite, allanite, titanite and pyrrhotite (Plates 2-5-6, 7 and 8) and galena (Plate 2-5-9) in the mineralized rock suggests that the crystallization of these phases was more or less contemporaneous. Although it should be noted that while pyrrhotite is often overgrown by allanite, galena is often intergrown with the allanite grains.

Based on relative REE concentrations, Richards (1989) reported some correlation in concentrations of individual stratigraphic horizons in the Pritchard Formation (USA) and those in the Aldridge Formation, suggesting that the Sullivan horizon is also recognizable in the Belt Basin. He concluded that the similarity between Pritchard and Aldridge tourmalinite rare-earth concentration indicated a similar origin and that rare-earth elements could be used for stratigraphic correlation. Our work indicates significant rare-earth variation between tourmalinized and chlorite-altered rocks and hence we maintain that alteration type is the main variable that influences rare-earth mobilization in Sullivan mine rocks.

A siltstone with comparably high rare-earth concentration (S-11, Figure 2-5-3) was collected from the upper part of altered Lower Aldridge Formation on North Star Hill. This fine-grained rock is characterized by a high pyrrhotite content and biotite alteration. Allanite grains generally occur either in the biotite, or are intergrown with pyrrhotite.

DISCUSSION AND CONCLUSIONS

This preliminary study is a precursor to a comprehensive geochemical investigation of REE concentration and mobility associated with alteration and mineralization in various rock types at the Sullivan deposit and the surrounding area, and an investigation concerning the role of the Moyie sills in mineralization (Hamilton *et al.*, 1982; Hoy, 1989).

The significance of the presence of allanite in the chlorite-altered mineralized footwall, and in the albite-chlorite alteration zone at the mine is twofold by recognizing a high REE gradient (accompanied by allanite concentration) or significant REE fluctuation, we may define a possible zone of mineralization, distinguishing it from the 'barren' alteration zones; and possible dating of allanite by U-Pb geochronology may define the age of mineralization. The reported occurrence of allanite in the granophyric zones of the Purcell (Moyie) sills (Bishop, 1974) is not surprising, as rare earths are common constituents (often as monazite) of some carbonaceous sediments. Therefore, the melting or partial melting of included sediments in the gabbro, and the contemporaneous (?) crystallization of allanite with the emplacement and subsequent deuteric alteration (epidotization of feldspars) of the sills suggests the scavenging of rare earths from remelted sediments. The crystallization of allanite under such specific conditions does not negate the importance of its association with mineralization. More significant is the allanite vein reported by Campbell and Either (1984), who recognized large (300 µm) allanite grains crosscutting tourmalinized Aldridge sediments. This is in agreement with our observations with respect to the hydrothermal origin of the minerals around the ore. Because REE tend to favor precipitation under reducing conditions (Schandl and Gorton, 1991), we would expect a REE gradient (enrichment and/or fluctuation) around sulphide orebodies. Rare-earth element enrichment around several Archean massive sulphide deposits has been reported by Campbell *et al.* (1984) and Schandl and Gorton (1991), and a current study funded by the Ontario Geological Survey Research Grant Program is under way to investigate the impact of this rare-earth element halo on exploration

Plate 2-5-5. Allanite and pyrrhotite in chlorite. Field: 0.8 mm. Plane polarized light.

Plate 2-5-7. Allanite rims pyrrhotite. Field: 0.8 mm. Plane polarized light.

Plate 2-5-6. Titanite (large centre grain) and small allanite grains (with pleochroic halos) in chlorite. Field: 0.8 mm. Plane polarized light.

Plate 2-5-8. Allanite intergrown with pyrrhotite in chlorite. Field: 0.8 mm. Plane polarized light.

Plate 2-5-9. Allanite intergrown with galena, in chlorite. Field: 0.8 mm. Plane polarized light.

(Schandl *et al.*, 1991). In this preliminary study, the textural relationship between allanite, sphalerite, galena and chlorite suggests that mineralization was contemporaneous with the mobilization of rare-earth elements and with the crystallization of allanite in the localities studied. The source of rare-earth elements may have been the "metamorphic monazite" (Heubschman, 1973) or other rare-earth element-rich minerals in the carbon-rich horizons of the Lower and Middle Aldridge. Work is in progress for detailed rare-earth element studies of the Moyie sills and the altered zones in the Lower and Middle Aldridge sediments, and the U-Pb geochronology of hydrothermal alteration around the Sullivan orebody.

ACKNOWLEDGMENTS

We thank Cominco Ltd. for its permission to collect samples from the Sullivan mine. Special thanks to Dr. John Lydon of the Geological Survey of Canada for his helpful suggestions concerning this project and to Dr. Trygve Höy for his help in collecting samples outside the mine. Funding of the project by the Department of Energy, Mines and Resources (Canada) and National Science and Engineering Research Council to M.P. Gorton is gratefully acknowledged.

REFERENCES

Barnes, S.J. and Gorton, M.P. (1984): Trace Element Analysis by Neutron Activation with a Low Flux Reactor (SLOWPOKE II): Results for International Reference Rocks; *Geostandard Newsletter*, Volume 8, No. 1, pages 17-23.

Bishop, D.T. (1974): Petrology and Geochemistry of the Purcell Sills in Boundary County, Idaho; *in* Belt Symposium, Volume 2; *University of Idaho and Idaho Bureau of Mines and Geology*, pages 15-66.

Campbell, F.A. and Ethier, V.G. (1984): Composition of Allanite in the Footwall of the Sullivan Orebody, British Columbia; *Canadian Mineralogist*, Volume 22, pages 507-511.

Campbell, I.H., Lesher, C.M., Coad, P., Franklin, J.M., Gorton, M.P. and Thurston, P.C. (1984) Rare Earth Element Mobility in Alteration Pipes Below Massive Sulphide Cu-Zn Sulphide Deposits; *Chemical Geology*, Volume 45, pages 181-202.

Delaney, G. (1975): Internal Report to Cominco Ltd.

Hamilton, J.M, Bishop, D.T., Morris, H.C. and Owens, O.E. (1982): Geology of the Sullivan Orebody, Kimberley, B.C., Canada; *in* Precambrian Sulphide Deposits, Hutchinson, R.W., Spence, C.D. and Franklin, J.M., Editors, *Geological Association of Canada*, Special Paper 25, pages 598-665.

Heubschman, R.P. (1973): Correlation of Fine Carbonaceous Bands across a Precambrian Stagnant Basin; *Journal of Sedimentary Petrology*, Volume 43, pages 688-699.

Höy, T.O. (1989): The Age, Chemistry and Tectonic Setting of the Middle Proterozoic Moyie Sills, Purcell Supergroup, Southeast British Columbia; *Canadian Journal of Earth Sciences*, Volume 26, pages 2305-2317.

Leitch, C.H.B. (1991): Preliminary Fluid Inclusion and Petrographic Studies of Parts of the Sullivan Stratiform Sediment-hosted Pb-Zn Deposit, Southeastern British Columbia; *in* Current Research, Part A, *Geological Survey of Canada*, Paper 91-1A, pages 91-101, 1991

Leitch, C.H.B. and Turner, R.J.W. (1991): The Vent Complex of the Sullivan Stratiform Sediment-hosted Zn-Pb Deposit, British Columbia: Preliminary Petrographic and Fluid Inclusion Studies *in* Current Research, Part E, *Geological Survey of Canada*, Paper 91-1E, pages 33-44.

Leitch, C.H.B., Turner, R.J.W. and Höy, T (1991): The District-scale Sullivan–North Star Alteration Zone, Sullivan Mine Area, British Columbia: A Preliminary Petrographic Study; *in* Current Research, Part E, *Geological Survey of Canada*, Paper 91-1E, pages 45-57.

Richards, B.D. (1989): Rare Earth Element Geochemistry of Proterozoic Prichard/Aldridge Formations as an Indicator for Occurrences of Stratiform Massive Sulfide Mineralization; Program with Abstracts, 85th Annual Meeting, Cordilleran Section, 42nd Annual meeting of Rocky Mountains Section; *The Geological Society of America*, Volume 21, No. 5, page 3383.

Schandl, E.S. and Gorton, M.P. (1991): Post-ore Mobilization of Rare Earth Elements at Kidd Creek and Other Archean Massive Sulfide Deposits; *Economic Geology*, Volume 26, No.7.

Schandl, E.S., Davis, D.W., Gorton, M.P. and Wastenays, H.A. (1991): Geochronology of Hydrothermal Alteration Around Volcanic-hosted Massive Sulphide Deposits in the Superior Province; *Ontario Geoscience Grant Program*, Summary of Research.

NOTES

British Columbia Geological Survey
Geological Fieldwork 1991

SILVER-BEARING MINERALS OF THE SILVER QUEEN (NADINA) MINE, OWEN LAKE, WEST-CENTRAL BRITISH COLUMBIA (93L)

By Christopher T. Hood and Alastair J. Sinclair
The University of British Columbia
Craig H.B. Leitch
The Geological Survey of Canada

KEYWORDS: Economic geology, silver-bearing minerals, Silver Queen mine, ore mineralogy, vein deposits.

INTRODUCTION

The Silver Queen (Nadina, Bradina) deposit of New Nadina Explorations Ltd. is located near Houston, 100 kilometres southeast of Smithers in the Bulkley Valley region of central British Columbia. The mine, which produced 98.28 kilograms of gold, 5225 kilograms of silver, 405 000 kilograms of copper, 703 000 kilograms of lead, 5 million kilograms of zinc and 15 000 kilograms of cadmium from 190 700 tonnes of ore over a brief period from 1972 to 1973, has current reserves of approximately 500 000 tonnes grading 3 grams per tonne gold and 200 grams per tonne silver, 0.23 per cent copper, 0.92 per cent lead and 6.20 per cent zinc (Nowak, 1991). Metallurgical problems arising from a complex mineralogy contributed to closure of the mine. The purpose of this study is to define the nature of the precious metal mineralization at Silver Queen mine and consider how the deposition of these minerals is related to the formation of the deposit.

GEOLOGY OF THE SILVER QUEEN DEPOSIT

Detailed geology of the area surrounding the Silver Queen mine has been presented by Leitch *et al.* (1990) and is summarized here only briefly. Rocks hosting the deposit are subdivided into five major units plus three types of dike with units numbered sequentially from oldest to youngest. A basal reddish purple polymictic conglomerate (Unit 1) is overlain by fragmental rocks ranging from thick crystal tuff (Unit 2) to coarse lapilli tuff and breccia or lahar (Unit 3); this is succeeded upwards by a thick feldspar-porphyritic andesite flow unit (Unit 4), intruded by microdiorite sills (Unit 5) and other feldspar porphyry (Unit 5a) and quartz porphyry (Unit 5b) dikes and stocks.

The stratified rocks form a gently northwest-dipping succession, with the oldest rocks exposed near Riddeck Creek to the south and the youngest in Emil Creek to the north. All the units are cut by dikes that can be divided into three groups: amygdaloidal dikes (Unit 6), bladed feldspar porphyry dikes (Unit 7), and diabase dikes (Unit 8). The succession is unconformably overlain by basaltic to possibly trachyandesitic volcanics that crop out in Riddeck Creek and farther south. These volcanics may be correlative with the Goosly Lake Formation (Church and Barakso, 1990).

Mineralized veins cut the amygdaloidal, fine-grained plagioclase-rich dikes (Unit 6), and are cut by the series of dikes with bladed plagioclase crystals (Unit 7). The former are generally strongly altered close to the veins whereas the latter are unaltered and are possibly correlative with the Ootsa Lake Group Goosly Lake volcanics of Eocene age (50 Ma). The unaltered, feldspar porphyry dikes cut the amygdaloidal dikes, and both are cut by the slightly younger diabase dikes (Unit 8).

ANALYTICAL PROCEDURE

This work is part of an exhaustive mineralogical study of the veins and altered wallrock of the Silver Queen property based on extensive use of x-ray diffraction, a scanning electron microscope - energy dispersive system (SEM-EDS), and quantitative analyses with the Cameca SX-50 wavelength dispersive electron microprobe. Operating conditions for the SEM-EDS studies were: polished specimens were run with no tilt on the energy dispersive spectrum, and the tungsten filament was used with 30-kilovolt accelerating voltage and 2.7-amp filament current. The beam current was 0.5 nanoamperes, giving a 0.5-micron (500 angstrom) beam width or resolution for backscattered electrons.

For the electron microprobe analyses, operating conditions were: 20-kilovolt accelerating voltage, 10 nanoamperes beam current and 1.0-micron beam diameter (approximately 5 micron diameter of spot-size resolution on the polished surface). Counting times were 30 seconds for peaks and 15 seconds for background. Standards used were pure metals (Ag, Bi, Mn, Cd, Ge, In) or compounds (HgTe, GaAs), natural pyrrhotite, galena, sphalerites (for Zn, S, Fe) and synthetic tetrahedrites (for Cu, S, Sb, As and Zn).

All data were reduced using a PAP correction program that corrected for atomic number, absorption and fluorescence, supplied by the probe manufacturer. Routine analyses of standards were within ±5 per cent of the accepted values. The precision of microprobe analysis is difficult to estimate, as there is no possibility of re-analyzing exactly the same point (significant "burns" occur in some minerals – especially sulphosalts, micas and carbonates). However, repeated analyses of the same grain in several locations showed that fluctuations were usually less than 5 per cent.

VEIN DEPOSITS

More than 20 separate epithermal, polymetallic veins are known in four main areas of the Silver Queen property (Leitch *et al.*, 1990): Camp-Portal vein area, main No. 3 vein area, George Lake vein and Cole Lake area; lesser veins are found in the Chisholm and Tailings Pond areas. The No. 5 and Switchback veins are included with the

Portal vein system to the west of the No. 3 vein. The No. 3 vein system is apparently the largest and is by far the best known and most easily accessible because of extensive underground development. More detailed descriptions of individual veins are provided by Leitch *et al.* (1990) and Hood (1991). The various veins have been a veritable mineralogical "gold mine" with a variety of unusual minerals having been reported (*e.g.*, Bernstein, 1987; Harris and Owens, 1973).

TABLE 2-6-1
MINERAL SPECIES IDENTIFIED AT SILVER QUEEN MINE
(this study)

PHASE	COMPOSITION	QUALITATIVE ABUNDANCE*
Ore Minerals		
Pyrite	FeS_2	C
Marcasite	FeS_2	R
Arsenopyrite	FeAsS	R
Pyrrhotite	FeS_1-x	T
Sphalerite	ZnS	C
Galena	PbS	C
Tetrahedrite	$Cu_{12}Sb_4S_{13}$	C
Tennantite	$Cu_{12}As_4S_{13}$	C
Freibergite	$(Cu,Ag)_{12}Sb_4S_{13}$	R
Bismuthinite	Bi_2S_3	T
Cuprobismutite	$CuBiS_2$	T
Proustite	Ag_3AsS_3	T
Pyrargyrite	Ag_3SbS_3	R
Covellite	CuS	T
Chalcocite	Cu_2S	T
Chalcopyrite	$CuFeS_2$	C
Bornite	Cu_5FeS_4	T
Aikinite	$CuPbBiS_3$	R
Matildite	$AgBiS_2$	R
Berryite	$Pb_2(Cu,Ag)_3Bi_5S_{11}$	R
Pearceite	$(Ag,Cu)_{16}(As,Sb,Bi)_2S_{11}$	R
Polybasite	$(Ag,Cu)_{16}(Sb,As)_2S_{11}$	T
Arsenpolybasite	$(Ag,Cu)_{16}(Sb,As)_2S_{11}$	T
Seligmannite	$PbCuAsS_3$	R
Bournonite	$PbCuSbS_3$	R
Gustavite	$Ag_3Pb_5Bi_{11}S_{24}$	T
Geocronite	$Pb_5(As,Sb)_2S_8$	T
Acanthite	Ag_2S	T
Electrum	$Ag_{0.3}Au_{0.7}$	R
Oxides		
Hematite	Fe_2O_3	C
Magnetite	Fe_3O_4	T
Rutile/Anatase	TiO_2	T
Gangue Minerals		
Barite	$BaSO_4$	C
Hinsdalite	$(Pb,Sr)Al_3(PO_4)(SO_4)(OH)_6$	R
Svanbergite	$(Sr,Ca)Al_3(PO_4)(SO_4)(OH)_6$	R
Quartz	SiO_2	C
Calcite	$CaCO_3$	C
Mn-siderite	$(Fe,Mn)CO_3$	C
Rhodochrosite	$MnCO_3$	C
Dolomite	$MgCO_3$	R
Bitumen	(C,H,O)	R

* "C" represents minerals occurring in several or all locales in amounts greater than 2 volume percent.
* "R" represents minerals occurring in a few locales, in some cases greater than 2 volume percent.
* "T" represents minerals occurring in only a few locales, generally in trace quantities.

Ore Mineralogy

An outline of the mineralogy of the veins has been presented by Hood *et al.* (1991) who recognize a complex paragenesis with several stages of mineralization. The observed minerals are summarized in Table 2-6-1, with a general indication of relative abundances. Other minerals reported at Silver Queen include boulangerite (Marsden, 1985), guettardite meneghinite (Weir, 1973) and wurtzite (Bernstein, 1987). Hood (1991) has defined four well developed paragenetic stages in the No. 3 vein:

1. early quartz-pyrite ± barite
2. layered sphalerite-carbonate ± galena
3. galena-sulphosalt-chalcopyrite
4. late quartz-calcite

The principal sulphides are pyrite, galena and sphalerite with lesser amounts of chalcopyrite and tetrahedrite-tennantite scattered throughout. In addition, there are a variety of rare minerals, some of which are relatively abundant locally, many of which are silver-bearing, and are the principal focus of this report.

Silver Minerals

TETRAHEDRITE-TENNANTITE

Minerals of the tetrahedrite-tennantite ("fahlore") series are by far the most important silver-bearing phase at the Silver Queen deposit. Tetrahedrites (and other sulphosalt minerals) occupy a single paragenetic interval in the "Stage III" assemblage (Hood, 1991) and are commonly intergrown with galena, chalcopyrite and other sulphosalt minerals. Fracture infillings of fahlores are widespread in chalcopyrite and sphalerite, and the series commonly occurs as a matrix for pyrite and sphalerite vein breccias.

Tetrahedrite is also present as irregular masses up to several millimetres across in veins with elevated silver contents (*e.g.*, Camp veins).

Compositionally, tetrahedrite-series minerals show a broad range at the Silver Queen mine (Table 2-6-2). Silver-

TABLE 2-6-2
TETRAHEDRITE COMPOSITIONS*

Element	1	2	3	4	5	6
Cu	42.21	43.27	42.78	36.26	33.13	24.37
S	27.56	27.82	28.26	24.96	24.65	23.33
Zn	8.00	8.07	6.35	7.74	5.66	4.31
Fe	0.55	0.60	1.95	0.20	1.91	2.26
Sb	0.40	0.27	0.75	22.59	25.02	25.66
As	18.14	18.98	19.06	3.98	2.16	1.44
Pb	0.00	0.00	0.56	0.00	0.00	0.00
Ag	0.40	0.30	0.10	3.72	6.52	18.61
Bi	3.00	0.62	0.05	0.68	0.27	0.00
Hg	0.00	0.00	0.05	0.00	0.00	0.00
Total	100.26	99.93	99.91	100.13	99.32	99.98

1: Bi-rich tennantite, deep north No. 3 vein.
2: low-Bi tennantite, deep north No. 3 vein.
3: tennantite from south No. 3 vein.
4: Ag-rich tetrahedrite from south No. 3 vein.
5: tetrahedrite from shallow north No. 3 vein.
6: freibergite from Owl vein.
* values given as weight per cents

rich compositions are found in the north, deep in the southern parts of the No. 3 system, and in smaller veins most distant from the No. 3 vein. Silver contents of up to 18 per cent have been determined for tetrahedrites from the Cole and Owl veins. Variations in bismuth, antimony and zinc contents were also noted in Silver Queen tetrahedrites (Hood, 1991) and in a number of cases remarkably zoned crystals were observed (Plate 2-6-1).

MATILDITE

Matildite is uncommon in the No. 3 system, but is the most important sulphosalt mineral in the Portal vein system. It is present as symplectic intergrowths with galena and forms masses up to 3 millimetres across (Plate 2-6-2). Matildite also occurs with aikinite, electrum and berryite in the chalcopyrite-rich Portal veins.

PEARCEITE-POLYBASITE

Minerals of the pearceite-polybasite series are relatively rare at the Silver Queen deposit, but there is a wide degree of compositional variation among those that are (Table 2-6-3). Polybasite occurs deep in the southern part of the No. 3 vein as small (less than 50 microns) irregular grains intergrown with tetrahedrite and proustite-pyrargyrite. More arsenic-rich compositions are present in the Portal and Camp veins, where the minerals occur as anhedral to subhedral grains up to 1 millimetre in diameter. An unusual bismuthian pearceite is also present, occurring as small veinlets cutting chalcopyrite and other sulphosalts. In the Camp veins, pearceite is commonly symplectically intergrown with pyrargyrite, galena and argentian tetrahedrite and may form up to 50 per cent of the silver-bearing assemblage. It has also been noted in the northernmost parts of the Cole and No. 3 systems, and in the Chisholm veins.

PROUSTITE-PYRARGYRITE

The proustite-pyrargyrite (ruby silver) series is limited in distribution at the Silver Queen deposit, attaining peak abundance in the northern part of the Camp vein system. In the Camp veins, end-member pyrargyrite (*see* Table 2-6-3) occurs as symplectic intergrowths with galena, tetrahedrite and pearceite, with individual masses up to 1 millimetres across identified in polished section. Pyrargyrite also occurs as much finer grained material in the north part of the No. 3 system, Owl vein and Cole Lake veins. As with the Camp veins, pyrargyrite grains are commonly intergrown with galena, argentian tetrahedrite and pearceite.

More arsenic-rich compositions have been found only at the southern end of the No. 3 system, where proustite occurs as small (less than 100 microns) exsolved grains in massive galena. Geocronite and an as yet unidentified silver-antimony-lead sulphosalt are also present with the proustite.

TABLE 2-6-3
PEARCEITE-POLYBASITE AND RUBY SILVER COMPOSITIONS*

Element	1	2	3	4
Cu	11.30	8.58	0.12	0.13
S	16.51	16.54	17.67	17.51
Zn	0.00	0.00	0.05	0.00
Fe	0.44	0.00	0.00	0.00
Sb	0.34	0.65	21.83	19.61
As	6.57	5.48	0.67	1.82
Pb	0.00	0.00	0.00	0.00
Ag	64.40	65.86	59.77	59.76
Bi	0.26	3.21	0.13	0.00
Hg	0.05	0.00	0.00	0.00
Total	99.88	100.32	100.24	98.93

1: pearceite from small vein between No. 3 and George Lake systems.
2: bismuthian pearceite from No. 5 vein.
3: pyrargyrite from Camp veins.
4: pyrargyrite from Owl vein.
* values given as weight per cents

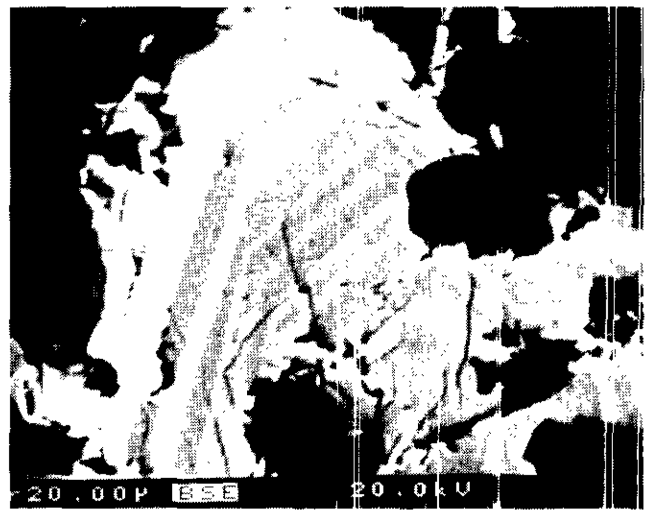

Plate 2-6-1. Backscattered electron photomicrograph of oscillatory zoned tetrahedrite from the northern No. 3 vein. Zonation is controlled by variation between antimony-rich (light) and arsenic-rich (dark) compositions. Scale bar at lower left is 20 microns.

Plate 2-6-2. Symplectic intergrowths of galena and matildite from chalcopyrite-rich Portal vein material. Note large, light-coloured electrum grain in upper right corner. Scale bar at lower right is 10 microns.

BERRYITE

Berryite (Table 2-6-4) was first identified at the Silver Queen mine by Harris and Owens (1973) and locally forms an important constituent of the sulphosalt assemblage in chalcopyrite-rich veins. Deep in the northern part of the No. 3 vein, berryite occurs as laths up to 0.3 millimetre long in a chalcopyrite matrix. Bismuthian tennantite and galena commonly replace the laths along cleavage and grain margins, although symplectic intergrowths with these minerals have also been noted (Plate 2-6-3). Berryite is also present in the Portal vein system, where it occurs with galena, matildite and gustavite.

GUSTAVITE

Gustavite (Table 2-6-4) is a relatively rare mineral at Silver Queen, restricted to the chalcopyrite-rich Portal veins. The mineral occurs as masses (in chalcopyrite) up to 0.5 millimetre across and is associated with berryite and galena, locally forming up to 50 per cent of the sulphosalt assemblage.

ELECTRUM

Electrum occurs throughout the No. 3 and associated veins and appears to be the only gold-bearing phase at Silver Queen mine. In general the mineral is present as small (less than 50 microns) rounded inclusions in galena or galena-sulphosalt intergrowths and is commonly associated with fine-grained pyrite. Locally, individual grains are up to 160 microns across and occur in embayments in larger pyrite grains associated with the host galena (Plate 2-6-4). Electrum grains are less commonly hosted by chalcopyrite, tetrahedrite, pyrite or sphalerite.

Compositionally, electrum from Silver Queen is quite silver rich, with grains from the No. 3 and Portal veins in the range of 600 to 720 fine. Electrum from the Copper vein is even more silver rich, containing gold with a fineness of approximately 500.

DISCUSSION

Precious metal values in the Silver Queen deposit result from the occurrence of electrum and the sulphosalt minerals tetrahedrite-tennantite, matildite, berryite, pearceite-polybasite, gustavite and proustite-pyrargyrite. Silver was also detected in trace amounts in galena and aikinite. The fahlores (tetrahedrite-tennantite series minerals) are the most important silver minerals, containing up to 18 weight per cent silver and locally forming up to 10 to 15 per cent by volume of the vein. Silver contents are highest in the northern part of the No. 3 vein and in veins farthest from the central No. 3 and George Lake structures. The other silver sulphosalts are less abundant, with berryite, matildite and gustavite confined to veins where chalcopyrite is a major part of the vein assemblage (*e.g.*, No. 5, deep in north No. 3 and in the Portal veins). Pearceite-polybasite and proustite-pyrargyrite are most abundant in silver-rich veins along the

TABLE 2-6-4
BERRYITE AND GUSTAVITE COMPOSITIONS*

Element	1	2	3	4
Cu	6.37	6.43	6.30	0.19
S	17.52	17.69	17.44	16.95
Zn	0.00	1.23	0.00	0.00
Fe	0.04	0.24	0.00	0.00
Sb	0.00	0.00	0.00	0.00
As	0.00	0.00	0.00	0.00
Pb	20.37	20.13	20.76	23.67
Ag	7.29	8.20	7.62	8.60
Bi	48.75	46.01	47.60	49.91
Hg	0.00	0.00	0.00	0.00
Total	100.34	99.93	99.72	99.32

1 and 2: berryite from chalcopyrite-rich No. 3 vein.
3: berryite from the No. 5 vein.
4: gustavite from the Portal veins.
* values are as weight per cents.

Plate 2-6-3. Backscattered electron photomicrograph of berryite grain (medium gray) undergoing replacement by galena (pale coloured). From the deep north No. 3 vein. Scale bar at lower right is 4 microns.

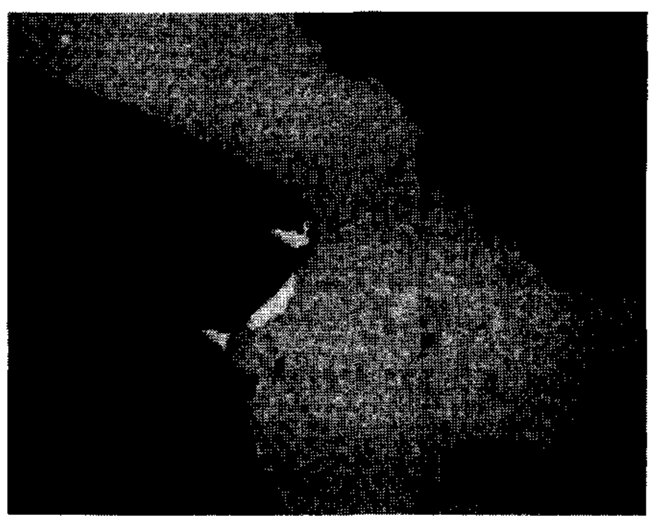

Plate 2-6-4. Electrum grains (white) occurring in embayments along the margin of large euhedral pyrite grain. Medium gray matrix is intergrown galena-matildite. From chalcopyrite-rich Portal vein material. Scale bar on lower right is 20 microns.

margins of the deposit. Symplectic intergrowths with galena are common for all silver sulphosalt species.

Electrum is the only gold mineral identified in the Silver Queen deposit, where it occurs as rare, but widely dispersed inclusions in galena or, less commonly, in sulphosalt minerals or pyrite. Electrum grains range in size from less than 5 microns to over 100 microns in diameter.

Sulphosalt minerals at the Silver Queen mine are interpreted to have been emplaced during the waning stages of a hydrothermal cycle under temperatures and pressures of less than 250°C. and 50 000 kilopascals (500 bars) (Hood, 1991). Sulphide and sulphosalt deposition was apparently controlled by mixing of hot, acidic waters with a cooler, more dilute meteoric fluid, with mineralogic zonation related to the stability of the metal-transporting species as the metal-charged fluids were carried away from the fluid source. Sulphosalt concentrations in the No. 3 and smaller veins thus represent sites of preferred deposition by copper, lead, bismuth and silver. To a lesser extent, the nature of the wallrock also appears to have influenced the deposition of sulphosalts in the No. 3 vein.

Silver sulphosalts tend to be concentrated along the outer margins of the deposit, corresponding to high silver-contents in tetrahedrite and the presence of abundant barite. As a result, the "peripheral" veins are interpreted to represent sites most distant from the fluid source (*e.g.*, Wu and Petersen, 1977) and where the influence of the cooler, more oxidized waters was most extreme (Hayba *et al.*, 1985). This particular occurrence is of importance when considering future exploration for silver and gold-rich parts of the vein system.

ACKNOWLEDGMENTS

The Owen Lake project is supported by a cooperative research grant from the Natural Science and Engineering Research Council and by industrial participants, initially Pacific Houston Resources Inc. and more recently New Nadina Explorations Ltd.. The authors thank M.L. Thomson, X. Cheng and M. Nowak for their helpful advice during evolution of the mineralogical part of the study. W. Cummings and J. Hutter are also thanked for their assistance during field work, and G. Carlson for his continuing interest and support.

REFERENCES

Bernstein, L.R. (1987): Mineralogy and Petrography of Some Ore Samples from the Silver Queen Mine, Near Houston, British Columbia; unpublished report; *Mineral Search*, Menlo Park, California, 13 pages.

Church, B.N. and Barakso, J.J. (1990): Geology, Lithogeochemistry and Mineralization of the Buck Creek Area, British Columbia; *B.C. Ministry of Energy Mines and Petroleum Resources*, Paper 1990-2.

Harris, D.C. and Owens, D.R. (1973): Berryite, a Canadian Occurrence; *Canadian Mineralogist*, Volume 11, pages 1016-1018.

Hayba, D.O., Bethke, P.M., Heald, P. and Foley, N.K. (1985): Geologic, Mineralogic, and Geochemical Characteristics of Volcanic-hosted Epithermal Precious-metal Deposits; *Reviews in Economic Geology*, Volume 2, pages 129-167.

Hood, C.T.S. (1991): Mineralogy, Paragenesis, and Mineralogic Zonation of the Silver Queen Vein System, Owen Lake, Central British Columbia unpublished M.Sc. thesis, *The University of British Columbia*, 273 pages.

Hood, C.T.S., Leitch, C.H.B. and Sinclair, A.J. (1991): Mineralogic Variation Observed at the Silver Queen Mine, Owen Lake, Central British Columbia (93L/2); *in* Geological Fieldwork 1990. *B.C. Ministry of Energy, Mines and Petroleum Resources*, Paper 1991-1, pages 185-191.

Leitch, C.H.B., Hood, C.T.S., Cheng, X. and Sinclair, A.J. (1990): Geology of the Silver Queen Mine Area, Owen Lake, Central British Columbia (93 L); *in* Geological Fieldwork 1989, *B.C. Ministry of Energy, Mines and Petroleum Resources*, Paper 1990-1, pages 287-295.

Marsden, H.W. (1985): Some Aspects of the Geology, Mineralization, and Wallrock Alteration of the Nadina Zn-Cu-Pb-Ag-Au Vein Deposit, North-central British Columbia; unpublished B.Sc. thesis, *The University of British Columbia*, 90 pages.

Nowak, M. (1991): Ore Reserve Estimation. Silver Queen Vein, Owen Lake Area, British Columbia; unpublished M.A.Sc thesis, *The University of British Columbia*, 204 pages.

Weir, B. (1973): Mineralogical and Milling Study of the Nadina Mine; unpublished report, *The University of British Columbia*, 23 pages.

Wu, I. and Petersen, U. (1977): Geochemistry of Tetrahedrite-Tennantite at Casapalca, Peru; *Economic Geology*, Volume 72, pages 993-1016.

NOTES

FLUID INCLUSION STUDY OF VEIN MINERALS FROM THE SILVER QUEEN MINE, CENTRAL BRITISH COLUMBIA (93L/2)

Margaret L. Thomson and Alastair J. Sinclair
The University of British Columbia

KEYWORDS: Economic geology, fluid inclusions, Silver Queen mine, epithermal deposit, Eocene mineralization

INTRODUCTION

Silver Queen mine in central British Columbia, is located approximately 35 kilometres south of Houston and 3 kilometres east of Owen Lake (Figure 2-7-1). Although currently inactive, it was worked briefly in the early 1970s for gold, silver, copper, zinc, lead and cadmium. The deposit is hosted by Cretaceous rocks of the informal Tip Top Hill group (78.3±2.67 Ma, K-Ar whole rock), with the age of mineralization bracketed by pre and post-mineralization dikes at 51.1±1.8 Ma and 51.9±1.8 Ma (K-Ar whole rock, Leitch *et al.*, 1990). Detailed descriptions of the regional and deposit geology are found in Lang (1929), Church (1970), Church and Barakso (1990) and Leitch *et al.* (1990).

The deposit is a complex epithermal vein system with ore generally restricted to delicately banded quartz-carbonate-sulphide-bearing veins (Plate 2-7-1). Hood *et al.* (1991) and Hood (1991) define four characteristic assemblages which represent early to late stages of mineral deposition within the veins. Stage I is characterized by the assemblage quartz-pyrite-hematite-barite, Stage II by the assemblage sphalerite and manganese-iron-rich carbonate, Stage III by quartz-chalcopyrite-tetrahedrite-galena and Stage IV by the assemblage quartz-barite-pyrite-calcite. Stages I and IV also contain bitumen as a coexisting mineral with barite. Rarely is a single vein comprised of all four stages; two consecutive stages are most common.

The composition and temperature of the fluid at the time of mineral deposition are estimated for the various paragenetic stages by measuring the homogenization temperatures of liquid and vapour phases and freezing point depression temperatures or temperatures of the disappearance of the last melt for the common minerals. These measurements provide important constraints for the interpretation of the geochemical and thermal evolution of the hydrothermal system that formed the Silver Queen deposit

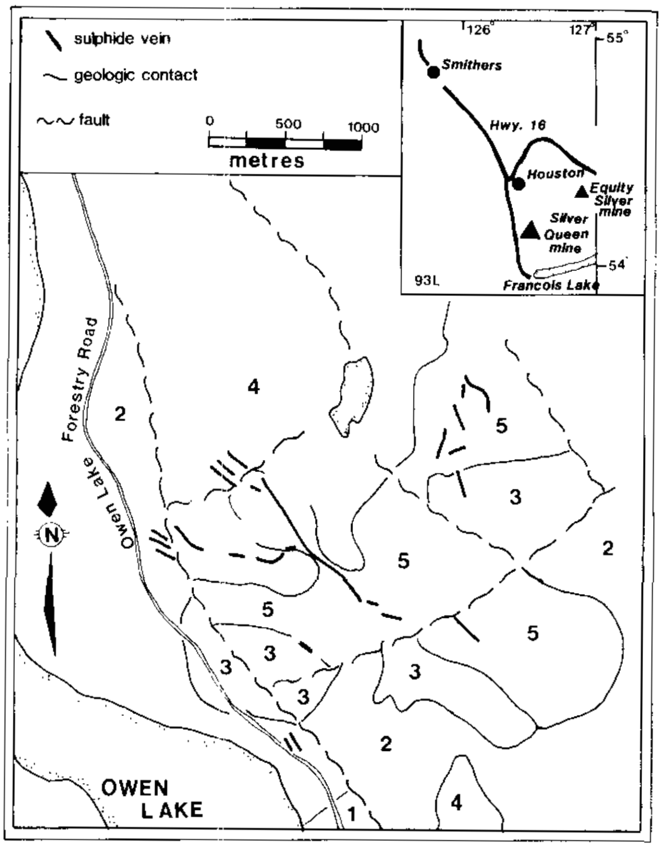

Figure 2-7-1. Location and simplified geologic map of the Silver Queen mine area.

FLUID INCLUSIONS

Fluid inclusions within minerals represent fluid which has been trapped either by irregularities during the growth of the host crystal, that is primary inclusions, or by the healing of later fractures to form secondary inclusions. Fracturing may also occur during crystal growth and healing of these fractures can produce pseudosecondary inclusions. In practise, distinguishing primary, pseudosecondary or secondary inclusions is not always straightforward. Generally, primary inclusions are found along well-defined growth zones, secondary inclusions occur as distinct trails which

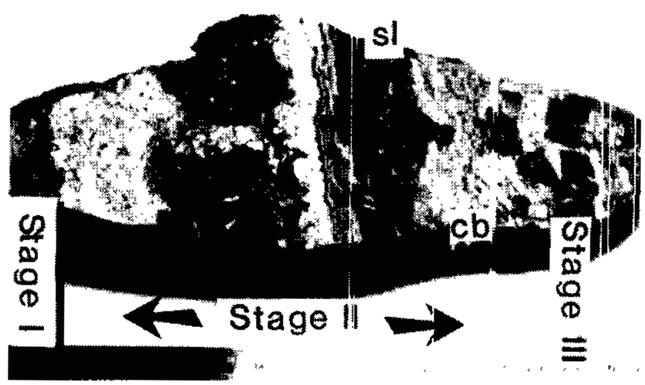

Plate 2-7-1. Photograph of typical ore vein within the Silver Queen mine. The left side of the sample (light grey) represents Stage I pyrite-quartz assemblage. The sample is dominated by Stage II sphalerite and carbonate, with minor Stage III carbonate to the right.

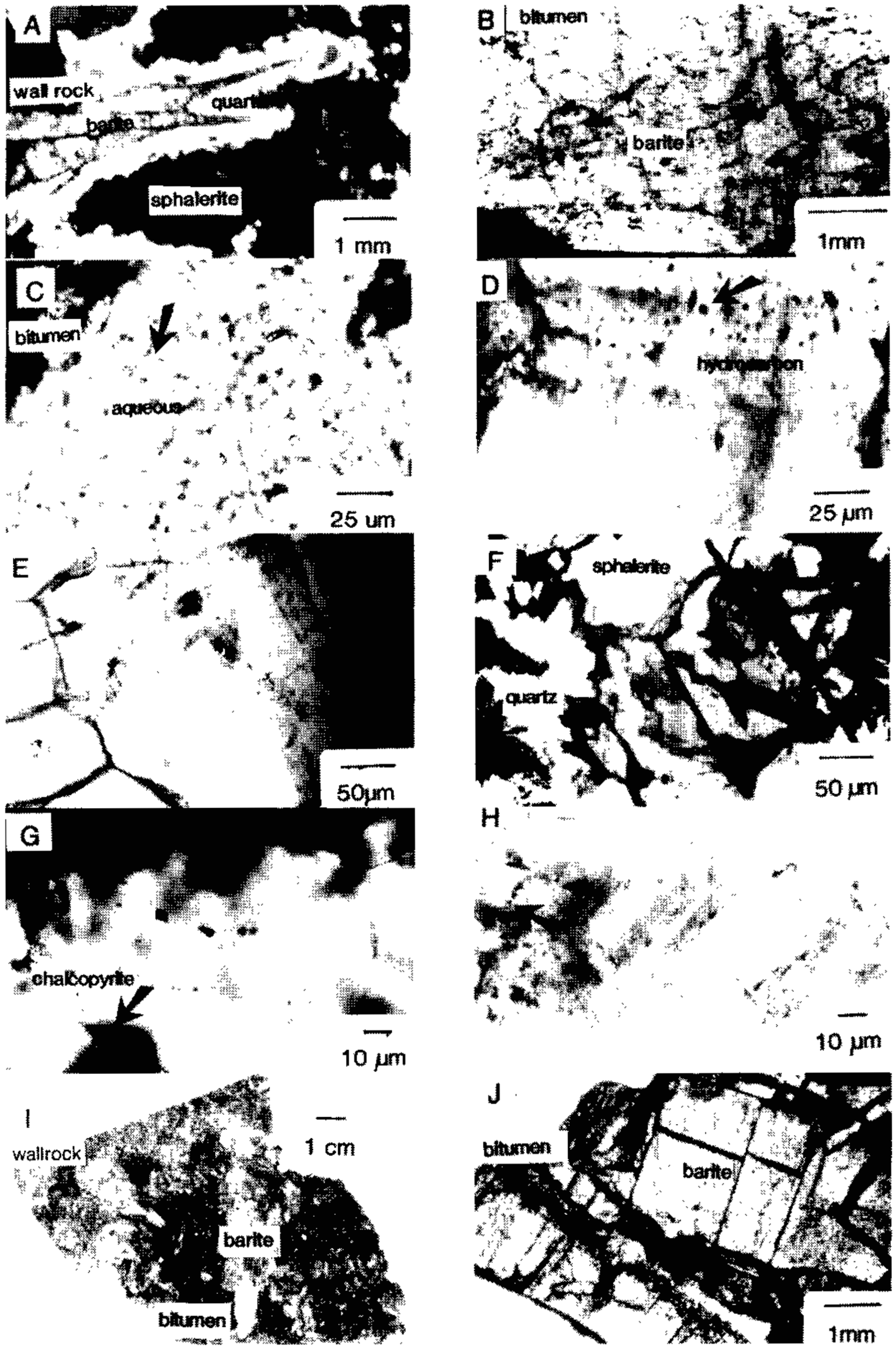

Plate 2-7-2. (a) Stage I barite blades oriented perpendicular to the vein wall. (*Photomicrograph slightly out of focus*); (b) Stage I barite with included bitumen; (c) colourless, aqueous, primary or pseuosecondary fluid inclusion within Stage I barite (arrow points to fluid inclusion with clear liquid and vapour phase); (d) amber-coloured, hydrocarbon-filled fluid inclusions within Stage I barite (arrow points to fluid inclusion with liquid and vapour phase); (e) Stage I, subhedral quartz crystals cut by trails of secondary aqueous fluid inclusions, dark inclusions are hematite; (f) Stage II sphalerite intergrown with euhedral quartz crystals; (g) primary or pseudosecondary fluid inclusions within Stage II sphalerite, fine inclusions of chalcopyrite (arrow) occur within sphalerite; (h) Stage III carbonate illustrating chevron-shape of banding and nature of primary fluid inclusions (arrow); (i) core sample of Stage IV barite with bitumen; (j) Stage IV barite, note blocky shape compared to needle shape of Stage I barite.

cross grain boundaries and pseudosecondary inclusions form as trails which are restricted to single grains and do not cross grain boundaries (*c.f.* Roedder, 1984).

The trapped fluid is commonly aqueous; however, in this study hydrocarbon-rich fluids are also present. Vapour and solid phases may also be present. The vapour may contain a mixture of water, carbon dioxide and methane or other gases, although water is usually the dominant phase. In most cases, the solid inclusion phases are alkali salts precipitated from the liquid (Roedder, 1984).

Homogenization temperatures (T_h) and melting temperatures (T_m) are the two data sets which were determined from the samples studied. Homogenization temperature represents the temperature at which the isovolume line intersects the liquid-vapour line. As most fluid has been trapped in inclusions at pressures and temperatures above the liquid-vapour curve, a correction for pressure is applied to T_h to determine the trapping temperature (T_t) as described by Potter (1977).

The melting temperature (T_m) provides an indication of the composition of the fluid. The freezing temperature of an aqueous solution containing dissolved salts is depressed relative to the freezing temperature of pure water. This temperature can be interpreted in terms of the percentage of NaCl dissolved in the solution that gives a freezing point depression temperature identical to the experimental value. The values presented are calculated after Roedder (1984). In every case, an attempt was made to make two determinations for every fluid inclusion, but this was not always possible. In some cases melting temperatures were not determined because of inability to clearly see a change in the inclusion during the heating of a super-cooled inclusion.

METHODOLOGY

For this study doubly polished rock plates were prepared on standard size thin-section glass. Fluid inclusions in quartz, barite, carbonate and sphalerite were examined. A Fluid Inc. adapted United States Geological Survey gas-flow heating and freezing stage system located at the Geological Survey of Canada (Vancouver) was used. Temperature calibration using SYN-FLINC® as described by Reynolds (1988; unpublished manual) results in an accuracy of 0.4°C from 56.6 to 660°C and a precision of ±1 per cent up to 200°C and ±2 per cent above 200°C.

The problem of the susceptibility of aqueous inclusions within barite to stretching when overheated past the homogenization temperature (Ulrich and Bodnar, 1988), and when frozen (Keenan *et al.*, 1978) was taken into consideration. Individual barite blades averaged 5 to 10 millimetres in length, allowing several chips to be taken from a single blade. The samples were frozen first and heated a maximum of three times. After heating, the ratio of volume of vapour to volume of liquid was observed to determine if stretching had occurred. If the inclusion had stretched, the vapour: liquid volume ratio would have decreased. No significant change was noted in any of the samples.

No melting temperatures were obtained for the hydrocarbon inclusions. Cooling to −90°C produced no visible freezing behavior within the liquid and subsequent warming produced no changes either.

SAMPLES

Fluid inclusions from six samples representing the four paragenetic stages were measured as follows: Stage I, barite and quartz; Stage II, sphalerite and carbonate; Stage III, sphalerite and carbonate; Stage IV, barite. Fluid inclusions in quartz from the wallrock of a Stage I vein were also measured. A summary of the inclusion descriptions can be found in Figure 2-7-2.

STAGE I INCLUSIONS

Stage I barite occurs as tapered blades, 1 to 8 millimetres long, rooted in and oriented perpendicular to the vein wall (Plate 2-7-2a, b). Clear aqueous and amber-coloured hydrocarbon inclusions occur within single blades (Plate 2-7-2c, d). The blades are clouded by evenly distributed, rectangular aqueous inclusions, 3 to 15 microns wide (average 5 μm), interpreted to be either primary or pseudosecondary. Primary or pseudosecondary hydrocarbon inclusions are less common, larger than the aqueous inclusions (average 15 μm) and tend to occur in patches. Trails of secondary aqueous and hydrocarbon inclusions clearly crosscut grain boundaries. They are rounded to oblong, and are smaller than the primary inclusions (3–10 μm wide).

Stage I quartz occurs as euhedral crystals, 1 to 3 millimetres wide, infilling hematite blades. Primary inclusions, 3 to 7 microns wide, occur with growth zones 0.5 millimetre wide, parallel to the hexagonal crystallographic outline. Secondary inclusions form distinct trails which crosscut boundaries of quartz grains and are parallel to vein walls (Plate 2-7-2e). The inclusions range in width from less than 4 microns to 8 microns, and average about 5 microns wide

STAGE	MINERAL	TYPE	SIZE	SHAPE	L:V
I	BARITE	AQ (P-PS)	3-15 (5)		5-10 (6)
		H (P-PS)	6-15 (10)		5-20 (10)
	QUARTZ	AQ (P)	3-7 (3)		10 (8)
		AQ (S)	4-8 (5)		6-10 (8)
		WR	3-5 (5)		5-10 (5)
II	SPHALERITE	AQ (P)	5-15 (10)		15-30 (20)
	CARBONATE	AQ (P)	5 (8)		15 (15)
III	SPHALERITE	AQ (P)	3-20 (5)		5-15 (8)
	X	AQ (PS)	3-15 (5)		5-10 (5)
	CARBONATE	AQ (PS)	3-5 (5)		5
IV	BARITE	AQ (P-PS)	3-10 (4)		10-20 (15)
		H (P-PS)	6-20 (6)		5-15 (8)

Figure 2-7-2. Summary of descriptive data determined for fluid inclusions in minerals from the four paragenetic stages in the Silver Queen veins. Bracketed values represent mean value. AQ, aqueous; P, primary; PS, pseudosecondary; HC, hydrocarbon; L:V, liquid to vapour ratio.

Stage II Inclusions

Stage II sphalerite occurs as bands 1 to 3 millimetres wide that parallel the vein wall. An intergrowth with euhedral quartz gives the sphalerite bands a wormlike outline (Plate 2-7-3f). The sphalerite is transluscent, zoned from colourless to honey coloured, with 0.5-millimetre bands of densely packed, large chalcopyrite blebs 1 micron wide (Plate 2-7-2g). Inclusions which occur singly with irregular distribution are interpreted as primary and those which occur in trails are pseudosecondary. The primary inclusions are irregular in shape, generally elongate (Plate 2-7-2g) and range in size from 3 to 20 microns long (averaging 10 μm). Pseudosecondary inclusions are rounded and range in size from 1 to 10 microns.

Carbonate occurs dominantly as patches of chevron-shaped bands 1 to 5 millimetres wide (Plate 2-7-2h). Most fluid inclusions in carbonate are difficult to measure because of high internal reflections and small size ($<1\ \mu m$). Primary fluid inclusions, 1 to 10 microns wide, are best developed and measurable along the growth zones of the bands.

Stage III Inclusions

Stage III sphalerite is massive, occuring as subhedral grains 1 to 10 millimetres wide, mostly isolated in carbonate matrix. Stage III sphalerite is brecciated, with grains clearly broken and rotated in a carbonate-quartz matrix. The inclusion style is the same as that for the Stage II sphalerite.

Stage III carbonate is massive, with no clear banding developed. Fluid inclusions occur evenly distributed, and range in size form 1 to 5 microns wide.

Stage IV Inclusions

Stage IV barite occurs as large (5-15 mm long) blades randomly oriented within the veins, with bitumen generally forming the matrix (Plate 2-7-2j). Fluid inclusions form in zones, generally within the core of a blade. Both aqueous and amber-coloured hydrocarbon inclusions are present. The aqueous inclusions are primary or pseudosecondary, with a rectangular to angular shape, and range from 3 to 10 microns long. The hydrocarbon inclusions are also primary or pseudosecondary, rounded to irregular in shape, and range from 6 to 20 microns long.

RESULTS

A total of 186 temperature measurements were completed, with the results summarized in Figures 2-7-3 and 4.

There is no independant geobarometer available to calculate the load pressure during deposition of the minerals studied. Quartz textures, although in no way a rigourous geobarometer, can be used to suggest the relative depth of deposition. Chalcedony may form a sinter in the surface or near-surface environment (Bodnar *et al.*, 1985) and as no sinter is found at the Silver Queen mine it is assumed that the vein formed at depth. Epithermal deposits occur within the upper 1.5 kilometres of the crust, therefore we can assume that the load pressure probably did not exceed 50000 kilopascals and was probably somewhat less. Given this maximum pressure, the temperature correction for the pressure differential (after Potter, 1977) of those inclusions with a T_h of approximately 220°C and salinity of 6.5 per cent NaCl equivalent is a maximum of 40°C, and for those inclusions with a T_h of 100°C and salinity of 2 per cent NaCl equivalent, a maximum of 50°C. Homogenization temperatures represent the minimum trapping temperature and the true trapping temperature is from zero to 50°C higher. Because of this uncertainty, reference will be made to the homogenization temperature in the following discussion.

Stage I fluid is relatively saline with a mode of 6.4 per cent NaCl equivalent and hot, with two populations of T_h at 260°C and 210°C. The primary inclusions in vein quartz and wallrock alteration quartz are more saline and hotter than the secondary inclusions in the quartz.

Stage II fluid shows a similar range of homogenization temperatures and salinity as Stage I. The peak T_h are slightly cooler, with modes at 230°C and 180°C and salinity is slightly elevated with a mode of 7.5 per cent NaCl equivalent.

Stage III homogenization temperatures are equivalent to the secondary inclusions in the vein quartz of Stage I, however, the salinity shows a complete range with the mode equivalent to that of Stage II fluids at 7.5 per cent NaCl equivalent. The limited sampling of fluid inclusions within brecciated sphalerite shows no significant difference between it and the *in situ* sphalerite.

Stage IV fluids are less saline and cooler than the other stages, although a broad compositional range is indicated. The homogenization temperature of hydrocarbon fluid is less than that of the aqueous fluid inclusions.

DISCUSSION

The variation in salinity of the aqueous fluid inclusions within and between each mineral stage suggests the presence of two distinct aqueous fluids within the system. The early stage fluid is relatively more saline than the later fluid. In hydrothermal systems saline fluids ($>25\%$ NaCl equivalent) are generally associated with a heat source, commonly an intrusive body (Henly, 1985). Such fluids are more saline than the strongest brines encountered in the Silver Queen samples. Weakly ($<1.7\%$ NaCl equivalent) to nonsaline inclusions are generally associated with meteoric fluids (Henly, 1985). It is suggested that mixing of these two fluids could result in salinity values noted in this study.

Independant evidence of a meteoric source for the weakly saline fluid comes from the hydrocarbon inclusions and associated bitumen. Carbon isotope values from bitumen of $\delta^{13}C \approx -27$ per mil from Stages I and IV indicate the source of the hydrocarbon to be the same and to be terrestrial plant material (Thomson *et al.*, in press). The difference in salinity between the two periods of hydrocarbon trapping and deposition represents a process of differential mixing with the more saline fluid.

Mineral deposition in the sulphide-bearing Stages II and III (Hood *et al.*, 1991) appears to be related to more saline fluids. This is consistent with the model of chloride as a complexing agent, transporting metals to the site of deposition (Barnes, 1979). Interestingly, the deposition of sphalerite appears to be insensitive to temperature, forming in a range from 255°C in Stage II to 85°C in Stage III. Corroborating the lower temperature of ore deposition in Stage III is the occurrence of the galena-matildite pair which is limited to a low-temperature stability range (Hood, 1991).

Boiling, or mixing of two fluids are the two common mechanisms invoked for the deposition of metals in epithermal deposits (Bodner *et al.*, 1985). When boiling occurs the steam phase and liquid phase are trapped in separate inclusions, producing a spatially related population of liquid-rich and vapour-rich inclusions (Roedder, 1984). Complicating this interpretation, however, is the possibility that the same texture was produced through secondary necking of a primary inclusion. During necking the vapour from the primary inclusion is not equally distributed into the newly formed pseudosecondary inclusion. Clearly care must be taken when interpreting the textures. In this study, there is no significant variation in the liquid:vapour ratio within a single population of fluid inclusions, suggesting that boiling probably did not occur within the system. This further supports a model of mixing of the two fluids.

The overall homogenization temperature, and therefore the trapping temperature, show a general decrease from Stage I to Stage IV. The similar homogenization temperatures and salinities of Stage III and the Stage I secondary fluid inclusions suggest that the early stage mineral assemblages were accessible to later stage fluids, probably through intermittent brecciation and veining.

Stage II is characterized by the presence of abundant manganese-iron carbonates, however, there is no evidence of the presence of measurable carbon dioxide within the attendant fluid. This absence of visible carbon dioxide in inclusions indicates its low partial pressure in the ore fluid (Fournier, 1985).

INTERPRETATION

The fluid inclusion data summarized here indicate two probable sources of fluid. One which was relatively hot and saline and one which was cooler and weakly to nonsaline. The hot, saline fluid is most likely related to a magmatic body interpreted to be at depth, as evidenced by the intimate association of dikes with the ore veins (Thomson and Sinclair, 1991). The cooler fluid is probably meteoric in origin,

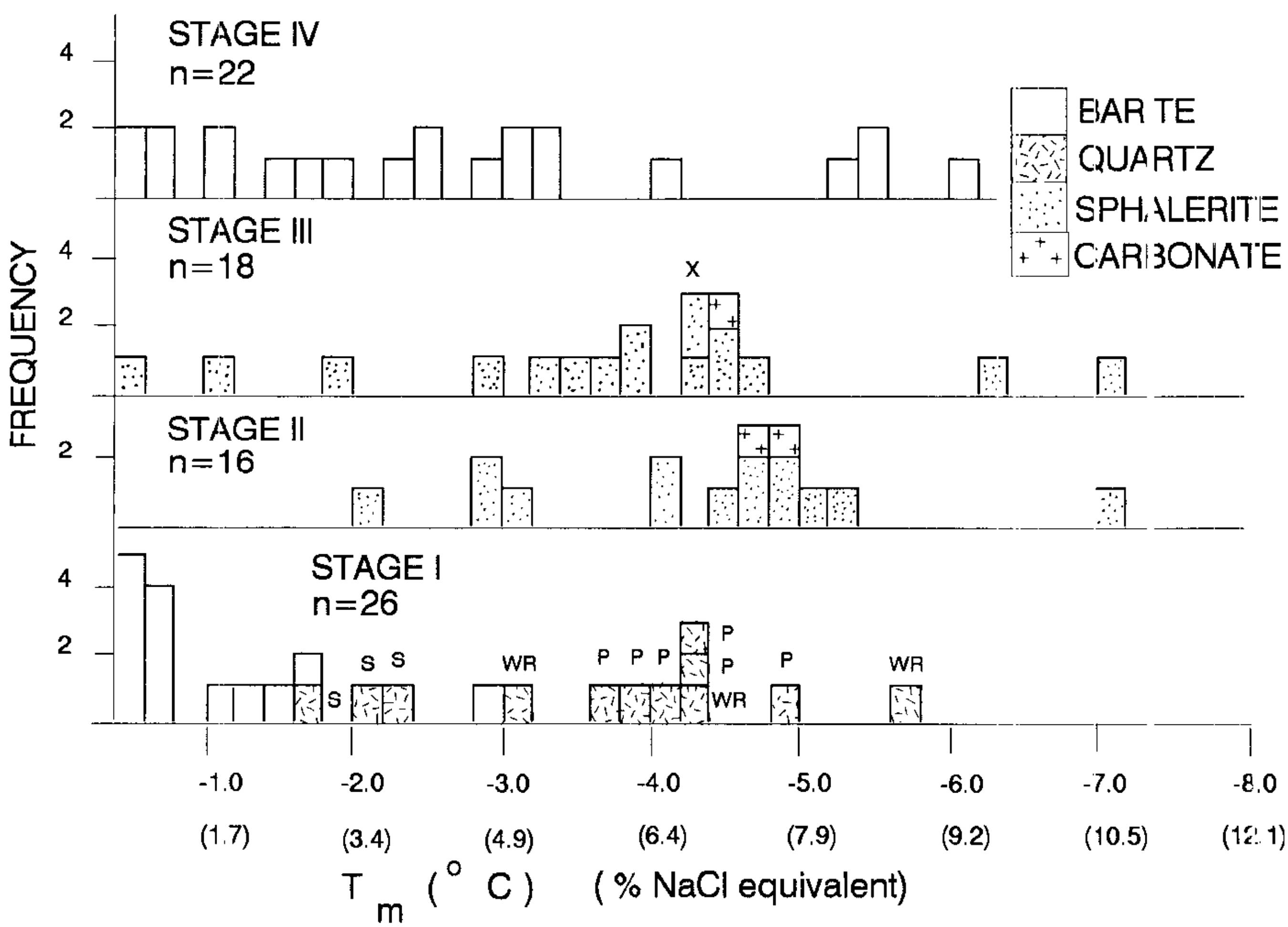

Figure 2-7-3. Histogram of homogenization temperatures. Patterns denote minerals studied. P, primary; S, secondary; and x, breccia.

heated by the magmatic body. Initial mixing of these two fluids resulted in the deposition of metals within the veins. With time, the mixed fluid became dominated by cooler, weakly saline fluid, indicating either the exhaustion of hot saline fluid or the sealing of the transport path.

Thomson and Sinclair (1991) have shown physical evidence of continuous fracturing and brecciation within the Silver Queen veins. The present study corroborates this by showing that a single crystal can contain several types, and therefore several generations of fluid inclusions. This will have significant impact on the choice of mineral grains for future stable isotope studies. Randomly choosing any grain may result in stable isotope data which represent a mixture, not end-member representatives of the fluid sources.

The Equity Silver mine, approximately 20 kilometres to the northeast of Silver Queen, is of comparable age and geology (Church and Barakso, 1990). Wojdak and Sinclair (1984) describe results of a fluid inclusion study of the Equity Silver ores and a comparison with Silver Queen data is interesting. The Equity Silver ore assemblages of arsenopyrite-sphalerite-chalcopyrite and chalcopyrite-tetrahedrite are broadly comparable to the Stage III and Stage II assemblages respectively at the Silver Queen deposit (Hood *et al.*, 1991). The homogenization temperatures of the Equity Silver mine assemblages are approximately 320 to 400°C and 260 to 310°C, a full 100°C hotter than those of the comparable Silver Queen assemblages. The melting temperatures or per cent NaCl equivalents of the Equity Silver inclusions are, however, remarkably similar to the comparable assemblage in the Silver Queen deposit, ranging from 3 to 10 per cent and 3 to 8 per cent for the two assemblages. It appears that the Equity Silver orebody may represent a deeper depositional environment, and in particular may have formed closer to the heat source than Silver Queen orebody.

CONCLUSIONS

- *Two fluids are involved in ore deposition at the Silver* Queen mine. One is saline and relatively hot and the other is weakly saline and relatively cool.
- The weakly saline fluid is probably meteoric in origin. Evidence comes from the presence of associated hydrocarbons derived from terrestrial plants.
- The source of the hotter, more the saline fluid is probably related to a magmatic body at depth.
- Fluid ingress and veining occurred repeatedly, overprinting earlier vein assemblages. This has implications for stable isotope analysis of vein minerals. Detailed examination of the samples is important to

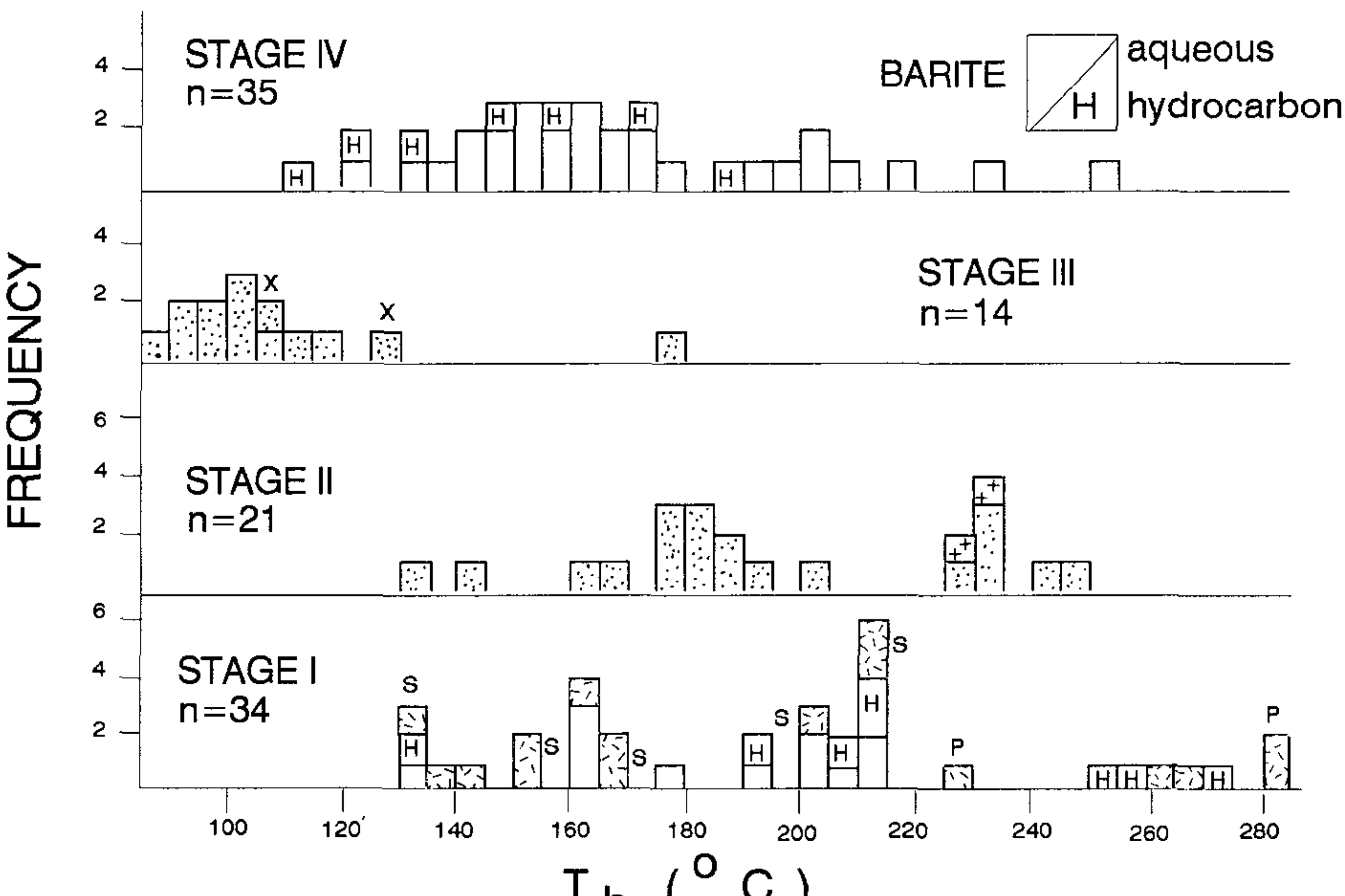

Figure 2-7-4. Histogram of melting temperatures with per cent NaCl equivalent as determined by equations given by Roedder (1984).

confirm if more than one episode of mineral deposition has affected the sample, allowing for possible re-equilibration.

- The temperature of ore deposition ($\approx$250°C) at the Silver Queen mine is about 100°C cooler than for comparable stages of mineralization at the Equity Silver mine, although the salinities of the fluids are similar (3-10% NaCl equivalent). This suggests that the Equity Silver orebody formed at a greater depth, closer to the magmatic heat source.

ACKNOWLEDGMENTS

The opportunity to work on this project comes through a joint industry (Pacific Houston Resources Inc.) and National Science and Engineering Research Council research grant to AJS. Dr. C.H.B. Leitch provided valuable assistance in techniques of fluid inclusion study. Y. Doumma provided well-crafted fluid inclusion plates for study. Editing by J.M. Newell improved the readability of the paper.

REFERENCES

Barnes, H.L. (1979): Solubilities of Ore Minerals; *in* Geochemistry of Hydrothermal Ore Deposits, Barnes, H.L., Editor, *John Wiley & Sons*, pages 404-460.

Bodnar, R.J., Reynolds, T.J. and Kuehn, C.A. (1985): Fluid Inclusion Systematics in Epithermal Systems; *in* Geology and Geochemistry of Epithermal Systems; Berger, B.R. and Bethke, P.M., Editors, *Society of Economic Geologists*, Reviews in Economic Geology, Volume 2, pages 73-98.

Church, B.N. (1970): Nadina (Silver Queen); *in* Geology, Exploration and Mining in British Columbia 1969, *B.C. Ministry of Energy, Mines and Petroleum Resources*, pages 126-139.

Church, B.N. and Barakso, J.J. (1990): Geology, Lithochemistry and Mineralization in the Buck Creek Area, British Columbia; *B.C. Ministry of Energy, Mines and Petroleum Resources*, Paper 1990-2, 95 pages.

Fournier, R.O. (1985): Carbonate Transport and Deposition in the Epithermal Environment; *in* Geology and Geochemistry of Epithermal Systems, Berger, B.R. and Bethke, P.M., Editors, *Society of Economic Geologists*, Reviews in Economic Geology, Volume 2, pages 63-72.

Henly, R.W. (1985): The Geothermal Framework for Epithermal Deposits; *in* Geology and Geochemistry of Epithermal Systems, Berger, B.R. and Bethke, P.M., Editors, *Society of Economic Geologists*, Reviews in Economic Geology, Volume 2, pages 1-24.

Hood, C.T.S. (1991): Mineralogy, Paragenesis, and Mineralogic Zonation of the Silver Queen Vein System, Owen Lake, Central British Columbia; unpublished M.Sc. thesis; *The University of British Columbia*, 275 pages.

Hood, C.T., Leitch, C.H.B. and Sinclair, A.J. (1991): Mineralogic Variation Observed at the Silver Queen Mine, Owen Lake, Central British Columbia; *in* Geological Fieldwork 1990, *B.C. Ministry of Energy, Mines and Petroleum Resources*, Paper 1991-1, pages 185-191.

Keenan, J.H., Keyes, F.G., Hill, P.G. and Moore, J.G. (1978): Steam Tables, Thermodynamic Properties of Water Including Water Vapor, Liquid and Solid Phase (SI units); *Wiley Interscience*, 156 pages.

Lang, A.H. (1929): Owen Lake Mining Camp, British Columbia; Summary Report, 1929, Part A; *Geological Survey of Canada*, 93 pages.

Leitch, C.H.B., Hood, C.T., Cheng, X.C. and Sinclair, A.J. (1990): Geology of the Silver Queen Mine Area, Owen Lake, Central British Columbia (93L); *in* Geological Fieldwork 1989, *B.C. Ministry of Energy, Mines and Petroleum Resources*, Paper 1990-1, pages 287-295.

Potter, R.W. II (1977): Pressure Corrections for Fluid Inclusion Homogenization Temperatures Based on the Volumetric Properties of the System NaCl-H_2O; *United States Geological Survey*, Journal of Research, Volume 5, pages 603-607.

Roedder, E. (1984): Fluid Inclusions; *in* Reviews in Geology, *Mineralogical Society of America*, Volume 12, 644 pages.

Thomson, M.L. and Sinclair, A.J. (1991): Syn-hydrothermal Development of Fractures in the Silver Queen Mine Area, Owen Lake, Central British Columbia (93L/2); *in* Geological Fieldwork 1990, *B.C. Ministry of Energy, Mines and Petroleum Resources*, Paper 1991-1, pages 191-197.

Thomson, M.L., Mastalerz, M., Sinclair, A.J. and Bustin, R.M. (in press): Implications of Bitumen and Hydrocarbon Fluid Inclusions to Fluid Source and Thermal History of Polymetallic, Epithermal Vein Deposits, Central British Columbia; *Mineralium Deposita*.

Ulrich, M.R. and Bodnar, R.J. (1988): Systematics of Stretching of Fluid Inclusions II: Barite at 1 Atmosphere Confining Pressure; *Economic Geology*, Volume 81, pages 1037-1046.

Wojdak, P.J. and Sinclair, A.J. (1984): Equity Silver-Copper-Gold Deposit: Alteration and Fluid Inclusion Studies; *Economic Geology*, Volume 79, pages 969-990.

NOTES

British Columbia Geological Survey
Geological Fieldwork 1991

THE LEXINGTON PORPHYRY, GREENWOOD MINING CAMP, SOUTHERN BRITISH COLUMBIA: GEOCHRONOLOGY (82E/2E)

By B.N. Church

KEYWORDS: Geochronology, Lexington, copper-gold porphyry, Precambrian basement, zircon dating.

INTRODUCTION

This report provides the results and interpretation of U-Pb analyses of zircon from the Lexington porphyry at the City of Paris mine in the Greenwood mining camp. The Greenwood camp is in Quesnel Terrane in the eastern part of the Intermontane Belt of southern British Columbia (Figure 2-8-1).

The geology and history of the Greenwood mining camp has been reviewed by Little (1983), Church (1986) and Fyles (1990). The Lexington copper-gold porphyry deposit and associated veins have been the target of exploration and development since 1890 on both sides of the International Boundary (Figure 2-8-2). In 1900 development at the City of Paris mine, 10 kilometres southeast of Greenwood, yielded 1900 tonnes of ore grading 13.7 grams per tonne gold, 71 grams per tonne silver and 3.12 per cent copper. In a similar geological setting, the Lone Star mine in Washington State produced 5900 tonnes of ore (1890-1920) that yielded 1.1 grams per tonne gold, 6.5 grams per tonne silver and 2.6 per cent copper; an additional 360 000 tonnes was mined from the same area in an open-pit operation in 1977-78.

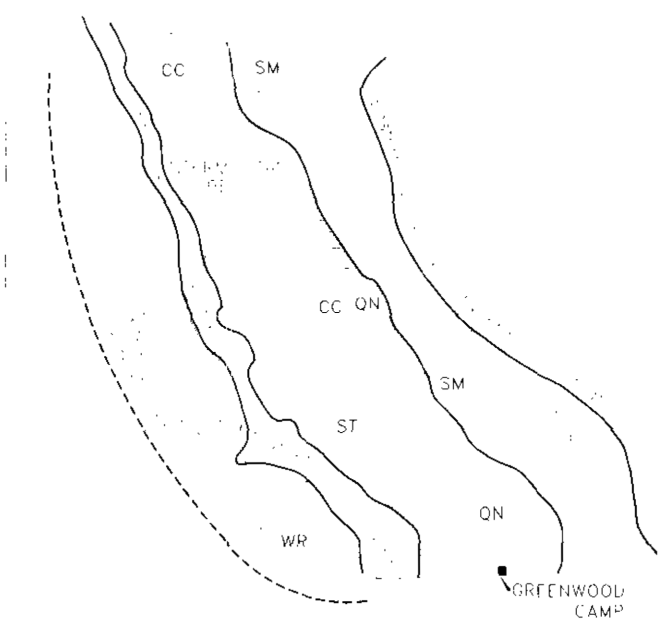

Figure 2-8-1. Major tectonic belts and terranes in the Canadian Cordillera. Key to abbreviations CC = Cache Creek Terrane, SM = Slide Mountain Terrane, WR = Wrangellia, ST = Stikinia, QN = Quesnellia (Price *et al.*, 1985).

GEOLOGICAL SETTING

The Lexington intrusion is an elongate quartz porphyry emplaced in a shear that extends 3 kilometres southeast from the headwaters of Goosmus Creek, through the City of Paris mine, across the International Boundary to the Lone Star mine in Washington. The intrusion follows a major zone of serpentinite and appears to be related to a larger quartz feldspar porphyry on the same break, exposed to the west on Gidon Creek and Hippolite Creek. These bodies cut Paleozoic units including chert, schist, argillite, limestone and greenstone of the Knob Hill and Mount Attwood groups (Figure 2-8-2).

The age of the Lexington porphyry was previously thought to be Cretaceous or earliest Tertiary by Little (1983), however, analyses of diamond-drill core samples submitted by the author to P. van der Heyden of The University of British Columbia give an Early Jurassic and a Precambrian age (Table 2-8-1 and Figure 2-8-3). The lower concordia intercept (200 Ma) indicates the age of intrusion of the porphyry; the upper concordia intercept (2445 Ma) is believed to be the result of a relict zircon fraction assimilated from (early Proterozoic) basement rocks.

DISCUSSION

The Intermontane tectonic belt is underlain by at least four allochthonous oceanic and off-shore island-arc terranes that evolved separately in middle and late Paleozoic and early Mesozoic time and were subsequently accreted to the North American craton. Knowledge of the temporal and spacial conditions of accretion is incomplete, however, it is known that the eastern terranes onlap the continental rocks and that this onlapping or docking was mostly achieved by middle Mesozoic (Price *et al.*, 1985).

In the Greenwood area the Knob Hill, Attwood (Paleozoic) and Brooklyn (Triassic) groups comprise multiple slabs of oceanic and transitional crust partly delaminated from their mantle and lithospheric base and overthrust onto the margin of the Precambrian craton. On the basis of strontium isotope studies (Armstrong *et al.* 1991), early Proterozoic rocks are believed to outcrop and subcrop in the Grand Forks area and to the east, and as far west as the Okanagan valley.

The Lexington porphyry is evidently contaminated by or rooted in the Precambrian basement rocks. This is suggested by an inherited zircon fraction dated 2445 Ma in core samples. Intrusion of the porphyry into the thrusted terrane in the early Jurassic, at 200 Ma, appears to pin the position of the terrane at this date and suggests that accretionary docking of oceanic rocks on the continental craton was completed by this time. This is in close agreement with the interpretations of Monger (1984).

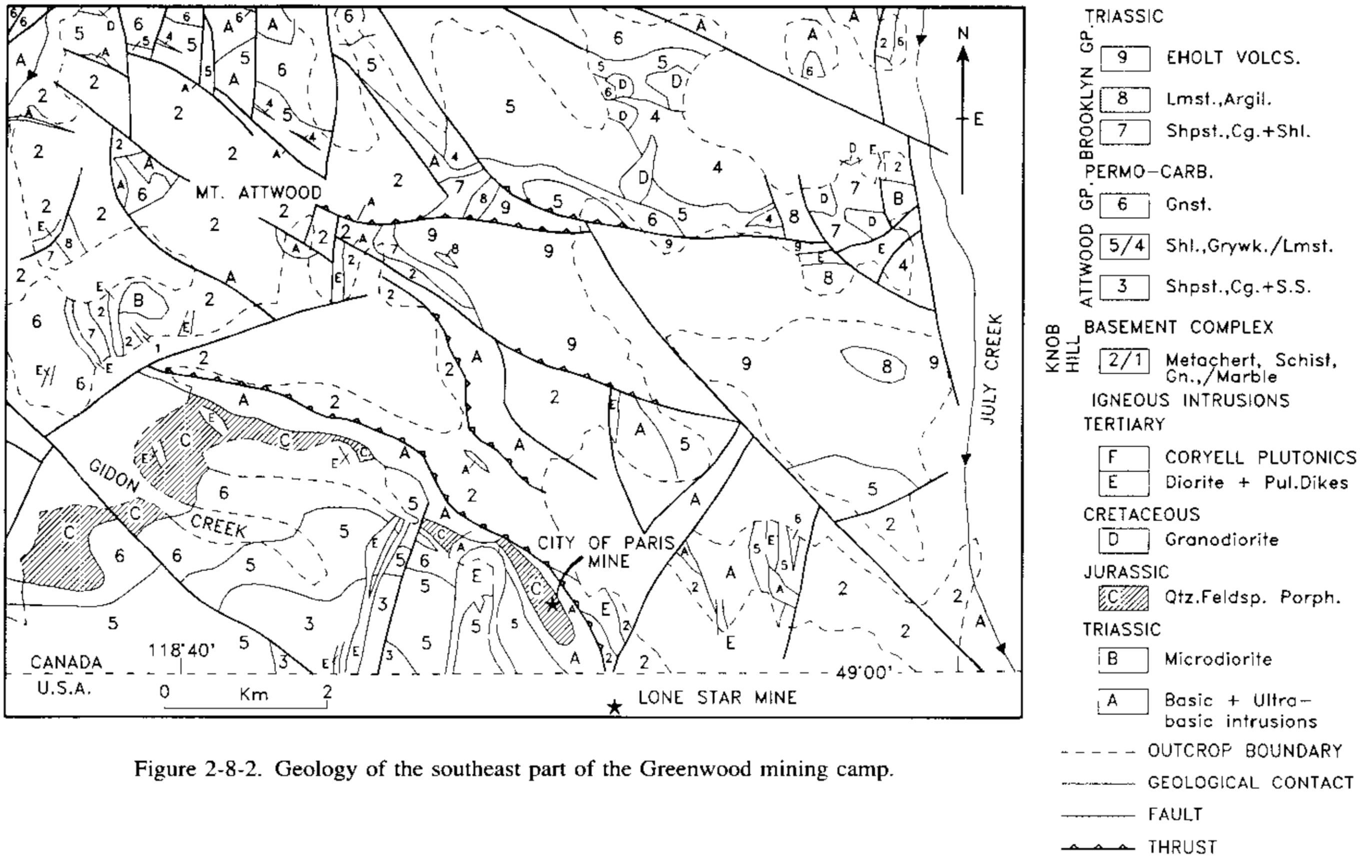

Figure 2-8-2. Geology of the southeast part of the Greenwood mining camp.

TABLE 2-8-1
URANIUM-LEAD ZIRCON DATA FOR LEXINGTON QUARTZ PORPHYRY

Sample No.	Location	Sample Properties	Weight (mg)	Concentration Observed (ppm) U	Pb	$^{206}Pb/^{204}Pb$	Atomic Ratios[3,4] $^{206}Pb/^{238}U$	$^{207}Pb/^{235}U$	$^{207}Pb/^{206}Pb$	Model Ages (Ma)[4] $^{206}Pb/^{238}U$	$^{207}Pb/^{235}U$	$^{207}Pb/^{206}Pb$	Concordia Intercepts low	high
FLY 86-1	49°0.5' 118°36.5'	nm,<100μm	0.8	130.6	4.0	1438	0.03141±0.00023	0.2177±0.0028	0.05027±0.0050	199.4±1.4	200.0±2.3	207.5±23.1	200	2445
		m, 100-200μm	4.6	166.7	5.4	1555	0.03219±0.00024	0.2302±0.0033	0.05187±0.0061	204.3±1.5	210.4±2.7	279.6±26.5		
		m,>200μm	2.4	197.5	6.3	2808	0.03175±0.00023	0.2286±0.0020	0.05223±0.0024	201.5±1.4	209.1±1.6	295.5±10.2		

Note: Sample submitted by B.N. Church, analysis performed by P. Van der Heyden.

A cluster of other Early or Middle Jurassic felsic intrusions in the Nelson area, that may be related to the Lexington porphyry, has been noted by Dunne and Höy (1992, this volume). These include the Rossland monzonite and the smaller Aylwin and Lectus bodies. Although these are slightly younger than the Lexington body, they are similarly mineralized and show early Proterozoic zircon inheritance. It may be that felsic intrusions of this character in this region of the Quesnel Terrane are favoured for porphyry-gold mineralization, however, data are insufficient to be conclusive.

ACKNOWLEDGMENTS

Many thanks are owing J.T. Fyles of Kettle River Resources Ltd. for assisting in collecting samples and to P. van der Heyden of The University of British Columbia for zircon analyses and dating. The author acknowledges with appreciation drafting services provided by A. Pettipas and review of the manuscript by D.V. Lefebure, J.M. Newell and B. Grant.

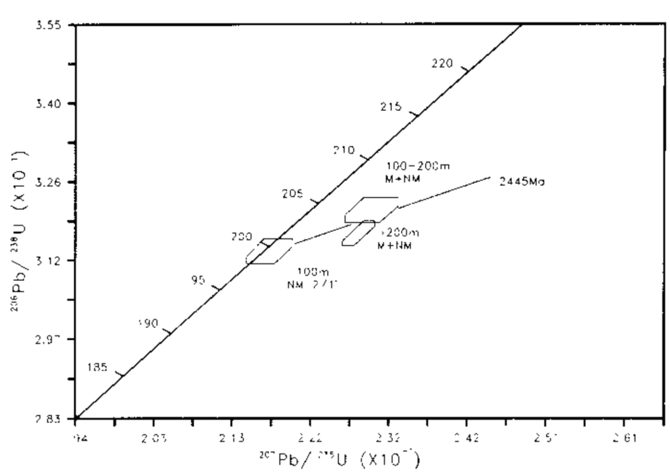

Figure 2-8-3. U-Pb concordia diagram for the Lexington porphyry. Lower intercept at 200 Ma is interpreted to be crystallization age of intrusion; the upper intercept at 2445 Ma is inherited from basement rocks.

REFERENCES

Armstrong, R.L., Parrish, R.R., van der Heyden, P., Scott, K., Runkle, D. and Brown, R.L. (1991): Early Proterozoic Basement Exposures in the Southern Canadian Cordillera: Core Gneiss of Frenchman Cap, Unit I of the Grand Forks Gneiss, and the Vaseaux Formation; *Canadian Journal of Earth Sciences*, Volume 28, Number 8, pages 1169 to 1201.

Church, B.N. (1986): Geological Setting and Mineralization in the Mount Attwood – Phoenix Area of the Greenwood Mining Camp; *B.C. Ministry of Energy, Mines and Petroleum Resouces*, Paper 1986-2, 65 pages.

Dunne, K.P.E. and Höy, T. (1992): Petrology of Lower Middle Jurassic Intrusions, Rossland Group, Trail Map-area; *in* Geological Fieldwork 1991, Grant, B. and Newell, J.M., Editors, *B.C. Ministry of Energy, Mines and Petroleum Resources*, Paper 1992-2 this volume.

Fyles, J.T. (1990): Geology of the Greenwood – Grand Forks Area, British Columbia; *B.C. Ministry of Energy, Mines and Petroleum Resources*, Open File 1990-25, 19 pages.

Little, H.W. (1983): Geology of the Greenwood Map-area, British Columbia; *Geological Survey of Canada*, Paper 79-29, 37 pages.

Monger, J.W.H. (1984): Cordilleran Tectonics A Canadian Perspective; *Bulletin de la Societé Geologique de la France*, Volume 26, pages 255 to 278.

Price, R.A., Monger, J.W.H. and Roddick, J.A. (1985): Cordilleran Cross-section; Calgary to Vancouver; *in* Field Guides to Geology and Mineral Deposits in the Southern Canadian Cordillera; *Geological Society of America*, Cordilleran Section Meeting, Vancouver B.C., May '85, pages 3-1 to 3-85.

NOTES

British Columbia Geological Survey
Geological Fieldwork 1991

STREAM-SEDIMENT PETROGRAPHY USING THE COARSE FRACTION OF STREAM SEDIMENTS

By Jay W. Page
Westex Exploration Ltd.

KEYWORDS: Economic geology, petrography, stream-sediments, alteration.

INTRODUCTION

The mining industry has traditionally relied upon stream-sediment geochemistry as a primary exploration technique. Its value in this regard is largely unquestioned and it is an important part of any regional program. However, there are limitations on its use in some environments, notably the British Columbia Coast Range.

In the Coast Range, many of the high-energy mountain streams, particularly the first and second-order streams, have little, if any, fine silt in their stream beds. This is a problem for conventional geochemistry because normally only the fines (−80-mesh fraction) are analyzed. The technique of sampling moss mats (Matysek and Day, 1988) has partly addressed this problem by increasing the range of materials that can be sampled. A second problem also exists in the Coast Range: active glaciation generates large quantities of silt that can dilute most geochemical signatures below detection. Both of these factors create significant sampling problems.

Interpretation of stream-sediment geochemistry in the Coast Range is difficult. Although it is largely underlain by plutonic rocks, there are many roof pendants which are the focus of most exploration activity. Contact metamorphic effects along the margins of these pendants has created numerous small skarns and quartz veins, many of which contain minor amounts of base metals. This mineralization generates numerous base metal anomalies, which may obscure more subtle geochemical signatures of economic mineralization. Compounding this problem is the fact that the primary exploration targets in the Coast Range are the volcanogenic massive sulphide deposits - a deposit type for which stream-sediment geochemistry is poorly suited unless mineralization is exposed on the surface.

Additional factors in the Coast Range include the extremely rugged terrain, the high rainfall and the dense coastal forest. Exploration is difficult and expensive. Stream-sediment geochemistry is routinely carried out, despite its widely recognized limitations, because there is moderately good access to streams for boat and helicopter-supported programs. However, in spite of the ease of access provided by helicopters and the advances in stream-sediment geochemistry over the past several decades, there have been few new discoveries. Most known occurrences were found by prospectors years ago, and most of the old mines and the better known properties are in the accessible areas of the islands (*e.g.*, Little Billie mine, Surf Inlet mine), or near access routes through the mountains (*e.g.*, Britannia mine).

Clearly there is a need for a regional technique which, like stream-sediment geochemistry, can detect mineralization from a distance, and can evaluate large areas with a limited number of samples in an economical and efficient fashion. The technique should be able to provide information to aid the interpretation of stream-sediment geochemical anomalies and be capable of evaluating areas where sampling problems exist.

A technique with the potential to satisfy these requirements is "stream-sediment petrography", here defined as the identification and interpretation of drainage-basin geology based on the microscopic examination of stream sediments. For the explorationist, this is a technique which can identify rock and mineral fragments in stream sediments which are normally associated with ore deposits, and can provide information about mineralogical anomalies, such as alteration zones, which may be important to the interpretation of geochemical anomalies.

Alteration zones are commonly the result of hydrothermal processes and are associated with many ore deposits. Generalizations about hydrothermal processes and wallrock alteration are not warranted in the context of this paper, other than to note that the alteration mineral assemblage often reflects additions or losses of the rock-forming elements, such as potassium, sodium, silica, magnesium and iron. These subtle changes in composition can be detected by soil geochemistry. However, a stream sediment is essentially a sample of a large area, and as there may actually be very little variation in the bulk chemistry of an area, these changes in the rock-forming elements are not usually identified by stream-sediment geochemistry. However, stream-sediment petrography does have the potential to detect these changes in mineral composition.

This paper describes the results of a study to develop a method of stream-sediment sample preparation suitable for binocular microscope examination and techniques to enhance the detection of alteration minerals in stream sediments.

COARSE FRACTION STUDY

The coarse fraction as defined for this study is the +80-mesh fraction; that is, material that does not pass through a screen which has a nominal opening of 180 microns. Such material is present in virtually all stream-sediment samples, but because it is coarser than the material used for analysis, it is usually discarded.

There are a number of reasons for choosing the coarse fraction, among them being the need to base interpretations on mineral associations, so the presence of rock fragments, as opposed to monomineralic grains, is essential. Also, the identification of alteration often depends upon being able to see grain boundaries. Another consideration is that many sediment particles are coated with a rind of hydroxides. These particles must be large enough so that fresh rock is exposed in the centre when they are cut. There are also practical considerations, including the relative difficulty of examining small grains under a microscope, and the abundance of coarse material in the high-energy Coast Range streams.

Conventional stream-sediment geochemistry is a four-step process, consisting of: sample collection, sample preparation, analysis and interpretation. Stream-sediment petrography follows a similar process, albeit with a different type of preparation, and analysis is by microscope. The present study has focused primarily on the sample preparation and microscope examination steps.

Sample collection has not been addressed in the coarse fraction study. Field studies are needed to determine the characteristics and behaviour of alteration minerals in the fluvial environment before a specific type of sample site can be recommended. For the time being, it is assumed that samples for stream-sediment petrography will be collected from the active channel in the same manner as samples for geochemical analysis. The possibility that moss-mat samples contain a bias toward heavy minerals at the expense of lighter alteration minerals likewise has not been investigated.

The study utilized samples from two sources. Test samples were created from crushed and sieved altered rock, and stream sediments were obtained from the Geological Survey Branch. The test samples were made up from material such as: silicious pyritic ore from the Britannia mine and from the H-W orebody at Myra Falls on Vancouver Island; epidote and chlorite alteration envelopes from Gambier Group quartz veins; chlorite and sericite schists from the Gambier Group and the Eagle Bay assemblage; rhyolite from Westmin's Price and H-W orebodies; a high-potassium rhyolite from the Gambier Group; pyrite in quartz veins from the Harrison Formation; and orthoclase from the Beaverdell granite. This material was mixed in various concentrations with a quartz-plagioclase sand from Scuzzy Creek and with chlorite schist from the Gambier Group.

The test samples were augmented by stream sediments from the Geological Survey Branch sample library. These samples consisted of the −18 and +80-mesh fraction left over from recent Regional Geochemical Surveys in southwestern British Columbia. Samples were selected from a variety of deposit types, and included: the Britannia mine (volcanogenic massive sulphide), the OK porphyry (porphyry copper), the Merry Widow (skarn), Mount Washington Copper (porphyry copper), and Lara (volcanogenic massive sulphide). The lack of coarse material in the samples and limited sample density in the deposit areas precluded detailed studies of each area. The samples did, however, provide an opportunity to test the preparation techniques on stream sediments collected around ore deposits.

The coarse fraction study did not directly address the fourth step in the evaluation process – interpretation. The significance of alteration minerals in stream sediments must be based upon comparisons with stream sediments collected around well-known deposits. This information can only be determined from detailed field studies.

Sample Preparation

A variety of preparation techniques was investigated at various stages of the study. There were two objectives: to determine the best possible technique in terms of accuracy and repeatability, and to develop a technique which could be carried out in any medium-sized exploration camp, which at the same time did not significantly compromise the quality of information. Both objectives were achieved and are described below. It is worth noting that the technology for producing polished sections for the study of ore minerals is well developed and could produce excellent samples for stream-sediment petrography. However, in general, polished sections are too small to contain a representative-sized stream-sediment sample, and the equipment needed to prepare them would never be considered suitable for use in a field camp.

SIEVING

Choosing an appropriate sieve size is of considerable importance, and as noted above, the greater amount of information in rock fragments must be balanced against the more representative nature of samples of finer fractions. In the coarse fraction study, three sieve sizes were examined: −5 to +20-mesh, −10 to +35-mesh, and −20 to +40-mesh (U.S. standard sieve sizes). In the following discussion, reference to "fine material" is to sediment smaller than 1 millimetre in size, such as the −20 to +40-mesh fraction.

The Geological Survey Branch samples contained large amounts of coarse organic material, which considering that all the samples from Vancouver Island were moss mats, was not surprising. These organics were easily removed by lightly blowing over a shallow pan after dry sieving. However, if fine organics are a problem, then wet sieving may be the best solution. It is important to have clean sediment particles to ensure a good bond with the casting resin.

RESIN CASTING

Early tests with loose sediment demonstrated that it was not suitable for staining, and identification of minerals present in low concentrations was difficult. Casting the sample and working with a polished surface proved to be far superior in terms of the ease and accuracy of the microscopic identification.

Tests were carried out on a variety of potential casting media, including polyester resin, epoxy resin, plaster of paris and several cements. The following criteria were used to evaluate each medium:

- It must be inexpensive, easy to prepare and set quickly. It must be relatively inert and not react with the sample, the mould, or with any of the chemicals used in staining.
- It must be strong enough to hold the sediment fragments firmly during the cutting and polishing operation.

- It must not smear over the fragment faces during cutting and polishing, preventing them from being etched and stained.
- It must polish well and provide good contrast with the sediment fragments.

Both the polyester resin and the epoxy resin produced acceptable results. The polyester resin was chosen over the epoxy because it is less expensive and easier to mix and work with. This resin is a clear, waxable polyester resin of the type used by the fibreglass industry.

A variety of casting moulds were experimented with. The most suitable was found to be the petri dish. These inexpensive plastic dishes, which are normally used for growing biological cultures, are ideal for casting samples. They are about 9 centimetres in diameter, 1 centimetre deep and have a flat bottom. With a surface area of about 58 square centimetres on the prepared sample, a large number of sediment particles (approximately 20 000 in the −20 +40-mesh sieve interval) are exposed. The prepared sample disk is about 8.5 centimetres in diameter and this is approximately the maximum size that can easily be accommodated on a microscope stage.

The petri dish has a capacity of 62 cubic centimetres, although, an acceptable sample can be prepared from as little as 10 cubic centimetres (about 25 grams) of sediment. The sample is mixed with resin in a disposable cup, and poured into a dish in sufficient quantity to cover the bottom. The dish is then topped up with resin. A sample-disk thickness of 1 centimetre is necessary for strength and ease of handling. After the resin has set, the petri dish must be removed – a process which is made much easier by waxing the dish with a non–silicone-based paste wax prior to casting.

POLISHING

Several techniques of preparing the sample surface were tested, with mixed results. The type of finish has a large effect on the quality of information obtained and it is the critical step in the sample preparation process. The best results were produced by a commercial vibrating lap and this was apparent at an early stage in the testing. However, much of the testing was directed at developing a technique suitable for use in a field camp.

The vibrating lap was used with 220 and 600-grit silicon carbide abrasive and tin oxide polishing compound. A 1 kilogram weight was placed on each sample during grinding and polishing to speed-up the process. The lap yielded the best overall results in terms of the accuracy and ease of identification of all of the minerals studied. The only disadvantage of this technique is that it is very slow. A 15-inch lap can only produce about 8 samples per 24-hour period.

Alternative techniques, with a higher production rate and suitable for field use were investigated. They included sawing samples into slabs with a rock saw, and preparing the sample surface with a variety of sanding and grinding media.

Rock saws can produce samples which are quite adequate for identifying gross lithological features, such as common rock types, and for identifying distinctive minerals such as epidote and pyrite if they comprise at least several per cent of the sample. The surface can be etched and stained to identify the presence of potassium minerals, although identifying the actual mineral may be difficult. Larger sample sizes are needed for sawing, typically about 200 cubic centimetres, and the best results are obtained with coarse fragments (larger than several millimetres in diameter). Material smaller than 1 millimetre produced poor results in the study due to the particles being plucked out of the resin.

The sawn samples can be polished with a vibrating lap, although there is no advantage gained by having cut the samples. Sawing produces neither a flat nor a smooth surface. Additionally, the forceful cutting action of a saw shatters brittle minerals such as quartz and pyrite. The mineral identification techniques use the resin surface as a reference, based on the assumption that the resin and mineral surfaces were smooth and contiguous prior to etching. The shattering caused by sawing creates negative relief which must removed before it can be polished. This increases the time needed for the 220-grit grinding, because an entire layer of mineral grains must be removed. In addition, pieces of the shattered minerals break free and contaminate the grinding media with oversize material, resulting in the need to replace the grit frequently.

A more useful polishing technique uses a sanding head. This is a flat disk, covered with sandpaper and fixed to an electric motor. Tests were carried out with a 15-centimetre diameter sanding head attached to a 0.25 horsepower electric motor which rotated at 1725 rpm. The samples, cast in petri dishes, were sanded with silicon carbide sandpaper in the sequence: 80, 120, 240, 320, 400 and 600. The first three in the sequence were sanded dry, the remainder wet. The paper was backed with a neoprene pad 5 millimetres thick.

Moderately good results were obtained using this method, and they were comparable to the polished samples produced by the vibrating lap. In terms of mineral identification and staining, sanding produced surfaces that were adequate for the −20 to +40-mesh fraction marginal for the −10 to +35-mesh fraction and poor for the −5 to +20-mesh fraction. The coarser sizes are more difficult to prepare because the large grains are resistant to abrasion, while the relatively soft resin between the grains is worn away, leaving pits. The sanding technique proved to be poor for preparing samples containing more than several per cent sulphides. In contrast, the polished samples produced by the vibrating lap were excellent in all three sizes, and were much better for sulphide-rich samples.

The fine size material (<1 mm in diameter) can be rough polished using the 80, 120 and 240-grit dry-sanding sequence and this is adequate for identifying most minerals. This technique could be useful in a field camp setting because a sample can be prepared in about 5 minutes. The higher quality 600-grit polish requires much more time and effort and does not produce significantly more useful samples. If the fine grain sizes are of interest (such as in the detection level studies described later) and time is a constraint, then the best approach is to use the sanding technique to identify the interesting samples which can then be polished using the vibrating lap.

ETCHING AND STAINING

After the sample surface has been polished, it is etched with hydrofluoric acid and stained with sodium cobaltinitrite. The purpose of the etching is twofold: it prepares a fresh surface on potassium minerals so they can react with the sodium cobaltinitrite, and it variably etches the rock and mineral fragments allowing quartz to stand out in positive relief from the rest of the fragment. This is the primary method used to identify silicification, quartz-sericite schist, rhyolite and potassic alteration.

An important factor controlling the identification of these features is the length of time the sample is etched with hydrofluoric acid. Etching tests carried out on standard samples indicated that a 20-second etch time with 48 per cent hydrofluoric acid produced the best results on polished samples. All samples were stained by dipping them in a concentrated solution of sodium cobaltinitrite for 60 seconds. Shorter etching times reduced the contrast between quartz and most other minerals, although a 5-second etch time was able to remove the polish from most non-quartz minerals, allowing them to be readily identified with a hand lens. Etching in excess of 30 seconds bleached most minerals beyond recognition and reduced the effectiveness of the staining.

Sample Examination

Samples were systematically examined under a binocular microscope using reflected light. It was found that 10-power was best for estimating percentages of easily identified minerals, and 30-power was useful for examining most fragments. A 45-power lens is useful for the occasional detailed examination of individual fragments smaller than approximately 20-mesh (850 microns). The value of the binocular microscope over the monocular microscope becomes readily apparent when examining the relief created by the acid etching, or when viewing fractures, cleavages and crystal shapes visible in the clear resin below the sample surface.

Many of the mineral properties used to identify hand specimens are also useful for identifying stream-sediment fragments. The binocular examination is augmented by the use of hydrochloric acid (for identifying carbonates), a magnet, and a needle (for testing hardness). It is difficult to identify metallic minerals with any confidence. Exhaustive test procedures for the metallic minerals are described by Short (1940). Samples prepared using a vibrating lap are polished to approximately the same standard as conventional polished sections, and detailed examinations of metallic minerals could be carried out with a reflecting light microscope. Similarly, thin sections can be cut from the sample disks for detailed petrographic work.

MINERAL IDENTIFICATION

The following list of minerals were chosen for study because they are commonly associated with alteration zones and ore deposits. The list is not exhaustive; further work in stream-sediment petrography will no doubt broaden the scope to include other minerals and refine the techniques of identification. The features listed are those characteristics that were observed in the study and are based on a limited number of samples. All of the samples were etched and stained as described above.

Pyrite

- Brass-yellow colour, metallic lustre when polished, fine pebbled finish when viewed under 30-power.
- Chipped edges and conchoidal fractures common on edges of fragments.
- Cubic crystal form and striated crystal faces may be seen in resin below the surface.
- Hard, cannot be scratched by a needle.
- Rarely contained in rock fragments smaller than 1 millimetre.
- Surfaces may appear black (due to pyrite powder) if prepared using the sanding technique.

Chalcopyrite

- Distinctive greenish yellow colour.
- Polishes poorly, with broken edges, and has an irregular felted appearance on surfaces.
- Soft, can be easily scratched by a needle.

Magnetite

- Polishes to a silvery-grey colour with a metallic lustre, turns to a dark grey colour with a dull lustre after hydrofluoric acid etching.
- Magnetic.
- Hard, cannot be scratched by a needle.

Calcite

- Effervescence when exposed to hydrochloric acid.
- Rhombohedral cleavage may be visible below the surface in resin.
- Soft, easily scratched.

Epidote

- Distinctive green colour.
- Little effect from hydrofluoric acid etching.
- Hard, cannot be scratched by a needle.

Chlorite

- Medium to dark green colour.
- Soft, but if associated with quartz or epidote, it may appear to be hard.
- High relief when etched, but this may not be apparent if associated with quartz or epidote.

Quartz

- Stands out in positive relief from the rest of the rock fragment after etching.
- Commonly has a glassy appearance.
- Polishes to a high lustre, polish turns to a slightly pebbled surface when etched for 20 seconds.
- Hard, cannot be scratched by a needle.
- Conchoidal fracture commonly visible in resin below the sample surface.

Potassium-rich Minerals and Rocks

These minerals and rocks are identified as a group by the yellow potassium cobaltinitrite stain. All stained surfaces have been etched leaving negative relief.

- ORTHOCLASE: Identified by rich yellow stain which often has a frambroidal habit. The stain commonly leaves an irregular, linear pattern of yellow lines on a glassy background. The prominent c-axis cleavage may be visible below the surface of the resin.
- SERICITE: Identified in schistose fragments by tiny, pale yellow, wispy streaks which may form most of the fragment. A pronounced foliation is common, even in tiny fragments. Often associated with fine-grained quartz which stands out in positive relief.
- RHYOLITE: Included under potassic rocks because it is primarily identified by its potassium stain. A rhyolite in this context is defined as a fine-grained rock composed of potassium feldspar, quartz and plagioclase. The stain is subtle, being pale yellow and very wispy in appearance. Glassy quartz, either as small crystals or tiny threads, stands out in positive relief. Plagioclase is chalky white. The fragment may have a directed fabric defined by glassy shards, or it may have a spherulitic texture.

Alteration

The interpretation of alteration requires mineralogical evidence to support a change in the mineral assemblage of a rock. In stream-sediment petrography this information can only be obtained from rock fragments. Most of the minerals discussed above can be identified as alteration minerals based on a binocular microscope examination. However, the evidence of alteration is often subtle and it may be difficult to interpret with confidence. Evidence to support alteration includes:

- A mineral, commonly found in alteration zones, appears to crosscut other mineral grain boundaries or foliations. This may include tiny veinlets of quartz, or small indistinct crystals of orthoclase which may give a mottled appearance.
- Variations in the mineral assemblage which suggest selective replacement of a mineral in some fragments.

It is difficult to distinguish regional metamorphic effects from local effects and accurate interpretation requires knowledge of the local geology.

Sieve Size and Detection Levels

The sieve intervals chosen in the study contained a wide range of sizes and this is evident in the number of particles exposed on the prepared surface of the sample disks. The −5 to +20-mesh sample averaged 60 fragments per square centimetre or approximately 3400 per disk, the −10 to +35-mesh fraction averaged 110 and 6200 fragments, and the −20 to +40-mesh fraction averaged 350 and 20 000 fragments.

There is an important trade-off between the size of material being examined (sieve interval), the amount of information contained in the average-sized fragment (rock or mineral grains), the detection levels, and the difficulty of the examination. Clearly, how these factors are rationalized will depend upon the individual circumstances of each field area and exploration program. The average grain size of the rocks of interest in the drainage area has a large bearing on what is the best sieve interval for interpretative study. Fine-grained sedimentary or volcanic rocks can be easily studied from fragments averaging 1 millimetre in diameter, coarse-grained granites cannot.

For the explorationist, detection of a given indicator mineral will, at least initially, be a higher priority than interpretation. The chance of identifying a mineral present only in trace amounts, is obviously much better in a sample where there is a large number of particles. The polished surface of the sample disk is essentially a sample of the stream sediment sample, and by selecting a fine sieve interval, we can introduce a bias that is favourable to detection. Detection level examinations can be easily carried out using the −18 to +35-mesh size (1 mm to 500 μm). If these fragments are too small to provide information necessary for interpretation, coarser material, which is more appropriate to the grain size of the rocks in the drainage area, can be examined later.

In the study, test samples were made up using measured amounts of pyrite and epidote mixed with Scuzzy Creek sand. Both the pyrite and epidote were easily detected at concentrations as low as 1 part per 1000 in both the −10 to +35 and −20 to +40-mesh fractions. Polishing the sample surface improved the ease of detection considerably.

DEPOSIT STUDIES

Stream-sediment samples from the vicinity of several ore deposits in southwestern British Columbia were examined after completing the study of test samples. Only the −18 to +40-mesh fraction (1 mm to 425 μm) was examined. As mentioned earlier the low sample density, the lack of information about background conditions, and the limited range of sediment sizes precludes any firm conclusions. Interpretation of stream-sediment petrographic identifications must be based on comparisons with studies of stream-sediments in areas of known mineralization. However, several observations can be made that support the usefulness of the technique and offer encouragement for further studies; these are:

- Some of the creeks draining the Mount Washington, Britannia and Merry Widow areas contain small grains of pyrite and chalcopyrite in concentrations which range from 1:1000 to 1:10 000.
- The Merry Widow skarn is easily distinguished by the large amount of magnetite in the sediments, up to approximately 5 per cent.
- There appears to be an increase in potassium-rich minerals in the vicinity of the Britannia mine.
- There appears to be an increase in epidote and quartz in the vicinity of mineralization in most of the areas.

APPLICATION TO EXPLORATION

Stream-sediment petrography may be of significant value to exploration in the British Columbia Coast Range, and it may have widespread application in other environments. It can evaluate areas where sampling problems limit the use of geochemistry, and it can compliment the use of stream-sediment geochemistry by providing information about the presence of mineralogical anomalies, such as alteration zones. When integrated with geochemistry in regional exploration, it may be able to predict the type of mineralization generating geochemical anomalies and it can provide a second-level screen to help establish priorities for follow-up field programs.

The coarse fraction, utilized in stream-sediment petrography, is already contained in most stream-sediment samples collected by industry, but it is usually thrown away. This material contains valuable information which can be obtained for little additional cost, especially when compared to the cost of additional fieldwork. Stream-sediment petrography is a cost-effective method of enhancing the usefulness of stream-sediment samples in regional exploration programs.

DISCUSSION

Stream-sediment petrography has the potential to detect alteration minerals in stream sediments, and initial studies have been encouraging. However, the significance of the results is still speculative. Detailed studies of sediments from streams around ore deposits are needed to provide standards for comparison. This work should not be carried out in isolation from research on the weathering of altered rocks and their transport characteristics.

Alteration zones are larger than the orebodies they surround and they are potentially a much larger target to explore for. This is an important consideration now that most exploration targets are blind orebodies. Altered rocks may weather more quickly than fresh rocks and as a consequence, sediments may be biased toward the altered areas, to the benefit of the explorationist. Another consideration is that altered rocks may weather into small particles *in situ*, or may disintegrate a short distance after entering the stream environment. As a result, stream-boulder prospecting may be ineffective for locating some types of alteration unless the prospector is close to the source. Detecting alteration zones by a microscopic examination of stream sediments may be the only way to identify the alteration from a distance. However, some types of alteration, such as clay alteration, may erode only into very fine particles which may not be detected in the coarse fraction. The range of alteration minerals to which this technique can be applied has not yet been fully defined.

The stream petrographic techniques are best suited for identifying alteration minerals, although it has been demonstrated that economic minerals, such as chalcopyrite, can be identified. In exploration, common sense dictates that the economic minerals themselves are often the best indicator minerals. Stream-sediment petrography relies on the skill of the person examining the sample, and the results are at best semiquantitative. The economic minerals are probably best identified by geochemistry, especially if detection can be enhanced by techniques such as heavy-liquid separation. In situations where samples from high-energy streams have no fines, the coarse fraction can be crushed and analyzed, and the geochemical results will probably be comparable to the petrographic work.

Stream-sediment petrography is able to identify minerals commonly associated with alteration, however the linkage with alteration zones is not easily established. The techniques identified in this study require further refinement. The identification of alteration zones through the use of stream-sediments may then be of significant value in mining exploration.

ACKNOWLEDGMENTS

The assistance of Paul Matysek in securing funding for this study is gratefully acknowledged. Credit for the original suggestion of staining stream sediments to determine alteration is given to R.R. (Dick) Culbert. Funding for this study was provided by the British Columbia Geoscience Research Grant Program, grant number RG91-28.

REFERENCES

Matysek, P.F. and Day, S.J. (1988): Geochemical Orientation Surveys: Northern Vancouver Island, Fieldwork and Preliminary Results, *in* Geological Fieldwork 1987, *B.C. Ministry of Energy, Mines and Petroleum Resources*, Paper 1988-1, pages 493-502.

Short, M.N. (1940): Microscopic Determination of the Ore Minerals, *United States Department of the Interior*, Geological Survey Bulletin 914, Second Edition, 314 pages.

THE REGIONAL GEOCHEMICAL SURVEY PROGRAM: SUMMARY OF ACTIVITIES

By W. Jackaman, P.F. Matysek and S.J. Cook

KEYWORDS: Regional Geochemical Survey, reconnaissance, multi-element, stream sediment, stream water, anomalies, claim status, Mount Waddington, Hope, Ashcroft, Pemberton, Taseko Lakes, Bonaparte Lake.

INTRODUCTION

The British Columbia Regional Geochemical Survey (RGS) program marked the completion of its fifteenth year with the successful release of seven RGS Open File data packages on June 27, 1991. Unprecedented in size, this release included results from two 1990 surveys conducted in NTS map sheets Fernie (82G) and Kananaskis Lakes (82J) and, as part of the RGS Archive Program, new analytical data from five previously released joint federal-provincial surveys from map sheets Penticton (82E), Nelson (82F), Lardeau (82K), Vernon (82L) and Seymour Arm (82M). To date, over 250 map and digital data packages have been purchased by mineral explorationists and other earth scientists. These packages present multi-element determinations for stream sediments and waters, field observations, sample location information, bedrock associations, statistics and data analyses for 8431 sample sites covering 100 000 square kilometres in southeastern British Columbia. Contact with companies involved in the release has determined that new mineralized showings have already been discovered in the

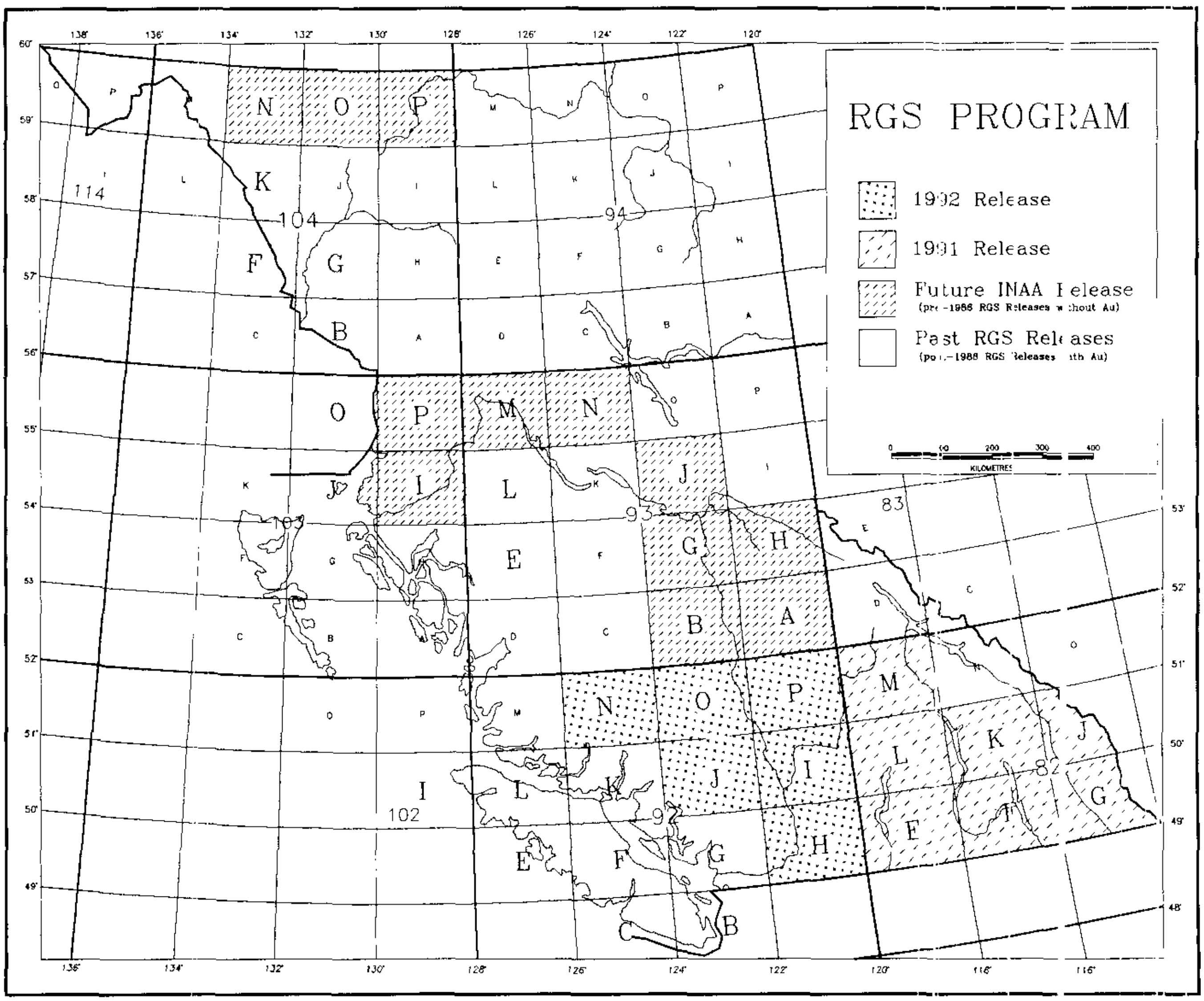

Figure 3-2-1. Current status of RGS program.

Coyote Creek watershed (82J/3) near Invermere and Howell Creek (82G/2) in the Flathead district. The Mineral Titles Branch has noted that claim staking throughout the survey area increased with over 1000 new claim units being recorded immediately after the release.

During the past five years, the RGS program has significantly increased the rate at which survey results have been disseminated. Consequently, the RGS database has quickly expanded to its present size of over 1.4 million analytical determinations for 38 000 sample sites (Figure 3-2-1, Table 3-2-1). Due to the amount of data contained within this extensive data set, explorationists are faced with the formidable challenge of screening the data for sites that reflect mineralization. To assist in the assessment of the data, and to ensure that *bona fide* anomalies are not being overlooked or forgotten, this report will re-evaluate precious and base metal results from the 1991 release, and provide survey information and preliminary data evaluation for the forthcoming 1992 release. Specifically this paper will:

- Identify and determine the claim status of precious-metal (Au-Ag-As-Sb), base-metal (Cu-Pb, Zn-Ag), single-element gold and single-element zinc anomalies from the 1991 RGS release.

TABLE 3-2-1
SUMMARY OF RGS DATABASE

MAP	RGS OF	GSC OF	YEAR	SAMPLES	ROUTINE	INAA	ADDITIONAL ANALYSES	RELEASE YEAR
82E	RGS 29	OF 409	1976	1631	•	•		1991 INAA RELEASE
82F	RGS 30	OF 514	1977	1394	•	•	Sn,Hg	1991 INAA RELEASE
82G	RGS 27		1990	922	•	•	Sn,W,Hg,As,Sb,Cd,V,LOI,F,Bi,Cr	1991 RGS RELEASE
82J	RGS 28		1990	583	•	•	Sn,W,Hg,As,Sb,Cd,V,LOI,F,Bi,Cr	1991 RGS RELEASE
82K	RGS 31	OF 515	1977	1297	•	•	Sn,W,Hg	1991 INAA RELEASE
82L	RGS 32	OF 410	1976	1385	•	•		1991 INAA RELEASE
82M	NGR 33	OF 516	1977	1219	•	•	Hg	1991 INAA RELEASE
92B/C	RGS 24	OF 2182	1989	599	•		Sn,W,Hg,As,Sb,Cd,V,LOI,F,Bi,Cr,Au	1990 RGS RELEASE
92E	RGS 21	OF 2038	1988	386	•		Sn,W,Hg,As,Sb,Ba,Cd,V,LOI,F,Bi,Cr,Au	1989 RGS RELEASE
92F	RGS 25	OF 2183	1989	909	•		Sn,W,Hg,As,Sb,Cd,V,LOI,F,Bi,Cr,Au	1990 RGS RELEASE
92G	RGS 26	OF 2184	1989	922	•		Sn,W,Hg,As,Sb,Cd,V,LOI,F,Bi,Cr,Au	1990 RGS RELEASE
92H	RGS 07	OF 865	1981	995	•	•	Hg,W,As,Sb	1992 INAA RELEASE
92I	RGS 08	OF 866	1981	606	•	•	Hg,W,As,Sb	1992 RGS RELEASE
92J	RGS 09	OF 867	1981	853	•	•	Hg,W,As,Sb	1992 INAA RELEASE
92K	RGS 22	OF 2039	1988	1216	•		Sn,W,Hg,As,Sb,Ba,Cd,V,LOI,F,Bi,Cr,Au	1989 RGS RELEASE
92L/102I	RGS 23	OF 2040	1988	1144	•		Sn,Hg,W,As,Sb,Ba,Cd,V,LOI,F,Bi,Cr,Au	1989 RGS RELEASE
92N	RGS 34		1991	874	•	•	Sn,W,Hg,As,Sb,Cd,V,LOI,F,Bi,Cr	1992 INAA RELEASE
92O	RGS 03	OF 774	1979	935	•	•	Hg,W,AS	1992 INAA RELEASE
92P	RGS 04	OF 775	1979	914	•	•	Hg,W,AS	1992 INAA RELEASE
93A	RGS 05	OF 776	1980	1299	•	•	Hg,W,As,Sb	FUTURE INAA RELEASE
93B	RGS 06	OF 777	1980	757	•	•	Hg,W,As,Sb	FUTURE INAA RELEASE
93E	RGS 16	OF 1360	1986	1112	•		Hg,W,As,Sb,Ba,Cd,LOI,Au	1987 RGS RELEASE
93G	RGS 13	OF 1214	1984/85	1095	•		Sn,W,Hg,As,Sb,Ba,Cd,V,LOI	FUTURE INAA RELEASE
93H	RGS 14	OF 1215	1984/85	1119	•		Sn,W,Hg,As,Sb,Ba,Cd,V,LOI	FUTURE INAA RELEASE
93J	RGS 15	OF 1216	1985	1088	•		Sn,W,Hg,As,Sb,Ba,Cd,V,LOI	FUTURE INAA RELEASE
93L	RGS 17	OF 1361	1986	1093	•		Sn,W,Hg,As,Sb,Ba,Cd,V,LOI,F,Au	1987 RGS RELEASE
93M	RGS 10	OF 1000	1983	1100	•	•	Hg,W,As,Sb	FUTURE INAA RELEASE
93N	RGS 11	OF 1001	1983	1124	•	•	Hg,W,As,Sb	FUTURE INAA RELEASE
103I/J	RGS 01	OF 772	1978	2234	•	•	Hg,W,AS	FUTURE INAA RELEASE
103O/P	RGS 02	OF 773	1978	1883	•	•	Hg,W,AS	FUTURE INAA RELEASE
104B	RGS 18	OF 1645	1987	661	•		Sn,W,Hg,As,Sb,Ba,Cd,V,LOI,F,Bi,Cr,Au	1988 RGS RELEASE
104F/G	RGS 19	OF 1646	1987	1218	•		Sn,W,Hg,As,Sb,Ba,Cd,V,LOI,F,Bi,Cr,Au	1988 RGS RELEASE
104K	RGS 20	OF 1647	1987	847	•		Sn,W,Hg,As,Sb,Ba,Cd,V,LOI,F,Bi,Cr,Au	1988 RGS RELEASE
104N	NGR 28	OF 517	1977	936	•	•	Sn,W,Hg	FUTURE INAA RELEASE
104O	NGR 41	OF 561	1978	946	•	•		FUTURE INAA RELEASE
104P	NGR 42	OF 562	1978	848	•	•		FUTURE INAA RELEASE
TOTAL				38144				

ROUTINE SEDIMENT ANALYTICAL SUITE : Zn, Cu, Pb, Ni, Co, Ag, Mn, Fe, Mo, U

ROUTINE WATER ANALYTICAL SUITE : U, F, pH

INAA SEDIMENT ANALYTICAL SUITE : Au, Sb, As, Ba, Br, Ce, Cs, Cr, Co, Hf, Fe, La, Lu, Mo, Ni, Rb, Sm, Sc, Na, Ta, Tb, Th, W, U, Yb, Zr

- Detail the forthcoming 1992 RGS release, including the 1991 reconnaissance stream-sediment and water survey of NTS map sheet Mount Waddington (92N), and new analytical data from five previously released joint federal-provincial surveys of NTS map sheets Hope (92H), Ashcroft (92I), Pemberton (92J), Taseko Lakes (92O) and Bonaparte Lake (92P). A summary of survey parameters (sample collection, preparation and analytical procedures), physiography, geology, mineral potential and exploration targets in the survey areas will be presented.
- Statistically evaluate gold, copper, lead and zinc data from the surveys conducted in map sheets 92H, I, J, O and P, and breakdown the number of anomalous sites found within key lithological units.

1991 RGS RELEASE

IDENTIFICATION AND CLAIM STATUS OF RGS ANOMALIES

METHODOLOGY

The seven 1:250 000-scale regional geochemical surveys (NTS 82/E, F, G, J, K, L and M) in southeastern British Columbia released in 1991 cover 8060 stream-sediment sites with over 300 000 analytical determinations. Systematic evaluation of such large multi-element geochemical databases presents a challenge to explorationists in identifying samples related to economic mineralization, as considerable variation in background metal concentrations may exist between geological units. This study develops a methodology to distinguish sites reflecting potential economic mineralization in the combined survey areas (RGS 27, 28, 29, 30, 31, 32 and 33), and identifies those sites on which no mineral claims have been staked, in order to guide and stimulate exploration activity in the region. An interpretive technique developed by Matysek *et al.* (1991a, b, c, d, e, f, g; Figure 3-2-2) rates individual samples and identifies those sites characterized by multi-element signatures associated with particular mineral deposit types. Stream-sediment geochemistry typically reflects the underlying geology of the watershed, and natural background metal variations must be taken into account to distinguish anomalous samples. Briefly, the method consists of calculating 90th, 95th and 98th percentile threshholds for each metal in each geological unit containing ten or more sample sites in the adjoining survey areas; and then assigning metal anomaly ratings to individual samples exceeding these thresholds. Those samples exceeding the 98th percentile for any given geological unit are assigned an anomaly rating of 3. Those samples having concentrations between the 95th and 98th percentiles for a geological unit are assigned an anomaly rating of 2, while those between the 90th and 95th percentiles are assigned a rating of 1. Element ratings for base metal (Cu-Pb-Zn-Ag) and precious metal (Au-Sb-As-Ag) associations are summed for each site, and anomalous samples are deemed to be those with a top rating of at least 10 of a possible 12 in either association. Threshold tables and evaluation charts for anomalous samples are provided in data booklets for individual RGS releases (Matysek *et al.*, 1991a, b, c, d, e, f, g).

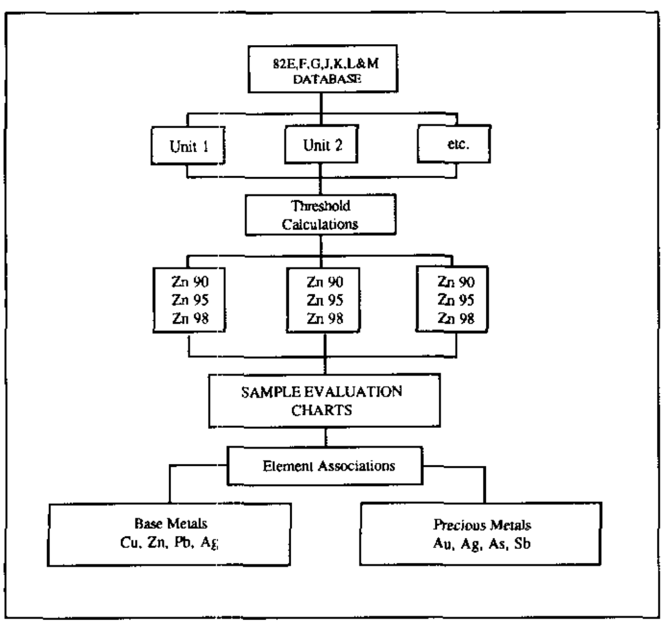

Figure 3-2-2. Flow chart for anomaly identification.

RESULTS

Eighteen base metal and twenty precious metal top-rated anomalies were identified in the combined survey areas (Table 3-2-2; Figure 3-2-3). In addition, zinc and gold concentrations in sediments were ranked and the highest 20 sites of each (Table 3-2-3) arbitrarily identified as anomalous. Upon elimination of coincident anomalies, 51 sites were identified as anomalous. Of these, one site lies within the Purcell Wilderness Conservancy and will not be further considered. A breakdown of the remaining 50 sites by anomaly type (base metals, precious metals, zinc and gold) and mineral claim status (Table 3-2-4) shows that only two of the sites are anomalous in all four categories, and only six sites for three categories. Fifteen of the eighteen base metal anomalies are coincident with precious metal anomalies. However, the majority of gold anomalies are unrelated to either of these associations; 18 of the 20 highest gold values are anomalous for gold alone. Similarly, half of the top 20 zinc values are anomalous for zinc only.

Highest gold values in stream sediments are concentrated in Intermontane Belt and Kootenay Arc lithologies in southern NTS 82E and F, particularly Paleozoic-Mesozoic metasedimentary and metavolcanic rocks in the vicinity of the Rossland and Greenwood gold camps. Combined base and precious metal anomalies are associated with both Triassic-Jurassic and Lower Paleozoic Kootenay Arc metasedimentary rocks. The greatest concentrations of combined anomalies and zinc anomalies is in the New Denver area. Most precious metal anomalies, however, occur in Proterozoic metasedimentary rocks of the Purcell anticlinorium, and associated felsic intrusions. Two high zinc values are the only anomalies associated with sedimentary rocks of the Foreland Belt.

TABLE 3-2-2
TOP-LEVEL BASE AND PRECIOUS METAL ANOMALY LISTINGS: NTS 82E, F, G, J, K, L AND M (N=8060 SITES)

Anomaly Type	NTS	Sample	UTM Zone	UTM East	UTM North	Geological Unit	Site Contamination	Zn ppm	Cu ppm	Pb ppm	Ag ppm	Au-1 ppb	Au-2 ppb	Sb ppm	As ppm	Hg ppb
Base Metal (Cu-Pb-Zn-Ag) Anomalies (n=18)	82E06	767296	11	351007	5475967	EKgd	Possible	278	26	90	5.8	53	-	2.2	50.9	-
	82F03	773064	11	481982	5435428	TJv	None	7800	330	2450	2.8	624	-	22.8	1450.0	220
	82K01	771055	11	559097	5541834	HSL	None	174	44	650	2.8	38	-	26.1	115.0	40
	82K11	773155	11	473356	5611360	lPs	Probable	875	136	355	7.8	209	281	13.0	95.0	110
	82K13	773173	11	457892	5624788	lPs	None	580	66	345	3.6	49	-	16.6	50.3	180
	82K11	773208	11	467169	5616823	lPs	None	2620	182	1120	6.0	110	-	24.4	91.1	300
	82K15	773300	11	505142	5645061	Hs	None	11200	210	2500	4.8	99	-	56.6	1740.0	40
	82K15	773303	11	501611	5644065	Hs	Probable	88000	1200	20000	29.0	446	-	566.0	5370.0	310
	82K11	775230	11	489279	5612332	lEs	None	320	50	140	1.3	15	-	3.6	40.0	30
	82K01	775386	11	549862	5559138	HSL	None	800	42	270	3.6	67	-	18.4	370.0	50
	82K03	775546	11	499803	5542966	Ms	None	1175	116	565	2.6	25	-	6.8	160.0	50
	82K03	777009	11	488813	5539481	TJs	Probable	7000	134	4500	5.2	39	-	19.1	90.6	150
	82K03	777010	11	490723	5543459	TJs	Probable	1980	78	1300	8.0	73	-	18.3	104.0	70
	82K03	777012	11	488339	5543137	TJs	Probable	3080	70	1500	8.4	27	-	9.2	44.0	60
	82K03	777016	11	483510	5540765	TJs	Probable	9400	148	1750	5.8	27	-	20.6	1330.0	140
	82K03	779090	11	478346	5538642	EKgd	Probable	2800	56	2450	3.0	200	-	10.2	25.0	70
	82M04	763047	11	301802	5665253	lPs	Possible	2600	328	1060	3.6	110	-	131.0	77.2	-
	82M04	767042	11	316121	5660510	lPs	Possible	580	92	840	2.0	16	-	4.1	195.0	-
Precious Metal (Au-Sb-As-Ag) Anomalies (n=20)	82E06	767296	11	351007	5475967	EKgd	Possible	278	26	90	5.8	53	-	2.2	50.9	-
	82F03	773064	11	481982	5435428	TJv	None	7800	330	2450	2.8	624	-	22.8	1450.0	220
	82F06	779045	11	478678	5478512	Jg	Mining Activity	156	280	87	2.8	120	-	10.0	20.0	130
	82K01	771055	11	559097	5541834	HSL	None	174	44	650	2.8	38	-	26.1	115.0	40
	82K11	773155	11	473356	5611360	lPs	Probable	875	136	355	7.8	209	281	13.0	95.0	110
	82K13	773173	11	457892	5624788	lPs	None	580	66	345	3.6	49	-	16.6	50.3	180
	82K11	773208	11	467169	5616823	lPs	None	2620	182	1120	6.0	110	-	24.4	91.1	300
	82K15	773300	11	505142	5645061	Hs	None	11200	210	2500	4.8	99	-	56.6	1740.0	40
	82K15	773303	11	501611	5644065	Hs	Probable	88000	1200	20000	29.0	446	-	566.0	5370.0	310
	82K09	773250	11	540166	5594320	HSU	None	78	80	130	3.0	13	-	35.6	134.0	100
	82K01	775386	11	549862	5559138	HSL	None	800	42	270	3.6	67	-	18.4	370.0	50
	82K01	775387	11	549540	5562672	HSM	None	495	26	105	1.8	34	-	7.9	122.0	50
	82K03	775528	11	495395	5544067	PTv	None	200	58	31	1.2	110	-	2.4	18.0	30
	82K03	775546	11	499803	5542966	Ms	None	1175	116	565	2.6	25	-	6.8	160.0	50
	82K09	775274	11	539836	5603025	EKqm	None	66	10	33	1.6	14	-	1.5	11.0	60
	82K11	775230	11	489279	5612332	lEs	None	320	50	140	1.3	15	-	3.6	40.0	30
	82K03	777010	11	490723	5543459	TJs	Probable	1980	78	1300	8.0	73	-	18.3	104.0	70
	82K03	777016	11	483510	5540765	TJs	Probable	9400	148	1750	5.8	27	-	20.6	1330.0	140
	82K03	779090	11	478346	5538642	EKgd	Probable	2800	56	2450	3.0	200	-	10.2	25.0	70
	82M04	763047	11	301802	5665253	lPs	Possible	2600	328	1060	3.6	110	-	131.0	77.2	-

UNIT	DESCRIPTION	UNIT	DESCRIPTION
eoTV	Tertiary basalt, andesite, volcaniclastic and flow rocks, minor sediments	lEs	Lower Cambrian quartzite, limestone, phyllite, argillite
TJv	Triassic-Jurassic greenstone, tuff, sediments	Hs	Proterozoic (Hadrynian) sandstone, conglomerate, limestone, grit, volcanic rocks
TJs	Triassic-Jurassic shale, argillite, limestone, conglomerate, schist, sandstone	HSU	Proterozoic (Helikian) quartzite, argillite, dolomite, limestone, siltstone
PTv	Permian-Triassic greenstone, basalt, andesite, lava, tuff, breccia, serpentinite	HSM	Proterozoic (Helikian) limestone, argillite, quartzite, andesite, breccia, tuff
PPT	Carboniferous-Permian argillite, quartzite, greenstone, limestone, conglomerate	HSL	Proterozoic (Helikian) quartzite, argillite, siltstone
Ms	Carboniferous-Permian slate, argillite, chert, schist, conglomerate, limestone	EKgd	Cretaceous granodiorite, quartz diorite; lesser quartz monzonite
DTs	Devonian-Triassic shale, sandstone, limestone, chert	Jg	Jurassic granodiorite, quartz diorite; lesser quartz monzonite
lPs	Lower Paleozoic argillite, limestone, schist, phyllite, greenstone	Dg	Devonian gneissic granitic rocks

(after Okulitch and Woodsworth, 1977)

Figure 3-2-3. Legend of geological units.

A large proportion of RGS anomalies remain open for staking. Stream watersheds of nine of the fifty-one anomalous sites were unstaked as of mid-October, 1991, with an additional eight only partially staked (Table 3-2-4). A summary listing of unstaked or partially staked anomalous sites, including location, lithology, presence or absence of similar mineral occurrences, site contamination status, mineral claim status and selected element concentrations is shown in Table 3-2-5. Single-element gold anomalies comprise the majority (6 of 9) of the unstaked sites; nearly all base metal, zinc and coincident base and precious metal anomalies occur on ground already staked. In two instances, top 10 anomalies of gold and zinc were staked following the Regional Geochemical Survey releases in June, 1991. However, stream sediments with somewhat lower gold concentrations appear to have been overlooked. Watersheds of all but one of the ten highest gold concentrations (470-3530 ppb) have been staked, but 70 per cent of those in the range 335-446 ppb are either unstaked or partially staked. The greatest concentration and variety of unstaked anomalies (5 out of 12) occur in NTS 82K. Four of these (one combined base/precious metals, two precious metal, and one gold anomaly) occur in Purcell Group rocks with associated felsic intrusions.

The use of percentile thresholds based on geological groupings, and of a multi-element association rating system, facilitates the recognition of multi-element base and precious metal stream-sediment anomalies in the 8060-site adjoining RGS survey areas of southeastern British Columbia. Of the 51 anomalous sites defined by this method and by the top 20 ranked gold and zinc concentrations, stream watersheds of nine sites were available for staking as of October, 1991. Watersheds of an additional eight anomalous sites were only partially staked.

TABLE 3-2-3
TOP 20-RANKED ZN AND AU CONCENTRATIONS: NTS 82E, F, G, J, K, L AND M (N=8060 SITES)

Anomaly Type	NTS	Sample	UTM Zone	UTM East	UTM North	Geological Unit	Site Contamination	Zn ppm	Cu ppm	Pb ppm	Ag ppm	Au-1 ppb	Au-2 ppb	Sb ppm	As ppm	Hg ppb
Zn	82K15	773303	11	501611	5644065	Hs	Probable	**88000**	1200	20000	29.0	446	-	566.	5370.0	310
(Top 20 Sites)	82K15	773300	11	505142	5645061	Hs	None	**11200**	210	2500	4.8	59	-	56.	1740.0	40
	82K03	777016	11	483510	5540765	TJs	Probable	**9400**	148	1750	5.8	27	-	20.	1330.0	140
	82F03	773064	11	481982	5435428	TJv	None	**7800**	330	2450	2.8	624	-	22.	1450.0	220
	82F14	777317	11	476637	5538211	TJs	Possible	**7200**	56	1800	5.4	19	-	27.	44.0	250
	82K03	777009	11	488813	5539481	TJs	Probable	**7000**	134	4500	5.2	29	-	19.	90.6	150
	82K02	779146	11	507313	5563930	lEs	Possible	**6000**	22	37	0.1	2	-	0.6	2.6	20
	82J03	901143	11	609924	5541841	DTs	None	**5550**	27	10	0.5	2	6	14.	21.0	70
	82F14	779202	11	482233	5538069	TJs	Possible	**4200**	84	31	0.6	4	-	8.1	31.0	20
	82K03	777015	11	484844	5541900	TJs	Probable	**3680**	60	49	1.4	7	-	2.2	17.0	20
	82K08	779151	11	554206	5590335	Hs	Possible	**3440**	42	1450	8.2	5	-	13.	28.0	760
	82K03	777012	11	488339	5543137	TJs	Probable	**3080**	70	1500	8.4	27	-	9.2	44.0	60
	82E13	765096	11	300403	5516362	Jg	Possible	**2900**	66	59	0.1	4	-	0.5	2.4	-
	82K03	779096	11	478346	5538642	EKgd	Probable	**2800**	56	2450	3.0	200	-	10.	25.0	70
	82K11	*773208*	*11*	*467169*	*5616823*	*lPs*	*None*	***2620***	*182*	*1120*	*6.0*	*110*	-	24.	*91.1*	300
	82M04	763047	11	301802	5665253	lPs	Possible	**2600**	328	1060	3.6	110	-	131	77.2	-
	82J06	901034	11	630392	5579867	DTs	Forestry	**2480**	13	5	0.2	2	-	1.2	1.8	70
	82G05	905249	11	586291	5456692	HSL	None	**2300**	68	540	0.5	5	-	2.0	8.0	60
	82E12	763100	11	288817	5512648	Jg	None	**2025**	175	23	1.2	3	-	0.6	3.1	-
	82K03	777010	11	490723	5543459	TJs	Probable	**1980**	78	1300	8.0	73	-	18.	104.0	70
Au	82E03	767057	11	341290	5440939	PPT	None	1800	470	790	0.4	**3530**	-	1.	75.4	-
(Top 20 Sites)	*82F03*	*773055*	*11*	*490504*	*5442888*	*lPs*	*Possible*	*82*	*20*	*30*	*0.1*	***1650***	-	0.	6.6	40
	82E05	763040	11	303084	5461434	PPT	None	45	57	24	0.1	**1020**	1040	0.	2.8	-
	82E02	765120	11	387137	5437312	PPT	Possible	83	780	3	0.6	**848**	-	5.	130.0	-
	82E03	767043	11	342666	5437494	EKgd	None	306	65	138	0.1	**809**	-	0.	6.9	-
	82K05	779102	11	431743	5589580	Dg	None	68	16	21	0.1	**786**	-	0.	1.7	40
	82F06	779074	11	480200	5470445	TJv	None	140	76	12	0.2	**626**	-	3.	35.0	50
	82F03	773064	11	481982	5435428	TJv	None	7800	330	2450	2.8	**624**	-	22.	1450.0	220
	82E12	765111	11	299984	5488103	Jg	Possible	35	7	1	0.1	**507**	-	0.	2.3	-
	82E05	763043	11	302758	5463500	eoTv	Possible	39	31	10	0.1	**470**	-	0.	2.6	-
	82K15	773303	11	501611	5644065	Hs	Probable	88000	1200	20000	29.0	**446**	-	566.0	5370.0	310
	82F01	771113	11	551956	5436128	HSL	Possible	40	18	17	0.1	**445**	-	1.	7.6	20
	82K08	775364	11	539844	5574178	HSU	None	52	26	26	0.1	**413**	-	2.	26.0	70
	82L01	765279	11	409799	5547468	EKgd	None	88	50	2	0.1	**403**	-	1.	8.6	-
	82G05	901003	11	573071	5473731	HSL	Mining Activity	27	15	6	0.1	**374**	318	1.	5.1	30
	82F05	777049	11	427779	5472806	EKgd	Possible	78	32	18	0.2	**365**	-	1.	10.0	30
	82L01	767268	11	397822	5552168	PPT	None	110	43	6	0.1	**361**	-	2.	91.9	-
	82M08	775164	11	424619	5683683	lPs	None	112	28	44	0.1	**348**	2	0.	4.1	30
	82K02	773132	11	503126	5554007	lPs	None	68	42	14	0.1	**340**	-	0.	13.0	10
	82E12	769387	11	296569	5499432	Jg	None	29	17	1	0.1	**335**	-	0.	2.7	-

TABLE 3-2-4
ANOMALOUS SITES ACCORDING TO ANOMALY TYPE AND MINERAL CLAIM STATUS (AS OF MID-OCTOBER, 1991).

	Anomaly Type	Sites	Sites Off-Limits to Staking	Sites Staked	Sites Partially Staked	Sites Unstaked
Coincident Anomalies	Base Metals/Precious Metals/Au/Zn	2	-	2	-	-
	Base Metals/Precious Metals/Zn	6	-	5	1	-
	Base and Precious Metals	7	1*	4	2	-
	Base Metals and Zn	2	-	2	-	-
Single Target Anomalies	Base Metals	1	-	1	-	-
	Precious Metals	5	-	2	1	2
	Zn	10	-	7	2	1
	Au	18	-	10	2	6
	Total	*51*	*1*	*33*	*8*	*9*

* **Purcell Wilderness Conservancy**

TABLE 3-2-5
UNSTAKED AND PARTIALLY STAKED STREAM SEDIMENT ANOMALIES

Anomaly Type	NTS	Sample	UTM Zone	UTM East	UTM North	Geological Unit	Adjacent Occurrences	Site Contamination	Mineral Claim Status	Zn ppm	Cu ppm	Pb ppm	Ag ppm	Au ppb	Sb ppm	As ppm	Hg ppb
Base Metals, Precious Metals and Au.	82K15	773300	11	505142	5645061	Hs	Yes	None	Partially Staked	11200	210	2500	4.8	99	56.6	1740.0	40
Base Metals and Precious Metals	82K13	773173	11	457892	5624788	lPs	Yes	None	Partially Staked	580	66	345	3.6	49	16.6	50.3	180
	82K03	775546	11	499803	5542966	Ms	Yes	None	Partially Staked	1175	116	565	2 6	25	6.8	160.0	50
	82K01	775386	11	549862	5559138	HSL	No	None	*Staking forbidden**	800	42	270	3.6	67	18.4	370.0	50
Precious Metals	82K09	775274	11	539836	5603025	EKqm	No	None	Unstaked	66	10	33	1.6	14	1.5	11 0	60
	82K01	775387	11	549540	5562672	HSM	No	None	Unstaked	495	26	105	1.8	34	7.9	122.0	50
	82K03	775528	11	495395	5544067	PTv	No	None	Partially Staked	200	58	31	1.2	110	2.4	18.0	30
Zn	82J06	901034	11	630392	5579867	DTs	No	Forestry	Unstaked	*2480*	13	5	0.2	2	1 2	1.8	70
	82K02	779146	11	507313	5563930	lEs	Yes	Possible	Partially Staked	*6000*	22	37	0.1	2	0 6	2.6	30
	82K08	779151	11	554206	5590335	Hs	Yes	Possible	Partially Staked	*3440*	42	1450	8.2	6	13.6	28.0	1760
Au	82E12	765111	11	299984	5488103	Jg	No	Possible	Unstaked	35	7	1	0.1	*507*	0.6	2.3	-
	82F01	771113	11	551956	5436128	HSL	No	Possible	Partially Staked	40	18	17	0.1	*445*	1.3	7.6	20
	82K08	775364	11	539844	5574178	HSU	No	None	Unstaked	52	26	26	0.1	*413*	2.4	26.0	70
	82L01	765279	11	409799	5547468	EKgd	Yes	None	Partially Staked	88	50	2	0.1	*403*	1.0	8.6	-
	82F05	777049	11	427779	5472806	EKgd	No	Possible	Unstaked	78	32	18	0.2	*365*	1 2	10.0	30
	82M08	775164	11	424619	5683683	lPs	No	None	Unstaked	112	28	44	0.1	*348*	0.4	4.1	30
	82K02	773132	11	503126	5554007	lPs	No	None	Unstaked	68	42	14	0.1	*340*	0.6	13.0	10
	82E12	769387	11	296569	5499432	Jg	No	None	Unstaked	29	17	1	0.1	*335*	0.6	2.7	-

* **Purcell Wilderness Conservancy**

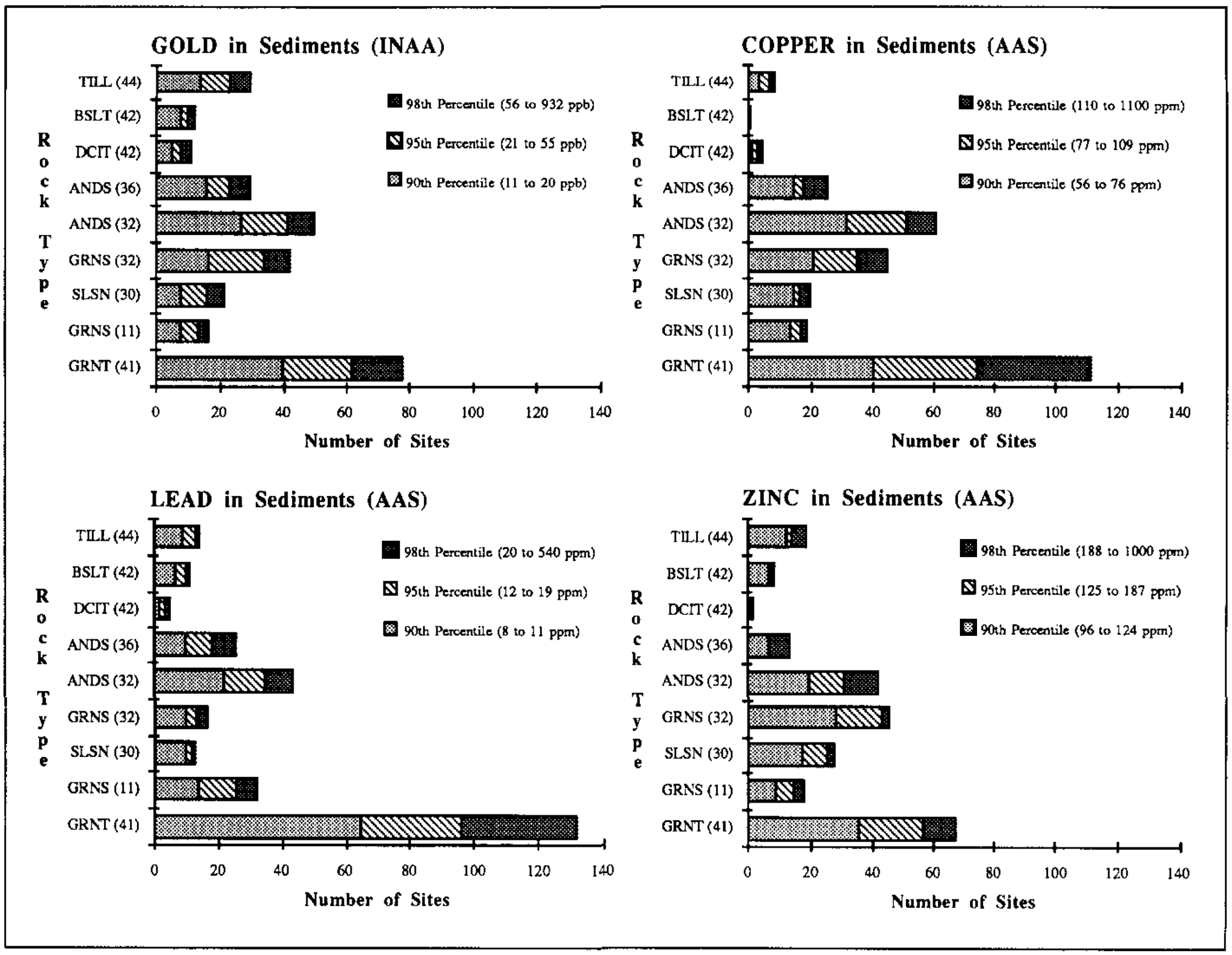

Figure 3-2-4a. Proportion of gold and base metal sample sites within key geological units.

1992 RGS RELEASE

Regional Summary

PHYSIOGRAPHY AND GEOLOGY

The six map areas included in the 1992 RGS release cover a region of over 90 000 square kilometres in south-central British Columbia. The survey areas are located within the the Coast Mountain and Interior Plateau physiographic regions (Holland, 1976), and the diverse geological environments associated with the Coast and Intermontane tectonic belts.

The Coast Mountains are an extremely rugged and heavily glaciated mountain range. Summit elevations commonly exceed 2500 metres and extend above deeply cut U-shaped valley floors that average 1200 metres in elevation. Numerous alpine glaciers and extensive ice fields cover a large proportion of the survey area. The slopes tend to be steep and are typically exposed bedrock or a thin cover of till, colluvium and talus. Thick deposits of glacialfluvial material are found at the lower elevations. Streams at higher elevations tend to form a trellised drainage pattern and braided streams commonly occupy in the valley floors. Stream sediment is primarily composed of fine to course-grained material. The sediment associated with the numerous glacier-fed streams also contains a high glacial flour component.

A narrow transitional zone separates the Coast Mountains from the semi-arid and subdued terrain of the Fraser and Thompson plateaus. These plateau areas consist of flat to gently rolling hills ranging between 1200 and 1500 metres in elevation and are covered by a thick layer of glacial drift. In the southern Thompson Plateau, resistant bedrock occasionally rises above 1800 metres in elevation. Low-energy, glacially deranged stream channels tend to produce sediment material having a moderate to high organic content.

The Coast Plutonic Complex, composed of Cretaceous granites and granodiorites, dominates the western half of the survey area. Within the Coast Complex, roof pendants of gniess, amphibolite, metasediments and metavolcanics represent metamorphosed remnants of volcanic-arc rocks (Roddick and Tipper, 1985).

The boundary between the Coast and Intermontane tectonic belts includes successions of Upper Jurassic to Lower Cretaceous volcanic and sedimentary rocks of the Tyaughton-Methow trough, and Permian to Middle Jurassic chert, argillite, basalt and alpine-type ultramafic rocks of the Bridge River and Hozameen terranes (Wheeler *et al.*, 1988).

The Intermontane Belt to the east is occupied by the Stikine Terrane which is comprised of Devonian to Permian arc volcanics and platform carbonates overlain by Triassic and Lower Jurassic arc volcanics, volcaniclastic, chert and arc-derived clastic rocks which are intruded by comagmatic plutonic rocks. The Cache Creek Terrane comprised of Mississippian to Upper Triassic oceanic volcanics and sediments borders the Stikine Terrane to the south-east. The southeast corner of the survey area is within the Quesnel Terrane which contains Upper Triassic to Lower Jurassic arc volcanics, volcaniclastic and comagmatic intrusive rocks overlain by Jurassic arc-derived clastic rocks (Wheeler *et al.*, 1988).

MINERAL POTENTIAL AND EXPLORATION TARGETS

The number of favourable geological environments found throughout the survey area, combined with a long and successful history of mineral exploration, has established this region as having an excellent potential for a variety of mineral deposits containing high-grade base and precious metal mineralization.

Based on the status of mineral occurrence (Table 3-2-6) and a review of exploration activity from assessment reports filed over the last five years (Table 3-2-7), most exploration activity has been focused on mineral deposits located on map sheets 92H and 92I and to a lesser extent 92J. Although

GEOLOGY LEGEND

SEDIMENTARY AND VOLCANIC ROCKS

QUATERNARY

Pleistocene to Recent

TILL (44)	Till, gravel, silt, clay.

TERTIARY

Miocene and/or Pliocene

BSLT (42)	Varicoloured vesicular valley basalt, brown amygdaloidal plateau basalt.

Eocene to Oligocene

DCIT (42)	Sheba Group, Kamloops Group, Skull Mtn. Formation; dacite, trachyte, basalt, andesite, rhyolite and related breccias.

MESOZOIC

Cretaceous

ANDS (36)	Kingsvale Group, Spences Bridge Group, Gambier Group, Fire Lake Group; varicoloured andesitic, basaltic and acidic pyroclastic and flow rocks.

Triassic to Cretaceous

SLSN (30)	Tyaughton Group, Relay Mtn. Group, Jackass Mtn. Group, Taylor Creek Group and Kingsvale Group; siltstone, greywacke, conglomerate and shale.

Triassic

ANDS (32)	Cadwallader Group, Bridge River Group, Nicola Group, Tulameen Group; andesite, basalt, greywacke, agglomerate, breccia.
GRNS (32)	Cadwallader Group (Pioneer Formation), Bridge River Group, Nicola Group; greenstone, chert, argillite.

PALEOZOIC

Windermere to Permian

GRNS (11)	Cariboo Group, Slide Mtn. Group (Fennell Formation, Eagle Bay Assemblage); greenstone, andesitic and basaltic flow rocks and tuff, schist, chert, argillite, shale, limestone.

PLUTONIC ROCKS

MESOZOIC AND YOUNGER

GRNT (41)	Raft, Baldy Mtn., Thuya, Takomkane, Guichon Creek, Mount Lytton Batoliths; Scuzzy, Spuzzum and Needle Peak Plutons; Coast, Otter, Lightning Creek and Copper Mtn. Intrusions; granite, granodiorite, quartz monzonite, quartz diorite, diorite.

Generalized geology from GSC Open Files 865 (92H), 866 (92I), 867 (92J), 774 (92O) and 775 (92P). The four-letter mnemonic name indicates rock type and the two-digit number refers to age.

Figure 3-2-4b. Legend.

TABLE 3-2-6
MINERAL OCCURRENCE STATUS

Map	Showing	Prospect	Dev. Prospect	Producer	Past Producer	Total
92H	464	61	21	7	41	594
92I	464	26	16	8	45	559
92J	136	48	17	1	22	224
92N	44	3	0	0	0	47
92O	87	16	6	0	8	117
92P	154	5	6	0	5	170

TABLE 3-2-7
SUMMARY OF EXPLORATION ACTIVITY FROM FILED ASSESSMENT REPORTS

	1990 (219)			1989 (209)			1988 (268)			1987 (211)			1986 (283)			
Map	I	II	III	I	II	III	I	II	III	I	II	III	I	II	III	Total
92H	14	34	10	16	31	13	10	47	20	9	43	12	19	47	18	343
92I	11	24	22	9	28	14	11	28	19	8	26	11	15	41	13	280
92J	7	21	2	7	19	5	8	35	9	4	26	9	9	44	16	221
92N	0	1	0	1	3	0	5	5	2	1	0	0	0	2	0	20
92O	1	33	2	4	16	10	5	18	7	5	16	7	4	14	5	147
92P	3	26	8	1	19	13	7	23	9	5	20	9	6	20	10	179
Total	36	139	44	38	116	55	46	156	66	32	131	48	53	168	62	

I : Prospecting; minor geological mapping, orientation sampling.
II : Intermediate Exploration Stage; detailed geophysical, silt, soil and rock surveys.
III : Advanced Exploration Stage; drilling, trenching, underground development.
( ) : Total number of Assessment Reports filed for that year.

map sheets 92O and 92P have not received the same level of attention there has been a slight increase in activity during recent years. Map sheet 92N remains relatively unexplored with only 47 known mineral occurrences and 20 filed assessment reports.

Within the Intermontane Belt, porphyry copper deposits containing precious metal values are currently the primary exploration target. During 1990 the majority of active exploration projects located within the survey area were on porphyry copper-gold targets. Gold-bearing skarn mineralization found in the Hedley area, volcanogenic massive sulphide deposits similar to the Chu Chua property and precious metal epithermal deposits such as the Elk property have all been identified as important exploration targets in the eastern half of the survey area.

The Coast Belt portion of the survey area has received a relatively low level of exploration attention. Activity has been concentrated in areas south of Taseko Lake and to the north of Whitesail Lake and only a small number of active exploration properties are located in the survey area between these two districts. Mesothermal and epithermal precious metal vein mineralization has been identified as the most common type of deposit found in the area (McLaren, 1990). Examples of this style of mineralization include properties located in the Bralorne and Gold Bridge areas. Other primary exploration targets include porphyry copper-molybdenum-gold deposits such as the Fish Lake and Poison Mountain properties, and volcanogenic massive sulphide mineralization similar to the Britannia deposit.

RGS Program – Mount Waddington (92N)

STREAM-SEDIMENT AND STREAM-WATER SURVEY

The Mount Waddington map sheet covers one of a few remaining areas in British Columbia which continues to be relatively unexplored. A reconnaissance stream-sediment and water survey was conducted during the 1991 field season in order to develop a greater understanding of the mineral potential of this frontier region and to provide geoscientific information to aid in the resolution of the numerous land-use discussions currently in progress.

McElhanney Engineering Services Limited was selected by competitive bid to carry out the sample collection component of the 1991 RGS program in the Mount Waddington map area. The base camp and dry facility were established at White Saddle Air Services' facility on Bluff Lake and a field camp was located at the head of Bute Inlet on Scar Creek. The vast majority of samples were collected by two teams consisting of a helicopter pilot, one crew chief and one sampler. Both White Saddle Air Services and Vancouver Island Helicopters provided air support for the program. Ministry representation by the senior author was maintained throughout the fast-paced 18-day program to ensure all aspects of the sample collection, data recording, sample drying, packing and shipping were in accordance with standards set by the National Geochemical Reconnaissance Program.

A total of 874 stream-sediment and stream-water samples were collected. The survey covered an area of approximately 15 000 square kilometres at an average density of one sample site every 17.6 square kilometres. The majority of the samples were collected from sites located within the Coast Mountains; less than 100 sites were in the plateau region. Discounting areas such as the large ice fields and the sparsely sampled plateau, the area covered by the survey is actually closer to 12 000 square kilometres and the density was one site every 14 square kilometres. Eighty-seven per cent of the sites were accessed by helicopter, seven per cent by truck and six per cent by boat. The program also included the collection of nine sediment and water samples in the southern tip of Tweedsmuir Provincial Park.

In general, sample sites were restricted to primary and secondary drainage basins having catchment areas of less than 10 square kilometres. Contaminated or poor-quality sample sites were avoided by choosing an alternative stream or by sampling a minimum of 60 metres upstream from the identified problem. At each sample site fine-grained stream sediment weighing 1 to 2 kilograms was collected within the active (subject to flooding) stream channel and placed in kraft-paper bags. In an attempt to minimize the glacial flour component of samples collected from glacial streams, the coarser grained material below the surface layer was sampled. Unfiltered water samples free of suspended materials were collected in 250-millilitre bottles. Field observations regarding sample media, sample site and local terrain were recorded and, to assist follow-up, aluminum tags inscribed with a unique RGS sample identification number were fixed to permanent objects, when available, at each site. Field-site checks were conducted by the Ministry representative to monitor, control and assess sample-collection procedures.

FIELD SAMPLE PREPARATION

Samples were field processed at the Bluff Lake base camp. Sediment samples were dried at a temperature less than 50°C and all sediment material finer than 1 millimetre was recovered by seiving each sample through a −18-mesh ASTM screen. Samples were assessed for quality and content of fine-grained sediment and those which appeared deficient in fine-grained material were routinely sieved through a −80-mesh screen (less than 177 microns). Sites yielding organic-rich samples and samples containing less than 40 grams of −80-mesh stream-sediment material were resampled.

LABORATORY SAMPLE PREPARATION

In order to complete sample preparation, the field-processed sediment samples were shipped to Rossbacher Analytical Laboratory in Burnaby and the water samples to the Ministry laboratory in Victoria. Sediment samples were sieved to −80-mesh ASTM fraction and analytical duplicate samples and control reference materials were inserted into each analytical block of 20 sediment samples. At this stage, a quantity of −80-mesh sediment and a representative sample of the +80 to −18-mesh fraction was archived for future studies. Control reference water standards were inserted into each analytical block of 20 water samples.

ANALYTICAL PROCEDURES

The standard methods and specifications for analysis of RGS stream sediments and waters are summarized in Table 3-2-8. Barringer Laboratories (Calgary, Alberta) has been contracted to provide this analytical work. In addition to the routine analytical suite of elements, the 1991 program will also include the analysis of sulphates in stream waters.

The determination of elements (Table 3-2-9) by instrumental neutron activation analysis will be carried out by Activation Laboratories (Ancaster, Ontario). This analytical technique involves irradiating the sediment samples, which on average weigh 10 grams, for 20 minutes in a neutron flux of 10^{11} neutrons per square centimetre per second. After a decay period of approximately one week, gamma-ray emissions for the elements are measured using a gamma-ray spectrometer with a high resolution, coaxial germanium detector. The counting time is 15 minutes per sample and the results are accumulated on a computer and converted to concentrations.

Field site duplicates, blind analytical duplicates and control reference materials are used in each analytical block of 20 samples to ensure that analytical data satisfy National Geochemical Reconnaissance Program quality control guidelines.

RGS ARCHIVE PROGRAM (92H, I, J, O, P)

The RGS Archive Program involves the analysis by instrumental neutron activation of stream-sediment samples collected during past joint federal-provincial Regional Geochemical Surveys, for gold and other previously undetermined elements of interest. Last year's RGS release represented the initial delivery of new analytical results generated by this program. In a continuing effort to disseminate new analytical results for the over 24 000 stream-sediment samples retrieved from the Geological Survey of Canada storage facilities in Ottawa, the current RGS Archive Program includes the production of RGS Open File reports for surveys which were originally conducted in map sheets 92H, I, J, O and P during 1979 and 1981. Becquerel Laboratories (Toronto, Ontario) has provided the INAA data for map sheets 92H, I, O and P, and under the direction of the Geological Survey of Canada, the INAA data for map sheet 92J samples were provided by Bondar Clegg Laboratories (Ottawa, Ontario).

A total of 4301 stream-sediment and stream-water samples were collected in south-central British Columbia during the 1979 and 1981 surveys. The samples were taken at an average density of one sample every 13 square kilometres and covered an area in excess of 78 000 square kilometres. The field and analytical data from the original programs were co-published by the British Columbia Ministry of Energy, Mines and Petroleum Resources and the Geological Survey of Canada in the early 1980s. These data packages consisted of a data booklet listing raw data and summary statistics, plus a single sample-location map.

The RGS Open Files due for release in 1992 will include the new analytical data as determined by INAA, and the original sample site information and analytical results for Zn, Cu, Pb, Ni, Co, Ag, Mn, Ag, Mo, U, W, Hg, As and Sb

TABLE 3-2-8
ANALYTICAL METHODS AND SPECIFICATIONS FOR ROUTINE RGS SUITE OF ELEMENTS

Element	Detection Limits	Sample Weight	Digestion Technique	Determination Method	
Cadmium	0.2 ppm				
Cobalt	2 ppm				
Copper	2 ppm		3 mL HNO_3 let sit overnight,		
Iron	0.02 %	1 g	add 1 mL HCl in 90°C water		
Lead	2 ppm		bath, for 2 hrs. cool, add 2 mL	A A S	
Manganese	5 ppm		H_2O, wait 2 hrs.		
Nickel	2 ppm				atomic absorption spectrophotometry using air-
Silver	0.2 ppm				acetylene burner and standard solutions for calibration,
Zinc	2 ppm				background corrections made for Pb, Ni, Co, Ag, Cd
Molybdenum	1 ppm	0.5 g	Al added to above solution		
Barium	10 ppm		HNO_3 - HCl - HF taken to		
Vanadium	5 ppm	1 g	dryness, hot HCl added to leach		
Chromium	5 ppm		residue		
Bismuth Antimony	0.2 ppm 0.2 ppm	2 g	HCl - $KClO_2$ digestion, KI added to reduce Fe, MIBK and TOPO for extraction	A A S - H	organic layer analyzed by atomic absorption spectrophotometry with background correction
Tin	1 ppm	1 g	sintered with NH_4I, HCl and ascorbic acid leach	A A S	atomic absorption spectrophotometry
Arsenic	1 ppm	0.5 g	add 2 mL KI and dilute HCl to 0.8M HNO_3 • 0.2M HCl	A A S - H	2 mL borohydride solution added to produce AsH_3 gas which is passed through heated quartz tube in the light path of atomic absorption spectrophotometer
Mercury	10 ppb	0.5 g	20 mL HNO_3 • 1 mL HCl	A A S - F	10% stannous sulphate added to evolve mercury vapour, determined by atomic absorption spectrometry
Tungsten	1 ppm	0.5 g	K_2SO_4 fusion, HCl leach	C O L O R	colorimetric: reduced tungsten complexed with toluene 3, 4 dithiol
Fluorine	40 ppm	0.25 g	$NaCO_3$ - KNO_3 fusion, H_2O leach	I O N	citric acid added and diluted with water, fluorine determined with specific ion electrode
Uranium	0.5 ppm	1 g	nil	N A D N C	neutron activation with delayed neutron counting
LOI	0.1 %	0.5 g	ash sample at 500°C	G R A V	weight difference
pH - water	0.1 pH unit	25 mL	nil	G C E	glass - calomel electrode system
U - water	0.05 ppb	5 mL	add 0.5 mL fluran solution	L I F	place in Scintrex UA-3
F - water	20 ppb	25 mL	nil	I O N	fluorine ion specific electrode

TABLE 3-2-9
ADDITIONAL ELEMENTS ANALYZED BY INNA

Element	Detection Limit	Element	Detection Limit
Gold	2 ppb	Molybdenum	1 ppm
Antimony	0.1 ppm	Nickel	10 ppm
Arsenic	0.5 ppm	Rubidium	5 ppm
Barium	100 ppm	Samarium	0.5 ppm
Bromine	0.5 ppm	Scandium	0.5 ppm
Cerium	10 ppm	Sodium	0.1 %
Cesium	0.5 ppm	Tantalum	0.5 ppm
Chromium	5 ppm	Terbium	0.5 ppm
Cobalt	5 ppm	Thorium	0.5 ppm
Hafnium	1 ppm	Tungsten	2 ppm
Iron	0.2 %	Uranium	0.2 ppm
Lanthanum	5 ppm	Ytterbium	2 ppm
Lutetium	0.2 ppm	Zirconium	200 ppm

in stream sediments and U, F and pH in waters. Data packages will be comprised of a data booklet and a second booklet containing a variety of 1:500 000-scale maps. Data booklets will present survey details, raw data listings, summary statistics and data interpretations. Map booklets will contain sample location maps, bedrock geology and surficial geology maps, symbol and value maps for each element and multi-element anomaly maps. The raw data will also be available as ASCII files on 5.25-inch high-density diskettes.

PRELIMINARY DATA EVALUATION

New analytical data for gold in sediments together with the original analytical results for copper, lead and zinc in sediments have been evaluated in order to:

- Illustrate a method of data evaluation incorporated in recent RGS publications.
- Demonstrate data confidence by showing that gold and base metal anomalies are associated with regions of known mineral potential.
- Provide explorationists with some background information to assist in their follow-up of the 1992 release of archive data.
- Further promote the upcoming release of previously unavailable analytical data for gold as well as other elements of interest.

This data reduction technique involves a statistical assessment of gold and base metal stream-sediment data which have been sorted on the basis of underlying geology (Table 3-2-10). Only those geological units having greater than 100 sample sites have been considered. The geological units utilized are the four-letter mnemonic names indicating rock type and a two-digit number refering to age that are listed in the original Open File publications. In contrast, the forthcoming 1992 release will use the geological formations associated with the 1:1 000 000 Geological Atlas Series compiled by Roddick *et al.* in 1979. Figure 3-2-5 further defines the data set by illustrating the proportion of anomalous (greater than the 90th percentile) gold and base metal samples located within each geological unit. The following summary of this statistical breakdown can be made for the gold and base metal concentrations.

GOLD (NEW DATA)

Stream-sediment samples from 3767 sites provided sufficient material to be analyzed by instrumental neutron activation for gold and 25 other elements. A total of 1285 of these sites (34%) reported gold concentrations greater than the 2 ppb detection limit. The mean gold value is 8 ppb, and the 90th, 95th and 98th percentile concentrations are 11, 21 and 56 ppb, respectively. The maximum gold determination reported was 932 ppb.

With reference to Table 3-2-10 and Figure 3-2-4, anomalous gold values tend to be particularly associated with the Triassic Cadwallader (Bralorne properties), Bridge River (Bridge River gold camp) and Nicola (Highland Valley mining camp) groups. The Paleozoic Fennell Formation (Chu Chua property) and Eagle Bay assemblage (Samatosum mine) are also characterized by a high proportion of anomalous sites. Although the Mesozoic and younger plutonic rocks contain 80 sites with anomalous concentration of gold, the actual number of anomalous sites is less than 7 per cent of the total number of sites found within this extensive geological unit (n=1214). Better resolution of lithologies comprising this unit would assist in the identification of the mineralized host at these anomalous sites.

BASE METALS (1979 AND 1981 DATA)

Original copper, lead and zinc analyses by atomic absorption consisted of a total data set of 4010 sample sites. Over 99 per cent of these sites reported copper concentrations greater than the 2 ppm detection limit. The mean copper value is 33 ppm, and the 90th, 95th and 98th percentile concentrations are 56, 77 and 110 ppm, respectively. The maximum copper determination reported was 1100 ppm. A total of 2458 sample sites (61%) reported lead concentra-

TABLE 3-2-10
SUMMARY STATISTICS

GOLD	ALL	TILL (44)	BSLT (42)	DCIT (42)	ANDS (36)	ANDS (32)	GRNS (32)	SLSN (30)	GRNS (11)	GRNT (41)
N	3767	333	272	232	244	326	150	224	121	1214
MEAN	7.87	7.03	4.61	4.70	9.59	10.49	14.42	12.31	11.94	[illegible]
SD	32.00	26.07	16.89	12.51	31.76	35.50	25.49	56.75	35.2	24.62
CV	4.07	3.71	3.66	2.66	3.31	3.38	1.77	4.61	2.95	4.00
MIN	2	2	2	2	2	2	2	2	2	2
MAX	932	357	211	130	276	406	170	588	247	348

COPPER	ALL	TILL (44)	BSLT (42)	DCIT (42)	ANDS (36)	ANDS (32)	GRNS (32)	SLSN (30)	GRNS (11)	GRNT (41)
N	4010	336	280	234	260	359	150	228	127	1298
MEAN	32.79	21.32	17.75	23.84	39.98	41.97	55.27	35.04	36.8	29.99
SD	44.18	16.00	10.20	19.87	66.19	44.65	39.46	31.68	23.4	53.90
CV	1.35	0.75	0.58	0.83	1.66	1.06	0.71	0.90	0.6	1.80
MIN	2	4	4	7	5	3	11	10	[illegible]	2
MAX	1100	130	98	240	920	560	380	400	15	1100

LEAD	ALL	TILL (44)	BSLT (42)	DCIT (42)	ANDS (36)	ANDS (32)	GRNS (32)	SLSN (30)	GRNS (11)	GRNT (41)
N	4010	336	280	234	260	359	150	228	127	1298
MEAN	4.79	2.62	4.04	2.57	4.19	4.00	3.70	3.24	6.5	4.59
SD	44.18	2.60	29.78	2.92	8.47	5.04	5.58	2.79	7.8	16.76
CV	1.35	0.99	7.37	1.14	2.26	1.26	1.51	0.86	1.2	3.55
MIN	2	2	2	2	2	2	2	2	[illegible]	2
MAX	540	20	500	26	128	50	45	26	5	330

ZINC	ALL	TILL (44)	BSLT (42)	DCIT (42)	ANDS (36)	ANDS (32)	GRNS (32)	SLSN (30)	GRNS (11)	GRNT (41)
N	4010	336	280	234	260	359	150	228	127	1298
MEAN	62.20	50.63	50.13	49.92	68.86	67.68	88.55	72.28	68.7	50.08
SD	50.37	38.05	33.33	23.59	74.26	43.33	37.31	31.48	63.4	45.93
CV	0.18	0.75	0.67	0.47	1.08	0.64	0.42	0.44	0.9	0.92
MIN	7	9	12	16	10	16	25	12	1	7
MAX	1000	380	445	320	1000	390	255	270	49	800

tions greater than the 2 ppm detection limit. The mean lead value is 5 ppm, and the 90th, 95th and 98th percentile concentrations are 8, 12 and 20 ppm, respectively. The maximum lead determination reported was 540 ppm. All of the sample sites reported zinc concentrations greater than the 2 ppm detection limit. The mean zinc value for the total data set is 62 ppm, and the 90th, 95th and 98th percentile concentrations are 96, 125 and 188 ppm respectively. The maximum zinc value reported was 1000 ppm.

Evaluation of the copper and zinc anomalies produced similar rock-type associations that were identified with the gold data. Although lead also has a similar association, lead anomalies are much more common in the Paleozoic Fennell Formation, Eagle Bay assemblage and plutonic rocks.

ACKNOWLEDGMENTS

Acknowledgments are extended to all government agencies and private companies who contributed to the successful completion of the 1991 RGS and RGS Archive programs.

REFERENCES

Holland, S.S. (1976): Landforms of British Columbia, A Physiographic Outline; *B.C. Ministry of Energy, Mines and Petroleum Resources*, Bulletin 48.

Matysek, P.F., Jackaman, W., Gravel, J.L., Sibbick, S.J. and Feulgen, S. (1991a): British Columbia Regional Geochemical Survey – Fernie (NTS 82G); *B.C. Ministry of Energy, Mines and Petroleum Resources*, RGS 27.

Matysek, P.F., Jackaman, W., Gravel, J.L., Sibbick, S.J. and Feulgen, S. (1991b): British Columbia Regional Geochemical Survey – Kananaskis Lakes (NTS 82J); *B.C. Ministry of Energy, Mines and Petroleum Resources*, RGS 28.

Matysek, P.F., Jackaman, W., Gravel, J.L., Sibbick, S.J. and Feulgen, S. (1991c): British Columbia Regional Geochemical Survey – Penticton (NTS 82E); *B.C. Ministry of Energy, Mines and Petroleum Resources*, RGS 29.

Matysek, P.F., Jackaman, W., Gravel, J.L., Sibbick, S.J. and Feulgen, S. (1991d): British Columbia Regional Geochemical Survey – Nelson (NTS 82F); *B.C. Ministry of Energy, Mines and Petroleum Resources*, RGS 30.

Matysek, P.F., Jackaman, W., Gravel, J.L., Sibbick, S.J. and Feulgen, S. (1991e): British Columbia Regional Geochemical Survey – Lardeau (NTS 82K); *B.C. Ministry of Energy, Mines and Petroleum Resources*, RGS 31.

Matysek, P.F., Jackaman, W., Gravel, J.L., Sibbick, S.J. and Feulgen, S. (1991f): British Columbia Regional Geochemical Survey – Vernon (NTS 82L); *B.C. Ministry of Energy, Mines and Petroleum Resources*, RGS 32.

Matysek, P.F., Jackaman, W., Gravel, J.L., Sibbick, S.J. and Feulgen, S. (1991g): British Columbia Regional Geochemical Survey – Seymour Arm (NTS 82M); *B.C. Ministry of Energy, Mines and Petroleum Resources*, RGS 33.

McLaren, G.P. (1990): A Mineral Resource Assessment of the Chilko Lake Planning Area; *B.C. Ministry of Energy, Mines and Petroleum Resources*, Bulletin 81.

Roddick, J.A., Tipper, H.W. (1985): Geology, Mount Waddington (92N) Map Area; *Geological Survey of Canada*, Open File 1163.

Roddick, J.A., Muller, J.E. and Okulitch, A.V. (1979): Fraser River – Sheet 92 – Geological Atlas Series; *Geological Survey of Canada*, Open File 1386A.

Wheeler, J.O., Brookfield, A.J., Gabrielse, H., Monger, J.W.H., Tipper, H.W. and Woodsworth, G.J. (1988): Terrane Map of the Canadian Cordillera; *Geological Survey of Canada*, Open File 1894.

DISTRIBUTION AND MORPHOLOGICAL CHARACTERISTICS OF VISIBLE GOLD IN HARRIS CREEK (82L/2)

By Zhihui Hou and W. K. Fletcher
The University of British Columbia

KEYWORDS: Applied geochemistry, stream sediments, gold particles, Corey Shape Factor.

INTRODUCTION

The distribution and morphology of gold particles from stream sediments, glacial tills and soils have been used to assess their distance from source (Antweiler and Campbell, 1977; Averill, 1988; Petts *et al.*, 1991; Nikkarinen, 1991; Averill and Huneault, 1991; Grant *et al.*, 1991). Here we present preliminary data on the distribution and morphology of gold in Harris Creek, southern British Columbia.

LOCATION AND GEOLOGY

Harris Creek is a gravel-bed river 25 kilometres east of Vernon in southern British Columbia (Figure 3-3-1). The catchment basin has an area of 225 square kilometres, of which about 60 per cent is between 1300 and 2000 metres above sea level on the dissected plateau of the Okanagan Highland. A simplified geological map, after Jones (1959), is shown in Figure 3-3-2. The area had a complex history during the Fraser glaciation when an ice sheet advancing from the north first impounded a lake in the Harris Creek catchment basin and then over-rode the glaciolacustrine sediments deposited in the lake (Ryder, 1991; Ryder and Fletcher, 1991). The lake was subsequently re-established as the ice sheet melted and retreated.

Our previous studies of gold in Harris Creek have shown that: preferential accumulation of gold in bar-head cobble-gravels counteracts the effects of downstream anomaly decay (Day and Fletcher, 1989, 1991; Fletcher, 1990), and transport of particulate gold only occurs during late spring when brief periods of high discharge caused by nival floods disrupt the cobble framework and release trapped gold (Fletcher and Wolcott, 1991).

STUDY METHODS

After removal of boulders a preliminary field concentrate was prepared by panning 40 kilograms of sediment, collected from bar-head sites (Figure 3-3-2) to obtain a near-black magnetite-rich sand. The field concentrate was then further upgraded in the laboratory with a gold pan. The magnetic fraction, which makes up about 90 per cent of the

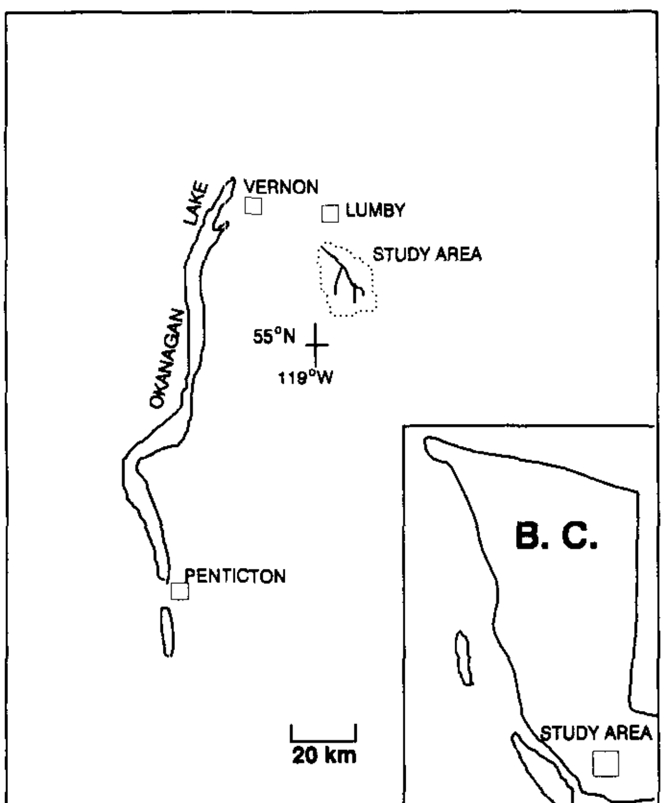

Figure 3-3-1. Location of study area.

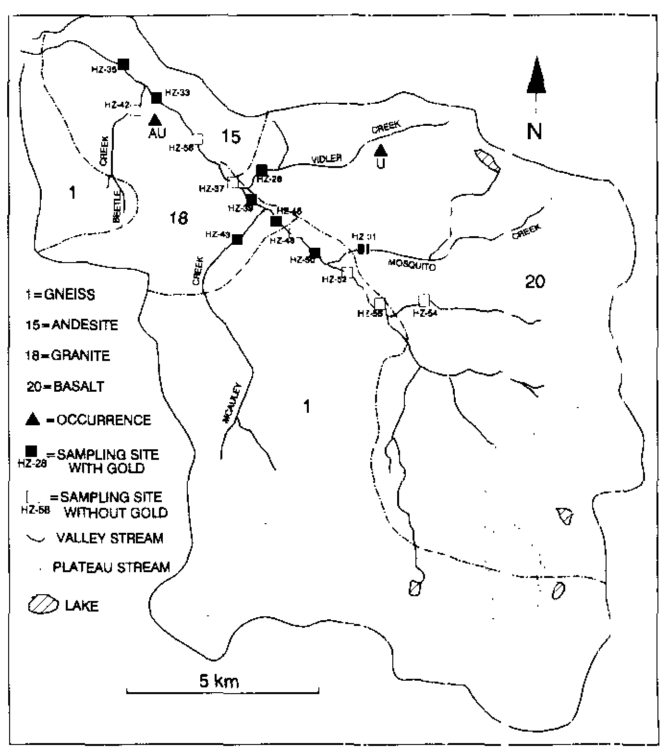

Figure 3-3-2. Catchment basin geology and sampling sites [geology simplified after Jones (1959)].

concentrate, was removed with a hand magnet. Gold particles were picked out of the nonmagnetic fraction under a binocular microscope.

The form and the size of the gold grains was investigated using the microscope and a Nanolab-7 scanning electron microscope. Grain size (d) was estimated as the geometric mean of the diameters of the intermediate and long axes [$d=(D_i*D_l)^{0.5}$, where D_i and D_l are the diameters of the intermediate and long axes, respectively. Particle shape is described using the Corey Shape Factor ($CSF=D_s/(D_i*D_l)^{0.5}$ where D_s is the smallest diameter]. The value of the Corey Shape Factor of flakes is from 0.1 to 0.3; the value of blocky grains from 0.5 to 0.7; and the value of near-spherical grains is 0.8 or larger. Grain roundness is a measure of the curvature of the corners and edges expressed as a ratio to the average curvature of the particle as a whole. It was estimated using Wadell's (1932) chart which has twelve sets of standard images with roundness values from 0.13 to 0.66: the roundness values of angular silhouettes varies from 0.13 to 0.35; subrounded ones from 0.35 to 0.60; and rounded ones from 0.60 to 0.66.

RESULTS AND DISCUSSION

Gold was found in Mosquito Creek (HZ-31) and at all but three sites on Harris Creek downstream from its confluence with Mosquito Creek (Table 3-3-1, Figure 3-3-2). Gold grains were also found in Vidler Creek (HZ-28) and McAuley Creek (HZ-43), but not in Beetle Creek or the headwaters of Harris Creek. There seems to be a slight increase in the abundance of gold grains downstream with the greatest number (3) at sites HZ-33 and HZ-35 on the main trunk.

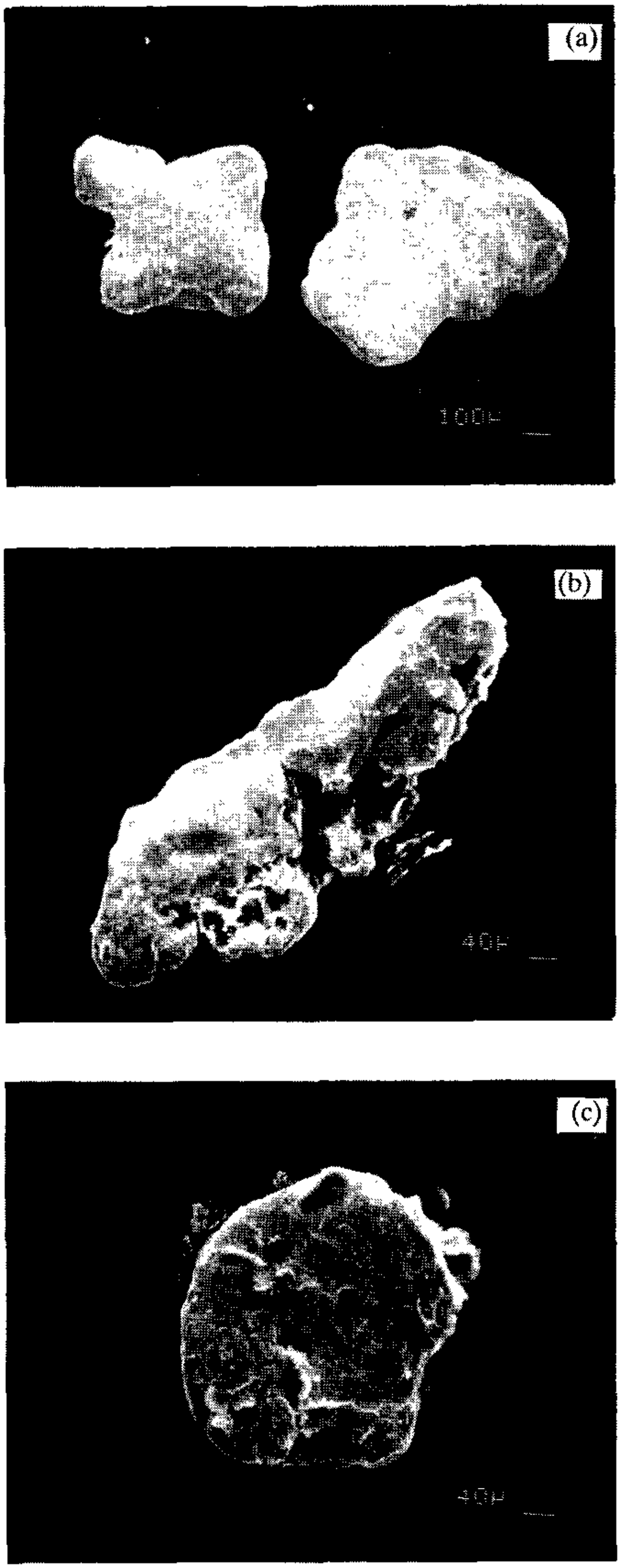

Plate 3-3-1. SEM photographs of (a) blocky shapes in HZ-35 with CSF 0.6 and 0.7, and roundness 0.3 and 0.6; (b) rod-like shape in HZ-46 with CSF 0.6, and roundness 0.4; and (c) spherical shape in HZ-50 with CSF 0.8, and roundness 0.6.

TABLE 3-3-1
SUMMARY OF DESCRIPTIVE CHARACTERISTICS OF VISIBLE GOLD FROM HARRIS CREEK

Sample number	Distance downstream (km)	Gold grains	Size (μm)	CSF	Roundness
Gold particles in the tributaries					
HZ-31	Mosquito Creek	2	348	0.3	0.2
			441	0.3	0.2
HZ-43	McAuley Creek	2	500	0.1	0.2
			292	0.5	0.5
HZ-28	Vidler Creek	1	297	0.3	0.5
Gold particles in the trunk stream					
HZ-50	1.0 km	1	353	0.8	0.6
HZ-46	2.4	2	430	0.6	0.4
			446	0.5	0.4
HZ-39	3.1	1	320	0.5	0.4
HZ-33	6.9	3	330	0.2	0.2
			393	0.7	0.3
			411	0.5	0.3
HZ-35	8.1	3	790	0.7	0.6
			669	0.6	0.3
			290	0.5	0.5

Note: $Size=(D_i*D_l)^{0.5}$, $CSF=D_s/(D_i*D_l)^{0.5}$ where D_s, D_i and D_l are the diameters of the short, intermediate and long axes, respectively.

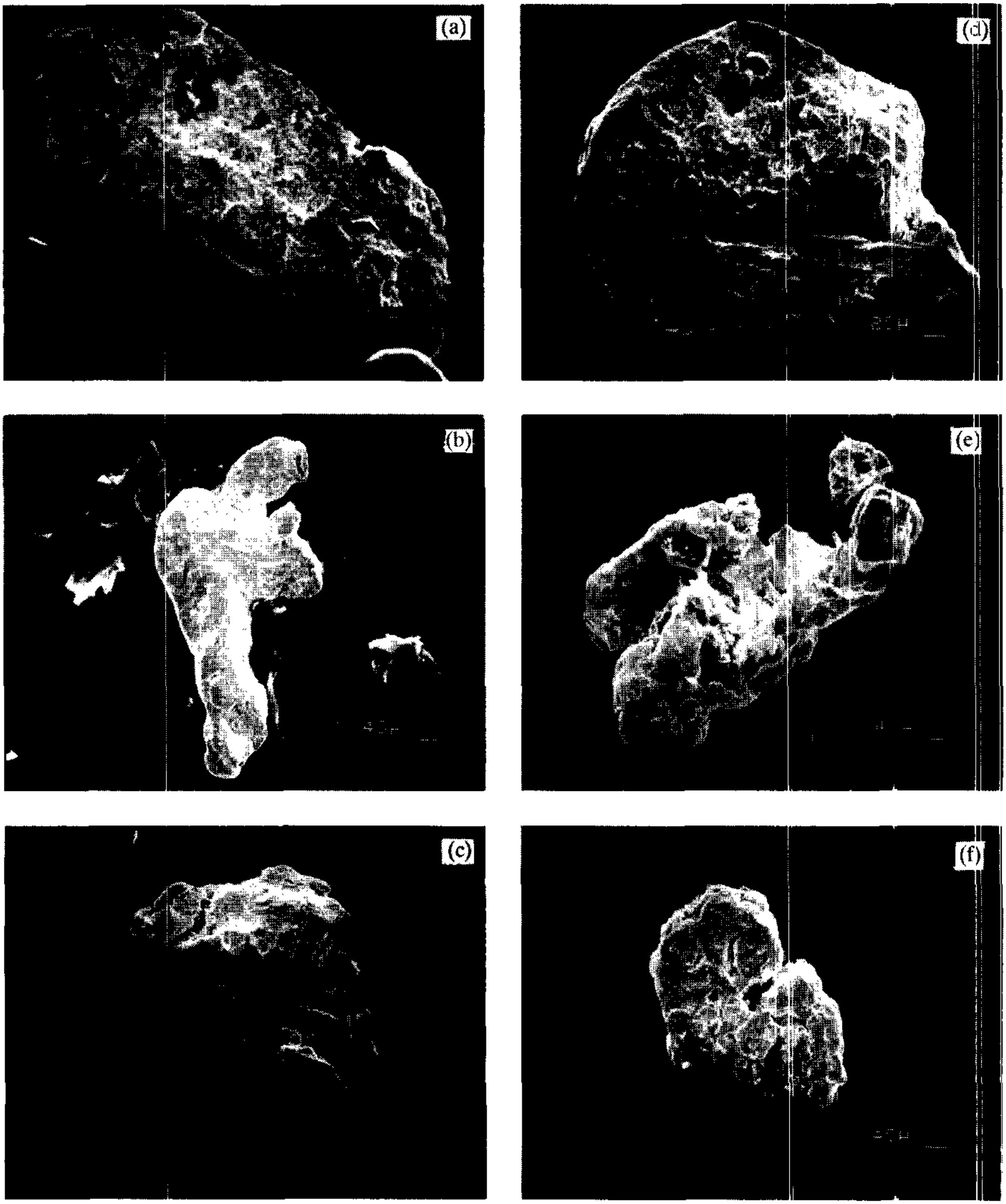

Plate 3-3-2. SEM photographs of (a) gold in HZ-43 with angular edges and blade shape, CSF 0.1, and roundness 0.2; (b) gold grain in HZ-31 with angular edges, smooth surface and flake shape, CSF 0.3, and roundness 0.2; (c) gold in HZ-33 with curled edges, CSF 0.5, and roundness 0.3; (d) gold in HZ-39 with striated surface, CSF 0.5, and roundness 0.4; (e) gold in HZ-46 with crumpled edges and porous surface, CSF 0.5, and roundness 0.4; and (f) gold in HZ-33 with scaly and porous surface, CSF 0.7, and roundness 0.3.

Size of the gold particles varies from 290 to 790 millimetres with both the maximum and minimum sizes being found in the downstream sample HZ-35. Based on their Corey Shape Factor, gold grains below the confluence with Mosquito Creek are blocky (Plate 3-3-1a) and rod-like (CSF 0.5 to 0.7; Plate 3-3-1b) or near-spherical (CSF 0.8; Plate 3-3-1c). Blades (Plate 3-3-2a) and flakes (Plate 3-3-2b) of gold (CSF 0.1-0.3) are more typical of the tributary streams. Roundness of the gold grains varies erratically, but those in Mosquito Creek (and perhaps McAuley Creek) appear to be less rounded than those from the trunk stream.

Dilabio (1990) proposed a nongenetic, descriptive classification of the shapes and surface textures of gold (Table 3-3-2). No pristine gold grains were found. However, gold particles in McAuley Creek and Mosquito Creek have blade and flake shapes with angular edges (Plate 3-3-2a, b) that approach pristine. Gold particles in the trunk stream having curled edges (Plate 3-3-2c) and moderately striated surfaces (Plate 3-3-2d) are classified as "modified"; and others having crumpled edges and porous surfaces (Plate 3-3-2e), and scaly, felty and porous surfaces (Plate 3-3-2f) are classified as "reshaped".

Although gold is widely distributed in the Harris Creek catchment basin, too few gold grains were found to make definitive statements about trends in their abundance and morphology. Nevertheless, it appears that abundance, size, sphericity, roundness, and degree of modification and reshaping may increase downstream. In contrast, grains in McAuley Creek and Mosquito Creek are more flake-like and pristine with lower roundness and CSF values.

The presence of gold in McAuley, Mosquito and Vidler creeks suggests that there may be several distinct bedrock sources of gold. Possibilities include: placer gold in uraniferous channel-gravels below Miocene plateau basalts in the Vidler Creek and Mosquito Creek catchment basins (Day, 1987); and a source in granodiorite and gneiss for the delicate gold grains found in McAuley Creek. The near-pristine character of these grains suggests proximity to their source. However, because of the complex glacial history of the Harris Creek catchment basin, it is also possible that the widespread distribution of gold results partly from its dispersion throughout the catchment basin as a result of glacial and glaciolacustrine processes.

The (slight) increase in abundance and size of gold grains downstream is consistent with the observation of Day and Fletcher (1989) that trapping of gold by bar-head cobble-gravels counteracts downstream anomaly dilution in Harris Creek. Field evidence and bedload transport theory both indicate that this process is most effective for coarse gold (Day and Fletcher, 1991).

TABLE 3-3-2
CLASSIFICATION OF SHAPES AND SURFACE TEXTURES OF GOLD GRAINS (AFTER DILABIO (1990)

Class	Shape	Surface texture
Pristine	—block —rod —wire —leaf —crystal —star —globule	—smooth surface —angular edges —grain moulds clearly visible —thin edges not curled —some striae
Modified	—all shapes damaged	—pristine shapes visible —leaf edges and wires bent —blunted and thickened edges —grain moulds preserved where protected. —moderately striated —felty texture where damaged
Reshaped	—folded rod wire, flake —rounded block —typical discoid placer flake —nugget	—pristine shapes destroyed —well-rounded grain outline —moderately striated —porous, scaly, felty or spongy

CONCLUSIONS

Preliminary studies of the distribution and morphology of gold in the Harris Creek catchment basin suggest that there may be several bedrock sources of gold. Alternatively, gold may have been widely dispersed by glacial processes. The downstream increase in abundance of coarse gold is consistent with earlier field observations and bedload transport theory.

ACKNOWLEDGMENTS

We thank S. Babakaieff, J. Borges, L.A. Groat and B. Cranston for their assistance. The study is part of an ongoing program funded by grants to WKF from Noranda Exploration Ltd.; the Geoscience Research Grant Program of the British Columbia Ministry of Energy, Mines and Petroleum Resources; a Research Agreement with the Geological Survey of Canada; and a Natural Science and Engineering Research Council of Canada operating grant.

REFERENCES

Antweiler, J. and Campbell, W. (1977): Application of Gold Compositional Analyses to Mineral Exploration in the United States; *Journal of Geochemical Exploration*, Volume 8, pages 17-29.

Averill, S. (1988): Regional Variations in the Gold Content of Till in Canada; *in* Prospecting in Areas of Glaciated Terrain 1988, MacDonald, D.R. and Mills, K.A., Editors, *Canadian Institute of Mining and Metallurgy*, London, Ontario, pages 271-284.

Averill, S.A. and Huneault, R. (1991): Using Silt-sized Visible Gold Grains to Explore for Gold Deposits Concealed by Quaternary Overburden: Nevada vs. Canada; *Explore*, Number 72, Pages 1-12.

Day, S.J. (1987): Sampling Stream Sediments for Gold in Mineral Exploration, Southern British Columbia; unpublished M.Sc. thesis, *The University of British Columbia*, 232 pages.

Day, S.J. and Fletcher, W.K. (1989): Effect of Valley and Local Channel Morphology on the Distribution of Gold in Stream Sediments from Harris Creek, British Columbia, Canada; *Journal of Geochemical Exploration*, Volume 32, pages 1-16.

Day, S.J. and Fletcher, W.K. (1991): Concentration of Magnetite and Gold at Bar and Reach Scales in a Gravel-bed Stream, British Columbia, Canada; *Journal of Sedimentary Petrology*, Volume 61, No. 6.

DiLabio, R.N.W. (1990): Classification and Interpretation of the Shapes and Surface Textures of Gold Grains from Till on the Canadian Shield; *Geological Survey of Canada*, Paper 90-1C, pages 323-329.

Fletcher, W.K. (1990): Dispersion and Behavior of Gold in Stream Sediments; *B.C. Ministry of Energy, Mines and Petroleum Resources*, Open File 1990-28, 28 pages.

Fletcher, W.K. and Wolcott, J. (1991): Transport of Magnetite and Gold in Harris Creek, British Columbia, Canada, and Implication for Exploration; *Journal of Geochemical Exploration*, Volume 41, pages 253-274.

Grant, A.H., Lavin, O.P. and Nichol, I. (1991): The Morphology and Chemistry of Transported Gold Grains as an Exploration Tool; *Journal of Geochemical Exploration*, Volume, 40, pages 73-94.

Jones, A.G. (1959): Vernon Map-area, British Columbia; *Geological Survey of Canada*, Memoir 296.

Nikkarinen, M. (1991): Size, Form and Composition of Gold Grains in Glacial Drift in Ilomantsi, Eastern Finland; *Journal of Geochemical Exploration*, Volume 39, pages 295-320.

Petts, G.E., Coats, J.S. and Hughes, N. (1991): Freeze-sampling Method of Collecting Drainage Sediments for Gold Exploration; *The Institution of Mining and Metallurgy*, Transactions, Volume 100, pages B28-B32.

Ryder, J.M. (1991): Quaternary Geomorphology and Terrain Map of the Harris Creek Area (82L/2); *B.C. Ministry of Energy, Mines and Petroleum Resources*, Open File 1990-18.

Ryder, J.M. and Fletcher, W.K. (1991): Exploration Geochemistry – Sediment Supply to Harris Creek (82L/2); *in* Geological Fieldwork 1990, *B.C. Ministry of Energy, Mines and Petroleum Resources*, Paper 1991-1, pages 301-306.

Wadell, H. (1932): Volume, Shape, and Roundness of Rock Particles; *Journal of Geology*, Volume 40, pages 443-451.

NOTES

NEOTECTONIC INVESTIGATIONS ON VANCOUVER ISLAND (92B, F)

**By P.T. Bobrowsky, B.C. Geological Survey Branch
and J.J. Clague, Geological Survey of Canada**

KEYWORDS: Geological hazards, neotectonics, Quaternary, Shoemaker Bay, tsunami, C^{14}, Port Alberni, Tofino, Island View Beach, Gyro Park, earthquakes, sedimentology.

INTRODUCTION

Quaternary geologic studies were undertaken by staff of the British Columbia Geological Survey Branch and Geological Survey of Canada at several locations during 1991. These studies are part of a multi-year program aimed at assessing the Holocene seismicity, neotectonism and sea level history of Vancouver Island and adjacent mainland British Columbia (Clague and Bobrowsky, 1990). This research will provide information on the probability and likely impacts of catastrophic natural events such as earthquakes and tsunamis. The 1991 field activities of this joint provincial-federal research effort consisted of three parts: a scientific cruise in Saanich Inlet in February; excavations near Port Alberni in June; and sonic drilling and excavation near Victoria and Port Alberni in September (Figure 3-4-1). A second cruise in Saanich Inlet to obtain air-gun seismic reflection data is tentatively planned for late 1991. The objective of the Saanich Inlet cruise was to recover sediment cores which might provide a record of late Holocene earthquakes. Cores up to 11 metres in length, spanning approximately the last 2000 years, were retrieved at five locations. These cores supplement three others collected and described previously (Bobrowsky and Clague, 1990). Detailed micropaleontological, sedimentological and geochronological analyses are currently in progress (Blaise, 1992).

Shovel excavations were made in undisturbed marsh sediments near Port Alberni to document historic and prehistoric tsunamis. Samples for Cs^{137} and C^{14} dating and micropaleontological analysis were collected and are now being processed; the results will be presented in a future publication. The Port Alberni work developed from the authors' discovery of possible tsunami deposits near Tofino in 1990 (Bobrowsky and Clague, 1991b). At the time of publication of the Tofino results, an absence of C^{14} dates precluded an adequate synthesis of some of the data. Two new dates of 7070±120 years B.P. (AECV-1205C) and 7900±100 years B.P. (GSC-5106) obtained from tree stumps rooted in marine muds below mean sea level now permit an expanded interpretation of Holocene sea level fluctuations in this area (Bobrowsky and Clague, 1991a). Briefly, these new dates, coupled with evidence for late Holocene raised shorelines (Friele, 1991) indicate a middle Holocene transgression followed by regression during the late Holocene (Figure 3-4-2).

Observations and preliminary results of the third component of our 1991 fieldwork (sonic drilling) are presented below.

DRILL SITES

Sonic drilling was done at three sites: Island View Beach (48°35'N, 123°22'W) on the east side of Saanich Peninsula; Gyro Park (48°28'N, 123°18'W) at Cadboro Bay, north of Victoria; and Shoemaker Bay (49°15'N, 124°50'W) directly west of Port Alberni (Figure 3-4-1). One hole was drilled at Island View Beach north of the park access road on the west side of a Holocene spit complex (CIA-91-171). Some 500 metres of wetland separates the drill site from eroded Pleistocene bluffs to the west. Two holes were drilled at Gyro Park, one at the southern edge of the park at the upper limit of the beach (CIA-91-172) and the other approximately 10 metres northeast of the parking lot and 20 metres northwest of the park washrooms (CIA-91-173). Two holes were also drilled at Shoemaker Bay, one on a road extending into the marsh area some 100 metres south of the Alberni pulpmill water pipeline (CI4A-91-174) and the other approximately 500 metres to the west of the first, at the edge of the marsh (CIA-91-175) (Plate 3-4-1).

METHODS

Drilling was done with a truck-mounted rotosonic drill operated by Sonic Drilling Ltd. of Surrey, B.C. (Plate 3-4-2). This machine uses high-frequency vibrations to retrieve intact sediment cores up to 6 metres in length and 10 centimetres in diameter. Rapid penetration of the sediment is achieved by the vibratory action of the drill pipe which causes soil particles to fluidize at the drill bit and along the pipe edge. Intact sediment slides into the pipes as drilling progresses. Individual core sections are extruded into plastic sleeves for storage, transport or on-site examination (Plate 3-4-3).

Extruded cores were split in the field and described in detail. Description includes observations on the type and texture of the sediment, primary and secondary structures, the thickness of lenses, laminae and beds, the nature of the bounding contacts, and the type and distribution of organic material. Photographs were taken of all cores. Samples were collected for C^{14} dating, geochemistry and micropaleontological analysis.

RESULTS

At Island View Beach (CIA-91-171), continuous core was recovered to a depth of 14 metres (Figure 3-4-3). Most of the sediment consists of clean, medium to coarse sand with scattered small rounded pebbles. Lenses and layers of sandy gravel are present throughout the sequence, and a silt bed 1 metre thick occurs at 9 to 10 metres depth. Basal contacts of muddy and gravelly interbeds are generally sharp. Three samples, comprising wood and shell, were recovered from the silt bed for C^{14} dating.

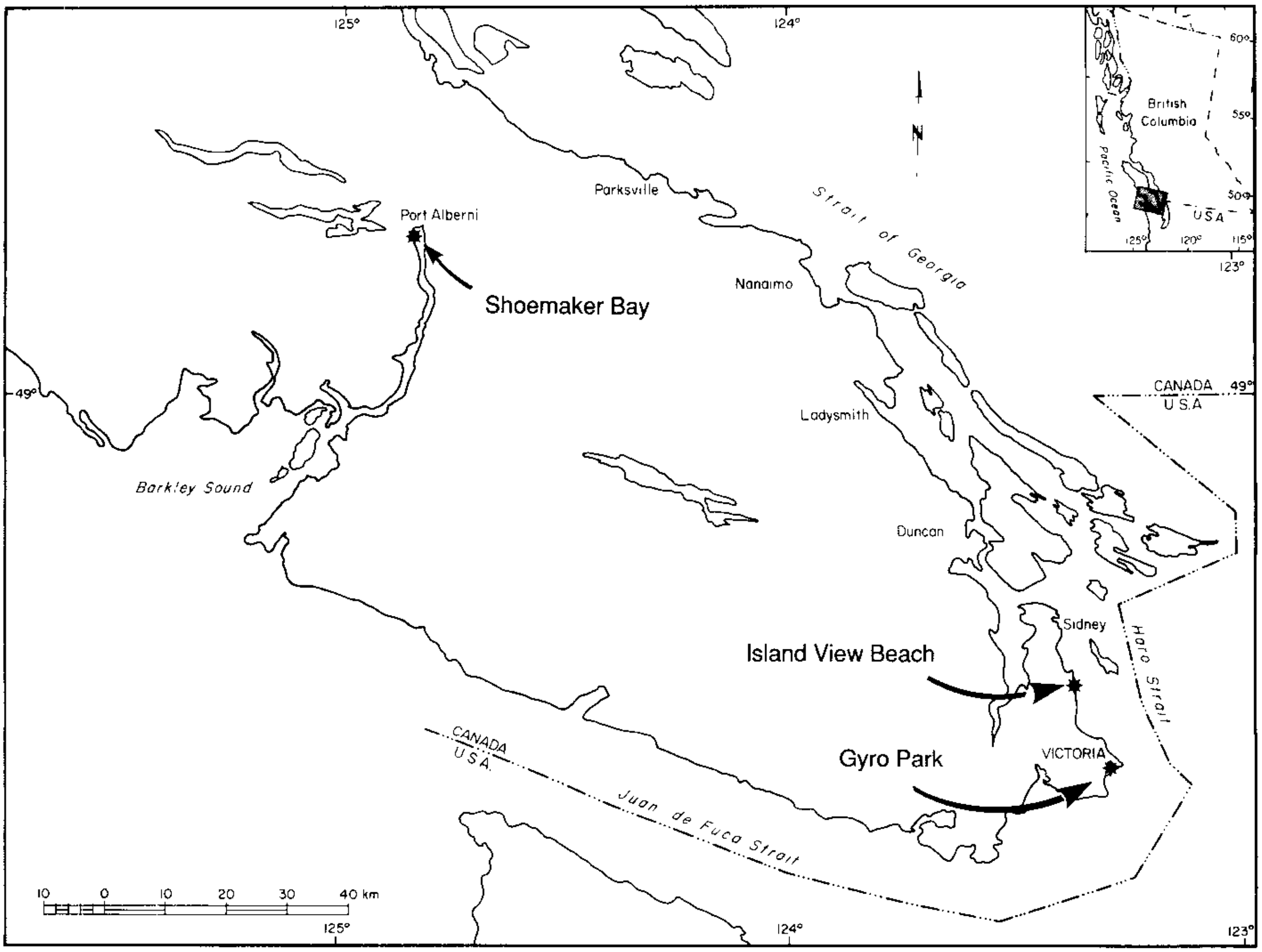

Figure 3-4-1. Location map of 1991 drilling sites.

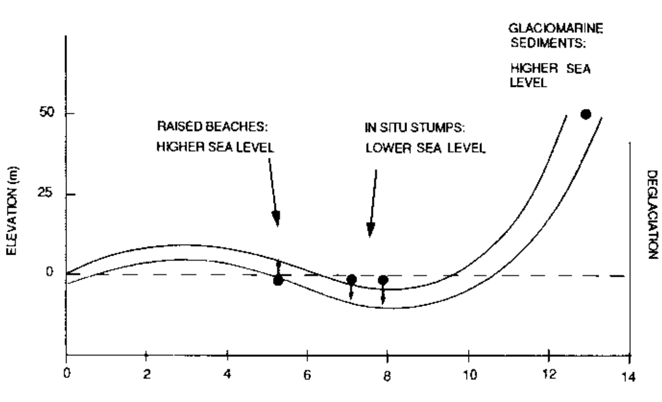

Figure 3-4-2. Sea-level curve for the Tofino area. Interpretation based on radiocarbon dates by the authors and raised shoreline data by Friele (1991).

Cores were collected to 7.9 metres depth at the Gyro Park beach site (CIA-91-172). The sequence, from top to bottom, is: approximately 3 metres of well sorted coarse sand and gravel (modern beach facies), 3 metres of Holocene peat, and approximately 2 metres of pebbly sand and sandy gravel. The basal contacts of the units are gradational. Eight samples for foraminiferal analysis and two wood samples for C^{14} dating were collected from the lower part of the peat unit and from a thin muddy zone just below the peat. The second set of cores at Gyro Park (CIA-91-173) totalled 12.5 metres in length (Figure 3-4-4). Five major units are recognized; from top to bottom, these are: approximately 0.5 metre of fill, 2.5 metres of compacted peat, 6.5 metres of sand and gravel, 3 metres of silty clay and sandy silt, and shelly pebbly sand. All contacts, except that between the fill and peat, are gradational.

About 27 metres of sediment were cored at the first Shoemaker Bay drill site (CIA-91-174). Approximately 3 metres of road fill abruptly overlies 2 metres of silty mud with sandy interbeds, which in turn sharply overlies 22 metres of alternating lenses and beds of sandy gravel and pebbly sand. Six wood samples were collected at depths of 4.5 to 6 metres for C^{14} dating. The second Shoemaker Bay drill hole cored 11.5 metres (CIA-91-175; Figure 3-4-5). The upper 3.7 metres is road fill. This sharply overlies about 0.5 metre of muddy peat and organic mud containing sandy

Plate 3-4-1. General view of drilled marsh sediments at Shoemaker Bay area Port Alberni.

interbeds. This unit grades downwards over a short distance into 0.8 metre of sedgy sand with scattered stones. The remaining 6.5 metres of the sequence consists of massive fossiliferous muddy silt intercalated with thin beds of clean sand. One thick (*ca.* 60 cm) pebbly sand bed occurs at a depth of 8 to 9 metres. Eight C^{14} samples were recovered from the sediments at depths ranging from 5 to 11.5 metres.

DISCUSSION

The stratigraphy at Island View Beach supports the earlier sea-level interpretations of Clague (1989). The predominantly coarse sediments record a lengthy period of intertidal and perhaps shallow subtidal sedimentation at a time when sea level was lower than at present. The sediments are part of a complex spit that was deposited by waves and longshore currents. The source of the sediments is Pleistocene bluffs at Cowichan Head to the south. Interbeds of fine sediment (silt and clay) indicate periods of quiescence, whereas coarser gravel beds record episodic storms.

At Gyro Park, the lowest cored sediments contain a marine shelly fauna and thus record a marine depositional environment (probably shallow subtidal or intertidal). Overlying interbeds of sand and gravel were deposited in an inshore or foreshore environment. Subsequent emergence of the site is indicated by the accumulation of peat. The uppermost unit of sand and gravel at site CIA-91-172 indicates that a transgression has occurred in the last few thousand years.

The thick sand and gravel sequence at drill site CIA-91-174 at Shoemaker Bay is probably fluviodeltaic in origin and may have been deposited, in part, during a period when sea level was lower than today. Of greater interest, however, are the sharply bounded layers of sand in the overlying mud unit. These may be tsunami deposits and are the focus of our ongoing work in this area.

ACKNOWLEDGMENTS

The drilling was done by R. Foussy (Sonic Drilling Ltd.).

REFERENCES

Blaise, A. (1992): Holocene Sediments from Saanich Inlet, British Columbia, and their Neotectonic Implications; *in* Current Research, Part A, Cordillera and Pacific Margin, *Geological Survey of Canada*, Paper 92-1A, in press.

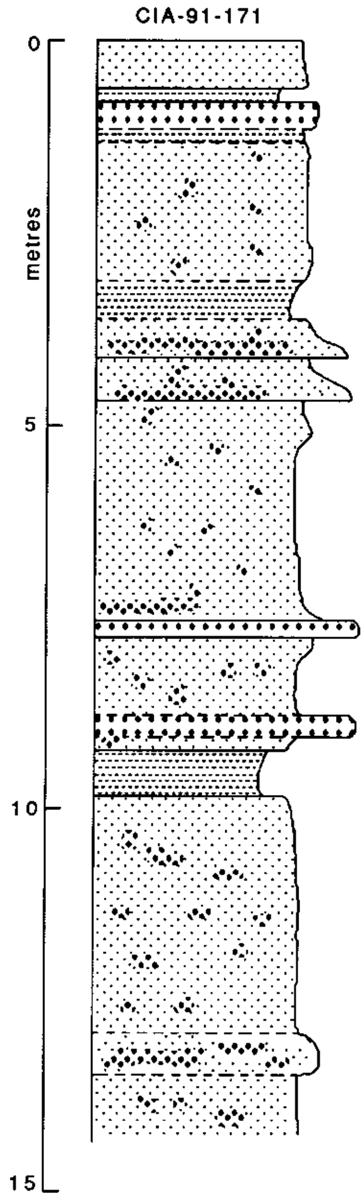

Figure 3-4-3. Composite core stratigraphy at Island View Beach (CIA-91-171).

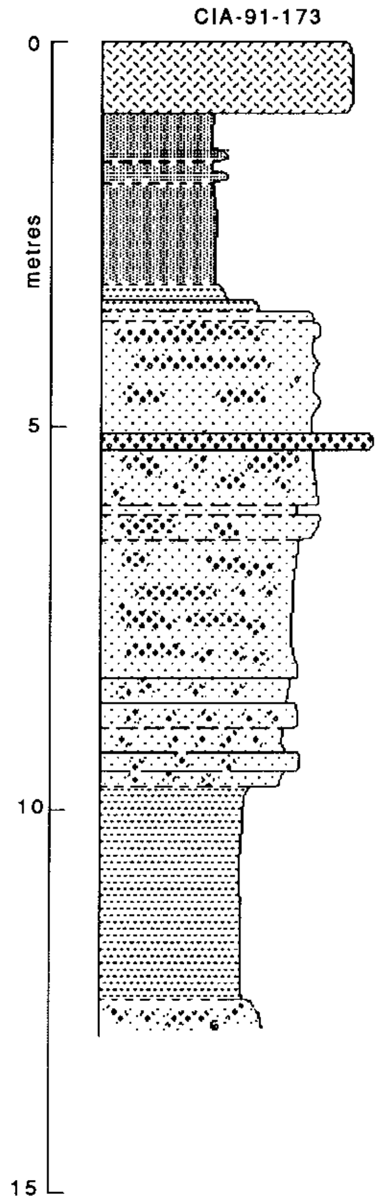

Figure 3-4-4. Composite core stratigraphy at Gyro Park (CIA-91-173).

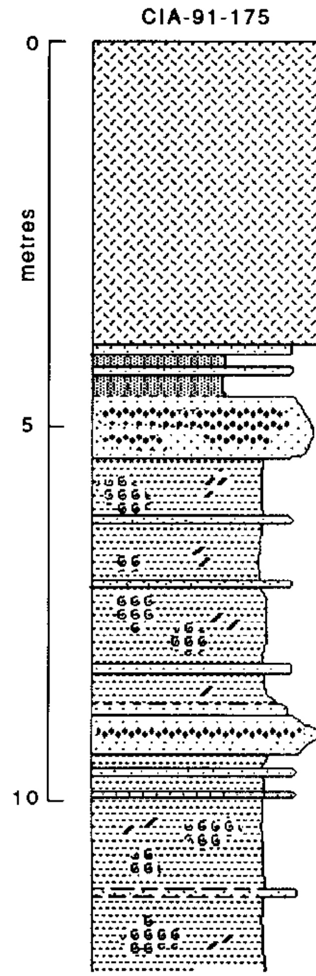

Figure 3-4-5. Composite core stratigraphy at Shoemaker Bay (CIA-91-175).

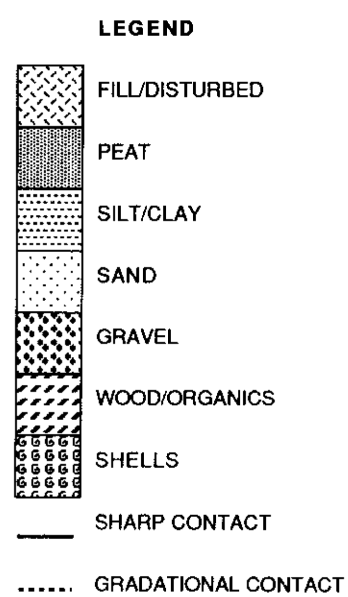

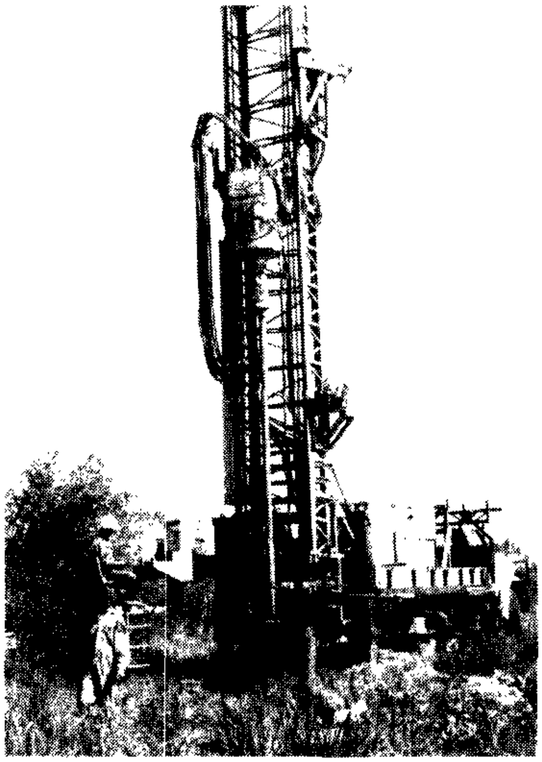

Plate 3-4-2. View of sonic drill used in neotectonic study to obtain solid core of unconsolidated sediment.

Bobrowsky, P.T. and Clague, J.J. (1990): Holocene Sediments from Saanich Inlet, British Columbia, and their Neotectonic Implications; *in* Current Research, Part E. *Geological Survey of Canada*, Paper 90-1E, pages 251-256.

Bobrowsky, P.T. and Clague, J.J. (1991a): Late Glacial and Post-glacial History of the Tofino Area, British Columbia; *Canadian Quaternary Association*, Biennial Meeting, Programs and Abstracts, page 16.

Bobrowsky, P.T. and Clague, J.J. (1991b): Neotectonic Investigations on Western Vancouver Island, British Columbia (92F/4); *in* Geological Fieldwork 1990, *B.C. Ministry of Energy, Mines and Petroleum Resources*, Paper 1991-1, pages 307-313.

Clague, J.J. (1989): Late Quaternary Sea Level Change and Crustal Deformation, Southwestern British Columbia; *in* Current Research, Part E, *Geological Survey of Canada*, Paper 89-1E, pages 234-236.

Clague, J.J. and Bobrowsky, P.T. (1990): Holocene Sea Level Change and Crustal Deformation, Southwestern British Columbia; *in* Current Research, Part E, *Geological Survey of Canada*, Paper 90-1E, pages 244-250.

Friele, P.A. (1991): Holocene Relative Sea-level Change: Vargas Island, British Columbia; unpublished M.Sc. thesis, *Simon Fraser University*, 106 pages.

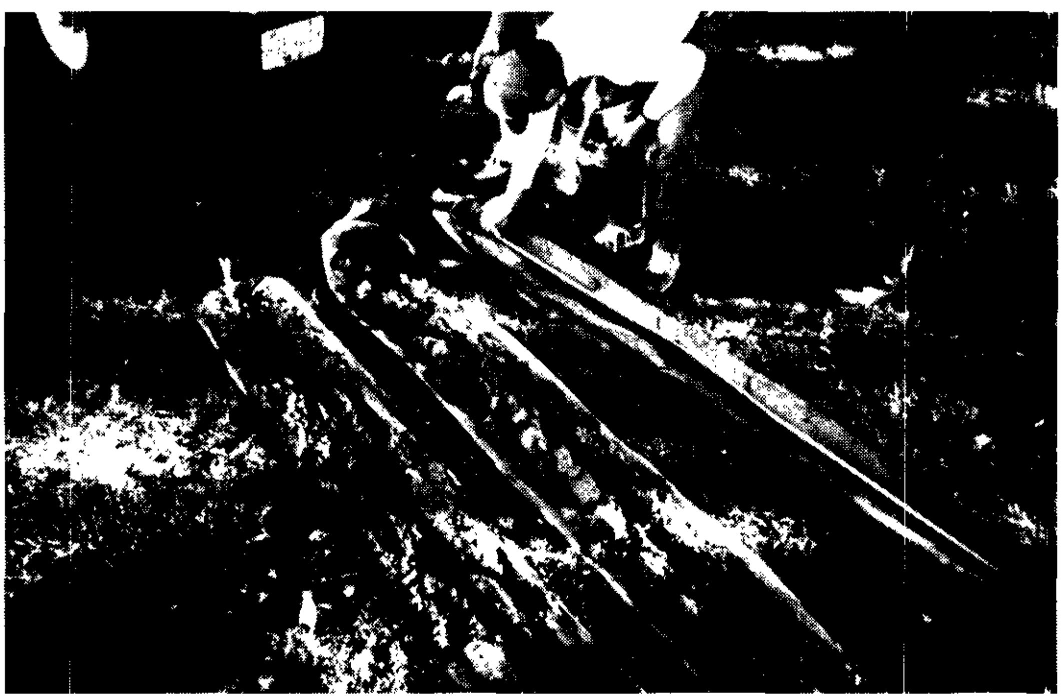

Plate 3-4-3. Extruded core being examined during sectioning and logging at the drill site.

NOTES

AN EVALUATION OF THE POTENTIAL AGGREGATE RESOURCES FOR SOOKE LAND DISTRICT, B.C. (92B/5)

By J.R. Goff and S.R. Hicock
The University of Western Ontario

KEYWORDS: Surficial geology, aggregate, Sooke, sedimentation model.

INTRODUCTION

This study details potential aggregate resources within the Sooke Land District (Figure 3-5-1). A model which charts the interactions between Middle and Late Pleistocene ice-sheets and ice-marginal sedimentation was developed to assist in the process of identifying potential aggregate sources. Information concerning general bedrock and surficial geology has been derived from published sources (Muller, 1980; Senyk, 1972). More detailed data on surficial geology have been obtained from airphoto interpretation, ground survey, laboratory analysis and further published and unpublished sources.

Urban areas in the study area are within one hour's drive of Victoria and have considerable potential for future commercial and residential development. Ongoing improvements to Highway 14 are indicative of the need for further aggregate resources, a demand which will not decline in the foreseeable future. The urban areas of Sooke, Milnes Landing and Saseenos, have limited extraction potential, but aggregate resources located in these areas are also discussed on the premise that economic priorities often change.

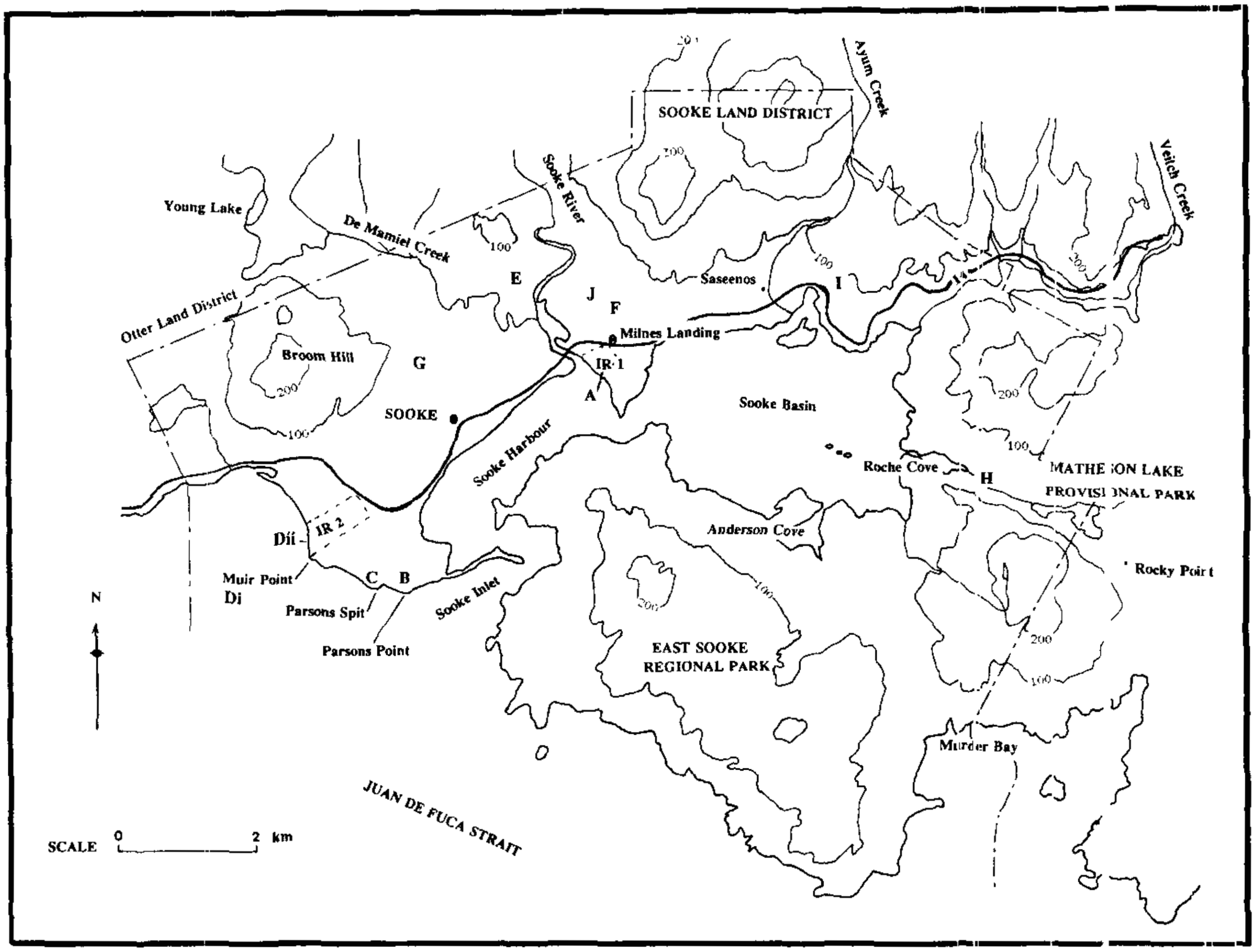

Figure 3-5-1. Sooke Land District — physiographic map (contours in metres; based on Energy, Mines and Resources, Canada, 1981).

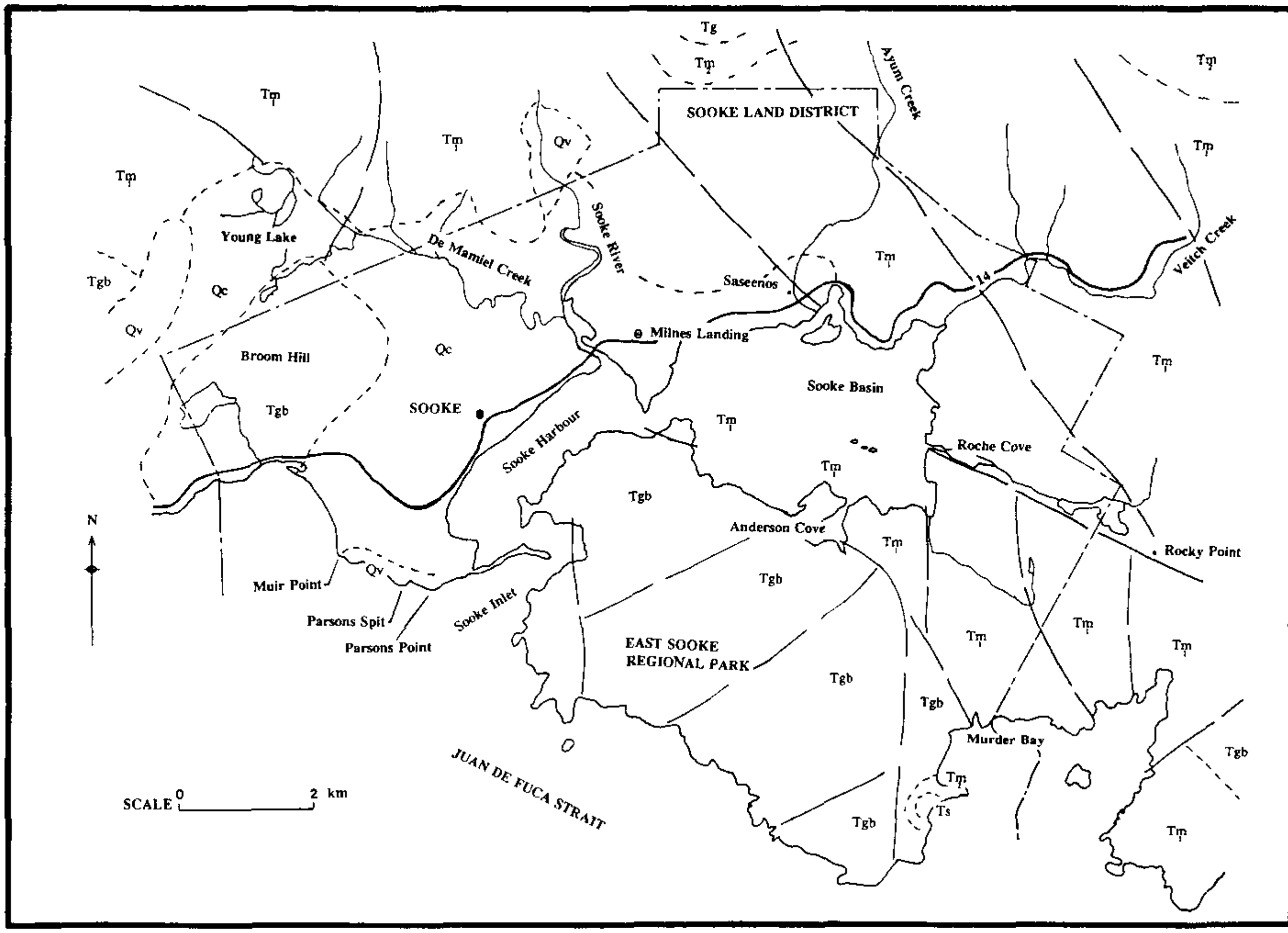

QUATERNARY

Qc — CAPILANO SEDIMENTS: sand, gravel; silt, clay

Qv — VASHON DRIFT: gravel, sand, till

TERTIARY
Miocene ?

Ts — SOOKE FORMATION: conglomerate, sandstone, shale

Eocene (and older ?)

Tg — CATFACE PLUTONIC SUITE: quartz dolerite, agmatite

Tm — METCHOSIN VOLCANICS: Tm_1: pillow basalt, breccia, tuff; Tm_2: mainly basaltic lava

Tgb — SOOKE GABBRO: mainly gabbro

Geological boundary, approximate

Fault, approximate

Highway

Figure 3-5-2. Sooke Land District — geology map (based on Muller, 1980).

BEDROCK GEOLOGY — GENERAL

The geology of Sooke Land District is dominated by two rock types: Sooke gabbro and Metchosin volcanics (Figure 3-5-2). Sooke gabbro constitutes the bedrock in the Broom Hill – East Sooke Regional Park area, while to the northeast, the remainder of the Sooke Land District is underlain by Metchosin volcanics.

SURFICIAL GEOLOGY AND GENERAL PHYSIOGRAPHY

Located in the southwest corner of Vancouver Island, the Sooke Land District is centred on Sooke Inlet. This physiographic relationship is reflected by a radial drainage pattern into Sooke Basin (Figure 3-5-1). The geology map (Figure 3-5-2) identifies some Quaternary deposits, namely: Capilano sediments (sand, gravel, silt and clay) and Vashon drift (gravel, sand and till) to the north and south of Sooke. Senyk's (1972) general terrain map provides further data, but results of ground surveys carried out during this study suggest that some refinement is needed and it is not reproduced. Sediment provenance and physiographic observations are combined to identify potential aggregate sources both in and around the Sooke Land District area.

Unconsolidated surficial materials are largely of Pleistocene or Recent age. Sedimentation by Pleistocene ice masses, meltwater and more recent subaerial processes has resulted in complex depositional sequences which have been only partially interpreted (Clapp, 1912; Bretz, 1920; Mayers and Bennett, 1973; Alley, 1979; Alley and Chatwin, 1979; Hicock, 1980, 1990; Thorson, 1980; Clague, 1981; Hicock and Armstrong, 1983; Hicock *et al.*, 1983; Hicock and Dreimanis, 1985; Alley and Hicock, 1986).

The following subsections detail the main physiographic features of relevance to potential aggregate sources. Site-specific data are discussed in more detail in the section titled Aggregate Resource Development. Finally, this information is collated under Sedimentation Model to produce a model of Middle and Late Pleistocene ice-sheet and ice-marginal sedimentation and the subsequent evolution of Holocene deposits.

Glacial Landforms and Deposits

Ground and airphoto surveys reveal no obvious depositional landforms, although till and diamicton were recovered from several sites. In general, glacial sediments have either been covered by even younger deposits or have been substantially eroded leaving isolated "till" islands. Deposits related to pre-Sangamonian (Illinoian ?) and Late Wisconsinan glaciations are exposed in coastal bluffs at Muir Point (Clague, 1981; Hicock and Armstrong, 1983). However, at Parsons Spit the lower, pre-Sangamonian till is no longer exposed above the beach. Moreover, the Late Wisconsinan till is discontinuous and is not found beyond the southwestern margin of Muir Point. Further evidence of glacial deposition is apparent on both banks of Ayum Creek, inland from the delta for about 2 kilometres. Although heavily incised and reworked by fluvial processes, this deposit generally retains its integrity as a till island surrounded by colluvially covered bedrock and recent fluvial sediments.

On the west side of Sooke River, ice-marginal deposits rest upon lacustrine sediments. This is indicative of glacial activity in the valley, although supplementary evidence appears to have been effectively removed by paraglacial processes during ice retreat. These deposits (and the underlying lacustrine sediments) have been sharply truncated at their southern end.

Evidence for erosional activity by glacier ice can be found in the widened valleys of Sooke River, Ayum and Veitch creeks. Of particular interest are two subglacial channels situated in the southeast of the Sooke Land District (Murder Bay to Anderson Cove, and Rocky Point to Roche Cove). Both are oriented northwest along fault lines; the more easterly valley incorporating the railway-line footpath and Matheson Lake (Provincial Park) is longer and wider than the other.

Sooke Basin, Harbour and Inlet are the best indicators of glacial erosion in this area. Their probable genesis was glacial scour by the combined ice flows of valley glaciers (Sooke River, Ayum and Veitch creeks) and the Juan de Fuca lobe. Ice streaming, associated with subglacial lubrication (from the two channels to the southeast of Sooke Basin), would have produced faster flowing ice into the basin than along the strait. Confinement by the valley glaciers of Ayum and Veitch creeks would have produced local ice build-up, rising compressive flow and subsequent scour. Sooke Inlet and Harbour, were probably created by ice flows redirected by the Sooke River glacier, following slowdown of the ice mass in Sooke Basin. This is considered to have occurred early in the glacial history of the area, perhaps pre-Sangamonian (Illinoian ?), because later deposits suggest a more passive glacial environment, closer to the limits of ice advance.

Stream Deposits Related to Glaciation

The complex glacial history of this area produced correspondingly complicated postglacial meltwater and fluvial sequences. Landforms are generally poorly defined, but deposits are extensive. Sand and gravel deposits of the Muir Point Formation are characterized by massive bedding structures as well as other paleocurrent indicators (imbrication structures, stoss-lee features and stone orientation). These deposits are exposed in the coastal bluffs between Parsons Point and Muir Point. The formation separates pre-Sangamonian and Late Wisconsinan tills. It pinches out before reaching the northern end of the bluffs. Here the Late Wisconsinan till unconformably overlies the pre-Sangamonian till. Furthermore, the sand and gravel beds are not found to the southeast of Sooke Inlet. Results of the ground survey and model development show that these deposits are derived from several sources. The lower section preserves evidence of derivation from the east northeast: the upper section from the south-southeast.

Muir Point also has meltwater deposits associated with a later period of ice-marginal conditions. These are located between Muir Point and the flanks of Broom Hill, but are thickest across the coastal frontage of Sooke Indian Reserve 2 (IR 2). Model development assisted in the identification of contemporaneous meltwater terraces on the east flank of Broom Hill which can be seen on aerial photographs (*e.g.*, much of the Sooke golf course and residential areas to the north of Sooke are built on these terraces). The sharp truncation of the Sooke River ice-marginal deposits suggests that the contemporaneous sediments of Sooke Indian Reserve 2 and the golf course terraces are evidence of a meltwater outburst, either along the edge of a retreating glacier, or by the breaching of stagnant ice. Deltaic deposits to the north of Milnes Landing indicate that Sooke River meltwater flowed into a small, temporary lake at about the same time. The sharp truncation of the west side of this delta confirms an outburst origin for the sediments on Sooke Indian Reserve 2. Additional evidence is difficult to assess because the southern boundary of this delta has been buried by subsequent fluvial deposition in Sooke Basin. In spite of this, aerial photographs show a marked break of slope, which would be a probable result of lake drainage to the west.

Two predominant meltwater deposits (lower section Muir Point and Sooke Indian Reserve 2) contain paleocurrent indicators showing that deposition was from the east. These could be the result of catastrophic outburst events produced by the draining of ice-dammed lakes. Russel *et al.* (1990) point out that these events involve rapid moraine erosion (*i.e.*, erosion of pre-Sangamonian and Late Wisconsinan tills, Muir Point ?) and that lake sediments are heavily incised (*e.g.*, Sooke River). Researchers agree that ice-dammed lakes were formed in side valleys adjacent to the Juan de Fuca lobe (Alley and Chatwin, 1979; Clague, 1981). Submerged "moraine" deposits in Juan de Fuca Strait may be evidence of this ice-marginal activity (*e.g.*, Mayers and Bennett, 1973; Solheim and Pfirman, 1985). This may explain the multi-genetic origin of the intertill sand and gravel deposit at Muir Point, the lowest unit representing a lag deposit (from lake outburst?), followed by backwater sedimentation and, finally, meltwater and outwash associated with the Vashon ice advance.

Recent Fluvial Sedimentation

Compared with the zones of meltwater deposition, recent fluvial sedimentation is minor. Relatively small deposits are found in conjunction with contemporary fluvial sources. These are listed in Table 3-5-1.

Recent Sooke River deposits are found mainly in a delta extending south, beyond the earlier meltwater sediments. However, most of this site is covered by residential and industrial development. In-channel and riparian deposits are found up-river, but all easily accessible sources associated with the Sooke River have been utilized. On the other hand, De Mamiel Creek valley has not been exploited. The creek flows into Sooke River from the west, cutting through the meltwater terraces discussed above. The valley is noteworthy, not only as a potential aggregate source within the Sooke Land District, but also as a possible source immediately to the north in the Otter Land District, in the vicinity of Young Lake. This site was not visited during the ground survey, but subsequent airphoto analysis and map interpretation indicates that sand and gravel deposits (which are buried by ice-marginal and lacustrine sediments in the De Mamiel Creek and Sooke River area) may well be exposed in the Otter Land District.

TABLE 3-5-1
RECENT FLUVIAL DEPOSITS

Site	Grid Reference	Deposit Location
Anderson Cove	512 565 517 564	Intermittent channel deltas
Ayum Creek	513 598	In-channel, riparian, deltaic
Doerr Creek	530 567	Deltaic, riparian (colluvially covered upstream)
Kemp Stream	432 576	In-channel, riparian
Veitch Creek	533 597	In-channel, riparian (colluvially covered upstream)

Colluvial Deposits

A considerable area of the Sooke Land District is covered by a colluvial veneer of varied thickness. Senyk (1972) indicates that this is underlain by fluvial gravels in several areas. Our ground survey suggests that these fluvial deposits are discontinuous and occur only as a thin layer. Recent fluvial sedimentation is considered to be more significant than this patchy, thin lag deposit of ice-retreat origin.

AGGREGATE RESOURCE DEVELOPMENT

Potential Aggregate Resources

The first priority of this study was to ascertain potential aggregate resources for the Sooke Land District. In order to provide the most useful information, a potential aggregate inventory, based upon sites analysed during the ground survey, is detailed below. Figure 3-5-1 indicates the locations of Sites A to J, and a summary is given in Table 3-5-2. Figure 3-5-3 graphically displays particle-size analyses of samples taken from potential aggregate sources.

SITE A

Sediments at the mouth of Sooke River are comprised of stable, well-drained, reasonably compact, deltaic deposits. The site is less than 0.5 kilometre from Highway 14, but is in an area of residential development near Sooke Indian Reserve 1 (IR 1). Old gravel pits within this area are almost exhausted, and the area of potential aggregate resource is correspondingly small. This site does not appear to be economically viable.

SITE B

Situated at Parsons Point, this site consists of a coastal bluff exposure of approximately 5 metres of interbedded sands and gravels. The upper 3 metres is predominantly sand and is compact, stable and relatively impermeable. Underneath are uncemented gravels, less compact, but stable. Beneath this, a cemented, poor-quality gravel is exposed as a raised beach – this is discussed in more detail under Site C. Paleocurrent indicators and bedding structures demonstrate that the upper sands and gravels were deposited by flows from the southwest and the east. This exposure of aggregate represents a thin strip of accessible material which extends northwest into Sites C and Di for approximately 2 kilometres. However, while its inland projection probably lies beneath most of this peninsula, residential development precludes access. At least three subdivision roads extend almost as far as the coastal bluffs along this strip, but coastal frontage is under private residential ownership. Coastal erosion is evident as far as Muir Point, and while the deposits are inherently stable, these is some undercutting. Extraction is not recommended here.

SITE C

Comments regarding Site B are equally applicable to Site C and only a technical description of the quality of aggregate deposits will be provided. Twelve metres of sands and gravels are underlain by a pre-Sangamonian till sequence. The upper section, again predominantly sand, is compact and clean. Paleocurrent indicators show that they were deposited by flows from the south-southeast and east, suggesting a similar origin to those at Site B. A review of the particle size information (Figure 3-5-3a) confirms this. Underlying gravels are the same cemented, poor-quality deposits which comprise the raised beach at Site B. Fabric analysis and paleocurrent indicators demonstrate an easterly origin and clast provenance (sub-rounded Leech River Formation, Metchosin volcanics and Karmutsen Formation) shows that some pebbles have been transported from the Shawnigan Lake region. In the sedimentation model discussed below these gravels are considered to be an outburst lag deposit from a glacially dammed lake, probably laid down at the beginning of the Sangamonian. This explanation provides an answer to the depositional history of the overlying multisourced sediments. The lower section, composed predominantly of organic-rich silt and sand with some peat (Alley and Hicock, 1986) represents a post-outburst backwater swamp deposit. The upper section, a mixture of organic-rich silt, sand and gravel is indicative of local reworking of the underlying sediment by meltwater flows from the southeast.

Access problems are similar to Site B although they are exacerbated by the increasing height of the coastal bluffs. This is partly a function of increasing stability brought about by the emergence of a resistant till layer at the base of the bluffs, but also the complete exposure of the overlying cemented gravels. Once again, extraction is not recommended.

SITE Di

This is part of a continuing sequence that becomes gradually more complex from Site B to Site D. At Muir Point the sands and gravels are sandwiched between underlying pre-Sangamonian and overlying Late Wisconsinan tills. However, these sand and gravel deposits pinch out and are no longer visible at the northwestern end of the section, where the Late Wisconsinan till rests unconformably on the pre-Sangamonian till (some 200 metres farther up the coast the bluffs rapidly decrease in height and are replaced by an outwash plain, Site Dii). Sand-filled tension fractures are

TABLE 3-5-2
SUMMARY OF STUDY SITES

Site	Location	Physical Features	Access	Suitability
A	487 588	New delta: surface deposit	**Good:** Highway 14	**Poor:** area developed
B	460 558	Coastal bluff: surface deposit	**Moderate:** residential area	**Moderate:** upper compact/clean; lower: uncemented
C	453 557	Coastal bluff: surface deposit	**Moderate:** residential area	**Moderate:** upper compact/clean; lower: cemented gravel
Di	443 563	Coastal bluff: exposed buried deposit	**Poor:** high bluffs, residential	**Moderate:** ltd. cementation, fairly clean
Dii	443 565	Outwash surface: surface deposit	**Moderate:** Sooke IR 2 road	**Good:** clean, noncompact
E	473 606	Fluvial terrace: exposed buried deposit	**Good:** loose-surface road	**Good:** Clean, noncompact
F	488 601	Old delta: surface deposit	**Good:** hard-surface road	**Good:** clean, noncompact
G	462 591	Fluvial terraces: surface deposit	**Good:** hard-surface road	**Good:** clean, noncompact
H	540 573	Valley floor: surface deposit	**Moderate:** via railway footpath	**Moderate:** veneer deposit, noncompact, fairly clean
I	520 604	"Till" island: surface deposit	**Good:** new road in subdivision	**Moderate:** fine sand only, compact
J	487 603	Old delta: surface deposit	**Good:** hard-surface road	**Good:** clean, noncompact

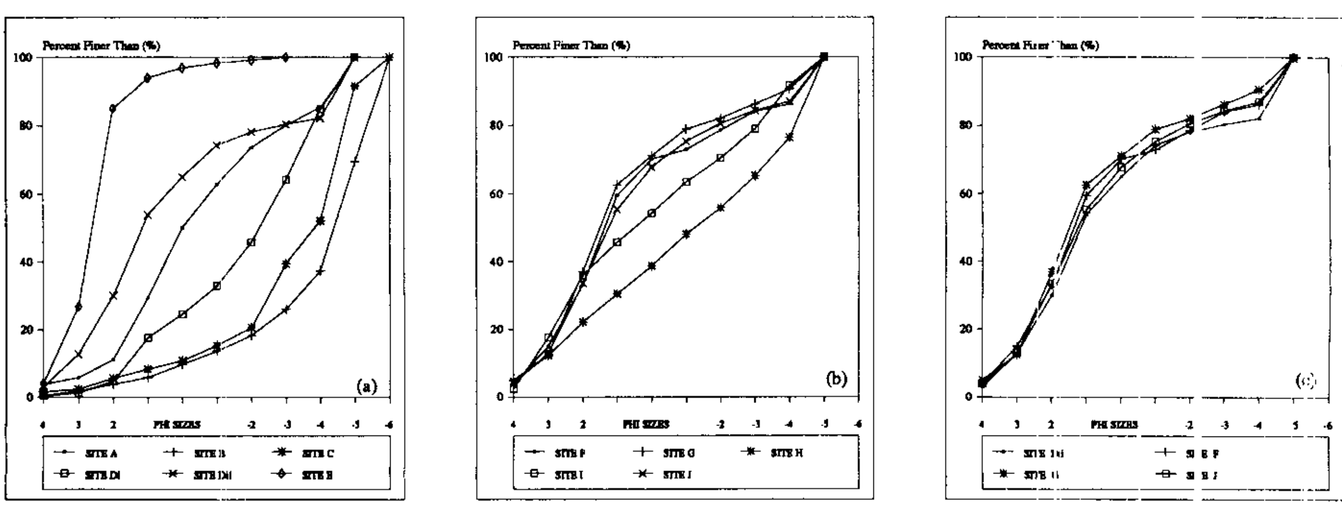

Figure 3-5-3. Particle-size distribution (sample sizes in excess of 20 kg in accordance with suggested criteria; Church *et al.*, 1987).

visible in the upper layers of the underlying pre-Sangamonian till, indicating a northwesterly ice movement (Hicock and Dreimanis, 1985). Deformation structures within the sands and gravels indicate some overloading by the Late Wisconsinan (Vashon) till. Particle-size analyses indicate that these sands and gravels are slightly coarser than those at Sites B and C, suggesting increased water percolation through the sediment along stress fractures. Muir Point is a coastal bluff susceptible to wave action. Although it is well drained and only a short distance from a paved road, it suffers from the same access problems as Sites B and C. No action is recommended here.

SITE Dii

An outwash plain under Sooke Indian Reserve 2 is the seaward margin of what was probably a meltwater outburst resulting from a combination of water from a glacially dammed lake and paraglacial Sooke River water. Vashon ice in Juan de Fuca Strait may have been sufficiently active to rework the Sangamonian sands and gravels to the southwest (Site Di) causing them to pinch-out, but the Vashon till at Site Di appears to have been passively deposited. It may have been deposited mainly by meltout from stagnant ice which temporarily dammed Sooke Inlet as valley glaciers retreated northeast, allowing lake build-up to occur in Sooke Basin. Alternatively, deposition may have occurred by lodgement as Juan de Fuca ice retreated after valley glaciers, causing a similar blockage. Eventual catastrophic breaching of the stagnant Juan de Fuca ice removed any underlying till and deposited sands and gravels to a depth of at least 3 metres at Site Dii. As can be seen from particle-size analyses (Figure 3-5-3c), Sites Dii, F, G and J have very similar compositions, corroborating this theory.

Site Dii has an easily accessible supply of aggregate (there is a paved road into Sooke Indian Reserve 2) of unspecified depth, which can be traced inland as far as Sooke River. Clearly most of the urban growth of Sooke overlies this source, but at Site Dii these surface deposits are clean, noncompacted and readily extractable. The exact areal extent of the accessible outwash plain is difficult to assess, but it could be about 1 square kilometre. Accessibility and aggregate quality are both good and extraction appears to be economically feasible.

SITE E

Fine ice-marginal and lacustrine sediments overlie sand deposits of unknown depth (in excess of 3 metres). The exposure, which is adjacent to a loose gravel road has been heavily incised by meltwater flows. This scenario is compatible with the suggested outburst theory and the track of the flood event. Sediments are noncompacted, easily accessible and close to De Mamiel Creek. Extraction would be facilitated by their occurrence as a river terrace, although the deposit is of limited areal extent because of truncation to the south and west by meltwater activity. Gradual physiographic constriction northwards along Sooke River valley is also a factor. The deposit could prove to be economically viable as an isolated extraction site for fine sands only.

SITE F

Interbedded sand and gravel deltaic beds are exposed to a depth of 10 metres at Site F. The beds dip south and have a particle-size distribution linking them with a westerly outburst event. We believe that these delta beds are the remains of the paraglacial Sooke River exit into a temporary ice-dammed lake occupying Sooke Basin. Ice-marginal and lacustrine deposits at Site E overlie paraglacial Sooke River sediments and show the extent of this lake. Rapid ice retreat up Sooke River valley built a delta into the lake, with marginal delta deposits being laid down beneath lacustrine sediments. The aggregate in the deltaic beds has been extracted to a limited extent in the past and is now adjacent to and partially covered by commercial and residential properties. Although the aggregate is clean and noncompact, in view of the northward expansion of the community of Milnes Landing this is not a good site for extraction. Road access is good, but extraction would be constrained by surrounding properties.

SITE G

Terraces exposed near Sooke golf course are as high as 10 metres in places and have a similar particle-size distribution to other post Late Wisconsinan outburst sites. Extraction is precluded at this location because of commercial and residential site coverage associated with the urban spread of Sooke.

SITE H

A continuous sand and gravel veneer, 1 to 5 metres thick, is situated between Roche Cove and Matheson Lake. This channel is of subglacial origin and the deposit is probably a lag from meltwater flows. The veneer overlies bedrock and is itself covered in places by some colluvial material. It is noncompacted, but due to some colluvial mixing is less clean than other sites. Pebble provenance shows that subrounded clasts of Sooke gabbro are of local origin, and rounded clasts of Wark gneiss are from the Victoria area. Access is reasonable along the railway-line footpath, but extraction is not recommended because some of the deposit is within the boundaries of Matheson Lake Provincial Park.

SITE I

Ice retreat northeast along the Ayum Creek valley deposited this sediment in an ice-marginal, lacustrine environment and as such the particle-size distribution is fine (Figure 3-5-3b). This appears to be a turbidite deposit, with many clasts found countersunk (dropstones) and transverse to flow direction (by rolling). Access is by a new subdivision road, and some residential construction already partially covers the site. Extraction seems to be precluded because of proposed and ongoing development. It represents the southern extent of a heavily incised, reworked till island which is compacted and relatively impermeable. Areal extent may be as large as 1.5 square kilometres although much is colluvially-covered and less accessible.

SITE J

Situated only a few hundred metres northwest of Site F, Site J is a continuation of the paraglacial Sooke River delta and was examined to assess the extent of the deposit. Particle size and aggregate qualities are similar to the other location, although there is no evidence of past extraction. Pebble provenance from both sites shows a similar origin to those at Sites C and D, with subrounded clasts of Leech River Formation and Metchosin volcanic lithologies. There has, as yet, been less urban development in the vicinity, although access is through a residential area. Residential development is more concentrated to the north, along Sooke River valley, and as such, the site has limited extraction potential. In view of the constricted area available for extraction, no action is recommended.

SEDIMENTATION MODEL

In order to thoroughly analyse the aggregate deposits in the Sooke District it was necessary to compile a sedimentary history of the area. Previous researchers have identified a pre-Sangamonian till (Illinoian ?) at Muir Point (Hicock, 1980; Hicock and Armstrong, 1983), making it necessary to consider both ice-sheet and ice-marginal sedimentation processes. An essential part of this operation required the development of a model which showed the interactions of these processes. This model was instrumental in predicting the location of Sites E, F and H.

DISCUSSION

A pre-Sangamonian till at Muir Point (probably Illinoian – Westlynn glaciation, although it may be older; Hicock, 1980) represents the chronological starting point for this model. The till was deposited by an ice sheet which moved west-northwest along the Juan de Fuca Strait. Although little is known about earlier Pleistocene time, as the Juan de Fuca lobe moved northwest it would have risen out of the physiographic trough to the south and east of Vancouver Island, while undergoing compressive flow (Hicock *et al.*, 1983). A similar process, on a smaller scale, must have occurred as the ice over-rode the area to the southeast of Sooke Basin (East Sooke Regional Park - Matheson Lake Provincial Park). This scoured the land surface (which remains largely colluvially-covered bedrock today) accentuating weaknesses within the bedrock. This is particularly evident in the two subglacial channels carved along recognized fault lines. Occupation of these troughs by subglacial meltwater created lubrication for a faster moving ice stream into the Sooke Basin area.

However, glaciers flowing southwest along Ayum and Veitch Creek valleys; (Alley and Chatwin, 1979) blocked the northwesterly progress of this ice stream, inducing compressive flow and dissipating its energy by scouring out the Sooke Basin (effectively creating a low-lying cirque). General ice flow out of Sooke Basin was diverted southwest by a strong Sooke River valley glacier, thereby scouring out Sooke Harbour and Inlet. Here, ice flow and entrained rock debris joined the northwest-moving Juan de Fuca lobe (Figure 3-5-4a). Tension fractures, shear planes and till wedges in deposits along the eastern coast of Juan de Fuca Strait (at Muir Point) indicate that the till was deformed by two phases of ice-sheet advance to the northwest (Hicock, 1980; Hicock and Dreimanis, 1985).

During deglaciation, valley glaciers retreated more rapidly than the Juan de Fuca lobe, forming an ice-dammed lake in Sooke Basin. Evidence for a catastrophic outburst is found in the lower cemented gravels at Muir Point, which appear to represent a lag deposit, with paleocurrent indicators showing a westerly flow direction. It seems likely that valley deglaciation, and associated paraglacial activity, was waning by the time this occurred because no related meltwater deposits of any significance overlie these gravels. It is possible that Sooke Inlet was blocked by stagnant ice, and that the sedimentary evidence was removed by the outburst (Russel *et al.*, 1990; Figure 3-5-4b).

Overlying sediments show that this event was followed by a quiescent period during which organic-rich silt and sand were deposited (Alley and Hicock, 1986). Radiocarbon dates indicate that a backwater-swamp environment existed for tens of thousand years. A mixture of sand, gravel, diamicton and organic-rich silt overlies these deposits (Alley and Hicock, 1986). The heterogenous nature of these sediments points to fluvial reworking of distal nonorganic deposits (diamicton and gravel) followed by proximal activity (organic-rich sand and gravel), possibly associated with the late Wisconsinan advance (Vashon till) from the southeast along Juan de Fuca Strait. A more passive regime is proposed for this advance because of the preserved sand and gravel sequence at Muir Point, although this disappears at the northwestern margin of the site. This can be explained if one assumes that overlying Vashon till was mainly formed by stagnant ice meltout. Previous sand and gravel sediments occupying this site were gradually washed out (prior to the area being ice-covered) by westerly flowing meltwater from the valley glaciers to the northeast. A thin sand layer between the pre-Sangamonian and Late Wisconsinan tills may indicate such an event. This fits with the explanation of the subsequent outwash plain found immediately northwest of Muir Point.

Several surficial deposits were laid down during the deglaciation of the late Wisconsinan ice mass. A combination of subglacial low-pressure zones caused by the decaying ice front (*e.g.*, Hooke *et al.*, 1990), and a simple lag deposit, produced a sedimentary veneer on the Matheson Lake – Roche Cove valley floor. More significant, from an aggregate point of view, is the extensive Sooke River outburst. Valley glacier retreat was slow, with Ayum Creek and Sooke River showing evidence of ice-marginal deposits in their lower reaches, close to another ice-dammed lake in Sooke Basin. However, sufficient deglaciation had taken place in the Sooke River valley to create a fairly extensive delta into the lake. Either ice-margin collapse or catastrophic breaching of a stagnant ice blockage caused both lake drainage and temporary redirection of Sooke River flows to the west. As suggested above, these events commonly lead to the rapid erosion of morainal deposits and the deep incision of lacustrine sediments (*e.g.*, Russel *et al.*, 1990; Fitzsimons, 1990). Evidence for the erosional nature of this event is found in the terraces to the north of Sooke, the southern and eastern truncation of deposits at Site E and the southerly truncation of the old Sooke River delta (Figure 3-5-4c). Headward erosion by De Mamiel Creek to the northwest from Sooke River breached the terraces and undoubtedly caused sediment redistribution, redirecting

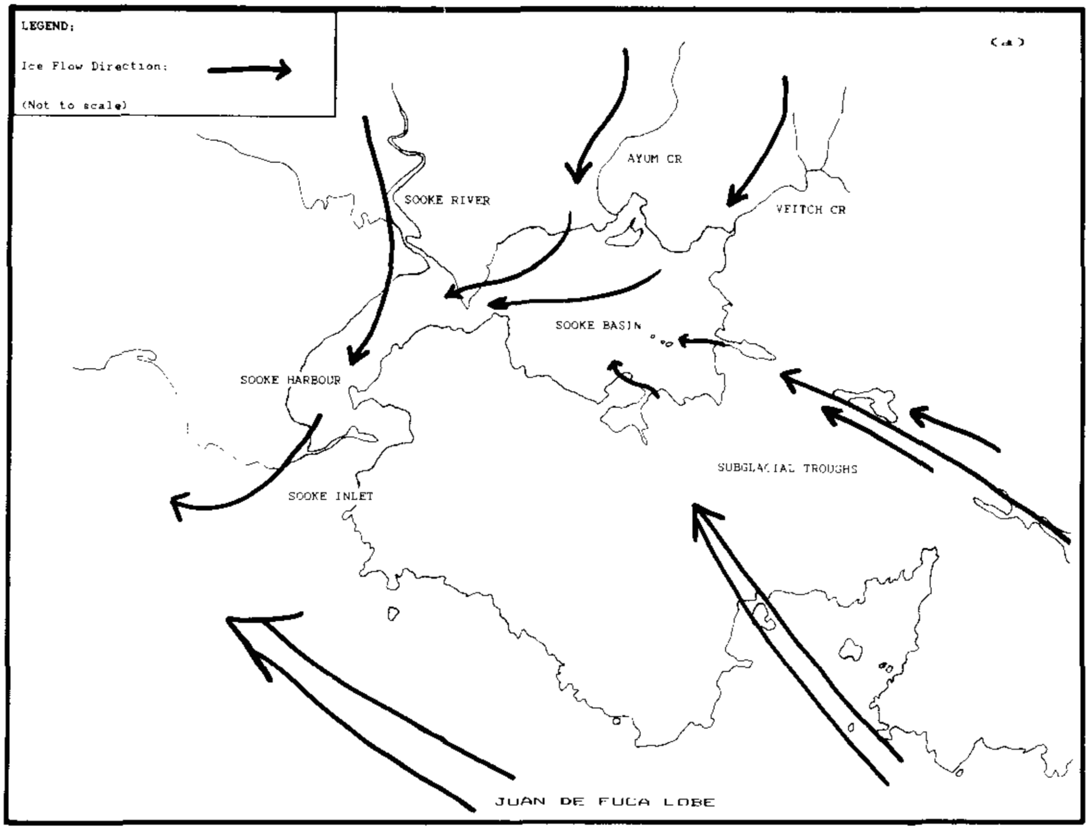

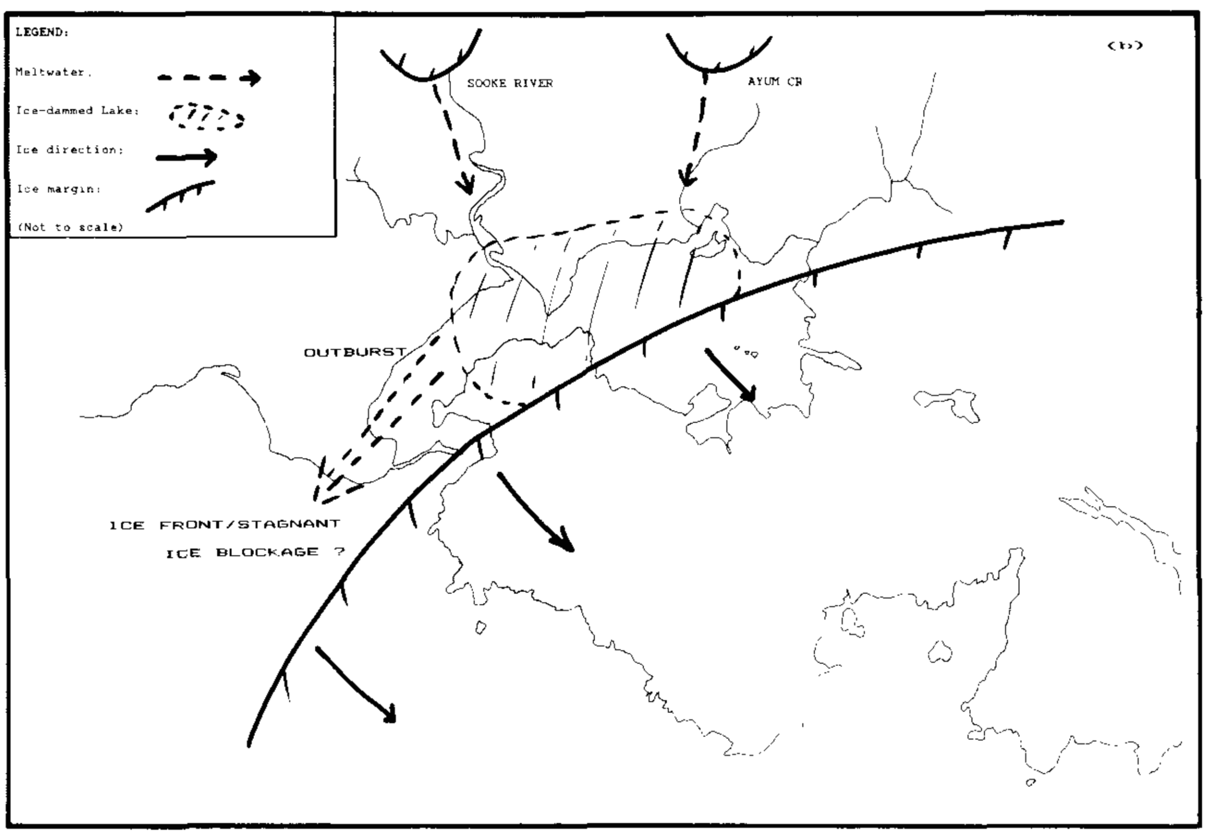

Figure 3-5-4. Sedimentation model: (a) Pre-Sangamonian, (b) Early Sangamonian, (c) Late Wisconsinan ice retreat, (d) Recent changes.

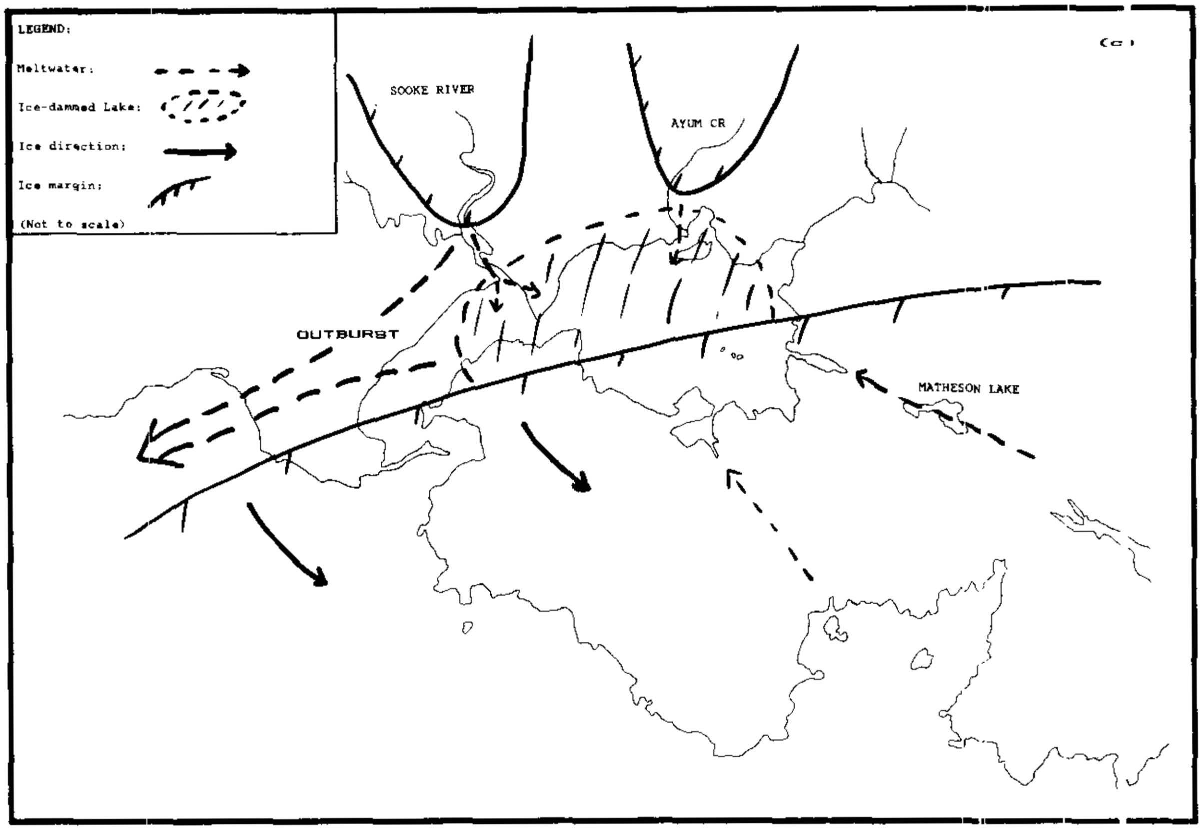

LEGEND:
Meltwater:
Ice-dammed Lake:
Ice direction:
Ice margin:
(Not to scale)
(c)
SOOKE RIVER
AYUM CR
OUTBURST
MATHESON LAKE

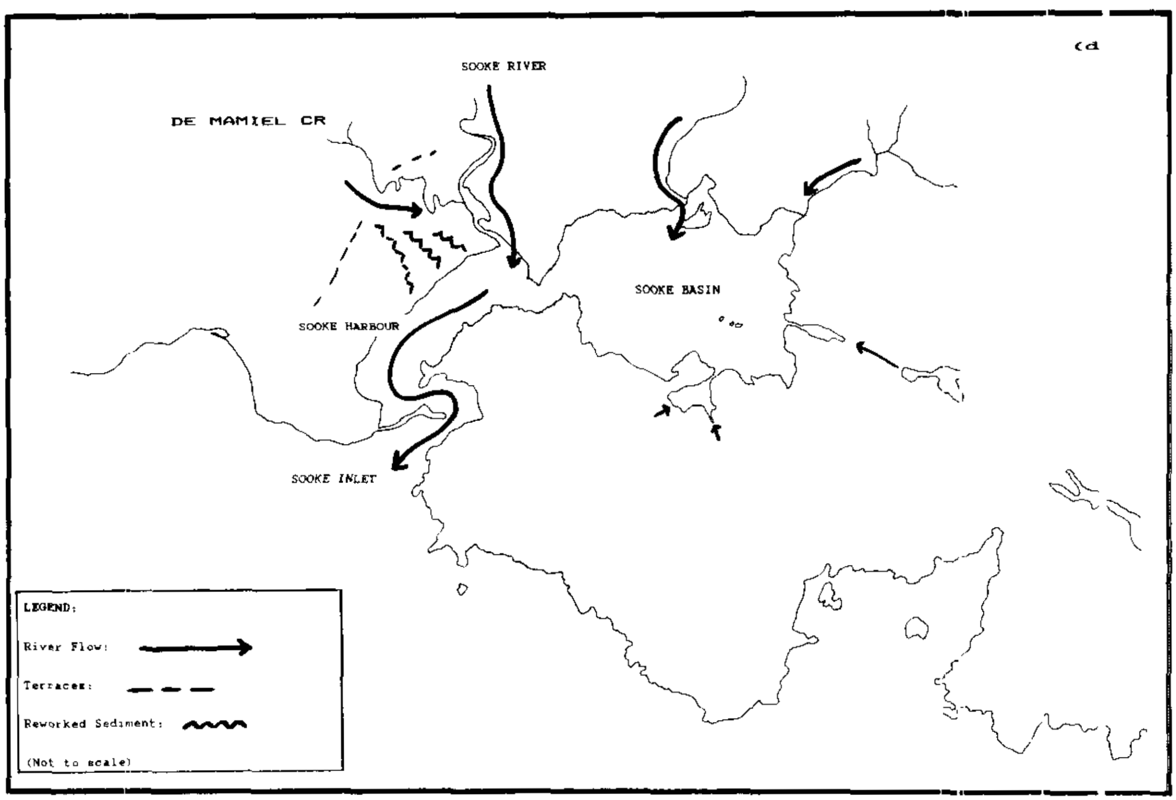

(d
SOOKE RIVER
DE MAMIEL CR
SOOKE BASIN
SOOKE HARBOUR
SOOKE INLET
LEGEND:
River Flow:
Terraces:
Reworked Sediment:
(Not to scale)

Sooke River flows to the south into the drowned cirque of Sooke Basin. Subsequent drainage of Sooke Basin, by dominant Sooke River flows to the south, has reopened Sooke Harbour and Inlet (Figure 3-5-4d).

CONCLUSIONS

With few exceptions, potential aggregate resources in the Sooke Land District area are poor and difficult to extract. The Sooke River outwash deposit is a significant potential resource with several potential extraction sites. Possible extraction sites include:

- Site Dii — Sooke Indian Reserve 2 (good).
- Site E — De Mamiel Creek – Sooke River interfluve (good).
- Site H — Matheson Lake – Roche Cove (limited by site-specific problems).
- Site I — New Ayum Creek sub-concession (fine sand only — moderate).
- Site J — North Milnes Landing (limited by adjacent buildings — good).

The findings of this study show that the importance of developing a sedimentation model cannot be overemphasized. The model helped identify possible aggregate sites and, because airphoto analysis was inconclusive, these locations were later confirmed by ground survey.

REFERENCES

Alley, N.F. (1979): Middle Wisconsinan Stratigraphy and Climatic Reconstruction, Southern Vancouver Island, British Columbia; *Quaternary Research*, Volume 11, pages 213-237.

Alley, N.F. and Chatwin, S.C. (1979): Late Pleistocene History and Geomorphology, Southwestern Vancouver Island, British Columbia; *Canadian Journal of Earth Sciences*, Volume 16, pages 1645-1657.

Alley, N.F. and Hicock, S.R. (1986): The Stratigraphy, Palynology, and Climatic Significance of Pre-Middle Wisconsinan Pleistocene Sediments, Southern Vancouver Island, British Columbia; *Canadian Journal of Earth Sciences*, Volume 23, 369-382.

Bretz, J.H. (1920): The Juan de Fuca Lobe of the Cordilleran Ice Sheet; *Journal of Geology*, Volume 28, 333-339.

Church, M., McLean, D.G. and Wolcott, J.F. (1987): River Bed Gravels: Sampling and Analysis; *in* Sediment Transport in Gravel-bed Rivers; Thorne, C.R., Bathurst, J.D. and Hey, R.D., Editors, *John Wiley and Sons Ltd.*, pages 43-78.

Clague, J.J. (1981): Late Quaternary Geology and Geochronology of British Columbia, Part 2: Summary and Discussion of Radiocarbon-dated Quaternary History; *Geological Survey of Canada*, Paper 80-35, 41 pages.

Clapp, C.H. (1912): Southern Vancouver Island; *Geological Survey of Canada*, Memoir No. 13, 208 pages.

Energy, Mines and Resources Canada (1981): Sooke, British Columbia; *Surveys and Mapping Branch*, Map No. 92B/5, 1:50 000-scale.

Fitzsimons, S.J. (1990): Ice-marginal Depositional Processes in a Polar Maritime Environment, Vestfold Hills, Antarctica: *Journal of Glaciology*, Volume 36, pages 279-286.

Hicock, S.R. (1980): Pre-Fraser Pleistocene Stratigraphy, Geochronology, and Paleoecology of the Georgia Depression, British Columbia; unpublished Ph.D. thesis, *The University of Western Ontario*, London, 230 pages.

Hicock, S.R. (1990): Last Interglacial Muir Point Formation, Vancouver Island, British Columbia; *Géographie Physique et Quaternaire*, Volume 44, pages 337-340.

Hicock, S.R. and Armstrong, J.E. (1983): Four Pleistocene Formations in Southwest British Columbia: Their Implications for Patterns of Sedimentation of Possible Sangamonian to Early Wisconsinan Age; *Canadian Journal of Earth Sciences*, Volume 20, pages 1232-1247.

Hicock, S.R. and Dreimanis, A. (1985): Glaciotectonic Structures as Useful Ice-movement Indicators in Glacial Deposits: Four Canadian Case Studies; *Canadian Journal of Earth Sciences*, Volume 22, pages 339-346.

Hicock, S.R., Dreimanis, A. and Broster, B.E. (1983): Submarine Flow Tills at Victoria, British Columbia: Reply; *Canadian Journal of Earth Sciences*, Volume 20, pages 510-513.

Hooke, R. LeB., Laumann, T. and Kohler, J. (1990): Subglacial Water Pressures and the Shape of Subglacial Conduits; *Journal of Glaciology*, Volume 36, pages 67-71.

Mayers, I.R. and Bennett, L.C. Jr. (1973): Geology of the Strait of Juan de Fuca; *Marine Geology*, Volume 15, pages 89-117.

Muller, J.E. (1980): Geology: Victoria Map Area, Vancouver Island and Gulf Islands, B.C.; *Geological Survey of Canada*, Map No. 92 B/NW and part of B/SW, Open File 701.

Russel, A.J., Aitken, J.F. and De Jong, C. (1990): Observations on the Drainage of an Ice-dammed Lake in West Greenland, *Journal of Glaciology*, Volume 36, pages 72-74.

Senyk, J. (1972): Sooke Terrain Map; *Environment Canada*, Map No. 92B/5 Terrain.

Solheim, A. and Pfirman, S.L. (1985): Sea-floor Morphology Outside a Grounded, Surging Glacier, Brsvellbreen, Svalbard; *Marine Geology*, Volume 65, pages 127-143.

Thorson, R.M. (1980): Ice Sheet Glaciation of the Puget Lowland, Washington, During the Vashon Stade (Late Pleistocene); *Quaternary Research*, Volume 13, pages 303-321.

British Columbia Geological Survey
Geological Fieldwork 1991

PRELIMINARY RESULTS OF DRIFT EXPLORATION STUDIES IN THE QUATSINO (92L/12) AND THE MOUNT MILLIGAN (93N/1E, 93O/4W) AREAS

By Dan E. Kerr and Steve J. Sibbick

KEYWORDS: Applied geochemistry, drift exploration, surficial geology, Island Copper, Mount Milligan, till, glaciofluvial outwash, soil geochemistry, dispersal trains, porphyry copper-gold.

INTRODUCTION

This report describes the preliminary results of the Quatsino project (1991 field season) which entails a drift exploration study of the Island Copper mine area and the Quatsino map sheet (92L/12), and an investigation of regional glacial dispersal in the Mount Milligan area (Figure 3-6-1). Both projects are part of the British Columbia Geological Survey Branch's drift prospecting program designed to demonstrate the utility of a combined surficial geology–exploration geochemistry program in the search for drift-covered mineral deposits in areas of glaciated terrain. The program's main goals are:

- *To define regional Quaternary stratigraphy and glacial* history.
- To document glacial dispersal patterns from known mineral occurrences.
- To produce 1:50 000-scale surficial geology and RGS-style interpretive maps for use in mineral exploration.
- To develop interpretive drift-exploration models.

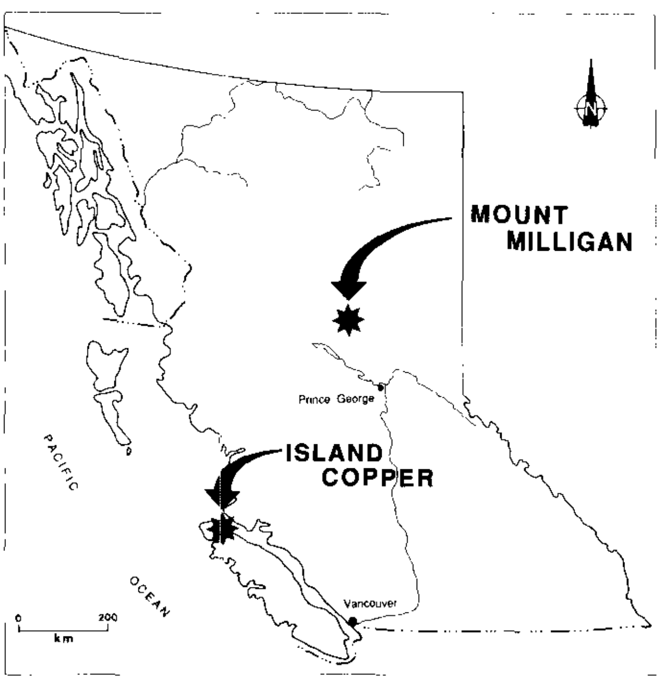

Figure 3-6-1. Location of the Island Copper and Mount Milligan deposits.

The Quatsino project is an evaluation of the use of drift sampling as a regional mineral exploration tool. The Quatsino map sheet, centred over the North Island copper belt, was chosen due to the high mineral potential of this area, the presence of known mineral deposits suitable for drift prospecting case studies, the variable drift thickness and the poor understanding of the regional Quaternary glacial history.

The drift sampling program in the Mount Milligan area will document regional patterns of geochemical dispersal trains in an area of high mineral potential and aid in the determination of regional sampling densities. This work complements the detailed surficial geological and geochemical dispersion studies carried out at the Mount Milligan deposit during the 1990 field season (Kerr, 1991; Kerr and Bobrowsky, 1991; Gravel and Sibbick, 1991).

METHODS

QUATSINO PROJECT

Preliminary airphoto interpretation of the surficial geology of the Quatsino map sheet at a scale of 1:50 000 was *undertaken prior to fieldwork.* Access was mainly by logging road, and by traverses on foot along streams which provided opportunities for stratigraphic studies. A helicopter was used to gain access to isolated locations. Surficial sediment types were initially plotted on 1:15 000 and 1:20 000-scale maps supplied by Western Forest Products Limited and the British Columbia Ministry of Forests. Ice-flow directions were obtained from till fabrics at 13 sites across the map area; other ice-flow indicators (striae, fluted bedrock, drumlins) were measured at numerous locations. Approximately 28 detailed stratigraphic sites were investigated, including 2 glaciomarine and marine deltas. A marine shell sample was collected, for radiocarbon analysis, at 6 metres below sea level from the pit wall of the Island Copper mine.

Sampling for the Quatsino project consisted of 194 drift samples collected across the map area from road cuts, hand-dug pits and stream banks, at an approximate density of one sample per 5 square kilometres (Figure 3-6-2). The unoxidized C-horizon, commonly 1 to 2 metres below the surface, was sampled whenever possible. Of the 194 samples, 134 samples consisted of till, 48 of colluvium, 11 of glaciofluvial sediment and 1 of glaciomarine material. At three-quarters of the sites, 25 pebbles were collected for lithological analyses and provenance studies. Each sample will be analysed by instrumental neutron activation analysis (INAA) and inductively coupled plasma analysis (ICP) for 40 elements.

An orientation survey was conducted around the Island Copper copper-gold-molybdenum mine, for a distance of 6

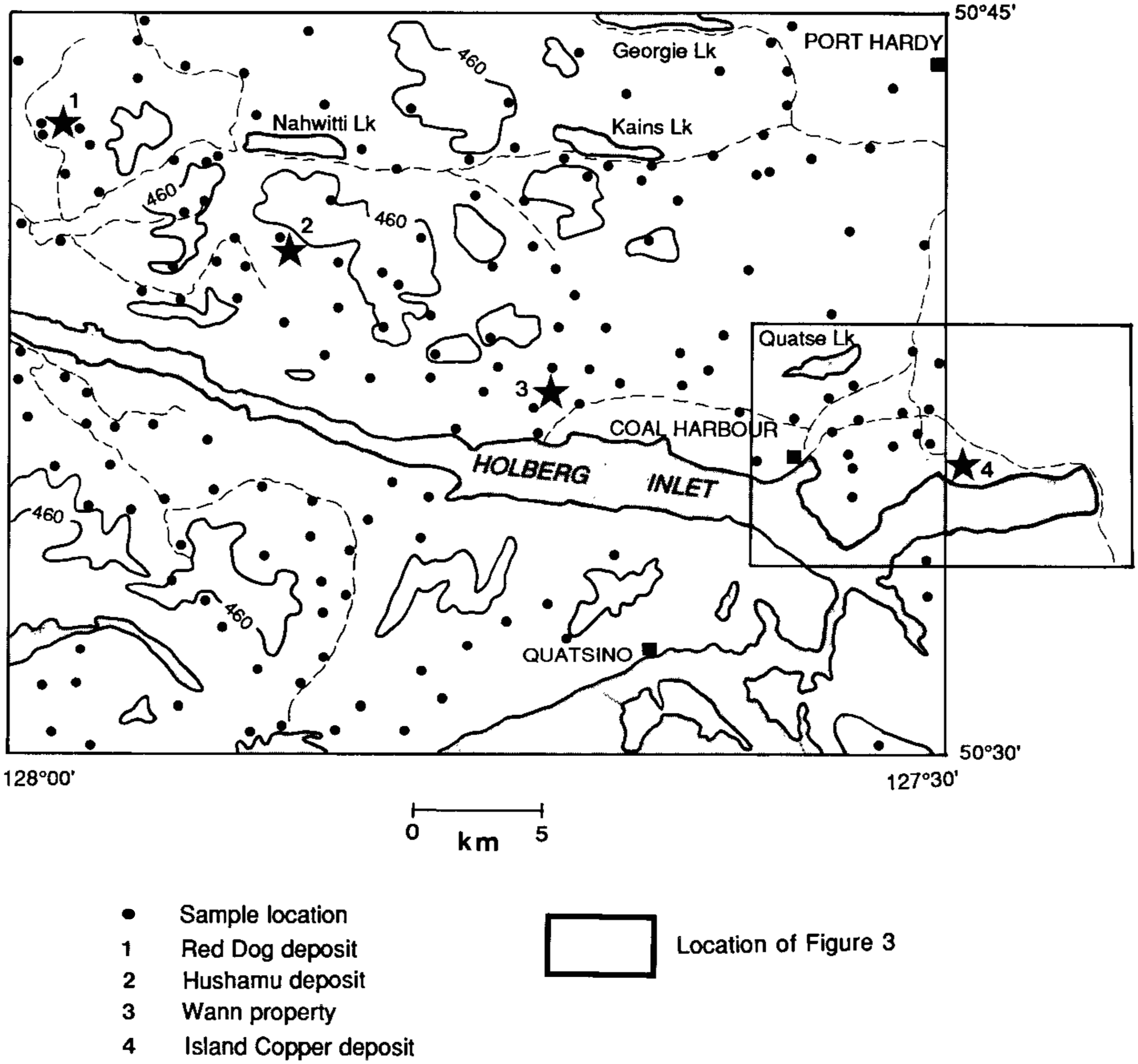

Figure 3-6-2. Geochemical sample locations and mineralized areas under investigation in the Quatsino map area (92L/12).

kilometres down-ice of the deposit (Figure 3-6-3). Near the deposit, surficial sediment cover is up to 75 metres thick, obscuring much of the bedrock near the orebody. Approximately 37 till samples were collected, providing a sampling density of one sample per square kilometre. Additional samples were collected from surficial sediments at the Red Dog and Hushamu deposits for comparative geochemical studies.

Mount Milligan

In 1991, regional-scale sampling of till was carried out down-ice from the Mount Milligan porphyry copper-gold deposit for a distance of 20 kilometres to the east-northeast (Figure 3-6-4). About 125 till samples were collected from 112 hand-dug pits within a 150 square kilometre area. The unoxidized C-horizon was preferentially sampled at depths of 0.5 to 1.5 metres. Sampling was concentrated in two distinct areas where till is the predominant surficial sediment: in the vicinity of the deposit and in the region to the east of Rainbow Creek. The intervening area, consisting of glaciofluvial outwash, was not sampled due to its different generic characteristics in comparison with till. Soil samples of the oxidized B-horizon developed in till were acquired at each site in order to contrast any differences resulting from the underlying unoxidized C-horizon. Pebble samples were also collected from each site for provenance studies. Three size fractions (−250+125, −125+62.5 and −62.5

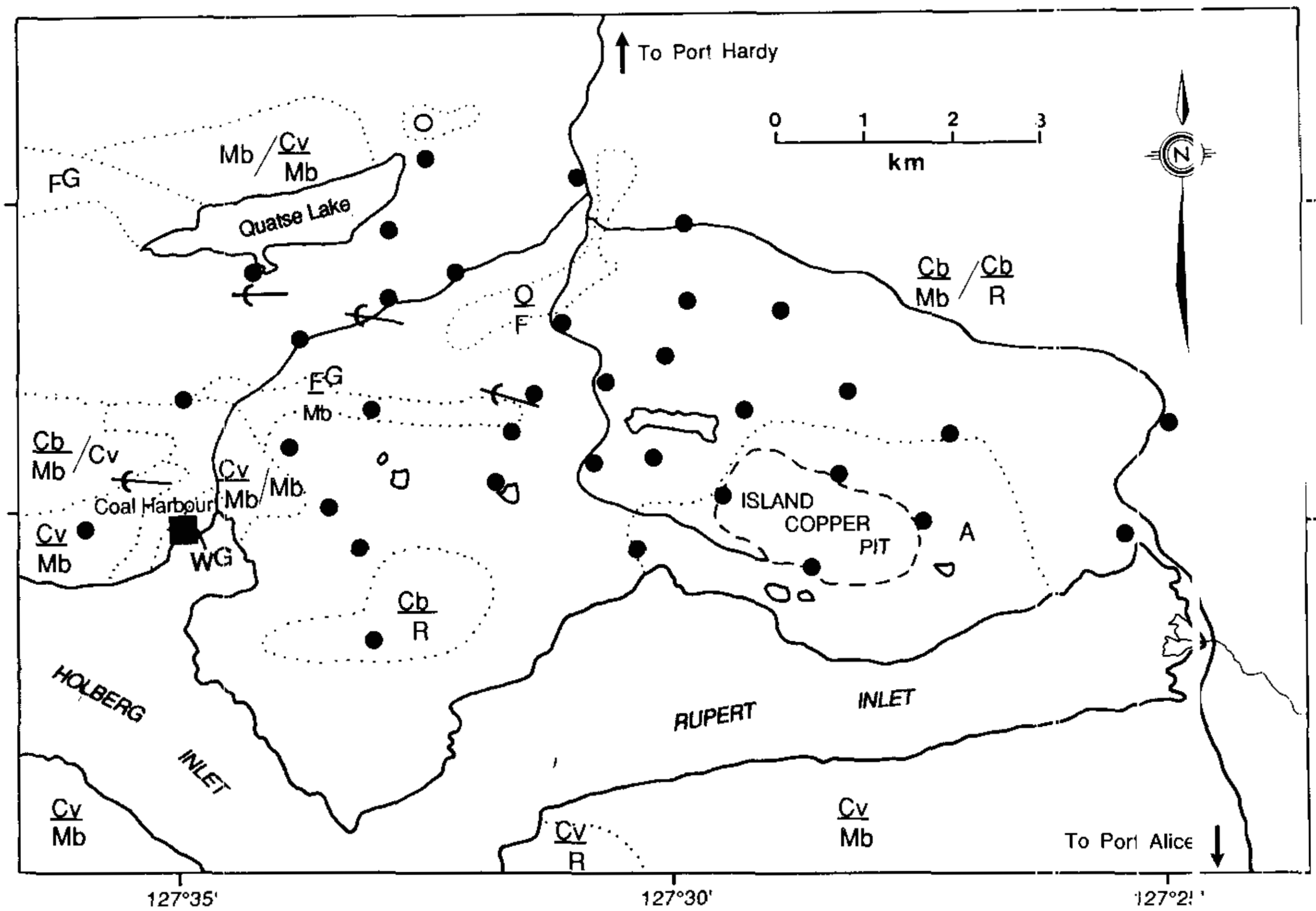

A	Anthropogenic material	O	Organics
Cv, Cb	Colluvium veneer, blanket	WG	Glaciomarine sediments
F	Fluvial sediments	R	Bedrock
FG	Glaciofluvial outwash	●	Sample location
Mb	*Morainal (till) blanket*	⟶	*Striae*

Figure 3-6-3. Detailed surficial geology and geochemical sample location map of the Island Copper area.

microns) of each sample will be analysed by instrumental neutron activation analysis (INAA) and inductively coupled plasma analysis (ICP) for 40 elements.

RESULTS

Quatsino Project

The Quatsino map area (Plate 3-6-1) was last glaciated during the Late Wisconsinan (Fraser glaciation) about 20 000 to 10 000 years ago. Howes (1983) has reported evidence for two glaciations based on the presence of two distinct tills in the north-central regions of Vancouver Island. However, the present authors have found evidence for only one glaciation within the study area. Regional ice-flow direction during the last glaciation was generally toward the northwest, originating from the Coast Mountains and crossing Queen Charlotte Strait. There is, however, considerable variation in glacier flow direction on a local scale; during the initial stages of the glacial advance, individual tongues of ice followed pre-existing valleys, some ice lobes flowing to the west, southwest and south. As opposed to the Nimpkish Valley to the south where small alpine glaciers developed, there is no evidence for any local ice sources in the Quatsino area.

Field mapping shows that surficial materials consist of minor glaciomarine and marine sediments along coastal lowlands below 25 to 30 metres elevation. Widespread deposits of till (Plate 3-6-2), attaining tens of metres in thickness in valleys, are common in both highlands and lowlands. Glaciofluvial outwash, consisting of sand and gravel 1 to 15 metres thick, is generally restricted to valley bottoms. Isolated pockets of silty clay glaciolacustrine sediments occur in valleys where glacial meltwaters were once ponded by stagnant lobes of ice. Colluvium derived from till and weathered bedrock is found not only on steeper slopes, but as a ubiquitous veneer (<1 m) or blanket (>1 m) which covers most other types of surficial sediment types (Plate 3-6-3).

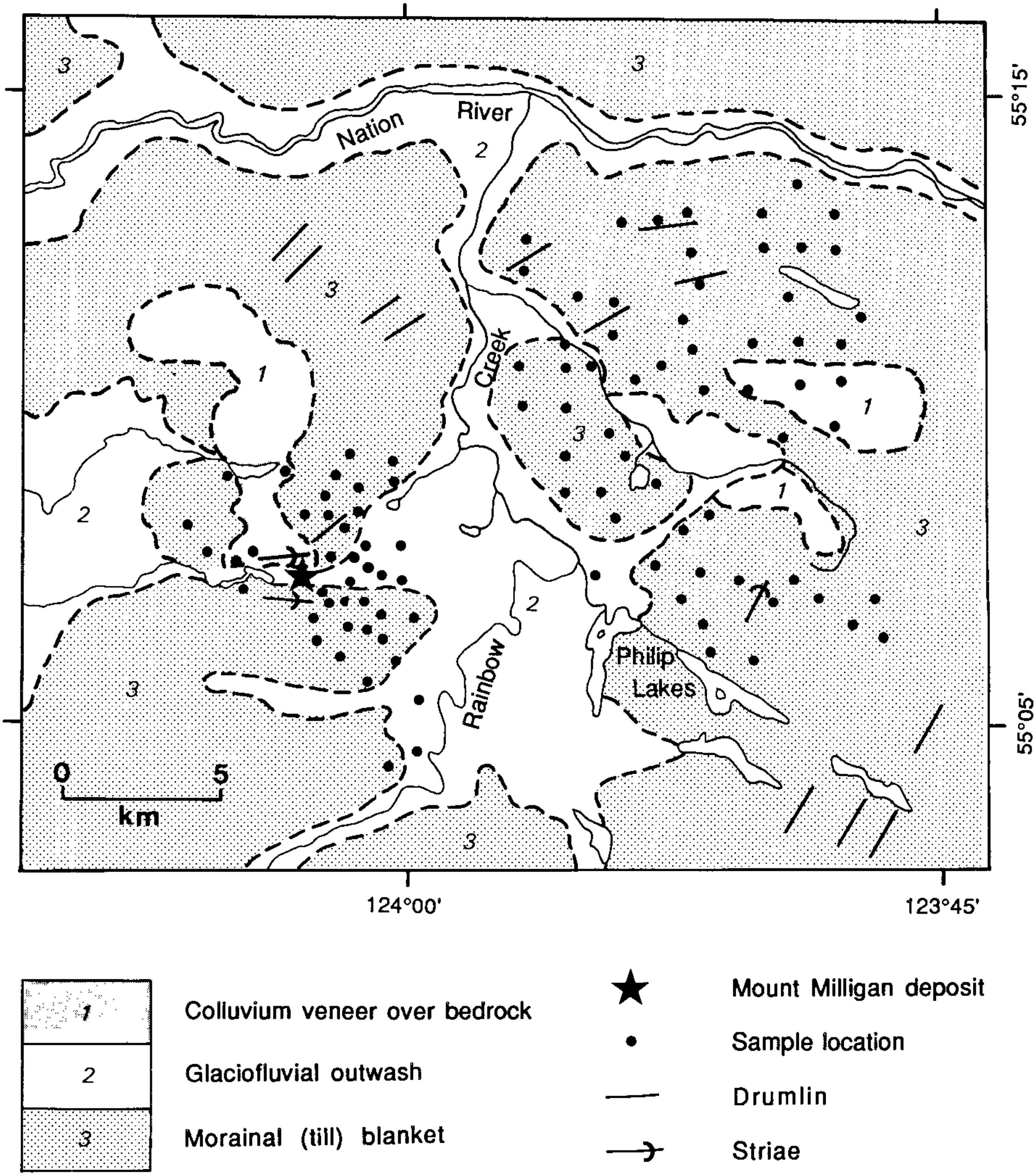

Figure 3-6-4. Generalized surficial geology and geochemical sample location map of the Mount Milligan deposit area.

Plate 3-6-1. Aerial view of Quatsino area relief north of Holberg Inlet, looking north: note fluted landforms developed in till, trending northwest in the foreground, Pemberton Hills in background.

Plate 3-6-2. Striated bedrock (309) overlain by massive till; trowel for scale.

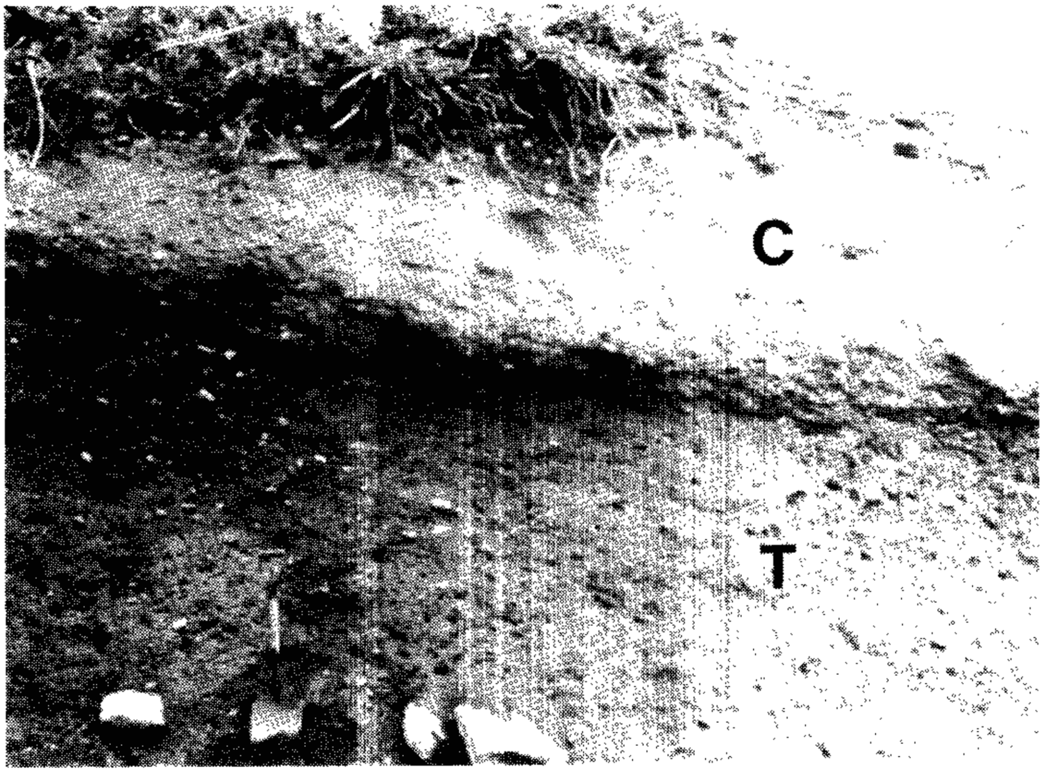

Plate 3-6-3. Massive till (T) sharply overlain by colluvium blanket (C); shovel for scale.

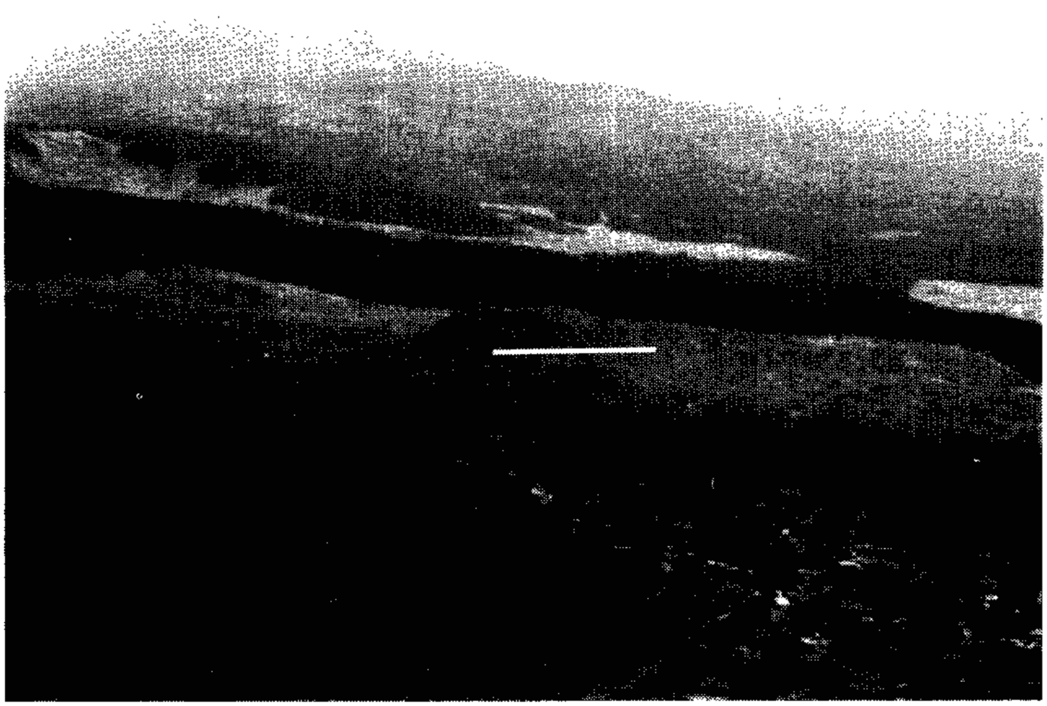

Plate 3-6-4. Aerial view of the subdued relief east of the Mount Milligan property, looking north. Glaciofluvial veneer over till in extensively drilled mineralized areas in foreground and till in centre/background. Note northeast-trending drumlin in centre and Mount Milligan in distance.

Mount Milligan

The last glacial episode in the Mount Milligan region occurred 20 000 to 10 000 years ago during the Late Wisconsinan. Regional ice movement during this event was primarily to the northeast, as interpreted from ice-flow indicators such as well-developed striae scoured into bedrock and drumlinoid features developed in and on unconsolidated sediments.

The sample area (Figure 3-6-4; Plate 3-6-4) can be divided into two general surficial units: a broad, predominantly morainal (till) blanket which is dissected by a central corridor of glaciofluvial outwash. The till was deposited during the last ice advance and is commonly hummocky and drumlinized. Glacial striae, drumlins and other fluted landforms in the southern and western map areas indicate that, on a local scale, ice was initially funnelled through the narrow east-west-oriented valleys between the highlands north and south of the Mount Milligan deposit, and then flowed toward the northeast during full glacial conditions. South of the Nation River, ice flow was reoriented towards the east, as suggested by the drumlinized features which reflect a gradual change in flow direction. In general, the till consists of a dense diamicton composed of very poorly sorted angular to well-rounded pebbles to cobbles in a sand-silt-clay matrix.

A large concentration of glaciofluvial sand and gravel dominates the central part of the map area along Rainbow Creek. This outwash-sediment complex consists of sinuous esker ridges up to 10 kilometres long, kame deposits and a series of broad overlapping outwash fans. Together with outwash sediments along the Nation River and smaller east-west glaciofluvial corridors in the western map area, this complex forms part of a larger regional glaciofluvial system. The stratified sands and gravels in the Rainbow Creek area and elsewhere were deposited by glacial meltwaters during phases of ice retreat. These sediments represent the end product of a long period of glacial and fluvial erosion, transportation and reworking of many types of surficial sediments from an area hundreds of square kilometres in size.

Drift thickness is highly variable, ranging from less than 1 metre on rocky highlands, to over 80 metres in the Rainbow Creek area. Detailed drilling around the Mount Milligan deposit has helped to define topographic bedrock lows toward the northeast. Further drilling, however, would be required to determine the extent and trend of these buried valleys.

ACKNOWLEDGMENTS

The authors wish to thank Lorne Warner and Dale Sketchley of Placer Dome Inc., John Fleming of BHP-Utah Mines Ltd. and Peter Dasler of Moraga Resources for logistical support during the field season, as well as Western Forest Products Limited, Tribune Timber Limited and W.D. Moore Logging Limited for their hospitality and assistance in the field.

REFERENCES

Gravel, J. and Sibbick, S. (1991): Mount Milligan: Geochemical Exploration in Complex Glacial Drift; *in* Exploration in British Columbia 1990, *B.C. Ministry of Energy, Mines and Petroleum Resources* Exploration Part B, pages 117-134.

Howes, D. (1983): Late Quaternary Sediments and Geomorphic History of Northern Vancouver Island, British Columbia; *Canadian Journal of Earth Sciences*, Volume 20, pages 57-65.

Kerr, D. (1991): Surficial Geology of the Mount Milligan Area, NTS 93N/1E, 930/4W; *B.C. Ministry of Energy, Mines and Petroleum Resources*, Open File 1991-7.

Kerr, D. and Bobrowsky, P.T. (1991): Quaternary Geology and Drift Exploration at Mount Milligan and Johnny Mountain, British Columbia; *in* Exploration in British Columbia 1990, *B.C. Ministry of Energy, Mines and Petroleum Resources*, Part B, pages 135-152.

NOTES

SOIL GEOCHEMISTRY OF THE KEMESS SOUTH PORPHYRY GOLD-COPPER DEPOSIT (94E/2E)

By S.J. Sibbick, Geological Survey Branch, C.M. Rebagliati, D.J. Copeland, El Condor Resources Limited, and R.E. Lett, Geological Survey Branch

KEYWORDS: Applied geochemistry, Kemess, porphyry gold-copper, supergene enrichment, soil profiles, element distribution, geochemical dispersion.

INTRODUCTION

As part of the British Columbia Geological Survey drift prospecting program, a geochemical orientation survey was conducted at the Kemess South porphyry copper-gold deposit. The goal of the drift prospecting program is to establish drift exploration methodologies appropriate for the province through the examination of glacial and postglacial processes which influence geochemical dispersion.

The Kemess South deposit was chosen for a study of the interaction between an oxidizing orebody and the overlying transported surficial deposits. Soil geochemical response to the deposit is strong; concentrations greater than 500 ppm copper and 150 ppb gold directly overlie the deposit in an area measuring 800 by 300 metres (Coffin and Mertens, 1988). During the 1991 field season, the relationship between the Kemess South deposit and the overlying soils was studied to determine if the geochemical anomalies overlying it are a result of physical or hydromorphic (chemical) transport.

A blanket of enriched (supergene) copper mineralization, overlain in places by a copper-depleted oxidized cap, is developed within the Kemess South deposit. Ney *et al.* (1976) provide a detailed review of the process and occurrence of supergene porphyry copper mineralization in the Canadian Cordillera. Within a porphyry copper deposit, the process of supergene enrichment results in a distinct vertical zonation. In the oxidized zone copper minerals are either nonexistent or consist of copper oxides and native copper. Iron oxide minerals are common and include limonite, hematite, jarosite, goethite and a variety of amorphous iron oxides (Anderson, 1982). Underlying the oxidized zone, supergene copper minerals consist mainly of chalcocite and covellite. Pyrite and chalcopyrite are the most common primary sulphides in the hypogene zone.

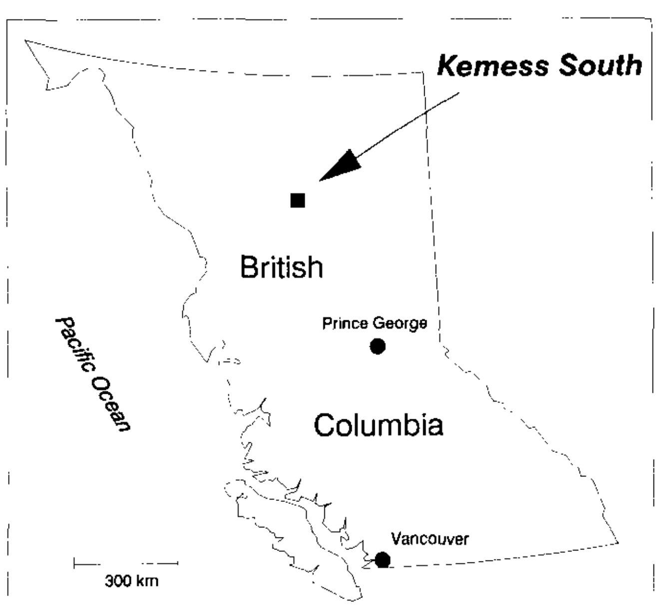

Figure 3-7-1. Location of the Kemess South deposit.

PROPERTY OVERVIEW

LOCATION AND ACCESS

The Kemess South deposit is located at latitude 57°00'N, longitude 126°45'W (NTS 94E/02W), 7 kilometres east of Thutade Lake and 550 kilometres northwest of Prince George (Figure 3-7-1). Access to the property, by the Omineca Mining Road, is possible from either Mackenzie or Fort St. James. The property may also be reached by air via the Sturdee airstrip, approximately 25 kilometres to the northwest.

LOCAL GEOLOGY AND MINERALIZATION

The Kemess South property is underlain mainly by mafic volcanic rocks of the Upper Triassic Takla Group and poorly exposed sedimentary strata of the Permian Asitka Group (Figure 3-7-2). Stocks, dikes and a sill-like body of porphyritic quartz monzodiorite and tonalite intrude these rocks. Cann and Godwin (1980) have assigned a Lower Jurassic age to similar intrusions on the Kemess North property 5 kilometres to the north. Gold-copper mineralization at Kemess South is hosted by a sill-like body of quartz monzodiorite porphyry, up to 245 metres thick, and sometimes extends a short distance into the underlying Takla volcanics. Drilling has confirmed the deposit extends over an area exceeding 1100 by 600 metres. The main hypogene sulphide minerals, in order of abundance, are pyrite, chalcopyrite, bornite and a trace of molybdenite. They occur as disseminated grains and fracture fillings and within quartz stockwork veins.

A zone of supergene enrichment, ranging up to 66 metres thick, is preserved in the southwestern part of the deposit. It is partly covered by a thin layer of sedimentary and volcanic rocks which resemble the Cretaceous-Tertiary Sustut Group, possibly the basal member of the Eocene Brothers Peak Formation. Within the supergene zone, the quartz monzodiorite is weathered to a brick-red colour, imparted by a ubiquitous mixture of hematite, limonite and indeterminate iron oxide and clay minerals. Where the leached cap

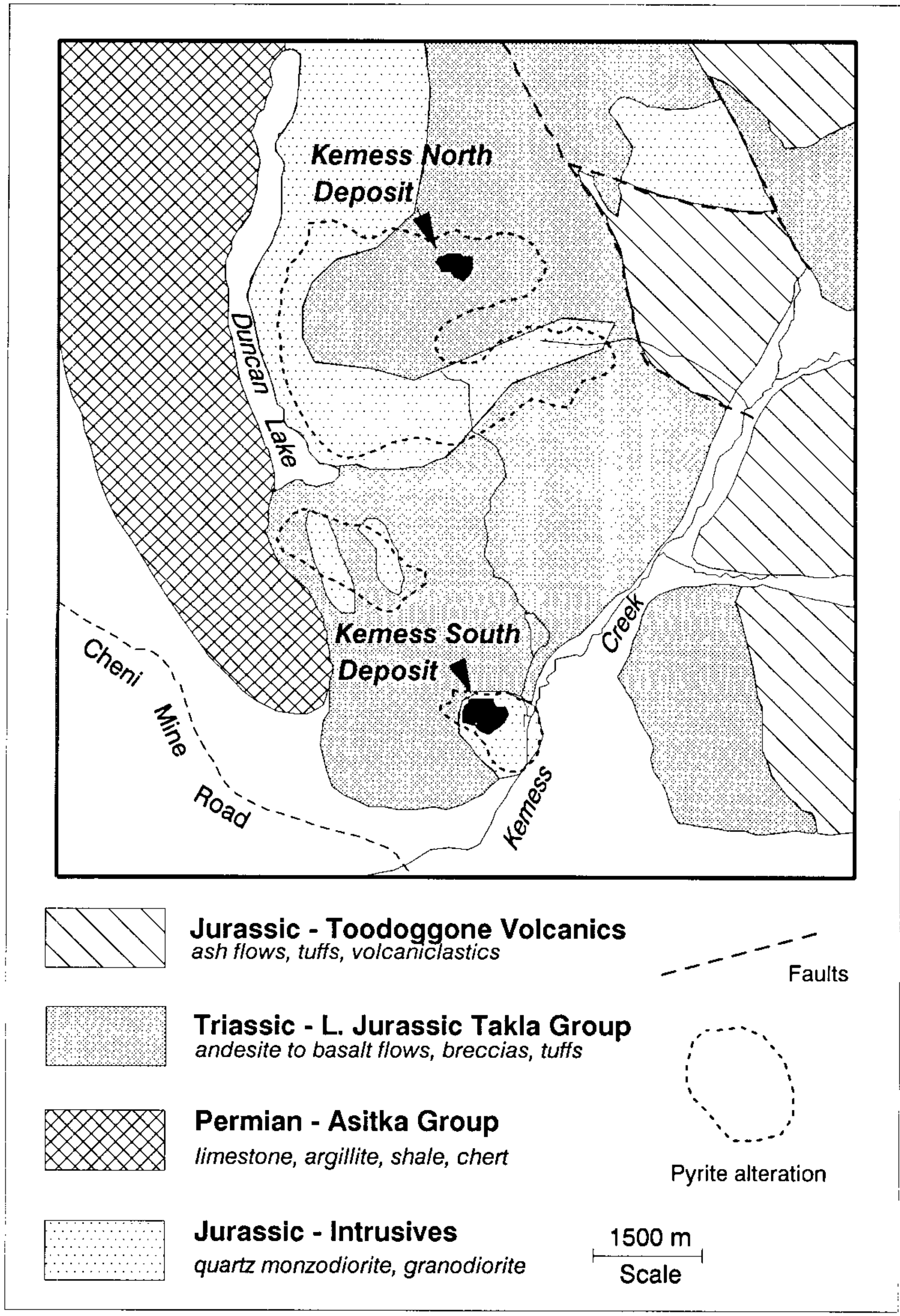

Figure 3-7-2. Geology of the Kemess South area.

of the supergene zone has been preserved, all original textures have been destroyed. However, the quartz stockwork remains readily discernible. Drilling below the leached cap reveals native copper and chalcocite to be the major supergene copper minerals. Copper oxide, carbonate and silicate minerals are minor constituents. Significant concentrations of chalcocite occur in a narrow zone at the transition between supergene and hypogene ore. Locally significant quantities of copper are found within secondary iron minerals. The downward limit of secondary iron minerals marks the abrupt appearance of hypogene sulphides. There is no noticeable change in the concentration of gold in the supergene zone relative to the protore.

Within the mineralized zone the quartz monzodiorite hostrock is replaced by a secondary mineral assemblage of potassium feldspar and intense sericite-chlorite alteration. Most primary mafic silicate minerals have been replaced by biotite and chlorite. Takla volcanic rocks in the footwall are characterized by a propylitic alteration assemblage comprising chlorite, calcite and pyrite. Laterally outwards from the intrusion, propylitic alteration in the Takla volcanics is comprised of epidote and pyrite.

Surficial Geology

Surficial deposits overlying the Kemess South deposit are of a variable nature and thickness. A veneer of colluvium and till interspersed with pockets of hard-packed till filling lows in the bedrock topography covers the northern, upslope area of the deposit. Towards Attichika Creek the veneer of colluvium and till grades into a thick blanket of till and glaciofluvial sediment which masks the bedrock topography. The Attichika Creek valley is blanketed with extensive deposits of till and glaciofluvial outwash, together with several stagnant ice features. Talus, felsenmeer and bedrock predominate at higher elevations near the deposit. Glacial striae to the south indicate that the direction of regional ice movement during the last (Fraser) glaciation was towards the east and southeast (Lord, 1948). However, glacial features in the vicinity of the property suggest ice flowed in a southerly direction, a result of control by local topography.

Physiography and Climate

The property lies in the Swannell Ranges of the Omineca Mountains. Local relief ranges from 1200 to 1900 metres and is represented by a mixture of steep to precipitous slopes and flat valley bottoms. Located at an elevation of 1300 metres, the deposit subcrops near the base of a moderate to steeply sloping northwest-trending ridge which rises approximately 300 metres above the adjoining Attichika Creek valley. Glaciation has rounded peaks less than 1800 metres in height while bedrock above this height is still comparatively rugged. Humo-ferric podzols are the most prevalent soil type developed above the deposit and in the vicinity. Remnants of late Teritary erosion surfaces were noted by Holland (1976) in the McConnell and Wrede Ranges to the southeast. Treeline is at approximately 1500 metres.

METHODS

Sample Collection

Twenty-eight 1-kilogram samples of soil, saprolite or rock were collected from five profiles ranging from [illegible] to 3 metres in depth along an east-west traverse across the deposit (Figure 3-7-3). Four of the profiles were developed on mineralized bedrock and one profile sampled a thick unit of till. At each location, B-horizon, till, saprolite or rock were sampled at regular intervals down profile, or on either side of significant physical changes in the profile. Two field duplicates were taken.

Sample Preparation

Samples were sent to the Geological Survey Branch Analytical Sciences Laboratory in Victoria for sample preparation. All samples were dried at 50°C. Soil and saprolite samples were dry sieved to −80+230 mesh (−177−63 µm) and −230-mesh (−63 µm) fractions. The −80+230-mesh fraction was wet sieved to remove any adhering fines and then dried at 50°C. Bedrock samples were cleaned with compressed air, crushed and pulverized to −100 mesh (−150 µm). Representative splits of each sample fraction were prepared for analysis. Control reference standards GXR2 and GXR4 were inserted into each sample batch to allow monitoring of quality control.

Sample Analysis

COPPER, MOLYBDENUM, GOLD, IRON AND ALUMINUM

Subsamples of the −80+230 and −230-mesh fractions were submitted to Chemex Labs, Ltd. in North Vancouver and subjected to a total dissolution using a hot, concentrated perchloric-nitric-hydrofluoric acid ($HClO_4$-HNO_3-HF) digestion. Analyses were carried out for copper by atomic absorption spectroscopy (AAS) and for aluminum, iron and molybdenum by inductively coupled plasma - atomic emission spectroscopy (ICP-AES). Gold analyses were conducted on five grams of each −80+230 and −230-mesh sample by instrumental neutron activation analysis (INAA) at Activation Laboratories in Ancaster, Ontario.

SEQUENTIAL PARTIAL EXTRACTIONS FOR COPPER

Sequential partial extractions for copper were performed at the Analytical Sciences Laboratory on 0.5-gram subsamples of the −230-mesh fraction in the following order:

(1) 1 M ammonium acetate (CH_3COONH_4) at pH 7.2

(2) 0.1 M hydrochloric acid (HCl)

(3) Aqua regia (3HCl:1HNO_3)

Solutions derived from these extractions were analysed for copper by atomic absorption spectroscopy. Sequential partial extractions provide a method for identifying the residence sites of metals within samples. Each extraction technique liberates metals from particular minerals either by dissolution of the mineral or by the exchange of that metal with another cation. Neutral (pH 7.2) ammonium acetate acts to remove weakly bonded metals in exchange sites. For example, copper cations (Cu^{+2}) weakly held to a mineral will be displaced by free NH_4^{+2} cations in the ammonium

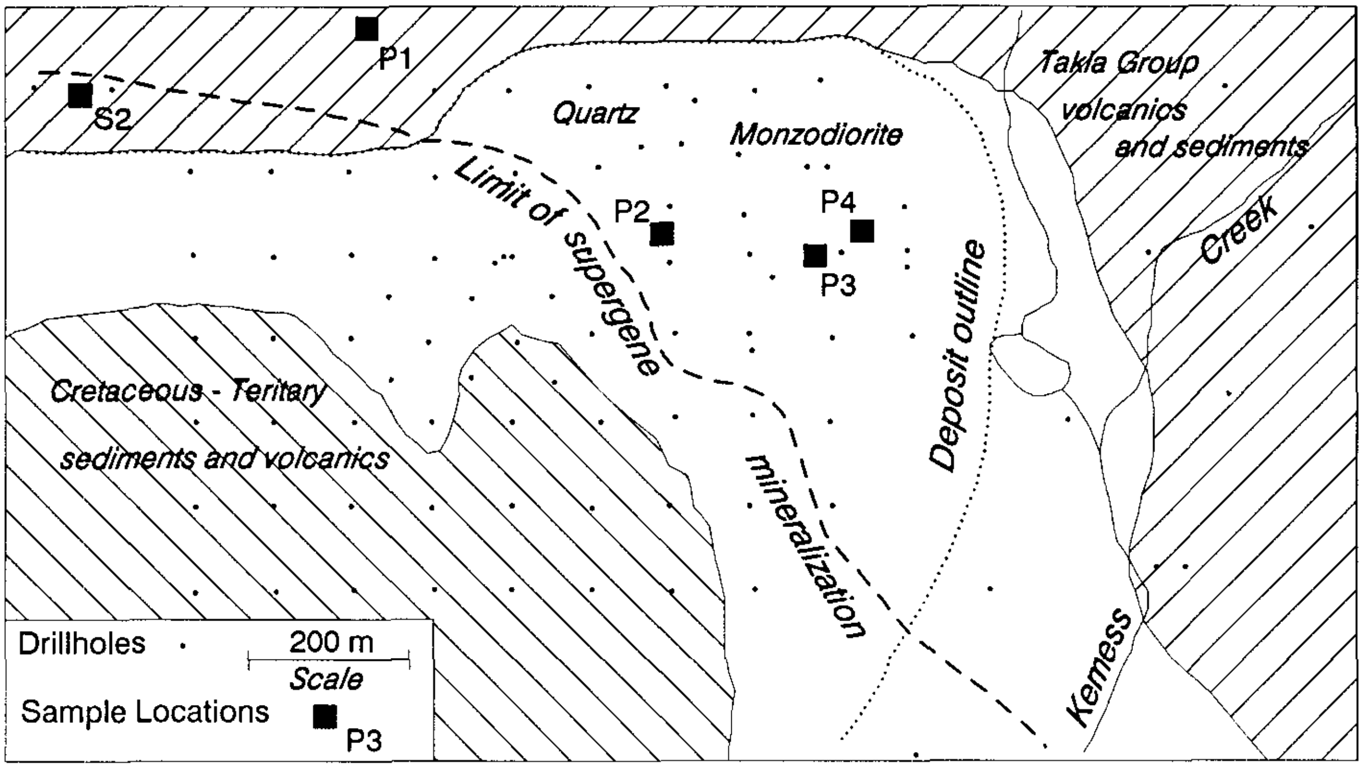

Figure 3-7-3. Geology of the Kemess South deposit.

acetate solution. Dilute hydrochloric acid (0.1 M HCl) will release exchangeable metals and metals associated with clays, manganese oxides and organic matter, and will also partly decompose sulphides and carbonates (Fletcher, 1981). Aqua regia readily dissolves sulphides and iron oxides while leaving silicates relatively uneffected. Results of these extractions were compared with the copper results for the total acid digestion discussed above.

RESULTS

PROFILE DESCRIPTIONS

Diagrams of the five sampled profiles are shown in Figure 3-7-4. Profile S2 is a 3.5-metre section topped by a gleyed organic-rich A-horizon 25 centimetres thick. The B-horizon soil is developed within a layer of colluvium containing angular clasts which extends to a depth of 75 centimetres. Within the B-horizon, a reddish Bf-horizon grades into an underlying dark brown BC-horizon at a depth of 60 centimetres. Underlying the colluvium is a compact, brick-red hematitic saprolite unit containing abundant clay between strongly weathered rock clasts. Minor amounts of malachite-bearing clasts are visible within this unit which grades into the lower unit at a depth of 180 centimetres. This lowermost saprolite is buff coloured and consists of rotted bedrock with clays filling the interstices between rock fragments. It is more compact than the overlying saprolite and contains a higher proportion of malachite-bearing clasts. Locally high concentrations of hematite and jarosite endow a brick-red or pale yellow colour to the unit. Mineralized quartz monzodiorite and a volcaniclastic unit, tentatively indentified as belonging to the Toodoggone Group (L.J. Diakow, personal communication, 1991), underlies the saprolite. Both rock types contain native copper, chalcocite and malachite.

Profile P1 is a 250-centimetre section. A thin (5–10 cm) A-horizon is underlain by a 40-centimetre B-horizon. The B-horizon grades downwards into a unit of oxidized, tan-coloured till which extends to the bottom of the profile. Clasts within the till consist primarily of subrounded fragments of dark grey chert; approximately 10 per cent of the clasts are iron stained.

The 1-metre section of Profile P2 is composed of 40 centimetres of saprolitic quartz monzodiorite overlain by a 60-centimetre B-horizon and a thin (<5 cm) A-horizon. The contact between the saprolite and B-horizon is gradational over approximately 10 centimetres. Within the B-horizon, a reddish Bf-horizon grades into an underlying, dark brown BC-horizon at a depth of 35 centimetres.

Profile P3 is a 2.5-metre section. A thin (<5 cm) A-horizon is underlain by a 50-centimetre B-horizon. The B-horizon is subdivided into an upper Bf and a lower BC-horizon by a gradational contact at approximately 30 centimetres. Below the B-horizon is a transitional unit 60 centimetres thick consisting of a dark brown, clay-rich sandy material. Both the upper and lower contacts of this unit are gradational over 20-centimetre intervals. Underlying this transitional unit is 70 centimetres of brick-red, clay-rich hematitic saprolite composed of rotted quartz monzodiorite. At 180 centimetres, the hematitic saprolite changes abruptly to a relatively pristine quartz monzodiorite containing pyrite (3%) and chalcopyrite (1%).

Profile P4 is a 2.5-metre section. A thin (<5 cm) A-horizon is underlain by a B-horizon 40-centimetres thick which grades into an 80-centimetre unit of till (C horizon). The till is dark grey and contains subangular to subrounded clasts of which approximately 10 per cent are iron stained. Underlying the till is 110 centimetres of brick-red clay-rich hematitic saprolite, similar to that found in Profile P3. At a depth of 230 centimetres, the saprolite abruptly changes to a relatively pristine quartz monzodiorite containing visible pyrite (3%) and chalcopyrite (1%), similar to that in Profile P3.

Element Distributions Within Profiles

COPPER

Copper concentrations for both size fractions are highest within the saprolite samples from Profile S2, ranging from 10 700 to 36 800 ppm (1.07 to 3.68%; Table 3-7-1 and Figure 3-7-5a). The lowest copper values are found in the till profile P1, with concentrations varying from 53 to 1099 ppm. Profiles P2, P3 and P4, each containing saprolitic or pristine quartz monzodiorite, have copper concentrations ranging from 398 to 3582 ppm with the quartz monzodiorite samples (P3-180, P4-240) reporting the lowest values (572 and 398 ppm, respectively). Systematic variation in copper content with depth is not prevalent; only Profiles S2 and P2 show an increase with depth whereas Profiles P1, P3 and P4 show little variation.

GOLD

The highest gold values are found within the −230-mesh fraction of Profile P2, ranging from 1820 to 2880 ppb (Table 3-7-1 and Figure 3-7-5b). Gold contents from both size fractions of the till profile P1 are consistently the lowest, varying from 1 ppb to 930 ppb. Concentrations are uniformly higher within the −230-mesh fractions of Profiles P2, P3 and P4, and generally higher within the −230-mesh fractions of Profile P1 than in their corresponding −80+230-mesh fractions. Except for the B-horizon sample, gold contents are highest within the −80+230-mesh fraction of Profile S2. Duplicate pairs for sample P4-30 show a small degree of variation; 9.6 per cent for gold in the −80+230-mesh fraction and 5.4 per cent for gold in the −230-mesh fraction. No consistent variation with depth was observed for gold within the profiles.

MOLYBDENUM

Molybdenum values are highest within the −230-mesh fraction of Profile P3 and peak (449 ppm) within the coarse-grained, sandy transitional unit between the overlying B-horizon soils and underlying saprolitic quartz monzodiorite (Table 3-7-1 and Figure 3-7-5c). As with gold, molybdenum values are consistently higher within the −230-mesh fraction of Profiles P2, P3 and P4 than in their corresponding −80+230-mesh fractions. Copper and molybdenum behave sympathetically, a feature especially prevalent in Profiles P2, P3 and P4.

IRON

Maximum iron concentrations are found within the −230-mesh fraction of Profile P3; sample P3-150 contains 14.23 per cent iron, whereas the transitional unit reports values of 12.15 and 13.03 per cent iron for samples P3-70 and P3-100, respectively (Table 3-7-1 and Figure 3-7-5d). Profile P1 contains the lowest iron value (2.[illegible]7%) and displays the least variation between samples. Iron content corresponds to gross variations in copper and molybdenum for both size fractions of Profiles P2, P3 and P4. A similar correlation is not observed in Profiles S2 and P1.

ALUMINUM

Aluminum values are greatest within the -230-mesh fractions of the three lowermost saprolite samples of Profile S2 (up to 12.45%) and the saprolite samples of Profile P3 (up to 10.86%; Table 3-7-1 and Figure 3-7-5e) Unlike iron, variations in aluminum do not appear to correspond to variations in copper and molybdenum for Profiles P2, P3 and P4. However, variations in the aluminum content of the −230-mesh fraction do correspond to variations in copper and molybdenum for the saprolite samples of Profile S2.

Partial Extractions For Copper

Results of partial extractions for copper are shown in Table 3-7-2. Figure 3-7-6 presents the percentages of partially extractable copper as a function of the total copper content for each profile. Maximum amounts of ammonium acetate extractable copper are found in samples from Profile S2 whereas Profile P1 generally contains the lowest and most uniform levels of exchangeable copper. Excluding bedrock samples P3-180 and P4-240, the proportion of exchangeable copper increases with depth in Profiles P2, P3 and P4. Copper extractable using 0.1 M hydrochloric acid is also highest in Profile S2; up to 61.75 per cent of the copper present in sample S2-200 is extractable. Samples from Profile P1 contain nearly uniform levels of extractable copper, whereas Profiles P2, P3 and P4 contain increasing amounts of extractable copper with depth. Aqua regia extractable copper accounts for over 80 per cent of the copper in the samples, with the exception of sample P1-30 and, notably, all Profile S2 samples and the saprolite samples from Profiles P3 and P4.

DISCUSSION

Concentrations of copper, molybdenum, gold, iron and aluminum are higher in the −230-mesh fraction than the −80+230-mesh fraction, reflecting the original grain size of sulphides in the deposit, the greater abundance of secondary clays and oxide minerals in the fraction and the hydromorphic redistribution of metals to these secondary minerals. The sympathetic variation of copper, molybdenum, iron and aluminum within the profiles reflects the incorporation of these elements in secondary minerals developed during weathering. Copper and molybdenum concentrations in the −230-mesh fraction of Profile S2, developed within the supergene zone, appear to correlate more strongly with aluminum than with iron. In contrast, the copper and molybdenum contents of Profiles P2, P3 and P4, developed outside of the zone of supergene enrichment but within oxidized bedrock, correlate with variations in iron.

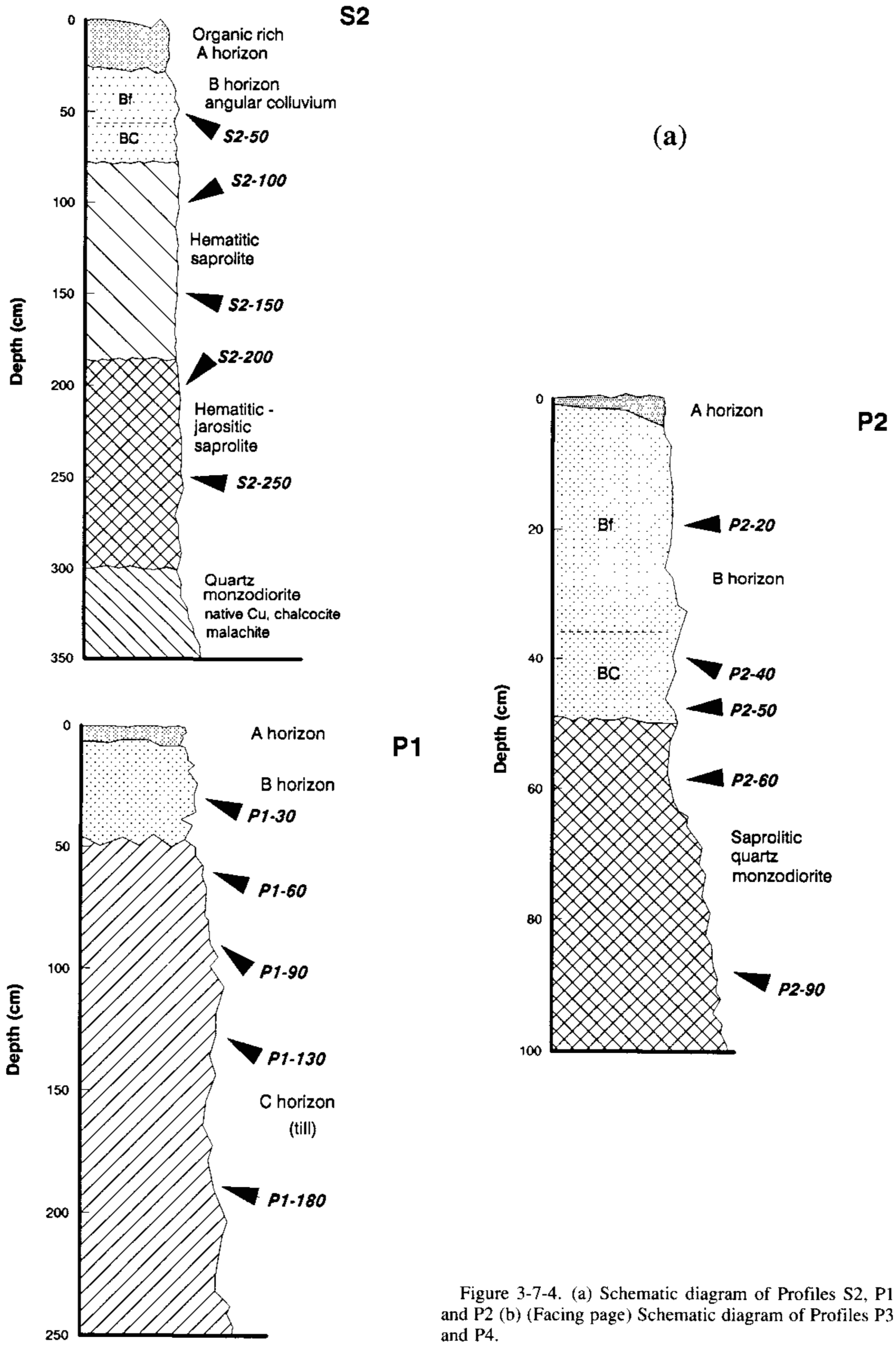

Figure 3-7-4. (a) Schematic diagram of Profiles S2, P1 and P2 (b) (Facing page) Schematic diagram of Profiles P3 and P4.

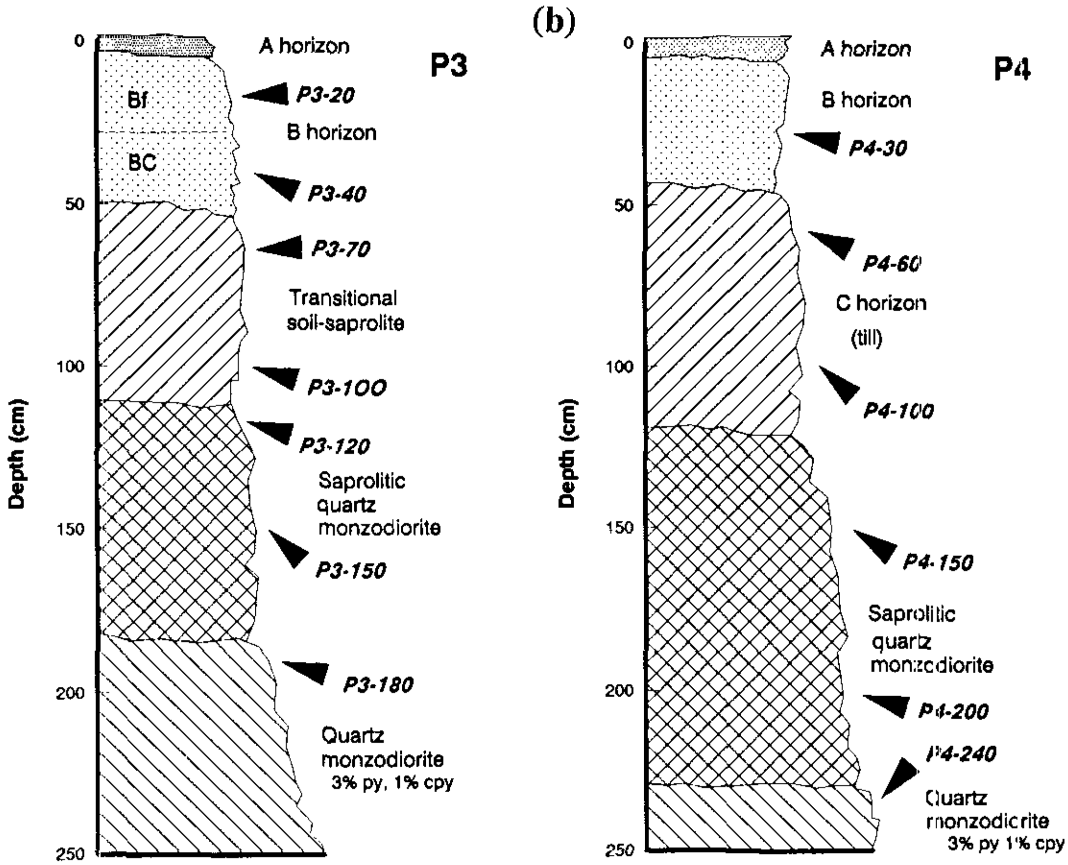

Partial extraction results indicate mineralogical differences between the supergene profile S2, the saprolite profiles P2, P3 and P4 and the till profile P1. Further, variation in the percentage of partially extractable copper with depth reveals changes in the mineralogy of the profile. With the exception of the supergene profile samples S2-150 and S2-200, aqua regia extracts most of the contained copper. Coupled with the lack of sulphides in the profiles (excluding bedrock samples P3-180 and P4-240), this implies that the principal residence site for copper is within iron oxides. Profile P1 contains similar proportions of exchangeable copper (ammonium acetate extractable) and weak hydrochloric acid extractable copper at all depths, reflecting the uniform nature of the till. The consistent increase in exchangeable copper and weak hydrochloric acid extractable copper with depth in Profiles P2, P3 and P4 indicates that the proportion of secondary copper-bearing minerals increases down profile and drops off sharply once competent bedrock is reached. Profile S2 contains the highest levels of exchangeable copper and weak hydrochloric acid extractable copper; the presence of abundant clays, iron oxides, jarosite and malachite suggests that these secondary minerals are also residence sites of copper.

Significant levels of exchangeable copper (3.54%) and weak hydrochloric acid extractable copper (21.67%) in the B-horizon of Profile S2 indicate the presence of copper either within or adsorbed onto secondary minerals, implying that hydromorphic transport of copper has occurred or is ongoing. Profiles P1, P2, P3 and P4, with B-horizons containing less than 1 per cent exchangeable copper and less than 10 per cent copper extractable by weak hydrochloric acid, appear to have a lesser component of hydromorphically transported copper. However, the similarity of copper contents of the B and C-horizons in Profile P4 with the underlying saprolite suggests that some degree of hydromorphic transport has occurred.

Unlike copper, gold values do not appear to have been effected by weathering and the development of a supergene enrichment zone. Molybdenum contents appear to mimic iron values for Profiles P2, P3 and P4, suggesting the presence of ferrimolybdite ($Fe_2(MoO_4)_3 \cdot 8H_2O$) which is insoluable in oxidizing, acidic solutions (Anderson, 1982). The stronger association of molybdenum and copper with aluminum in the −230-mesh fraction of Profile S2 indicates that these elements may be associated more with secondary clays than iron oxides.

CONCLUSIONS

The principal residence sites for copper within soils and the saprolitic hypogene bedrock of Profiles P2, P3 and P4 are secondary iron oxide minerals. Within the upper leached cap of the supergene zone (Profile S2), which has been exposed to Holocene (postglacial) weathering, oxidation of sulphides has resulted in the development of secondary minerals which retain upwards of 70 per cent of the copper,

TABLE 3-7-1
CONCENTRATIONS OF GOLD, COPPER, MOLYBDENUM, IRON AND ALUMINUM FOR THE -80+230 AND -230-MESH FRACTIONS

			Minus 80+230 mesh data					Minus 230 mesh data				
Sample	**Depth (cm)**	**Media**	**Au (ppb)**	**Cu (ppm)**	**Mo (ppm)**	**Fe (%)**	**Al (%)**	**Au (ppb)**	**Cu (ppm)**	**Mo (ppm)**	**Fe (%)**	**Al (%)**
S2 - 50	50	Bf	37	1353	2	5.75	6.73	56	2580	3	4.47	6.54
S2 - 100	100	sap.	1220	825	70	6.67	6.97	148	838	4	5.44	8.80
S2 - 150	150	sap.	2670	10900	19	3.76	7.00	709	10700	19	4.46	11.06
S2 - 200	200	sap.	840	19400	29	4.32	6.87	544	21700	35	2.68	12.45
S2 - 250	250	sap.	271	36800	21	5.65	6.06	190	14200	14	5.09	10.37
P1 - 30	30	Bf	6	212	8	3.37	6.33	10	164	8	3.91	7.54
P1 - 60	60	till	6	77	1	2.87	6.02	21	127	1	3.95	7.50
P1 - 90	90	till	1	55	<1	2.85	6.22	20	123	3	4.33	7.70
P1 - 90D	90	till	930	930	72	6.43	6.75	11	1099	43	5.57	8.82
P1 - 130	130	till	1	53	3	3.06	6.32	14	122	2	4.40	7.99
P1 - 180	180	till	49	59	1	2.95	6.22	20	138	<1	4.48	7.93
P2 - 20	20	Bf	575	747	34	6.12	7.26	1820	1077	40	5.61	8.90
P2 - 40	40	BC	32	901	72	6.37	6.80	1820	1348	93	6.48	8.85
P2 - 50	50	BC	1090	376	3	4.20	6.19	2000	1141	76	5.70	9.25
P2 - 60	60	sap.	1060	1137	98	5.61	8.33	2880	1448	128	6.90	9.53
P2 - 90	90	sap.	783	2818	259	7.59	7.10	1850	3774	386	10.60	8.71
P3 - 20	20	Bf	457	962	138	6.82	7.71	972	1669	139	6.98	9.25
P3 - 40	40	BC	510	1919	276	7.50	7.97	1070	2749	312	9.40	9.02
P3 - 70	70	trans.	426	1819	242	6.26	8.45	1340	3354	419	12.15	8.79
P3 - 100	100	trans.	375	1878	244	6.81	8.69	1070	3582	449	13.03	8.89
P3 - 120	120	sap.	437	1003	76	3.70	8.37	769	2100	133	6.97	10.86
P3 - 150	150	sap.	324	913	98	4.75	8.82	762	2746	395	14.23	10.48
P3 - 180	180	rock	650	572	58	3.87	8.80	650	572	58	3.87	8.80
P4 - 30	30	Bf	411	837	32	4.60	6.99	551	1286	40	4.71	7.76
P4 - 30D	30	Bf	455	790	25	4.41	6.80	521	1350	43	5.08	7.64
P4 - 60	60	till	483	738	16	4.48	6.47	596	1338	23	4.37	7.55
P4 - 100	100	till	451	832	20	4.26	6.75	976	1406	30	4.73	7.53
P4 - 150	150	sap.	315	797	24	4.48	6.95	527	1346	44	5.10	7.70
P4 - 200	200	sap.	460	1404	149	6.06	7.95	896	2513	271	10.66	8.58
P4 - 240	240	rock	438	398	77	3.38	8.79	438	398	77	3.38	8.79

TABLE 3-7-2
SEQUENTIAL PARTIAL EXTRACTION DATA FOR COPPER
IN THE –230-MESH FRACTION OF EACH SAMPLE

SAMPLE DATA			EXTRACTION (ppm)				% EXTRACTED		
Sample	Media	Depth (cm)	NH4 Acetate	0.1M HCl	Aqua Regia	Total digestion	NH4 Acetate	0.1M HCl	Aqu Regi
S2-50	Bf	50	93	570	1790	2630	3.54	21.67	68.0
S2-100	sap.	100	44	187	610	835	5.27	22.40	73.0
S2-150	sap.	150	1210	6300	2250	10700	11.31	58.88	21.0
S2-200	sap.	200	1560	13400	5800	21700	7.19	61.75	26.7
S2-250	sap.	250	1230	4300	8000	14200	8.66	30.28	56.3
P1-30	Bf	30	1	14	110	164	0.61	8.54	67.0
P1-60	till	60	1	11	114	127	0.79	8.66	89.7
P1-90	till	90	1	11	116	123	0.81	8.94	94.3
P1-90d	till	90	1	11	120	1100	0.09	1.00	10.9
P1-130	till	130	1	12	108	122	0.82	9.84	88.5
P1-180	till	180	1	17	125	138	0.72	12.32	90.5
P2-20	Bf	20	10	51	940	1075	0.93	4.74	87.4
P2-40	BC	40	6	29	1200	1350	0.44	2.15	88.8
P2-50	BC	50	8	28	1040	1140	0.70	2.46	91.2
P2-60	sap.	60	21	60	1340	1450	1.45	4.14	92.4
P2-90	sap.	90	80	300	3340	3770	2.12	7.96	88.5
P3-20	Bf	20	3	14	1340	1670	0.18	0.84	80.2
P3-40	BC	40	12	66	2580	2750	0.44	2.40	93.8
P3-70	trans.	70	34	200	3000	3350	1.01	5.97	89.5
P3-100	trans.	100	39	319	3150	3580	1.09	8.91	87.9
P3-120	sap.	120	48	258	1540	2100	2.29	12.29	73.3
P3-150	sap.	150	63	460	1860	2750	2.29	16.73	67.6
P3-180	R	180	4	29	583	572	0.70	5.07	101.9
P4-30	Bf	30	6	62	1130	1250	0.48	4.96	90.4
P4-30d	Bf	30	6	56	1180	1350	0.44	4.15	87.4
P4-60	till	60	10	73	1100	1340	0.75	5.45	82.0
P4-100	till	100	15	84	1190	1450	1.03	5.79	82.0
P4-150	sap.	150	25	125	1080	1375	1.82	9.09	78.5
P4-200	sap.	200	61	370	1970	2510	2.43	14.74	78.4
P4-240	R	240	8	33	370	398	2.01	8.29	92.9
Standards									
GXR4			277	1410	4800	na	na	na	n
GXR4			278	1790	4240	6620	4.20	27.04	64.0

LEGEND
Bf - soil BC - transitional B-C horizon soil sap. - saprolite
R - bedrock trans. - transitional (soil to saprolite)

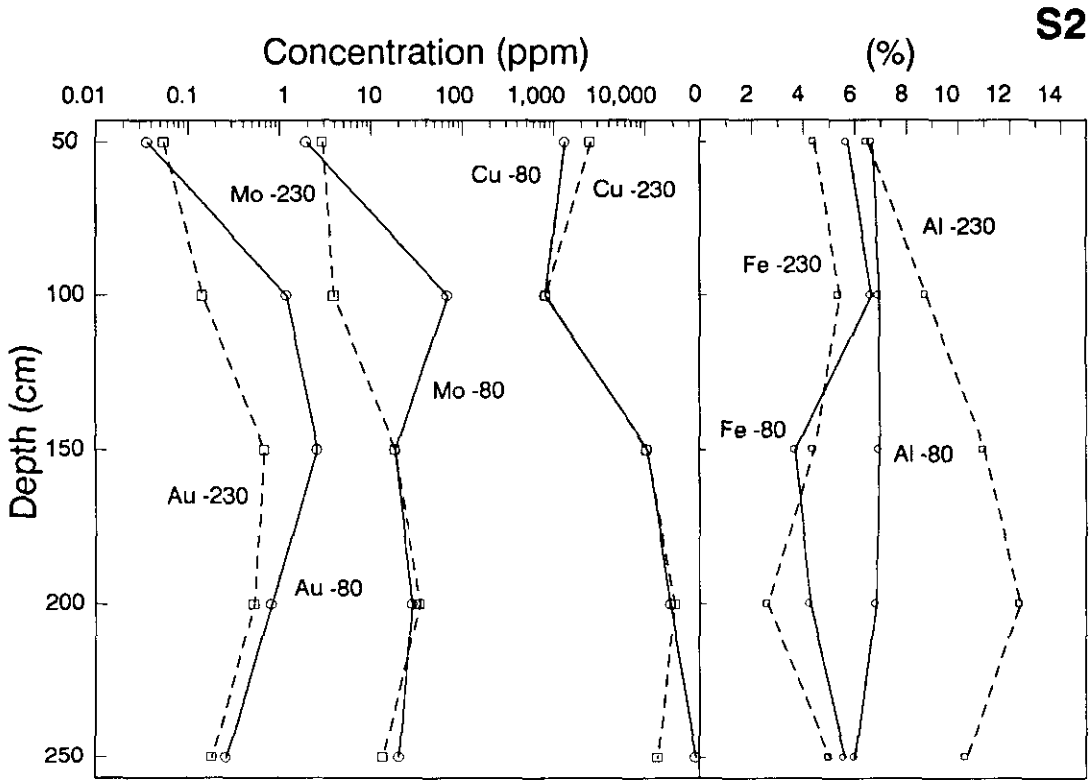

(a)

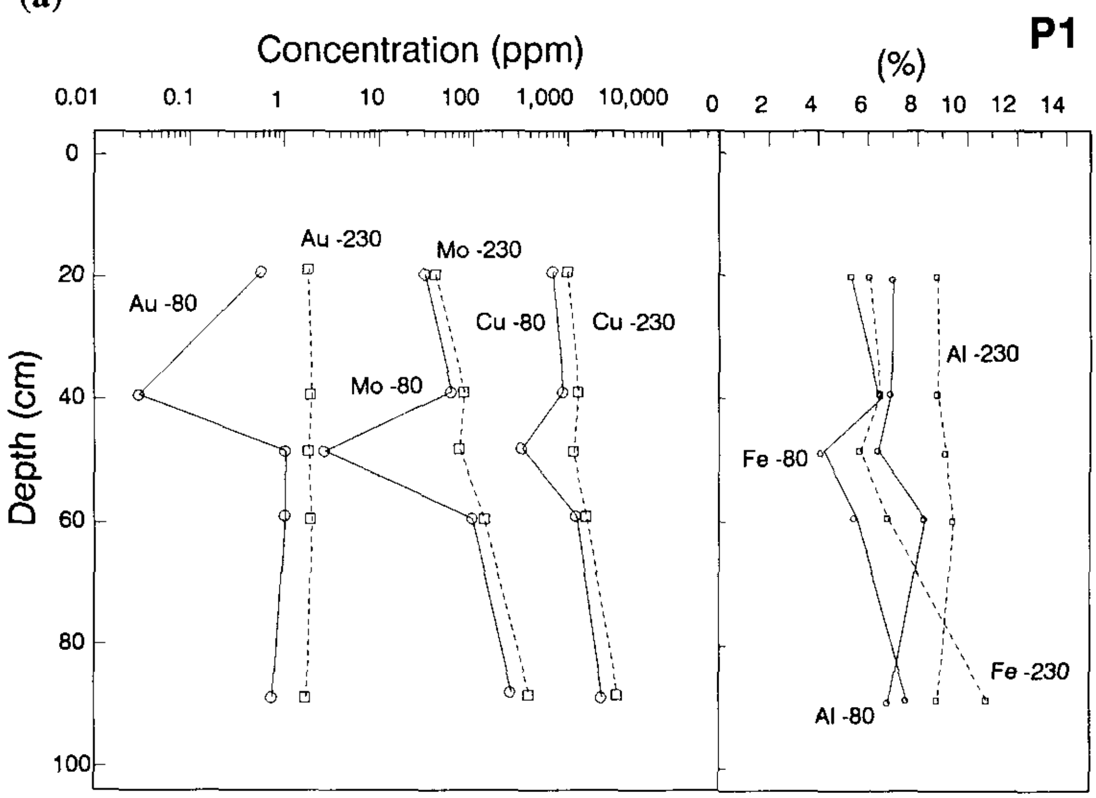

Figure 3-7-5. (a) Plots of Au, Mo, Cu, Fe and Al concentrations with depth for Profiles S2 and P1 (b) Plots of Au, Mo, Cu, Fe and Al concentrations with depth for Profiles P2 and P3 (c) Plots of Au, Mo, Cu, Fe and Al concentrations with depth for Profile P4.

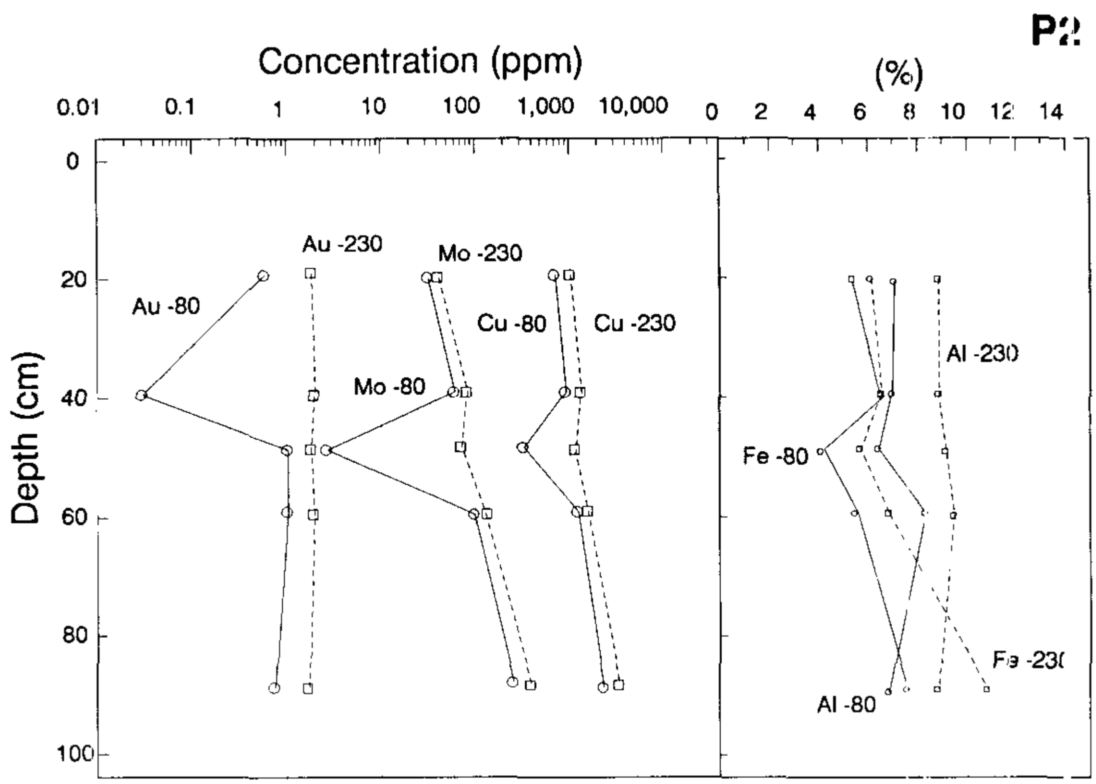
P2
Concentration (ppm)
(%)
Depth (cm)
Au -230
Mo -230
Au -80
Cu -80
Cu -230
Mo -80
Al -230
Fe -80
Fe -230
Al -80

(b)

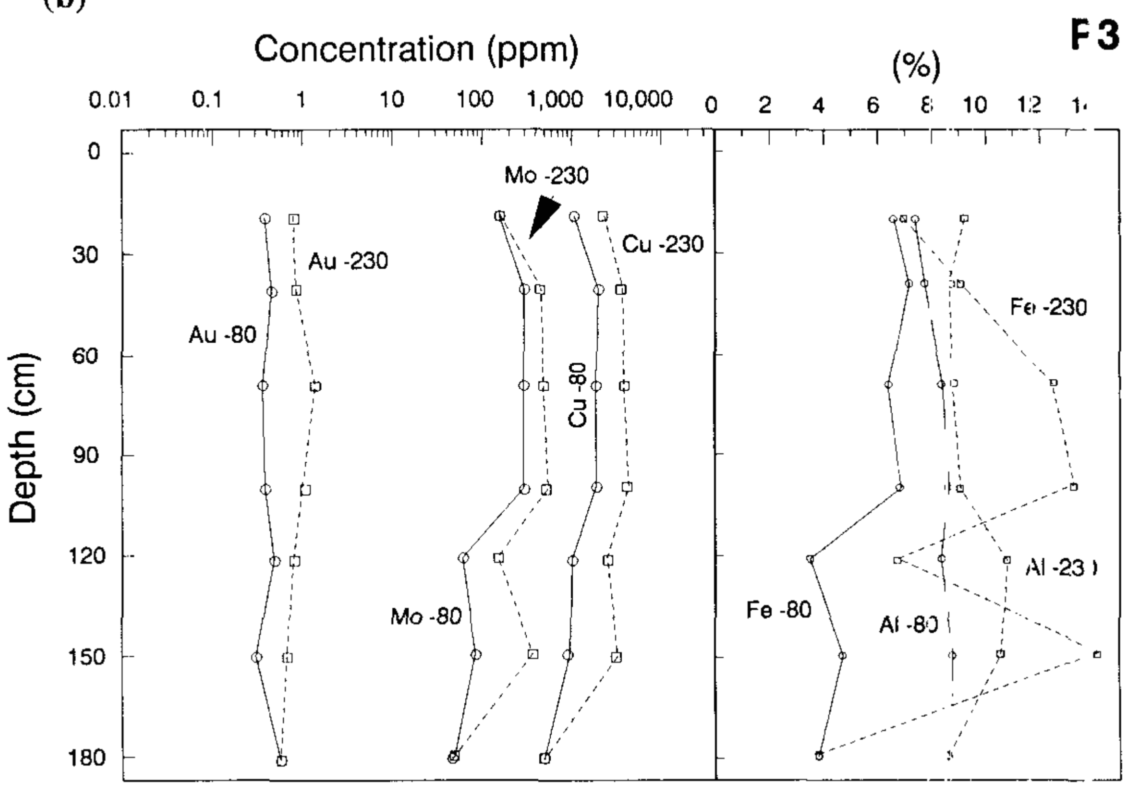
P3
Concentration (ppm)
(%)
Depth (cm)
Mo -230
Cu -230
Au -230
Fe -230
Au -80
Cu -80
Al -230
Mo -80
Fe -80
Al -80

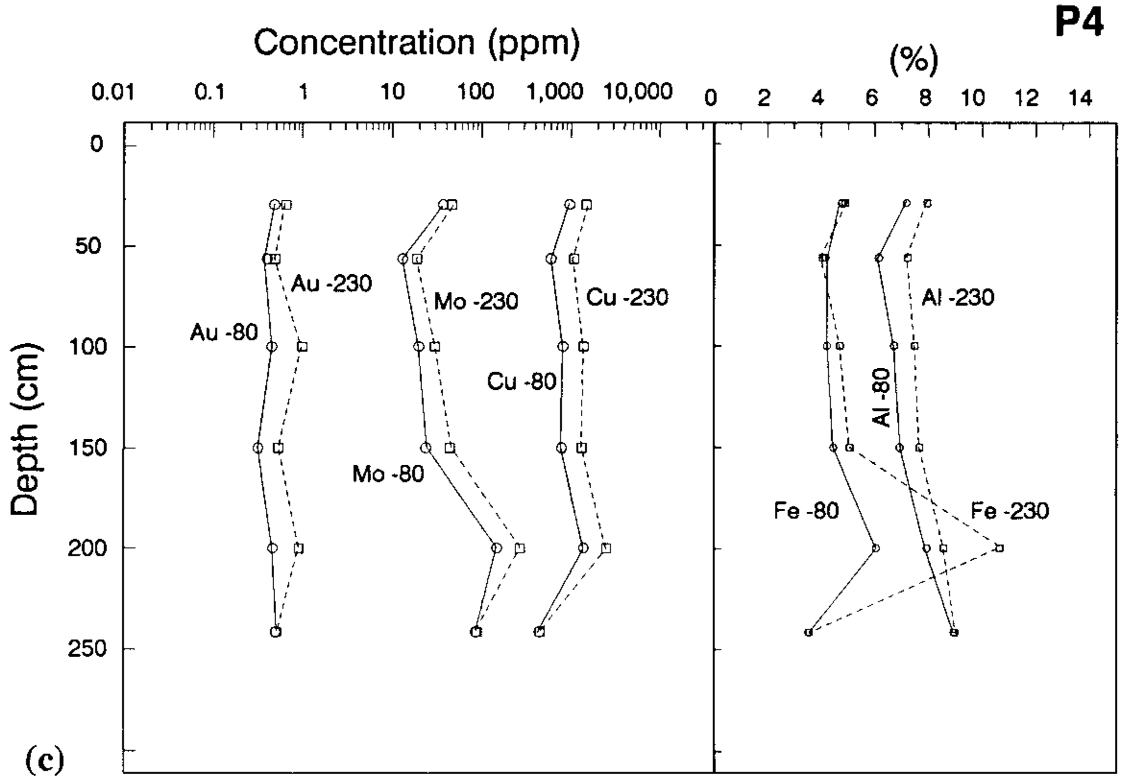

probably present as native copper, chalcocite, malachite or adsorbed onto clays and iron oxides. Hydromorphic transport has increased the copper content of soils over mineralized bedrock at the Kemess South deposit. The degree of hydromorphic transport is significantly greater over the supergene enriched zone of the deposit than over the weathered hypogene bedrock.

ACKNOWLEDGMENTS

Advice and assistance in the field were provided by Mike Harris and Brian Bower of El Condor Resources Limited. Sample preparation and analysis was conducted by Joanne Doris, Kathy Colborne and Bish Bhagwanani. Larry Diakow, Paul Matysek and John Newell provided insightful editorial comments.

REFERENCES

Anderson, J.A. (1982): Characteristics of Leached Capping and Techniques of Appraisal; *in* Advances in Geology of the Porphyry Copper Deposits, Titley, S.R., Editor, *The University of Arizona Press*, 560 pages.

Cann, R.M. and Godwin, C.I. (1980): Geology and Age of the Kemess Porphyry Copper-Molybdenum Deposit, North-central British Columbia; *Canadian Institute of Mining and Metallurgy Bulletin*, Volume 73, pages 94-99.

Coffin, D. and Mertens, H. (1988): Assessment Report on the Kemess Creek Property Ron #4 and DU Claims, Omineca Mining Division; *B.C. Ministry of Energy, Mines and Petroleum Resources*, Assessment Report 16852, 75 pages.

Fletcher, W.K. (1981): Analytical Methods in Geochemical Prospecting; Handbook of Exploration Geochemistry, Volume 1, Govett, G.V.S., Editor, *Elsevier*, 255 pages.

Holland, S.S. (1976): Landforms of British Columbia; *B.C. Ministry of Energy, Mines and Petroleum Resources*, Bulletin 48, 139 pages.

Lord, C.S. (1948): McConnell Creek Map-area, Cassiar District, British Columbia; *Geological Survey of Canada*, Map 962A.

Ney, C.S., Cathro, R.J., Panteleyev, A. and Rotherham, D.C. (1976): Supergene Copper Mineralization; *in* Porphyry Deposits of the Canadian Cordillera, Sutherland Brown, A., Editor, *Canadian Institute of Mining and Metallurgy*, Special Volume 15, pages 72-79.

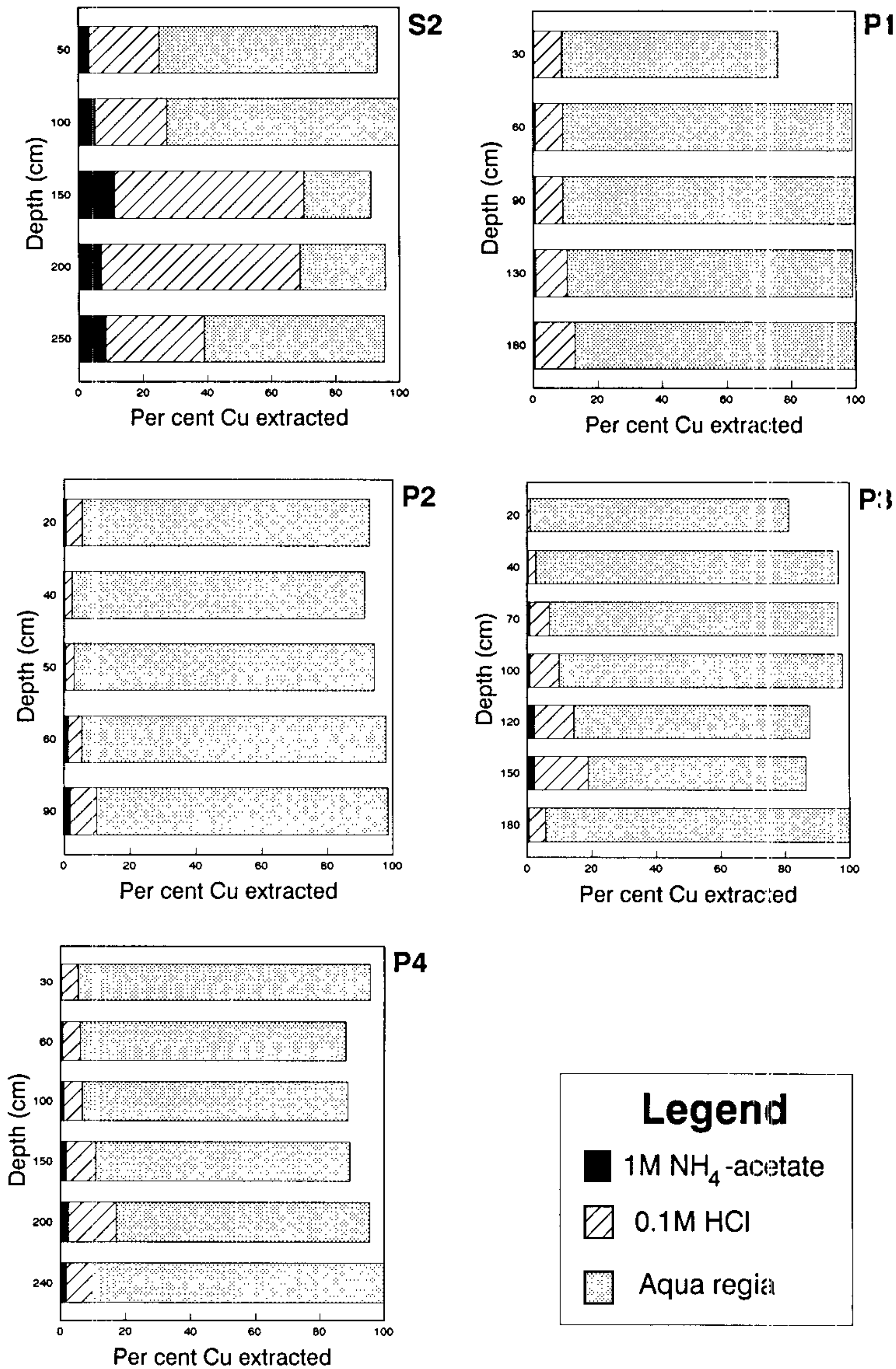

Figure 3-7-6. Plots of partial extraction results with depth, by profile.

NOTES

British Columbia Geological Survey
Geological Fieldwork 1991

QUATERNARY STUDIES IN THE PEACE RIVER DISTRICT, 1990: STRATIGRAPHY, MASS MOVEMENTS AND GLACIATION LIMITS (94P)

By P.T. Bobrowsky and C.P. Smith

KEYWORDS: Surficial geology, Quaternary, Pleistocene, Peace River, sedimentology, stratigraphy, C^{14}, mass movements, landslide dam, debris flows, Halfway River slide, Laurentide erratics, surficial maps.

INTRODUCTION

Quaternary geologic research was undertaken in 1991 in the Peace River region of northeastern British Columbia following reconnaissance studies in 1990 (Figure 3-8-1). The objectives of this work were to:

- Assess the Quaternary economic potential of the area, including aggregate and peat resources, through the production of detailed surficial geological maps (1:50 000 scale) suitable for industry use.
- Provide a practical database (surficial maps) of use to municipal, regional and provincial governments, which will be helpful in future land-use planning.
- Examine the nature of mass movements common to the area, which negatively effect the economic and social well being of the region.
- Contribute to the provincial Quaternary database by detailing the stratigraphic and sedimentologic history of the region.

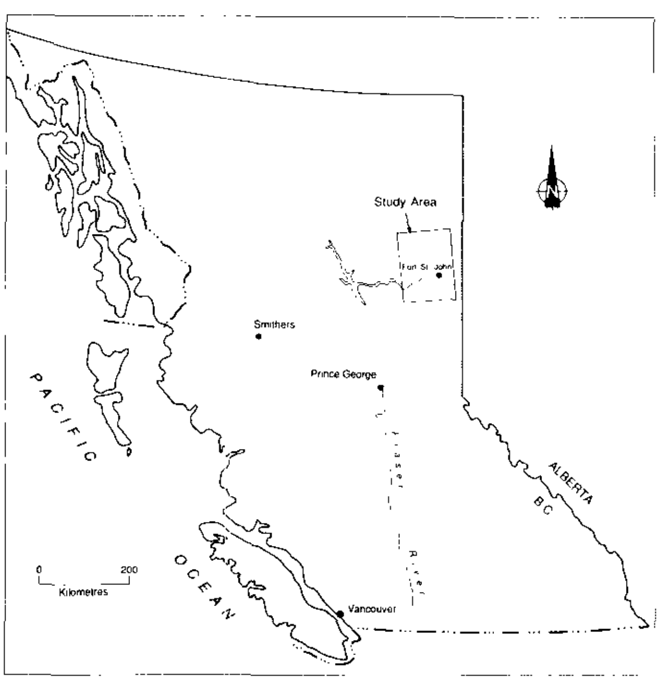

Figure 3-8-1. Surficial geology program, Peace River project study area.

Previous geologic work and surficial map coverage in the Peace River District has been reviewed elsewhere (Bobrowsky *et al.*, 1991 and references therein). With respect to the objectives of the present study Catto (1991, 1992) provides recent surficial coverage of eight map sheets in the area. The distribution and characteristics of surficial materials are discussed at length by the author, as are the economic and land-use implications for future development. A detailed compilation of field studies following completion of laboratory studies will appear in a separate publication. Given the above, the purpose of this paper is to provide preliminary results addressing the latter two project objectives. To meet this goal, brief comment is provided regarding three items:

- Subsurface mapping (stratigraphy and sedimentology).
- The areal distribution of Canadian Shield erratics.
- The morphologic characteristics of two recent mass movements.

STUDY AREA

The general study area encompasses a broad region of northeastern British Columbia which extends from the Rocky Mountain Foothills, at about longitude 122°15'W eastward to the provincial border with Alberta at longitude 120°W, and further delimited to the north at latitude 57°N and the south at latitude 55°N. Specifically stratigraphic studies were restricted to subsurface exposures occurring along the Peace River and its adjoining tributaries including the Beatton, Halfway and Kiskatinaw rivers. Mapping of erratic distribution included subsurface occurrences from stratigraphic studies, but also involved mapping of occurrences on the present land surface easily accessed by road or on foot. Mass movement research was also restricted to river and creek localities. The bedrock geology and physiography of the area has been reviewed previously (Bobrowsky *et al.*, 1991).

METHODOLOGY

Reconnaissance fieldwork during 1990 and extensive work during 1991 resulted in the identification of 77 localities suitable for detailed study. Fieldwork during 1991 consisted of three parts:

- Detailed examination of the stratigraphic and sedimentologic characteristics of subsurface exposures bordering the Peace River and its tributaries.
- Regional mapping documenting the surficial location of Canadian Shield erratics in the district.
- Cursory study of recent and prehistoric mass movements.

Subsurface studies involved examination of exposed sediments including the documentation of deposit characteristics such as elevation, thickness, nature of contacts, vertical and lateral extent, structures, texture, sorting, lithology and pebble fabrics. Sampling consisted of collecting bulk sediment samples (>4 kg) for textural and geochemical analysis and pebble samples for provenance studies, each sample consisting of 100 clasts. Radiocarbon samples ranged from 1.8 to 177 grams, limited in size only by the amount of material available. Both wood and bone were collected. Several samples are still being processed but a number of dates are available (Table 3-8-2). Pebble-fabric measurements consisted of trend and plunge measurements along the a-axis of clasts with a:b:c dimensions approaching 1.5:1:1. The number of clasts measured for fabric study ranged from 25 to 50 per sample.

Mapping of erratic distribution involved documenting the presence of distinct pink granite and granitic gneiss stones which originated on the Canadian Shield. Presence or absence of the diagnostic lithologies in the pebble counts of subsurface studies assisted in this mapping, but the bulk of information was obtained through systematic coverage along roads. Given the large area of examination, this type of survey proved most cost effective.

Mass movement studies were concerned with establishing the timing of the failure event(s). Organic materials were collected for C^{14} dating at exposed failure planes or shear zones for several slides along the river valleys. Detailed measurements for two recent mass-movement deposits were also established.

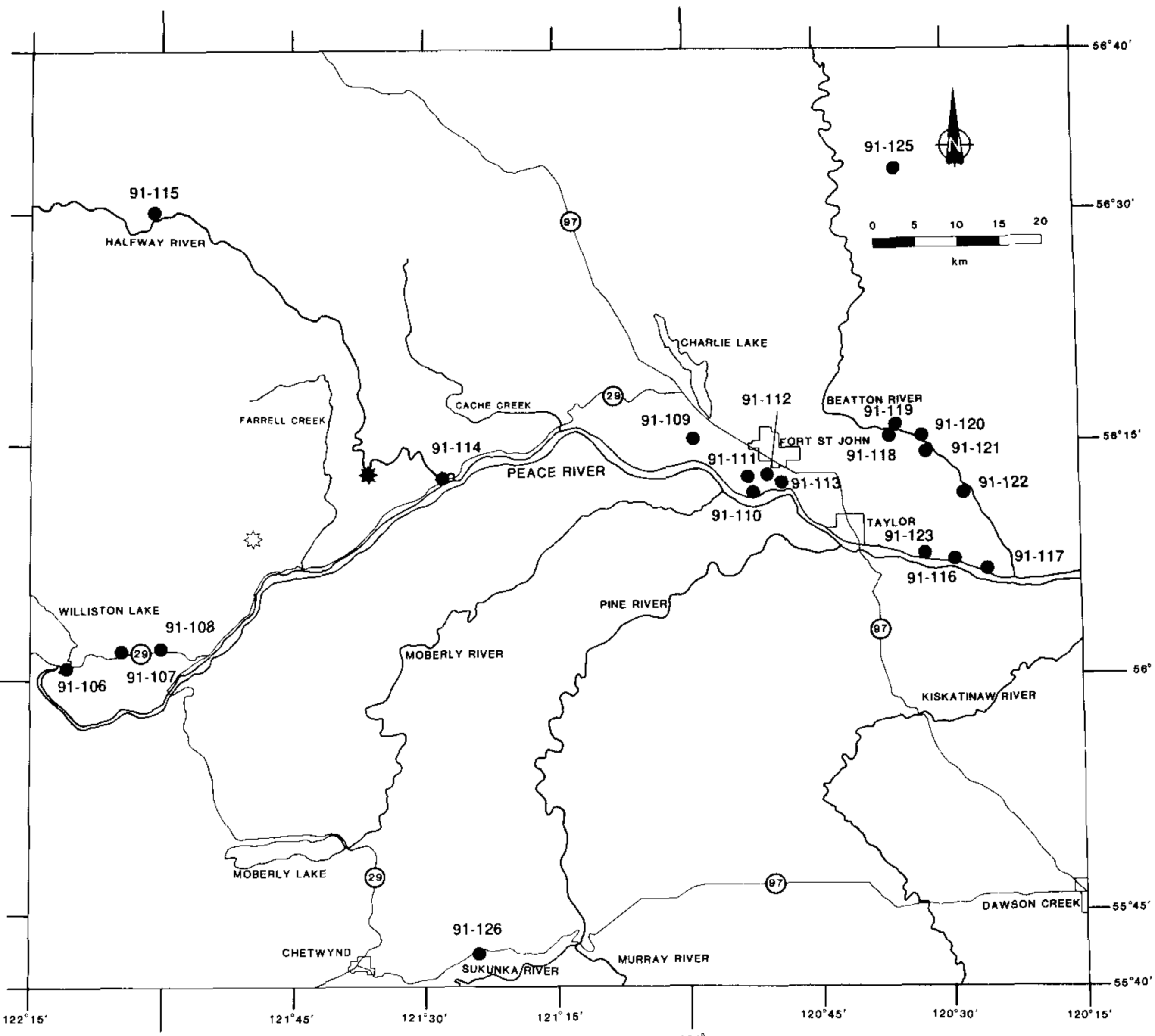

Figure 3-8-2. Location map of 1991 Quaternary localities in the Peace River study area. Coordinates for the sites given in Table 3-8-1. Closed star indicates location of Halfway River slide (PTB90-43) and open star indicates location of mud flow (PTB90-09).

TABLE 3-8-1
LOCATION OF 1991 STUDY SITES IN PEACE RIVER AREA

Locality	Latitude	Longitude	UTM	Elevation	NTS No.
91-106	56°01.0′	122°11.0′	ET 509078	700	94 B/1
91-107	56°01.6′	122°04.2′	ET 580093	738	94 B/1
91-108	56°01.9′	122°01.0′	ET 614099	708	94 B/1
91-109	56°14.9′	120°59.4′	FT 246353	716	94 A/2
91-110	55°11.8′	120°51.5′	FT 328298	487	94 A/2
91-111	55°12.5′	120°51.1′	FT 333311	625	94 A/2
91-112	55°12.8′	120°48.7′	FT 357317	625	94 A/2
91-113	55°12.3′	120°47.7′	FT 368309	625	94 A/2
91-114	55°12.8′	120°28.2′	ET 949307	487	94 A/3
91-115	56°30.4′	122°03.2′	ET 594621	655	94 B/9
91-116	56°07.7′	120°35.2′	FT 502229	403	94 A/2
91-117	56°07.2′	120°28.7′	FT 567221	533	94 A/1
91-118	56°15.7′	120°36.8′	FT 477376	426	94 A/7
91-119	56°15.7′	120°36.4′	FT 482377	419	94 A/7
91-120	56°15.2′	120°33.4′	FT 513366	426	94 A/7
91-121	56°14.4′	120°31.7′	FT 532352	411	94 A/2
91-122	56°12.1′	120°27.8′	FT 574311	403	94 A/1
91-123	56°08.0′	120°35.4′	FT 498234	533	94 A/2
91-124	56°07.6′	120°04.8′	FT 814238	548	94 A/1
91-125	56°33.0′	120°35.5′	FT 478698	693	94 A/10
91-126	55°42.6′	121°22.0′	FS 025749	722	94 P/11

TABLE 3-8-2
S.G.U. RADIOCARBON DATES IN PEACE RIVER AREA

Locality	Age	Lab. No.	Comments
90-02	10240 ± 160	AECV-1206C	Bone; postglacial gravels
90-04	110 ± 90	AECV-1213C	Wood; along shear zone of slide
90-06	420 ± 140	AECV-1437C	Wood; under diamicton (laboratory considers the sample unreliable and contaminated)
90-12	3400 ± 90	AECV-1204C	Wood/charcoal; paleosol underlies resedimented diamicton
90-47	2660 ± 90	AECV-1214C	Wood; along shear zone of slide
91-116	910 ± 80	AECV-1438C	Wood; 20 cm above shear zone of slide
91-122	830 ± 70	AECV-1439C	Wood; along shear zone of slide

TABLE 3-8-3
SUMMARY STATISTICS FOR THREE-DIMENSIONAL PEBBLE-FABRIC ANALYSIS

Fabric	Trend	Plunge	S1	S2	S3	N
PTB90-06	116.4°	13.1°	0.6986	0.1857	0.1157	50
PTB90-09A	286.0°	00.1°	0.7895	0.1804	0.0301	30
PTB90-09B	245.5°	02.9°	0.8579	0.0967	0.0454	25
PTB90-10	098.2°	05.7°	0.5001	0.3610	0.1389	50
PTB90-15	325.8°	18.9°	0.6489	0.2775	0.0736	50
PTB90-18	273.6°	04.3°	0.8552	0.1018	0.0429	25
PTB90-26	339.7°	03.7°	0.9024	0.0615	0.0361	50
PTB90-28A	355.7°	00.18	0.8015	0.1127	0.0858	50
PTB90-28B	027.8°	09.6°	0.6587	0.2709	0.0704	50
PTB90-37A	082.7°	01.4°	0.8907	0.0696	0.0397	50
PTB90-37B	222.5°	08.4°	0.8845	0.0876	0.0279	20
PTB90-37C	029.6°	02.1°	0.8141	0.1276	0.0583	25
PTB91-111	315.8°	29.4°	0.8675	0.0814	0.0511	50
PTB91-115	083.3°	12.6°	0.7372	0.1752	0.0876	25

STRATIGRAPHIC STUDIES

Twenty-one new localities were examined in addition to the 56 sites noted last year; with site elevations ranging from 403 to 738 metres above mean sea level (Figure 3-8-2). Table 3-8-1 lists the coordinates and elevations of the new sites. A total of 26 diamicton and sand bulk samples obtained from 14 sections are currently being processed for textural characteristics. Additionally, 21 pebble samples (100 clasts each) collected from 16 sections are also undergoing lithologic identification. A total of 14 pebble fabrics were determined on diamictons from 10 sections (Table 3-8-3). Descriptive observation of the various sediments supports the interpretations offered previously regarding the nature of diamicton, gravel, sand and fine (silt and mud) deposits (Bobrowsky *et al.*, 1991). Several examples of structureless, stratified and massive diamictons with interbeds were observed this year. Genesis is interpreted to be variable and case specific ranging from basal till to debris-flow accumulations. Similar variability is evident for the sand and gravel deposits, with diverse examples of massive, stratified, normal and reverse-graded accumulations recorded during 1991. A detailed discussion of the Quaternary stratigraphy and sedimentology of the Peace River District will appear in a separate publication, when analytical results from C^{14}, grain size and lithologic samples are available. Nonetheless, based on existing data, it now appears that for the Quaternary history of the region, the Model II scenario of Bobrowsky *et al.* (1991) is more likely to be the case than Model I (*i.e.*, Mathews 1978, 1980).

ERRATIC DISTRIBUTION

Part of the regional mapping objectives included observations on the areal distribution of diagnostic Laurentide erratics. Mathews (1980) interpreted the distribution of Canadian Shield granites in terms of the maximum extent of Late Wisconsinan Laurentide ice advance. Within our study area, Mathews' estimated western limit parallels the Alaska Highway in the north, extends about 17 kilometres west of Fort St. John in the central region and trends south some 30 kilometres west of Dawson Creek (Figure 3-8-3). Since this early work, access to remote areas has improved, allowing better coverage for distributional studies of erratics. As a result of this improved access, the western limit of Canadian Shield granites and gneisses now occurs at 56°30′N and 122°14′W in the north and 55°42′N and 121°12′W in the southern parts of the study area. The interpolated maximum limit therefore extends from the Wagner Ranch at the confluence of the Halfway and Graham rivers, continues southward to Hudson Hope and then bends slightly southeastward to approximately 30 kilometres east of Chetwynd. The newly proposed limit extends the previous estimate westward by about 60 kilometres.

MASS MOVEMENTS

Quaternary sediments in British Columbia are very prone to mass movement phenomena. Since 1856, processes including debris torrents, natural damming from landslides, piping-related subsidence, soil creep, slumping and many others are considered to have been directly and indirectly responsible for about 365 deaths and costs exceeding $500 million in Canada alone (Evans, 1989). One of the most historically active mass movement areas in this province, which is dominated by Quaternary sediments, is the Peace River District. Indeed, one study documented 212 sizable prehistoric slides occurring within unconsolidated sediments of the Peace River valley between Hudson Hope and the Alberta border (Thurber Consultants Ltd., 1976). The two end-members of the mass movement continuum are discussed in this paper in relation to the Peace River; namely, a large but rare landslide damming event and a small mud flow event.

Landslides which result in temporary or permanent damming of rivers have been documented in several areas in British Columbia. The earliest Canadian Cordillera event recorded, occurred on October 14, 1880 at about 2100 hours, when a landslide (volume = 15×10^6 m^3) south of Ashcroft blocked the Thompson River for about 44 hours (Evans, 1984). The cause of the slide appears to have been irrigation practices. On May 26, 1973, a landslide occurred on the south bank of the Peace River, directly west of the village of Attachie, some 60 kilometres west of Fort St. John. Between 11 and 17 million cubic metres of material failed along a 750-metre length of slope and temporarily dammed the Peace River for about 12 hours (Coulter, 1973; Thurber Consultants Ltd., 1981). This rapid debris flow, which lasted about 10 minutes, generated a water wave which ran up the opposite bank approximately 15 metres above river level (Coulter, 1973).

Several failures which have temporarily dammed rivers have occurred in northeastern British Columbia in the last few years. On May 5, 1990, at approximately 2300 hours, a failure occurred at Quintette coal mine (54°59′N; 121°03.5′W) and dammed the Murray River for about 12 hours. Waste rock, till and glaciolacustrine silts totalling

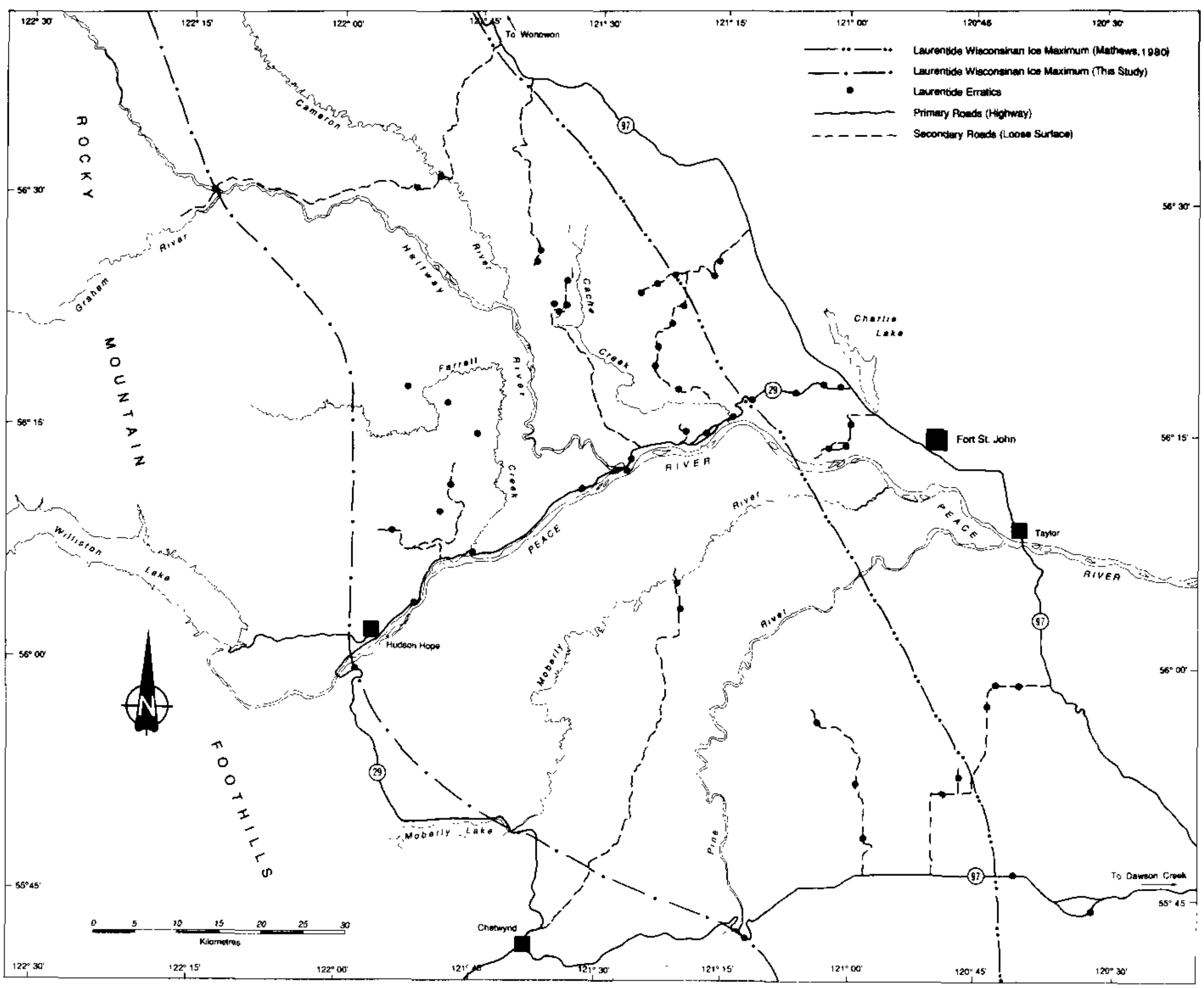

Figure 3-8-3. Map of Laurentide erratic distribution in northeastern British Columbia documented in this study. Note position of previous Laurentide boundary on the east side of the figure, relative to the new position to the west.

2.53 million cubic metres inexplicably failed at the mine dump. About 15 kilometres south of Fort Nelson (58°26'W; 122°52'N), on November 19, 1990 at 0230 hours, an unknown volume of Pleistocene sediments (till and glaciolacustrine silt) failed and dammed the Prophet River for 44.5 hours; apparently as a result of heavy rain. Finally, on August 20, 1989, at about 1500 hours, a landslide occurred on the Halfway River (56°13.4'N; 121°36.1'W) approximately 9.5 kilometres northeast of the Attachie slide. About 1.88 million cubic metres of unconsolidated material temporarily dammed the river for 6 hours (Plate 3-8-1). Details of this latter event are described below.

Heavy rainstorms, intense cloudbursts and concomitant runoff events often generate localized mass movements in steep and channelized terrain. The most significant type of movement consists of water-charged slurries of debris called debris torrents (~debris flows, mud flows, debris avalanches), but less significant variations including sediment-laden water floods and slumps can also occur. In North America, the average number of deaths due to mass movements is about 25 per year (Skermer, 1984). In western Canada, the impact of these common, small-scale events varies from negligible to devastating. For example, in British Columbia, rainstorms in early July, 1983, triggered 14 debris torrents between Hope and Chilliwack that severed transportation for 3 days (Evans and Lister, 1984). One estimate of debris torrent damage for western Canada places the death toll at 17 and the damage costs in excess of $100 million for the period 1962 to 1984 (VanDine, 1985).

HALFWAY RIVER SLIDE

At approximately 1500 hours, on August 20, 1989, some 5.5 kilometres north of Highway 29, Pleistocene terrace sediments on the south side of the Halfway River catastrophically failed (Figure 3-8-2, Plate 3-8-1). The resultant debris flow of about 1.88 million cubic metres temporarily dammed the river for up to 6 hours, at which point overtopping of the dam was followed by breaching. The area of the river dammed by sediment measures approximately 100 by 440 metres. During the period of damming, the course of the Halfway was diverted northward across the vegetated floodplain and point bar on the opposite side of the river. The event can be considered a Type I landslide dam of Costa and Schuster (1988). The affected area of the flow is described in relation to three zones: an upper failure zone; a middle transitional zone; and a lower accumulation zone (Figure 3-8-4).

The slide motion originated on the first and second Pleistocene terrace surfaces some 275 metres south of the former shoreline. The back scarp of the upper failure zone is 330 metres from the lower terrace edge (line A of Figure 3-8-5), 690 metres from the present river shoreline and at an elevation of 65 metres above river level (Plate 3-8-2). The depth of the upper displaced mass averages 12 metres, whereas the width is about 270 metres (line B, Figure 3-8-5). The basal shear zone of the displacement coincides with Wisconsinan glacial diamicton which overlies Cretaceous silty shales of the Shaftesbury and/or Gates forma-

Plate 3-8-1. Aerial view to south of Halfway River landslide. Photograph taken August 21, 1989 one day after the failure. Note the volume and lateral extent of debris still blocking normal river flow. (Photo courtesy of D. Lister. MoTH).

tions. A considerable portion of the remobilized sediment remains in the upper failure zone, providing local relief up to 6 metres in height. A second debris mass originated at the south end of the transitional zone (275 metres from the water; Plate 3-8-3). The back scarp of the second failure (transitional zone) follows the edge of the lower Pleistocene terrace along a surface which is 320 metres long and 20 metres high (Figure 3-8-5). Sediment in the transitional zone consists of glaciolacustrine silt and clay and silt-rich diamicton derived from the upper terraces. A series of deep gullies and secondary failure scarps characterize the topographic surface in this zone. Relief reaches 8 metres over the disturbed topography. Several trees survived destruction during the sediment gravity-flow process, resulting in a vegetated medial ridge running parallel to the flow axis (Plate 3-8-3). The broad fan-shaped accumulation zone originally covered an area measuring 190 by

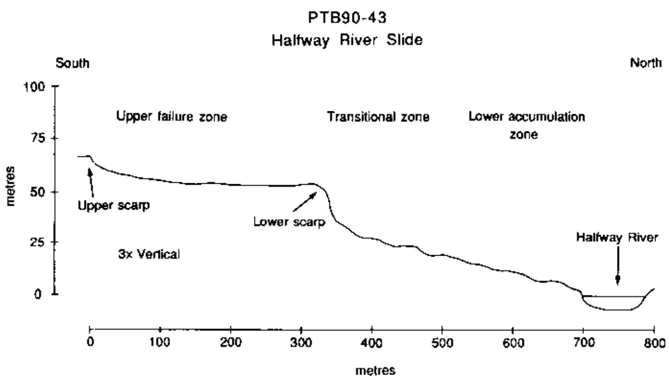

Figure 3-8-4. Longitudinal cross-section of locality PTB90-43 (Halfway River slide); failure occurred at 1500 hours on August 20, 1989. Mass movement is schematically divided into three parts: upper failure zone, transitional zone and lower accumulation zone.

385 metres before fluvial erosion reclaimed much of the river's original course (lines E and F, Figure 3-8-5). The toe of the debris flow now forms a steep and actively calving front some 7 metres above the water surface (Plate 3-8-4). A series of overlapping debris-flow noses along the margin of the accumulation zone provide a stacked terrace-like morphology to the failure.

We are unable to confirm the history of events preceding the failure, but the long-term triggering mechanism for slope failure proposed for the Attachie slide (*cf.* Thurber Consultants Ltd., 1981) warrants attention as a likely analogue to the Halfway River slide. A long history of jointing and cracking in the unconsolidated sediments on the upper terrace preceded the failure. Large and partially vegetated tensional cracks paralleling the terrace edge are evident east of the upper failure zone (Plate 3-8-2). Both attributes (size and vegetation) of the cracks suggest a prolonged period of distress, as well as active accommodation of the sediment to tensile stress. Several syndepositional cracks are further evident within the central basin of the upper failure zone. Prolonged ponding in the pre-failure cracks, water infiltration and eventual saturation of the unconsolidated sediment covering the bedrock apparently reached a critical threshold suitable for the rapid motion to take place on August 20. The precipitation records for the area do not support a rain-induced triggering mechanism as a spontaneous event, however, the long-term increasing pore-water pressure in the area may have reduced the effective internal shear resistance enough to trigger the failure (Figure 3-8-6). At the point of initial movement, the distressed sediments most likely underwent quick disintegration and began to flow in a fluid-like manner. Although there was no precipitation on the day of the event (Figure 3-8-6), the amount of water draining from the upper terraces (evident in Plate 3-8-1), as well as eyewitness accounts of the event, support the contention that a considerable amount of internal pore water was released from the Quaternary sediments.

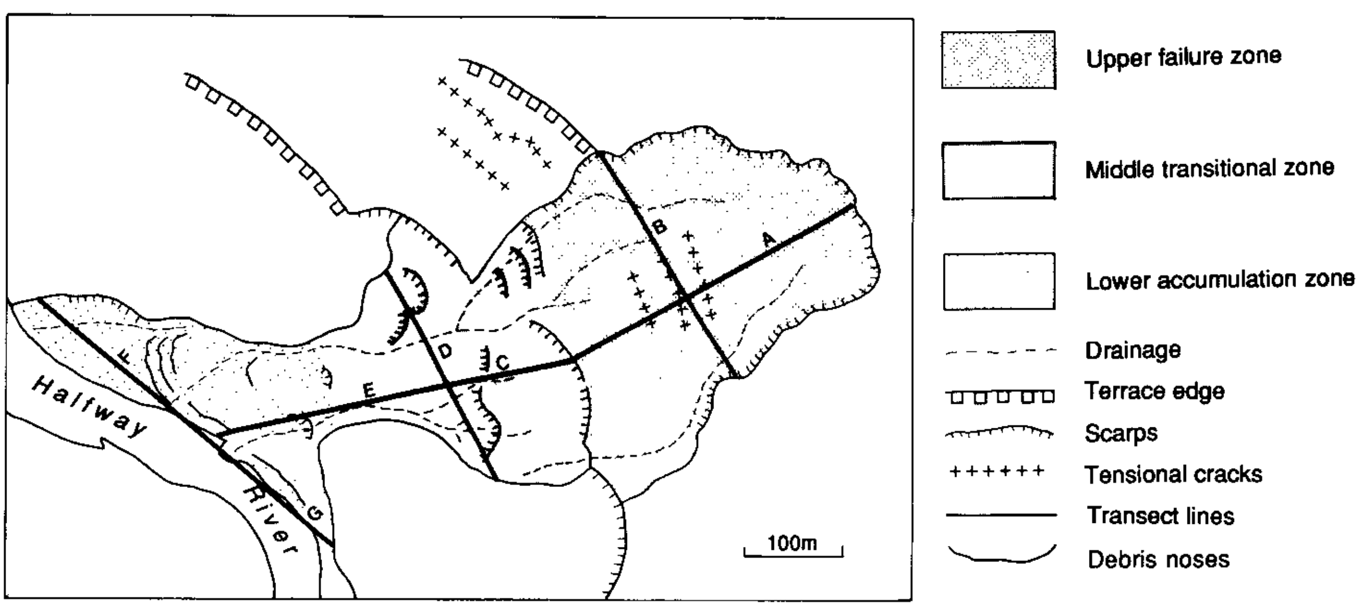

Figure 3-8-5. Plan view figure of Halfway River slide. Compare to series of photostereograms provided.

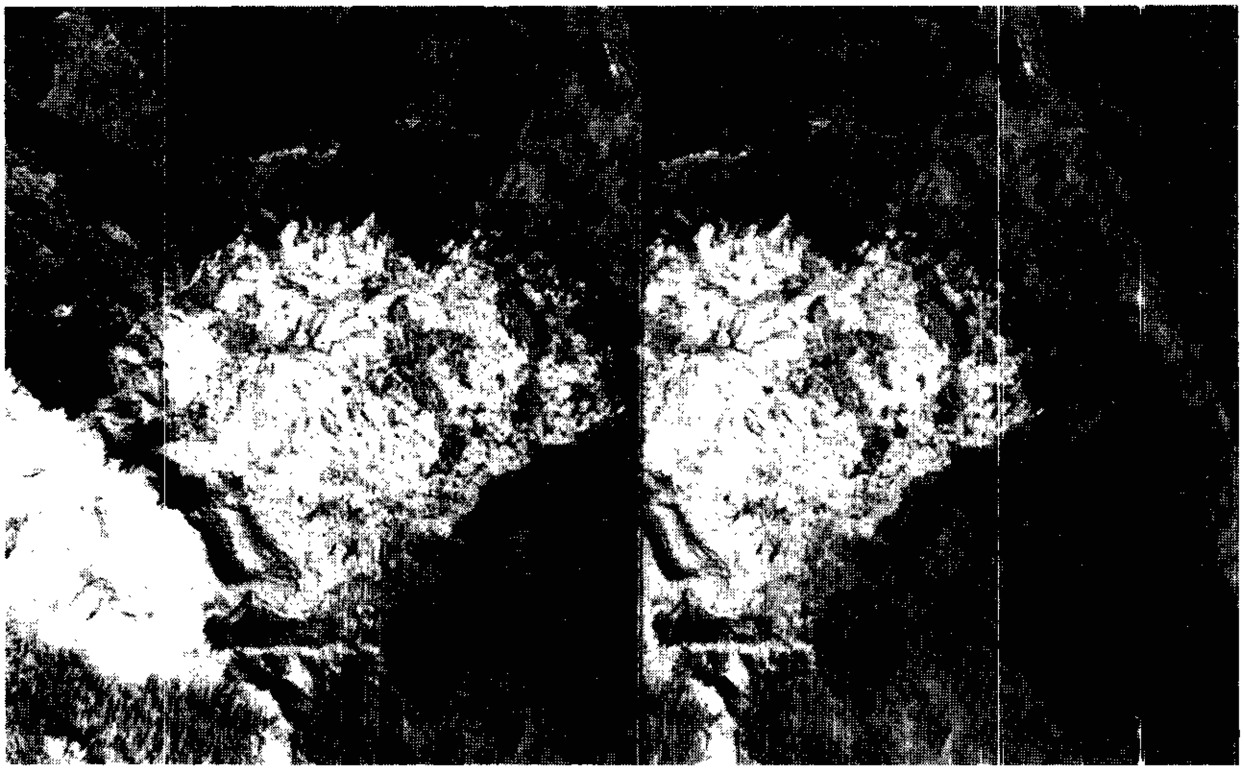

Plate 3-8-2. Photostereogram of the Halfway River slide, northeastern British Columbia. Upper failure zone.
See Figure 3-8-5 for scale and details.

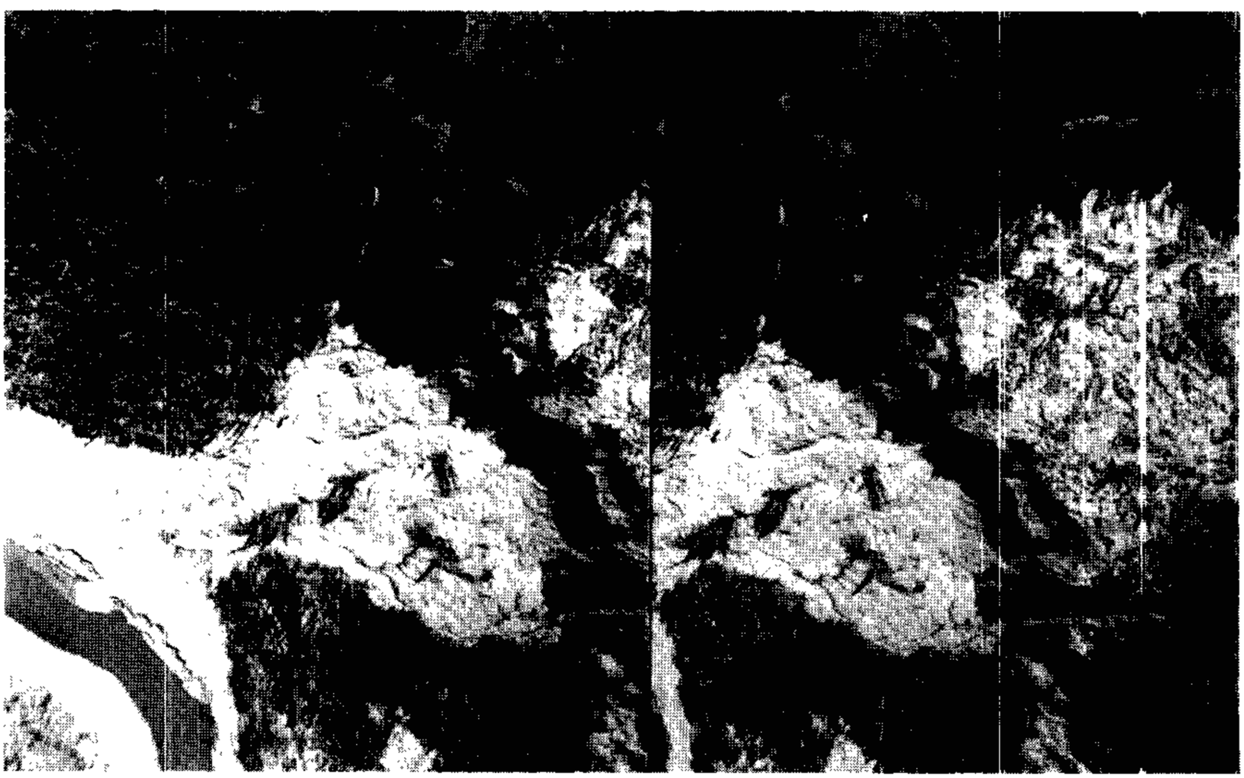

Plate 3-8-3. Photostereogram of the Halfway River slide, northeastern British Columbia. Transitional zone.
See Figure 3-8-5 for scale and details.

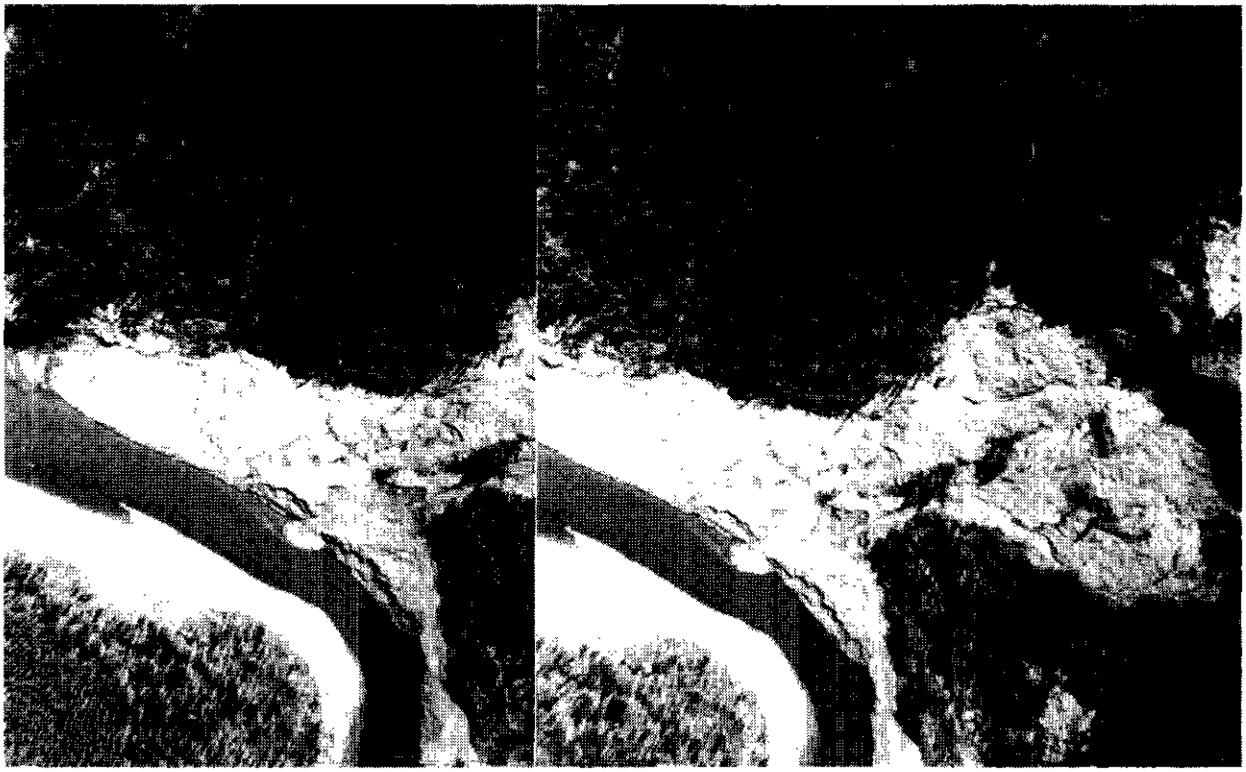

Plate 3-8-4. Photostereogram of the Halfway River slide, northeastern British Columbia. Lower accumulation zone. See Figure 3-8-5 for scale and details.

Plate 3-8-5. View down slope from end of elevated conduit gully toward nick point and amphitheatre feature.

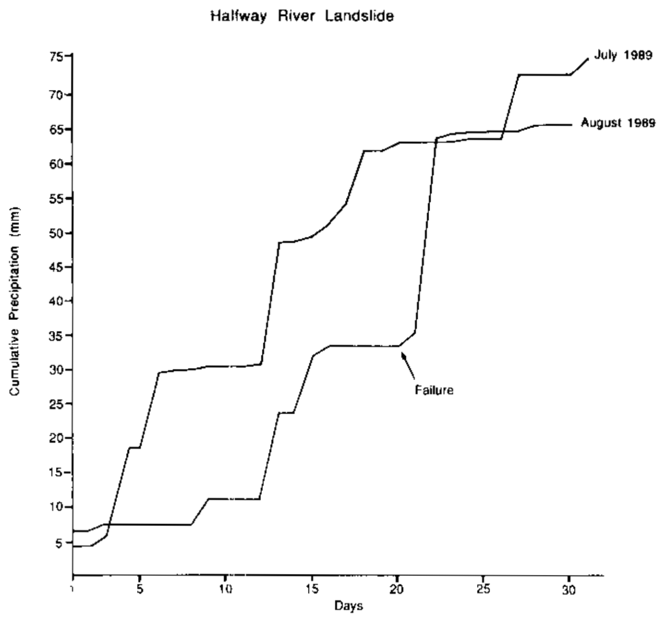

Figure 3-8-6. Precipitation record for the period preceding the Halfway River slide in northeastern B.C.

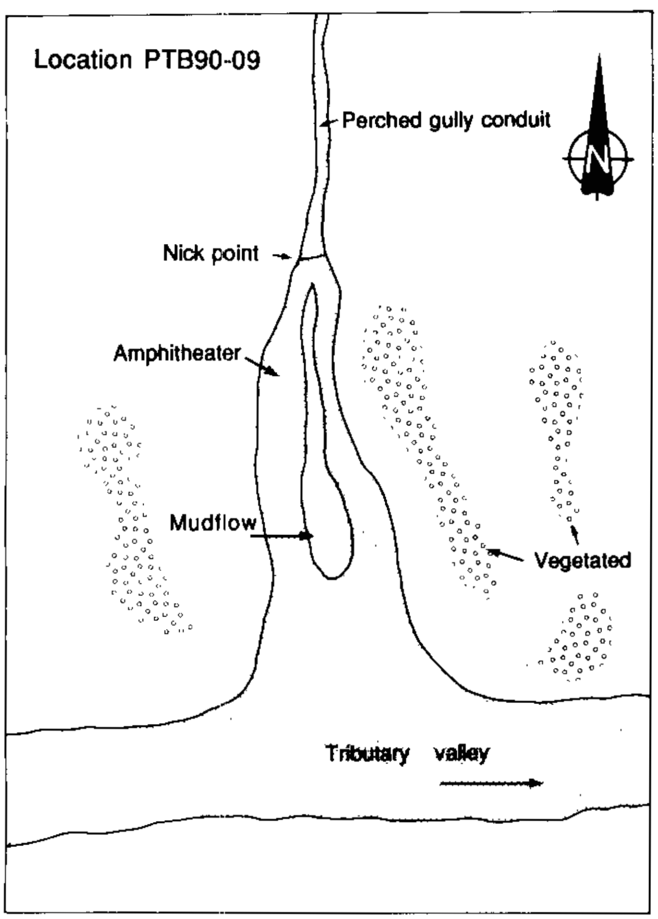

Figure 3-8-7. Conceptual plan view of locality PTB90-09 described in detail by Bobrowsky *et al.* (1991). Note location of (a) elevated conduit gully, (b) amphitheatre and (c) main tributary.

Mud Flow

On the evening of July 4, 1991, during a local rainstorm depositing 3.8 millimetres of precipitation, a small mud flow was deposited in a gully of a tributary valley containing a well-exposed stratigraphic section (Section PTB90-09 described in Bobrowsky *et al.*, 1991; Figure 3-8-7). The precipitation record for the area indicates that rainfall for that day, as well as for the preceding weeks, was essentially average for the time of year. Meteorological conditions often cited as generating debris flows can be discounted; instead, sediment disturbance by us during mapping is a more likely antecedent cause of this event which was finally triggered by the local rainstorm.

The geomorphology of the site consists of a gully 3 metres deep (A) which borders an open field on an upper terrace adjacent to a main tributary valley (C) Figure 3-8-7; Plate 3-8-5). The elevated gully (A) serves as a water conduit to a small amphitheatre-like erosional feature (B) which "represents the adjustment of the landscape to recurrent intervals of erosion by running water and slope failure" (Eisbacher and Clague, 1984:15). The elevated gully intersects the amphitheatre at a nick point 2 metres above the highest point of the sloped surface (Figure 3-8-8). The amphitheatre has a horizontal length of 55 metres and a height of 27.2 metres in relation to the main tributary valley (Figure 3-8-8).

A mud-flow scar and deposit occur within the amphitheatre feature. The plug-nose of the deposit is up to 1.5 metres thick and 4.5 metres wide (Plate 3-8-6). The outer edge of the plug is not well defined as the deposit actually continues down-slope to a lower sediment dump of lighter and finer grained material, but an approximate limit is 55 metres from the edge of the nick point. Debris in the plug consists of small to medium-sized angular blocks of hardened mud, a few fragments of which are over 1 metre in maximum dimension. These blocks represent sheared and fragmented pieces of the adjoining chute-channel walls. Their emergence at the surface of the flow is probably a result of intergranular dispersive forces, buoyancy of larger fragments and forward push of debris from behind (*cf.* Eisbacher and Clague, 1984). The up-slope end of the plug gradually grades into a tail feature which extends almost up to the amphitheatre edge at the base of the nick point (Plate 3-8-7). This proximal sediment accumulation consists mainly of large pebble to cobble-sized clast. Most of the clasts are remnants of the flow which lagged behind as the channel-flow forces diminished. Additional washing by rain further winnowed the fine sediments from this pebble-cobble lag. Lateral margins of the chute are defined by a levee, which represents the zone of laminar flow and sediment spill-over (Plate 3-8-8). The debris levees range in thickness from less than 5 centimetres to 70 centimetres. From crest to crest, the chute width averages 3.1 metres, whereas the depth ranges from 0.30 to 1.60 metres, averaging about 1.2 metres.

Much of the original sediment is derived from the bank walls of the conduit gully directly above the nick point (Plate 3-8-5). During the course of our work in the days preceding the mud flow event, our mapping of the section had severely lessened the sediment strength and integrity of

Plate 3-8-6. View up slope of mud-flow nose. Pick for scale is 65 centimetres long. Note angular nature and size of debris blocks. Note also marginal undercutting of slope on right side of photo (arrow).

Plate 3-8-7. View up slope of mud-flow channel scar. Arrow points to horizontal scale which is 3.1 metres in length. Note relation of marginal levee, slickensided surface and central washed-pebble lag deposit.

the gully walls. The precipitation on July 4 was sufficient to trigger sediment avalanching of the walls into the gully. The debris must have then cascaded over the nick point and was rafted down-slope for an additional 55 metres.

IMPLICATIONS

Stratigraphic and sedimentologic results which tend to support the Model II scenario of Bobrowsky *et al.* (1991) can be briefly viewed in relation to the extended erratic distribution data. The earliest glacial deposits in the region are clearly of Montane or Cordilleran origin, whereas the second glacial event has often been considered to be of both western and eastern ice provenance. However, the westward extension of the Laurentide ice maximum to the margin of the foothills discounts the possibility of ice coalescence near Fort St. John.

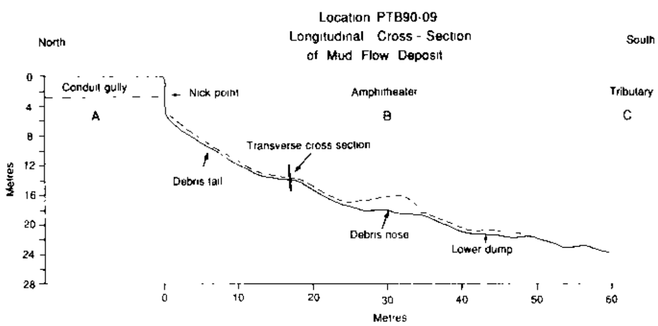

Figure 3-8-8. Longitudinal cross-section of PTB90-09 and mud flow deposited in the afternoon of July 4, 1991.

Throughout the Holocene, including today, the Peace River District has proven to be the centre of a variety of mass movement phenomena. Many of these events were and continue to be either threatening or costly. The large mass movement on the Halfway River which temporarily dammed the flow of water could have been disastrous under different circumstances. Rainfall historically proves to be a prime impetus for triggering slope failures (*cf.* Church and Miles, 1987; Evans and Clague, 1989). Long-term water accumulation appears to be a good explanation for the Halfway River slide. Precipitation for August, 1989 (Halfway River slide) was 64.9 millimetres which is over twice the 22.9 millimetre total for May, 1973 (Attachie slide). Neither month-end precipitation total reflects heavy rain.

Intensified study of the unstable slopes, failed slopes and slide deposits should be undertaken in the Peace region. For example, the slope movement adjacent to the Attachie slide currently ranges from 28 to 82 millimetres per year (D.R. Lister, personal communication, 1987). Although not exceptional (Big Slide near Quesnel has movement rates as high as 271 millimetres per year), this ongoing movement illustrates the continued threat that is posed by the immature landscape that typifies the Peace District. A number of measures can be adopted to assess and respond to mass movement threats (*cf.* Hungr *et al.*, 1987). Unfortunately, only a few of these measures are being actively pursued in the region. Continued geologic research is warranted.

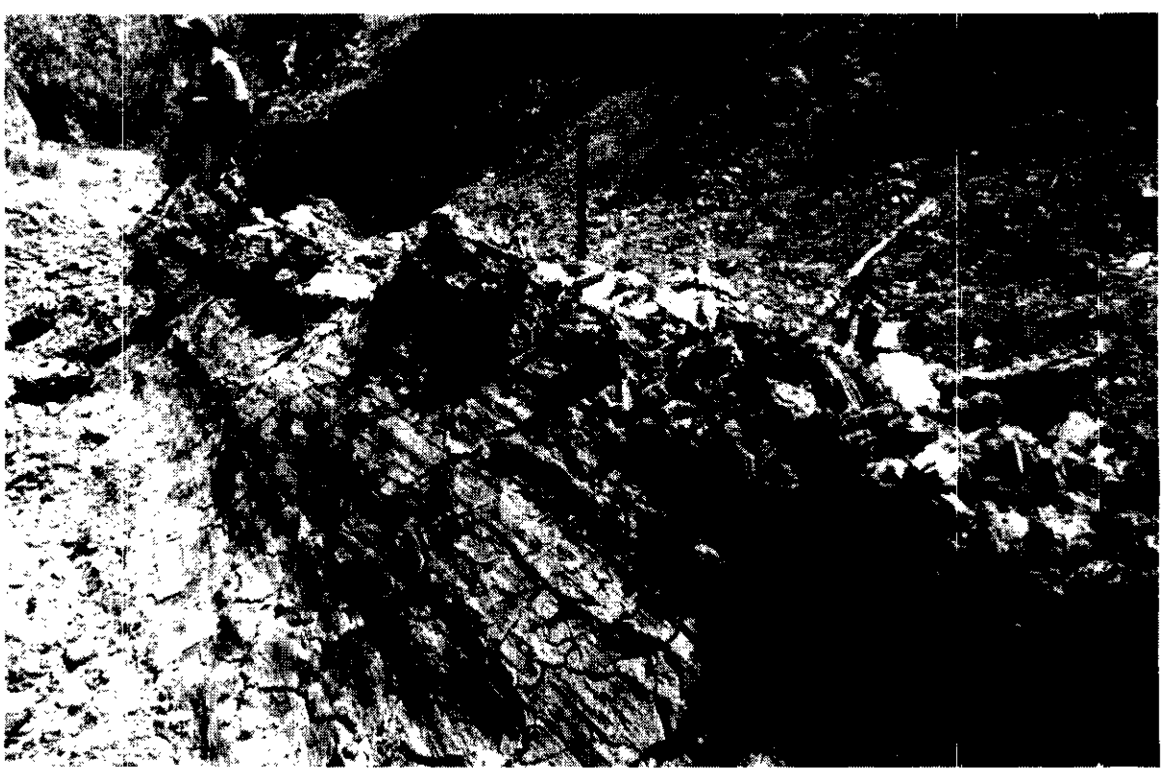

Plate 3-8-8. View down slope of mud-flow scar and deposit at locality PTB90-09. Note slickensided channel wall and prominent levee.

ACKNOWLEDGMENTS

We appreciate the assistance of Mr. Len Eklund for his jet-boat services in helping us access the Halfway River slide. Mr. K. Walde led us to several useful fossil localities. Don Lister and Doug VanDine provided data on the Attachie slide. Mr. J. Stalker and Mr. R. Sauvlet provided useful data on other large landslide dams in the region. Art Roberts provided air support for the Halfway River slide study. Steve Sibbick and John Newell provided useful editorial comments on the manuscript. B.C. Hydro provided access to several field locations as well as unpublished data.

REFERENCES

Bobrowsky, P.T., Catto, N.R. and Levson, V. (1991): Reconnaissance Quaternary Geological Investigations in Peace River District, British Columbia (93P, 94A); *in* Geological Fieldwork 1990, *B.C. Ministry of Energy, Mines and Petroleum Resources,* Paper 1991-1, pages 345-358.

Catto, N.R. (1991): Quaternary Geology and Landforms of the Eastern Peace River Region, British Columbia, NTS 94A/1, 2, 7, 8; *B.C. Ministry of Energy, Mines and Petroleum Resources,* Open File 1991-11, 19 pages.

Catto, N.R. (1992): Quaternary Geology and Landforms of the Eastern Peace River Region, British Columbia, NTS 93P/9, 10, 15, 16; *B.C. Ministry of Energy, Mines and Petroleum Resources,* Open File, in press.

Church, M. and Miles, M.J. (1987): Meteorological Antecedents to Debris Flow in Southwestern British Columbia; Some Case Studies; *in* Debris Flows/Avalanches: Process, Recognition and Mitigation, Costa, J.E. and Wieczorek, G.F., Editors; *Geological Society of America, Reviews in Engineering Geology,* Volume VII, pages 63-79.

Costa, J.E. and Schuster, R.L. (1988): The Formation and Failure of Natural Dams; *Geological Society of America Bulletin,* Volume 100, pages 1054-1068.

Coulter, T.S. (1973): Report on the Stability of the South Bank of the Peace River near Halfway River (Attachie Slide); unpublished report, *B.C. Ministry of Transportation and Highways,* 8 pages.

Eisbacher, G.H. and Clague, J.J. (1984): Destructive Mass Movements in High Mountains: Hazard and Management; *Geological Survey of Canada,* Paper 84-16, 230 pages.

Evans, S.G. (1984): The 1880 Landslide Dam on Thompson River, near Ashcroft, British Columbia; *in* Current Research, Part A, *Geological Survey of Canada,* Paper 84-1A, pages 655-658.

Evans, S.G. (1989): Landslides and Related Processes in the Canadian Cordillera; *Landslide News,* June, Number 3, pages 3-6.

Evans, S.G. and Clague, J.J. (1989): Rain-induced Landslides in the Canadian Cordillera, July 1988; *Geoscience Canada,* Volume 16, pages 193-200.

Evans, S.G. and Lister, D.R. (1984): The Geomorphic Effects of the July 1983 Rainstorms in the Southern Cordillera and their Impact on Transportation Facilities; *in* Current Research, Part B, *Geological Survey of Canada,* Paper 84-1B, pages 223-235.

Hungr, O., Morgan, G.C., VanDine, D.F. and Lister, D.R. (1987): Debris Flow Defenses in British Columbia; *in* Debris Flows/Avalanches: Process, Recognition and Mitigation, Costa, J.E. and Wieczorek, G.F., Editors; *Geological Society of America, Reviews in Engineering Geology,* Volume VII, pages 201-222.

Mathews, W.H. (1978): Quaternary Stratigraphy and Geomorphology of Charlie Lake (94A) Map-area, British Columbia; *Geological Survey of Canada,* Paper 76-20, 25 pages, includes Map 1460A.

Mathews, W.H. (1980): Retreat of the Last Ice Sheets in Northeastern British Columbia and Adjacent Alberta; *Geological Survey of Canada,* Bulletin 331, 22 pages.

Skermer, N.A. (1984): M Creek Debris Flow Disaster; *Ontario Hydro Landslide Symposium,* pages 187-194.

Thurber Consultants Ltd. (1976): Site C and E Lower Peace River and Tributaries, Shoreline Assessment; unpublished report, *B.C. Hydro and Power Authority,* File No. 15-2-37A, 53 pages.

Thurber Consultants Ltd. (1981): Site C Reservoir, A Report on Field Inspection of Overburden Landslides; unpublished report, *B.C. Hydro and Power Authority,* File No. 15-2-169A, 15 pages.

VanDine, D.F. (1985): Debris Flows and Debris Torrents in the Southern Canadian Cordillera; *Canadian Geotechnical Journal,* Volume 22, pages 44-68.

British Columbia Geological Survey
Geological Fieldwork 1991

QUATERNARY GEOLOGY OF THE ATLIN AREA (104N/11W, 12E)

By V. M. Levson

KEYWORDS: Economic geology, surficial geology, Atlin, placer gold, stratigraphy, auriferous gravels, exploration.

INTRODUCTION

This paper reports on the preliminary results of an investigation of the Quaternary and placer geology of the Atlin mining district in northwest British Columbia. The area was selected for study because it supports the second largest placer mining industry in the province and has a long history of placer gold production. In addition, dwindling reserves in recent years have resulted in the shutdown of major mining operations such as the Queenstake mines on Spruce and Pine creeks. The Atlin area also offers good exposure of Pleistocene gold-bearing strata as well as dating control provided by interbedded basalts. Gold production from the district, recorded for the 50 year period after discovery in 1897, was approximately 20 000 kilograms (Holland,1950). The locations of active mechanized mining and exploration projects are shown in Figure 3-9-1.

PREVIOUS WORK

Early reports on the geology of the Atlin area were provided by Gwillim (1901, 1902). The placer geology of the region was investigated by Black (1953) and Proudlock and Proudlock (1976). Debicki (1984) provided an overview of the placer mining industry in the region. The Quaternary history of the Fourth of July Creek valley just north of the map area was investigated by Tallman (1975). Anderson (1970) constructed a geobotanical chronology of the Atlin area covering the last 11 000 years. Lacelle (1985) investigated the surficial geology of the shoreline region of Atlin Lake in the vicinity of Atlin townsite and produced a terrain materials map of the Atlin 1:250 000 NTS mapsheet (Lacelle, 1989). The bedrock geology was initially mapped by Aitken (1959) and Monger (1975). Regional bedrock maps were compiled by Lefebure and Gunning (1989), Bloodgood *et al.* (1989a and 1990) and Ash and Arksey (1990a) and discussed by Ash and Arksey (1990 b, c), Bloodgood and Bellefontaine (1990) and Bloodgood *et al.* (1989b). MacKinnon (1986) completed a mineralogical study of placer concentrates from four mines in the area.

METHODS

Preliminary airphoto interpretation of the surficial geology of NTS mapsheets 104N/11W and 104N/12E was conducted and field checked at 180 sites in conjunction with stratigraphic and sedimentologic studies of gold-bearing Cenozoic deposits in the region. Property visits and geologic descriptions of 16 active and recently active mines offering good section exposure were completed. Sections in the active mines were mapped and lithologic, pebble-fabric and sedimentological studies were conducted. Samples were collected for textural, mineralogical and geochemical analysis. Pollen, basalt and wood samples were also collected at several sites for stratigraphic control. Gold production in each stratigraphic unit was determined, where possible, by discussions with miners. Heavy mineral concentrates were collected from gold-bearing lithofacies within a number of stratigraphic units in the Spruce Creek area, using a small test sluice, and from commercial operations at several other sites.

SURFICIAL GEOLOGY

BEDROCK AND COLLUVIAL DEPOSITS

A generalized surficial geology map of the area is given in Figure 3-9-1. Mountain areas, typically but not exclusively above 1500 metres elevation, are characterized by a thin colluvial veneer with about 30 per cent bedrock exposure, mainly on steep slopes. Bedrock outcrops comprise up to 70 per cent of the mountainous areas on the east shore of Atlin Lake and the northeast shore of Surprise Lake, and up to 50 per cent of the uplands immediately north of Atlin townsite. More gentle slopes at high elevations may have a thin blanket of glacially derived diamicton, resedimented by slope processes after initial deposition.

Many high-elevation areas in the region are subject to rapid mass movements (rock falls and debris flows) and snow avalanches. Noteworthy is a large landslide deposit that extends from the east side of Ruby Mountain across the Ruby Creek valley (Plate 3-9-1). Failed materials are mainly Pleistocene vesicular basalts and scoria. Landslide debris typically consists of angular bedrock material ranging in size from sand to large boulders. Some surficial sediments are also incorporated in the slide debris.

Periglacial features such as solifluction lobes, stone stripes (Plate 3-9-2), nivation hollows and cryoturbated soils are common, especially in the northwest part of the map area and to a lesser extent along the high mountains in the south. Talus deposits are common below most bedrock cliffs and rock glaciers occur in some high cirques (Plate 3-9-3).

GLACIAL DEPOSITS

Lower slopes and valley bottoms throughout the area are blanketed by morainal deposits consisting of unsorted, massive diamicton. These glacial diamictons are typically matrix supported with clasts occurring in a mixture of sand, silt and clay. Clasts up to large boulders occur but the modal clast size is in the small to large pebble range. Clasts are of widely varied lithologies and commonly are striated and occasionally faceted. The presence of these glacial abrasion features and erratic lithologies indicates glacial transport. The diamictons are inferred to be tills deposited at the base of over-riding glaciers. They typically have planar erosional lower contacts (Plate 3-9-4) and are very dense. Where

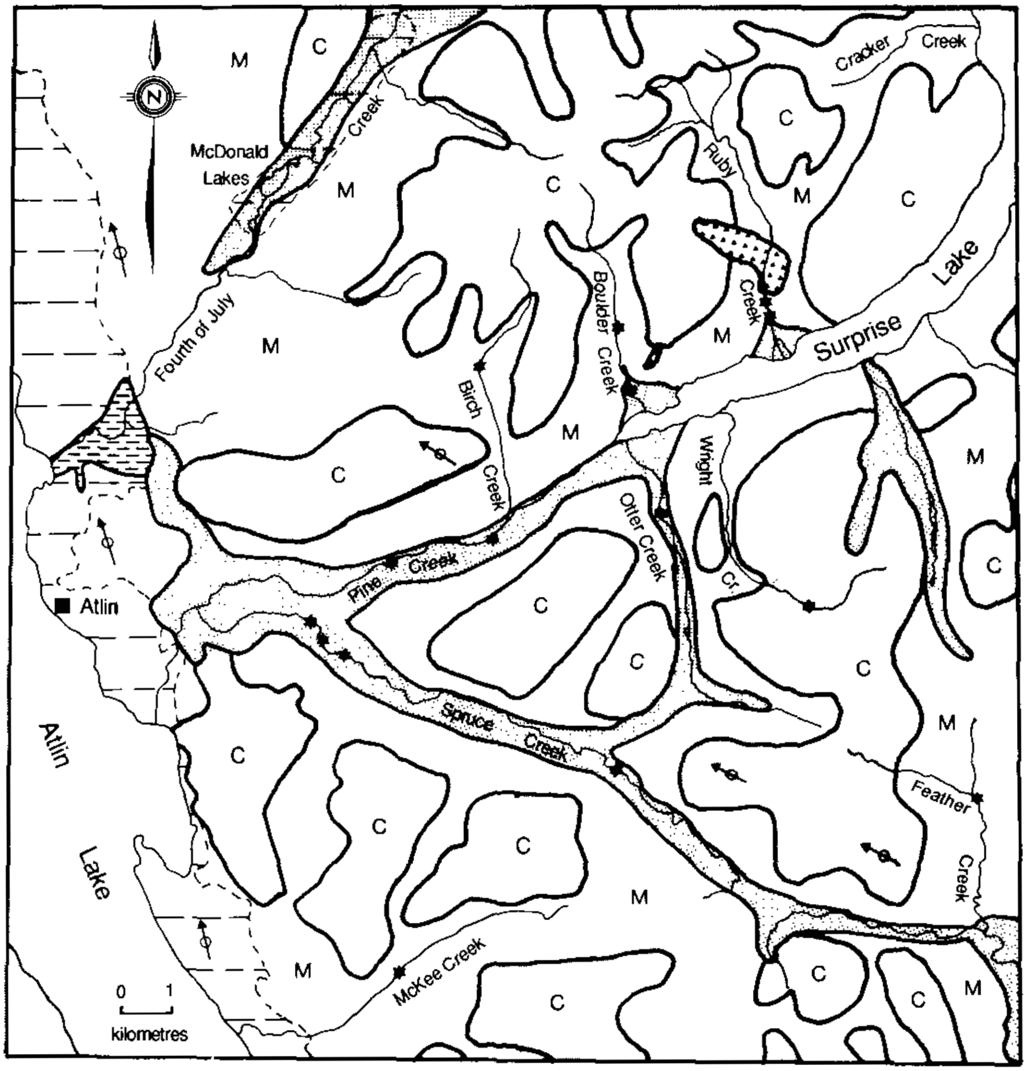

LEGEND

SURFICIAL MATERIALS:		TEXTURE:
M	MORAINAL (GLACIAL) DEPOSITS	mainly diamicton; some sand and gravel; minor exposed bedrock
	GLACIOLACUSTRINE SEDIMENTS	silt and clay; overlying diamicton and bedrock
	GLACIOFLUVIAL AND FLUVIAL DEPOSITS	gravel and sand; minor fines; some diamicton in alluvial fans
C	COLLUVIUM AND BEDROCK	diamicton and rubble; bedrock exposed mainly on upper slopes
	LANDSLIDE DEPOSITS	rubble and blocks (angular fragments); minor diamicton

REGIONAL ICE FLOW DIRECTION

APPROXIMATE UPPER LIMIT OF GLACIAL LAKE

ACTIVE PLACER MINE

Figure 3-9-1. Generalized surficial geology of the Atlin area (modified from Lacelle, 1989).

Plate 3-9-1. Airphoto of landslide deposits (L), moraines (dashed lines) and other landforms in the Ruby Creek valley. Note the area of intense mining activity (M) between the landslide and the alluvial fan (F) built into Surprise Lake at the mouth of Ruby Creek (British Columbia airphoto BC 5686 No. 86).

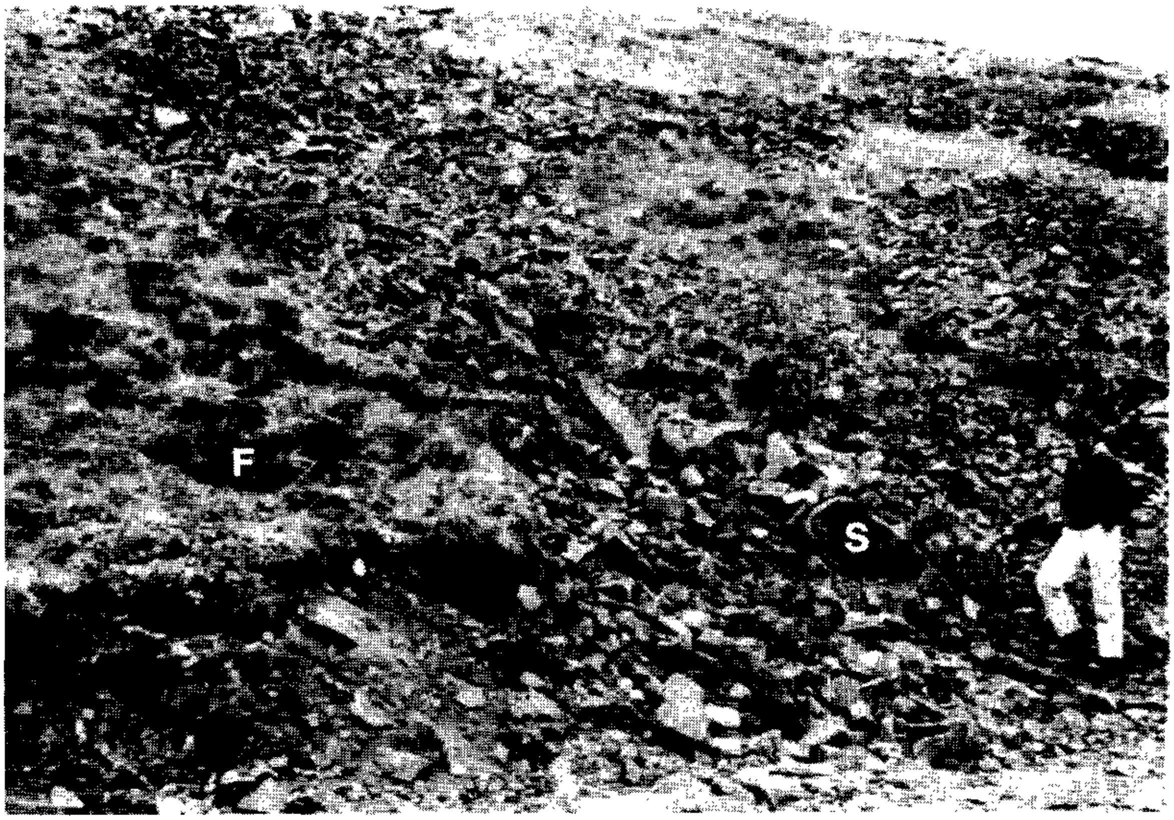

Plate 3-9-2. Cobble to boulder stone stripes (S) separated by finer grained colluvium (F) (with vegetation cover). Stone stripes and other periglacial features are common in high mountain areas throughout the region.

studied, these tills have a well-developed pebble fabric indicated by a strong preferred orientation of elongated clasts. Subglacial tills are typically compact, impermeable and poorly drained.

Tills are often overlain by 1 or 2 metres of poorly consolidated, sandy diamictons. These deposits occur mainly on slopes and probably are produced by colluviation of primary tills. They are comprised of glacially transported debris mixed with angular local materials and are commonly interbedded with thin lenses of sorted gravel, sand and silt. Debris-flow diamictons, comprised of similar materials and occurring on slopes from the surface to a depth of a few to several metres, were probably deposited in paraglacial environments shortly after deglaciation.

Glaciofluvial Deposits

Morainal deposits are locally incised by meltwater channels and commonly overlain by one to a few metres of glaciofluvial gravels and sands particularly in the Fourth of July Creek valley, along the southwest end of Surprise Lake and in the Boulder Creek, upper Spruce Creek and Feather Creek drainages.

Glaciofluvial deposits are most concentrated along the valley bottoms of Spruce, Pine, Otter and Fourth of July creeks. Well-developed glaciofluvial terraces occur in the lower Spruce Creek and Pine Creek valleys and merge with raised glaciofluvial delta complexes east and northeast of Atlin townsite. A large kettled delta complex also occurs in the Fourth of July Creek valley at the northern edge of the map area. An ice-contact kame complex occurs at the mouth of Otter Creek (Plate 3-9-5) and there are esker complexes in the lower and uppermost reaches of Spruce Creek. Glaciofluvial deposits consist mainly of moderately to well-sorted, well-stratified, non-cohesive gravels and sands. They typically have a high porosity and permeability and are well drained. Clasts are well rounded and generally in the pebble to cobble size range.

Glaciolacustrine Deposits

Glaciolacustrine sediments are uncommon surficial deposits in the map area but occur along the shore of Atlin Lake. The thickest sequence is at the mouth of Fourth of July Creek (Figure 3-9-1). Elsewhere they form a thin discontinuous veneer over morainal materials and bedrock. They are typically comprised of cohesive, impermeable silts and clays that are horizontally laminated to massive.

Fluvial and Other Deposits

Fluvial deposits are confined mainly to alluvial fans at the mouths of creeks entering the Surprise Lake valley, the Pine Creek fan-delta at Atlin Lake and narrow floodplains of streams throughout the area (Figure 3-9-1). They are similar to glaciofluvial deposits but tend to be finer grained and often are water saturated.

Bog and marsh deposits occur locally, particularly in the Atlin townsite area. Ephemeral salt-marsh deposits around the townsite contain as much as 43 per cent magnesium oxide (MgO) probably in the form of hydromagnesite (Young, 1915; Cummings, 1940). It is presumed that the hydromagnesite deposits formed as evaporite precipitates from saline pond waters fed by groundwaters rich in magnesium and other dissolved salts. Hydromagnesite with iron oxide cement and interbedded calcareous tufa occurs at a small spring on the north side of Atlin, near the lakeshore.

QUATERNARY AND ECONOMIC GEOLOGY OF PRODUCING PLACER DEPOSITS

BIRCH CREEK

The North Rim Resources mine on Birch Creek is currently exploiting gravels in the upper part of the creek where the flow changes from southwesterly to southerly (Figure 3-9-1). The auriferous gravels overlie waterworn bedrock and consist of clast-supported, pebble to cobble gravels. They are crudely imbricated, indicating a paleoflow towards 210°. Crude subhorizontal stratification is indicated by the presence of small to medium pebble lenses commonly 5 to 10 centimetres thick and approximately 25 centimetres wide. Up to 50 per cent of the beds have iron oxide staining, particularly small pebble lenses and open-work beds. Approximately 75 per cent of the clasts are subrounded to rounded, with the remainder consisting of angular rocks of local derivation. Four to five metres of overburden are exposed at the mine and consist of poorly sorted, massive to crudely stratified, sandy, cobble gravels interbedded with matrix-supported diamicton and lenses of horizontally laminated sand. Glacially abraded clasts are common, especially in diamicton beds.

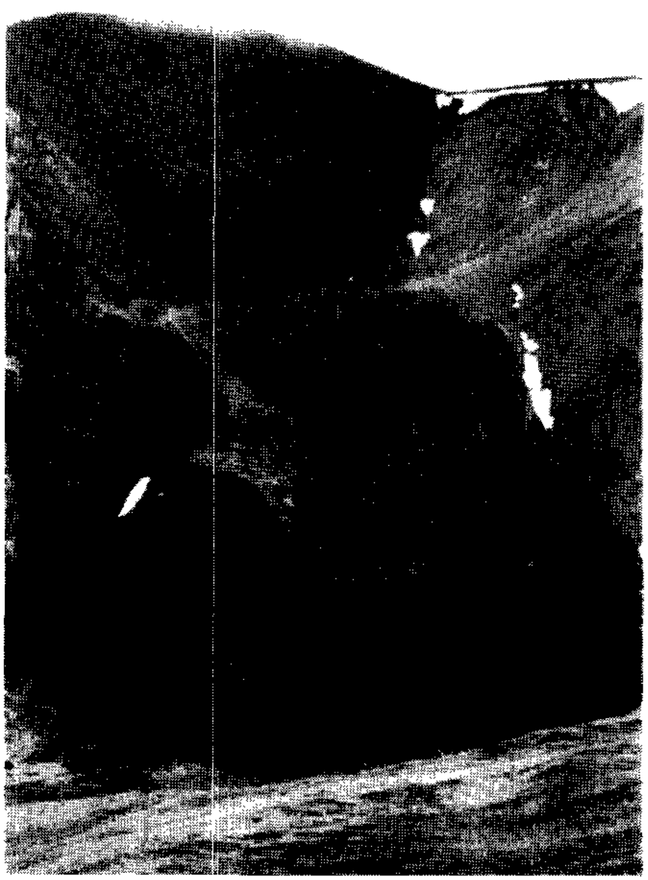

Plate 3-9-3. Rock glacier in a high cirque on the north side of Ruby Mountain.

Stratification, imbrication, clast rounding and the incorporation of local bedrock in the pay gravels all indicate fluvial transport and deposition in a high-energy erosive system. Gold nuggets vary from rounded to angular, also suggesting both local derivation and fluvial transport. Nuggets up to 155 grams (about 5 ounces) occur but approximately 60 to 70 per cent of the gold is finer than 1 millimetre in diameter. Irregularities in the bedrock surface, defined by near-vertical joints, act as natural riffles and are particularly rich in gold. Overburden sediments are interpreted as glacigenic debris flows and proximal outwash deposits.

The main paleochannel of Birch Creek was mined hydraulically in the past with some underground mining. For example, pay gravels under one extremely large boulder, excavated by recent mining, had been entirely removed by underground workings and the boulder was left supported only by timbers. Currently, the lower metre of the gravels and upper metre of the bedrock are being mined with a production cut-off of approximately 1 gram per cubic metre. Particularly large machinery and a specially engineered processing plant are currently utilized to mine and process the gravels due to the high silt and clay content and consolidation of the overburden. A possible buried channel on the east side of the creek was being investigated at the time of the property visit. The east side of the creek, throughout most of its length, has produced more gold than the west side (Gerry Schmidt, personal communication, 1991). Mining of unexploited gravels downstream from the current operation is planned.

BOULDER CREEK

Two small-scale operations are currently active on Boulder Creek. One is working alluvial-fan sediments at the downstream end of the creek. Exposures in test pits indicate that the fan sediments increase in thickness from 1.5 metres near the valley side to more than 8 metres nearer the fan centre. They consist of interbedded pebble, cobble and boulder gravels with crude horizontal bedding and weak imbrication. The gravels are clast supported and are locally open-work. They are characterized by numerous trough-shaped cobble and boulder concentrations a few to several metres wide. Clasts with evidence of glacial abrasion occur mainly in the lower 5 metres. The upper few metres exhibit trough-crossbedding with beds generally more than

Plate 3-9-4. Till (T) overlying glaciolacustrine (L) sediments on lower Otter Creek.

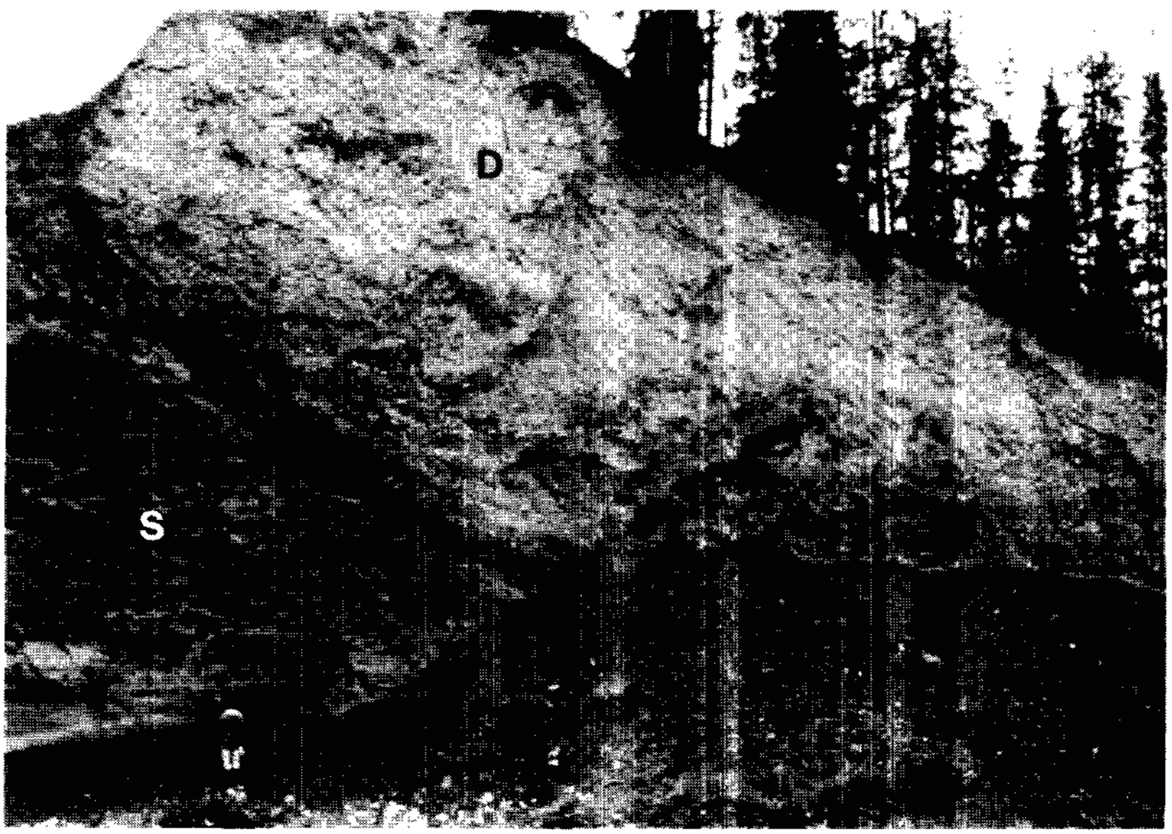

Plate 3-9-5. Exposure in part of a large ice-contact kame complex at the southwest end of Surprise Lake. Debris-flow deposits (D) unconformably overlie a faulted sand sequence (S).

5 metres wide and less than 0.5 metre thick. Exposed bedrock consists of oxidized basalt with numerous joints and small faults.

The bulk of sediments in the fan was probably deposited under paraglacial conditions and derived dominantly from glacial debris. The presence of crude imbrication, open-work beds, clast-supported strata and crossbedding suggests deposition by relatively fluid flows. Numerous trough-shaped, coarse-clast concentrations, interpreted as channel lags, and scour-and-fill structures indicate deposition in braided channels. Gold distribution is probably strongly facies-controlled with coarse gold concentrated along channel lags and finer gold more evenly distributed throughout the fan sequence. The gravels in the upper few metres show evidence of more fluvial reworking and probably have higher gold contents than the underlying deposits. Gold concentrations are expected to be highest in channels cut into bedrock near the fan apex. Buried fan-head channels associated with preglacial or interglacial stream courses of Boulder Creek are the best targets.

A second small operation on upper Boulder Creek is mining mainly old tailings in the channel bottom. Outcrops of original gravels are rare, with most remaining auriferous sediments being buried by thick glacial overburden and colluvium along the valley sides. At one outcrop, however, 2 metres of original pay gravels are exposed. They are heavily oxidized, massive to crudely stratified, cobble to boulder gravels interpreted as fluvial channel-fill gravels. They are overlain by 4 metres of bouldery, massive, matrix-supported diamicton of presumed glacial origin.

Feather Creek

The lowest exposed sediment observed at the Feather Creek mine is a matrix-supported, compact, oxidized, sandy-silt diamicton up to 8 metres thick, with interbedded lenses of well-sorted pale yellow (unoxidized) silts. Clasts are mostly angular, local rocks and some are striated. The diamicton is unconformably overlain by gold-bearing, unoxidized, clast-supported, cobble to boulder gravels grading locally into sandy gravelly diamicton. The upper part of the gravels has crude horizontal bedding, manganese and iron-stained open-work beds, small lenses of pebble gravel and more rounded to well-rounded clasts. Bedrock in the area is a pyritic basalt with silica and iron oxide filling vugs. It rises to within 3 metres of the surface upstream from the mining area and is exposed along the valley sides. Downstream from the minesite bedrock drops off as much as 20 metres, indicating the possible presence of a deep paleochannel. Buried paleochannel placers in the area have been mined underground in the past.

The gold-bearing unoxidized gravels are interpreted as Holocene stream deposits. Most of the recovered gold is flattened and rounded and predictably comes from the basal portion of these gravels where it has been reconcentrated from the underlying sediments. Glaciers overriding the area probably eroded and incorporated gold from the bedrock and possibly also from pre-existing fluvial placer deposits in the area. During deglaciation, resedimentation of glacial debris occurred to form debris-flow diamicton deposits, poorly sorted fluvial gravels and local waterlain silts. A dominantly local derivation for the sediments is indicated by the large proportion of angular clasts and by the presence of some fragile gold forms (Plate 3-9-6). Oxidation of fine-grained diamicton and silty sediments is probably a relict feature resulting from the incorporation of oxidized bedrock as the sediments have a low permeability and are now in reducing conditions below the water table. The largest recently recovered nugget weighs approximately 28 grams.

McKee Creek

Exceptionally coarse gold has been recovered in the McKee Creek placers, mainly from buried paleochannel deposits (Plate 3-9-7). Gold-bearing strata in the area are overlain by a well-exposed Quaternary sequence consisting of over 30 metres of non-auriferous gravel, sand, silt and diamicton. Exposures at the upstream end of the mine area reveal a diamicton complex overlying horizontally stratified gravels and sands. Exposures farther downstream also have thick, horizontally laminated silt and clay units that grade vertically and laterally (to the southwest) into sand and gravel beds that dip consistently up valley (to the northeast) as much as 15° (Plate 3-9-8). They are erosionally truncated

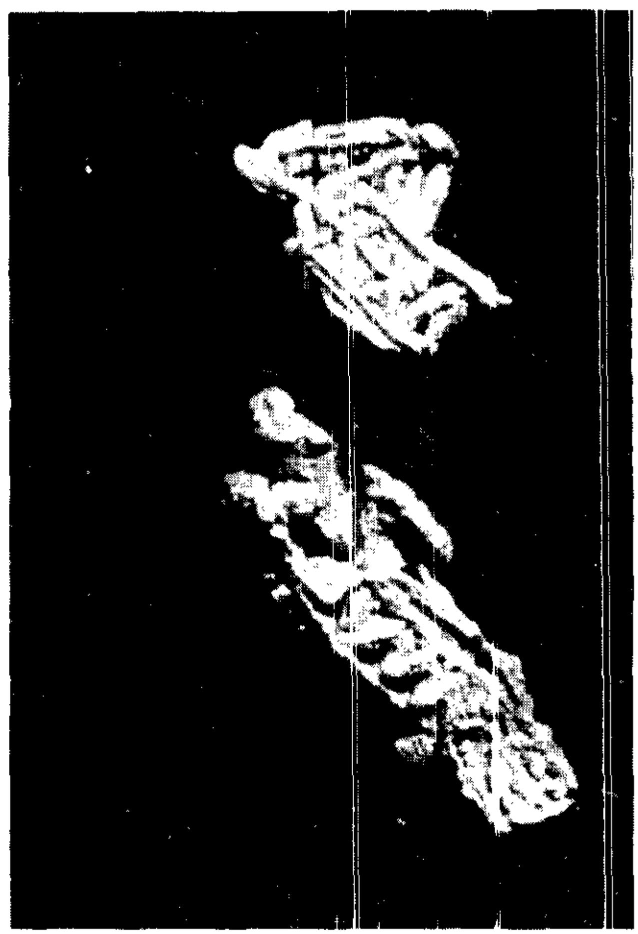

Plate 3-9-6. Locally derived gold nuggets from Feather Creek. (Small nugget is 1 cm long)

at the sharp base of a massive, compact diamicton with an exceptionally strong preferred fabric.

Study of these exposures indicates that gold was deposited in fluvial channel gravels in preglacial or interglacial times. Some of the lower gravels containing large boulders up to 2 metres in diameter have sedimentary characteristics indicative of high-energy hyperconcentrated flows (Plate 3-9-8). The presence of overlying glaciolacustrine silts and clays indicates that drainage in the McKee Creek valley was dammed, presumably by the advancing Atlin Lake valley glacier. Horizontally laminated fines, interpreted as bottomset beds, grade into dipping sand and gravel strata inferred to be foreset beds in a prograding glaciofluvial delta (Plate 3-9-8). The massive diamicton erosionally overlying the delta sequence is interpreted to be a till deposited at the base of the Atlin valley glacier as it expanded up the McKee Creek valley. Debris-flow and proximal outwash deposits shed off this glacier created the complex sequence of deposits exposed in higher parts of the valley. The uppermost part of the diamicton sequence represents till deposited during full glacial times and resedimented glacigenic debris deposited during and after deglaciation.

Mining in the area has included early hydraulic mining, open-pit mining and some underground activity. The most recent large operation exploited a buried channel remnant on the northwest side of the valley. There is potential for other channel remnants in the area as the bedrock rim has not yet been exposed along many parts of the valley side. A dry, boulder-gravel stream bed at the upper end of the mine area, on the southeast side of the valley, is the focus of current interest and has good potential for a shallow mining operation.

Otter Creek

The upper Otter Creek mine is the area's largest, with several large pieces of heavy mining equipment operating continuously. The open pit is nearly 2 kilometres in total length and provides excellent exposure of the Quaternary succession. The active highwall at the south end of the mine (Plate 3-9-9) reveals about 6 metres of gold-bearing sediments consisting of angular pebble to cobble gravel interbedded with poorly sorted, normally graded cobble to pebble gravel and diamicton. The upper part of the pay gravels has relatively high gold contents where large rounded boulders up to a few metres in diameter are concentrated. The bedrock surface under these bouldery gravels is well waterworn, undulatory and generally dips steeply towards the north and east. Overburden consists of 7 metres of crudely stratified large-pebble gravel, 10 metres of compact, massive, matrix-supported diamicton, grading up into 7 metres of very crudely stratified diamicton, capped by 4 metres of horizontally and trough cross-stratified gravels and sands.

The current mine is apparently working channel-margin deposits on the west side of the Otter Creek paleochannel. Poor sorting, numerous angular clasts and normal graded bedding in gravel and diamicton beds indicate a debris origin. The debris flows were locally derived and incorpor-

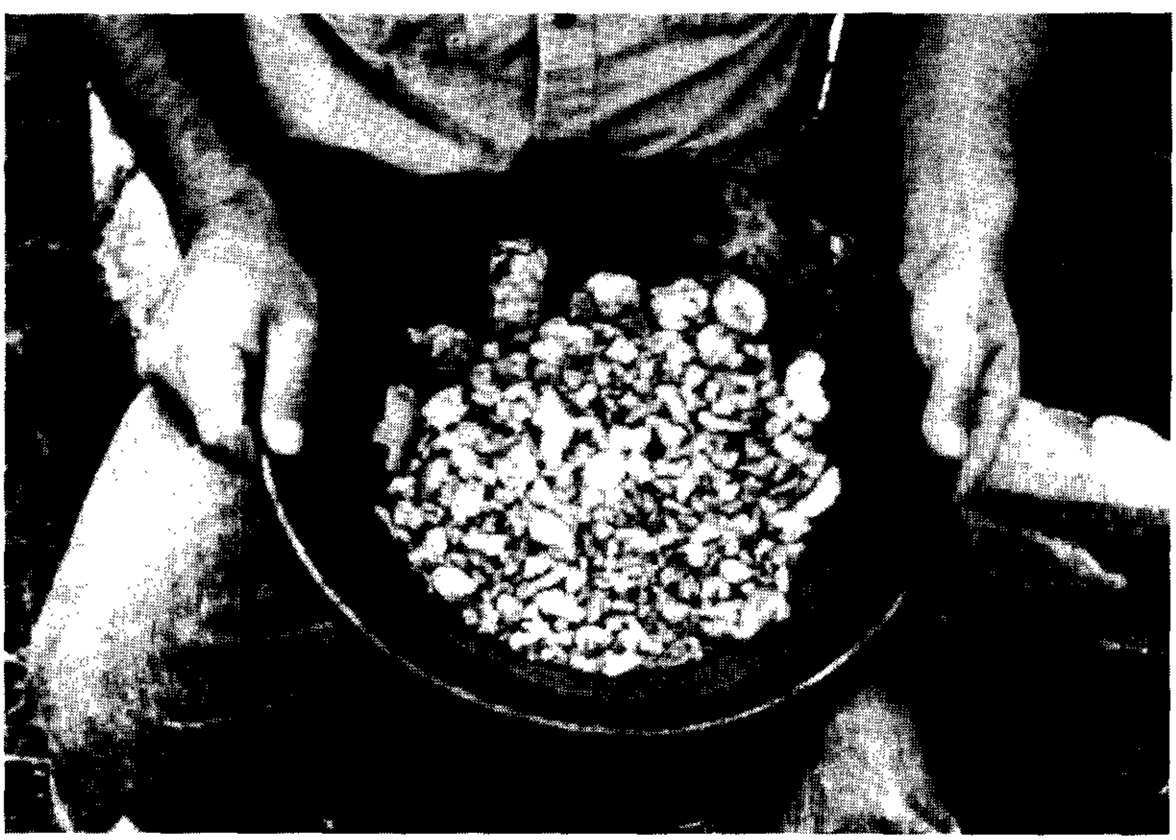

Plate 3-9-7. Coarse gold nuggets from McKee Creek paleochannel placers.

Plate 3-9-8. Glacigenic debris-flow and till deposits (T) unconformably overlying delta foreset and bottomset beds (D) and fluvial channel deposits (F) along lower McKee Creek. Exposure is 32 metres high. Large boulder at lower left is 2 metres in diameter.

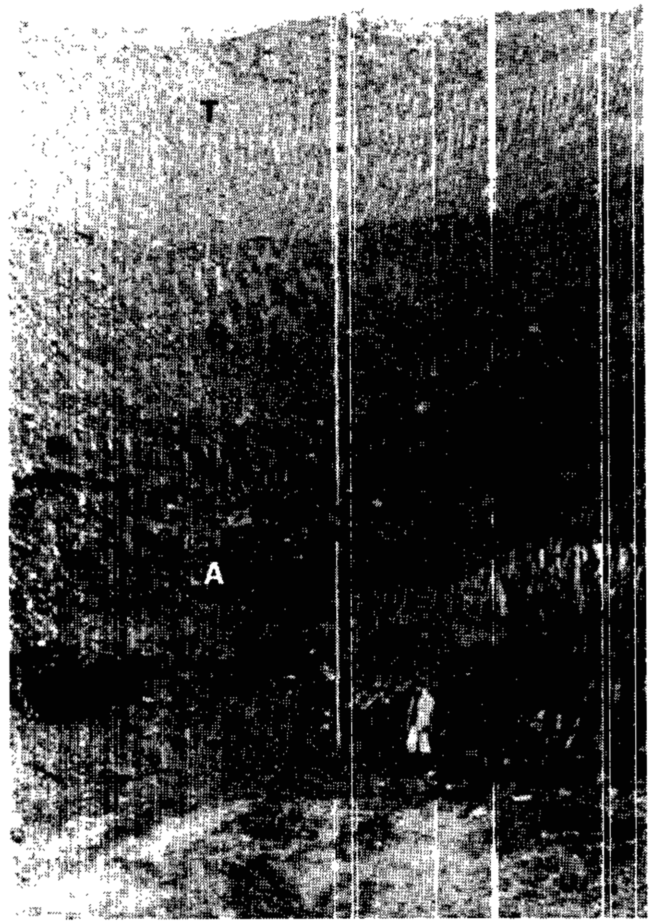

Plate 3-9-9. Gold-bearing gravels (A) overlain by non-auriferous gravels (G) and till (T) in the lower half of the active highwall at the Otter Creek mine.

ated gold from pre-existing auriferous colluvial and alluvial sediments. Boulder-gravel beds represent more typical channel deposits but their occurrence relatively high on a bedrock rim that dips steeply towards the east (paleochannel centre) as well as the north (downstream) indicates that deposition occurred along the channel margin and not in the thalweg (deepest part of the channel). The steep undulatory geometry of the bedrock is suggestive of a paleowaterfall and plunge pool.

Overburden deposits are interpreted as proglacial outwash stream gravels succeeded by till, postglacial debris-flow deposits, and finally Holocene fluvial channel gravels. Down valley, the complexity of the overburden succession increases with the addition of a deltaic gravel sequence (Plate 3-9-10), laminated glaciolacustrine silts and sands (Plate 3-9-4) and up to three auriferous gravel units interbedded with till deposits.

Pine Creek

Pine Creek is the second largest placer-producing stream in British Columbia and formerly supported a large mining community at Discovery, approximately 10 kilometres east of Atlin. Gold-bearing gravels in the area consist of massive to crude horizontally stratified boulder gravels. They are poorly sorted and mainly clast supported and contain discontinuous, poorly defined interbeds of diamicton with abundant silty-clay matrix. Discontinuous silty clay, granular gravel and pebbly sand strata also occur. The auriferous strata are overlain by a diamicton complex a few to several metres thick. The diamicton is locally crudely stratified and contains interbeds of sand and gravel. Elsewhere it is compact, massive, matrix supported and contains numerous striated clasts, sheared sand lenses and slickensided subhorizontal partings. Up to 5 metres of well-stratified sands and gravels, commonly with convoluted bedding, locally overlie the diamicton sequence.

The gold-bearing gravels are interpreted as fluvial channel and debris-flow deposits, possibly derived in part from the valley side. The overlying diamicton complex is inferred to be till and glacially derived debris-flow deposits. The uppermost sand and gravel sequence is interpreted as ice-contact and proximal outwash deposits. A large mine recently operated by Queenstake Resources Limited

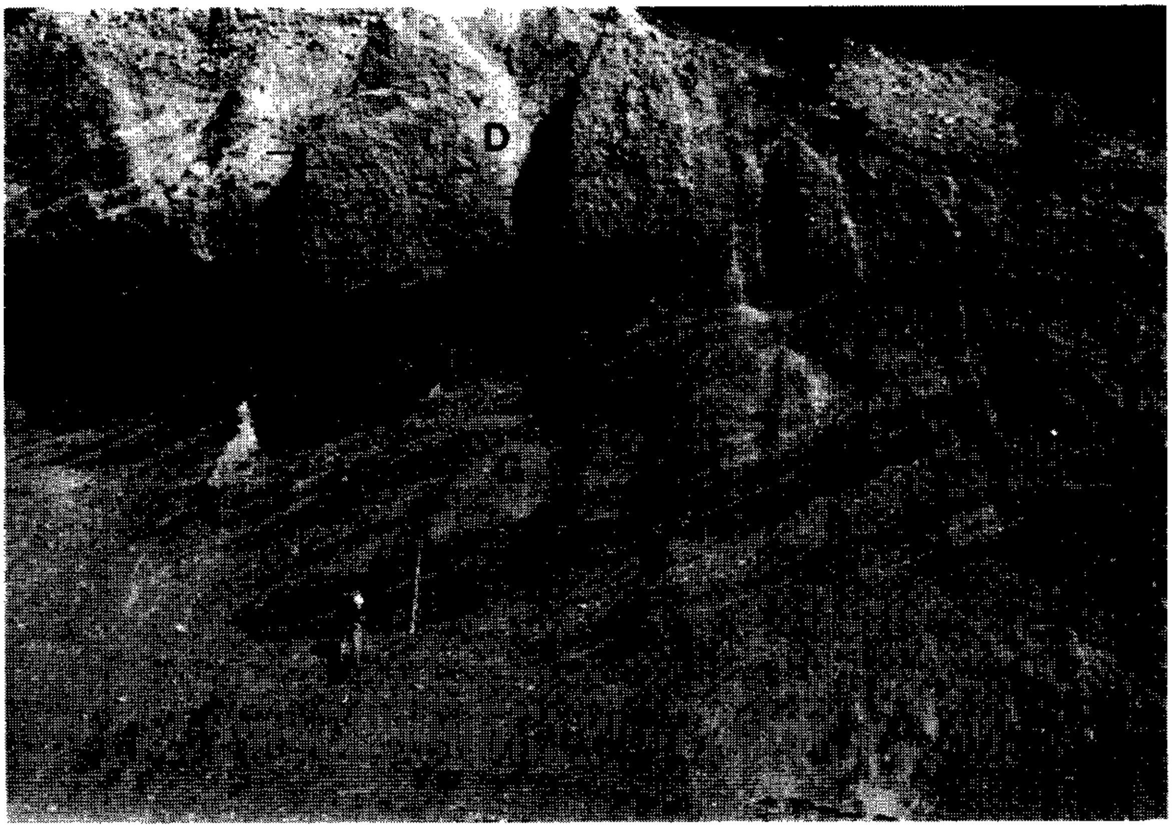

Plate 3-9-10. Delta foreset gravels (G) overlain by till and debris-flow deposits (D) on Otter Creek.

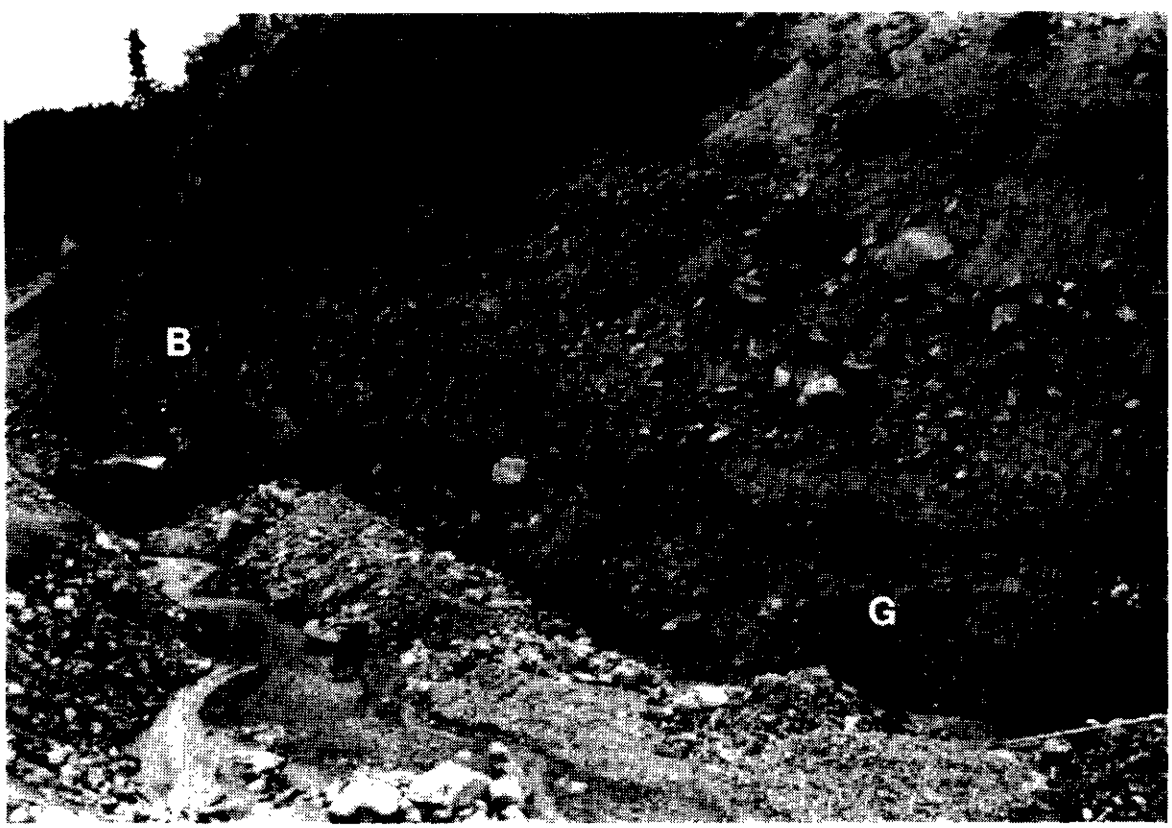

Plate 3-9-11. Excavating placer gravels (G) under Pleistocene basalts (B) on Ruby Creek.

exploited the lower gravel sequence in an area upstream from historical mining. There may be potential for further expansion of mining upstream, downstream and possibly also closer to the valley sides, but the thick glacial and glaciofluvial overburden inhibits exploration. Given the productivity of tributary creeks upstream from the Queenstake minesite, it seems probable that paleochannels of Pine Creek in that area would also be highly auriferous. However, depth of ice erosion and consequent preservation potential has not been documented.

RUBY CREEK

The Ruby Creek placer deposits have a unique geologic setting as they are overlain by Pleistocene basalts and rock avalanche deposits that originated in the Ruby Mountain area (Figure 3-9-1). The gold-bearing gravels are clast supported, mainly matrix filled and poorly to well sorted. They consist mainly of cobble and boulder gravels with some pebble beds and they exhibit horizontal stratification, clast clusters and crude imbrication. Clasts are mainly subrounded to well rounded and there are numerous well-rounded clasts of local granitic bedrock. The contact with the overlying basalts is locally marked by beds of stratified sand and fine gravel composed almost entirely of scoria. Large basalt 'clasts' also occur within the upper part of the gravels.

The auriferous gravels are interpreted as high-energy fluvial channel gravels and hyperconcentrated flood-flow deposits. Scoria-rich sand and gravel beds are interpreted as subaqueous volcaniclastic deposits formed during the initial phases of volcanic activity. The large basalt 'clasts' may also have formed subaqueously as lava pillows. Most of the basalt sequence, however, is columnar jointed and cooled relatively slowly. Glacial deposits locally overlie the columnar basalts as do postglacial landslide deposits. The latter are composed mainly of angular scoria and vesicular basalt rubble but locally contain large intraclasts of glacial diamicton.

Two mining operations are currently active at the lower end of Ruby Creek, both working gravels underlying basalts on the valley sides. The richest gravels are typically below the water table and undercutting the columnar basalts creates an additional mining challenge. The Bonnell operation is mainly utilizing natural slope and weathering processes active during the winter to remove the potentially hazardous overhanging basalts. The Russo operation is mechanically undercutting the gravels (Plate 3-9-11) and has done some underground mining, with plans for further underground developments.

Gold nuggets are typically about 2 millimetres in diameter and subrounded to angular. The largest recently recovered nugget was 180 grams (5.75 ounces) but nuggets up to 1.37 kilograms (44 ounces) have been reported. Gold grades in the lower metre of the pay gravels vary from 30 to 150 grams (3 to 5 ounces) per cubic metre and are up to 15 grams per cubic metre in the overlying 3 to 4 metres (Mike Bonnell, personal communication, 1991). Bedrock rises sharply on the valley walls and follows low-gradient benches along the valley-bottom margins which slope approximately 2° to 3° down valley. Gold contents are high where the bedrock is altered to a red granular sand or even a light-coloured silt. Ridges and knobs of unaltered bedrock are common.

SNAKE CREEK

Holocene fluvial gravels are mined on this small creek draining from a low pass on the east side of Spruce Mountain. The gold is relatively coarse with nuggets commonly 2 to 3 grams in weight, the largest recently recovered nugget weighed approximately 30 grams. Local bedrock consists of graphitic argillite with disseminated pyrite. A strong foliation strikes at 180° and dips 48° to the west. The bedrock is overlain by 4.5 metres of poorly sorted, large-cobble gravels interbedded with pebble gravels and horizontally laminated sands. The gravels are clast supported, matrix filled, horizontally bedded and crudely imbricated. They are overlain by a massive, matrix-supported sandy silt diamicton. Gold has been recovered mainly from the Holocene Snake Creek channel but the possibility of a deeper buried channel is indicated at one site along the present creek where an excavation revealed a sharp drop in the bedrock of more than several metres. The bedrock depression apparently crosses the creek obliquely and is buried by an additional several metres of glacial and glaciofluvial deposits to the east.

SPRUCE CREEK

Spruce Creek has produced more placer gold than any other creek in British Columbia, as well as the province's largest nugget weighing 2.6 kilograms (85 ounces). Most mining activity is currently concentrated at the lower end of the creek (Figure 3-9-1). Some open-pit mines higher up on the creek have heavy equipment on site but little current activity was seen other than hand operations. The main placer operation in the valley in recent years was the Queenstake mine on lower Spruce Creek. Several distinct stratigraphic units occur in the area, including possible preglacial, interglacial and postglacial deposits (Figure 3-9-2). Up to 4 metres of the lowermost auriferous gravels overlying bedrock have been mined. They are generally poorly sorted with a silty sand matrix, clast supported and crudely stratified. Gold also occurs in cobble and boulder beds in gravels that erosionally overlie the main, basal gold-bearing sequence, but in lower concentrations. These gravels are exposed just above water level at the northwest (downstream) end of the minesite (Figure 3-9-2). Stratigraphically higher gravel units are locally interbedded with diamicton and well-sorted sand beds and they are largely barren. The entire sequence is capped by massive diamicton beds and sands and gravels.

The gold-bearing gravels are interpreted as high-energy fluvial channel deposits. The paleochannel orientation is oblique to the trend of the modern valley as indicated by paleocurrent measurements (Figure 3-9-2). Drilling south and west of the property has been conducted in an attempt to delineate the buried channel geometry and extensive underground workings have been developed in the past to exploit the gravels. Gold occurs in lower concentrations and is

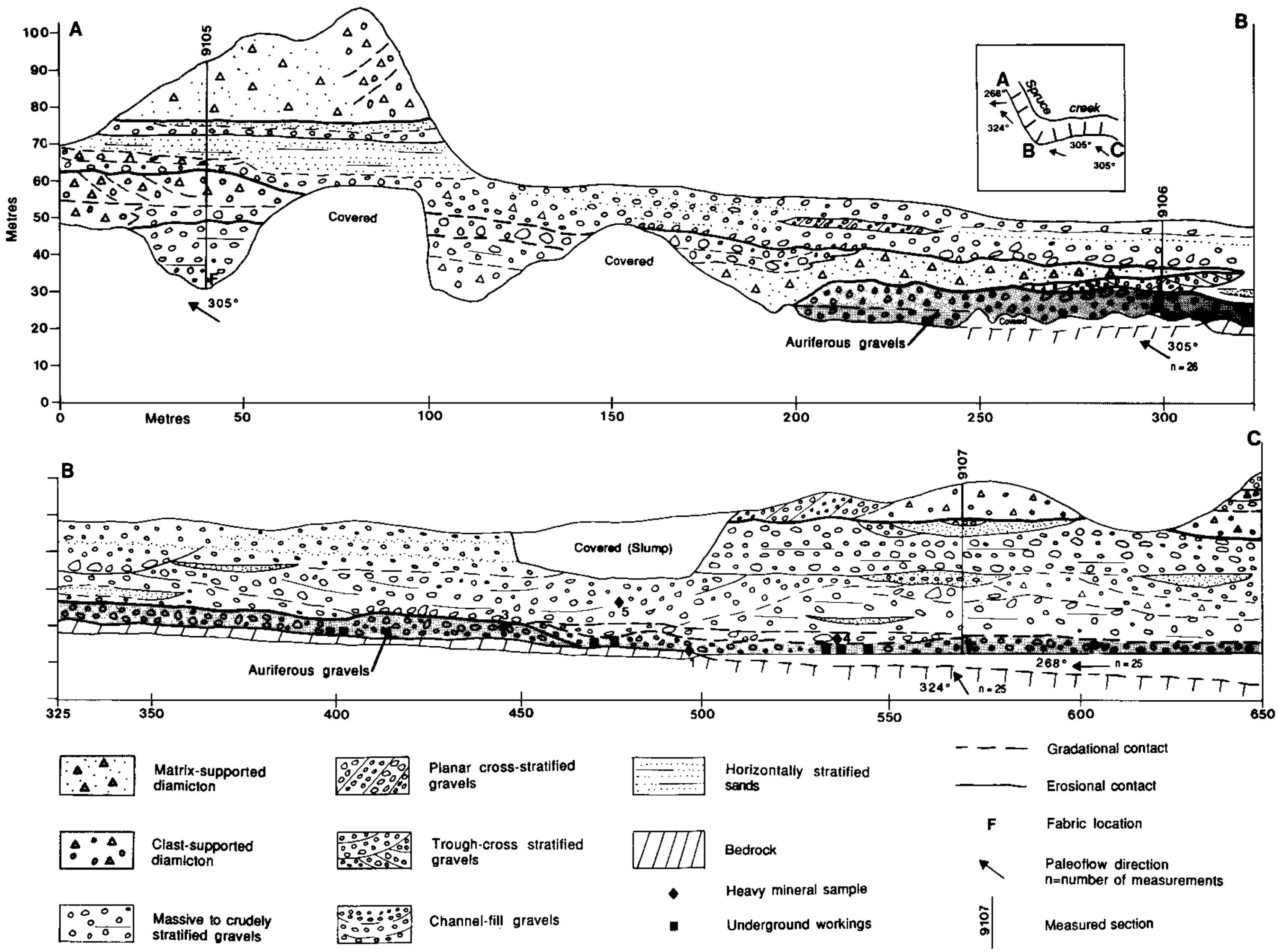

Figure 3-9-2. Longitudinal cross-section of Quaternary sediments exposed south and west of the former Queenstake Resources mine on Spruce Creek.

confined mainly to coarse gravel facies in younger gravel units, presumably because it was eroded from the older gravels and redeposited too quickly to allow significant reconcentration. Overlying gravels are believed to be glaciofluvial in origin and the uppermost diamictons are interpreted as till and ice-proximal debris-flow deposits. The uppermost sands and gravels comprise part of a postglacial, glaciofluvial esker and kame complex.

The Arnold Ellis mine, located just downstream from the area mined by Queenstake, has exploited mainly channel-bottom sediments missed by earlier operations and is currently mining basal cobble-gravels and the upper few metres of altered basaltic bedrock along the valley side. The gravels are heavily oxidized, clast supported and are poorly sorted with a high percentage of medium to coarse sand matrix. They locally grade into diamicton or very poorly sorted pebble gravel with a silty matrix. The underlying bedrock forms a bench that is defined by a ramp rising at a slope of about 15° from stream level onto a surface that dips gently (about 5°) toward the valley centre. The bedrock is locally strongly altered to red-coloured sand and silt-sized material that contains little placer gold. The gold-bearing gravels are overlain by about 5 metres of crudely imbricated, pebble to cobble gravels with crude horizontal stratification marked by coarse clast concentrations. These gravels are in turn overlain by 10 to 12 metres of massive diamicton grading up into crudely stratified diamicton with sandy interbeds.

The lower gravel sequence was probably deposited by sediment-rich flood flows with the basal gold-bearing gravels deposited during the final phases of channel degradation. The overlying barren gravels were probably deposited during valley aggradation, possibly induced by changes in base level and sediment input associated with the onset of glaciation. The capping diamictons are inferred to be till and other glacigenic sediments deposited during and immediately after glaciation.

Although the bulk of unmined placers in the Spruce Creek area are buried under thick overburden, some paleoplacers still remain in the valley bottom in areas where water problems have prevented mining. At the Springer Kyle property at the lower end of Spruce Creek (Figure 3-9-1), a channel 7 to 10 metres deep and approximately 20 metres wide has been mined in recent years and preliminary drilling results indicate the presence of another possible channel. An artesian aquifer, encountered in one hole at a depth of 8 metres, was still flowing at a rate of a several litres per minute a few weeks after drilling and indicates the probable presence of a highly porous gravel bed.

Oxidation of older gravel units in the Spruce Creek area is ubiquitous. It is often most intense in permeable strata but locally cross-cuts facies boundaries. It may reflect an early period of subaerial weathering, preferential incorporation and weathering of iron oxide rich bedrock, oxide precipitation from groundwater moving through permeable strata or hydrothermal alteration. Evidence for the latter is provided by zoned quartz veins in strongly altered bedrock and the presence of strongly altered clasts in the lower part of the gravels. Only the lowermost 0.5 to 4 metres of the oxidized gravels are highly auriferous, locally containing up to about 25 grams of gold per cubic metre. The gravels have been extensively mined underground and old workings are continuously encountered in modern open-pit mines (Figure 3-9-2).

WRIGHT CREEK

The only current operation on Wright Creek is in the upper part of the valley where a small mine run by Andy Didac is exploiting remnant channel gravels and Holocene alluvial fan sediments issuing from Eagle Creek, a small west-flowing tributary of Wright Creek (Plate 3-9-12). A maximum of about 4 metres of fan sediments are mined. Sandy, clast-supported, large-pebble gravels are overlain by cobble to boulder gravels with some diamicton interbeds. The lower few metres of the gravels contain approximately 0.5 gram of gold per tonne. Bedrock at the base of the fan consists of argillite with chert interbeds. Some gold-bearing gravels occurring on low bedrock terraces along Wright Creek are strongly cemented with iron and manganese oxides. Their hardness is comparable to the local bedrock and they may have been sufficiently resistant to have survived glaciation.

Lower Wright Creek was the site of an underground operation that temporarily exploited a rich gold-bearing gravel at approximately 30 metres depth but otherwise was unsuccessful due to water problems (Andy Didac, personal communication, 1991). The area has generated some recent interest as indicated by evidence of several deep drill holes. In addition, geophysical exploration for a possible buried channel between Wright and lower Otter creeks south of Surprise Lake is ongoing.

CONCLUSIONS

QUATERNARY HISTORY AND CHRONOLOGY

Glaciation of the Atlin area was preceded by an extensive period of fluvial valley incision during which many of the placer deposits in the area accumulated. Some of the placer deposits may be interglacial in age but most are probably preglacial. All are overlain by till deposits of the last glaciation. Infinite radiocarbon dates reported by Reeburgh and Springer-Young (1976) indicate that the gravels minimally predate the late Wisconsinan glaciation. Wood fragments from the bedrock-till interface in a underground placer mine on McKee Creek were dated at more than 36 000 years B.P. (AU-114) and peat at the base of compacted till at the mouth of Boulder Creek yielded a radiocarbon date of more than 31 000 years B.P. (AU-59).

In the Ruby Creek area, a period of Pleistocene volcanism occurred after deposition of the main gold-bearing gravel sequence. The lava, initially flowing into Ruby Creek, was deposited subaqueously, whereas subsequent flows cooled more slowly to form a thick sequence of columnar basalts.

The last glaciation largely obscured any evidence of earlier events, with the possible exception of some old glacigenic deposits at the lower end of Otter and Boulder creeks. Ice in the last glaciation initially moved into the Atlin region down major valleys from accumulation areas in

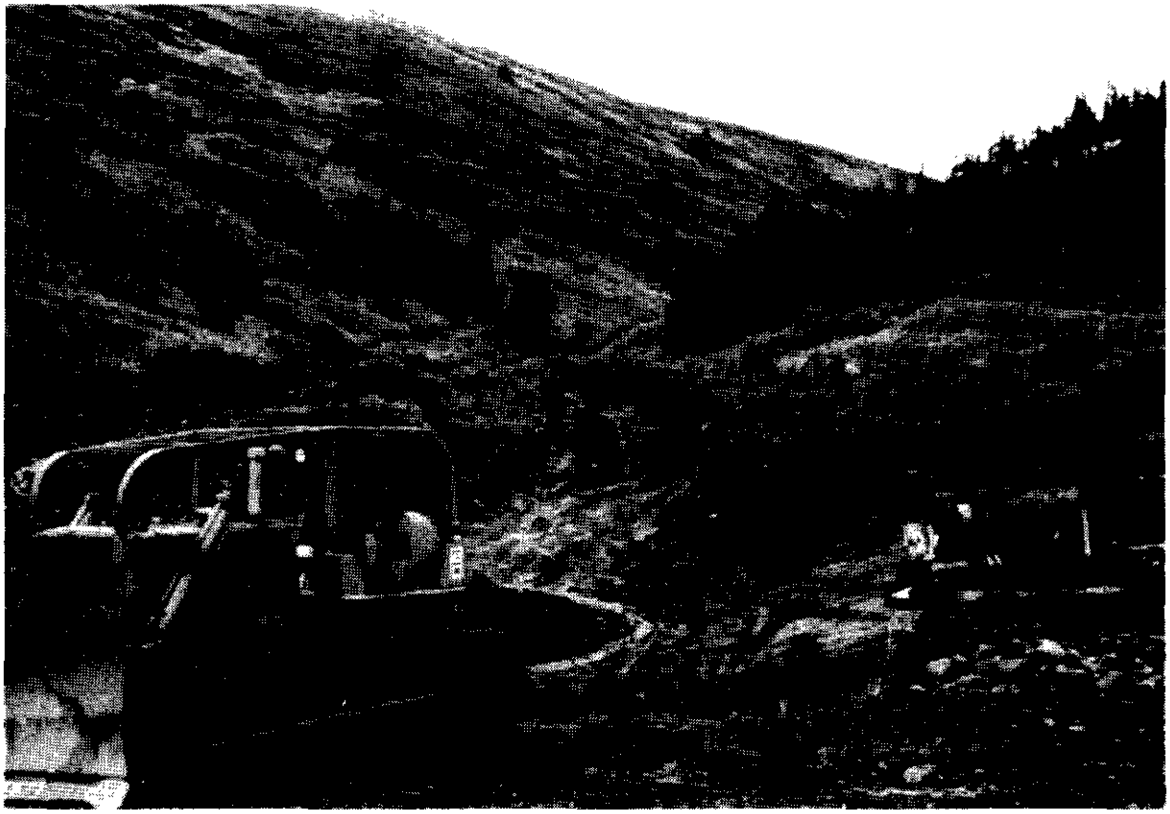

Plate 3-9-12. Small mine exploiting Holocene alluvial fan sediments at the mouth of Eagle Creek valley (background).

Plate 3-9-13. Glaciofluvial delta complex on lower Boulder Creek.

the Coast Range. Ice apparently occupied the Atlin Lake valley before smaller tributary valleys, resulting in damming of creeks such as McKee and Spruce. Ice damming in the Boulder and Otter Creek valleys may also have been caused by a glacier flowing up the Pine Creek valley. Prograding glaciofluvial delta complexes (Plate 3-9-13) formed in all these ice-dammed lakes. During full glacial times the region was almost entirely ice covered by a northeasterly flowing regional ice sheet resulting in a ubiquitous surficial cover of glacigenic sediments. Well-developed moraines are rare, but recessional moraines occur locally, as in the upper Ruby Creek valley (Plate 3-9-1).

During deglaciation ice-contact kame and esker complexes formed in a number of areas and a large glacial lake developed in the Atlin Lake valley. Outwash from Pine and Spruce creeks deposited glaciofluvial deltas northeast and east of Atlin. As the lake level dropped, deltas and correlative outwash terraces were constructed at successively lower levels. The highest lake level in the area, determined by the distribution of glaciolacustrine sediments and by maximum delta elevations, was at about 780 metres above sea level. A glacial lake also formed in the McDonald Lakes area (Figure 3-9-1) as a result of damming by Atlin valley ice retreating down the Fourth of July Creek valley (Tallman, 1975). The elevation of large pitted deltas along Fourth of July Creek northeast of McDonald Lakes indicates a maximum glacial lake level higher than 1000 metres above sea level.

During and following deglaciation, previously deposited glacigenic sediments were extensively reworked by colluvial processes under paraglacial conditions. Resedimented glacigenic deposits are common at the base of steep slopes. Similarly, paraglacial alluvial-fan sedimentation was probably very active during deglaciation and has continued to the present. Holocene glacial activity was restricted to high cirques in the northeast part of the map area. At high elevations, periglacial processes have played a large role in the evolution of geomorphic features throughout much of the Holocene (Tallman, 1975). Rock glaciers, solifluction lobes and stone stripes are common high-elevation features. At least one major postglacial landslide has occurred in the area. Fluvial terrace, floodplain and active channel deposits have also formed along valley bottoms during the Holocene. Postglacial sediments currently supporting placer mines are uncommon but locally include Holocene alluvial fan and fluvial deposits.

Future Placer Prospects

In identifying potentially productive placer settings from geomorphic and stratigraphic points of view, it is necessary to first consider the potential for bedrock in the area to yield gold to the placer environment. For example, a probable connection between altered ultramafic rocks (listwanites) and lode and placer gold production in the Atlin area has recently been suggested (Ash and Arksey, 1990 b, c). These studies suggest that areas with placer potential may occur downstream from known ultramafic outcrops or in areas where it can be determined by geological inference that ultramafic rocks previously occurred and have since been eroded. Such inferences can be made, for example, on the basis of structural cross-sections or simply by the presence of altered ultramafic clasts or related mineral suites in the placer deposits under investigation.

In addition to specific potential developments discussed above for each of the main placer mining areas, a number of other general areas with placer potential can be suggested. Although the Pine Creek valley has been extensively mined, it is wide and there is good potential for undiscovered buried channels, particularly to the north and east of previously mined areas. On the north side of the valley, broad, linear topographic lows are recognizable on airphotos and may represent surface expressions of former gold-bearing paleochannels. Similarly, the area between the Birch Creek confluence and Surprise Lake has not been mined and, given the historical productivity of upstream tributaries such as Otter, Boulder and Ruby creeks, it seems probable that paleochannels in that area would also be gold bearing

Good potential for rich buried-channel placer deposits also exists in the Spruce Creek valley. In addition to the area downstream and west of the Queenstake property, much of the valley upstream of the Nolan underground mine has good potential. Depth of ice erosion and thick glacial and glaciofluvial overburden are the main factors limiting the location and exploitation of these deposits.

Confined channel gravels below Pleistocene basalts and rock avalanche deposits in the Ruby Mountain area have good potential. Undiscovered paleochannel deposits on this creek and on others such as Boulder and Birch creeks, will mostly be small channel remnants on the valley sides, but there is local potential for more extensive deposits in areas where these valleys widen. Similarly, the broad alluvial flat on Wright Creek, downstream from the point where it bends from a northwest to a northerly trend, has good potential for deeply buried fluvial channel deposits. The valley is narrow and oriented obliquely to the regional ice-flow direction and therefore may have escaped deep glacial erosion.

Although postglacial placers are less productive than buried channel deposits and have not been heavily exploited to date, they may have potential for efficient mining operations with improved recovery systems. Large-volume, relatively low-grade surface placers include alluvial fan deposits at the mouths of Boulder, Ruby and Birch creeks and to a lesser extent fans on lower Otter, Wright and McKee creeks. In addition, fluvial terrace deposits such as are recognized on upper Spruce Creek and in the Wilson Creek area just south of the study area have potential.

Other regions with placer potential, not investigated in this study, include Davenport, Lincoln, Consolation and Volcanic creeks north of the map area, Cracker Creek to the northeast and Burdette, O'Donnel and Bull creeks to the south. Productive placers have also been recorded in the Graham Creek area west of the study area. Further study of these placer deposits is needed to identify their extent and potential.

ACKNOWLEDGMENTS

The author would like to particularly thank Heather Blyth for capable assistance and valuable discussions during the field component of this program. As part of this study a field conference on placer deposits was held in Atlin and presentations by Chris Ash, Randy Clarkson, Dennis Lieutard, Mary Lou Malott and Steve Morison are appreciated. Chris Ash contributed valuable information on potential lode sources in the area. The author also thanks all of the miners in the region for providing information and access to properties. Financial, logistic and other support from the Atlin Placer Mining Association, the Yukon Geological Services Division, Finning Tractor, Shirley Connolly, Jeri Johnson and Barb Levson are also greatly appreciated. This study is part of a joint research endeavor of the British Columbia Geological Survey Branch and the Yukon Exploration and Geological Services Division to investigate the geology of economically important placers in the Atlin area. The manuscript was reviewed by John Newell and Dan Kerr. Figure 3-9-2 was drafted by Chris Smith.

REFERENCES

Aitken, J.D. (1959): Atlin Map Area, British Columbia; *Geological Survey of Canada*, Memoir 307, 89 pages and Map 1082A, 1:250 000.

Anderson, J.H. (1970): A Geobotanical Study in the Atlin Region in Northwestern British Columbia and South-central Yukon Territory; unpublished Ph.D. thesis, *Michigan State University*, East Lansing, 380 pages.

Ash, C.H. and Arksey, R.L. (1990a): Tectonic Setting of Listwanite - Lode Gold Deposits in Northwestern British Columbia (104N/12); *B.C. Ministry of Energy, Mines and Petroleum Resources*, Open File 1990-22, 1:20 000.

Ash, C.H. and Arksey, R.L. (1990b): The Atlin Ultramafic Allochthon: Ophiolitic Basement within the Cache Creek Terrane: Tectonic and Metallogenic Significance (104N/12); *in* Geological Fieldwork 1989, *B.C. Ministry of Energy, Mines and Petroleum Resources*, Paper 1990-1, pages 365-374.

Ash, C.H. and Arksey, R.L. (1990c): The Listwanite - Lode Gold Association in British Columbia; *in* Geological Fieldwork 1989, *B.C. Ministry of Energy, Mines and Petroleum Resources*, Paper 1990-1, pages 359-364.

Black, J.M. (1953): Report on the Atlin Placer Camp; *B.C. Ministry of Energy, Mines and Petroleum Resources*, Miscellaneous File Copy Report, Victoria, 71 pages, out of print.

Bloodgood, M. A. and Bellefontaine, K.A. (1990): The Geology of the Atlin Area (Dixie Lake and Teresa Island) (104N/6 and parts of 104N/5 and 12); *in* Geological Fieldwork 1989, *B.C. Ministry of Energy, Mines and Petroleum Resources*, Paper 1990-1, pages 205-215.

Bloodgood, M. A., Bellefontaine, K.A., Gertz, I.C. and Maddison, L. (1990): The Geology of the Dixie Lake and Teresa Island Map Area (104N/5, 6); *B.C. Ministry of Energy, Mines and Petroleum Resources*, Open File 1990-6, two 1:50 000 sheets.

Bloodgood, M.A., Rees, C.J. and Lefebure, D.V. (1989a): Geology of the Atlin Area (104N/11W, 12E); *B.C. Ministry of Energy, Mines and Petroleum Resources*, Open File 89-15, two 1:50 000 sheets.

Bloodgood, M.A., Rees, C.J. and Lefebure, D.V. (1989b): Geology and Mineralization of the Atlin Area, Northwestern British Columbia (104N/11W and 12E); *in* Geological Fieldwork 1988, *B.C. Ministry of Energy, Mines and Petroleum Resources*, Paper 1989-1, pages 311-322.

Cummings, J.M. (1940): Saline and Hydromagnesite Deposits of British Columbia; *B.C. Ministry of Energy, Mines and Petroleum Resources*, Bulletin 4, 160 pages.

Debicki, R.L. (1984): An Overview of the Placer Mining Industry in the Atlin Mining Division, 1978 to 1982; *B.C. Ministry of Energy, Mines and Petroleum Resources*, Paper 1984-2, 21 pages.

Gwillim, J.C. (1901): Report on the Atlin Mining District, British Columbia; *Geological Survey of Canada*, Annual Report, Volume 12 (1899), Report B.

Gwillim, J.C. (1902): Glaciation in the Atlin District, British Columbia; *Journal of Geology*, Volume 10, pages 182-185.

Holland, S.S. (1950): Placer Gold Production of British Columbia; *B.C. Ministry of Energy, Mines and Petroleum Resources*, Bulletin 28, 89 pages. (Reprinted in 1980).

Lacelle, L.E.H. (1985): Terrain Capability for Residential Settlements: Atlin, British Columbia; *B.C. Ministry of Environment*, Working Report, 43 pages.

Lacelle, L.E.H. (1989): Atlin Terrain Materials (104N); *B.C. Ministry of Environment*, 1:250 000-scale map.

Lefebure, D.V. and Gunning, M.H. (1989): Geological Compilation Map of the Atlin Area (104N/11W, 12E); *B.C. Ministry of Energy, Mines and Petroleum Resources*, Open File 1989-24, two 1:20 000 sheets.

MacKinnon, H.F. (1986): Examination of Concentrates from Atlin B.C. Placers: Economic Implications; unpublished B.Sc. thesis, *Carleton University*, Ottawa, 199 pages.

Monger, J.W.H. (1975): Upper Paleozoic Rocks of the Atlin Terrane, Northwest British Columbia and South-central Yukon; *Geological Survey of Canada*, Paper 74-47, 63 pages.

Proudlock, P.J. and Proudlock, W.M. (1976): Stratigraphy of the Placers in the Atlin Placer Mining Camp, British Columbia; *B.C. Ministry of Energy, Mines and Petroleum Resources*, Miscellaneous File Copy Report, Victoria, 69 pages, out of print.

Reeburgh, W.S. and Springer-Young, M. (1976): University of Alaska Radiocarbon Dates; *Radiocarbon*, Volume 18, Number 1, pages 1-15.

Tallman, A.M. (1975): The Glacial and Periglacial Geology of the Fourth of July Creek Valley, Atlin Region, Cassiar District, Northwestern British Columbia; unpublished Ph.D. thesis, *Michigan State University*, East Lansing, 178 pages.

Young, G.A. (1915): Hydromagnesite Deposits of Atlin B.C.; *Geological Survey of Canada*, Annual Summary Report for 1915, pages 50-61.

AN EQUATION FOR ESTIMATION OF MAXIMUM COALBED-METHANE RESOURCE POTENTIAL

By Barry D. Ryan

KEYWORDS: Coalbed methane, resource estimation, equations, computer calculations, relationships, coalification gradient.

INTRODUCTION

This is a technical note on coalbed methane resource estimation. There is extensive literature on the subject of coalbed methane in coal. Many useful references can be found in the special publication by the American Association of Petroleum Geologists (1989).

There has been considerable interest in estimating methane gas content of deeply buried coal. In some coal basins the recovery of coalbed methane from wells penetrating coal seams is a reality and is economic. The potential maximum coalbed methane resource of many other coal basins is being calculated using available seam thickness, rank and depth data.

Often the method used to estimate the maximum methane resource per tonne of *in situ* coal relies on the empirical curves introduced by Eddy *et al.* (1982; Figure 4-1-1). These curves provide estimates of the lost and desorbed gas from coals of different ranks and at different depths. Lost and desorbed methane is an approximation of the maximum methane resource. The lost and desorbed gas content can be read from the appropriate rank curve based on the depth of the sample. The process is convenient for a few determinations but becomes increasingly awkward when rank is defined by a wide range of mean maximum reflectance ($\bar{R}_{max}$) measurements and data are required for a large number of depths.

DISCUSSION

A single equation that relates $\bar{R}_{max}$ and depth to maximum recoverable methane would make the process much

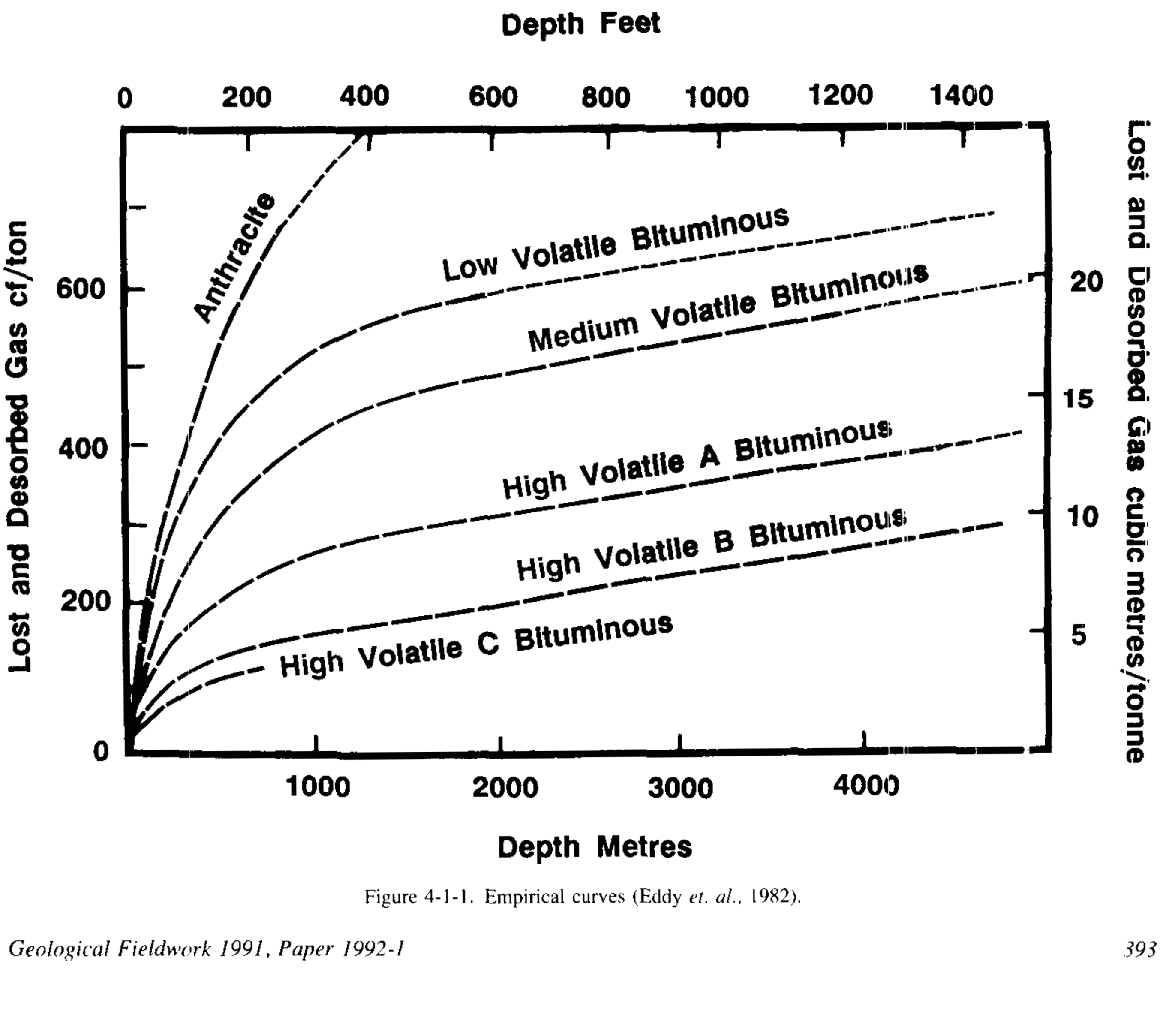

Figure 4-1-1. Empirical curves (Eddy *et. al.*, 1982).

TABLE 4-1-1
EQUATIONS FOR RELATING COALBED METHANE *TO DEPTH AND MEAN MAXIMUM REFLECTANCE* OF VITRINITE

EQUATION A

$$R = \bar{R}_{max}\% \times K$$
$$C = \text{depth} \times R\hat{\ }\ 2.5 - 0.2$$
$$B = \text{Ln}(\ C\ )\ /\ 2.30259 - 1.095)\ /\ 0.003913$$
$$GAS = B \times (100 - M - A)\ /\ 100\ /\ 32.037$$

$\bar{R}_{max}\%$ = Mean maximum reflectance of vitrinite in oil.
K = 0.98 for mid-rank, 0.89 for lower limit and 1.25 for upper limit.
Ln = natural logarithm
Depth in metres
GAS in cubic centimetres per gram

EQUATIONS FOR THE FIVE RANK CURVES IN FIGURE 1

1/	HVB-C	GAS = (104.85 = 0.0514 × D - 770.4 / D)/32.037
2/	HVB-B	GAS = (122.74 = 0.155 × D - 1203.6 / D)/32.037
3/	HVB-A	GAS = (267.62 + 0.09613 × D - 11499.3 / D)/32.037
4/	MVB	GAS = (466.57 + 0.09974 × D - 25923.2 / D)/32.037
5/	ANTH	GAS = (786.2 + 0.089 × D - 40290.1 / D)/32.037

KARWEIL CUMULATIVE GAS EQUATION

$$CGAS = -325.6\ \text{Ln}(VM\ /\ 37.8)$$

CGAS = Cumulative gas in cubic centimetres per gram
VM = Volatile matter; dry ash-free basis

TABLE 4-1-2
VALUES OF LOST PLUS DESORBED GAS VERSUS DEPTH FROM THE RANK CURVES IN FIGURE 1

RANK Average $\bar{R}_{max}$ Depth (Metres)	HVB C *0.52%* g/cc	HVB B *0.64%* g/cc	HVB A *0.82%* g/cc	MVB *1.30%* g/cc	LVB *1.80%* g/cc	ANTH *3.50%* g/cc
200	3.47	4.37	7.09	11.02	14.08	18.73
300	3.68	4.78	8.18	12.89	16.04	21.29
400	3.87	5.18	8.68	14.02	17.14	22.60
500	4.03	5.59	9.11	14.64	17.19	23.50
600	4.18	5.93	9.61	14.98	18.39	24.07
700	4.37	6.24	9.93	15.45	18.73	24.41
800	4.53	6.68	10.27	15.95	19.13	25.13
900	4.68	6.99	10.61	16.39	19.51	25.66
1000	4.84	7.43	11.02	16.73	19.82	26.22
1100	5.03	7.77	11.27	17.26	20.26	
1200	5.18	8.12	11.58	17.70	20.54	
1300	5.34	8.62	11.92	18.04	21.01	
1400	5.49	8.87	12.33	18.39	21.32	
1500	5.68	9.11	12.74	18.73	21.63	

Abbreviations:
$\bar{R}_{max}$ Mean maximum reflectance of vitrinite in oil.
HVB High-volatile bituminous.
MVB Medium-volatile bituminous.
ANTH Anthracite.

TABLE 4-1-3
RANGES OF $\bar{R}_{max}$ FOR DIFFERENT RANKS (FROM WARD, 1984) AND DIVERGENCE OF EQUATION A FROM RANK CURVES IN TABLE 4-1-1

Rank	Low	$\bar{R}_{max}$ Mid	High	Equation A Errors Absolute	 Normative
HVB-C	0.47	0.52	0.57	ND	ND
HVB-B	0.57	0.64	0.71	−4	+6
HVB-A	0.71	0.90	1.10	+13	+13
MBV	1.10	1.30	1.50	−0.2	+1.0
LVB	1.5	1.8	2.05	−0.5	+0.6
SEMI-A	2.05	2.5	3.0	ND	ND
ANTH	3.0	3.5	ND	+0.04	+1.5

Errors represent the average divergence from the appropriate rank equation in Table 4-1-1 when the mid-range $\bar{R}_{max}$ value is used in Equation A.

less tedious and amenable to computerization. Such an equation is introduced here (Equation A, Table 4-1-1). It reproduces the original five rank curves in Figure 4-1-1 quite well, except for R_{max} values of less than 0.6 per cent.

Approximate readings of depth in metres and gas content in grams per cubic centimetre can be read from the five rank curves in Figure 4-1-1 (Table 4-1-2). Data were input into a curve-fitting computer program and for each rank the best-fit curve with the resultant constants defined (Table 4-1-1, Equations 1 to 5). In all cases an equation of the type Y = (A + B) × (X + C) / × fitted the data very well. In fact the R^2 correlation factors for the five curve fits varied from 0.996 to 1.0. These five equations therefore provide an accurate way of representing the five rank curves in Figure 4-1-1. These equations can be used to model the gas content *versus depth relationship for coal with a rank represented by* one of the five curves. Unfortunately it is difficult to relate the constants in each equation to changes of $\bar{R}_{max}$ from curve to curve so that the equations are not useful when coal rank is not represented by one of the five curves.

Equation A was developed to provide a single equation capable of predicting the gas content for coal from any depth and of any rank. In fact the equation works quite well for reflectances greater than 0.6 per cent and depths greater than 100 metres. It was first used in resource calculations for the Tuya River coal basin (Ryan, 1990). Obviously if Equation A is valid, then it should reproduce the five rank curves in Figure 4-1-1. The range and average ($\bar{R}_{max}$) values that define each rank of coal (Ward, 1984) are in Table 4-1-3. The mid- ($\bar{R}_{max}$) values were entered in Equation A. With the help of a computer program, predictions of gas content versus depth derived from Equation A were checked against those provided by the appropriate rank equation (Equations 1 to 5, Table 4-1-1).

The program incorporates Equation A and Equations 1 to 5. *It calculates the average divergence of Equation A from* the appropriate rank equation when the correct mid-range ($\bar{R}_{max}$) value (Table 4-1-3) is entered in Equation A. The divergence is calculated as an average, taking into account sign (absolute divergence), in which case random fluctuations about the rank curve will result in a zero divergence. The normative average divergence is also calculated. In this case fluctuations about the rank curve are summed and averaged irrespective of sign. The absolute average divergences range from −4.0 to +13.0 per cent and the normative average divergences from 0.6 to 13.0 per cent.

If the mid-point $\bar{R}_{max}$ values are used in Equation A then the five rank curves in Figure 4-1-1 are reproduced fairly accurately except for the high-volatile A bituminous rank curve. The mid-point $\bar{R}_{max}$ value for high-volatile A bituminous coal is 0.90 per cent; Equation A produces a good fit to the curve if a value of 0.82 per cent is used. Because Equation A fits the five rank curves quite well it reasonable to suppose that it can also model the depth versus gas content relationship for all intervening ranks of coal.

It is easy to adjust constant K in Equation A to enable the equation to model the five rank curves assuming that they represent the minimum $\bar{R}_{max}$ values for that rank, for example to model the lower limit of each rank, K = 0.89, or to model the upper limit of each rank, K = 1.25. It is also possible to add a constant to Equation A that takes account of the effect of ash and moisture; the simplest assumption is that the five curves are at the same ash basis as the samples being modelled. If the five curves are for ash-free coal, then an adjustment of (100-M-A)/100 must be made where A = ash per cent and M = moisture per cent of the coal being modelled.

Equation A makes it easier to use the relationships explicit in the five rank curves. These curves are only approximations of actual coalbed methane resource potential. Using Equation A does not make the resource evaluation more accurate. It simply makes the process of initial order-of-magnitude resource calculations easier to perform when a lot of coal rank, depth and seam thickness data are available.

Generally coal rank increases with depth; it is therefore unrealistic to model a constant rank coal from 0 to 1500 metres. In fact the rank should increase with depth. Equation A can be modified with a term that allows for the consideration of a coalification gradient. Coalification gradients are expressed as the change in $\bar{R}_{max}$ per 100 metres. If a start-depth, mean maximum reflectance value and coalification gradient are specified, then a gas content versus depth profile can be calculated that cuts across the equi-rank curves.

Another way of estimating *in situ* lost and adsorbed methane was introduced by Kim (1977). This method uses proximate coal-quality data and information about the level of saturation of the coal. It is possible to computerize the Kim equations and compare results with those obtained from Equation A and the five rank equations. Generally results compare quite well. Exact comparisons between the Kim equations and Equation A are difficult because of the "degree of saturation" constant required by the Kim equation but not present in equation A. Karweil (1969) introduced an equation (reproduced in Meissner, 1984) for estimating cumulative methane generation for coals with volatile contents less than 37.8 per cent. Meissner (1984) also developed a series of equations that describe the relationship between volatile matter and mean maximum reflectance. It is possible to predict the cumulative methane generated by a coal for which the lost and adsorbed gas content is also calculated by using the equations of Karweil and Meissner. Obviously the difference between cumulative methane generated and methane retained is the gas available to charge adjacent reservoirs.

A computer program has been written that incorporates the equations in Table 4-1-1 and is available on request. An example of the output is included as Figure 4-1-2. It permits simple modelling of maximum potential methane resource under different conditions of depth, rank, ash content, moisture content and coalification gradient.

CONCLUSIONS

A simple equation is introduced that facilitates the initial estimation of maximum potential methane resource for coal from a wide range of depths and for a wide range of ranks. Recoverable reserves are often 50 to 10 per cent of initial resource estimates. In many cases a useful estimate of recoverable coalbed methane requires drilling and desorption tests.

REFERENCES

American Association of Petroleum Geologists (1989): Studies in Geology, Series 17.

METHANE RETENTION USING EQUATION A AND GENERATION USING KARWEIL

DEPTH METRES	DEPTH FEET	METHANE RETAINED SCF	METHANE RETAINED c/g	METHANE GENERATED c/g	REFLECTANCE R MAX	VOLATILES VM DAF %
100.00	328.08	232.00	7.24	27.52	1.10	31.11
200.00	656.16	323.56	10.10	31.74	1.15	30.20
300.00	984.24	382.31	11.93	36.08	1.20	29.29
400.00	1312.32	427.21	13.33	40.56	1.25	28.38
500.00	1640.40	464.27	14.49	45.18	1.30	27.46
600.00	1968.48	496.19	15.49	49.96	1.35	26.55
700.00	2296.56	524.45	16.37	54.91	1.40	25.64
800.00	2624.64	549.93	17.17	60.04	1.45	24.72
900.00	2952.72	573.23	17.89	65.36	1.50	23.81
1000.00	3280.80	594.74	18.56	70.89	1.55	22.90
1100.00	3608.88	614.77	19.19	76.64	1.60	21.98
1200.00	3936.96	633.53	19.77	82.64	1.65	21.07
1300.00	4265.04	651.21	20.33	88.90	1.70	20.16
1400.00	4593.12	667.93	20.85	95.46	1.75	19.25
1500.00	4921.20	683.82	21.34	102.33	1.80	18.33

Figure 4-1-2. Example of output from program incorporating equations found in Table 4-1-1.

Eddy, G.E., Rightmire, C.T. and Byren, C.W. (1982): Relationship of Methane Content of Coal Rank and Depth: Theoretical vs. Observed; *Society of Petroleum Engineers, Department of the Interior*, Proceedings, Unconventional Gas Recovery Symposium, Pittsburg, Pennsylvania, SPE/DOE 10800, pages 117-122.

Karweil, J. (1969): Aktuelle Problem der Geochemic der Kohle; *in* Advances In Geochemistry (1968); Schenk P.A. and Havernaar I., Editors, *Oxford Pergamon Press*, pages 59-84.

Kim, A.G. (1977): Estimating Methane Content of Bituminous Coalbeds from Adsorption Data; *U.S. Bureau of Mines*, Report of Investigations 8245.

Meissner, F.F. (1984): Cretaceous and Lower Tertiary Coals as Sources for Gas Accumulations in the Rocky Mountain Area; *in* Hydrocarbon Source Rocks of the Greater Rocky Mountain Region, Woodward, J., Meissner, F.F. and Clayton, J.L., Editors, *Rocky Mountain Association of Geologists*, 1984 Symposium, pages 401-431.

Ryan, B.D. (1990): Geology and Potential Coal and Coalbed Methane Resource of the Tuya River Coal Basin, British Columbia; *in* Geological Fieldwork 1990, *B.C. Ministry of Energy, Mines and Petroleum Resources*, Paper 1991-1, pages 419-429.

Ward, C.R. (1984): Coal Geology and Coal Technology; *Blackwell Scientific Publications*, page 96.

RELATIONSHIPS BETWEEN COAL QUALITY PARAMETERS IN BRITISH COLUMBIA COALS

By D.A. Grieve

KEYWORDS: Coal quality, British Columbia, vitrinite reflectance, volatile matter, hydrogen/carbon ratio, rheology, calorific value, ash content.

INTRODUCTION

One of the main objectives of the Coal Quality Project in the British Columbia Geological Survey Branch is to demonstrate how British Columbia coals fit into accepted coal classification systems, and to derive the implied technical utilization potential of our coals. The quality of a given coal can, for many purposes, be considered to be made up of three components, its grade, rank and type (Snyman, 1989), and most classification systems utilize one or more of these components. One proposed system, the so-called "Alpern" classification (Alpern *et al.*, 1989), uses indicators of all three components.

Grade refers to the amount, type and association of mineral matter in coal. Ash content and washability characteristics are two familiar coal properties which are largely dependent on grade. Washability of British Columbia coals is discussed by Holuszko (1992, this volume). Rank refers to the position of a given coal within the metamorphic gradation from peat to meta-anthracite. Many coal properties vary with rank (vitrinite reflectance, ultimate carbon and volatile matter are three examples), but vitrinite reflectance is considered to be useable over a wider range of ranks than any of the others (Bustin *et al.*, 1985). Vitrinite reflectance increases with increasing rank. Type refers to the organic constituent make-up of a coal, and a maceral analysis is the best and most direct way of determining coal type.

As a preliminary step in this endeavour, a series of x-y graphs (scatterplots) demonstrating correlations between

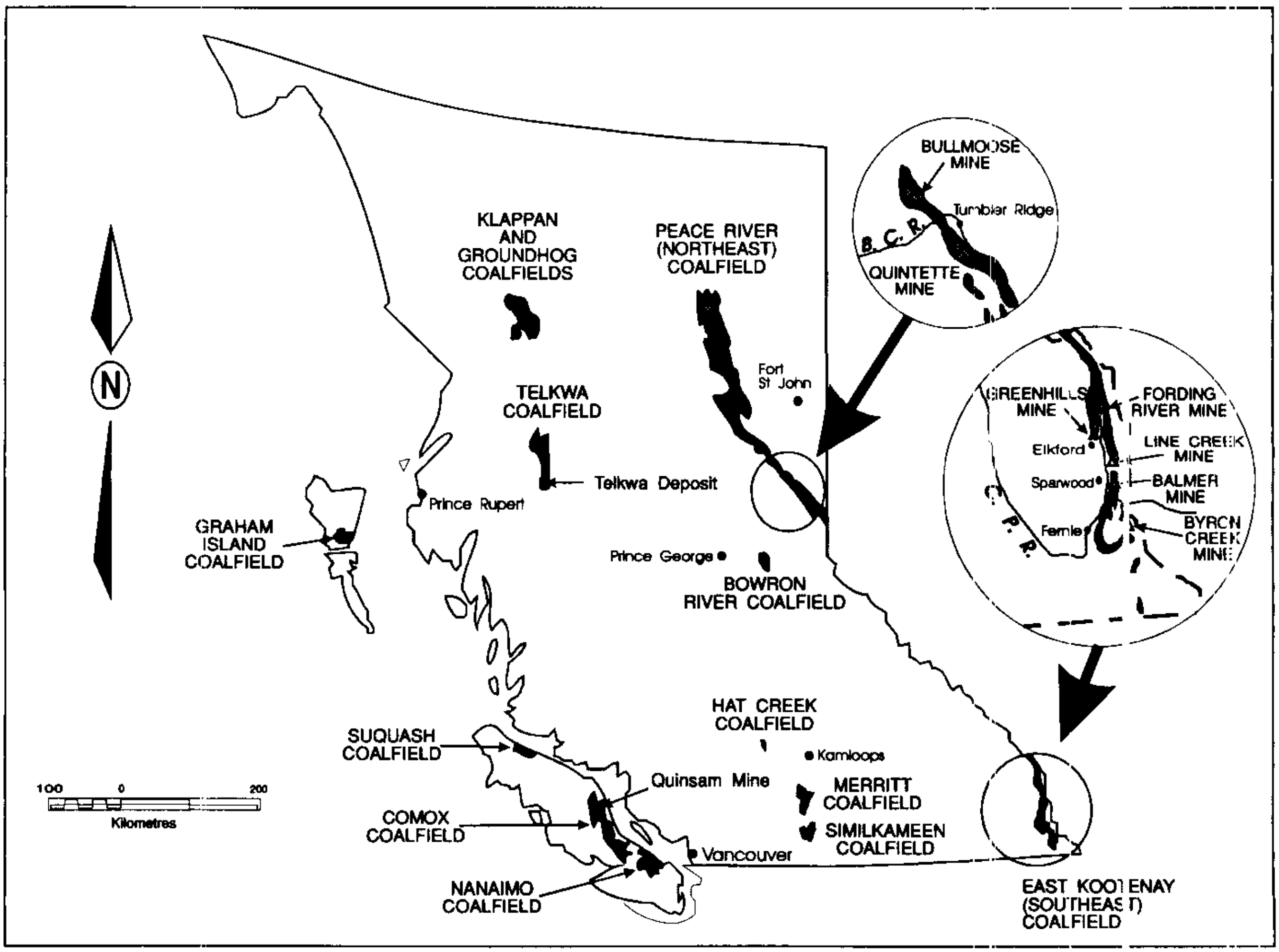

Figure 4-2-1. Locations of British Columbia coal deposits.

coal quality parameters has been generated, together with corresponding regression lines and correlation coefficients. The emphasis is on vitrinite reflectance. Establishment of these relationships will ultimately lead to identification of the coal quality parameters and classification systems which are most appropriate to our coals.

There are three sources of the data presented here: exploration assessment reports, the British Columbia Coal Quality Catalog (2nd edition; Grieve, in press) and analyses of raw run-of-mine coal samples collected at all operating coal mines in the province in 1990. The sources of individual data points are not identified, ensuring confidentiality.

GEOLOGICAL SETTING

British Columbia coal deposits range from Late Jurassic to Tertiary in age, and occur in three of the six major tectonic belts. Coalfields and deposits considered in this article include the Peace River or northeast coalfield, the East Kootenay or southeast coalfields, the Telkwa deposit, the Klappan coalfield, the Hat Creek coalfield and the Comox coalfield (Figure 4-2-1). They represent the whole range of ages and tectonic settings of British Columbia coals.

Coal in the East Kootenay coalfields belongs to the Mist Mountain Formation of the Jurassic-Cretaceous Kootenay Group, and occurs in the Front Ranges of the Rocky Mountains. Gates and Gething Formation coals from the Peace River coalfield are Early Cretaceous in age, and occur in the Foothills of the Rocky Mountains. The Intermontane tectonic belt contains the Klappan coalfield and Telkwa deposit of northwestern British Columbia, and the Hat Creek coalfield of south-central British Columbia. The Klappan coalfield is hosted by the Jurassic-Cretaceous Bowser Lake Group, and the Telkwa deposit by the Early Cretaceous Skeena Group. Hat Creek coal is Eocene in age, and contained in the Kamloops Group. Lastly, the Insular tectonic belt contains the Quinsam mine in the Comox coalfield, where coals are Late Cretaceous in age and belong to the Nanaimo Group.

SAMPLING AND ANALYSIS

A total of 36 raw run-of-mine coal samples was collected at all eight of the province's coal mines in the summer of 1990 (*see* Table 4-2-1 for a list of samples, and Figure 4-2-1 for mine locations). The samples, which were approximately 30 kilograms in weight, were collected from piles of excavated coal in the pits, and each sample represents one seam. In the case of the underground coal sample from Quinsam mine, the pile of coal on the surface at the end of the conveyor was sampled.

Samples were processed and analyzed for chemical and rheological properties according to ASTM standard conditions and procedures. Representative splits of −20-mesh coal were supplied to the author for petrographic analysis, using vitrinite reflectance techniques developed by Kilby (1988).

TABLE 4-2-1
LIST OF RAW RUN-OF-MINE COAL SAMPLES COLLECTED AT ACTIVE MINES IN 1990

Sample	Property	Pit	Seam
90-01	Balmer	Camp 8 Ext.	8UX
90-02	Balmer	A	A
90-03	Balmer	Baldy 8UA	7RC
90-04	Balmer	Adit 29E	10 (Balmer)
90-05	Balmer	Adit 29E	8UC
90-06	Line Creek	Main	10A
90-07	Line Creek	Main	10B
90-08	Line Creek	Main	9
90-09	Line Creek	North Line	7
90-10	Line Creek	North Line	8
90-11	Greenhills	Cougar 2	20
90-12	Greenhills	Cougar 2	16 (upper 1/2)
90-13	Greenhills	Cougar 2	16 (lower 1/2)
90-14	Greenhills	Cougar 3	17
90-15	Greenhills	Bighorn	10
90-16	Greenhills	Falcon	1
90-17	Byron Creek	14	1 (Mammoth)
90-18	Byron Creek	12	1 (Mammoth)
90-19	Byron Creek	14	1 (Mammoth)
90-20	Fording	Taylor	4
90-21	Fording	Taylor	5
90-22	Fording	Taylor	11 upper
90-23	Fording	Eagle	15
90-24	Fording	Eagle South	14-2
90-25	Fording	Eagle South	13
90-26	Fording	Brownie	9
90-27	Bullmoose		A1
90-28	Bullmoose		B
90-29	Bullmoose		C
90-30	Bullmoose		D
90-31	Bullmoose		E
90-32	Quintette	Deputy	J
90-33	Quintette	Mesa	E
90-34	Quintette	Wolverine	F
90-35	Quinsam	Underground	1
90-36	Quinsam	Surface	1

MAXIMUM VERSUS RANDOM REFLECTANCE

The set of 36 samples was subjected to determination of petrographic rank (vitrinite reflectance). As both mean maximum ($\bar{R}_{max}$) and mean random ($\bar{R}_m$) reflectance are routinely determined in our lab, it is possible to compare these parameters over the range of ranks of productive coal seams in the province. Figure 4-2-2 shows their relationship, and indicates that there is almost perfect correlation between them (r=0.997). The regression equation is:

$$\bar{R}_{max} = -0.0632 + 1.107\ \bar{R}_m.$$

There is some suggestion that the slope of the regression line is diminishing at the high rank end.

Given the high coefficient, this equation can serve as a reliable conversion formula for British Columbia high-volatile A and medium-volatile bituminous coals. Its application to petrographic rank boundaries is provided under "Discussion and Summary."

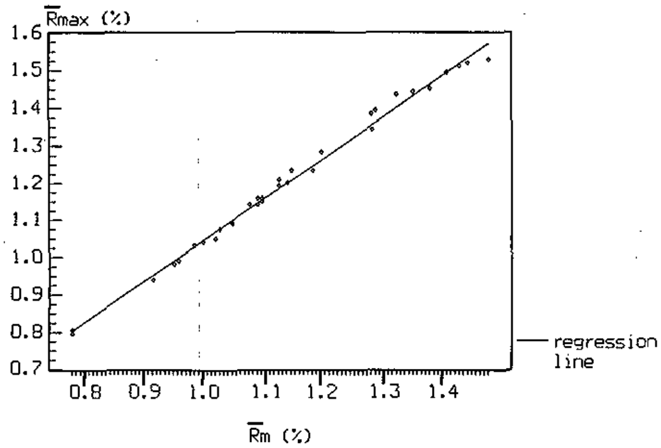

Figure 4-2-2. $\bar{R}_{max}$ versus $\bar{R}_m$ for raw run-of-mine samples collected at active coal mines in 1990. The regression equation and correlation coefficient are given in the text.

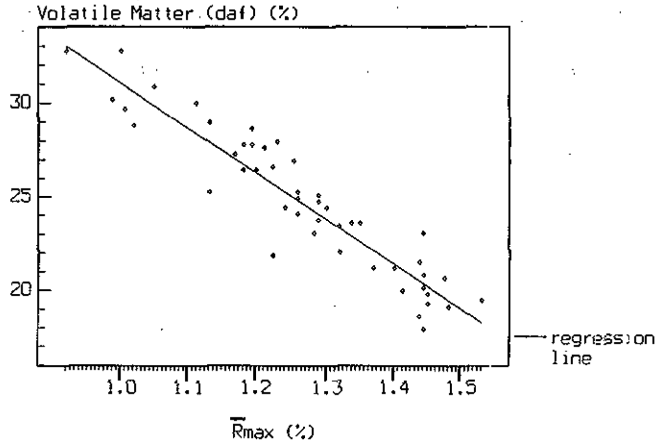

Figure 4-2-5. $\bar{R}_{max}$ versus volatile matter for clean Mist Mountain Formation coals in the East Kootenay coalfields. All data are from assessment reports. *See* Table 4-2-2 for correlation coefficient.

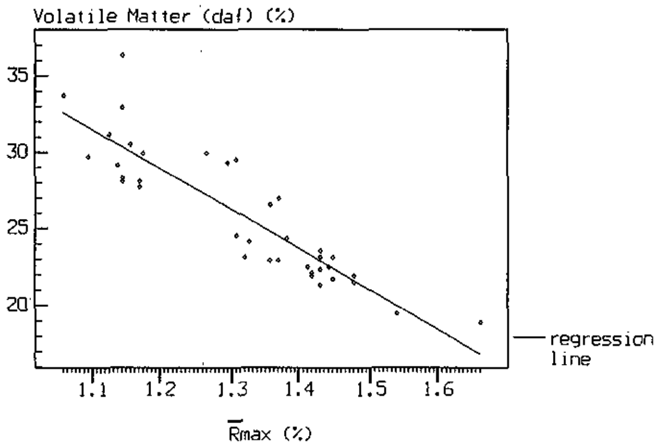

Figure 4-2-3. $\bar{R}_{max}$ versus volatile matter (daf) for clean Gething Formation coals in the Peace River coalfield. All data are from assessment reports. *See* Table 4-2-2 for correlation coefficient.

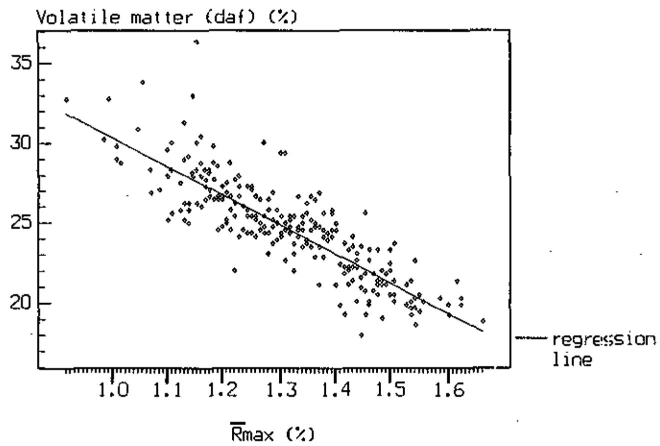

Figure 4-2-6. Combination of all data in Figures 4-2-3 to 5, representing clean coal in the Peace River and East Kootenay coalfields. *See* Table 4-2-2 for correlation coefficient.

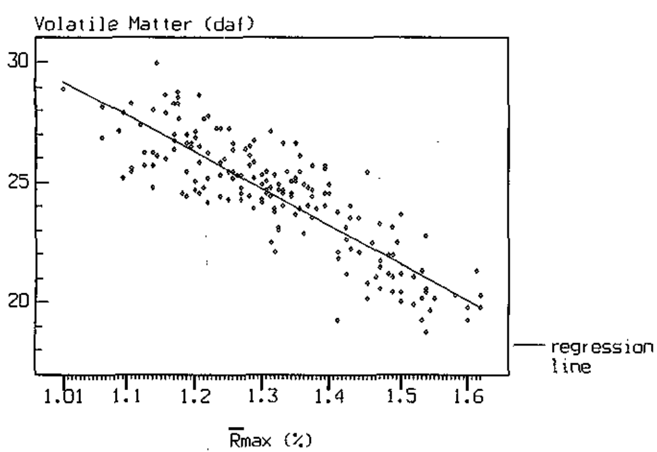

Figure 4-2-4. $\bar{R}_{max}$ versus volatile matter (daf) for clean Gates Formation coals in the Peace River coalfield. All data are from assessment reports. *See* Table 4-2-2 for correlation coefficient.

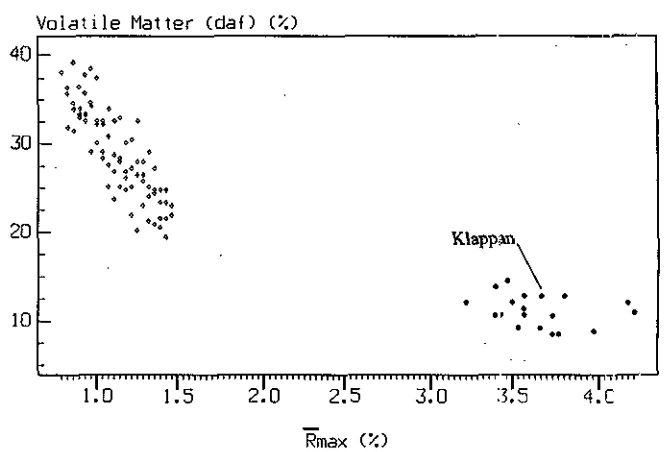

Figure 4-2-7. $\bar{R}_{max}$ versus volatile matter (daf) for raw coals from the Peace River, East Kootenay and Klappan coalfields. All data are from assessment reports.

VITRINITE REFLECTANCE VERSUS VOLATILE MATTER

Volatile matter on a dry, mineral matter free (dmmf) basis is the parameter used in the ASTM classification of coal by rank for coals of high-volatile A bituminous rank and higher (ASTM D388:1984). During coalification, as rank increases, volatile matter decreases, and thus there is an inverse relationship between vitrinite reflectance and volatile matter. A series of five graphs has been generated to explore this relationship in British Columbia coals (Figures 4-2-3 to 7). Correlation results for the Gething, Gates and Mist Mountain formations, assuming the relationships are linear over the observed rank range, are summarized in Table 4-2-2. Volatile matter has been converted to a dry, ash-free (daf) basis rather than the dmmf basis specified by the ASTM rank classification. This is because reliable formulae for converting ash to mineral matter contents have not been developed for British Columbia coals. All the data in Figures 4-2-3 to 7 have been taken from assessment reports. Most represent analyses of drill-core samples; no rotary-drill samples are included. With very few exceptions the drill-core recovery for all samples included is greater than 65 per cent. Both raw and clean coal data were collected, but as much as possible, clean coal data are presented here, as the correlation coefficients are consistently higher in clean coal.

Figure 4-2-3 shows the $\bar{R}_{max}$ versus volatile matter (daf) relationship for clean Gething Formation coals (Peace River coalfield). The correlation coefficient (r) is −0.89, and the degree of scatter is attributable to a number of factors. To begin with, volatile matter is controlled not only by rank, but also by type of coal. That is, at a given rank level, two coals of differing maceral compositions will have different volatile contents, with the more reactive-rich coal having the higher volatiles. Another factor is the varying amount and nature of mineral matter, as a portion of the volatile matter in any coal is derived from the inorganic fraction. Thirdly, these reflectance readings were generated by three or more different labs, which introduces potential systematic analytical errors of up to ±0.1 per cent $\bar{R}_{max}$ (Bustin *et al.*, 1985).

Figure 4-2-4 shows the $\bar{R}_{max}$ versus volatile matter (daf) relationship for clean Gates Formation coals (Peace River). The correlation coefficient is −0.85 and the comments concerning the origin of data scatter noted for Figure 4-2-3 apply here also.

TABLE 4-2-2
CORRELATION COEFFICIENTS (r)
VITRINITE REFLECTANCE VS. VOLATILE MATTER (DAF) IN CLEAN COALS OF THE PEACE RIVER AND EAST KOOTENAY COALFIELDS*

Coalfield	r	Critical r (99%)
Peace River (Gething)	−0.89	0.41
Peace River (Gates)	−0.85	0.19
East Kootenay	−0.93	0.36
Combined data	−0.84	0.16

* All data are from assessment reports

Figure 4-2-5 shows the $\bar{R}_{max}$ versus volatile matter (daf) relationship for clean East Kootenay coals. The correlation coefficient is −0.93 and the origins of scatter are also the same as for the data in Figure 4-2-3. If the clean coal data from the Peace River and East Kootenay coalfields are combined (Figure 4-2-6), the correlation coefficient is −0.84.

Figure 4-2-7 shows the $\bar{R}_{max}$ versus volatile matter (daf) relationship for raw coals from the Klappan coalfield, together with raw coals from the Peace River and East Kootenay coalfields for comparison. The Klappan coals are characterized by reflectance values above 3.0 per cent and volatile matter contents under 14 per cent. At this high rank level (anthracitic) reflectance is clearly not a good predictor of volatile matter.

VITRINITE REFLECTANCE VERSUS CARBON AND HYDROGEN

Correlations between $\bar{R}_{max}$ and chemical analytical results obtained on the 36 samples (Table 4-2-1) are shown in Table 4-2-3. Carbon and hydrogen contents in coal are determined, together with oxygen, nitrogen and sulphur, during an ultimate analysis. Carbon content, when expressed on a daf or dmmf basis, increases with rank, while hydrogen content decreases. Both can be used as rank indicators, and they are the two basic components of the well-known Seyler coal classification system (Carpenter,

TABLE 4-2-3
CORRELATION COEFFICIENTS (r)*
VITRINITE REFLECTANCE VS. CHEMICAL PARAMETERS IN RAW RUN-OF-MINE SAMPLES COLLECTED FROM ACTIVE COAL MINES IN 1990

Volatile Matter (daf)	−0.84
C (daf)	0.59
H (daf)	−0.68
H/C	−0.75
O (daf)	−0.56
O/C	−0.56

* Critical value of r is 0.41 at the 99 per cent confidence level.

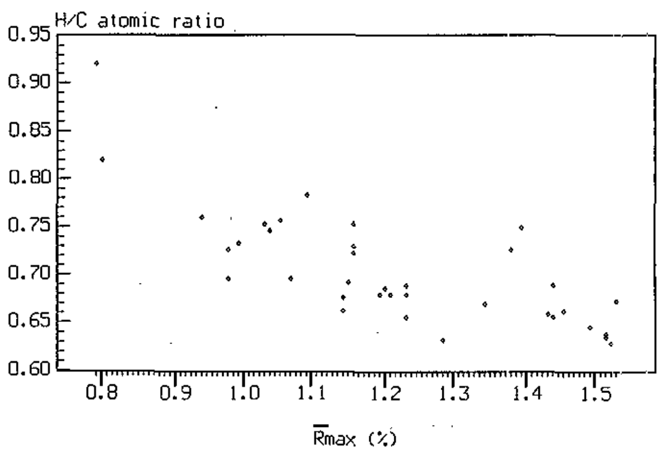

Figure 4-2-8. $\bar{R}_{max}$ versus the ratio H/C for raw run-of-mine samples collected at active coal mines in 1990. *See* Table 4-2-3 for correlation coefficient.

1988). Table 4-2-3 shows a significant positive correlation between carbon (daf) and $\bar{R}_{max}$ (r=0.59), and a significant negative correlation between hydrogen (daf) and $\bar{R}_{max}$ (r=−0.68). When expressed as the ratio hydrogen/carbon the negative correlation with $\bar{R}_{max}$ becomes stronger (r=−0.75). This relationship is shown in Figure 4-2-8. This suggests that the hydrogen/carbon ratio is probably a better rank indicator than either element by itself for coals currently being produced in British Columbia, although it is still not as good an indicator as volatile matter (daf; r=−0.84 in Table 4-2-3). The last relationship was considered in some depth in the previous section, based on larger data populations.

VITRINITE REFLECTANCE VERSUS RHEOLOGICAL PROPERTIES

The set of 36 samples was tested for fluidity and dilatation properties. Correlation coefficients between $\bar{R}_{max}$ and Geiseler fluidity parameters are shown in Table 4-2-4 and between $\bar{R}_{max}$ and dilatation parameters are shown in Table 4-2-5. In the former case one sample did not soften, and so the matrix is based on 35 samples. In the latter case, all 36 samples contracted, but only 12 had a positive net dilatation. Therefore, the correlations involving maximum dilatation and temperature of maximum dilatation are based on only 12 sets of results.

The temperatures recorded during the fluidity test, namely the temperatures of initial softening, maximum fluidity and resolidification, are positively correlated to a significant degree with $\bar{R}_{max}$ (Table 4-2-4). Figures 4-2-9 and 4-2-10 show the relationship between $\bar{R}_{max}$ and temperatures of initial softening (r=0.64) and maximum fluidity (r=0.77), respectively. In other words, critical temperatures of fluidity increase with rank of coal, through the rank range represented. The fluid temperature range of these samples is not correlated to $\bar{R}_{max}$, and the actual value of the fluidity, in dial divisions per minute, is only marginally correlated, in a negative manner, with $\bar{R}_{max}$.

None of the parameters derived from the dilatation analysis show significant correlation with $\bar{R}_{max}$ (Table 4-2-5).

TABLE 4-2-4
CORRELATION COEFFICIENTS (r)*
VITRINITE REFLECTANCE VS. GEISELER FLUIDITY IN RAW RUN-OF-MINE SAMPLES COLLECTED FROM ACTIVE COAL MINES IN 1990

Initial softening temp.	0.64
Temp. of maximum fluidity	0.77
Temp. of resolidification	0.58
Fluid range	−0.35
Maximum fluidity	−0.46

* Critical value of r is 0.42 at the 99 per cent confidence level.

TABLE 4-2-5
CORRELATION COEFFICIENTS (r)*
VITRINITE REFLECTANCE VS. DILATATION IN RAW RUN-OF-MINE SAMPLES COLLECTED FROM ACTIVE COAL MINES IN 1990

Softening temp.	0.31
Maximum contraction	0.06
Temp. of maximum dilatation	−0.02
Maximum dilatation	0.15

* Critical values of r at the 99 per cent confidence level — softening temperature and maximum contraction: 0.41; maximum dilatation and temperature of maximum dilatation: 0.661.

CALORIFIC VALUE VERSUS ASH CONTENT

Calorific value on a moist, mineral matter free (mmmf) basis is the rank parameter used in the ASTM classification for low-rank coals (up to high-volatile A bituminous). It increases with increasing rank over the low-rank range. When not expressed on an ash-free or mineral matter free basis, however, calorific value can be a very good indicator of the grade of a coal deposit (Cameron, 1989). As the amount of inorganic material, expressed as ash or mineral matter, increases, the calorific value of a coal decreases. A

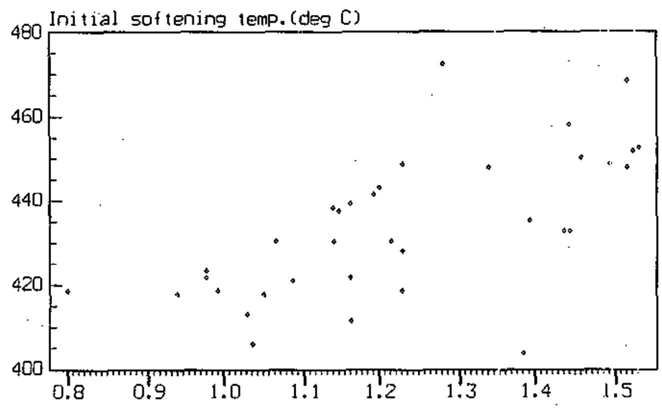

Figure 4-2-9. $\bar{R}_{max}$ versus initial softening temperature for raw run-of-mine samples collected at active coal mines in 1990. *See* Table 4-2-4 for correlation coefficient.

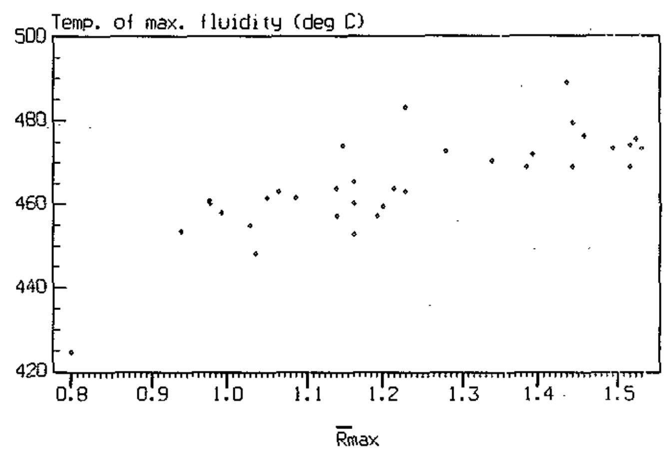

Figure 4-2-10. $\bar{R}_{max}$ versus temperature of maximum fluidity for raw run-of-mine samples collected at active coal mines in 1990. *See* Table 4-2-4 for correlation coefficient.

series of six graphs showing the relationship between calorific value and ash content has been generated for raw coals in five British Columbia coalfields (Figures 4-2-11 to 16). Results are summarized in Table 4-2-6. All the data are originally from assessment reports, but are not intended to be a comprehensive collection of the data available for each deposit. They mainly represent drill-core samples, with the exception of the East Kootenay data (Figure 4-2-13), which represent bulk and channel samples. The East Kootenay and Hat Creek data (Figure 4-2-14) are expressed on a dry basis, while the data for the other coalfields are expressed on an air-dried (ad) basis.

The results show very strong inverse relationships between ash content and calorific value for raw coals from all coalfields. Correlation coefficents are all between −0.9 and −1.0, with some being extremely close to the latter value (Table 4-2-6). The poorest correlation, which is for data from the Telkwa deposit (Figure 4-2-15), represents the smallest range in ash values. It is a safe and obvious assumption that coal grade is a major factor influencing calorific value of raw coals in British Columbia.

In order to compare the various coalfields, calorific values at an arbitrary 15 per cent raw-ash content have been predicted, based on the calorific value versus ash relationships shown in Figures 4-2-11 to 16. The predictions are presented for discussion purposes only and are not intended to be rigorous or realistic, because they do not include the statistical uncertainty of the predictions, and because product coals are obviously much higher in moisture than air-dried or dry coals. In the case of Hat Creek, moreover, the 15 per cent ash level is lower than in any potential unbeneficiated product.

The predicted values are as follows: Gething Formation, Peace River, 29.01 megajoules per kilogram (ad); Gates Formation, Peace River, 30.09 (ad); East Kootenay, 29.23 (dry); Hat Creek, 25.33 (dry); Telkwa, 28.59 (ad); Klappan, 29.09 (ad). Note that the East Kootenay value would be reduced by only 1 to 2 per cent if recalculated on an air-dried basis. These results indicate that the predicted cal-

TABLE 4-2-6
CORRELATION AND REGRESSION COEFFICIENTS CALORIFIC VALUE VS. ASH CONTENT, RAW BRITISH COLUMBIA COALS*
(MEGAJOULES/KILOGRAM)

Coalfield	r	Critical r (99%)	Intercept	Slope
Peace River (Gething) *ad basis*	−0.94	0.42	34.41	−0.36
Peace River (Gates) *ad basis*	−0.99	0.83	35.80	−0.38
East Kootenay *dry basis*	−0.99	0.68	34.58	−0.36
Hat Creek *dry basis*	− 0.999	0.80	30.97	−0.38
Telkwa *ad basis*	−0.92	0.71	34.18	−0.37
Klappan *ad basis*	−0.99	0.42	34.95	−0.39

* All data are from Grieve (in press)

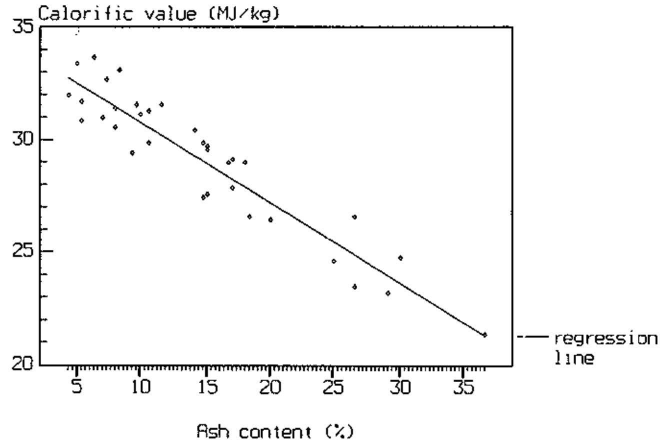

Figure 4-2-11. Calorific value (air-dried) versus ash content for raw coals from the Gething Formation in the Peace River coalfield. Data are taken from Grieve (in press). *See* Table 4-2-6 for results of linear regression analysis.

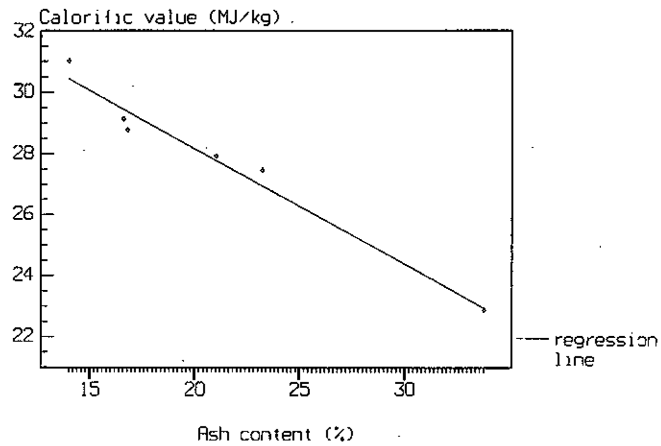

Figure 4-2-12. Calorific value (air-dried) versus ash content for raw coals from the Gates Formation in the Peace River coalfield. Data are taken from Grieve (in press). *See* Table 4-2-6 for results of linear regression analysis.

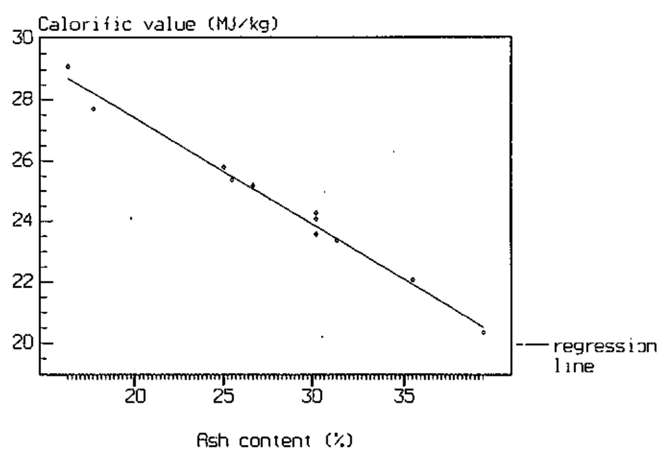

Figure 4-2-13. Calorific value (dry) versus ash content for raw coals from the Mist Mountain Formation in the East Kootenay coalfields. Data are taken from Grieve (in press). *See* Table 4-2-6 for results of linear regression analysis.

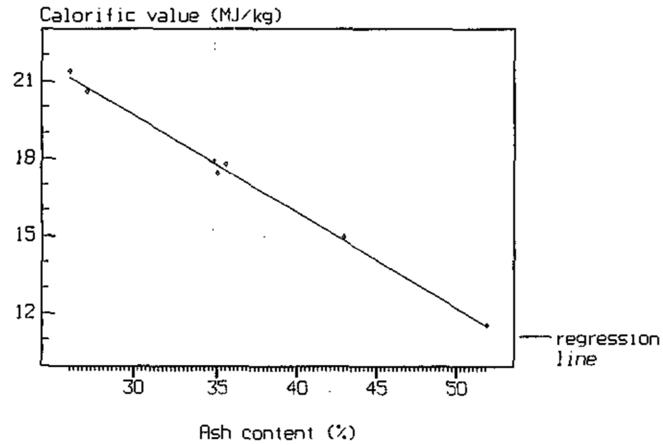

Figure 4-2-14. Calorific value (dry) versus ash content for raw coals from the Hat Creek coalfield. Data are taken from Grieve (in press). *See* Table 4-2-6 for results of linear *regression analysis.*

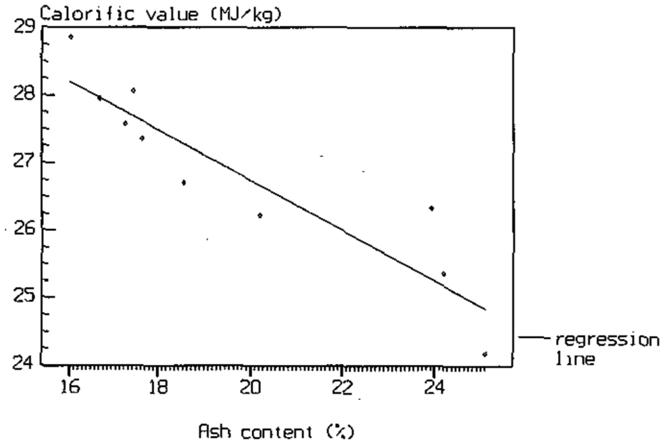

Figure 4-2-15. Calorific value (air-dried) versus ash content for raw coals from the Telkwa deposit. Data are taken from Grieve (in press). *See* Table 4-2-6 for results of linear *regression analysis.*

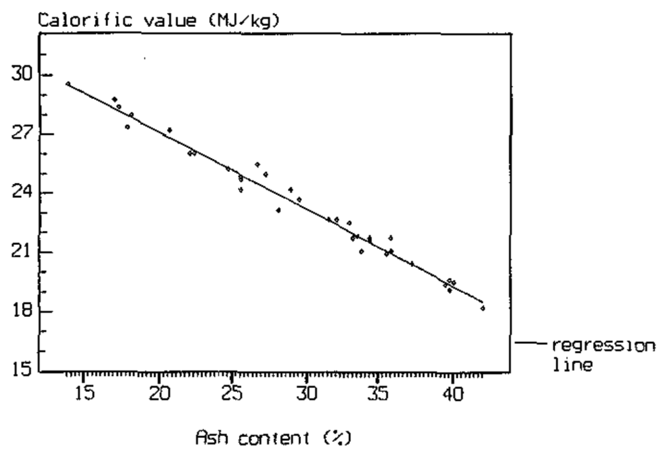

Figure 4-2-16. Calorific value (air-dried) versus ash content for raw coals from the Klappan coalfield. Data are taken from Grieve (in press). *See* Table 4-2-6 for results of linear regression analysis.

orific values of raw, air-dried coals from the Peace River, East Kootenay, Telkwa and Klappan coalfields, at the given ash level of 15 per cent, are all on the order of 29 to 30 megajoules per kilogram. The deposit with the lowest average rank of this group, Telkwa, has the lowest predicted calorific value, while the Gates Formation has the highest. This general similarity in predicted values does not imply that coals from these four regions will behave similarly in actual usage. There are significant differences between them in volatile matter, mineral matter composition and coal type; all these factors have a potentially large influence on coal behaviour during combustion.

DISCUSSION AND SUMMARY

Given that vitrinite reflectance is a widely used and applicable coal rank parameter, correlation results obtained in this study (Table 4-2-3) suggest that volatile matter content (daf), the hydrogen/carbon ratio, hydrogen content (daf) and carbon content (daf), in order of decreasing effectiveness, are to some extent also rank indicators in the high-volatile A through medium-volatile bituminous range in British Columbia coals.

The correlations between $\bar{R}_{max}$ and volatile matter content (daf) in the Rocky Mountain coalfields are strongly negative (−0.84 to −0.93; Tables 4-2-2 and 3). Despite these high correlations the reflectance versus volatile matter (daf) relationships illustrated by Figures 4-2-3 to 5 display a considerable amount of scatter and can not be used to predict the volatile matter content of specific reflectance levels, except in a very approximate way. The sources of these uncertainties were summarized earlier. As an example of their influence, based on inspection of the actual data points shown in Figure 4-2-4, a clean Gates Formation coal with a reflectance of 1.3 per cent might have between 22 and 27 per cent volatile matter content (daf).

It is also inappropriate to use the graphs in Figures 4-2-3 to 6 to determine reflectance values corresponding to rank category boundaries. These should only be determined on vitrinite concentrates or coals with uniformly high vitrinite contents. A good evaluation of variations in fixed carbon (dmmf) with reflectance in Western Canadian coals was published recently by Cameron (1989). He recommends using 0.95 per cent $\bar{R}_m$ as the boundary between ASTM high-volatile A and medium-volatile bituminous coals, and 1.45 per cent for the ASTM medium-volatile/low-volatile bituminous boundary. Using the relationship between $\bar{R}_{max}$ and $\bar{R}_m$ established earlier in this paper, these values can be converted to 0.99 and 1.54 per cent $\bar{R}_{max}$. This is a slightly wider range for medium-volatile coals than I have used previously (1.1 to 1.5 per cent), but I consider Cameron's new boundaries to be valid and applicable.

Fluidity and dilatation tests have been shown to be inappropriate measures of the coking potential of Western Canadian coals (Price and Gransden, 1987). Nevertheless, the actual temperatures of fluid behaviour of an individual coal are very important parameters in coke production from coal blends. This is because there must be overlap between the fluid temperature ranges among the various coals in the blend. These preliminary results show that critical fluidity temperatures are partly dependent on rank of coal.

Strong inverse relationships, with correlation coefficients ranging from −0.92 to −0.999, between ash content and calorific value for raw British Columbia coals (Table 4-2-6) substantiate the well-known dilutant effect of ash on calorific value. Crude predictions based on these relationships suggest that at 15 per cent ash, raw coals of high-volatile A bituminous through anthracitic rank have calorific values (ad basis) that are on the order of 29 to 30 megajoules per kilogram.

ACKNOWLEDGMENTS

I am very grateful to staff at all eight of British Columbia's coal mines for permission and assistance in collecting samples in the summer of 1990. Joanne Schwemler carried out all vitrinite reflectance analyses. Ongoing discussions with colleagues Maria Holuszko, Barry Ryan and Ward Kilby are very beneficial to this study.

REFERENCES

Alpern, B., Lemos de Sousa, M.J. and Flores, D. (1989): A Progress Report on the Alpern Coal Classification; *International Journal of Coal Geology*, Volume 13, pages 1-19.

Bustin, R.M., Cameron, A.R., Grieve, D.A. and Kalkreuth, W.D. (1985): Coal Petrology – Its Principles, Methods and Applications, 2nd Edition; *Geological Association of Canada*, Short Course Notes, Volume 3, 230 pages.

Cameron, A.R. (1989): Relationship of Petrographic and Chemical Parameters in Coal Rank Evaluation for Western Canadian Coals; *in* Advances in Western Canadian Coal Geoscience, *Alberta Research Council*, Information Series No. 103, Pages 225-232.

Carpenter, A.M. (1988): Coal Classification; *IEA Coal Research*, London, 104 pages.

Grieve, D.A. (in press): British Columbia Coal Quality Catalog, 2nd Edition; *B.C. Ministry of Energy, Mines and Petroleum Resources*, Information Circular.

Holuszko, M.E. (1992): Washability Characteristics of British Columbia Coals; *in* Geological Fieldwork 1991, Grant, B. and Newell, J.M., Editors, *B.C. Ministry of Energy, Mines and Petroleum Resources*, Paper 1992-1, this volume.

Kilby, W.E. (1988): Recognition of Vitrinite with Non-uniaxial Negative Reflectance Characteristics; *International Journal of Coal Geology*, Volume 9, pages 267-285.

Price, J.T. and Gransden, J.F. (1987): Metallurgical Coals in Canada: Resources, Research and Utilization; *Canada Centre for Mineral and Energy Technology (CANMET)*, Report 87-2E, 71 pages.

Snyman, C.P. (1989): The Role of Coal Petrography in Understanding the Properties of South African Coal; *International Journal of Coal Geology*, Volume 14, pages 83-101.

WASHABILITY OF PEACE RIVER AND EAST KOOTENAY COALS

By M.E. Holuszko

KEYWORDS: Coal geology, coal quality, washability, degree of washing, washability number, liberation characteristics, coal petrography, mineral matter, lithotypes.

INTRODUCTION

This study is concerned with the washability characteristics of British Columbia coals from different seams, geological formations, coalfields and regions. In the initial stage of the project, compilation of washability data from all over the province was completed. Analysis of the data and relating it to known geological conditions as well as seam characteristics became the major task of the project. Classical washability parameters were used together with the washability number and degree-of-washing parameters. A comparison of coal washability from different regions was also a part of the washability analysis process. Special emphasis was put on comparing the washability numbers between coal seams, as this parameter appears to be a better indicator of ease of washing of a coal seam. It defines the boundary between free mineral matter and mineral matter intergrown with coal. It also gives a scale of difficulties associated with cleaning, to a specific clean-coal product.

Coals discussed in this paper are from two major British Columbia coalfields: the northeast or Peace River area and the southeast or East Kootenay area (Figures 4-3-1 and 2). Due to complex geological conditions in both regions, local changes in coal quality are quite common. Variations are not only within the formations, but also among the individual seams. Therefore, using washability numbers for comparison is even more desirable, as they provide a single numeric measure of the variation.

BACKGROUND

The washability of any particular coal seam is directly related to the amount and type of mineral matter associated with the coal matter (macerals). The mode of association is a result of the sedimentation conditions that prevailed during formation of the coal seam.

Coal seams have their origin in peat-forming swamps and marshes. These swamps and marshes are formed from different plant communities, each having its own set of biological and geochemical conditions. Mixtures of macerals and minerals are formed in these environmentally distinct areas. The individual ecosystems control the formation and composition of different layers within the coal seam, referred to as lithotypes.

The compositional characteristics of lithotypes control the coal quality within the seams. Many physical, chemical and mechanical properties of coal are governed by the lithotype composition (Jeremic, 1980; Falcon and Falcon, 1987; Hower *et al.*, 1987; Hower, 1988; Hower and Lineberry, 1988). Stratigraphically, each seam represents a separate sequence of lithotypes, with specific coal quality in terms of type and grade.

From the washability point of view, the important aspects of coal quality are the amount and type of mineral matter found within the coal seam. The variation in mineral matter content is not only due to the association of macerals with minerals (lithotypes), but also due to mining methods, which may result in out-of-seam dilution. This effect, however, is reflected in a lower yield of clean product from a given seam.

An important factor in coal quality variability is folding and faulting of seams, resulting in shearing of coal. Shearing leads to increased friability of coals and results in a disproportionate amount of fines and poor washability characteristics (Bustin, 1982), as is the case in many of the coal-bearing formations in western Canada. The poor washability of sheared coals is especially evident when the shearing plane is close to the contact of a seam. This results in dissemination of comminuted floor or roof rock through the coal, as pointed out by Bustin, and difficulty arises in distinguishing and separating sheared rock from the coal seam.

The ease of washing, as traditionally measured by yield of clean coal, amount of near-gravity material and other washability parameters, is not always the best measure of the intrinsic character of a particular coal seam (Sarkar and Das, 1974; Sarkar *et al.*, 1977; Sanders and Brooks, 1986; Holuszko and Grieve, 1990). For example, clean coal yield is strongly influenced by the amount of out-of-seam dilution. Furthermore, yield-ash and density-yield relationships are coal dependent, and cannot be reliably used to compare washability of various coal seams, especially if the coals are of different origin.

The introduction of washability number by Sarkar and Das (1974) made it possible to classify and correlate coal seams in accordance with their inherent washability characteristics. The washability number appears to be the only parameter not affected appreciably by any large increase in extraneous mineral matter in the raw coal. When used in conjunction with other washability parameters it becomes a very useful tool to assess the ease of washing of coal.

OBJECTIVES

The aims of the project are threefold:

- To compile available washability data and create a computer database file for future use.
- To analyze the data in order to look for relationships between the washability characteristics and other inherent properties of coal, such as its rank and type.
- To accommodate washability parameters such as washability number and degree of washing into the new classification system (Alpern *et al.*, 1989) as an alternative to the yield of clean coal at preselected ash levels. Yield of clean coal is a purely technical term used to describe the final product and does not reflect the natural characteristics of coal.

PEACE RIVER COALFIELD

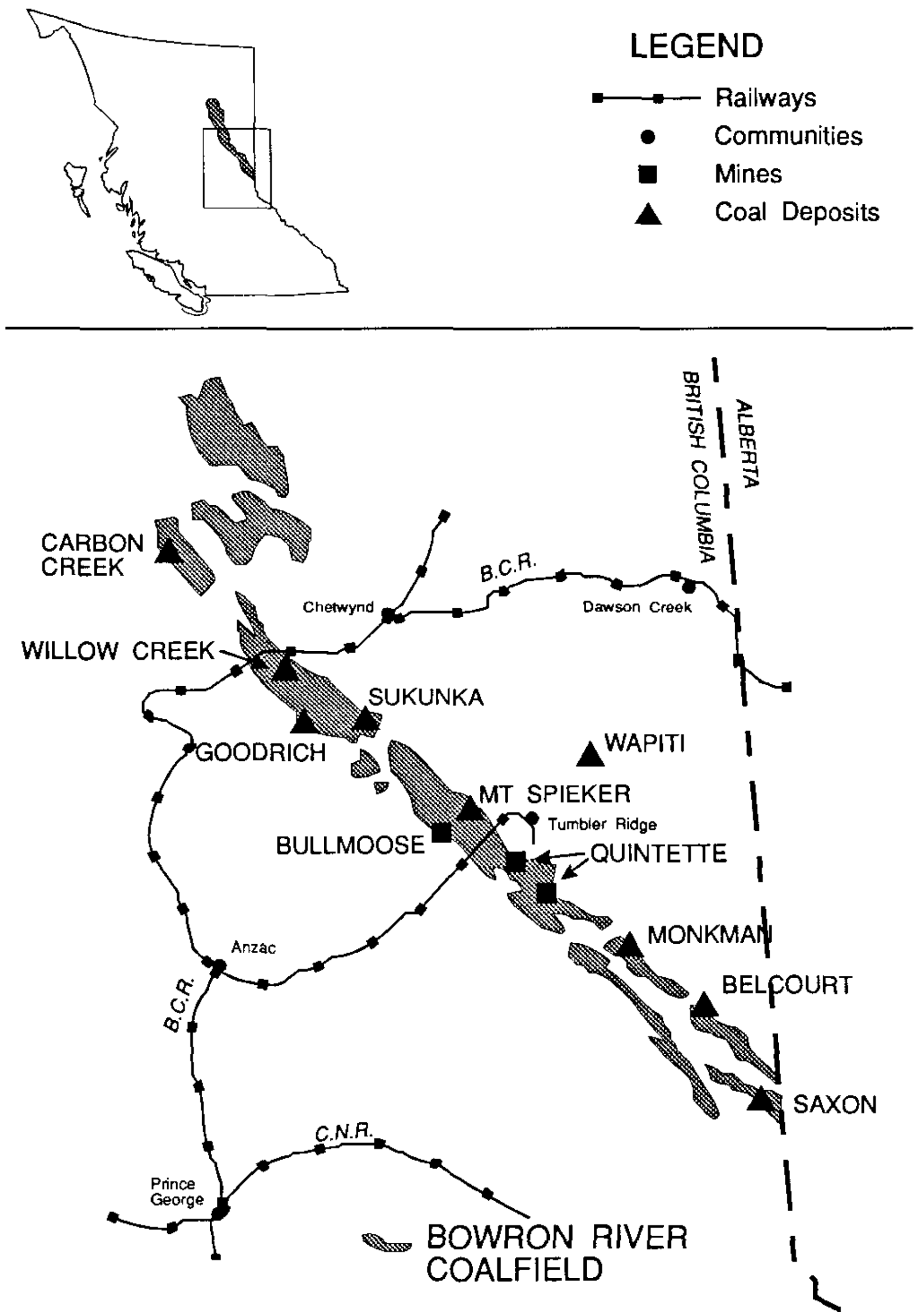

Figure 4-3-1. Coal deposits and location of mines in the study area; Peace River coalfield of northeast British Columbia.

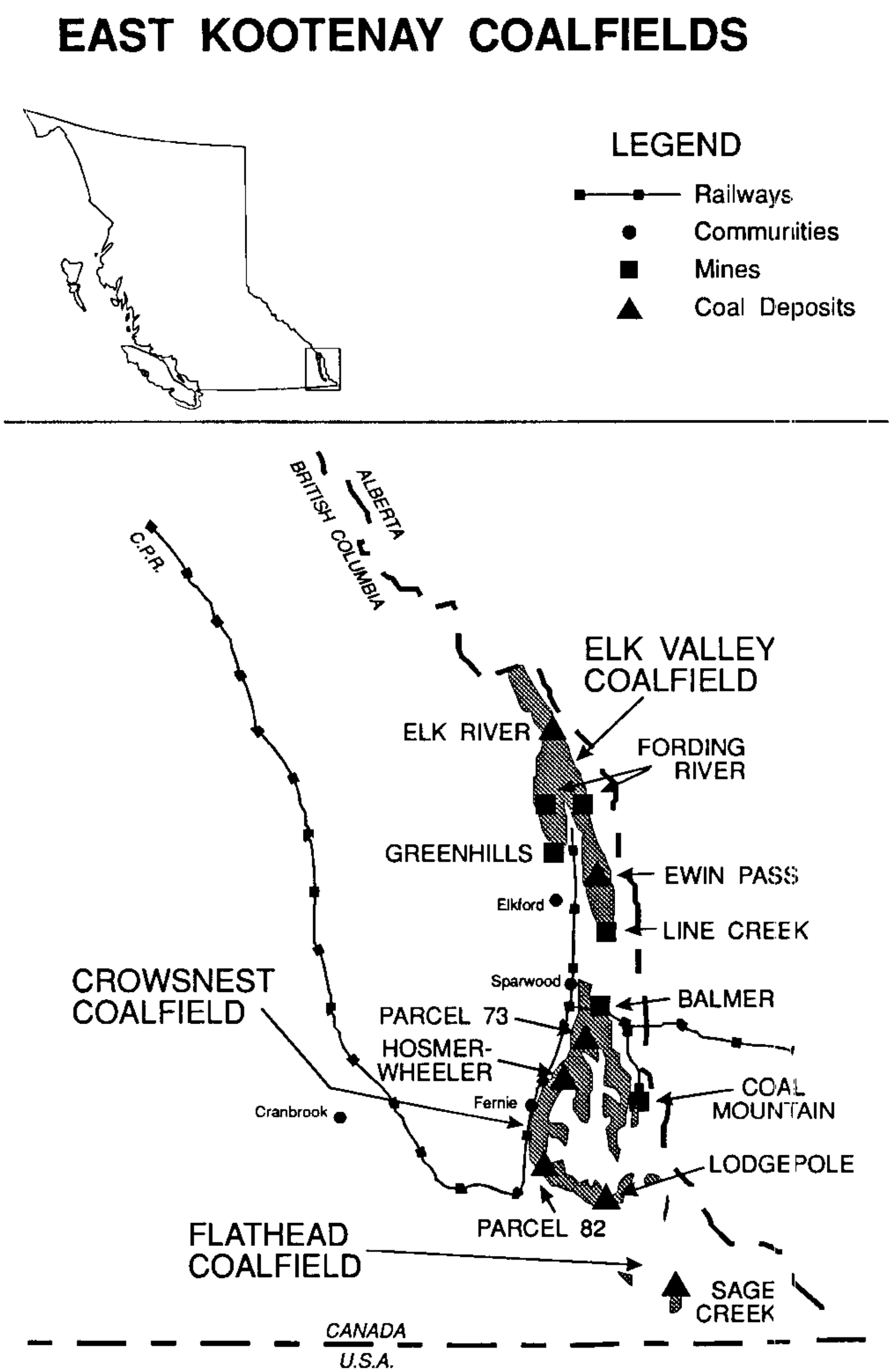

Figure 4-3-2. Coal deposits and locations of mines in the study area; East Kootenay coalfield of southeast British Columbia.

After compiling washability data from various British Columbia coalfields it became possible to compare washability characteristics of coal seams from different regions. The comparison of the two major coal-producing coalfields, Peace River and East Kootenay, is the subject of this paper.

GEOLOGICAL SETTINGS

Coal deposits in the Peace River and East Kootenay regions produce all of the metallurgical coal in the province. The coal measures lie within the Rocky Mountain Front Ranges and Foothills of British Columbia. The northeast British Columbia (Peace River) coalfield contains coals of Early and Late Cretaceous age, whereas the coal deposits in the southeast (East Kootenay) are of Jurassic-Cretaceous age. Coal-bearing strata throughout the region were deposited in deltaic and alluvial plain environments. Tectonism associated with mountain building has resulted in strongly faulted and folded coal measures. The coals are mainly medium to low-volatile bituminous in rank, and are generally very suitable for good quality coke (Smith, 1989).

PEACE RIVER COALFIELD

Coal deposits of the Peace River coalfield are found within the northern inner Foothills belt, which extends northwestwards for more than 300 kilometres from the Alberta - British Columbia border east of Prince George (Figure 4-3-1). The coal deposits occur in four different geological formations, but the major coal measures of the region are in the Early Cretaceous Gething Formation of the Bullhead Group and Early Cretaceous Gates Formation of the Fort St. John Group. The Gates Formation contains 70 per cent of commercially attractive coal measures (Smith, 1989). Coals of the Jurassic-Cretaceous Minnes Group and the Late Cretaceous Wapiti Formation are generally considered to be economically unattractive.

Structurally, the area is characterized by folding and thrust faulting, resulting in thickening of some of the coal seams. The least structural deformation is observed in the coal seam in the Wapiti Formation. In terms of coal quality, most of the seams in the region are classified as medium volatile with excellent coking characteristics and low sulphur, usually less than 1 per cent. The rank of coals in the Gates and Gething formations is in the range from high-volatile A to low-volatile, whereas the Wapiti Formation coal is of much lower rank, high-volatile C.

Early Cretaceous Gates Formation seams are characterized by relatively low vitrinite and high inertinite contents with negligible liptinite (Lamberson *et al.*, 1991; Marchioni and Kalkreuth, 1991). The lithotype composition of coal seams is highly variable, reflecting various depositional conditions during peat formation. In some seams banded lithotypes are predominant, in others brighter lithotypes are the most abundant, but generally banded lithotypes are characteristic of the Gates coals. The dull appearance of some lithotypes is due either to the presence of mineral matter, or an abundance of inertodetrinite and mineral matter, particularly quartz (Marchioni and Kalkreuth, 1991) or close proximity to clastic partings. According to Lamberson *et al.* (1991) differences in lithotype stratigraphy are due to variations in ground-water level as well as differences between wetland types. These lithotypes represent a continuous change in depositional environment from forest swamps (dry and wet) to dry herbaceous or shrubby marshes.

Coal seams from the upper part of Gething Formation are in general composed predominantly of bright lithotypes. The reported maceral analysis for these seams has shown that they are rather low (66%) in vitrinite content and high in inertinite macerals, mainly semifusinite and micrinite. The mineral matter content is exceptionally low. The carbonate minerals (mostly calcite) occur in cleats and fill cavities in semifusinite and fusinite; clays occur more rarely and are associated with massive vitrinite (Cook, 1972).

The coal at the base of the Late Cretaceous Wapiti Formation is the only seam in this formation with possible economic potential. It contains a great deal of mineral matter both from the dirt bands (partings) and inherent in the coal.

EAST KOOTNEY COALFIELD

The coal-bearing strata in southeast British Columbia are confined to the Mist Mountain Formation of the Jurassic-Cretaceous Kootenay Group. Mist Mountain coals are between high and low-volatile bituminous rank (Smith, 1989). Coal beds comprise 8 to 12 per cent of the stratigraphic thickness of the formation (Grieve, 1985). Coal seams in the lower part of the formation tend to be thicker and more continuous, and in some instances structural deformation has resulted in substantial thickening of seams (Grieve, 1985; Smith, 1989).

Structural deformation of coals in the Mist Mountain Formation has tremendous impact not only on the mining methods used but also on the coal quality. Faulting and folding have created many problems in terms of correlation of the seams, and in many cases discontinuity of the seams has complicated mine planning and development. The quality of coal has been deteriorated as a result of shearing (Bustin, 1982).

Petrographic composition of the Mist Mountain coals varies from inertinite-rich to vitrinite-rich, from the base to the top of the formation (Cameron, 1972; Grieve, 1985). This reflects a systematic variation in depositional environments, changing from an upper to a lower delta plain (Cameron, 1972). In terms of lithotype composition this is reflected by a brightening-upward (increasing in bright lithotypes) tendency in these coals.

SAMPLE SELECTION FOR WASHABILITY STUDY

Washability data for bulk samples from across the province were compiled from the Ministry's collection of coal exploration assessment reports. Data from the southeast and northeast coalfields were chosen for comparison here, as the majority of commercially producing seams are found in these two coalfields. Economically, the most significant coal seams are in the Gates and Mist Mountain formations, therefore, the study was limited to seams in these formations. For a list of samples see Table 4-3-1. The following criteria for sample selection were applied:

- Only bulk samples representing run-of-mine coal were used.
- A limit was imposed on ash content of raw coal to avoid biases caused by out-of-seam dilution; only samples with ash content of less than 35 per cent were considered.
- The washability data of attritted samples were preferred to the data on crushed samples (the non-attritted sample data were used when in accordance with the particular coal preparation plant practice).
- Samples do not necessarily represent the whole coalfield; they are rather considered to be representative of the seams which are contributing to coal production within the studied regions.
- A restriction was also imposed on the top-size of the samples; the upper limit of the top-size was restricted to maxima of 150 and 50 millimetres; a lower size limit of 0.50 millimetre was uniform for all the samples.
- *Crushed samples were used for the liberation studies;* in these tests the washability of the coal at a larger top-size was compared with the same coal crushed to significantly lower sizes.

METHODS

To compare washability characteristics of different coal seams, the following **washability parameters** were used: yield of clean coal curve, corresponding yield of rejects, and the near-gravity material-distribution curve. For convenience of comparison seams from both coalfields were assigned to categories according to the yield of their clean coal product at 10 per cent ash. These categories were as follows: yield of clean coal in the range of **90 to 100** per cent; **70 to 90** per cent; and **less than 70** per cent.

A statistical approach was used to determine the number of seams from each of the coalfields falling into the different categories.

The degree of washing (N) and washability number (Wn) were also used to further examine the inherent washability characteristics of coal seams. The degree of washing at any specific gravity cut-point is expressed as follows:

$$N=\frac{w(a-b)}{a}$$

where:

a=the ash content of the raw coal (feed)

b=the ash content of the clean coal at a given density of separation

w=the yield of clean coal at a given density of separation

For a given coal, depending on the rank, type and mineral matter associated with it, there will always be a density of separation which will maximize the yield of the cleanest product possible. The optimum degree of washing (N_{opt}) is then obtained by plotting degree-of-washing values (N) versus the density of separation, and finding the maximum value. Degree-of-washing plots were constructed for three yield-of-clean-coal ranges.

The ash content of the clean coal at the optimum degree of washing has specific significance in characterizing the coal. Therefore, it is advisable to express the washability number as the ratio of the degree of washing to the clean-coal ash at the optimum level (Sarkar and Das, 1974; Sarkar *et al.*, 1977; Sanders and Brooks, 1986). The washability number can be expressed as follows:

$$Wn=10\left(\frac{N_{opt}}{b_{opt}}\right)$$

where:

b_{opt}=ash content at N_{opt}.

The degree of washing and washability number take into account not only the ash content of the raw coal but also yield and ash of clean coal. The washability number describes the inherent washability characteristics of a coal far better than any of the classical washability parameters. The washability index was first introduced by Sarkar and Das (1974) to outline patterns of depositional conditions of Indian coal seams. In other studies, using the washability number as the comparative measure was recommended (Sarkar *et al.*, 1977; Sanders and Brooks, 1986).

For the present study, the washability numbers were calculated for the arbitrarily devised yield-of-clean-coal categories. This allowed comparison of the coal seams falling into the same range in terms of yield of clean coal at the selected ash level (10% ash) from different regions.

RESULTS

The washability results discussed in this paper are not considered to represent the final coal product quality from the studied areas. They are an attempt to make meaningful comparisons between various coal seams and find a way of predicting the changes in washability characteristics in relation to various geological conditions.

YIELD OF CLEAN COAL AND QUALITY OF REJECTS

The clean-coal curve plotted as cumulative ash content at any given density of separation, versus cumulative yield, predicts the theoretical yield of clean coal at a given ash level. This is a strictly technical parameter which has a major influence on the economics of the mined seam. However, comparable yields of clean coal at a preselected ash level may be obtained with varying degrees of diffi-

TABLE 4-3-1
LIST OF PROPERTIES REPRESENTING PEACE RIVER AND EAST KOOTENAY COALFIELDS

PEACE RIVER	EAST KOOTENAY
Bullmoose	Balmer
Belcourt	Elk River
Quintette	Ewin Pass
Mount Spieker	Ewin Creek
Sukunka	Fording
Wapiti	Greenhills
	Horseshoe Ridge
	Line Creek

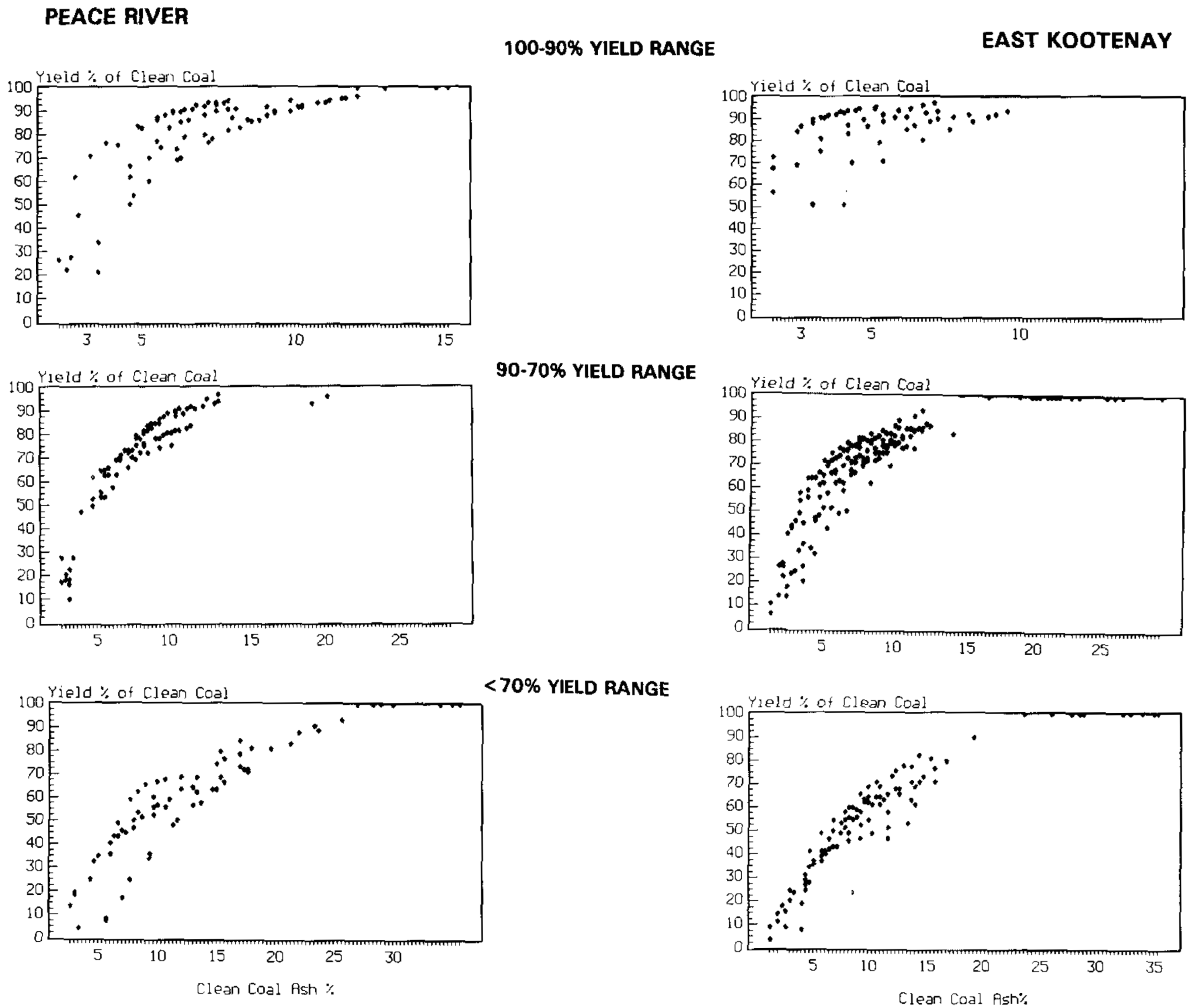

Figure 4-3-3. The ranges of variation for cumulative clean-coal curves for seams falling within specified yield ranges from Peace River coalfield and East Kootenay coalfield.

culty, due to different inherent coal characteristics. Clean-coal curves were plotted for a number of seams from the two coalfields. The Peace River coalfield was represented by 24 seams from three geological formations. The majority of seams, however, are from the Gates Formation. The East Kootenay coalfield was represented by 35 seams. These seams were assigned to different categories according to their yield of coal product at 10 per cent ash, and clean-coal curves were plotted in the corresponding ranges for seams from both coalfields (Figure 4-3-3).

For coals from the Peace River coalfield, eight seams out of twenty-four were in the range of 100 to 90 per cent yield at 10 per cent ash, nine seams were in the second highest range, 90 to 70 per cent yield at 10 per cent ash, and the remaining were assigned to the lowest range. The raw ash as well as the top-size of the samples from both coalfields is reported in Table 4-3-2.

For the seams representing East Kootenay coalfield only six out of thirty-five examined fell into the high-yield category, eighteen were in the middle range, and eleven were in the lowest yield range. The ranges of ash content and top-size of the raw coal samples from both coalfields are also given in Table 4-3-2.

The clean-coal curves within three ranges of yields for both regions, show quite a wide range of coal characteristics. This is particularly noticeable for the high-yield range for both formations. Similarly, the quality of rejects varies significantly for seams in the same yield category. The cumulative-reject curves for different categories of clean-coal yield for seams from the two coalfields are shown in Figure 4-3-4.

There is no consistent trend between the yield categories of the seams studied and their stratigraphic position in the Gates Formation sequence. For the Mist Mountain Formation, seams from the upper part of the formation appear to have somewhat higher yields of clean coal at 10 per cent ash as compared to those in the middle and lower part of the formation.

A comparison of the washability characteristics using the clean-coal curve is quite difficult, as the yield-ash relationship is very much coal dependent, and suffers from many drawbacks. Above all, it is not a quantitive measure.

Near-Gravity Material as a Measure of "Ease of Washing"

The amount of material in the range ±0.1 of density of separation is considered to be a more quantitive measure for comparing the "ease of washing". Difficulties of washing are categorized on the basis of the amount of near-gravity material at the density of separation for the desired clean-coal product (Leonard, 1979). The ±0.1 specific gravity range approach assumes that all material lying within this range contributes to difficulties in washing. However, this assumption may not be accurate for washing in more efficient separators, operating within much narrower ranges (*e.g.*, ±0.05 s.g.). Figure 4-3-5 depicts the amount of near-gravity material (±0.1 s.g.) for seams from both studied coalfields.

The amount of near-gravity material close to the density of separation rates coal seams from Peace River as moderately difficult to very difficult to wash. The designation "moderately difficult" was assigned to the two highest clean-coal ranges and "very difficult" to the lowest range. The coal seams from East Kootenay coalfield are classified as "simple" for the highest yield range (Figure 4-3-5), moderately difficult for the second highest range and difficult for the coal seams in the lowest yield category.

Degree of Washing and Washability Number

Degree-of-washing plots were derived for the designated ranges of yield of clean coal for seams from the Peace River and East Kootenay coalfields (Figure 4-3-6). Very similar ranges of optimum degree of washing were found for the same yields of clean coal from both coalfields. Table 4-3-3 lists optimum degree-of-washing values, and washability

TABLE 4-3-2
DISTRIBUTION OF COAL SEAMS FROM PEACE RIVER AND EAST KOOTENAY ACCORDING TO THEIR YIELD OF CLEAN-COAL PRODUCT AT 10 PER CENT ASH REPORTED WITH RAW ASH AND TOP-SIZE RANGES

	PEACE RIVER COALFIELD			EAST KOOTENAY COALFIELD		
RANGE of YIELD at 10% ASH	NUMBER of SAMPLES	RAW COAL ASH RANGE	TOP SIZE mm	NUMBER of SAMPLES	RAW COAL ASH RANGE	TOP SIZE mm
100 - 90	8(24)	11.82-14.85	100(4) 75(3) 50(1)	6(35)	8.37-13.42	100(6)
90-70	9(24)	15.42-28.41	150(4) 100(4) 75(1)	18(35)	16.21-28.45	100(8) 50(10)
<70	7(24)	21.11-35.00	100(6) 75(1)	11(35)	23.57-35.00	100(6) 50(5)

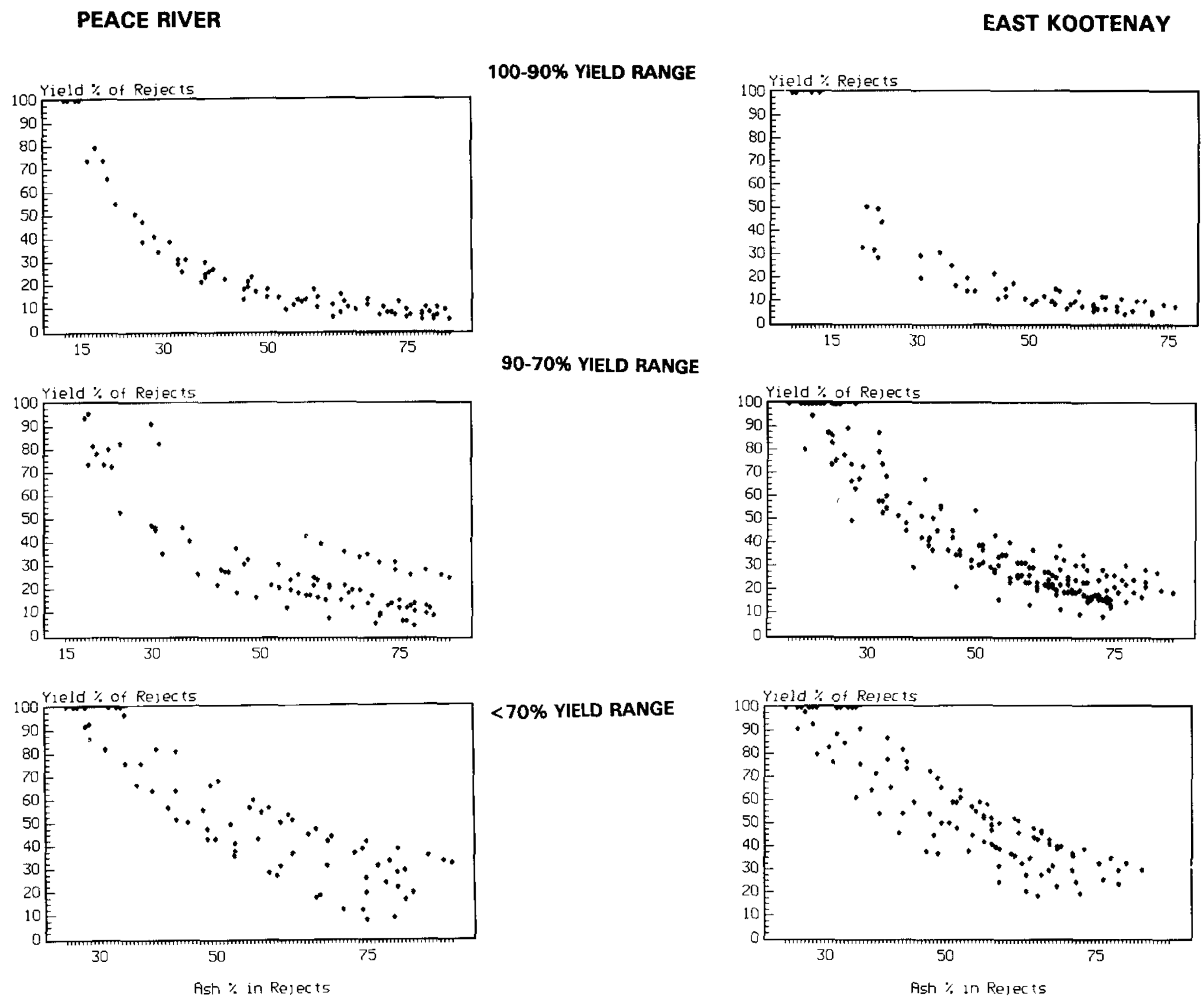

Figure 4-3-4. The ranges of variation for cumulative reject curves for seams falling within specified yield ranges from Peace River coalfield and East Kootenay coalfield.

numbers with the corresponding ash of clean coal and rejects, and the density at the optimum cut points.

The optimum cut point for the Peace River seams with highest yield of clean coal appears to be at a slightly higher density than for East Kootenay coal seams. The washability numbers associated with the various clean-coal yield ranges imply that Peace River coals are much more difficult to wash to the same clean-coal product levels than the East Kootenay coals. The average washability number for Peace River coals is 88 compared to 136 for East Kootenay coals. For the second range 64 compares with 71. For the third range the washability numbers are not significantly different.

The important conclusion to be drawn from the data in Table 4-3-3 is that even when the clean coal products at narrow yield ranges are compared within the same coalfield, the washability characteristics vary greatly. In other words, the difficulties in achieving the same coal product vary tremendously between different seams. This is evident from the wide range of washability numbers within designated yield ranges of clean coal.

The variation in washability numbers within the same geological formation varies from 39 to 185, with no consistency or relation to stratigraphic position. The washability number of two adjacent seams can be just as variable (72 to 142).

Liberation Patterns

The washability of any coal seam is very much dependent on the top-size of its representative sample. Liberation of coal from mineral matter is usually achieved by reducing the size of coal by breaking or crushing. During breakage coal particles separate from inclusive minerals, usually along the bedding planes. The way in which coal separates from ash-forming impurities depends on the type and mode of occurrence of minerals as well as the type of coal. The easiest to separate are the epigenetic minerals, whereas epiclastic and syngenetic minerals are more difficult to remove by physical methods (Cook, 1981; Falcon and Falcon, 1983; Holuszko and Grieve, 1990).

For coals with epigenetic minerals concentrated along the cleats, reducing the size will lead to an easy physical separation of liberated minerals, and result in an increase in the yield of clean coal. For minerals of epiclastic origin (chiefly clays and quartz) liberation-separation may be difficult, as coarse crushing will not liberate the coal from associated minerals.

Figure 4-3-7 illustrates liberation patterns for four different coal seams from the Peace River coal field. All four coals are from the Gates Formation. A reduction in the top-size of the run-of-mine sample resulted in a substantial increase in the yield of clean coal (a); some increase in the yield of clean coal (b); almost no increase in the yield of clean coal (c); and no increase in the yield of clean coal (d). This is reflected in the increase of the washability number, for coals a, b, and c, and a slight decrease in value for the fourth coal.

The liberation characteristics of the four coals are quite different, indicating wide variations in the mode of occurrence of mineral matter in these seams. From the analysis of washability numbers, it is seen that only in the case of seams (a) and (b) can the ease of washing and recovery of clean coal be improved by size reduction. For seam (c) the reduction in size has almost no positive effect on the washability number. An interesting trend is observed in seam (d), where crushing to a smaller size leads to a decrease in ease of washing. However, there is no indication of a decrease in the yield of clean coal. This implies that the washability number detects changes in ease of washing better than the clean-coal curve does.

Systematic computation of washability numbers at various levels of crushing will aid in assessing the mode of association of mineral matter with coal, and the extent of liberation of mineral matter from coal.

SUMMARY AND CONCLUSIONS

This comparative study of washability of coal samples from two major British Columbia coalfields resulted in the following conclusions:

TABLE 4-3-3
CHARACTERISTICS AT OPTIMUM "DEGREE OF WASHING" FOR SEAMS FROM THE PEACE RIVER AND EAST KOOTENAY COALFIELDS

RANGE of YIELD at 10% ASH	DEGREE of WASHING MIN - MAX	DEGREE of WASHING AVG	ASH in CLEAN COAL at Nopt MIN - MAX	ASH in CLEAN COAL at Nopt AVG	ASH in REJECTS MIN - MAX	ASH in REJECTS AVG	DENSITY of SEPARATION	WASHABILITY NUMBER MIN-MAX	WASHABILITY NUMBER AVG
PEACE RIVER COALFIELD									
100-90	40.4-56.7	*47.3*	3.5-6.2	*5*	16.5-46.7	*32.1*	1.42	48-163	*83*
90-70	40.8-51.9	*45.8*	5.7-8.5	*7.3*	25.6-73.91	*51.3*	1.48	54-90	*64*
<70	30.3-47.5	*37.5*	9.3-14.5	*11.5*	45.01-75.9	*56.8*	1.57	21-51	*33*
EAST KOOTENAY COALFIELD									
100-90	41.3-55.0	*49.9*	2.9-5.4	*4*	20.9-34.4	*24.7*	1.36	76-185	*136*
90-70	39.6-54.2	*48*	5.4-9.4	*7.1*	27.5-76.8	*52.6*	1.49	45-10	*71*
<70	29.6-44.3	*39.3*	8.6-13.8	*10.4*	38.8-68.1	*56.9*	1.55	22-51	*39*

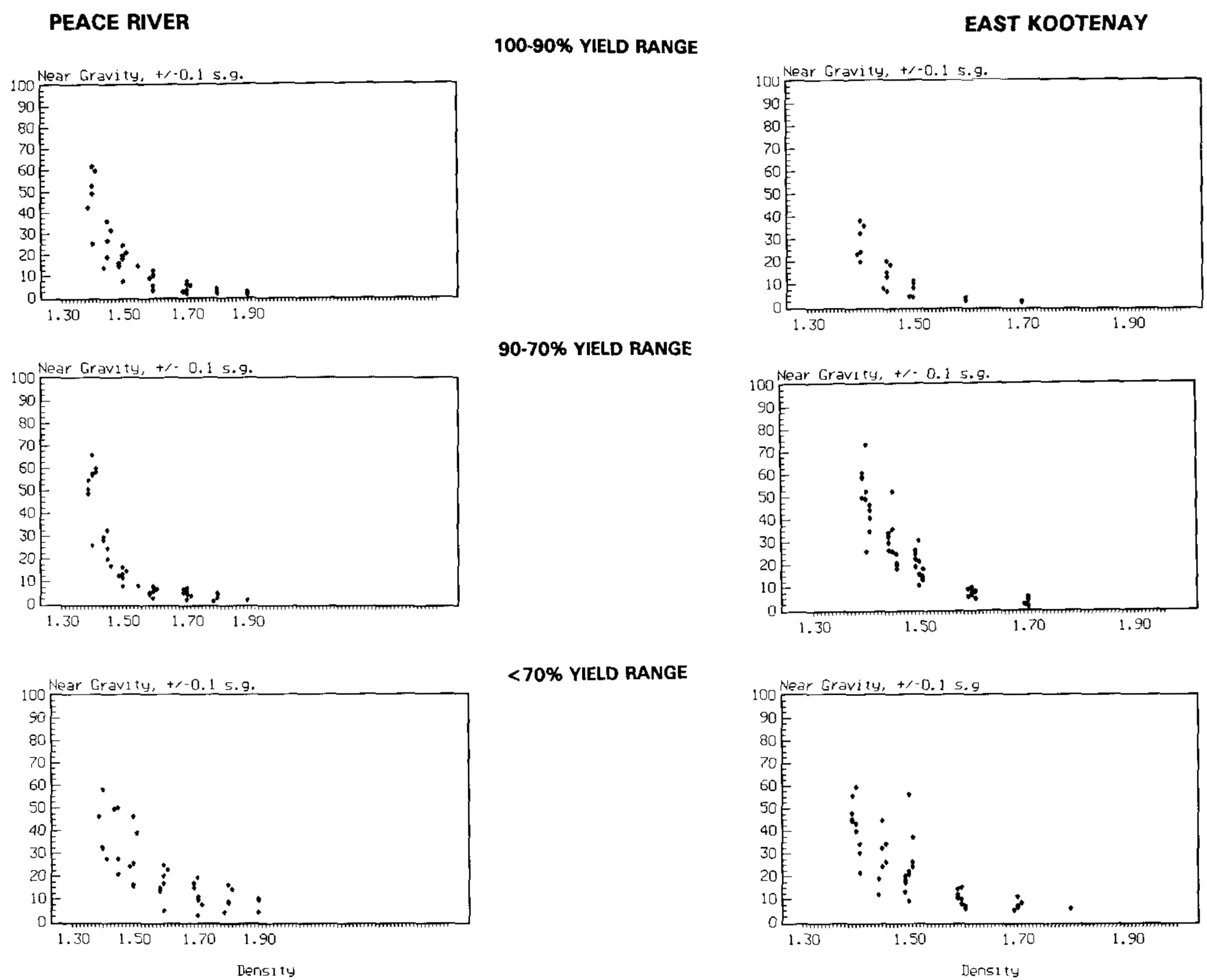

Figure 4-3-5. The range of variation for the amount of near-gravity material (±0.1 s.g.) for specified yield of clean coal ranges in Peace River and East Kootenay coals.

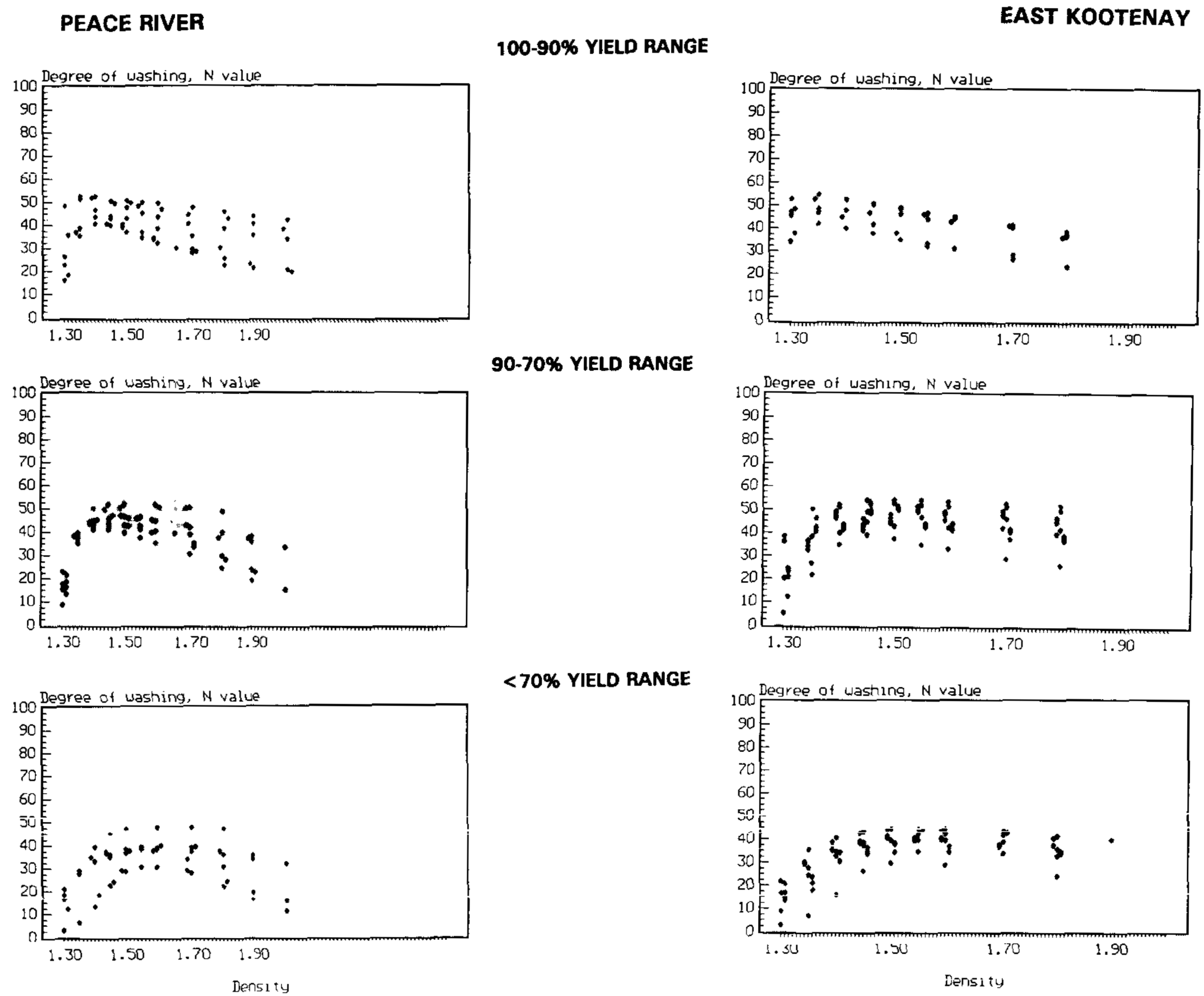

Figure 4-3-6. The range of variation for the degree of washing, for specified yield of clean coal ranges in Peace River and East Kootenay coals.

- Washability characteristics of seams from both the Peace River and East Kootenay coalfields are variable to the same extent. Seventeen out of twenty-four samples from the Peace River coalfield yielded more than 70 per cent of clean-coal product at 10 per cent ash, as compared to twenty-four out of thirty-five from East Kootenay.
- The quality of rejects is highly variable for samples falling into the three different ranges of clean-coal yield at 10 per cent ash, in both coalfields.
- From the amount of near-gravity material (±10 s.g.) at the density of separation required for good quality clean coal, the East Kootenay seams yielding the most clean-coal product were classified as simple to wash, whereas the seams from Peace River falling into the same category were found to be moderately difficult to wash.
- The "optimum degree of washing" and the ash content of clean coal were found to be very similar for seams from both coalfields, however, washability numbers obtained for different ranges of yield of clean coal were found to be much greater for the East Kootenay coalfield than for Peace River. This was especially true for the seams yielding the most clean coal (100–90% yield range), which were from the upper half of the Mist Mountain Formation. The higher washability numbers for the East Kootenay seams implies that these seams can be washed much more easily to the same clean coal product than their counterparts from Peace River.
- There is no significant trend or correlation between the washability number and stratigraphic position in the Gates Formation coals.
- The great variation in washability numbers within both coalfields indicates diversity in ease of washing among these seams.
- Examples of different liberation patterns of coal during size reduction confirms significant variation in washing characteristics; the washability number is a better indicator of the liberation characteristics of coal than the clean-coal curve derived from classical washability parameters.

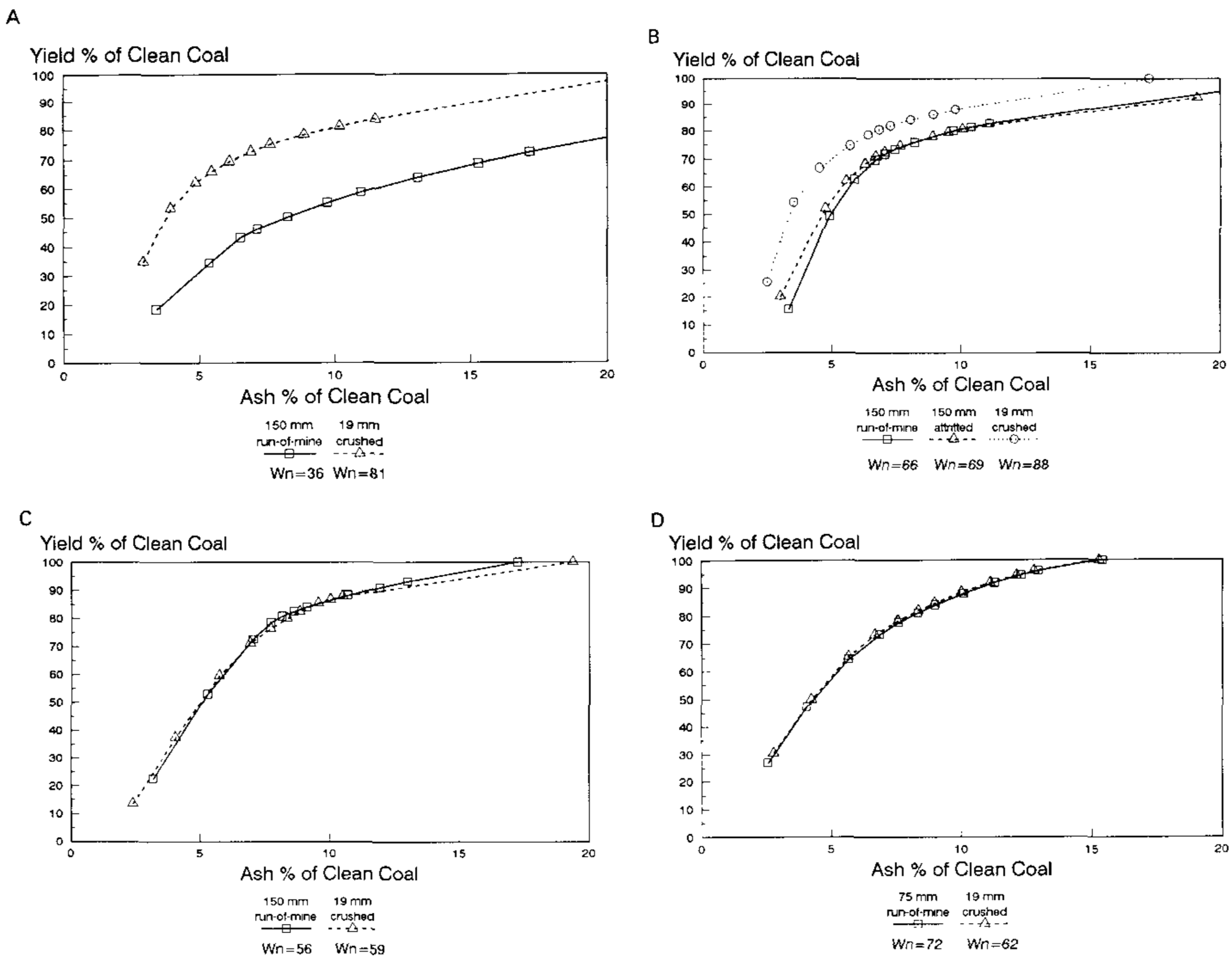

Figure 4-3-7. Liberation patterns for four coals from the Peace River coalfield.

FUTURE PLANS

The quality of any seam is very closely related to its lithotype composition. Lithotypes are useful indicators not only of the original environment of coal formation, but also of the physical and mechanical properties of coal. It is important to examine the extent to which lithotypes can be indicative of the washability characteristics of a given coal seam.

In the future this study will focus on lithotype and petrographic analyses of various coal seams in order to elucidate their influence on washability characteristics. To this end, a number of lithotype samples were collected from the East Kootenay coalfield during 1991. The sampling program was arranged in cooperation with Dr. Alex Cameron of the Institute of Sedimentary Petroleum and Geology in Calgary. Lithotype sampling of Peace River coal seams is planned for next year. The emphasis will be on finding a way of predicting the ease of washing from lithotype composition. A further aim of this project is to investigate the viability of adopting the washability number for use in the new International Coal Classification System (Alpern *et al.*, 1989).

Systematic analysis of the possible applications of the degree of washing and washability number to the improvement of various technical procedures (e.g. sampling, blending) and coal preparation technologies will also be a part of this project.

ACKNOWLEDGMENTS

I wish to express my gratitude to the geology staff at all the province's coal mines for their cooperation, especially the staff of Greenhills and Line Creek mines for their assistance in this year's sampling program and supplying additional coal quality data. A special thanks is also due to David Grieve and Ward Kilby, who read an earlier version of this paper and contributed to its improvement.

REFERENCES

Alpern, B., Lemos De Sousa, M.J. and Flores, D. (1989): A Progress Report on the Alpern Coal Classification; *in* Coal: Classification, Coalification, Mineralogy, Trace-element Chemistry, and Oil and Gas Potential, Lyons, P.C. and Alpern, B., Editors, *Elsvier*, Amsterdam.

Bustin, R.M. (1982): The Effect of Shearing on the Quality of Some Coals in the Southeastern Canadian Cordillera; *Canadian Institute of Mining and Metallurgy*, Bulletin, Volume 75, No. 841, pages 76-83.

Cameron, A.R. (1972): Petrography of Kootenay Coals in the Upper Elk River and Crowsnest Areas, British Columbia and Alberta; *Research Council of Alberta*, Information Series No. 60, pages 31-45.

Cook, A.C. (1972): Report on Samples of Coal from Sukunka, Canada; *Clifford McElroy and Associates Pty. Ltd.*, internal report, January 1972.

Cook, A.C. (1981): What Are We Trying to Separate?; *Separation Science and Technology*, Volume 16 (10), pages 1545-1569.

Falcon, L.M. and Falcon, R.M.S. (1987): The Petrographic Composition of Southern African Coals in Relation to Friability, Hardness and Abrasive Indices; *Journal of the South African Insititute of Mining and Metallurgy*, Volume 87, No. 10, pages 323-336.

Grieve, D.A. (1985): Coalfields of the East Kootenay Region, Southeastern British Columbia; *Canadian Institute of Mining and Metallurgy*, Coal in Canada, Special Volume 31, pages 203-211.

Holuszko, M.E. and Grieve, D.A. (1990): Washability Characteristics of British Columbia Coals; *in* Geological Fieldwork 1990, *B.C. Ministry of Energy, Mines and Petroleum Resources*, Paper 1991-1, pages 371-379.

Hower, J.C. (1988): Additivity of Hardgrove Grindability: A Case Study; *Journal of Coal Quality*, Volume 7, pages 68-70.

Hower, J.C., Grease, A.M. and Klapheke, J.G (1987): Influence of Microlithotype Composition on Hardgrove Grindability for Selected Eastern Kentucky Coals; *International Journal of Coal Geology*, Volume 7, pages 68-70.

Hower, J.C. and Lineberry, G.T. (1988): The Interaction of Coal Lithology and Coal Cutting on the Breakage Characteristics of Selected Kentucky Coals; *Journal of Coal Quality*, Volume 7, pages 88-95.

Jeremic, M.L. (1980): Coal Strengths in the Rocky Mountains; *World Coal*, Volume 6, No. 9, pages 40-43.

Lamberson, M.N., Bustin, R.M. and Kalkreuth, W. (1991): Lithotype (Maceral) Composition and Variation as Correlated with Paleo-wetland Environments, Gates Formation, Northeastern British Columbia, Canada; *International Journal of Coal Geology*, Volume 18, pages 87-124.

Leonard, J.W. (1979): Coal Preparation. 4th Edition, *American Institute of Mechanical Engineers*, New York.

Marchioni D. and Kalkreuth, W. (1991): Coal Facies Interpretations Based on Lithotype and Maceral Variations in Lower Cretaceous (Gates Formation) Coals of Western Canada; *International Journal of Coal Geology*, Volume 18, pages 125-162.

Sanders, G.J. and Brooks, G.F. (1986): Preparation of the "Gondwana" Coals. 1. Washability Characteristics; *Coal Preparation*, Volume 3, pages 105-132.

Sarkar, G.G. and Das, H.P. (1974): A World Pattern of the Optimum Ash Levels of Cleans from the Washability Data of Typical Coal Seams; *Fuel*, Volume 53, pages 74-84.

Sarkar, G.G., Das, H.P. and Ghose, S. (197?): Sedimentation Patterns: Do They Offer Clues to Coal Quality?; *World Coal*, pages 10-13.

Smith, G.G. (1989): Coal Resources of the Rocky Mountain Front Ranges and Foothills; British Columbia and Alberta; Coal Resources of Canada, *Geological Survey of Canada*, Paper 89-4, pages 50-68.

NOTES

British Columbia Geological Survey
Geological Fieldwork 1991

GEOLOGY AND ENERGY RESOURCE POTENTIAL OF THE TSABLE RIVER AND DENMAN ISLAND (92F/10, 11)

By C.G. Cathyl-Bickford, Consulting Geologist

KEYWORDS: Coal geology, stratigraphy, coal resources, coalbed gas, Comox Formation, Trent River Formation, Tsable River, Denman Island.

INTRODUCTION

Continued strong interest in the coal deposits and associated natural gas occurrences of eastern Vancouver Island and the northern Gulf Islands has stimulated the reexamination of critical geological relationships. The aim of this study is to provide accurate geological data to assist government and industry in assessing the remaining resource potential of the Vancouver Island coalfields, as well as identifying potential for new discoveries of natural gas associated with the coal measures.

This report presents preliminary results of one month's detailed geological mapping near Tsable River and on Denman Island.

LOCATION AND ACCESS

The study area includes Denman Island and part of the eastern coastal lowland of Vancouver Island, between Rosewall Creek in the south and Union Bay in the north (Figure 4-4-1). This area lies near the geographic centre of the Comox sub-basin of the Late Cretaceous Georgia Basin.

Access to the area is provided by a few paved highways and side roads, as well as a dense network of unpaved logging roads. Many of the bridges and culverts on the logging roads were washed out during torrential rains in the autumn of 1990, preventing vehicular access to large parts of the area.

Forestry is presently the only land-use near Tsable River, while land-use on Denman Island is divided between tree farms, dairy farms and rural residential subdivisions.

PREVIOUS WORK

The first recorded geological mapping in the study area was by J. Richardson (1873) of the Geological Survey of Canada. Coal deposits near Tsable River (Williams, 1924) were studied in detail by McKenzie (1922) and Buckham (1957). Denman Island was mapped by Usher (1952), Allmaras (1978) and Bell (1960). Remapping of the study area by the British Columbia Geological Survey began in 1987, and has continued through the autumn of 1991. (Bickford and Kenyon, 1988; Bickford *et al.*, 1990; Kenyon and Bickford, 1989).

STRATIGRAPHY

The coal measures of eastern Vancouver Island and the Gulf islands are part of the Nanaimo Group of Turonian to Maastrichtian age (England, 1990; Haggart, 1991). The rocks occupy the western erosional margin of the Late Cretaceous Comox sub-basin of Georgia Basin. The Comox sub-basin contains the Tsable River, Cumberland, Campbell River and Quinsam coalfields, together with several other minor coal showings (Bickford and Kenyon, 1988; Bickford *et al.*, 1990; Saunders *et al.*, 1974; Table 4-4-1).

TABLE 4-4-1
LITHOSTRATIGRAPHY OF LATE CRETACEOUS ROCKS WITHIN THE STUDY AREA

Formation:	Map Unit:	Member:	Description: Unit:
Lambert	15	—	Mudstone and siltstone; minor sandstone and argillaceous limestone. >115 m
			Abrupt contact
Denman	14	Norman Point	Sandstone; minor siltstone. 25 to 40 m.
			Intertonguing contact
	13	Graham	Conglomerate; minor sandstone and siltstone. 65 to 80 m
			Erosional contact
	12	Madigan	Sandstone; minor conglomerate and siltstone. 55 to 75 m
			Intertonguing contact
Trent River	11	Willow Point	Mudstone and siltstone; minor sandstone. 120 to 150 m.
			Abrupt contact
	10	Baynes Sound	Sandstone and siltstone; minor conglomerate. 10 to 60 m.
			Abrupt contact
	9	Royston	Mudstone and siltstone; minor sandstone. 50 to 220 m.
			Intertonguing contact
	8	Tsable	Mud-matrix conglomerate and pebbly siltstone. 5 to 140 m.
			Erosional contact
	7	Browns	Sandstone. 0 to 45 m.
			Intertonguing contact
	6	Puntledge	Mudstone and siltstone; minor sandstone. 100 to 130 m.
			Abrupt contact
	5	Cowie	Sandstone. 2 to 15 m.
			Abrupt contact
	4	Cougarsmith	Mudstone and siltstone; minor sandstone. 8 to 22 m.
			Intertonguing contact
Comox	3	Dunsmuir	Sandstone; minor siltstone and coal. 120 to 190 m.
			Erosional contact
	2	Cumberland	Siltstone, shale and coal; minor sandstone and gritstone. 30 to 90 m.
			Intertonguing contact
	1	Benson	Conglomerate; minor red shale and siltstone. 0 to 220 m.
			Erosional contact
Pre-Cretaceous Basement Complex:			
Karmutsen	V		Basalt, basaltic breccia and tuff.

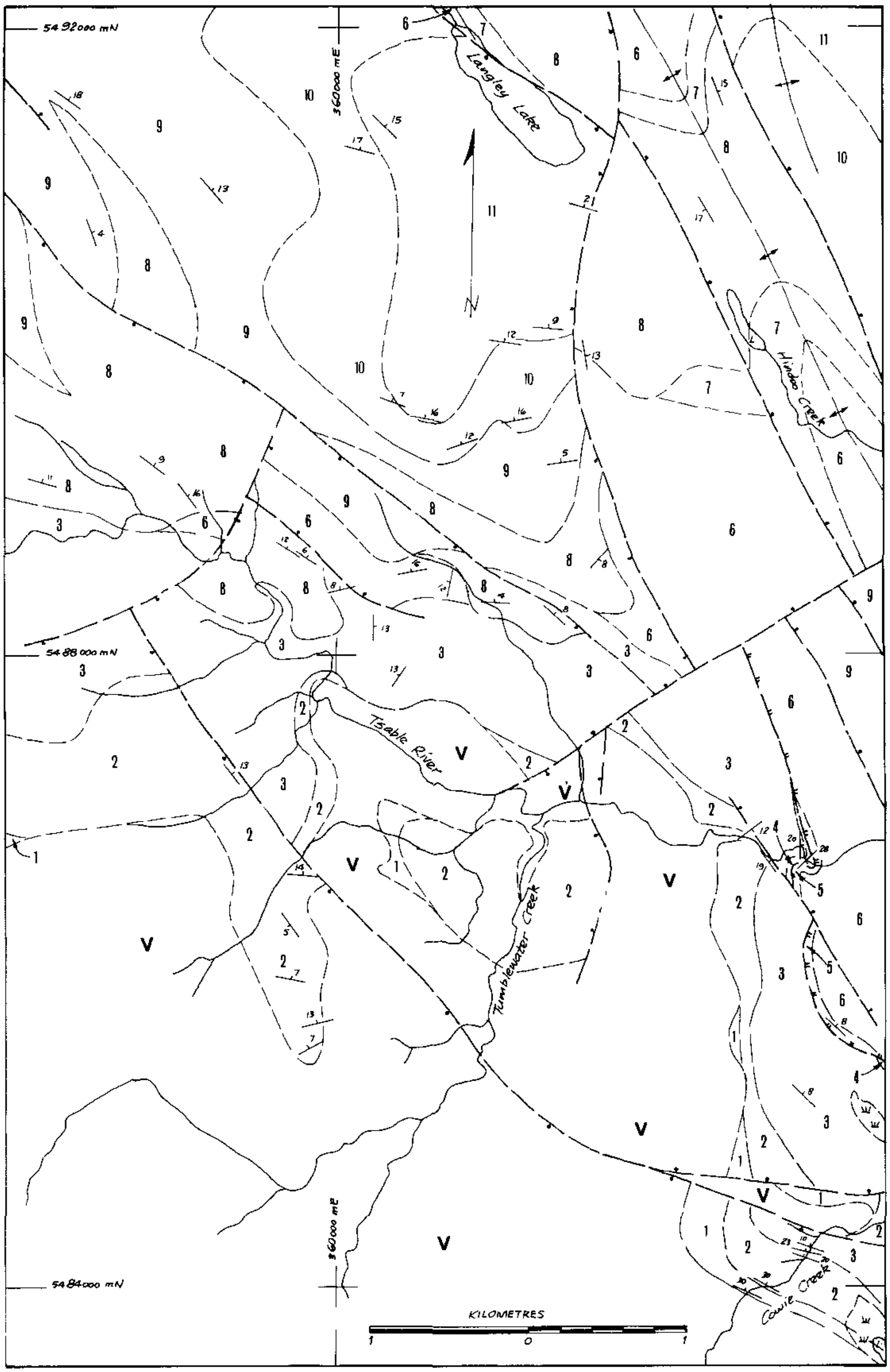

Figure 4-4-1. Geological map of the Tsable River and Denman Island study area.

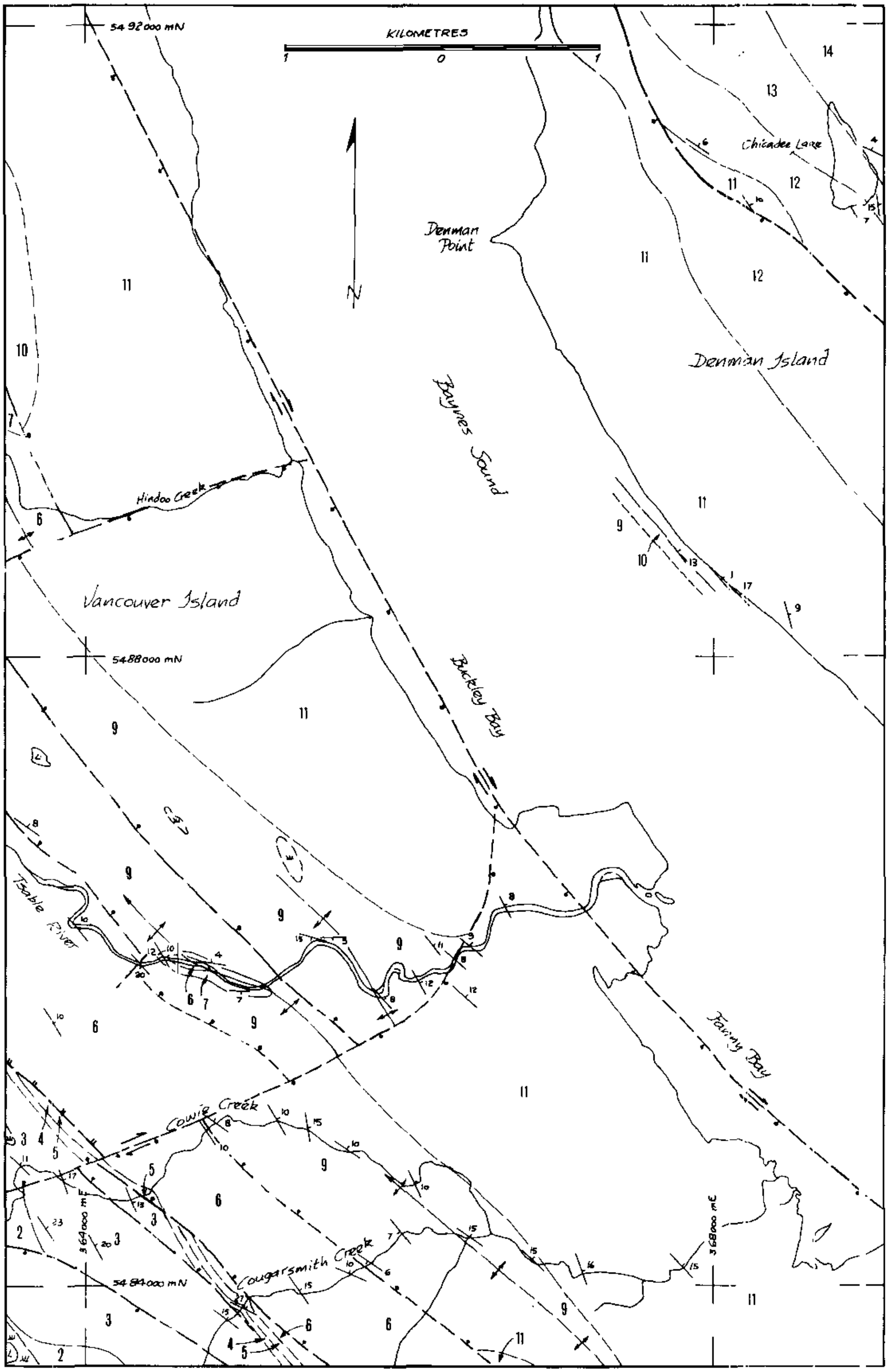
KILOMETRES
1 0 1
5492000 mN
5488000 mN
5484000 mN
364000 mE
368000 mE
N
Denman Point
Denman Island
Chickadee Lake
Baynes Sound
Buckley Bay
Fanny Bay
Vancouver Island
Hindoo Creek
Tsable River
Cowie Creek
Cougarsmith Creek

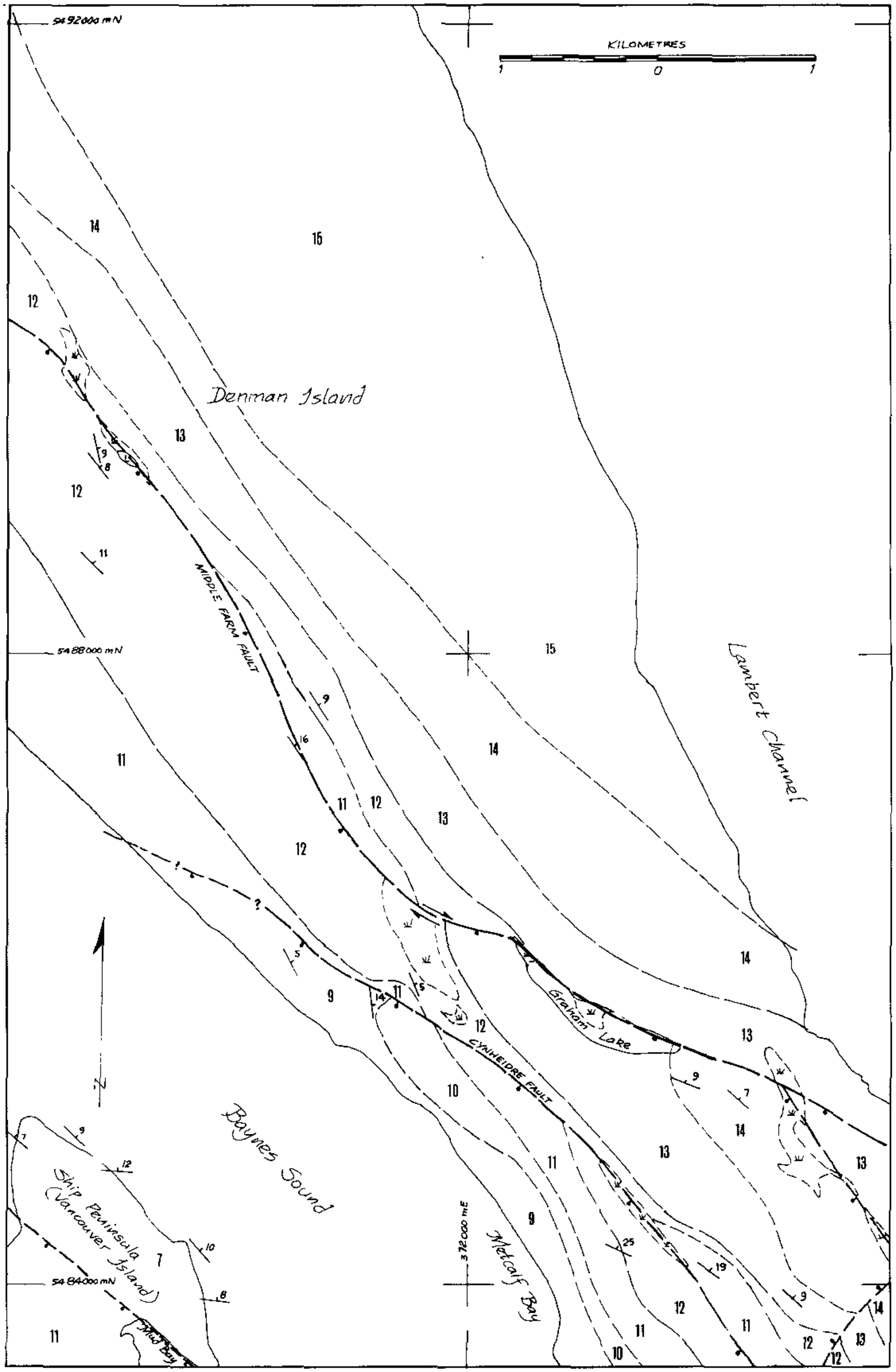
KILOMETRES
1
0
1
5492000 mN
5488000 mN
5484000 mN
372000 mE
Denman Island
Lambert Channel
Baynes Sound
Ship Peninsula
(Vancouver Island)
Metcalf Bay
Graham Lake
MIDDLE FARM FAULT
CYNHEIDRE FAULT
Mud Bay
N

Subdivision of the Trent River Formation

The Trent River Formation is divided into seven members within the study area. In order from base to top of the formation, they are the Cougarsmith, Cowie, Puntledge, Browns, Tsable, Royston, Baynes Sound and Willow Point members.

The Cougarsmith member (Unit 4) is a new unit, comprising the basal mudstones and siltstones of the Trent River Formation, in those areas where the overlying Cowie sandstones are present. The name Cougarsmith is derived from Cougarsmith Creek, where a nearly complete section of the member is exposed. The Cougarsmith member is 18 to 22 metres thick in the area between Tsable River and Cougarsmith Creek. The Cougarsmith mudstones and siltstones were probably deposited in sheltered lagoons on the landward side of barrier islands or offshore bars.

The Cowie member (Unit 5) is also a new unit, comprising thick-bedded to massive sandstones which overlie the Cougarsmith member. These sandstones were first recognized as an informal, unnamed unit by McKenzie (1922). The name Cowie is derived from Cowie Creek, near the centre of the presently mapped extent of the member. The member is 12 to 15 metres thick in the area between Tsable River and Cougarsmith Creek. The Cowie sandstones were probably deposited as a complex of barrier islands or offshore bars.

The Baynes Sound member (Unit 10) was first proposed by England (1989) for sandstones and conglomerates on the western shore of Denman Island southeast of Denman Point. Sandstones and conglomerates, probably correlative with the Baynes Sound member, are also exposed on hills to the east and west of Langley Lake on Vancouver Island, where they were previously mapped by Bickford and Kenyon (1988) as the Protection Formation. The name Baynes Sound is derived from the body of water which lies between Vancouver and Denman Islands. The Baynes Sound member is 15 to 60 metres thick near Langley Lake, and 10 to 25 metres thick on Denman Island. It was probably deposited in a submarine fan, with the conglomerates possibly representing submarine channel fills.

The Willow Point member (Unit 11) is a new unit, comprising sedimentary rocks previously mapped as the Cedar District Formation in the Comox sub-basin (Bickford, *et al.*, 1990). It consists of dark grey mudstone and siltstone with occasional thin, graded beds of sandstone. The name Willow Point is derived from Willow Point on the east coast of Vancouver Island, southeast of the town of Campbell River. The member is 120 to 150 metres thick on the western side of Denman Island (Davidson *et al.*, 1965; Mahannah, 1964), where it is well exposed in wave-cut benches and sea cliffs. It was probably deposited in a distal submarine fan environment.

Subdivision of the Denman Formation

The Denman Formation has been divided into three members, following suggestions made by Bell (1960) and Allmaras (1978). From bottom up, the three members are named Madigan, Graham and Norman.

The Madigan member (Unit 12) is a new unit, comprising thick-bedded to massive, medium to coarse-grained, light grey to greenish grey sandstones with occasional thick interbeds of siltstone and minor pebble conglomerate. The Madigan sandstones are generally poorly sorted, and locally contain very coarse disseminated grains of quartz sand. The name Madigan is derived from the historic Madigan farm in the central valley of Denman Island. The member is 55 to 75 metres thick on the western side of Denman Island, where it forms a prominent east-dipping cuesta ridge. It was probably deposited below wave base, in a continental shelf environment.

The Graham member (Unit 13) is a new unit, comprising thick-bedded to massive, locally trough-crossbedded conglomerates, with occasional thin to medium lenticular interbeds of sandstone and siltstone. The name Graham is derived from Graham Lake on Denman Island, where the conglomerates are well exposed. Clast sorting in the Graham conglomerates is fair to good; clasts are well rounded and consist of large pebbles to cobbles of basalt with minor granodiorite, sandstone, shale and red chert. Framework a-b imbrication is locally well developed. Indicated paleocurrent directions range from 025° to 200°, averaging 114°. The basal contact of the Graham member is generally erosional, while its top contact is gradational by intertonguing with the overlying Norman Point sandstones. The member is 65 to 80 metres thick on Denman Island. It was probably deposited in submarine channels, incised within older continental-shelf deposits.

The Norman Point member (Unit 14) is also a new unit, comprising medium to thick-bedded, medium to coarse-grained, light grey sandstone with occasional interbeds of dark grey siltstone. The name Norman Point is derived from the point of land south of Ford Cove on Hornby Island, where the sandstones are well exposed. The top contact of the Norman Point with the overlying Lambert Formation is abrupt. The Norman Point member is 25 to 35 metres thick on eastern Denman Island, and at least 40 metres thick at Norman Point. It was probably deposited below wave base, in a continental-shelf environment.

STRUCTURAL GEOLOGY

The dominant structural feature of the study area is an east-dipping homocline within the sedimentary rocks of the Nanaimo Group. The regional dip of the sedimentary rocks is 10° to 15° northeast. The homocline is disrupted by three sets of faults as well as local folds.

Set 1 consists of subparallel, northwest-striking faults, which have various combinations of extensional and dextral strike-slip displacement. Near Tsable River, most of the northwest-striking faults dip steeply to the northeast, with the exception of several faults on the north bank of the Tsable River, southwest of Langley Lake, which dip to the southwest. On Denman Island, the northwest-striking faults dip steeply to the southwest, and have extensional offset down to the southwest. Taken as a whole, the northwest-striking faults may be the surface manifestation of a 'flower structure', underlain at depth by a major strike-slip shear zone.

Set 2 consists of near-vertical cross-faults which strike to the northeast and east, and appear to be younger than the northwest-striking faults. The cross-faults have apparent sinistral strike-slip displacements ranging from less than 100 to perhaps 1000 metres.

Set 3 consists of bedding-plane shear zones, which are of indeterminate age relative to the other two fault sets. Bedding-plane shears are well exposed in shales and coal beds in the canyons of Tsable River and Cowie Creek and were also encountered in the underground workings of Tsable River colliery.

Sedimentary rocks of the Nanaimo Group are sheared, cleaved and strongly jointed adjacent to the faults, particularly adjacent to the northwest-striking faults.

COAL RESOURCE POTENTIAL

The Comox No. 2 and No. 3 coal beds are of mineable thickness in the Tsable River area. The cover over these two coal beds increases rapidly to the east and northeast of their outcrops, and is approximately 550 metres thick along the western shore of Baynes Sound, and 675 to 950 metres thick on Denman Island. Previous coal mining operations on Vancouver Island have worked at depths as great as 540 metres, although at these depths the miners encountered severe strata control problems such as floor heave and spontaneous outbursts of gas and coal. It is unlikely that coal will be mined beneath Baynes Sound or Denman Island within the foreseeable future.

Considerable exploratory drilling has been done along the outcrop of the Comox coal beds between Tsable River and Cougarsmith Creek. Most boreholes have been shallower than 300 metres, and current industrial interest in the area appears to be concentrated on the open-pit mining potential of the Comox coals.

The Comox No. 2 coal bed lies near the top of the Cumberland member of the Comox Formation. It was extensively worked in the Tsable River colliery, which was abandoned in 1966 due to exhaustion of accessible reserves. The Comox No. 2 coal bed is a composite of up to five individual coal plies, separated by thin partings of grey silty mudstone and black carbonaceous to coaly mudstone. Some of the coaly mudstone partings are sheared and soft, and they locally grade into low-density canneloid mudstone stony coal.

The coal of the No. 2 bed is bright to bright banded, and is generally blocky and hard. Some plies of platy or laminated coal are occasionally present within the coal bed; such platy coal makes a noticeable contribution to the waste dump at Tsable River colliery, where it was rejected as being unmarketable due to its "shaly" appearance. The No. 2 coal bed ranges in thickness from 1.2 to 4.2 metres within the mined area, and boreholes indicate similar thicknesses elsewhere in the study area. The lower part of the bed often consists of inferior, dirty or "bony" coal, with ash contents greater than 25 per cent.

The Comox No. 3 coal bed lies near the middle of the Cumberland member. The rock parting between the No. 2 and No. 3 coal beds is 10 to 20 metres thick, and consists of a coarsening-upward unit of mudstone, sandy siltstone and sandstone. The coal bed is a composite of at least three individual coal plies, separated by thin partings of black carbonaceous and coaly mudstone. The partings are generally sheared and flaky, while the coal itself is bright banded, and locally sheared and platy.

Boreholes indicate that the No. 3 coal bed is 1.0 to 4.1 metres thick within the study area (Saunders *et al.*, 1974). The upper and lower contacts of the coal bed are often gradational, marked by thin interbeds of coal and mudstone.

The Comox coals at Tsable River are of high-volatile A bituminous rank. Significant down-dip increase in coal rank at Tsable River is unlikely, given the predeformational timing of coalification in the area (Kenyon and Bickford, 1989).

Most of the drilling within the Tsable River coalfield has been confined to the vicinity of the outcrops of the Comox coal beds. Very little drilling has been done to establish the down-dip continuity of the coals at depths greater than approximately 300 metres. The few deep boreholes suggest that the Comox coals may become dirtier to the east (Buckham, 1957) and the aggregate thickness of coal may be somewhat less than that near the outcrops.

Buckham (1957) reported an unclassified reserve of 6.2 million tonnes for coal in place along the outcrop belt between Tsable River and Cougarsmith Creek.

GAS RESOURCE POTENTIAL

Gas has been reported from a few deep coal exploration boreholes in the Tsable River area. The best show was in the Alvensleben Tsable River ATR-1 borehole (Cathyl-Bickford, 1991), which encountered gassy coal at a depth of approximately 550 metres. Drilling of ATR-1 was suspended in 1914 due to excessive gas pressure in the hole. The borehole was subsequently put into service as an unlicensed gas well, serving a forestry camp, and continued to produce gas until its casing was sheared off by a landslide in 1984.

Given sufficient maturation, an organic-rich source rock will generate hydrocarbons which will migrate to fill all accessible pore spaces. In order to form a significant gas accumulation, the source rock must be in communication with a reservoir rock within an effective trap. The source of the Tsable River gas is probably the coal beds of the Comox Formation. The coals, having attained a high-volatile A bituminous rank, are sufficiently mature to have generated significant quantities of thermogenic methane due to progressive devolatilization of the coal during burial and heating with the subsiding Georgia Basin.

Although black, carbonaceous to coaly mudstones are associated with the coals, the overall thickness and organic matter content of the mudstones are much less than those of the coals. Mudstones are therefore not expected to have been significant sources of gas within the study area.

Gas which has been generated by a maturing coal bed is partially adsorbed by the coal, while a portion of the gas is released by the coal and exists in the free state within micropores and fractures in the coal bed (Das *et al.*, 1991). The fate of the free gas depends upon the nature of the roof and floor of the coal bed from which it was generated. If the coal is bounded by permeable rocks such as conglomerate or sandstone, the free gas will migrate from the coal bed and either accumulate in a structural or stratigraphic trap elsewhere in the basin, or be lost by escape to the atmosphere.

Possible carrier beds and reservoirs for coal-sourced gas include the sandstones of the Dunsmuir and Cowie members. The Cowie member is of particular interest as it displays good to excellent framework sorting, and has fair to good intergranular porosity. The Dunsmuir sandstones are interbedded with coals and carbonaceous mudstones, and are therefore in effective communication with sources of gas. The Cowie sandstones are stratigraphically isolated, and it is more difficult to envisage an effective migration pathway from the Comox coals into the Cowie sandstones without involving vertical migration of gas along faults. The sandstones and conglomerates of the Benson and Cumberland members are either too discontinuous or too poorly sorted to constitute effective reservoirs for gas.

Adequate seals over the Dunsmuir and Cowie sandstones are provided by the mudstones and siltstones of the Trent River Formation. Significant structural traps are probably present on the upthrown sides of the major northwest-trending faults on Denman Island.

Drilling depths to the top of the Dunsmuir sandstone under Denman Island will be approximately 500 to 800 metres. Although these are shallow depths compared with most gas fields, they are typical of the depth range of most coalbed gas prospects.

Production of coalbed gas by desorbtion may be practicable wherever the coal is at depths greater than 200 metres, regardless of the presence or absence of a structural or stratigraphic trap (Das *et al.*, 1991). Such traps may, however, enhance the development potential of coalbed gas wherever porous reservoir rocks are in contact with coal beds. Close association of clastic reservoir rocks and coal beds affords improved economics for coalbed gas production (Wyman, 1984), as gas may diffuse into adjacent reservoir rocks if a pressure differential is established during production, thus increasing the effective drainage area of each coalbed gas well.

ACKNOWLEDGMENTS

Lodging was provided by Dennis Lavalle and Sandy Melnyk on Denman Island, and by Jane Larsen and Kelly Brooks in Courtenay. Seth Brooks and Tallis Jovanka provided cheerful assistance in the field. John Eden at Macmillan Bloedel provided the key for gated logging roads near Tsable River. Anne Corddry of the Denman Island Forestry Committee and David Shaw at Fletcher Challenge accommodated an endless series of requests for prints of base maps. William Hodge and Mike Gallo of the British Columbia Ministry of Environment, Lands and Parks provided water-well records which were essential to deciphering the geology of drift-covered areas. Kate Slater and John Newell provided technical criticism and editing for this article.

REFERENCES

Allmaras, J.M. (1978): Stratigraphy and Sedimentology of the Late Cretaceous Nanaimo Group, Denman Island, British Columbia; unpublished M.Sc. thesis, *Oregon State University.*

Bell, G.L. (1960): Geological Report of the Hornby and Denman Islands Areas, Permits 796 and 799; *Charter Oil Company Limited*, unpublished report.

Bickford, C.G.C. and Kenyon, C. (1988): Coalfield Geology of Eastern Vancouver Island; *in* Geological Fieldwork 1987, *B.C. Ministry of Energy, Mines and Petroleum Resources*, Paper 1988-1, pages 441-450.

Bickford, C.G.C., Hoffman, G.L. and Kenyon, C. (1990): Geological Investigations in the Coal Measures of the Oyster River, Mount Washington and Cumberland Areas, Vancouver Island; *in* Geological Fieldwork 1989, *B.C. Ministry of Energy, Mines and Petroleum Resources*, Paper 1990-1, pages 431-437.

Buckham, A.F. (1957): Report on Cowie Creek Area, *Canadian Collieries Resources Ltd.*, unpublished report.

Cathyl-Bickford, C.G. (1991): Coal Geology and Coalbed Methane Potential of Comox and Nanaimo Coal Fields, Vancouver Island, British Columbia; *in* Coalbed Methane of Western North America, Schwochow, S.D., Murray, D.K. and Fahy, M.F., Editors, *Rocky Mountain Association of Geologists*, pages 155-162.

Das, B.M., Nikols, D.J., Das, Z.U. and Hucka, V.J. (1991): Factors Affecting Rate and Total Volume of Methane Desorbtion from Coalbeds; *in* Coalbed Methane of Western North America, *Rocky Mountain Association of Geologists*, pages 69-76.

Davidson, A., Peach, H.B. and Ferrie, D.J. (1965): Upper Cretaceous and Tertiary Sediments, Eastern Vancouver Island and Gulf Islands, British Columbia; *Shell Canada Limited*, unpublished report.

England, T.D.J. (1989): Lithostratigraphy of the Nanaimo Group, Georgia Basin, Southwestern British Columbia; *in* Report of Activities, *Geological Survey of Canada*, Paper 1989-1E, pages 197-206.

England, T.D.J. (1990): Late Cretaceous to Paleogene Evolution of the Georgia Basin, Southwestern British Columbia; unpublished Ph.D. thesis, *Memorial University of Newfoundland.*

Haggart, J.W. (1991): A New Assessment of the Age of the Basal Nanaimo Group, Gulf Islands, British Columbia; *in* Report of Activities, *Geological Survey of Canada*, Paper 91-1E, pages 77-82.

Kenyon, C. and Bickford, C.G.C. (1989): Vitrinite Reflectance Study of Nanaimo Group Coals of Vancouver Island; *in* Geological Fieldwork 1988, *B.C. Ministry of Energy, Mines and Petroleum Resources*, Paper 1989-1, pages 543-552.

Mahannah, R.S. (1964): Report on 1963 Surface Geological Mapping along the East Coast of Vancouver Island, the Alberni Area, and the Gulf Islands, B.C. *Shell Canada Limited*, unpublished report.

McKenzie, J.D. (1922): The Coal Measures of Cumberland and Vicinity, Vancouver Island; *Canadian Institute of*

Mining and Metallurgy, Transactions, Volume 25, pages 382-411.

Richardson, J. (1873): Report on the Coal Fields of Vancouver and Queen Charlotte Islands; *Geological Survey of Canada*, Report of Progress, 1872-1873, pages 32-65.

Saunders, C.R., Howey, H.O. and Campbell, D.D. (1974): Report on the Reserves and Mining Costs of the Comox Coalfield, Vancouver Island, B.C.; *Dolmage Campbell and Associates Ltd.*, unpublished report.

Usher, J.L. (1952); The Ammonite Faunas of the Upper Cretaceous Rocks of Vancouver Island, British Columbia; *Geological Survey of Canada*, Bulletin 21.

Williams, T.B. (1924): The Comox Coal Basin; unpublished Ph.D thesis, *University of Wisconsin*.

Wyman, R.E. (1984): Gas Resources in Elmworth Coal Seams; *American Association of Petroleum Geologists*, Memoir 38, pages 173-187.

SUBSURFACE THERMAL COAL SAMPLING SURVEY, MERRITT COAL DEPOSITS, SOUTH-CENTRAL BRITISH COLUMBIA (92I/2)

By A. Matheson

KEYWORDS: Coal geology, Merritt, diamond drilling, core sampling, coal quality, coalbed methane.

INTRODUCTION

The province-wide subsurface coal-sampling survey started in 1988 in the Comox coalfield. In 1989 the program was cosponsored by the Institute of Sedimentary and Petroleum Geology and focused on the Telkwa coalfield. This was followed by drilling in the Bowron River coal deposit in 1990. The focus of the 1991 drilling was the Merritt coal deposit (Figure 4-5-1). A total of 354 metres was drilled, with a core diameter of 3.5 centimetres. Two holes were spudded in the Coal Gully area, one on Coldwater Hill, one at Diamond Vale and another at Normandale, for a total of five diamond-drill holes (Figure 4-5-2). The drilling program was conducted, as in previous years, by Neills Mining Company using a Prospector 89 drill manufactured by Hydrocore Drill Ltd.

Several coal exposures had been sampled and analyzed in 1987, under the direction of Dr. Fari Goddarzi of the Institute of Sedimentary and Petroleum Geology. The coal seams and bands recovered from the drill cores are being prepared for analysis.

LOCATION OF THE STUDY AREA

The Merritt coal deposits are located 90 kilometres south of Kamloops on the Coquihalla Highway. Situated in the Nicola Valley, south-central British Columbia (Figure 4-5-1), the occurrences surround the town of Merritt stretching 8 kilometres east-west and 5 kilometres north-south. The locations of the mined areas are indicated on Figure 4-5-2. The Quilchena deposit was not sampled in this study due to financial constraints.

EXPLORATION AND PRODUCTION HISTORY

The earliest reference to coal in the Nicola Valley area, near the present town of Merritt, appeared in the "British Colonist", Victoria, British Columbia, on August 20, 1896, reporting on its use for a forge in Victoria. The coal was generally mined by the local inhabitants for domestic purposes. Regular production from the Middlesboro Collieries on Coal Gully Hill began in 1906. A total of 2.93 million tonnes was produced underground from the Merritt coal deposits until mining ceased in 1963. Middlesboro Collieries mined 92 per cent of the total, from the Coal Gully area and a large area of Coldwater Hill. Other collieries mined the Diamond Vale (mining ceased in 1912, after an explosion resulted in the deaths of seven men), Normandale and Sunshine areas. A very small amount was taken out of Quilchena by a local rancher for domestic purposes.

At present Imperial Metals Corporation holds the freehold coal rights to the Coal Gully Hill and Coldwater areas. Renewed interest in coal in 1980 and 1981 resulted in Crows Nest Resources Ltd. taking up coal licences and options on freehold lands in the area. Mapping was carried out from the Coal Gully Hill deposit to Quilchena, 27 holes were drilled and a trench excavated at Quilchena. Due to rapid weathering and the character of the rocks in the area, nearly all the adits have caved and trenches have filled with rubble. No further exploration has been carried out since that time.

GEOLOGICAL SETTING

The Tertiary (Eocene) coal measures of the Coldwater Formation overlie and are bounded by volcanic rocks of the Upper Triassic Nicola Group. A tongue of younger Pliocene valley basalt outcrops in the northeast corner of the study area, covering the Nicola volcanics, and runs southwestwards, covering a portion of the Coldwater Formation. Pleistocene and Recent unconsolidated sediments, both glacial and fluvial, cover much of the valley floor (White, 1946).

The Coldwater Formation is a sequence of nonmarine conglomerate, sandstone, shale and coal. It occupies one of several early Tertiary basins in the Cordilleran Intermontane Belt. The lake in which deposition occurred was part of a drowned valley system, probably conforming with the present topography. The coal formed in the early stages of lake development.

The conglomerate, grit and sandstone are largely composed of quartz and feldspar, derived mainly from local granitic sources. The shales are thinly bedded and are associated with the coal horizons of the sequence. The basal conglomerate is composed mainly of Nicola rock fragments. Calcareous horizons occur throughout the sedimentary sequence.

Due to the thick Pleistocene cover in the valley, the structural pattern of the underlying sediment is unclear. In the west, where the geology is better known as a result of the mining and exploration activity, there are moderately tight northwest-trending folds, offset by numerous strike faults. To the east, the dips become more gentle and the coal deeper. In the centre of the basin the sediments appear to have been less disturbed by tectonic activity. In the southeast sector, near the eastern boundary, the beds strike northeast and the folds are more open. The eastern boundary of the Coldwater sediments is a fault contact with the Nicola volcanics. (Read, 1988; Figure 4-5-2)

COAL MEASURES

The thickness of the coal measures varies up to 300 metres at the western rim of the basin where the coal

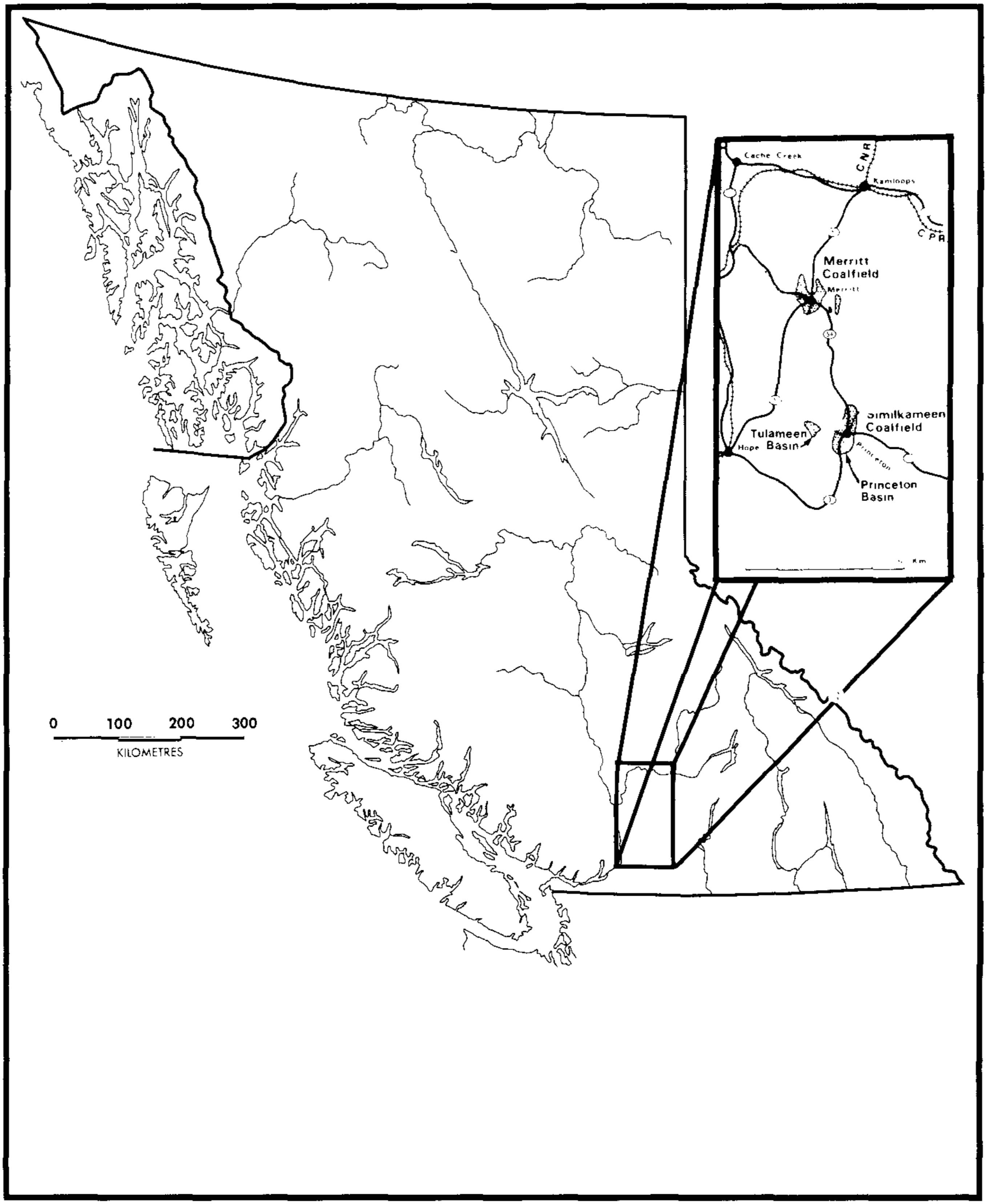

Figure 4-5-1. Location map showing the Merritt and Similkameen coalfields and the Tulameen and Princeton basins.

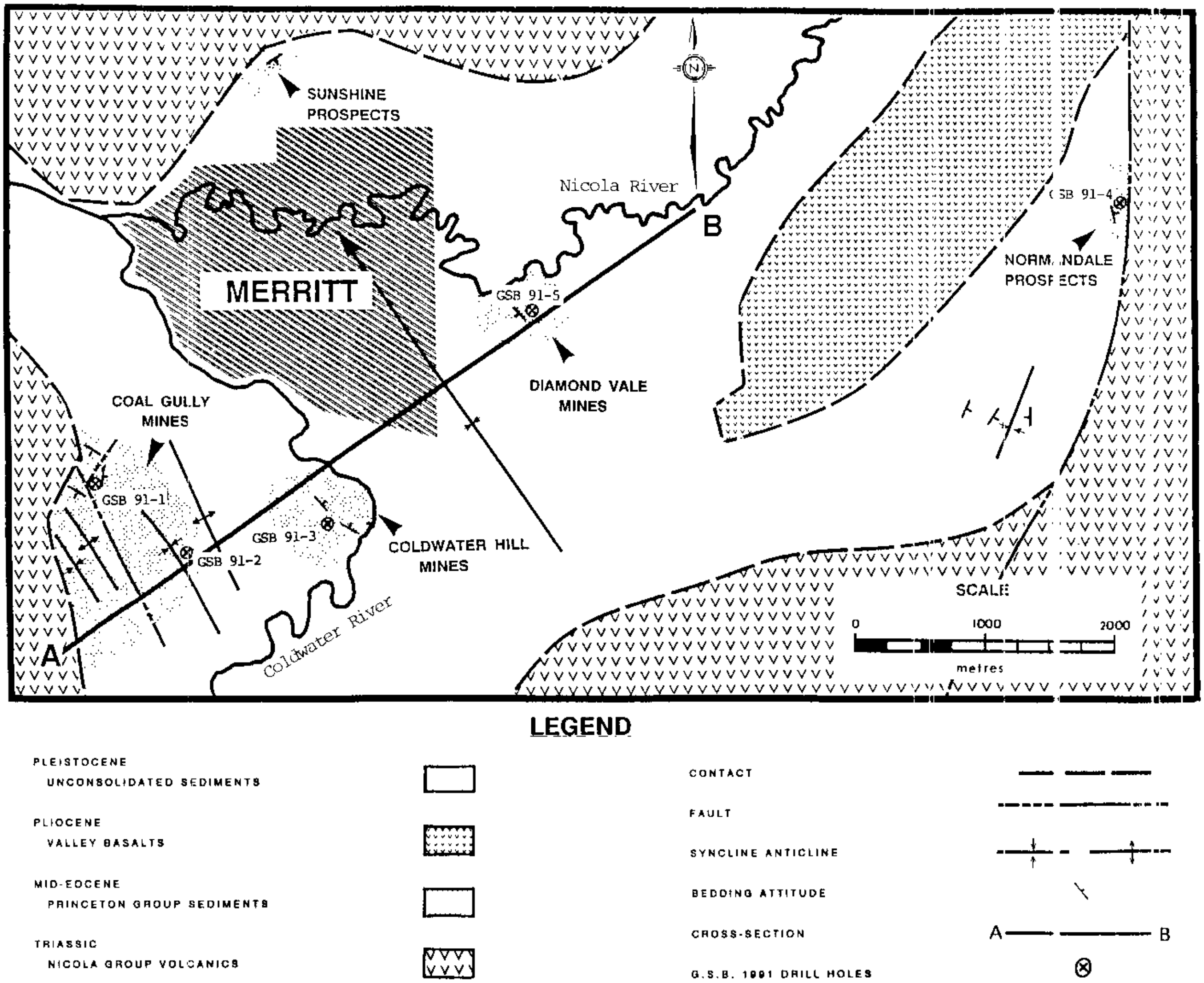

Figure 4-5-2. Detailed geology of the Merritt area showing drill-hole locations.

zones tend to be thicker and more numerous than in the eastern part of the basin. In the Coal Gully area, where the strata are quite steeply folded, seven coal zones have been reported. Starting from the lowest in the succession, the thicknesses of the zones are as follows: No. 1 is 7.9 metres, No. 5 is 1.5 metres, No. 4 is 7.6 metres, No. 8 is 2.44 metres, No. 6 is 1.8 metres, No. 3 is 0.76 metre and No. 2 is 1.8 metres (Swaren, 1977).

To the east and the south, the coal zones generally diminish in thickness, however, No. 5 zone increases to 3 metres and 2.2 metres respectively and the No. 3 zone increases to 1.3 metres. The zones pinch and swell, and the intervals between them may vary up to 30 metres.

Drilling in the Coldwater Hill area in 1991 confirmed that No. 6 zone, previously reported absent in this area, does occur, but thins to about 1.1 metres. The beds form the southwest limb of a broad symmetrical syncline, striking northwestwards and dipping to the northeast at an average of 35° at outcrop.

In the Diamond Vale mine, zones 2, 3 and 5 were mined. The lower zones, 8, 4, 5 and 1 were not exploited due to depth. The mine is on the northeast limb of the syncline and coal seams dip to the southwest at an average of 40° at outcrop. East of the Diamond Vale mine, two strike-slip faults have been identified by drilling (Figures 4-5-3 and 4), but little more is known about this area.

The coal is interbedded with shale and rooted quartz arenite, in parts calcareous, with coalspar and horizons exhibiting burrowing and bioturbation. The typical depositional environment ranged from back-barrier lagoons to mixed sand and mud flats, corresponding to areas of low to moderate energy, and subject to variable current velocities.

COAL QUALITY

The coal is reported to vary form high-volatile C to A bituminous in rank. A typical proximate analysis, on an as-received basis, is: moisture, 5 per cent; ash, 9 per cent;

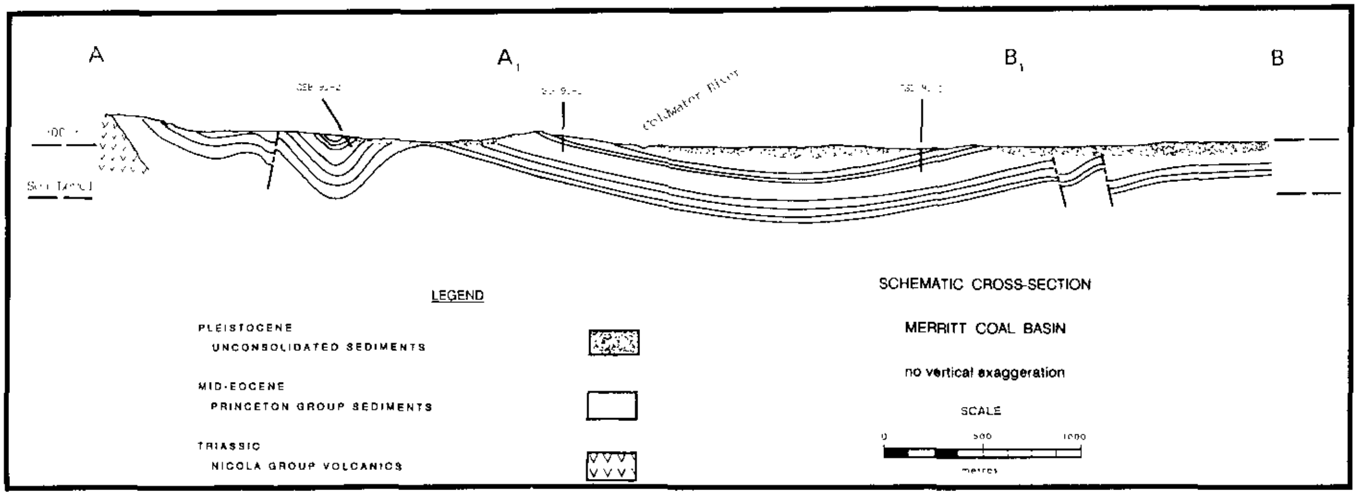

Figure 4-5-3. Schematic cross-section of the Merritt coal basin.

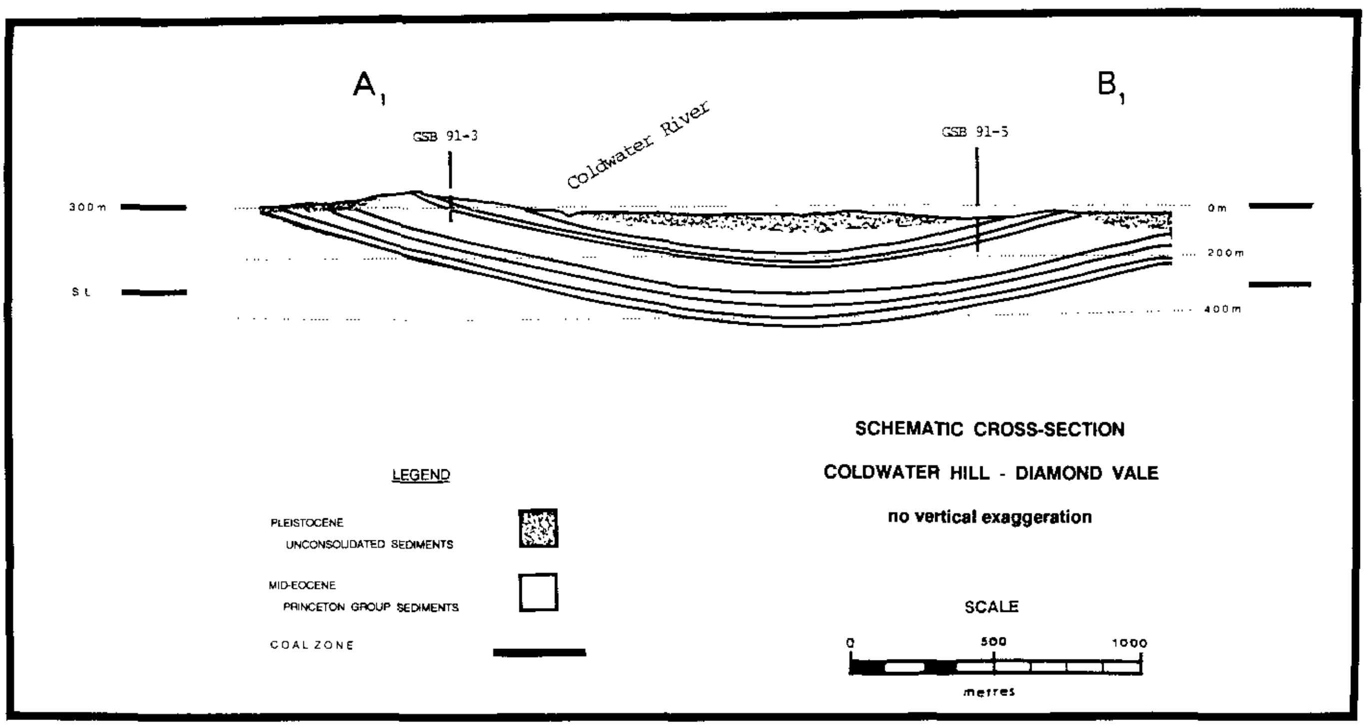

Figure 4-5-4. Schematic cross-section of a portion of the Merritt coal basin in the vicinity of Coldwater River. Location of drill-holes GSB91-3 and 5 indicated. *See* Figures 4-5-3 for complete section.

volatile matter, 34 per cent; fixed carbon 52 per cent; (*B.C. Ministry of Energy, Mines and Petroleum Resources*, Information Circular 1990-5).

Sulphur at 0.6 per cent is low. The heating value is about 30 000 kilojoules per kilogram. The Hardgrove grindability index is about 57. Amber is often present but is not abundant.

Friability may be higher than suggested by the Hardgrove index and rank, probably due to the effects of tectonism.

DRILLING AND SAMPLING

There were several major constraints in selecting drilling sites. Water was not readily available and in several cases had to be pumped from a source over 800 metres away. The water required for drilling at Normandale had to be brought in by truck from Nicola Lake 6 kilometres away. There are no accurate mine plans available, and as a result drill sites had to be carefully selected to avoid any break through into old workings. Finally, burning coal of unknown extent at Coldwater Hill had to be avoided.

The sandstone is poorly consolidated and cavities occur as a result of dissolution (Plate 4-5-1). Consequently there was frequent caving and loss of water circulation while drilling. Hole GSB-91-4 at Normandale had to be abandoned at 60 metres due to constant caving jamming the drill rods.

Two holes were collared on Coal Gully Hill. A vertical hole (GSB-91-1; total depth 83.2 metres) intersected the No. 4 zone (Plate 4-5-2). Due to the very broken character of the coal in the core, only 4.25 metres (true thickness) of core was recovered from the zone measuring 8 metres (true thickness) at outcrop. Hole GSB-91-2, was angled at 60° from the horizontal at an azimuth of 220. Number 2, 3 and 6 zones were intersected before the hole was stopped at 60.2 metres. A vertical hole on Coldwater Hill, GSB-91-3 (depth 45 metres), intersected the No. 3 and No. 6 zones. The final hole, GSB-91-5, drilled at Diamond Vale (depth 91.3 m), intersected coal zones Nos. 2, 3 and 6. Most previous reports on this area indicate the existence of only six coal zones, however, No. 6 zone has been intersected in three holes and though it may not be continuous, it does bring the total to seven zones.

SAMPLE ANALYSIS

All coal samples will be crushed to −2(mesh. Petrographic rank determinations will be carried o it in-hous by the vitrinite reflectance method. Minera ogy of low-temperature ash samples wil be dete mine l using x-ray defraction. The following analyses will be c rried out by a private laboratory under the joint auspices of he Geological Survey Branch and the Institute of Sed mentary and Petroleum Geology: proximate; ultimate; s ilphur forms; calorific value; ash analysis; chlorine, fluorin e and mercury contents; and ash fusion.

Dr. Fari Goodarzi sampled the remainde of the core, after the coal had been removed, and these samples were sent to the Institute of Sedimentary and Petro leum Geology

Plate 4-5-1. Poorly consolidated sandstone with cavities due to dissolution.

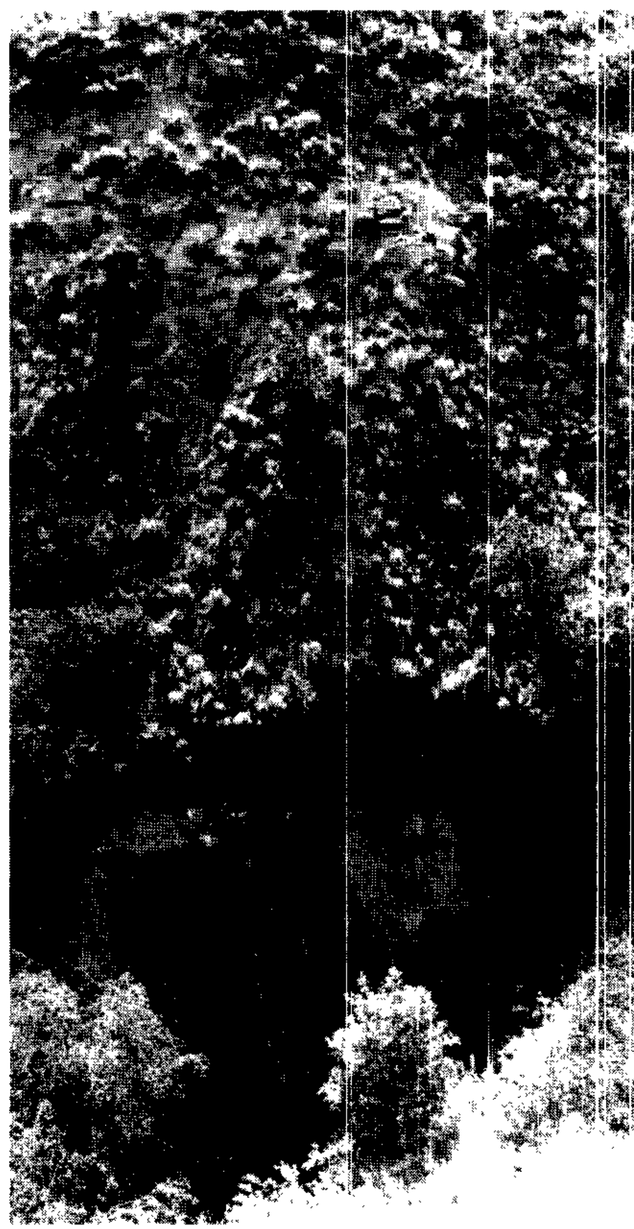

Plate 4-5-2. No. 4 zone at Gully Hill inter ected by drill hole GSB-91-1.

in Calgary, primarily for petrographic examination of the carbonaceous material in the siltstones and shales, and for trace element determination, which will be done on the coal, using primarily neutron activitation.

METHANE POTENTIAL

Methane is inherent in all coals and is desorbed when the gas pressure exceeds that of the hydrostatic head. Blocky coals, which desorb 60 per cent of their total gas, have less than 57 per cent fixed carbon and have an average Hardgrove index of less than 70. Friable coals, which desorb 94 per cent of their total gas, have greater than 57 per cent fixed carbon and have an average Hardgrove index greater than 70 (McCullough *et al.*, 1980). Further analysis is necessary to resolve the nature of the Merritt coals.

As a general rule, retention of methane in coal seams increases with the rank and depth of the coal (Ryan, 1991)

The Merritt basin, underlain by coal measures, covers an area of about 40 square kilometres. An area of 15 square kilometres was selected for the examination of coalbed methane potential, from Coldwater Hill to Diamond Vale. The coal measures form a symmetrical open syncline, 3 kilometres wide, which plunges to the northwest for about 5 kilometres. All seven seams are present. The average thicknesses of the coal zones recorded from drill logs are as follows: No. 1 is 2.5 metres, No. 5 is 2.8 metres, No. 4 is 2.4 metres, No. 8 is 0.6 metre, No. 6 is 0.7 metre, No. 3 is 1.3 metres and No. 2 is 1.1 metres.

Calculations are based on the mean cross-section A1-B1 (Figure 4-5-3) and the graph showing methane retention by rank and depth (Eddy *et al.*, in Ryan, 1991). The total potential volume of this particular area amounts to about 31 billion cubic feet of gas (Table 4-5-1). It is not possible to calculate the gas potential of the remaining 60 per cent of the field due to lack of geological data.

CONCLUSION

Badly broken core, abundant slickensiding and cavities in the sandstone created by solution, resulted in an overall core loss of 12 per cent, considerably greater than that of previous years. The core loss was highest in the coal zones, where it averaged 18 per cent. Methane desorption tests were not possible due to the broken nature of the core. Further drilling, north, northeast and east of the Diamond Vale mine, would resolve the structure, identify the coal measures and delineate the resources.

It is improbable that the Merritt coal deposits would be capable of supporting a viable mining operation in the future, but an interesting alternative energy resource may be the extraction of methane from the coal measures, providing a valuable source of fuel for the inhabitants of Merritt and the surrounding countryside.

TABLE 4-5-1
MERRITT COAL DEPOSITS COLDWATER HILL – DIAMOND VALE COAL RESOURCES AND POTENTIAL COALBED METHANE RESOURCES

	DEPTH IN METRES			TOTALS
FROM	0	200	400	0
TO	200	400	500	500
TOTAL COAL (million tonnes)	77.39	123.27	28.34	229
TOTAL METHANE (million cubic feet)	10 835	16 025	3 968	30 828
REFLECTANCE	.75			

ACKNOWLEDGMENTS

The author would like to thank Mansour Sadre for his invaluable assistance and provocative stimulus in the field; Dr. Fari Goodarzi for his keen interest, participation and support of the program; his colleagues in the Coal Unit and Anna Peakman for her stenographic support. The author would, in addition, like to extend his appreciation to the local ranchers, Mrs. Greta Garthwaite, Mr. Dave Chutter and Messrs Ewalt for their very kind assistance, and to Imperial Metals Corporation for permission to drill on their freehold properties.

SELECTED BIBLIOGRAPHY

Diamond, W.P. and Levine, J.R. (1985): Direct Method Determination of the Gas Content of Coal: Procedures and Results; *United States Department of the Interior, Bureau of Mines*, Report of Investigations 8515.

Dolmage, Campbell & Associates Ltd. (1975): Coal Resources of British Columbia, Nicola Coalfield; *Dolmage, Campbell & Associates Ltd.*, pages 4-26 to 4-30.

Eddy, G.E., Rightmire, C.T. and Byern, C.W. (1982): Content of Coal Rank and Depth; Relationship of Methane; *Society of Petroleum Engineers/Department of Environment*, Proceedings of the Unconventional Gas Recovery Symposium, Pittsburg, Pennsylvania, pages 117-122.

Graham, P.S.W. (1977): The Geology and Coal Potential of Tertiary Sedimentary Basins, Interior British Columbia; Merritt, Quilchena; *Geological Survey of Canada*, pages 10-14.

McCullough, C.M., Levine, J.R., Kissell, F.N. and Duel M. (1980): Measuring the Methane Content of Bituminous Coal Beds; *United States Department of the Interior, Bureau of Mines*, Report of Investigations 8043.

Read, P.B. (1988): Tertiary Stratigraphy and Industrial Minerals, Merritt Basin, Southern British Columbia; (92I/1 & 2); *B.C. Ministry of Energy, Mines and Petroleum Resources*, Open File 88-15.

Ryan, B.C. (1991): Geology and Potential Coal and Coalbed Methane Resource of the Tuya River Coal Basin; *in* Geological Fieldwork 1990, *B.C. Ministry of Energy, Mines and Petroleum Resources*, Paper 1991-1, pages 419-429.

Swaren, R. (1977): unpublished Exploration Report; Imperial Oil Ltd.

White, W.H. (1946): Report on the Merritt Coalfield; *B.C. Ministry of Energy, Mines and Petroleum Resources*, Report to the B.C. Minister of Mines 1946, pages A250-A279.

PINE VALLEY MAPPING AND COMPILATION PROJECT (93O/9, 10; 93P/12)

By P.C. Jahans

KEYWORDS: Coal geology, Pine Valley, Peace River coalfield, stratigraphy, structural geology, coal occurrences.

INTRODUCTION

This project is a continuation of the British Columbia Geological Survey Branch's 1:50 000-scale mapping program in the Peace River coalfield. The study area is adjacent to the Burnt River and Carbon Creek map-areas (Hunter and Cunningham, 1991; Cunningham and Sprecher, 1992, this volume). The objective is to produce Open File maps for NTS map sheet 93O/9, the northeast half of 93O/10 and the southwest half of 93P/12.

Computer methods were used extensively in data handling, compilation and map drafting. The geological maps will be in digital format for reproduction and distribution. Several in-house software modules were developed and, in conjunction with commercial packages, will be used to produce these maps.

LOCATION

The map area is located in northeastern British Columbia immediately west of the town of Chetwynd (Figure 4-6-1). It lies between latitudes 55°30' and 55°45' and is bordered on the west by the Front Ranges of the Rocky Mountains. The area is generally covered by thick vegetation except for the ridges in the west, and is divided by the east-flowing Pine River. Access to most of the area consists of a network of logging and drilling roads, cut-lines, seismic lines and transmission-line roads. Elevation ranges from about 600 to over 1900 metres.

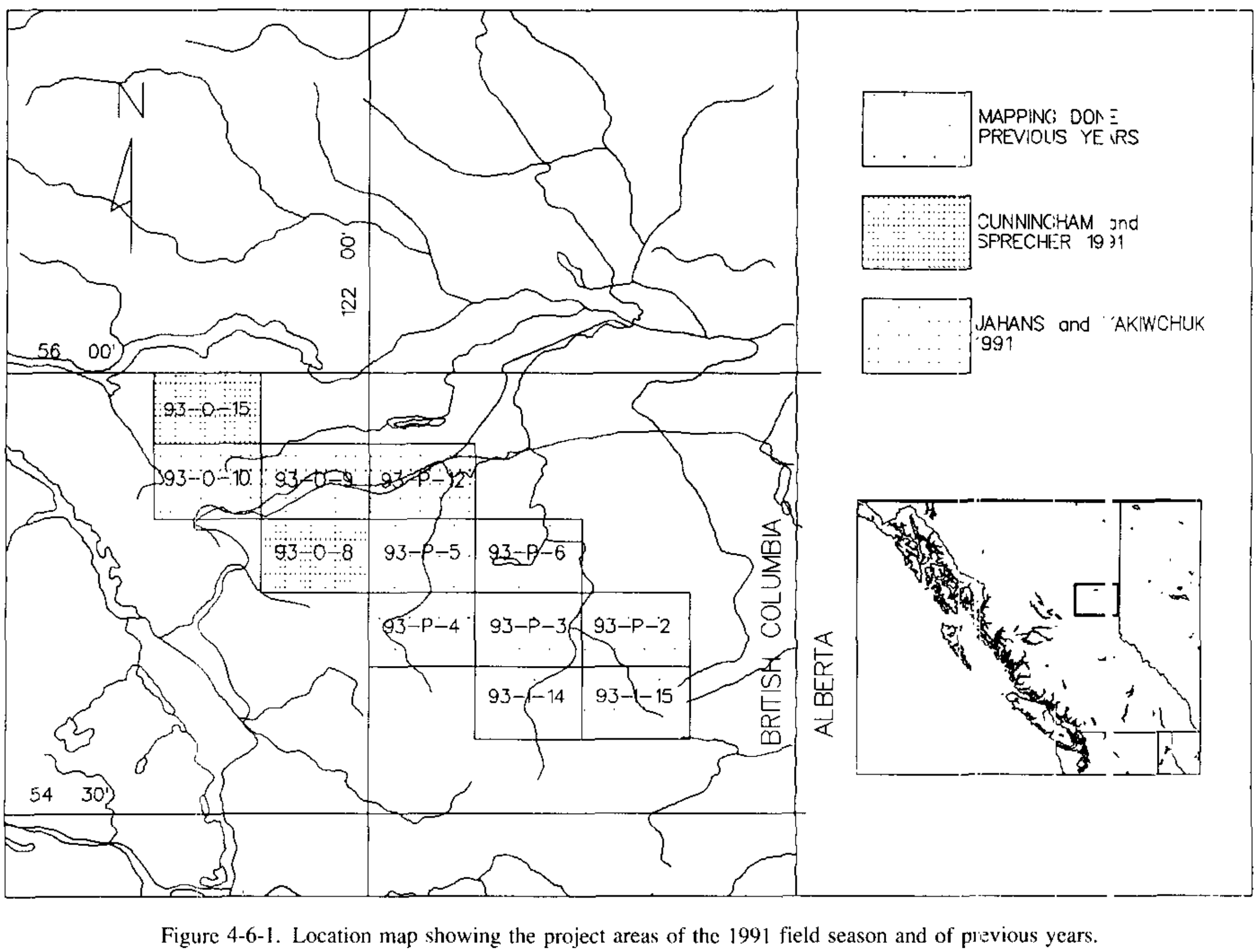

Figure 4-6-1. Location map showing the project areas of the 1991 field season and of previous years.

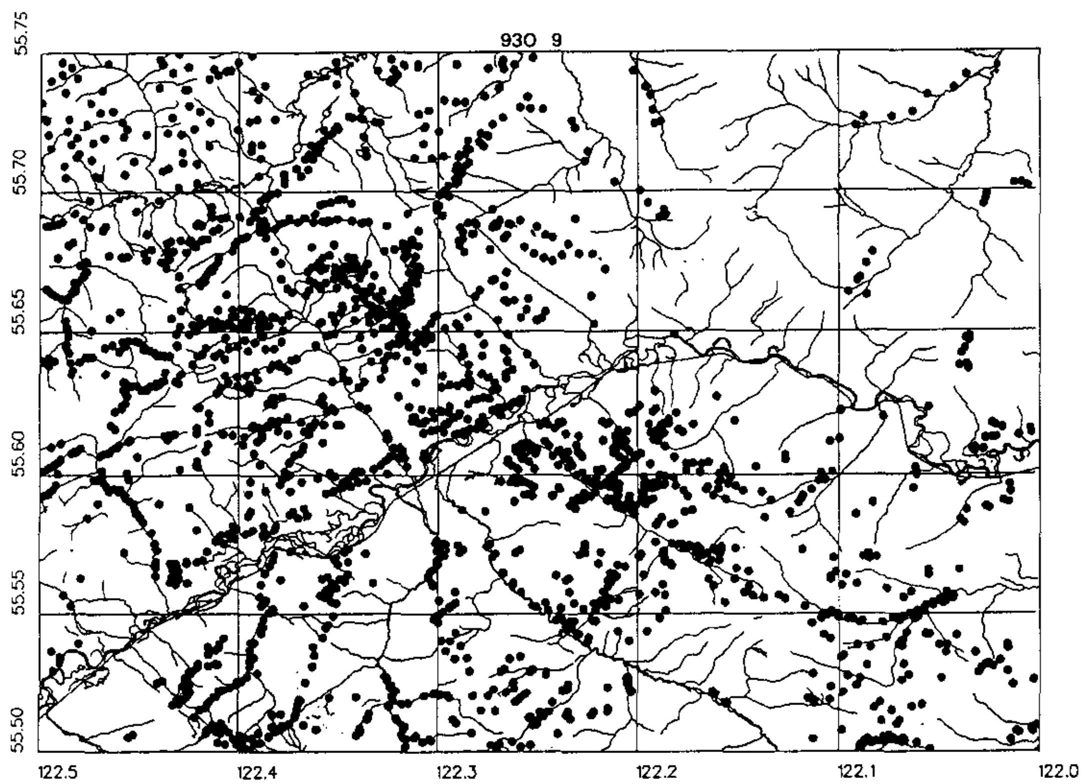

Fig. 2a

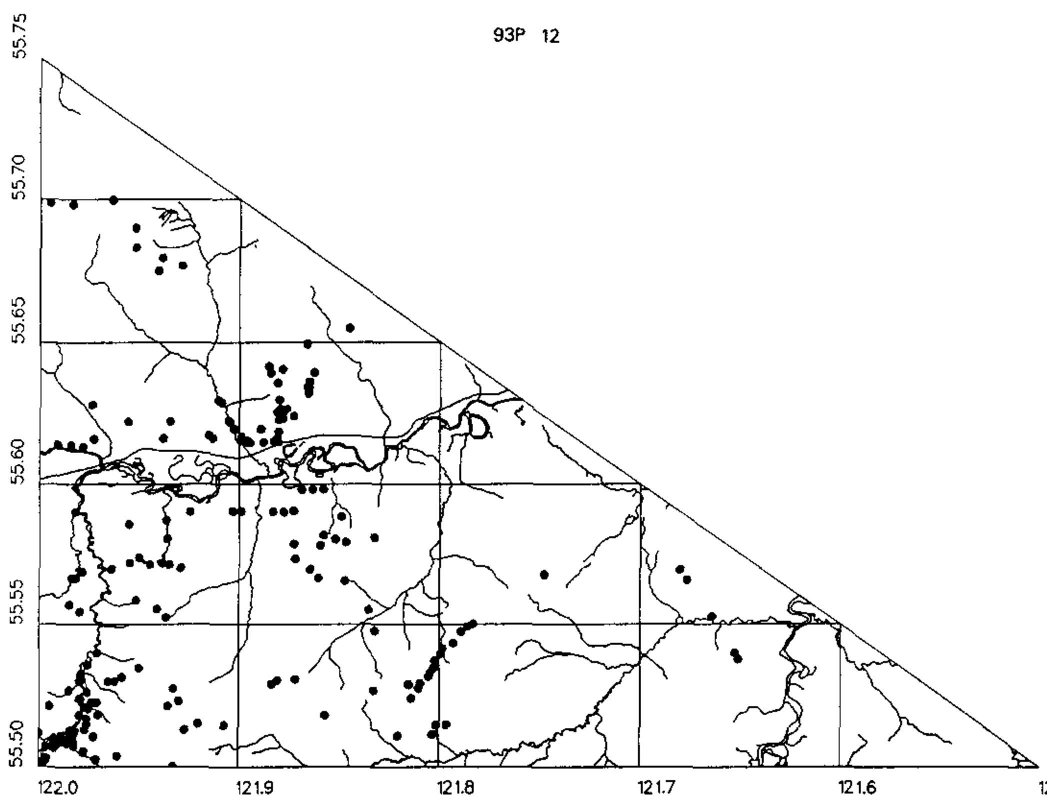

Fig. 2b

Figure 4-6-2. Outcrop distribution in the map sheets (a) 93O/9 and (b) 93P/12. Outcrops represented here are a compilation from previous work and the 1991 field season.

PREVIOUS WORK

Parts of the map area have been studied in detail by several coal and petroleum exploration companies as well as by researchers from the provincial (McKechnie, 1955; Hughes, 1964, 1967) and federal governments (Stott, 1967, 1968, 1973, 1982). This project is a compilation of the past summer's fieldwork and recent detailed mapping by coal company geologists.

1991 FIELD ACTIVITIES

Mapping during the 1991 field season focused on areas with little or no coverage on existing maps. Coverage is generally good near the Pine River and in most of the western parts of the 93P/12 and 93O/9 map sheets. Transport was by four-wheel-drive vehicle, mountain bicycle, helicopter and hiking on foot (Figure 4-6-2). Aerial photographs were used for navigation and in geological interpretation.

DATA

The integration of outcrop data collected during this field season with the extensive information obtained from provincial government coal and petroleum files and from various industry sources was accomplished using computer techniques. Base maps with contour, cadastral, drainage and cultural information were obtained as digital TRIM files.

During the field season, outcrop data were recorded in the traditional way and then entered into computer files at the field office in Chetwynd. Maps showing topographic contours, roads, cut-lines and drainage were plotted at various scales for use in the field in conjunction with aerial photographs. If time permitted, preliminary geological interpretations of each day's fieldwork were added to the database. Extensive use of CAD-based graphical mapping software facilitated the efficient presentation of data and drawing of geological maps.

STRATIGRAPHY

The map area is underlain by rocks ranging in age from Triassic and Jurassic in the southwest to Cretaceous in the northeast. Marine clastic rocks make up the Jurassic Fernie Formation and Lower Cretaceous Minnes Group. Alternating marine to nonmarine clastics and marine shales dominate the rest of the Cretaceous. Formation names and general thicknesses with brief lithological descriptions are given in Table 4-6-1.

MINNES GROUP

The Minnes Group, divisible into the Monteith, Beattie Peaks, Monach and Bickford formations, consists mainly of interbedded sandstones, siltstones and shales. The Beattie Peaks and the Bickford are the more argillaceous of these formations with minor coal seams present in the Bickford. Towards the west, the sand content of the Beattie Peaks Formation increases to the point where it becomes increasingly difficult to distinguish between it and the underlying Monteith and overlying Monach formations.

The ridge-forming Monteith and Monach formations are dominated by arenaceous strata. Very light grey to white quartzitic sandstones occur in both units. Two such beds, usually 2 to 6 metres thick, provide useful marker horizons near the top of the Monach Formation.

The Bickford Formation consists of interbedded fine-grained sandstones, siltstones, dark grey mudstones and silty shales. Thin coal seams, generally less than 1 metre thick, are present in this unit.

BULLHEAD GROUP

The Bullhead Group includes the Cadomin and Gething formations. The ridge-forming Cadomin Formation consists of well-rounded, poorly sorted chert pebbles and very coarse grained sandstones and grits. Its thickness varies and the proportion of conglomerate tends to decrease to the northwest.

The Gething Formation is generally a recessive unit and exposures are rare. Similar in composition to the Bickford Formation, it consists of interbedded sandstones, siltstones, mudstones and silty shales. The Gething Formation, however, contains more shale and thick coal seams, has better developed cyclothems, and is finer grained. Coal seams are generally from 1 to 3 metres thick but are up to 4 metres thick in places. Abundant plant imprints and the occasional fossilized tree stump are observed in outcrop.

FORT ST. JOHN GROUP

The Fort St. John Group is divided into the Moosebar, Gates, Hulcross, Boulder Creek, Hasler, Goodrich and Cruiser formations. At two locations in the Crassier Creek area, a bed of conglomerate and sandstone, 2 to 4 metres thick, separates the Moosebar from the Gething and is believed to represent, or be stratigraphically equivalent to, the Bluesky Formation. The Moosebar Formation is a very recessive and poorly exposed unit. It is distinguished by its dark grey to black shale content and interbedded sideritic siltstones and concretions.

The remaining formations are easily distinguishable in the field. Prominent ridges formed by Gates, Boulder Creek and Goodrich sandstones and conglomerates together with the topographic lows formed by the recessive marine shales of the Hulcross and Hasler formations, combine to form a distinctive profile easily recognized in the east-central portion of map sheet 93O/9.

Unlike the area to the south, the Gates Formation is thin and lacks significant coal seams. There is an abrupt change from the sandy sediments of the Gates to the dark marine shales of the Hulcross Formation. The Hulcross is similar to the Moosebar Formation and its contact with the basal sandstones of the Boulder Creek Formation is gradational. The Boulder Creek sandstones and conglomerates separate the Hulcross from the Hasler, another dark grey marine shale which is often difficult to distinguish from other shale units.

TABLE 4-6-1
TABLE OF FORMATIONS FOR THE PINE RIVER VALLEY AREA. ADAPTED FROM STOTT (1982)

Series	Group	Formation/Thickness	Description
Upper Cretaceous	Smoky	Dunvegan 107-300 m	Fine- to coarse-grained carbonaceous sandstone and shale; minor coal.
	Fort St. John	Cruiser 107-244 m	Dark grey marine shale with sideritic concretions and interbedded siltstones and sandstones.
Lower Cretaceous		Goodrich 15-411 m	Fine- to medium grained crossbedded sandstone; interbedded shale, mudst.
		Hasler 152-459 m	Dark grey marine shale with sideritic concretions; siltier in lower half.
		Boulder Creek 73-171 m	Fine-grained, well sorted sandstone; massive conglomerate; non-marine sandstone and mudstone.
		Hulcross 0-131 m	Dark grey marine shale with sideritic concretions and interbedded siltstones.
		Gates 67-274 m	Fine-grained, marine and non-marine sandstones; conglomerate, sh. & mudst.
		Moosebar 30-304 m	Dark grey marine shale with sideritic concretions; sandst. and congl. at base.
	Bullhead	Gething 22-549 m	Fine grained, carbonaceous sandst.; coal, carbonaceous shale; some conglomerate.
		Cadomin 14-213 m	Massive chert & quartzite pebble conglomerate, and med. to coarse gr. sandst.
	Minnes	Bickford 0-427? m	Interbedded fine-grained sandst.; silty sh.; coal.
		Monach 0-304 m	Fine- to coarse grained, argill. to q'tzose sandst.
		Beattie Peaks 0-396 m	Interbedded silty shales and fine-grained sandst.
		Monteith 0-610 m	Fine- to coarse grained, quartzose sandstone.
Jurassic		Fernie 0-579 m	Calcareous and phosphatic shales; thinly interbedded sandst, siltst, & shale.

A persistent argillaceous sandstone with interbedded dark grey shales, which has been called the Walton Member of the Boulder Creek Formation, separates the Boulder Creek from the Hasler. The Walton Member is distinguished by the presence of abundant rootlets and other plant remains. Although it is known to contain coal (Hughes, 1967; Stott, 1982), no coal seams were found during this field season.

Next in succession are the recessive dark grey shales of the Hasler Formation. The lower half of this unit has a distinctly siltier composition and is more resistant. Gradationally overlying the Hasler are the fine-grained, well-sorted sandstones of the Goodrich Formation. Reddish brown weathering, and abundant large-scale crossbedding are its characteristic features. Fossiliferous marker horizons are present.

The dark grey shales and interbedded siltstones of the Cruiser Formation overly the Goodrich gradationally. This unit is very similar to the Hasler Formation. To the east, where the Goodrich pinches out in the subsurface, the Hasler and Cruiser are together assigned to the Shaftesbury Formation. In the eastern half of the map area, the Cruiser Formation underlies most of the upper slopes.

Smoky Group

The Dunvegan Formation is the youngest mapped formation, conformably overlying the Cruiser Formation and forming many of the easternmost cliffs in the map area. It is made up of interbedded carbonaceous sandstones, siltstones and shales. The sandstones are often micaceous and plant debris is abundant. Minor coal measures, generally less than 1 metre thick, are found in some locations. *Unio* and *Inoceramus* are common and distinguishing fossils.

STRUCTURE

The map area lies in the Rocky Mountain Foothills. This region is characterized, as is most of the Rocky Mountain fold and thrust belt, by northwesterly trending folds and southwest-dipping thrust faults (McMechan, 1985; McMechan and Thompson, 1989). The Foothills are subdivided into inner and outer belts. The outer Foothills are characterized by low amplitude, long-wavelength, easily mapped folds involving Fort St. John and Dunvegan strata (Figure 4-6-3).

Deformation in the inner Foothills is characterized by tighter, higher amplitude folds involving Gething and older strata. The boundary between the outer and inner Foothills in the map area runs through Crassier Creek. Folds in the Gething Formation are difficult to analyze because of their complexity and small scale, and because of the poor exposure. The alternation of resistant and recessive units of the Minnes Group and the prominence of the Cadomin Formation provide good structural markers in the western parts of the inner Foothills belt.

Although numerous small faults are visible in outcrop in the outer Foothills, there is little evidence for large thrust faults. The inner Foothills, in contrast, contain many small- and large-scale faults. The linearity of their surface traces in areas with considerable topographic relief indicates relatively steep dips. There is some evidence for minor east-dipping thrust faults in the map area, especially the outer Foothills, though no major fault traces were found. The east-dipping contact between the Moosebar and the Gates on Dokie Ridge appears disconformable towards the northwest, and nearly pinches out the Gates Formation (Plate 4-6-1). Exposures are very poor and access is limited, so it is unconfirmed whether this feature represents local thinning of the Gates or the presence of an east dipping thrust fault.

Drilling has indicated the presence of blind thrusts in the region, and regional structural sections have shown the likelihood of major detachment zones in Upper Jurassic to Lower Cretaceous strata as well as at the base of Middle Devonian shales (McMechan, 1985). A triangle zone appears to be present.

COAL OCCURRENCES AND ECONOMIC GEOLOGY

Coal seams up to 3 metres thick are found in the Gething Formation and others up to 1 metre thick are present in the Bickford Formation. Minor coal occurrences are visible as thin seams less than a metre thick, in the Dunvegan, Goodrich and Cadomin formations. No significant coal was seen in the Gates Formation in the map area, although there are economic deposits in the Gates to the south at Bullmoose and Quintette mines.

There is no exploration for coal currently underway in the study area. Previous exploration was carried out by numerous coal and petroleum companies which mainly targeted the Gething Formation, although some interest was taken in the thinner seams of the Bickford Formation (referred to as the Brenot Formation by Hughes, 1964 and 1967, and many coal companies), and in the reported coal measures of the Walton Member (Hughes 1967; Stott, 1982). Vitrinite reflectances from coal samples suggest this area would be of potential interest for coalbed methane exploration (Hunter and Cunningham, 1991; Cunningham and Sprecher, 1992, this volume).

In contrast to coal, exploration for natural gas is very active. This season, several new wells were drilled and seismic lines cut in and around the study area. Main targets were the deep Triassic carbonates, which crop out in the west and form part of the Front Ranges.

SUMMARY

The importance of the Gates Formation as a coal-bearing unit is diminished in this map area compared to southern regions, while the Gething Formation, and to lesser extent, the Bickford Formation and Walton Member have been targets for coal exploration. Although there is potential for coalbed methane, current exploration activities are limited to conventional gas plays. Known coal deposits are not economic at this time.

Evidence for blind thrusts and east-dipping faults indicates the possible existence of a triangle zone. Regional geological mapping is essential in the construction of accurate, balanced cross-sections for resource exploration in the Rocky Mountain Foothills.

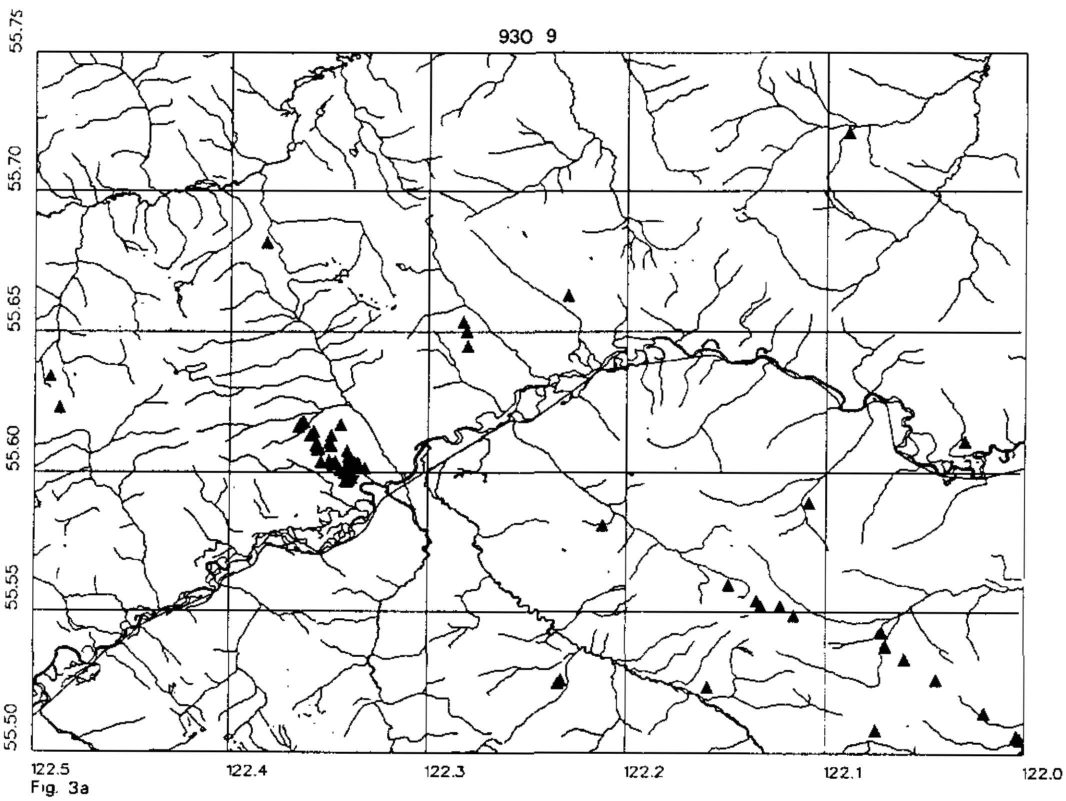

Fig. 3a

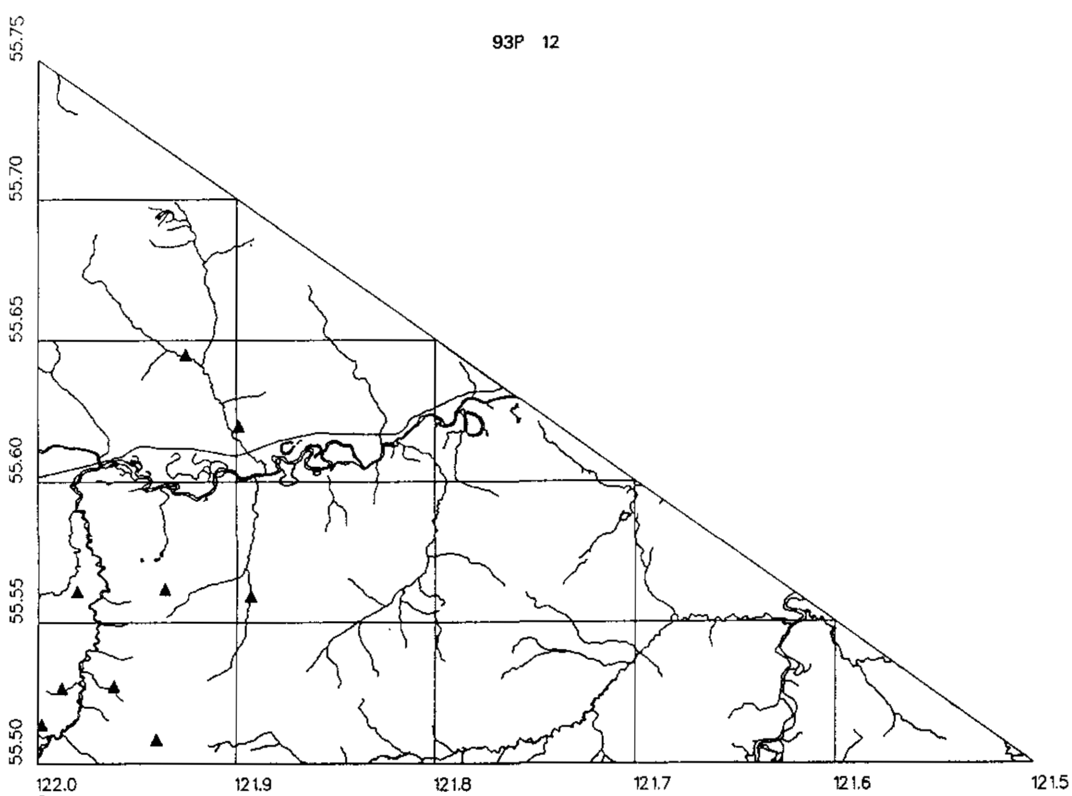

Fig. 3b

Figure 4-6-3. Drillhole locations in maps sheets (a) 93O/9 and (b) 93P/12.

This project is a continuation of the Peace River Coalfield Digital Mapping Project. Computer methods have enabled efficient data compilation and interpretation, in both the office and the field. Geological maps at a 1:50 000 scale will be available as Open Files in early 1992.

ACKNOWLEDGMENTS

The author wishes to thank Ward Kilby and John Cunningham for their invaluable advice and discussion throughout the project, and Kevin Yakiwchuk for his enthusiastic and tireless assistance in the field. Our comfortable accommodations in Chetwynd were provided by Robert and Jean Pohl. Special thanks go to Dr. Henry Charlesworth whose guidance, support and criticisms are gratefully acknowledged.

REFERENCES

Cunningham, J.M. and Sprecher, B. (1992): Peace River Coalfield Digital Mapping Program (930/8, 15); *in* Geological Fieldwork 1991, Grant, B. and Newell, J.M., Editors, *B.C. Ministry of Energy, Mines and Petroleum Resources*, Paper 1992-1, this volume.

Hughes, J.E. (1964): Jurassic and Cretaceous Strata of the Bullhead Succession in the Peace River Foothills; *B.C. Ministry of Energy, Mines and Petroleum Resources*, Bulletin 51, 73 pages.

Hughes, J.E. (1967): Geology of the Pine Valley, Mount Wabi to Solitude Mountain, Northeastern British Columbia; *B.C. Ministry of Energy, Mines and Petroleum Resources*, Bulletin 52, 137 pages.

Hunter, D.J. and Cunningham, J.M. (1991): Burnt River Mapping and Compilation Project (93P/5, 6); *in* Geological Fieldwork 1990, *B.C. Ministry of Energy, Mines and Petroleum Resources*, Paper 1991-1, pages 407-414.

McKechnie, N.D. (1955): Coal Reserves of the Hasler Creek – Pine River Area, British Columbia; *B.C. Ministry of Energy, Mines and Petroleum Resources*, Bulletin 36, 32 pages.

McMechan, M.E. (1985): Low-taper Triangle-zone Geometry: An Interpretation for the Rocky Mountain Foothills, Pine Pass – Peace River Area, British Columbia; *Bulletin of Canadian Petroleum Geology*, Volume 33, No. 1, pages 31-38.

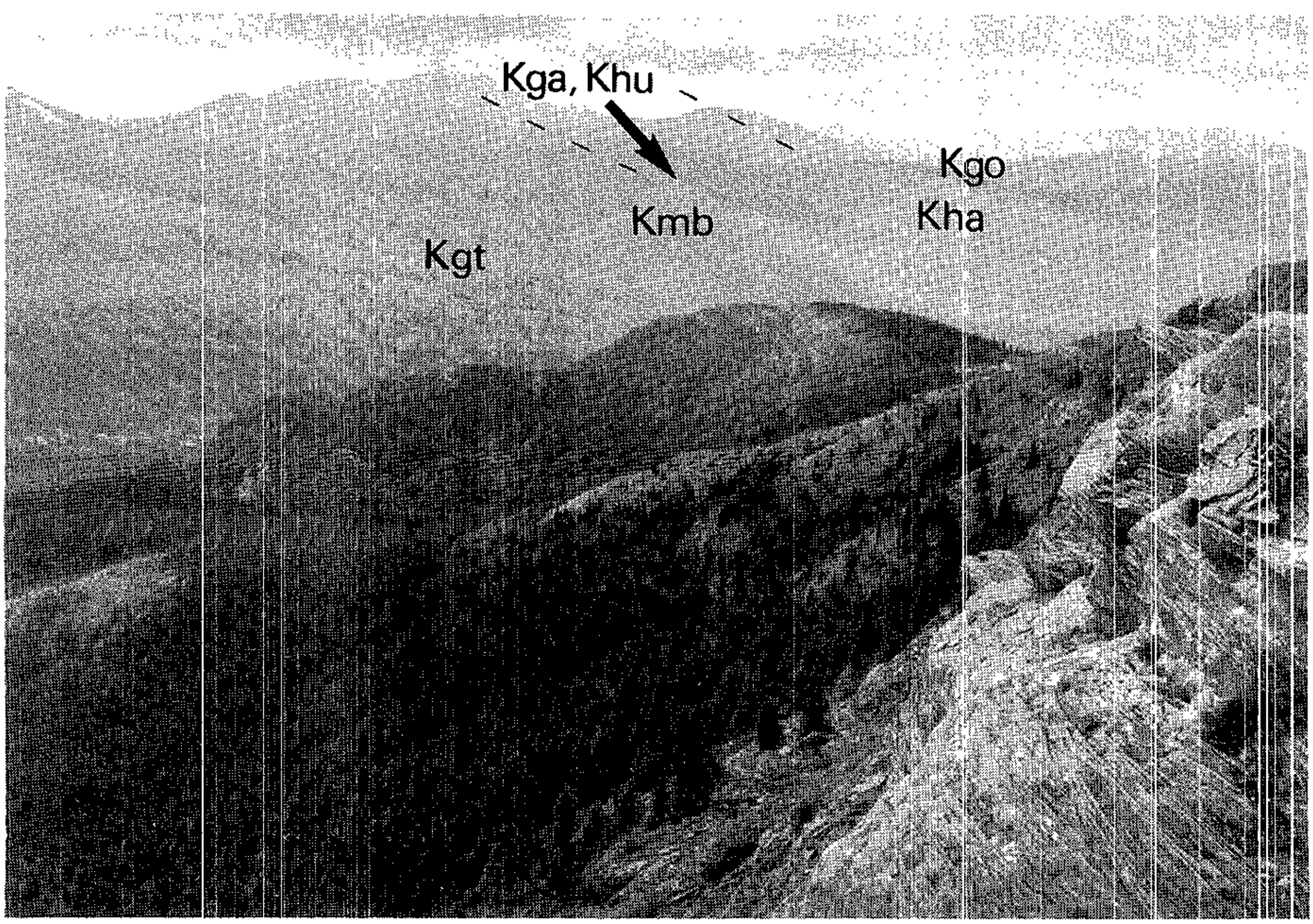

Plate 4-6-1. Photograph looking northwest showing east-dipping strata of the outer Foothills (foreground and right) overlying tightly folded strata in the Crassier Creek valley (background-left). Crossbedded sandstones of the Goodrich Formation (foreground) overly shales of the Hasler Formation. An apparently disconformable contact between the Moosebar and Gates formations indicates the possible existence of an east-dipping thrust fault (*see* text).

McMechan, M.E. and Thompson, R.I. (1989): Structural Style and History of the Rocky Mountain Fold and Thrust Belt; *in* Western Canada Sedimentary Basin, A Case History; Ricketts, B.D., Editor, *Canadian Society of Petroleum Geologists*, pages 47-71.

Stott, D.F. (1967): The Cretaceous Smoky Group, Rocky Mountain Foothills, Alberta and British Columbia; *Geological Survey of Canada*, Bulletin 132, 133 pages.

Stott, D.F. (1968): Lower Cretaceous Bullhead and Fort St. John Groups between Smoky and Peace Rivers, Rocky Mountain Foothills, Northeastern British Columbia; *Geological Survey of Canada*, Bulletin 152, 279 pages.

Stott, D.F. (1973): Lower Cretaceous Bullhead Group Between Bullmoose Mountain and Tetsa River, Rocky Mountain Foothills, Northeastern British Columbia; *Geological Survey of Canada*, Bulletin 219, 228 pages.

Stott, D.F. (1982): Lower Cretaceous Fort St. John Group and Upper Cretaceous Dunvegan Formation of the Foothills and Plains of Alberta, British Columbia, District of Mackenzie and Yukon Territory; *Geological Survey of Canada*, Bulletin 328, 124 pages.

PEACE RIVER COALFIELD DIGITAL MAPPING PROGRAM (93O/8, 15)

By J.M. Cunningham and B. Sprecher

KEYWORDS: Coal geology, Peace River coalfield, Le Moray Creek, Carbon Creek, stratigraphy, coal rank, structural geology, GIS, computer-aided mapping, coalbed methane.

INTRODUCTION

This project continued the 1:50 000-scale digital mapping and compilation program in the Peace River coalfield of northeastern British Columbia.The area mapped in this ongoing study reflects a continuing interest in the coal-bearing strata and structural relationships found in the Rocky Mountain Foothills. The regional northwest structural trends have necessitated the inclusion of half-map sheets for completeness. The areas mapped this year are located to the west and north of the map sheets completed in previous years (Figure 4-7-1). Two crews, each consisting of a geologist and an assistant, completed the mapping. Peter Jahans and Kevin Yakiwchuk mapped sheets 93P/12 and 93O/9 (Jahans, 1992, this volume). This article will deal with the work done by the authors on the Le Moray Creek (93O/8) and the Carbon Creek map sheets (93O/15).

The goal of the digital mapping and compilation project is to produce geology maps and databases in digital format. This will allow distribution of the computer files containing maps with the edited and refined data, as well as all the original raw data used in drawing the maps. Users will have the option of examining and manipulating the data.

An important aim of this year's study was to integrate the use of geographic information systems (GIS), in this case QUIKMap®, into the field mapping program. The data gathered in the field were combined with information compiled from previous Open File publications, coal assessment reports and petroleum borehole data, into a computer database. This database will be used in conjunction with QUIKMap software and TRIM© base-map data to generate computer-drafted geology maps. The maps will be released

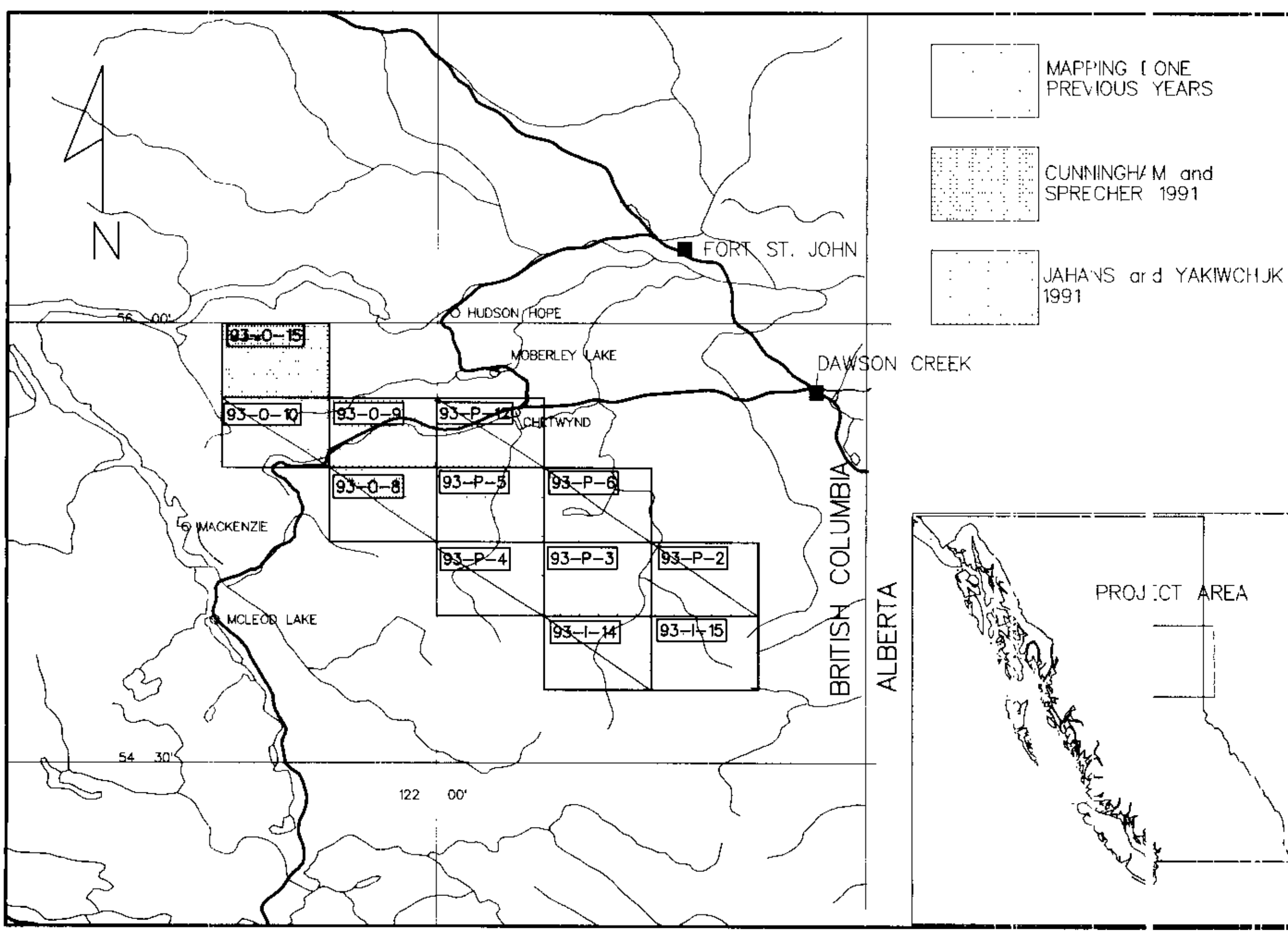

Figure 4-7-1. Location map showing the areas mapped as part of this year's study. Areas mapped in the previous years are also indicated.

SERIES	GROUP	MAP CODE	FORMATION	THICK (M)	LITHOLOGY
UPPER CRETACEOUS	FORT ST. JOHN	uKCR	CRUISER	150	Dark grey marine shale with sideritic concretions; some sandstone.
LOWER CRETACEOUS	FORT ST. JOHN	KGO	GOODRICH	150	Fine-grained, crossbedded sandstone; shale and mudstone.
		KHA	HASLER	300	Silty dark grey marine shale with sideritic concretions; siltstone in lower part.
		KBC	BOULDER CREEK	120	Fine-grained, well-sorted sandstone; massive conglomerate; nonmarine sandstone and mudstone and coal.
		KH	HULCROSS	100	Dark grey marine shale with sideritic concretions.
		KG	GATES	130	Fine-grained, marine and nonmarine sandstones; conglomerate; coal; shale and sandstone.
		KM	MOOSEBAR	130	Dark grey marine shale with sideritic concretions; glauconitic sandstone and pebbles at base.
	BULLHEAD	KGE	GETHING	1000	Fine to coarse-grained, brown, calcareous carbonaceous sandstone; coal; carbonaceous shale, and conglomerate.
		KCD	CADOMIN	200	Massive conglomerate containing chert and quartzite pebbles and sandstone.
	MINNES	KBI	BICKFORD	200	Sandstone; fine-grained and silty shale, carbonaceous in part; coal.
		KMC	MONACH	120	Fine grained argillaceous sandstones; massive fine to coarse-grained quartzose sandstones and quartzites.
		KBP	BEATTIE PEAKS	290	Interbedded fine-grained sandstone and silty shales.
		JKMT	MONTEITH	320	Fine-grained sandstones; white, fine to coarse-grained quartzose sandstones.
JURASSIC		JF	FERNIE	200	Calcareous and phosphatic shales; rusty weathering shales; glauconitic siltstone; sideritic shales; and in upper part thinly interbedded sandstone, shale, and siltstone.
TRIASSIC		TRS	(UNDIVIDED)	600	Limestone; dolomite; calcareous siltstone and sandstones; some anhydrite.

Table 4-7-1. Stratigraphic Table. Formation thicknesses given are average.

in 1992 as Open File map sheets 93O/15, 93O/9 and half-map sheets 93O/8, 93P/12 and 93O/10.

LOCATION AND ACCESS

The areas mapped on the Carbon Creek and the Le Moray sheets covered approximately 1300 square kilometres in the Rocky Mountain Foothills of northeastern British Columbia. Elevations in the region range from 700 to 2000 metres, with treeline at 1500 to 1600 metres. Vegetation varies from mature stands of pine and spruce to alpine tundra at the higher elevations.

The town of Chetwynd provided a convenient base for the study. The Le Moray Creek map area to the west of Chetwynd was reached by the John Hart Highway (No. 97), and the Carbon Creek map area to the north by Highway 29. In both areas a network of gravel roads, logging roads and old well-roads provides local access using a four-wheel-drive truck. Mountain bikes were used where roads were impassable by truck. Most of the cut lines, seismic lines, creeks and streams could be traversed only on foot.

This was the first year that mountain bikes were used on this project. They proved durable enough to handle the rough terrain and negotiating washouts and deadfalls was easier than with motorized bikes. Mountain bikes appear to be a viable alternative to the use of small four-wheel-drive all-terrain vehicles and motorcycles and they require minimum maintenance, no fuel and have a low impact on the environment.

STRATIGRAPHY

Strata ranging in age from Early Cretaceous to Jurassic are exposed in the map area. Progressively older formations are exposed southwestward. The succession includes both marine and nonmarine sediments of the Fort St. John, Bullhead and upper Minnes groups. These overlie the older, predominantly marine sediments found in the rest of the Minnes Group and the Fernie Formation. Triassic carbonate rocks of the Rocky Mountain Front Ranges are exposed in the southwest half of the Le Moray Creek map area and along the western edge of the Carbon Creek map area. The formations found in the region are summarized in Table 4-7-1.

PREVIOUS WORK

The stratigraphic nomenclature used for the study area is that of the Geological Survey of Canada and is derived from the work of D.F. Stott (1967, 1968, 1973, 1982). This nomenclature is used to maintain continuity with previous years' mapping on this project (Hunter and Cunningham, 1991a, b; Kilby and Johnston, 1988a, b, c; Kilby and Hunter, 1990; Hunter, 1990; Kilby and Wrightson, 1987a, b, c). Detailed descriptions of the stratigraphy are provided by Stott (1967, 1968, 1973, 1982) and Hughes (1964, 1967). The stratigraphy of the Bullhead Group and younger strata in the area has also been described by Kilby and Wrightson (1987a, b, c), Kilby and Johnston (1988a, b, c) as well as Hunter and Cunningham (1991a). Descriptions of the Gething Formation in the Carbon Creek region can be found in Gibson (1985).

Previous mapping in the Carbon Creek area includes work by Legun (1987, 1988). This mapping covered much of the map sheet, so work in the Carbon Creek area concentrated on areas in the south and west, where new road access provides additional information that was not available to previous workers. Detailed descriptions of the Minnes and Bullhead Group strata in the area are provided by Legun (1986, 1987, 1988).

Because previous descriptions of the stratigraphy are quite extensive, only a brief description which highlights the variations in the study area will be provided here.

FERNIE FORMATION

The Jurassic Fernie Formation consists predominantly of dark grey to black marine shales. The upper 25 to 50 metres is composed of interbedded sandstones, siltstones and shales, is more resistant, and is more readily preserved in roadcut outcrops than the rubbly, recessive marine shales below.

MINNES GROUP

MONTEITH FORMATION

The Monteith Formation is Jurassic to Early Cretaceous in age. It consists of very resistant, massive, clean, fine to medium-grained marine sandstones and quartzites with minor shales and argillaceous sandstones. It forms resistant ridges throughout most of the map area.

BEATTIE PEAKS FORMATION

The Early Cretaceous Beattie Peaks Formation comprises thinly bedded, fine-grained sandstones, siltstones and silty shales. In the Le Moray Creek area it is typically recessive. To the north, in the Carbon Creek map area, the formation consists of cleaner sandstones and quartzites and becomes less recessive.

MONACH FORMATION

The Monach Formation is Early Cretaceous in age and consists of resistant, medium to coarse-grained, clean sandstones and quartzites with minor shale. It forms resistant ridges through much of the map area. In the south, in the Le Moray Creek map area, the upper contact of the Monach is often marked by a white, coarse-grained quartzite.

STRATIGRAPHIC VARIATIONS IN THE LOWER PART OF THE MINNES GROUP

The Monteith and Monach formations often appear very similar in outcrop and sometimes can only be distinguished on the basis of stratigraphic position. Hughes (1967) suggests that the Monach, Beattie Peaks and Monteith not be separated into formations in the western part of the Pine Valley, where there are no thick quartzites to mark the top of the Monach or Monteith, and there is an increasing amount of sandstone in the Beattie Peaks Formation. To some extent, this is apparent in the western half of the Carbon Creek area. Here, it becomes increasingly difficult to distinguish between the three formations, although the Beattie Peaks sandstone beds tend to be more thinly bedded than those found in the Monach or Monteith formations.

BICKFORD FORMATION

The Early Cretaceous Bickford Formation, defined by Stott, consists of fine to medium-grained, brown laminated sandstones interbedded with dark grey shales and silty shales. It is sometimes carbonaceous, with some thin coal seams. In the Le Moray Creek map area, the unit contains numerous coal seams varying from a few centimetres to over a metre thick; woody imprints and fossils are also found. In the Carbon Creek area there is much less coal but some woody fossils and imprints are present. The unit is similar to the Gething Formation, and to the Brenot Formation described by Hughes (1964, 1967). The criteria used by Hughes to define and describe the Brenot Formation may be more suitable for mapping this unit in the Le Moray Creek area.

BULLHEAD GROUP

CADOMIN FORMATION

The Cadomin Formation is a resistant conglomerate unit of Early Cretaceous age and consisting predominantly of beds of well-rounded chert-pebble conglomerate, very coarse grained cherty sandstones and grits, together with recessive beds of carbonaceous mudstone, fine-grained sandstone and thin coal seams.

In the Carbon Creek map area, the prominent conglomeratic units of the Cadomin, observed in the Le Moray Creek area to the south, are no longer present. Here the

Cadomin generally consists of thick-bedded, medium to coarse-grained resistant sandstones and gritty to pebbly sandstones, carbonaceous shales, dark grey shales, some grits and minor coal. This unit is similar to the description of the Dresser Formation defined by Hughes (1964). The criteria used to define the Dresser Formation may be more suitable for mapping the unit in this area.

GETHING FORMATION

The Early Cretaceous Gething Formation comprises interbedded fine to medium-grained brown sandstones, dark grey shales, mudstones and siltstones, with carbonaceous shales and coal. It also contains conglomerates and grits. Carbonaceous material, woody fossils and imprints, and leaf fossils and imprints, are locally abundant and are generally found in argillaceous sandstones and sandy siltstones. Coal seams are generally about 1 to 1.5 metres thick, but reach up to 3 metres thick.

STRATIGRAPHIC VARIATIONS IN THE BICKFORD FORMATION AND BULLHEAD GROUP

Hughes (1967) suggests that in the western foothills, especially west of Mount Bickford in the Pine Valley, it becomes difficult and impractical to divide the Gething, Cadomin and Bickford formations. Although the lithological criteria that define the formations in the Le Moray Creek area do not always suffice in the Carbon Creek area, it is possible to separate these units into mappable formations by recognizing the variations in lithology that are present.

The presence of grits and conglomerates in the Gething, together with a decrease in distinct coarse-grained units in the Cadomin, can make it difficult to distinguish between these two units in the Carbon Creek area. Here, the Cadomin can be very similar in appearance to the lower part of the Gething. The contact is marked by some thick, coarse-grained sandstone and pebbly sandstone units near the top of the Cadomin. Conglomerate is found in the upper Gething (Gibson, 1985).

The Bickford Formation is more recessive with less coal than to the south in the Le Moray Creek area. There is a greater proportion of thick sandstones in the Cadomin and it is still more prominent than the Bickford in this area.

FORT ST. JOHN GROUP

Strata of the Fort St. John Group are exposed only in the northeast corner of the Carbon Creek map area. The Moosebar and Gates formations form most of the outcrops exposed along roadcuts and creeks. No coal or carbonaceous sediments were found in the Gates. The Boulder Creek Formation lacks the massive conglomeratic units seen in the prominent ridges to the south in previous years' mapping. Near the Peace River it consists mostly of sandstone and shale (Stott, 1982).

STRUCTURE

The northwesterly structural trend found in the Rocky Mountain thrust and fold belt is reflected in the study area. Traces of fold axes and faults on the map follow this regional trend.

Most of the areas mapped this summer are within the inner foothills, and the style of structural deformation reflects this. The broad, gentle folds and box folds observed in previous years to be fairly typical of the outer foothills deformational style are not common here. The folding is tighter, with more steeply dipping limbs; it is often associated with the thrust faulting that can be traced at surface. Fold axes trends are very shallow. Eigen vector analysis of all the outcrop orientations was completed using TRIPOD®, an interactive structural analysis package for use on microcomputers, indicating a regional fold axis with a trend of 136° and a very gentle plunge of only about 1° Figure 4-7-2). Fold axes may undulate in gentle waves with wavelengths of several kilometres as plunges change from southwest to northeast and back again, along an axial trace. Initial analysis suggests that the folding is cylindrical in domains limited in scale to several square kilometres.

The Carbon Creek area is dominated by two major synclines that can be traced over much of the map area. The Carbon Creek syncline in the east and the West Carbon Creek syncline in the west, expose significant coal seams in

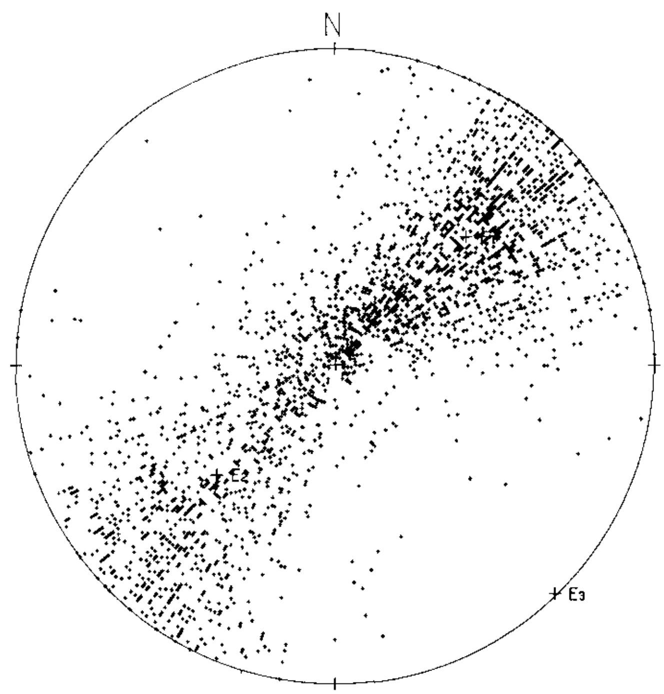

EQUAL AREA SCATTER PLOT
PI DIAGRAM

NUMBER OF OUTCROPS = 3027

TREND	PLUNGE	EIGENVALUE/3027
45.4	42.0	0.5773
227.0	48.0	0.3765
136.1	0.8	0.0462

Figure 4-7-2. Pi diagram showing poles to bedding for all outcrops in the Carbon Creek - Le Moray Creek database. Distribution of poles and eigen-vector analysis indicate a regional fold axis with trend 136° and 1° plunge.

the Gething Formation. In the Le Moray Creek map area the Goodrich synclinorium exposes coal-bearing Gething in the north-central part of the area and Brenot on the southeast.

Linear fault traces that crosscut topographical contours indicate most faults are steeply dipping. Most of these faults are west-dipping thrusts. The Pardonet fault, along the western edge of the Carbon Creek area, is a the major thrust fault in the region and marks the boundary of the Rocky Mountain Foothills to the east and the Rocky Mountain Main Ranges to the west. Triassic carbonates have been uplifted and exposed in the hangingwall to overlie Lower Cretaceous and Jurassic rocks. The Carbon thrust, east of Carbon Creek, brings Minnes Group and Fernie Formation strata into contact with rocks of the Fort St. John Group. East-dipping thrust faults have been mapped in the north-central Carbon creek area by Legun (1987, 1988). The only major normal fault is the Burnt normal fault in the Le Moray Creek map area.

DATA COMPILATION AND COMPUTER-AIDED GEOLOGIC MAPPING

The data compiled from coal assessment reports (exploration maps, coal boreholes, exploration reports) in COALFILE©, as well as oil and gas drill-hole data obtained through the Petroleum Branch, were entered into a computer database. Formation boundaries and structural traces were also digitized from several coal assessment report maps using QUIKMap so that geological traces could be displayed in conjunction with outcrop data. QUIKMap provided a convenient means to combine, organize, edit and display large quantities of data. The database compiled for the Carbon Creek and Le Moray map areas currently contains over 3700 outcrops and 369 drill holes, including the outcrop data gathered from traverses during this summer's field season (Figures 4-7-3 and 4). TRIM data (produced by the Ministry of Environment, Lands and Parks) provide a digital base-map, including contour, cadastral, drainage and cultural information.

A computer brought into the field was used to combine the compiled data and the TRIM topographic data to plot base-maps used with 1:20 000-scale airphotos for mapping. Outcrop data collected in the field was periodically added to the outcrop database. Using the compiled data and the field data in conjunction with QUIKMap made the microcomputer an on-site, interactive tool integrated into the field mapping process, as opposed to merely an electronic file cabinet for geological data.

The database will continue to be updated until the Open File maps are produced. Eventually the data files and the geology map QUIKMap files produced for the study area will also be made available for distribution. Much of the raw, unedited data that cannot be displayed on the final printed map will also be made available. With the outcrop data, borehole picks, and formation and structural traces stored in digital form, more detailed structural analysis can be carried out using computers.

Geographic information systems software like QUIKMap will make it possible to produce a complete geological compilation map by combining and assessing all the information in the database prior to the field season. Such a compilation map would provide a geological base map that would highlight those areas needing further investigation. This would maximize the use of the time available during a short field season, leading to increased productivity By incorporating the new information gathered each day with the compilation base map, it is now possible to produce a first-draft geology map on the computer while still in the field (Figure 4-7-5).

ECONOMIC GEOLOGY

The only producing coal mines in the Peace River coalfield are at Bullmoose and Quintette, to the south of the areas mapped this summer. The two operations are mining the coal measures of the Gates Formation although the Gething Formation has also attracted exploration attention.

Previous Exploration

CARBON CREEK AREA

The region mapped this year includes several properties that have been explored for their coal potential. Utah Mines Ltd. acquiried the Carbon Creek property in 1971, and the West Carbon Creek property in 1978. The two properties covered the West Carbon Creek and Carbon Creek synclines in the north half of the Carbon Creek map sheet between the Pardonet fault in the west and the Carbon fault in the east. Exploration continued until 1982 and included mapping, trenching and drilling programs. In 1980, Gulf Canada Resources Ltd. acquired the Whiterabbit block, which included the south end of the West Carbon Creek syncline extending across Carbon Creek. Gulf surrendered the coal leases for the Whiterabbit block in 1982.

The primary exploration targets were the coal seams found in the Gething Formation that is exposed in the core of both Carbon Creek synclines.

LE MORAY CREEK AREA

Gulf Canada Resources acquired the Goodrich property in 1979. It covered most of the Le Moray Creek map sheet east of the Le Moray Creek valley and was the target of extensive mapping, trenching and drilling programs. In 1982, a test adit was driven into a Gething coal seam in the Lossan mine area, north of Brazion Creek. Coal seams in the Bickford Formation (the uppermost formation of the Minnes has been mapped as the Brenot by Gulf Canada Resources) were the primary target in the southeast corner of the Le Moray Creek area. Exploration continued until 1984.

Coal Occurrences

Significant coal seams in the area are found in the Gething Formation. Coal seams are also present in the upper Minnes (Bickford), although these tend to be thinner and of less importance than Gething coals. The thin and discontinuous seams of the Cadomin have yet to prove to be of economic interest. Although economic coal seams are found in the Gates Formation to the south, no coal was noted in the Gates Formation exposed in the northeast corner of the Carbon Creek map area.

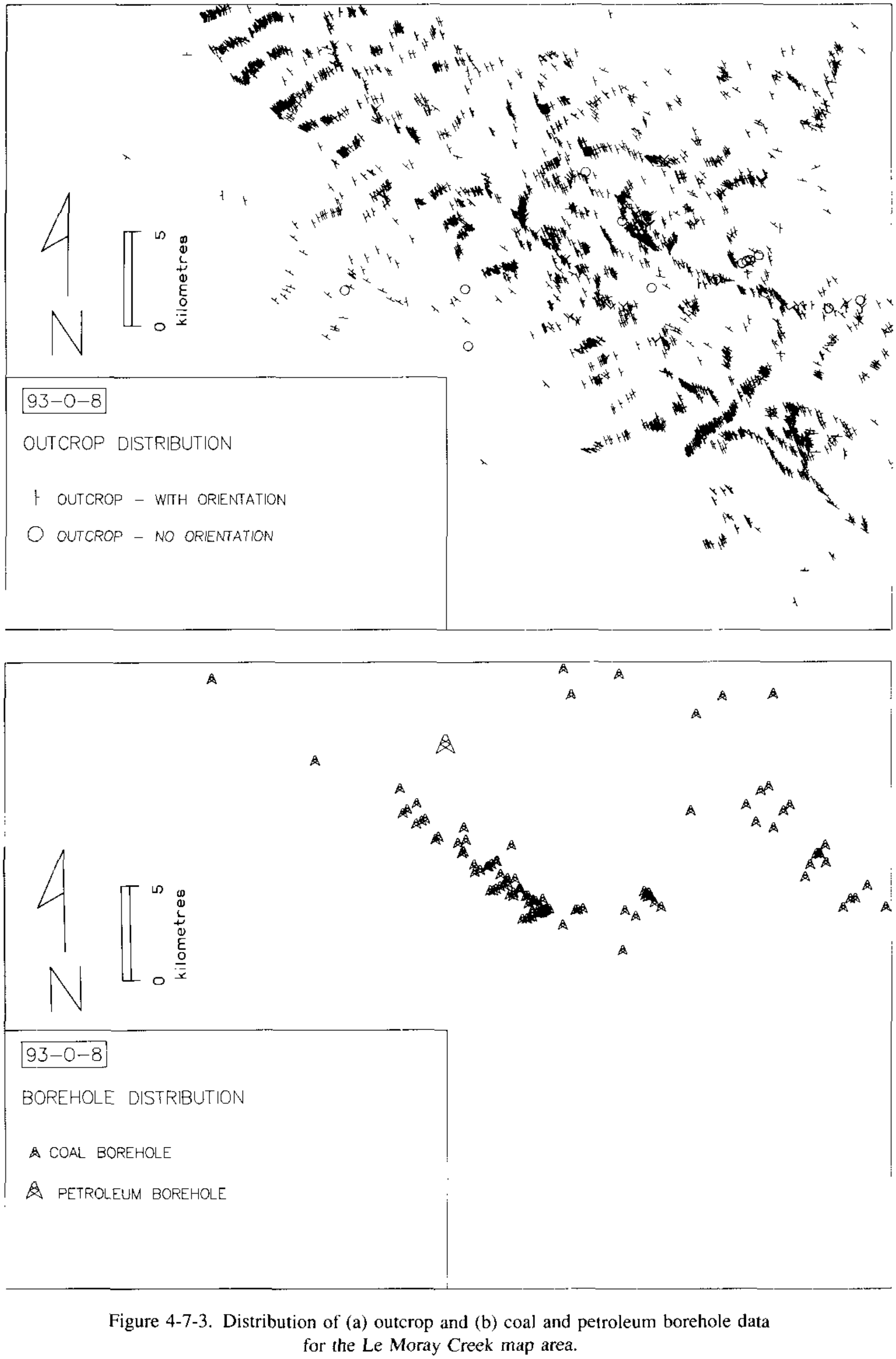

Figure 4-7-3. Distribution of (a) outcrop and (b) coal and petroleum borehole data for the Le Moray Creek map area.

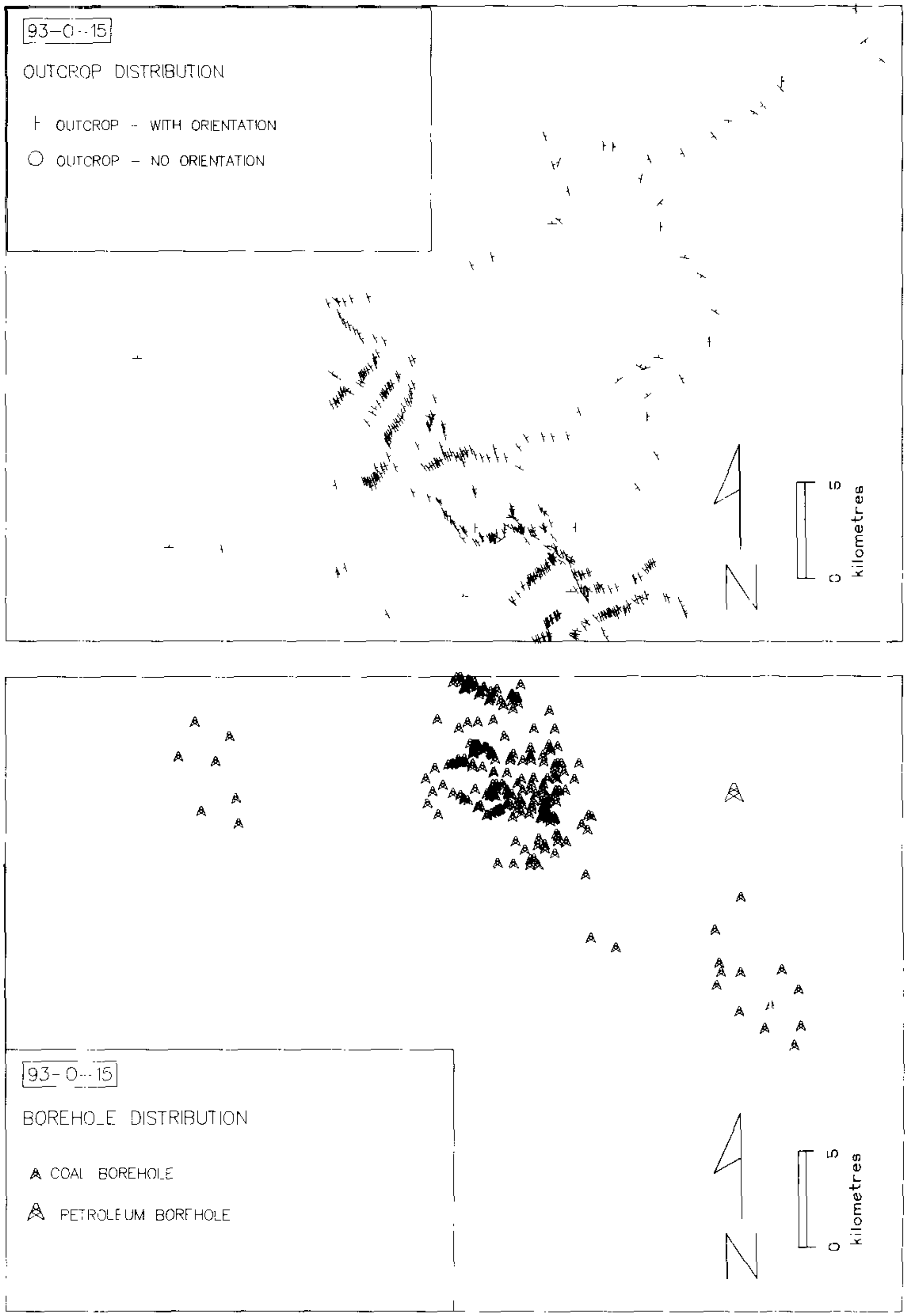

Figure 4-7-4. Distribution of (a) outcrop and (b) coal and petroleum borehole data for the Carbon Creek map area.

Coal samples were taken from seams in outcrops of the Gething and Bickford formations. Samples were prepared and analyzed using the methods outlined by Kilby (1986, 1989). Mean random vitrinite reflectance values (R_m) have been measured on some of the samples and range from 0.99 to 1.65. These samples fall in the high to low-volatile bituminous rank, using the American Standard Testing Materials classification (Stach, 1982).

Coal samples were taken from the Gething Formation in the Le Moray Creek and Carbon Creek areas. The seams that were sampled were between 0.2 and 1 metre thick. Coal seams in the Gething Formation in the Carbon Creek area are known to vary from a few centimetres to over 4 metres thick, and show marked lateral variations in thickness (Gibson, 1985). In the Le Moray Creek area, Gething coal seams may be up to 5.5 metres thick, however, the average thickness ranges from 0.5 to 1 metre thick over the whole area.

The coal samples from the Gething Formation that have been analyzed have R_m values from 0.83 to 1.57. The samples which showed the least amount of weathering in outcrop had reflectance values of 1.35 to 1.57 (medium-volatile bituminous to low-volatile bituminous rank).

The coals sampled in the Bickford Formation are from the Le Moray Creek map area, north of Brazion Creek. The seams that were sampled are 0.2 to 1 metre thick. Seams as thick as 3 metres can be found here. No significant seams were noted in the Bickford Formation in the Carbon Creek area.

Mean random reflectance values for Bickford coal samples range from 1.17 to 1.65. The single sample with reflectance of 1.17 appeared weathered in outcrop. The other samples varied from 1.46 to 1.65, placing them at the low-volatile bituminous rank, or near the boundary of the medium and low-volatile bituminous rank.

Current Exploration Activity

There is no current exploration for coal in the area. Vitrinite reflectance values in the bituminous range, and the number of coal-bearing formations, suggest this area would be of potential interest for developing coalbed methane production. The thicker seams of the Gething Formation are one possible target, although the thin but numerous seams of the Bickford may also be of interest.

There was a great deal of conventional gas exploration activity in the region this summer. Several wells are already in production, with several more nearing production. New wells are currently being drilled and more are proposed in both the Le Moray Creek and Carbon Creek map areas.

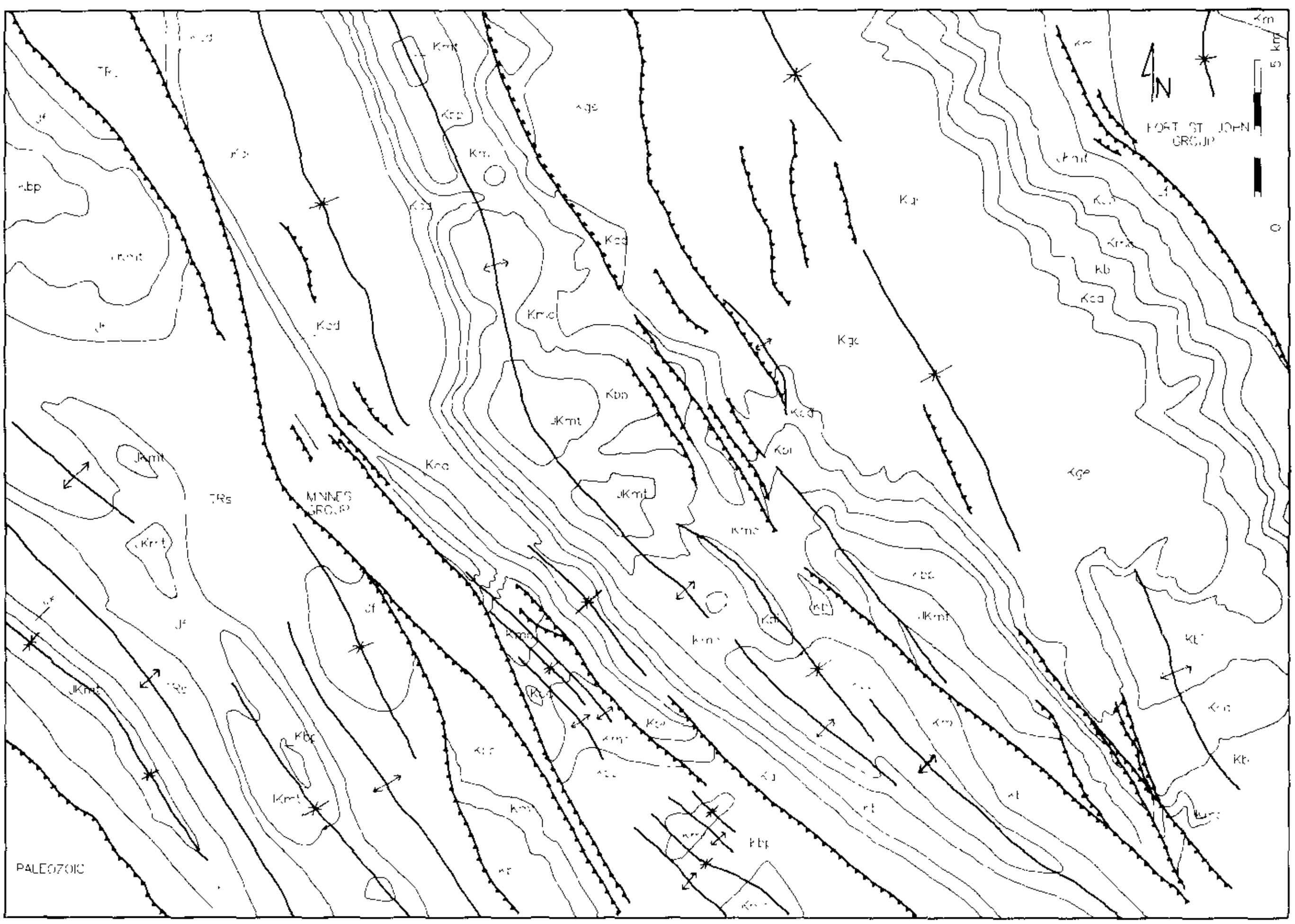

Figure 4-7-5. First draft of geologic map for the Carbon Creek area, combining compiled data and maps with the data collected in the field. Software such as QUIKMap will allow the first-draft maps to be completed on the computer while still in the field.

Targets are generally the deeper Triassic limestones which only outcrop in the Rocky Mountain Main Ranges. Regional mapping can indicate structural trends which may be expressed at deeper levels as structural traps and so be an important consideration in selecting targets for gas exploration.

ACKNOWLEDGMENTS

The authors thank Ward Kilby for his valuable input into the project. Joanne Schwemler provided the coal sample preparation and vitrinite reflectance observations. Accomodations in Chetwynd were once again provided by Robert and Jean Pohl, whose hospitality was greatly appreciated.

REFERENCES

Gibson, D.W. (1985): Stratigraphy and Sedimentology of the Lower Cretaceous Gething Formation, Carbon Creek Coal Basin, Northeastern British Columbia; *Geological Survey of Canada*, Paper 80-12.

Hughes, J.E. (1964): Jurassic and Cretaceous Strata of the Bullhead Succession in the Peace River Foothills; *B.C. Ministry of Energy, Mines and Petroleum Resources*, Bulletin 51.

Hughes, J.E. (1967): Geology of the Pine Valley, Mount Wabi to Solitude Mountain, Northeastern British Columbia; *B.C. Ministry of Energy, Mines and Petroleum Resources*, Bulletin 52.

Hunter, D.J. and Cunningham, J.M. (1991a): Burnt River Mapping and Compilation Project (93P/5, 6); *in* Geological Fieldwork 1990, *B.C. Ministry of Energy, Mines and Petroleum Resources*, Paper 1991-1, pages 407-414.

Hunter D.J. and Cunningham, J.M. (1991b): Geology of the Burnt River and Gwillim Lake (Southwest Half) Areas, Northeast British Columbia, NTS 93P/5, 6; *B.C. Ministry of Energy, Mines and Petroleum Resources*, Open File 1991-4.

Jahans, P.C. (1992): Pine Valley Mapping and Compilation Project (930/9, 10; 93P/12); *in* Geological Fieldwork 1991, Grant, B. and Newell, J.M., Editors, *B.C. Ministry of Energy, Mines and Petroleum Resources*, Paper 1992-1, this volume.

Kilby, W.E. (1986): Biaxial Reflecting Coals in the Peace River Coalfield (93O, P, I); *in* Geological Fieldwork 1985, *B.C. Ministry of Energy, Mines and Petroleum Resources*, Paper 1986-1, Pages 127-137.

Kilby, W.E. (1989): Tectonically Altered Coal Rank, Boulder Creek Formation, Northeastern British Columbia, (93P/3); *in* Geological Fieldwork 1988, *B.C. Ministry of Energy, Mines and Petroleum Resources*, Paper 1989-1, Pages 565-570.

Kilby, W.E. and Hunter, D.J. (1990): Tumbler Ridge, Northeastern British Columbia (93P/2, 3, 4; 93I/14, 15); *in* Geological Fieldwork 1989, *B.C. Ministry of Energy, Mines and Petroleum Resources*, Paper 1990-1, pages 455-459.

Kilby, W.E. and Johnston, S.T. (1988a): Kinuseo Mapping and Compilation Project (93I/14, 15; 93P/3); *in* Geological Fieldwork 1987, *B.C. Ministry of Energy, Mines and Petroleum Resources*, Paper 1988-1, pages 463-470.

Kilby, W.E. and Johnston, S.T. (1988b): Bedrock Geology of the Kinuseo Creek Area, Northeast British Columbia, NTS 93I/15; *B.C. Ministry of Energy, Mines and Petroleum Resources*, Open File 1988-21.

Kilby, W.E. and Johnston, S.T (1988c): Bedrock Geology of the Kinuseo Falls Area, Northeast British Columbia, NTS93I/14; *B.C. Ministry of Energy, Mines and Petroleum Resources*, Open File 1988-22.

Kilby, W.E. and Wrightson, C.B. (1987a): Bullmoose Mapping and Compilation Project (93P/3, 4); *in* Geological Fieldwork 1986, *B.C. Ministry of Energy, Mines and Petroleum Resources*, Paper 1987-1, pages 373-378.

Kilby, W.E. and Wrightson, C.B. (1987b): Bedrock Geology of the Bullmoose Creek Area, Northeast British Columbia, NTS 93P/3; *B.C. Ministry of Energy, Mines and Petroleum Resources*, Open File 1987-6.

Kilby, W.E. and Wrightson, C.B. (1987c): Bedrock Geology of the Sukunka River Area, Northeast British Columbia, NTS 93P/4; *B.C. Ministry of Energy, Mines and Petroleum Resources*, Open File 1987-7.

Legun, A. (1983): Stratigraphy and Sedimentology Notes on the Bullhead Mountain - Peace River Canyon, Carbon Creek Area, Northeastern British Columbia, (93O/15, 16; 94B/1, 2); *in* Geological Fieldwork 1982, *B.C. Ministry of Energy, Mines and Petroleum Resources*, Paper 1983-1, pages 93-97.

Legun, A. (1985): Geology of the West Carbon Creek Area, (93O/15); *in* Geological Fieldwork 1984, *B.C. Ministry of Energy, Mines and Petroleum Resources*, Paper 1985-1, pages 227-232.

Legun, A. (1987): Geology of the Carbon Creek Area, NTS 93O/15; *B.C. Ministry of Energy, Mines and Petroleum Resources*, Open File 1987-21.

Legun, A. (1988): Geology and Coal Resources of the Carbon Creek Map Area; *B.C. Ministry of Energy, Mines and Petroleum Resources*, Paper 1988-3.

Stach, E. (1982): Coal Petrology; *Gebruder Borntraeger Publishing*, 535 pages.

Stott, D.F. (1967): The Cretaceous Smoky Group, Rocky Mountain Foothills, Alberta and British Columbia; *Geological Survey of Canada*, Bulletin 132.

Stott, D.F. (1968): Lower Cretaceous Bullhead and Fort St. John Groups between Smoky River and Peace Rivers, Rocky Mountain Foothills, Northeastern British Columbia; *Geological Survey of Canada*, Bulletin 152.

Stott, D.F. (1973): Lower Cretaceous Bullhead Group between Bullmoose Mountain and Tetsa River, Rocky Mountain Foothills, Northeastern British Columbia; *Geological Survey of Canada*, Bulletin 219.

Stott, D.F. (1982): Lower Cretaceous Fort St. John Group and Upper Cretaceous Dunvegan Formation of the Foothills and Plains of Alberta, British Columbia, District of Mackenzie and Yukon Territory; *Geological Survey of Canada*, Bulletin 328.

NOTES

COAL RANK VARIATIONS IN THE TELKWA COALFIELD, CENTRAL BRITISH COLUMBIA (93L/11)

By Barry D. Ryan

KEYWORDS: Coal rank, coal quality, Telkwa coalfield, medium volatile, bituminous, coking coal, anthracite, thrusts.

INTRODUCTION

The Telkwa coalfield, which is centred on Smithers in central British Columbia, extends for about 50 kilometres along the Bulkley River from north of Smithers to south of Telkwa (Figure 4-8-1). This paper presents 286 mean maximum reflectance measurements of vitrinite from coal samples from outcrop and drill holes in the coalfield. The data are analyzed and the significance of variations in coal rank vertically through the stratigraphy and laterally within single seams is discussed. Analysis of mean maximum reflectance of vitrinite data ($\bar{R}_{max}$) provides some insights into the depositional and post-depositional history of the Telkwa coalfield. It also indicates that there may be resources of metallurgical coal and anthracite in the field.

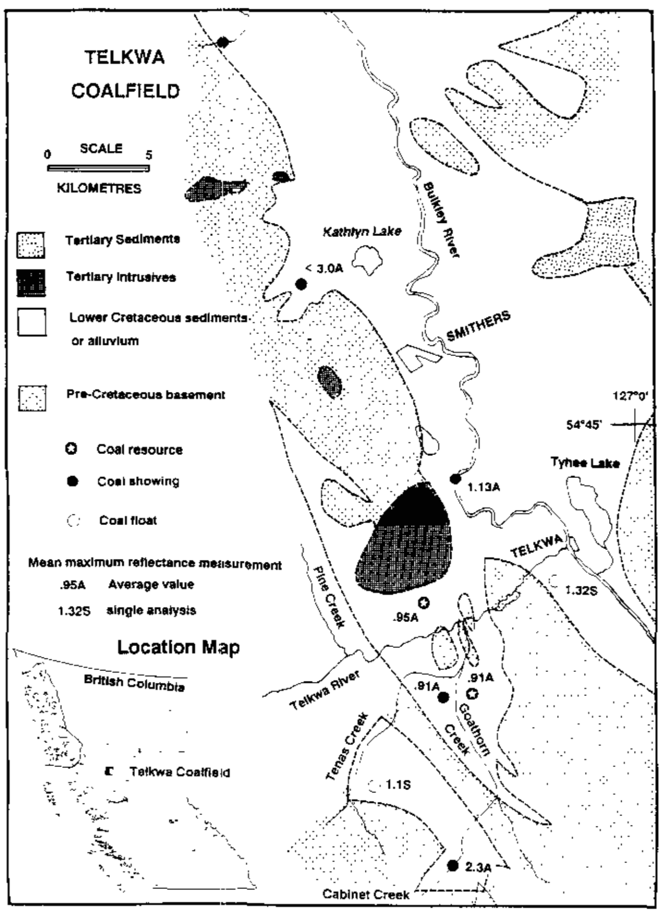

Figure 4-8-1. Regional geological map of the Telkwa coalfield.

Telkwa coalfield geology is discussed in several papers (Koo, 1983; Palsgrove and Bustin, 1989) and is covered by regional geology maps of MacIntyre *et al.* (1989) and Tipper (1976). Coal-bearing rocks in the coalfield belong to the Skeena Group of Lower Cretaceous age and are assigned to the Red Rose Formation of Albian age and possibly also to the older Kitsun Creek Formation of Hauterivian age.

Much of the basin is covered by alluvium. Coal outcrops northwest of Smithers, south of Smithers in the Bulkley River, north of the Telkwa River east of Pine Creek, east and west of Goathorn Creek and at the headwaters of Tenas and Cabinet creeks (Figure 4-8-1). The known coal outcrops are widely separated and restricted to the west side of the Bulkley River, leaving room for additional exploration. Cretaceous rocks east of the Bulkley River are coarser grained, indicating that they are either a different unit within the Skeena Group or that there is a facies change from nonmarine in the west to shallow-marine in the east.

RECENT EXPLORATION HISTORY

The Telkwa coal exploration property, which occupies less than 10 per cent of the whole field, is 15 kilometres south of Smithers and is centred on the confluence of the Telkwa River and Goathorn Creek. Most exploration to date has been on the Telkwa coal property both in the Goathorn Creek area and east of Pine Creek. Measured coal resources for these two areas, and probable coal resources in the Cabinet Creek area, have been estimated at 30 million tonnes. The Telkwa coal property was intensively explored by Crowsnest Resources Limited during the period from 1978 to 1990 when over 350 exploration holes were drilled and a large test-pit excavated. The exploration activity is recorded in a number of geological assessment reports covering the years 1978 to 1989 and in Prospectus, Stage 1 and Stage 2 submissions to the B.C. Ministry of Energy, Mines and Petroleum Resources.

The Cretaceous stratigraphy at the Telkwa coal property was divided into four units by Palsgrove and Bustin (1989). The lowest unit, which is 20 to 100 metres thick, rests unconformably on Lower Jurassic volcanic rocks of the Telkwa Formation, Hazelton Group. It is a nonmarine, coarse clastic unit which contains a single coal zone composed of up to six coal bands together referred to as Seam 1 or Coal Zone 1. Often, one of these bands contains a radioactive marker apparent on downhole geophysical logs and probably represents a layer of volcanic ash. The cumulative coal thickness varies up to 7 metres in the area considered for development (Figure 4-8-2).

Unit 2 is composed of 60 to 170 metres of shallow-marine mudstones and siltstones. It is lithologically monotonous and contains no coal.

Unit 3 consists of mudstones, siltstones, coal and sandstones and averages 90 metres in thickness. It contains the

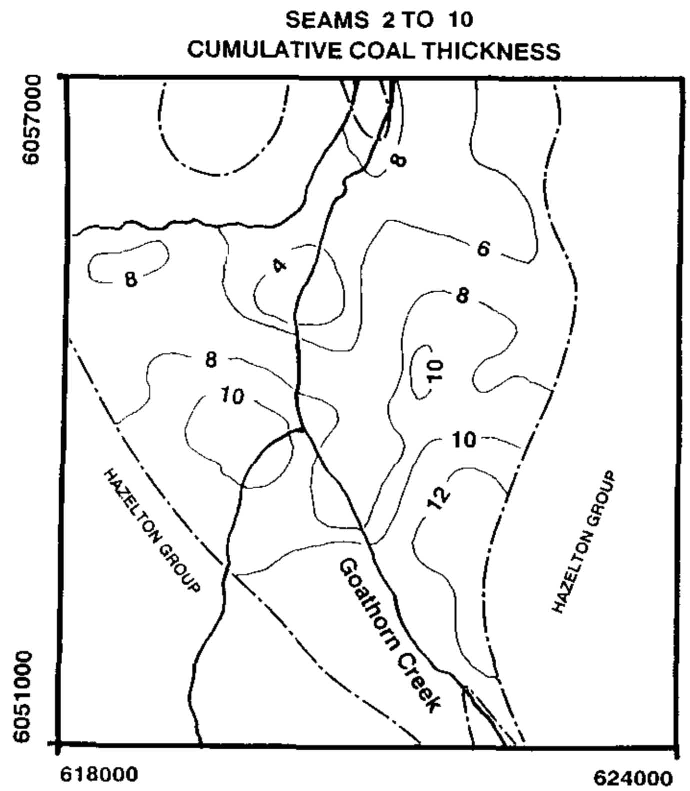

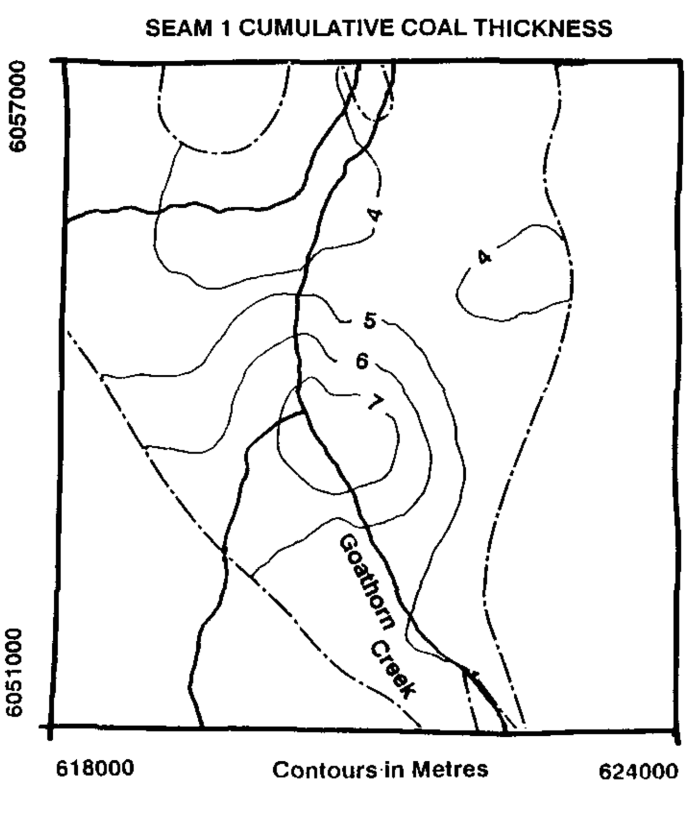

Figure 4-8-2. Cumulative coal thickness for the upper seams (2 to 10) and Seam 1; Goathorn Creek area.

major coal-bearing zone comprising Seams 2 to 10. The cumulative coal thickness ranges from 6 to 14 metres in the area considered for development (Figure 4-8-2). Unit 3 is overlain by the sandstone-rich Unit 4 of unknown thickness.

An understanding of the structural geology of the Telkwa coal property is based largely on information from drilling and geophysical surveys. Bedding generally dips gently southeast or east and is disrupted by at least two generations of faulting. Early faults are east-dipping thrusts; late steep-dipping faults trend northwest or northeast.

DATA SOURCES AND ANALYTICAL TECHNIQUES

Samples used in this study are from:

- Coal outcrop samples collected by the author during the summers of 1990 and 1991 (Table 4-8-1).
- Drill-core samples in the Geological Survey Branch (GSB) rock-sample collection originally collected by J. Koo (Table 4-8-2).
- Drill-core samples from holes drilled, logged and sampled by Matheson and Van Den Bussche (1990) as part of the GSB subsurface coal-sampling program (Table 4-8-2).

All samples were analyzed for mean maximum reflectance by JoAnne Schwemler. Polished pellets of 20-mesh sized coal grains were prepared and the reflectance in oil of at least 50 grains was measured from each pellet.

It is important to understand the component errors in the total reproducibility error for a single sample analysis. The error of the optical procedure is usually considered to be about 0.01 per cent at one standard deviation (Bustin, 1983). The same paper lists a set of duplicate analyses made by different laboratories, the one standard deviation of these inter-laboratory analyses is 0.06 per cent; reproducibility within a single laboratory should be considerably better.

Sampling bias and natural variations within the seam also influence the scatter of values obtained from a suite of related samples. Matheson and Van Den Bussche (1990)

TABLE 4-8-1
TELKWA COALFIELD
OUTCROP COAL SAMPLES

SAMPLE	EAST	NORTH	COMMENTS	SEAM	TYPE	R Max
90-150	620980	6047480	Cabinet Cr	u	oc	2.20
90-150	620980	6047480	Cabinet Cr	u	oc	2.30
90-154	620960	6047240	Cabinet Cr	u	oc	2.33
90-155	620980	6047160	Cabinet Cr	u	oc	2.36
90-155	620980	6047160	Cabinet Cr	u	oc	2.44
90-29	620750	6066250	Bulkley R	u	oc	1.27
90-15	620100	6066100	Bulkley R	u	oc	1.00
90-121	621040	6053280	Goathorn Cr	u	oc	0.94
90-134	616200	6051200	Tenas Cr	?	f	1.10
90-72	625180	6059900	NE Goathorn Cr	?	f	1.32
90-131	619800	6056000	Goathorn Cr	1	oc	0.85
90-133	620500	6055520	Goathorn Cr	1	oc	0.85
90-100	620820	6057280	Goathorn Cr	1	s	0.88
90-97	620760	6057480	Goathorn Cr	1	s	0.81
90-92	620340	6058540	Goathorn Cr	1	s	0.80
90-120	617860	6057560	Telkwa R	1	oc	0.88
90-123	621240	6052740	Goathorn Cr	1	oc	0.90
90-123	621240	6052740	Goathorn Cr	1	oc	0.88
90-88	617940	6057800	Telkwa R	1	oc	0.98

u = seams 2 to 10
oc = outcrop
f = float or bloom
s = coal spar

sampled and analyzed the 1989 drill core on 20-centimetre increments. This suite of analyses is presented in Table 4-8-4. Up to 29 samples from a single seam were analyzed providing a good estimate of the reproducibility of a single sample value. The average standard deviation of a single value from a seam is 0.043 per cent. Consequently in-seam variation and sampling bias must account for something less than 0.043 minus the error in the optical measurement (0.01 per cent).

The analysis technique of the GSB (Kilby, 1988) provides a value of the mean maximum reflectance of vitrinite in oil, classifies the shape of the reflectance-indicating surface (RIS) and quantifies its degree of eccentricity.

The reflectance data are presented in Tables 4-8-1, 3 and 4. Figure 4-8-3 illustrates the shape and type of RIS by seam. The pie diagram is the top triangular segment of a parent triangle diagram in which each corner represents one of the axes of the RIS. Increasing bireflectance is represented by increases in RAM and changes in eccentricity by RST; a negative RST value of 30 indicates a uniaxial negative RIS and positive value of 30 indicates a uniaxial positive RIS, The terms RST and RAM are defined as follows:

TABLE 4-8-2
TELKWA COALFIELD
LOCATION OF DRILL HOLES PROVIDING SAMPLES USED FOR MEAN MAXIMUM REFLECTANCE MEASUREMENT

HOLE	EASTING	NORTHING	ELEVATION (metre)	DEPTH (metre)
216	618656	6059476	786	138
218	618791	6059835	780	103
224	620653	6054054	773	249
231	619511	6054312	762	330
232	621777	6053797	779	98
236	619821	6054776	733	178
237	619986	6054858	730	151
239	620020	6055035	726	159
243	621396	6053108	829	148
246	621653	6052344	840	164
247	621870	6053110	860	258
248	621840	6052041	852	283
250	622070	6052083	869	173
251	621583	6052867	872	354
252	622346	6052072	887	374
255	621656	6053469	802	200
256	622016	6052584	890	292
259	621075	6054410	747	87
260	621019	6055019	698	155
267	619565	6054091	762	250
268	621643	6054395	745	301
272	621633	6055142	708	121
316	621087	6054904	713	88
318	621012	6055277	715	118
326	621077	6053440	793	84
327	621074	6053287	794	101
337	621527	6054500	733	124
343	621343	6055300	699	173
344	621626	6055420	694	149
345	619642	6053981	764	136
347	619649	6054196	760	136
GSB-89-1	620305	6054860	660	28.5
GSB-89-2	620260	6054970	655	25.0
GSB-89-3	620410	6055285	645	52.0
GSB-89-4	620420	6055320	645	25.0
GSB-89-5	620455	6055705	645	45.6
GSB-89-7	620530	6055720	635	10.3
GSB-89-8	618015	6057665	575	33.4
GSB-89-9	618000	6057700	580	43.3

$$RST = 30 - \arctan(X/Y)$$
$$RAM = (X\text{^}2 + Y\text{^}2)\text{^}1/2$$
$$R = \bar{R}_{max} + R_{int} + R_{min}$$
$$X = (\tfrac{1}{3} - \tfrac{R_{min}}{R} / \cos(30) - y\tan(30))$$
$$Y = \bar{R}_{max}/R - \tfrac{1}{3}$$

Much of the scatter of individual maximum reflectance measurements seen in (Figure 4-8-4) is related to the real spread of individual maximum reflectance values within the sample. In fact, in a uniaxial RIS the dispersion of individual maximum reflectance measurements is a direct measure of this spread in the coal and could probably be used to make inferences about coking potential.

At Telkwa, lower rank coal samples from Seams 10 and 6 generally have low bireflectance (RAM) and moderate biaxial eccentricity (RST); higher rank coals have greater bireflectance and more extreme eccentricity, often approaching uniaxial negative RIS patterns. Increasing bireflectance with rank has been described in the literature by a number of authors (*e.g.*, McCartney and Ergun, 1967). Trends in eccentricity with rank are not well developed at Telkwa although some of the high-rank Cabinet Creek coals have uniaxial negative RIS.

Some coal samples do not define a coherent RIS pattern. Coalspar collected from outcrop samples usually has a scattered pattern (Figure 4-8-4). These samples represent coal fragments incorporated in sandstones of Unit 1 (Table

TABLE 4-8-3
TELKWA COALFIELD
CROWSNEST RESOURCES DRILL HOLES, MEAN MAXIMUM REFLECTANCE DATA

HOLE	SEAM 1 R Max/Depth (metre)		SEAM 2 R Max/Depth (metre)		SEAM 6 R Max/Depth (metre)		SEAM 10 R Max/Depth (metre)	
216	-		0.94	48.80	0.90	22.90	-	
218	-		0.95	75.00	0.91	47.20	-	
224	0.90	212.20	-		-		-	
224	0.94	248.30	-		-		-	
231	0.90	306.98	0.98	180.00	-		0.84	106.60
232	-		0.93	79.68	-		-	
236	0.92	153.23	-		-		-	
237	0.89	128.80	-		-		-	
237	1.03	139.34	-		-		-	
239	0.89	40.76	-		-		-	
243	-		0.90	67.70	-		-	
244	-		-		0.84	76.60	-	
246	-		0.89	94.68	-		-	
247	-		0.92	204.78	0.84	154.0[illegible]	0.81	115.14
248	0.99	267.30	-		-		-	
250	-		-		0.84	74.43	-	
251	-		0.86	131.08	0.94	107.8[illegible]	0.80	64.96
252	1.24	352.70	1.00	166.60	-		-	
255	-		0.99	179.83	-		-	
256	-		0.90	257.74	0.96	202.5[illegible]	-	
259	-		-		0.88	18.67	-	
260	0.87	117.02	0.84	22.55	-		-	
267	-		1.02	154.54	0.96	130.8[illegible]	0.87	81.46
268	-		-		-		0.85	102.95
277	-		0.93	88.08	0.86	53.95	-	
316	-		-		0.82	71.65	-	
318	0.88	91.85	-		-		-	
326	-		0.92	47.32	-		-	
327	-		0.87	76.30	-		-	
337	-		0.90	91.63	-		-	
343	-		1.55	139.55	0.84	104.1[illegible]	-	
344	-		0.86	123.52	-		-	
345	-		1.51	102.20	0.97	77.00	-	
347	-		1.03	40.52	0.89	25.30	-	

HOLE	SEAM 2		SEAM 3		SEAM 5		SEAM 6	
800c	0.976	?	0.901	?	0.957	?	0.963	?

TABLE 4-8-4
TELKWA COALFIELD
GEOLOGICAL SURVEY BRANCH
DRILL HOLES, COAL INTERSECTIONS
AND *MEAN MAXIMUM REFLECTANCE DATA*

HOLE	TOP (metre)	BOTTOM (metre)	THICKNESS (metre)	AV R Max	COUNT	SD
89-1	3.05	4.88	1.83	0.899	29	0.038
89-1	6.10	6.25	0.15	0.983	1	
89-1	7.62	8.08	0.46	0.908	2	
89-1	9.68	11.28	1.60	0.932	8	0.053
89-1	16.91	17.83	0.92	0.912	4	0.030
89-1	24.46	25.83	1.37	0.922	7	0.029
89-2	2.13	3.51	1.38	0.846	6	0.035
89-2	4.88	5.71	0.83	0.902	4	0.048
89-2	6.55	7.92	1.37	0.955	7	0.048
89-2	13.34	13.66	0.32	0.926	4	0.009
89-2	20.12	20.52	0.40	0.933	2	
89-2	20.73	21.79	1.06	0.946	5	0.040
89-3	4.88	5.18	0.30	0.875	1	
89-3	29.26	29.72	0.46	0.868	2	
89-3	30.34	30.48	0.14	0.904	1	
89-3	40.77	40.92	0.15	0.968	1	
89-4	6.43	6.95	0.52	0.871	4	0.02
89-4	12.34	12.95	0.61	0.878	4	0.026
89-5	15.3	15.83	0.53	0.851	2	
89-5	19.6	20.45	0.83	0.916	2	
89-7	3.7	3.9	0.20	0.847	1	
89-7	5.50	5.95	0.45	0.865	2	
89-8	8.30	14.05	5.85	0.956	29	0.061
89-8	14.8	15.67	0.87	0.967	4	0.049
89-8	18.78	21.70	2.92	1.005	11	0.056
89-8	26.82	27.82	1.00	0.989	4	0.051
89-8	28.9	29.9	1.00	1.004	5	0.039
89-9	13.81	18.12	4.31	0.952	22	0.066
89-9	18.4	19.72	1.32	0.963	7	0.048
89-9	20.85	21.75	0.90	0.976	5	0.054
89-9	23.35	23.47	0.12	1.00	1	
89-9	24.3	27.22	2.92	0.986	15	0.04
89-9	32.6	33.55	0.93	1.008	5	0.066
89-9	34.4	35.5	1.10	0.991	6	0.032
89-9	36.9	37.1	0.20	0.932	1	
89-9	42.4	42.97	0.57	0.962	3	
			AVERAGES	0.946	217	0 043

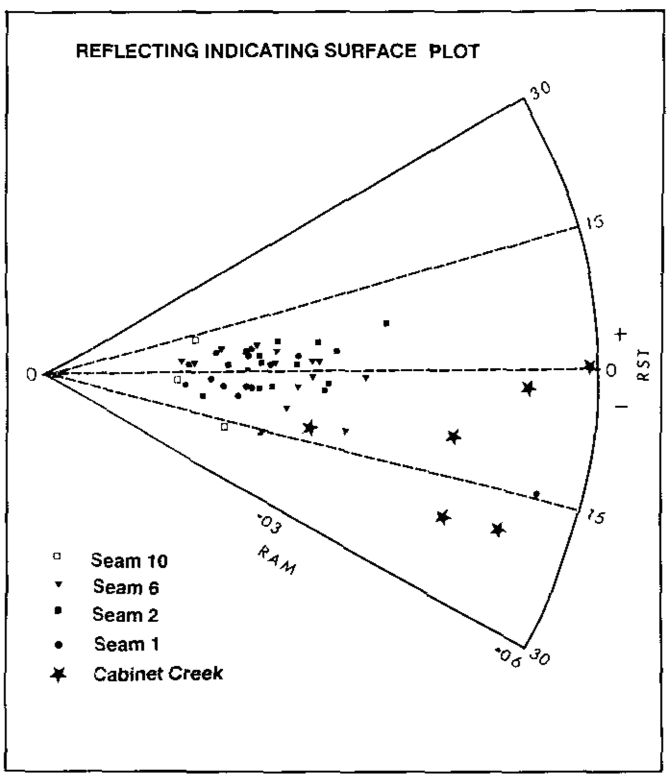

Figure 4-8-3. Plot of the relative shape of the reflectance indicating surface (RIS) for Telkwa coals.

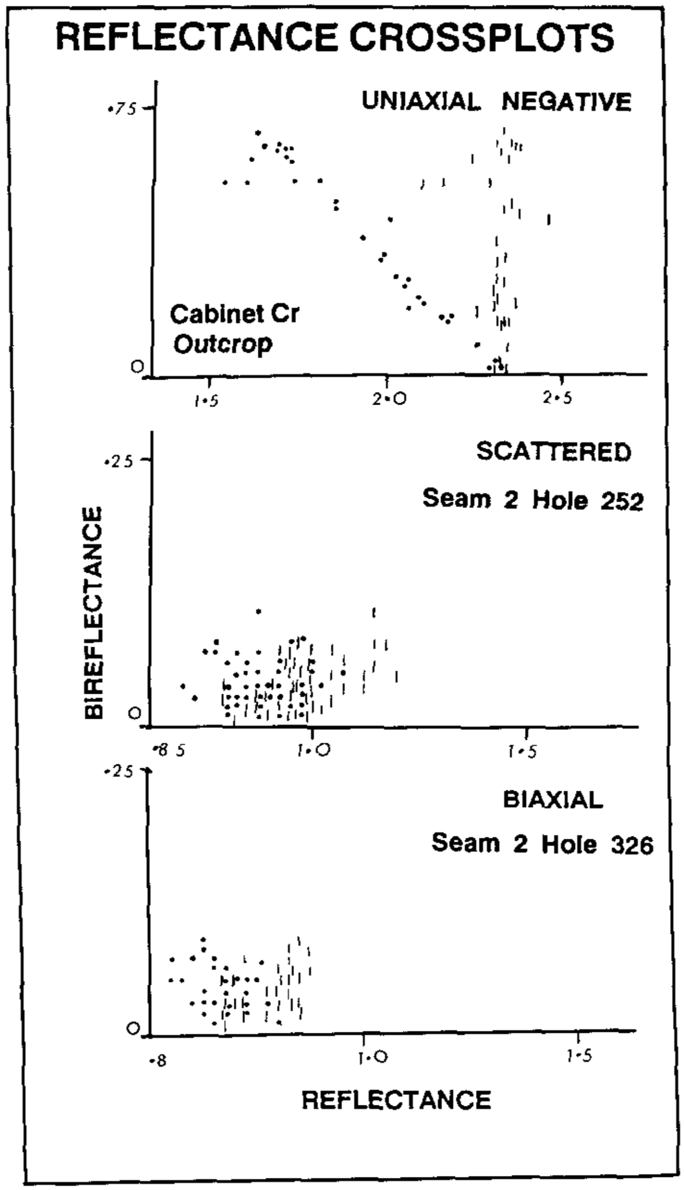

Figure 4-8-4. Examples of reflectance measurement populations for samples, illustrating different RIS.

4-8-1). Based on the angular shape of the fragments, they appear to have been included in the sediment as coal and not pieces of vegetation later compressed and coalified in place. This raises the possibility that coal seams older than Seam 1 were being eroded during deposition of Unit 1. The $\bar{R}_{max}$ values for the coalspar samples are similar to Seam 1 values indicating that the coalspar must be either from Seam 1 or from older coal that was of lower rank than Seam 1 when eroded and deposited in Unit 1. The scatter on the RIS plot probably results from mixing grains of slightly different rank and also the effects of weathering which generally tend to decrease $\bar{R}_{max}$ values (Bustin, 1982).

A few drill-core samples also have scattered RIS patterns. In four out of six cases the $\bar{R}_{max}$ values are higher than would be predicted by the accompanying volatile matter analysis for the seam. One possible explanation for this is that the spot sample used for reflectance measurement was taken from close to an in-seam fault whereas the sample used for quality analysis was a whole-seam composite sample. The high $\bar{R}_{max}$ values may be caused by heating associated with the faulting; an effect which is usually local in extent (Bustin, 1983). Oxidation and lowering of reflectance values is more likely and this probably explains the low values for the other two samples.

The reflectance data were analyzed with the help of a number of computer programs. Files of $\bar{R}_{max}$ coal-seam data with UTM locations were entered into GEOEAS®, a variogram, kriging and contouring computer program distributed in the public domain by the United States Environmental Protection Agency (1988). This software was used to grid the data. Programs generated in-house were then used to calculate area-weighted averages for the data, construct AutoCAD® DXF files and generate contour files compatible with QUIKMap®; a geographical information system (Environmental Sciences Limited, 1990). The series of programs allows for geostatistical analysis resource evaluation and display of results.

To round off discussion of the reflectance data, use was made of a database of Telkwa coal quality. The database consists of over 3000 lines, each line representing a set of analyses of a single sample. Data are derived from all ten seams sampled from over 350 holes, many of which were cored. They are analyzed with the help of a number of in-house programs tailored to the manipulation of coal-quality data.

VERTICAL COALIFICATION GRADIENTS

Change of $\bar{R}_{max}$ with stratigraphic depth can provide information on unconformities or faults in the coalfield. The timing of coalification with respect to folding and faulting can be analyzed using isorank surfaces.

Prior to this study few $\bar{R}_{max}$ data existed for the Telkwa coalfield. Spot analyses established that the coal is high-volatile A bituminous in rank but there were insufficient data to extend the discussion. Additional data required core samples of coal seams. Unfortunately most core samples obtained during the 1978 to 1989 exploration no longer exist so use was made of samples in the GSB collection and samples obtained by GSB drilling. These samples provide reasonable representation of Units 1 and 3 but poor representation of Unit 2. The coalification gradient through Unit 2 can only be estimated from holes that intersect Seam 2, Unit 2 and Seam 1. With the exception of some holes drilled in the early part of the 1982 exploration program, most were targeted to core either Unit 1 or Unit 3 but not the intervening marine Unit 2.

In general, two samples from different seams in the same drill hole were selected to provide $\bar{R}_{max}$ depth pairs. Most of depth pairs are for Unit 3 or Unit 1 and there is only one pair from Hole 231 (Table 4-8-2) which drills through Unit 2 and includes Seams 2 and 1. The $\bar{R}_{max}$ and depth paired data for the drill holes are in Tables 4-8-3 and 4.

Unit 3 is represented by a number of depth pairs for Seams 10, 6 and 2. Most represent depth differences of less than 50 metres and changes of $\bar{R}_{max}$ of less than 0.10 (Table 4-8-3). The average gradient is 0.15 per cent per 100 metres. The reproducibility of a single measurement is about 0.043 as discussed earlier (Table 4-8-4). There is some uncertainty in the exact depths recorded for some of the drill-core samples, consequently a 2.0-metre error is assumed for sample depths. The errors in $\bar{R}_{max}$ and depth make it impossible to calculate meaningful gradients for data pairs usually representing changes in $\bar{R}_{max}$ of less than 0.1 and change in depth of less than 60 metres. Therefore no comments can be made about local gradients at each hole.

It is possible to estimate the regional coalification gradient of Unit 3 by stacking the individual depth pairs in such a way as to allow a consideration of sample error. Table 4-8-5 lists the changes in $\bar{R}_{max}$ and depth for all the data pairs. Each pair can be represented as a two data-point line, one point is the origin and the second point is X = (lower depth − upper depth) and Y = (lower $\bar{R}_{max}$ − upper $\bar{R}_{max}$). When ten pairs are overlain on the plot there will be ten overlapping points at the origin and ten other points scattered through the plot. One standard deviation errors of 0.043 for $\bar{R}_{max}$ and 2.0 metres for depth are assigned to the data points. A best-fit least-squares line is fitted through the data using the method of York (1969). Errors in $\bar{R}_{max}$ and depth are considered to be uncorrelated. The resultant best-fit line is a good estimate of the average coalification gradient and the process provides an estimate of the error in the slope (coalification gradient) and intercept (approximately 0.0).

Data from Unit 3 are plotted in Figure 4-8-5. The best-fit line has a gradient of 0.114±0.028 per cent per 100 metres and an intercept of 0.007. The line intersects the one stan-

TABLE 4-8-5
TELKWA COALFIELD
NORMALIZED MEAN MAXIMUM
REFLECTANCE GRADIENTS

HOLE	STARTING POINT X1	Y1	END POINT X2	Y2	GRADIENT
SEAM 2					
218	0	0	0.04	27.[illegible]	0.14
224	0	0	0.04	36.[illegible]	0.11
231	0	0	0.14	73.[illegible]	0.19
247	0	0	0.03	38.[illegible]2	0.08
247	0	0	0.11	89.[illegible]4	0.12
251	0	0	0.14	42.[illegible]	0.33
251	0	0	0.06	66.[illegible]2	0.09
260	0	0	0.03	94.[illegible]7	0.03
267	0	0	0.09	49.[illegible]4	0.18
267	0	0	0.15	73.[illegible]8	0.21
272	0	0	0.07	34.[illegible]3	0.21
316	0	0	0.0	59.[illegible]5	0.0
347	0	0	0.14	15.[illegible]2	0.91
SEAM 1					
GSB-89-1	0	0	0.03	21.[illegible]8	0.14
GSB-89-2	0	0	0.1	18.[illegible]4	0.54
GSB-89-3	0	0	0.093	35.[illegible]2	0.26
GSB-89-8	0	0	0.048	18.[illegible]2	0.26

X = R Max difference   Y = Depth difference in metres

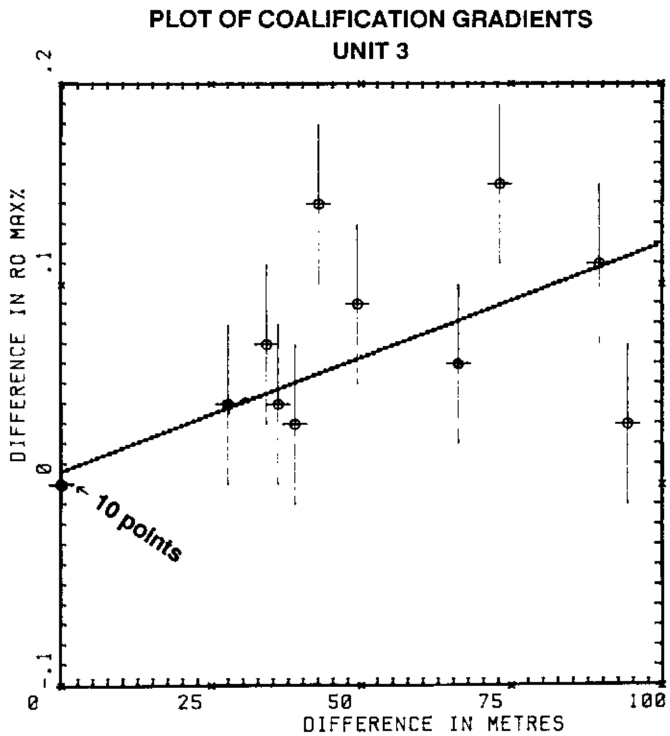

Figure 4-8-5. Stacked coalification gradients for Unit 2.

dard deviation error fields of more than two-thirds of the data. The data scatter can therefore be explained by statistical scatter about the line and any variations in coalification gradient from hole to hole that might exist are masked.

A coalification gradient of 0.114 per cent per 100 metres is similar to gradients calculated for the Lower Cretaceous Mist Mountain Formation in southeast British Columbia (Hacquebard and Cameron, 1989); data in Table 3 in their paper provide an average gradient of 0.114 per cent per 100 metres for sections in the Elk Valley area. The gradient in Unit 3 at Telkwa is somewhat greater than the coalification gradient of 0.06 per cent per 100 metres in the Seaton coal basin north of Smithers (Ryan, 1991).

Most of the short holes appear to penetrate Unit 1. The average coalification gradient for the short holes in Unit 1 is 0.3 per cent per 100 metres (Table 4-8-5). The depth increments used to calculate this gradient are small but the estimate is still reliable because of the large number of $\overline{R}_{max}$ measurements averaged to provide final data points (Table 4-8-4). As for data from Unit 3, data pairs from Unit 1 can be stacked and a best-fit least-squared line fitted through the data. A gradient of 0.27±0.11 per cent per 100 metres and an intercept of 0.002 are calculated. This gradient is significantly higher than that for Unit 3.

ESTIMATE OF THE COALIFICATION GRADIENT FOR UNIT 2

There are no useful $\overline{R}_{max}$ data available to calculate a gradient for Unit 2. It is possible to estimate $\overline{R}_{max}$ values from measurements of volatile matter. If this is done then volatile matter analyses of coal samples from the early 1982 holes which penetrate the total thickness of Unit 2 can be used to estimate Unit 2 coalification gradient. A number of papers discuss the relationship between volatile matter (VM) on a dry ash-free basis (daf) or dry mineral matter free basis (dmmf) and $\overline{R}_{max}$ (Bustin *et al.*, 1983; Meissener, 1984). In the Telkwa area VM analyses exist for the seams also analyzed for reflectance and it is possible to generate correlation plots.

Volatile matter data can be corrected to an ash or mineral matter free basis in a number of ways. One empirical way is to:

1. Regress all VM data against ash data on a seam-by-seam basis to derive the best-fit linear relationships.
2. Use the slope of the lines to correct individual VM measurements to an equivalent individual VM ash-free value.

The slope of the line will equal the Y intercept (VM ash free) if the ash acts only as a dilutant. If the mineral matter and any sulphides add inorganic volatile matter to the VM analysis then the slope will be decreased by a component equal to the gassiness of the mineral matter.

The VM intercept and slope derived from 167 analyses of Seam 2 are 29.3 per cent (or 0.293) and 0.168. The fact that the slope is much less than the intercept indicates that the mineral matter is gassy. Eighty-four samples of Seam 1 data provide an intercept value of 30.9 per cent and slope value of 0.30, indicating a non-gassy mineral matter. Non-gassy mineral matter is often associated with a reactive-rich coal (Slaghuis *et al.*, 1990).

Once a method is developed to provide VM(af) values it is possible to investigate their relationship to $\overline{R}_{max}$ on a

TABLE 4-8-6
TELKWA COALFIELD
CORRELATION BETWEEN MEAN MAXIMUM REFLECTANCE AND VOLATILE MATTER
(ASH FREE BASIS)

SEAM 6			SEAM 2			SEAM 1		
HOLE	R Max	VC %	HOLE	R Max	VC %	HOLE	R Max	VC %
216	0.40	29.5	218	0.95	28.0	224	0.92	30.1
218	0.91	29 4	231	0 99	26.6	231	0.90	33 1
247	0.84	29 1	243	0.90	28.5	237	0.96	30 1
250	0.84	26.6	246	0.89	29.3	239	0.89	33 0
251	0.94	29.5	247	0.92	30.7	248	0.99	31 2
256	0.96	25 3	251	0.86	31.0	252	1.24	27 2
259	0.88	29 5	255	0.87	28.7	260	0 87	34 1
267	0.96	25 9	256	0.90	30.3	318	0.88	32.5
272	0.86	30.2	260	0.84	28.9			
316	0.82	31 0	267	1.02	25.5			
343	0 84	30 8	272	0.93	22 3			
345	0.97	26.3	326	0.92	29.1			
347	0 89	27 6	327	0 87	28 0			
			337	0 90	28 5			
			344	0.86	30.1			
			347	1.03	27.2			

SEAM				COUNT	COREL	SL/In
	VM	=	29 6 - 0.176 x A	134	-0 41	0.59
6	VC%	=	VM + 0 176 x A			
	R%c	=	1 53 - 0 022 x VC	12	-0.82	
	VM	=	29 3 - 0 168	167	-0 54	0 64
2	VC%	=	VM + 0 168 x A			
	R%c	=	1 31 - 0 014 x VC	16	-0 54	
	VM	=	30 9 - 0.304 x A	84	-0 46	1
1	VC%	=	VM + 0 304 x A			
	R%c	=	2 46 - 0.0479 x VC	8	-0 88	

VM = Volatile matter % at A = ash percent
Corel = corellation coefficient
SN/In = slope/intercept x 100

R Max = Mean maximum reflectance measured.
VC % = Volatile matter corrected to an ash free basis using the equations below
R%c = calculated mean maximum reflectance

seam-by-seam basis using the existing $\bar{R}_{max}$ measurements. There are eight VM(af), $\bar{R}_{max}$ pairs for Seam 1, sixteen pairs for Seam 2 and thirteen pairs for Seam 6 (Table 4-8-6). Lines were fitted through each data suite (Figure 4-8-6).

It is now possible, using the VM versus ash relationships and the VM(af) versus $\bar{R}_{max}$ relationships for each seam, to convert any Seam 2 or 1 VM measurement to an estimate of $\bar{R}_{max}$. This is done for all the holes that intersect Seams 2 and 1 and the coalification gradients are calculated (Table 4-8-7). An average gradient of 0.04 per cent per 100 metres is determined which is significantly lower than that for either Unit 1 or Unit 3.

The method of deriving the coalification gradient for Unit 2 is fraught with assumptions and errors, in fact a number of other approaches were attempted; all predicted a low to very low coalification gradient through Unit 2. One method of correcting VM to VM(dmmf) uses the Parr Equation (mineral matter = 1.08 × ash % + 0.55 × sulphur %; Ward, 1984). This equation assumes that all mineral matter is equally gassy, although variations are allowed for differences in sulphur dioxide derived from pyritic sulphur. This is not the case at Telkwa for Seams 6, 2 and 1, as indicated by the different ratios of slopes of lines for the VM versus ash plots divided by the intercept value of the line (Table 4-8-6).

Coalification gradients increase exponentially with depth. England and Bustin (1986) indicate that an equation of the type $D = A \times \log((0.938 \times \bar{R}_{max} + 0.001) \times 100)) - B$ describes coalification gradients in deep oil wells in

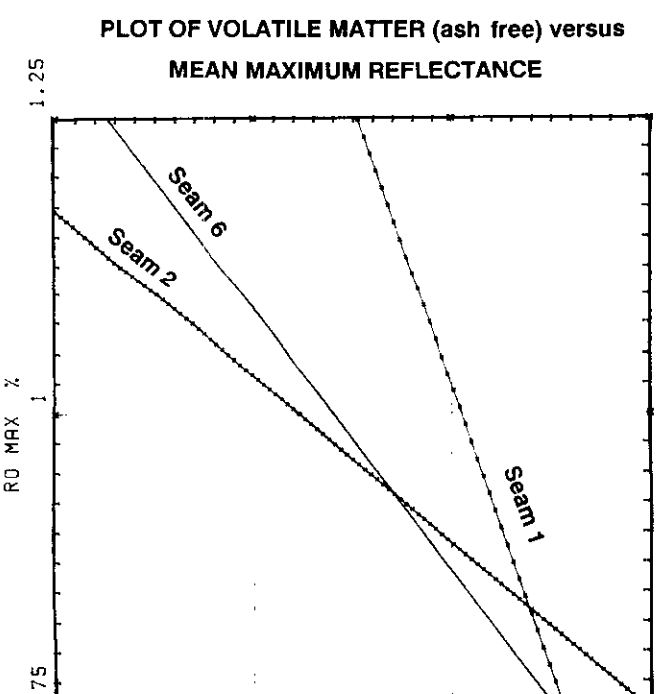

Figure 4-8-6. Mean maximum reflectance versus calculated volatile matter on an ash-free basis, Seams 6, 2 and 1. Contours of $\bar{R}_{max}$% calculated from VM data.

Alberta. If the gradient at Telkwa increases exponentially with depth then the true gradient through Unit 2 should be greater than the Unit 3 gradient of 0.11 per cent per 100 metres. This could be achieved by maintaining the difference in $\bar{R}_{max}$ values between Seams 2 and 1 but dividing by a depth increment of 60 metres instead of 130 metres (the average present separation of Seams 2 and 1). A decrease in thickness of Unit 2 by two-thirds to explain the coalification gradient implies that the thickness of Unit 2 has been increased by post-coalification thrusting from approximately 60 metres to 130 metres.

Thrust faulting does occur in Unit 3 in the area drilled, but no thrusts of sufficient magnitude have been mapped. If Unit 2 is thickened by thrusts there should be areas where the original thickness of about 40 metres is preserved: such areas could have increased exploration potential. The low gradient through Unit 2 may indicate a high thermal conductivity for the unit but this is unlikely.

LATERAL VARIATIONS IN THE COALIFICATION GRADIENTS

Most of the $\bar{R}_{max}$ values available for the Telkwa coalfield are from the Goathorn Creek area with a limited amount of data for the rest of the field. The rank of coal in the Lake Kathlyn prospect west of Smithers (Figure 4-8-1) has been increased to meta-anthracite by adjacent intrusions (Dowling, 1915). South of Smithers, along the Bulkley River, two $\bar{R}_{max}$ measurements (Table 4-8-1) indicate a rank of medium-volatile bituminous ($\bar{R}_{max}$ greater than 1.0 per cent). The rank of coal in Unit 3 north of the Telkwa River, in the area drilled by Crowsnest Resources Limited, averages high-volatile A bituminous ($\bar{R}_{max}$ = 0.95, average of four analyses, Table 4-8-1). Locally the rank is increased by a Tertiary intrusion outcropping to the north, but the average rank is not much higher than the rank at Goathorn Creek where the $\bar{R}_{max}$ data range from 0.8 to 1.0 per cent.

TABLE 4-8-7
TELKWA COALFIELD
CALCULATED MEAN MAXIMUM REFLECTANCE (R%c)
FOR SEAMS 2 AND 1
COALIFICATION GRADIENTS THROUGH UNIT 2

			SEAM 2		SEAM 1		
HOLE	EASTING	NORTHING	DEPTH (metre)	R%c	DEPTH (metre)	R%c	GRADIENT
219	621616	6054106	151.2	0.89	275.5	0.94	0.04
220	621378	6053784	82.2	0.90	231.2	0.94	0.02
223	621047	6053853	55.8	0.90	154.9	0.94	0.04
225	621252	6053453	29.6	0.89	190.7	1.00	0.07
227	621386	6053449	61.2	0.86	218.2	0.95	0.06
231	619511	6054312	179.8	0.94	305.8	0.87	-0.06
234	619710	6054451	62.1	0.92	178.2	1.10	0.16
251	621583	6052867	131.1	0.88	267.7	0.96	0.06
260	621019	6055019	56.8	0.91	16.5	0.83	-0.01
265	619687	6054626	98.9	0.92	263.1	1.02	0.06
268	621643	6054395	140.4	0.91	266.4	0.92	0.01
			AVERAGE	0.90		0.95	0.04

Note: average separation of 2 seam to 1 seam = 120 metres.

Gradient = R Max difference per 100 metres
R%c = calculated mean maximum reflectance

Seam1: R%c = 1.31 - 0.014 (VM + 0.168 x A)
Seam 2: R%c = 2.46 - 0.0479 (VM + 0.0309 x A)

VM = Volatile matter percent
A = Ash percent

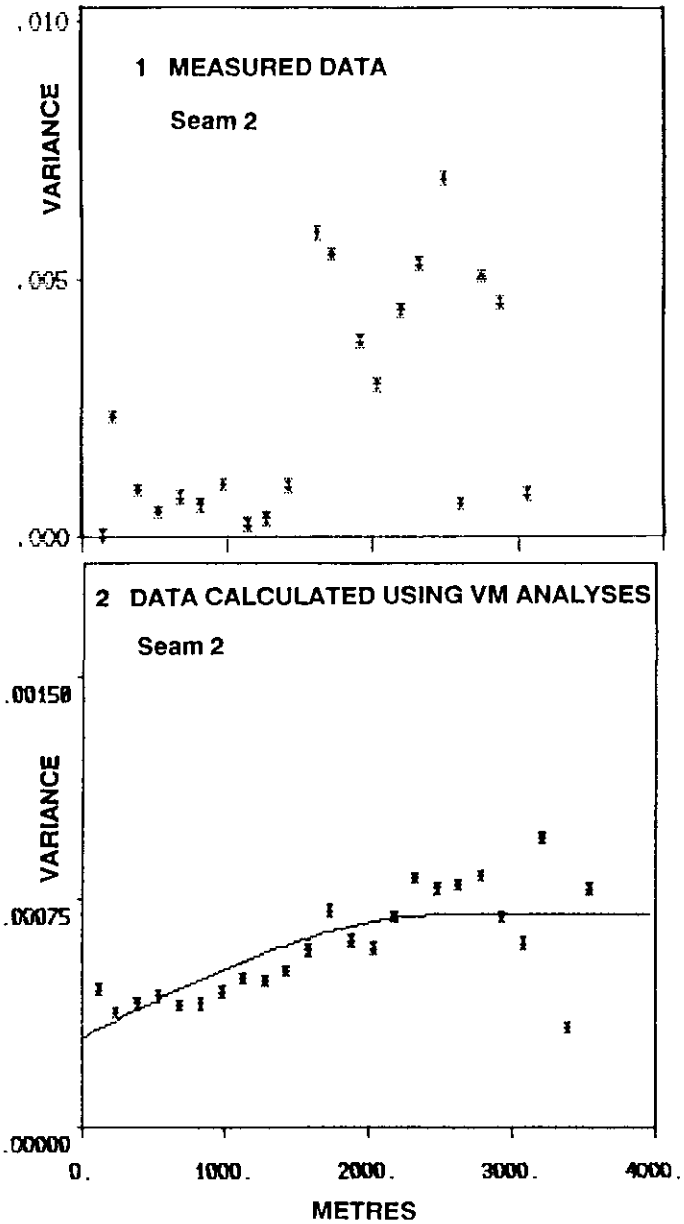

Figure 4-8-7. Variograms for mean maximum reflectance data and calculated mean maximum reflectance data; Seam 2.

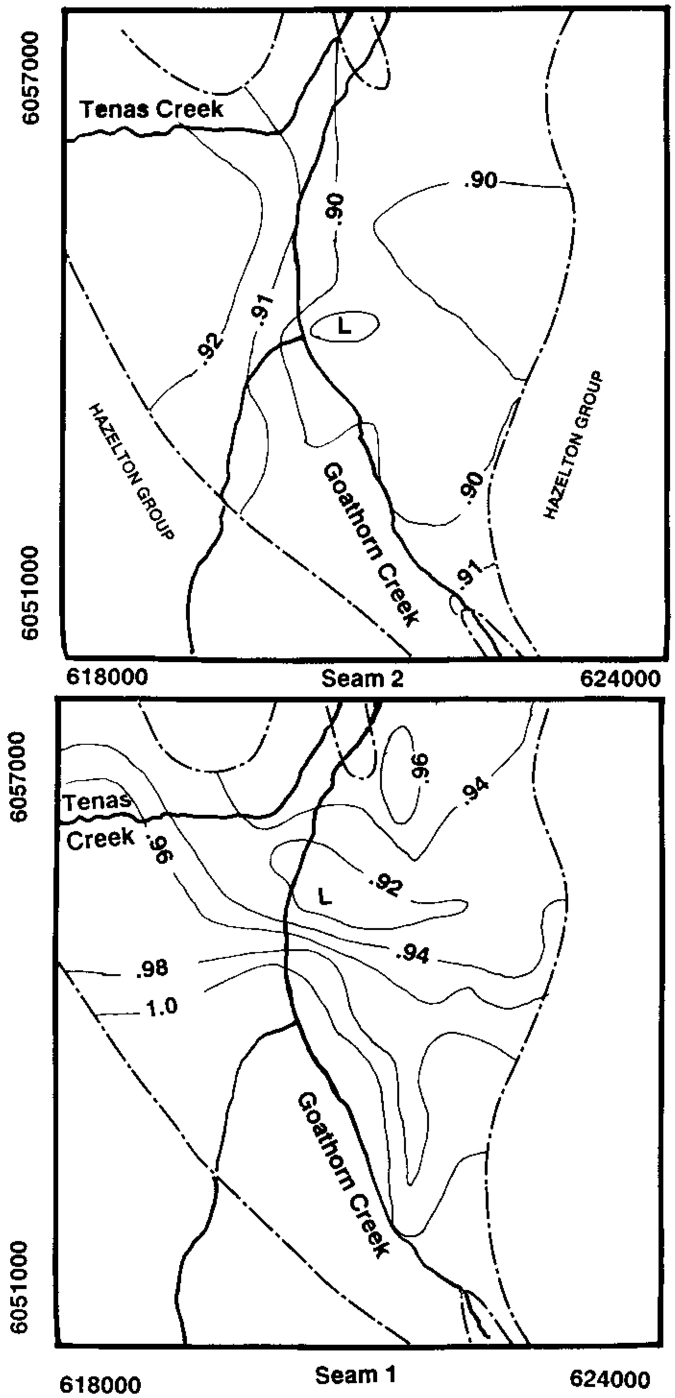

Figure 4-8-8. Contours of calculated mean maximum reflectance data for Seams 2 and 1.

A single $\bar{R}_{max}$ measurement on float collected from northeast of the Goathorn Creek area is 1.32 per cent, indicating the possible presence of coal of medium-volatile rank south of the Telkwa River and northeast of the present Goathorn Creek exploration area. The $\bar{R}_{max}$ value of a sample from a subcrop of coal bloom exposed by logging activity southeast of the headwaters of Tenas Creek is 1.10 per cent, indicating the presence of medium-volatile bituminous coal.

An outlier of the Telkwa coalfield outcrops at Cabinet Creek. A number of seams are exposed in the creek and three drill holes in the area intersect coal assigned to Unit 1. Mean maximum reflectance measurements of outcrop samples indicate a rank of semi-anthracite (Table 4-8-1); in fact Dowling (1915) describes an adit probably located near Cabinet Creek that intersected anthracite. The quality available from the three rotary-drill holes indicates a rank of at least low-volatile bituminous based on ash and VM analyses of chip samples. Two of these holes intersected 6 and 11 metres of fine-grained igneous rock in the sedimentary section. No intrusive rocks were seen in outcrop nor are any Tertiary plutons mapped in the area. The high rank at Cabinet Creek could be caused by: post-Cretaceous heat sources, a deeper stratigraphic section than the Goathorn Creek area, or a higher heat-flux from the pre-Cretaceous basement. The preference of the author is for the third possibility.

The rank of coal through the Telkwa coalfield is obviously more variable than previously thought. The coalfield has the potential to be a source of medium-volatile metallurgical coal as well as an anthracite thermal product.

In-seam lateral variations of coal rank in the Goathorn Creek area were investigated using the GEOEAS software. Variogram diagrams were constructed for Seams 10, 6, 2 and 1. In all cases no variogram models could be fitted through the data and no regional trends contoured. Despite this, the data were gridded to obtain area-weighted average $\bar{R}_{max}$ values for each seam. Values of 0.83, 0.88, 0.91 and 0.91 per cent were obtained for Seams 10, 6, 2 and 1. The similarity of average values for Seams 2 and 1 supports the previous suggestion of a low coalification gradient through Unit 2. It should be noted that in averaging Seam 1 data where there is more than one $\bar{R}_{max}$ value in a hole, the minimum depth value was used.

The beds in the Goathorn Creek area dip gently to the east and it is important to see if present depth has any influence on the coalification gradient. A plot of all Seam 2 reflectance data versus present depth revealed no positive correlation; a line through seventeen points has a slope of 0.01 per cent per 100 metres, an intercept $\bar{R}_{max}$ value of 0.91 per cent and a correlation coefficient of 0.15. It appears that coalification predates folding, thrusting and tilting.

The reflectance data for Seams 2 and 1 cover a limited area; if the method of converting VM measurements into estimated $\bar{R}_{max}$ values is used, then a much larger database covering a larger area is available. Variograms for calculated values of Seams 2 and 1 indicate some regional trends. Figure 4-8-7 illustrates variogram plots measured $\bar{R}_{max}$ data and calculated $\bar{R}_{max}$ data for Seam 2. No variogram model can be fitted to the measured data but a spherical variogram model fits to the larger database of calculated values. The calculated databases for Seams 2 and 1 were kriged, gridded and contoured (Figure 4-8-8).

Figures 4-8-2 and 8 are redrafted printer-output with some distortion in the Y axis. There is considerable random scatter in the data but the two contour diagrams (Figure 4-8-8) show some similarities. Coal rank tends to be high in the southeast and southwest but low in the centre of the map (east of Goathorn Creek and north of the area proposed for development).

Sediments in a small graben in the central part of the basin, away from the fault-bounded margins, might experience less maturation. The area-weighted average for the calculated $\bar{R}_{max}$ values for Seams 2 and 1 are 0.91 per cent and 0.99 per cent which, for an average separation of 130 metres indicates a gradient of 0.06 per cent per 100 metres which is similar to the previously estimated coalification gradient for Unit 2.

ECONOMIC IMPLICATIONS

The Telkwa property has been considered for development as a thermal coal mine for a number of years. Certainly most of the area intensively explored is high-volatile A bituminous in rank. New data indicate that medium-volatile bituminous coal may subcrop near Tenas Creek and in other areas. This leads to the possibility of a metallurgical coal which is a more valuable product. The semi-anthracite in the Cabinet Creek area could be developed as a smokeless high-calorie thermal product for local as well as international markets. Many houses in the area burn wood in stoves for heat; anthracite, a smokeless fuel could be an environmentally acceptable replacement as long as the sulphur content is moderate.

The coalbed-methane potential for Telkwa will be the subject of another study. Gas content increases with rank and the medium-volatile rank at Tenas Creek and semi-anthracite rank at Cabinet Creek should increase the methane resource estimate for the area.

The use of volatile matter to estimate $\bar{R}_{max}$ has an interesting spin-off. Comparison of the VM(af) versus $\bar{R}_{max}$ lines for the different seams provides information about the relative reactivity of the seams and the relative vitrinite contents. Seam 1 has a higher volatile matter content than Seams 6 and 2, at the same rank, indicating that it is the most reactive coal and, at a rank approaching medium-volatile bituminous, may be suitable for coking. Stauss *et al.* (1976) graph the relationship between $\bar{R}_{max}$ vitrinite plus liptinite content and VM (daf). Using the average VM ash-free values derived for Seam 2 (29.3 per cent) and Seam 1 (30.9 per cent) and average $\bar{R}_{max}$ values for Seam 2 (0.91) and Seam 1 (0.99) the diagram predicts vitrinite plus liptinite contents of 30 per cent for Seam 2 and 60 per cent for Seam 1. These predictions are approximate, in part because the VM ash-free values in this study have to be corrected to a dry basis before using the graph.

An $\bar{R}_{max}$ value of 0.99 and 60 per cent reactives for Seam 1 predicts a free swelling index (FSI) value of 4 using the petrographic composition versus $\bar{R}_{max}$ diagram introduced by Pearson (1980). The Telkwa coal-quality database contains some FSI data. Weighted averages of ash and FSI for each seam are as follows:

Seam 6: 10 per cent ash, FSI = 2, count 64 holes;

Seam 2: 13 per cent ash, FSI = 1.5, count 65 holes;

Seam 1: 15 per cent ash, FSI = 3.8, count 36 holes;

The predicted FSI of 4 is in reasonable agreement with the actual average value of 3.8. Based on these inferences Seam 1 classifies as a G4-type coking coal (Pearson, 1980).

Seam 1 generally has the lowest sulphur content of all the seams but maybe difficult to wash. Often vitrinite-rich seams with good metallurgical properties such as fluidity, also have higher ash and are difficult to wash. It should be emphasized that Seam 1, which does not feature in present surface-mining proposals, has potential as a metallurgical coal. The next stage of this study will include petrography to check and extend the above analysis.

CONCLUSIONS

Coal in the Telkwa coalfield varies from high-volatile A bituminous to semi-anthracite. The area most intensively explored is underlain mainly by high-volatile A bituminous coal. Medium-volatile bituminous coal and semi-anthracite are also present and may eventually be developed as reserves. The coalification gradients range from 0.114 per cent per 100 metres for Unit 3 to 0.27 per cent per 100 metres for Unit 1. The gradient in the intervening Unit 2 appears to be low, a possible explanation is the presence of as yet unrecognized thrusts within the unit. Major lateral variations of in-seam rank are not present in the Goathorn area. Apparent minor variations may reflect the local basin structure with higher rank near the margins and lower rank in the centre.

Volatile matter (ash free basis) versus $\bar{R}_{max}$ relationships indicate that the lowest seam in the section is the most reactive and corroborate the correlation between gassiness of mineral matter and reactive content in the coal.

Coalspar material collected from Unit 1 may be derived from coal older than Seam 1 but of equal or lower rank.

ACKNOWLEDGMENTS

The author wishes to thank JoAnne Schwemler for performing the reflectance measurements. David Grieve acted as a sounding board. Anna Peakman and Mike Fournier typed the tables.

REFERENCES

Bustin, R.M. (1982): The Effect of Shearing on the Quality of Some Coals in the Southeastern Canadian Cordillera; *Canadian Institute of Mining and Metallurgy*, Volume 75, pages 76-83.

Bustin, R.M. (1983): Heating During Thrust Faulting; Friction or Fiction?; *Tectonophysics*, Volume 95, pages 309-328.

Bustin, R.M., Cameron, A.R., Grieve, D.A. and Kalkreuth, W.D. (1983): Coal Petrology; Its Principles, Methods, and Applications; *Geological Association of Canada*, Short Course Notes, Volume 3.

Dowling, D.B. (1915): Coalfields of British Columbia; *Geological Survey of Canada*, Memoir 309.

England, T.D.S. and Bustin, R.M. (1986): Thermal Maturation of the Western Canadian Sedimentary Basin South of the Red Deer River (1) Alberta Plains; *Bulletin of Canadian Petroleum Geology*, Volume 34, pages 71-90.

Environmental Sciences Limited (1990): QUIKMap; *ESL Environmental Sciences Limited*, Sidney, B.C.

Hacquebard, P.A. and Cameron, A.R. (1989): Distribution and Coalification Patterns in Canadian Bituminous and Anthracite Coals; *International Journal of Coal Geology*, Volume 13, pages 207-260.

Kilby, W.E. (1988): Recognition of Vitrinite with Non-uniaxial Negative Reflectance Characteristics; *International Journal of Coal Geology*, Volume 9, pages 267-285.

Koo, J. (1983): The Telkwa, Red Rose and Klappan Coal Measures in Northwestern British Columbia; *in* Geological Fieldwork 1983, *B.C. Ministry of Energy, Mines and Petroleum Resources*, Paper 1984-1, pages 81-90.

McCartney, J.T. and Ergun S. (1967): Optical Properties of Coals and Graphite; *Bureau of Mines, United States Department of the Interior*, Bulletin 641.

MacIntyre, D., Desjardins, P., Tercier, P.O. and Koo, J. (1989): Geology of the Telkwa River Area (NTS 93L/11); *B.C. Ministry of Energy, Mines and Petroleum Resources*, Open File 1989-16.

Matheson, A. and Van Den Bussche, B. (1990): Subsurface Coal Sampling Survey Central British Columbia; *in* Geological Fieldwork 1989, *B.C. Ministry of Energy, Mines and Petroleum Resources*, Paper 1990-1, pages 445-448.

Meissener, F.F. (1984): Cretaceous and Lower Tertiary Coals as Sources for Gas Accumulations in the Rocky Mountain Area; *in* Hydrocarbon Source Rocks of the Greater Rocky Mountain Region, Woodward, J., Meissener, F.F. and Clayton, J.L., Editors, *Rocky Mountain Association of Geologists*, 1984 Symposium, pages 401-431.

Palsgrove, R.J. and Bustin, R.M. (1989): Stratigraphy and Sedimentology of the Lower Skeena Group, Telkwa Coalfield, Central British Columbia (93L/11); *in* Geological Fieldwork 1989, *B.C. Ministry of Energy, Mines and Petroleum Resources*, Paper 1990-1, pages 449-454.

Pearson, D.E. (1980): The Quality of Western Canadian Coking Coal; *Canadian Institute of Mining and Metallurgy*, Bulletin, Volume 73, pages 1-15.

Ryan, B.D. (1991): Geology and Potential Coal and Coalbed-methane Resources of the Seaton Coal Basin; *in* Exploration in British Columbia 1990, *B.C. Ministry of Energy, Mines and Petroleum Resources*, pages 153-167.

Slaghuis, J.H., Ferreira, L.C. and Judd, M.R. (1990): Volatile Matter in Coal: Effect of Inherent Mineral Matter; *Fuel*, Volume 70, pages 468-470.

Stauss, P.G., Russell, N.J., Bennett, A.J.R. and Atkinson, C.M. (1976): Coal Petrography as an Exploration Aid in the West Circum-Pacific; *in* Coal Exploration, Muir, W.L.G., Editor, *Miller Freeman Publications*, pages 401-443.

Tipper, H.W. (1976): Smithers Map Area 93/L; *Geological Survey of Canada*, Open File Map 351.

United States Environmental Protection Agency (1988): GEOEAS Geostatistical Environmental Assessment Software; *Environmental Monitoring Systems Laboratory*, Las Vegas, Nevada, 89193-3478.

Ward, C.R. (1984): Coal Geology and Coal Technology; *Blackwell Scientific Publications*, pages 60-73.

York, D. (1969): Least Squares Fitting of a Straight Line with Correlated Errors; *Earth and Planetary Science Letters*, Volume 5, pages 320-324.

GEOLOGY OF DOLOMITE-HOSTED MAGNESITE DEPOSITS OF THE BRISCO AND DRIFTWOOD CREEK AREAS, BRITISH COLUMBIA

By George J. Simandl and Kirk D. Hancock

KEYWORDS: Economic geology, industrial minerals, magnesite, Mount Nelson Formation, Evaporites, Precambrian.

LOCATION AND HISTORY

The magnesite deposits of the Brisco and Driftwood Creek areas are located approximately 30 and 50 kilometres, respectively, northwest of Radium Hot Springs (Figure 4-9-1). Most of the deposits are accessible by forestry roads. The first magnesite discovery in the area dates back to the early Sixties. Some of the deposits have been investigated by drilling, trenching and bulk sampling. Up to the present, no commercial production has resulted from these activities.

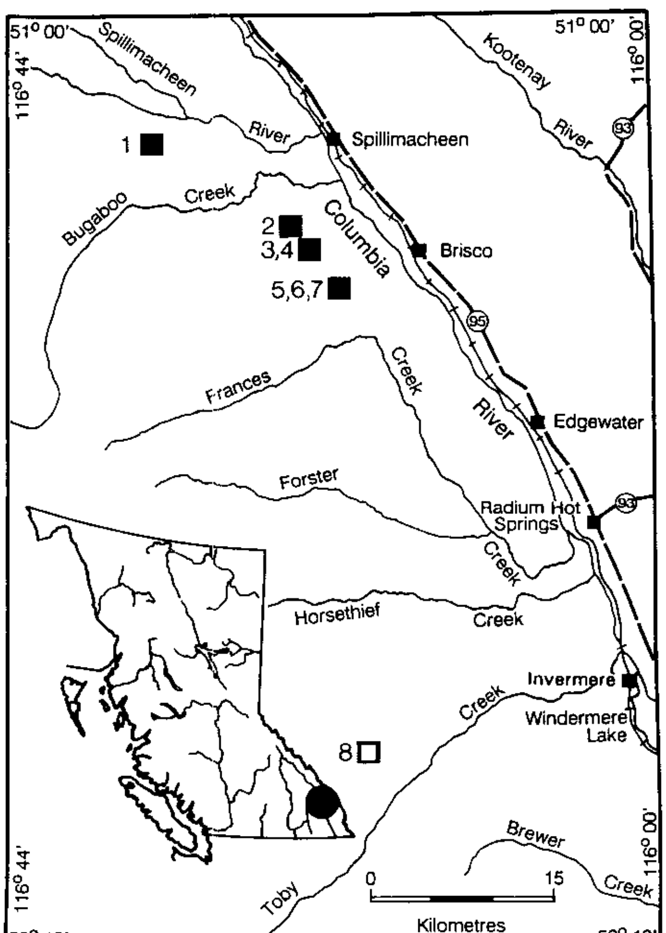

Figure 4-9-1. Location of the Brisco and Driftwood Creek magnesite deposits. 1-Driftwood Creek, 2-Red Mountain, 3-Topaz Lake, 4-Cleland Lake, 5-Dunbar, 6-Jab, 7-Botts Lake, 8-deposits described by Pope (1990).

REGIONAL GEOLOGIC SETTING

The Brisco and Driftwood Creek deposits are situated west of the Rocky Mountain Trench fault (Figure 4-9-2). They are hosted by dolomites of the Helikian Mount Nelson Formation of the Purcell Supergroup within the Purcell anticlinorium. Stratigraphic sections applicable to the area of the magnesite deposits were established by Walker (1926), Reesor (1973) and Bennett (1985). The geology of the Toby and Horsethief Creek areas has been described by Pope (1989, 1990). Only the Mount Nelson and Toby Creek formations will be described below. The upper part of the Mount Nelson Formation hosts the magnesite deposits.

The Mount Nelson Formation is separated from the overlying Toby Formation of the Windermere Supergroup (Hadrinian) by an unconformity (Reesor 1973, Pope 1989). This unconformity records the East Kootenay orogenic event which consisted of regional uplift and thermal metamorphism dated at 750–850 Ma and submarine volcanic activity within the Purcell anticlinorium (Pope, 1989).

The magnesite deposits are located within an area affected by low-grade regional metamorphism (Reesor, 1973; Bennett, 1985). All known magnesite occurrences are located outside the contact metamorphic aureole of Middle Cretaceous intrusions (Figure 4-9-2).

STRATIGRAPHY OF THE MOUNT NELSON AND TOBY FORMATIONS

MOUNT NELSON FORMATION

In the Toby – Horsethief Creek map area, the Mount Nelson Formation (Figure 4-9-3) is at least 1320 metres thick and is the uppermost unit of the Purcell Supergroup (Pope, 1990). It is divided into seven members. The descriptions below, in order from oldest to youngest are summarized from Pope (1990).

The "lower quartzite" is 50 to 150 metres thick, white, well-sorted, thin-bedded (<20 cm), ripple-laminated, fine to medium-grained quartz arenite.

The "lower dolomite sequence" is characterized by its grey colour and a light grey weathered surface, laminated beds 20 to 50 centimetres thick, soft sediment features, cryptalgal laminations and laterally linked hemispherical stromatolites. This dolomite also contains black argillite layers 1 to 2 centimetres thick and oolitic laminae. The top of the sequence is the cream-coloured, cherty "cream marker dolomite", 20 metres thick.

The "middle dolomite sequence" comprises the "middle quartzite", "orange dolomite" and "white markers". The "middle quartzite" has a characteristic apple-green colour. It consists of graded, crossbedded and massive arenites, siltstones and argillites. Beds are 10 to 50 centimetres thick

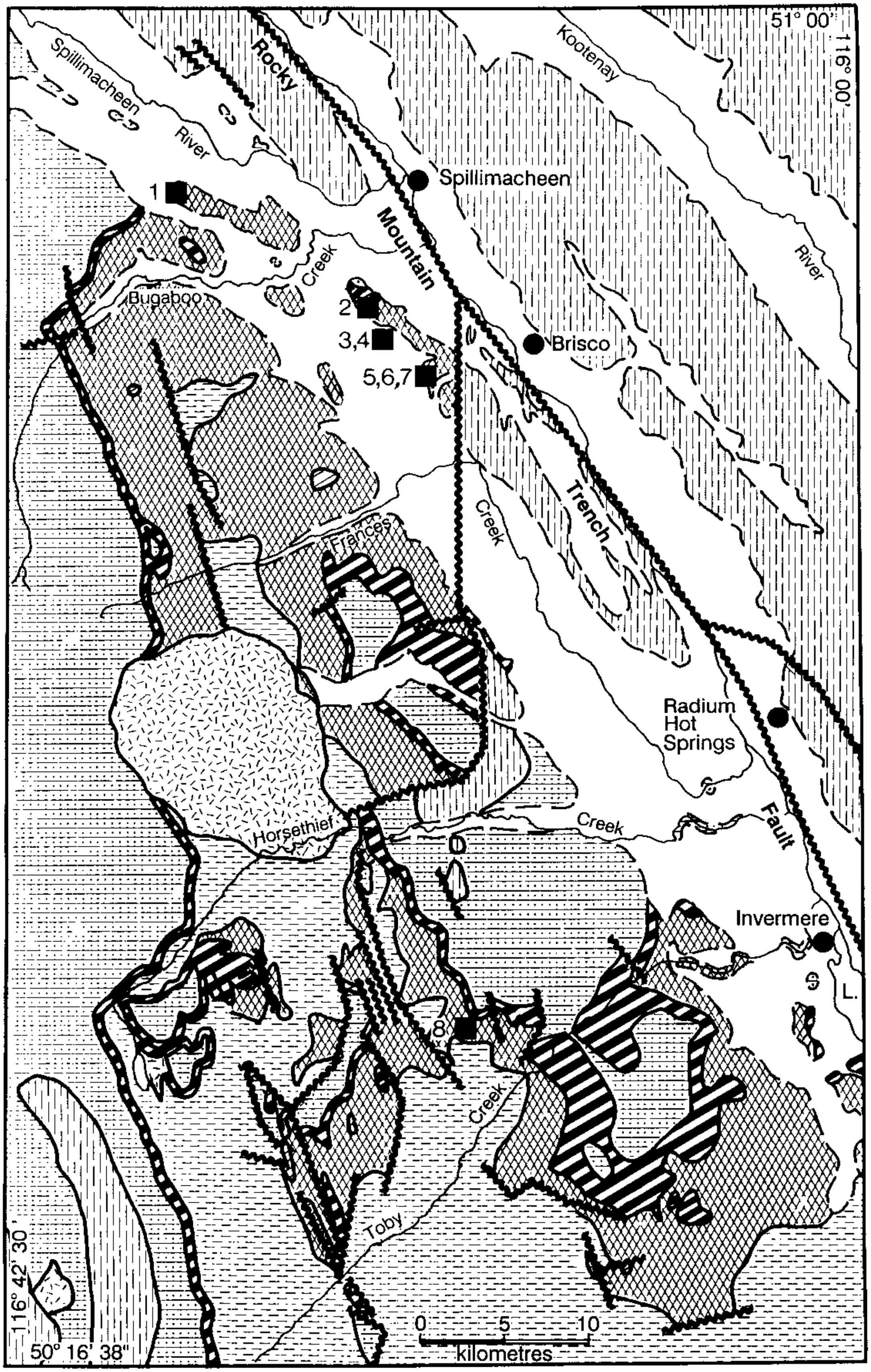

Figure 4-9-2. Regional geology and geological setting of the magnesite deposits hosted by Mount Nelson Formation. Simplified from Reesor (1973).

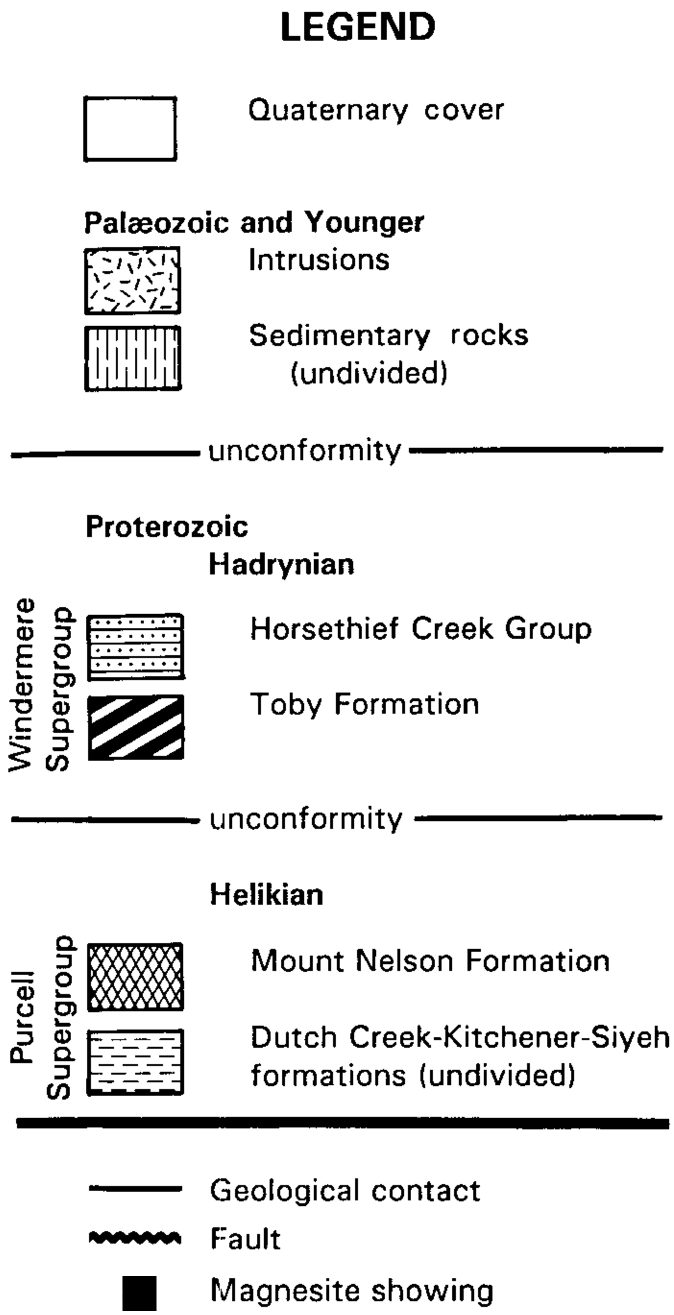

with undulate bases and truncated tops. The orange dolomite consists of well-bedded silty or light beige to dark grey dolomites weathering orange-brown or orange-buff. Stromatolitic textures, cryptalgal laminations, chert intercalations, halite casts, solution-collapse breccias and dewatering features have been described in this unit.

The "white markers" sequence is less than 70 metres thick and comformably overlies the orange dolomite. It consists of cream to medium grey dolomites and locally contains white magnesite beds up to 1 metre thick as well as purple, green and buff dolomitic mudstones and beds with dolomite-replaced halite crystals.

The "purple sequence" comformably overlies the white markers. It consists of dolomites as well as dolomitic siltstones and sandstones consisting of 20 per cent quartz, 70 per cent dolomicrite and 10 per cent hematite. These rocks contain halite casts and grade upward into purple shales with green reduction spots. Several mudchip breccias and monomictic conglomerates occur within this sequence. The upper part of the purple sequence is referred to as "purple shale unit". It consist of purple argillites with or without green reduction spots and laminae. The purple sequence is separated from the overlying upper middle dolomite by a conglomerate consisting of angular to rounded dolomite and quartzite clasts of variable dimensions, cemented by purple sandy argillite.

The "upper middle dolomite" is 80 metres thick and similar to the lower main dolomite, however, it contains abundant allochems (oncolites and oolitic peloidal and pisolitic laminations) replaced by chert.

The "upper quartzite" is over 260 metres thick. It is a cliff-forming, well-sorted, quartz-cemented and medium to coarse-grained arenite, characterized by massive bedding and poorly preserved sedimentary features.

The "upper dolomite" has a conformable gradational contact with the upper quartzite. Pale beige to dark grey, dolomite beds, 10 to 50 centimetres thick, are interbedded with quartz and dolomite-pebble conglomerates and dolomitic sandstones. The unit is characterized by abundant chert layers, cryptalgal structures replaced by black chert and by a distinctive, laminated, strongly contorted and locally brecciated blue-grey dolomite. The contact with underlying quartzite is transitional and consists of interbeds of purple argillite, quartzite and dolomite.

Toby Formation

The Toby Formation forms the base of the Windermere Supergroup. It consists of five major lithofacies: boulder breccia, diamictite, sparse-clast diamictite, siltstone and argillite, and submarine basic volcanics which are described by Reesor (1973) and Pope (1989). These lithofacies exhibit rapid facies changes.

The boulder breccia facies forms lenticular bodies at the base of the Toby Formation. Clasts are of local provenance and consist of underlying lithologies of the Mount Nelson Formation (Pope, 1989).

The diamictite facies consists of rounded quartzite and subangular dolomite clasts supported by a sandy argillite matrix. The sparse clast diamictite consists of graded, poorly sorted argillites that contain isolated, rounded quartzite clasts.

The volcanic component of the Toby Formation is a "conglomerate" containing clasts of the same range of composition and size as previously described lithofacies, but the matrix is vesicular andesite flow (Reesor, 1973; Bennett, 1985). The Toby Formation is commonly interpreted as a "syn-rift" deposit (Pope, 1989).

GEOLOGY OF THE MAGNESITE DEPOSITS

The descriptions of the Driftwood Creek – Brisco magnesite deposits presented below are based mainly on the 1991

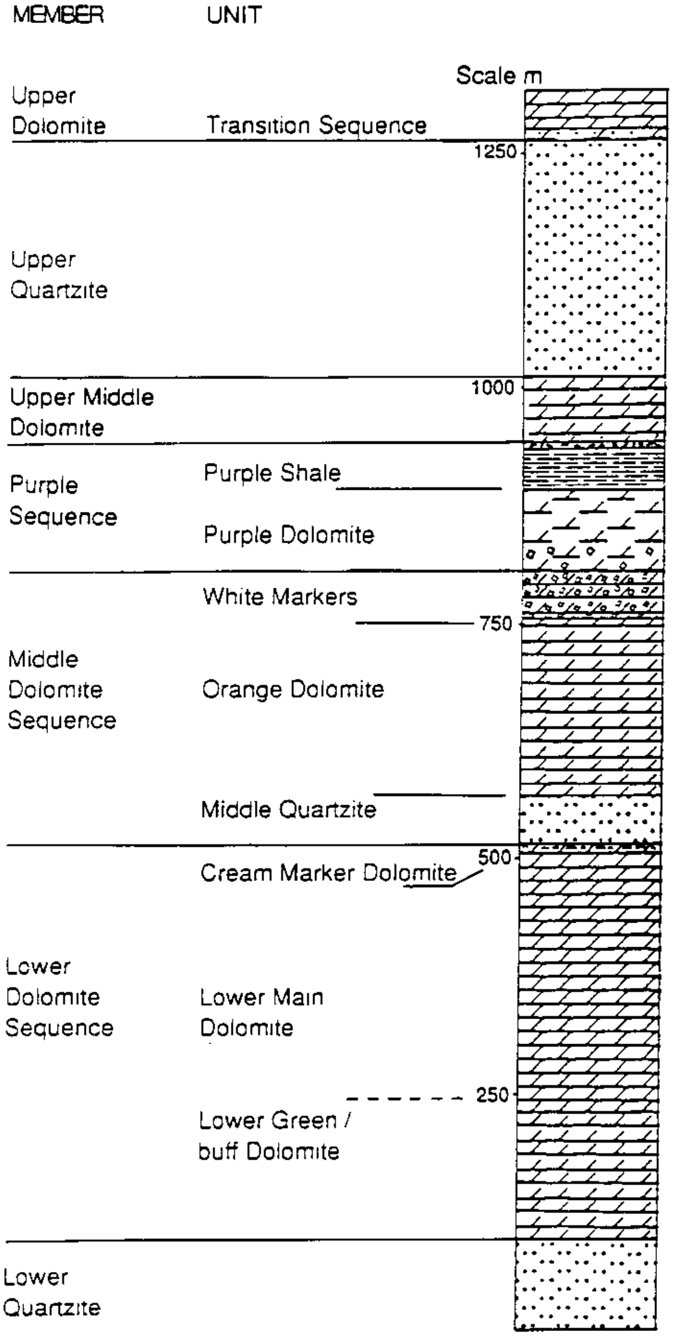

Figure 4-9-3. Stratigraphy of the Mount Nelson Formation. (Pope, 1990)

field investigations, however, where required, deposit descriptions are supplemented by published information by McCammon (1964) and Grant (1987). Mineralogical descriptions are based on field observations. The deposits were extensively sampled in 1991. Chemical analyses of these samples are not available at the time of writing and all quoted analyses are from Grant (1987).

All deposits are hosted by dolomites of the Mount Nelson Formation. The mineralization consists of sparry or coarse-grained magnesite. With the exception of the Red Mountain deposit, detailed stratigraphy in the proximity of magnesite deposits is impossible to establish due to the poor exposure.

Driftwood Creek

The Driftwood Creek deposit is exposed on ridges, on the east side of Driftwood Creek (Figure 4-9-2). The northern part of the deposit was drilled and test pitted by Kaiser Resources Ltd. in 1978 (Morris, 1978) and mapped by Hora (1983). Present work documents a string of stratabound magnesite lenses over a distance of 4 kilometres (Figure 4-9-4). The magnesite-hosting horizon continues farther south and is covered by overburden to the north. The sparry carbonate with least silica impurities lies south of the area investigated by Kaiser Resources. The geology of the Driftwood Creek deposit is illustrated by Figure 4-9-4 and lithologies are described below:

Phyllite and quartzite (Unit D1, Figure 4-9-4) outcrop in the southeastern part of the map area. This unit consists mainly of dark grey argillite with moderately well developed planar cleavage and phyllitic sheen. Grain size is usually smaller than 0.062 millimetre, however, locally white mica specks up to 0.5 millimetre appear on some cleavage faces. Interbeds of soft, probably feldspathic, greenish sandstone (0.062–0.125 mm), less than 50 centimetres thick, are common.

Massive orthoquartzite (Unit D2) is typically white but locally greenish. It consists mainly of rounded, silica-cemented grains measuring 0.125 to 0.5 millimetre in diameter. It is crosscut by numerous, white quartz veins, up to several centimetres wide, and by narrow iron oxide stained fractures less than 0.5 millimetre wide.

Green or buff-weathering dolomitic argillites and siltstones (Unit D3) overlie the massive orthoquartzite. Individual beds are usually 10 to 25 centimetres thick. Both the green and buff-weathering rocks contain dolomite.

Black dolomite (Unit D4) is generally massive and aphanitic and weathers buff. However, some of the beds, 10 centimetres to 2 metres thick, may weather pale grey or greyish white. This rock may contain cryptalgal laminations or isolated stromatolites up to 20 centimetres in diameter (Plate 4-9-1). The dolomite reacts moderately with hydrochloric acid when powdered and is crosscut by abundant quartz veinlets a few millimetres to several centimetres wide.

Greenish grey and locally purplish orthoquartzite (Unit D5) weathers grey, greenish or beige. Massive beds are up to 50 centimetres thick and laminated beds are up to 30 centimetres thick. Quartz grains are moderately well sorted, rounded, less than 0.25 millimetre in diameter and silica cemented. Loadcast textures indicate the sequence is upright.

Dark grey dolomite (Unit D6) is similar to unit D4. It weathers beige or light grey.

Fine-grained, dolomitic siltstone and silty dolomites (Unit D7) are characterized by diffuse centimetre-scale, greenish to purplish or almost salmon-pink rainbow-like colour transitions. Broken rock has sharp edges and nearly conchoidal fractures. The rock is hard and in most cases can not be scratched by a hammer. It reacts strongly with hydrochloric acid if crushed and consists mainly of quartz and dolomite. Softer, more weathered, purplish beds also con-

Plate 4-9-1. Stromatolite in the dolomite which hosts and underlies magnesite; Driftwood Creek deposit.

Plate 4-9-2. Dolomite breccia; pale grey dolomite fragments cemented by sparry dolomite. Sulphide grains appear black; Driftwood Creek deposit.

tain chlorite. Proportions of rock-forming minerals are highly variable from bed to bed.

Laminated dark grey dolomite (Unit D8) is medium to dark grey and weathers buff. It is commonly massive and aphanitic to fine grained, however, where locally recrystalized it is coarser (0.25-0.5 mm). When crushed, it reacts with hydrochloric acid. Differential weathering emphasizes fine, sub-millimetre laminations.

Stromatolitic dolomite (Unit D9) most commonly forms the footwall of the magnesite deposit. It is pale grey in colour and weathers orange-brown or red-brown. A feature characteristic of this unit is an abundance of hemispherical stromatolites measuring 10 to 40 centimetres across, commonly discernible only on the weathered surface. When crushed, the rock reacts strongly with hydrochloric acid. It consists of dolomite (<0.125 mm, >90 %) and calcite (<0.125 mm, 0–5%). Commonly it is cut by silica veinlets up to 3 millimetres wide which form less than 10 per cent of the rock. Sparry calcite veins up to 10 centimetres wide were observed in one outcrop only. This rock is locally brecciated where it outcrops adjacent to or below the magnesite lenses. The angular breccia clasts may be elongate or equidimensional and vary in size from a few millimetres to 20 centimetres across. These are interpreted as dissolution and collapse breccias. Clasts are cemented by light grey or white, sparry dolomite (Plate 4-9-2). The sparry cement commonly contains 1 to 3 per cent pyrite crystals up to 4 millimetres across. The dolomite fragments also contain fine-grained, disseminated sulphides.

Magnesite and sparry carbonate (Unit D10) form stratabound lenses and pockets. They are either white, pale grey or beige and weather buff. The unit is characterized by coarse to sparry crystals (Plate 4-9-3) and locally contains light green interbeds less than 1 centimetre in thickness. The interbeds are either regular or disrupted by growth of sparry magnesite crystals within the coarsest magnesite-rich zones. Vestiges of hemispherical stromatolites are observed locally in finer grained magnesite-bearing rocks. Chert, quartz veinlets and dolomite are the most common impurities. Calcite, pyrite, and talc (?) are typically present in trace amounts. The abundance and proportion of impurities change irregularly both along strike and across bedding.

Cherty dolomite (Unit D11) occupies the hangingwall of the magnesite deposits and locally forms parts of the footwall. The chert is generally dark grey to black and weathers either grey or beige. It forms either lenses (Plate 4-9-4) and layers 0.5 to 20 centimetres thick or angular clasts 0.5 to 2 centimetres across. Where interbedded with dolomite,

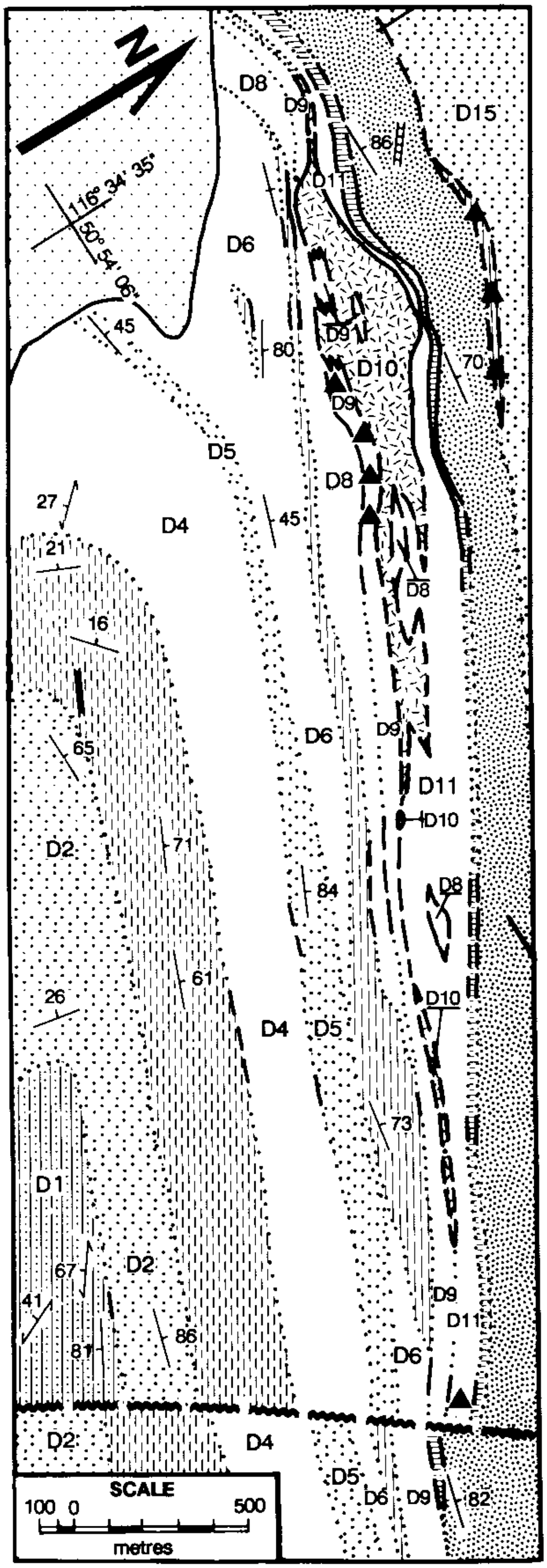

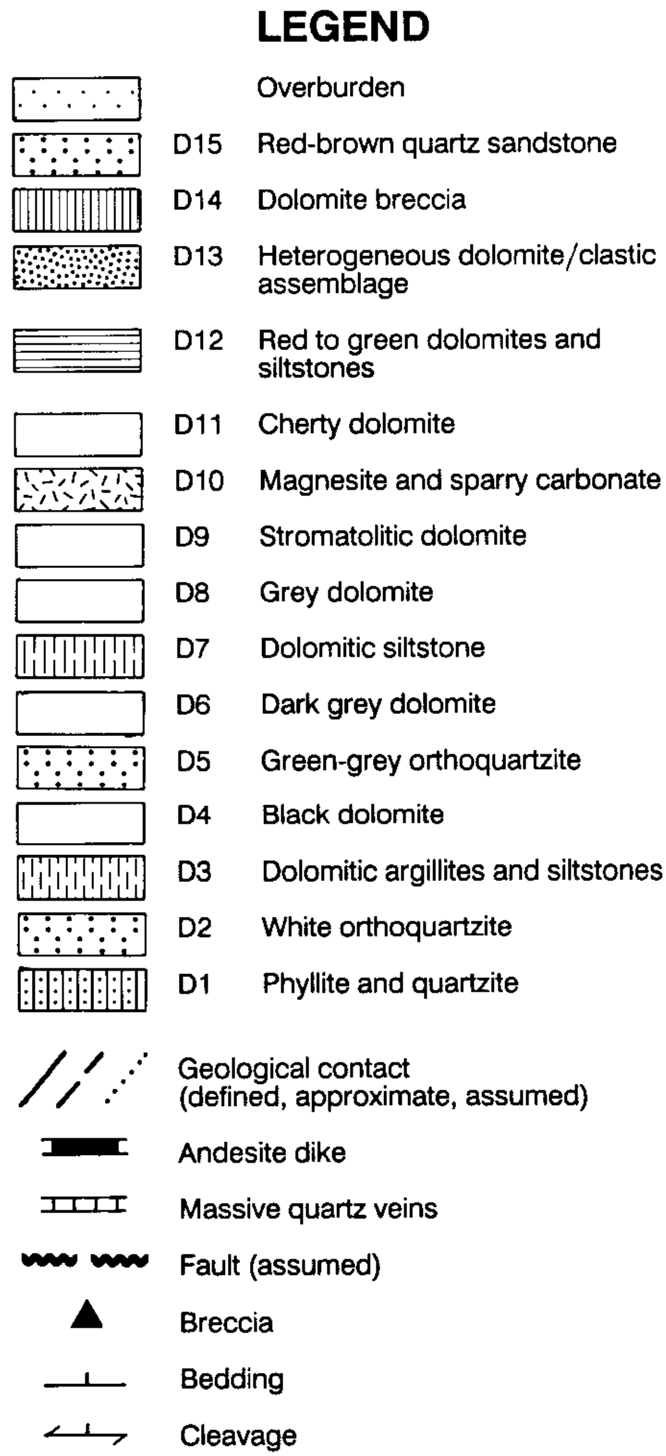

Figure 4-9-4. Geology of the Driftwood Creek deposit.

chert has distinctive positive relief on weathered surfaces. Dolomite is pale to medium grey and weathers beige, light grey or buff. It reacts strongly with hydrochloric acid if crushed.

Red to green dolomites and siltstones (Unit D12) overlie cherty dolomite. The fine-grained red to purple dolomites, minor limestones, silty dolomites, and dolomitic siltstones and shales are characterized by brown to red and pitted weathered surfaces (Plate 4-9-5). These rocks may be inter-

Plate 4-9-3. Sparry magnesite, granola-like texture; Driftwood Creek deposit.

Plate 4-9-4. Chert lenses interbedded with dolomites immediately overlying magnesite; Driftwood Creek deposit.

bedded on centimetre to decimetre scale. Dolomite pseudomorphs after halite are the most distinctive features. Shales and siltstones, and to some extent dolomites, change colour along strike from red-purple in the south to green in the north.

The heterogeneous dolomite-siltstone assemblage (Unit D13) consists of a wide variety of lithologies such as cherty dolomites, red to purple dolomites, dark grey massive dolomites and a variety of dolomitic siltstones either purple, brown or green in colour. Due to poor exposure, the correlation between these units on the map scale is impossible.

Dolomite breccia (Unit D14) consists of dolomitic chert and quartz arenite fragments in a matrix dark grey, fine-grained dolomite weathering grey. When powdered it reacts strongly with hydrochloric acid. In general the breccia is clast supported and polymictic, with fragments consisting of laminated or massive dark grey dolomite. Dark grey chert and white arenite fragments are angular and less than one centimetre in diameter. Over 75 per cent of dolomite fragments are also angular, but some of the clasts larger than 3 centimetres are subrounded. Both matrix and fragments are locally crosscut by fibrous quartz veinlets. Where the breccia is monomictic, the fragments consist exclusively of dolomite. This breccia is at least 25 metres thick.

Massive, white, grey or beige sandstone (Unit D15) weathers light shades of red-brown. Locally it contains silty, olive-coloured layers with well-developed, planar, paper-thin, spaced cleavage. Near the contact with the underlying dolomitic unit this rock consists of well-rounded quartz grains 0.25 to 0.5 millimetre in diameter. Outcrops higher in the sequence contain well-rounded quartz grains up to 6 millimetres in diameter and lithic clasts up to 2 centimetres across. In some outcrops quartz grains are at least partially recrystallized and the rock could be called quartzite. Regardless of size, the grains are, at least in part, cemented or stained by iron oxides and/or coated by clay. Quartz constitutes over 85 per cent of the rock, lithic fragments from 0 to 14 per cent, clays and iron oxides 1 per cent.

Based on the above information, the magnesite-bearing horizon (Unit D10) in the Driftwood Creek area probably corresponds to the white markers unit underlying the purple sequence of the Mount Nelson Formation (Figure 4-9-3).

Red Mountain Deposit

The Red Mountain deposit is located on Figures 4-9-1 and 2. The coarse to sparry magnesite-bearing zone outcrops near the top of Red Mountain. It was traced over 400 metres along strike and has an orientation of approximately 075° with a dip of 45° south. Thickness of the zone is variable and locally exceeds 20 metres.

Two stratigraphic sections were measured perpendicular to the strike near the easternmost limit of the deposit. Section A is correlated with section B along the twin conglomerate marker (Figure 4-9-5). Section B, which is not mineralized, is longer and will be described first. It includes the top of the Mount Nelson Formation and the base of the Toby Formation.

The base of the section consists of pale grey or beige quartzite which weathers beige, grey or white (Unit I). It is exposed for 51 metres. The coarser grained portion of this unit, 37 metres thick, appears at least partly recrystallized and is characterized by a blocky appearance. The longest fracture faces are perpendicular to the bedding. The quartzite consists of well-sorted, well-rounded quartz grains from 0.125 to 0.5 millimetre in diameter depending on individual beds. Other minerals observed in trace quantities are disseminated pyrite (1 mm, <0.5%), iron oxide stains and clays coating or cementing quartz grains (<0.5%).

The upper part of this unit consists mainly of beds, 0.5 metre thick, containing quartz grains varying from 0.125 to 0.75 millimetre in diameter. These beds are interbedded with fine-grained sandstone and siltstone beds from 2 to 20 centimetres thick with grain sizes of less than 0.125 millimetre. Other characteristics are similar to the basal portion of the unit.

A red to purple sequence of shales and siltstones (Unit II), identified on Figure 4-9-5b as red beds, overlies the quartzite. The grain size is typically less than 0.065 milli-

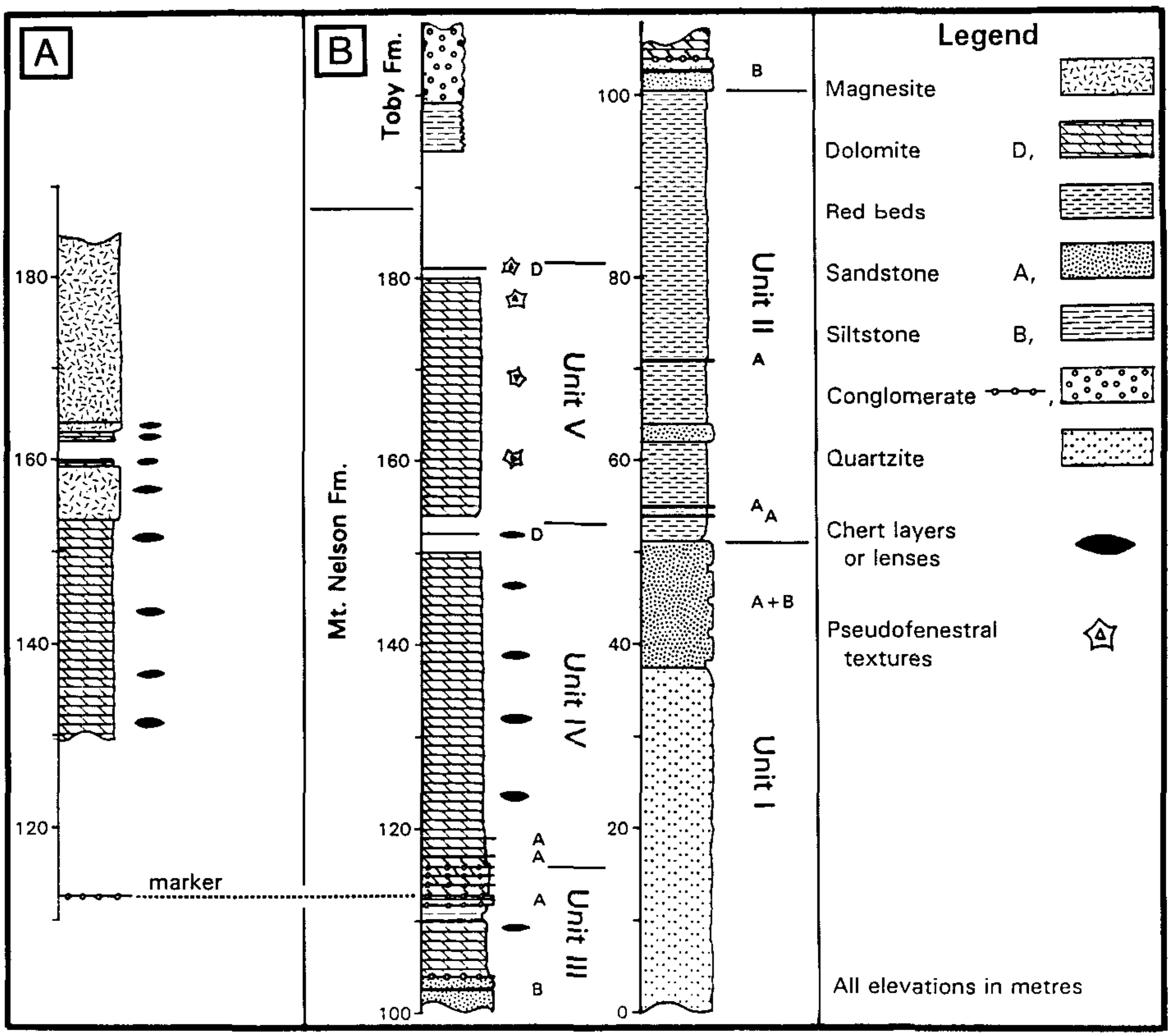

Figure 4-9-5. Stratigraphic setting of the Red Mountain deposit. Section A is magnesite-bearing equivalent of Section B.

metre. However, locally, rounded quartz grains up to 0.75 millimetre in diameter form layers less than 1 centimetre thick within the siltstones. The rock does not react with hydrochloric acid even if crushed. A few thicker and isolated quartzite beds are present within this unit. The first sign of a change from an oxidizing to a reducing environment appears at 87.5 metres above the base of the section, in the form of irregular green patches and lenses within the red-purple shales.

Unit III extends from 100.2 metres to 118.8 metres above the base of the section. It consists of a variety of sandstones, siltstones, conglomerates and minor argillite interbedded with dolomite.

Sandstone dominates the stratigraphic interval from 100.2 to 104.0 metres. The first continuous bed of green shale appears at 102.1 metres. This bed contains four dolomitic layers 1 centimetre thick marking the first appearance of dolomite in the section. Isolated angular clasts of white quartzite, measuring approximately 3 centimetres across, are observed within the dolomite at 104 metres. These clasts consist of arenite (99% quartz) with grain size of 0.125 millimetres.

Fine-grained green siltstone is exposed from 109.9 to 111.7 metres. It weathers light green. The grain size does

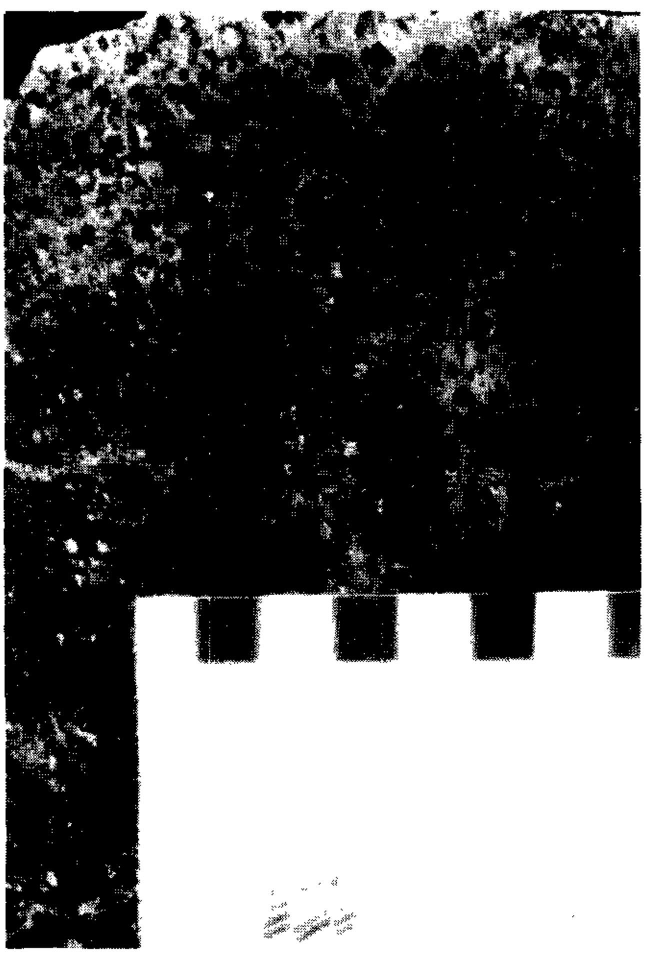

Plate 4-9-5. Weathered-out dolomite cast after halite; Driftwood Creek deposit.

not exceed 0.062 millimetre except for scattered feldspathic and lithic grains of up to 0.125 millimetre in diameter

A sequence of conglomerate and siltstone beds enclosed by dolomite overlies the fine-grained green siltstone. The conglomerates are matrix supported with angular to subrounded clasts ranging from 0.5 to 20 centimetres across. The clasts are quartz arenite with grain sizes of 0.25 to 0.5 millimetre. The matrix is a coarse, 0.25 to 1.0-millimetre quartz sand. Iron oxides and calcite stain or cement the matrix. A twin quartz-conglomerate marker, 1.1 metres thick, consists of two conglomerate beds separated by a thin green siltstone layer approximately 10 centimetres thick. The top of the twin conglomerate marker was used to relate sections A and B (Figure 4-9-5). Three other conglomerate beds, each about 10 centimetres thick, are present at 113.7, 114.8 and 115.9 metres.

Dolomite is present throughout this unit and contains minor, thin, green siltstone and sandstone layers. The dolomite is medium grey and weathers beige or pale grey. It reacts strongly with hydrochloric acid if crushed. Grain size varies from aphanitic to 0.062 millimeter. The first isolated lens of chert, less than 3 centimetres thick, appears at 107.6 metres.

The thick succession of cherty dolomite (Unit IV) starts at 118.8 metres and extends to 150 metres with one more metre exposed at 151.8 metres. The dolomite is medium to dark grey, fine grained to aphanitic and thickly bedded to laminated. Parallel ripple marks are preserved in some of the dolomite beds. Black chert forms interbeds and discontinuous, lobate lenses within the dolomite. Thickness of chert beds and lenses is from a few millimetres to a maximum of 20 centimetres.

Overburden covers the interval 152.8 to 154.0 metres. Distinctive pseudofenestral dolomite (Unit V) extends from 154.0 to 181.0 metres. This dolomite is grey on fresh surface and weathers white to light grey. It is fine grained and generally massive. The pseudofenestral texture is seen as very irregular, complexly shaped features commonly outlined by a thin, black or dark grey border with a core of white or medium grey dolomite or rarely calcite. Concentric layers of dolomite, in shades of grey, are present within some of these pseudofenestrae. Locally the pseudofenestrae have polygonal outlines and are interpreted as fillings within a dissolution breccia.

The Toby Formation is exposed from 94 metres to 208 metres. The lower 5.3 metres consists of brown-weathering, well-cleaved shale. On fresh surfaces the rock is dark to medium grey with grain size less than 0.062 millimetre. Calcite forms a thin coating on the planar cleavage. Scattered, discontinuous layers of dolomite, less than 2 centimetres thick, are present in the shale. They are grey, weather light buff and have a slight positive relief above the surrounding shale.

Above the brown shale to the top of the exposure is a polymictic conglomerate, typical of the Toby Formation. The conglomerate is matrix supported. The clasts form 40 per cent of the rock, range from 1 to 20 centimetres in diameter and are subangular to rounded. Clasts consist of fragments of rocks from the underlying Mount Nelson Formation. They consist of black chert, pseudofenestral dolomite and grey dolomite together with green, grey and white quartz arenite. Magnesite clasts were were not observed. The matrix is the same as the underlying shale. Cleavage is developed exclusively in the matrix.

Comparison between Sections A and B clearly indicates that cherty dolomite and pseudofenestral dolomite are host-rocks and stratigraphic equivalents of the magnesite. This relationship is further supported by the preservation of the cherty layers and lenses within the sparry magnesite-bearing rock. The footwall contact between sparry magnesite and cherty dolomite is irregular. Carbonate pseudomomorphs after lenticular gypsum crystals are present within the dolomite near this contact. The lateral lithological change between sparry magnesite and cherty and pseudofenestral dolomite is not exposed.

Magnesite-bearing rock is sparry and light grey on fresh surface. It is characterized by a knobby, rough, buff-coloured weathered surface. When crushed, the rock reacts moderately with hydrochloric acid. Grain size varies from 0.1 millimetre to 2 centimetres. The rock consists mainly of magnesite. Typical impurities are dolomite (1-25%), calcite, rusty stains along fractures and occasional shaly layers. Near contacts with dolomite, magnesite-bearing rock contains layers of black chert 1 to 15 centimetres thick which form up to 30 per cent of the rock. The chemical composition of the rock is given in Table 4-9-1.

The Red Mountain deposit overlies the purple and green shales of the Mount Nelson Formation (Figure 4-9-5), indicating that it is located higher in the stratigraphy than the Driftwood Creek deposit.

Plate 4-9-6. Pseudofenestral features. Open spaces filled be white dolomite separated from the host dolomite by dark gray rims. Topaz Lake deposit.

Topaz Lake Deposit

This magnesite deposit, located south of Topaz Lake, was staked in 1960 and 61 and consists of several showings

TABLE 4-9-1
CHEMICAL COMPOSITION OF THE MAGNESITE-BEARING ROCKS OF THE BRISCO AND DRIFTWOOD CREEK AREAS

DEPOSIT	MgO	CaO	SiO_2	Fe_2O_3	Fe (Total)	Al_2O_3	CO_2
Red Mountain	39.50	0.76	14.72	0.88	-	-	43.40
Topaz Lake	42.79	1.04	6.48	0.87	-	-	46.72
	43.34	0.51	5.54	1.02	-	-	47.60
	44.85	0.73	3.47	0.95	-	-	49.20
Cleland Lake	38.20	7.89	4.51	1.00	-	-	47.74
Jab	44.02	0.47	8.99	0.99	-	-	43.82
Botts Lake	35.97	8.57	8.69	0.12	-	-	46.02
Dunbar Creek	41.41	2.84	3.97	2.07	-	-	47.48
	42.28	2.67	3.22	1.03	-	-	48.28
Driftwood Creek	42.50	4.20	2.50	-	0.77	0.06	-
	40.00	6.00	4.60	-	0.82	0.13	-

(McCammon, 1964; Grant 1987). The largest is exposed over an area of 38 800 square metres (Figure 4-9-6). The contact between magnesite-bearing rock and the footwall is irregular and subhorizontal. Drilling indicates a thickness of magnesite of up to 30 metres (Grant, 1987). The footwall of the deposit, where exposed, consists of dark grey to black, fine-grained dolomite. When powdered, this dolomite effervesces strongly on contact with hydrochloric acid. It commonly displays spectacular pseudofenestral textures (Plate 4-9-6). However, drilling indicated that outcropping magnesite is underlain by cherty dolomite (Grant, 1987), suggesting that the footwall contact is discordant.

Sparry magnesite-bearing rock is white to light grey and weathers beige. Crystal size varies from 1 to 20 millimetres. Observed impurities are dolomite (0-20%), calcite veinlets and fracture fillings (<5%), disseminated pyrite (<0.5 mm, trace) and quartz grain aggregates (1-2 cm, <1%). It reacts weakly or not at all with hydrochloric acid even if crushed. However, near the contact with fine-grained dolomite, powdered sparry carbonate reacts moderately with acid when crushed, indicating a substantial dolomite component. These sparry zones with lower magnesite content are identified on Figure 4-9-6 as a distinct unit. The chemical composition of the magnesite-bearing rock from the main showing is given in Table 4-9-1. Smaller magnesite occurrences nearby are described by Grant (1987).

Based solely on textural and lithologic similarities, both the Cleland Lake and Red Mountain deposits are tentatively interpreted as part of the same magnesite horizon.

Cleland Lake Deposit

This magnesite deposit is exposed along a low ridge at the south end of Cleland Lake (Figure 4-9-7). The minimum thickness of the magnesite zone is 20 metres (Figure 4-9-8). Most of the sparry magnesite rock is coarse grained and, when crushed, reacts moderately with hydrochloric acid. It is beige to pale grey and weathers buff. It consists of magnesite (1-5 mm, 60-95%), sparry dolomite (1-10 mm, 3-40%), local silica concentrations in the form of veinlets and sandy layers (<5%) and disseminated pyrite (<2 mm, <0.5%). Composition of the magnesite-bearing rock is given in Table 4-9-1. Some sparry carbonate zones have a high dolomitic component and are referred to as sparry carbonate (Figure 4-9-7). Near the contact of magnesite with overlying red or grey fine-grained dolomite, the magnesite zone is fine grained and layered.

Fine-grained, pale grey dolomite is a stratigraphic equivalent of the sparry magnesite in the southern part of the study area.

The hangingwall consists of a thin layer of pale to dark grey, fine-grained carbonate, which is in turn overlain by a thick sequence of red to purple dolomites and dolomitic siltstones (Figure 4-9-8). These purple rocks contain abundant dolomite casts after halite and dolomite-replaced halite hopper crystals. They are reduced in the northwestern part of the map area, where their colour changes to green and they contain pyrite crystals up to 1 centimetre in size.

Disseminated fine-grained sphalerite, bornite and an unidentified opaque mineral were observed approximately

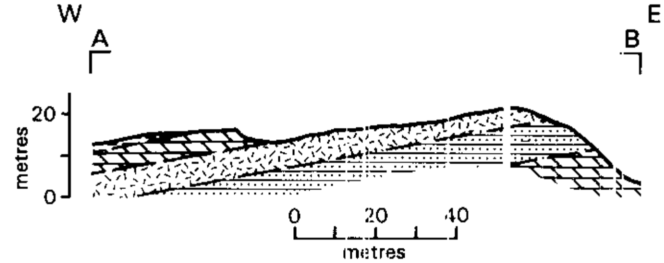

Figure 4-9-8. Cleland Lake deposit; vertical cross-section; for location and legend see Figure 4-9-7.

620 metres southeast of the magnesite showing. This metalliferous mineralization is hosted by silicified, light grey dolomite which is believed to be the stratigraphic equivalent of the magnesite horizon.

Based on the lithologic succession: magnesite and red silty dolomite containing halite hopper crystals, the Cleland Lake deposit is probably hosted by the stratigraphic equivalent of the white markers unit described by Pope (1989) which underlies the purple sequence (Figure 4-9-3).

Jab Deposit

Staked in 1961, the Jab deposit is the oldest known magnesite showing in the Brisco area. Magnesite-bearing rocks form a knoll about 130 metres long, up to 55 metres wide and up to 20 metres high (Figures 4-9-9 and 10). The magnesite-bearing rock is white on fresh surfaces and weathers beige. It is sparry, however, the size of magnesite crystals diminishes progressively from several centimetres in the north to finer and sugary (1-3 mm) in the south part of the knob. Most of the primary sedimentary features of the protolith were destroyed during recrystallization, however relicts of hemispherical, laterally linked stromatolites are preserved in two fine-grained outcrops. In the southern part of the knoll, magnesite layers 2 to 5 centimetres thick are separated by vestiges of thin (<5 mm) silty beds now partially transformed to talc or serpentine.

Visual examination indicates that magnesite-bearing rock consists mainly of magnesite (>85%). Impurities are dolomite (<10%), disseminated pyrite (trace) and vestiges of the talc or serpentinized green silt layers (0-5%). Silica veinlets and quartz crystals (0-3%) are less abundant than in other deposits of the Brisco area.

The magnesite-bearing knoll (Figure 4-9-9) is isolated and none of the nearby trenches reached bedrock. The knoll was bulk sampled and drilled. A drill hole over 80 metres deep terminated in magnesite (McCammon, 1962). The orientation of the borehole is not known. Although the overburden in the area appears to be thick, this deposit warrants further exploration and testing. The interpretation of structural measurements taken on the vestiges of bedding planes suggests that the magnesite knoll is part of a larger fold structure plunging 16° towards 324°.

The lack of outcrops in the immediate area of the deposit precludes stratigraphic correlation, however stromatolitic textures and green centimetre-scale layers of sedimentary origin were also observed in magnesite-bearing rocks of the

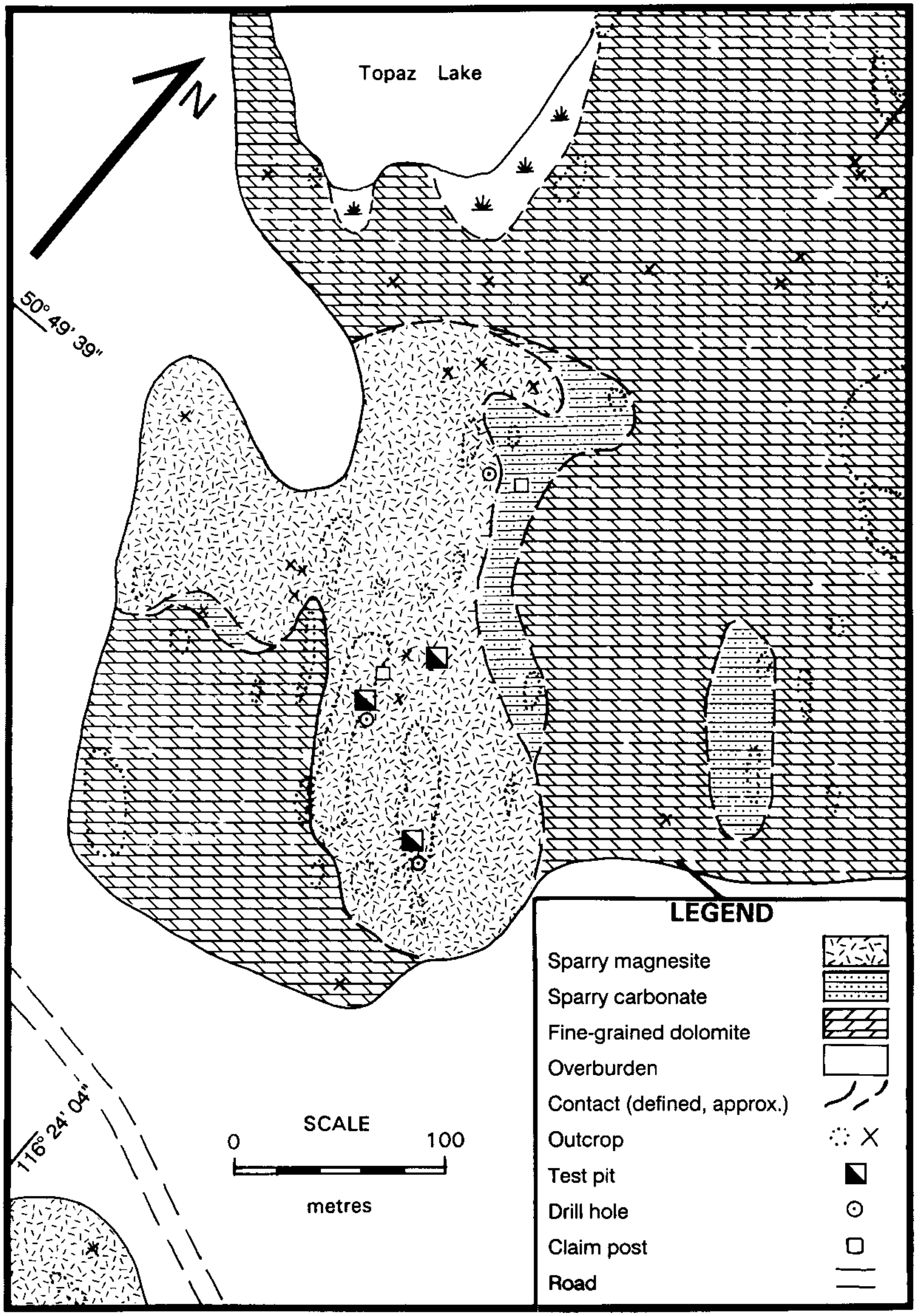

Figure 4-9-6. Geology of the Topaz Lake deposit.

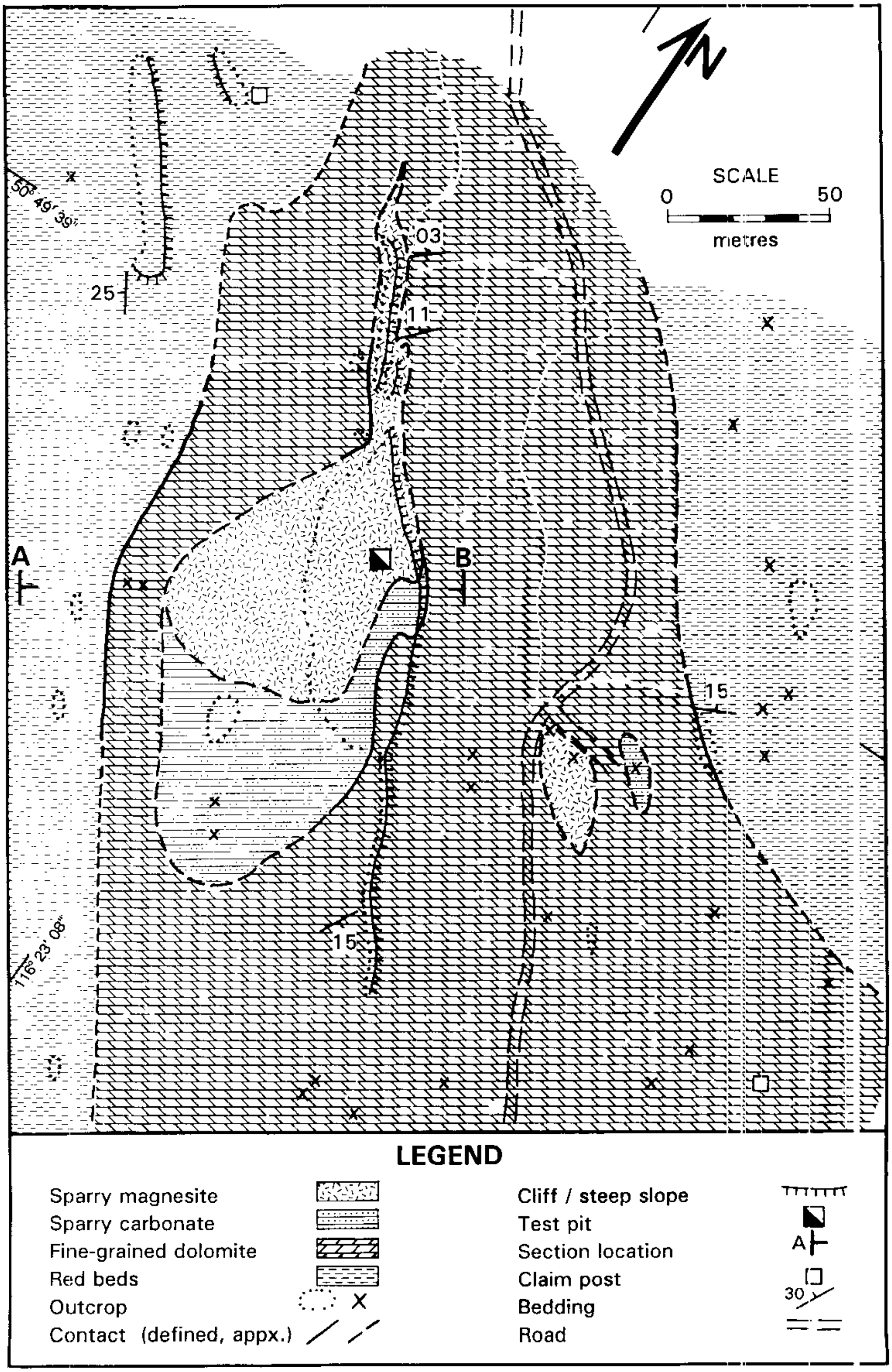

Figure 4-9-7. Geology of the Cleland Lake deposit.

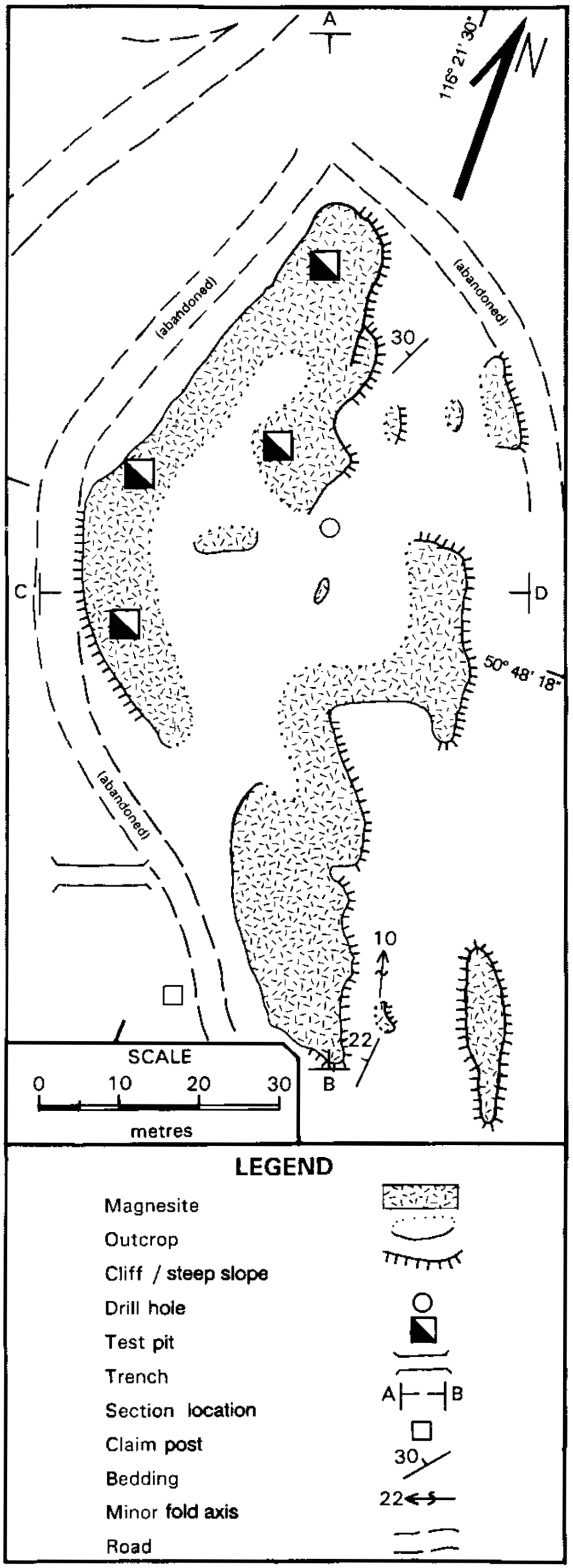

Figure 4-9-9. Geology of the Jab deposit.

Driftwood Creek deposit. These similarities suggest that the Jab and Driftwood Creek deposits may be part of the same stratigraphic horizon.

Dunbar Creek Deposit

The Dunbar Creek showings are hosted by a sequence of stromatolitic and cherty dolomites. Most of the showings have irregular shape and variable grade. They are described by McCammon (1964). When crushed, the magnesite-bearing rock reacts moderately to poorly with hydrochloric acid. Magnesite content varies from 50 to 90 per cent. Impurities are dolomite (5-30%), calcite veinlets and fracture fillings (0-5%), disseminated pyrite (trace), cherty layers over 1 centimetre thick (0-15%) and disturbed veinlets of quartz less than 5 centimetres wide (0-1%). A thick stromatolitic sequence underlies the deposit and cherty layers are abundant in adjacent dolomite. It is possible that the Dunbar deposit lies on the same stratigraphic horizon as the Driftwood Creek deposit, which is tentatively interpreted as the equivalent of the white markers unit (Figure 4-9-3).

Botts Lake Deposit

The Botts Lake deposit is located on Figures 4-9-1 and 2. Magnesite outcrops were traced over a distance of 118 metres along strike. A magnesite-bearing unit is at least 10 metres thick (Figure 4-9-11), strikes 130° and dips 47° east. The footwall consists of hard, aphanitic to fine-grained, dark grey to black dolomite which weathers pale grey. When crushed, this dolomite reacts moderately to strongly with hydrochloric acid. It appears massive on fresh surfaces, however, careful examination of the weathered surface reveals submillimetre-scale laminations. It is cut by pale grey dolomite and milky white quartz veinlets (<5 mm thick).

Light to medium grey dolomite which weathers pale fawn in colour overlies the dark dolomite. It fractures along irregular, lumpy surfaces. It does not react with hydrochloric acid unless crushed and is cut by hairline fractures containing clay and/or calcite.

Pale grey dolomite, which possibly contains minor amounts of magnesite, may represent the transition between dolomite and the magnesite-bearing horizon. If crushed it reacts moderately with acid. The rock appears massive on the fresh surface, however, suggestions of diffuse 3 to 5-millimetre layers are seen on the weathered surfaces. Grain size does not exceed 0.5 millimetre.

The magnesite-bearing rock is snow white and weathers white or light grey. Crushed rock will effervesce moderately to poorly when in contact with hydrochloric acid. The rock appears textureless on fresh surfaces. Laboratory work is required to identify the origin of local, irregular, "sponge-like" shapes revealed by differential weathering. Field estimates indicate that the rock consists of a mixture of dolomite (40 to 70%) and magnesite (30 to 60%) and is expected to have a lower magnesia content than other magnesite deposits of the Brisco area. Traces of enargite (Cu_3AsS_4) were found in hairline fractures within this horizon.

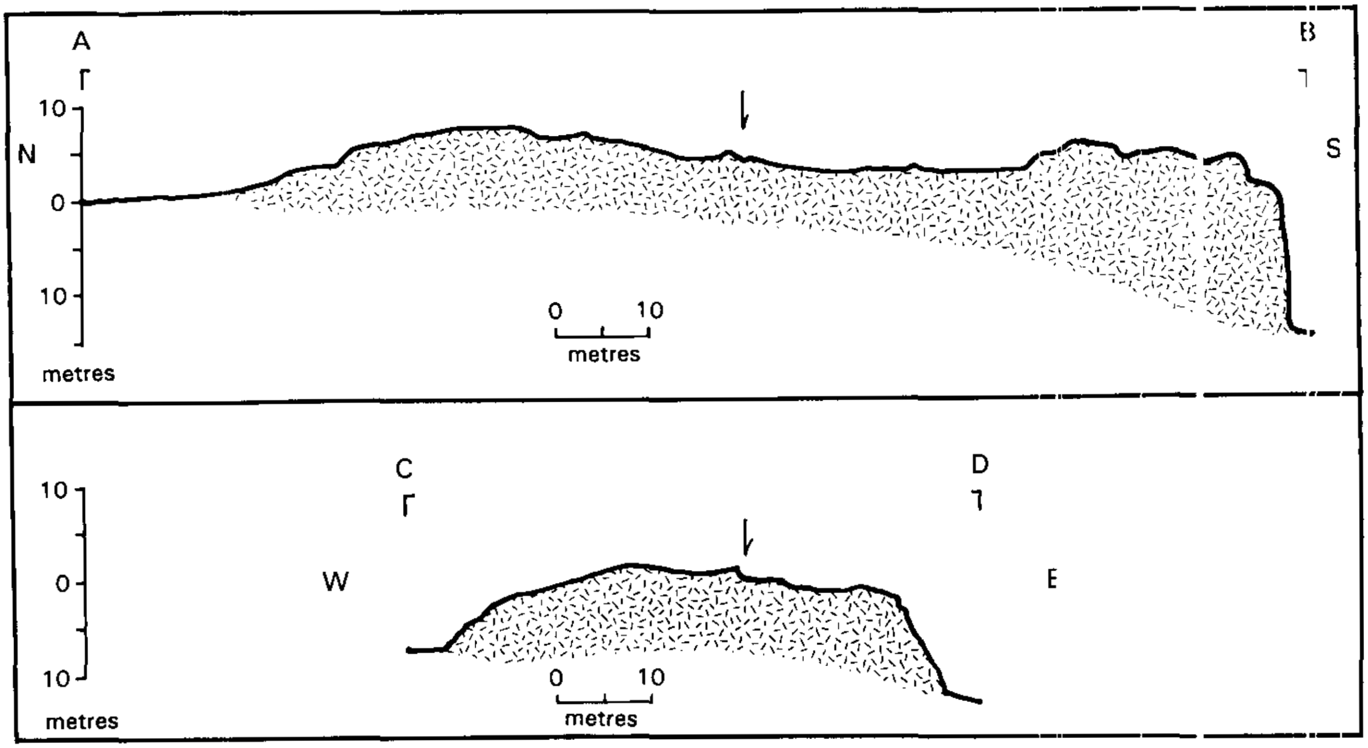

Figure 4-9-10. Vertical sections across the Jab deposit; *see* Figure 4-9-9 for location and legend.

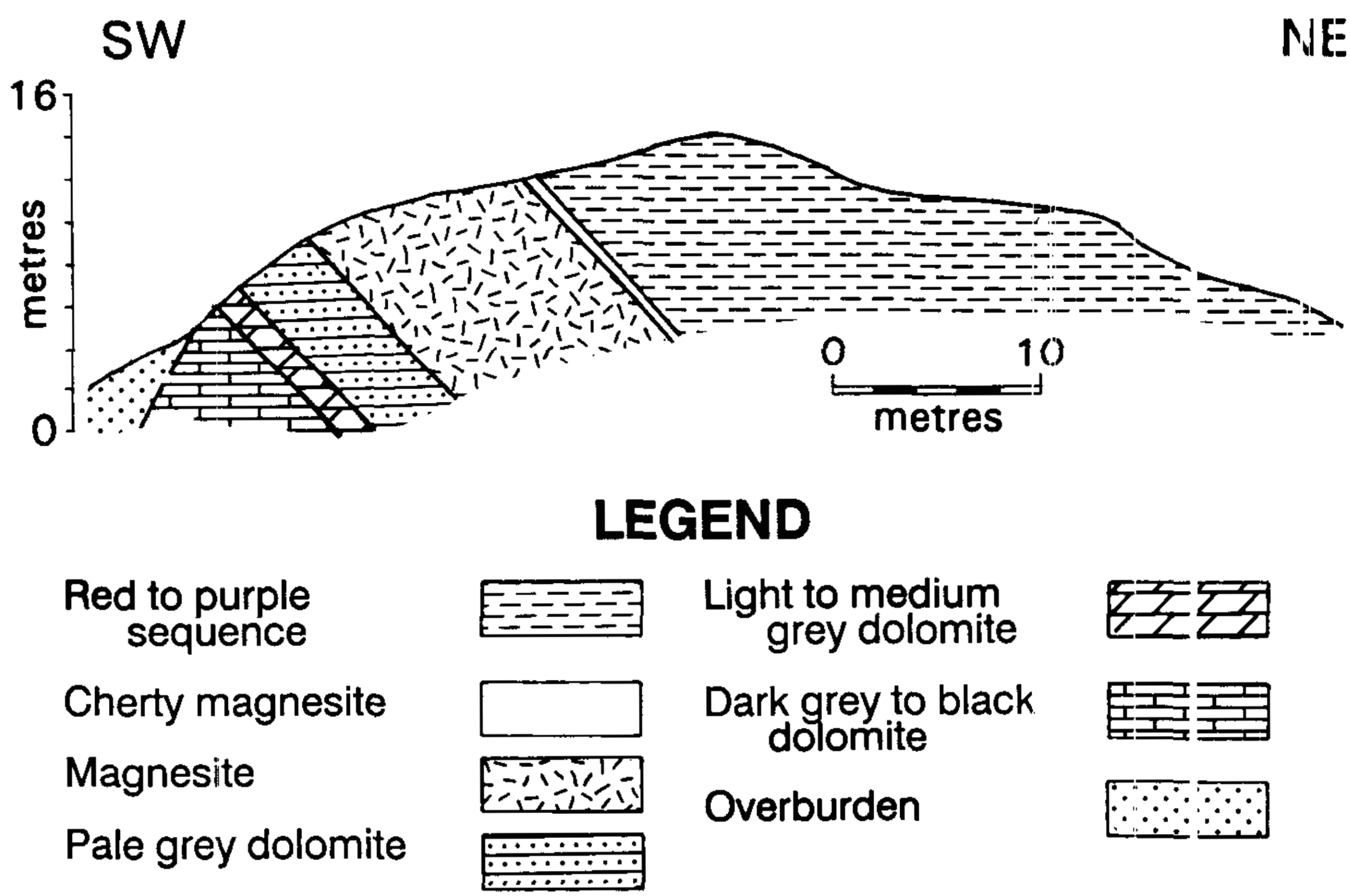

Figure 4-9-11. Geology of the Botts Lake deposit.

Chert is exposed in the hangingwall of the magnesite-bearing unit (Figure 4-9-11). The thickness of this horizon appears to increase along strike to the south.

Red to purple silty dolomite and dolomitic argillite overly the chert-bearing horizon. These rocks are characterized by a red to rusty brown, locally pitted, weathered surface, halite casts and intraformational breccias. Locally, red argillite contains ellipsoid-shaped reduction features usually less than 5 centimetres along the longest axis. Based on the relative position of the lithologic units, magnesite and red-purple dolomite containing halite pseudomorphs, it is suggested that the Botts Lake showing corresponds stratigraphicaly to the white markers unit (Figure 4-9-3).

Other Magnesite Deposits

Two magnesite showings reported in the Invermere area (Pope, 1989, 1990), are located on Figure 4-9-2. They consist of impure magnesite and are less than 1 metre thick. They are hosted by the white markers unit (Figure 4-9-3) in the upper part of the Mount Nelson Formation (Pope, 1990).

SUMMARY AND DISCUSSION

All the magnesite deposits in the Brisco and Driftwood Creek areas are dolomite hosted and stratabound. They are located within the upper half of the Mount Nelson Formation. Most are lenticular and seem to form chains as illustrated by the Driftwood Creek example (Figure 4-9-4).

All deposits are stratigraphically associated with red to purple dolomites, cherty dolomites (Plate 4-9-4), stromatolitic dolomites (Plate 4-9-1), dissolution breccias (Plate 4-9-2) and other rocks containing dolomite pseudomorphs after halite (Plate 4-9-5) and lenticular gypsum crystals. Locally, stromatolitic textures are preserved, even within magnesite-bearing rocks. Most of the above features are indicative of the evaporitic depositional environment.

Origin

The current working hypothesis for the origin of the magnesite deposits in the Brisco and Driftwood Creek areas is based mainly on the field evidence indicating an evaporitic depositional environment and published information concerning magnesite genesis. The link between the evaporitic environment and magnesite in the Brisco area was first suggested by Bennett (1985).

Although magnesite can not precipitate directly from aqueous solutions under normal near-surface conditions (Lippman, 1973), magnesium hydrates or hydroxyhydrates commonly form in evaporitic environments (Morse and Mackenzie, 1990). The Brisco and Driftwood Creek deposits may have formed by recrystallization of such magnesite precursors, or by cyanobacterial magnesite precipitation in evaporitic basins or lakes having high Ph (8.5-10). The biomineralization of magnesite by cyanobacteria was documented on the laboratory scale by Thompson and Ferris (1990). The presence of magnesite is well documented in modern marine environments for example in Coorong Lakes, South Australia (Warren, 1990) and Sebkha El Melah, Tunisia (Perthuisot, 1980). The evaporitic model was proposed on many occasions in the past to explain the origin of ancient sediment-hosted magnesite deposits. Unfortunately in most cases the analogy was not convincingly documented or the concept was misused. In this case metalliferous minerals would represent an overprint.

Two alternative hypotheses for the formation of the magnesite deposits in the Brisco and Driftwood Creek area should not be discounted before completion of ongoing laboratory studies. They are: (a) formation of magnesite by replacement of dolomite, as proposed for the Mount Brussilof magnesite deposit (Simandl and Hancock, 1991), and (b) formation of magnesite by the inflow of hydrothermal fluids into closed basins as previously proposed for some Yugoslavian deposits (Fallick *et al.*, 1991).

Replacement of dolomite by magnesite can not be prematurely ruled out in the study area. Evaporitic rocks are easier to dissolve than carbonates. Preferential dissolution of evaporitic rock may result in the development of karst features and extensive zones of dissolution breccia along evaporitic horizons. Late diagenetic or hydrothermal fluids similar to those forming Mississippi Valley-type base metal deposits could move preferentially through these highly permeable zones, replacing fine-grained dolomite and evaporitic minerals by sparry magnesite and dolomite, overprinting primary evaporitic textures.

Magnesite deposits of hydrothermal exhalative origin are described in Yugoslavia. These deposits are fine-grained magnesite-dolomite beds and lenses hosted by Miocene lacustrine sediments related to silicic volcanism (Fallick *et al.*, 1991). The hydrothermal model is a viable hypothesis for magnesite deposition in the Brisco area because syn-rift vesicular andesites containing clasts from the Mount Nelson Formation documented along the unconformity separating the Mount Nelson and Toby formations (Reesor, 1973; Bennett, 1985; Pope, 1989). Furthermore the origin of the chert associated with the magnesite deposits is not yet established. Chert may be evaporitic with or without a hydrothermal component.

Exploration Implications

Regardless of the origin of the fluids involved in magnesite genesis (evaporitic, diagenetic or hydrothermal), the carbonates of the Mount Nelson Formation represent a favourable exploration environment for Brisco-type deposits, particularly stratigraphic equivalents of chert-bearing rocks adjacent to red or purple-colored dolomites and dolomitic siltstones with dolomite pseudomorphs after halite.

The Toby conglomerate is a well-documented marker that can be used by prospectors to delimit the Mount Nelson Formation which hosts all known magnesite occurrences in the area (Figure 4-9-2).

Two magnesite showings reported in the Invermere area are also hosted by the white markers sequence of the upper Mount Nelson Formation (Pope, 1990), indicating that the formation is prospective for magnesite at least from Invermere to Driftwood Creek.

Laboratory studies are in progress to test the previously described hypothesis concerning the origin of magnesite deposits in the Brisco and Driftwood Creek areas. A deposit model is required to identify the areas with highest exploration potential.

The occurrence of enargite within magnesite-bearing rock at Botts Lake showing, and of sphalerite and bornite near the Cleland Lake magnesite showing may represent a post-magnesite hydrothermal overprint. However, a possible genetic link with magnesite mineralization should not be discounted. Enargite, sphalerite and bornite are reported in association with a wide variety of geological environments including exhalative hydrothermal deposits (Guilbert and Park, 1985) and Mississippi Valley-type base metal deposits (Hagni, 1976; Vos *et al.*, 1989). The possible metallogenic significance of these new base metal showings should not be overlooked.

ECONOMIC POTENTIAL

Field investigations indicate that several of the magnesite deposits in the Brisco and Driftwood Creek areas have grades similar to deposits currently mined in Europe, however, their silica content is higher than that of the famous Mount Brussilof deposit.

Magnesite-bearing rocks in the Brisco – Driftwood Creek area have simple mineralogy and coarse textures, suggesting that they may be either upgraded by traditional concentrating methods or used as source material for products not requiring high-purity feed.

Furthermore, as illustrated by the Driftwood Creek example, concentration of impurities such as quartz and chert varies substantially along strike, indicating that extensions of other known deposits may have higher grades than outcropping portions. Most of the deposits are open either along strike or to depth.

Laboratory tests will contribute significantly to determining the possible applications for magnesite from these deposits.

ACKNOWLEDGMENTS

Enriching discussions with Dr. S.Paradis of the Geological Survey of Canada and Dr. A. Panteleyev from the British Columbia Ministry of Energy, Mines and Petroleum Resources are acknowledged. Enargite, sphalerite and bornite were positively identified by Dr. M. Chaudhry of the British Columbia Ministry of Energy, Mines and Petroleum Resources using x-ray diffraction. Mr. J.M. Newell, Dr. D.V. Lefebure, Ms. P. Kelly and Mr. Z.D. Hora of the British Columbia Ministry of Energy, Mines and Petroleum Resources kindly edited this manuscript.

REFERENCES

Bennett, S.M.H. (1985): Tectonics, Sedimentation and Mineralization on the East Flank of the Purcell Anticlinorium, Southeast British Columbia, Canada; unpublished Ph.D. thesis, *University of London*, 461 pages.

Fallick, A.E., Ilich, M. and Russell, M. (1991): A Stable Isotope Study of the Magnesite Deposits Associated with the Alpine-type Ultramafic Rocks of Yugoslavia; *Economic Geology*, Volume 86, pages 847-861.

Grant, B. (1987): Magnesite, Brucite and Hydromagnesite Occurrences in British Columbia; *B.C. Ministry of Energy, Mines and Petroleum Resources*, Open File 1987-13, 68 pages.

Guilbert, M.J. and Park, C.F. Jr. (1985): The Geology of Ore Deposits; *W.H. Freeman and Company*, New York, 985 pages.

Hora, Z.D. (1983): Magnesite – Driftwood Creek Area; *in* Geological Fieldwork 1983, *B.C. Ministry of Energy, Mines and Petroleum Resources*, Paper 1984-1, pages 213-214.

Hagni, R.D. (1976): Tri-State Ore Deposits: The Character of their Host Rocks and their Genesis; *in* Handbook of Strata-bound and Stratiform Ore Deposits, Volume 6, Wolf, K.H., Editor, *Elsevier Scientific Publishing Company*, Amsterdam, 585 pages.

Lippman, F. (1973): Sedimentary Carbonate Minerals; *Springer-Verlag*, New York, 228 pages.

McCammon, J.W. (1962): untitled map; *B.C. Ministry of Energy, Mines and Petroleum Resources* Property File map 082K-NE-014.

McCammon, J.W. (1965): The Brisco Magnesite Area; *B.C. Ministry of Energy, Mines and Petroleum Resources;* Annual Report 1964, pages 194-199.

Morse, J.W. and Mackenzie, F.T. (1990): Geochemistry of Sedimentary Carbonates; Developments in Sedimentology, Volume 48, *Elsevier*, 707 pages.

Morris, R.J. (1978): Fish Magnesite Deposit; *B.C. Ministry of Energy, Mines and Petroleum Resources*, Assessment Report 8760.

Perthuisot, J.P. (1980): Sebkha El Melah near Zarzis: A Recent Paralic Salt Basin (Tunisia); *in* Evaporite Deposits, *Editions Technip*, Paris, pages 12-17.

Pope, A.J. (1989): The Tectonics and Mineralization of the Toby – Horsethief Creek Area, Purcell Mountains, Southeast British Columbia, Canada; unpublished Ph.D. thesis, *University of London*, 350 pages.

Pope, A.J. (1990): The Geology and Mineral Deposits of the Toby – Horsethief Creek Map Area, Northern Purcell Mountains, Southeastern British Columbia; *B.C. Ministry of Energy, Mines and Petroleum Resources*, Open File 1990-26, 54 pages.

Reesor, J.E. (1973): Geology of the Lardeau Map Area, Purcell Mountains, Southeastern British Columbia; *Geological Survey of Canada*, Memoir 369, 118 pages.

Simandl, G.J. and Hancock K.D. (1991): Geology of the Mount Brussilof Magnesite Deposit, Southeastern British Columbia; *in* Geological Fieldwork 1990, *B.C. Ministry of Energy, Mines and Petroleum Resources*, Paper 1991-1, pages 269-278.

Thompson, J.B. and Ferris, F.G. (1990): Cyanobacterial Precipitation of Gypsum, Calcite, and Magnesite from Natural Alkaline Lake Water; *Geology*, Volume 18, pages 995-998.

Vos, R.L., Hagni, R.D. and Gregg, J.M. (1989): Sequential Deposition of Zoned Dolomite and its Relationship to Sulfide Mineral Paragenetic Sequence in the Viburnum Trend, Southeast Missouri; *Carbonates and Evaporites*, Volume 5, pages 195-209.

Walker, J.F. (1926): Geology and Mineral Deposits of the Windermere Map-area, British Columbia; *Geological Survey of Canada*, Memoir 148.

Warren J.K. (1990): Sedimentology and Mineralogy of Dolomitic Coorong Lakes, South Australia; *Journal of Sedimentary Petrology*, Volume 60, pages 843-858.

DETECTION AND MAPPING OF REGIONAL-SCALE LINEAMENTS USING NOAA AVHRR SATELLITE IMAGERY

By Karl Kliparchuk and Peter von Gaza
Advanced Satellite Productions, Inc.

KEYWORDS: Regional geology, satellite imagery, regional-scale lineaments, remote sensing.

INTRODUCTION

Satellite remote sensing technology has played an increasingly large role in the search for mineral resources over the past two decades (*e.g.*, Goetz *et al.*, 1983). This has been primarily through the use of Landsat Multispectral Scanner (MSS) imagery and, more recently, Landsat Thematic Mapper (TM) imagery. The MSS scans in four spectral regions with a ground resolution of 80 metres, whereas the TM scans in seven spectral regions and has 30-metre ground resolution. These two types of imagery have provided geologists with a valuable tool for investigating surface materials and lineaments. Many studies have shown that though satellite data is generally not successful at locating specific targets for mineral exploration, it is a valuable reconnaissance tool and in many cases is an invaluable aid in more detailed investigations.

Most of the investigations of satellite imagery for mineral exploration to date, especially in areas covered by dense vegetation, have focused on techniques for identifying lineaments. Geologists have realized for some time that many mining districts and individual ore deposits occur along or near linear trends. These faults and fractures may represent conduits through which hydrothermal fluids migrated, and therefore control the spatial distribution of potential ore deposits. Contemporary mineral exploration geologists spend a considerable amount of time and funds seeking and developing techniques for identifying lineaments. The ability to view extensive areas using Landsat imagery has provided geologists with a useful technique for mapping potential fracture and fault patterns, especially in areas where very little is known about the geological environment.

Current trends in mineral exploration in British Columbia, especially in reconnaissance studies, indicate that the recognition of structural zones is, in many cases, a prime objective. This is due in part to the fact that the province is heavily vegetated and the clearly visible alteration patterns associated with deposits in more arid regions are not easily recognized.

The use of lineament mapping from the Landsat imagery for mineral exploration is well documented, although examples from British Columbia were not located. A recent study by Mortensen and von Gaza (in press) which used TM thermal-band data for regional analysis of lineaments in the Klondike district, Yukon, demonstrated that significant, but previously unrecognized structural patterns could be identified and should influence exploration models in the region. Another paper by von Gaza (1988b) demonstrated the value of TM data for mapping lineaments in the Wheaton River district, Yukon.

Standard investigations involving Landsat imagery generally centre on areas less than 100 by 100 kilometres. Most recent studies have focused on using TM data at scales up to 1:50 000. The use of Landsat Thematic Mapper or Multispectral Scanner data would be cumbersome and extremely expensive if applied to a province wide study. It would take approximately 50 to 60 Landsat scenes to compose a mosaic of the province. Alternatively, satellite data from the National Oceanic and Atmospheric Administration's Advanced Very High Resolution Radiometer (AVHRR) is relatively inexpensive and a single scene covers an extensive area (*e.g.*, total imagery cost was approximately $350 for this study). To date, no documentation of attempts to map regional lineaments with AVHRR imagery has been located.

OBJECTIVES

The purpose of this study is to investigate the potential use of AVHRR data as a tool for mapping regional-scale lineaments in British Columbia. The general objectives of this research are to determine:

- If remotely sensed satellite imagery with coarse spatial resolution (*e.g.*, 1 kilometre by 1 kilometre) is valuable in mapping regional-scale lineaments.
- The extent of correspondence between the detected lineaments and the major tectonic features in British Columbia.
- If previously unmapped major lineaments can be identified and whether these lineaments potentially add to the structural knowledge of British Columbia.

STUDY AREA

The study area for this research consisted of the entire province of British Columbia. The Canadian Cordillera within British Columbia comprises five tectonostratigraphic regions (Insular Belt, Coast Belt, Intermontane Belt, Omineca Belt and Foreland Belt) that broadly correspond to the physiographic subdivisions (Western System, Cascade Mountains, Interior System and Eastern System).

The Foreland and Omineca belts are separated by the Rocky Mountain Trench. This is one of the three trenches occurring in the Canadian Cordillera, with the others being the Tintina and Shakwak trenches in the Yukon. The Rocky Mountain Trench extends from Flathead Lake nearly 200 kilometres south of the International Boundary, northwestwards for 1600 kilometres, until it disappears in the Liard Plain. The Tintina Trench begins 300 kilometres northwest of the Liard River and extends for 725 kilometres before entering Alaska. Strong structural control is suggested by the linearity of the features and the occasional displacement in their alignment. Some researchers have theorized that the Rocky Mountain Trench began as a series of Tertiary faults that developed into graben. The graben were expanded and preserved as a continuous valley by stream erosion (Bird, 1980).

DATA

Designed to assist in weather prediction and monitoring, meteorological satellites employ sensors which have a very coarse spatial resolution compared to land-oriented satellites. The trade-off of coarse spatial resolution is highly repetitive coverage. The passive sensors aboard the satellites collect reflected and emitted electromagnetic energy from the earth's surface and atmosphere.

The National Oceanic and Atmospheric Administration (NOAA) series of meteorological satellite data was used in this study. Several generations of NOAA satellites have been launched. The NOAA-6 through NOAA-12 missions contain the Advanced Very High Resolution Radiometer (AVHRR). The swath width of the AVHRR instrument is 2400 kilometres with a ground resolution of 1.1 kilometres at nadir. To provide the global coverage, the satellite orbits the earth at an altitude of 833 kilometres. The system daily provides one image in the visible portion of the spectrum and two images in the infrared portions of the spectrum. One of the infrared images is generated at the same time as the visible light image.

The AVHRR scans four portions of the spectrum:

1. 0.58 – 0.68 nm Green to red light,
2. 0.72 – 1.10 nm Photographic near-infrared light,
3. 3.55 – 3.93 nm Near-thermal infrared light,
4. 10.5 – 11.5 nm Far-thermal infrared light.

Figure 5-1-1 shows the divisions of the electromagnetic spectrum together with the ranges of the sensors on the AVHRR. For more information on AVHRR data the reader is referred to Lillesand and Kiefer (1987).

Data from the NOAA-9 mission were used in this study. This satellite crosses the equator, moving southward, at 2:30 p.m. daily and provides repeat coverage every 12 hours. It passes over Canada at approximately 1:00 p.m. Summer imagery was chosen for this research because the sun is at the highest point above the horizon, which minimizes shadowing. Although shadowing helps to detect topographically expressed lineaments in remotely sensed imagery, an excessive amount may result in misinterpretation.

The image of British Columbia was created from a mosaic of images from July 11 to July 31, 1988. Multiple images were required to create the final composite image due to the presence of cloud cover in parts of the province. The mosaic was rectified to the Lambert conformal map projection and resampled to a pixel (a picture element) size of 1.0 kilometre. Due to time and financial constraints, the researchers only acquired datasets for Channels 1, 2 and 3 from the NOAA-9 AVHRR.

METHODOLOGY

Simple Image Enhancement

The initial interpretation of lineaments consisted of a visual inspection of the image bands which had been linearly contrast stretched and edge enhanced. High-pass filtering (*i.e.*, edge enhancement) is a technique that applies a local operation to a pixel and its neighbours. The result of the local operation is then placed in the central pixel's location. For this study a three by three kernel was created with weights of 1.88 at the centre and -0.11 at the edges. This kernel is moved throughout the original image bands, row by row, and the central value in the output image is created by multiplying each coefficient in the kernel by the corresponding brightness value in the original image, then adding together all the resulting products.

Only those linear features which were clearly discernible on the computer screen were recorded. Figure 5-1-2 shows a down-sampled view of the three AVHRR bands after contrast stretching and edge enhancement.

Non-topographic Hill Shading

An alternate approach to enhancing lineaments is the non-topographic hill-shading technique (von Gaza, 1988a). In digital images the tonal differences used in visually identifying lineaments, as expressed by topography and spectral differences between surface materials, are not always easily detected. Tonal differences however are manifest in the digital image topology as breaks in slope and can be enhanced for visual identification by illumination from a single synthetic light source. This is done by treating the

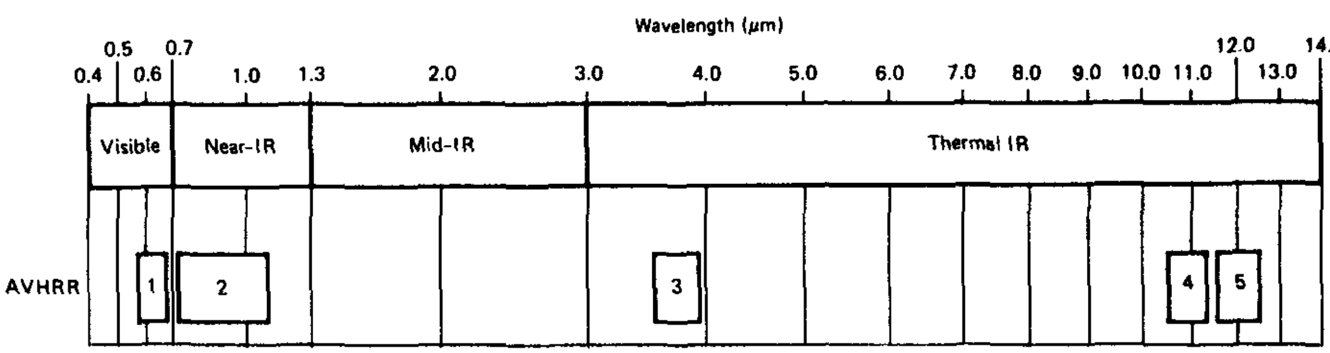

Figure 5-1-1. The divisions of the electromagnetic spectrum and sensing ranges of the sensors for the AVHRR.

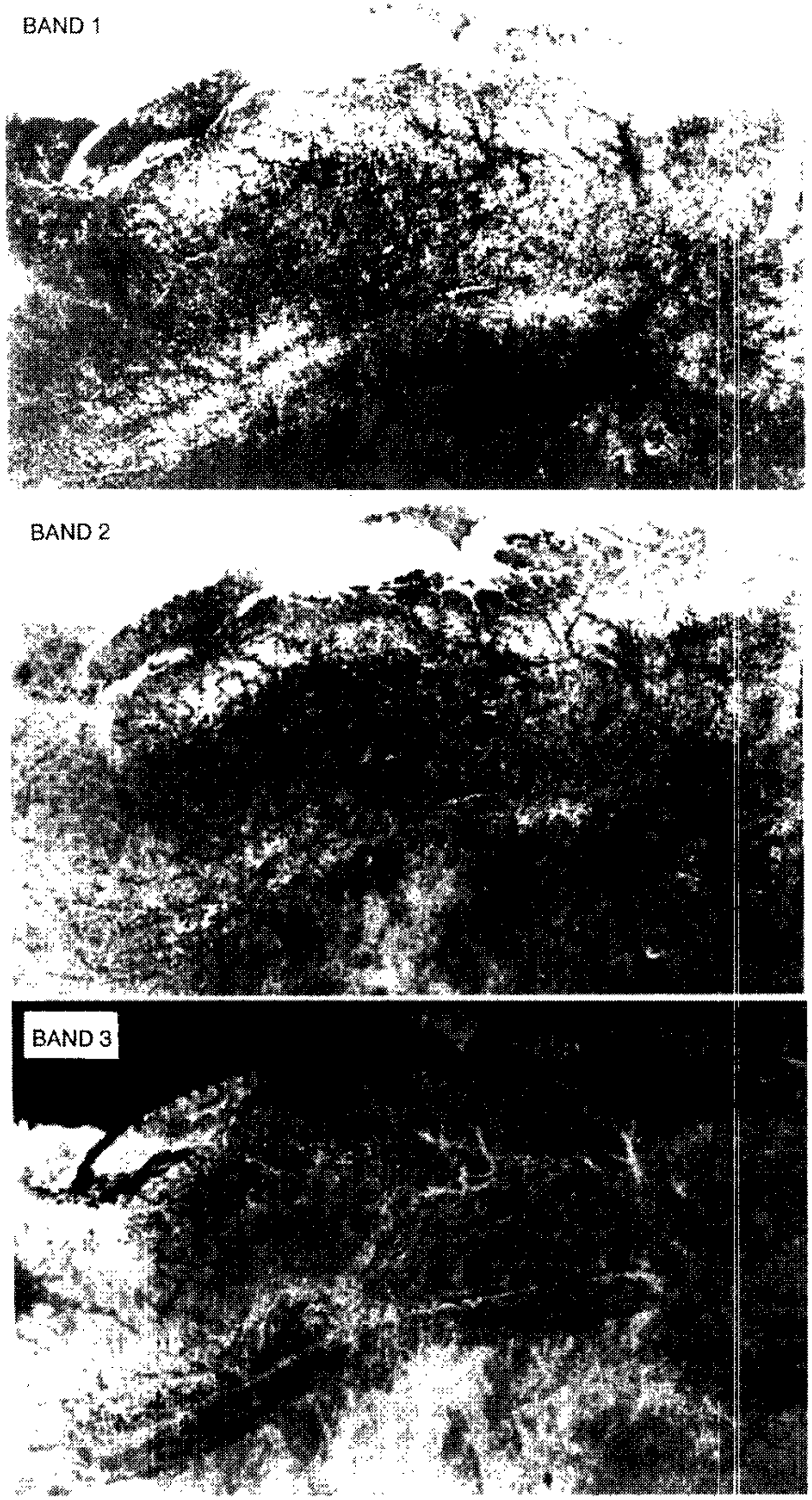

Figure 5-1-2. A down-sampled view of the three AVHRR bands after contrast stretching and edge enhancement.

digital image data as a digital elevation model (DEM) and illuminating the dataset with a hypothetical "sun". Shading of the dataset is calculated using a Lambertian reflectance model. The user interactively specifies the solar azimuth and solar elevation which provides best definition of the lineaments. This technique is basically a refinement of standard directional filtering techniques used in image processing.

In an effort to enhance the visual expression of inherent lineaments in the data, two images were produced using the hill-shading technique. Two hill-shaded images were created for each band, with the first image having a pseudo solar azimuth of 0° and the second a pseudo-solar azimuth of 75°. Two images were created with different solar azimuths in order to avoid directional biases. The authors' experience suggests that more than two viewing angles are not necessary as long as the directions are carefully chosen.

Near orthogonal azimuths were selected in order to maximize the amount of different information presented in the datasets. At the sun azimuth of 0°, patterns which trend in an east-to-west direction are emphasized, while at a sun azimuth of 75°, patterns trending north to south are emphasized. The sun azimuth of 75° was chosen to emphasize the known major lineament patterns in British Columbia. The solar inclination (angle above the horizon) was set to 30°. This value was selected through trial and error. Figure 5-1-3 shows a part of the hill-shaded image from Band 3, with the sun azimuth at 75° and the solar inclination set to 30°.

The lineaments derived from visual interpretation of the contrast-stretched and edge-enhanced bands were stored together with the lineaments extracted from the hill-shaded image bands as rasterized maps.

Figure 5-1-3. A part of the hill-shaded image from Band 3 (sun azimuth = 75° and solar inclination = 30°)

Digitization of Known Major Lineaments

The Tectonic Assemblage Map of the Canadian Cordillera (Tipper *et al.*, 1981) published by the Geological Survey of Canada was digitized for its curvilinear features. The scale of this map is 1:2 000 000 and it is in the Lambert conformal map projection. The interpreted lineaments from the three AVHRR bands were plotted on a raster output device together with the lineaments digitized from the tectonic assemblage map. The plots of the interpreted lineaments were overlain on the tectonic assemblage plot, one at a time, and the areas of coincidence and divergence were located.

Plots of Known Mining Sites

Some known mining sites were plotted on the tectonic assemblage map in order to compare their location to the location of the known major lineaments. This plot was then compared to the location of the lineaments derived from the interpreted AVHRR imagery.

ANALYSIS OF RESULTS

The interpreted lineaments for the three AVHRR bands are presented in Figure 5-1-4. The major lineaments from the tectonic assemblage map were more readily identified from the contrast-stretched imagery while the more subtle linear patterns were more easily recognized on the hill-shaded imagery. Due to the coarse resolution and the need for ancillary datasets (*e.g.*, aeromagnetic data), we did not attempt to rank the interpreted lineaments or describe whether they were surficial or deep.

Description of Band 1

The Band 1 image has very little tonal or topographic information. Major topographic features are not easily seen, with the exception of the Rocky Mountain Trench. The image, with the exception of snow, is very dark and shows little or no contrast between ground-cover types. It was very difficult to detect any linear patterns in the northwest corner of the image because of snow cover in that geographic area.

Lineaments detected in this band were primarily from the contrast-stretched raw image. Inspection of hill-shaded images from Band 1 did not add significantly to the number of lineaments mapped. The effects of atmospheric scattering also probably contributed to detection of fewer lineaments in the Band 1 image. Solar radiation in the visible portion of the electromagnetic spectrum is more strongly scattered and can result in hazy images with a muddy appearance. Most of the lineaments plotted from Band 1 are long and the lineament pattern is evenly distributed across the province. Overall, this band is not good for detecting topographically expressed lineaments.

Description of Band 2

The raw image from Band 2 shows more scene contrast than Band 1 but also has a significant amount of high-frequency noise. Most of the noise appears as very bright pixels which represent snow. The expression of major topographic features is apparent and there is a better differentiation between ground-cover types. The Band 2 image is generally sharper than Band 1 because it was recorded in the near-infrared portion of the spectrum, which is less affected by atmospheric scattering. The greater tonal range of the image is primarily due to the fact that near-infrared light is reflected more strongly by vegetation than visible light.

More lineaments were detected in the Band 2 image than in the Band 1 image. In contrast to Band 1, it was found that the hill-shaded image was more useful for detecting the possible presence of lineaments. Most of the linear features in Band 2 are located in the southern half of the AVHRR image. The presence of snow in the northwest, as in Band 1, masks the expression of potential lineaments.

Description of Band 3

The Band 3 image is the most useful and the easiest to interpret. Major province-wide topographic features are easily identified and differences in surface materials that are hardly visible in Band 1 and 2 are very evident in Band 3. Areas of snow and water are black and thus the visual annoyance of bright pixels is avoided. The hill-shaded Band 3 image proved to be the best for detecting and mapping lineaments. Most of the lineaments in Band 3 are located in the northern half the AVHRR image and along the Rocky Mountains.

The primary reason that Band 3 is most useful is that emitted thermal radiation is the least affected by atmospheric scattering, resulting in a sharper image. Both Bands 1 and 2 depend on the amount of reflected radiation from ground cover. whereas Band 3 response is governed by the thermal emittance from the ground cover. In the Band 3 image of Figure 5-1-2, snow and water are black (coldest), sparsely vegetated. dry areas are white (warmest) and more vegetated areas are grey (warm).

Band 3 depicts the amount of heat re-radiated from the earth's surface. As most of the ground cover in British Columbia is vegetation, the amount of solar absorption can be taken as a constant. The amount of heat from the surface also depends on the direction of the surface in relation to the position of the sun. North-facing slopes receive less direct solar radiation than south-facing slopes and therefore appear darker (colder). This dependence of thermal emission on terrain suggests that Band 3 can be effectively used to map changes in slope magnitude and direction.

Concordance of Interpreted Lineaments With Known Major Lineaments

We have determined that there are some areas of coincidence between the Tectonic Assemblage Map and the interpreted lineaments from the AVHRR imagery Figure 5-1-4). The areas of coincidence occur mainly along the Rocky Mountain Trench and the Fraser fault. Most of these lineaments were derived from visual inspection of the contrast-stretched image bands.

Few lineaments from Band 1 matched the Tectonic Assemblage Map. A part of the northern Rocky Mountain Trench near Williston Lake, the southern part of the Rocky Mountain Trench and a segment of the Fraser fault were detected on the Band 1 imagery. Some unnamed faults on Vancouver Island and south of Prince Rupert were also matched.

There were more matches of lineaments from Band 2. The northern part of the Rocky Mountain Trench near Williston Lake, the southern part of the Rocky Mountain Trench and the Fraser fault were successfully identified. There was coincidence along the Yalakom fault and the lineament also showed an east-southeast extension into the interior of British Columbia. There were also matches to other unnamed faults south of the Rocky Mountain Trench and on Vancouver Island.

The lineaments derived from Band 3 had the most agreement with the Tectonic Assemblage Map. A significant part of the Northern Rocky Mountain Trench, the northern part of the Pinchi fault and most of the Fraser fault were mapped from the Band 3 image. There are also matches to other unnamed lineaments east of the Northern Rocky Mountain Trench, on Vancouver Island and south of the southern part of the Rocky Mountain Trench.

Areas of Contrast With the Known Major Lineaments

Lineaments which were not detected by the Band 1 imagery include the Yalakom fault, the Pinchi fault, the central and most of the northern part of the Rocky Mountain Trench. Among the Band 2 lineaments, there was no match along the Pinchi fault. The southern part of the Pinchi fault and the entire Yalakom fault was not detected from the Band 3 imagery. Nonetheless, if the interpretations from all three AVHRR bands are combined into a single map, most the major lineaments can be successfully mapped.

Many lineaments in all three bands cross-cut the linears on the Tectonic Assemblage Map. It is significant that this cross-cutting pattern is common to all three bands. The possible reasons for this contrast merits further investigation.

Agreement With Known Mining Sites

A plot of known mining sites, Figure 5-1-5, shows that many of the mines are not located on or along regional-scale lineaments, as marked by the Tectonic Assemblage Map. These same mining sites also do not coincide with lineaments mapped from the AVHRR data. Some mining sites which are located near the lineaments derived from AVHRR

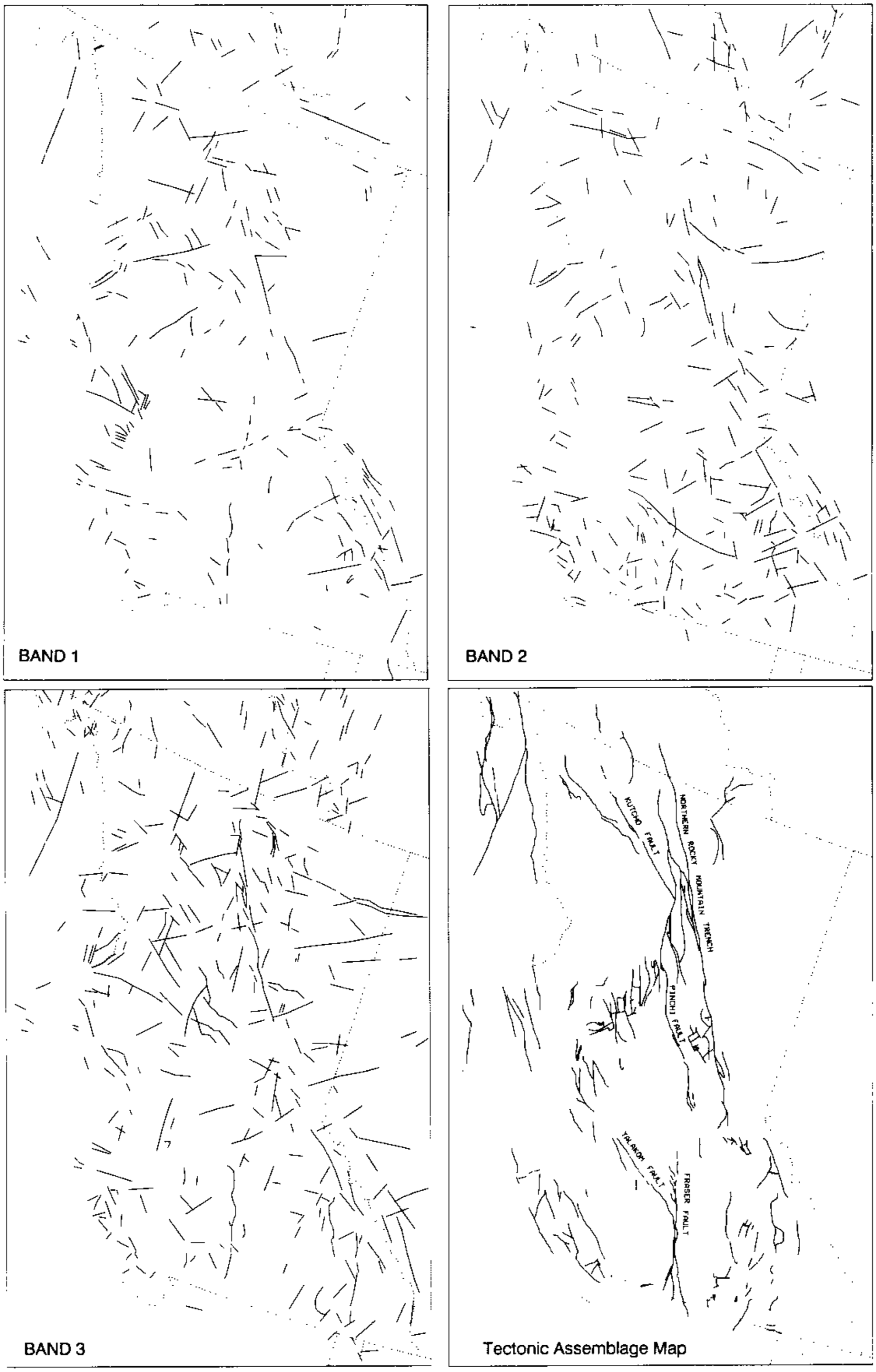

Figure 5-1-4. The interpreted lineaments for the three AVHRR bands and the lineaments from the Tectonic Assemblage Map.

imagery are Myra Falls (Westmin Resources Ltd.), Johnny Mountain mine (Skyline Explorations Ltd.), Babine Lake (Noranda Inc.), Beaverdell (Teck Corporation), Princeton (Similco Mines Ltd.) and Hedley (International Corona Corporation). The Myra Falls mine is located close to lineaments detected in all three AVHRR bands.

CONCLUSIONS

The interpretation of the contrast-stretched and edge-enhanced imagery and the hill-shaded imagery provided useful, complementary information. Known major linear features were easily detected and mapped using contrast-stretched imagery, while hill-shaded imagery allowed detection of more subtle linear features. Users of NOAA AVHRR imagery should use both methods for detecting lineaments.

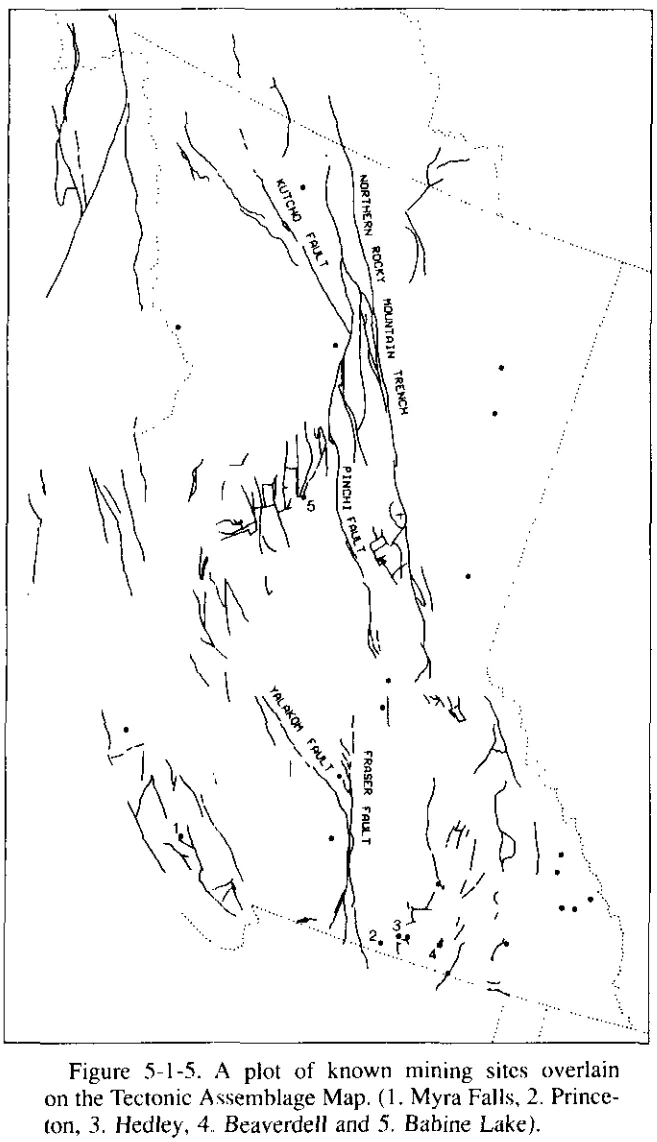

Figure 5-1-5. A plot of known mining sites overlain on the Tectonic Assemblage Map. (1. Myra Falls, 2. Princeton, 3. Hedley, 4. Beaverdell and 5. Babine Lake).

The most detailed information was derived from the Band 3 image. This image had the most readily identifiable details of the three bands. It also appears that the ability to differentiate gross ground-cover types is better using the thermal band than either the reflected visible or reflected infrared bands. If other users intend to map lineaments with AVHRR imagery, it is suggested that the Band 3 image be used in preference to the other two bands.

The major lineaments shown on the Tectonic Assemblage Map are more readily identified from the contrast-stretched imagery while the more subtle linear patterns are more easily derived from the hill-shaded imagery. The areas of coincidence between the interpreted lineaments and the lineaments from the Tectonic Assemblage Map occurred mainly along the Rocky Mountain Trench and the Fraser fault. Many linears in all three bands cross-cut the linears from the Tectonic Assemblage Map.

ACKNOWLEDGMENTS

We acknowledge the Geological Survey Branch of the British Columbia Ministry of Energy, Mines and Petroleum Resources for funding this research through the British Columbia Geoscience Research Grant Program, grant number RG91-02.

REFERENCES

Bird, J.B. (1980): The Natural Landscapes of Canada, Second Edition; *John Wiley & Sons*, Canada, pages 224, 225.

Goetz, A.F.H., Rock, B.N. and Rowan, L.C. (1983): Remote Sensing for Exploration: An Overview; *Economic Geology*, Volume 78, pages 573-590.

Lillesand, T.M. and Kiefer, R.W. (1987): Remote Sensing and Image Interpretation. Second Edition; *John Wiley & Sons*, Canada, pages 590-601.

Mortensen, J.K. and von Gaza, P. (in press) The Application of TM Thermal Imagery for Regional Lineament Analyses in the Klondike District, Yukon: *in* Yukon Geology, Volume 3, Exploration and Geological Services Division, *Yukon Indian and Northern Affairs Canada.*

Tipper, H.W., Woodsworth, G.J. and Gabrielse, H., Coordinators (1981): Tectonic Assemblage Map of the Canadian Cordillera and Adjacent Parts of the United States of America; *Geological Survey of Canada*, Map 1505A.

von Gaza, P. (1988a): The Perception and Enhancement of Depth in Monoscopic Remotely Sensed Images; unpublished M.Sc. thesis, *University of Alberta.*

von Gaza, P. (1988b): Enhanced Landsat Thematic Mapper Imagery for Mineral Exploration in the Wheaton District, Southern Yukon; unpublished M.Sc. thesis, *University of Alberta.*

NOTES

British Columbia Geological Survey
Geological Fieldwork 1991

RESOURCE ASSESSMENT USING A GEOGRAPHICAL INFORMATION SYSTEM: A PILOT STUDY IN THE SMITHERS AREA*

By E.C. Grunsky, D.G. MacIntyre, B.C. Ministry of Energy, Mines and Petroleum Resources
and
T.A. Richards, Prospecting Ltd.

KEYWORDS: Geographic information system, mineral resource assessment, Land Information Strategic Plan, Knowledge-based systems, multivariate data.

INTRODUCTION

Data that can be used for mineral resource assessment include, but are not limited to, geological maps, satellite imagery, regional geochemical data, mineral occurrence data, geophysical data, mineral titles data, digital elevation-contour data, planimetry and structural information, all of which can be digitized. Geologists now routinely acquire data using portable computers in base camps and in the field and this has been a common practice within the British Columbia Geological Survey Branch for a number of years (MacIntyre, 1991). Geological data are commonly stored in CAD-based files that record points, lines and polygons that describe geological features. Additional information that includes structural measurements and other descriptive features of field data are commonly stored in database management systems that have associated geographical coordinates. An integrated mapping program that has tied both the geological vector-based data with the attributes that describe the features at specific geographic locations has been implemented by the Ontario Geological Survey (Brodaric and Fyon, 1989). Such systems are a step towards an integrated approach to data capture and management in ways that were not previously possible.

The integration of spatially based data with attributes associated in a database management system is the foundation of a Geographical Information System (GIS). The development of GIS technology and software is a step toward an integrated system of data collection, management and, most importantly, analysis. The analytical tools that are being developed for spatial data are the most important features of GIS packages.

The use of spatially based digital data is not unique to geoscience. The proliferation of spatially based data prompted the British Columbia government to implement the Corporate Land Information Strategic Plan in order to provide a framework through which geographically based data could be stored, managed and disseminated within the land information infrastructure (DMR Group, 1989). The Geological Survey Branch will be participating in the implementation of the land information infrastructure and must be able to store, manage, model and disseminate geoscience information gathered or created by the Branch in digital form.

The Geological Survey Branch has embarked on a pilot project, funded by the Canada - British Columbia Partnership Agreement on Mineral Development to implement and assess the usefulness of a GIS. The main goal is to capture and integrate the wealth of digital information available for a mineral resource assessment study in the Smithers area. The implementation of a GIS will also be used to meet the requirements and assist in the implementation of the land information strategic plan. As geological data are, for the most part, geographically based, the use of a GIS is particularly well suited to geological applications. A previous study by Bartier and Keller (1990) integrated stream-sediment geochemistry with bedrock geology using a GIS and was shown to be a superior means of examining the data.

The assessment of spatially based data using automatic methods is not new. Previously, studies of spatially related geological phenomena were applied to particular datasets that were assembled for specific applications (*e.g.*, geochemical datasets). Assessments of gold deposits in the Abitibi belt of Ontario were carried out by Agterberg and Kelly (1971). They modelled the probability of a gold deposit occurring within a given area, based on the distribution of gold deposits over the entire area. More recently, studies of data integration and assessment using GIS have been carried out in other provinces and countries (George and Bonham-Carter, 1989; Bonham-Carter *et al.*, 1988; Rock *et al.*, 1990). The main purpose of data integration is to co-register spatially based information so that the data can be interrogated using automatic or manual techniques of analysis.

Resource assessment of spatially based data requires the integration of information onto a common set of georeferenced coordinates and the ability to examine and evaluate the data by choosing one or more "layers" of information. One of the most challenging problems is accurate coding of the data. Most maps and digital data are coded with the Universal TransMercator projection (UTM) coordinates which, in North America, are based on the 1927 North American Datum (NAD27). This datum is determined from parameters which define flattening of the geoid. Adoption of the 1983 North American Datum (NAD83) has resulted in a new set of parameters for geocoding. Converting between the two standards is not a difficult procedure (B.C. Ministry of Lands and Parks, 1991), however, knowing which datum was used is important. Errors introduced in coding will cause errors in data modelling and analysis, particularly with raster-based images where the offset between two layers can result in shifts of several pixels.

* Canada - British Columbia Partnership Agreement on Mineral Development.

SELECTION OF THE GEOGRAPHICAL INFORMATION SYSTEM

Aronoff (1989) presents a general overview of geographical information systems. The review describes their concepts, features and capabilities. Van Driel and Davis (1989) and Agterberg and Bonham-Carter (1989) contain papers that describe methods of data integration and the application of GIS to specific geological problems. Bartier (1991) has reviewed the requirements and features for a successful GIS implementation for use in mineral resource evaluation in British Columbia. The choice of the right GIS is complex. Bruce and Davidson (1991) outline a systematic process for selecting a system based on user requirements. Image analysis systems which are raster-based can complement vector and raster-based GIS packages (Bonham-Carter, 1989) particularly when satellite imagery is used.

The Geological Survey Branch selected a commercial microcomputer-based GIS package, TERRASOFT® as the initial GIS package for resource assessment (Note: *the Branch does not endorse the use of any particular commercial Geographical Information System*). The selection of the TERRASOFT system was based on the comparison of four GIS packages in which the cost, ease of implementation, ease of training and compatibility with the land information infrastructure strategy of the British Columbia government were the main considerations. The package is being evaluated through the Mineral Resource Assessment Study and may not be the only GIS package that will be used.

GEOGRAPHICAL INFORMATION MANAGEMENT, DATA INTEGRATION AND RESOURCE ASSESSMENT OF THE SMITHERS (93L) AREA

Richards (in preparation) has developed a systematic set of guidelines for a manual mineral potential assessment that are based on a study of the Smithers area map sheet (93L) (Tipper and Richards, 1976; Richards and Tipper, *in preparation*). The guidelines were derived from a mineral potential evaluation scheme devised by McLaren (1990) and based on the presence of anomalous regional geochemistry, the presence of mineralization and conditions of favourable geology. Richards' scheme departs from McLaren's in that the assessment of mineral potential is not based on the presence or absence of known mineral occurrences or regional geochemical data. It is instead, primarily based upon the fundamental premises of the geological controls on the formation of hydrothermal mineral deposits, and mineral deposit models. The presence of mineral deposits and regional geochemistry are secondary factors. The quality of the map created by this scheme is dependent upon the quality of the geological map used to derive the mineral potential map.

The assessment process follows three stages:

(1) Creation of a base map using the fundamental characteristics required for the formation of hydrothermal mineral deposits. The basic premises that control the deposition of a hydrothermal mineral deposit are: (a) all hydrothermal mineral deposits require a conduit for the flow of hydrothermal solutions, (b) they all require a porous medium for mineral deposition and (c), they all require a heat source. The base map is created by outlining features that may represent conduits, depositional sites, sources of heat, and includes faults, linears, and their intersections and their proximity to intrusive bodies.

(2) Creation of one map, derived from a set of mineral potential maps based upon the geologic controls implied by the various mineral deposit models. Included in the Smithers study were the models that define epithermal, mesothermal, prophyry, volcanogenic massive sulphide and shale-hosted mineral deposits. Known mineral deposits and regional geochemistry may modify this map.

(3) Creation of a final mineral potential map by combining the two base maps. Known mineral deposits modify the final map.

The final map combines all the stratigraphic, structural, intrusive and metamorphic elements that control hydrothermal mineralization, as well as known mineralization (Richards and Desjardins, *in preparation*), all plotted on a single plane – the mineral potential map. These systematic rules define the foundation for a knowledge-based or expert-system approach using a GIS.

Considering the attributes required to define the potential presence of a mineral deposit, the Smithers area is a logical choice for a GIS-based assessment of the mineral resource potential. The area is well mapped by the Geological Survey Branch and the Geological Survey of Canada, and has been the subject of various studies carried out by universities and exploration geologists. The area also includes a wide variety of mineral deposits related to a number of metallogenic events (at least three: Jurassic, Late Cretaceous and Eocene). In addition, regional geochemical survey and MINFILE® data are available for the area. Terrain resource information data (TRIM) from the Ministry of Lands and Parks are available in digital form. Numerous land-use issues are being considered in the area.

KNOWLEDGE-BASED SYSTEMS AND RESOURCE ASSESSMENT

Resource assessment of multiple datasets requires a systematic approach based on a structured analysis of the information. The analysis procedure requires integration of both qualitative (*e.g.*, rock texture) and quantitative data (geochemical analysis). Most systems have the ability to manage three-dimensional data with varying degrees of complexity. Historically, the most common applications of three-dimensional data are in ore deposit modelling. More recently, digital elevation models (DEM) have been incorporated into a few limited geological studies. For the initial part of this study, our investigations will be restricted to the two-dimensional map plane.

Geological data can be composed of points, lines and polygons. Points usually define locations where specific attributes are recorded, as in a geochemical analysis representing several elements, or it may be a structural measurement such as a strike and dip. Qualitative attributes may represent features such as the texture of a rock or a visual estimate of clast abundance recorded within a very small area which can be considered to be a single point. Data attributes that are recorded for a point may also represent attributes associated with a polygon within which the point lies. The most common linear features on geological maps are faults, which represent the surface trace of three-dimensional planes. The attributes that may define features such as the type of fault can be useful in map-pattern assessment and have an influence on the way that relationships of patterns are perceived.

Polygons represent areas that describe a particular rock type or geologic unit. They can have attributes that contain qualitative (rock texture), quantitative (geochemical abundances) or binary (present/absent) information. This information may also be univariate (only rock texture was observed) or multivariate (several elements within a geochemical analysis). The complexity of relationships based on the attributes of polygons may require the use of a knowledge-based or expert system to decipher less obvious trends.

The spatial analysis of multivariate quantitative data has been described by Brower and Merriam (1989), Grunsky and Agterberg (1988), Royer (1988) and Wackernagel (1988). Their methods are capable of reducing the number of variables required to describe systematic relationships within the data. They are commonly applied to multielement geochemical data and can assist in interpreting the multi-element signatures by reducing the number of maps required to view systematic trends in the data (magmatic trends, alteration trends, etc.).

Assessment of qualitative (descriptive) data presents a challenge. Currie and Ady (1989a) discuss the importance of the semantic relationships between geological units (*e.g.*, dike *intrudes* sediment). Thus, the relationships between various data types require a set of rules that describe the semantic relationship between them. Once the semantic rules are established, then a meaningful interpretation or analysis can be performed. In normal manual analysis the semantic relationships are implicitly understood or intuitively perceived by the investigator. In an automatic analysis scheme, these relationships must be encoded into the system. Inclusion of the semantic relationships has been termed "extended GIS" (Currie and Ady, 1989b). This requires an elaborate set of rules for evaluation.

Evaluation of binary coded data (present or absent) for mineral resource evaluation can be carried out by the "weights of evidence" modelling method (Agterberg, 1989; Bonham-Carter *et al.*, 1988, Bonham-Carter and Agterberg, 1990). The possiblity of finding mineral deposits can be assessed by using the presence or absence of features that define the conditions for the formation of a mineral deposit.

PROJECT PLAN

Data have been imported into the TERRASOFT system from the digital topographic data files of the Ministry of Lands and Parks. These include contour data, streams, lakes, glaciers, and road data. A digital elevation model will also be incorporated into the system. Data that define the land-use boundaries of the area have also been entered. A database consisting of mineral titles information will also be incorporated. The geological data are currently being digitized from existing maps and converted from the UTM coordinates of NAD27 to NAD83. Regional geochemical data from the Smithers area (Matysek, 1988 and the mineral inventory database (MINFILE) will be imported into the system. The use of the regional geochemical data will require a catchment-basin analysis and would also benefit from the incorporation of the digital elevation model. The acquisition of aeromagnetic and landsat satellite imagery is currently being investigated.

The mineral resource assessment of the data will be carried out using the analysis facilities available with the TERRASOFT GIS package. Additional spatial analysis and knowledge-based interrogation will be developed within TERRASOFT or exported to other systems where appropriate. It is planned that the mineral resource assessment will use the systematic criteria established by Richards (*in preparation*), as a model for determining the mineral potential of the area. Many of the analytical methods mentioned above show promise as resource assessment tools and the use of GIS as a practical tool for resource potential evaluation will be studied.

REFERENCES

Agterberg, F.P. (1989): Systematic Approach to Dealing with Uncertainty of Geoscience Information in Mineral Exploration; *in* Application of Computers and Operations Research in the Mineral Industry 21st International Symposium, *American Society of Mining Engineers*, pages 165-178.

Agterberg, F.P. and Bonham-Carter, G.F., Editors, (1989): Statistical Applications in the Earth Sciences: *Geological Survey of Canada*, Paper 89-9.

Agterberg, F.P. and Kelly, A.M. (1971): Geomathematical Methods for Use in Prospecting: *Canadian Mining Journal*, Volume 92, No. 5, pages 61-7?.

Aronoff, S. (1989): Geographical Information Systems: A Management Perspective; *WDL Publications*, Ottawa.

Bartier, P.M. (1991): Investigation into Development and Implementation of Natural Resources Geographical Information Systems (GIS): Case Study Geological Survey of British Columbia; unpublished M.Sc. thesis, *University of Victoria*.

Bartier, P.M. and Keller, C.P. (1991): Integrating Bedrock Geology with Stream-sediment Geochemistry in a Geographic Information System (GIS): Case Study NTS 92H; *in* Geological Fieldwork 1990, *B.C. Ministry of Energy, Mines and Petroleum Resources* Paper 1991-1, pages 315-321.

B.C. Ministry of Lands and Parks (199): NAD27 to NAD83 Conversion in British Columbia, National Transformation, Version 1.1, includes 1 diskette, unpaginated.

Bonham-Carter, G.F. (1989): Comparison of Image Analysis and Geographic Information Systems for Integrating Geoscientific Maps, *in* Statistical Applications in the Earth Sciences, Agterberg, F.P. and Bonham-Carter, G.F., Editors, *Geological Survey of Canada*, Paper 89-9, pages 141-155.

Bonham-Carter, G.F. and Agterberg, F.P. (1990): Application of Microcomputer-based Geographical Information System to Mineral-potential Mapping; *in* Microcomputer Applications in Geology 2, Hanley, J.T. and Merriam, D.F., Editors, *Computers & Geology*, Volume 6, pages 49-74.

Bonham-Carter, G.F., Agterberg, F.P. and Wright, D.F. (1988): Integration of Geological Datasets for Gold Exploration in Nova Scotia; *Photogrammetry and Remote Sensing*, Volume 54, No. 11, pages 1585-1592.

Brodaric, B. and Fyon, J.A. (1989): OGS FIELDLOG: A Microcomputer-based Methodology to Store Process and Display Map-related Data; *Ontario Geological Survey*, Open File Report 5709, 73 pages, 1 magnetic diskette.

Brower, J.C. and Merriam, D.F. (1989): Geological Map Analysis and Comparison by Several Multivariate Algorithms; *in* Statistical Applications in the Earth Sciences, Agterberg, F.P. and Bonham-Carter, G.F., Editors, *Geological Survey of Canada*, Paper 89-9, pages 123-134.

Bruce, B. and Davidson, D. (1991): GIS for Decision Makers: An Exercise in Operational Risk Management; *Proceedings of the Eighth Thematic Conference on Geological Remote Sensing*, Denver, Colorado, April 29 - May 2, 1991.

Currie, A. and Ady, B. (1989a): GEOSIS Project: Knowledge Representation and Data Structures for Geoscience Data; *in* Statistical Applications in the Earth Sciences, Agterberg, F.P. and Bonham-Carter, G.F., Editors, *Geological Survey of Canada*, Paper 89-9, pages 111-116.

Currie, A. and Ady, B. (1989b): Extended GIS – An Enriched Model Used to Represent Geoscience Spatial Data; *Proceedings of the GIS National Conference*, Ottawa, 1989.

DMR Group (1989): A Corporate Land Information Strategic Plan for the Government of British Columbia: Land Information Infrastructure.

George, H. and Bonham-Carter, G.F. (1989): An Example of Spatial Modelling of Geological Data for Gold Exploration, Star Lake Area, Saskatchewan; *in* Statistical Applications in the Earth Sciences, Agterberg, F.P. and Bonham-Carter, G.F., Editors; *Geological Survey of Canada*, Paper 89-9, pages 157-169.

Grunsky, E.C. and Agterberg, F.P. (1988): Spatial and Multivariate Analysis of Geochemical Data from Metavolcanic Rocks in the Ben Nevis Area, Ontario; *Mathematical Geology*, Volume. 20, No. 7, pages 825-861.

McLaren, G.P. (1990): A Mineral Resource Assessment of the Chilko Lake Planning Area; *B.C. Ministry of Energy, Mines and Petroleum Resources*, Bulletin 81.

MacIntyre, D.G. (1991): Computer Assisted Mapping in the British Columbia Geological Survey – Progress to Date and Predictions for the Future; Proceedings of the Second Canadian Conference on Computer Applications in the Mineral Industry, Vancouver, Canada, September 15-18, 1991, Volume II, Poulin, R., Pakalnis, R.C.T and Mular, A.L., Editors; *The University of British Columbia* and the *Canadian Institute of Mining, Metallurgy and Petroleum*, pages 61-68.

Matysek, P.F. (1988): Regional Sediment and Water Geochemical Reconnaissance Data, British Columbia, NTS 93L; *B.C. Ministry of Energy, Mines and Petroleum Resources*, Regional Geochemical Survey RGS-17, *Geological Survey of Canada*, Open File 1361.

Richards, T.A. *(in preparation)*: An Outline of Guide Lines for the Construction of Regional Mineral Potential Maps; *B.C. Ministry of Energy, Mines and Petroleum Resources*.

Richards, T.A. and Tipper, H.W. (*in preparation*): Smithers Map-sheet (93L); *Geological Survey of Canada*, Open File Series, 1:250 000.

Richards, T.A. and Desjardins, P.J. (*in preparation*): Mineral Inventory, Smithers Map-area (93L), 1991; *B.C. Ministry of Energy Mines and Petroleum Resources*.

Rock, N.M.S., Shellabear, J.N., Wheatley, M.R., Poulinet, R. and Groves, D.I. (1990): Microcomputers in Mineral Exploration: A Database For Modeling Gold Deposits in the Yilgarn Block of Western Australia; *in* Microcomputer Applications in Geology 2, Hanley J.T., Merriam, D.F., Editors, *Computers & Geology*, Volume 6, pages. 199-222.

Royer, J.J. (1988): Geochemical Data Analysis; *in* Statistical Treatments for Estimation of Mineral and Energy Resources, Fabbri, A.G., Chung, C.F. and Sinding-Larsen R., Proceedings NATO Conference, Il Ciocco, Italy, July 1986, *Reidel*, Dordrecht, pages 89-112.

Tipper, H.W. and Richards, T.A. (1976): Smithers Map-sheet (93L); *Geological Survey of Canada*, Open File 351, 1:250,000.

Van Driel, J.N. and Davis, J.C., Editors (1989): Digital Geologic and Geographic Information Systems; *in* Short Course in Geology: Volume 10, *American Geophysical Union*, 62 pages.

Wackernagel, H. (1988): Geostatistical Techniques for Interpreting Multivariate Spatial Information; *in* Statistical Treatments for Estimation of Mineral and Energy Resources; Fabbri, A.G., Chung, C.F. and Sinding-Larsen R., Proceedings NATO Conference, Il Ciocco, Italy, July 1986, *Reidel*, Dordrecht, pages 393-409.

Mineral Deposit Research Unit
The University of British Columbia

The Mineral Deposit Research Unit (MDRU) is a University-Industry-Government collaborative research unit within the Department of Geological Sciences, The University of British Columbia.

Research described in the following papers is funded by the MDRU Iskut project "Metallogensis of the Iskut River area, northwestern British Columbia" which is supported by the Natural Sciences and Engineering Council and the following companies: BP Resources Canada Ltd., Cominco Ltd., International Corona Corporation, Ecstall Mining Corporation, Granges Inc., Homestake Mineral Development Company, Kennecott Canada Inc., Lac Minerals Ltd., Newhawk Gold Mines Ltd., Noranda Exploration Co. Ltd., Placer Dome Inc., Prime Equities Inc. and Teck Corporation.

GEOCHRONOMETRY OF THE ISKUT RIVER AREA – AN UPDATE (104A and B)

By A. James Macdonald
Mineral Deposit Research Unit, U.B.C.
Peter van der Heyden, Geological Survey of Canada
David V. Lefebure and Dani J. Alldrick
British Columbia Geological Survey Branch

(MDRU Contribution 004)

KEYWORDS: Regional geology, Hazelton Group, Iskut River area, U-Pb geochronometry, metallogeny, intrusions.

INTRODUCTION

The Mineral Deposit Research Unit's (MDRU) project "Metallogeny of the Iskut River Area, Northwestern British Columbia" (Macdonald *et al.*, 1991) is employing high-precision, U-Pb zircon geochronometry to augment the understanding of the relative and absolute timing of intrusive and extrusive events associated spatially with base and precious metal mineralization. Researchers are working together with geologists from the federal and provincial Geological Surveys, and with mining and exploration company geologists active in the area. Data gathered during this study will be integrated with paleontological studies in progress (*e.g.*, Nadaraju and Smith, 1992) to further refine our understanding of stratigraphic relationships and timing. In this contribution, we report four new U-Pb results for zircons from plutons in the Iskut River area; three are from the lower Iskut River district, in the vicinity of the Snip mine and Johnny Mountain and Inel properties; one is from the Eskay Creek area.

EXISTING DATABASE

Alldrick *et al.* (1986, 1987), Anderson (1989), Anderson and Bevier (1990), Anderson *et al.* (1991), Anderson and Thorkelson (1990) and Bevier and Anderson (1991) have summarized the K-Ar and U-Pb isotopic data available for the Iskut River and adjacent areas (*e.g.*, Stewart) comprising northwest Stikinia (Wheeler and McFeely, 1987). In brief, these data indicate four principal plutonic events (Table 6-1-1); Anderson and Bevier (1990) suggest that at least the first three of these have associated extrusive equivalents.

TABLE 6-1-1
PLUTONIC EVENTS, SUITES AND RELATED EXTRUSIVE EQUIVALENTS (ANDERSON AND BEVIER, 1990)

Plutonic Event	Plutonic Suite	Extrusive Equivalent
230-226 Ma (Late Triassic)	Stikine	Stuhini Group
211-187 Ma (Late Triassic to Early Jurassic)	Texas Creek	Hazelton Group
179-172 Ma (Middle Jurassic)	Three Sisters	Salmon River *Formation*
55-51 Ma (Tertiary)	Coast Plutonic Complex	

Anderson and Thorkelson (1990) and Bevier and Anderson (1991) propose a widespread unconformity in northwestern Stikinia separating Toarcian (Harland *et al.*, 1989) and younger (Middle Jurassic) rocks from underlying Early Jurassic strata, attributed to late Early Jurassic contractional deformation.

SAMPLE DESCRIPTIONS – PETROLOGY AND GEOCHEMISTRY

Four samples collected during the MDRU 1990 field program from the Iskut area were analyzed in 1991:

(1) Iskut River (Bronson) stock, on the Iskut Joint Venture property.
(2) Red Bluff porphyry, collected from the Snip property.
(3) Inel stock, on the Inel property.
(4) Eskay porphyry, on the Eskay Creek/GNC properties.

Refer to Figure 6-1-1 for property locations.

ISKUT RIVER (BRONSON) STOCK

Britton *et al.* (1990b) describe the Iskut River stock as follows:

"Phaneritic intrusions of probable early Jurassic age include ... the Iskut River stock. ... A common feature of these intrusions is the presence of coarse (up to 5 cm) potassium feldspar phenocrysts."

The sample of the Iskut River stock collected in 1990 by A.J.M. (AJM-ISK90-333) from the Iskut Joint Venture property (Prime Resources Group Inc., American Ore Ltd., Golden Band Resources Inc.; Figure 6-1-1) is a plagioclase-phyric, locally alkali feldspar phyric, monzodiorite, based upon thin section estimates (plagioclase 60%, poikilitic potassium feldspar 25%, quartz 10% and biotite 5%). The chemical composition of the rock given in Table 6-1-2 yielded a low An:[An+Or] ratio (<10) and a quartz - alkali feldspar syenite classification (Streckeisen and LeMaitre, 1979). Plagioclase euhedra are zoned, with sericitized cores and rims of less altered feldspar, and are locally contained within poikilitic potassium feldspar.

RED BLUFF PORPHYRY

Britton *et al.* (1990b) described the Red Bluff porphyry (which outcrops on both Cominco Ltd. and Prime Resources Group Inc.'s Snip property and Skyline Gold Corporation's Johnny Mountain holdings, Figure 6-1-1) as a potassium feldpar phyric, Early Jurassic intrusion (*see* description of Iskut River stock). The sample collected by A.J.M. (AJM-ISK91-041) from the 130-metre haulageway in the Snip mine is an altered, sheared, feldspar-megacrystic intrusive rock that is not an ideal candidate for U-Pb geochronometry due to abundant (1 to 5%) pyrite as an alteration product. The Red Bluff porphyry and spatially associated mineralization is the subject of a companion study being conducted by Ettlinger (in preparation). In addition, Rhys and Godwin (1992, this volume) are investigating the structural geology of the Snip mine, including the Red Bluff porphyry, as part of an M.Sc. thesis by Rhys in progress at The University of British Columbia.

TABLE 6-1-2
LITHOGEOCHEMICAL DATA [Wt. %]

	AJM-ISK90-333 Iskut River Stock	AJM-ISK90-162 Inel Stock	AJM-ISK90-111 Eskay Porphyry	DJA-90-PZ1 Eskay Porphyry
SiO_2	62.7	69.8	67.8	64.1
TiO_2	0.42	0.29	0.48	0.58
Al_2O_3	17.4	16.5	14.7	16.4
Fe_2O_3	4.09	2.62	3.53	3.69
MgO	1.39	0.69	0.26	0.25
MnO	0.05	0.09	0.05	0.07
CaO	4.45	0.19	0.12	0.14
Na_2O	3.97	2.96	1.82	2.40
K_2O	3.86	5.48	8.8	9.86
P_2O_5	0.17	0.08	0.15	0.17
H_2O	0.8	1.8	1.6	1.1
CO_2	[dl]	0.04	[dl]	[dl]
TOTAL	99.3	100.54	99.31	98.76

Note: 1. [dl] = below detection limit
2. Total iron as Fe_2O_3
3. Analyses by X-Ray Assay Laboratories, Don Mills, Ontario

Inel Stock

Britton *et al.* (1990b) describe the Inel felsite stock (property location, Figure 6-1-1) as follows:

"Synvolcanic intrusions are thought to be comagmatic and coeval with extrusive rocks. Examples include felsite stocks on the ... Inel property. These are leucocratic to holofelsic, cream to tan, porphyritc rocks with fine feldspar and quartz phenocrysts set in an aphanitic groundmass. Contacts are altered and sheared, but the stocks appear to form sill-like bodies that are crudely conformable with enclosing strata. On the Inel property the felsite stock is associated with a small felsite dike swarm."

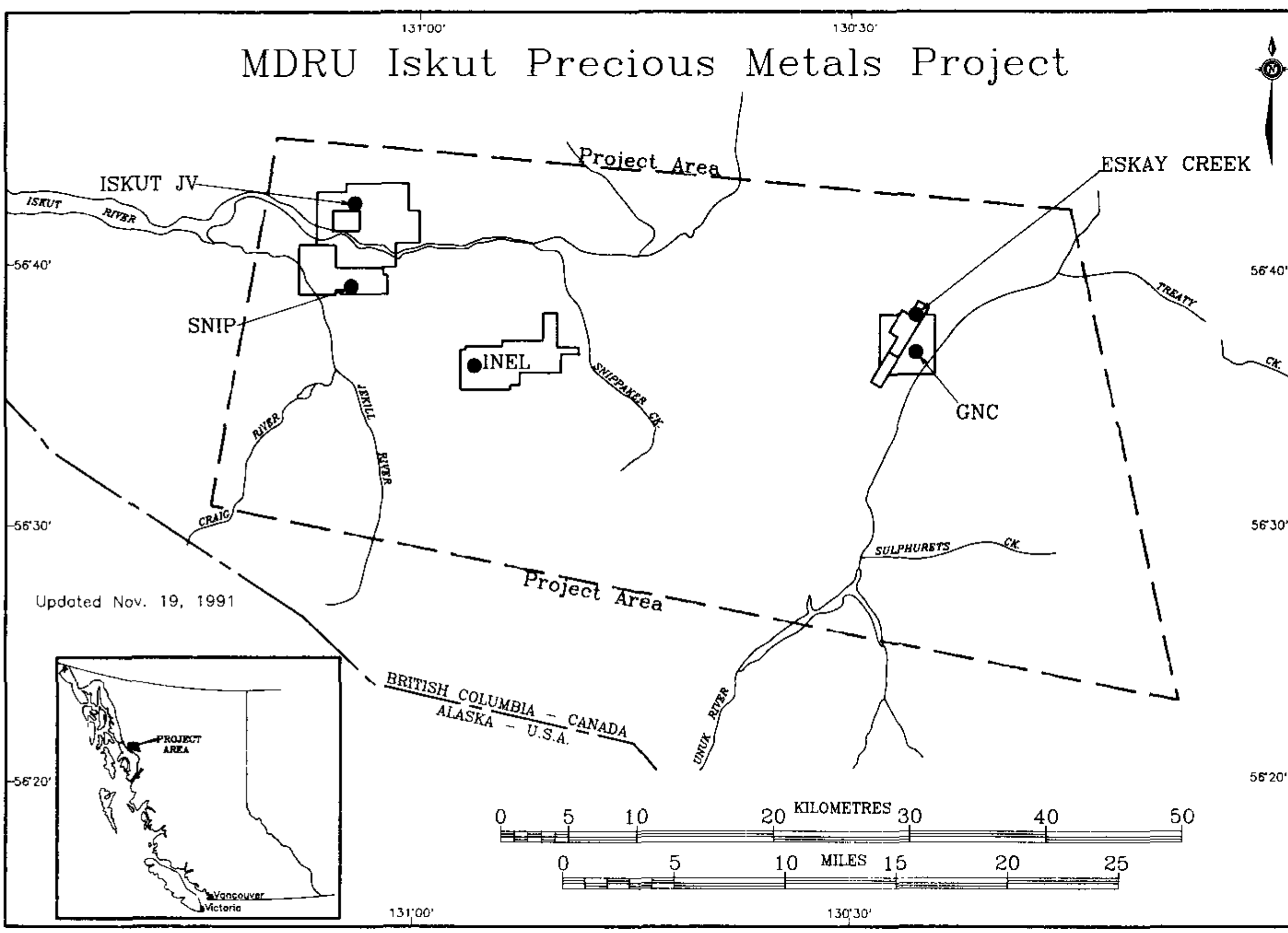

Figure 6-1-1. Location map of the Iskut River Project area, showing properties from which samples described in this report were collected.

The Inel stock is also spatially associated with diatreme-like, igneofragmental breccia dikes that cut overlying strata, indicative of vigorous devolatilization of a magma body, which may have consolidated to form the Inel stock, or a related, blind intrusion.

Sample AJM-ISK90-162 was collected from the Gulf International Minerals Ltd. exploration campsite (1990) on the Inel property and contains altered feldspar (15%) and quartz (5%) phenocrysts in a fine-grained quartz-feldspar groundmass. A quartz monzodiorite composition is indicated (Streckeisen and LeMaitre, 1979) from the chemical composition (Table 6-1-2).

ESKAY PORPHYRY

A sill-like body (C. Edmunds, International Corona Corporation, personal communication, 1991) of feldspar porphyry crops out approximately 1 kilometre east of the 22 zone at Eskay Creek, and straddles the claim boundary between the Eskay Creek and GNC properties (both properties operated by International Corona Corporation; Figure 6-1-1). Britton *et al.* (1990a), relying also on Donnelly (1976), described the body thus:

"... granodiorite porphyry ... [with] subhedral phenocrysts of oligoclase, up to 1 millimetre long, (36%), anhedral quartz, 0.3 millimetre diameter, (11%) and 1 millimetre, subhedral grains of orthoclase (8%), ... are set in a fine-grained quartz-feldspar matrix. Plagioclase is extensively replaced with chlorite and sericite. Its bulk composition is similar to dacitic pyroclastics seen higher in the section. It may represent a synvolcanic plug or a thick dacitic flow."

Exploration diamond drilling conducted in 1990 by Prime Resources Group Inc. demonstrated the local presence of potassium feldspar megacrysts, up to 2 centimetres in long dimension (V.P. Van Damme, Project Geologist, personal communication, 1990). Along the northern and western margins inclusions, rafts and complex interfingering of porphyry and hornfelsed argillite country rock occurs within the "Porphyry zone".

Two samples from the Eskay porphyry were selected for lithogeochemical analysis: AJM-ISK90-111, collected from outcrop by A.J.M. and DJA-90-PZ1, collected from talus blocks at the base of a cliff by D.J.A. The latter sample was also selected for U-Pb geochronometry (see below). Sample AJM-ISK90-111 is an amphibole (5%) plagioclase (20%) potassium feldspar (20%) porphyry. Phenocrysts up to 3.2 millimetres occur in an altered groundmass (<0.1 mm) of (?) quartz and feldspar; amphibole is also completely altered. Sample DJA-90-PZ1 is similar, with coarser grain size (phenocrysts to 1 cm) and more abundant plagioclase (approximately 30%) compared to potassium feldspar (10%), and with accessory biotite (<5%) and pyrite (1-2%). Both rocks are compositionally similar (Table 6-1-2) and are classified as alkali-feldspar granites (Streckeisen and LeMaitre, 1979).

Early Jurassic potassium feldspar megacrystic plutons (*e.g.*, phases of the Iskut River, Red Bluff and Eskay bodies) are texturally similar to rocks described in the Stewart area ("Premier porphyries", a component of the Texas Creek plutonic suite, Table 6-1-1; *e.g.*, Alldrick, 1987; Brown, 1987), that show a spatial and temporal relationship with the Silbak Premier gold, silver and base metal deposit. Grove (1971) and, more recently, Anderson (1989) and Britten and Alldrick (1990) suggested that there may be a genetic relationship between the Premier-like igneous bodies and precious metal mineralization (with or without base metals) in both the Stewart and Iskut areas. This hypothesis will be tested further as part of MDRU's Iskut project.

U-Pb GEOCHRONOMETRY ANALYTICAL PROCEDURES

All work was carried out in the geochronometry laboratory at the Department of Geological Sciences, The University of British Columbia. Zircon-rich heavy mineral concentrates were recovered using standard crushing, grinding, wet shaking (Wilfley table) and heavy liquid separation techniques. Abundant pyrite in the Wilfley concentrate from sample AJM-ISK91-41 (Red Bluff porphyry) was removed from heavy silicates by flotation using warm 7N HNO_3. Pure zircon populations from nonmagnetic size fractions were handpicked in ethanol. Zircons from sample DJA-90-PZ-1 (Eskay porphyry) were separated by hand from abundant pyrite in the heavy fraction and were treated with HNO_3 only during final zircon washing. Abrasion of all zircon fractions was done using the procedure of Krogh (1982), and zircons were handpicked from the abrasion mixture. Zircon dissolution was done in microcapsules using the technique of Parrish (1987), and uranium and lead chemistry procedures were modified from the technique developed by Krogh (1973).

Uranium and lead concentrations were determined using a ^{205}Pb-^{233}U-^{235}U mixed spike (Parrish and Krogh, 1987). Uranium and lead were loaded together on single rhenium filaments using H_3PO_4 and silica gel and analyzed in a VG Isomass 54R solid-source mass spectrometer in single collector mode (Daly photomultiplier). Analytical precision was better than 0.1 per cent for ^{207}Pb:^{206}Pb and ^{208}Pb:^{206}Pb, and better than 0.3 per cent for ^{205}Pb:^{207}Pb. Precisions for ^{204}Pb:^{205}Pb were as much as 1 per cent due to small ^{204}Pb ion beam currents (in the 10-16 A range). Total procedural blanks were approximately 40 picograms lead and 30 picograms uranium, based on repeated analyses of blanks during the period our analyses were carried out.

Lead:uranium and lead:lead errors for individual zircon fractions were obtained by individually propagating all calibration and analytical uncertainties through the date calculation and summing the individual contributions to total variance. Errors on individual U-Pb dates are quoted at the 2 sigma level (95% confidence interval). The U-Pb analytical data are given in Table 6-1-3.

DISCUSSION OF RESULTS

The Iskut River (Bronson) stock is either Early Jurassic or Late Triassic in age. This uncertainty is due to noncolinearity of the error ellipse for the +149-micron fraction relative to the ellipsoids for the other three fractions, all of which clearly show the effects of lead loss (Figure 6-1-2c). A best-fit chord through the three colinear points has an upper intercept of $225^{+100}/_{-40}$ Ma; the lower intercept is 142 Ma, but no significance is attached to this date. A best-fit chord through all four points and 0 Ma intersects concordia at 203±4 Ma. The youngest and oldest $^{207}Pb/^{206}Pb$ dates for the four fractions are 197±8 Ma and 208±2 Ma, respectively. We interpret the age of the Iskut River (Bronson) stock to lie between 197 and 225 Ma, based on the youngest $^{207}Pb/^{206}Pb$ date and the upper intercept for the three colinear points.

Zircons from the Red Bluff porphyry have a minimum age of 195±1 Ma, but are not likely to be much older. The effect of lead loss is evident from dispersion of three error ellipsoids along concordia (Figure 6-1-2b). This dispersion may be due to lead loss during a hydrothermal mineralizing event shortly after emplacement and crystallization of the intrusion (note that the sample contained significant pyrite). This interpretation is speculative and the problem of timing of lead loss from Red Bluff zircons will require further investigation. The error ellipse for the coarse, +149-micron fraction plots below concordia, and its errors are relatively large due to low-intensity ion beams (a result of sample loss during column chemistry), but its $^{206}Pb{:}^{238}U$ date is within error of the oldest concordant fraction. The anomalously high Pb:Pb date for this fraction may reflect minor inheritance of older radiogenic lead.

The Inel stock is 190±3 Ma old, based on the upper intercept with concordia of a best-fit chord through all four points, forced through 0 Ma (Figure 6-1-2d). Forcing the

TABLE 6-1-3
U-Pb ANALYTICAL DATA[1]

Sample Fraction[2]	Wt (mg)	U (ppm)	Pb[3]	Isotopic abundance[4] $^{206}Pb=100$ 208	207	204	6/4[5]	Isotopic ratios[6] ±2σ errors $^{206}Pb^*/^{238}U$	$^{207}Pb^*/^{235}U$	$^{207}Pb^*/^{206}Pb$
								Dates (Ma)[7] ±2σ errors		
AJM-ISK90-333 Iskut River (Bronson Stock)[8]										
−74	0.8	580	16.8	9.18	5.11	0.0074	8199	0.02944±16	0.20310±124	0.05003±16
NM2/2 ABR								**187.0±1.0**	**187.7±1.0**	**196.5±7.8**
−134+74	1.9	470	13.9	8.59	5.25	0.0161	5379	0.03020±14	0.20877±106	0.05013±6
NM2/2 ABR								**191.8±1.0**	**192.5±0.8**	**201.1±3.1**
−149+134	3.5	428	12.6	7.71	5.04	0.0017	31665	0.03038±14	0.21004±94	0.05015±6
NM2/2 ABR								**192.9±0.8**	**193.6±0.8**	**201.7±2.8**
+149	3.8	380	10.9	7.18	5.14	0.0075	11031	0.02976±20	0.20632±142	0.05029±4
NM2/2 ABR								**189.0±1.2**	**190.5±1.2**	**208.4±2.0**
AJM-ISK91-041 Red Bluff porphyry[9]										
−74	1.2	437	13.2	10.60	5.42	0.0290	3001	0.03018±16	0.20788±120	0.04995±10
NM2/2 ABR								**191.7±1.0**	**191.8±1.0**	**192.9±4.3**
−149+134	1.4	341	10.3	7.98	5.21	0.0142	5341	0.03077±16	0.21208±120	0.04999±14
NM2/2 ABR								**195.4±0.6**	**195.3±1.0**	**194.4±6.4**
+149	0.9	317	10.0	10.27	6.37	0.0886	1037	0.03099±30	0.21644±268	0.05066±38
NM2/2 ABR								**196.7±2.0**	**198.9±2.2**	**225.2±17.4**
−134+74	3.1	376	11.4	9.94	5.57	0.0388	2443	0.03040±18	0.20972±140	0.05003±18
NM2/2 ABR								**193.0±1.2**	**193.3±1.2**	**196.6±8.0**
AJM-ISK90-162 Inel stock[10]										
−74	5.3	590	18.4	21.29	5.34	0.0241	4002	0.02843±18	0.19536±132	0.04983±6
NM2/2 ABR								**180.7±1.2**	**181.2±1.2**	**187.3±3.2**
−134+74	2.2	521	17.1	22.52	6.31	0.0896	1084	0.02910±14	0.20054±112	0.04999±14
NM2/2 ABR								**184.9±0.8**	**185.6±1.0**	**194.4±6.4**
−149+134	0.8	487	15.2	17.92	5.51	0.0357	2400	0.02927±14	0.20135±116	0.04989±18
NM2/2 ABR								**186.0±1.0**	**186.3±1.0**	**189.7±8.2**
+149	0.3	484	18.7	28.75	10.98	0.4077	236	0.02956±24	0.20326±308	0.04987±62
NM2/2 ABR								**187.8±1.4**	**187.9±2.6**	**189.1±28.8**
DJA-90-PZ-1 Eskay porphyry[11]										
−74	0.5	489	15.3	21.63	5.21	0.0143	4213	0.02856±14	0.19670±94	0.04997±8
NM2/2 lightly abraded								**181.5±0.8**	**182.3±0.8**	**193.0±2.0**
−134+74	1.5	328	10.1	18.18	5.07	0.0059	9475	0.02909±14	0.19990±98	0.04984±8
NM2/2 ABR								**184.8±0.8**	**185.0±0.8**	**187.6±4.0**
−149+134	2.2	279	8.6	16.66	5.13	0.0102	7214	0.02920±16	0.20035±114	0.04977±10
NM2/2 ABR								**185.5±1.0**	**185.4±1.0**	**184.1±4.4**
+149	5.5	220	6.7	15.03	5.18	0.0131	6648	0.02913±22	0.20024±146	0.04986±10
NM2/2 ABR								**185.1±1.4**	**185.3±1.2**	**188.4±4.2**

NOTES:

[1] Complete analytical data, including the measured $^{206}Pb/^{204}Pb$ errors, the mole % blank Pb and the $Pb^*/(Pb^*+Pb_{common})$ ratios in the analyses, the assumed Stacey-Kramers common Pb ages and their errors, and the correlation coefficients for the Pb/U ratios, are recorded on UBC Geochronometry Laboratory data sheets.

[2] −149+74 = size range in microns; all fractions are nonmagnetic on Frantz isodynamic separator at 2 A and 2° side tilt; all fractions were abraded to remove outer rims.

[3] radiogenic + common Pb.

[4] radiogenic + common Pb, corrected for 0.15%/amu fractionation and for 40 pg Pb blank with composition 208:207:206:204=37.30±0.75:15.50±0.34:17.75±0.19:1.

[5] $^{206}Pb/^{204}Pb$ measured, corrected for 0.15%/amu fractionation.

[6] corrected for fractionation (0.12%/amu for U, 0.15%/amu for Pb), blank Pb (see note 4 above), and for common Pb using the Stacey and Kramers (1975) growth curve; errors are 2 sigma, only last digits are shown.

[7] decay constants used in age calculation : $\lambda^{238}U=1.55125\times10^{-10}$, $\lambda^{235}U=9.8485\times10^{-10}$; $^{238}U/^{235}U=137.88$ (Steiger and Jager, 1977). Errors are 2 sigma.

[8] collected by AJM, Latitude : 56° 40′ 32″ N, Longitude : 131° 06′ 30″ W; UTM zone 370800 E, 6283270N.

[9] collected by AJM, Latitude : 56° 40′ 0″ N, Longitude : 131° 07′ 37″ W; UTM zone 371300 E, 6282340 N.

[10] collected by AJM, Latitude : 56° 37′ 45″ N, Longitude : 130° 57′ 18″ W; UTM zone 379800 E, 6275700 N.

[11] collected by DJA, Latitude : 56° 38′ 23″ N, Longitude : 130° 26′ 40″ W; UTM zone 411650 E, 6277350 N

chord through 0 Ma is reasonable given the roughly similar Pb:Pb dates of all four fractions, which have clearly suffered some lead loss. The analytical errors for the coarse, +149-micron fraction are somewhat large, due to low-intensity ion beams (small sample load, also reflected in low ^{206}Pb:^{204}Pb ratio), but this does not affect the age interpretation for this sample.

Sample DJA-90-PZ-1 of the Eskay porphyry yields an age of 186±2 Ma based on mutual overlap of three error ellipsoids with concordia (Figure 6-1-2a). A fourth, lightly abraded, very fine grained fraction plots below concordia, probably due to minor lead loss. The good analytical quality of the data suggests that the age of the Eskay porphyry is early Toarcian.

SUMMARY

Interpreted ages for the Inel stock and Red Bluff porphyry (190±3 and 195±1Ma, respectively) fall well within the range of Early Jurassic plutonism coeval with Hazleton arc volcanic rocks (205-187 Ma, Table 6-1-1). The interpreted age for the Eskay porphyry (186±2 Ma) is slightly younger than the age range of the Early Jurassic event, although the difference is minimal; at this time, we interpret the Eskay porphyry to be a member of the Early Jurassic Texas Creek suite, thus extending the known time span for this plutonic event in the Iskut River area.

The age of the Iskut River (Bronson) stock is uncertain, due to the highly discordant and variable nature of the data set; it is likely that the stock has an age between 225 and 197 Ma (Late Triassic to Hettangian/Sinemurian). Further work will be required to improve this estimate.

ACKNOWLEDGMENTS

We are grateful for the assistance of the following property operators for providing permission and logistical help to map and sample as part of this study: Cominco Ltd. and Cominco Metals (Snip mine), Prime Equities Inc. (Iskut Joint Venture and Eskay Creek), International Corona Corporation (Eskay Creek) and Gulf International Minerals Ltd. (Inel). An original version of the manuscript has been improved greatly from review by Lindsay Bottomer (Prime Equities Inc.) Robert G. Anderson and Mary Lou Bevier

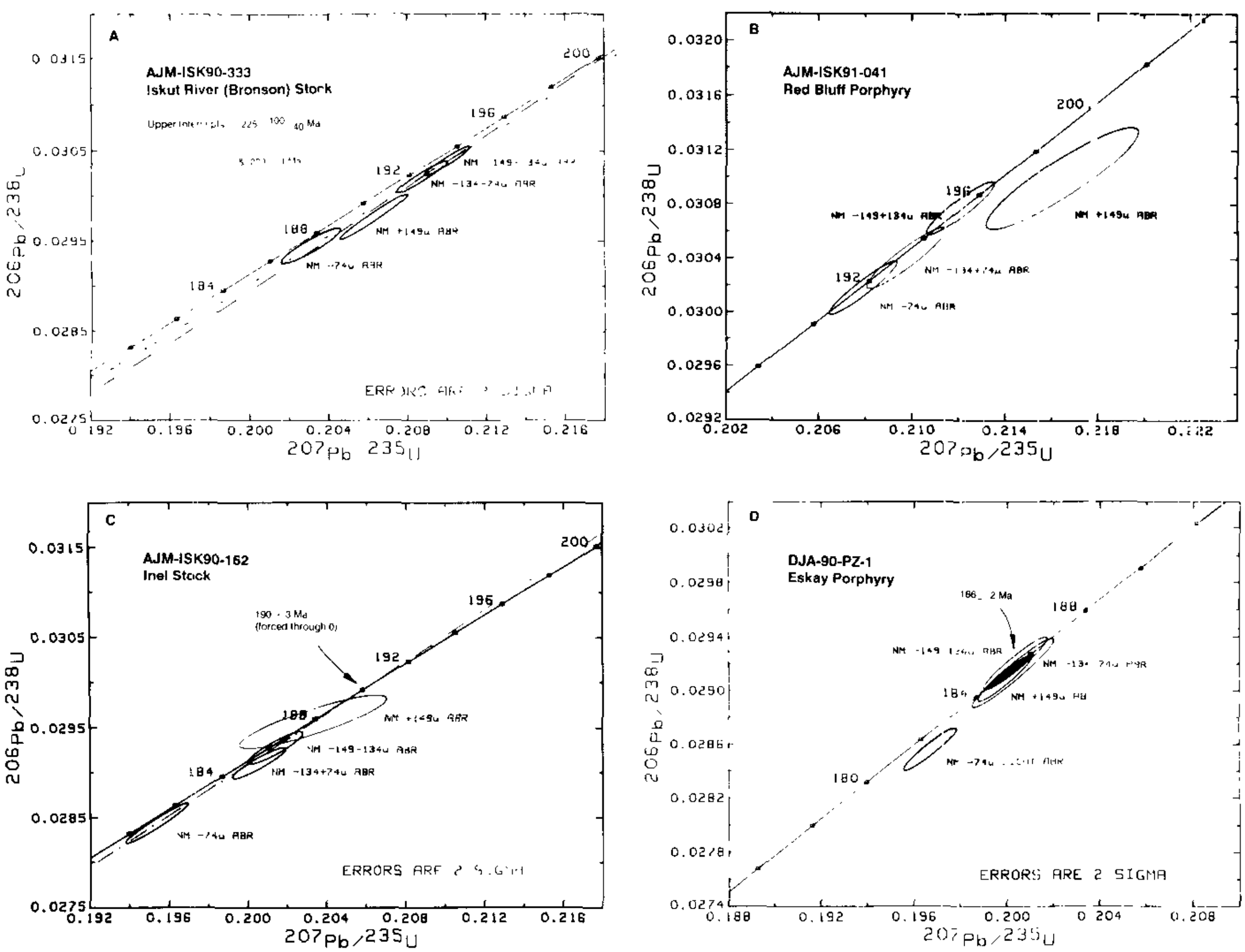

Figure 6-1-2. ^{206}Pb:^{238}U Vs. ^{207}Pb:^{235}U concordia graphs for (a) Eskay Creek porphyry (b) Red Bluff porphyry (c) Iskut River (Bronson) stock (d) Inel stock.

(Geological Survey of Canada), and the editorial staff of the British Columbia Geological Survey Branch and, in particular, John Newell.

Funding for the MDRU Project "Metallogenesis of the Iskut River Area" is provided by thirteen exploration and mining companies, a Science Council of British Columbia Research and Technology Grant, and a Natural Science and Engineering Council Research CRD Grant.

REFERENCES

Alldrick, D.J. (1987): Geology and Mineral Deposits of the Salmon River Valley, Stewart Area (104A/B); *B.C. Ministry of Energy, Mines and Petroleum Resources*, Open File 1987-22.

Alldrick, D.J., Brown, D.A., Harakal, J.L., Mortensen, J.K. and Armstrong, R.L. (1987): Geochronology of the Stewart Mining Camp; *in* Geological Fieldwork 1986, *B.C. Ministry of Energy, Mines and Petroleum Resources*, Paper 1987-1, pages 81-92.

Alldrick, D.J., Mortensen, J.K. and Armstrong, R.L. (1986): Uranium-Lead Age Determinations in the Stewart Area; *in* Geological Fieldwork 1985, *B.C. Ministry of Energy, Mines and Petroleum Resources*, Paper 1986-1, pages 217-218.

Anderson, R.G. (1989): A Stratigraphic, Plutonic and Structural Framework for the Iskut River Map Area, Northwestern British Colmbia; *in* Current Research, Part E, *Geological Survey of Canada*, Paper 89-1E, pages 145-154, 1989

Anderson, R.G. and Bevier, M.L. (1990): A Note on Mesozoic and Tertiary K-Ar Geochronometry of Plutonic Suites, Iskut River Map Area, Northwestern British Columbia; *in* Current Research, Part E, *Geological Survey of Canada*, Paper 90-1E, 1990, pages 141-147.

Anderson, R.G., Bevier, M.L. and Reichenbach (1991): Jurassic Magmatism in NW Stikinia and North Central Wrangellia, British Columbia, Abstracts with Programs, *Geological Society of America*, Annual Meeting. October 1991, San Diego, California, Volume 23, Number 5, page A190.

Anderson, R.G. and Thorkelson, D.J. (1990): Mesozoic Stratigraphy and Setting for Some Mineral Deposits in Iskut River Map Area, Northwestern British Columbia; *in* Current Research, Part E, *Geological Survey of Canada*, Paper 90-1E, pages 131-140.

Bevier, M.L. and Anderson, R.G. (1991): Jurassic Geochronometry in NW Stikinia (56-57° N), British Columbia; Abstracts with Programs, *Geological Society of America*, Annual Meeting, October 1991, San Diego, California, Volume 23, Number 5, page A191.

Britten, R.M. and Alldrick, D.J. (1990): Gold Deposits in the Iskut-Stikine, Northwestern B.C.; abstract in *Geological Association of Canada/Mineralogical Association of Canada*, Annual General Meeting, Vancouver, May, 1990, Program with Abstracts, page A15.

Britton, J.M., Blackwell, J.D. and Schroeter, T.G. (1990a): Eskay Creek (104B 008); *in* Exploration in British Columbia 1989, *B.C. Ministry of Energy, Mines and Petroleum Resources*, pages 197-223.

Britton, J.M., Fletcher, B.A. and Alldrick, D.J. (1990b): Snippaker Map Area (104B/6E, 7W, 10W, 11E); *in* Geological Fieldwork 1989, *B.C. Ministry of Energy, Mines and Petroleum Resources*, Paper 1990-1, pages 115-125.

Brown, D.L. (1987): Geological Setting of the Volcanic Hosted Silbak Premier Mine, Northwestern British Columbia (104A/4, 104B/1); unpublished M.Sc. thesis, *The University of British Columbia*, 1987, 203 pages.

Donnelly, D.A. (1976): A Study of the Volcanic Stratigraphy and Volcanogenic Mineralization on the KAY Claim Group, Northwestern British Columbia; unpublished B.Sc. thesis, *The University of British Columbia*, 59 pages.

Grove, E.W. (1971): Geology and Mineral Deposits of the Stewart Area, British Columbia; *B.C. Ministry of Energy, Mines and Petroleum Resources*, Bulletin 58, 219 pages.

Harland, W.B., Armstrong, R.L., Cox, A.V., Craig, L.E., Smith, A.G. and Smith D.G. (1989): A Geologic Time Scale 1989; *Cambridge University Press.*

Krogh, T.E. (1973): A Low Contamination Method for Hydrothermal Decomposition of Zircon and Extraction of U and Pb for Isotopic Age Determinations; *Geochimica et Cosmochimica Acta*, Volume 37, pages 485-494.

Krogh, T.E. (1982): Improved Accuracy of U-Pb Ages by the Creation of More Concordant Systems Using an Air Abrasion Technique; *Geochimica et Cosmochimica Acta*, Volume 46, pages 637-649.

Macdonald, A.J., Ettlinger, A.D. and Thompson, J.F.H. (1991): Metallogeny of the Iskut River Area, Northwestern British Columbia, Canada; Abstracts with Programs; *Geological Society of America*, Annual Meeting, October 1991, San Diego, California, Volume 23, page A413.

Nadaraju, G. and Smith, P.L. (1992): Jurassic Biochronology of the Iskut River Map Area: a Progress Report; *in* Current Research, Paper 1992-1A, *Geological Survey of Canada*, in press.

Parrish, R.R. (1987): An Improved Micro-capsule for Zircon Dissolution in U-Pb Geochronology; *Isotope Geoscience*, Volume 66, pages 99-102.

Parrish, R.R. and Krogh, T.E. (1987): Synthesis and Purification of ^{205}Pb for U-Pb Geochronology; *Isotope Geoscience*, Volume 66, pages 103-110.

Rhys, D.A. and Godwin, C.I. (1992): Preliminary Interpretation of the Snip Mine (104B/11): *in* Geological Fieldwork 1991, Grant, B. and Newell, J.M., Editors, *B.C. Ministry of Energy, Mines and Petroleum Resources*, Paper 1992-1, this volume.

Stacey, J.S. and Kramers, J.D. (1975): Approximation of Terrestrial Lead Isotope Evolution by a Two-stage Model; *Earth and Planetary Science Letters*, Volume 26, pages 207-221.

Steiger, R.H. and Jager, E. (1977): Subcommission on Geochronology: Convention on the Use of Decay Constants in Geo- and Cosmochronology; *Earth and Planetary Science Letters*. Volume 36, pages 359-362.

Streckeisen, A., and LeMaitre, R.W.L. (1979): A Chemical Approximation to the Modal QAPF Classification of the Igneous Rocks; *Neues Jahrbuch fuer Mineralogie*, Abhandlunguer, Stutgaart, Volume 136, pages 169-206.

Wheeler, J.O. and McFeely P. (1987): Tectonic Assemblage Map of the Canadian Cordillera and Adjacent Parts of the United States of America; *Geological Survey of Canada*, Open File 1565.

NOTES

SILVER-GOLD VEIN MINERALIZATION, WEST ZONE, BRUCEJACK LAKE, NORTHWESTERN BRITISH COLUMBIA (104B/8E)

By Stephen Roach, Newhawk Gold Mines Ltd. and
A. James Macdonald, Mineral Deposit Research Unit,
The University of British Columbia

(MDRU Contribution 003)

KEYWORDS: Economic geology, Hazelton Group, Stikine assemblage, Sulphurets, metallogeny, structure, gold, silver, Brucejack Lake, vein.

INTRODUCTION

The West zone is one of over 20 mineralized zones and showings on the Sulphurets property (Newhawk Gold Mines Limited, 60%; Granduc Mines Limited, 40%), located 65 kilometres north of Stewart, British Columbia (Figures 6-2-1). Intial fieldwork was completed by the senior author in 1989 (Roach, 1990), comprising grid mapping of lithologies and alteration assemblages in the West Zone and the recording of structural data (attitudes of veins and principal fabrics). In 1991, the co-author extended mapping to include traverses in the Brucejack Lake area in a 2-kilometre radius around the West zone. In addition, 14 diamond-drill holes on a section through the centre of the West zone were studied and sampled extensively in 1991. This report discusses the geology and structure observed at surface in the West zone. Further objectives of the study are to define:

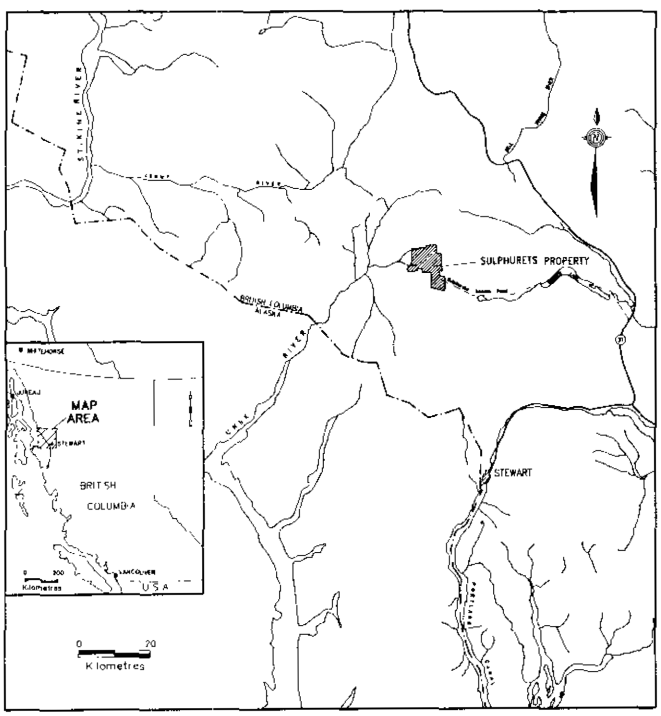

Figure 6-2-1. Location map, Stewart-Iskut River district, northwestern British Columbia.

- Lithostratigraphic relationships between hostrocks to precious metal vein mineralization.
- Alteration mineralogy and chemistry around mineralized zones.
- Hypogene mineralogy of the vein systems in the Brucejack Lake area.
- An examination of vein material to assess applicability for fluid inclusion studies.

HISTORY OF THE SULPHURETS PROPERTY

The Sulphurets property covers approximately 85 square kimometres (Figure 6-2-2). A small fractional claim (500 by 20 m), located 5 kilometres north of the West zone, is owned by a third party. Exploration for placer gold in the Unuk River valley and subsidiary valleys such as that occupied by Sulphurets Creek, was first recorded in the 1880s, although there are no production data. In 1935, prospectors located copper mineralization in the area now referred to as the Main Copper zone (Figure 6-2-2). Prospecting in the Brucejack Lake area continued intermittently until 1959, when gold and silver mineralization was first reported. In 1960, Granduc Mines Ltd. staked most of the area comprising the current property and began an exploration program for porphyry copper mineralization, employing airborne and ground geophysics in addition to reconnaissance geology; as a result copper mineralization was discovered on the ridge between the Mitchell and Sulphurets glaciers and gold and silver mineralization at the base of the Iron Cap area (Bridge *et al.*, 1981). Exploration continued sporadically on the property from 1961 to 1974, with the focus on diamond drilling of anomalies identified by geophysical and geochemical prospecting techniques. During the period 1961-1963 R.V. Kirkham completed an M.Sc. thesis comprising geological mapping of the bulk of the property (Kirkham, 1963). The Brucejack Lake area was prospected in 1975. Relatively little exploration activity occurred at Sulphurets until 1980, when Esso Minerals Ltd. optioned the property from Granduc, conducted detailed and reconnaissance geological mapping and geochemical sampling throughout the property, and diamond drilling, which focused principally on the West and Shore zones (Figure 6-2-2). In 1985, Newhawk Gold Mines Ltd and Lacana Mining Corporation optioned the property from Granduc and continued with intensive exploration on the West zone, driving an exploration decline to the 1150-metre level, approximately 250 metres below surface (Roach, 1990) providing access for extensive underground diamond drilling and reserve delineation.

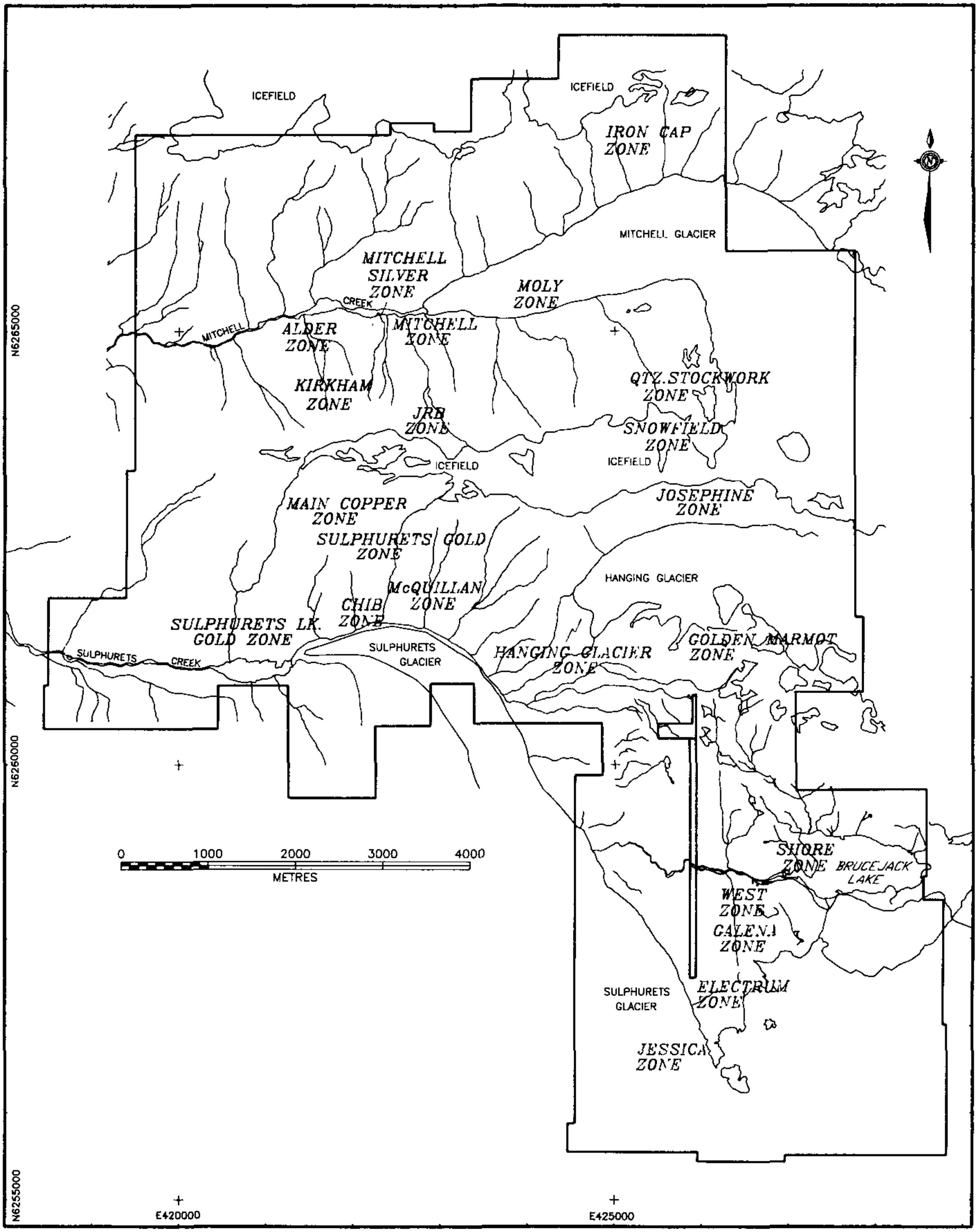

Figure 6-2-2. Sulphurets property, with location of mineralized zones.

In 1989, Newhawk commissioned an independent report of *in situ* ore reserves by Watts, Griffis and McOuat, Consulting Geologists and Engineers of Toronto. Using a cut-off grade of 0.2 ounces per ton (approximately 6.9 g/t Au) and a minimum true width of 5 feet (approximately 1.5 metres), proven and probable reserves were announced (Newhawk Gold Mines, Press Release, February 6, 1990) as 715 400 tons (approximately 650000 tonnes) at a gold grade of 0.431 ounces per ton (14.8 g/t) and a silver grade of 19.7 ounces per ton (675 g/t). Based upon the ore reserve, International Corona Corporation, which holds a 42 per cent interest in Newhawk, conducted a feasibility study for the West zone, concluding that the project was uneconomic under existing conditions (Newhawk Gold Mines, Press Release, October 25, 1990). The decline was allowed to flood in 1990.

REGIONAL GEOLOGY

LITHOSTRATIGRAPHY

The Sulphurets property and surrounding area is within the Stikine Terrane (Wheeler and McFeely, 1987) and is underlain by Upper Triassic and Lower to Middle Jurassic Hazleton Group volcanic, volcaniclastic and sedimentary rocks (Grove, 1986). The lithostratigraphic assemblage in the Sulphurets area has been described by Kirkham (1963), Britton and Alldrick (1988), Alldrick and Britton (1991) and Kirkham *et al.* (in preparation), and comprises a package, from oldest to youngest, of alternating siltstones and conglomerates (lower Unuk River Formation, Norian to Hettangian); alternating intermediate volcanic rocks and siltstones (upper Unuk River Formation, Hettangian to Pliensbachian); alternating conglomerates, sandstones, intermediate and mafic volcanic rocks (Betty Creek Formation, Pliensbachian to Toarcian); felsic pyroclastic rocks and flows, including tuffaceous rocks ranging from dust tuff to tuff breccias and localized welded ash tuffs (Mount Dilworth Formation, Toarcian); and, finally, alternating siltstones and sandstones (Salmon River and Bowser formations, Toarcian to Bajocian). Britton and Alldrick (1988) also describe at least three intrusive episodes in the area: intermediate to felsic plutons that are probably coeval with volcanic and volcaniclastic supracrustal rocks; small stocks related to the Cretaceous Coast Plutonic Complex; minor Tertiary dikes and sills. Regional geological mapping (*e.g.* Britton and Alldrick, 1988; Anderson, 1989) has demonstrated the continuity of lithologies and formations from well-constrained areas, such as the Stewart mining camp to the south (*e.g.* Alldrick *et al.*, 1987) to the Sulphurets area. In the immediate Sulphurets area, however, age constraints are poor at present, although considerable work in progress is addressing this problem, for example, by using high-precision U-Pb and K-Ar geochronometry.

Researchers include Anderson, Kirkham and Bevier (Geological Survey of Canada), Alldrick, Britton and co-workers (British Columbia Geological Survey), Bridge (M.A.Sc. candidate, The University of British Columbia), Margolis (Ph.D. candidate, University of Oregon), and the authors of this study. In addition, Smith and Nadaraju of The University of British Columbia are conducting paleontological studies in the area. It is anticipated that a more tightly constrained framework for the relative and absolute ages of rocks in the Sulphurets area will be forthcoming in the near future.

STRUCTURE

Britton and Alldrick (1988) and Kirkham *et al.* (in preparation) have described the regional structural geology; in brief, the Hazleton Group lithologies display fold styles ranging from gently warped (*e.g.*, a mapped synform to the south and east of Brucejack Lake, Alldrick and Britton, 1988) to tight disharmonic folds in the Salmon River and Bowser formations. Synvolcanic, synsedimentary and syn-intrusive faults are suspected but are yet to be documented fully (Kirkham *et al.*, in preparation); Britton and Alldrick (1988), however, describe a syndepositional fault to the northeast of the Sulphurets property. Northerly striking, steep normal faults are recognised (*e.g* Britton and Alldrick, 1988), although certain prominent northerly striking lineaments, such as the Brucejack lineament (Kirkham, 1963, 1991), immediately west of the West zone, display evidence for little, if any, motion, at least in the Brucejack Lake area. Kirkham *et al.* (in preparation) note that elsewhere along this linear, hydrothermal alteration zones are truncated. Minor thrust faults, dipping westerly, are common in the region and are important in the northern and western parts of the Sulphurets property in regard to interpretation of mineralized zones. Ongoing research by the Geological Survey of Canada and by Peter Lewis of the Mineral Deposit Research Unit at The University of British Columbia will add significantly to the near-term structural understanding of the area.

During the 1991 field season, an intermediate to felsic flow-dome complex has been defined at the southeast corner of Brucejack Lake, first identified, apparently, by G. Albino and J. Margolis (International Corona Corporation; personal communication, 1990). The rock is flow banded, locally flow folded and intrudes heterogeneous, bedded to massive pyroclastic rocks, locally red, maroon or green coloured, and locally potassium feldspar and plagioclase-hornblende-porphyritic flows, ascribed to the upper Unuk River and Betty Creek formations by Alldrick and Britton (1988). The flow-banded unit has gradational contacts with a voluminous breccia unit, comprising clasts of identical composition to the intrusive phase, in a hematitic, muddy and locally finely laminated matrix. The morphology and geometry of the breccias suggests conformity with enclosing flow rocks, including potassium feldspar and plagioclase-hornblende-phyric flows; the breccias are interpreted as volcanic ejecta, cemented by subaqueous, iron-rich pelitic material. Higher in the section to the south of Brucejack Lake, the flow-banded intermediate to felsic unit rests in apparent stratigraphic contact upon marooon, blocky tuff. These field relationships indicate that the flow-banded unit passes up-section from intrusive at depth, to complex interdigitations with related ejecta at intermediate levels, to extrusive at the highest observed level.

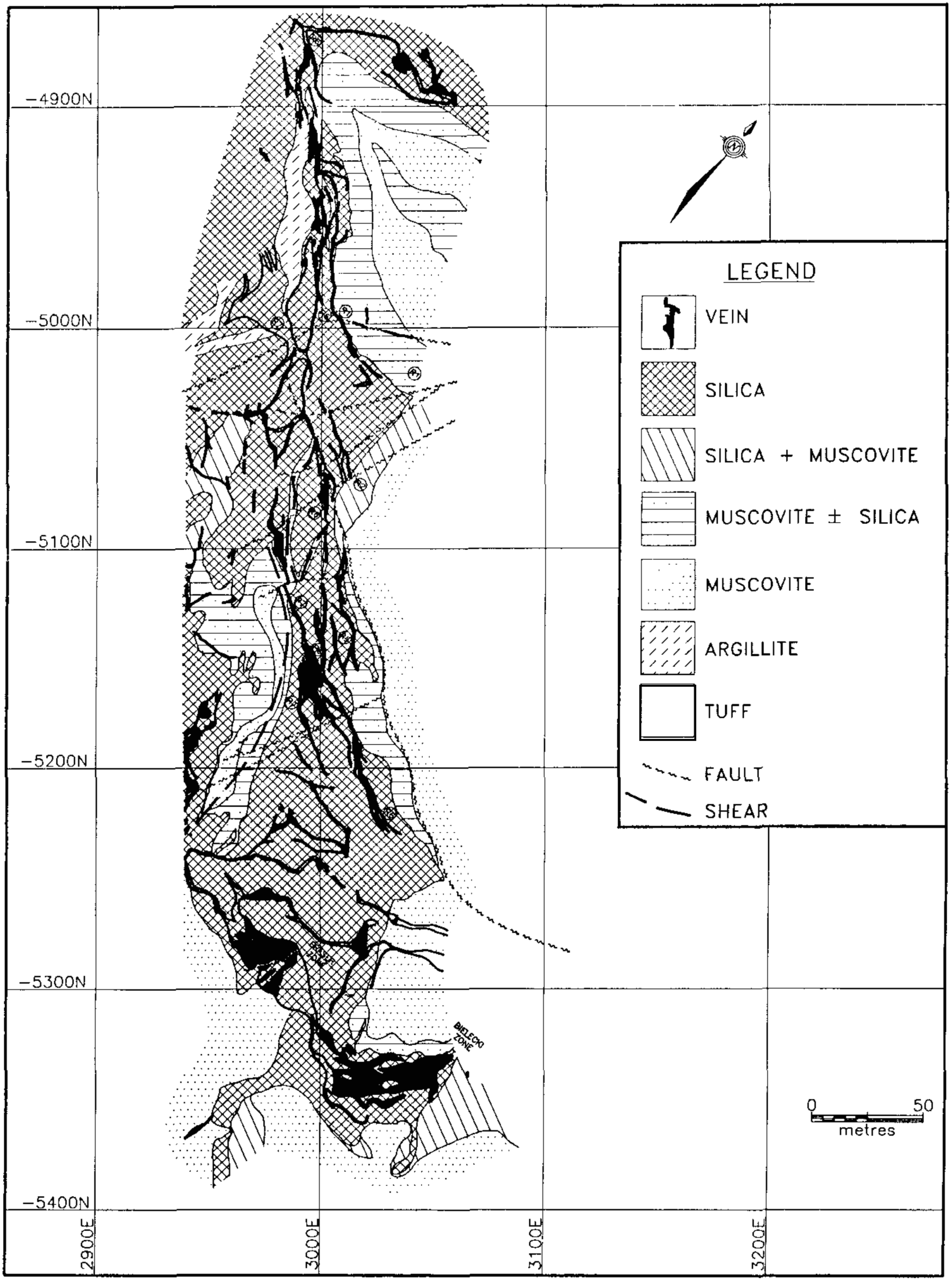

Figure 6-2-3. Map of the West zone (modified from Roach, 1990), showing distribution of mineralized and hydrothermally altered zones.

GEOLOGY OF THE WEST ZONE

Rocks underlying the West zone are considered by Britton and Alldrick (1988), and Alldrick and Britton (1988) to be confined to the Unuk River Formation and consist of a band of generally northwesterly-trending volcanic and sedimentary rocks 400 to 500 metres wide, sandwiched between two plagioclase and hornblende-phyric intrusive bodies (Kirkham, 1991). The hostrocks are dominantly intermediate volcanic (pyroclastic) rocks to the northeast of the zone, and intermediate volcaniclastic rocks and minor argillaceous rocks to the southwest (Roach, 1990; Figure 6-2-3). Geological relationships and original characteristics of the host lithologies are obscured in the vicinity of the mineralized rocks, as a result of intense hydrothermal alteration and the development of penetrative fabric(s).

In the immediate vicinity of the West zone, intermediate tuffs and tuff breccias have been strongly silicified and (?) potassium feldspar altered, brecciated and fractured, with subsequent silica influx into the zones of brecciation and fracturing, resulting in vein and stockwork zones containing up to 20 per cent quartz, over widths to 35 metres on surface (Figure 6-2-3). Roach (1990) has identified a well-developed zonation of hypogene alteration about the mineralized zone, up to 100 metres wide at surface. From the core of the West zone to its mappable outer margins, the alteration assemblages, with the first mineral listed being dominant, are:

1. Quartz ± sericite ± carbonate
2. Sericite ± quartz ± carbonate
3. Chlorite ± sericite ± carbonate
4. Clay

In addition, diamond-drill core reveals the presence of considerable potassium feldspar and at least two carbonate species. Few petrographic and mineralogic data on the alteration mineralogy are currently available, and are a focus of on-going work.

WEST ZONE MINERALIZATION

The West zone comprises at least ten quartz vein and veinlet shoots (Figures 6-2-3 and 4), named R1, R2, R4, R5, R6, R7, R8, UTC, Bielecki and Eraser; the nearby Old Yeller zone is approximately 150 metres to the south-southeast. Some shoots do not outcrop and are known only from underground development and exploration (Figure 6-2-4). Description in this paper is restricted to geological relationships exposed on surface and in diamond-drill core. The R6 shoot is the most extensive within the West zone, exposed along a strike length of 250 metres, and ranges in thickness from 0.3 to 6 metres. Ore shoots tend to have greater down-plunge extent (to the northeast) than in the strike dimension (Kirkham *et al.*, in preparation); the structural geology of various elements of the West zone is described in the next section. With the exception of R7, the other shoots with prefix R are structures that splay off R6; these relationships are amplified later in this paper.

Gangue mineralogy in the veins is dominated by quartz, with accessory potassium feldspar, albite and sericite, and minor carbonate (at least two varieties noted in core: white calcite and an orange, calcium-magnesium carbonate, probably kutnohorite; R.H. Sillitoe, personal communication, 1991), barite, apatite and rutile (Harris, 1989). Sulphides in the veins include, in decreasing order of abundance, pyrite, sphalerite, chalcopyrite and galena; silver is present as tetrahedrite, pyrargyrite, polybasite, electrum and native silver, with rare stephanite and acanthite; native gold has been described, although electrum is the principal auriferous phase (Harris, 1989; Kirkham *et al.*, in preparation). At least six vein and veinlet assemblages have been documented macroscopically in this study based upon crosscutting relationships observed in diamond-drill core; from earliest to latest, they are:

1. Potassium feldspar and quartz microveinlets (1 mm in width)
2. Quartz-carbonate veins and veinlets – generation (i)
3. Pyrite-sphalerite-galena veinlets
4. Quartz-carbonate veins and veinlets – generation (ii)
5. Quartz (alone) veins and veinlets – generation (i)
6. Quartz (alone) veins and veinlets – generation (ii)

This preliminary paragenesis is to be confirmed by petrography and will form the basis for a study of the applicability of the West zone material for microthermometric analysis of fluid inclusions. Petrography and lithogeochemistry will also be used to characterize the hypogene alteration related to West zone mineralization.

STRUCTURE OF WEST ZONE AREA

The West zone has an overall southeasterly strike, approximately 140°, although internal structural elements such as veins, veinlet arrays and associated penetrative fabric(s) are complex and variable (Figures 6-2-3 and 4). Most of the structural data presented in this paper were collected predominantly by the senior author in 1989, during a surface mapping program conducted by Newhawk Gold Mines (Roach, 1990); additional data, collected by the co-author in 1991, are also included. The dominant fabric in the rocks at some distance (100 m) from the West zone dips steeply and strikes to the south-southeast (160°; Figure 6-2-5). Approaching the West zone, the fabric is rotated to between 110° and 130°, throughout a zone approximately 130 metres wide, that correlates spatially with the most altered and highly strained hostrocks. The sense of rotation suggests sinistral shear in the West zone, based upon typical geometries of structural elements in a shear zone (*e.g.*, Tchalenko, 1970). These relationships are, however, complicated by development of a northeasterly (30° to 70°) fabric over a zone 40 metres wide to the northeast of the high-strain rocks (Figure 6-2-5).

The majority of veins observed on surface dip steeply to the northeast and strike approximately parallel to the trend of the zone (*i.e.*, 140°), although locally exhibiting sygmoidal terminations (Figures 6-2-4 and 5). Veins of this geometry are "central shear veins" and "oblique shear veins", using the terminology of Hodgson (1989a, b). Subsidiary, second-order veins branch off the principal veins, and strike between 100° and 130°; again, this vein geometry supports a

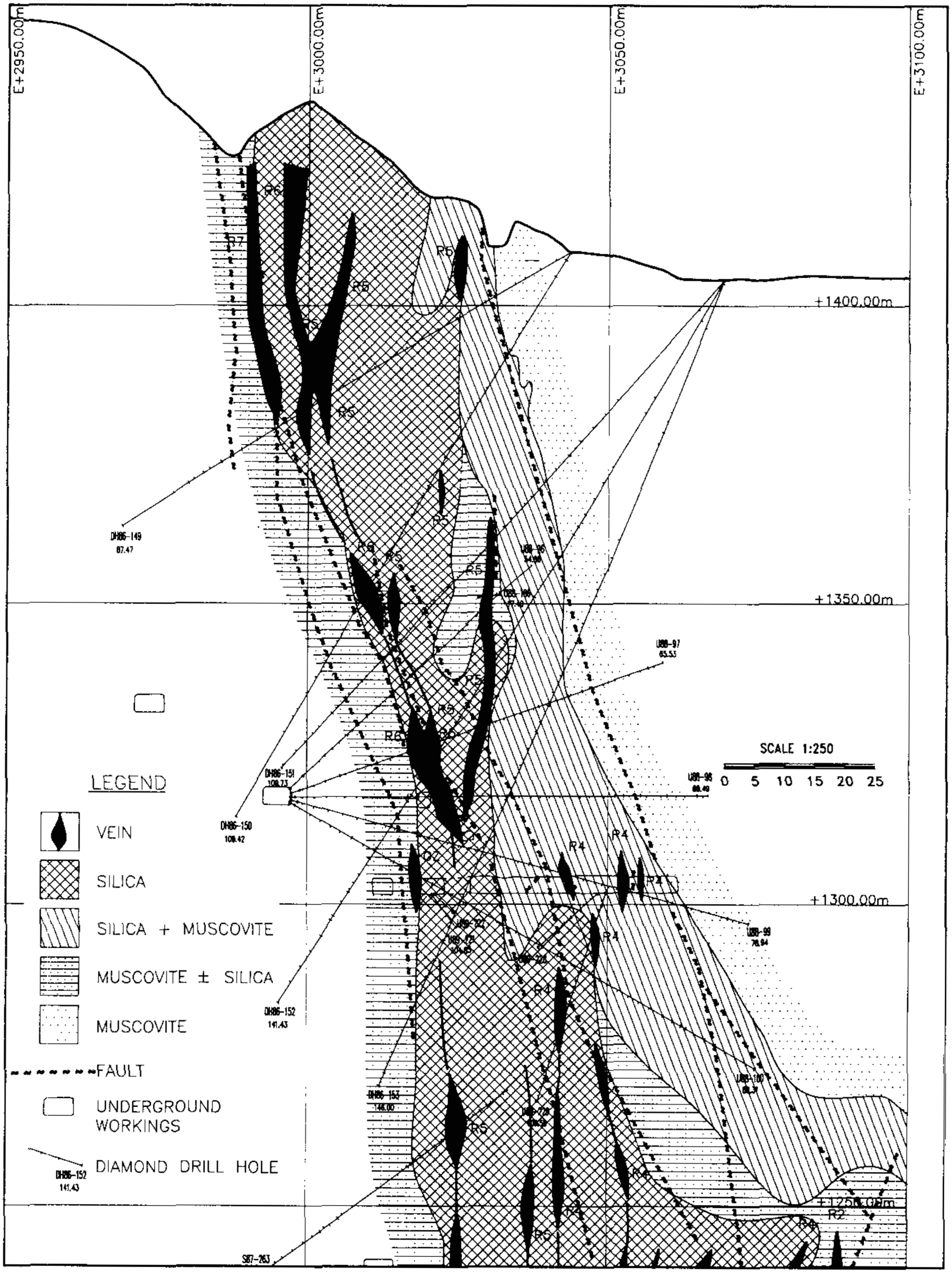

Figure 6-2-4. Cross-section 51+00 S, West zone.

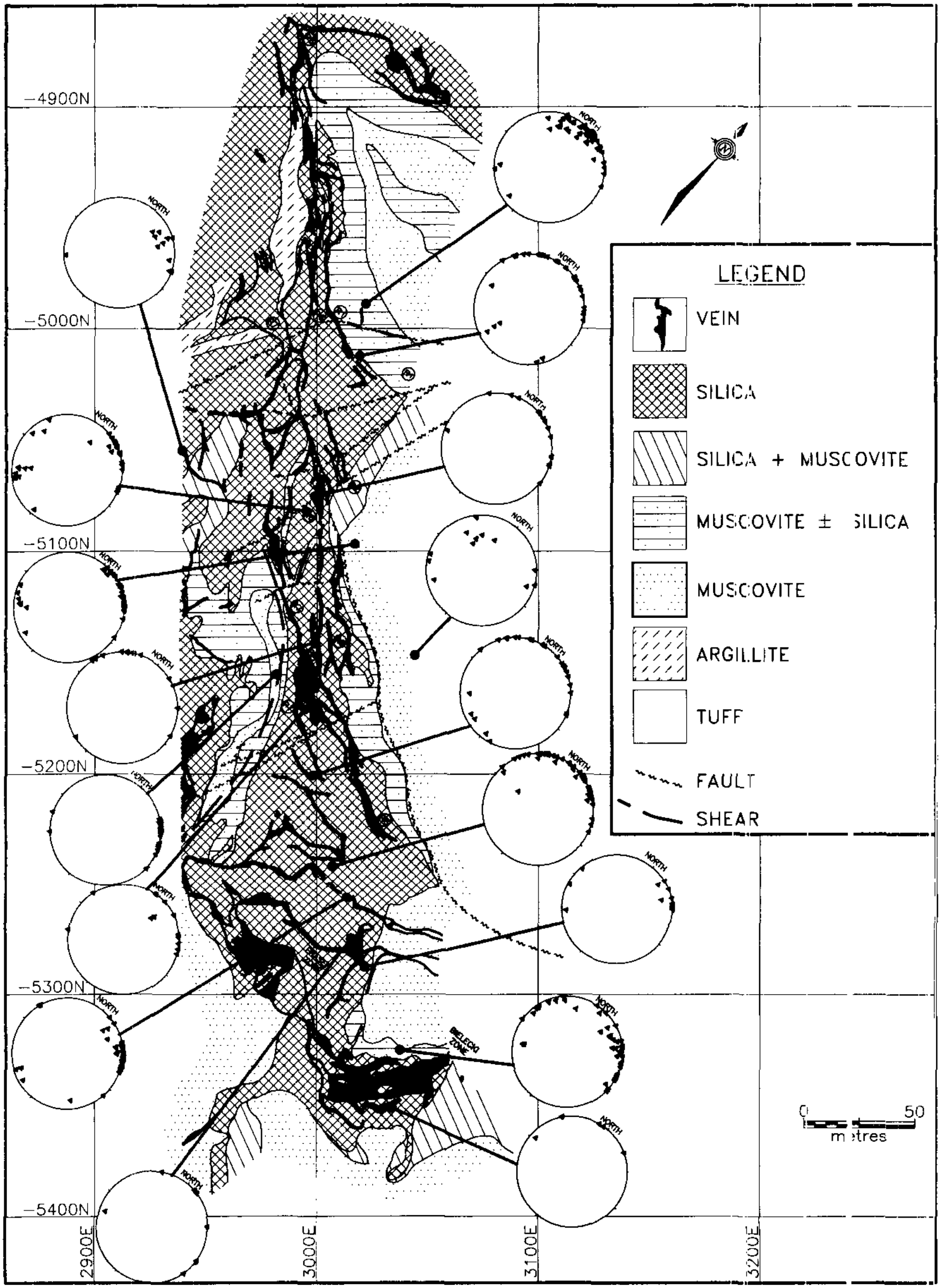

Figure 6-2-5. Lower hemisphere projections of poles to structural elements within and adjacent to the West zone.

sense of sinistral shear. In addition, a few veins follow northeast structures, oblique to the general trend, and dip steeply to the southeast and northwest (note that attitudes at depth differ from those at surface – the vein system tends to steepen and dip to the southwest; B. Way, Newhawk Gold Mines Ltd., personal communication, 1991). Individual veins and composite vein sets exposed on surface in the West zone exhibit evidence of crack-seal fill with slivers of altered wallrock included within veins; and also vein fill in an extensional environment, subjected to contemporaneous folding and localized brecciation during crystallization of gangue minerals, for example quartz and carbonate (Roach, 1990; Kirkham *et al.*, in preparation; and this study); observed features at surface include (from apparently least strained to most strained): vug fills of quartz with unbroken crystal terminations; vug fills in small-scale (5–10 cm wavelength) folds; extension gash veins; second-order central or oblique veins; sigmoidal central or oblique veins, locally conjugate arrays of sigmoidal veins and veinlets. These geometric relationships between veins are observed on several scales – from hand-specimen to map scale (note, for example, the sigmoidal, enechelon and branching vein geometries in Figures 6-2-3, 6-2-4), and are consistent with fluid influx (and hydrothermal alteration) during predominantly ductile deformation, interrupted periodically by brittle failure in response to a fluctuating fluid pressure (*e.g.*, Sibson *et al.*, 1975).

SUMMARY

Vein-hosted, gold-silver mineralization in the West zone at Brucejack Lake, is contained within a zone of intensely altered and strained volcanic and volcaniclastic rocks. Alteration is zoned about the mineralized veins and veinlet arrays, from a central silicified zone, passing outwards to sericite, to chlorite and finally to clay; accessory sericite and carbonate are found throughout each alteration facies. The geometry of structural elements observed on surface in the West zone described here is compatible with high strain zones, as synthesized by, for example, Hodgson (1989b).

ACKNOWLEDGMENTS

The authors wish to thank the owners and management of Newhawk Gold Mines Ltd. for permission to publish this work. The co-author also wishes to acknowledge the considerable logistical and technical assistance received from Newhawk; in particular from, Fred Hewett, Barry Way and Dave Visagie. We are most grateful for much assistance from geologists visiting the West zone during 1991: including, R.V. Kirkham (G.S.C., Ottawa), J. Margolis (Ph.D. candidate, University of Oregon) and R.H. Sillitoe (London). We also thank Tim Kirby (Newhawk Gold Mines) for providing digitized diagrams and Kirk Simpson (Ibex Drafting) for diagram preparation. The co-author has benefited from discussions with Peter Lewis of the Mineral Deposit Research Unit concerning structural geology at Brucejack Lake; the paper has been improved by reviews by Brian Grant and John Newell.

This paper is dedicated to the memory of Phil Malone.

REFERENCES

Alldrick, D.J. and Britton, J.M. (1988): Geology and Mineral Deposits of the Sulphurets Area; *B.C. Ministry of Energy, Mines and Petroleum Resources*, Open File Map 1988-4

Alldrick, D.J. and Britton, J.M. (1991): Sulphurets Area Geology; *B.C. Ministry of Energy, Mines and Petroleum Resources*, Open File 1991-21.

Alldrick, D.J., Brown, D.A., Harakal, J.E., Mortensen, J.K. and Armstrong, R.L. (1987): Geochronology of the Stewart Mining Camp; *in* Geological Fieldwork 1986, *B.C. Ministry of Energy, Mines and Petroleum Resources*, Paper 1987-1, pages 81-92.

Anderson, R.G. (1989): A Stratigraphic, Plutonic, and Structural Framework for the Iskut River Map Area, Northwestern British Columbia; *in* Current Research, Part E, *Geological Survey of Canada*, Paper 89-1E, pages 145-154.

Bridge, D.A., Ferguson, L.J. and Brown, M.G. (1981): 1980 Exploration Report on the Sulphurets Property, Skeena Mining Division, B.C.; unpublished internal report, *Granduc Mines Ltd., Esso Resources Canada Ltd. and Sidney F. Ross.*

Britton, J.M. and Alldrick, D.J. (1988): Sulphurets Map Area; *in* Geological Fieldwork 1987, *B.C. Ministry of Energy, Mines and Petroleum Resources*, Paper 1988-1, pages 199-209.

Grove, E.W. (1986): Geology and Mineral Deposits of the Unuk River - Salmon River - Anyox Area; *B.C. Ministry of Energy, Mines and Petroleum Resources*, Bulletin 63, 434 pages.

Harris, J.F. (1989): Petrographic Report 1989-1; unpublished report, *Newhawk Gold Mines Ltd.*

Hodgson, C.J. (1989a): Patterns of Mineralization; *in* Mineralization and Shear Zones, Bursnall, J.T., Editor, *Geological Association of Canada*, Short Course Notes, Volume 6, pages 51-88.

Hodgson, C.J. (1989b): The Structure of Shear-related, Vein-type Gold Deposits; A Review: *Ore Geology Reviews*, Volume 4, pages 231-273

Kirkham, R.V. (1963): The Geology and Mineral Deposits in the Vicinity of the Mitchell and Sulphurets Glaciers, Northwestern British Columbia; unpublished M.Sc. thesis, *The University of British Columbia*, 122 pages.

Kirkham, R.V. (1991): Provisional Geology of the Mitchell-Sulphurets Region, Northwestern British Columbia (104B/8, 9); *Geological Survey of Canada*, Open File 2416.

Kirkham, R.V., Ballantyne, S.B. and Harris, D.C. (in preparation): Sulphurets area, British Columbia – Preliminary Geology, Geochemistry, and Mineralogy of a Deformed Porphyry Copper, Molybdenum, Precious Metal System.

Roach, S. (1990): 1989 Surface Exploration Program; unpublished internal report, *Newhawk Gold Mines Ltd.*

Sibson, R.H., Moore, J.M. and Rankin, A.H. (1975): Seismic Pumping – A Hydrothermal Fluid Transport Mechanism; *Geological Society*, London, Journal, Volume 131., pages 653-659.

Tchalenko, J.S. (1970): Similarities Between Shear Zones of Different Magnitudes; *Geological Society of America*, Bulletin, Volume 81, pages 1625-1640.

Wheeler, J.O. and McFeely P. (1987): Tectonic Assemblage Map of the Canadian Cordillera and Adjacent Parts of the United States of America; *Geological Survey of Canada*, Open File 1565.

NOTES

British Columbia Geological Survey
Geological Fieldwork 1991

PRELIMINARY GEOLOGY OF THE KERR COPPER-(GOLD) DEPOSIT, NORTHWESTERN BRITISH COLUMBIA (104B/8)

David J. Bridge and Colin I. Godwin
Mineral Deposit Research Unit
The University of British Columbia

(MDRU Contribution 005)

KEYWORDS: Economic geology, porphyry, Kerr, Sulphurets, copper, gold, Stuhini Group, Unuk River Formation.

INTRODUCTION

The Kerr porphyry copper-(gold) deposit, owned by Placer Dome Inc., is in the Sulphurets gold camp 60 kilometres north of Stewart, British Columbia. Reserves calculated in 1989 by the previous owner, Western Canadian Mining Corporation, are 66 million tonnes averaging 0.8 per cent copper and 0.33 gram per tonne gold using a 0.5 per cent copper cut off. Access to the deposit is by helicopter from Tide Lake airstrip 50 kilometres north of Stewart. The deposit was diamond drilled extensively by Western Canadian Mining Corporation from 1987 to 1989 and by Placer Dome Inc. in 1990.

REGIONAL GEOLOGY

The Kerr deposit is hosted by Late Triassic to Early Jurassic island-arc rocks of Stikinia (Alldrick, 1989). The stratigraphic units are characterized by rapid facies changes typical of submarine island arcs. Regional deformation during the Cretaceous (Evenchick, 1991) deformed the volcanic and sedimentary units into westerly dipping thrust slices. These slices are stacked onto each other, exposing the oldest units in thrust wedges and tightly folded anticlines. The lowermost unit exposed in the area is the eastern facies of the Late Triassic Stuhini Group (Anderson and Thorkelson, 1990). The eastern facies consists of hornblende or pyroxene-phyric andesitic and basaltic volcanic conglomerates, and orange and black-weathering laminated siltstone and greywacke. Boulder to cobble conglomerates with shale and siltstone layers form a transitional unit between the underlying Stuhini Group and the overlying Early Jurassic Unuk River Formation (Anderson and Thorkelson, 1990). The Unuk River Formation in the Sulphurets gold camp consists of pyroclastic rocks of andesitic composition, possibly derived from diorite subvolcanic intrusions that are spatially related to porphyry copper deposits (Britton and Alldrick, 1988).

DEPOSIT GEOLOGY

The geology of the Kerr deposit is obscured by intense alteration and deformation. The 'deformed zone' outlined on Figure 6-3-1 is an area of foliated, sericite-altered volcanic and intrusive rock. A band of intense alteration and mineralization outcrops parallel to the edges of the deformed zone. Correlation of rock units between drill holes and on surface is hampered by complex structures in the deformed zone and poor outcrops on the eastern edge of the deposit. Lithologies exposed along the eastern margin of the deposit are regionally upright with local overturning. The absolute ages of the various units are not well constrained, but relative ages have been determined from surface mapping, crosscutting relationships and differences in intensity of deformation and alteration.

SEDIMENTARY AND VOLCANIC UNITS

Bedded ash-tuff forms the lowermost continuous rock unit exposed in the deposit area. It crops out along the eastern edge of the deformed zone and as a small unit below Kerr Peak (Figure 6-3-1). The unit consists of very fine grained siliceous layers interbedded with crossbedded coarser layers.

Volcanic conglomerate with chert clasts conformably overlies the bedded ash-tuff along the eastern edge of the deformed zone (Figure 6-3-2). Heterolithic clasts, up to 7 centimetres in diameter, change in composition from dominantly ash-tuff fragments at the bottom of the unit to porphyritic intermediate volcanic rocks and grey chert pebbles at the top.

Conglomerate and minor sandstone and siltstone overlie the volcanic conglomerate along the eastern margin of the deposit. The conglomerate is distinguished from the volcanic conglomerate by its black calcareous matrix with euhedral to subhedral feldspar crystals and rare cobbles of dull grey, fossiliferous limestone. The relative abundance of feldspar crystals increases up section until the unit appears to be a crystal tuff with a black calcareous matrix. The conglomerate unit fines upward into interbedded grey sandstone and siltstone that is exposed below Kerr Peak and as subcrops 100 metres south of the old camp.

Laminated argillite and rusty weathering siltstone conformably overlie the interbedded grey sandstone. This unit crops out around the old camp and as a sliver of rock below Kerr Peak. Contorted bedding, possibly due to soft-sediment deformation, is characteristic of this unit. Abundant load casts and graded bedding define a steep easterly dip on section 10600N (Figure 6-3-2). Bedding in the sediment is parallel to the bedding in the ash tuff.

Epiclastic conglomerate underlies Kerr Peak southwest of the deposit. This unit is in fault contact with underlying black argillite. Clasts in this conglomerate are 1 to 30 centimetres in diameter, and are elongate parallel to an east-striking, steep westerly dipping penetrative fabric. The clasts are matrix supported and comprise: plagioclase por-

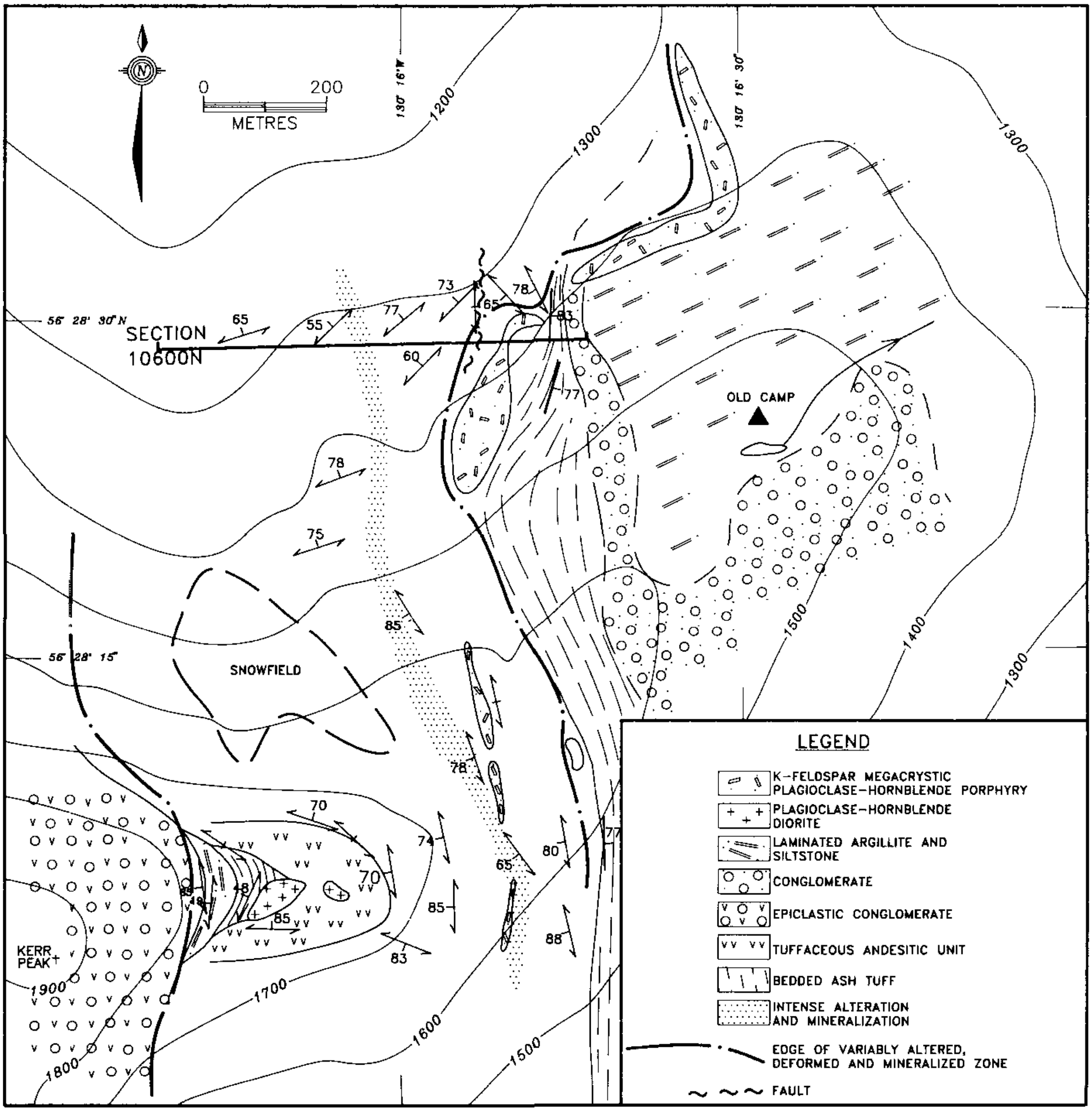

Figure 6-3-1. Simplified surface geology from this study of the Kerr deposit. Small dikes have been omitted for clarity. Rock units (volcanic rocks, pre and syn-mineral dikes) in the variably altered, deformed and mineralized zone have been omitted in places because of intense deformation, alteration and weathering that has obscured the relationships between individual units.

phyry (30% of the unit), hornblende porphyry (10%), aphanitic felsic volcanic rock (10%), and epidotite (5%). The matrix (45%) consists of plagioclase fragments (20%) and altered ash. The rock is weakly propylitized, possibly as a result of lower greenschist metamorphism (Britton and Alldrick, 1988). Age and stratigraphic position relative to units described above is uncertain. Anderson and Thorkelson (1990) mapped this unit as part of the Late Triassic Stuhini Group.

A pale brown weathering tuffaceous andesitic unit, is exposed surrounding the bedded tuff below Kerr Peak. It consists of bedded feldspar-phyric crystal tuff and a monolithic fragmental rock consisting of clasts of aphanitic tuff in a fine-grained feldspar-rich matrix.

Intrusive Units

Several distinctive pre to post-mineral dikes and stocks comprise 70 per cent by volume of rock in the deposit (Figure 6-3-2). Their relative age was determined from crosscutting relationships, distribution of sulphides and veins, and extent of deformation and alteration.

PRE-MINERAL DIKE?

A fine-grained plagioclase and hornblende-phyric unit is shown only on Figure 6-3-2. It hosts most of the copper mineralization in the Kerr deposit. Extensive alteration and deformation have obscured its original identity. One by two millimetre euhedral laths of plagioclase, hornblende and minor pyroxene comprise 30 to 70 per cent of the rock. The unit may be a premineral intrusive rock.

SYN-MINERAL DIKES

Plagioclase hornblende diorite occurs as a dike that is up to 100 metres wide (Figure 6-3-2). It strikes north and dips west, parallel to the trend of the copper mineralization. This unit consists of 2 by 4 millimetre phenocrysts of plagioclase (30%) and hornblende (10%) in a fine-grained matrix. The plagioclase hornblende diorite is interpreted to be a syn-mineral dike because it cuts and hosts pyrite and minor chalcopyrite-bearing banded quartz veins. Unmineralized magmatic breccias locally form margins to this intrusion. Small dikes of plagioclase hornblende diorite cut silicified unmineralized heterolithic hydrothermal breccia near the surface at the western corner of section 10600N (Figure 6-3-2).

Feldspar-megacrystic plagioclase hornblende porphyry forms a westerly trending dike 1 to 5 metres thick, but is not visible at map scale. It cuts bedded tuff below Kerr Peak and is in chill contact with plagioclase hornblende diorite. The unit is interpreted to be a late syn-mineral dike because it hosts polymetallic quartz veins and postdates the plagioclase hornblende diorite.

POST-MINERAL DIKES

Augite-hornblende-plagioclase porphyry crops out 500 metres east of Kerr Peak as a 10 by 50 metre lozenge in strongly altered and deformed tuffaceous rocks. It is too small to show on the figures. Alteration consists of epidote replacement of fine plagioclase laths and epidote veins.

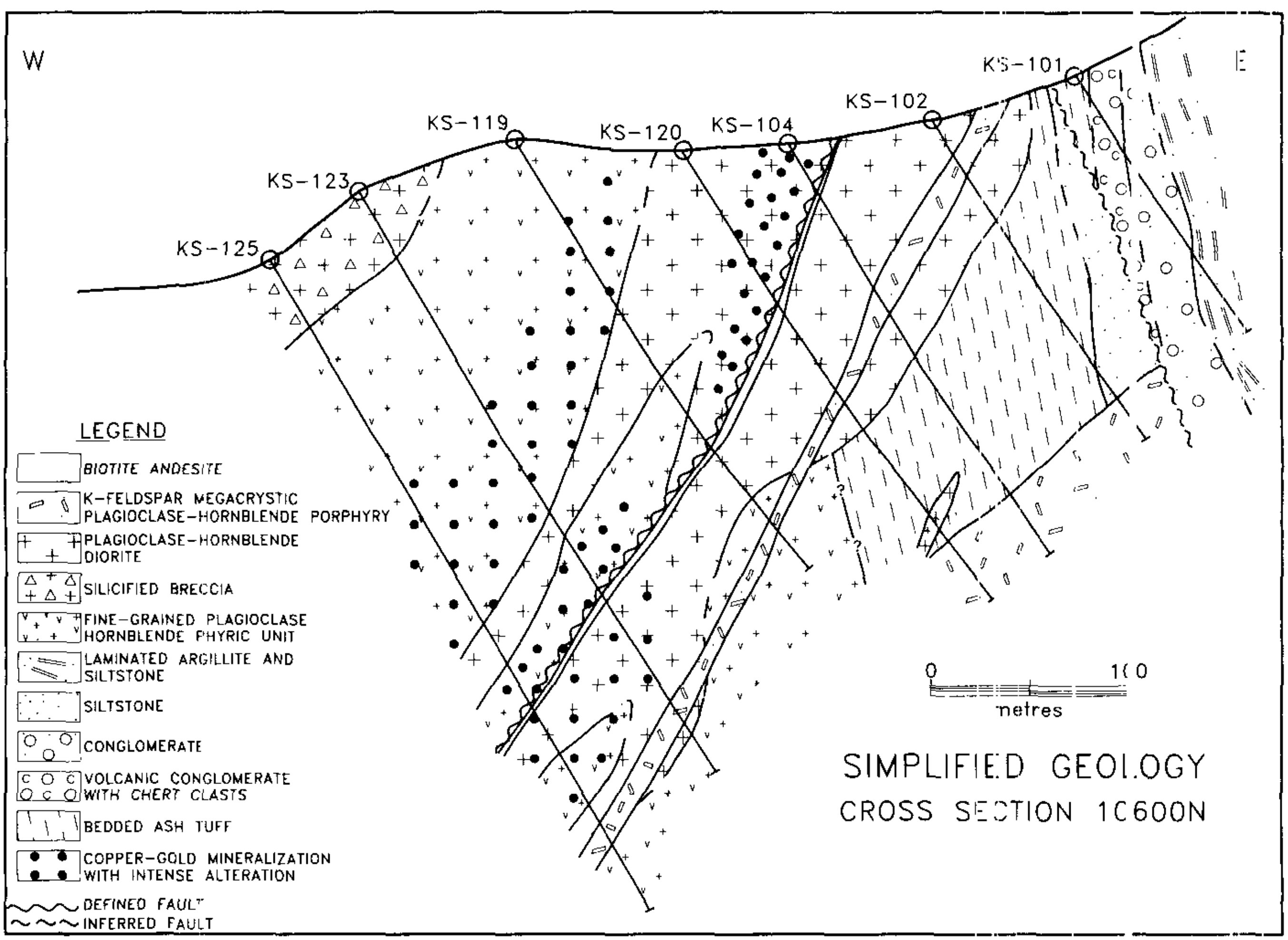

Figure 6-3-2. Simplified cross-section from this study showing distribution of altered lithologies and areas of intense mineralization.

Potassium feldspar megacrystic plagioclase hornblende porphyry strikes north and dips to the west (Figures 6-3-1 and 2). The potash feldspar megacrysts are euhedral, up to 20 millimetres in length in a matrix of plagioclase laths and minor hornblende. The dike is boudinaged and surrounded by strongly altered tuffaceous and intrusive rocks.

Green, aphanitic andesite dikes strike east and dip steeply south but they are volumetrically insignificant. These dikes are concentrated in the deformed zone where they are intensely folded with their fold axes parallel to the north-trending fabric.

Biotite andesite dikes are up to 2 metres wide and follow major late faults which parallel the trend of the mineralization and earlier intrusions (Figure 6-3-2). This unit is characterized by minor biotite books in a magnetic, dark reddish brown aphanitic matrix. Quartz and pink potassium feldspar crystals with corroded edges are concentrated in the centre of these dikes.

MINERALIZATION AND ALTERATION

Copper and gold mineralization on cross-section 10600N is concentrated above the fault hosting the biotite andesite dike (Figure 6-3-2). Minor mineralization is present below the fault.

Five distinct vein types have been identified, from oldest to youngest:

- banded, grey to milky white quartz veins with minor pyrite and chalcopyrite,
- magnetite and specular hematite with minor disseminated chalcopyrite and pyrite,
- pyrite and minor chalcopyrite with minor quartz gangue,
- anhydrite, quartz and calcite with pyrite, chalcopyrite and tetrahedrite, and
- pink gypsum veinlets with selvages of chalcopyrite and minor molybdenite.

These veins form stockworks in the plagioclase and hornblende-phyric unit above the plagioclase hornblende diorite dike. Alteration of the host unit varies repeatedly over 10 metre intervals. Each alteration interval has a texturally destructive chlorite and magnetite or pyrite 'core' assemblage, flanked successively by green sericite and pyrite, and white and yellow sericite with quartz and pyrite. This small-scale zonation reflects the overall alteration pattern across the deformed zone. The stippled region marked on Figure 6-3-1 represents an area of chlorite and green sericite alteration. It is crosscut by white gypsum veinlets. These may have formed during deformation, by remoblization from earlier anhydrite and pink gypsum veins. Mineralization intersected by drill hole KS-120 below KS-104 (Figure 6-3-2) in the plagioclase hornblende diorite dike consists of banded quartz veins cut by pyrite and chalcopyrite veinlets.

Minor polymetallic veins occur around the periphery of the plagioclase hornblende diorite locally cutting feldspar-megacrystic plagioclase hornblende porphyry. They consist of milky white quartz and carbonate with pyrite, chalcopyrite, tetrahedrite, sphalerite and galena.

DEFORMATION

A strong northerly trending foliation follows the trace of the area of intense alteration and mineralization (Figure 6-3-1). It dips to the west, parallel to the dip of the plagioclase hornblende diorite dike and megacrystic plagioclase hornblende porphyry dike. All post-mineral dikes are strongly deformed except for the biotite andesite dikes. They intruded along relatively late major faults that were subsequently reactivated.

DISCUSSION AND CONCLUSIONS

The Kerr deposit is interpreted to be an Early Jurassic copper-(gold) porphyry system that was deformed during the Cretaceous (Evenchick, 1991). This interpretation is supported by the observation that post-mineral dikes are extensively folded and boudinaged parallel to a strong northerly trending foliation. Regional mapping by Britton and Alldrick (1988), Alldrick (1989) and Anderson and Thorkelson (1990) suggests that the deposit is hosted by the Late Triassic Stuhini Group. However, the footwall cannot be directly correlated with published stratigraphy of the Stuhini Group or of the Early Jurassic Unuk River Formation. Further geological mapping in the vicinity of the Kerr deposit is required.

Intense copper mineralization on cross-section 10600N occurs as quartz, magnetite and sulphide stockworks in lenses within the plagioclase hornblende diorite dike and in its hangingwall. Anhydrite and gypsum veins are concentrated in the strongly altered plagioclase and hornblende-phyric unit. The relationship between these stockworks and the syn-mineral plagioclase hornblende diorite dike will be investigated by a detailed petrographic study.

ACKNOWLEDGMENTS

Fieldwork for this study was supported in part by generous financial and technical assistance provided by Placer Dome Inc. Special thanks are extended to E. Kimura, J. Kowalchuk, R. Pease and G. Shevchenko for stimulating technical discussions about the mineralization and structure of the Kerr deposit. This project is part of the Mineral Deposit Research Unit study "Metallogenesis of the Iskut River Area, Northwestern B.C.".

REFERENCES

Alldrick, D.J. (1989): Volcanic Centres in the Stewart Complex (103P and 104A, B); *in* Geological Fieldwork 1988, *B.C. Ministry of Energy, Mines and Petroleum Resources*, Paper 1989-1, pages 233-240.

Anderson, R.G. and Thorkelson, D.J. (1990): Mesozoic Stratigraphy and Setting for Some Mineral Deposits in Iskut River Map Area, Northwestern British Columbia; *in* Current Research, Part E, *Geological Survey of Canada*, Paper 90-1F, pages 131-139.

Britton, J.M. and Alldrick, D.J. (1988): Sulphurets Map Area (104A/5W, 12W; 104B/8E, 9/E); *in* Geological Fieldwork 1987, *B.C. Ministry of Energy, Mines and Petroleum Resources*, Paper 1988-1, pages 199-209.

Evenchick, C.A. (1991): Structural Relationships of the Skeena Fold Belt West of the Bowser Basin, Northwest British Columbia; *Canadian Journal of Earth Sciences*, Volume 28, pages 973-983.

ESKAY CREEK AREA, STRATIGRAPHY UPDATE (104B/9, 10)

By R.D. Bartsch
Mineral Deposit Research Unit
The University of British Columbia

(MDRU Contribution 006)

KEYWORDS: Economic geology, stratigraphy, Eskay Creek, alteration, structure, Mount Dilworth Formation, Betty Creek Formation.

INTRODUCTION

Mapping at 1:5000-scale of an area near the Eskay Creek precious and base metal deposits initiated in 1991 emphasizes documentation of facies variations within the Lower to Middle Jurassic rocks of the Hazelton Group. This work is an integral part of the Mineral Deposit Research Unit's Iskut River Metallogeny project and is the basis of M.Sc. thesis research by the author at The University of British Columbia.

The study area is centred within the northern half of the Unuk map area (Alldrick *et al.*, 1989) and extends south and southwest of the Eskay Creek deposit (Figure 6-4-1). It includes properties held by International Corona Corporation, Granges Inc., American Fibre Corporation/Silver Butte Resources Ltd. (formerly Consolidated Silver Butte Mines Ltd.) and Prime Equities Inc.

Previous work in the Unuk and adjacent Snippaker and Sulphurets map areas was compiled by Britton (1990) who describes the stratigraphic nomenclature for this part of the Intermontane Belt. Current observations from geologists with Granges Inc. and American Fibre Corporation are incorporated in this update.

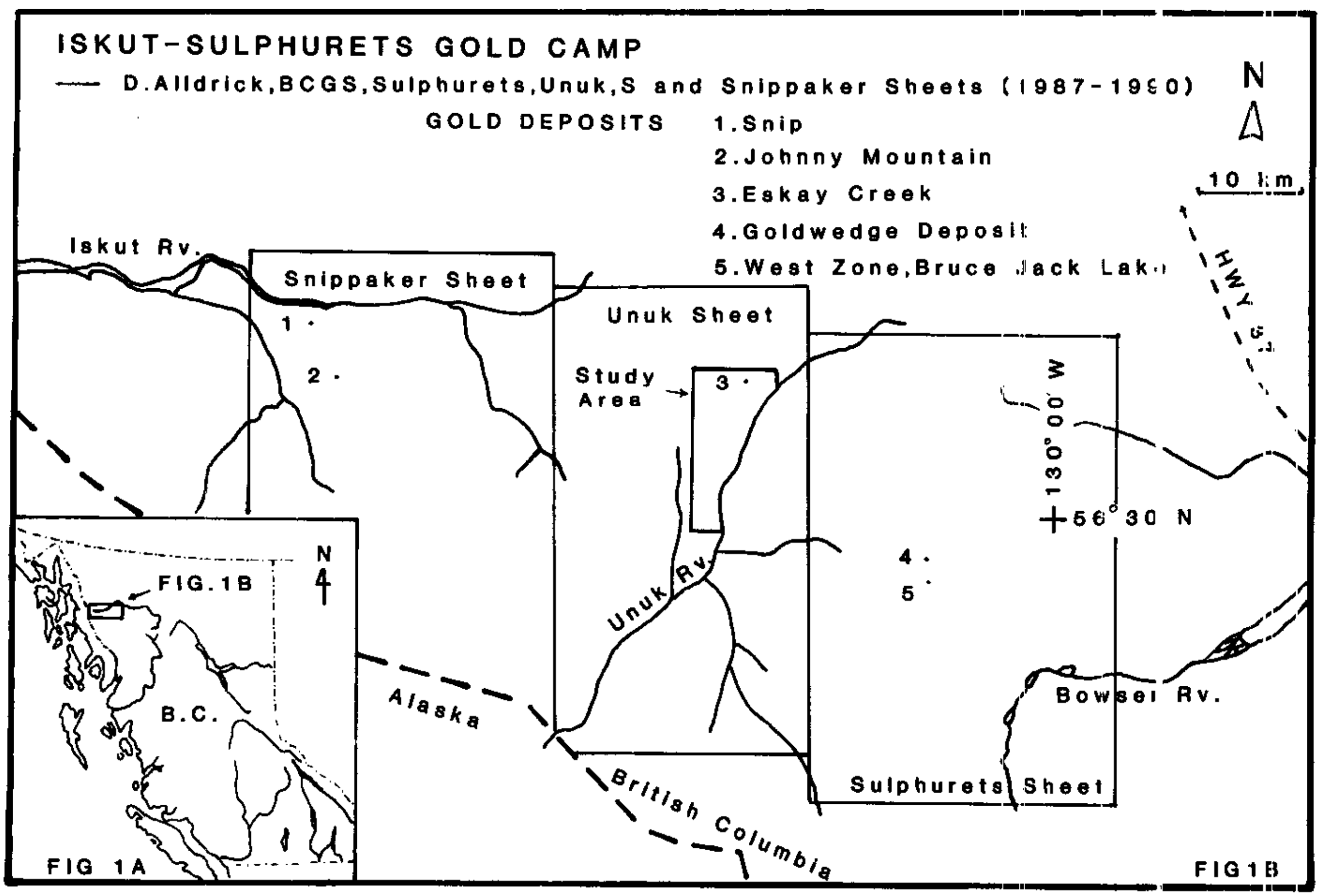

Figure 6-4-1. Iskut-Sulphurets gold camps: study area. (Modified from Alldrick *et al.*, 1989.)

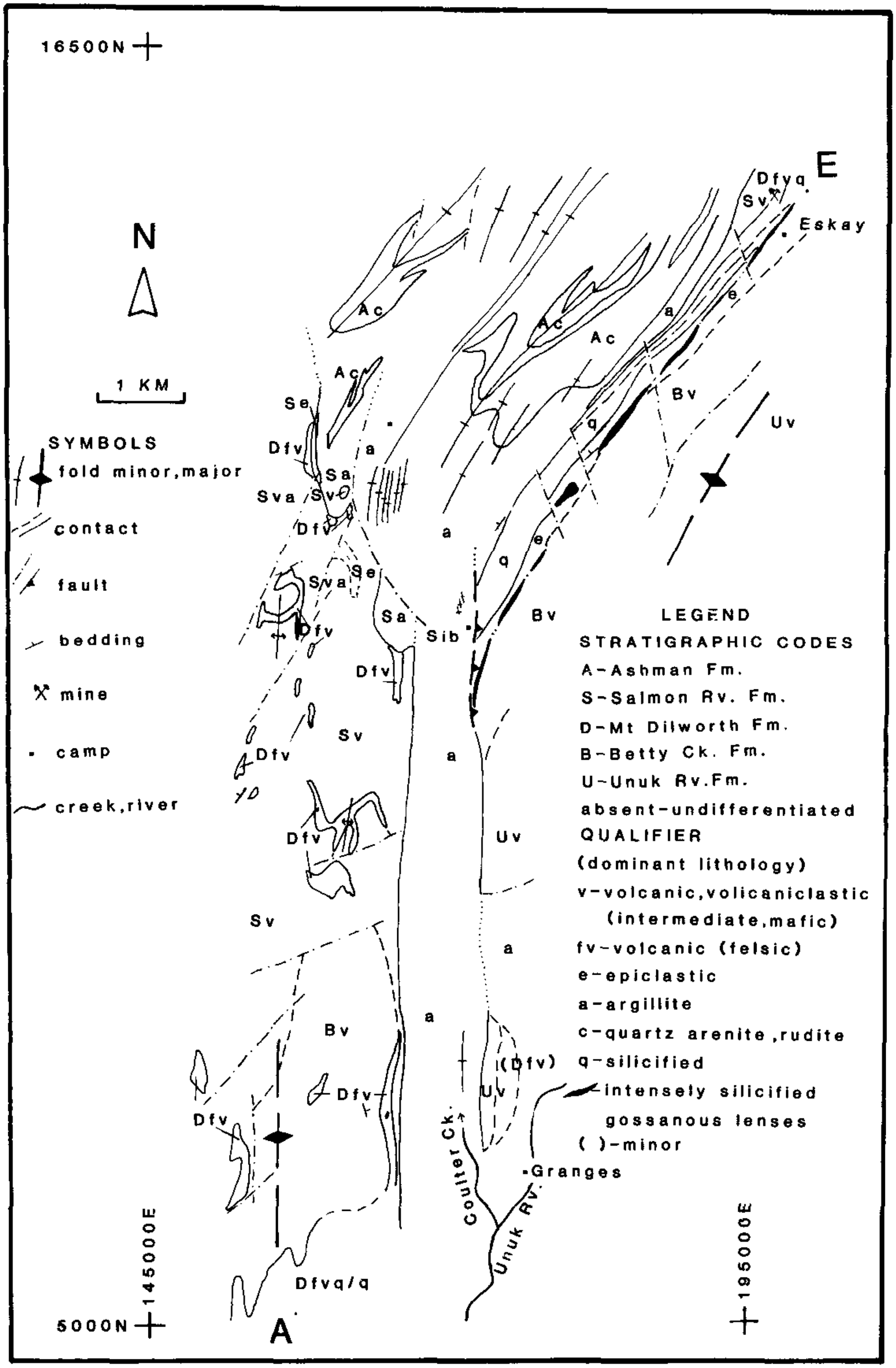

Figure 6-4-2. Simplified geological map of the Eskay Creek area. Structural detail within the northern Bowser Lake Group sediments from Lewis (1992, this volume).

STRATIGRAPHY UPDATE

Six regionally mappable units are defined by Britton *et al.* (1989) in the study area and are tentatively correlated with the Unuk River, Betty Creek, Mount Dilworth, Salmon River and Ashman formations. Significant variations are observed in the distribution of the units defined on the regional 1:50 000-scale mapping (Alldrick *et al.*, 1989) and problems in definition of stratigraphic intervals have arisen.

Stratigraphic intervals are best characterized by the nature of the volcanic rock component. Similar epiclastic rocks occur at different stratigraphic intervals. Regionally extensive fault and stratigraphically controlled alteration dominated by silica replacement often obscures the stratigraphy. Disconformable relationships between formations are common. Individual units display considerable facies variations and contact relationships (depositional and structural) are complex. Experience gained during the 1991 field season suggests that the Hazelton Group rocks can best be mapped in terms of facies.

Within the study area the Unuk River and Betty Creek formations are not easily distinguished. The definitive maroon coloration of the Betty Creek Formation seen in the Stewart area are absent. Both formations comprise green chloritic volcaniclastic rocks, andesitic tuffs, flows and flow breccias and minor shales, sandstones and carbonates. Andesite flows within the Unuk River Formation are characterized by feldspar and/or pyroxene phenocrysts, however this feature is not ubiquitous and the boundary between the formations is indistinct.

The Mount Dilworth Formation disconformably overlies the Unuk River and Betty Creek formations and comprises dacitic to rhyolitic rocks which vary systematically from an imaginary curvilinear baseline extending from Eskay Creek to Alice Lake (E-A; Figure 6-4-2). Close to the baseline the interval is distinguished by flow breccias; clasts within the breccias are flow banded. Farther northwest the stratigraphic interval is marked by discontinuous layers of lapilli breccia (subaerial) and subsequently by heterolithic debris-flow breccias.

Thickness is greatest and continuity is best close to the baseline, maximum thickness is estimated at 25 metres; to the northwest the interval is 1 to 5 metres. Trends comparable to those in the Mount Dilworth Formation are evident in the underlying stratigraphy in the dominance of massive andesite flows near the baseline varying to volcaniclastic, epiclastic and argillite lithologies to the northwest.

Field recognition of the felsic rocks (and lateral variations) is blurred by alteration and relies on identification of poorly preserved primary textures. The imaginary baseline defines the most intense alteration which is characterized by quartz and/or potassium feldspar, sericite and pyrite, imparting a grey-green cherty appearance to the rocks. Within the stratigraphy between SIB and Eskay Creek camps (Figure 6-4-2) the silica alteration zone attains a true thickness of 125 metres and extends between both camps. Textures within the lower 100 metres of the alteration zone are indicative of intermediate and mafic volcanic rocks, including pillow and pahoehoe textures. Unaltered intermediate flows immediately underlie felsic volcanic rocks to the south. Indisputable silicified pahoehoe-textured volcanics are laminated (flow banded). Flow banding has been used to distinguish altered rhyolites throughout the area and highlights the problems associated with recognizing protoliths.

The SIB-Eskay alteration zone is capped by a thin (<10 m thick) black-matrix breccia concordant with the alteration zone and overlying argillite contact and discordant to the stratigraphic contacts. Discrete, narrow (<30 cm) black-matrix breccias and black veinlets cut the underlying silicified volcanic rocks. The breccias comprise cherty, pale grey-green angular fractured clasts; clasts are matrix supported and matrix and fracture infill is gradational from black cherty carbonaceous siltstone to black (carbonaceous?) quartz. Within the stratigraphic interval between the SIB and Eskay camps (Figure 6-4-2), minimally altered, well-bedded feldspathic sandstones, conglomerates, fossiliferous siltstones and minor carbonates mark the transition from green chloritic volcanic and volcaniclastic rocks of the Betty Creek Formation to the east and the silica alteration zone to the west. The sediments are dominated by argillites to the north and pinch out to the south. To the west, similar epiclastic rocks are interbedded with and overlie the Mount Dilworth Formation.

The Salmon River Formation comprises andesite flows and tuffs and volcaniclastic, epiclastic and minor carbonate rocks and argillite. The northwesterly variations within the felsic rocks are mimicked by a transition within the younger rocks from andesite flows which are massive, columnar jointed and brecciated, to pillowed flows; and from a dominance of volcaniclastic to epiclastic rocks and argillite. In the absence of the felsic marker it is difficult to distinguish the upper and lower intermediate and mafic volcanic units. Lateral equivalents of the mineralized, contact argillite at Eskay Creek crop out in the northeast and comprise thin, finely laminated cherty siltstones intercalated with pillowed andesites. Massive argillites in the centre of the map area may include distal equivalents of the Betty Creek and Salmon River formations and, in the absence of volcanic rocks and paleontological control, are indistinguishable from overlying Bowser Lake Group argillites. Qualitatively the argillites in the lower part of the sequence are more carbonaceous and pyritic than argillites in the upper part of the sequence and contain minor carbonate interbeds. Quartz sandstones, grits and conglomerates consisting of white and black cherty clasts are interbedded with the Bowser Lake Group argillites and are good local markers. These sediments onlap the Salmon River and Mount Dilworth formation volcanic rocks to the northwest and northeast where they contain minor feldspathic horizons. Britton *et al.* (1989) correlate this unit with the Ashman Formation of Tipper and Richards (1976), and define it as the base of the Bowser Lake Group. The break between the distal facies of the Salmon River and Bowser Lake formations is a major problem to be resolved.

STRUCTURE AND MINERALIZATION

The distribution of the units is interpreted to represent a triplet of regional folds with fold axes rotated northeasterly to northerly progressively to the south. Argillites, sandstones and conglomerates of the Salmon River Formation and Bowser Lake Group occupy a central synform. Deformation increases to the south in parallel with the gradual rotation of fold axes (Lewis, 1992, this volume). Within the zone of inflection the eastern limb of the synform is truncated by high and low-angle faults with some associated ramping of the volcanic rocks over argillites.

Two periods of faulting are distinguishable. Early faults are associated with varying alteration and mineralization. Small displacements of the contact between the Salmon River and Mount Dilworth formations occur on these faults, however, no significant alteration or epigenetic mineralization is visible in outcrops of the younger rocks, indicating some reactivation of the structures. Within the SIB-Eskay stratigraphy these early structures are prominent as minor faults crosscutting and subparallel to bedding and a major fault zone (Tony's fault named informally after Tom MacKay's horse) also subparallel to stratigraphy.

Recognition of Tony's fault is based on discordance between a linear, subvertical, intense alteration zone and bedding in adjacent epiclastic rocks which varies in orientation, with dips dominantly 45° to 70° northwest. Tony's fault is spatially related to the prominent silica alteration zone and to the imaginary baseline describing variations within the stratigraphy. The core of this fault zone comprises massive lenses of microcrystalline quartz measuring up to 500 by 25 metres which have both diffuse and sharp contacts. The lenses step left-laterally to the north, converging with the silica alteration zone at the Eskay Creek camp, and are enveloped by a continuously mineralized and strongly foliated alteration halo. The strong foliation within the alteration envelope is restricted to sericitic and chloritic alteration zones and is not visible in intensely silicified lenses. The dominant foliation is parallel to axial surfaces of regional folds (post Bowser Lake Group; Lewis, 1992, this volume) and its pronounced development in this zone may simply reflect strain partitioning into the 'slippery' phyllosilicate alteration assemblage. The fault crops out as a line of discontinuous gossanous bluffs from Eskay to SIB camps. Steps within the fault are associated with minor crosscutting mineralized faults which coincidentally control the outcrop distribution of pillowed andesites and cherty siltstones of the Salmon River Formation (contact zone). Mineralization within the faults is dominated by pyrite with or without galena, chalcopyrite and sphalerite.

Late unmineralized faults are related to folding and are best expressed by the truncation of the eastern limb of the regional synform at SIB camp; the stratigraphy and the major gossanous fault zone extending from SIB to Eskay camps are cut off.

FUTURE WORK

There is an intimate relationship between faulting, regionally extensive, stratigraphically controlled alteration and variations within the upper Hazelton Group stratigraphy. Highlighted lithological variations indicate a northerly and northwesterly transition from proximal to distal and subaerial to marine volcanic facies. A focus of future work will be to assimilate field data in terms of facies and determination of protoliths obscured by intense alteration. Further mapping is required to the north and northwest to correlate stratigraphy in the vicinity of the Eskay deposit with regional stratigraphy.

ACKNOWLEDGMENTS

I am grateful to International Corona Corporation, Granges Inc., American Fibre Corporation, Silver Butte Resources Ltd., Prime Equities Inc. and their respective staffs for ongoing logistical and technical support of this study. Thanks are also extended to Western Mining Corporation Limited and its generous study-leave program which enabled me to take two years leave to come from Australia to undertake an M.Sc. Assistance from Dr. A. Sinclair, my supervisor, Dr. J. MacDonald, the manager of the Iskut Project and co-workers in the Mineral Deposit Research Unit is deeply appreciated.

REFERENCES

Alldrick, D.J., Britton, J.M., Webster, I.C.L. and Russell, C.W.P. (1989): Geology and Mineral Deposits of the Unuk Area (104B/7E, 8W, 9W, 10E); *B.C. Ministry of Energy, Mines and Petroleum Resources*, Open File 1989-10.

Britton, J.M. (1990): Stratigraphic Notes from the Iskut-Sulphurets Area; *in* Geological Fieldwork 1990; *B.C. Ministry of Energy, Mines and Petroleum Resources*, Paper 1991-1, pages 131-137.

Britton, J.M., Webster I.C.L. and Alldrick D.J. (1989): Unuk Map Area (104B/7E, 8W, 9W, 10E); *in* Geological Fieldwork 1988, *B.C. Ministry of Energy, Mines and Petroleum Resources*, Paper 1989-1, pages 241-250.

Lewis, P.D. (1992): Structural Geology of the Prout Plateau Region, Iskut River Map Area, British Columbia; *in* Geological Fieldwork 1991, Grant, B. and Newell, J.M., Editors, *B.C. Ministry of Energy, Mines and Petroleum Resources*, Paper 1992-1, this volume.

Tipper, H.W. and Richards, T.A. (1976): Jurassic Stratigraphy and History of North-central British Columbia; *Geological Survey of Canada*, Bulletin 270, 73 pages.

STRUCTURAL GEOLOGY OF THE PROUT PLATEAU REGION, ISKUT RIVER MAP AREA, BRITISH COLUMBIA (104B/9)

By Peter D. Lewis
Mineral Deposit Research Unit
The University of British Columbia

(MDRU Contribution 001)

KEYWORDS: Structural geology, Prout Plateau, Eskay Creek, Hazelton Group, Bowser Lake Group.

INTRODUCTION

The Iskut River map area contains several important mineral deposits and has been the focus of numerous recent geological studies, including government sponsored regional surveys (Alldrick and Britton, 1988; Britton and Alldrick, 1988; Anderson, 1989; Alldrick *et al.*, 1989, 1990; Britton *et al.*, 1989b, 1990; Anderson and Thorkelson, 1990) and extensive property-scale mapping conducted by mining companies. Despite the large amount of exploration work within the area, its structural history is poorly understood and even the stratigraphic framework is only established at a basic level. A regional-scale structural and stratigraphic framework is essential to further evaluate the metallogeny of the area, and will be useful for designing strategies for future exploration programs.

A regional study of the structural evolution of the Iskut River area is one important aspect of the multifaceted Iskut River metallogeny project currently being conducted by the Mineral Deposit Research Unit at the University of British Columbia. This study began with geologic mapping in the Unuk River map area during the 1991 field season. Long-term objectives are to provide a regional structural and stratigraphic framework for the area, which will then be integrated with property-scale studies focusing on relationships between mineralization and deformation. These goals will be achieved through 1:20 000-scale geological mapping of key areas which feature well-exposed rocks and potentially significant structural and stratigraphic relationships. Deposit-scale mapping by other MDRU researchers, and property maps provided by MDRU industry members will

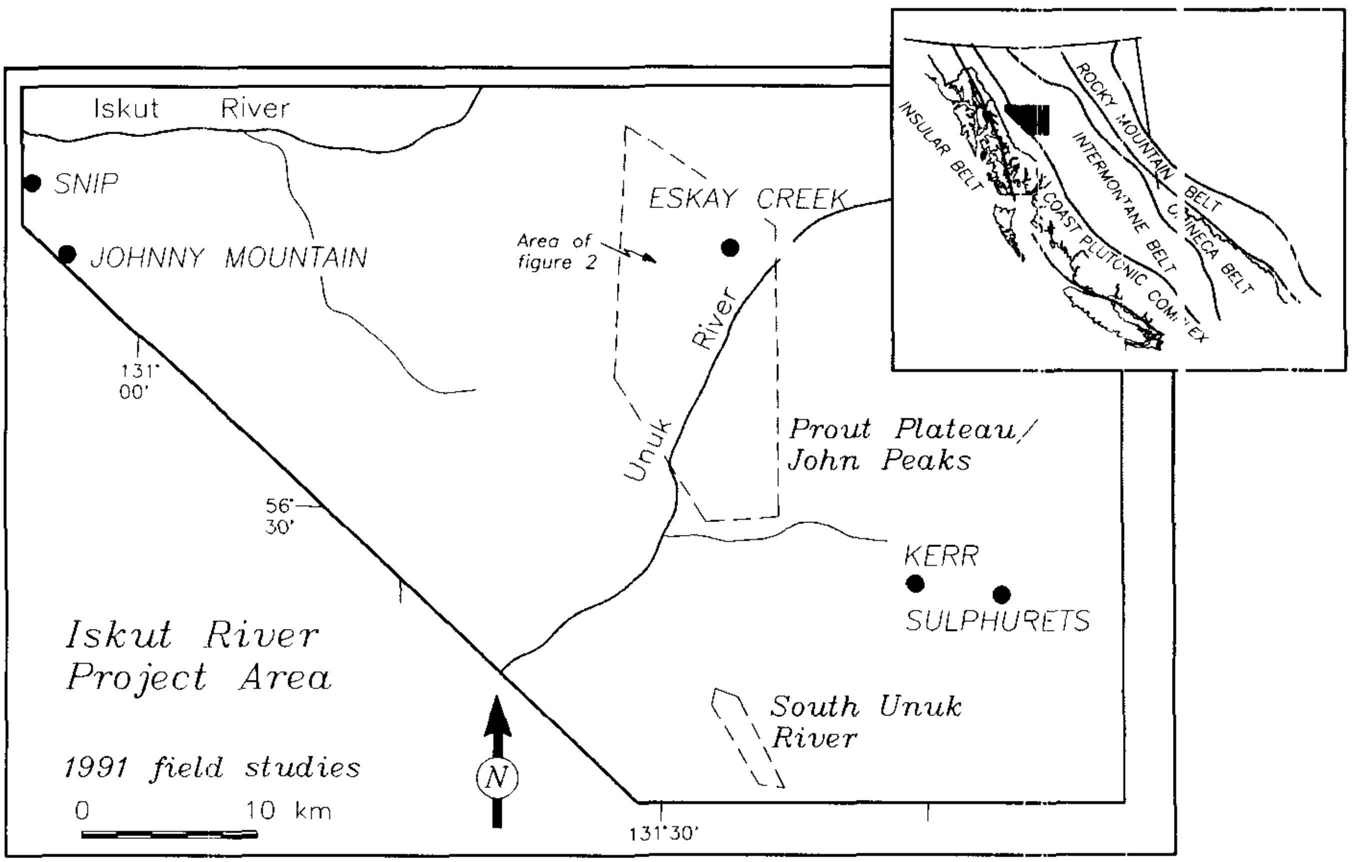

Figure 6-5-1. Location of the Iskut River map area within the five tectonic belts of the Canadian Cordillera, and locations of areas examined during the 1991 field season.

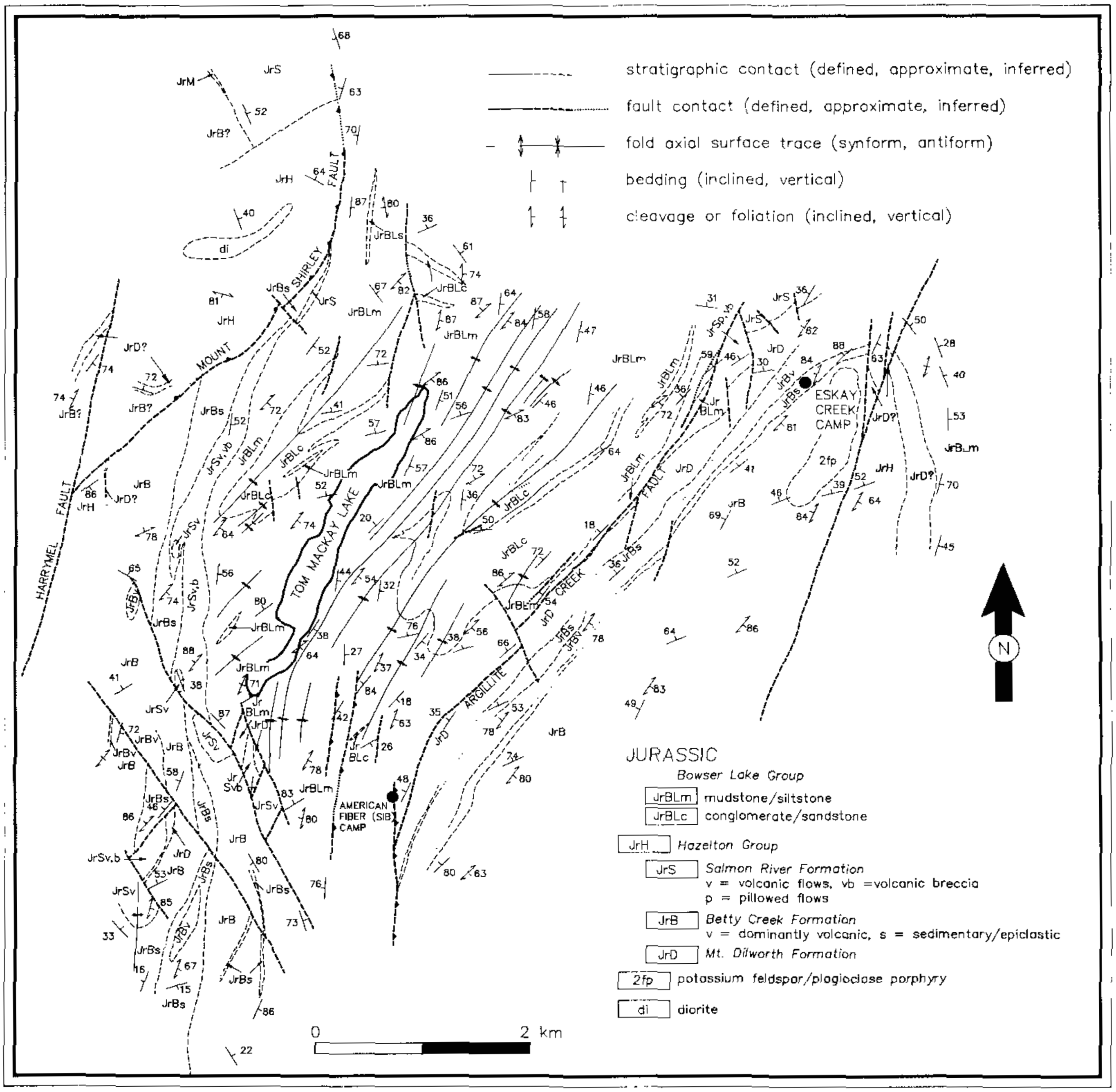

Figure 6-5-2. Simplified geologic map of the Prout Plateau area, based on 1991 fieldwork.

be combined with the new regional mapping to provide the most up-to-date geologic compilation of the Iskut River area.

Mapping during the 1991 field season concentrated on the John Peaks and Prout Plateau areas and exposures of the South Unuk River fault (Figure 6-5-1). Preliminary results from the Prout Plateau area are discussed in this paper; other work will be presented in future reports.

GENERAL GEOLOGY

The Prout Plateau is underlain by rocks of two major stratigraphic divisions. Rocks of the lower division belong to a regionally extensive sequence of Lower Jurassic volcanic and epiclastic rocks of the Hazelton Group more than 2 kilometres thick. Hazelton Group rocks are conformably overlain by argillites, sandstones and conglomerates of the Middle and Upper Jurassic Bowser Lake Group. Intrusive rocks are volumetrically minor, and include potassium feldspar-plagioclase-hornblende porphyritic dikes and stocks (Premier porphyry) and scattered aphyric dikes of varied composition. The stratigraphy and alteration history of Hazelton and Bowser Lake rocks in the Prout Plateau area is the subject of R. Bartsch's M.Sc. thesis at The University of British Columbia, and preliminary results from his study appear elsewhere in this volume (Bartsch, 1992).

Rocks of the Bowser Lake Group form the lowest overlap assemblage within the Bowser Basin, which occupies much of the northern Intermontane Belt. The Prout Plateau area contains some of the most westerly exposures of this important rock package, and geological relationships with older rocks there will probably be critical to unravelling the tectonic history of the Bowser Basin. The plateau also lies near the boundary between the Skeena fold belt to the east (Evenchick, 1991) and the Coast Plutonic Complex to the west, and mapping here will contribute to understanding of the transition between these major tectonic features.

Existing geological maps (Grove, 1986; Alldrick *et al.*, 1989) show the structural geology of the plateau area as dominated by a major north to northeast-trending syncline-anticline-syncline fold sequence. Faults mapped or inferred in the area, although continuous for several kilometres, do not offset stratigraphic contacts appreciably. One notable exception is the Unuk-Harrymel fault, which skirts the western edge of the Unuk River map area and has inferred east-side-down displacement (Britton *et al.*, 1989b). The Hazelton Group – Bowser Lake Group contact is exposed for several tens of kilometres along the limbs of the fold triplet sequence, making the area ideal for examining transitions in structural style between the two units. The Early to Middle Jurassic age range of the units also provides the opportunity to evaluate the regional affects of a proposed Early Jurassic deformation event in the Iskut River area (Bevier and Anderson, 1991).

RESULTS OF THE 1991 FIELDWORK

STRATIGRAPHY

An analysis of Hazelton Group stratigraphy in the Prout Plateau area is presently being conducted by R. Bartsch (Bartsch, 1992) and only a brief summary is presented here. The Lower to Middle Jurassic Hazelton Group in the Iskut River area is conventionally divided, in ascending order, into the Unuk River, Betty Creek, Mount Dilworth and Salmon River formations (Anderson, 1989). Existing maps show that the upper three of these units are exposed in the Prout Plateau area. However, lithofacies within these formations are very variable and laterally discontinuous, leading to correlation difficulties. In general, the lowest rocks exposed consist of epiclastic and volcanic strata which have historically been correlated with the Betty Creek Formation. In the Eskay Creek area (Figure 6-5-2), four units are mappable within this sequence: a lower volcanic and epiclastic unit of intermediate composition, an overlying package of epiclastic sandstone, siltstone, conglomerate and local fossiliferous carbonate, an upper intermediate to felsic volcanic unit ("footwall dacite" at Eskay Creek, Britton *et al.*, 1989a), and a thin, laterally discontinuous mudstone-siltstone package. These four map units can be traced the length of the Eskay Creek and SIB properties with only minor fault offsets (Figure 6-5-2), but are not individually mappable in the Mount Shirley area to the west. Felsic fragmental and massive volcanic flows and pyroclastic rocks, presently correlated with the Mount Dilworth Formation, overlie the epiclastic and volcanic succession in most, but not all locations. Uppermost Hazelton Group rocks consist of basaltic to andesitic flows of the Salmon River Formation. These rocks include pillowed flows, volcanic breccias and massive flows, and contain variable amounts of interbedded mudstone. On the north slope of Mount Shirley, extensive areas of pillowed flows, tentatively assigned to the Salmon River Formation, contain thinly bedded felsic tuffaceous intervals. Lithologies of the Salmon River Formation grade in a north to south direction from pillowed flows, to broken pillow breccias and volcanic breccias, to massive flows.

The base of the Bowser Lake Group is mapped at the top of the highest occurrence of volcanic rocks within the Salmon River Formation. Although this boundary is easily mapped on the Prout Plateau, in surrounding regions where the Salmon River Formation consists entirely of fine-grained sedimentary rocks, it can be a difficult distinction to make, and some workers advocate placing the Hazelton Group – Bowser Lake Group boundary below the Salmon River Formation (Kirkham *et al.*, in preparation). At Prout Plateau, the Bowser Lake Group is distinguished by thick sequences of rhythmically bedded mudstone and siltstone, which enclose laterally discontinuous sandstone and chert-pebble conglomerate layers. Thickest accumulations of coarse clastic rocks occur adjacent to the Eskay Creek area. Although these units are several hundred metres thick near Eskay Creek, they pinch out completely a few kilometres to the west.

STRUCTURAL GEOLOGY

BOWSER LAKE GROUP

The present structural geometry of the Prout Plateau area reflects folding and faulting associated with significant amounts of east-west shortening in both Bowser Lake Group and Hazelton Group strata. Bowser Lake Group rocks are best exposed in a major north-plunging syncline which encloses the Tom Mackay Lake area (Figure 6-5-2). Lithologies here are dominated by thick sequences of thinly bedded siltstone and mudstone, with lesser conglomerate and sandstone layers.

In general, intensity of deformation and amounts of shortening increase southward toward the pinch-out of Bowser Lake strata in the hinge of the syncline. At Tom Mackay Lake and northwards, second order folds within the major syncline are symmetric, have wavelengths of 400 to 800 metres, and have rounded to subangular hinges with interlimb angles of about 90°. Faults in this area have only minor offset, but some unrecognized layer-parallel slip is likely. Simple estimates of the amount of shortening based on fold geometry, indicate a minimum of approximately 40 per cent east-west shortening; total shortening will also include a component of penetrative strain leading to cleavage formation, and this estimate therefore represents a minimum value.

The contact between the Hazelton Group and the Bowser Lake Group near Tom Mackay Lake is either faulted or conformable, depending on the locality. Bedding truncations, missing stratigraphy and localized tectonism in Bowser Lake Group rocks along the east side of Mount Shirley indicate that the west side of the syncline is cut by a

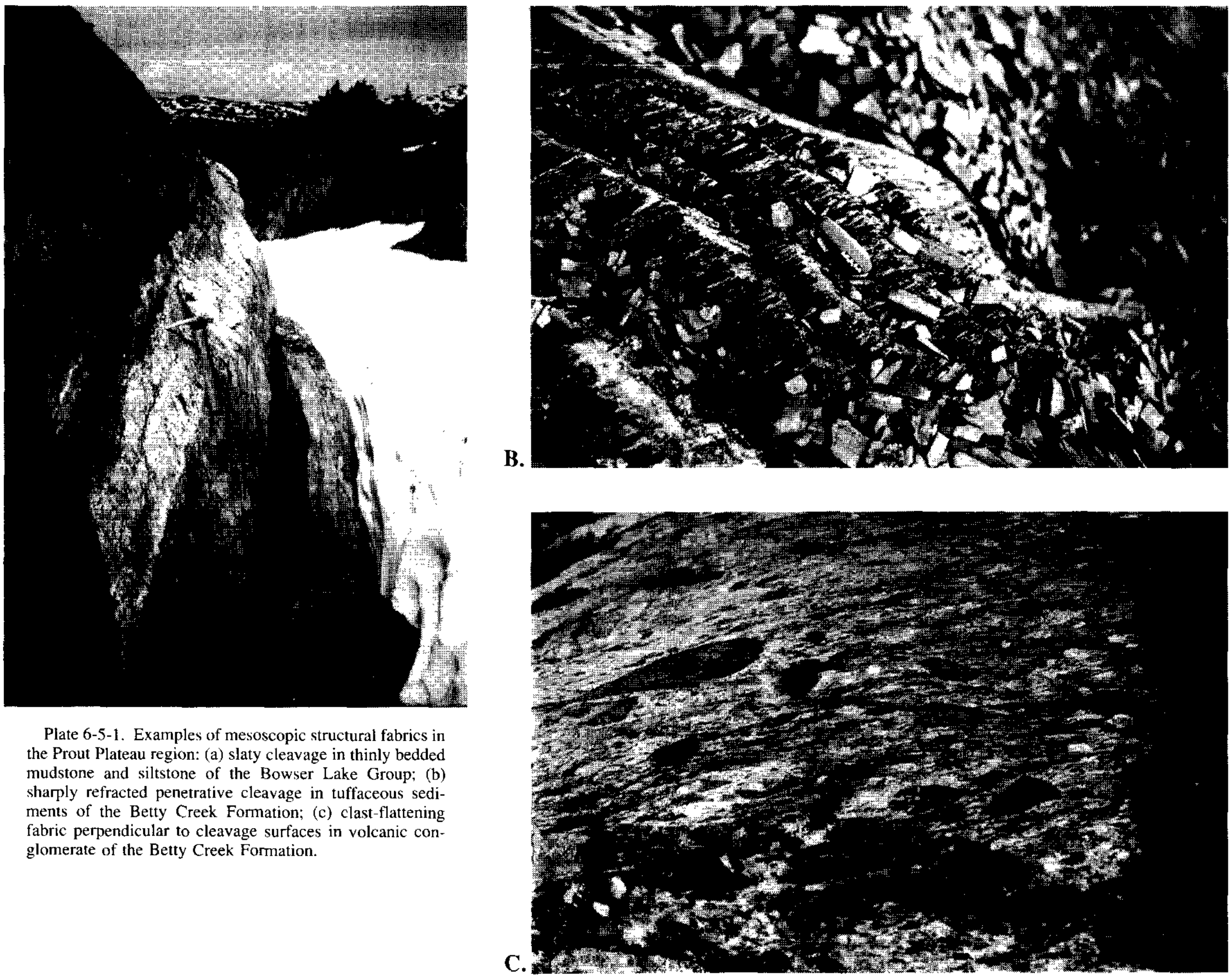

A.

B.

C.

Plate 6-5-1. Examples of mesoscopic structural fabrics in the Prout Plateau region: (a) slaty cleavage in thinly bedded mudstone and siltstone of the Bowser Lake Group; (b) sharply refracted penetrative cleavage in tuffaceous sediments of the Betty Creek Formation; (c) clast-flattening fabric perpendicular to cleavage surfaces in volcanic conglomerate of the Betty Creek Formation.

steeply west-dipping fault in that area. Southward, this fault joins, or is cut by, the Harrymel fault, and the two rock packages are conformable. On the eastern limb of the western syncline, the contact between the Bowser Lake and Hazelton groups is the Argillite Creek fault. Both the faulted contact and stratification within these units dip steeply to the northwest. Speculation that the contact is an unconformity is not supported, given the lack of a basal shallow-water deposit in the younger sequence, the apparent truncation and tectonism in overlying units and the rapid thickening of the rhythmically bedded siltstone-mudstone package southward (Figure 6-5-2).

South of Tom Mackay Lake, toward the syncline closure, Bowser Lake Group strata are more strongly deformed, but the poorer exposure at lower elevations makes mapping of continuous structures difficult. At the south end of the lake, fold axial surfaces are more closely spaced than farther north, and fold limbs are locally overturned. In this same area, folds with a strong westerly asymmetry are cut by westerly directed thrust faults, and axial surfaces swing to a more northerly orientation. Shortening amounts are difficult to estimate due to uncertainty in determining fault cut-off locations, but fold geometry alone requires in excess of 50 per cent east-west shortening. Contacts with Hazelton Group rocks are different from those found farther north as well: on the west syncline limb, steeply dipping faults striking 150° truncate folds in the Bowser Lake Group and juxtapose the sedimentary strata against lower parts of the Hazelton Group to the west. These faults are not usually exposed in outcrop, but are easily recognized by structural or stratigraphic truncation and topographic expression. The simplest interpretation of movement history involves hundreds of metres of east-side-down displacement. On the eastern limb, the contact is faulted along Coulter Creek where the contact between the two units dips gently to moderately eastward. The geometry here is consistent with a west-vergent thrust fault contact placing Hazelton Group rocks over Bowser Lake Group strata.

The Bowser Lake Group has not been mapped in detail southward through the syncline closure, but projection of structural styles south down Coulter Creek suggests a strongly tectonized, fault-bounded package of sediments within the fold core, an inference corroborated by reconnaissance examinations (R. Bartsch, personal communication, 1991). The faulted fold-closure probably lies near the confluence of Coulter Creek and the Unuk River, where the bounding faults merge.

HAZELTON GROUP

Hazelton Group rocks are best exposed in the anticline core east of Tom Mackay Lake and on the western edge of the Prout Plateau, south of Mount Shirley. In general, they are more massive and stratigraphic markers are less continuous than in the overlying Bowser Lake Group; consequently mappable structures are more difficult to define. Hazelton Group units are broadly folded and are cut by several generations of steeply dipping faults. South of Mount Shirley, two sets of faults are common: earlier faults are subvertical, strike 030° to 050°, and expose older strata on their northwest sides. More regionally continuous, steeply dipping faults striking 145° to 155° truncate the older faults, and generally expose older strata on their southwest sides. In places these younger faults separate the Bowser Lake Group from the Hazelton Group. Slip-direction indicators are lacking for both sets of faults. Broad, north to northwest-trending folds in the Hazelton Group are cut and offset by the northwest-striking faults, resulting in locally complex contact distribution patterns along the ridge south of Mount Shirley. Mapping along the flanks of this ridge in the Harrymel and Coulter Creek valleys by R. Bartsch (personal communication, 1991) suggests that the ridge forms the core of a regional antiform and that Hazelton strata form dip slopes along the flanks.

East of the Tom Mackay syncline, a monoclinal section of northwest-dipping Hazelton Group strata extends across the Eskay Creek and SIB properties. Stratigraphic markers can be traced continuously across both claim groups, with only minor apparent left-lateral offsets along northerly striking faults. There is probably some faulting parallel to stratigraphic layering, but it is not mappable at 1:20 000 scale. Regional maps show this northwest-dipping panel forming the west limb of a major northwest-trending anticline. This interpretation is supported by the occurrence of southeast-facing Bowser Lake Group argillites and mudstones along the lower reaches of Eskay Creek and in the Unuk River valley. The transition from west-facing to east-facing beds, however, occurs within a structurally complex, poorly exposed area and coincides with a major northeast-striking fault. This fault obscures the fold hinge and has undetermined offset. The apparent lack of continuity of Hazelton Group felsic volcanic rocks across the hinge (Figure 6-5-2; Alldrick *et al.*, 1989) is probably related to this faulting.

MESOSCOPIC STRUCTURAL FEATURES

The most prominent mesoscopic structural features in Bowser Lake Group and Hazelton Group strata are well-developed, steeply dipping, north to northeast-striking cleavage fabrics. These cleavages are parallel to axial surfaces of macroscopic folds and the few mesoscopic folds scattered through the area. The form and visual appearance of cleavage correlates strongly with host lithology. A strong slaty cleavage is present at highest structural levels in bedded mudstone and siltstone of the Bowser Lake Group (Plate 6-5-1a). Coarse sandstone and conglomerate layers within this unit contain weakly to moderately developed spaced cleavage, best developed in fold hinges. Dissolution of clasts along cleavage surfaces is apparent in some exposures and is indicative of a pressure solution mechanism of cleavage formation in these areas.

Lithologically variable Hazelton Group rocks contain a wide variety of structural fabrics. At highest levels, volcanic breccias and pillowed flows of the Salmon River Formation contain no visible penetrative fabrics, and pillow shapes appear unstrained. However, interlayered mudstones are disharmonically folded and locally are strongly tectonized. Lower in the section, felsic volcanic flows contain a weak to moderate anastomosing foliation at Eskay Creek. Epiclastic sedimentary rocks contain weak to strong penetrative cleavage which refracts sharply across lithologic interfaces (Plate 6-5-1b). Coarse volcanic conglomerates contain strongly oblate clasts, with shortest dimensions perpendicular to cleavage planes (Plate 6-5-1c). Axial ratios in these clasts range up to 3:3:1. Clast elongation is rare and, where it occurs, is in a down-dip orientation.

Mesoscopic folds occur in scattered locations throughout the Prout Plateau area, and are usually north to northeast-plunging structures coaxial to the macroscopic folds. Minor fold asymmetry is variable and consistent with that expected for folds which are second order to the major structures. Fault drag folds are common along some of the major faults (*e.g.*, Argillite Creek fault, Mount Shirley fault) where their geometry is probably controlled by movement on adjacent structures.

DISCUSSION

Structures in the Prout Plateau area developed during a period of east-west contraction, during which approximately 50 per cent shortening was accommodated by rocks of the Hazelton and Bowser Lake groups. The cuspate syncline and lobate anticline structural form of the Bowser Lake Group - Hazelton Group contact is typical of folded multilayers with high competence contrasts. An arcuate swing in structural trend from northeasterly (north of Tom Mackay Lake) to northerly (south of Tom Mackay Lake) reflects either a reorientation of originally rectilinear features, or a variation in fold orientation during initial deformation. The latter interpretation is favoured because of the lack of overprinting mesoscopic features in outcrop; original arcuate trends may have been caused locally by emplacement of the structurally competent block formed by Mount Shirley against the northern part of the Prout Plateau syncline. North of Mount Shirley, where the Mount Shirley fault loses definition, structural trends are again more northerly (Read *et al.*, 1989), supporting this interpretation. However, maps of areas to the east suggest this swing to northeasterly structural trends may be part of a more regional northeast-trending fold set along the western edge of the Skeena fold belt.

Timing of deformation is only approximately constrained by the initial mapping. Major folds in the Prout Plateau area occur in rocks of both the Hazelton and the Bowser Lake groups. The wide age range of these packages, from Early to Late Jurassic, suggests that major Early to Middle Jurassic deformation documented elsewhere in the Cordillera did not have a strong impact on structural development of the Iskut River area. Evidence for Middle Jurassic deformation is limited to an intra-Hazelton Group unconformity around John Peaks (unpublished mapping, this study; Henderson *et al.*, 1992) and a Toarcian unconformity, to the north, on Troy Ridge (R.G. Anderson, personal communication, 1991). Most regional folding apparently followed deposition of the Bowser Lake Group sedimentary sequence, in latest Jurassic time or later. This timing is consistent with Cretaceous to Early Tertiary shortening to the east within the Skeena fold belt (Evenchick, 1991) and the folds in the Prout Plateau area can reasonably be considered to be the westernmost manifestation of this fold belt.

Initial mapping in the area surrounding John Peaks has revealed structural styles consistent with those described for the Prout Plateau area. This area is dominated by a major west-vergent thrust fault within the Hazelton Group, which places an overturned folded sequence of Mount Dilworth Formation and older rocks onto an upright sequence of Salmon River Formation argillites and pillowed flows. Subsequent work will involve tracing regional structures between the two areas, and extending mapping to the south and east into the Sulphurets area.

ACKNOWLEDGMENTS

International Corona Corporation, American Fibre Ltd. and Prime Resources Group Inc. are acknowledged for granting permission to work on their respective properties and to publish this paper. The work and ideas presented benefited greatly from discussions with Rod Kirkham, Bob Anderson, Jack Henderson, Mariette Henderson, Tom Wright, Dani Alldrick, Jim Britton and other MDRU project participants. Susan Taite critically reviewed an early version of the manuscript. Funding for this study is provided under the MDRU project "Metallogenesis of the Iskut River Area".

REFERENCES

Alldrick, D.J. and Britton, J.M. (1988): Geology and Mineral Deposits of the Sulphurets Area (104A/5, 104A/12, 104B/8, 104B/9); *B.C. Ministry of Energy, Mines and Petroleum Resources*, Open File 1988-4.

Alldrick, D.J., Britton, J.M., MacLean, M.E., Hancock, K.D., Fletcher, B.A. and Hiebert, S.N. (1990): Geology and Mineral Deposits of the Snippaker Area, (104B/6E, 7W, 10W, 11E); *B.C. Ministry of Energy, Mines and Petroleum Resources*, Open File 1990-16.

Alldrick, D.J., Britton, J.M., Webster, I.C.L. and Russell, C.W.P. (1989): Geology and Mineral Deposits of the Unuk Map Area, (104B/7E, 8W, 9W, 10E); *B.C. Ministry of Energy, Mines and Petroleum Resources*, Open File 1989-10.

Anderson, R.G. (1989): A Stratigraphic, Plutonic, and Structural Framework for the Iskut River Map Area, Northwestern British Columbia; *in* Current Research, Part E, *Geological Survey of Canada*, Paper 89-1E, pages, 145-154.

Anderson, R.G. and Thorkelson, D.J. (1990): Mesozoic Stratigraphy and Setting for Some Mineral Deposits in Iskut River Map Area, Northwestern British Columbia; *in* Current Research, Part E, *Geological Survey of Canada*, Paper 90-1E, pages 131-139.

Bartsch, R.M. (1992): Eskay Creek Area, Stratigraphy Update; *in* Geological Fieldwork 1990, Grant, B. and Newell, J.M., Editors, *B.C. Ministry of Energy, Mines and Petroleum Resources*, Paper 1992-1, this volume.

Bevier, M.L. and Anderson, R.G. (1991): Jurassic Geochronometry in Northwest Stikinia (56-57° N), British Columbia; *in* Program with Abstracts, *Geological Society of America*, Annual Meeting, San Diego.

Britton, J.M. and Alldrick, D.J. (1988): Sulphurets Map Area (104A/5W, 12W, 104B/8E, 9E); *in* Geological Fieldwork, 1987, *B.C. Ministry of Energy, Mines and Petroleum Resources*, Paper 1988-1, pages 199-209.

Britton, J.M., Blackwell, J.D. and Schroeter, T.G. (1989a): Eskay Creek (104B 008); *in* Exploration in British Columbia 1989, *B.C. Ministry of Energy, Mines and Petroleum Resources*, pages 197-223.

Britton, J.M., Fletcher, B.A., and Alldrick, D.J. (1990): Snippaker Map Area (104B/6E, 7W, 10W, 11E); *in* Geological Fieldwork 1989, *B.C. Ministry of Energy, Mines and Petroleum Resources*, Paper 1990-1, pages 115-125.

Britton, J.M., Webster, I.C.L. and Alldrick, D.J. (1989b): Unuk Map Area (104B/7E, 8W, 9W, 10E); *in* Geological Fieldwork 1988, *B.C. Ministry of Energy, Mines and Petroleum Resources*, Paper 1989-1, pages 241-250.

Evenchick, C.A. (1991): Structural Relations of the Skeena Fold Belt West of the Bowser Basin, Northwest British Columbia; *Canadian Journal of Earth Sciences*, Volume 28, Number 6, pages 973-983.

Grove, E.W. (1986): Geology and Mineral Deposits of the Unuk River - Salmon River - Anyox Area; *B.C. Ministry of Energy, Mines and Petroleum Resources*, Bulletin 63, 152 pages.

Henderson, J.R., Kirkham, R.V., Henderson, M.N., Payne, J.G., Wright, T.O. and Wright, R.L. (1992): Stratigraphy and Structure of the Sulphurets Area, British Columbia (104B/8, 9); *in* Current Research, Part A, *Geological Survey of Canada*, Paper 92-1A, in press.

Kirkham, R.V., Ballantyne, S.B. and Harris, D.C. (in preparation): Sulphurets Area, British Columbia -- Preliminary Geology, Geochemistry and Mineralogy of a Deformed Copper, Molybdenum, Precious Metal System.

Read, P.B., Brown, R.L., Psutka, J.F., Moore, J.M., Journeay, M., Lane, L.S. and Orchard, M.J. (1989): Geology, More and Forrest Kerr Creeks (Parts of 104B/10, 15, 16 and 104C/1, 2); *Geological Survey of Canada*, Open File 2094.

NOTES

PRELIMINARY GEOLOGY OF THE 21A ZONE, ESKAY CREEK, BRITISH COLUMBIA (104B/9W)

By T. Roth and C.I. Godwin
Mineral Deposit Research Unit
The University of British Columbia
(MDRU Contribution 007)

KEYWORDS: Economic geology, Eskay Creek, massive sulphides, Stikinia, Hazelton Group, gold, silver, 21A zone.

INTRODUCTION

The Eskay Creek deposit (56°38′N; 130°27′W), in northwestern British Columbia, is approximately 80 kilometres north of Stewart. The deposit, known as the 21 zone, is hosted in bimodal volcanics of the Lower Jurassic Hazelton Group, within the Stikine Terrane, near the western margin of the Intermontane Belt. The 21 zone has been subdivided into the 21A and 21B zones on the basis of differing ore mineralogies and gold grades. Both zones are hosted by similar lithologies.

Published reserves for the 21 zone are 3.95 million tonnes (4.36 million tons) grading 26.4 grams per tonne (0.77 oz/ton) gold and 998 grams per tonne (29.12 oz/ton) silver (The Northern Miner, January 28, 1991). The bulk of these reserves are in the 21B zone. As this paper goes to press, reserves have been revised downwards (Globe and Mail, December 17, 1991). New tonnage and grade estimates are not available, but projected gold recovery is now approximately 62 000 kilograms (2 million oz.), a reduction of one-third from earlier estimates, largely as a result of using a cut-off grade of 13.7 grams per tonne gold. The 21A zone is estimated to contain approximately 1.41 million tonnes (1.56 million tons) of probable and possible reserves grading 7.2 grams per tonne (0.21 oz/ton) gold and 116.6 grams per tonne (3.4 oz/ton) silver at a cut-off grade of 1.4 grams per tonne (0.04 oz/ton) (Roscoe Postle Associates Incorporated quoted in Britton *et al.*, 1990).

This report presents preliminary observations of the 21A Zone. Data were collected during the summer of 1991 as part of an M.Sc. study by Roth. Drill core from three sections through the zone, spaced at 100 metre intervals, was re-logged to develop a detailed geological framework for the deposit (Figure 6-6-1). Several mineralized intervals between these sections were re-logged to evaluate changes along strike. Samples were collected for petrographic and geochemical analysis.

REGIONAL GEOLOGY

Four tectonostratigraphic assemblages have been defined in the area of the deposit (Anderson, 1989): the Paleozoic Stikine assemblage, the Triassic to Jurassic volcanic-plutonic complexes, the Middle and Upper Jurassic Bowser overlap assemblage, and the Tertiary Coast Plutonic Complex. The Triassic to Jurassic strata include the Upper Triassic Stuhini Group and the Lower Jurassic Hazelton Group (Anderson, 1989; Anderson and Thorkelson, 1990). Regional geology is also summarized by Britton *et al.* (1990).

GEOLOGY OF THE 21A ZONE

The Eskay Creek property is underlain by Lower to Middle Jurassic Hazelton Group volcanics and sediments. A summary of the property geology is provided by Britton *et al.* (1990). The general geological features of the 21 zone deposit have been described by Blackwell (1990). Features of the 21A zone are detailed below.

Stratigraphy observed in drill core from the 21A zone drill core is illustrated in Figure 6-6-2. The strata strike northeast and dip moderately northwest. The sequence from footwall dacitic volcanics, upwards to felsic volcanics and into hangingwall basaltic volcanics, is consistent throughout the zone. The major volcanic units are generally separated by argillite, which occurs at the top of both the dacite and the rhyolite units. The contact between the footwall rhyolite and the hangingwall basaltic volcanics has been called the contact unit (Blackwell, 1990; Britton *et al.*, 1990). Argillite within the contact unit is referred to as the "contact argillite".

This stratigraphic sequence may represent two cycles of volcanism. The lower dacites and rhyolites would represent the progressively increasing felsic top of a volcanic cycle. The contact argillite reflects a hiatus between cycles, and is followed by basaltic volcanics that represent the mafic beginning of the next cycle.

Footwall dacite, the lowermost unit in the 21A zone (Figure 6-6-2), is a sequence of medium to dark green volcaniclastics, lapilli and ash tuffs. It has a minimum thickness of 60 metres. The volcaniclastics contain fragments of mixed provenance and are interbedded with shales, siltstones and coarser clastics. Volcanic textures and grading are locally preserved. A pinkish beige commonly amygdaloidal dacitic flow or breccia occurs locally near the top of the sequence. The dacitic sequence is generally separated from the rhyolitic package by a thin, black shale (0 to 10 m thick).

Footwall rhyolite overlies the dacitic unit and ranges from 70 to 210 metres in thickness (Figure 6-6-2). The unit consists dominantly of grey mottled, altered and devitrified material. Though many of the textures have been obliterated, well-preserved flow banding, breccias and volcaniclastics are present. Massive, siliceous light grey aphanitic rhyolite also occurs, most commonly in the lower portion of the sequence. Most of the rhyolite appears to consist of fragmental material. Clasts may be well preserved in a mottled and indistinguishable grey matrix that is

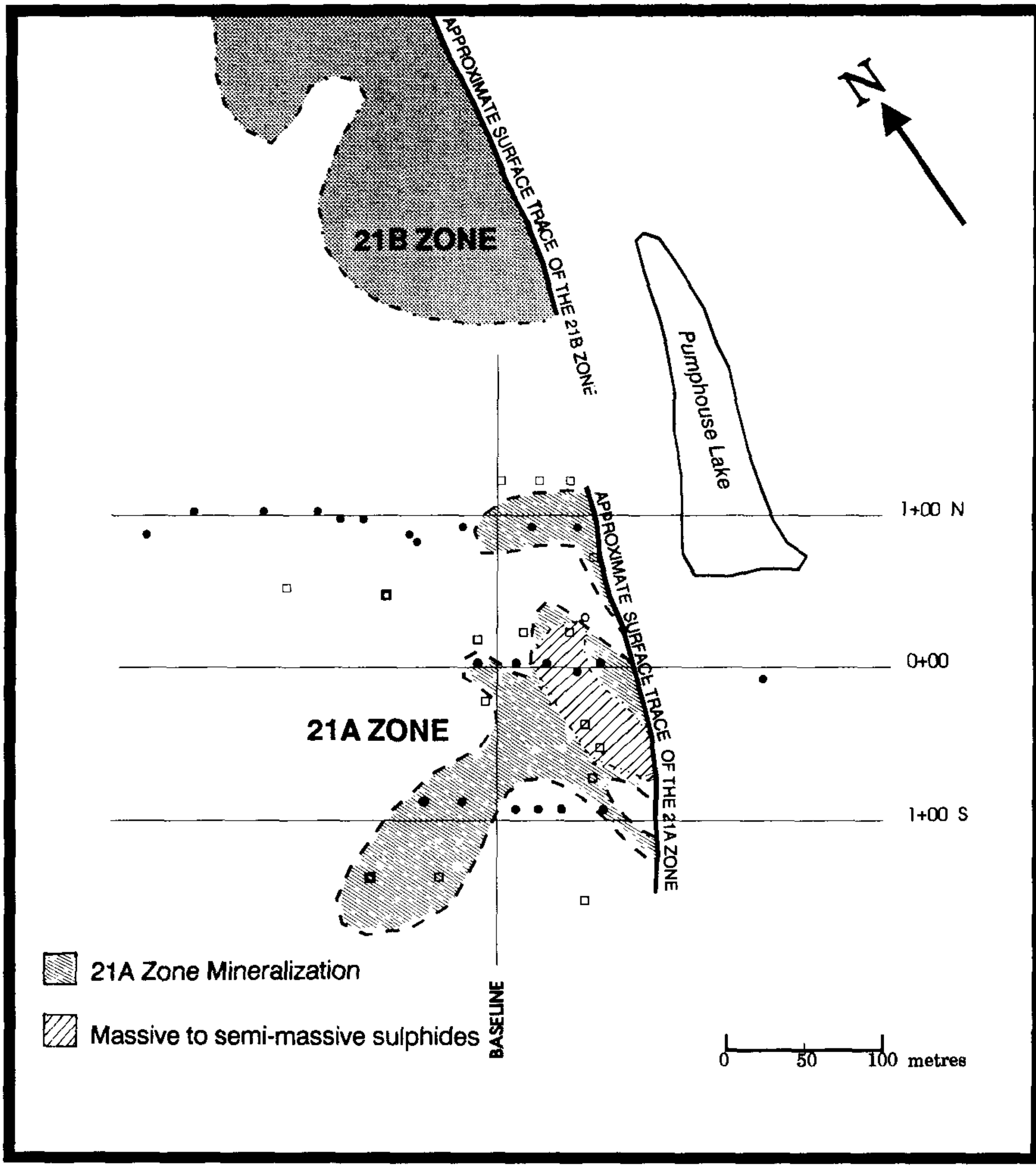

Figure 6-6-1. Schematic diagram of the distribution of gold mineralization in the Eskay Creek 21A zone, with locations of re-logged drillholes. Squares and dots mark intersections with the contact argillite. Dots = holes on detailed sections; Open squares = mineralized intersections logged off-section).

devitrified and altered. Excellent breccia textures, often with rotated flow-banded clasts, are predominantly monolithic; but variably altered clasts, and mixed massive siliceous and flow-banded clasts occur locally.

Fine-grained, possibly tuffaceous intervals occur most commonly near the top of the rhyolitic sequence, but also in the middle to lower part. Strong to intense sericitic alteration has obliterated many primary textures, but relict clasts are commonly observed. Textures in the Eskay Creek footwall are discussed further by Ettlinger (1992, this volume).

The upper contact of the rhyolite is difficult to define, partly due to sericitic alteration. The sequence locally grades upwards into the overlying argillite. In several drill holes, thin beds of siliceous black argillite are interbedded with intervals of grey to very dark grey, sericitic material. Clasts of argillite are locally included in a very soft, fine-grained, greenish matrix or in a black carbonaceous matrix. Elsewhere, variably altered rhyolite clasts occur in a black argillaceous matrix. This change from dominantly rhyolitic material to dominantly black argillaceous material was formerly termed the "transition zone" (Blackwell, 1990) and was considered to be part of the lower part of the contact unit. In this study, grey to dark grey sericitic intervals have been included as a subunit of the rhyolite sequence. The clastic material was logged as separate subunits of the rhyolite or argillite, based on dominant lithology.

Contact argillite, from 0 to 15 metres thick, occurs between the rhyolite package and the overlying basaltic volcanics (Figure 6-6-2). The upper contact is sharp. The argillite is black and mostly thinly bedded to laminated with silty or tuffaceous pyritic layers. It is variably calcareous, hard and cherty, or soft and graphitic (possibly bituminous). Beds of black limestone and fossil belemnites occur locally, but not necessarily together.

Basaltic volcanics form the uppermost sequence of the 21A zone stratigraphy (Figure 6-6-2). In drill core, the volcanics range from dark green to tan; their minimum thickness is 125 metres. Flows and some sills are intercalated with laminated to thin-bedded argillites with silty or tuffaceous layers and black chert; some of these units may represent distal turbidites. The silty to tuffaceous layers usually contain pyrite or pyrrhotite. Volcanic textures observed include pillowed flows and pillow breccias, massive, crystalline to porphyritic flows, amygdaloidal flows, hyaloclastites and debris flows. Brecciated intervals have a fine-grained calcareous and siliceous matrix.

ALTERATION

Alteration is prevalent in the footwall rhyolite. The rocks are altered extensively to quartz, sericite and pyrite, as well as chlorite and clay. Moderate to intense, pervasive sericitic and chloritic alteration are significant and abundant. The altered material is very soft, medium to dark grey or green, and contains ubiquitous very fine grained, disseminated pyrite. In some places, this alteration is also accompanied by secondary clay alteration – especially in zones of faulting or shearing. Silicification in the footwall rhyolite is pervasive to patchy. Narrow quartz veins with white, siliceous envelopes locally replace and obliterate flow-banded textures.

The hangingwall basaltic volcanics exhibit propylitic alteration. Barren calcite veins are common throughout the hangingwall sequence. This alteration may reflect either regional lower greenschist facies metamorphism or weak, late hydrothermal effects from the mineralizing event for the 21A zone.

MINERALIZATION

The bulk of gold mineralization in the 21A zone is in the lower part of the contact argillite and the upper portion of the footwall rhyolite (Figure 6-6-2). Gold and silver-rich mineralization also occurs locally in veins and veinlets throughout the footwall rhyolite. Sporadic precious metal values are present at the top of the underlying dacitic sequence.

The most striking mineralization and highest gold values within the 21A zone are found in a stratabound lens of massive to semimassive stibnite, arsenopyrite realgar, orpiment and cinnabar at the base of the contact argillite (Figure 6-6-2). This lens represents a volumetrically small portion of gold-bearing mineralization in the 21A zone (Figure 6-6-1). Veins containing realgar and cinnabar, generally with calcite and/or quartz selvages, cut the lower contact argillite or the upper part of the footwall rhyolite close to the high-grade lens.

Much of the gold and silver mineralization in the 21A zone is associated with strongly to intensely altered, fine-grained, sericitized material in the upper part of the rhyolite (Figure 6-6-1). Sulphides in this zone are usually very fine grained and include pyrite, sphalerite, galena and tetrahedrite. This type of mineralization is also found locally in the middle portion of the footwall rhyolite.

The footwall rhyolite also hosts stockwork veins and veinlets of sphalerite, galena, tetrahedrite, pyrite and minor chalcopyrite. For the most part, these sulphides are not usually associated with significant precious metal assay values.

Minor gold mineralization occurs locally at the top of the dacitic sequence. The dacitic flow units locally host vein pyrite and semimassive pyrite, both associated with minor amounts of sphalerite and galena (Figure 6-6-1). The origin of the semimassive pyrite is not clear.

SUMMARY

The 21A zone at Eskay Creek occurs near the top of a felsic cycle of volcanism. The gold and silver mineralization is dominantly within both the top of the felsic rhyolitic package and the base of the overlying argillite. It occurs locally lower in the rhyolite sequence. Mineralization associated with massive lenses of arsenic, antimony and mercury minerals appears to be restricted to a volumetrically small part of the zone.

Data collected this summer will better define the distribution of, and relationships among, mineralization, alteration and lithology. A petrographic study will identify the fine-grained host minerals and sulphides and establish their relationships. This work will be enhanced by x-ray diffraction, microprobe and geochemical studies.

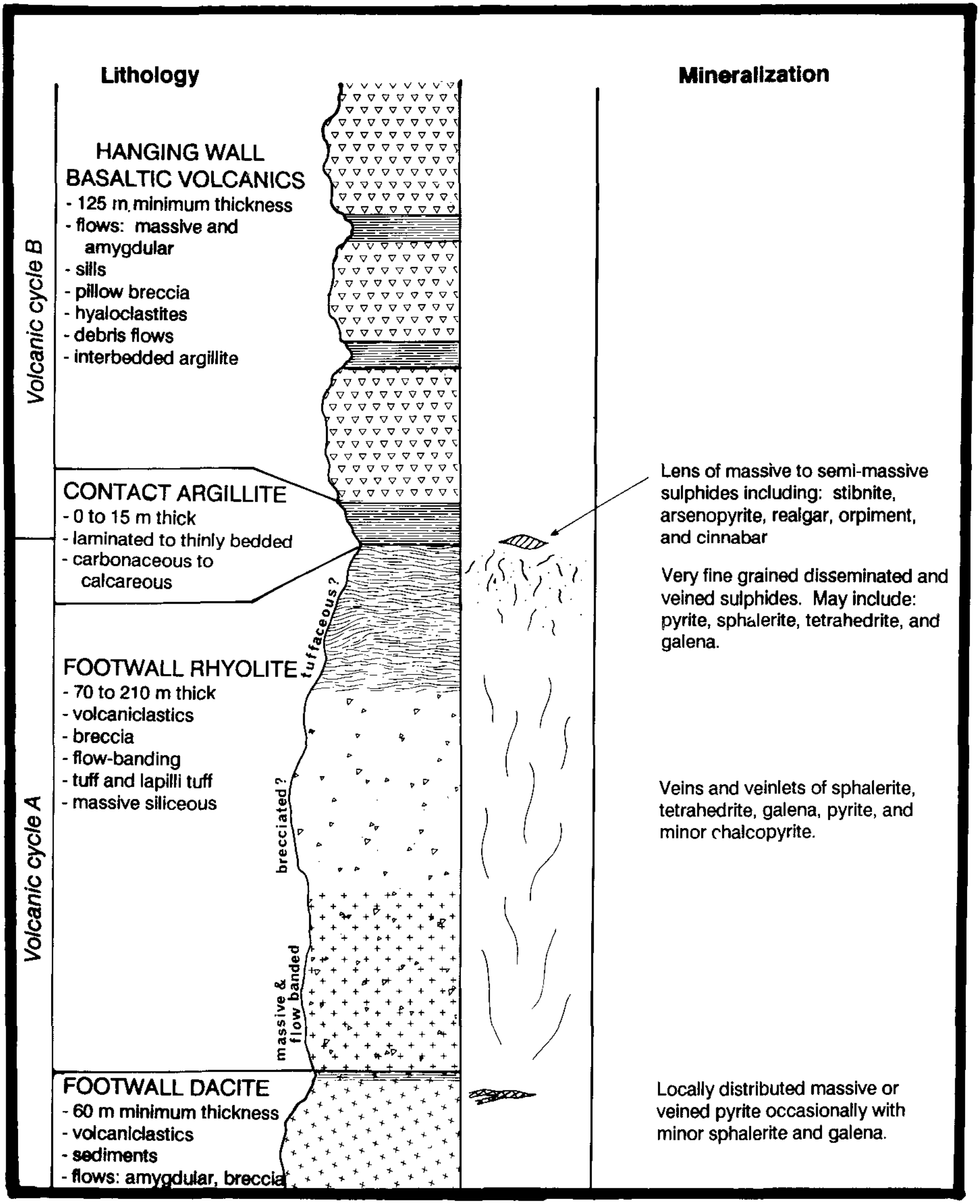

Figure 6-6-2. Schematic stratigraphic section of the Eskay Creek 21A zone showing general lithology, textures and mineralization.

ACKNOWLEDGMENTS

We would like to thank International Corona Corporation, particularly K. Rye, C. Edmunds, D. Kuran and F. Fowler, for their support and input this summer. Members of the Mineral Deposit Research Unit (MDRU) Iskut research team provided helpful discussions and regional insights. This M.Sc. thesis study forms part of the MDRU project, "Metallogenesis of the Iskut River Area, Northwestern B.C.". Additional funding to Roth is provided through a National Science and Engineering Research Council postgraduate scholarship.

REFERENCES

Anderson, R.G. (1989): A Stratigraphic, Plutonic and Structural Framework for the Iskut River Map Area (NTS 104B), Northwestern British Columbia; *in* Current Research, Part E, *Geological Survey of Canada,* Paper 89-1E, pages 145-154.

Anderson, R.G. and Thorkelson, D.J. (1990): Mesozoic Stratigraphy and Setting for some Mineral Deposits in the Iskut River Map Area, Northwestern British Columbia; *in* Current Research, Part E, *Geological Survey of Canada,* Paper 90-1E, pages 131-139.

Blackwell, J.D. (1990): Geology of the Eskay Creek 21 Deposits; *in* The Gangue, Number 31, *Mineral Deposits Division, Geological Association of Canada,* April 1990, pages 1-4.

Britton, J.M., Blackwell, J.D. and Schroeter, T.G. (1990): 21 Zone Deposits, Eskay Creek, Northwestern British Columbia; *in* Exploration in British Columbia 1989, *B.C. Ministry of Energy, Mines and Petroleum Resources,* Pages 197-223.

Ettlinger, A.D. (1992): Footwall Alteration, 21 zone, Eskay Creek; *in* Geological Fieldwork 1991, Grant, B. and Newell, J.M., Editors, *B.C. Ministry of Energy, Mines and Petroleum Resources,* Paper 1992-1, this volume.

NOTES

British Columbia Geological Survey
Geological Fieldwork 1991

HYDROTHERMAL ALTERATION AND BRECCIATION UNDERLYING THE ESKAY CREEK POLYMETALLIC MASSIVE SULPHIDE DEPOSIT (104B/9W)

By Art D. Ettlinger
Mineral Deposit Research Unit, The University of British Columbia

(MDRU Contribution 008)

KEYWORDS: Economic geology, Eskay Creek, hydrothermal alteration, brecciation, devitrification, hydrofracturing, pseudobreccia.

INTRODUCTION

The Iskut River area of northwestern British Columbia (Figure 6-7-1) has been a centre of extensive mineral exploration activity since the discovery of the Eskay Creek polymetallic massive sulphide-gold deposit during late 1988. Since that time, over 650 diamond-drill holes in the 21A and 21B ore zones at Eskay Creek, have identified a geologic reserve in excess of 3 million ounces of gold and 125 million ounces of silver (Northern Miner, Jan. 28, 1991). This makes Eskay Creek one of the most significant exploration discoveries in western Canada in the past ten years.

Most of the exploration activity, including surface and underground diamond drilling and bulk sampling for metallurgical studies, has focused on the 21B zone which contains the bulk of quoted geologic reserves. The 21A zone (*see* Roth and Godwin 1992; this volume), which lies approximately 0.5 kilometre along strike to the southwest of the 21B zone (Figure 6-7-1), displays similar hydrothermal alteration and brecciation, but contains a trace element association enriched in mercury, antimony and arsenic that is not commonly observed in the 21B zone. Both zones are hosted by a similar lithologic sequence and occur at the same stratigraphic level. A distinct style of brecciation and hydrothermal alteration appears to be associated with spectacular gold assays on core from several mineralized intercepts in diamond-drill hole CA89-109 (Prime Capital Corporation, News Release #44, 21 Sept. 1989). Hole CA89-109 is located within the 21B zone, near the centre of the deposit (Figure 6-7-1).

The observations presented in this paper are the result of logging approximately 3800 metres of diamond-drill core from the 21A and 21B zones, and surface sampling followed by limited petrographic analysis. This work is part of an ongoing study of Iskut River metallogenesis by the Mineral Deposit Research Unit, The University of British Columbia. Further research at Eskay Creek will more completely address questions relating to the distribution and significance of the different alteration patterns and their relationship to gold-sulphide mineralization.

ESKAY CREEK GEOLOGY

The Eskay Creek deposit is situated within the Stikine Terrane on the eastern margin of the Coast Plutonic Complex. A framework for the geology of the Iskut River district has been established by researchers of the Geological Survey of Canada (Anderson, 1989; Anderson and Bevier, 1990; Anderson and Thorkelson, 1990) and the British Columbia Geological Survey Branch (Alldrick and Britton, 1988; Alldrick *et al.*, 1989, 1990). These workers place the hostrocks of the deposit within the Lower Jurassic Hazelton Group, a heterogeneous, bedded sequence of predominantly marine sedimentary and volcaniclastic rocks

Early descriptions of the ore deposit and surrounding geology are given by Idziszek *et al.* (1990), Blackwell (1990), and Britton *et al.* (1990). The bulk of base metal sulphide and precious metal mineralization forming the 21 zone deposits is hosted by laminated, carbonaceous argillite and underlying rhyolite breccia (Britton *et al.* 1990). Stratiform sulphides in the "contact unit" (Blackwell, 1990), occur at the base of a flow-sill complex, informally known as the hangingwall andesite unit. The hangingwall sequence largely consists of fine-grained, medium-green pillowed flows, flow breccia and hyaloclastite. Sills, with chilled aphanitic contacts, are massive and commonly porphyritic. These submarine volcanic rocks contain numerous, discontinuous lenses of fossiliferous, laminated black argillite. Volcanic flow structures and mud infilling in underlying flow-top breccias indicate the sequence youngs upwards.

An unbedded, intensely altered accumulation of rhyolite and rhyolite breccia underlies the stratiform sulphides and is the host to stockwork and disseminated base metal sulphide and gold-silver mineralization (Blackwell, 1990). The rhyolite varies in thickness from 30 to 110 metres, averaging 80 metres (Britton *et al.*, 1990). Due to alteration, primary volcanic textures are rare. This felsic volcanic sequence, informally known as the footwall rhyolite (Blackwell, 1990), is underlain by dacitic ash and lapilli tuff, volcanic agglomerate and epiclastic rocks in excess of 100 metres thick. This sequence, referred to as the footwall dacite unit, is widely pyritic and locally contains base metal massive sulphides, but is not currently known to host economic gold-silver mineralization.

PRIMARY DEPOSITIONAL TEXTURES

Hydrothermal alteration and related brecciation have destroyed much of the original rock fabric and volcanic minerals within the footwall rhyolite. A volumetrically small amount of rock, displaying primary flow, pyroclastic or epiclastic textures, is preserved. Massive flow-banded rhyolite, autoclastic flow-breccia and heterolithic tuff-breccia are the most common volcanic features observed (Plate 6-7-1a, b, c). Most of the footwall consists of a mottled light grey, massive featureless rock which is very hard and intensely silicified (Plate 6-7-1d). It is uncertain

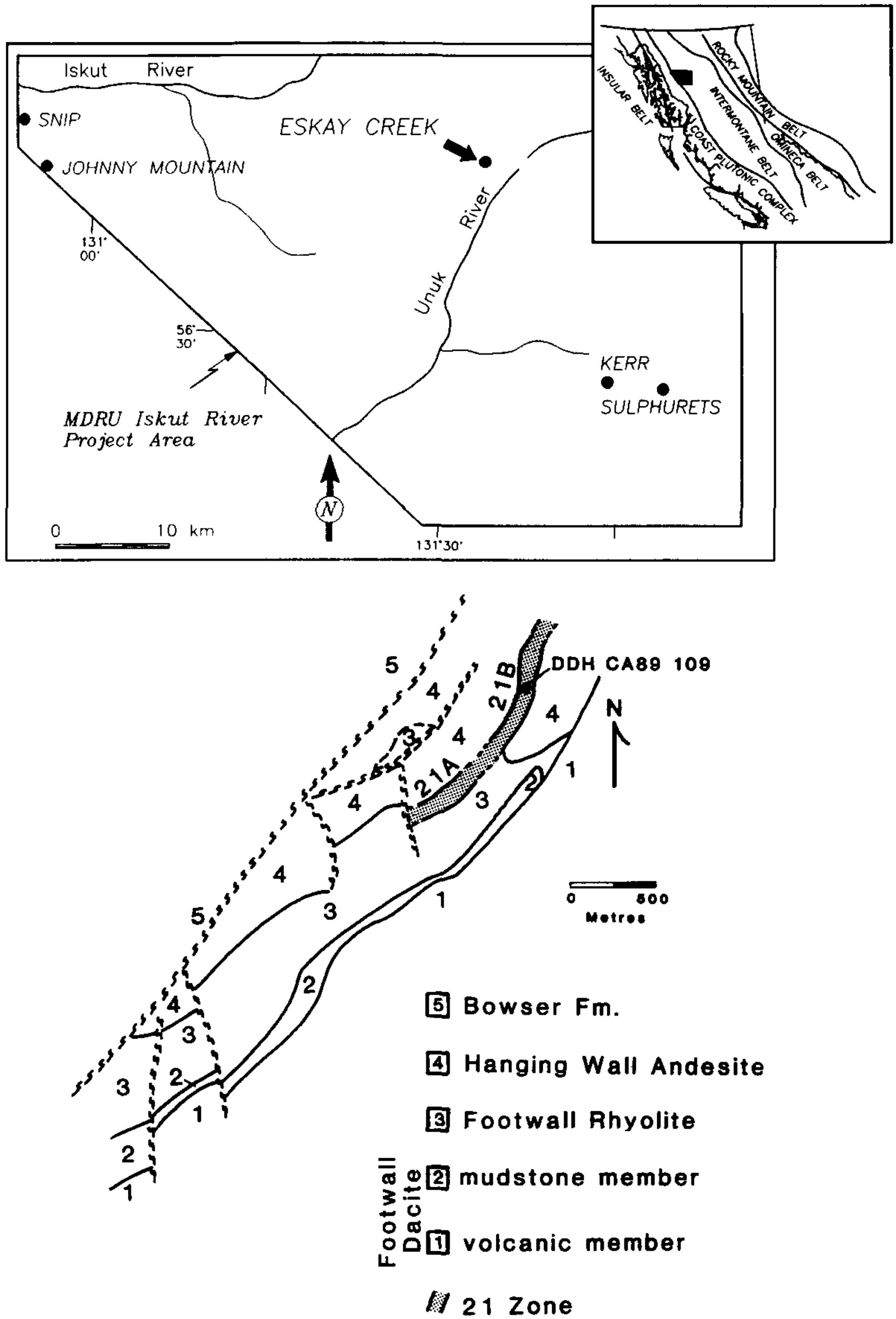

Figure 6-7-1. Location map and general geology of the Eskay Creek deposit.
Geology adapted from Rebagliati and Haslinger, 1991.

whether this facies represents original, massive silicic lava or some other intensely altered protolith.

FOOTWALL ALTERATION

Several styles of hydrothermal alteration and brecciation are present in the footwall beneath the Eskay Creek deposit. Silicification of the footwall rhyolite is intense and widespread, both immediately below, and extending away from the ore zones. Phyllosilicate alteration is in part related to silicification, with a second style limited to the area of massive sulphide mineralization. Fine-grained pyrite occurs with the silicification and phyllosilicate alteration. Solid hydrocarbons, scattered throughout all lithologies hosting 21-zone mineralization, appear most abundantly in the footwall rhyolite underlying the 21B zone.

Breccia textures are common in the footwall rhyolite. Brecciated rocks are present throughout the sequence, but they appear to be most abundant in the upper half of the rhyolite, underlying the contact argillite.

SILICIFICATION AND PHYLLOSILICATE ALTERATION

Quartz is by far the most abundant alteration mineral underlying the Eskay Creek deposit. Virtually all of the rhyolite underlying the 21 zone, as exposed in drill core and on the surface, is intensely silicified. In rare cases, an intense stockwork of millimetre-wide quartz veinlets is developed (Plate 6-7-2). In most of the footwall, however, quartz flooding results in a very hard, mottled grey rock, with little recognizable texture or fabric preserved (Plate 6-7-1d). The timing of silicification is uncertain; earliest silicification appears to be associated with brecciation (see below) and persists temporally through deposition of at least some of the sulphides.

At least two styles of phyllosilicate alteration are present. Petrographic analysis indicates sericite is a persistent component in silicified zones throughout the footwall. It commonly occurs with pyrite, forming a widespread quartz-sericite-pyrite alteration blanket underlying the 21 zone. Preliminary x-ray diffraction analysis indicates muscovite and illite are the major sericite components. Small amounts of phlogopite and clinochlore are also present.

A more intense phase of phyllosilicate alteration, resulting in a soft, highly incompetent rock, appears to be spatially related to semimassive and massive sulphide mineralization. Zones of intense, sheared sericite and dark green to black clinochlore (Blackwell, 1990) alteration are most abundant within the upper half of the footwall rhyolite, directly beneath the 21A and 21B zones. Scattered, disseminated sphalerite is generally associated with the clinochlore alteration.

ALTERATION BRECCIAS

Breccia textures are a common feature of the footwall rhyolite. Other than the volcaniclastic tuff breccias noted above, brecciation may also result from hydrothermal alteration of the rhyolite. The distribution and intensity of these "alteration breccias" are highly variable. These textures can be identified and distinguished from true pyroclastic rocks, by the following criteria:

- Fragments are monolithic with individual fragments appearing to be in-place. This results in a mosaic fabric to the rock.
- Fragments have highly irregular or finely scalloped margins, resorption textures or gradational boundaries with the breccia matrix.
- Fragments and unbrecciated hostrock, are cut by stockwork veinlets of similar composition to the enclosing matrix.
- Breccia distribution is highly irregular and discontinuous, making correlation between adjacent drill holes difficult or impossible.

Plate 6-7-3a and b illustrate the process by which the hydrothermal breccias form. As a precursor to actual breccia formation, massive, silicified rhyolite is cut by a stockwork of black, very hard veinlets which consist dominantly of black silica (Plate 6-7-3a). In some cases, migration of veinlet material into the wallrock along subparallel offshoots is observed. In areas of increased stockwork veining, discrete rhyolite fragments are formed, bounded on all sides by veinlet material (Plate 6-7-3b). At this early stage of breccia formation, individual fragments are commonly cut by veinlets of similar colour, hardness and texture as the matrix (Plate 6-7-3b).

Matrix-supported breccias represent completion of the brecciation process (Plate 6-7-4a, b). Plate 6-7-4a is an example of the mosaic fabric formed by clusters of fragments displaying jigsaw-like boundaries. Plate 6-7-4b shows the highly irregular, finely scalloped nature of fragment margins. Some of the larger fragments are surrounded by the faint outlines of smaller rhyolitic fragments, resulting in the appearance of a somewhat gradational boundary with the matrix. In each of these cases, the breccias are monolithic and adjacent fragments share similar characteristics of colour, hardness, texture and alteration. They appear continuous on a megascopic scale.

A distinct style of brecciation and subsequent silicification is observed in core from diamond-drill hole CA89-109, and surrounding drill holes. Both footwall and hangingwall rocks are fragmented, with individual fragments showing displacement or rotation. Within the footwall, rhyolitic and sulphide fragments are coated with white sparry quartz (Plate 6-7-5) which can be observed growing into open vugs now filled with black silica. This open-space filled texture appears to be unique to this part of the 21 zone.

PYROBITUMEN

Solid, relatively hard hydrocarbons, assumed to be pyrobitumen, occur throughout the Eskay Creek deposit. In most cases, the pyrobitumen is filling late fractures within both hangingwall and footwall units. It also occurs with quartz or carbonate and has a black, resinous lustre, commonly with a conchoidal fracture. Fractures filled with pyrobitumen are most common in silicified rhyolite underlying mineralization in the area of drill-hole CA89-109 (Plate 6-7-6).

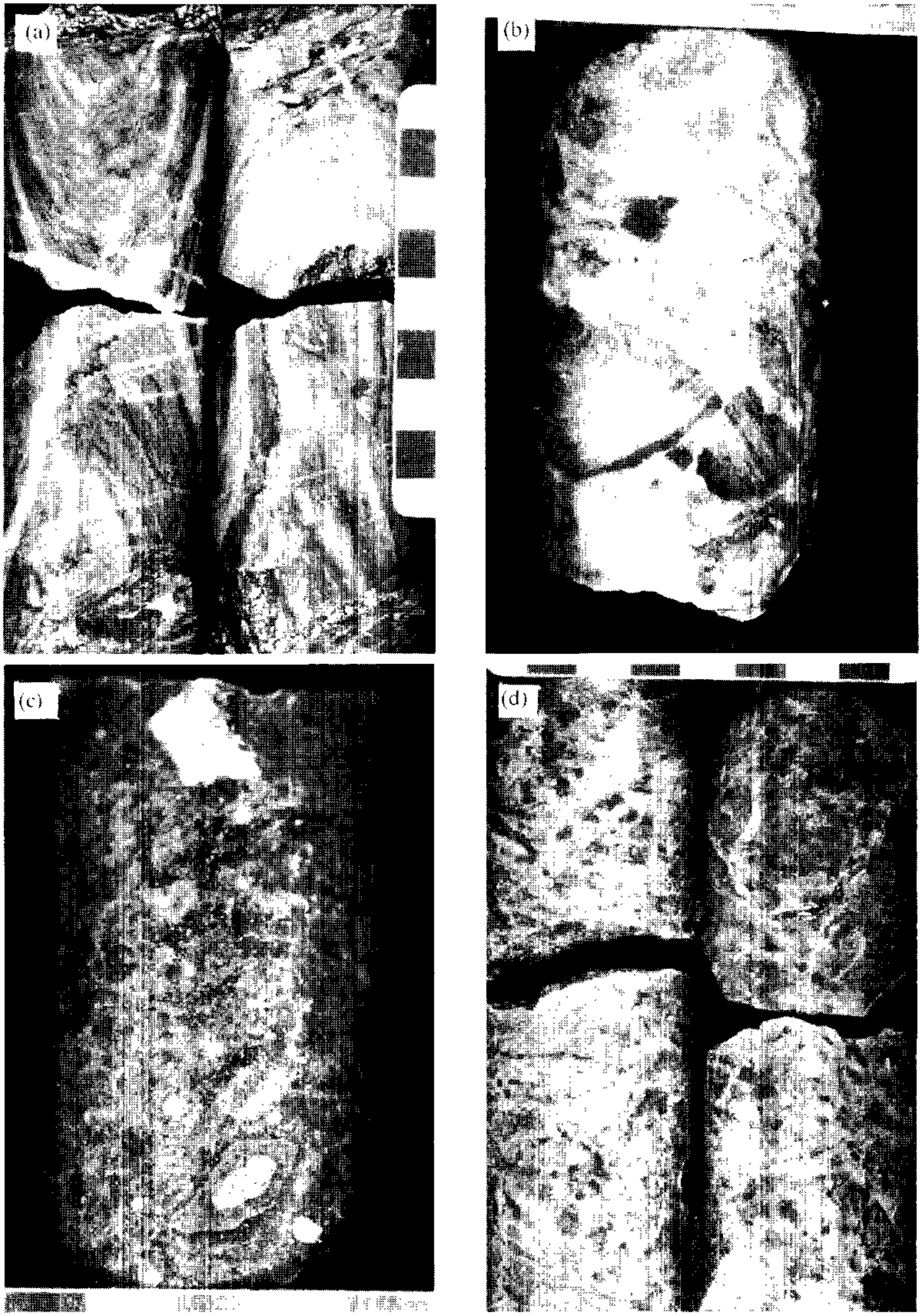

Plate 6-7-1. Primary depositional features observed in the footwall rhyolite. A. Massive flow-banded rhyolite, 21B zone (CA90-490-205.7). B. Autoclastic flow-breccia, note discordance in flow banding between individual fragments, 21B zone (CA90-273-156.6). C. Heterolithic tuff-breccia containing variably altered rhyolitic and exotic lithic fragments, 21B zone (CA90-345-184.2). D. Typical massive, featureless silicified rhyolite, 21B zone (CA90-271-140.6). NQ-size drill core in each photograph.

Petrographic analysis indicates pyrobitumen is a ubiquitous, finely disseminated phase in the hangingwall. In the footwall, it appears to coat sericite folia within the quartz-sericite-pyrite alteration zone beneath the deposit. Other habits include fine stringers associated with intensely silicified rhyolite, and coarse, broken clots in quartz-sulphide veins cutting footwall rhyolite. A wide range of reflectance values (R_0=0.81–13.98) indicates a variety of hydrocarbon maturity levels (Ettlinger and Roth, 1991).

DISCUSSION

The identification of primary volcanic textures in the footwall to sulphide-gold mineralization at Eskay Creek is complicated by intense hydrothermal alteration and related brecciation overprinting these rocks. Devitrification of felsic volcanic rocks can also result in the formation of breccia textures in rocks that were originally massive, relatively homogenous lavas. Allen (1988) describes several false pyroclastic textures found in silicic lavas hosting zinc-copper-lead massive sulphide deposits in the Benambra area of southeastern Australia. Pseudopyroclastic breccias con-

Plate 6-7-2. Closely spaced stockwork quartz veinlets in footwall rhyolite, 21A zone (CA90-273-152.6). NQ-size drill core.

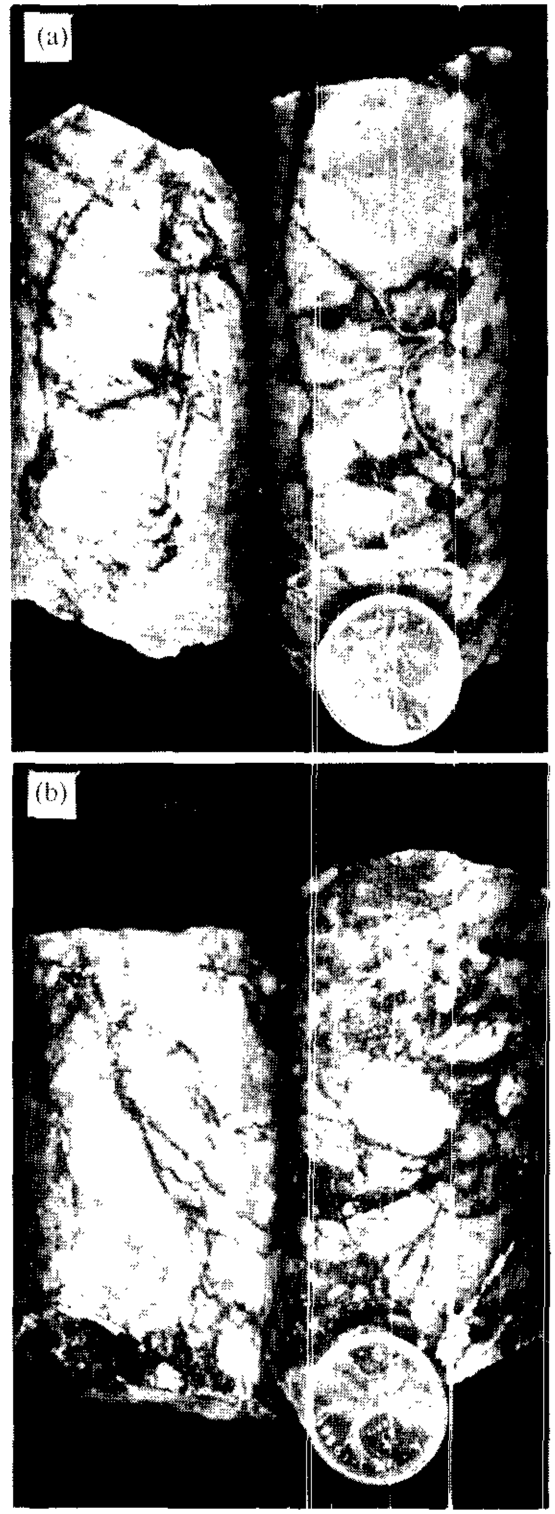

Plate 6-7-3. Early stages of hydrothermal veining and brecciation, 21B zone. A. Massive, silicified rhyolite is cut by stockwork veinlets of black silica. Top core piece also illustrates subparallel offshoots of veinlet material migrating into host rhyolite (CA90-216-121.7). B. Increased stockwork veinlet density results in formation of individual fragments, many containing veinlets of material similar in texture and composition to the matrix (CA90-421-95.6). NQ-size core.

Plate 6-7-4. Matrix-supported breccia in footwall rhyolite representing advanced stages of hydrothermal alteration, 21B zone. A. Light-coloured rhyolite fragments displaying a jigsaw, mosaic fabric (CA90-437-174.4). B. Light-coloured rhyolite fragments display highly irregular, finely scalloped margins, sometimes gradational into the dark grey matrix (CA90-421-114.0). Both examples contain fragments cut by veinlets of matrix material. NQ-size drill core.

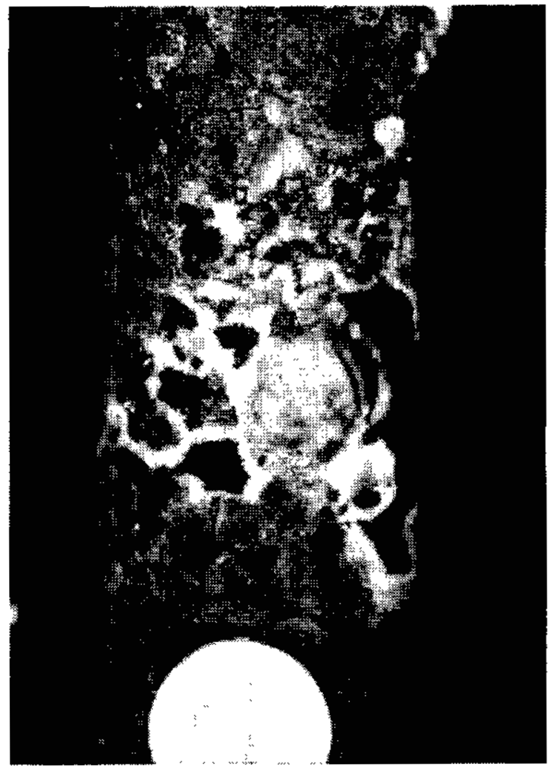

Plate 6-7-5. Footwall breccia, 109 area of 21B zone (CA90-424-173.4). White, sparry quartz coating fragments of rhyolite, sphalerite and pyrite. This quartz appears to grow into open vugs now filled with silica (black areas).

Plate 6-7-6. Pyrobitumen-filled fractures in footwall rhyolite. Diamond-drill hole CA90-627, 144 metres. NQ-size drill core.

taining apparent lithic or pumice fragments, and thinly bedded and lapilli tuffs are all shown to have formed through the process of devitrification and progressive hydrothermal alteration of mostly massive rhyolitic flows. The formation of these textures can result in misidentification of volcanic facies. Consequently, Allen suggests that the overall significance of explosive silicic volcanism in areas of volcanic-hosted massive sulphide deposits may have been over estimated.

The role devitrification processes have played in formation of the breccia textures observed at Eskay Creek is not yet known. The large amount of altered rhyolitic rock, and sporadic presence of perlitic cracks and spherulites observed in the footwall rhyolite, suggests that devitrification processes were in operation. There is, however, clear evidence that some of these breccias have formed through the process of replacement veining, where fragmental textures result from progressive replacement of the rock fabric along fractures. Unreplaced rock forms *in situ* remnant islands that resemble fragments. This is in contrast to the well known process of chemical brecciation (Sawkins, 1969) which results in hydrofracturing and generally outward movement of the fragments. Textures resulting from replacement veining are also described in skarn deposits (Ray *et al.*, 1988).

Recognition of the processes forming the footwall breccias at Eskay Creek is critical for the construction of a genetic model for this deposit. Recent descriptions of the 21B zone are characteristic of a volcanogenic massive sulphide model. The epithermal-style silicification and brecciation found in the vicinity of drill-hole CA89-109, however, suggests the classic volcanogenic model must be modified.

ACKNOWLEDGMENTS

Financial and logistical support by Prime Resources Group, Inc. and International Corona Corporation are gratefully acknowledged. Many interesting geologic discussions with Gerry McArthur, Jerry Blackwell and the Prime Exploration crew were helpful in many ways. Also acknowledged are stimulating discussions with James Stewart and Alex Kusic of International Corona Corporation. Thanks go to Tina Roth (MDRU) for sharing many interesting ideas concerning the 21A zone. Peter Lewis' (MDRU) help with AutoCad is appreciated. This study forms part of the Mineral Deposit Research Unit project "Metallogenesis of the Iskut River area, northwestern British Columbia".

REFERENCES

Alldrick, D.J. and Britton, J.M. (1988): Geology and Mineral Deposits of the Sulphurets Area (104A/5, 12; 104B/8, 9); *B.C. Ministry of Energy, Mines and Petroleum Resources*, Open File 1988-4.

Alldrick, D.J., Britton, J.M., Webster, I.C.L. and Russell, C.W.P. (1989): Geology and Mineral Deposits of the Unuk Area (104B/7E, 8W, 9W, 10E); *B.C. Ministry of Energy, Mines and Petroleum Resources*, Open File 1989-10.

Alldrick, D.J., Britton, J.M., MacLean, M.E., Hancock, K.D., Fletcher, B.A. and Hiebert, S.N. (1990): Geology and Mineral Deposits of the Snippaker Area (104B/6E, 7W, 10W, 11E); *B.C. Ministry of Energy, Mines and Petroleum Resources*, Open File 1990-16.

Allen, R.L. (1988): False Pyroclastic Textures in Altered Silicic Lavas, with Implications for Volcanic-associated Mineralization; *Economic Geology*, Volume 83, pages 1424-1446.

Anderson, R.G. (1989): A Stratigraphic, Plutonic and Structural Framework for the Iskut River Map Area (NTS 104B), Northwestern British Columbia; *in* Current Research, Part E, *Geological Survey of Canada*, Paper 89-1E, pages 145-154.

Anderson R.G. and Bevier, M.L. (1990): A Note on Mesozoic and Tertiary K-Ar Geochronometry of Plutonic Suites, Iskut River Map Area, Northwestern British Columbia; *in* Current Research, Part E, *Geological Survey of Canada*, Paper 90-1E, pages 141-147.

Anderson, R.G. and Thorkelson, D.J. (1990): Mesozoic Stratigraphy and Setting for some Mineral Deposits in the Iskut River Map Area, Northwestern British Columbia; *in* Current Research, Part E, *Geological Survey of Canada*, Paper 90-1E, pages 131-139.

Blackwell, J. (1990): Geology of the Eskay Creek #21 Deposits; *Mineral Deposits Division, Geological Association of Canada*, The Gangue, Number 31, April, pages 1-4.

Britton, J.M., Blackwell, J.D. and Schroeter, T.G. (1990): #21 Zone Deposits, Eskay Creek, Northwestern British Columbia; *in* Exploration in British Columbia 1989; *B.C. Ministry of Energy, Mines and Petroleum Resources*, pages 197-223.

Ettlinger, A.D. and Roth, T. (1991): Host Rock Geochemistry and Alteration in the Eskay Creek 21A Zone, Northwestern British Columbia, Canada; *in* Abstracts with Programs, *Geological Society of America* Annual Meeting, San Diego, October 1991, page 413.

Idziszek, C., Blackwell, J., Fenlon, R., McArthur, G. and Mallo, D. (1990): The Eskay Creek Discovery; *Mining Magazine*, March 1990, pages 172-173.

Ray, G.E., Dawson, G.L. and Simpson, R. (1988): Geology, Geochemistry and Metallogenic Zoning in the Hedley Gold-skarn Camp (92H/08; 82E/05); *in* Geological Fieldwork 1987, *B.C. Ministry of Energy, Mines and Petroleum Resources*, Paper 1988-1, pages 59-80.

Rebagliati, C.M. and Haslinger, R. (1991): SB Property; *in* 1991 "Snapshot" Review, *British Columbia & Yukon Chamber of Mines*, Cordilleran Roundup.

Roth, T. and Godwin, C.I. (1992): Preliminary Geology of the 21A Zone, Eskay Creek, B.C. (104B/9W); *in* Geological Fieldwork 1991, Grant, B. and Newell, J.M., Editors, *B.C. Ministry of Energy, Mines and Petroleum Resources*, Paper 1992-1, this volume.

Sawkins, F.J. (1969): Chemical Brecciation, an Unrecognized Mechanism for Breccia Formation?; *Economic Geology*, Volume 64, pages 613-617.

NOTES

ADVANCED ARGILLIC ALTERATION AT TREATY GLACIER, NORTHWESTERN BRITISH COLUMBIA (104B/9)

By John F.H. Thompson and Peter D. Lewis
Mineral Deposit Research Unit
The University of British Columbia

(MDRU Contribution 002)

KEYWORDS: Economic Geology, Iskut, Treaty Glacier, Hazelton, advanced argillic, alunite, sulphur.

INTRODUCTION

Treaty Glacier is located in northwestern British Columbia within the Suphurets map area (Alldrick and Britton, 1988), approximately 75 kilometres north of Stewart. The Sulphurets map covers the eastern part of the area being studied by the Mineral Deposit Research Unit of the University of British Columbia under the project: "Metallogenesis of the Iskut River Region, Northwestern British Columbia". Access is by helicopter from Stewart, Tide Lake airstrip, Bob Quinn Lake or exploration camps in the Eskay Creek - Sulphurets region.

The Treaty Glacier and the South Treaty Glacier surround a large nunatak. A prominent red-brown-weathering gossan occurs on the west side of the nunatak (mineral occurrence 44, Alldrick and Britton, 1988). This gossan (the "main gossan" in this paper) has been of interest to mining companies for a number of years and currently lies at the centre of the Treaty Creek property of Tantalus Resources Ltd. and Teuton Resources Corporation. Alldrick and Britton (1988) reported the presence of alunite and native sulphur within the gossan. A second area of grey and locally limonite-stained bluffs occurs on the north side of the Treaty Glacier, and is referred to here as the "north gossan". Natroalunite and sartorite [$PbAs_2(Sb)S_4$] have been reported from the north gossan (Kirkham *et al.*, in preparation).

Alunite and natroalunite form over a considerable temperature range during low-pH alteration in oxidizing, sulphur-rich environments. Together with pyrite and native sulphur, they comprise an assemblage that is characteristic of acid-sulphate advanced argillic alteration associated with two distinct settings:

- Acid-leach zones developed as blankets in the near surface from the condensation of volatiles released during boiling in geothermal systems.
- Vertically extensive alteration zones developed in and above magmatic-hydrothermal systems due to the release, disproportionation and condensation of magmatic gases.

Both environments may be related to mineralization, but gold mineralization is only associated with the latter (White and Hedenquist, 1990). The origin and timing of alteration is, therefore, important for understanding the metallogenesis of the region (Macdonald *et al.*, 1991).

Fieldwork in 1991 focused on establishing the general geological setting, the morphology and structural style of both the main and north gossans. The preliminary mineralogy, based on limited petrological and x-ray diffraction analyses, and scanning electron microscope and microprobe analyses are also reported. Follow-up geochemical studies are planned. Fieldwork in 1992 will attempt to resolve questions of timing and structural relationships highlighted by the initial work.

GEOLOGICAL SETTING

The Treaty Glacier area is underlain by sedimentary rocks of the Bowser Lake Group and volcanic and epiclastic rocks of the Hazelton Group (Alldrick and Britton, 1988). These rocks are complexly folded and faulted, and their structural history is the topic of ongoing studies at the Mineral Deposit Research Unit and Geological Survey of Canada. Most of the Treaty nunatak, and both the main and north gossans, lie on the upper plate of a regional, southeast-directed thrust fault which places Hazelton Group strata on top of rocks of the Bowser Lake Group (Figure 6-8-1). This thrust fault is exposed discontinuously along the southeastern edge of the nunatak, where fault duplex geometry, minor drag folds and slickensides are all consistent with southeastward movement. Upper plate rocks consist of volcanic and sedimentary rocks of the Salmon River Formation, felsic volcanic rocks of the Mount Dilworth Formation and epiclastic rocks of the Betty Creek Formation. Broad northwest-trending folds and several sets of steeply-dipping faults deform these units. Contacts of the main gossan cut across lithologic boundaries, suggesting that all three map units are affected by alteration. However, the extensive alteration within the gossan makes identification and mapping of geologic contacts between units difficult.

The north gossan is approximately 2 kilometres north of the main gossan and is separated from it by the Treaty Glacier and a section of unaltered rocks at the north end of the nunatak. The northern contact of the north gossan is obscured by a gully which separates it from an unaltered and unfoliated feldspar porphyry. A prominent series of east-trending outcrops higher on the south-facing slope exposes pyritic but texturally well-preserved volcanic fragmental rocks of probable felsic composition. These are overlain to the north by minor grits and shales, suggesting that the two units represent the Mount Dilworth and Salmon River formations, respectively, as mapped by Alldrick and Britton (1988). The east end of the gossan is faulted against unaltered and unfoliated clastic rocks, probably of the Bowser Lake Group.

THE ALTERATION SYSTEM

MAIN GOSSAN

The main gossan covers an area of approximately 1 square kilometre on west-facing slopes below an icefield which occupies the central part of the nunatak (Figure 6-8-1). Exposure is good in the upper part of the gossan and poor on the lower slopes.

The hostrocks are predominantly epiclastic with extensive weak to moderate propylitic alteration. The epiclastic rocks are locally cut by quartz-sericite-pyrite veins and individual beds are selectively replaced by similar sericite-pyrite alteration. The central part of the main gossan is dominated by outcrops of quartz-sericite schist with variable amounts of pyrite and no obvious primary texture. The rock is cut by steeply dipping mafic dikes which strike 80° to 110°. The dikes are subparallel to foliation, moderately boudinaged and propylitically altered. To the north of the central icefield, there are prominent outcrops of quartz-sericite-pyrite schist with irregular pods of silica and brecciated quartz. Rare outcrops show textures suggesting porphyritic and fragmental protoliths. This part of the main gossan is covered by abundant float of strongly laminated and crenulated quartz±pyrite±native sulphur rock, including a massive pile of disaggregated material at the toe of the central ice field. This distinctive lithology has only been found in one small, isolated outcrop in the southern part of the gossan. Adjacent outcrops, 5 to 10 metres away, are quartz-sericite schists. Both the laminated quartz and quartz-sericite schist contain a strong foliation and secondary crenulation. Contacts of the gossan are gradational from sericitic to propylitic alteration with a corresponding increase in textural preservation.

NORTH GOSSAN

The north gossan forms major grey to brown-weathering bluffs adjacent to the north side of the glacier. The bluffs consist of laminated quartz-pyrite with individual siliceous laminae ranging from 1 to 50 millimetres in thickness. Pyrite is disseminated throughout the rock and locally occurs as individual bands of fine pyrite up to 30 millimetres across. The laminated quartz is folded into spectacular chevron crenulations (Plate 6-8-1). The proportion of siliceous material increases upwards in the gossan, and is accompanied by a textural transition from fine laminations, to thicker pods and bands, to massive grey to white microcrystalline silica at the highest levels. There is no evidence for primary texture in the laminated or massive siliceous rocks.

ALTERATION MINERALOGY

Preliminary petrography of outcrop and float samples from the main gossan, supported by limited x-ray diffrac-

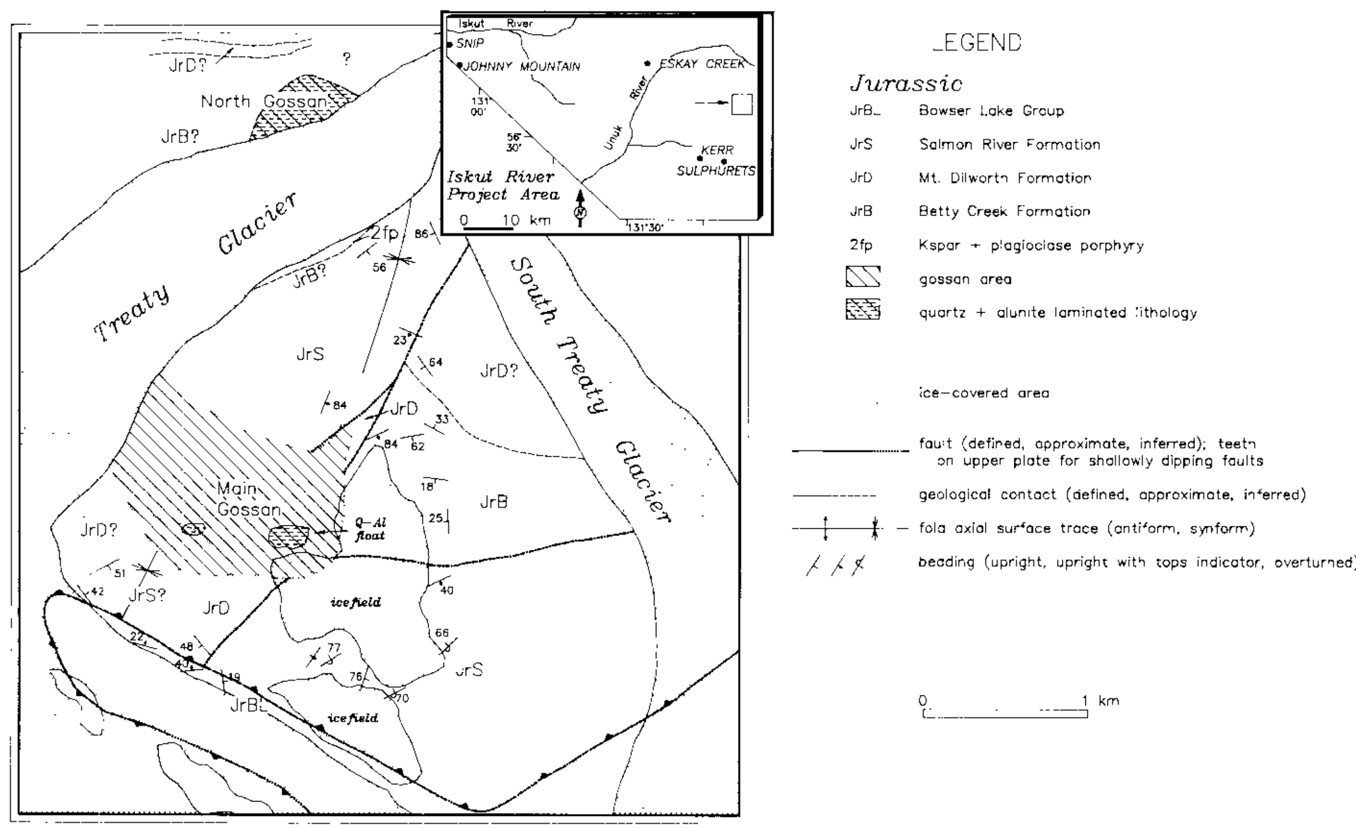

Figure 6-8-1. Generalized geology of the Treaty Glacier area based on this study, Alldrick and Britton (1988), Kirkham (personal communication), and mapping by Tantalus Resources Ltd. and Teuton Resources Corporation.

tion, scanning electron microscope and microprobe analyses, indicates that the laminated quartz rock consists of quartz±alunite interbanded with pyrite±sericite. One sample of float also contains pyrophyllite with laths of diaspore. The alunite consistently produces natroalunite x-ray diffraction peaks although initial microprobe analyses have returned a considerable range of X_{Na} (mole ratio Na/Na+K), 0.38 to 0.74. The sericite is illite or hydromuscovite. Native sulphur occurs locally in the laminated rock as discontinuous veins which cut the laminae, Kirkham *et al.* (in preparation) also report natroalunite and sartorite from the north gossan.

Primary textures are visible in some samples and include individual quartz grains or phenocrysts, quartz-rich clasts and rhombohedral ghosts of possible pseudomorphs of amphibole. Preliminary petrography supports field evidence for multiple protoliths.

Structural Fabrics

The sericitic foliation and the quartz-pyrite both present structural fabrics imprinted on altered rocks of the Treaty gossan. Sericitic foliation is almost ubiquitous in the main gossan but absent from the north gossan. This subvertical foliation is broadly folded and has variable strikes from 045° to 135°. The quartz-pyrite-alunite layering is well developed in the north gossan but is limited to one small outcrop and patches of float on the main gossan. In all locations the laminated layering is refolded by crenulations (Plate 6-8-2). In the main gossan outcrop, laminations are parallel to sericitic foliation in the adjacent rocks and the overprinting crenulations are parallel to axial surfaces of mesoscopic folds in the sericitic rocks. In the north gossan area, subvertical crenulation fabrics strike southeast and deform a subvertical primary lamination which strikes north to northeast.

Microscopic fabrics within the quartz-alunite-pyrite laminated lithology suggest the primary fabric is a post-alteration feature. Samples from float boulders in the main gossan show a strong grain-elongation fabric parallel to compositional layering within the quartz-rich bands. Aspect ratios of quartz-ribbon grains approach 10: (Plate 6-8-2). In some samples, less elongate quartz grains are consistently inclined at 10° to 20° to the primary layering. Pyrite grains commonly have symmetric quartz pressure shadows which show elongation parallel to the primary layering. Alunite shows no evidence of intracrystalline strain, but grains in alunite-rich layers often have weak preferred orientations, with longest dimensions inclined at small angles to the external compositional layering.

Plate 6-8-1. Outcrop of laminated quartz-alunite-pyrite rock on the north gossan, showing strong crenulation.

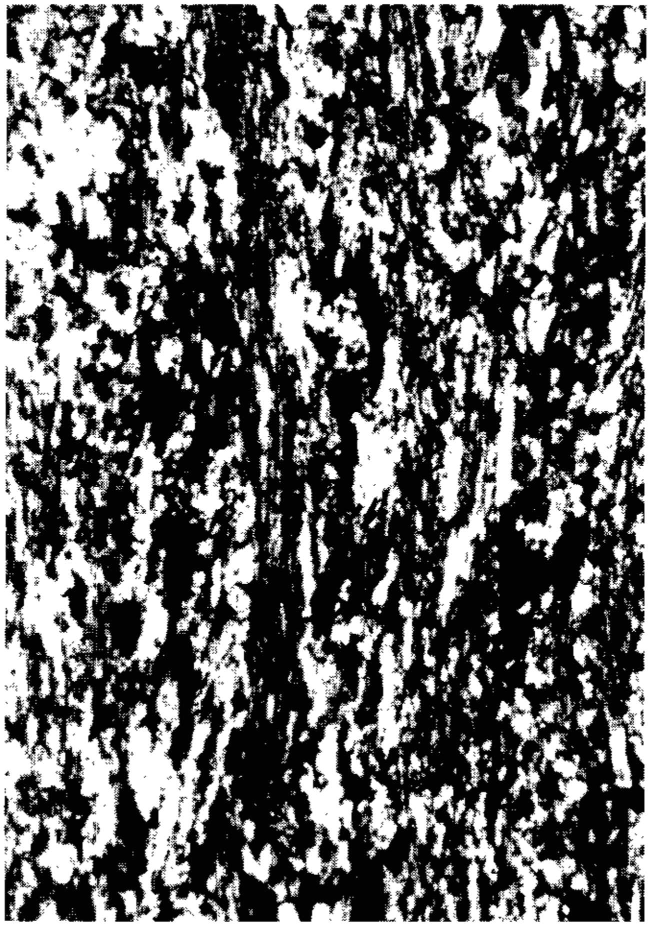

Plate 6-8-2. Photomicrograph of laminated quartz-alunite-pyrite rock showing elongated ribbon quartz and parallel alunite laths of tectonic origin. The field of view is 2.5 millimetres across.

DISCUSSION

The main gossan on the Treaty Glacier nunatuk is dominated by quartz-sericite-pyrite alteration with minor zones of quartz-alunite/natroalunite-pyrite$\pm$sulphur$\pm$pyrophyllite $\pm$diaspore. The alteration system is developed in a variety of hostrocks with selective alteration of fragmental units on the periphery of the system. The quartz-sericite alteration passes outwards into propylitic alteration, also developed in a variety of hostrocks. Preliminary stratigraphic interpretation indicates that the system affects Betty Creek Formation or equivalent intermediate fragmental rocks, Mount Dilworth Formation felsic fragmental rocks, which may be quartz phyric in this area, and pillowed basalts and andesites possible belonging to the Salmon River Formation. If the latter interpretation is correct, it suggests that the alteration system formed or was active until late in the Early Jurassic. Mafic dikes cut sericitic alteration but are partially altered. The dikes are deformed and there is no evidence, to date, for post-deformation alteration.

The north gossan contains laminated quartz-alunite/natroalunite-pyrite and zones of massive silicification. Contacts between the north gossan and surrounding unaltered rocks are faulted or obscured. Lack of foliation or crenulation in these surrounding units either reflects this structural juxtaposition, or the relatively incompetent nature of the quartz-alunite rock. Future fieldwork will attempt to resolve these questions. The protolith for the north gossan is uncertain. The possibility that the lamination reflects a primary banding in a tuffaceous or flow-banded rhyolite protolith cannot be ruled out at this time.

Mesoscopic and microscopic structural characteristics of the laminated quartz-alunite lithology strongly suggest that the laminations represent a tectonic fabric, imposed after alteration and overprinted by a younger crenulation fabric. Concentration of strain along discrete quartz-rich layers, and asymmetric grain-elongation fabrics indicate that a moderate to large component of noncoaxial strain contributed to fabric development.

Fieldwork and initial follow-up has established the following constraints for the formation of the Treaty Glacier alteration system:

- The alteration is dominantly sericitic or phyllic with local zones of acid-sulphate advanced argillic alteration and peripheral propylitic alteration.
- The presence of pyrophyllite-diaspore implies temperatures in excess of 280°C at the time of formation or during post-alteration metamorphism (Hemley *et al.*, 1980). There is no evidence for the latter.
- The system was deformed post-alteration.
- The alteration effects a variety of rock types and there is no evidence for any paleosurface features.

Preliminary conclusions are that alteration relates to the upper part of a magmatic-hydrothermal system which was subsequently deformed. The predominance of natroalunite, and its range of X_{Na} based on initial work, are also consistent with magmatic-hydrothermal environments (Stoffregen and Cygan, 1990; Thompson and Peterson, 1991). These types of systems occur elsewhere in the Sulphurets region and typically show similar timing relationships (Kirkham *et al.*, in preparation; J. Margolis, personal communication, 1991). To date, exploration on the gossan has not been successful but the owners of the Treaty property have discovered numerous precious and base metal rich veins throughout their property. At this stage, no conclusions can be drawn on the relationship of these veins to the Treaty Glacier alteration system or on the potential for mineralization within or below the alteration.

ACKNOWLEDGMENTS

We acknowledge Tantalus Resources Ltd. and Teuton Resources Corporation for granting permission to work on the Treaty property and to publish this paper. The work and ideas benefit from discussions with Rod Kirkham (Geological Survey of Canada) and Dani Alldrick (British Columbia

Geological Survey Branch). The work is funded from the Mineral Deposit Research Unit.

REFERENCES

Alldrick, D.J. and Britton, J.M. (1988): Geology and Mineral Deposits of the Sulphurets Area; *B.C. Ministry of Energy, Mines and Petroleum Resources*, Open File 1988-4.

Hemley, J.J., Montoya, J.W., Marinenko, J.W. and Luce, R.W. (1980): Equilibria in the System Al_2O_3-SiO_2-H_2O and Some General Implications for Alteration/Mineralization Processes; *Economic Geology*, Volume 75, pages 220-228.

Kirkham, R.V., Ballantyne, S.B and Harris, D.C. (in preparation): Sulphurets Area, British Columbia: Preliminary Geology, Geochemistry and Mineralogy of a Deformed Porphyry Copper, Molybdenum, Precious Metal System.

Macdonald, A.J., Ettlinger, A.D. and Thompson, J.F.H. (1991): Metallogeny of the Iskut River Area, Northwestern British Columbia, Canada; *Geological Society of America*, Abstracts with Program, Volume 23, Number 5, page 413.

Stoffregen, R.E. and Cygan, G. (1990): An Experimental Study of Na-K Exchange Between Alunite and Aqueous Sulfate Solutions; *American Mineralogist*, Volume 75, pages 209-220.

White, N.C. and Hedenquist, J.W. (1990): Epithermal Environments and Styles of Mineralization: Variations and Their Causes and Guidelines for Exploration; *Journal of Geochemical Exploration*, Volume 36, pages 45-474.

Thompson, A.J.B. and Petersen, E.U. (1991) Alunite Compositions and Textures: Indicators of the Environment of Formation; *Geological Society of American Bulletin*, Volume 23, Number 5, page A229.

NOTES

PRELIMINARY STRUCTURAL INTERPRETATION OF THE SNIP MINE (104B/11)

By David A. Rhys and Colin I. Godwin
Mineral Deposit Research Unit
The University of British Columbia

(MDRU Contribution 009)

KEYWORDS: Economic geology, structural geology, Snip, Twin zone, shear vein, mesothermal gold.

INTRODUCTION

The Snip mine, on the south side of the Iskut River, is 70 kilometres east of Wrangell, Alaska, and 110 kilometres northwest of Stewart, British Columbia. The mine is jointly owned by Cominco Ltd. (60%) and Prime Resources Group Inc. (40%). Production began in January, 1991, at a rate of 360 tonnes per day.

Gold-bearing quartz veins were first discovered by Cominco prospectors. Limited trenching on the showings in 1966 yielded mixed results and the claims were allowed to lapse. Cominco restaked the area in 1980 as the Snip claim group. Delaware Resources Corporation, now Prime Resources Group Inc., funded an intensive exploration program on the property between 1986 and 1990 as part of a joint venture agreement with Cominco (Nichols, 1989). The exploration program delineated a reserve of 960 000 tonnes at a grade of 28.5 grams per tonne gold (A. Samis, personal communication, 1991).

The deposit is within the Stikine Terrane at the eastern margin of the Coast Plutonic Complex. The regional geology is outlined in Britton *et al.* (1990).

During 1991, Rhys spent 98 days at Snip doing 1:500-scale structural mapping in the accessible mine workings and on surface. In addition, over 500 drill intersections of the Snip orebody were re-logged for mineral zoning and ore-type distribution studies. Extensive sampling was done for detailed petrography, structural analysis, fluid inclusion microthermometry, alteration, stable isotope analysis and geochronology.

LOCAL GEOLOGY

Two major lithologic units are exposed in the area of the Snip mine (Figure 6-9-1). The host unit is a thick sequence of tuffaceous biotitic feldspathic greywacke. This is intruded by an elongate orthoclase-porphyritic quartz monzonite stock.

The greywackes contain rare interbeds of graded siltstone and matrix-supported pebble conglomerate, which suggest a turbiditic origin for portions of the sequence. Bedding is upright and dips moderately to steeply northwesterly.

The quartz monzonite stock, known as the Red Bluff porphyry, forms a prominent cliff along the west side of Bronson Creek (Figure 6-9-1). A large alteration zone flanks this intrusion to the southwest (Kerr, 1948). The intrusion comprises lenses of orthoclase porphyry in a rock composed of sheeted quartz veinlets with magnetite bands in a magnetic, siliceous dark grey matrix. A U-Pb zircon minimum age of 195±1 Ma was obtained from a sample of orthoclase porphyry collected from the 130 haulage level of the Snip workings (Macdonald *et al.*, 1992)

CHARACTER OF THE SNIP OREBODY

Ore at the Snip mine is contained within a shear-vein system termed the Twin zone (Nichols, 1987) which strikes 120° and dips 30° to 60° southwest (Figure 6-9-2). It has been traced by drilling for 500 metres, both horizontally and vertically. Thickness varies to a maximum of 13 metres, and averages approximately 2.5 metres. In the eastern and lowest parts of the mine, the Twin zone dies out in a series of discontinuous quartz-carbonate-sulphide stringers. Erosion has removed the westernmost and upper parts of the orebody.

An unmineralized basic biotitic dike, termed the biotite spotted unit (BSU of Nichols, 1989; *also see* Figure 6-9-2), intrudes the Twin zone above the 280 level (Figure 6-9-2), and commonly obliquely cuts fabrics and veins developed in the zone. Below this level, the dike diverges into the hangingwall. It typically contains 15 per cent black to dark green felted biotite spots, 0.5 to 4 millimetres long, in a fine-grained biotitic matrix. It has a pervasive phyllitic foliation that parallels its margins. Common elongation of the biotite spots defines a lineation on the foliation that plunges 35° southwest. The phyllitic foliation locally grades into a schistosity on the dike margins. In such cases it can be difficult to distinguish foliated dike from biotitic Twin zone mineralization.

The Twin zone has a pronounced internal banding of four different ore types, all of which carry gold:

Biotite mineralization consists dominantly of two varieties of biotite: black (Mg, Fe) biotite, and the green, iron end-member of the biotite group, annite (McLeod *in* Nichols, 1989). Alternating laminae of schistose biotite/annite and calcite, 1 to 15 millimetres thick, are common, but some drill holes intersect intervals of almost pure annite. Quartz is locally abundant as augen or foliation-parallel veinlets (Figure 6-9-3A and 6-9-3C). Total sulphide content, mainly pyrite and minor pyrrhotite, seldom exceeds 2 per cent. Streaks of pink calcite and potassium feldspar occur in some annite-rich areas. These areas are also associated with high molybdenite (up to 2%) and gold (generally greater than 120 g/t) content. The streaks may represent slivers of potassically altered wallrock.

A gradual transition, 3 to 25 centimetres wide, from weakly foliated biotitic greywacke to schistose biotite ore occurs in some drillholes. Remnant carbonate/potassium feldspar altered wacke grains are often present in annite-rich sections of this ore type. These observations suggest that the biotite ore may have formed by progressive wallrock alteration.

Carbonate mineralization occurs as bands of granular calcite and lesser iron carbonate, often with patches of potassically altered wallrock. Bands and stringers of sphalerite are common, but seldom exceed 1 per cent of the volume of the carbonate ore. Disseminated pyrite occurs in most drill intersections. Streaks of black biotite and annite commonly comprise 5 to 25 per cent of the carbonate ore and there is a complete compositional gradation from the carbonate ore to the biotite ore, indicating they are closely related genetically.

Massive sulphide mineralization contains a high diversity of sulphide minerals. Massive sulphides occur in foliation-parallel veins of predominantly massive pyrite 5 centimetres to more than 1 metre thick. Massive pyrrhotite is present locally. Other significant sulphides include, in decreasing order of abundance, arsenopyrite, sphalerite, chalcopyrite and galena. Streaks of magnetite occur in some pyrite veins with 1 to 5 per cent disseminated pyrrhotite. Both black biotite and annite streaks are associated with the sulphides, but seldom exceed more than 10 per cent of the vein volume. Calcite is interstitial to sulphide grains in most veins and quartz eyes are common in pyrrhotite-rich ore. Both chalcopyrite and fine (<mm) visible gold are commonly spatially associated with the quartz.

Quartz mineralization consists of foliation-parallel quartz veins containing the same sulphide species as the massive sulphide veins, but sulphide content seldom

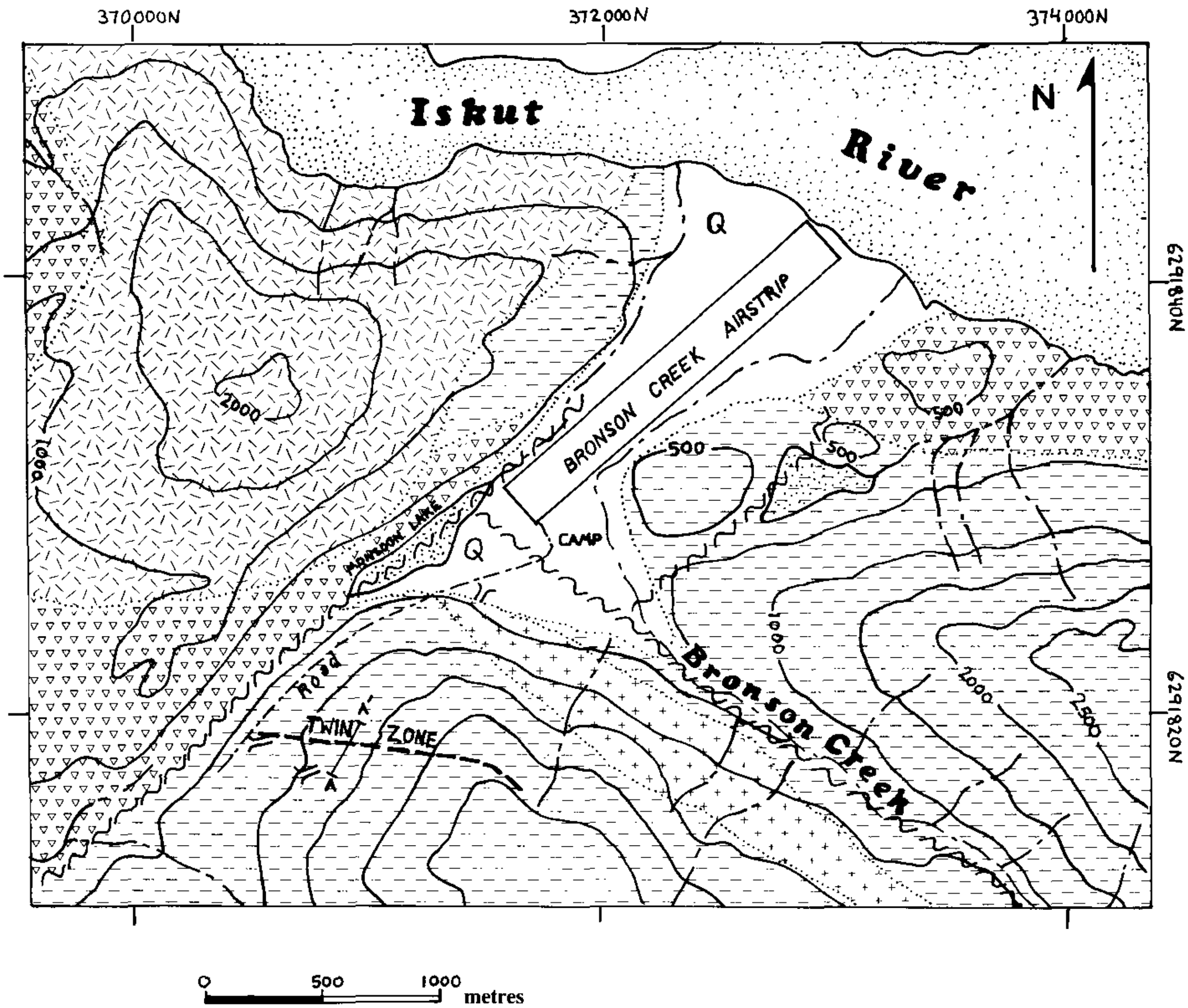

Figure 6-9-1. Local geology of Snip mine area, British Columbia. Base map after Nichols (1989) and geology modified after Alldrick *et al.* (1990).

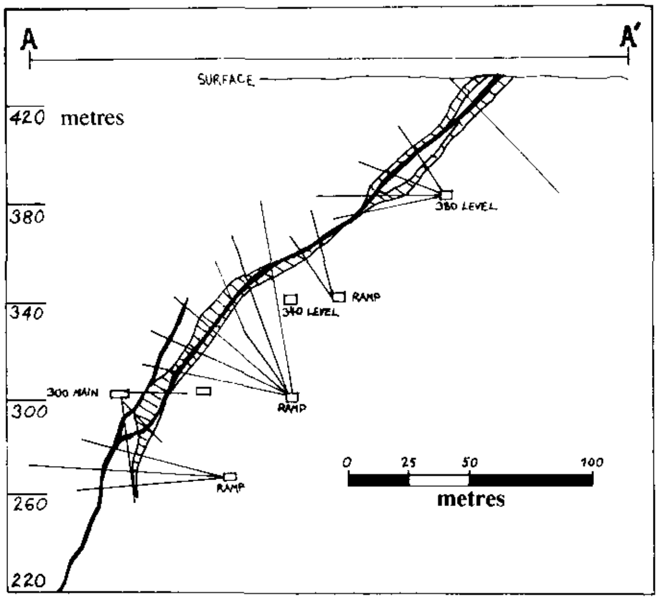

Figure 6-9-2. Cross-section through the Twin zone at 4512.5 east, *Snip mine grid, showing the relationship of the* biotite spotted unit (BSU). The BSU is shown in black and the Twin zone is hatched. Section is parallel to the 030° azimuth. Underground-drill intersections and workings are shown. Modified from a section drawn by A. Samis (Cominco Ltd.).

exceeds 2 per cent. The relative abundance of pyrite is generally less than that in massive sulphide mineralization; other sulphides, notably pyrrhotite and chalcopyrite, are proportionally more abundant. Annite, and less abundantly, black biotite, commonly comprises 5 per cent of the quartz veins, but locally forms up to 50 per cent of the vein. Bladed quartz-annite intergrowth is common in veins with abundant annite (*Figure 6-9-3B). Blades are generally perpendicular* to the vein walls.

Quartz veins are invariably strongly fractured and have been previously described as "crackle quartz" (Nichols, 1989). Fractures are usually filled with calcite and/or iron carbonate, giving the quartz veins a carbonate content of 1 to 4 per cent. Annite and sulphides may also occur as fracture fill. Visible gold is usually associated with or enclosed in sulphides and annite as fine, free gold, but may also occur as disseminations in unfractured quartz.

Progressive increase in sulphide content over distances of 1 to 2 metres commonly produces a gradation from quartz to sulphide vein mineralization, implying a genetic relationship between these two ore types.

Individual drill intersections of the Twin zone consist of one or more of the four ore types, often layered in an apparent stratigraphy. All ore types occur throughout the Twin zone, but sulphide veins are more abundant in the eastern part of the orebody (Nichols, 1989). Slivers of greywacke are also common within the Twin zone.

ALTERATION

The Twin zone rarely exhibits a well-developed alteration halo. In many instances, especially in sections of carbonate or quartz ore, no alteration envelope is apparent. Sulphide mineralization, however, commonly has an envelope of felted black biotite with disseminated pyrite or pyrrhotite 1 to 50 centimetres wide. In some locations, this biotitic envelope forms an inner halo within an outer zone of potassically altered wacke.

The greywackes throughout the mine have abundant black biotite alteration. The biotite is predominantly fract*ure controlled and, less commonly, pervasive. Biotite-filled* fractures commonly contain pyrite and have bleached potassium feldspar envelopes, mimicking the progressive alteration envelopes that surround some sulphide mineralization in the Twin zone. Siltstone interbeds in the greywackes appear most strongly altered: some graded beds have a matrix composed entirely of pale pink potassium feldspar. Patches of potassium feldspar flooded greywacke with up to 60 per cent potassium feldspar are often found in drill core (Nichols, 1988).

Southwest-dipping laminated biotite-carbonate-quartz-sulphide-filled shear zones of variable thickness (2 cm to 1.2 m) occur throughout the mine workings up to the contact with the Red Bluff porphyry. They are spaced 7 to 15 metres apart and have the same internal structure and similar mineralogy to the Twin zone. The abundance of these shear zones suggests a large hydrothermal system was active in the area at the time of the formation of the Twin zone. Their spacing may be sufficient to explain the pervasive biotite and potassium feldspar alteration in areas distant from the Twin zone.

INTERNAL STRUCTURE OF THE TWIN ZONE

Structures internal to the Twin zone suggest it formed as a dilatent shear zone with a predominantly normal sense of movement.

Drag folds commonly occur in all Twin zone mineralization types (Figures 6-9-3A, 6-9-3C). Fold amplitudes range from 2 centimetres in biotite and carbonate mineralization to 20 to 70 centimetres in the more competent quartz vein mineralization. Fold axes are contained within the Twin zone boundary plane orientation. Most fold axes are either subhorizontal or southwesterly plunging, but there is a range of intermediate plunge directions. Folds with subhorizontal axes verge down-dip and are common in all mineralization types. Folds with southwesterly plunging axes verge both east and west, and are common in the biotite and carbonate ore types. The dual west and east vergence of folds developed in the relatively incompetent carbonate and biotite ores suggests the presence of sheath folds (Cobbold and Quinquis, 1980) formed by progressive deformation of initially rectilinear fold axes. Figure 6-9-3 illustrates both down-dip verging (Figure 6-9-3A) and west-verging (Figure 6-9-3B) folded quartz veins in biotite mineralization.

Sulphide veins commonly have undulose margins, but rarely exhibit clear folds. In some stopes, these undulations form apophyses that project up to 1.5 metres into the wall-rock and terminate at a point (Figure 6-9-4). Cleavage in adjacent biotite or carbonate ore commonly curves around these structures, itself defining folds. Well-rounded pyrite grains are common and suggest intergranular flow.

C-S fabrics are locally developed in the biotite and carbonate mineralization. In these locations, flattening (S) fabrics have shallow to subhorizontal dips, whereas the shear (C) fabrics parallel the margins of the shear zone, consistent with a normal shear sense. Asymmetric quartz augen indicate a compatible shear sense. Synthetic Riedel shears, although not common, occur in the Twin zone (Figure 6-9-3D). These have a 60° to 75° southwest dip and record a normal sense of motion.

A striation lineation with an oblique southwesterly down-dip plunge is defined by biotite throughout the Twin zone. Pyrite is commonly streaked along the lineation. The southwesterly plunging drag-fold axes and the elongate biotite spots in the biotite spotted unit parallel this lineation.

STRUCTURAL FEATURES OUTSIDE THE TWIN ZONE

The internal structural features of the Twin zone also occur in the southwest-dipping laminated shear zones that are present throughout the mine. A subhorizontal cleavage is locally developed for up to several metres into the hangingwall and footwall of the larger shear zones. This cleavage also occurs locally in the footwall of the Twin zone. The hangingwall, however, is not exposed. The cleavage commonly curves to steeper dips adjacent to the shear veins, consistent with drag folding due to normal motion on these zones.

Two orientations of extension veins with moderate northeast and southeast-dipping orientations occur abundantly through the greywacke sequence. They cut fabrics developed in the Twin zone and laminated shear zones, and the biotite spotted dike. Both vein sets consist of blocky to

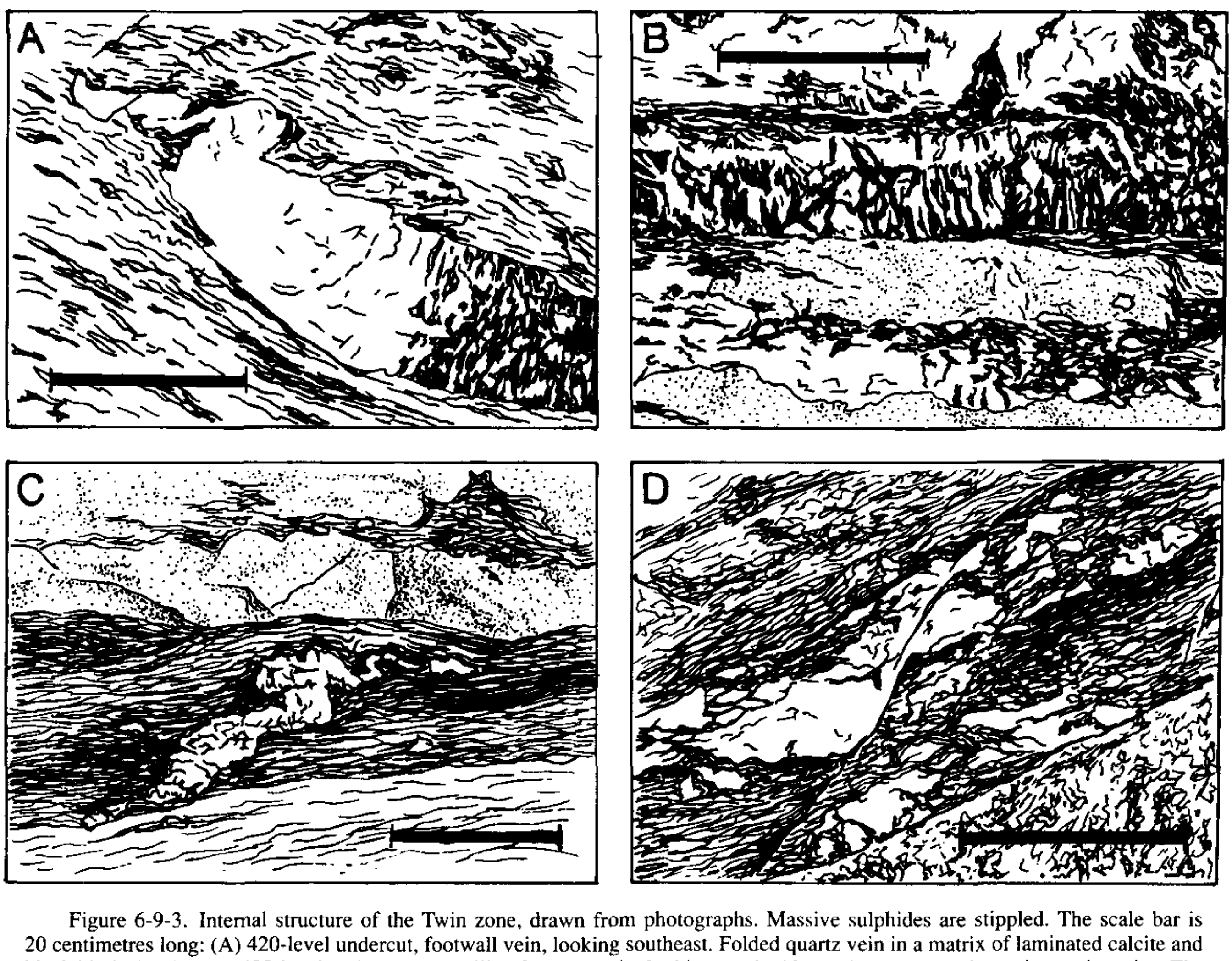

Figure 6-9-3. Internal structure of the Twin zone, drawn from photographs. Massive sulphides are stippled. The scale bar is 20 centimetres long: (A) 420-level undercut, footwall vein, looking southeast. Folded quartz vein in a matrix of laminated calcite and black biotite/annite; (B) 420-level undercut, west pillar, footwall vein, looking north. Alternating quartz and massive pyrite veins. The quartz veins exhibit a coarse bladed intergrowth of annite and quartz; (C) 340-level undercut access, east wall, footwall vein, looking north. West-verging folded quartz veinlet in a band of black biotite ore. Massive pyite veins and footwall greywacke appear in the upper and lower portions of the picture, respectively; (D) 340-level undercut access, west wall, footwall vein, looking northwest. A synthetic Riedel shear normally offsets a large quartz augen in a matrix of black biotite ore. Below are footwall greywackes.

Figure 6-9-4. 150 vein, 400-level west access, looking southeast. Two massive pyrite-pyrrhotite veins are separated by strongly biotite-altered greywacke. Note the undulose margin of the sulphide vein on the left side of the picture, and the tongue of sulphide that joins the two veins. Drawn from photographs. The scale bar is 1 metre long.

fibrous quartz, calcite, green mica (probably annite), iron carbonate and pyrite, with rarer epidote, pyrrhotite, chalcopyrite and galena. Typical veins are 30 centimetres to 1 metre long and 1 to 4 centimetres wide, and occur at a spacing of 0.5 to 1.0 metre. Where observed, fibres are generally perpendicular to the vein walls. The southeast-dipping vein set frequently forms conjugate en echelon arrays with varying degrees of sigmoidal folding indicative of a reverse sense of shear. Crosscutting relationships indicate that the southeast-dipping set, which is also the most abundant, is younger than the northeast-dipping set. The extension veins are often boudinaged, with subhorizontal, linear boudin axes striking south-southeast. Where they cut laminated shear veins and Twin zone fabrics, the extension veins often show minor normal offset.

The Red Bluff porphyry is intersected for 120 metres by the mine haulage level, and has a strong southwest-dipping foliation throughout. Orthoclase phenocrysts are augenized and flattened parallel to a phyllitic fabric. Locally, elongated phenocrysts are sigmoidally folded. The asymmetry of these folded phenocrysts and occasional drag folding of quartz-magnetite sheeted veinlets suggest a normal sense of movement. A striation lineation developed by micas on the foliation plunges westerly. Southeast-dipping extension veins cut these fabrics.

Brittle fault sets cut all other structural features in the mine. Displacement appears variable, but one northeast-striking set offsets the Twin zone by approximately 80 metres of oblique-reverse displacement, based on offset, thickened portions of the orebody and a consistent slickenside orientation. These faults are filled with gouge which sometimes contains vuggy quartz-calcite-ankerite-pyrite veins. They commonly have bleached envelopes 1 to 2 metres wide.

DISCUSSION AND CONCLUSIONS

Down-dip verging folds, probably sheath folds, C-S structures, synthetic Riedel shears, asymmetric augen, subhorizontal cleavage, and a striation lineation, are common to both the Twin zone and laminated shear zones; all indicate an oblique normal sense of motion. Deformation is relatively localized and brittle-ductile, and is confined to the southwest-dipping phyllitic and schistose foliation (S_1) within the laminated shear and Twin zone. In contrast, widespread fabric development within the Red Bluff porphyry indicates more distributed deformation.

The relative abundance of sheath folds in biotite and carbonate mineralization types is probably related to the competency of these rock types. Preferential fold development in biotite and carbonate mineralization types suggests they were less competent during deformation than other mineralization types such as the quartz vein.

The presence of both deformed and undeformed quartz veins (Figure 6-9-3A and 6-9-3B) suggests that several generations of syntectonic quartz veining formed during Twin zone formation. Periodic intervals of extremely high hydrostatic pressure during deformation may have caused dilatency along the cleavage of the zone, allowing the formation of veins parallel to the pre-existing biotite cleavage. A similar mechanism of hydrostatic pressure cycling has been suggested for the formation of crack-seal type veins in comparable deposits, such as Bralorne (Leitch, 1990).

The two extension vein sets record a later phase of deformation than the event which formed the Twin zone. Their moderate to gentle easterly dips, sigmoidal arrays with reverse shear sense, and crosscutting relations with S_1 fabrics indicate they formed in a different stress field than the Twin zone and laminated shear zones. Limited normal movement along Twin zone and laminated shear zones after the formation of the extension veins is indicated by their slight displacement. This phase of movement may have caused the boudinage of the gash veins.

Intrusion of the biotite spotted unit probably occurred late during the first phase of movement on the Twin zone, as it has developed penetrative fabrics similar to those in the zone. Extension veins which cut this dike indicate it must have been in place before the widespread extension veining event.

ACKNOWLEDGMENTS

The work and ideas presented benefited greatly from discussions with Cominco geologists Al Samis, Earl Masarsky and Ian Paterson, and with Peter Lewis, Al Sinclair, James Macdonald and John Thompson at The University of British Columbia. We thank Merlyn Royea and Ray Merrifield of Cominco Ltd. for their hospitality, and permission to work and stay at the Bronson camp. Ken Donner and Dale Craig of Cominco are also thanked for their support. Cominco generously provided food and accommodation for Rhys between June and September. Funding for this study is provided under the Mineral Deposit Research Unit project "Metallogenesis of the Iskut River Area".

REFERENCES

Alldrick, D.J., Britton, J.M., MacLean, M.E., Hancock, K.D., Fletcher, B.A. and Hiebert, S.N. (1990): Geology and Mineral Deposits of the Snippaker Map Area (104B/6E, 7W, 10W, 11E); *B.C. Ministry of Energy, Mines and Petroleum Resources*, Open File 1990-16.

Britton, J.M., Fletcher, B.A. and Alldrick, D.J. (1990): Snippaker Map Area (104B/6E, 7W, 10W, 11E); *in* Geological Fieldwork 1989, *B.C. Ministry of Energy, Mines and Petroleum Resources*, Paper 1990-1, pages 115-125.

Cobbold, P.R. and Quinquis, H. (1980): Development of Sheath Folds in Shear Regimes; *Structural Geology*, Volume 2, pages 119-126.

Kerr, F.A. (1948): Lower Stikine and Western Iskut River Map Areas, British Columbia; *Geological Survey of Canada*, Memoir 246, 94 pages.

Leitch, C.H.B. (1990): Bralorne: A Mesothermal, Shield-type Vein Gold Deposit of Cretaceous Age in Southwestern British Columbia; *Canadian Institute of Mining and Metallurgy*, Bulletin, Volume 83, Number 941, pages 53-80.

Macdonald, J., van der Heyden, P., Alldrick, D.J., Anderson, R.G. and Lefebure, D. (1992): Geochronometry of the Iskut River Area – An Update; *in* Geological Fieldwork 1991, Grant, B. and Newell, J.M., Editors, *B.C. Ministry of Energy, Mines and Petroleum Resources*, Paper 1992-1, this volume.

Nichols, R.F. (1987): Snip Property, 1986 Year-end Report; unpublished company report, Cominco Ltd.

Nichols, R.F. (1989): Snip Property, Final Project Report; unpublished company report, Cominco Ltd.

SELECTED RECENT EXTERNAL PUBLICATIONS BY B.C. GEOLOGICAL SURVEY BRANCH STAFF

Note: The following publications are by British Columbia Geological Survey Branch staff, or by staff in co-operation with other industry, government or university researchers.

Andrew, K.P.E. and Höy, T. (1990): Structural Models for Precious Metal Deposits in Jurassic Arc Volcanic Rocks of the Rossland Group, Southeastern B.C.; *Geological Association of Canada*, Cordilleran Section, Program with Abstracts, Vancouver, B.C.

Bobrowsky, P.T. (1991): Quaternary Geology of the Northern Rocky Mountains and Foothills of Western Canada; *XIIIth INQUA Congress*, Program with Abstracts, page 29.

Bobrowsky, P.T. and Clague, J.J. (1990): Holocene Sediments from Saanich Inlet, British Columbia, and their Neotectonic Implications; *in* Current Research, Part E, *Geological Survey of Canada*, Paper 90-1E, pages 251-256.

Bobrowsky, P.T. and Clague, J.J. (1990): Possible Evidence for Holocene Earthquakes in Saanich Inlet; *Canadian Quaternary Association – American Quaternary Association*, Joint Meeting 1990, Program and Abstracts, page 14.

Bobrowsky, P.T. and Clague, J.J. (1991): Late Glacial and Post-glacial History of the Tofino Area, British Columbia; *Canadian Quaternary Association*, Biennial Meeting 1991, Program and Abstracts, page 16.

Bobrowsky, P.T. and Rutter, N.W. (1990): Geologic Evidence for an Ice-free Corridor in Northeastern British Columbia, Canada; *in* Current Research in the Pleistocene, *University of Maine*, Volume 7, pages 133-135.

Bobrowsky, P.T. and Rutter, N.W. (1990): The Cordilleran Ice Sheet: Rocky Mountain Sector; *Geological Association of Canada – Mineralogical Association of Canada*, Program with Abstracts, A12, 15 pages.

Bobrowsky, P.T. and Rutter, N.W. (1992): Quaternary Geology of the Canadian Rocky Mountains; *in* Geographie Physique et Quaternaire, *Les Presses de l'Universite de Montreal*, Volume 46(1), in press.

Bobrowsky, P.T., Catto, N.R., Brink, J., Spurling, B.E., Gibson, T.H. and Rutter, N.W. (1990): Archaeological Geology of Western and Northwestern Canada; *in* Archaeological Geology of North America, Decade of North American Geology, Lasca, N.P. and Donahue, J.E., Editors, *Geological Society of America*, Centennial Special Volume 4, Boulder, Colorado.

Bobrowsky, P.T., Gravel, J., Matysek, P., Kerr. D. and Sibbick, S. (1991): Exploring for Cu-Au Porphyry Deposits in the Quesnel Trough: Unravelling the Quaternary Blanket; *Canadian Institute of Mining Bulletin*, Volume 84(847), page 88.

Brown, D.A., Logan, J.M., Gunning, M.H., Orchard, M.J. and Bamber, W.E. (1991): Stratigraphic Evolution of the Paleozioc Stikine Assemblage in the Stikine and Iskut Rivers Area, Northwestern British Columbia; *Canadian Journal of Earth Sciences*, Volume 28, pages 958-972.

Church, B.N. and Jessop, A.M. (1991): Geothermal Drilling in the Summerland Basin, British Columbia; *Geological Survey of Canada*, Open File 2348, 14 pages.

Clague, J.J. and Bobrowsky P.T. (1990): Holocene Sea Level Change and Crustal Deformation Southwestern British Columbia; *in* Current Research, Part E, *Geological Survey of Canada*, Paper 90-1E, pages 245-250.

Diakow, L.J., Panteleyev, A. and Schroeter T.G. (1991): Jurassic Epithermal Deposits in the Toodoggone River Area, Northern British Columbia: Examples of Well Preserved Volcanic-hosted, Precious Metal Mineralization; *Economic Geology*, Volume 86, Number 3, pages 529-554.

Ettlinger, A.D., Ray, G.E. and Meinert, L.D. (1989): Tectonic Controls on Precious Metal Enriched Skarn Mineralization in British Columbia; *in* Deep Structure of the Pacific Ocean and its Continental Surroundings: *Symposium Proceedings*, Blagoveshchensk, Russia, August 18-24 1988.

Grieve, D.A. (1991): Biaxial Vitrinite Reflectance in Coals of the Elk Valley Coalfield, Southeastern British Columbia, Canada. *International Journal of Coal Geology*, Volume 19.

Hall, R.L., Poulton, T.P. and Diakow, L. (1991): Lower Bajocian (Middle Jurassic) Ammonite and Bivalves from the Whitesail Lake Area, West-Central British Columbia; Contributions to Canadian Paleontology, *Geological Survey of Canada*, Bulletin 412, pages 133-167.

Hamilton, W.N. and Hora, Z.D. (1987): Opportunities Exist for Industrial Mineral Development in British Columbia and Alberta; *Mining Engineering*, Volume 39, Number 12, pages 1061-1067.

Höy, T. (1984) The Purcell Supergroup near the Rocky Mountain Trench, Southeastern British Columbia; *Montana Bureau of Mines and Geology*, Special Publication 90, pages 36-38 (extended abstract).

Höy, T. (1988): Early Tectonic and Magmatic Evolution of the Middle Proterozoic Purcell Basin, Southeastern Canadian Cordillera; *Geological Association of Canada, Pacific Section*, Program and Abstracts, page 16.

Höy, T. (1989): The Purcell Supergroup and the Sullivan Massive Sulfide Deposit, Southeastern British Columbia; *in* Geological Guidebook for Washington and Adjacent Areas, Joseph, N. and Reed, K., Editors, *Washington Division of Geology and Earth Resources*, Information Circular 86, pages 56-62, 69-72.

Höy, T. and Andrew, K. (1988): Geology, Geochemistry and Mineral Deposits of the Lower Jurassic Rossland Group, Southeastern British Columbia; *Canadian Institute of Mining and Metallurgy,* Twelfth District 6 Meeting, Program and Abstracts, page 11.

Höy, T. and Andrew, K. (1989): Structure, Stratigraphy and Mineral Deposits of the Rossland Group, Nelson Area, Southeastern British Columbia; *in* Geological Guidebook for Washington and Adjacent Areas, Joseph, N. and Reed, K., Editors, *Washington Division of Geology and Earth Resources,* Information Circular 86, pages 63-67, 79-80.

Höy, T. and Godwin, C.I. (1988): Significance of a Galena Lead Isotope Cambrian Date for the Stratiform Cottonbelt Deposit in the Monashee Complex, Southeastern British Columbia; *Canadian Journal of Earth Science,* Volume 25, Number 9, pages 1534-1541.

Höy, T. and Kwong, Y.T.J. (1986): The Mount Grace Carbonatite – an Nb and Light Rare Earth Element Enriched Marble of Probable Pyroclastic Origin in the Shuswap Complex, Southeastern B.C.; *Economic Geology,* Volume 81, pages 1374-1386.

Höy, T. and Van der Heyden, P. (1988): Geochemistry, Geochronology, and Tectonic Implications of Two Quartz Monzonite Intrusions, Purcell Mountains, Southeastern British Columbia; *Canadian Journal of Earth Sciences,* Volume 25, pages 106-115.

Höy, T., Berg, N., Fyles, J.T., Delaney, G.D., McMurdo, D. and Ransom, P.W. (1985): Stratabound Base Metal Deposits in Southeastern British Columbia; *in* Field Guides to Geology and Mineral Deposits in the Southern Canadian Cordillera, Templeman-Kluit, D., Editor, *Geological Society of America,* Cordilleran Section Fieldtrip 13, 32 pages.

Höy, T., Gibson, G. and Berg, N.W. (1984): Copper-zinc Deposits Associated with Basic Volcanism, Goldstream Area, Southeastern British Columbia; *Economic Geology,* Volume 79, Number 5, pages 789-814.

Hora, Z.D. (1990): Industrial Minerals in British Columbia-New Developments, New Discoveries and New Opportunites; *Canadian Institute of Mining and Metallurgy,* Bulletin, Volume 83, Number 933, pages 74-78.

Hora, Z.D. (1990): Industrial Minerals in British Columbia: Present Producers and Further Development Opportunities; *in* Industrial Rocks and Minerals of the Pacific Northwest, Geitgey, R.P. and Vogt, B.F., Editors, Proceedings of the 25th Forum on the Geology of Industrial Minerals, *State of Oregon, Department of Geology and Mineral Industries,* Special Paper 23, pages 45-50.

Jones, L.D., McArthur J.G. and McPeek, C.B. (1991): MINFILE – A Mineral Deposit Information System; *in* Proceedings of the *Second Canadian Conference on Computer Applications in the Mineral Industry* (CAMI), Poulin, R., Pakalnis, R.C.T. and Mular, A.L., Editors, September 15-18, 1991, Vancouver, Canada, pages 85-96.

Kenyon, C. (1991): Coalbed Methane Potential of Vancouver Island, British Columbia; *in* Washington Geology, *Washington Department of Natural Resources,* Volume 19, No. 4, pages 19-20.

Kerr, D.E. (1991): Drift Exploration in Areas with Thick Quaternary Cover in British Columbia, Canada; *XIII INQUA Congress,* Program with Abstracts, page 162.

Kilby, W.E. (1991): Vitrinite Reflectance Measurement – Some Technique Enhancements and Relationships; *International Journal of Coal Geology,* Volume 19.

Leitch, C.H.B., Turner, R.J.W. and Höy, T. (1991): The District-scale Sullivan Mine Area, British Columbia; *in* Current Research, Part E, *Geological Survey of Canada,* Paper 91-1E, pages 45-57.

Levson, V.M. (1990): Geologic Settings of Buried Placer Gold Deposits in Glaciated Regions of the Canadian Cordillera; *Geological Association of Canada – Mineralogical Association of Canada,* Joint Annual Meeting, May 16-18, 1990, Vancouver, B.C., program with Abstracts, Volume 15, page A76.

Levson, V.M. (1990): Late Glacial Paleoenvironments in the Rocky Mountains, Jasper, Canada; Implications for Human Habitation; *in* Current Research in the Pleistocene, *University of Maine,* Volume 7, pages 138-140.

Levson, V.M. (1990): Late Glacial Paleoenvironments in the Rocky Mountains, Jasper, Canada; Implications for Human Habitation; *in* Current Research in the Pleistocene, *University of Maine,* Volume 7, pages 138-140.

Levson, V.M. (1990): Transition from Non-glacial to Glacial Conditions in the Canadian Cordillera: The Sedimentary Record; First Joint Meeting of the *Canadian Quaternary Association and the American Quaternary Association,* Waterloo, June 4-6, 1990. Program and Abstracts, page 23.

Levson, V.M. (1991): The Bullion Mine; A Large Buried-valley Gold Placer; *The Cariboo Miner,* Volume 2, pages 8-9.

Levson, V. and Kerr, D.E. (1991): Quaternary Studies and Gold Exploration in the British Columbia Intermontane Belt; *CANQUA 1991,* Program with Abstracts, page 25.

Levson, V.M. and Kerr, D.E. (1991): Quaternary Studies and Gold Exploration in the British Columbia Intermontane Belt; *in* Late Glacial and Post-glacial Events in Coastal and Adjacent Areas, *Canadian Quaternary Association,* Program and Abstacts, page 25.

Levson, V.M. and Morison, S. (1991): Quaternary Gold Placers in the Canadian Cordillera; *International Union for Quaternary Research,* XIII International Congress, Abstracts, page 191.

McMillan, W.J., Pantaleyev, A. and Höy, T. (1986): Mineral Deposits in British Columbia: a Review of their Tectonic Settings; *in* Geoexpo/86 Exploration in the North American Cordillera, Elliott, I.L. and Smee, B.W., Editors, *Association of Exploration Geochemists* and *Cordilleran Section, Geological Association of Canada,* pages 1-18.

Nixon, G.T., Cabri, L.J. and Laflamme, J.H.G. (1989): Provenance of Platinum Nuggets in Tulameen Placer Deposits; *Geological Society of Finland,* Bulletin 61(1), page 45.

Nixon, G.T., Cabri, L.J. and Laflamme, J.H.G. (1990): Platinum-Group-Element Mineralization in Lode and Placer Deposits Associated with the Tulameen Alaskan-Type Complex, British Columbia; *Canadian Mineralogist*, pages 503-535.

Pell, J. and Hora, Z.D. (1990): Rifting, Alkaline Rocks and Related Magmatic Deposits in the Southern Canadian Cordillera; *in* Program with Abstracts, 8th IAGOD Symposium, *International Association of the Genesis of Ore Deposits*, August 12-18, Ottawa.

Pell, J. and Höy, T. (1989): Carbonatites in the Canadian Cordillera; *in* Carbonatites, Genesis and Evolution, Bell, K., Editor, *Unwyn Hyman*, London, pages 200-220.

Ray, G.E., Coombes, S., MacQuarrie, D.R., Niels, R.J.E., Shearer, J.T. and Cardinal, D.G. (1985): Precious Metal Mineralization in Southwestern British Columbia; *Geological Society of America*, Field Trip 9, Guidebook, pages 9-1 to 9-31.

Ray, G.E. (1986): The Hozameen Fault System and Related Coquihalla Serpentine Belt of Southwestern British Columbia; *Canadian Jounal of Earth Sciences*, Volume 23, pages 1022-1041.

Ray, G.E. (1986): Harrison Lake Gold; *The Northern Miner Magazine*, March 1986, pages 17-19.

Ray, G.E., Shearer, J.T. and Niels, R.J.E. (1983): Carolin Gold Mine; *in* Some Gold Deposits in the Western Canadian Cordillera, *Geological Association of Canada*, MAC/CGU, May 1983, Field Trip Guidebook No. 4, pages 40-64.

Ray, G.E., Shearer, J.T. and Niels, R.J.E. (1986): The Geology and Geochemistry of the Carolin Gold Deposit, Southwestern British Columbia, Canada: *Proceedings of the "Gold 86" International Symposium on the Geology of Gold Deposits*, Toronto, pages 470-487.

Ray, G.E. (1990): Precious Metal Enriched Skarns of British Columbia; *The Gangue*, No. 30, January 1990, pages 2-4.

Ray, G.E. (1991): Vein Gold Mineralization Related to Mid-Tertiary Plutonism, Harrison Lake, British Columbia; *Economic Geology*, Volume 86, pages 833-891.

Sibbick, S.J. and Fletcher, W.K. (1991): Application of Cyanidation to Gold Exploration in Glaciated Terrain, British Columbia, Canada; *in* Exploration Goechemistry 1990 – Proceedings of Third International Joint Symposium, Mrna, F. Editor, *International Association of Geochemistry and Cosmochemistry (IAGC) and Association of Exploration Geochemists (AEG)*, pages 350-357.

Sibbick, S.J. and Fletcher, W.K. (1991): Distribution and Behavior of Gold in Soils and Tills at the Nickel Plate Mine, Southern British Columbia; *in* Abstracts with Programs, 15th International Geochemical Exploration Symposium, Reno, Nevada, *The Association of Exploration Geochemists*, page 45.

Smyth, R.W. (1990): British Columbia's Approach to the Challenges of Exploration and Mining in an Environmentally Conscious Province; in Pacific Rim Congress 90, Gold Coast, Queensland, Australia, *The Australasian Institute of Mining and Metallurgy*, Proceedings, Volume III, page 411.

Turner, R.J.W., Leitch, C.H.B., Ames, D.E., Höy, T., Franklin, J.M. and Goodfellow, W.D. (1991): Character of Hydrothermal Mounds and Adjacent Altered Sediments, Active Hydrothermal Areas, Middle Valley Sedimented Rift, Northern Juan de Fuca Ridge, Northeastern Pacific: Evidence from ALVIN Push Cores; *Geological Survey of Canada*, Current Research, Part E, Paper 91-1E, pages 99-108.

NOTES

UNIVERSITY RESEARCH IN BRITISH COLUMBIA

THE UNIVERSITY OF BRITISH COLUMBIA

Alldrick, D. (1991): Geology and Ore Deposits of the Stewart Mining Camp, British Columbia; Ph.D. (103O, P)

Cook, S.J. (1991): The Distribution and Behaviour of Platinum in Soils of the Tulameen Ultramafic Complex, Southern British Columbia: Applications to Geochemical Exploration for Chromitite Associated Platinum Deposits; M.Sc. (92H)

Heah, T.S.T. (1991): Latest Cretaceous to Eocene Extension along the Eastern Margin of the Central Gneiss Complex, Coast Belt, Shames River Area, near Terrace, British Columbia; M.Sc. (103I)

Hesthammer, J. (1991): Stratigraphy and Structural Styles in Central Graham Island, Queen Charlotte Islands, British Columbia; M.Sc. (103F)

Hood, C.T. (1991): Mineralogy, Paragenesis, and Mineralogic Zonation of the Silver Queen Vein System, Owen Lake, Central British Columbia; M.Sc. (93M, L)

Indrelid, J. (1991): Stratigraphy, Structural Geology and Petroleum Potential of the Cretaceous and Tertiary Rocks in the Central Graham Island, Queen Charlotte Islands, British Columbia; M.Sc. (103F)

Lewis, P.D. (1991): Structural Geology and Processes of Deformation in the Mesozoic and Cenozoic Evolution of the Queen Charlotte Islands; Ph.D. (103F, G, C)

Palty, J. (1991): Uppermost Hettangian to Lowermost Pliensbachian (Lower Jurassic Biostratigraphy and Ammonoid Fauna of the Queen Charlotte Islands, British Columbia; M.Sc. (103F, G, C)

Palsgrove, R.J. (1991): Stratigraphy, Sedimentology and Coal Quality of the Lower Skeena Group, Telkwa Coalfield, Central British Columbia; M.Sc.

Sperling, A. (1991): A Risk-Cost-Benefit Framework for the Design of Dewatering Systems in Open Pit Mines; Ph.D.

Taite, S.P. (1991): The Geology of the Central Moresby Island Region, Queen Charlotte Islands, (Haida Gwaii) British Columbia; M.Sc. (103C)

Von Sacken, R. (1991): New Data and Re-evaluation of the 1965 Hope Slide; M.Sc. (91H)

UNIVERSITY OF ALBERTA

Shaw, R.P. (1990): The Geology and Geochemistry of Gold Mineralization at Athabasca Pass, Central Rocky Mountains, British Columbia, Canada; M.Sc.

THE UNIVERSITY OF WESTERN ONTARIO

MacLean, P.J. (1991): Characterization of Pyrite from Gold Deposits, Axial Seamount; Ph.D.

UNIVERSITY OF CALGARY

MacLeod, S.E. (1991): Sedimentology and Paleontology of an Upper Jurassic-Lower Cretaceous Shelf to Alluvial Plain Coal-bearing Sequence, Northwest British Columbia, Canada; Ph.D.

Spiteri, R.R. (1991): Modelling the Deformation of the Alberta Foreland Basin using Finite Elements; M.Sc.

WESTERN WASHINGTON UNIVERSITY

Buddington, A.M. (1990): The Similkameen Batholith of North-Central Washington and South-Central British Columbia: The Petrotectonic Significance of an Alkaline/Calc-Alkaline Magma; M.Sc.

UNIVERSITY OF TORONTO

Peter, J.M. (1991): Comparative Geochemical Studies of the Upper Triassic Windy Craggy and Modern Guaymas Basin deposits: A Contribution to this Understanding of Massive Sulphide Formation in Volcano-sedimentary Environments; Ph.D.

UNIVERSITY OF WASHINGTON

Tyson, T.M. (1991): Structure, Plutonism and Metamorphism of the Cairn Needle Area, Southern Coast Mountains, British Columbia: Implications for Mid-Cretaceous Orogenesis; M.Sc. (92H, 92G)

UNIVERSITY OF OTTAWA

Beaudoin, G. (1991): Ag-Pb-Zn-Au Veins of Kokanee Range, British Columbia; Ph.D.

Stewart, D. (1991): Stratigraphy and Sedimentology of the Chancellor Succession (Middle to Upper Cambrian), Southeastern Canadian Rocky Mountains; Ph.D.

CARLETON UNIVERSITY

Bender, L.K. (1990): Aluminous Schists of the Shuswap Metamorphic Complex, Southern British Columbia; B.Sc.

Carr, S.D. (1991); Late Cretaceous-early Tectonic Evolution of the Southern Omineca Belt, Canadian Cordillera; Ph.D.

Coleman, M.E. (1991): Eocene Dextral Strike-Slip and Extensional Faulting in the Bridge River Terrane, Southwest British Columbia; M.Sc.

Coleman, V.J. (1991) The Monashee Decollement at Cariboo Alp and Regional Kinematic Indicators, Southeastern British Columbia; M.Sc.

Gareau, S. (1991): Geology of the Scotia-Quaal Metamorphic Belt, Coast Plutonic Complex, British Columbia; Ph.D.

Harrap, R.M. (1991): Stratigraphy and Structure of the Monashee Terrane in the Mount English Area, West of Revelstoke, B.C.; M.Sc.

Kaip, A. (1991): Synsedimentary Deformation and Depositional Environmemt of the Prodeita-slope Assemblage, Ashman Formation, Bowser Lake Group, North Central British Columbia; B.Sc.

Lindsay, D. (1991): Geology, Geochemistry and Petrography of the Moochie Cu-Au Occurrence Nelson, British Columbia; B.Sc.

Marsden, H.W. (1991): Stratigraphic, Structural and Tectonic Setting of the Shasta Au-Ag Deposit, North-Central British Columbia; M.Sc.

Waque, P. (1991): Mineral Assemblages, Textural Relationships of Sulphide-sulphate Hydrothermal Chimney 1924-6 Form Axial Seamount, Juan de Fuca ridge; B.Sc.

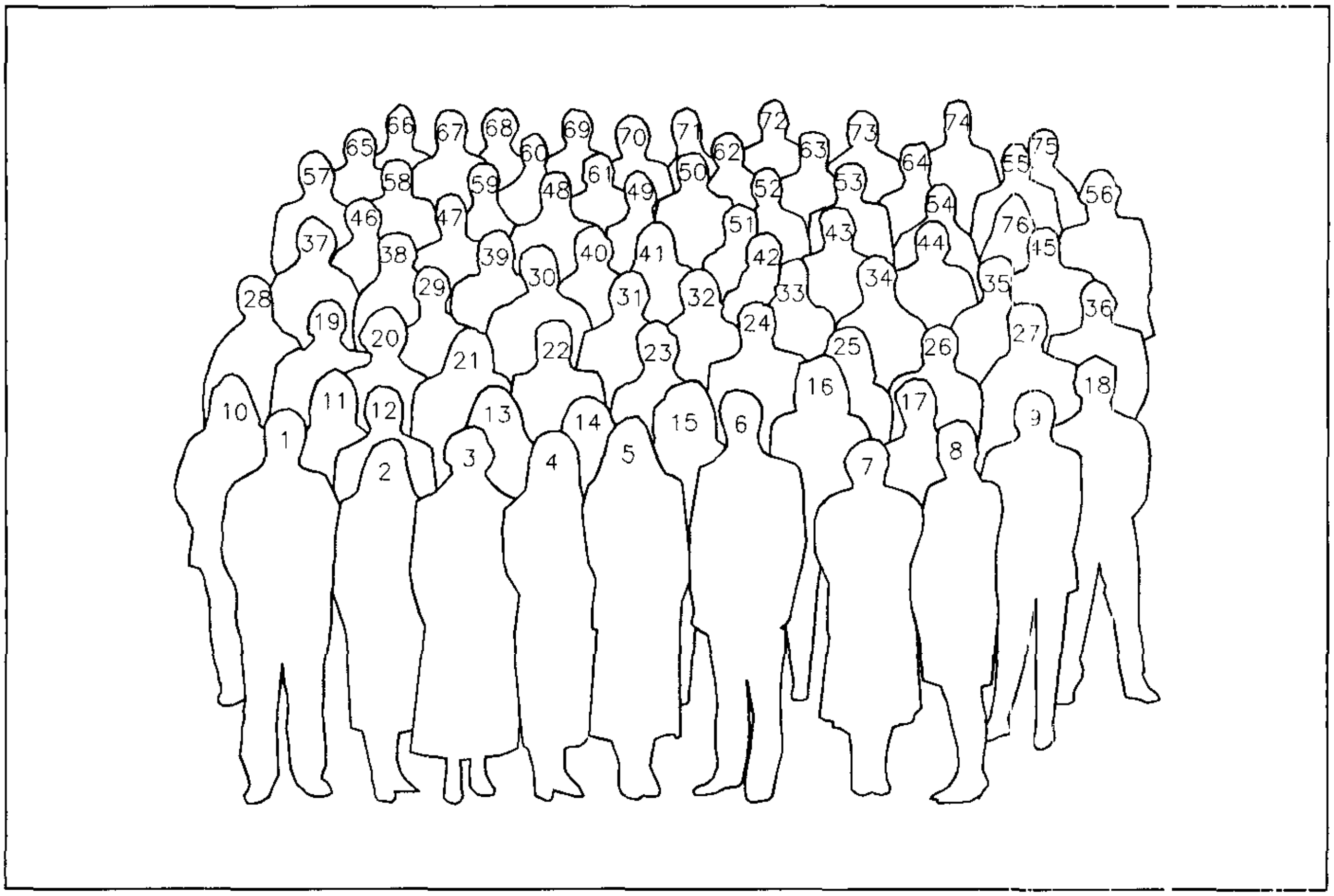

GEOLOGICAL SURVEY BRANCH PERSONNEL

1. John Cunningham
2. Laura deGroot
3. Julie Hutchins
4. Janet Trenamen
5. Claudia Logan
6. Ron Smyth
7. Sheila Arnett
8. Shirley Marshall
9. Shielagh Banfield
10. Moira Smith
11. Anna Peakman
12. Bill McMillan
13. Cindy McPeek
14. Pauline Loos
15. Candace Kenyon
16. Linda Jensen
17. Mary-Lou Malott
18. Victor Koyanagi
19. Bev Brown
20. Donna Blackwell
21. Shannon Ferguson
22. Tom Schroeter
23. Brian Grant
24. Dani Alldrick
25. Joanne Schwemler
26. Maria Holuszko
27. Andre Panteleyev
28. Mitch Mihalynuk
29. Bob Lane
30. George Simandl
31. Jim Logan
32. Joni Borges
33. Jan Hammack
34. Don MacIntyre
35. Ian Webster
36. Ray Lett
37. Mike Fournier
38. Nick Massey
39. Dorthe Jakobsen
40. Larry Jones
41. Kathy Colbourne
42. Vic Levson
43. Wayne Jackaman
44. Derek Brown
45. Talis Kalnins
46. David Ballantyne
47. Gary Payie
48. Chris Ash
49. Eric Grunsky
50. Gib McArthur
51. Bish Bhagwanani
52. George Owsiacki
53. Dave Lefebure
54. Barry Ryan
55. Alex Matheson
56. Dave Grieve
57. Andre Legun
58. Danny Hora
59. Peter Bobrowsky
60. Gerry Ray
61. Trygve Höy
62. Bob Gaba
63. Paul Wilton
64. Rick Meyers
65. Alan Wilcox
66. Bruce Madu
67. Steve Cook
68. Rob MacDonald
69. Jim Britton
70. Vic Preto
71. Steve Sibbick
72. Larry Diakow
73. James Pardy
74. Kirk Hancock
75. Ron Arksey
76. Joanne Nelson

NOTES

NOTES

Vern A. Burkhardt
Queen's Printer for British Columbia©
Victoria, 1992